UNITED STATES PATENT AND TRADEMARK OFFICE

BEFORE THE PATENT TRIAL AND APPEAL BOARD

ZHUHAI COSMX BATTERY CO., LTD.,
Petitioner

v.

NINGDE AMPEREX TECHNOLOGY LIMITED,
Patent Owner

Case IPR2023-00587
Patent No. 10,964,987

DECLARATION OF SAMUEL P. GIDO, PhD

TABLE OF CONTENTS

I. INTRODUCTION 1

II. BACKGROUND AND QUALIFICATIONS 2

III. LEVEL OF ORDINARY SKILL IN THE ART 7

IV. MATERIALS CONSIDERED AND RELIED UPON 8

V. LEGAL STANDARDS 9

A. Claim Construction 9

B. Anticipation 10

C. Obviousness 10

VI. STATE OF THE ART 12

VII. OVERVIEW OF PRIOR ART 38

A. Nishikawa 38

B. Iwai 39

C. Honda 45

VIII. THE ’987 PATENT 46

IX. CLAIM CONSTRUCTION 47

X. THE CHALLENGED CLAIMS ARE UNPATENTABLE 48

A. Ground 1: *Nishikawa* Would Have Anticipated Claims 1-2 and 4-9 48

1. Claim 1 48

2. Claim 2: The separator according to claim 1, wherein the porous layer has a thickness of 0.2 μm to 10 μm. 54

3. Claim 4: The separator according to claim 1, wherein a volume ratio of the inorganic particles to the binder is in a range from 0.2 to 3.0. 54

4. Claim 5: The separator according to claim 1, wherein the porous layer has a porosity of 20% to 90%. 60

5. Claim 6: The separator according to claim 1, wherein the inorganic particles are one or more selected from the group consisting of alumina, silica, magnesia, titanium oxide, hafnium dioxide, tin oxide, zirconia, cerium dioxide, nickel oxide, zinc oxide, calcium oxide, boehmite, aluminum hydroxide, magnesium hydroxide, calcium hydroxide, and barium sulfate. 60

6. Claim 7: The separator according to claim 1, wherein the binder is one or more selected from the group consisting of polyvinylidene fluoride, vinylidene fluoride-hexafluoropropylene copolymer, polyamide, polyacrylonitrile, polyacrylate, polyacrylic acid, polyacrylates, sodium carboxymethylcellulose, polyvinylpyrrolidone, polyvinyl ether, polymethyl methacrylate, polytetrafluoroethylene and polyhexafluoropropylene. 61

7. Claim 8: An energy storage device, comprising the separator according to claim 1. 62

8. Claim 9: The energy storage device according to claim 8, wherein the energy storage device is a lithium-ion battery. 62

B. Ground 2: *Nishikawa* Would Have Rendered Obvious Claims 10-16 63

1. Claim 10 63

2. Claim 11: The method according to claim 10, wherein the solid content in the coating solution is in a range from 7% to 25%. 72

3. Claim 12: The method according to claim 10, wherein the coagulating solution comprises a second solvent and a third solvent, and the second solvent has a mass percentage of 20% to 60% 72

4. Claim 13: The method according to claim 10, wherein the first solvent is one or more independently selected from the group consisting of N-methylpyrrolidone, dimethylacetamide and dimethylformamide 73

5. Claim 14: The method according to claim 10, wherein the porous substrate comprises a polymer film, a multilayer polymer film, or a non-woven fabric formed by any one or more of the following polymers: polyethylene, polypropylene, polyethylene terephthalate, polyphthaloyl diamine, polybutylene terephthalate, polyester, polyacetal, polyamide, polyimide, polyetheretherketone, polyaryletherketone, polyetherimide, polyamide imide, polybenzimidazole, polyethersulfone, polyphenylene oxide, cycloolefin copolymer, polyphenylene sulfide, and polyethylene naphthalene 74

6. Claim 15: The method according to claim 14, wherein the polyethylene is at least one selected from the group consisting of high density polyethylene, low density polyethylene, and ultrahigh molecular weight polyethylene 74

7. Claim 16: The method according to claim 12, wherein the second solvent is one or more independently selected from the group consisting of N-methylpyrrolidone, dimethylacetamide and dimethylformamide, and the third solvent is one or more selected from the group consisting of deionized water, ethanol, propanol, acetone, dimethyl carbonate and diethyl carbonate 75

C. Ground 3: *Nishikawa* and *Honda* Would Have Rendered Obvious Claim 17 76

1. Claim 17: The separator according to claim 1, wherein the porous layer has pores formed by the binder, at least a part of the inorganic particles are embedded in the pores. 76

D. Ground 4: *Iwai* Anticipates Claims 1-2 and 4-9 78

1. Claim 1 78

2. Claim 2: The separator according to claim 1, wherein the porous layer has a thickness of 0.2 μm to 10 μm. 88

3. Claim 4: The separator according to claim 1, wherein a volume ratio of the inorganic particles to the binder is in a range from 0.2 to 3.0. 88

4. Claim 5: The separator according to claim 1, wherein the porous layer has a porosity of 20% to 90%. 92

5. Claim 6: The separator according to claim 1, wherein the inorganic particles are one or more selected from the group consisting of alumina, silica, magnesia, titanium oxide, hafnium dioxide, tin oxide, zirconia, cerium dioxide, nickel oxide, zinc oxide, calcium oxide, boehmite, aluminum hydroxide, magnesium hydroxide, calcium hydroxide, and barium sulfate. 93

6. Claim 7: The separator according to claim 1, wherein the binder is one or more selected from the group consisting of polyvinylidene fluoride, vinylidene fluoride-hexafluoropropylene copolymer, polyamide, polyacrylonitrile, polyacrylate, polyacrylic acid, polyacrylates, sodium carboxymethylcellulose, polyvinylpyrrolidone, polyvinyl ether, polymethyl methacrylate, polytetrafluoroethylene and polyhexafluoropropylene. 93

7. Claim 8: An energy storage device, comprising the separator according to claim 1. 94

8. Claim 9: The energy storage device according to claim 8, wherein the energy storage device is a lithium-ion battery. 95

E. Ground 5: *Iwai* Would Have Rendered Obvious Claim 3 95

1. Claim 3: The separator according to claim 1, wherein the pores have an average pore size of 0.3 μm to 20 μm. 95

XI. CONCLUSION 1

LIST OF EXHIBITS

Exhibit	Description
Ex. 1001	U.S. Patent No. 10,964,987
Ex. 1002	Prosecution History of U.S. Patent No. 10,964,987
Ex. 1003	Declaration of Dr. Samuel Gido
Ex. 1004	Curriculum Vitae of Dr. Samuel Gido
Ex. 1005	Nishikawa et al., U.S. Patent No. 7,976,987
Ex. 1006	Iwai et al., U.S. Patent App. Pub. No. 2014/0248525
Ex. 1007	Honda et al., U.S. Patent App. Pub. No. 2015/0263325
Ex. 1008	Jurgen O. Besenhard (ed.), Handbook of Battery Materials (1999)
Ex. 1009	Seo et al., U.S. Patent No. 8,318,360
Ex. 1010	Lee et al., U.S. Patent No. 7,662,517
Ex. 1011	Sigma-Aldrich Safety Data Sheet for Aluminum hydroxide fine powder pure, hydrargillite
Ex. 1013	Sigma-Aldrich Safety Data Sheet for Poly [N,N′-(1,3-phenylene) isophthalamide]
Ex. 1017	Patnaik, Handbook of Inorganic Chemicals (2002)
Ex. 1018	Ahmad et al., Synthesis of Polyvinylidene Fluoride (PVDF) Membranes for Protein Binding: Effect of Casting Thickness, Journal of Applied Polymer Science (2013)
Ex. 1019	Katayama et al., U.S. Patent App. Pub. No. 2010/0221965

LIST OF APPENDICES

Appendix	Description
A	Showa Denko Webpage on HIGILITE® (Machine Translation)
B	Lin et al., Poly(m-phenylene isophthalamide) (PMIA): A potential polymer for breaking through the selectivity-permeability trade-off for ultrafiltration membranes, *Journal of Membrane Science* 518 (2016) 72-78.
C	Huang et al., Ionic Conductivity of Microporous PVDF-HFP/PS Polymer Blends, *Journal of The Electrochemical Society*, 148 (3) A279-A283 (2001).
D	Kynar Flex 2801 Technical Data Sheet
E	Kynar Flex 2751 Technical Data Sheet
F	U.S. National Transportation Safety Board, Incident Report NTSB/AIR-14/01, PB2014-108867. Auxiliary Power Unit Battery Fire, Japan Airlines Boeing 787-8, JA829J, Boston, Massachusetts January 7, 2013.
G	Prosini et al., A novel intrinsically porous separator for self-standing lithium-ion batteries, *Electrochimica Acta* 48 (2002) 227-233.
H	Hotza et al., Review: aqueous tape casting of ceramic powders, *Materials Science and Engineering* A202 (1995) 206-217.
I	Huang, Separator technologies for lithium-ion batteries, *J. Solid State Electrochem.* (2011) 15:649–662.
J	Arora et al., "Battery Separators" *Chem. Rev.* 2004, 104, 4419-4462.
K	Venugopal et al., Characterization of microporous separators for lithium-ion batteries, *J. Power Sources* 1999, 77, 34.
L	Kim et al., U.S. Patent No. 7,709,152
M	Park et al., U.S. Patent No. 7,695,870
N	Lee et al., U.S. Patent No. 7,638,241
O	"A basic guide to particle characterization," published by Malvern Instruments Ltd. (2015)
P	Choi et al., Enhancement of thermal stability and cycle performance in lithium-ion cells through the use of ceramic coated separators, *Journal of Power Sources*, Vol. 195, pp. 6192-6196, 2010.
Q	Shinohara et al., U.S. Patent No. 6,447,958
R	Zhang, A review on the separators of liquid electrolyte Li-ion batteries, *Journal of Power Sources* 164 (2007) 351–364
S	Isaacson et al., U.S. Patent No. 3,558,764

T	Larsen et al., U.S. Patent No. 3,351,495
U	Lundquist et al., U.S. Patent No. 4,650,730
V	Yu et al., U.S. Patent No. 5,565,281
W	Yu et al., U.S. Patent No. 5,952,120
X	Carlson et al., U.S. Patent No. 6,306,545
Y	Kim et al., Characteristics of PVdF-HFP/TiO2 composite membrane electrolytes prepared by phase inversion and conventional casting methods, *Electrochimica Acta* 51 (2006) 5636–5644.

I, Samuel Gido, of Amherst, Massachusetts, declare that:

I. INTRODUCTION

1. My name is Samuel Gido, and I have been retained by counsel for Petitioner Zhuhai CosMX Battery Co., Ltd. ("Petitioner") as an expert witness to provide assistance regarding U.S. Patent No. 10,964,987 ("the '987 Patent"). Specifically, I have been asked to consider the validity of claims 1-17 of the '987 Patent (the "challenged claims") in view of prior art, anticipation and obviousness considerations, and the understanding of a person of ordinary skill in the art at the time of the invention ("POSA") as it relates to the '987 Patent. I have personal knowledge of the facts and opinions set forth in this declaration and believe them to be true. If called upon to do so, I would testify competently thereto.

2. I am being compensated for my time at my standard consulting rate. I am also being reimbursed for expenses that I incur during the course of this work. My compensation is not contingent upon the results of my study, the substance of my opinions, or the outcome of any proceeding involving the challenged claims. I have no financial interest in the outcome of this matter or on the pending litigation between Petitioner and Patent Owner.

3. My analysis here is based on my years of education, research and experience, as well as my investigation and study of relevant materials, including those cited herein.

4. I may rely upon these materials, my knowledge and experience, and/or additional materials to rebut arguments raised by the Patent Owner. Further, I may also consider additional documents and information in forming any necessary opinions, including documents that may not yet have been provided to me.

5. My analysis of the materials in this proceeding is ongoing and I will continue to review any new material as it is provided. This declaration represents only those opinions I have formed to date. I reserve the right to revise, supplement, and/or amend my opinions stated herein based on new information and on my continuing analysis of the materials already provided.

II. BACKGROUND AND QUALIFICATIONS

6. I have been on the faculty at the University of Massachusetts at Amherst since 1993. I am currently Associate Professor of Polymer Science and Engineering. I have broad expertise across the fields of polymers (plastics), polymer-nanoparticle composites, fluorinated polymers, polyolefins, porous materials, phase separations, and coating processes. I am an expert in and experienced user of a range of materials characterization techniques including scattering, and spectroscopies, but with a particular emphasis on microscopy, especially electron microscopy. Over the years I have studied materials for a broad range of applications including: batteries, fuels cells, adhesives, non-stick coatings, elastomers, composites and nanostructures. In addition to academic research, I have done research for, and/or consulted for a

range of companies including: W.L. Gore, Boston Scientific, FujiFilm (Japan), Kureha Chemical Industry (Japan), Loctite Corp. (now Henkle), Rexam Graphics, St. Gobain, and Scapa Tape.

7. I studied for my bachelor's degree in Chemical Engineering at Princeton University, and graduated *Magna Cum Laude* in 1988. While at Princeton I did research at the nearby Textile Research Institute (https://www.triprinceton.org/what-we-offer) ("TRI"), where I focused on applying foamed coatings to porous substrates. I completed a bachelor's thesis on this topic; the title of my thesis was: "Foam Flow Through Porous Media: Image Analysis Development & Investigation of Microscopic Flow Mechanism." TRI also provided my first involvement in using scanning electron microscopy (SEM) to coatings and porous materials.

8. After graduating from Princeton in 1988, I moved on to a doctoral program at the Massachusetts Institute of Technology (MIT). My home department at MIT was Chemical Engineering, but I also was part of the interdisciplinary Program in Polymer Science and Technology (PPST, http://polymerscience.mit.edu/). I did my research and doctoral thesis under the direction of Prof. Edwin L. Thomas, who was in the Materials Science and Engineering Department at MIT. Prof. Thomas is a world-renowned expert in the study of polymer structure using electron microscopy. Therefore, my training and

research at MIT focused on the use of electron microscopy, including SEM and transmission electron microscopy (TEM), to study a range of different topics including plastics, rubbers, copolymers, polymer-ceramic composites, phase behavior, and phase separations. After receiving my Ph.D. in 1993, I moved on to begin my career as an Assistant Professor in the Polymer Science and Engineering Department at the University of Massachusetts at Amherst. Over my academic career I have received millions of dollars of research funding from government (U.S. Army, National Science Foundation, U.S. Department of Education), foundations (Bill and Melinda Gates Foundation, W. M. Keck Foundation), and industry.

9. I have focused on a bottom-up concept of new materials design for advanced applications. In particular, I have worked on development of new molecular structures for the control of nanometer and micrometer length scale structure and morphology, directed toward improving properties such as: mechanical strength, transport (diffusion) of gases and liquids in porous materials, electrical properties, and adhesion. A large part of this research is on controlling the phase separation behavior (coagulation) of material to form unique, functional structures. One particular published study was on using phase separation to produce porous structures in high density polyethylene. *See* Ex. 1004 (Peer-Reviewed Publication 65).

10. I have numerous publications and a U.S. Patent on fluorinated polymers

for a range of applications, including in separators for batteries and fuel cells. I have done research on materials for batteries and fuel cells, including fluorinated polymers and polymer particle composites, with funding from Kureaha (Japan), and the U.S. Army. In these studies, we developed polymer chemistries, nanometer and micrometer scale composite structures and porous structures, and coating processes to enhance ion conductivity in the separator layers. Additionally, I have worked and continue to work as a consultant for W. L. Gore, a leading company in fluorinated polymers. I have consulted for industry on the topic of coating processes, particularly for Rexam Graphics and Scapa Tape. I was also a co-founder of a startup company, Smart Surfaces LLC, that developed environmentally friendly, non-stick coatings for boats (and other structures in a marine environment) to prevent fouling with marine organisms. Smart Surfaces was sold to FujiFilm in 2006, and I continued to consult for the resultant company: FujiFilm Smart Surfaces LLC. These coatings, were silicone based, contained ceramic filler particles, and cured by a coagulation (phase separation) process.

11. I did a research project for Loctite Corporation in which I used electron microscopy to study adhesive polymer layers filled with inorganic reinforcing particles. And I did research for Boston Scientific, which resulted in a U.S. Patent, on polymer coatings for heart stents, using a number of techniques including electron microscopy. These coatings contained filler particles, a particulate drug, and we

studied the diffusion of this drug through the coating layer.

12. One of the best ways to really understand a topic is to teach it to someone else. I have taught and continue to teach topics, relevant to this matter, to our advanced graduate students (doctoral candidates) in the Polymer Science and Engineering Department at the University of Massachusetts at Amherst. In past years I have taught PSE 608 Introduction to Polymer Engineering, which includes topics such as mechanical properties, coatings processes, and diffusion of ions in materials. I have also taught in the past and am currently teaching PSE 602 Polymer Characterization Laboratory, in which the students gain practical laboratory experience with techniques of importance in this matter including SEM, and static laser light scattering (aka laser diffraction) for size determination. I teach PSE 608 Physical Chemistry of Polymers I and PSE 789 Physical Chemistry of Polymers II. In this sequence of classes, I cover, among other things, phase behavior and phase separations (coagulation), and the theory of laser light scattering. I also teach PSE 721 Polymer Morphology. This class focuses on nanometer and micrometer size structure in polymers and composites, as well as the use of electron microscopy to study materials structure. In PSE 608 and also in PSE 721, polyethylene is repeatedly used as an example for in depth discussion of polymer structure, and characterization methods. I also teach a seminar class for freshman, FFYS 191POLY The Polymer Age, which focuses on popular and societal impacts of polymers. In this class, I

present a seminar on lithium ion batteries with a particular focus on the materials used in their construction and the safety issues related to separators.

III. LEVEL OF ORDINARY SKILL IN THE ART

13. In rendering the opinions set forth in this declaration, I was asked to consider the patent claims and the prior art through the eyes of a person of ordinary skill in the art ("POSA") at the time of the alleged invention, which I understand is asserted to be as early as April 11, 2018. I understand that determining the ordinary skill in the art includes looking, among other considerations, at (i) the type of problems encountered in the art; (ii) prior art solutions to those problems; (iii) rapidity with which innovations are made; (iv) sophistication of the technology; and (v) educational level of active workers in the field. I understand that a POSA is not a specific real individual, but rather is a hypothetical individual having the qualities reflected by the factors above. I understand that a POSA would also have knowledge from the teachings of the prior art, including the art cited below.

14. Taking these factors into consideration, on or before April 11, 2018, a POSA of the '987 Patent would have had at least a bachelor's degree or equivalent degree from an accredited institution in chemistry, chemical engineering, materials science, or a similar discipline covering relevant principles of organic and inorganic chemistry, polymer processing, ceramic materials, and ceramic processing, as well as three or more years of experience in electrochemical energy storage devices,

lithium-ion battery technology, separators, characterizations and analyses of particle size, film thickness, and/or materials compositions, battery performance characterization, or other applications of polymer chemistry, ceramic chemistry, and ceramic processing. More education could substitute for less experience, and vice versa.

15. With bachelors and PhD degrees in Chemical Engineering, and years of experience working in the fields of polymers, polymer-filler composites, polymer processing, coatings, batteries and other energy storage devices, electron microscopy and laser diffraction, I meet and surpass the definition of a POSA in this matter. Before April 11, 2018, my level of skill in the art was at least that of a POSA. I am qualified to provide opinions concerning what a POSA would have known and understood at that time, and my analysis and conclusions herein are from the perspective of a POSA as of that date.

IV. MATERIALS CONSIDERED AND RELIED UPON

16. In reaching the conclusions described in this declaration, I have relied on the documents and materials cited herein as well as those identified in this declaration, including the ’987 Patent, the prosecution history of the ’987 Patent, and prior art references cited herein. These materials comprise patents, related documents, and printed publications. Each of these materials is a type of document that experts in my field would have reasonably relied upon when forming their

opinions.

17. In quoting the cited references, all emphasis is added unless otherwise noted.

18. I have also relied on my education, training, research, knowledge, and personal and professional experience in the relevant technologies and systems that were already in use prior to, and within the timeframe of the earliest asserted invention date of the claimed subject matter in the ’987 Patent, which is April 11, 2018.

V. LEGAL STANDARDS

19. I am not a lawyer. My understanding of the legal standards to apply in reaching the conclusions in this declaration is based on discussions with counsel for Petitioner and my reading of the documents submitted in this proceeding. In preparing this declaration, I have tried to faithfully apply these legal standards to the challenged claims.

A. Claim Construction

20. I have been instructed that the terms appearing in the ’987 patent should be interpreted in view of the claim language itself, the specification, the prosecution history of the patent, and any relevant extrinsic evidence. The words of a claim are generally given their ordinary and customary meaning, which is the meaning that the term would have to a POSA at the time of the invention, which I have assumed

here is April 11, 2018. While claim limitations cannot be read in from the specification, the specification is the single best guide to the meaning of a disputed term. I have followed these principles in reviewing the claims of the ’987 patent and forming the opinions set forth in this declaration.

B. Anticipation

21. I have been told that under 35 U.S.C. § 102, a patent claim is invalid if its subject matter was patented or described in a printed publication before the effective filing date of the claimed invention. I have been told that this is referred to as invalidity by anticipation. I have been told that a patent claim is anticipated under § 102 if a single prior art reference discloses, either expressly or inherently, all limitations of the claimed invention.

C. Obviousness

22. I understand that the existence of each and every element of the claimed invention in a prior art does not necessarily prove obviousness and that most, if not all, inventions rely on building blocks of prior art. But I have been told that under 35 U.S.C. § 103, a patent claim may be obvious if the differences between the subject matter sought to be patented and the prior art are such that the subject matter as a whole would have been obvious at the time the invention was made to a POSA to which said subject matter pertains. I have been told that a proper obviousness analysis requires the following:

a. Determine the scope and content of the prior art;

b. Ascertain the differences between the prior art and the claims at issue;

c. Resolve the level of ordinary skill in the pertinent art; and

d. Consider evidence of secondary indicia of non-obviousness (if available).

23. I have been told that the relevant time for considering whether a claim would have been obvious to a POSA is the time of invention. For my obviousness analysis, counsel for Petitioner instructed me to assume that the date of invention for the challenged claims is April 11, 2018. My opinions would not change if I assumed a later date of invention.

24. I have been told that a reference may be modified or combined with other references, or with a POSA's own knowledge, if the person would have found the modification or combination obvious. I have also been told that a POSA is presumed to know all the relevant prior art, and the obviousness analysis may take into account the inferences and creative steps that a POSA would employ.

25. I have been told that whether a prior art reference renders a patent claim obvious is determined from the perspective of a POSA. I have also been told that, while there is no requirement that the prior art contain an express suggestion to combine known elements to achieve the claimed invention, and while a suggestion to combine known elements to achieve the claimed invention may come from the prior art as a whole or individually and may consider the inferences and creative

steps a POSA would employ, as filtered through the knowledge of one skilled in the art, obviousness grounds cannot be sustained by mere conclusory statements and must include some articulated reasoning with some rational underpinning to support the legal conclusion of obviousness.

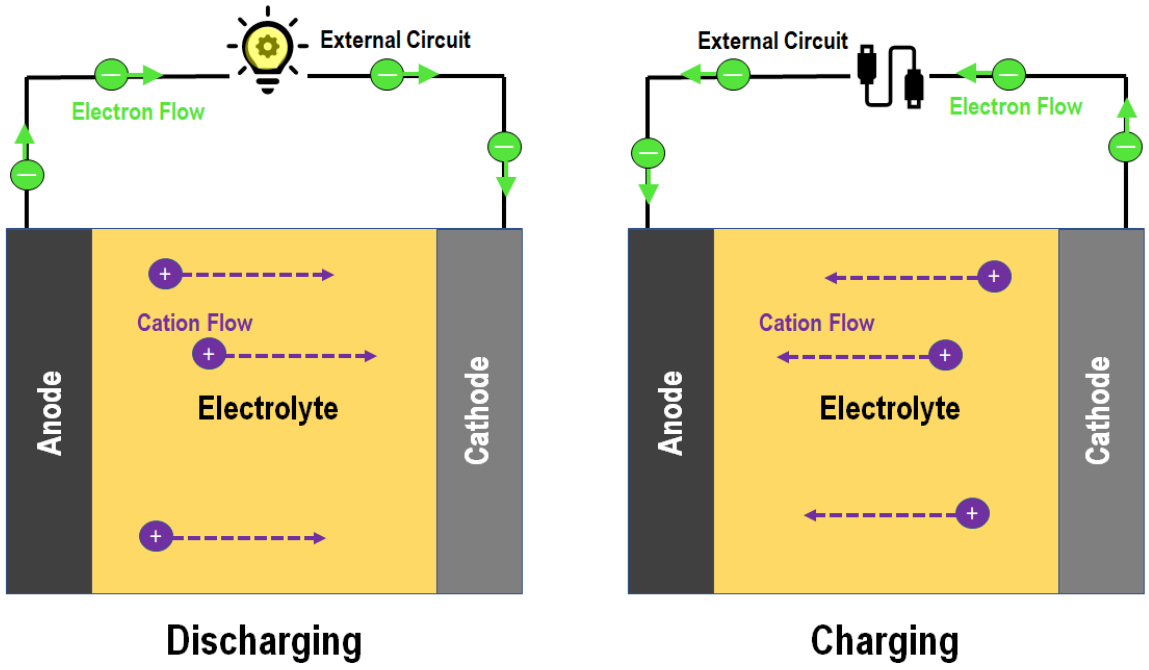
26. I have been told that there is no rigid rule that a reference or combination of references must contain a "teaching, suggestion, or motivation" to combine references. However, I also have been told that the "teaching, suggestion, or motivation" test can be used in establishing a rationale for combining elements of the prior art. I have also been told to be aware of distortions caused by hindsight bias, and that reading into the prior art the teachings of the invention at issue is improper.

VI. STATE OF THE ART

27. The most basic structure of any battery is illustrated below, in which an anode (negative electrode) and a cathode (positive electrode) are separated from one another and immersed in an electrolyte (medium capable of transporting ions). On discharging, positive ions, known as cations (atoms missing one or more electrons), diffuse through the electrolyte, from the anode across the gap to the cathode. In order to maintain electrical neutrality, electrons move separately through an external circuit from the anode to the cathode, where they are recombined with the cations to reform atoms. As the electrons make this journey through the external circuit they comprise an electrical current, which can be used to perform work, such as lighting

a lightbulb (as shown), or running an electric vehicle, computer, or smart phone. Charging the battery is the reverse process, in which an external voltage is used to push electrons through the external circuit back to the anode, creating cations at the cathode that migrate through the electrolyte to meet the electrons and reform the atoms at the anode.

General Battery Schematic



28. The term "battery" was coined by Benjamin Franklin in 1749 to refer to a rechargeable electrical power storage device he had built, which was actually an array of capacitors. Around 1799-1800, Italian scientist Alessandro Volta demonstrated the first true battery, consisting of alternating stacks of copper and zinc (the electrodes), separated by layers of cloth or cardboard soaked in brine or weak

acid (electrolyte). The rechargeable, or secondary, battery was invented in 1859 by Gaston Plante. This was a lead-acid battery similar to those still used today to start internal-combustion-powered vehicles. Plante also pioneered the spiral-rolled arrangement of electrodes and separator, still used in cylindrical batteries.

29. The first mass-produced and widely marketed battery was the Columbia Dry Cell, introduced by the National Carbon Company in 1896. It had a cylindrical shape, larger but recognizable to modern eyes. It also featured a cylindrically coiled cardboard separator between the anode and cathode. Alkaline batteries, the common disposable batteries still in common use, were invented in the 1950s and commercialized in 1959 by Union Carbide, the descendant of the National Carbon Company.

30. Lithium primary batteries (single use) were first conceived and studied in the 1960s. The 1970s and 1980s saw extensive development of lithium-ion secondary (rechargeable) batteries, culminating in the commercialization of the first lithium-ion battery by Sony in 1991. The 2019 Nobel Prize in Chemistry was awarded to three scientists who were instrumental in this work to develop practical lithium-ion batteries.

31. In a battery, the two electrodes, anode and cathode, must never touch. If they do, an electrical short circuit will result, discharging the battery so quickly that resistive heating from the high current inside the battery may cause a fire or

explosion, especially if the electrolyte fluid is combustible.

32. There are workable battery designs in which electrodes (for instance plates of metal and metal oxides) are suspended, apart from each another, in a bath of electrolyte fluid. A lead acid car battery is like this. But this is inefficient. The energy density of a battery (energy stored divided by the weight) is increased if the electrodes can be placed very close together, bearing in mind that they must also be prevented from ever actually contacting. Modern and emerging applications like electric vehicles and handheld electronics require high battery energy density.

33. To make batteries more energy dense, and thus more portable, separators are employed to act as a physical barrier as the electrodes are brought very close together. The production of modern battery configurations involves rolling long strips of electrodes into jellyroll structures to fit into cylindrical or prismatic cans, or squeezing multilayered sandwiches of electrodes into flat pouches. These processes force anode and cathode layers against one another and would cause them to touch if it were not for separator layers inserted between the electrodes.

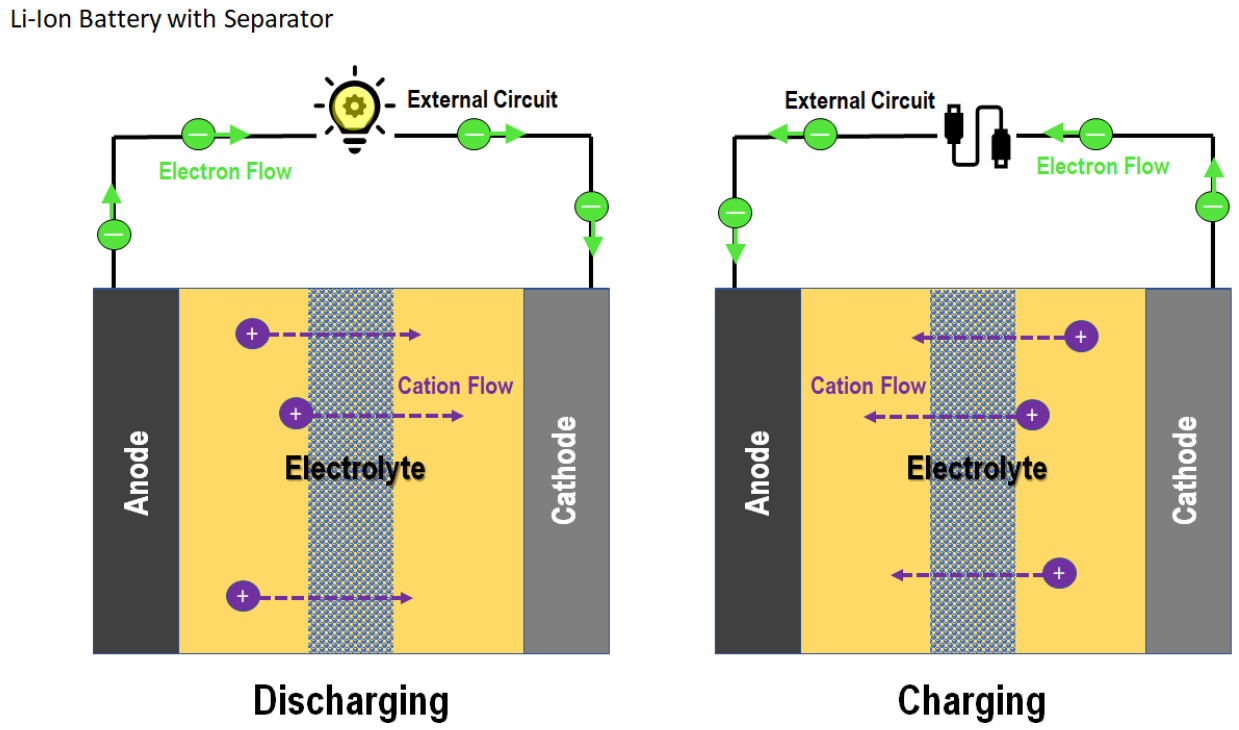
34. The separators must be electrically insulating with respect to current flow carried by electrons. They must be chemically stable in the strong oxidizing and reducing environment of battery electrochemistry. And they must facilitate the transport of cations (positively charged atoms). The separation function and the ion conduction function are usually accomplished by separate materials. For instance,

Volta's battery "pile" used cardboard separators soaked in a brine solution electrolyte.

35. Because of their high energy density and ability to withstand many discharging and charging cycles with little loss of capacity, lithium-ion batteries have become ubiquitous in the modern world. They power our smart phones, laptop computers, electric cars, and myriad other devices. They are beginning to be used to balance and back up our power grids to allow greater integration of green energy sources such as wind and solar. The rapid rise of these applications has led to a strong push over the past two decades, by industrial and academic researchers, to optimize lithium-ion batteries by, for example, improving energy density, charge and discharge rates, reliability and safety.

36. A schematic of the most common embodiment of the modern lithium-ion battery is shown below. A typical anode is formed of, for instance, a lithium carbon (graphite) intercalation compound coated onto a copper foil current collector. A typical cathode is formed of, for instance, lithium metal oxide dispersed in a polymer binder, coated onto an aluminum foil current collector. The anode and cathode are separated by a separator, which is typically a porous structure impregnated with a fluid electrolyte. The electrolyte fluid is generally a polar organic solvent, such as an organic carbonate liquid. Lithium cations are solubilized in this electrolyte solvent and can move between the electrodes by passing through the

separator.



37. In the 2000s, as lithium-ion batteries became ever more ubiquitous in portable devices, rare battery fires and explosions started to become a problem. With billions of these batteries being used in the world, even a rare problem produced a significant number of incidents. A famous case was the 2013 grounding of the Boeing 787 due to battery fires in Boston and Japan. *See, e.g.*, Appendix F. These fires in lithium-ion batteries result from short circuits in which the separator is breached. This can occur upon overcharging of the battery, in which lithium metal dendrites (sharp pointy structures) grow from the anode, pierce the separator, and contact the cathode. Short circuits can also result from damage to the battery such as

a puncture. Short circuits lead to thermal runaway, which is a feedback cascade of structural damage due to heating, from high current, producing even more damage, which leads to more current and more damage, rapidly escalating to a fire or explosion of the organic liquid electrolyte, which has combustibility similar to gasoline. Additionally: "Both shrinking and melting of the separator could result in physical contact of the electrodes so that direct chemical reactions between the strongly oxidative cathode material and the strongly reductive anode material occur, and the generated heat causes thermal runaway." Appendix R, 359.

38. Thus, over the last two decades, increasing the safety of battery separators has been a focus of extensive effort by those of skill in the art. One approach is to increase the mechanical robustness and high temperature stability of separators. For instance, the Evonik-Degussa SEPARION separator uses a porous non-woven fabric of polyethylene terephthalate (PET) fibers coated with ceramic particles, using a sol-gel process that does not use a polymer binder. PET has better high temperature stability than, for instance, polyolefins. Adding the ceramic coating further increases heat resistance. Appendix J, 4427.

39. It had been known for a long time (about a century) that adding inorganic particles to a polymer material can increase the strength and high temperature performance of the polymer. This was not a discovery of people working on battery separators, but rather comes from related, broader fields of

polymer processing, polymer compounding, and composite materials. For instance, car tires are black because the rubber (which is inherently white or slightly yellowish) is mixed with carbon black, an inorganic, particulate form of carbon. Without carbon black the rubber tires would be too soft and weak and would fail easily, especially at high temperatures experienced on a hot road in summer and exacerbated by repetitive, high-rate mechanical flexing. The inorganic filler particles improve the strength of the rubber and allow it to maintain its strength to higher temperatures. This is because the inorganic particles are themselves stable to very high temperature and because they reinforce the polymer molecules such that they are less likely to be degraded by high temperature, and to the degree that some degradation of the polymer occurs the presence of the inorganic filler mitigates the effect on properties.

40. Other high temperature resistant separators were produced in which inorganic, ceramic, particles were mixed with a polymer and cast to produce a free-standing film (*see, e.g.,* Appendix G, Appendix Q) or coated directly onto electrodes. The investigators who worked on these approaches in the 2000s and 2010s were importing, into the field of batteries, longstanding knowledge about polymer and ceramic properties and processing, especially knowledge of coating processes to produce thin films or tapes of polymer-ceramic slurries or mixtures. *See, e.g.,* Appendix H. This had already been used for a broad range of disparate applications, from porous coatings on specialty inkjet paper to capacitors.

41. Besides making battery separators stronger and more heat resistant, another approach to lithium-ion battery safety was to give separators a thermal shut-off functionality. This is achieved using uniaxially or biaxially stretched (oriented) porous, polyolefin separator films. The two polyolefin materials most often used in this capacity are polyethylene (PE) and polypropylene (PP). Different grades of PE are available and used in these applications, including low density polyethylene, high density PE (HDPE), and ultrahigh molecular weight PE (UHMWPE). In a dry process, solid films of polyolefin are mechanically stretched in one direction (uniaxial) or two directions (biaxial). This opens up voids or pores in the film. There is also a wet process for making polyolefin separators, based on a phase separation or a coagulation (phase inversion) process of the polyolefin from solvents, which also often incorporates stretching of the separator film.

42. The images below are scanning electron microscope (SEM) images of polyolefin separators produced by the dry (a) and wet (b) processes. Appendix I, Appendix J. Separator (a) has been uniaxially stretched (vertical direction) creating pores that are elongated in the direction of stretch, and separator (b) has more of a biaxial (in plane) orientation.

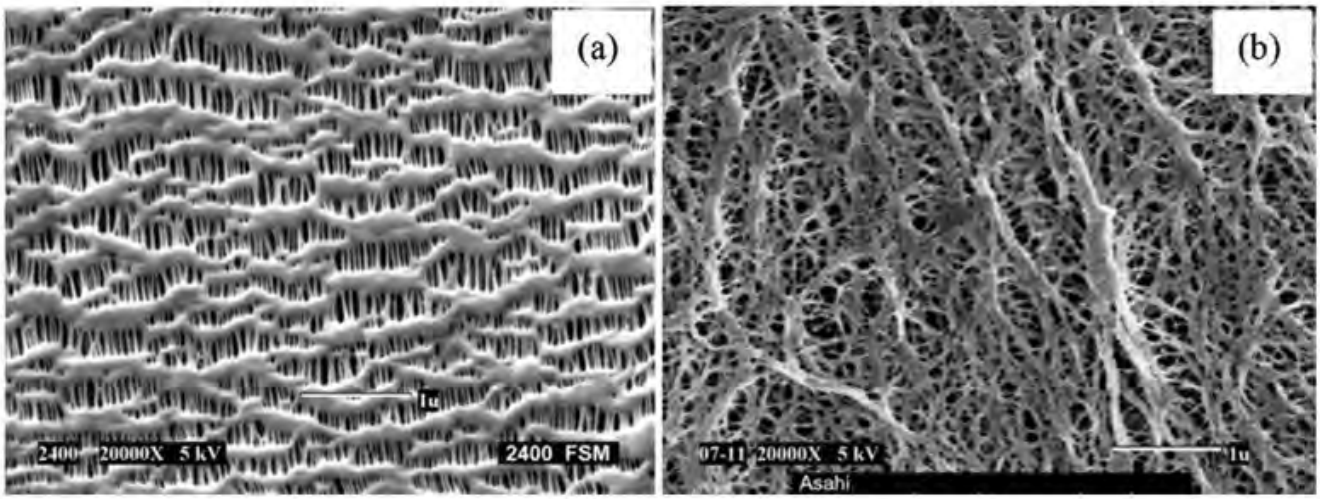


Fig. 4 Separators fabricated by the dry (a) and the wet (b) processes [7]

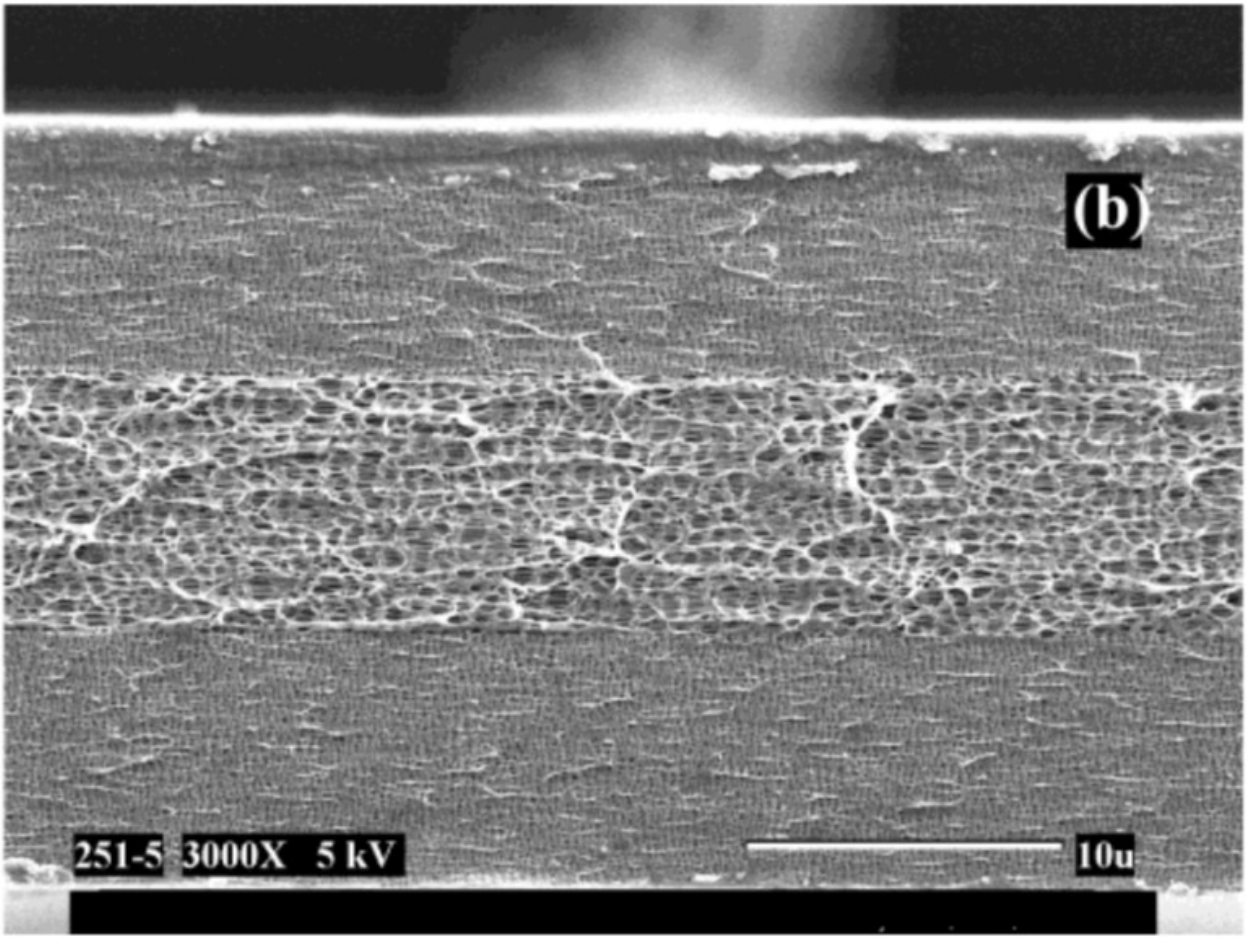
43. The melting point of HDPE and UHMWPE varies slightly with different resins and different processing histories, but is generally in the range of 120°C to 130°C. In the event of a short circuit or a puncture, a battery with a PE separator is resistant to a thermal runaway because the PE melts and as it does it shrinks to close off the pores. This converts the porous layer into a layer which is impermeable and electrically insulating. This restricts ion flow and short circuited electron current, and shuts down or at least slows the process to the point where the battery is less likely to burst into flames. Appendix I, Appendix J.

44. Although a PE separator can perform this shutoff function, the heat shrinkage of the PE tends to be more than is required to simply close off the pores and shut down the short circuit. A PE separator can shrink and distort to such a high degree that it loses its mechanical integrity, pulls the wider battery structure apart,

and bigger holes are opened up in the separator, exacerbating the thermal runaway. To address this shortcoming, multi-layer polyolefin separators were developed that have both PE and PP layers.

45. The image below is a cross-sectional SEM image of a three-layer separator (Celgard 2325) with two PP outer layers and an inner PE layer. Appendix J. PP has a higher melting point in the range of 160°C to 170°C. In the event of a short circuit and temperature increase, the PE layer of this separator melts around 130°C, closing off the pore structure. But the PP, which is well below its melting temperature, maintains its structural integrity. Only above the higher melting point of PP is this separator in danger of shrinking and distorting to the point where it fails catastrophically. This multilayer design, where one layer (PE) performs the shut off function, and the other (PP) holds the separator together, was an improvement in battery safety. *See, e.g.*, Appendix I, Appendix J, Appendix K. The technology for the production of microporous polyolefins films by mechanical stretching was developed in the 1960s and 1970s. *See, e.g.,* Appendix S (Isaacson et al., U.S. Patent No. 3,558,764 titled "Process for Preparing Microporous Film" (issued Jan 26, 1971). Microporous, polyolefin battery separators were also developed in the 1960s. *See, e.g.*, Appendix T (Larsen et al., U.S. Patent No. 3,351,495 titled "Battery Separator" (issued Nov. 7, 1967). The use of multilayer polyolefin separators for a thermal shut-off function in lithium ion batteries goes back to the 1980s. *See, e.g.,* Appendix U

(Lundquist et al., U.S. Patent No. 4,650,730 titled "Battery Separator" (issued Mar. 17, 1987). Research and development activity on these multilayer, thermal shutdown, polyolefin separators followed through the 1990s. *See, e.g.*, Appendix V (U.S. Patent No. 5,565,281 titled "Shutdown, Bilayer Battery Separator" (issued Oct. 15, 1996). And the three-layer PP-PE-PP separator of the type shown in the SEM image below was patented by Celgard in 1999. *See, e.g.*, Appendix W (Yu et al., U.S. Patent No. 5,952,120 titled "Method of Making a Trilayer Battery Separator" (issued Sept. 14, 1999).



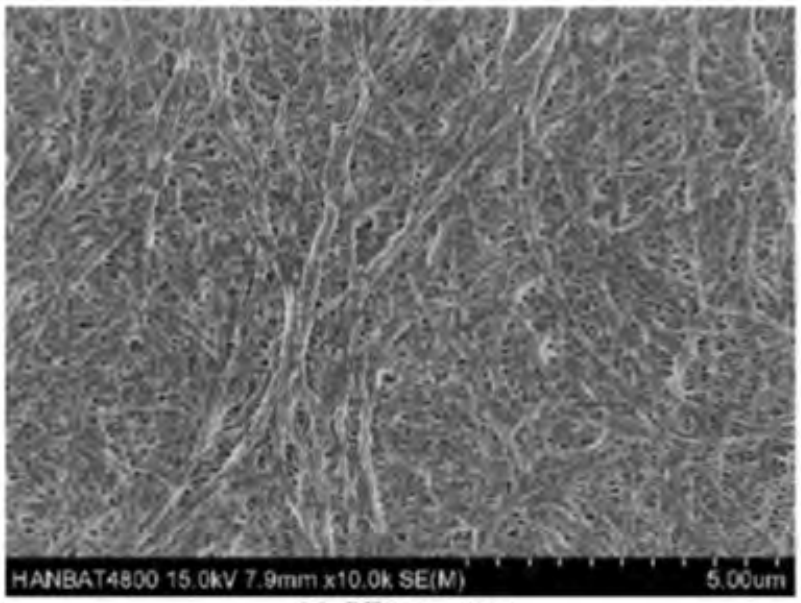
46. With the success of this multilayer composite structure for improved thermal shutoff in separators, it became logical to look for other even more temperature-stable material layers—beyond PP—to couple with the melting and shut-off function of the PE. For this POSAs turned to ceramic particle containing layers that were already known in the art to provide high temperature stable Li-ion battery separators as single free-standing layers or layers coated directly onto electrodes. These included porous ceramic layers, produced by sol-gel processes without polymer binder used as Li-ion battery separators. *See, e.g.*, Appendix X

(Carlson et al., U.S. Patent No. 6,306,545 titled "Separators for Electrochemical Cells" (issued Oct. 23, 2001). Single layer separator materials consisting of composites of ceramic particles and polymer binder were also used, including layers of metal oxide (titanium oxide) particles in a resin binder of polyvinylidene fluoride-hexafluoropropylene copolymer, in which porosity is created by a phase inversion process (addition of a non-solvent). *See, e.g.,* Appendix Y (Kim et al., "Characteristics of PVdF-HFP/TiO2 composite membrane electrolytes prepared by phase inversion and conventional casting methods," Electrochimica Acta 51 (2006) 5636–5644). This 2006 publication describes a stand-alone separator layer which has the same composition, similar structure and morphology, and is produced by a similar method as the porous layer in the '987 patent. And as noted above, coating a separator layer onto a porous polyoelefin substrate was known from roughly the 1990s.

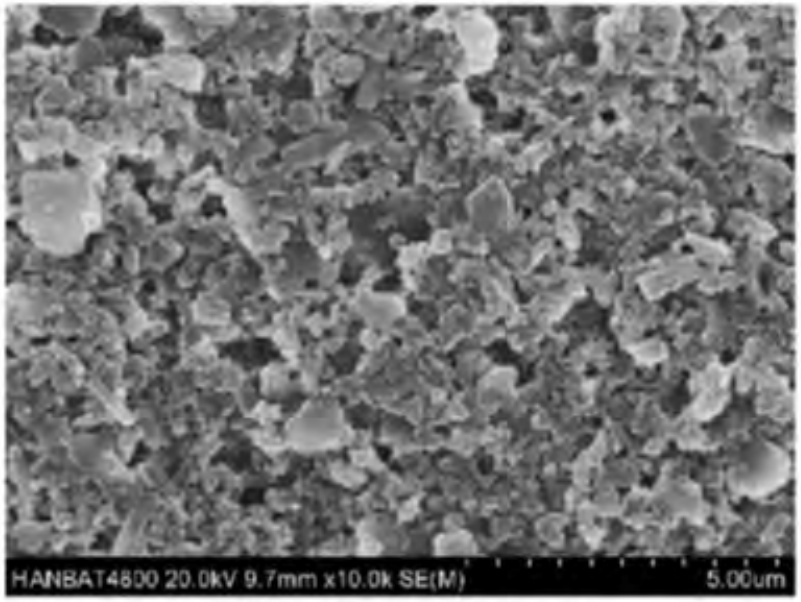
47. The approach of coating porous layers of ceramic particles and binder onto polyolefin separators was patented in 2009 and 2010 by LG Chem ("LG"). *See, e.g.,* Appendix L, Appendix M, Appendix N, Ex. 1009. LG's separators use a stretched, porous PE separator (for its thermal shutoff qualities) coated on one or both sides with a slurry of ceramic particles in polymer binder, with a solvent. Upon drying of the solvent, a porous layer of ceramic particles in polymer binder is left on the PE. This adds high-temperature structural integrity to the separator, above the

melting point of PE and exceeding the temperature limit of the PE-PP composite separators.

48. The images below are SEM images of the surface of an uncoated PE separator (a), and then the same separator with a ceramic-binder layer coated onto it (b). Appendix P. The surface is completely coated with the ceramic particles, which are bonded together by a binder polymer. The porosity of this separator layer comes from the pore space between the jagged ceramic particles. It is well understood that packings of particulate materials such as these ceramic particles generally only fill about half the volume. The interstitial space between the particles is connected into tortuous pores, which span the layer. Other examples of ceramic coated polyolefin separators soon followed.



(a) PE separator



(b) Ceramic-coated separator

Fig. 1. Scanning electron micrographs of the surface of a porous PE membrane and ceramic-coated separator (ACS-3).

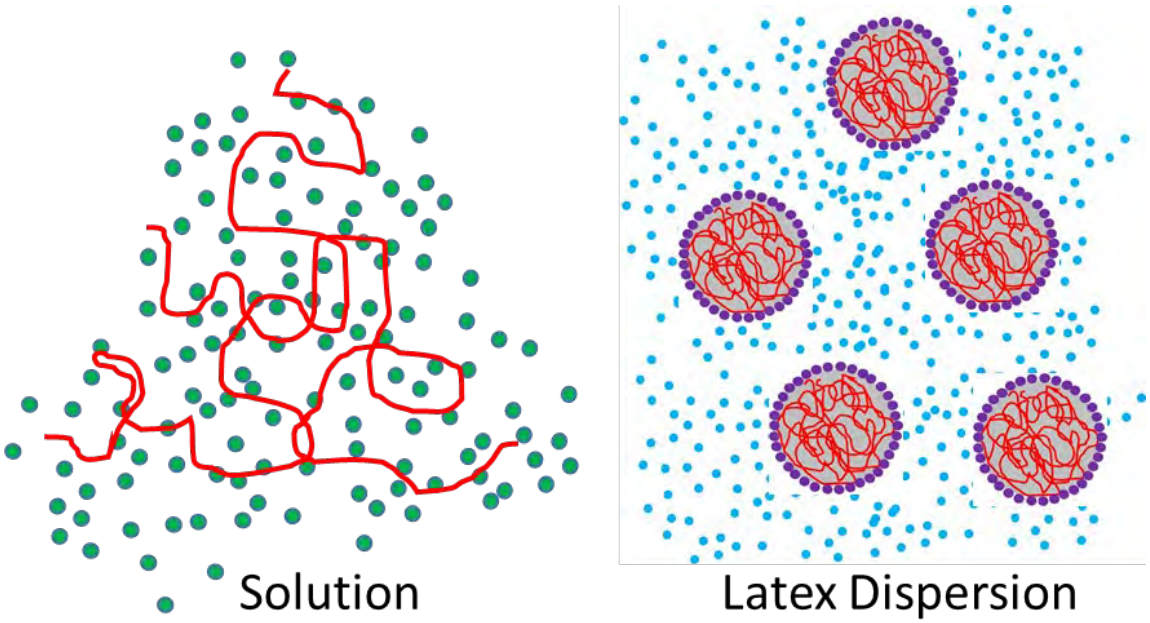
49. The properties of these ceramic particle and binder layers are influenced by the properties of the particles used, as well as the type of polymer binder. The main requirements for the particles are that they be stable at high

temperatures; chemically inert in the electrochemical environment of the battery cell; and able, through their packing, to enable a porous structure. To achieve these requirements, the particles are often some form of metal oxide, metal hydroxide, or other ceramic such as silica, silicon carbide, or a sulfate, such as barium sulfate. The particle size is also important to give the separator the required porosity and mechanical properties, such as handling properties during battery assembly and adhesion to adjacent electrodes.

50. Typically, the ceramic particles on ceramic coated battery separators are held together in a binder, which is a polymer, or more typically a mixture of polymers, along with smaller amounts of other components such as dispersing aids, or stabilizers, typically surfactants, or possibly chemical additives to adjust pH or other conditions. The ceramic particles and binder are generally mixed into a slurry—that is, a liquid containing dissolved components as well as dispersed particulate components—by adding the dry ingredients (binder polymer plus particles) into a solvent. The solvents used must be compatible with both the binder polymers and the inorganic particles. The solvent(s) is (are) often a polar organic solvent, or water, or mixtures of polar organic solvents, or mixtures of water with polar organic solvents.

51. Depending on the solvent used, the binder polymers are polymers that are soluble in polar organic solvents or in water. It is also possible to disperse binder

polymers that are not water soluble in water by using these polymers in the form of latex particles. The figure below illustrates the difference between a polymer in solution, on the left, and a polymer latex suspended in a solvent (often water), on the right. Here the polymer is shown as a red coil. In the solution, it is intimately mixed on a molecular scale with organic solvent molecules, shown in green. In the latex dispersion, by contrast, the polymer is compacted into nanometer sized balls or particles, which are essentially pure polymer in their interiors. These particles are surrounded by surfactant molecules, shown in purple, which stabilize the latex particles and compatibilize their interaction with an aqueous solvent (water or mostly water), shown in blue, which does not usually dissolve the particular type of polymer. The use of a latex polymer binder is not inherently different from the use of a dissolved polymer binder. Both methods disperse the binder in the coating slurry and both allow the binder to perform its function of forming a solid layer that embeds the ceramic particles.

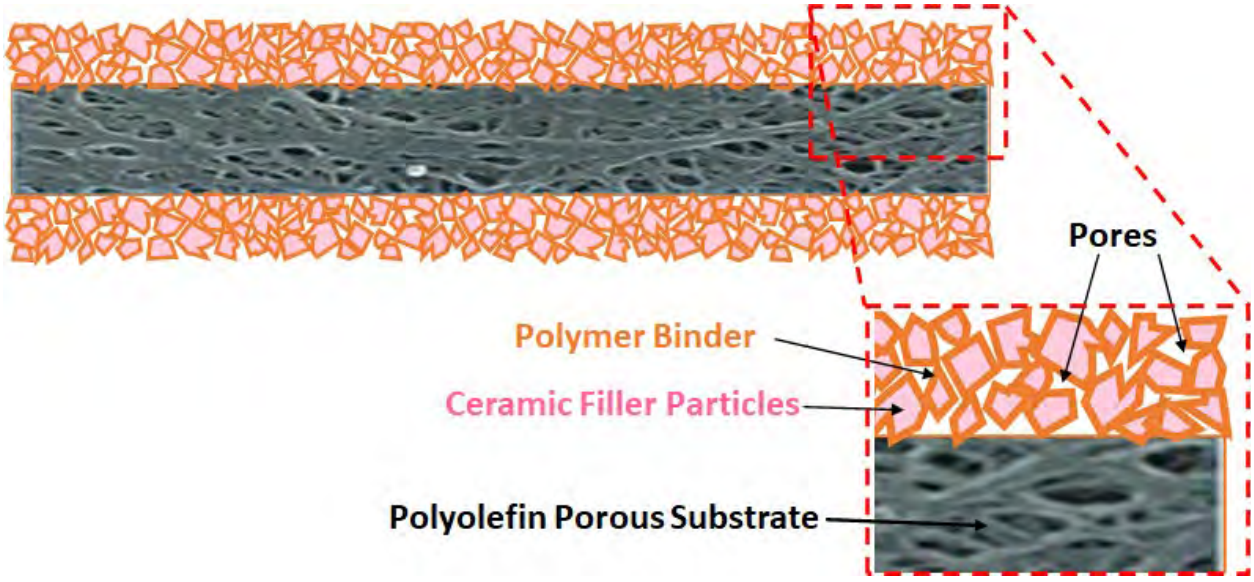


52. Some separators, such as those described in the patents in Appendices L-N and Exhibit 1009, use high particle loadings up to as much as 90% by weight, or more. In these ceramic coated separator layers, the binder is there as a glue to hold the particles together, but the structure of the layer is dominated by the particles, and the porosity is a result of the interstitial cavities between the relatively tightly packed particles. Other separators have been developed in which the amount of polymer binder in the ceramic particle containing layer is significantly greater, perhaps more than 50%. In these cases the particles are generally separated from one another and surrounded by binder. The ability of interstitial spaces in the particle packing to create porosity is greatly reduced. In these cases, it is necessary to generate porosity in the binder polymer itself. This is typically done by a solvent/non-solvent

coagulation, also known as a phase inversion processing method. Phase inversion is a generally known and widely used processing technique for polymers in general, and is the wet process used to make polyolefin separator layers, as discussed above. It has also been used to create porosity in ceramic-binder polymer layers on coated separators. From the 2000s, when polymer binder-ceramic particle composite separator layers were being developed, investigators understood that there was an interplay between parameters such as particle size, pore size, percent porosity, and layer thickness. In some approaches, like that of LG [Appendix L, Appendix M, Appendix N, Ex. 1009], the pore size and porosity are created by interstitial spaces between the pores, so the design choices made about particle size distribution influence pore size and porosity. In approaches based on phase inversion or coagulation of the binder to form pores, the choice of particle type and particle size also influences pore size and porosity, because the particles can act as nucleating sites for the phase separation that creates the pores.

53. Thus, well before 2018, separators regularly included a porous substrate, such as a polyolefin porous substrate, and a porous layer formed on one or both sides of the porous substrate, as illustrated below. It was likewise known to form the porous layer of a polymer binder, such as polyvinylidene fluoride, and inorganic particles, such as ceramic filler particles, as illustrated. As explained above, those in the art recognized that a polymer binder is non-conducting and can be

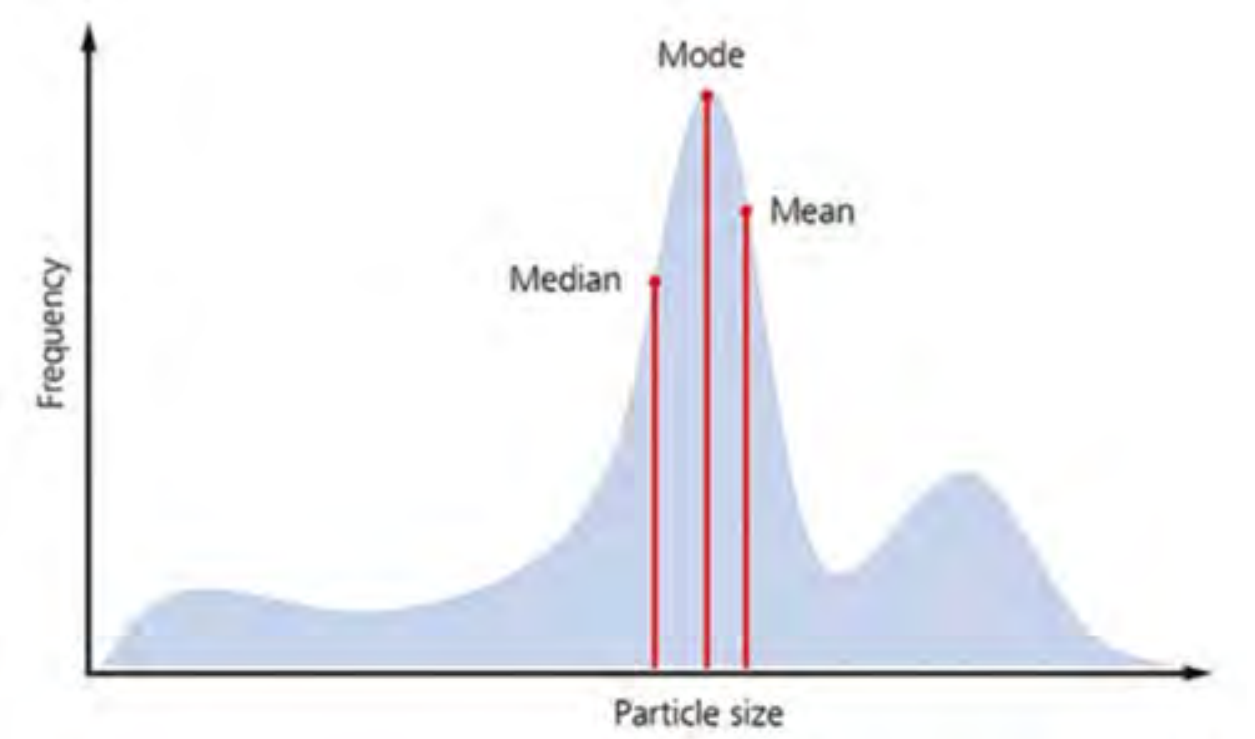
formed to be porous, while the addition of inorganic particles improves both mechanical strength and high-temperature stability.



54. The particles in any batch of ceramic particles come in a distribution of sizes, resulting from the process of making the particles, which typically involves pulverizing, grinding, or milling larger pieces of the materials. The figure below illustrates what a general particle size distribution might look like. Appendix O. The frequency of occurrence (*i.e.*, the relative number of particles) in the powder is plotted against size. As illustrated, it is possible that the distribution of sizes (typically diameter or radius) is multimodal, meaning there is more than one peak in

the distribution.

55. The distribution represents a large amount of complex information, and



POSAs often want, or need, to summarize this information in a more compact form, which typically involves averages. These averages are attempts to capture the essence of the distribution in a single number or a few numbers. The figure above illustrates a few such numbers, the median (middle point of distribution), mode (peak of the distribution), and mean (arithmetic average). Clearly, any one or all of these values, given in the absence of the graph of the distribution, does not really convey the complexity of the distribution.

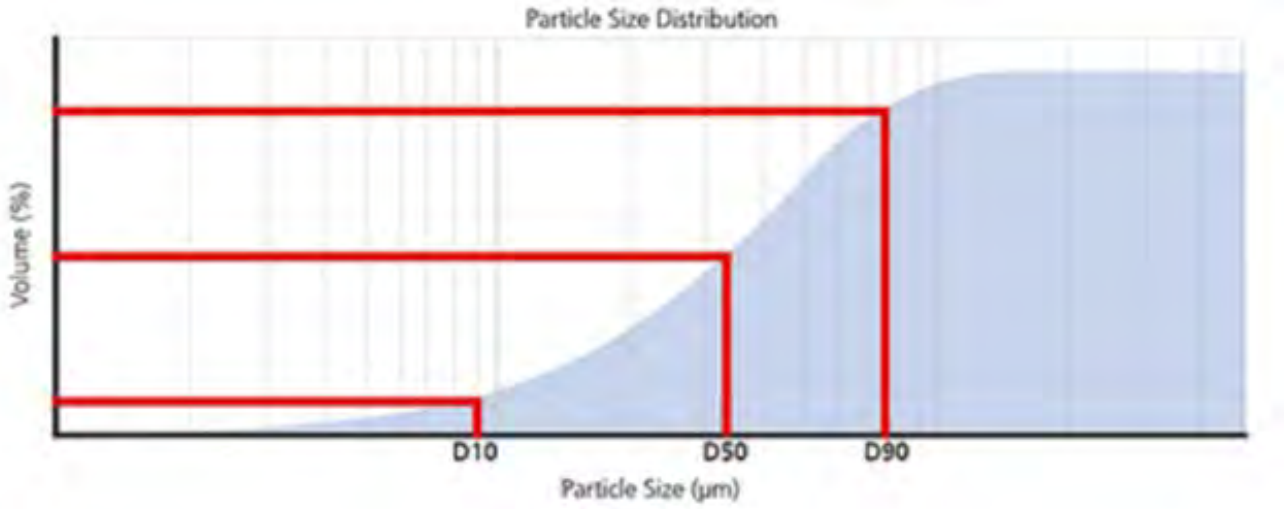
56. Another complicating factor for distributions of particle sizes is the fact that averages of distributions can be calculated by weighting (counting) the

contributions of various particles differently, according to different properties. The simplest average is a number weighted average in which each particle, no matter how big or small, is given the same importance in the average. But this type of number average tends to give too much weight to the smallest particles. There may be many of these small particles, but since they are small, their contribution to the total mass or volume of particles (and thus to material properties) may be less significant than a smaller number of large particles. Thus, practitioners in the field often use other types of averages, such as a surface area average, a mass average, or a volume average.

57. A mass average is calculated from the distribution above by multiplying (weighting) the frequency (number) of particles at each size by their mass. The smaller, less massive, particles now contribute less to the average than larger particles. The mass average size is generally larger than the number average size. For a distribution of particles that are all of the same material, the masses of the various particles are directly proportional to the volumes of the particles (because the mass is simply obtained by multiplying volume by the common density of all the particles). Thus, in such a distribution, the volume average of the distribution and the mass average of the distribution are the same. Light scattering, a technique commonly used to measure particle size, gives volume-weighted results. For this and other reasons, practitioners in the field are accustomed to using volume-weighted

averages to discuss particle size.

58. A common way to convey a bit more about the distribution of particle



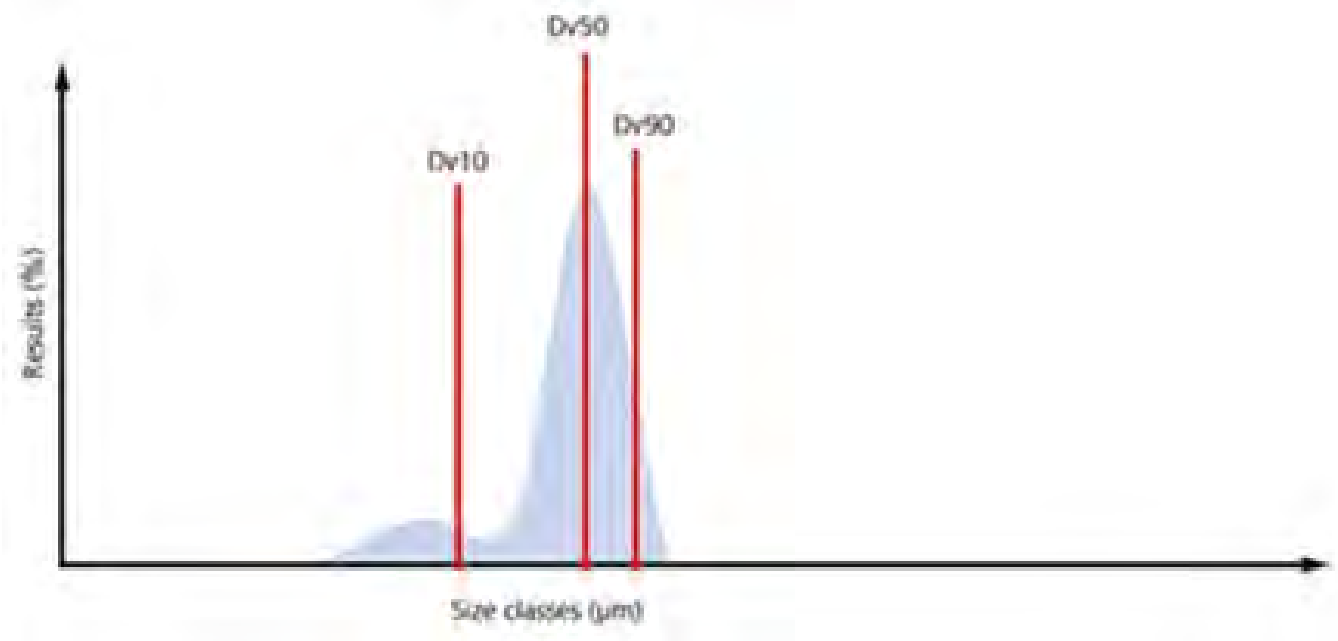
sizes than is conveyed by simple averages is to look at the properties of a cumulative size distribution. A volume-weighted cumulative particle size distribution is illustrated in the figure above. Appendix O. As shown, as particle size (here, particle diameter in microns (µm)) increases, a running total is plotted of the volume (as a percentage of the total volume of all the particles) of the particles up to that particle size. Eventually, at a large particle size, the cumulative distribution reaches a plateau (100%) because all the particles in the distribution are accounted for. Typically, such a cumulative distribution is characterized by the particle sizes at which the cumulative volume reaches particular percentages of the total. Shown in the figure are those most commonly used, namely, D10, D50, and D90.

59. D10 is the particle size (in an appropriate unit such as µm) at which

10% of the total particle volume is reached. D50 is the particle size at which 50% of the total particle volume is reached. And D90 is the particle size at which 90% of the total particle volume is reached.

60. It is actually possible to do this type of analysis of a cumulative size distribution on the different bases mentioned previously: number (frequency) basis, surface area basis, mass basis and volume basis. These different values are differentiated as follows (for the D50 case): Dn50, Ds50, Dm50, and Dv50. However, it is also common for POSAs to define D10, D50, and D90 in a particular context as being on one of these bases and simply use D10, D50, and D90.

61. Of course, even D10, D50, and D90 fail to fully convey the details of some distributions, such as the bimodal distribution shown below. Appendix O. But the fact that the D10 is shifted further to the small size than the D90 is to the large, for example, provides a clue to the asymmetry of the distribution. The value D90-D10 gives a rough indication of the breadth of the distribution and is often referred to as the span. The span may also be represented on relative or percentage basis as (D90-D10)/D50.



62. Prior to 2018, it was known in the art to adjust particle size—including as indicated through cumulative particle size values D10, D50, and D90—of the inorganic particles to achieve desirable separator properties. Another parameter those in the art knew to adjust was thickness of the porous layer. Moreover, it was recognized by those in the art that particle size and porous layer thickness were related parameters that were to be adjusted together. Finally, it was known in the art to adjust pore size and porosity of the porous layer. For instance, LG's series of patents, granted around 2010, on ceramic coated separators includes extensive teachings on particle size and how it relates to layer thickness: "In the organic/inorganic composite separator... the size of inorganic particles in the porous coating layer... is **preferably in the range from 0.001 to 10um, if possible, in order to form a coating layer in a uniform thickness** and ensure suitable porosity. If the

particle size is less than 0.001 um, a dispersing property is deteriorated, so it is not easy to control properties of the organic/inorganic composite separator. **If the particle size exceeds 10um, the thickness of the porous coating layer is increased, which may deteriorate mechanical properties**." Appendix M, 5:66-67, 6:1-9. Additionally, LG's patents taught that the pore size and porosity were important parameters for battery performance that were also influenced by particle size. "The pore size and porosity are mainly dependent on the size of inorganic particles... In case the pore size and porosity are respectively less than 0.001 um and 10%, the porous active layer may act as a resistance layer. In case the pore size and porosity are respectively greater than 10 um and 90%, mechanical properties may be deteriorated." Appendix L, 6:67, 7:1-9.

VII. OVERVIEW OF PRIOR ART

A. Nishikawa

63. U.S. Patent No. 7,976,987 (Ex. 1005) ("*Nishikawa*") issued July 12, 2011, and constitutes prior art under at least 35 U.S.C. §§ 102(a)(1) and (2).

64. *Nishikawa* describes a separator for use in a lithium-ion battery. *Nishikawa*, 1:8-18. *Nishikawa*'s separator includes an "microporous membrane" that is "laminated with a heat resistant porous layer." *Id.*, 2:47-52. *Nishikawa*'s porous layer includes both "inorganic filler" and a "resin." *Id.*

65. As shown below, *Nishikawa* describes Example 4 and Example 5

separators in which the porous layer has a D90 of the inorganic particles that is 1.05μm and 1.07μm, respectively. In *Nishikawa*'s Example 4 and 5 separators, the porous layer has a thickness of 3.15μm. *Id.*, Table 1, 16:25-29, 16:37-38. Thus, in *Nishikawa*'s Example 4 and 5 separators a ratio of the D90 of the inorganic filler to the thickness of the porous layer is 0.33 and 0.34, respectively—both of which are within a range from 0.3 to 3.0.

TABLE 2

	d10	d50	d90	α	Sliding property	Coating property
Example 4	0.38	0.75	1.05	0.89	good	good
Example 5	0.50	1.02	1.07	0.56	good	good
Example 6	1.50	8.0	22.0	2.56	good	poor
Example 7	5.10	23.0	58.0	2.30	good	poor

B. Iwai

66. U.S. Patent App. Pub. No. 2014/0248525 (Ex. 1006) ("*Iwai*") has a 35 U.S.C. § 371(c) date of April 17, 2014, and constitutes prior art under at least 35 U.S.C. §§ 102(a)(1) and (2).

67. *Iwai* describes a separator for use in a lithium-ion battery. *Iwai*, [0001]. *Iwai*'s separator includes a "porous substrate" and an "adhesive porous layer" that is "appl[ied] on one or both sides of the porous substrate." *Iwai*, [0021]. *Iwai*'s adhesive porous layer includes both "inorganic particles" and a "polyvinylidene-

fluoride resin." *Id.*, [0022]. *Iwai*, like others in the art, recognized that desirable properties of a separator could be achieved by adjusting particle size—as indicated through cumulative particle size values D10, D50, and D90—of the inorganic particles. In particular, *Iwai* taught that desirable adhesion of the separator could be achieved by keeping a "ratio a/r between an average thickness 'a' (μm) of the adhesive porous layer on one of the sides of the porous substrate and a volume average particle diameter 'r' (μm) of the" inorganic particles within a prescribed range. *Id.*, [0043]. While a POSA may typically understand the term "volume average particle diameter" to refer to the mean (arithmetic average) diameter of particles in the particle distribution, *Iwai* equates the "volume average particle diameter 'r' (μm)" with D50, stating "the volume average particle diameter (μm) of the filler is a particle diameter at 50% cumulative volume calculated from a smaller side in a volume particle size distribution." *Id.*, [0038]; *see also* [0160].

68. As shown in Table 1 below, *Iwai* describes an example separator, the Example 7 separator, in which the adhesive porous layer has a D50 of 1.2μm and a D90-D10 of 1.6μm. *Iwai*, [0039].

TABLE 1

	Average thickness a (μm) of adhesive porous layer	Resin type	Filler Type	Volume average particle diameter r (μm)	D90 – D10 (μm)	Content (% by mass)	a/r
Example 1	2.1	Resin A	Organic filler A	1.8	1.3	5	1.2
Example 2	1.1	Resin A	Organic filler A	1.8	1.3	20	0.6
Example 3	1.5	Resin A	Organic filler A	1.8	1.3	25	0.8
Example 4	3.5	Resin A	Organic filler A	1.8	1.3	1	1.9
Example 5	4.7	Resin A	Organic filler A	1.8	1.3	0.3	2.6
Example 6	3.0	Resin A	Organic filler B	3.0	2.0	20	1.0
Example 7	2.2	Resin A	Inorganic fillers C, D	1.2	1.6	10	1.8
Example 8	2.1	Resins A, B	Organic filler A	1.8	1.3	30	1.2
Comparative Example 1	1.3	Resin A	—	—	—	0	—
Comparative Example 2	3.1	Resin A	Inorganic filler D	0.8	1.1	40	3.9
Comparative Example 3	5.5	Resin A	Organic filler A	1.8	1.3	20	3.1
Comparative Example 4	2.0	Resin A	Organic filler E	5.0	3.6	1	0.4
Comparative Example 5	0.7	Resin A	Organic filler A	1.8	1.3	5	0.4
Comparative Example 6	5.0	Resin A	Organic filler E	5.0	3.6	5	1.0
Comparative Example 7	2.1	Resin A	Organic filler F	4.0	2.5	30	0.5

***Iwai*, Table 1 (cropped and annotated)**

69. From *Iwai*'s Table 1, a POSA would have recognized that D90 of the inorganic filler in *Iwai*'s Example 7 separator must be between 1.6μm and 2.8μm. In particular, a POSA would have recognized from the provided span, D90-D10, that D10 must be related to the D90 value as follows. Because Table 1 shows that, for Example 7, D90-D10 is 1.6, a POSA would have known that:

$$D90 - D10 = 1.6\mu m$$

70. Further, a POSA could have solved for D10 as follows:

$$D90 = 1.6\mu m + D10$$

$$D90 - 1.6\mu m = D10 \text{ (Equation 1)}$$

71. A POSA would also have recognized that D10 for *Iwai*'s Example 7 separator must be greater than 0μm. This is because D10 is "a particle diameter at which a cumulative volume of particles reaches 10% from a smaller side in a volume

particle size distribution." *Iwai*, [0039]. A POSA would have recognized that, because the particles at 10% of the cumulative volume cannot have a particle diameter less than 0μm, D10 must be greater than 0μm.

72. A POSA would likewise have recognized that D10 for *Iwai*'s Example 7 separator cannot be equal to or more than D50 for *Iwai*'s Example 7 separator. This is because D50 in *Iwai* is "a particle diameter at 50% cumulative volume calculated from a smaller side in a volume particle distribution." *Id.*, [0038]. A POSA would have recognized that the particle size at 10% of the cumulative volume cannot have a particle diameter that is equal to or more than the particle diameter at 50% of the cumulative volume. Therefore, D10 for *Iwai*'s Example 7 separator must be less than D50 for *Iwai*'s Example 7 separator. Because Table 1 shows that, for Example 7, D50 is 1.2μm, a POSA would have known that:

$$0\mu m < D10 < 1.2\mu m \text{ (Equation 2)}$$

73. Replacing D10 in Equation 2 per Equation 1, a POSA would have recognized:

$$0 < D90 - 1.6\mu m < 1.2\mu m$$

$$1.6\mu m < D90 < 2.8\mu m$$

74. Thus, a POSA would have recognized, D90 for *Iwai*'s Example 7 separator must be greater than 1.6μm and less than 2.8μm.

75. In *Iwai*'s Example 7 separator, the adhesive porous layer has a

thickness of 2.2μm. *Id.*, Table 1. Thus, a POSA would have understood, in *Iwai*'s Example 7 separator, a ratio of the D90 of the inorganic particles to the thickness of the porous membrane ($\frac{D90}{Thickness}$) must have a value in a range from $\frac{1.6\mu m}{2.2\mu m}$ =0.72 to $\frac{2.8\mu m}{2.2\mu m}$ =1.27, a value which falls within a range from 0.3 to 3.0.

76. Also from *Iwai*'s Table 1, a POSA would have recognized that D90 of the inorganic filler in *Iwai*'s Comparative Example 2 separator must be between 1.1μm and 1.9μm. In particular, a POSA would have recognized from the provided span, D90-D10, that D10 must be related to the D90 value as follows. Because Table 1 shows that, for Comparative Example 2, D90-D10 is 1.1, a POSA would have known that:

$$D90 - D10 = 1.1$$

77. Further, a POSA could have solved for D10 as follows:

$$D90 = 1.1 + D10$$

$$D90 - 1.1 = D10 \text{ (Equation 6)}$$

78. A POSA would also have recognized that D10 for *Iwai*'s Comparative Example 2 separator must be greater than 0. This is because D10 is "a particle diameter at which a cumulative volume of particles reaches 10% from a smaller side in a volume particle size distribution." *Iwai*, [0039]. A POSA would have recognized that, because the particles at 10% of the cumulative volume cannot have a particle

diameter less than 0, D10 must be greater than 0.

79. A POSA would likewise have recognized that D10 for *Iwai*'s Comparative Example 2 separator cannot be equal to or more than D50 for *Iwai*'s Comparative Example 2 separator. This is because D50 is "a particle diameter at 50% cumulative volume calculated from a smaller side in a volume particle distribution." *Id.*, [0038]. A POSA would have recognized that, because the particles at 10% of the cumulative volume cannot have a particle diameter that is equal to or more than the particle diameter of the particles at 50% of the cumulative volume, D10 for *Iwai*'s Comparative Example 2 separator must be less than D50 for *Iwai*'s Comparative Example 2 separator. Because Table 1 shows that, for Comparative Example 2, D50 is 0.8, a POSA would have known that:

$$0 < D10 < 0.8 \text{ (Equation 7)}$$

80. Replacing D10 in Equation 7 per Equation 6, a POSA would have recognized:

$$0 < D90 - 1.1 < 0.8$$

$$1.1 < D90 < 1.9$$

81. Thus, a POSA would have recognized, D90 for *Iwai*'s Comparative Example 2 separator must be greater than 1.1μm and less than 1.9μm.

82. In *Iwai*'s Comparative Example 2 separator, the adhesive porous layer has a thickness of 3.1μm. *Id.*, Table 1. Thus, a POSA would have understood, in

Iwai's Comparative Example 2 separator, a ratio of the D90 of the inorganic particles to the thickness of the porous membrane ($\frac{D90}{Thickness}$) must have a value in a range from 0.35 to 0.61. This is because, as shown below, a ratio of the lowest possible D90 value (1.1μm) to the thickness (3.1μm) is 0.35, while a ratio of the highest possible D90 value (1.9μm) to the thickness (3.1μm) is 0.61. The ratio thus has a value between 0.35 and 0.61, and thus a value which falls within the claimed range from 0.3 to 3.0.

$$\frac{1.1\mu m}{3.1\mu m} = 0.35$$

$$\frac{1.9\mu m}{3.1\mu m} = 0.61$$

C. Honda

83. U.S. Patent App. Pub. No. 2015/0263325 (Ex. 1007) ("*Honda*") has a 35 U.S.C. § 371(c) date of May 6, 2015, and constitutes prior art under at least 35 U.S.C. §§ 102(a)(1) and (2).

84. *Honda* describes a separator that includes a "porous substrate" and a "porous layer that is provided on one side or both sides of the porous substrate." *Honda*, [0021]-[003]. *Honda*'s porous layer, like *Nishikawa*'s and *Iwai*'s, includes a resin and inorganic filler. *Honda*, [0023], [0033]; *see also id.*, [0229]. *Honda* teaches an embodiment of the porous layer in which "a resin has a fibril shape to form a three-dimensional network structure, by which a filler is trapped by the

network structure." Honda, [0164] *see also id.*, [0228]. *Honda* states such a structure is "preferable." *Honda*, [0164]; *see also id.*, [0228].

85. I would consider *Nishikawa*, *Iwai*, and *Honda* to be from the same field of endeavor as the '987 patent, namely, separators for lithium-ion batteries. *See, e.g.*, '987 patent, 1:14-34; *Nishikawa*, Abstract; *Iwai*, [0001]-[0002]; *Honda*, [0001]-[0002]. Moreover, each is addressing a problem discussed in the '987 patent, such as improving adhesion, heat resistance, and cycle performance of a battery. '987 patent, Abstract, 4:57-62; *Nishikawa*, 2:35-41; *Iwai*, [0017]-[0018]; *Honda*, [0016].

VIII. THE '987 PATENT

86. Like *Nishikawa*, *Iwai*, and *Honda*, the '987 patent describes a "separator" for use in an "energy storage device," such as a lithium-ion battery. '987 patent, 1:14-24. Like the separators in *Nishikawa*, *Iwai*, and *Honda*, the claimed separator includes a porous substrate and a porous layer arranged on a surface of the porous substrate. *Id.*, 1:48-50. And like the porous layers in *Nishikawa*, *Iwai*, and *Honda*, the claimed porous layer includes both inorganic particles and a binder. *Id.*, 1:50-51.

87. The '987 patent requires that a ratio of Dv90 of the inorganic particles to the thickness of the porous layer be in a range from 0.3 to 3.0. *Id.*, 1:51-53. "[B]y controlling the ratio of Dv90 of the inorganic particles to the thickness of the porous

layer," the '987 patent states, "pores having a larger average pore size can be obtained." *Id.*, 5:13-16. When the ratio is in this range, the patent states, "the mechanical strength of the porous layer is increased, and the porous layer is prevented from undergoing pore blockage due to compression in the preparation or cycle process of the energy storage device." *Id.*, 5:28-35. As explained below, both *Nishikawa* and *Iwai* describe example separators for which a ratio of Dv90 of the inorganic particles to the thickness of the porous layer is in the range required by the '987 patent.

88. Claim 1, the sole independent claim, recites:

A separator, comprising:

a porous substrate; and

a porous layer arranged on a surface of the porous substrate,

wherein the porous layer comprises inorganic particles and a binder, and

a ratio of Dv90 of the inorganic particles to the thickness of the porous layer is in a range from 0.3 to 3.0.

IX. CLAIM CONSTRUCTION

89. I have applied the above-mentioned legal standard of claim construction here.

X. THE CHALLENGED CLAIMS ARE UNPATENTABLE

90. As described below, it is my opinion that each of the challenged claims is anticipated by or would have been rendered obvious by either *Nishikawa*, alone or in combination with *Honda*, and/or *Iwai* alone.

A. Ground 1: *Nishikawa* Would Have Anticipated Claims 1-2 and 4-9

1. Claim 1

91. *Nishikawa* anticipates claim 1.

a. 1[p] A separator, comprising:

92. *Nishikawa* describes "[a] separator." For example, *Nishikawa* describes a "separator for a nonaqueous secondary battery" and two example separators in Examples 4 and 5. *Nishikawa*, 2:47-52, 15:51-16:44, 22:10-52.

b. 1[a] a porous substrate; and

93. *Nishikawa* discloses "a porous substrate." In *Nishikawa*, the separator includes a "microporous membrane." *Nishikawa*, 2:47-52; *see also id.*, 8:57-67, 15:51-16:6[1]. A POSA would have understood *Nishikawa*'s microporous membrane

[1] *Nishikawa*'s Example 4 separator is "produced in the same manner as in Example 1, except that" the coating slurry is modified. *Nishikawa*, 22:37-40. *Nishikawa*'s Example 5 separator is "produced in the same manner as in Example 4 except that the inorganic filler was changed" from H-43M to H-42M,

to be a "porous substrate" for at least three reasons. First, this is because *Nishikawa* describes the microporous membrane as having "pores inside," which indicates it is "porous." Second, like embodiments of the porous substrate in the '987 patent, *Nishikawa*'s microporous membrane is formed of polyethylene and/or polypropylene, *compare Nishikawa*, 8:62-67 *with* '987 patent, 2:9-52. Third, just as the '987 patent describes a porous layer being "coat[ed] … onto a surface of [the] porous substrate," '987 patent, 2:25-26, *Nishikawa* describes a heat resistant porous layer being "coat[ed] … on both the surfaces of the microporous membrane," *Nishikawa*, 16:24-29. *Nishikawa*'s Example 4 and Example 5 separators each include a polyethylene microporous membrane onto which a heat resistant porous layer is coated. *Nishikawa*, 15:51-16:14, 22:37-38.

c. 1[b] a porous layer arranged on a surface of the porous substrate,

94. *Nishikawa* discloses "a porous layer arranged on a surface of the porous

---

where H-42M and H-43M are both commercially available aluminum hydroxide organic fillers having different particle size distribution as shown in Table 2. *Nishikawa*, 22:26-33, 22:46-51. Accordingly, throughout my declaration, citations to discussions of Example 1 are provided where they apply equally to Example 4 and Example 5.

substrate." In *Nishikawa*, the separator includes a "heat resistant porous layer" that is "laminated" onto both sides of the microporous membrane. *Nishikawa*, 2:47-52. *Nishikawa*'s Example 4 and Example 5 separators each include a heat resistant porous layer that is "coat[ed] … onto both the surfaces of the polyethylene microporous membrane." *Id.*, 16:25-35.

d. 1[c] wherein the porous layer comprises inorganic particles and a binder,

95. *Nishikawa* discloses "wherein the porous layer comprises inorganic particles and a binder."

96. Regarding inorganic particles, in *Nishikawa*, the heat resistant porous layer includes "inorganic filler." *Nishikawa*, 2:47-52. The heat resistant porous layer in each of *Nishikawa*'s Example 4 and Example 5 separators includes inorganic filler of aluminum hydroxide, like embodiments of the claimed "inorganic particles" described in the '987 patent. *Compare Nishikawa*, 22:26-33, 22:46-51 *with* '987 patent, 2:1-6. *Compare also Nishikawa*, 2:53-56 (listing materials for *Nishikawa*'s inorganic filler) *with* '987 patent claim 6 (listing materials for claimed "inorganic particles").

97. Regarding a binder, in *Nishikawa* the heat resistant porous layer includes a "heat resistant resin." *Nishikawa*, 2:47-52. A POSA would have understood *Nishikawa*'s heat resistant resin to be a "binder" for at least two reasons.

First, just as the '987 patent describes "pores formed by the binder" through which "diffusion" takes place, *Nishikawa*'s heat resistant resin has "pores inside … through which a gas or a liquid can pass," *compare* '987 patent, 3:59-61, 4:10-14 *with Nishikawa*, 7:41-45. Second, like embodiments of the binder in the '987 patent, *Nishikawa*'s heat resistant resin is formed of polyamide, *compare Nishikawa*, 3:5-9 *with* '987 patent, 2:9-52. *Compare also Nishikawa*, 7:49-57 (listing materials for *Nishikawa*'s heat resistant resin, including polyamide and carboxymethylcellulose (a form of cellulose)) *with* '987 patent claim 7 (listing materials for claimed "binder," including polyamide and cellulose). *Nishikawa*'s Example 4 and Example 5 separators each include polyamide heat resistant resin. *Nishikawa*, 22:26-35.

e. 1[d] a ratio of Dv90 of the inorganic particles to the thickness of the porous layer is in a range from 0.3 to 3.0.

98. *Nishikawa* discloses that "a ratio of Dv90 of the inorganic particles to the thickness of the porous layer is in a range from 0.3 to 3.0" because in each of *Nishikawa*'s Example 4 and Example 5 separators a ratio of a D90 of the inorganic filler to the thickness of the heat resistant porous layer is within the claimed range.

99. As shown below in Table 2, in *Nishikawa*'s Example 4 and Example 5 separators the heat resistant porous layer has a D90 of the inorganic filler that is 1.05μm and 1.07μm, respectively. A POSA would have understood "D90," as used by *Nishikawa* in Examples 4 and 5, to disclose the claimed "Dv90." As explained in

the State of the Art, it is possible for a cumulative size distribution to be on any of a number (frequency) basis, surface area basis, mass (i.e., weight) basis and volume basis, and these may be differentiated as (for the D50 case): Dn50, Ds50, Dm50, and Dv50, respectively. The ’987 patent uses a cumulative volume distribution (hence the “v” in “Dv90”). *Nishikawa* actually defines its D90 with reference to a cumulative weight distribution, *see Nishikawa*, 3:52-55. But a POSA would have recognized that where, as in *Nishikawa*’s Examples 4 and 5, the inorganic filler is of a single material (here, aluminum hydroxide, *see Nishikawa*, 22:26-35, 22:46-51), a cumulative volume distribution and a cumulative weight distribution will have the same D90 value. This is because, as a POSA would have known, volume is directly proportional to weight—in particular, mass is equivalent to volume multiplied with density. Where the inorganic filler is of a single material, the density relating each particle’s mass to each particle’s volume will be the same, such that Dm90 and Dv90 will have the same value. *Compare also Nishikawa*, 3:52-55 (defining “D90” as “an average particle diameter (μm) of weight accumulation of 90% by weight calculated from a smaller particle side in a particle size distribution”) *with* ’987 patent, 1:53-56 (defining “Dv90” as “a particle size which reaches 90% the cumulative volume from the side of small particle size in the granularity distribution on a volume basis.”).

TABLE 2

	d10	d50	d90	α	Sliding property	Coating property
Example 4	0.38	0.75	1.05	0.89	good	good
Example 5	0.50	1.02	1.07	0.56	good	good
Example 6	1.50	8.0	22.0	2.56	good	poor
Example 7	5.10	23.0	58.0	2.30	good	poor

100. In each of *Nishikawa*'s Example 4 and Example 5 separators, the heat resistant porous layer has a thickness of 3.15μm on each side of the microporous membrane. *Nishikawa*, Table 1, 16:24-44. I note that Table 1, shown below, lists the thickness of the heat resistant porous layer in Example 1 (which is, in this aspect, the same as Examples 4 and 5) as 6.3μm. In Example 1 (and Examples 4 and 5), there are heat resistant porous layers formed on both sides of the microporous membrane, *id.*, 16:24-44, and 6.3μm is the *total* thickness of both heat resistant porous layers. I know this because *Nishikawa* provides a total thickness of the separator as 17.8μm (*id.*, Table 1, 16:36-38) and provides a thickness of the microporous membrane as 11.5 (*id.*, Table 1, 16:6-8). Subtracting the thickness of the microporous membrane from the total thickness of the separator leaves 6.3μm, which must account for a thickness of *both* heat resistant porous layers. Thus, each of both heat resistant porous layers has half that thickness, namely, 3.15μm.

101. Thus, as summarized in *Nishikawa*'s Ratios Table below, in each of

Nishikawa's Example 4 and Example 5 separators a ratio of the D90 of the inorganic filler to the thickness of the heat resistant porous layer is any of 0.33 and 0.34, respectively.

***Nishikawa*'s Example**	**D90 (μm)**	**Thickness (μm)**	**Ratio ($\frac{D90}{Thickness}$)**
4	1.05	3.15	0.33
5	1.07	3.15	0.34

***Nishikawa*'s Ratios Table**

102. Thus, *Nishikawa* discloses two example separators in which a ratio of D90 of the inorganic filler to the thickness of the heat resistant porous layer "is in a range from 0.3 to 3.0."

2. Claim 2: The separator according to claim 1, wherein the porous layer has a thickness of 0.2 μm to 10 μm.

103. *Nishikawa* discloses "wherein the porous layer has a thickness of 0.2 μm to 10 μm." As explained above for claim element 1[d], in each of *Nishikawa*'s Example 4 and Example 5 separators, the heat resistant porous layer has a thickness of 3.15μm on each side of the microporous membrane. *Nishikawa*, Table 1, 16:24-44. This 3.15μm thickness is within the claimed range of 0.2 μm to 10 μm.

3. Claim 4: The separator according to claim 1, wherein a volume ratio of the inorganic particles to the binder is in a range from 0.2 to 3.0.

104. *Nishikawa* discloses "wherein a volume ratio of the inorganic particles

to the binder is in a range from 0.2 to 3.0," because a POSA would have understood from *Nishikawa* that each of the Example 4 and Example 5 separators has a "volume ratio of the inorganic particles to the binder" of 1.71, as explained below.

105. *Nishikawa* provides a mass ratio of the inorganic filler to the resin for the Example 4 and Example 5 separators, stating the poly-m-phenylene isophthalamide resin and the inorganic filler containing aluminum hydroxide "were mixed at a weight ratio of 25/75." *Nishikawa*, 22:26-29. From this, a POSA would have recognized the mass ratio of the inorganic filler to the resin is as follows:

$$\frac{M_{resin}}{M_{filler}} = \frac{25}{75}$$

106. Or, equivalently:

$$\frac{M_{filler}}{M_{resin}} = \frac{75}{25}$$

$$\frac{M_{filler}}{M_{resin}} = 3 \text{ (Equation 3)}$$

107. While Equation 3 provides a mass ratio, a POSA would have known how to determine a volume ratio from a mass ratio. In particular, a POSA would have known that a mass ratio is convertible to a volume ratio by multiplying the masses by a reciprocal of the densities, ρ, of the materials. This is shown in Equation 4, where "ρ_{filler}" refers to a density of the inorganic filler and "ρ_{resin}" refers to a mass of the resin, and "V_{filler}" refers to a density of the inorganic filler and "V_{resin}"

refers to a mass of the resin:

$$\frac{V_{filler}}{V_{resin}} = \frac{M_{filler}}{M_{resin}} \times \frac{\rho_{resin}}{\rho_{filler}} \text{ (Equation 4)}$$

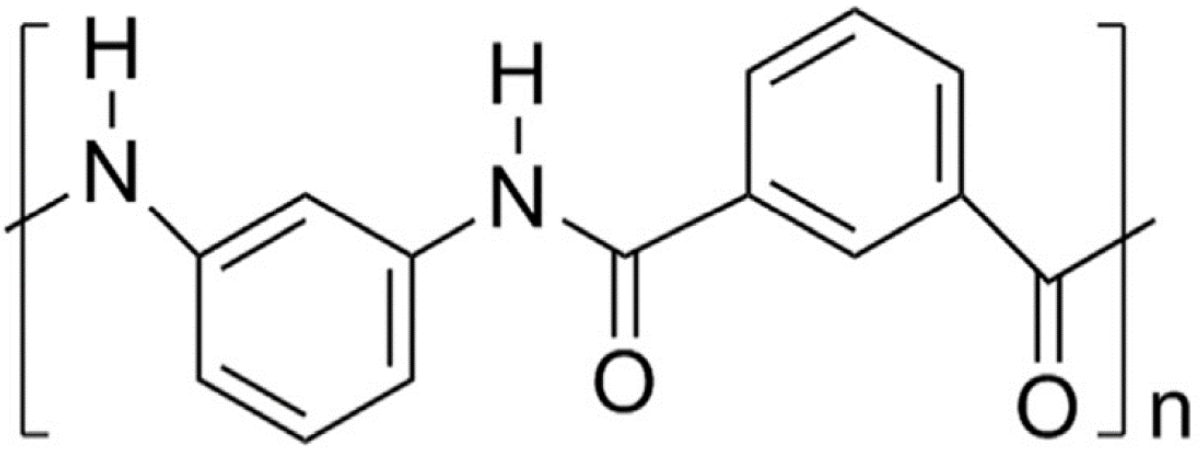
108. Replacing $\frac{M_{filler}}{M_{resin}}$ in Equation 4 per Equation 3 provides Equation 5 below:

$$\frac{V_{filler}}{V_{resin}} = 3 \times \frac{\rho_{resin}}{\rho_{filler}} \text{ (Equation 5)}$$

109. The separator of Example 4 in *Nishikawa* uses as an inorganic filler "aluminum hydroxide (H-43M, produced by Showa Denko K.K.)." *Nishikawa*, 22:28-29. The product information for Showa Denko's H-43M (obtained from http://www.sdsh-showadenko.com/product_03.php) indicates H-43M has a CAS Registry Number of 21645-51-2. *See* Appendix A. Using this CAS Registry Number, I obtained the Sigma-Aldrich Material Safety Data Sheet for CAS No. 21645-51-2 shown in Exhibit 1011. Exhibit 1011 is a true and accurate copy of a Material Safety Data Sheet for "Aluminum hydroxide fine powder pure, hydrargillite" from Sigma-Aldrich. Exhibit 1011 was downloaded by me from Sigma-Aldrich's website on February 17, 2023. Exhibit 1011 has a file name https://www.sigmaaldrich.com/US/en/sds/mm/1.01093. POSAs regularly employ CAS Registry Numbers and regularly rely on Material Safety Data Sheets as a reliable authority on the physical properties of a given material. Having determined that the H-43M product identified in *Nishikawa* is CAS No. 21645-51-2, a POSA

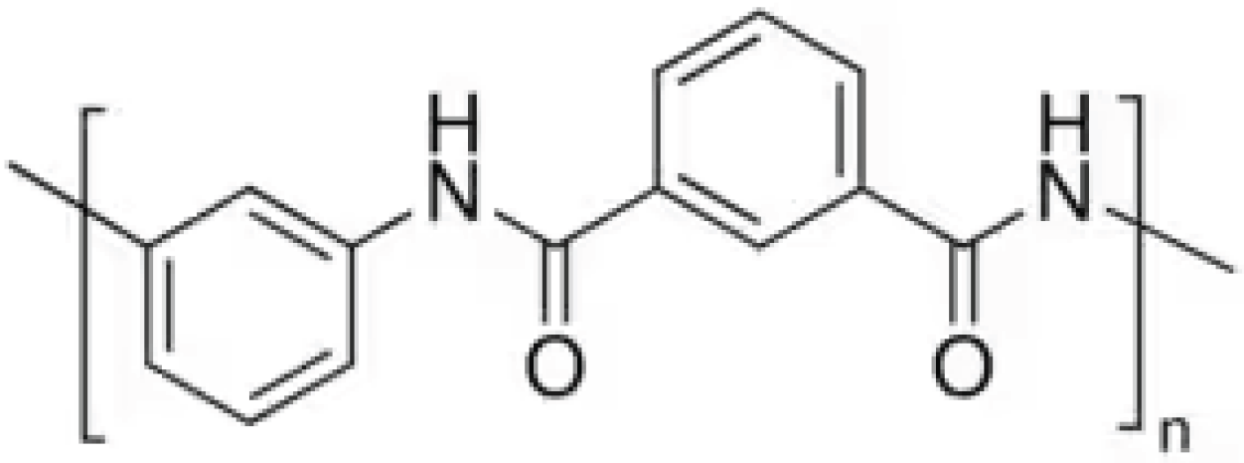
would have known that the H-43M product has a density ρ_{filler} of 2.42 g/cm^3, as listed in the Sigma-Aldrich Material Safety Data Sheet for CAS No. 21645-51-2. Ex. 1011, 5.

110. The separator of Example 4 in *Nishikawa* uses a poly-m-phenylene isophthalamide resin. *Nishikawa*, 22:26-27. As a POSA would have known, sometimes chemical compounds can be referred to by different names. Poly-m-phenylene isophthalamide is such a compound. As relevant here, poly-m-phenylene isophthalamide can also be referred to as poly [N,N′-(1,3-phenylene) isophthalamide]. This can be shown by, for example, comparing the chemical structures given these names. In an article by Lin et al. from the Journal of Membrane Science, for example, poly-m-phenylene isophthalamide is shown to have the chemical compound below. Appendix B, Figure 1.



111. And the Sigma-Aldrich Material Safety Data Sheet for poly [N,N′-

(1,3-phenylene) isophthalamide] (CAS Registry No. 25765-47-3) provides the chemical compound below. Exhibit 1013, 1.



112. As a POSA would recognize, these chemical compounds are identical. The brackets indicate a repeating unit of the structure which is repeated n times. This repeat unit can be specified in any way, so long as it includes everything that needs to be repeated. From the top structure to the lower structure, the brackets have been shifted so that the NH that appears on the far left (top), is instead accounted for on the far right (bottom). Both schematics show the same atoms connected in the same way. This indicates that poly-m-phenylene isophthalamide and poly [N,N′-(1,3-phenylene) isophthalamide] are alternative names for the same chemical compound. Having determined that the poly-m-phenylene isophthalamide identified in *Nishikawa* is the same chemical compound as poly [N,N′-(1,3-phenylene) isophthalamide], a POSA would have known that poly-m-phenylene isophthalamide has a density ρ_{resin} of 1.38 g/cm^3, as listed in the Sigma-Aldrich Material Safety Data

Sheet for poly [N,N′-(1,3-phenylene) isophthalamide] (CAS Registry No. 25765-47-3). Ex. 1013, 3.

113. So, plugging the values of ρ_{filler} and ρ_{resin} into Equation 5, a POSA would have arrived at a volume ratio for *Nishikawa*'s Example 4 separator of:

$$\frac{V_{filler}}{V_{resin}} = 3 \times \frac{\rho_{resin}}{\rho_{filler}} \text{ (Equation 5)}$$

$$\frac{V_{filler}}{V_{resin}} = 3 \times \frac{1.38}{2.42}$$

$$\frac{V_{filler}}{V_{resin}} = 1.71$$

114. Thus, *Nishikawa*'s Example 4 separator has a volume ratio of 1.71. This volume ratio of 1.71 is "in a range from 0.2 to 3.0," as claim 4 recites.

115. *Nishikawa*'s Example 5 separator has the same volume ratio of 1.71. This is because the only difference between Examples 4 and 5 is that the H-43M aluminum hydroxide of Example 4 has been switched to H-42M aluminum hydroxide, which has different particle size characteristics but is likewise the chemical compound have CAS Registry No. 21645-51-2. *See* Appendix A. Accordingly, a POSA would have known that the H-42M product likewise has a density ρ_{filler} of 2.42 g/cm^3, as listed in the Sigma-Aldrich Material Safety Data Sheet for CAS No. 21645-51-2. Ex. 1011, 5. Plugging the same density ρ_{filler} of 2.42 g/cm^3 into Equation 5 above yields the same volume ratio, namely, 1.71. This volume ratio

of 1.71 is "in a range from 0.2 to 3.0," as claim 4 recites.

116. Thus, a POSA would have understood *Nishikawa* to disclose that, in each of the separators of Examples 4 and 5, a volume ratio of the inorganic particles to the binder is 1.71, a value that is "in a range from 0.2 to 3.0."

4. Claim 5: The separator according to claim 1, wherein the porous layer has a porosity of 20% to 90%.

117. *Nishikawa* discloses "wherein the porous layer has a porosity of 20% to 90%." *Nishikawa* states "[t]he heat resistant porous layer preferably has a porosity of 60 to 90%." *Nishikawa*, 8:49-50.

5. Claim 6: The separator according to claim 1, wherein the inorganic particles are one or more selected from the group consisting of alumina, silica, magnesia, titanium oxide, hafnium dioxide, tin oxide, zirconia, cerium dioxide, nickel oxide, zinc oxide, calcium oxide, boehmite, aluminum hydroxide, magnesium hydroxide, calcium hydroxide, and barium sulfate.

118. *Nishikawa* discloses "wherein the inorganic particles are one or more selected from the group consisting of … aluminum hydroxide [and] magnesium hydroxide." The heat resistant porous layer in each of *Nishikawa*'s Example 4 and Example 5 separators includes inorganic filler of aluminum hydroxide. *Nishikawa*, 22:26-35, 22:46-52. *Nishikawa* additionally envisions that the inorganic filler may be magnesium hydroxide. *Id.*, 5:48-50.

6. Claim 7: The separator according to claim 1, wherein the binder is one or more selected from the group consisting of polyvinylidene fluoride, vinylidene fluoride-hexafluoropropylene copolymer, polyamide, polyacrylonitrile, polyacrylate, polyacrylic acid, polyacrylates, sodium carboxymethylcellulose, polyvinylpyrrolidone, polyvinyl ether, polymethyl methacrylate, polytetrafluoroethylene and polyhexafluoropropylene.

119. *Nishikawa* discloses "wherein the binder is one or more selected from the group consisting of … polyamide." The heat resistant porous layer in each of *Nishikawa*'s Example 4 and Example 5 separators includes a resin of poly-m-phenylene isophthalamide, which a POSA would have understood to be a polyamide. *Nishikawa*, 22:10-35, 22:46-51; *see also Nishikawa*, 7:49-55 (recommending a resin of polyamide). This is because, as shown in the chemical structure of poly-m-phenylene isophthalamide reproduced and annotated below, this polymer is linked together by amide linkages in its backbone. Appendix B. This is also reflected in the ending of the chemical name, poly-m-phenylene isophthal***amide***. Chemical names are constructed to tell the reader what kind of chemical functionality the compounds contain. *Compare also Nishikawa*, 7:49-57 (listing materials for *Nishikawa*'s heat resistant resin, including polyamide and cellulose, which is a category of chemical compounds that a POSA would have understood to encompass sodium carboxymethylcellulose) *with* '987 patent claim 7 (listing materials for claimed "binder," including polyamide and sodium carboxymethylcellulose).

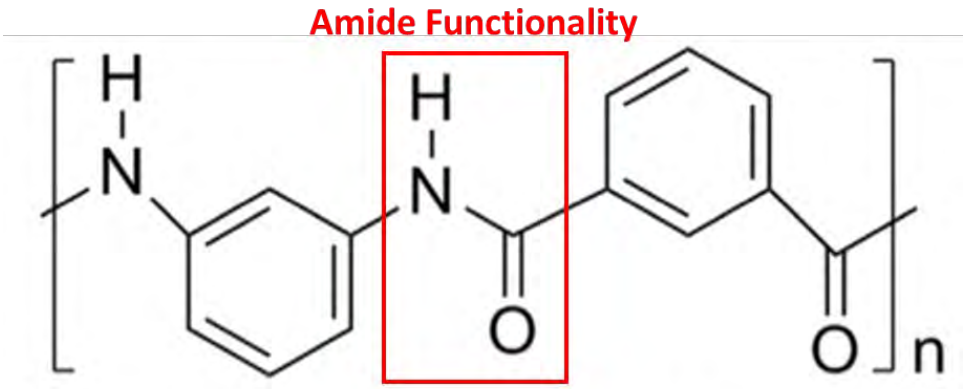


Fig. 1. Chemical structure of PMIA.

7. Claim 8: An energy storage device, comprising the separator according to claim 1.

120. *Nishikawa* discloses "[a]n energy storage device, comprising the separator according to claim 1." As explained above for claim 1, each of *Nishikawa*'s Example 4 and Example 5 separators discloses "the separator according to claim 1." And *Nishikawa* discloses using the example separators "for a nonaqueous secondary battery," which is one "energy storage device" described in the '987 patent. *Nishikawa*, 22:37-40, 22:46-51; '987 patent, 1:20-21 (describing "[n]on-aqueous secondary batteries").

8. Claim 9: The energy storage device according to claim 8, wherein the energy storage device is a lithium-ion battery.

121. *Nishikawa* discloses "wherein the energy storage device is a lithium-ion battery." As explained for claim 8, *Nishikawa*'s Example 4 and Example 5 separators are for a nonaqueous secondary battery, which *Nishikawa* states "is represented by a lithium ion secondary battery." *Nishikawa*, 1:14-18. A POSA would

likewise have known that a lithium-ion battery is a typical nonaqueous secondary battery.

B. Ground 2: *Nishikawa* Would Have Rendered Obvious Claims 10-16

1. Claim 10

122. *Nishikawa* would have rendered obvious claim 10.

a. 10[p] A method for preparing the separator of claim 1, wherein the method comprises steps of:

123. As explained above for claim 1, each of *Nishikawa*'s Example 4 and Example 5 separators discloses "the separator of claim 1." *Nishikawa* further discloses "[a] method for preparing" each of *Nishikawa*'s Example 4 and Example 5 separators. *Nishikawa*, 15:51-16:44 (Example 1), 22:10-42 (Example 4, same as Example 1 in some aspects), 22:46-52 (Example 5, same as Examples 1 and 4 in some aspects).

b. 10[a] mixing inorganic particles with a binder to generate a mixture; and 10[b] adding a first solvent into the mixture;

124. *Nishikawa* teaches "mixing inorganic particles with a binder to generate a mixture" and "adding a first solvent into the mixture." In particular, *Nishikawa* teaches that, to prepare each of the Example 4 and Example 5 separators, a poly-m-phenylene isophthalamide resin and an inorganic filler containing aluminum hydroxide "were mixed at a weight ratio of 25/75." *Nishikawa*, 22:26-29. A POSA

would have understood this to teach mixing the inorganic filler containing aluminum hydroxide with the poly-m-phenylene isophthalamide resin to generate a mixture.

125. *Nishikawa* further teaches that the resin and inorganic filler, once mixed together into the mixture, were "mixed [at a particular concentration] with a mixed solvent containing dimethylacetamide (DMAc) and tripropylene glycol (TPG) [in a particular weight ratio], thereby providing a coating slurry." *Nishikawa*, 22:26-33 (Example 4), 22:46-51 (Example 5 same as Example 4 in relevant aspects). The solvent *Nishikawa* describes, dimethylacetamide, is one embodiment of the claimed "first solvent" described in the '987 patent. *Compare Nishikawa*, 22:26-33 *with* '987 patent, 2:35-38. A POSA would have understood this to teach adding a solvent, the dimethylacetamide, to the mixture of the inorganic filler containing aluminum hydroxide with the poly-m-phenylene isophthalamide resin.

c. 10[c] stirring the mixture with the first solvent to obtain a uniform coating solution;

126. *Nishikawa* would have rendered obvious "stirring the mixture with the first solvent to obtain a uniform coating solution." *Nishikawa* teaches that the resin and inorganic filler, once mixed together, were "mixed [at a particular concentration] with a mixed solvent containing dimethylacetamide (DMAc) and tripropylene glycol (TPG) [in a particular weight ratio], thereby providing a coating slurry." *Nishikawa*, 22:26-33 (Example 4), 22:46-51 (Example 5 same as Example 4 in relevant aspects).

A POSA would have understood *Nishikawa*'s "mix[ing]" to be synonymous with—or at least to have rendered obvious—the claimed "stirring." This is so at least because stirring was a typical and widespread technique known to a POSA for mixing dry ingredients, like the resin and inorganic filler, into a solvent like the first solvent. For this reason, mixing by stirring would have been nothing more than the use of a known technique and would have yielded nothing more than predictable results.

127. A POSA would also have been motivated and found it obvious to make the "coating slurry" taught by *Nishikawa* "uniform." As *Nishikawa* explains, it is "favorable" for the heat resistant porous layer formed from the coating slurry to "hav[e] uniform minute pores," and a POSA would have recognized that uniformity in the coating slurry would lead to *Nishikawa*'s desired uniformity in the heat resistant porous layer formed from the coating slurry. Moreover, such uniformity was known to be desirable in the art, and a POSA would have known how to achieve such uniformity. As just one example, *Honda* recommends "enhancing the dispersibilities of the resin particles and inorganic filler" in a coating liquid, which a POSA would have recognized leads to greater uniformity. *See also* Ex. 1010, 10:50-53 (recommending a solvent that "facilitates uniform mixing"). Still further, a POSA would have known how to achieve such uniformity. POSAs producing coatings have long recognized the importance of a uniform coating solution, which

can also be referred to as a coating slurry or coating mixture. For instance, *Katayama* discusses the need for uniformity in the coating slurry: "[T]he inorganic fine particles … are likely to be settled in the slurry. In particular, if the particle size is 1 μm or less, the fine particles are likely to be agglomerated together. Thus, it may be difficult to maintain a stable dispersion state of the fine particles in the slurry. … When the slurry in which the fine particles are agglomerated or settled is applied to the base or the like, the application tends to be not uniform. The non-uniform application of the slurry reduces the evenness of the separator produced. Consequently, in the lithium secondary battery, the ionic conduction is not uniform within the separator, which may cause a deficiency such as a deposition of lithium during charging of the battery particularly at a high current density." Exhibit 1019, [0011]-[0013]. *Katayama* then teaches how to achieve this desired uniformity using mixing techniques, including ***stirring***: "… a method of using a slurry that is prepared by dispersing the insulating fine particles in a solvent with various types of mixing and **stirring** devices such as a disperser, an agitator, a homogenizer, a ball mill, an attritor, and a jet mill … ." *Id.*, [0113]. More generally, a POSA would have known, for example, that dispersion is achievable through commercially available dispersing devices in which desirable dispersion is achieved by controlling dispersion conditions such as a number of rotations, dispersion energy, and dispersion time.

128. As a POSA would have recognized in general, a uniform coating slurry

is fundamental to a successful coating process. This is true for at least three reasons. First, a POSA would have known, a non-uniform slurry will result in non-uniform coverage on the surface being coated. There may be bare patches, or bare streaks in the coating direction, and other places with too much (too thick) material. Since producing the coating slurry requires mixing dry powder ingredients with a liquid solvent, incomplete mixing may result in clumps of dry material suspended in the liquid. These would result in patches or streaks of dry powder in places on the coated surface. If the coating slurry is non-uniform, then the coating thickness may vary widely and there may be bare patches with no coating at all, or places covered with dry powder that falls off and leaves a bare patch. Second, a POSA would have recognized that a non-uniform coating slurry may gum up the coating equipment. This may cause the coating process to fail, and it may damage the coating equipment. Third, a POSA would have known that he or she should not even attempt to start a coating process until he or she is sure that the coating slurry is well mixed and uniformly dispersed. To do otherwise would risk failure of the coating process and potential damage to expensive equipment. Accordingly, for at least these reasons, a POSA would have been motivated and found it obvious to prepare a uniform coating slurry.

d. 10[d] coating the uniform coating solution onto a surface of a porous substrate to form a wet film;

129. *Nishikawa* teaches "coating the uniform coating solution onto a surface of a porous substrate to form a wet film." In *Nishikawa*, the coating slurry is "coat[ed] … on both the surfaces of the polyethylene microporous membrane." *Nishikawa*, 16:25-29 (Example 1); 22:37-40 (Example 4 same as Example 1 in relevant aspects), 22:46-51 (Example 5 same as Example 4 in relevant aspects). A POSA would have understood the coating slurry thus coated in *Nishikawa* to be "a wet film" because the term "slurry" used by *Nishikawa*, like the term "solution" used in the '987 patent, always refers to a wet fluid. And any coating process using a wet fluid (slurry or solution) necessarily produces a wet coating or wet film, at least before it is dried. (*Nishikawa* does disclose a drying step, but this is later in the process. *Nishikawa*, 16:31-32.) Finally, *Nishikawa* describes its own process as a "wet coating method." *Id.*, 7:58-63.

e. 10[e] [wherein the solid content in] the coating solution is in a range from 7% to 25%[2];

130. *Nishikawa* teaches "[wherein the solid content in] the coating solution

[2] This claim limitation reads only "the coating solution is in a range from 7% to 25%," but does not specify what aspect of the coating solution falls within this

is in a range from 7% to 25%" because a POSA would have recognized that each of *Nishikawa*'s Example 4 and Example 5 separators is prepared with a solid content in the coating slurry that "is in a range from 7% to 25%."

131. A POSA would have understood the "solid content" in claim 10 to refer to the solids composition of the coating solution. That would be the total amount of solids—i.e., the inorganic particles plus binder (and any other non-solvent, non-volatile components such as surfactants, viscosity modifiers, etc.) Put another way, the solid content in a coating solution (aka a coating slurry) is all the material that is left when the coating solution is completely dried, that is when all volatile components (solvents) are removed by drying. The solid content is then expressed as a percentage of the total amount of coating solution, which would include the total amount of solids as well as the solvent.

---

percentage range. I have been told that, for purposes of this IPR, Petitioner reads "the coating solution is in a range from 7% to 25%" as "wherein the solid content in the coating solution is in a range from 7% to 25%." *See, e.g.*, 2:30-31, 6:14-15, claim 11. Based on my knowledge of how a POSA would understand this claim language, I agree this is the best reading of claim 10. Accordingly, I have provided my opinions as to whether *Nishikawa* would have rendered obvious "wherein the solid content in the coating solution is in a range from 7% to 25%."

132. Claim 10 does not specify the basis on which this percentage is calculated. In theory, the solid content could be calculated based on weight (mass) or based on volume. A POSA would have understood claim 10 to refer to—or at least to include—a solid content calculated based on mass. This is because, in preparing such a coating solution, it is natural to weight out amounts of different components to be added. Measuring out amounts to be added on a volume basis, on the other hand, would be impractical as there are no simple ways to quickly determine volumes of materials, such as the powered ingredients being mixed. The nominal volume of a powder, when packed into a container, is much higher than the actual volume occupied by the material since packed particles only fill, very roughly, about half the space that the powder occupies (the balance being air). Were volumes to be needed for these components, a POSA would have to (i) weigh the ingredients to determine a mass of each ingredient and (ii) determine a volume for each ingredient by dividing the mass by the ingredient's density (e.g., as described above in connection with claim 4). For this reason, mass is the usual basis on which formulating and mixing these types of ingredients is done, and for this reason it is my opinion that a POSA would have understood claim 10 to refer to—or at least to include—a solid content calculated based on mass.

133. Each of *Nishikawa*'s Example 4 and Example 5 separators is prepared with a solid content in the coating slurry that "is in a range from 7% to 25%." For

Example 4, *Nishikawa* states that, in the coating slurry, the poly-m-phenylene isophthalamide resin has a concentration "of 5.5% by weight." *Nishikawa*, 22:26-35. *Nishikawa* also states that the poly-m-phenylene isophthalamide resin and the inorganic filler containing aluminum hydroxide "were mixed at a weight ratio of 25/75," meaning there is three times as much (by weight) inorganic filler as resin in the coating slurry. *Id*. From this, a POSA would have recognized that, in the coating slurry, the inorganic filler has a concentration of 16.5% by weight, as this is three times the 5.5% concentration by weight of the resin. As noted above, the "solid content" of the coating slurry, a POSA would have known, is simply the sum of the concentrations by weight of any solid content in the coating slurry—here in *Nishikawa*'s Example 4, the resin and the inorganic filler. Accordingly, a POSA would have understood that the solid content" of the coating slurry in Example 4 is the sum of the 5.5% concentration by weight of the resin and the 16.5% concentration by weight of the inorganic filler, namely, 22%. *Nishikawa*'s Example 5 has the same solid content, as it is the same as Example 4 in the relevant aspects. *Nishikawa*, 22:46-51. Thus, a POSA would have understood that each of *Nishikawa*'s Example 4 and Example 5 separators has a solid content of 22%, which is within the claimed range.

f. 10[f] wherein a ratio of Dv90 of the inorganic particles to the thickness of the porous layer is in a range from 0.3 to 3.0.

134. As explained above for claim element 1[d], *Nishikawa* discloses "wherein a ratio of Dv90 of the inorganic particles to the thickness of the porous layer is in a range from 0.3 to 3.0."

2. Claim 11: The method according to claim 10, wherein the solid content in the coating solution is in a range from 7% to 25%.

135. As explained above for claim element 10[e], *Nishikawa* teaches "wherein the solid content in the coating solution is in a range from 7% to 25%."

3. Claim 12: The method according to claim 10, wherein the coagulating solution comprises a second solvent and a third solvent, and the second solvent has a mass percentage of 20% to 60%.

136. *Nishikawa* teaches "wherein the coagulating solution comprises a second solvent and a third solvent, and the second solvent has a mass percentage of 20% to 60%."

137. *Nishikawa* describes a "coagulation bath," used in both Examples 4 and 5, in which the microporous membrane, coated with the coating slurry, is "immersed." *Nishikawa*, 16:29-31, 22:37-40 (Example 4 same as Example 1 in relevant aspects), 22:46-51 (Example 5 same as Example 4 in relevant aspects). *Nishikawa*'s coagulation bath, a POSA would have recognized, teaches the claimed "coagulating solution," in which the '987 patent likewise states the porous substrate, coated with

the coating solution, is "immers[ed]." '987 patent, 2:27-28.

138. *Nishikawa*'s coagulation bath includes dimethylacetamide, which is one of the embodiments of the "second solvent" in the '987 patent. *Compare Nishikawa*, 16:29-31 with '987 patent, 6:40-43. *Nishikawa*'s coagulation bath also includes water, which is one of the embodiments of the "third solvent" in the '987 patent. *Compare Nishikawa*, 16:29-31 *with* '987 patent, 6:43-46.

139. *Nishikawa* also teaches that the dimethylacetamide "has a mass percentage of 20% to 60%." This is because *Nishikawa*'s coagulation bath is described as having "a weight ratio of water / DMAc [dimethylacetamide] / TPG [tripropylene glycol] of 50/25/25," from which a POSA would understand the dimethylacetamide has a mass percentage of 25%. Thus, in each of *Nishikawa*'s Example 4 and Example 5 separators, the dimethylacetamide has a mass percentage of 25%, which is within the claimed range.

4. Claim 13: The method according to claim 10, wherein the first solvent is one or more independently selected from the group consisting of N-methylpyrrolidone, dimethylacetamide and dimethylformamide.

140. *Nishikawa* teaches "wherein the first solvent is one or more independently selected from the group consisting of … dimethylacetamide." In preparing each of the Example 4 and Example 5 separators, *Nishikawa* uses a solvent containing dimethylacetamide. *Nishikawa*, 22:26-33 (Example 4), 22:46-51

(Example 5 same as Example 4 in relevant aspects).

5. Claim 14: The method according to claim 10, wherein the porous substrate comprises a polymer film, a multilayer polymer film, or a non-woven fabric formed by any one or more of the following polymers: polyethylene, polypropylene, polyethylene terephthalate, polyphthaloyl diamine, polybutylene terephthalate, polyester, polyacetal, polyamide, polyimide, polyetheretherketone, polyaryletherketone, polyetherimide, polyamide imide, polybenzimidazole, polyethersulfone, polyphenylene oxide, cycloolefin copolymer, polyphenylene sulfide, and polyethylene naphthalene.

141. *Nishikawa* teaches "wherein the porous substrate comprises a polymer film … formed by … polyethylene." In each of *Nishikawa*'s Example 4 and Example 5 separators, the microporous membrane is a "polyethylene microporous membrane," formed of polyethylene. *Nishikawa*, 15:51-16:14 (Example 1), 22:36-37 (Example 4 uses "polyethylene microporous membrane" of Example 1), 22:46-51 (Example 5 same as Example 4 in relevant aspects). A POSA would have understood a "polyethylene microporous membrane" to be an example of a polymer film, polyethylene being a polymer and a membrane being a thin layer which is synonymous with a film.

6. Claim 15: The method according to claim 14, wherein the polyethylene is at least one selected from the group consisting of high density polyethylene, low density polyethylene, and ultrahigh molecular weight polyethylene.

142. *Nishikawa* teaches "wherein the polyethylene is at least one selected

from the group consisting of high density polyethylene, … and ultrahigh molecular weight polyethylene." This is because *Nishikawa* states that "preferred examples of polyethylene" for the microporous membrane "include high density polyethylene and a mixture of high density polyethylene and ultrahigh molecular weight polyethylene." *Nishikawa*, 8:63-67.

7. Claim 16: The method according to claim 12, wherein the second solvent is one or more independently selected from the group consisting of N-methylpyrrolidone, dimethylacetamide and dimethylformamide, and the third solvent is one or more selected from the group consisting of deionized water, ethanol, propanol, acetone, dimethyl carbonate and diethyl carbonate.

143. *Nishikawa* teaches that "the second solvent is … dimethylacetamide" and "the third solvent is … deionized water." In preparing each of the Example 4 and Example 5 separators, *Nishikawa*'s coagulation bath includes dimethylacetamide and water. *Nishikawa*, 16:29-31. A POSA would have understood *Nishikawa*'s use of water to teach "deionized water" at least because a POSA would have known it would be desirable to use pure water in *Nishikawa*, to avoid any complications from impurities, and deionized water would have been the most likely source of pure water for a POSA.

C. Ground 3: *Nishikawa* and *Honda* Would Have Rendered Obvious Claim 17

1. Claim 17: The separator according to claim 1, wherein the porous layer has pores formed by the binder, at least a part of the inorganic particles are embedded in the pores.

144. *Nishikawa* and *Honda* would have rendered obvious "wherein the porous layer has pores formed by the binder, at least a part of the inorganic particles are embedded in the pores."

145. *Nishikawa* describes "pores in the heat resistant porous layer," *Nishikawa*, 7:26-30. *Nishikawa* explains that "[t]he heat resistant porous layer of the invention contains the heat resistant resin, has numerous minute pores inside, and has a such a structure that the minute pores are connected to each other, thereby providing a porous layer, through which a gas or a liquid can pass from one surface to the other surface." *Id.*, 7:41-45. *Nishikawa* also explains that the "inorganic filler contribut[es] to the formation of pores" in the heat resistant porous layer, but does not explain how. *Nishikawa* does not further describe the structure of those pores.

146. *Honda* explains how inorganic filler can contribute to the formation of pores. In particular, *Honda* recommends a porous layer in which "a resin has a fibril shape to form a three-dimensional network structure, by which a filler is trapped by the network structure." *Honda*, [0164] *see also id.*, [0228]. A POSA would have recognized from *Honda* that such "a three-dimensional network structure" of the

resin would include "pores formed by the" resin. In particular, the pores are formed in the voids of the "three-dimensional network structure" *Honda* describes.

147. Thus, from *Honda*, a POSA would have recognized that one way for the "inorganic filler [to] contribut[e] to the formation of pores" in the resin of heat resistant porous layer—as *Nishikawa* envisions—is for the inorganic filler to be "trapped by" the pores in the resin, as *Honda* describes. Accordingly, from *Nishikawa* and *Honda*, a POSA would have been motivated and found it obvious for the inorganic filler to be "trapped by" the pores in the resin.

148. Thus, from *Nishikawa* and *Honda*, a POSA would have been motivated and found it obvious to implement *Nishikawa*'s heat resistant porous layer to have pores formed by the resin, with at least a part of the inorganic filler trapped in the pores, as *Honda* describes. A POSA would have understood such inorganic filler trapped in the pores to be "embedded in" the pores, at least because the '987 patent shows such "embedded" inorganic particles are trapped in the pores, as annotated Figure 1 of the '987 patent, below, shows.

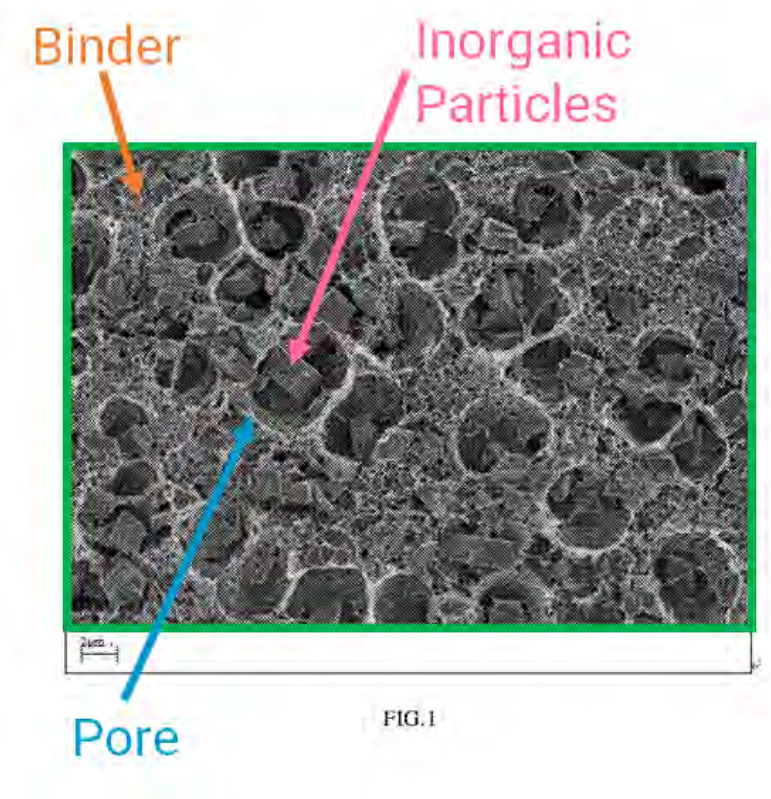


FIG.1

D. Ground 4: *Iwai* Anticipates Claims 1-2 and 4-9

1. Claim 1

149. *Iwai* anticipates claim 1.

a. 1[p] A separator, comprising:

150. To the extent this preamble is limiting, *Iwai* describes "[a] separator." *Iwai* describes a "separator for a non-aqueous secondary battery" and example separators in Example 7 and Comparative Example 2. *Iwai*, [0001], [0206]-[0208], [0215]-[0217].

b. 1[a] a porous substrate; and

151. *Iwai* discloses "a porous substrate." In *Iwai*, the separator includes a

"porous substrate." *Iwai*, [0020]; *see also id.*, [0046]-[0047]. Each of *Iwai*'s Example 7 and Comparative Example 2 separators includes a porous substrate. *Id.*, [0157] (Example 1 includes a "porous substrate"); [0206]-[0208] (Example 7 same as Example 1); [0215]-[0217] (Comparative Example 2 same as Example 1)[3].

c. 1[b] a porous layer arranged on a surface of the porous substrate,

152. *Iwai* discloses "a porous layer arranged on a surface of the porous

[3] *Iwai*'s Example 7 is "obtained in the same manner as in Example 1, except that" the "organic filler A" used in Example 1 is replaced with a mixture of "inorganic filler C," which is "a magnesium hydroxide filler having a volume average particle diameter of 1.6 μm," and "inorganic filler D" which is "a magnesium hydroxide filler having a volume average particle diameter of 0.8 μm," and "the average thickness a of the adhesive porous layer" was changed as shown in Table 1. *Iwai*, [0206]. *Iwai*'s Comparative Example 2 is "obtained in the same manner as in Example 1, except that the inorganic filler D was used instead of the organic filler A and that the average thickness of the adhesive porous layer" was changed as shown in Table 1. *Id.*, [0215]. Accordingly, throughout my discussion of Ground 4, citations to discussions of Example 1 are provided where they equally apply to Example 7 and Comparative Example 2.

substrate." In *Iwai*, the separator includes an "adhesive porous layer" that is "provided on one or both sides of the porous substrate." *Iwai*, [0021]; *see also id.*, [0063]. Each of *Iwai*'s Example 7 and Comparative Example 2 separators includes an adhesive porous layer that is "applied … to both sides of" the porous substrate. *Iwai*, [0189].

d. 1[c] wherein the porous layer comprises inorganic particles and a binder,

153. *Iwai* discloses "wherein the porous layer comprises inorganic particles and a binder."

154. Regarding inorganic particles, in *Iwai* the adhesive porous layer includes "filler" such as "inorganic filler." *Iwai*, [0087]-[0088]. The adhesive porous layer in each of *Iwai*'s Example 7 and Comparative Example 2 separators includes inorganic filler of magnesium hydroxide, which is one embodiment of the claimed "inorganic particles" described in the '987 patent. *Id.*, [0206] (Example 7), [0215] (Comparative Example 2), Table 1; '987 patent, 2:1-6. *Compare also Iwai*, [0092] (listing materials for *Iwai*'s inorganic filler) *with* '987 patent claim 6 (listing materials for claimed "inorganic particles").

155. Regarding a binder, in *Iwai* the adhesive porous layer includes a "resin" of "polyvinylidene-fluoride," which is one embodiment of the claimed "binder" described in the '987 patent. *Iwai*, [0022]; '987 patent, 2:7-13 The adhesive porous

layer in each of *Iwai*'s Example 7 and Comparative Example 2 separators includes the polyvinylidene-fluoride resin. *Id.*, [0187], Table 1. *Compare also Iwai*, [0074]-[0075] (listing materials for *Iwai*'s polyvinylidene-fluoride resin) *with* '987 patent claim 7 (listing materials for claimed "binder").

e. 1[d] a ratio of Dv90 of the inorganic particles to the thickness of the porous layer is in a range from 0.3 to 3.0.

156. *Iwai* discloses that "a ratio of Dv90 of the inorganic particles to the thickness of the porous layer is in a range from 0.3 to 3.0" because a POSA would have recognized that, in each of *Iwai*'s Example 7 and Comparative Example 2 separators, a ratio of a D90 of the inorganic filler to the thickness of the porous membrane must have a value that falls within the claimed range.

157. Table 1, below, shows *Iwai*'s Example 7 separator includes inorganic filler having a volume average particle diameter of 1.2μm. Table 1 also shows that D90-D10 for the inorganic filler—that is, a difference between the D90 of the inorganic filler and the D10 of the inorganic filler—in *Iwai*'s Example 7 separator is 1.6μm.

TABLE 1

	Average thickness a (μm) of adhesive porous layer	Resin type	Filler Type	Volume average particle diameter r (μm)	D90 – D10 (μm)	Content (% by mass)	a/r
Example 1	2.1	Resin A	Organic filler A	1.8	1.3	5	1.2
Example 2	1.1	Resin A	Organic filler A	1.8	1.3	20	0.6
Example 3	1.5	Resin A	Organic filler A	1.8	1.3	25	0.8
Example 4	3.5	Resin A	Organic filler A	1.8	1.3	1	1.9
Example 5	4.7	Resin A	Organic filler A	1.8	1.3	0.3	2.6
Example 6	3.0	Resin A	Organic filler B	3.0	2.0	20	1.0
Example 7	2.2	Resin A	Inorganic fillers C, D	1.2	1.6	10	1.8
Example 8	2.1	Resins A, B	Organic filler A	1.8	1.3	30	1.2
Comparative Example 1	1.3	Resin A	—	—	—	0	—
Comparative Example 2	3.1	Resin A	Inorganic filler D	0.8	1.1	40	3.9
Comparative Example 3	5.5	Resin A	Organic filler A	1.8	1.3	20	3.1
Comparative Example 4	2.0	Resin A	Organic filler E	5.0	3.6	1	0.4
Comparative Example 5	0.7	Resin A	Organic filler A	1.8	1.3	5	0.4
Comparative Example 6	5.0	Resin A	Organic filler E	5.0	3.6	5	1.0
Comparative Example 7	2.1	Resin A	Organic filler F	4.0	2.5	30	0.5

***Iwai*, Table 1 (cropped and annotated)**

158. From *Iwai*'s Table 1, a POSA would have recognized that D90 of the inorganic filler in *Iwai*'s Example 7 separator must be between 1.6μm and 2.8μm, as explained below.

159. **Volume average particle diameter.** *Iwai* defines "volume average particle diameter" as "a particle diameter at 50% cumulative volume calculated from a smaller side in a volume particle size distribution." *Iwai*, [0038]. As noted above, while a POSA may typically understand the term "volume average particle diameter" to refer to the mean (arithmetic average) diameter of particles in the particle distribution, by defining "the volume average particle diameter (μm) of the filler" as "a particle diameter at 50% cumulative volume calculated from a smaller side in a volume particle size distribution.," *Iwai* equates the "volume average particle

diameter 'r' (μm)" with D50, stating *Id.*, [0038]; *see also* [0160]. For *Iwai*'s Example 7 separator, the volume average particle diameter—that is, the D50—of the inorganic filler is 1.2μm.

160. **D10.** *Iwai* defines D10 as "a particle diameter at which a cumulative volume of particles reaches 10% from a smaller side in a volume particle size distribution." *Iwai*¸ [0039]. A POSA would have recognized that D10 for *Iwai*'s Example 7 separator must be greater than 0, because it would not be possible for particles at 10% of the inorganic filler volume to have a particle diameter of 0. Further, a POSA would have recognized that D10 for *Iwai*'s Example 7 separator must be less than the volume average particle diameter of the inorganic filler for *Iwai*'s Example 7 separator, because it would not be possible for the particle diameter at 10% cumulative volume to be more than the particle diameter at 50% cumulative volume. Thus, a POSA would have recognized that D10 for *Iwai*'s Example 7 separator must be less than 1.2μm.

161. **D90.** *Iwai*'s Table 1 shows D90-D10 for *Iwai*'s Example 7 separator as 1.6μm, as shown above. Thus, a POSA would have recognized:

$$D90 - D10 = 1.6$$

$$D90 = 1.6 + D10$$

$$D90 - 1.6 = D10 \text{ (Equation 1)}$$

162. Further, as explained above, a POSA would have recognized that D10

for *Iwai*'s Example 7 separator must be greater than 0 and less than 1.2μm:

$$0 < D10 < 1.2 \text{ (Equation 2)}$$

163. Replacing D10 in Equation 2 per Equation 1, a POSA would have recognized:

$$0 < D90 - 1.6 < 1.2$$

$$1.6 < D90 < 2.8$$

164. Thus, a POSA would have recognized, D90 for *Iwai*'s Example 7 separator must be greater than 1.6μm and less than 2.8μm. A POSA would have recognized that "D90," as used by *Iwai*, is synonymous with "Dv90," as used in the '987 patent, at least because *Iwai* and the '987 patent define them synonymously. *Compare Iwai*, [0040] (defining "D90" as "particle diameter at which a cumulative volume of particles reaches 90% from a smaller side in a volume particle size distribution") *with* '987 patent, 1:53-56 (defining "Dv90" as "a particle size which reaches 90% the cumulative volume from the side of small particle size in the granularity distribution on a volume basis.").

165. Thus, a POSA would have understood that, in *Iwai*'s Example 7 separator, the D90 of the inorganic particles must be greater than 1.6μm and less than 2.8μm. Further, Table 1 shows that the thickness of the adhesive porous layer in *Iwai*'s Example 7 separator is 2.2μm. Thus, as summarized in *Iwai*'s Ratios Table below, in *Iwai*'s Example 7 separator the ratio of the D90 of the inorganic particles

to the thickness of the porous membrane must be greater than 0.72 and less than 1.27.

166. Similar calculations show that, in *Iwai*'s Comparative Example 2 separator, the ratio of D90 of the inorganic filler to the thickness of the porous membrane must also have a value that falls within the claimed range.

167. Table 1, above, shows *Iwai*'s Comparative Example 2 separator includes inorganic filler having a volume average particle diameter of 0.8μm. Table 1 also shows that D90-D10 for the inorganic filler—that is, a difference between the D90 of the inorganic filler and the D10 of the inorganic filler—in *Iwai*'s Comparative Example 2 separator is 1.1μm.

168. From *Iwai*'s Table 1, a POSA would have recognized that D90 of the inorganic filler in *Iwai*'s Comparative Example 2 separator must be between 1.6μm and 2.8μm, as explained below.

169. **Volume average particle diameter.** For *Iwai*'s Comparative Example 2 separator, the volume average particle diameter of the inorganic filler is 0.8μm.

170. **D10.** A POSA would have recognized that D10 for *Iwai*'s Comparative Example 2 separator must be greater than 0, because it would not be possible for particles at 10% of the cumulative volume of inorganic filler particles to have a particle diameter of 0. Further, a POSA would have recognized that D10 for *Iwai*'s Comparative Example 2 separator must be less than the volume average particle

diameter of the inorganic filler for *Iwai*'s Comparative Example 2 separator, because it would not be possible for the particle diameter at 10% cumulative volume to be more than the particle diameter at 50% cumulative volume. Thus, a POSA would have recognized, D10 for *Iwai*'s Comparative Example 2 separator must be less than 0.8μm.

171. **D90.** *Iwai*'s Table 1 shows D90-D10 for *Iwai*'s Comparative Example 2 separator as 1.1μm, as shown above. Thus, a POSA would have recognized:

$$D90 - D10 = 1.1$$

$$D90 = 1.1 + D10$$

$$D90 - 1.1 = D10 \text{ (Equation 6)}$$

172. Further, as explained, a POSA would have recognized that D10 for *Iwai*'s Comparative Example 2 separator must be greater than 0 and less than 0.8μm:

$$0 < D10 < 0.8 \text{ (Equation 7)}$$

173. Replacing D10 in Equation 7 per Equation 6, a POSA would have recognized:

$$0 < D90 - 1.1 < 0.8$$

$$1.1 < D90 < 1.9$$

174. Thus, a POSA would have understood that, in *Iwai*'s Comparative Example 2 separator, a D90 of the inorganic particles must be greater than 1.1μm

and less than 1.9μm. Further, Table 1 shows that a thickness of the adhesive porous layer in *Iwai*'s Comparative Example 2 separator is 3.1μm. Thus, as summarized in the *Iwai*'s Ratios Table below, in *Iwai*'s Comparative Example 2 separator a ratio of the D90 of the inorganic particles to the thickness of the porous membrane must be greater than 0.35 and less than 0.61.

***Iwai*'s Example**	**D90 (μm)**	**Thickness (μm)**	**Ratio ($\frac{D90}{Thickness}$)**
Example 7	1.6 < D90 < 2.8	2.2	0.72 < Ratio < 1.27
Comparative Example 2	1.1 < D90 < 1.9	3.1	0.35 < Ratio < 0.61

***Iwai*'s Ratios Table**

175. Thus, *Iwai* discloses an example separator (Example 7) in which a ratio of D90 of the inorganic particles to the thickness of the porous membrane must have a value that falls between 0.72 and 1.27, and *Iwai* discloses an example separator (Comparative Example 2) in which a ratio of D90 of the inorganic particles to the thickness of the porous membrane must have a value that falls between 0.35 and 0.61. Put differently, inherent in *Iwai* is that each of *Iwai*'s Example 7 and Comparative Example 2 separators has a ratio of D90 of the inorganic particles to the thickness of the porous membrane having a value "in a range from 0.3 to 3.0." A POSA would have understood each of *Iwai*'s Example 7 and Comparative Example 2 separators to thus disclose, as claim 1 requires, a separator in which "a

ratio of Dv90 of the inorganic particles to the thickness of the porous layer is in a range from 0.3 to 3.0."

2. Claim 2: The separator according to claim 1, wherein the porous layer has a thickness of 0.2 µm to 10 µm.

176. *Iwai* discloses "wherein the porous layer has a thickness of 0.2 µm to 10 µm." As Table 1 shows, in *Iwai*'s Example 7 separator, the adhesive porous layer has a thickness of 2.2µm, and in *Iwai*'s Comparative Example 2 separator, the adhesive porous layer has a thickness of 3.1µm. *Iwai*, Table 1.

3. Claim 4: The separator according to claim 1, wherein a volume ratio of the inorganic particles to the binder is in a range from 0.2 to 3.0.

177. *Iwai* discloses "wherein a volume ratio of the inorganic particles to the binder is in a range from 0.2 to 3.0," because a POSA would have understood from *Iwai* that the separator of Comparative Example 2 has a volume ratio of 0.51, as explained below.

178. As Table 1 shows, the separator of Comparative Example 2 has "Filler" with "Content (% by mass)" of 40%. *Iwai*, Table 1. As *Iwai* explains, this "Content (% by mass)" refers to "[a] content of the filler in the coating liquid … with respect to a total mass of the polyvinylidene-fluoride resin and the filler." *Iwai*, [0189]. Thus, a POSA would have understood from *Iwai* that, in the separator of Comparative Example 2, the inorganic filler accounts for 40% of the total mass of the

polyvinylidene-fluoride resin and the inorganic filler. This is reflected in Equation 8 below, where "M_{filler}" refers to the mass of the inorganic filler and "M_{resin}" refers to the mass of the polyvinylidene-fluoride resin:

$$\frac{M_{filler}}{M_{filler}+M_{resin}} = 0.4 \text{ (Equation 8)}$$

179. Taking the reciprocal of Equation 8 provides Equation 9:

$$\frac{M_{filler}+M_{resin}}{M_{filler}} = 2.5$$

$$M_{filler} + M_{resin} = 2.5M_{filler}$$

$$M_{resin} = 1.5M_{filler}$$

$$\frac{M_{resin}}{M_{filler}} = 1.5 \text{ (Equation 9)}$$

180. And taking the reciprocal of Equation 9 provides Equation 10:

$$\frac{M_{filler}}{M_{resin}} = 0.67 \text{ (Equation 10)}$$

181. While Equation 10 provides a mass ratio, a POSA would have known how to determine a volume ratio from a mass ratio. In particular, a POSA would have known that a mass is convertible to a volume by dividing the masse by the density, ρ, of the material. In general: V [volume] = M [mass] / ρ [mass/volume]. So, a ratio of the masses of two materials can be converted into the ratio of volumes by multiplying this mass ratio by the reciprocal density ratio. This is shown in Equation 11, where "ρ_{filler}" refers to the density of the inorganic filler and "ρ_{resin}"

refers to a density of the polyvinylidene-fluoride resin, and "V_{filler}" refers to the volume of the inorganic filler and "V_{resin}" refers to the volume of the polyvinylidene-fluoride resin:

$$\frac{V_{filler}}{V_{resin}} = \frac{M_{filler}}{M_{resin}} \times \frac{\rho_{resin}}{\rho_{filler}} \text{ (Equation 11)}$$

182. Replacing M_{filler}/M_{resin} in Equation 11 per Equation 10 provides Equation 12 below:

$$\frac{V_{filler}}{V_{resin}} = 0.67 \frac{\rho_{resin}}{\rho_{filler}} \text{ (Equation 12)}$$

183. The separator of Comparative Example 2 in *Iwai* uses an inorganic filler of magnesium hydroxide, which has a density ρ_{filler} of 2.36 g/cm^3. Ex. 1017, 525. The separator of Comparative Example 2 in *Iwai* uses a polyvinylidene-fluoride resin that is a vinylidene fluoride (VDF) / hexafluoropropylene (HFP) copolymer in which the VDF and HFP monomers are provided in a molar ratio of 98.9 to 1.1. *Iwai*, [0187] (Example 1), [0215] (Comparative Example 2 same as Example 1). A POSA would have known how to convert this molar ratio into a weight ratio or weight percentage based on the facts that (i) VDF has a molar mass of 64.034 g/mol and (ii) HFP has a molar mass of 150.021 g/mol. (VDF has the chemical formula $C_2H_2F_2$, and HFP has the chemical formula C_3F_6. The atomic weights of the constituent atoms are: C (12.011 g/mol), F (18.998 g/mol), and H (1.008 g/mol). Therefore, the molar mass of VDF is 2×12.011 + 2×18.998 + 2×1.008 = 64.034 g/mol. And the molar

mass of HFP is 3×12.011 + 6×18.998 = 150.021 g/mol) From this, it can be determined that there is 2.54% by weight of HFP and 97.46% by weight of VDF in the Comparative Example 2 binder copolymer.

184. From these percentages by weight, a POSA would have recognized that the polyvinylidene-fluoride resin in *Iwai*'s Comparative Example 2 has a density that is effectively the same as the density of pure polyvinylidene-fluoride. Polyvinylidene-fluoride hexafluoropropylene copolymer is a common material, and there are numerous examples of this material, with similar compositions to those used in *Iwai*'s examples, that are cited in the academic literature or available commercially. Densities for these copolymers are widely reported. The density of pure polyvinylidene fluoride is 1.78 g/cm^3. *See, e.g.*, Ex. 1018, 3440. Commercially available PVDF-HFP copolymers with 10% and 15% HFP by weight—much higher than the 2.54% HFP by weight of *Iwai*'s Comparative Example 2—are reported to have densities in the range of 1.7 to 1.8 g/cm^3, which is effectively the same as pure polyvinylidene-fluoride. *See, e.g.*, Appendix C, A280 (stating Kynar Flex 2801 has 10% by weight HFP and Kynar Flex 2751 has 15% by weight HFP); Appendix D (Kynar Flex 2801 Technical Data Sheet giving density as 1.78 g/cm^3); Appendix E (Kynar Flex 2751 Technical Data Sheet giving specific gravity as 1.7 - 1.8. A POSA knows that specific gravity is defined as the density of a material divided by the density of water, which is 1.0 g/cm^3. Thus this data sheet is telling a POSA that this

VDF-HFP copolymer with 15% HFP has a density of 1.7 to 1.8 g/cm^3, which again is no different from pure polyvinylidene chloride. From this, a POSA would have been able to identify a density ρ_{resin} of the resin in *Iwai*'s Comparative Example 2 to be effectively the same as the density of pure polyvinylidene fluoride, namely, 1.78 g/cm^3. *See, e.g.*, Appendix 1018, 3440.

185. Finally, plugging the values of ρ_{filler} and ρ_{resin} into Equation 13, a POSA would have arrived at a volume ratio for *Iwai*'s Comparative Example 2 separator of:

$$\frac{V_{filler}}{V_{resin}} = 0.67\frac{\rho_{resin}}{\rho_{filler}} \text{ (Equation 13)}$$

$$\frac{V_{filler}}{V_{resin}} = 0.67\frac{1.78}{2.36}$$

$$\frac{V_{filler}}{V_{resin}} = 0.51$$

186. Thus, a POSA would have understood *Iwai* to disclose that, in the separator of Comparative Example 2, a volume ratio of the inorganic particles to the binder is 0.51—a value that is "in a range from 0.2 to 3.0."

4. Claim 5: The separator according to claim 1, wherein the porous layer has a porosity of 20% to 90%.

187. *Iwai* discloses "wherein the porous layer has a porosity of 20% to 90%." *Iwai* discloses that "it is preferable that the adhesive porous layer has a porosity of from 30% to 60%." *Iwai*, [0066]. As *Iwai* explains, "in a case in which the porosity

is 30% or more, good ion permeability can be obtained." *Id. See also* Ex. 1008, 246 ("High porosity is desirable for unhindered ionic current flow.").

5. Claim 6: The separator according to claim 1, wherein the inorganic particles are one or more selected from the group consisting of alumina, silica, magnesia, titanium oxide, hafnium dioxide, tin oxide, zirconia, cerium dioxide, nickel oxide, zinc oxide, calcium oxide, boehmite, aluminum hydroxide, magnesium hydroxide, calcium hydroxide, and barium sulfate.

188. *Iwai* discloses "wherein the inorganic particles are one or more selected from the group consisting of alumina, … titanium oxide, hafnium dioxide, tin oxide, zirconia, … aluminum hydroxide, magnesium hydroxide, … and barium sulfate." The adhesive porous layer in each of *Iwai's* Example 7 and Comparative Example 2 separators includes inorganic filler of magnesium hydroxide. *Iwai*, [0206], [0215]. *Iwai* additionally envisions that the inorganic filler may be alumina, zirconia, and other metal oxides; aluminum hydroxide and other metal hydroxides; and barium sulfate. *Iwai*, [0092].

6. Claim 7: The separator according to claim 1, wherein the binder is one or more selected from the group consisting of polyvinylidene fluoride, vinylidene fluoride-hexafluoropropylene copolymer, polyamide, polyacrylonitrile, polyacrylate, polyacrylic acid, polyacrylates, sodium carboxymethylcellulose, polyvinylpyrrolidone, polyvinyl ether, polymethyl methacrylate, polytetrafluoroethylene and polyhexafluoropropylene.

189. *Iwai* discloses "wherein the binder is one or more selected from the

group consisting of polyvinylidene fluoride [and] vinylidene fluoride-hexafluoropropylene copolymer." The porous membrane in each of *Iwai*'s Example 7 and Comparative Example 2 separators includes as the polyvinylidene-fluoride resin a vinylidene fluoride-hexafluoropropylene copolymer. *Iwai*, [0187] (Example 1), [0206] (same as Example 1), [0215] (same as Example 1). *Iwai* additionally envisions that the polyvinylidene-fluoride resin may be polyvinylidene fluoride. *Iwai*, [0074].

7. Claim 8: An energy storage device, comprising the separator according to claim 1.

190. *Iwai* discloses "[a]n energy storage device, comprising the separator according to claim 1." Each of *Iwai*'s Example 7 and Comparative Example 2 separators discloses "the separator according to claim 1," as explained above for claim 1, and *Iwai* discloses using each of the Example 7 and Comparative Example 2 separators in a "lithium ion secondary battery," which is one "energy storage device" described in the '987 patent. *Iwai*, [0002]-[0003] (describing "a separator for non-aqueous secondary batter[ies] … which are represented by lithium-ion secondary batteries"), [0187]-[0199] (describing production of "test battery" in Example 1), [0207] (same for Example 7), [0216] (same for Comparative Example 2); '987 patent, 1:20-21 (describing "[n]on-aqueous secondary batteries, particularly lithium-ion batteries"), 2:17-18 ("the energy storage device is a lithium-

ion battery").

8. Claim 9: The energy storage device according to claim 8, wherein the energy storage device is a lithium-ion battery.

191. *Iwai* discloses "wherein the energy storage device is a lithium-ion battery." As explained for claim 8, *Iwai* discloses using each of the Example 7 and Comparative Example 2 separators in a "lithium ion secondary battery."

E. Ground 5: *Iwai* Would Have Rendered Obvious Claim 3

1. Claim 3: The separator according to claim 1, wherein the pores have an average pore size of 0.3 μm to 20 μm.

192. *Iwai* would have rendered obvious "wherein the pores have an average pore size of 0.3 μm to 20 μm." *Iwai* teaches that "the adhesive porous layer is a layer having a structure in which a large number of micropores are present inside thereof and the micropores connect to one another, which allows gas or liquid to pass therethrough from one side to the other side." *Iwai*, [0062]. From *Iwai*, a POSA would have been motivated and found it obvious to implement *Iwai*'s separator to have "an average pore size" within the claimed range for at least two reasons.

193. First, *Iwai* recognizes, like the '987 patent, that pore size must be adjusted to accommodate two competing concerns: the pores must be large enough to suppress "the blockage of pores." But the pores also need to be small enough to promote uniformity of ion flow, and to prevent "non-uniformity of the pores at the surface," which can undermine adhesion. *Iwai*, [0067]; *compare with* '987 patent,

5:28-35 ("pore blockage"), 5:43-49 ("non-uniform surface of the porous layer"). From these competing concerns described in *Iwai*, a POSA would have been motivated and found it obvious to implement each of *Iwai*'s Example 7 and Comparative Example 2 separators to address these concerns. And a POSA would have understood how to adjust pore size, as it was understood by 2018 that "pore size and the porosity are very important factors for the control of ion conductivity in a battery thus, are directly related to the quality of the battery." Ex. 1009, 4:34-37. *See also* Ex. 1010, 5:47-50 ("[T]he present inventors have recognized that controlling the porosity and pore size" of a porous layer "is one of the factors affecting the quality of a battery."). Thus, because *Iwai* teaches that pore size is a parameter to be adjusted to address these competing concerns, and adjustment of pore size would have been within a POSA's skill, a pore size within the claimed range would have been obvious to a POSA.

194. Second, while *Iwai* recommends a specific range of pore diameters—"from 20 nm to 100 nm," that is, from .02μm to .1μm—a POSA would still have found it obvious to adjust *Iwai*'s pore size outside this range, as pore size adjustment was widely understood, as explained in the State of the Art, and a POSA would not have found *Iwai*'s recommended range to be limiting. Rather, a POSA would have recognized that "micropore," as used by *Iwai* to describe the pores of its porous layer, was a term used in the art to refer to a broader range of pores, namely, those having

any size less than approximately 1µm. *See, e.g.*, Ex. 1008, 247 ("One distinguishes between microporous and microporous separators, the latter having to show pore diameters below 1 micron (µm), i.e., below one-thousandth of a millimeter."). Accordingly, a POSA would have found it obvious to adjust pore size for each of *Iwai*'s Example 7 and Comparative Example 2 separators within a broader micropore range up to at least 1µm, provided *Iwai*'s identified competing concerns of pore blockage and non-uniformity were addressed. As noted above, because *Iwai* teaches that pore size is a parameter to be adjusted to address these competing concerns, and adjustment of pore size would have been within a POSA's skill, adjusting *Iwai*'s pore size would have been obvious to a POSA.

XI. CONCLUSION

I declare that all statements made herein of my knowledge are true, that all statements made on information and belief are believed to be true, and that these statements were made with the knowledge that willful false statements and the like so made are punishable by fine or imprisonment, or both, under Section 1001 of Title 18 of the United States Code.

Dated: February 22, 2023 By: 

Samuel P. Gido
Amherst, Massachusetts

Appendix A

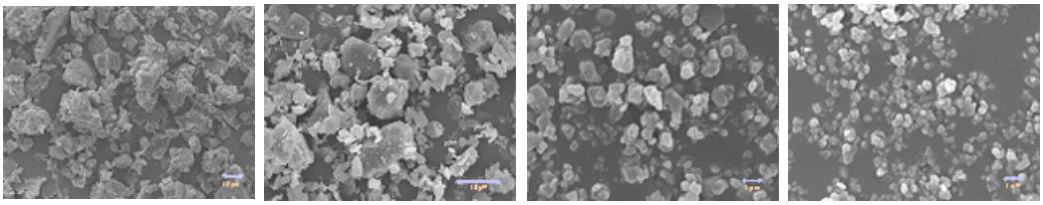
HIGILITE® (fine particles, particles)

Petrochemical Division
Functional Chemicals Division
Ceramics Division
Graphite Division
Aluminum Functional Components Division
High-tech Battery Materials Division
Basic Chemicals Division
レゾナック Optical Semiconductor Co., Ltd.
Original Electronic Functional Materials Division
レゾナック・パッケージング original packaging business promotion department

English name	HIGILITE®
Product nickname	• Aluminum hydroxide (fine particles, particles) / aluminum hydroxide • H-21 / H-21 • H-31 / H-31 • H-32 / H-32 • H-42 / H-42 • H-42M / H-42M • H-43 / H-43 • H-43M / H-43M • aluminum hydroxide <chemical name>

Product Description

Under the condition of 200～350℃, HIGILITE® will undergo violent dehydration reaction and absorb a lot of heat at the same time. Therefore, when HIGILITE® is used as a filler for rubber, plastic, and paper materials, even if heated, the temperature rise of the material is suppressed, the self-extinguishing property is improved, and the generation of smoke is suppressed at the same time. During this process, HIGILITE® will not produce toxic gas, and it can exert its excellent performance as a flame retardant filler. In addition, it improves the arc and creepage resistance of plastics. The main products that can meet the requirements of the above-mentioned applications are H-42M and H-43M of fine particles and particles.



HW H-32 H-42 H-43M

[Main application]

1. Polyaluminum chloride, sodium aluminate, various aluminum salts.
2. Flame retardant filler for latex compound and synthetic rubber.
3. Flame retardant filler for vinyl chloride, epoxy resin, polyester resin, polyurethane resin, polyolefin resin.
4. Catalysts and catalyst supports.
5. Internal filler for coated paper and flame retardant paper.

品名 / 品质项目		细粒			微粒			
		H-21	H-31	H-32	H-42	H-42M	H-43	H-43M
化学组成	附着水分 (%)	0.07	0.08	0.20	0.25	0.23	0.30	0.30
	$Al(OH)_3$ (%)	99.8	99.8	99.8	99.6	99.6	99.6	99.6
	Fe_2O_3 (%)	0.01	0.01	0.01	0.01	0.01	0.01	0.01
	SiO_2 (%)	0.01	0.01	0.01	0.01	0.01	0.01	0.01
	Na_2O (%)	0.17	0.17	0.17	0.34	0.33	0.40	0.34
	w-Na_2O (%)	0.02	0.02	0.02	0.10	0.05	0.13	0.07
+75μm量 (%)		0.20	0.04	—	—	—	—	—
+45μm量 (%)		—	—	0.10	0.02	0.01	0.02	0.02
粒度分布	平均粒径 (μm)	27	18	8	1.0	1.0	0.75	0.75
	−30μm (%)	56	76	96	100	100	100	100
	−20μm (%)	40	54	85	100	100	100	100
	−10μm (%)	23	31	58	100	100	100	100
	−5μm (%)	8	12	34	100	100	100	100
	−2μm (%)	2	4	12	98	98	100	100
	−1μm (%)	0	1	3	47	46	78	78
堆积密度 (g/cm^3)	轻装	1.0	0.9	0.7	0.2	0.2	0.2	0.2
	重装	1.4	1.2	1.1	0.5	0.5	0.4	0.4
白度		89	90	95	98	98	98	98
BET比表面积 (m^2/g)		1.3	1.4	2.0	5.0	5.0	6.7	6.7

Product related information

Properties

White powder

storage conditions, etc.

Keep dry

packaging

25kg paper bag, ton bag, etc.

Chemical Examination Law Number

(1)-17

CAS Reg#

CAS21645-51-2

Relevant laws and regulations (Japanese domestic law)

Dust damage prevention rules

Copyright (C) SHOWA DENKO (SHANGHAI) CO.,LTD. All rights reserved.

Appendix B

Journal of Membrane Science 518 (2016) 72–78

Contents lists available at ScienceDirect

Journal of Membrane Science

journal homepage: www.elsevier.com/locate/memsci

Poly(m-phenylene isophthalamide) (PMIA): A potential polymer for breaking through the selectivity-permeability trade-off for ultrafiltration membranes

Chun-Er Lin [a], Jun Wang [a], Ming-Yong Zhou [a], Bao-Ku Zhu [a,b,*], Li-Ping Zhu [a], Cong-Jie Gao [a,b]

[a] Key Laboratory of Macromolecule Synthesis and Functionalization (MOE), ERC of Membrane and Water Treatment (MOE), Department of Polymer Science and Engineering, Zhejiang University, Hangzhou 310027, China
[b] CIC-ZJ on Membrane and Water Treatment Technology, Zhejiang University of Technology, Hangzhou 310014, China

ARTICLE INFO

Article history:
Received 27 March 2016
Received in revised form
25 June 2016
Accepted 28 June 2016
Available online 30 June 2016

Keywords:
Poly(m-phenylene isophthalamide)
Ultrafiltration membrane
Permeability
Selectivity
Trade-off

ABSTRACT

The selectivity-permeability trade-off represents a limitation to the performance of ultrafiltration (UF) membranes. Theoretically, this trade-off is mainly determined by the pore structure, including the porosity, pore radius distribution and skin layer thickness. Benefiting from its high rigidity and high surface free energy, poly(m-phenylene isophthalamide) (PMIA) is proposed for preparing a high-performance UF membrane. In this work, PMIA membranes with various effective pore radii (6.58 nm, 6.84 nm and 9.28 nm) were fabricated via nonsolvent-induced phase separation (NIPS). Through selectivity-permeability analysis, the PMIA membrane was found to break through the trade-off between selectivity and permeability. Compared with other UF membranes, the PMIA membrane exhibited a high porosity, narrow pore radius distribution and excellent hydrophilicity, leading to its high performance in the filtration process. This phenomenon could probably be attributed to the high rigidity, which confined the motion of the PMIA chain to suppressing pore collapse during pore formation, as well as to the high surface free energy that caused the hydrophilicity. All of these results clearly indicated that PMIA might be the most appropriate polymer for fabricating the UF membrane.

© 2016 Elsevier B.V. All rights reserved.

1. Introduction

Ultrafiltration (UF) membranes are widely used in water purification [1], wastewater treatment [2], protein product concentration [3], hemodialysis [4], and more. Currently, commercial UF membranes are mostly made from polysulfone (PSf), celluloses, polycarbonate (PC), polyacrylonitrile (PAN), polyvinylidene fluoride (PVDF), polyvinyl chloride (PVC) and other inorganic materials. Each series contains membranes that have a range of pore size or molecular weight cut-off. Generally, the performance characteristics of UF membranes mainly contain permeability and selectivity that are inversely related. Because the steric (size exclusion) effect acts as the main separate mechanism [5], the selectivity of UF membrane is determined by pore radius (R) and pore radius distribution (σ) [6], while the permeability is governed mainly by the pore radius (R), porosity (ε) and skin layer thickness (δ_m). To identify the underlying relationship between the selectivity and permeability, Mehta and Zydney [7] developed a trade-off that known UF membranes cannot permeate.

Structurally, an ideal UF membrane should have a high porosity, narrow pore radius distribution and thin skin layer. Additionally, taking the surface property into consideration, hydrophilicity endows the UF membrane with excellent wettability, which effectively improves the water permeation in the filtration process [8,9]. The block copolymer (BCP) membrane, which is supposed to possess high selectivity due to its uniform pore size, has attracted substantial attention in recent years. Nevertheless, limited by their relatively low permeability, the benefits did not outweigh the limitations [10]. Additionally, the synthesis complexity and high cost of BCP make it difficult to produce on a large scale. Therefore, it is important to seek a suitable material for preparing a high-performance UF membrane.

Poly(m-phenylene isophthalamide) (PMIA), due to its hydrogen bond network, has excellent mechanical properties and an outstanding thermal stability [11]. The glass transition temperature (Tg) of PMIA is up to 558 K (shown in Table 1), resulting in a broad range of temperature and high rigidity, which is necessary for membranes with high porosity. Meanwhile, the PMIA membrane is supposed to be hydrophilic due to the high surface free energy provided by the amide bond. Additionally, its high solubility in a common organic solvent (such as DMF and DMAc) makes it

* Corresponding author at: Department of Polymer Science and Engineering, Zhejiang University, Hangzhou 310027, China.
E-mail address: zhubk@zju.edu.cn (B.-K. Zhu).

http://dx.doi.org/10.1016/j.memsci.2016.06.042
0376-7388/© 2016 Elsevier B.V. All rights reserved.

Table 1
Glass transition temperature and surface free energy of polymers.

Polymer	Glass transition temperature (K)	Surface free energy (mN m^{-1})	Δ (mN m^{-1})	Ref.
PMIA	558	50.5[a]	22.3	[13]
PSf	458	42.3	30.5	[14,15]
PP	~260	29	43.8	[14]
PAN	398	38.6	34.2	[14,16]
PTFE	303–399	19.5	53.3	[14,17]
PVC	344–371	41	31.8	[14,17]
PVDF	238	25	47.8	[14,17]
Nylon	320–330	44	28.8	[14,17]
Cellulose	503	56.7	16.1	[14,18]
Cellulose acetate	243–473	45.9	26.9	[14]
H_2O	/	72.8	/	[18]

Δ, the difference value of the surface free energy between polymers and water.

[a] 50.5, the surface free energy for PMIA, which was obtained from measurements using the two liquid method.

possible to prepare the PMIA membrane by nonsolvent-induced phase separation (NIPS), which is favorable for developing large scale UF membranes [12]. Therefore, PMIA may be a promising material for preparing UF membranes because of these prominent physiochemical properties. However, to the best of our knowledge, there are few (if any) reports about PMIA ultrafiltration membranes via NIPS.

In this work, PMIA ultrafiltration membranes with various effective pore radii (6.58 nm, 6.84 nm, and 9.28 nm) were prepared by varying the temperature of the coagulation bath during the NIPS process. As expected, the prepared PMIA membrane achieves remarkable performance, breaking through the selectivity-permeability trade-off, which can be ascribed to their excellent pore structure and surface hydrophilicity.

2. Materials and methods

2.1. Materials

Poly(m-phenylene isophthalamide) (PMIA) fiber was provided by DuPont Co., Ltd. (USA) and dried at 100 °C for 12 h before use. Its chemical structure is shown in Fig. 1. Dimethyl acetylamide (DMAc), dimethyl formamide (DMF), glycerin and bovine serum albumin (BSA) were purchased from Sinopharm Chemical Reagent Co. (Shanghai, China). A series of polyethylene glycols (PEGs, MW 10,000–100,000) were purchased from Sigma-Aldrich (USA). All solvents and chemicals were reagent grade and used as received. Ultrapure water (18 MΩ cm^{-1}, Millipore Milli-Q) was used in all aqueous solutions.

2.2. Membrane fabrication

The PMIA membranes were fabricated by the traditional phase inversion method. The casting solution was prepared by dissolving 12 g of PMIA in 88 g of mixed solution (DMAc/DMF/glycerin 1/1/0.8 wt/wt/wt) at 80 °C for 6 h. After filtration and removal of air bubbles by vacuum deaeration, the solution was cast on a glass substrate with a steel knife; then, the liquid film was immersed into a water coagulation bath at 30 °C, 50 °C or 70 °C. The formed membrane was peeled off and subsequently washed in water at 60 °C for 3 d to extract the residual solvent. The as-prepared PMIA membranes were designated M30, M50 and M70, with the digits indicating the temperature of coagulation baths. Before testing, PMIA membranes were stored in 10 mM phosphate buffer solution (PBS, pH=7.4) and 5 g/L BSA/PBS solution at 4 °C. For convenience, the PMIA membrane soaked in PBS is referred to as a PMIA/PBS membrane, while that in BSA/PBS solution is referred to as a PMIA/BSA membrane. To ensure equilibrium adsorption, the PMIA/BSA membrane was soaked for 24 h before use.

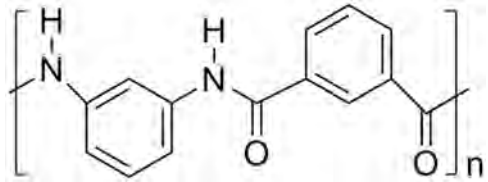


Fig. 1. Chemical structure of PMIA.

2.3. Membrane characterization

2.3.1. Membrane surface properties

The surface and cross-section morphology of the membrane was characterized by field emission scanning electronic microscopy (FE-SEM, Hitachi, S-4800, Japan). Images captured at a chosen magnification (50 k) were used to measure the membrane surface pore structure characteristics. With the help of ImageJ software (National Institutes of Health, NIH), binary images were acquired with the pores in black and surface in white at a chosen threshold level [19]. In this method, the pores on the surface should be disconnected from each other and were supposed to be circular. Thus, the porosity (ε_{sp}) and pore area can be directly obtained from the software. Then, based on these data, the average pore radius (R_{sa}) and pore density (N_{sp}) can be calculated.

The membrane surface zeta potential was determined from the streaming potential measurement with a SurPass Electrokinetic Analyser (Anton Paar, GmbH, Austria). This measurement was performed at 20 °C in 1 mM KCl solution with the solution pH values ranging from 2 to 10, and the zeta potential was calculated using the Helmholtz-Smoluchowski equation. The water contact angle of the membrane was measured with a contact angle meter system (OCA20, Dataphysics, Germany) in the sessile-drop mode at room temperature.

2.3.2. Pore structure characterization

Polyethylene glycols (PEGs, MW 10,000–100,000) were used as solutes in the feed solution with the solute concentration kept at 200 ppm by weight. The membrane was placed at the bottom of the stirred cell and compacted for 30 min at 0.015 MPa to reach a stable flux. After the stirred cell was filled with PEG solution, the experiment was conducted under 0.01 MPa at room temperature (20 ± 3 °C).

The rejection data for the PEG solution were plotted versus the solute radius on log-probability paper (shown in Fig. S1 in Supplementary information), showing straight lines fit with high correlation coefficients ($R^2 > 0.95$). By ignoring the concentration polarization as well as the steric and hydrodynamic interaction between pores and solutes, the average pore radius (R_a) and geometric standard deviation (GSD, σ_p) were determined. Then, the pore density (N) and porosity (ε) were calculated as descripted in Ref. [20]. Meanwhile, the effective pore radius (R_e) can be approximated using the Hagen-Poiseuille equation:

$$J_v = \frac{\varepsilon R_e^2 \Delta P}{8\eta\delta_m} \quad (1)$$

where J_v is the flux, ΔP is the pressure (Pa), η is the water viscosity (0.001 Pa s), δ_m is the skin layer thickness and ε is the porosity. The most probable pore radius (R_m) can be directly acquired from the probability density function curve, which was determined by the average pore radius and geometric standard deviation [6,20].

2.4. Filtration performance

All filtration experiments were conducted on a 47-mm-diameter Amicon UF cell (XFUF04701 Millipore) connected with a 500-mL reservoir containing and a N_2 gas cylinder at room temperature (20 ± 3 °C). The pressure in the stirred cell was controlled by the pressure regulator, which was connected to the N_2 gas cylinder. Each membrane was initially compacted for 30 min at 0.07 MPa to reach a stable flux.

The permeability (L_p, m s^{-1} Pa^{-1}) was evaluated by measuring the water (pH=6.5) flow rate via timed collection over a range of pressures from 0.01 to 0.05 MPa and calculated directly from the slope of the flux versus pressure data as:

$$L_p = \frac{J_v}{\Delta P} \tag{2}$$

where J_v is the volumetric filtrate flux (m s^{-1}).

After water filtration, the stirred cell was then filled with 5 g/L BSA/PBS solution, and the stirring speed was set to 600 rpm using a magnetic stirrer. After removing 2 mL of the sample to wash out the dead volume beneath the membrane, the filtrate samples were obtained for subsequent analysis. Meanwhile, the feed samples were collected directly from the stirred cell immediately before and after the experiment. The filtrate flow rates were evaluated using a digital balance and the protein concentration was determined by a UV/vis spectrophotometer (Shimadzu, UV-1601, Japan) at 280 nm.

Because the states for PMIA/PBS and PMIA/BSA were different, two methods were adopted for the rejection measurement. By adjusting the pressure in the stirred cell, the filtrate flow rate for the PMIA/PBS membrane was fixed to 1.5×10^{-5} m s^{-1} where the actual sieving coefficient (S_a) was close to the asymptotic sieving coefficient (S_∞) and a highly polarized condition was avoided [7]. As for the PMIA/BSA membrane, to minimize protein deposition, data were gained by monotonically increasing the flux (by increasing the applied pressure).

The observed sieving coefficient (S_o) was defined as:

$$S_o = \frac{C_f}{C_b} \tag{3}$$

where C_f and C_b are the solute concentrations in filtrate and bulk solution, respectively. Combined with the mass transfer coefficient (k), the actual sieving coefficient (S_a) can be calculated from the observed sieving coefficient (S_o) using a stagnant film model [5]:

$$S_a = \frac{S_o}{(1-S_o)\exp(J_v/k) + S_o} \tag{4}$$

The separation factor (α), which represented the selectivity of the membrane, was obtained from the asymptotic sieving coefficient (S_∞) by the following equation [7]:

$$\alpha = \frac{1}{S_\infty} \tag{5}$$

3. Results and discussion

3.1. Pore structure of the PMIA membrane

The surface morphology of the PMIA membrane (PMIA/PBS membrane) was observed by scanning electronic microscopy (SEM). As shown in Fig. 2(a), M30 was a typical ultrafiltration membrane with an estimated pore radius of approximately 10 nm. According to the binary image (Fig. 2(b)) transformed from the original SEM image, the surface pore structure parameters of M30 were obtained and are listed in Table 2. Moreover, the results also show that the PMIA membrane features a typical asymmetric structure consisting of a dense selective skin (approximately 0.1 μm) and finger-like macrovoids (see Fig. 2(c)) with a membrane thickness of approximately 130 μm. Because the skin layer thickness (δ_m) was equal to the dense selective skin thickness multiplied by the tortuosity factor (τ), the skin layer thickness for the PMIA membrane was calculated as 0.2 μm with a tortuosity factor (τ) of 2 [21], which was within the range of the skin layer thickness for UF membranes [20,22,23]. Additionally, as shown in Supplementary Fig. S2, both M50 and M70 have a similar structure, and their surface pore structure parameters are also presented in Table 2. In addition, the pore structure parameters of the PMIA membrane were calculated from the transport data with PEG solutes, as summarized in Table 2.

Clearly, as the temperature of the coagulating bath increased from 30 to 70 °C, the average pore radius of the PMIA membranes increased from approximately 5 to 9 nm and the porosity increased from approximately 5% to 10%. This observation can be attributed to the fact that a high temperature will enhance the mutual diffusivity between the non-solvent and casting solution to form large pores. By comparing the results obtained from the two different methods mentioned above, some differences can be found in the pore radius and porosity, which can be explained by the following reasons. First, because SEM sample preparation requires serial dehydration, capillary forces at the liquid-solid interface will cause the pore to shrink, which accounts for the slight reduction in the pore radius and porosity. Second, the surface pore measured by SEM is probably not the “sieve pore”, which has a decisive effect on the membrane filtration performance. Therefore, the pore structure, characterized by PEG filtration, can exactly reflect the actual structure of the PMIA membrane in the filtration process. Hence, on the basis of the average pore radius (R_a) and GSD (σ_p) acquired from PEG filtration, the pore radius distribution

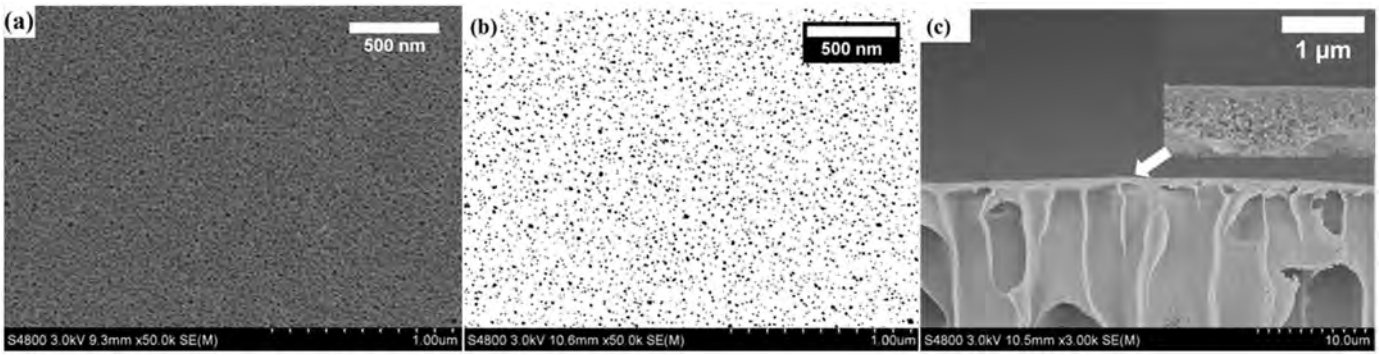


Fig. 2. SEM images of the (a) surface and (c) cross section for M30. (b) Binary image transformed from the SEM image of the surface of M30.

Table 2
Pore structure parameters of the PMIA membranes.

Name	R_{sa} (nm)	R_a (nm)	N_{sp} (μm^{-2})	N (μm^{-2})	ε_{sp} (%)	ε (%)
M30	5.46	6.26	686	632	5.15	5.65
M50	6.42	7.57	620	642	6.42	6.88
M70	7.15	8.73	605	644	8.97	9.23

R_{sa}, N_{sp} and ε_{sp} were obtained from SEM images, while R_a, N and ε were measured from PEG filtration.

and corresponding cumulative curves are shown in Fig. 3. The pore radius of the PMIA membrane is in the range of 3–15 nm, showing a narrow distribution.

3.2. Surface properties of the PMIA membrane

With a state water contact angle of approximately 65°, the PMIA membrane (PMIA/PBS membrane) demonstrated excellent hydrophilicity due to the high surface free energy of PMIA, implying an improvement in the permeability compared to hydrophobic UF membranes. Conversely, as shown in Fig. 4, the streaming potential measurement illustrated that the PMIA membrane has an isoelectric point around pH 4.5. This observation is common for polymeric UF membranes, such as PES and PVDF membranes, owing to the adsorption of hydroxide ions in aqueous electrolyte solution [24].

3.3. Selectivity-permeability analysis for the PMIA membrane

Here, the selectivity-permeability analysis developed by Mehta and Zydney is applied, as it is considered an effective method to analyze the performance of new ultrafiltration membranes [7]. The PMIA/PBS and PMIA/BSA membranes, which were in the same physical "state" [7], were both carefully evaluated.

As shown in Fig. 5, the permeability was obtained from the slope of flux versus pressure data. The value increased from approximately 2 to 4×10^{-9} m s^{-1} Pa^{-1} for the PMIA/BSA membranes, while that of the PMIA/PBS membranes improved from approximately 3 to 8×10^{-9} m s^{-1} Pa^{-1} as the temperature of the coagulation bath increased from 30 °C to 70 °C. This observation can mainly be attributed to the increase in the pore radius, as mentioned above. Moreover, the permeability for the PMIA/BSA membrane was much lower than that of the PMIA/PBS membrane, as the BSA adsorption greatly reduced the pore radius.

The relationships between the observed sieving coefficients (S_o) and filtrate flux of the PMIA/BSA membranes are shown in Fig. 6. Considering the effect of the concentration polarization, the actual sieving coefficients (S_a) were obtained from the observed sieving coefficients using Eq. (4). Thus, the asymptotic sieving coefficients (S_∞) can be determined by fitting the sieving coefficients to the hydrodynamic model using an optimization procedure [25,26] (Solver, Microsoft Excel). According to Eq. (5), the separation factors (α) of M30, M50 and M70 were calculated as 384, 139 and 114, respectively. As for the PMIA/PBS membranes, the sieving coefficients and separation factors are presented in Fig. 7. It can be seen that the separation factors for the PMIA/PBS membranes (10–200) were much lower than those of the PMIA/BSA membranes, as the BSA adsorption greatly reduced the pore radius. Nevertheless, both membranes show a similar decrease in the selectivity with increasing pore radius.

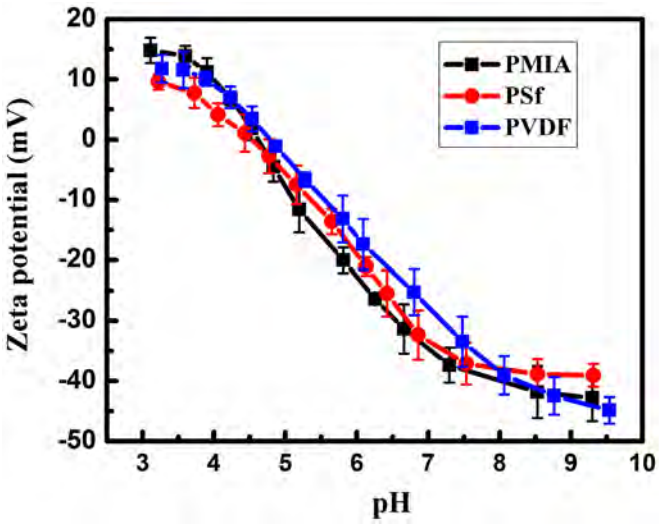


Fig. 4. Surface zeta potential for PMIA, PES and PVDF membranes at different pH values.

Fig. 8 shows two different selectivity-permeability trade-offs, respectively, for PMIA and other UF membranes [25,27–33]. Obviously, the PMIA membranes break through the original trade-off; the permeability at a given separation factor increases twofold while the separation factors at a given permeability are improved nearly 10 times. Therefore, based on theoretical calculation [7], a new upper bound (dashed curve) is plotted with $\varepsilon/\delta_m=2.5$ and $\sigma/\_r=0.18$, suggesting a high porosity and narrow pore radius distribution compared to the original parameter ($\varepsilon/\delta_m=1$ and $\sigma/\_r=0.2$, solid line). In spite of the different temperatures of the coagulation bath, all PMIA membranes show a similar trade-off between selectivity and permeability with the data clustering

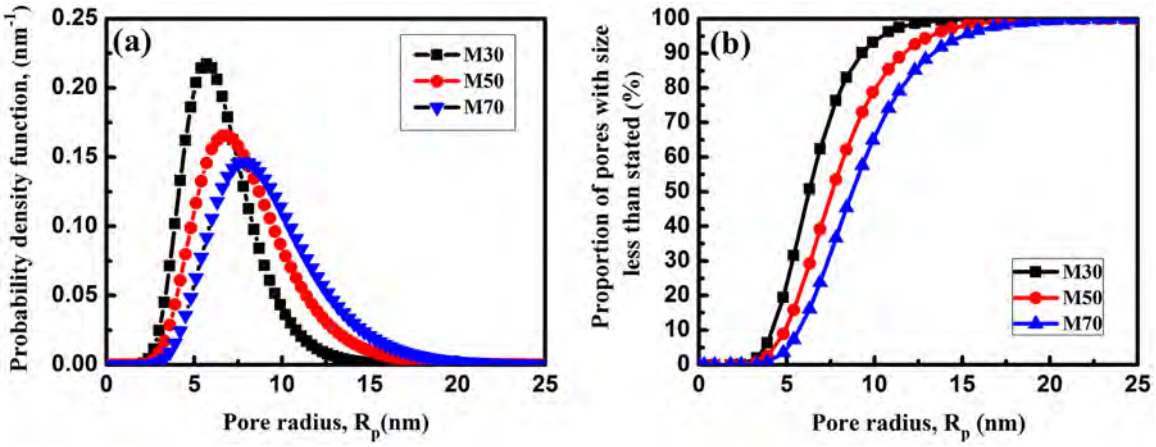


Fig. 3. (a) Pore radius distribution curves and (b) cumulative curves of PMIA membranes.

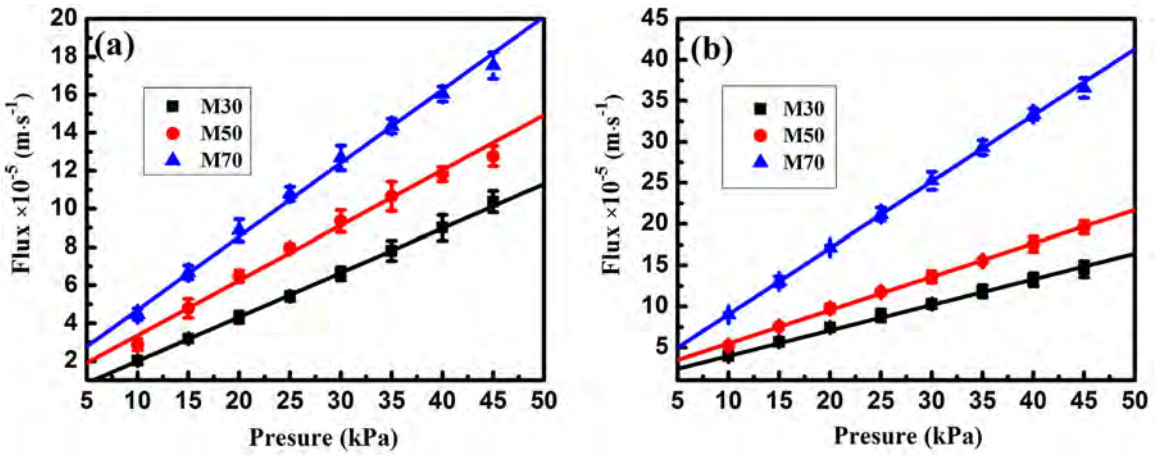


Fig. 5. Flux dependence of the applied pressure for the (a) PMIA/BSA membranes and (b) PMIA/PBS membranes.

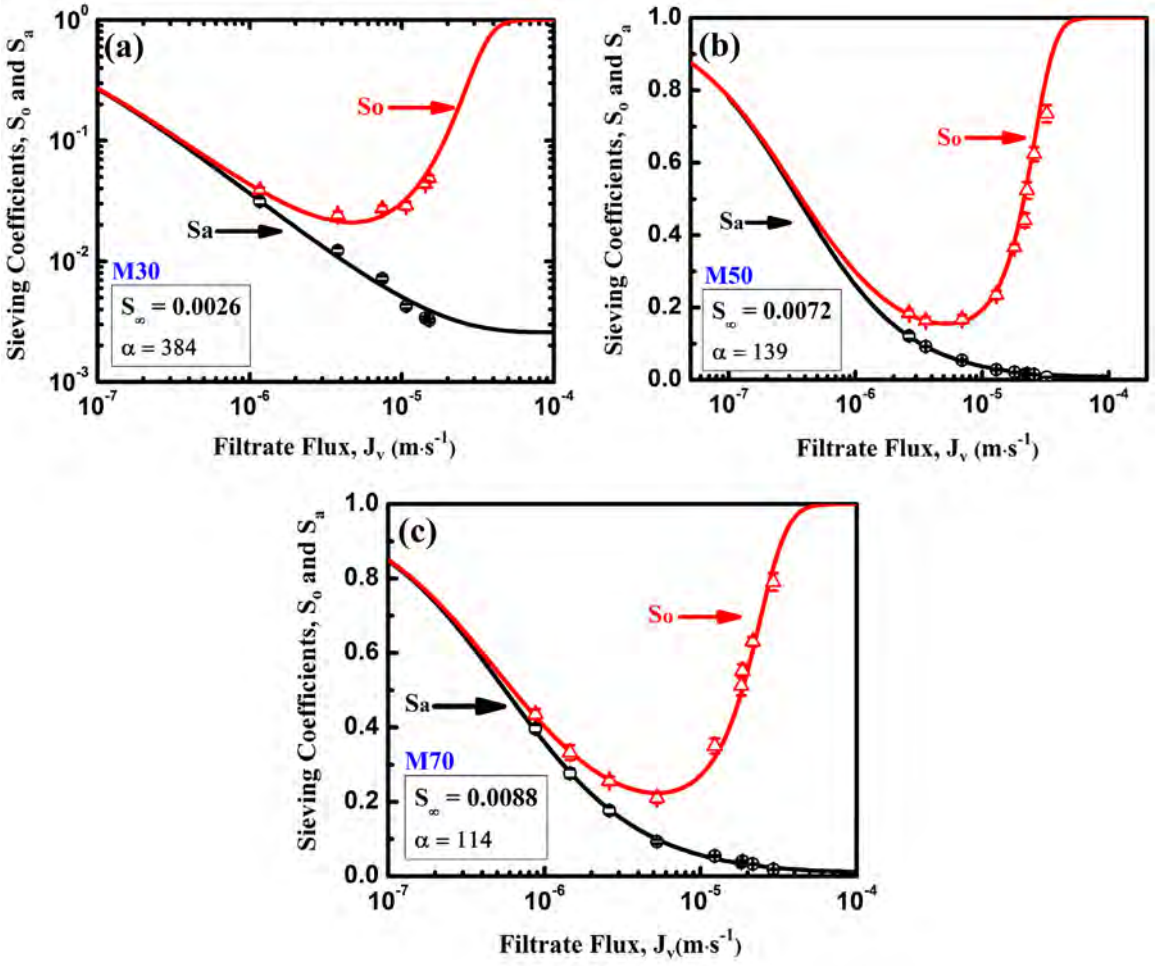


Fig. 6. Sieving coefficients as a function of the filtrate flux for the PMIA/BSA membranes. The solid lines represent the hydrodynamic model predictions with the optimized parameters.

along the dash curve regardless of whether they were adsorbed with BSA. Because the data of the other UF membranes are far from the new upper bound, the new selectivity-permeability trade-off is only suitable for PMIA membranes.

3.4. Comparisons between PMIA and other UF membranes

In this study, more attention is paid to the reasons for the excellent performance of the PMIA membrane. Therefore, six UF membrane types were chosen for comparison based on the original upper bound (solid line in Fig. 8). Their permeability and separation factors, as well as MWCO, were observed in previous studies, as shown in Table 3. The other parameters of the pore structure could be calculated from the MWCO and GSD (σ_p), with the GSD for the pore radius distribution appropriately valued as 2 [6,34,35].

As shown in Table 3, the effective pore radius (R_e) of the PMIA

CosMX Exhibit 1003, Page 116 of 512

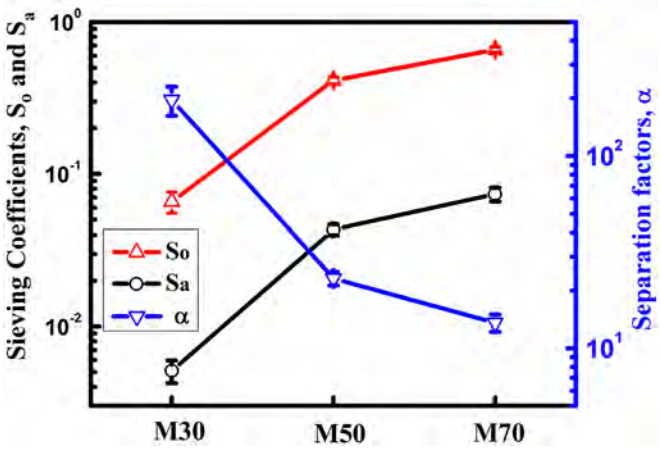


Fig. 7. Sieving coefficients and separation factors for the PMIA/PBS membranes.

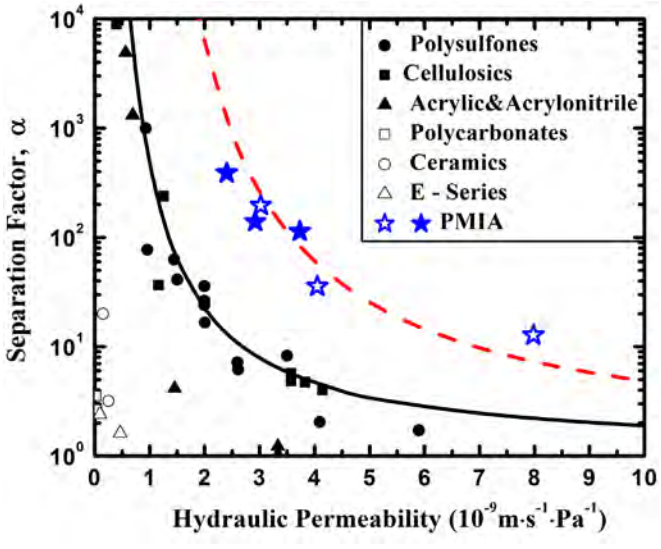


Fig. 8. Selectivity–permeability trade-off for ultrafiltration membranes, including PMIA and other UF membranes [7]. The curves represent the model calculations using a log–normal pore radius distribution with different parameters. The filled blue stars represent the PMIA/BSA membranes, while the hollow blue stars represent the PMIA/PBS membranes. (For interpretation of the references to color in this figure legend, the reader is referred to the web version of this article.)

membrane (6–9 nm) was smaller than that of the other UF membranes (10–24 nm); however, the porosity (6–10%) was much higher. Hence, depending on the Hagen-Poiseuille equation (Eq. (1)), the high porosity results in the large permeability of the PMIA membrane. Conversely, the selectivity is related to the most probable pore radius (R_m) and pore radius distribution (GSD, σ_p). Generally, a large R_m leads to a relatively small separation factor, while a small σ_p results in a large separation factor [6]. Therefore, the narrow pore radius distribution (σ_p=1.3–1.4) improves the separation factor for the PMIA membrane.

Compared with the other polymeric UF membranes, the high porosity and narrow pore radius distribution of the PMIA membrane were possibly generated from the rigid chain of PMIA. The high rigidity can confine the motion of the chain, containing the movement and rearrangement of the chain segment as well as the change in the conformation, during the membrane formation process. Furthermore, this effect could be effectively reinforced by the hydrogen bonding between the polymeric chains. Therefore, the pore collapse will be suppressed and membrane will have a higher porosity and narrower pore radius distribution compared to those of the membranes fabricated by polymer with a flexible chain, such as PVC and PVDF. As for the surface property, compared with the hydrophobic membrane prepared by PSf and PES whose chains are rigid, the hydrophilicity of the PMIA membrane undoubtedly improves its permeability. Hence, cellulose seems to be a suitable material for UF membranes due to its high glass translation temperature (rigid chain) and high surface free energy (hydrophilicity), as shown in Table 1. However, the insolubility in common organic solvents is one of its biggest disadvantages [38].

Accordingly, as a result of its rigid chain and high surface free energy, PMIA appears to be the most suitable polymer for UF membrane fabrication, which has been manifested by the breakthrough in the selectivity-permeability trade-off for the PMIA membrane.

4. Conclusions

In this work, PMIA was chosen to fabricate the ultrafiltration membrane due to its rigidity, high surface free energy and processability. Through selectivity-permeability analysis, the PMIA membrane was found to break through the selectivity-permeability trade-off, with permeability and separation factors ranging from 2.5 to 8×10^{-9} m s^{-1} Pa^{-1} and from 400 to 10, respectively. Compared with the other UF membranes, the high performance of the PMIA membrane was confirmed in terms of the high porosity, narrow pore radius distribution and excellent hydrophilicity. These superior properties could probably be attributed to the high rigidity, which confined the motion of the chain to suppress the pore collapse during membrane formation, as well as to the high surface free energy, which resulted in hydrophilicity.

Therefore, the PMIA membrane could be operated at a lower pressure than other UF membranes, decreasing the energy consumption. This membrane also has a broad range of temperatures available due to the high glass transition temperature. Furthermore, compared with the hydrophobic membrane, the PMIA

Table 3
Characteristic parameters of the pore structure and performance for different membranes.

Polymer	Name	R_m (nm)	R_e (nm)	σ_p	ε (%)	L_p (10^{-9} m s^{-1} Pa^{-1})	α	Ref.
PMIA	M30	5.66	6.58	1.36	5.65	3.06 (2.4)	196 (389)	This work
	M50	6.81	6.84	1.40	6.88	4.02 (2.92)	36 (139)	
	M70	7.83	9.28	1.39	9.23	7.92 (3.73)	13 (113)	
PSf	PTHK	2.55	12.25	~2	0.73	1.38	<90	[7,29]
Polyacrylonitrile	MX100	2.55	12.25	~2	0.78	1.46	<70	[7,29]
Cellulose	YM100	2.55	12.25	~2	1.14	2.15	<20	[7,29]
PES	OMEGA 100-K	2.55	12.25	~2	1.50	2.0	27	[25,36]
PES	OMEGA 50-K	2.10	10.21	~2	1.05	0.93	1000	[25,37]
PES	OMEGA 300-K	4.89	23.55	~2	2.95	4.1	2	[25,37]

The data for the PMIA membrane, in parentheses, were obtained from the PMIA/BSA membrane. The MWCO for PTHK, MX100, YM100, and OMEGA 100-K were 100 kDa, while those for OMEGA 50-k and OMEGA 300-k were, respectively, 50 and 300 kDa.

CosMX Exhibit 1003, Page 117 of 512

membrane, with hydrophilicity, is supposed to exhibit good anti-fouling properties. All of these great properties of the PMIA membranes demonstrate their potential for excellent performance in industrial applications. Hence, PMIA is probably the most suitable polymer for preparing ultrafiltration membranes.

Acknowledgments

The National 863 Program of China (grant number 2012AA03A602), the National 973 Program of China (grant number 2009CB623402) and the Nature Science Foundation Committee of China (grant number 20974094) are thanked for supporting this work.

Appendix A. Supporting information

Supplementary data associated with this article can be found in the online version at http://dx.doi.org/10.1016/j.memsci.2016.06.042.

Nomenclature

L_p	permeability of membranes (m s^{-1} Pa^{-1})
J_v	volumetric filtrate flux (m s^{-1})
ΔP	pressure (Pa)
k	mass transfer coefficient
S_o	observed sieving coefficient
S_a	actual sieving coefficient
S_∞	asymptotic sieving coefficients
C_f	solute concentration in filtrate (mol m^{-3})
C_b	solute concentration in bulk (mol m^{-3})
α	separation factor
R_a	average pore radius (nm)
R_{sa}	surface average pore radius (nm)
R_m	most probable pore radius (nm)
R_e	effective pore radius (nm)
R_s	solute radius (nm)
σ_p	geometric standard deviation
N	pore density
N_{sp}	pore density
ε	porosity
ε_{sp}	surface porosity
η	water viscosity (0.001 Pa s)
δ_m	skin layer thickness (μm)

References

[1] M.A. Shannon, P.W. Bohn, M. Elimelech, J.G. Georgiadis, B.J. Marinas, A. M. Mayes, Science and technology for water purification in the coming decades, Nature 452 (2008) 301–310.
[2] M. Marcucci, G. Nosenzo, G. Capannelli, I. Ciabatti, D. Corrieri, G. Ciardelli, Treatment and reuse of textile effluents based on new ultrafiltration and other membrane technologies, Desalination 138 (2001) 75–82.
[3] A.L. Zydney, Protein separations using membrane filtration: new opportunities for whey fractionation, Int. Dairy J. 8 (1998) 243–250.
[4] A.L. Zydney, Bulk Mass, Transport limitations during high-flux hemodialysis, Artif. Organs 17 (1993) 919–924.
[5] L.J. Zeman, A.L. Zydney, Microfiltration and Ultrafiltration: Principles and Applications, Marcel Dekker Inc., New York, 1996.
[6] S. Mochizuki, A.L. Zydney, Theoretical analysis of pore size distribution effects on membrane transport, J. Membr. Sci. 82 (1993) 211–227.
[7] A. Mehta, A.L. Zydney, Permeability and selectivity analysis for ultrafiltration membranes, J. Membr. Sci. 249 (2005) 245–249.
[8] Z. Yi, L.-P. Zhu, Y.-Y. Xu, Y.-F. Zhao, X.-T. Ma, B.-K. Zhu, Polysulfone-based amphiphilic polymer for hydrophilicity and fouling-resistant modification of polyethersulfone membranes, J. Membr. Sci. 365 (2010) 25–33.
[9] J.-H. Jiang, L.-P. Zhu, H.-T. Zhang, B.-K. Zhu, Y.-Y. Xu, Improved hydrodynamic permeability and antifouling properties of poly (vinylidene fluoride) membranes using polydopamine nanoparticles as additives, J. Membr. Sci. 457 (2014) 73–81.
[10] S.E. Querelle, E.A. Jackson, E.L. Cussler, M.A. Hillmyer, Ultrafiltration membranes with a thin poly styrene-b-poly isoprene selective layer, ACS Appl. Mater. Interfaces 5 (2013) 5044–5050.
[11] P. Nimmanpipug, K. Tashiro, O. Rangsiman, Factors governing the three-dimensional hydrogen-bond network structure of poly (m-phenylene isophthalamide) and a series of its model compounds (4): similarity in local conformation and packing structure between a complicated three-arm model compound and the linear model compounds, J. Phys. Chem. B 110 (2006) 20858–20864.
[12] J. Huang, K. Zhang, The high flux poly (m-phenylene isophthalamide) nanofiltration membrane for dye purification and desalination, Desalination 282 (2011) 19–26.
[13] M. Keating, High glass transitions of high-performance thermoplastics, Thermochim. Acta 319 (1998) 201–212.
[14] A. Kuo, Z. Pu, Polymer data handbook, Polymer Data Handbook, 1999.
[15] L. De Bartolo, A. Gugliuzza, S. Morelli, B. Cirillo, A. Gordano, E. Drioli, Novel PEEK-WC membranes with low plasma protein affinity related to surface free energy parameters, J. Mater. Sci.: Mater. Med. 15 (2004) 877–883.
[16] X. Zhao, Y. Su, W. Chen, J. Peng, Z. Jiang, Grafting perfluoroalkyl groups onto polyacrylonitrile membrane surface for improved fouling release property, J. Membr. Sci. 415 (2012) 824–834.
[17] A. Zosel, Adhesion and tack of polymers: influence of mechanical properties and surface tensions, Colloid Polym. Sci. 263 (1985) 541–553.
[18] P.E. Luner, E. Oh, Characterization of the surface free energy of cellulose ether films, Colloids Surf.: Physicochem. Eng. Asp. 181 (2001) 31–48.
[19] W. Sun, T. Chen, C. Chen, J. Li, A study on membrane morphology by digital image processing, J. Membr. Sci. 305 (2007) 93–102.
[20] S. Singh, K. Khulbe, T. Matsuura, P. Ramamurthy, Membrane characterization by solute transport and atomic force microscopy, J. Membr. Sci. 142 (1998) 111–127.
[21] F.P. Cuperus, Characterization of Ultrafiltration Membranes: Pore Structure and Top Layer Thickness, PhD Thesis, University of Twente, Enschede, The Netherlands, 1990.
[22] A. Kakuta, M. Kuramoto, M. Ohno, H. Kushida, A. Tanioka, K. Ishikawa, Freeze-dried cellulose acetate membrane fine structure observation, J. Polym. Sci.: Polym. Chem. Ed. 18 (1980) 3229–3243.
[23] A. Fane, C. Fell, A. Waters, The relationship between membrane surface pore characteristics and flux for ultrafiltration membranes, J. Membr. Sci. 9 (1981) 245–262.
[24] D.B. Burns, A.L. Zydney, Buffer effects on the zeta potential of ultrafiltration membranes, J. Membr. Sci. 172 (2000) 39–48.
[25] W.S. Opong, A.L. Zydney, Diffusive and convective protein transport through asymmetric membranes, AIChE J. 37 (1991) 1497–1510.
[26] L.D. Nghiem, A.I. Schäfer, M. Elimelech, Removal of natural hormones by nanofiltration membranes: measurement, modeling, and mechanisms, Environ. Sci. Technol. 38 (2004) 1888–1896.
[27] K.D. Miller, S. Weitzel, V. Rodgers, Reduction of membrane fouling in the presence of high polarization resistance, J. Membr. Sci. 76 (1993) 77–83.
[28] S. Nakatsuka, A.S. Michaels, Transport and separation of proteins by ultrafiltration through sorptive and non-sorptive membranes, J. Membr. Sci. 69 (1992) 189–211.
[29] R. Shukla, M. Balakrishnan, G.P. Agarwal, Bovine serum albumin-hemoglobin fractionation: significance of ultrafiltration system and feed solution characteristics, Bioseparation 9 (2000) 7–19.
[30] N.S. Pujar, A.L. Zydney, Electrostatic and electrokinetic interactions during protein transport through narrow pore membranes, Ind. Eng. Chem. Res. 33 (1994) 2473–2482.
[31] A. Fane, C. Fell, A. Waters, Ultrafiltration of protein solutions through partially permeable membranes—the effect of adsorption and solution environment, J. Membr. Sci. 16 (1983) 211–224.
[32] P. Prádanos, A. Hernández, Cross-flow ultrafiltration of proteins through asymmetric polysulfonic membranes: I. retention curves and pore size distributions, Biotechnol. Bioeng. 47 (1995) 617–625.
[33] L. Millesime, J. Dulieu, B. Chaufer, Fractionation of proteins with modified membranes, Bioseparation 6 (1996) 135–145.
[34] K.H. Youm, W.S. Kim, Prediction of intrinsic pore properties of ultrafiltration membrane by solute rejection curves: effects of operating conditions on pore properties, J. Chem. Eng. Jpn. 24 (1991) 1–7.
[35] T. Horiuchi, P. Malchesky, M. Emura, M. Usami, Y. Nose, Solute/pore changes in plasma filtration, Prog. Artif. Organs (1986) 877–882.
[36] S. Mochizuki, A.L. Zydney, Effect of protein adsorption on the transport characteristics of asymmetric ultrafiltration membranes, Biotechnol. Prog. 8 (1992) 553–561.
[37] B.C. Robertson, A.L. Zydney, Protein adsorption in asymmetric ultrafiltration membranes with highly constricted pores, J. Colloid Interface Sci. 134 (1990) 563–575.
[38] V.K. Thakur, S.I. Voicu, Recent advances in cellulose and chitosan based membranes for water purification: a concise review, Carbohydr. Polym. 146 (2016) 148–165.

CosMX Exhibit 1003, Page 118 of 512

Appendix C

Journal of The Electrochemical Society

The Electrochemical Society
Advancing solid state & electrochemical science & technology

Ionic Conductivity of Microporous PVDF-HFP/PS Polymer Blends

To cite this article: Haitao Huang and Stephanie L. Wunder 2001 *J. Electrochem. Soc.* **148** A279

View the article online for updates and enhancements.



This content was downloaded from IP address 128.119.168.112 on 20/02/2023 at 16:27

0013-4651/2001/148(3)/A279/5/$7.00 © The Electrochemical Society, Inc.

Ionic Conductivity of Microporous PVDF-HFP/PS Polymer Blends

Haitao Huang* **and Stephanie L. Wunder**[z]

Department of Chemistry, Temple University, Philadelphia, Pennsylvania, 19122 USA

Separators made from blends of poly(vinylidene fluoride-co-hexafluoropropylene) (PVDF-HFP) and polystyrene (PS) were microporous when cast from solvent/nonsolvent mixtures of acetone/dimethylcarbonate(DMC)/butanol(BuOH), where BuOH was the nonsolvent for both polymers. The ionic conductivities of these separators reached 2 $mScm^{-1}$ and could be increased to 4 $mScm^{-1}$ with addition of fumed silica. The morphology of the separators was characterized by scanning electron microscopy, nonsolvent (BuOH) and solvent (propylene carbonate, PC) uptake, and differential scanning calorimetry, and correlated with ionic conductivity measurements using 1 M $LiPF_6$ in ethylene carbonate/DMC/diethyl carbonate, in the ratio 4:5:1 by weight. The solvent filled the microporous network and caused the pore walls to swell. The greater the former contribution, which increased with increasing PS content, the higher the ionic conductivity. Passing two identical microporous films through a double-roll laminator at a temperature above the glass transition temperature, T_g, of PS (T_g = 95°C) and below the melt temperature, T_m, of PVDF-HFP (T_m = 133°C) preserved the microporous structure, with a conductivity decrease of only 20% compared with unlaminated films.
© 2001 The Electrochemical Society. [DOI: 10.1149/1.1346897] All rights reserved.

Manuscript submitted September 16, 2000; revised manuscript received November 26, 2000.

Hybrid or plasticized polymer electrolytes can be made from a polymer and solutions of lithium salts in organic solvents. Investigated polymers which incorporate liquid electrolytes include poly(vinylidene fluoride) (PVDF),[1-21] poly(methyl methacrylate) (PMMA),[20-26] polyacrylonitrile (PAN),[20,21,27,28] poly(vinyl chloride) (PVC),[20] poly(vinyl sulfone) (PVS),[29] poly(ethylene oxide) (PEO),[20,30,31] or their blends. Compared with ''dry'' polymer electrolytes (so-called solid polymer electrolytes), *e.g.*, PEO/lithium salt solid complexes, these plasticized, or gelled, polymer electrolytes possess higher ionic conductivity, about 10^{-3} Scm^{-1} at room temperature, and therefore may be useful for lithium or lithium-ion battery applications. Polymer electrolytes based on PVDF or its copolymer, poly(vinylidene fluoride-co-hexafluoropropylene) (PVDF-HFP), have received much attention, particularly since Gozdz *et al.*[5,6] at Bellcore proposed a technique in which the PVDF-HFP film matrix is prepared first and then reswollen in Li salt electrolyte solution at the last stage. In this so-called Bellcore technology, most of the processes of preparing the polymer electrolytes and cells do not require a moisture-free environment. This makes PVDF-based polymer electrolytes of practical interest and promising in near-term applications for lithium-ion batteries.

The ionic conductivity of PVDF-based polymers was first reported by Feuillade and Perche[1] in 1975, and then by Tsuchida *et al.*[2,3] in the early 1980s. The ionic conductivity of PVDF-based polymer electrolytes was initially 10^{-5} to 10^{-6} Scm^{-1} at room temperature,[2] while conductivities of over 10^{-3} Scm^{-1} are now obtained.[4-7,10,12-16] In the earlier studies, the PVDF-HFP copolymer was directly plasticized with liquid Li salt electrolytes. The polymer was dissolved in a low-boiling solvent (tetrahydrofuran, acetone, etc.) together with a nonaqueous lithium salt solution, *e.g.*, $LiClO_4$ in propylene carbonate (PC), to form a homogeneous gel after evaporation of the low-boiling solvent. At liquid electrolyte concentrations of over 60%, the ionic conductivity of the polymer gel exceeds 10^{-3} Scm^{-1} at room temperature.[4,6,10,11] Some gel polymer-liquid electrolyte systems have been described as single-phase homogeneous systems.[19] Alternatively, a mechanism of conduction in these gel systems has been suggested, in which there are two conduction domains, a swollen polymer phase of lower conductivity and a Li salt electrolyte solution phase of higher ionic conductivity.[17,18,22,23] At low polymer content, the gel electrolytes can be considered as consisting of a liquid electrolyte dispersed in a polymer matrix, with the lithium and counter ions migrating through the solvent. With increasing polymer content the contribution or volume fraction of the high conduction path decreases.[11] Strong interactions may exist between the polymer chains and the Li^+ ions or solvent molecules, leading to a decrease in the number of charge carriers and an increase in the activation energy of conduction.[22]

A two-phase structure has been proposed for PVDF-type polymers prepared according to the Bellcore process. The heterogeneous phase-separated polymer electrolyte[20] PVDF-HFP films were prepared by film casting using dibutyl phthalate (DBP) as a plasticizer. The DBP is removed with methanol, leaving a nanoporous structure in the polymer,[20] before the films are soaked in liquid electrolyte.[5,6] In addition, nanoparticle fumed silica (SiO_2) has been added into the composite film and it has been suggested that the interfacial regions around the nanoparticle filler[20] enhance electrolyte uptake. In our previous work, we demonstrated that when DBP was replaced with PEO oligomers, which were incompatible with the PVDF-HFP, the pore size increased from the nanometer to the micron size range, and as a result the conductivity of the films increased.[15] Microporous structures in PVDF or PVDF-HFP films using solvent/nonsolvent casting solutions have also been formed in our laboratory[16] as well as elsewhere.[7,12-14]

In porous polymer separators the amount of electrolyte uptake, the pore volume, size, interconnectivity, and the type of polymer that forms the pore walls are important factors in determining the ionic conductivity of the films. For polyolefin separators such as Celgard, where minimal swelling of the hydrophobic polymer occurs, the liquid electrolyte forms a one-phase system in the porous polymer network. In the polymer matrices that are more compatible with the polar solvents used as liquid electrolytes, there is also swelling of the polymer by the solvent.

In polymers such as polyacrylonitrile (PAN) and poly(methyl methacrylate) (PMMA), uptake of the polar solvents may result in their dissolution. In porous PVDF-type polymers, the semicrystalline nature of PVDF results in equilibrium swelling rather than dissolution. Desirable properties of these separators include the ability to bond to the electrode materials and to be wetted by the polar solvents used in lithium battery applications.

In this paper, the morphology and conductivity of films composed of PVDF-HFP blended with a second polymer, polystyrene (PS), are examined. PS was chosen because it was expected to be relatively nonadsorbing for the electrolyte solvent and would contribute to the mechanical stability of the separators. A solvent/nonsolvent casting process is used to produce microporous films. Correlation of pore structure with solvent uptake indicates that increased conductivity is obtained for separators containing increased PS content. A mechanism of conductivity in the microporous struc-

* Electrochemical Society Active Member.
[z] E-mail: slwunder@unix.temple.edu

CosMX Exhibit 1003, Page 121 of 512

tures is proposed, in which the more liquidlike electrolyte phase in the pores has higher conductivity than that of the swollen pore walls.

The ability of the PVDF-HFP/PS films to preserve their microporous structure after a simulated lamination step at elevated temperatures and pressure was investigated. When films were self-laminated in a temperature region above the glass transition temperature, T_g, of PS but below the melting temperature, T_m, of PVDF-HFP copolymers, the microporous morphology was preserved. To achieve bonding to the anode or cathode, PS would therefore have to be incorporated as part of the binder in the electrodes.

Experimental

Preparation of films from PVDF-HFP/PS polymer blends.—The PVDF-HFP copolymers used in this work were Kynar 2801 and 2751 from ELF Atochem, and contained, respectively, 10 and 15% by weight HFP. The PS used was purchased from Aldrich (Merck Index 14). Since the PS was not very soluble in acetone, it was dissolved in dimethyl carbonate (DMC, Aldrich) at elevated temperature (50-60°C) prior to mixing it, by slow dropwise addition, with the solution of PVDF-HFP in acetone. The solution became cloudy, and was kept in suspension by constant agitation using a Vortix Genie (Fisher). Subsequently, BuOH was added (or not as a control), the resulting blend slurry was doctor-bladed onto a polyester sheet and strong and self-supporting thin films were formed after solvent evaporation. The polymer in the casting slurry was between 14-16 wt%. Further drying of the films was carried out at room temperature under vacuum. The film thickness varied from 0.10 to 0.18 mm, although thinner films (60 μm) could be prepared. A Laminex model LX4 double-roll table-top laminator was used for self-lamination of the separators, using a speed of 1 cm s^{-1}; temperature was measured using a thermocouple. The residence time of the film in the heated zone was 20 s, and the pressure was estimated to be less than 100 psi.

Conductivity measurements.—The polymer blend films were soaked in an electrolyte containing 1 M $LiPF_6$ dissolved in ethylene carbonate/DMC/diethyl corbonate (EC/DMC/DEC) in the weight ratio 4:5:1 (Grant Chemical). The soaked films were sandwiched between two stainless steel blocking electrodes in a dry box. Ionic conductivity was measured on the sealed films outside the dry box using an ac impedance technique, in which a Schlumberger SI 1255 frequency response analyzer was coupled with an EG&G potentiostat/galvanostat model 273A. The amplitude of the ac voltage was 5 mV and the frequency ranged from 100 KHz to 100 Hz. Cole-Cole plots were characterized by slanted straight lines intercepting the real axis on the high-frequency side, from which the resistance was calculated, assuming an equivalent circuit in which a resistor is in series with a double layer capacitor. No effects due to interfacial resistance between the separator and the stainless steel electrodes were observed.

Characterization of microporous structure.—Cross-sectional views of the PVDF-HFP/PS blend films were observed using scanning electron microscopy (SEM, Philips model 501B). Solvent uptake was obtained by measurement of weight gain using thermogravimetric analysis (TGA) (TA Instruments, Hi-Res TGA 2950). TGA scans were run to 180°C. Although the boiling point of PC is 242°C, TGA scans showed that the PC was completely removed by 180°C; polymers without solvent uptake exhibited no weight loss over this temperature range, but decomposed at higher temperatures. Differential scanning calorimetry (DSC) measurements (TA Instruments DSC 2920) were obtained at a scan speed of 10°C/min. Specific surface area measurements were made using a single point BET technique (MONOSORS Surface Area Analyzer, model MS-12, Quantachrome Co.) with N_2/He as the adsorbing gas.

Table I. Composition of PVDF-HFP/PS blends.

Blend	%KYNAR 2801 (PVDF-10% HFP)	%KYNAR 2751 (PVDF-15% HFP)	%Polystyrene	Addition of butanol
1	60	40	0	No
2	60	40	0	Yes
3	80	0	20	No
4	80	0	20	Yes
5	50	40	10	Yes
6	40	40	20	Yes
7	30	40	30	Yes
8	20	40	40	Yes

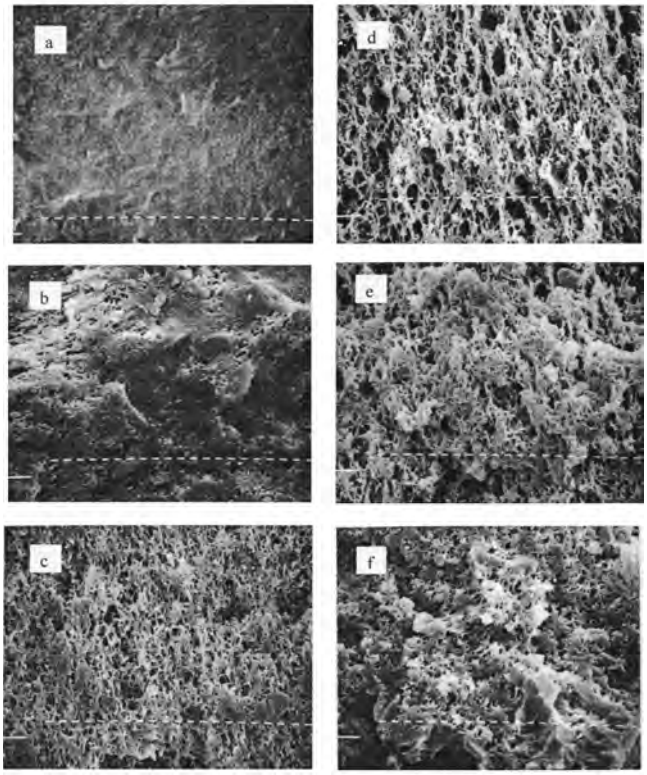


Figure 1. SEMs of the cross-sectional views of PVDF-HFP/PS films cast from solvent/nonsolvent mixtures: (a) 0% PS (sample #2); (b) 10% PS (sample #5); (c) 20% PS (sample #6); (d) 30% PS (sample #7); (e) 40% PS (sample #8); and (f) film made from 20% PS (sample #6) laminated at 120°C.

Results and Discussion

Formation of microporous structure.—The compositions of the PVDF-HFP/PS blend polymer films prepared with or without addition of BuOH are listed in Table I. The appearance of the pure PVDF-HFP films was transparent when cast without BuOH, and the transparency was reduced with the addition of BuOH in the casting solvent. The films became translucent when PVDF-HFP was blended with PS (tested up to 30% PS) and cast from acetone/DMC. The addition of BuOH resulted in PVDF-HFP/PS films that were opaque. The changes in transparency reflected a variation in the morphology of the polymer films, as observed by scanning electron microscopy (SEM). SEMs of the cross-sectional views of samples 2 and 5-8 are shown in Fig. 1.

Samples cast from the pure PVDF-HFP copolymers (with either 10% or 15% HFP) or their mixtures from acetone or from (by weight) 75% acetone/25% butanol (samples 1 and 2, respectively) are not microporous, as shown in Fig. 1a for sample 2; nanopores would not be observable at this magnification. Boudin *et al.*[13] observed a microporous morphology when PVDF homopolymer (Kynar 741) was cast from a solvent/nonsolvent (acetone/butanol) mixture. Michot *et al.*[14] found that the porosity of PVDF homopolymer

CosMX Exhibit 1003, Page 122 of 512

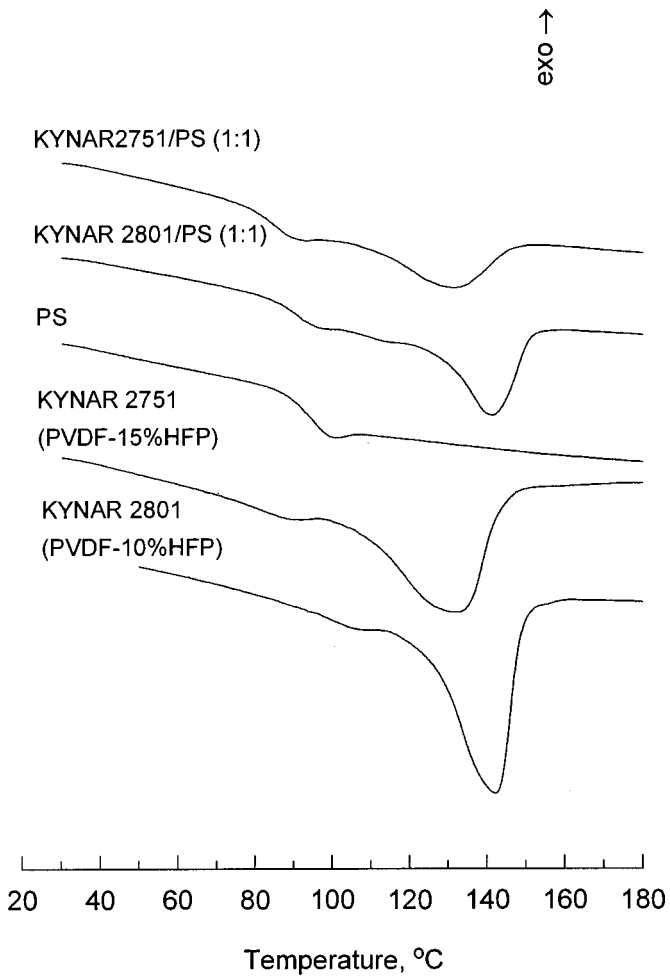


Figure 2. DSC curves of PVDF-HFP, PS, and PVDF-HFP/PS (1:1 by weight) polymer blends. Scan rate: 10°C min^{-1}.

was greater than for the copolymer PVDF-HFP (Kynar 2801) when both were cast from a single solvent [either acetone, tetrahydrofuran (THF) or methyl ethyl ketone (MEK)]. Pore formation in the polymer matrix is a result of phase separation between the polymer and solvent during the evaporation of solvent, and is driven by poor solubility of the polymer in the solvent. Crystallinity decreases polymer solubility and thus phase separation is enhanced with increased crystallinity of the polymer. Because HFP is known to reduce the crystallinity of PVDF, it is reasonable that no microsized pores formed in samples 1 and 2, whereas the PVDF homopolymer films[13,14] were microporous.

Comparison of PVDF-HFP(80%)/PS(20%) cast from acetone/DMC (sample 3) or from (by weight) 50%acetone/33.3%DMC/16.7%BuOH (No. 4 and No. 6) shows that only the samples cast from the solvent/nonsolvent mixtures exhibit a microporous morphology. The micrograph of sample 6 is shown in Fig. 1c, and is similar to that of sample 4 (not shown); small differences in the amount of HFP in the copolymer did not affect the results. All of the films containing PS and cast from acetone/DMC/BuOH mixtures exhibited a microporous morphology as shown in Fig. 1b-e. The porosity and pore volume of the films varied with the PS content, with pore sizes greater than 0.5 μm.

In our previous work,[16] we discussed the formation of porous structures from solvent/nonsolvent mixtures. BuOH is a nonsolvent for both PVDF-HFP and PS. Polymer precipitation in a nonsolvent is associated with phase inversion that creates pores. In addition, PS is not miscible with PVDF-HFP, as shown by the DSC results in Fig. 2. The PVDF-HFP/PS blends were made in weight ratios of 1:1.

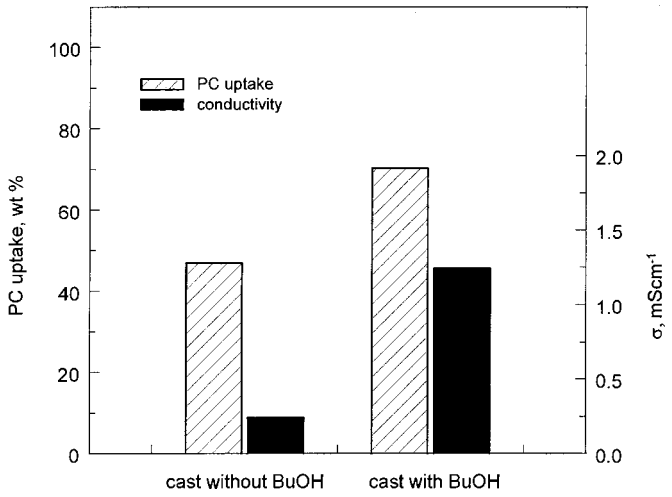


Figure 3. PC uptake and ionic conductivity of PVDF-HFP/PS (80:20 by weight) films prepared with and without BuOH added into casting solvent.

The temperature of the glass transition, T_g, of a PS film that was cast from cyclohexane/dimethyl carbonate (DMC) is 95.3°C, and the temperature of the melting points, T_m, of Kynar 2801 and 2751 are 142.4 and 132.9°C, respectively. For the Kynar 2801/PS blend, T_g appears at 91.6°C and T_m at 141.7°C. The Kynar 2751/PS blend exhibits a T_g and T_m, of 86.6°C and 131.6°C, respectively. While the slight lowering of T_g for the PS may indicate a small degree of mixing of PS with the PVDF-HFP amorphous segments, the blends are essentially incompatible. Therefore, complete phase separation of the polymers occurs in the blends. Phase separation between PS and PVDF-HFP and their co-precipitation in the nonsolvent BuOH both contribute to the formation of microporous structures in the PVDF-HFP/PS blend matrices.

Characterization of pore volume and solvent uptake.—The conductivity of plasticized polymer electrolytes is dominated mainly by the uptake of electrolyte solution by the polymer matrix. The liquid electrolyte is trapped in the pores,[13] and the pore walls can also be swollen by the electrolyte. In our previous work[16] we obtained the pore volume through a measurement of nonsolvent uptake. Since PVDF-HFP and PS do not swell in BuOH, as confirmed by TGA measurements of nonporous films, any increase in weight of the films after immersion in BuOH is a measure of the solvent trapped in the pores, and thus is related to the pore volume of the films. On the other hand, propylene carbonate (PC) uptake measures both pore volume and the swelling of the polymer matrix. TGA measurements confirm that PVDF-HFP can be swollen by PC, but that PS swelling in this solvent is minimal. Measurements of BuOH and PC uptake provide a means of separating the amount of electrolyte solution trapped by the pores and absorbed by the polymer. PC is used instead of the EC/DMC/DEC mixture because it has much lower volatility, thus making the weight uptake measurements more accurate.

To measure PC absorption, films were immersed in PC for 10 min and the TGA weight loss corresponding to the PC uptake was obtained using $(W_{PC+film} - W_{film})/(W_{PC+film})$; PC uptake increased with increasing time as discussed below. Figure 3 compares the PC uptake of PVDF-HFP/PS films cast with (sample 4, microporous) and without (sample 3, nonporous) butanol. There is a 50% increase in PC uptake for the porous film cast using nonsolvent. These two samples were composed of the same chemical components and differ only in their morphology. The results in Fig. 3 indicate that the solvent uptake depends on more than just the nature of the polymer. The increase in the amount of PC absorbed by sample 4 (microporous) is due to the liquid trapped in the pores.

To measure pore volume, films were immersed in butanol for 1 h, after which no further weight gain was observed, and uptake was

CosMX Exhibit 1003, Page 123 of 512

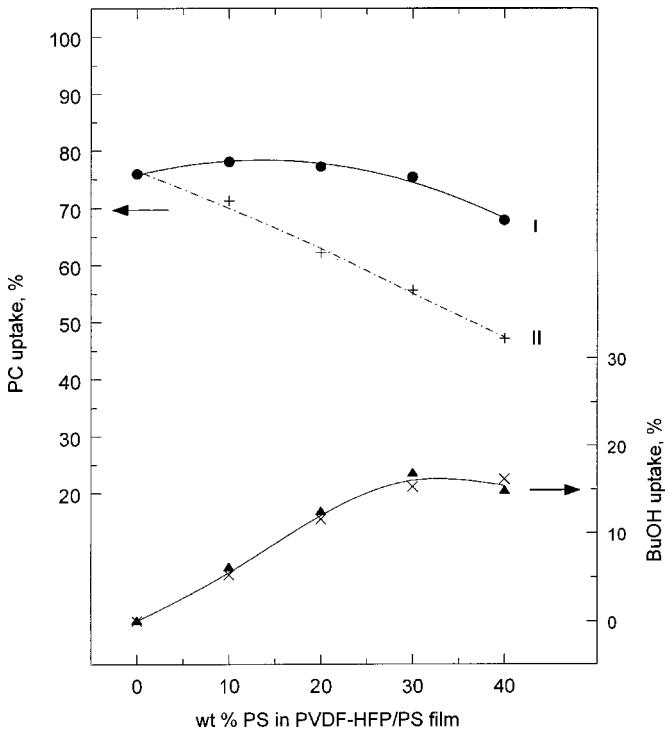


Figure 4. Solvent (BuOH or PC) uptake of PVDF-HFP/PS as a function of weight percent PS: PC-I: (●) experimental; II: +, calculated; BuOH, (▲) experimental; X calculated.

calculated from $(W_{\text{BuOH+film}} - W_{\text{film}})/(W_{\text{BuOH+film}})$. The results for a series of PVDF-HFP blends with increasing amounts of PS [sample 2, no PS, and samples 5-8 (▲)], are presented in Fig. 4, and show that pore volume increased with increased PS of the films, consistent with the SEM observations of Fig. 1.

The amount of PC uptake obtained from the same series of PVDF-HFP/PS blends with increasing PS content is shown in Fig. 4 [sample 2 (no PS) and samples 5-8 (●, connected with solid line I as guide)]. PC uptake decreased, although the porosity increased with increasing PS content for these films. Although this may appear contradictory to the results shown in Fig. 3, PC uptake in the blends is due to both the swelling of the polymer films and their porosity. Since PC uptake by PS is negligible, the decrease in PC uptake shown in line I reflects the increasing amount of PS in the blends.

The swelling of nonporous PVDF-HFP films by PC was measured for films cast without PS from acetone/butanol (75%/25% by weight) mixtures in the same ratios of Kynar 2801/Kynar 2751 as for samples 5-8. There was a slight increase in PC uptake as the ratio of PVDF-HFP 15%/PVDF-HFP 10% increased. As was the case for sample 2 (SEM Fig. 1a), these films exhibited no microporous morphology, so it is reasonable to assume that the PC uptake was due to PVDF-HFP swelling.

The contribution from swelling expected in PVDF-HFP/PS films (samples 5-8) was estimated by multiplying the value of PC uptake from PVDF-HFP by the weight percent of PVDF-HFP. Blends composed of nonporous PVDF-HFP/PS would then be expected to have PC uptakes given by line II in Fig. 4, that is PC uptake would decrease with increasing PS content. Because the uptake represented by line II is the amount of PC that swells the PVDF-HFP phase, the amount of PC trapped in the micropores can then be calculated from the differences between the PC uptake of lines I and II. The results of this calculation were converted into the expected amount of butanol uptake in the pores using the ratio of the densities between BuOH and PC, and presented in Fig. 3 (cross-hatched). The calculated values very closely match those directly measured from BuOH uptake (▲), and suggest that the model in which solvent uptake both fills the pores and swells the surrounding pore walls, depending on the nature of the solvent, is reasonable. The amount of PC uptake increased with increased soaking time, but contributed only to the swelling of the PVDF-HFP.

Self-lamination of microporous separators.—In order to determine whether the pore structure is preserved during a lamination step, two identical microporous films, composed of either 20%PS (sample 6) or 40%PS (sample 8), were self-laminated at three temperatures, between 90-100°C, between 120-125°C, and between 160-180°C, at pressures below 100 psi. Microporous films were opaque (white), as discussed above, whereas they appeared clear when no microporous structure existed. When the films were laminated at temperatures above ~160°C, they became transparent, and SEMs confirmed the lack of a microporous structure. At temperatures below about 90°C-100°C, the laminated films remained opaque, but did not adhere to each other. In the temperature range between 120 and 125°C, the laminated films remained opaque and did not come apart even after soaking in electrolyte solution at room temperature. SEMs confirmed the presence of the microporous morphology, as shown at the interface region in Fig. 1f for the sample prepared with 20%PS (sample 6). The temperature region in which the lamination produced self-adherent films that remained microporous was above the T_g of the PS component, but below the T_m of the PVDF-HFP component. Although the PS could dissolve in DMC at 60°C, it did not dissolve in the electrolyte solution at that temperature.

Ionic conductivity and conduction path.—Figure 3 also compares the conductivity between films with (sample 4) and without (sample 3) a microporous structure. For the latter, the conductivity is ~0.3 mScm^{-1}, similar to a PVDF-12% HFP film swollen with 50%1 M $LiPF_6$/EC/PC.[4] The microporous film exhibits a conductivity nearly five times higher, suggesting that it is the existence of micropores in the polymer matrix that enhances the conductivity. The ionic conductivity measurements for the polymer films discussed in Fig. 4 (samples 2 and 5-8) are presented in Fig. 5a, and verify the importance of the microporous structure. Ionic conductivity increases with increasing pore volume.

A mechanism in which two conduction paths exist has been proposed for gel polymer electrolytes,[22,23] and this mechanism is perhaps more appropriate for microporous polymer electrolytes. The simplest model is one in which the interconnected pores form a conduction path filled with pure liquid electrolyte, which has a higher conductivity than that of the liquid electrolyte that swells the surrounding pore walls. The ratio between the PC stored in the pores (the difference between lines II and I in Fig. 4) and the total PC uptake (line I in Fig. 4) is plotted against the content of PS in Fig. 5b. This ratio is a measure of how much of the absorbed liquid is in the higher conduction free liquid electrolyte path, and demonstrates that the greater this amount, the higher the conductivity of the films (Fig. 5a).

Figure 5c is a plot of the surface area of the pores measured by a single point Brunner-Emmett-Teller (BET) technique *vs.* the content of PS in samples 2 and samples 5-8. However, the surface area of the pores does not correlate as well as pore volume measurements with the variation in conductivity shown in Fig. 5a. This suggests that pore size and shape may need to be taken into account when using surface area as a measure of porosity, and more detailed, multipoint measurements are necessary.

Addition of fumed silica (SiO_2) to the films further increased their conductivity and improved their mechanical properties. For example, for films prepared based on the same polymer composition and casting solvents as for sample 6, a conductivity of nearly 4 mScm^{-1} was obtained with the addition of 35% SiO_2, and tough solid films less than 60 μm thick could be prepared. BuOH uptake and BET data obtained for films containing fumed SiO_2 were not straightforwardly related to pore volume or surface area, because fumed SiO_2 itself has very high surface area.

CosMX Exhibit 1003, Page 124 of 512

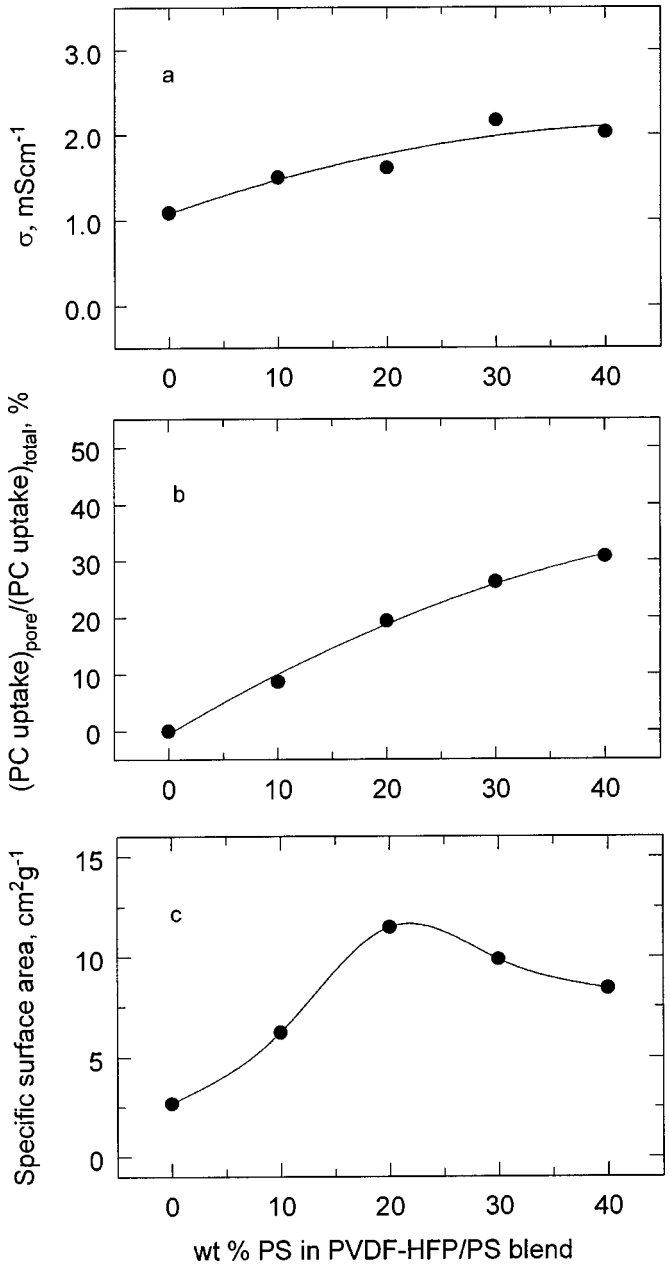


Figure 5. (a) Conductivity, (b) $(\text{PC uptake})_{\text{pores}}/(\text{PC uptake})_{\text{total}}$, and (c) specific surface area of PVDF-HFP/PS films as a function of weight percent PS.

The ionic conductivities of self-laminated separators that remained microporous were compared with the unlaminated films. The separator prepared with 20%PS (sample 6) had an initial conductivity of 1.62 mScm^{-1}, which decreased 20% to 1.28 mScm^{-1} after lamination. The separator prepared with 40%PS (sample 8) had an initial conductivity of 2.03 mScm^{-1}, which also decreased 20% to 1.62 mScm^{-1} after lamination. These results demonstrate that high conductivity separators can be prepared whose morphology and therefore high conductivity pathway can by maintained during the lamination procedure. This is in contrast to the published Bellcore process,[5,6] in which bonding via lamination of the anode, cathode, and polymer separator takes place before extraction of the plasticizer to avoid collapse of the pore structure.

Conclusions

High conductivity microporous separators can be prepared from PVDF-HFP/PS when cast from solvent/nonsolvent mixtures for the polymers. Film conductivity increased with increasing PS content. A two-phase model, with a higher conductivity path consisting of the liquid electrolyte in the interconnected pore structure and a lower conductivity path consisting of the swollen PVDF-HFP phase, was used to account for the conductivity trends. When the films were laminated in a temperature region above the T_g of PS but below the T_m of PVDF-HFP, they remained microporous, with conductivity decreases of only 20%. These results have ramifications for lithium-ion battery manufacturing technology. Microporous separators can be manufactured separately and post-laminated to anodes and cathodes while maintaining the microporous structure necessary for high conductivity. This is a departure from Bellcore technology,[5,6] where the plasticizer must be kept in the separator during the lamination step to avoid collapse of the pores.

Temple University assisted in meeting the publication costs of this article.

References

1. G. Feuillade and Ph. Perche, *J. Appl. Electrochem.*, **5**, 63 (1975).
2. E. Tsuchida, H. Ohno, and K. Tsunemi, *Electrochim. Acta*, **28**, 591 (1983).
3. E. Tsuchida, H. Ohno, and K. Tsunemi, *Electrochim. Acta*, **28**, 833 (1983).
4. A. S. Gozdz, C. N. Schmutz, J. M. Tarascon, and P. C. Warren, U.S. Pat. 5,418,091 (1995).
5. A. S. Gozdz, C. N. Schmutz, J. M. Tarascon, and P. C. Warren, U.S. Pat. 5,540,741 (1996).
6. J. M. Tarascon, A. S. Gozdz, C. Schmutz, F. Shokoohi, and P. C. Warren, *Solid State Ionics*, **86-88**, 49 (1996).
7. A. Du Pasquier, P. C. Warren, D. Culver, A. S. Gozdz, G. G. Amatucci, and J. M. Tarasov, Abstract 116, The Electrochemical Society Meeting Abstracts, Vol. 99-2, Honolulu, HI, Oct. 17-22, 1999.
8. K. M. Abraham, Z. Jiang, and B. Carroll, *Chem. Mater.*, **9**, 1978 (1997).
9. Z. Jiang, B. Carroll, and K. M. Abraham, *Electrochim. Acta*, **42**, 2667 (1997).
10. W. Huang and J. R. Akridge, *Mater. Res. Soc. Symp. Proc.*, **548**, 325 (1999).
11. A. M. Christie, L. Christie, and C. A. Vincent, *J. Power Sources*, **74**, 77 (1998).
12. X. Andrieu, C. Jehoulet, and F. Boudin, in Proceedings of the 38th Power Sources Conference, p. 266, Atlantic City, NJ (1998).
13. F. Boudin, X. Andrieu, C. Jehoulet, and I. I. Olsen, *J. Power Sources*, **81-82**, 804 (1999).
14. T. Michot, A. Nishimoto, and M. Watanabe, *Electrochim. Acta*, **45**, 1347 (2000).
15. H. Wang, H. Huang, and S. L. Wunder, *J. Electrochem. Soc.*, **147**, 2853 (2000).
16. H. Huang and S. L. Wunder, *J. Power Sources*, Submitted.
17. P. Mustarelli, E. Quartarone, C. Capiglia, C. Tomasi, and A. Magistris, *Solid State Ionics*, **122**, 285 (1999).
18. C. Capiglia, Y. Saito, H. Yamamoto, H. Kageyama, and P. Mustarelli, *Electrochim. Acta*, **45**, 1341 (2000).
19. M. Forsyth, P. M. Meakin, and D. R. MacFarlane, *Electrochim. Acta*, **40**, 2339 (1995).
20. J. Y. Sing, Y. Y. Wang, and C. C. Wan, *J. Power Sources*, **77**, 183 (1999).
21. K. Murata, S. Izuchi, and Y. Yoshihisa, *Electrochim. Acta*, **45**, 1501 (2000).
22. O. Bohnke, G. Frand, M. Rezrazzi, C. Rousselot, and C. Truche, *Solid State Ionics*, **66**, 97 (1993).
23. O. Bohnke, G. Frand, M. Rezrazzi, C. Rousselot, and C. Truche, *Solid State Ionics*, **66**, 105 (1993).
24. G. B. Appetecchi, F. Croce, and B. Scrosati, *Electrochim. Acta*, **40**, 99 (1995).
25. T. Iijima, Y. Toyoguchi, and N. Eda, *Denki Kagaku oyobi Kogyo Butsuri Kagaku*, **53**, 619 (1985).
26. Y. K. Yarovoy, H. P. Wang, and S. L. Wunder, *Solid State Ionics*, **118**, 301 (1999).
27. K. M. Abraham and M. Alamgir, *J. Electrochem. Soc.*, **137**, 1657 (1990).
28. K. M. Abraham and M. Alamgir, U.S. Pat. 5,219,679 (1993).
29. H. S. Choe, J. Giaccai, M. Alamgir, and K. M. Abraham, *Electrochim. Acta*, **40**, 2289 (1995).
30. G. B. Appetecchi, G. Dautzenberg, and B. Scrosati, *J. Electrochem. Soc.*, **143**, 6 (1996).
31. G. B. Appetecchi, F. Croce, and B. Scrosati, *J. Power Sources*, **66**, 77 (1997).

Appendix D

KYNAR FLEX®
2801-00

Kynar Flex® resins are fluorinated thermoplastic copolymers.

Outstanding characteristics: chemical resistance, imperviousness to UV, high barrier properties, high purity, good mechanical and thermo-mechanical properties. This product is **NSF/ANSI/CAN 61** certified.
Kynar Flex® 2801 resin is the powder form of the **Kynar Flex® 2800-00 resin.** To be used an additive in LLDPE to improve the extrusion rate.

PROPERTIES	VALUE	UNIT	TEST STANDARD
RHEOLOGICAL PROPERTIES			
Melt Volume-Flow Rate	0.5	cm³/10min	ISO 1133
Temperature	230	°C	-
	446	°F	
Load	5	kg	-
	11	lb	
Melt Flow Rate	3 - 8	g/10min	ASTM D1238
Temperature	230	°C	-
Load	12.5	kg	-
Melt Viscosity, 230°C, 100 s-1	23 - 27	kPoise	ASTM D3835
MECHANICAL PROPERTIES			
Tensile Modulus	700	MPa	ISO 527-1/-2
	102000	psi	
Tensile Modulus, 73 °F	552 - 896	MPa	ASTM D638
	80000 - 130000	psi	
Yield stress	27	MPa	ISO 527-1/-2
	3920	psi	
Tensile Strength at Yield, 73 °F	20 - 34.5	MPa	ASTM D638
	2900 - 5000	psi	
Yield strain	15	%	ISO 527-1/-2
Elongation at Yield, 73 °F	10 - 20	%	ASTM D638
Nominal Strain at Break	>50	%	ISO 527-1/-2
Tensile Strength at Break, 73 °F	17.2 - 34.5	MPa	ASTM D638
	2500 - 5000	psi	
Elongation at Break, 73 °F	100 - 300	%	ASTM D638
Taber Abrasion, CS 17 1000g:pad	16 - 19	mg/1000 cycles	ASTM-G195-13A
Hardness, Shore D, 73 °F	60 - 70	-	ASTM D2240
Flexural Modulus, 73 °F	483 - 758	MPa	ASTM D790
	70000 - 110000	psi	

Arkema France - A French "société anonyme", registered in the Nanterre (France) Trade and Companies Register under the number 319 632 790 SDC/11-2018
Source: automatically generated TDS from Material Database on 17-11-2022

KYNAR FLEX®
2801-00

Flexural Stength @ 5% Strain, 73 °F	20.7 - 34.5	MPa	ASTM D790
	3000 - 5000	psi	
Compressive Strength, 73 °F	31 - 41.4	MPa	ASTM D695
	4500 - 6000	psi	
Unnotched Impact Strength, 73 °F	No Break	kJ/m	ASTM D256
Notched Impact Strength, 73 °F	0.534 - 1.07	kJ/m	ASTM D256
	10 - 20	ftlb/in	
Coefficient of Friction, Static vs. Steel, 73 °F	0.33	-	ASTM D1894
Coefficient of Friction, Dynamic vs. Steel, 73 °F	0.33	-	ASTM D1894
THERMAL PROPERTIES			
Melting Temperature, 10°C/min	143	°C	ISO 11357-1/-3
Melting Point, 73 °F	140 - 145	°C	ASTM D3418
Glass Transition Temperature, 10°C/min	-40	°C	ISO 11357-1/-2
Glass Transition Temperature (Tg)	-41.1 - -39.4	°C	ASTM D7028
	-42 - -39	°F	
Temperature Rating	130	°C	UL RTI
	266	°F	
Temp. of Deflection Under Load, 1.80 MPa	48	°C	ISO 75-1/-2
	118	°F	
Heat Deflection Temperature, 264 Psi, 248 °F/hr	40 - 55	°C	ASTM D648
	104 - 131	°F	
Heat Deflection Temperature, 66 Psi, 248 °F/hr	60 - 75	°C	ASTM D648
	140 - 167	°F	
Vicat Softening Temperature, 50°C/h 50N	79	°C	ISO 306
	174	°F	
Coeff. of Linear Thermal Expansion, parallel	160	E-6/K	ISO 11359-1/-2
Coefficient of Thermal Expansion, 73 °F	12.6 - 18.5	10E-5/°C	ASTM D696
	7 - 10.3	10E-5/°F	
Burning Behav. at 1.5 mm Nominal Thickness	V-0	class	IEC 60695-11-10
Thickness Tested	1.5	mm	-
	0.0591	in	
Yellow Card available	yes	-	-
Burning Behav. at Thickness h	V-0	class	IEC 60695-11-10
Thickness Tested	0.8	mm	-
	0.0315	in	

Arkema France - A French "société anonyme", registered in the Nanterre (France) Trade and Companies Register under the number 319 632 790 SDC/11-2018
Source: automatically generated TDS from Material Database on 17-11-2022

KYNAR FLEX®
2801-00

Oxygen Index	43	%	ISO 4589-1/-2
Limiting Oxygen Index, 73 °F	42	%	ASTM D2863
Thermal Conductivity	0.144 - 0.18	W/(m K)	ASTM D433
	1 - 1.25	BTU in /(hr ft2 F)	
Specific Heat	745 - 958	J/(kg K)	DSC
	0.28 - 0.36	BTU/(lb·°F)	
Thermal Decomposition TGA, in air	375	°C	1% wt. loss
	707	°F	
Thermal Decomposition TGA, in nitrogen	410	°C	1% wt. loss
	770	°F	
Relative Thermal Index, Mechanical	130	°C	UL 746B
	266	°F	
Relative Thermal Index, Electrical	130	°C	UL 746B
	266	°F	
ELECTRICAL PROPERTIES			
Relative Permittivity, 1MHz	7	-	IEC 60250
Dielectric Constant, 1 kHz	3.5 - 10.6	-	ASTM D150
Dissipation Factor, 1MHz	2330	E-4	IEC 60250
Dissipation Factor, 100 kHz	0.02 - 0.21	-	ASTM D150
Volume Resistivity	2E12	Ohm*m	IEC 60093
Volume Resistivity, DC 68 °F, 65% R.H.	2E14	Ohm*cm	ASTM D257
Dielectric (Electric) Strength, 73°F	1.3 - 1.5	kV/mil	ASTM D149
OTHER PROPERTIES			
Water Absorption	0.03	%	Sim. to ISO 62
Density	1780	kg/m³	ISO 1183
	1.78	g/cm³	
Specific Gravity, 73 °F	1.77 - 1.8	-	ASTM D792
OPTICAL PROPERTIES			
Refractive Index @ sodium D line	1.41	-	ASTM D542

MAIN APPLICATIONS:

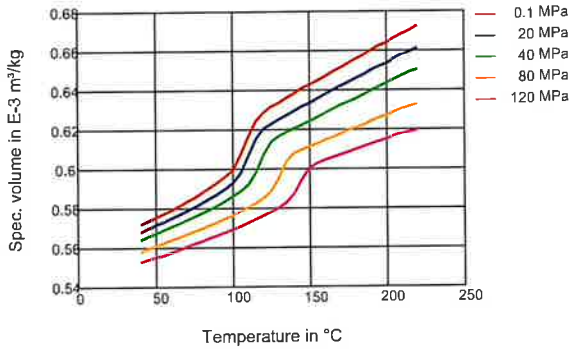
- corrosion protection in the chemical industry
- wire and cable
- coating (painting, co-extrusion)
- off shore

Arkema France - A French "société anonyme", registered in the Nanterre (France) Trade and Companies Register under the number 319 632 790 SDC/11-2018
Source: automatically generated TDS from Material Database on 17-11-2022

KYNAR FLEX®
2801-00

DIAGRAMS

SPECIFIC VOLUME-TEMPERATURE (PVT)



DELIVERY FORM

Powder

SPECIAL CHARACTERISTICS

Heat Stabilized, Light Stabilized

REGIONAL AVAILABILITY

North America, Europe, Asia Pacific, South and Central America, Near East/Africa

Headquarters:

Arkema France
420 rue d'Estienne d'Orves
92705 Colombes Cedex France
T +33 (0)1 49 00 80 80
arkema.com

Arkema Inc. – High Performance Polymers

900 First Avenue
King of Prussia, PA 19406
Tel.: +1 610 205 7000
hpp.arkema.com

Arkema France - A French "société anonyme", registered in the Nanterre (France) Trade and Companies Register under the number 319 632 790 SDC/11-2018
Source: automatically generated TDS from Material Database on 17-11-2022

The statements, technical information and recommendations contained herein are believed to be accurate as of the date hereof. Since the conditions and methods of use of the product and of the information referred to herein are beyond our control, ARKEMA expressly disclaims any and all liability as to any results obtained or arising from any use of the product or reliance on such information; NO WARRANTY OF FITNESS FOR ANY PARTICULAR PURPOSE, WARRANTY OF MERCHANTABILITY OR ANY OTHER WARRANTY, EXPRESSED OR IMPLIED, IS MADE CONCERNING THE GOODS DESCRIBED OR THE INFORMATION PROVIDED HEREIN. The information provided herein relates only to the specific product designated and may not be applicable when such product is used in combination with other materials or in any process. The user should thoroughly test any application before commercialization. Nothing contained herein constitutes a license to practice under any patent and it should not be construed as an inducement to infringe any patent and the user is advised to take appropriate steps to be sure that any proposed use of the product will not result in patent infringement.

Appendix E

KYNAR FLEX®
2751-00

Kynar Flex® resins are fluorinated thermoplastic copolymers.

Outstanding characteristics: chemical resistance, imperviousness to UV, barrier properties and high purity.
Kynar Flex® 2751-00 resin is a powder grade where maximum flexibility or impact strength is required.

PROPERTIES	VALUE	UNIT	TEST STANDARD
RHEOLOGICAL PROPERTIES			
Melt Volume-Flow Rate	1.9	cm³/10min	ISO 1133
Temperature	230	°C	-
	446	°F	
Load	5	kg	-
	11	lb	
Melt Flow Rate	4 - 14	g/10min	ASTM D1238
Temperature	230	°C	-
Load	12.5	kg	-
Melt Viscosity, 230°C, 100 s-1	20 - 25	kPoise	ASTM D3835
MECHANICAL PROPERTIES			
Tensile Modulus	450	MPa	ISO 527-1/-2
	65300	psi	
Tensile Modulus, 73 °F	552 - 896	MPa	ASTM D638
	80000 - 130000	psi	
Yield stress	21	MPa	ISO 527-1/-2
	3050	psi	
Tensile Strength at Yield, 73 °F	20 - 34.5	MPa	ASTM D638
	2900 - 5000	psi	
Yield strain	15	%	ISO 527-1/-2
Elongation at Yield, 73 °F	10 - 20	%	ASTM D638
Nominal Strain at Break	>50	%	ISO 527-1/-2
Tensile Strength at Break, 73 °F	17.2 - 34.5	MPa	ASTM D638
	2500 - 5000	psi	
Elongation at Break, 73 °F	100 - 300	%	ASTM D638
Taber Abrasion, CS 17 1000g:pad	16 - 19	mg/1000 cycles	ASTM-G195-13A
Hardness, Shore D, 73 °F	60 - 70	-	ASTM D2240
Flexural Modulus, 73 °F	483 - 758	MPa	ASTM D790
	70000 - 110000	psi	

Arkema France - A French "société anonyme", registered in the Nanterre (France) Trade and Companies Register under the number 319 632 790 SDC/11-2018
Source: automatically generated TDS from Material Database on 17-11-2022

KYNAR FLEX®
2751-00

Flexural Stength @ 5% Strain, 73 °F	20.7 - 34.5	MPa	ASTM D790
	3000 - 5000	psi	
Compressive Strength, 73 °F	31 - 41.4	MPa	ASTM D695
	4500 - 6000	psi	
Charpy Notched Impact Strength, +23°C	No Break	kJ/m²	ISO 179/1eA
Unnotched Impact Strength, 73 °F	No Break	kJ/m	ASTM D256
Notched Impact Strength, 73 °F	0.534 - 1.07	kJ/m	ASTM D256
	10 - 20	ftlb/in	
Coefficient of Friction, Static vs. Steel, 73 °F	0.33	-	ASTM D1894
Coefficient of Friction, Dynamic vs. Steel, 73 °F	0.33	-	ASTM D1894
THERMAL PROPERTIES			
Melting Temperature, 10°C/min	134	°C	ISO 11357-1/-3
Melting Point, 73 °F	140 - 145	°C	ASTM D3418
Glass Transition Temperature, 10°C/min	-40	°C	ISO 11357-1/-2
Glass Transition Temperature (Tg)	-41.1 - -39.4	°C	ASTM D7028
	-42 - -39	°F	
Temp. of Deflection Under Load, 1.80 MPa	40	°C	ISO 75-1/-2
	104	°F	
Heat Deflection Temperature, 264 Psi, 248 °F/hr	40 - 55	°C	ASTM D648
	104 - 131	°F	
Heat Deflection Temperature, 66 Psi, 248 °F/hr	60 - 75	°C	ASTM D648
	140 - 167	°F	
Coefficient of Thermal Expansion, 73 °F	12.6 - 18.5	10E-5/°C	ASTM D696
	7 - 10.3	10E-5/°F	
Burning Behav. at Thickness h	V-0	class	IEC 60695-11-10
Thickness Tested	0.8	mm	-
	0.0315	in	
Oxygen Index	43	%	ISO 4589-1/-2
Limiting Oxygen Index, 73 °F	42	%	ASTM D2863
Thermal Conductivity	0.144 - 0.18	W/(m K)	ASTM D433
	1 - 1.25	BTU in /(hr ft2 F)	
Specific Heat	745 - 958	J/(kg K)	DSC
	0.28 - 0.36	BTU/(lb·°F)	
Thermal Decomposition TGA, in air	375	°C	1% wt. loss
	707	°F	

Arkema France - A French "société anonyme", registered in the Nanterre (France) Trade and Companies Register under the number 319 632 790 SDC/11-2018
Source: automatically generated TDS from Material Database on 17-11-2022

KYNAR FLEX®
2751-00

Thermal Decomposition TGA, in nitrogen	410	°C	1% wt. loss
	770	°F	
ELECTRICAL PROPERTIES			
Dielectric Constant, 1 kHz	3.5 - 10.6	-	ASTM D150
Dissipation Factor, 100 kHz	0.02 - 0.21	-	ASTM D150
Volume Resistivity	2E12	Ohm*m	IEC 60093
Volume Resistivity, DC 68 °F, 65% R.H.	2E14	Ohm*cm	ASTM D257
Surface Resistivity, 73 °F	5.1E11 - 5.3E11	Ohm per square	ASTM D257
Dielectric (Electric) Strength, 73°F	1.3 - 1.5	kV/mil	ASTM D149
OTHER PROPERTIES			
Water Absorption	0.03 - 0.05	%	ASTM D570
Specific Gravity, 73 °F	1.7 - 1.8	-	ASTM D792
OPTICAL PROPERTIES			
Refractive Index @ sodium D line	1.41	-	ASTM D542

MAIN APPLICATIONS:

- flexible tubing
- corrosion protection in the chemical industry
- off-shore
- wire and cable

DELIVERY FORM

Powder

REGIONAL AVAILABILITY

North America, Europe, Asia Pacific, South and Central America, Near East/Africa

Headquarters:

Arkema France
420 rue d'Estienne d'Orves
92705 Colombes Cedex France
T +33 (0)1 49 00 80 80
arkema.com

Arkema Inc. – High Performance Polymers

900 First Avenue
King of Prussia, PA 19406
Tel.: +1 610 205 7000
hpp.arkema.com

Arkema France - A French "société anonyme", registered in the Nanterre (France) Trade and Companies Register under the number 319 632 790 SDC/11-2018
Source: automatically generated TDS from Material Database on 17-11-2022

The statements, technical information and recommendations contained herein are believed to be accurate as of the date hereof. Since the conditions and methods of use of the product and of the information referred to herein are beyond our control, ARKEMA expressly disclaims any and all liability as to any results obtained or arising from any use of the product or reliance on such information; NO WARRANTY OF FITNESS FOR ANY PARTICULAR PURPOSE, WARRANTY OF MERCHANTABILITY OR ANY OTHER WARRANTY, EXPRESSED OR IMPLIED, IS MADE CONCERNING THE GOODS DESCRIBED OR THE INFORMATION PROVIDED HEREIN. The information provided herein relates only to the specific product designated and may not be applicable when such product is used in combination with other materials or in any process. The user should thoroughly test any application before commercialization. Nothing contained herein constitutes a license to practice under any patent and it should not be construed as an inducement to infringe any patent and the user is advised to take appropriate steps to be sure that any proposed use of the product will not result in patent infringement.

Appendix F

Auxiliary Power Unit Battery Fire
Japan Airlines Boeing 787-8, JA829J
Boston, Massachusetts
January 7, 2013



Incident Report

NTSB/AIR-14/01
PB2014-108867

National Transportation Safety Board

NTSB/AIR-14/01
PB2014-108867
Notation 8604
Adopted November 21, 2014

Aircraft Incident Report

Auxiliary Power Unit Battery Fire

Japan Airlines Boeing 787-8, JA829J

Boston, Massachusetts

January 7, 2013

National Transportation Safety Board

490 L'Enfant Plaza, S.W.
Washington, D.C. 20594

National Transportation Safety Board. 2014. *Auxiliary Power Unit Battery Fire, Japan Airlines Boeing 787-8, JA829J, Boston, Massachusetts, January 7, 2013.* NTSB/AIR-14/01. Washington, DC.

Abstract: This report discusses the January 7, 2013, incident involving a Japan Airlines Boeing 787-8, JA8297, which was parked at a gate at General Edward Lawrence Logan International Airport, Boston, Massachusetts, when maintenance personnel observed smoke coming from the lid of the auxiliary power unit battery case, as well as a fire with two distinct flames at the electrical connector on the front of the case. No passengers or crewmembers were aboard the airplane at the time, and none of the maintenance or cleaning personnel aboard the airplane was injured. Safety issues relate to cell internal short circuiting and the potential for thermal runaway of one or more battery cells, fire, explosion, and flammable electrolyte release; cell manufacturing defects and oversight of cell manufacturing processes; thermal management of large-format lithium-ion batteries; insufficient guidance for manufacturers to use in determining and justifying key assumptions in safety assessments; insufficient guidance for Federal Aviation Administration (FAA) certification engineers to use during the type certification process to ensure compliance with applicable requirements; and stale flight data and poor-quality audio recording of the 787 enhanced airborne flight recorder. Safety recommendations are addressed to the FAA, The Boeing Company, and GS Yuasa Corporation.

The National Transportation Safety Board (NTSB) is an independent federal agency dedicated to promoting aviation, railroad, highway, marine, and pipeline safety. Established in 1967, the agency is mandated by Congress through the Independent Safety Board Act of 1974 to investigate transportation accidents, determine the probable causes of the accidents, issue safety recommendations, study transportation safety issues, and evaluate the safety effectiveness of government agencies involved in transportation. The NTSB makes public its actions and decisions through accident reports, safety studies, special investigation reports, safety recommendations, and statistical reviews.

The NTSB does not assign fault or blame for an accident or incident; rather, as specified by NTSB regulation, "accident/incident investigations are fact-finding proceedings with no formal issues and no adverse parties … and are not conducted for the purpose of determining the rights or liabilities of any person." 49 C.F.R. § 831.4. Assignment of fault or legal liability is not relevant to the NTSB's statutory mission to improve transportation safety by investigating accidents and incidents and issuing safety recommendations. In addition, statutory language prohibits the admission into evidence or use of any part of an NTSB report related to an accident in a civil action for damages resulting from a matter mentioned in the report. 49 U.S.C. § 1154(b).

For more detailed background information on this report, visit http://www.ntsb.gov/investigations/dms.html and search for NTSB accident ID DCA13IA037. Recent publications are available in their entirety on the Internet at http://www.ntsb.gov. Other information about available publications also may be obtained from the website or by contacting:

National Transportation Safety Board
Records Management Division, CIO-40
490 L'Enfant Plaza, SW
Washington, DC 20594
(800) 877-6799 or (202) 314-6551

NTSB publications may be purchased from the National Technical Information Service. To purchase this publication, order product number PB2014-108867 from:

National Technical Information Service
5301 Shawnee Rd.
Alexandria, VA 22312
(800) 553-6847 or (703) 605-6000
http://www.ntis.gov/

Contents

Figures iii

Tables iv

Abbreviations v

Executive Summary vii

1. Factual Information 1
1.1 Event History 1
1.2 Airplane Information 4
1.2.1 Battery Information 4
1.2.2 Battery and Related Component Information 10
1.2.3 Postincident Airplane Examination 11
1.2.4 Additional Airplane-Related Information 12
1.3 Flight Recorders 13
1.4 Incident Battery Examinations 15
1.4.1 External Observations 15
1.4.2 Radiographic Examinations of Incident Battery and Cells 17
1.4.3 Disassembly of Incident Battery 20
1.4.4 Battery Case Protrusion and Corresponding Cell Case Damage 23
1.4.5 Disassembly of Incident Battery Cells 24
1.5 Exemplar Battery Examinations and Testing 30
1.5.1 Radiographic Examinations of Exemplar Battery Cells 30
1.5.2 Cell Soft-Short Tests 31
1.5.3 Examinations of Cells From the Incident Airplane Main Battery 32
1.5.4 Cell-Level Abuse Tests 34
1.5.5 Rivet Observations During Cell- and Battery-Level Testing 37
1.5.6 Cold Temperature Cell- and Battery-Level Testing 39
1.5.7 Battery-Level Nail Penetration Tests 40
1.5.8 Additional Testing 41
1.6 Battery Manufacturing Information 42
1.6.1 Main and Auxiliary Power Unit Battery Development 42
1.6.2 Cell Manufacturing Process 45
1.7 System Safety and Certification 47
1.7.1 Type Certification Overview and Battery Special Conditions 47
1.7.2 Certification Plan 48
1.7.3 System Safety Assessment 49
1.8 Additional Information 52
1.8.1 Federal Aviation Administration Actions After Battery Incidents 52
1.8.2 Previously Issued Safety Recommendations 54

CosMX Exhibit 1003, Page 139 of 512

2. Analysis **56**
2.1 Failure Sequence 56
2.2 Emergency Response 58
2.3 Cell Manufacturing Concerns 58
2.4 Thermal Management of Large-Format Lithium-Ion Batteries 62
2.4.1 Battery Internal Heating During High-Current Discharge 62
2.4.2 Cell-Level Temperature and Voltage Monitoring 65
2.4.3 Thermal Safety Limits for Cells 66
2.5 Certification Process 67
2.5.1 Validation of Assumptions and Data Used in Safety Assessments Involving New Technology 68
2.5.2 Validating Methods of Compliance for Designs Involving New Technology 72
2.5.3 Certification of Lithium-ion Batteries and Certification of New Technology 74
2.6 Flight Recorder Issues 75
2.6.1 Stale Flight Data 75
2.6.2 Poor-Quality Cockpit Voice Recording 76

3. Conclusions **78**
3.1 Findings 78
3.2 Probable Cause 79

4. Recommendations **80**
4.1 New Recommendations 80
4.2 Previously Issued Safety Recommendations Classified in This Report 82

5. Appendixes **84**
Appendix A: Investigation and Hearing 84
Appendix B: Boeing 787 Type Certification Special Conditions 25-359-SC 86
Appendix C: Comments From the Bureau d'Enquêtes et d'Analyses pour la Sécurité de l'Aviation Civile 88

References **95**

CosMX Exhibit 1003, Page 140 of 512

Figures

Figure 1. Photograph of smoke emanating from the incident airplane's aft E/E bay. 3

Figure 2. Main and APU exemplar battery. 6

Figure 3. Electrode winding layout. 7

Figure 4. Exploded-view diagram of LVP65 lithium-ion cell construction. 8

Figure 5. Riveted header assembly. 9

Figure 6. Right aft corner of the battery lid and side 4 of the battery case. 16

Figure 7. Cross-sectional view of the APU battery. 18

Figure 8. Cross-sectional view of cell 5 aluminum current collectors. 19

Figure 9. Cross-sectional view of cell 6 aluminum current collectors. 20

Figure 10. Thermal damage to battery. 22

Figure 11. Lower and upper fixation trays. 23

Figure 12. Protrusion on the lower left of battery case side 3. 24

Figure 13. Cell 5 winding closest to cell 6. 27

Figure 14. Cell 6 winding closest to cell 5. 28

Figure 15. Results of cell-level internal short circuit abuse test. 36

Figure 16. Winding flattening process. 46

CosMX Exhibit 1003, Page 141 of 512

Tables

Table 1. Specifications for the main and APU battery and cells. 5

Table 2. Events surrounding APU shutdown. 14

CosMX Exhibit 1003, Page 142 of 512

Abbreviations

AC	advisory circular
ACO	aircraft certification office
AD	airworthiness directive
APSIF	UTC Aerospace Systems' Airplane Power Systems Integration Facility
APU	auxiliary power unit
ARAC	aviation rulemaking advisory committee
ARC	accelerating rate calorimetry
ARFF	aircraft rescue and firefighting
ARP	Aerospace Recommended Practice
ATP	acceptance test procedure
BCU	battery charger unit
BEA	Bureau d'Enquêtes et d'Analyses pour la Sécurité de l'Aviation Civile
BMU	battery monitoring unit
BOS	General Edward Lawrence Logan International Airport
CFR	*Code of Federal Regulations*
CT	computed tomography
CVR	cockpit voice recorder
DPA	destructive physical analysis
EAFR	enhanced airborne flight recorder
EASA	European Aviation Safety Agency
ECS	environmental control system
EDS	energy dispersive x-ray spectroscopy
E/E bay	electronic equipment bay

CosMX Exhibit 1003, Page 143 of 512

EICAS	engine indicating and crew alerting system
EPS	electrical power system
EUROCAE	European Organization for Civil Aviation Equipment
FAA	Federal Aviation Administration
FAI	first article inspection
FDR	flight data recorder
FHA	functional hazard assessment
FMEA	failure modes and effects analysis
FOD	foreign object debris
JAL	Japan Airlines
JTSB	Japan Transport Safety Board
KAI	Kanto Aircraft Instrument Company
NASA	National Aeronautics and Space Administration
NRT	Narita International Airport
NTSB	National Transportation Safety Board
ODA	organization designation authorization
SAE	Society of Automotive Engineers
SCD	specification control drawing
SEI	solid electrolyte interphase
SEM	scanning electron microscope
SPU	start power unit
TAK	Takamatsu Airport
TSO	technical standard order
UL	Underwriters Laboratories

CosMX Exhibit 1003, Page 144 of 512

Executive Summary

On January 7, 2013, about 1021 eastern standard time, smoke was discovered by cleaning personnel in the aft cabin of a Japan Airlines (JAL) Boeing 787-8, JA829J, which was parked at a gate at General Edward Lawrence Logan International Airport (BOS), Boston, Massachusetts. About the same time, a maintenance manager in the cockpit observed that the auxiliary power unit (APU) had automatically shut down. Shortly afterward, a mechanic opened the aft electronic equipment bay and found heavy smoke coming from the lid of the APU battery case and a fire with two distinct flames at the electrical connector on the front of the case. None of the 183 passengers and 11 crewmembers were aboard the airplane at the time, and none of the maintenance or cleaning personnel aboard the airplane was injured. Aircraft rescue and firefighting personnel responded, and one firefighter received minor injuries. The airplane had arrived from Narita International Airport, Narita, Japan, as a regularly scheduled passenger flight operated as JAL flight 008 and conducted under the provisions of 14 *Code of Federal Regulations* (CFR) Part 129.

The APU battery model is the same model used for the 787 main battery. On January 16, 2013, an incident involving the main battery occurred aboard a 787 airplane operated by All Nippon Airways during a flight from Yamaguchi to Tokyo, Japan. The airplane made an emergency landing at Takamatsu Airport (TAK), Takamatsu, Japan, shortly after takeoff. The Japan Transport Safety Board investigated this incident with support from the National Transportation Safety Board (NTSB).

Boeing was responsible for the overall integration and certification of the equipment in the 787's electrical power conversion subsystem, which is part of the airplane's electrical power system (EPS). Boeing contracted with Thales Avionics Electrical Systems to design the 787 electrical power conversion subsystem, which includes the main and APU batteries. Thales then subcontracted with various manufacturers for the main and APU battery system components, including GS Yuasa Corporation, which developed, designed, and manufactured the main and APU batteries.

Boeing was required to demonstrate that the 787's design complied with the Federal Aviation Administration's (FAA) Special Conditions 25-359-SC, "Boeing Model 787-8 Airplane; Lithium-Ion Battery Installation," which detailed nine specific requirements regarding the use of these batteries on the airplane. As part of the compliance demonstration with these requirements and 14 CFR Part 25 airworthiness standards, Boeing performed a safety assessment to determine the potential hazards that various failure conditions of EPS components could introduce to the airplane and its occupants. Boeing determined that the rate of occurrence of cell venting for the 787 battery would be about 1 in 10 million flight hours. However, at the time of the BOS and TAK incidents (both of which involved cell venting), the in-service 787 fleet had accumulated less than 52,000 flight hours.

After the BOS and TAK events and the FAA's subsequent grounding of the US 787 fleet, Boeing modified the 787 main and APU battery design and its installation configuration to include, among other things, a stainless steel enclosure for the battery case and a duct that vents

CosMX Exhibit 1003, Page 145 of 512

from the interior of the enclosure to the exterior of the airplane to prevent smoke from entering the occupiable space of the airplane. In April 2013, the FAA issued an airworthiness directive mandating the installation of the modified battery aboard US 787 airplanes before they could return to service.

The 787 main and APU battery design was also modified to mitigate the most severe effects of an internal short circuit (that is, cascading, cell-to-cell thermal runaway of other cells within the battery; excessive heat; flammable electrolyte release; and fire). The recommendations resulting from the safety issues identified during this investigation could help prevent such effects from occurring in future battery designs.

The NTSB identified the following safety issues as a result of this incident investigation:

- **Cell internal short circuiting and the potential for thermal runaway of one or more battery cells, fire, explosion, and flammable electrolyte release.** This incident involved an uncontrollable increase in temperature and pressure (thermal runaway) of a single APU battery cell as a result of an internal short circuit and the cascading thermal runaway of the other seven cells within the battery. This type of failure was not expected based on the testing and analysis of the main and APU battery that Boeing performed as part of the 787 certification program. However, GS Yuasa did not test the battery under the most severe conditions possible in service, and the test battery was different than the final battery design certified for installation on the airplane. Also, Boeing's analysis of the main and APU battery did not consider the possibility that cascading thermal runaway of the battery could occur as a result of a cell internal short circuit.

- **Cell manufacturing defects and oversight of cell manufacturing processes.** After the incident, the NTSB visited GS Yuasa's production facility to observe the cell manufacturing process. During the visit, the NTSB identified several concerns, including foreign object debris (FOD) generation during cell welding operations and a postassembly inspection process that could not reliably detect manufacturing defects, such as FOD and perturbations (wrinkles) in the cell windings, which could lead to internal short circuiting. In addition, the FAA's oversight of Boeing, Boeing's oversight of Thales, and Thales' oversight of GS Yuasa did not ensure that the cell manufacturing process was consistent with established industry practices.

- **Thermal management of large-format lithium-ion batteries.** Testing performed during the investigation showed that localized heat generated inside a 787 main and APU battery during maximum current discharging exposed a cell to high-temperature conditions. Such conditions could lead to an internal short circuit and cell thermal runaway. As a result, thermal protections incorporated in large-format lithium-ion battery designs need to account for all sources of heating in the battery during the most extreme charge and discharge current conditions. Thermal protections include (1) recording and monitoring cell-level temperatures and voltages to ensure that exceedances resulting from localized or other sources of heating can be detected and addressed before cell damage occurs and (2) establishing thermal safety limits for

CosMX Exhibit 1003, Page 146 of 512

cells to ensure that self-heating does not occur at a temperature that is less than the battery's maximum operating temperature.

- **Insufficient guidance for manufacturers to use in determining and justifying key assumptions in safety assessments.** Boeing's EPS safety assessment for the 787 main and APU battery included an underlying assumption that the effect of an internal short circuit within a cell would be limited to venting of only that cell without fire. However, the assessment did not explicitly discuss this key assumption or provide the engineering rationale and justifications to support the assumption. Also, as demonstrated by the circumstances of this incident, Boeing's assumption was incorrect, and Boeing's assessment did not consider the consequences if the assumption were incorrect or incorporate design mitigations to limit the safety effects that could result in such a case. Boeing indicated in certification documents that it used a version of FAA Advisory Circular (AC) 25.1309, "System Design and Analysis" (referred to as the Arsenal draft), as guidance during the 787 certification program. However, the analysis that Boeing presented in its EPS safety assessment did not appear to be consistent with the guidance in the AC. In addition, Boeing and FAA reviews of the EPS safety assessment did not reveal that the assessment had not (1) considered the most severe effects of a cell internal short circuit and (2) included requirements to mitigate related risks.

- **Insufficient guidance for FAA certification engineers to use during the type certification process to ensure compliance with applicable requirements.** During the 787 certification process, the FAA did not recognize that cascading thermal runaway of the battery could occur as a result of a cell internal short circuit. As a result, FAA certification engineers did not require a thermal runaway test as part of the compliance demonstration (with applicable airworthiness regulations and lithium-ion battery special conditions) for certification of the main and APU battery. Guidance to FAA certification staff at the time that Boeing submitted its application for the 787 type certificate, including FAA Order 8110.4, "Type Certification," did not clearly indicate how individual special conditions should be traced to compliance deliverables (such as test procedures, test reports, and safety assessments) in a certification plan.

- **Stale flight data and poor-quality audio recording of the 787 enhanced airborne flight recorder (EAFR).** The incident airplane was equipped with forward and aft EAFRs, which recorded cockpit audio data and flight parametric data. The EAFRs recorded stale flight data for some parameters (that is, data that appeared to be valid and continued to be recorded after a parameter source stopped providing valid data), which delayed the NTSB's complete understanding of the recorded data. In addition, the audio recordings from both EAFRs during the airborne portion of the flight were poor quality. The signal levels of the three radio/hot microphone channels were very low, and the recording from the cockpit area microphone channel was completely obscured by the ambient cockpit noise. These issues did not impact the NTSB's investigation because the conversations and sounds related to the circumstances of the

CosMX Exhibit 1003, Page 147 of 512

incident occurred after the airplane arrived at the gate and the engines were shut down, at which point the quality of the audio recordings was excellent.

The NTSB determines that the probable cause of this incident was an internal short circuit within a cell of the APU lithium-ion battery, which led to thermal runaway that cascaded to adjacent cells, resulting in the release of smoke and fire. The incident resulted from Boeing's failure to incorporate design requirements to mitigate the most severe effects of an internal short circuit within an APU battery cell and the FAA's failure to identify this design deficiency during the type design certification process.

As a result of this investigation, the NTSB makes safety recommendations to the FAA, Boeing, and GS Yuasa. The NTSB previously issued safety recommendations to the FAA regarding (1) insufficient testing methods and guidance for addressing the safety risks of internal short circuits and thermal runaway and (2) the need for outside technical knowledge and expertise to help the FAA ensure the safe introduction of new technology into aircraft designs.

CosMX Exhibit 1003, Page 148 of 512

1. Factual Information

1.1 Event History

On January 7, 2013, about 1021 eastern standard time,[1] smoke was discovered by cleaning personnel in the aft cabin of a Japan Airlines (JAL) Boeing 787-8, JA829J, which was parked at a gate at General Edward Lawrence Logan International Airport (BOS), Boston, Massachusetts. About the same time, a maintenance manager in the cockpit observed that the auxiliary power unit (APU) had automatically shut down.[2] Shortly afterward, a mechanic opened the aft electronic equipment bay (E/E bay) and found heavy smoke coming from the lid of the APU battery case and a fire with two distinct flames at the electrical connector on the front of the case.[3] None of the 183 passengers and 11 crewmembers were aboard the airplane at the time, and none of the maintenance or cleaning personnel aboard the airplane was injured. Aircraft rescue and firefighting (ARFF) personnel responded, and one firefighter received minor injuries. The airplane had arrived from Narita International Airport (NRT), Narita, Japan, as a regularly scheduled passenger flight operated as JAL flight 008 and conducted under the provisions of 14 *Code of Federal Regulations* (CFR) Part 129.

The captain of JAL flight 008 reported that the APU was turned on about 30 to 40 min before the airplane left the gate at NRT (about 0247Z) and was shut down after the engines started.[4] He stated that the flight, which departed NRT about 0304Z, was uneventful except for occasional moderate turbulence about 6.5 to 7 hours into the flight. Flight data recorder (FDR) data showed that the airplane touched down at BOS at 1000:24 and that the APU was started at 1004:10 while the airplane was taxied to the gate. The captain indicated that the APU operated normally. FDR data also showed that the airplane was parked at the gate with the parking brake set and both engines shut down by 1006:54.

The maintenance manager (the JAL director of aircraft maintenance and engineering at BOS) reported that the passengers had deplaned by 1015 and that the flight and cabin crewmembers had deplaned by 1020, at which time he and the cabin cleaning crew had entered

---

1 All times in this report are eastern standard time unless otherwise noted.

2 The APU battery provides power to start the APU during ground and flight operations. The APU controller monitors the parameters that are needed to operate the APU. The APU controller is powered by the APU battery bus, which receives its power from the APU battery. If the APU battery were to fail, then the APU battery bus would no longer receive power, and the APU would shut down.

3 The mechanic provided a written statement to the National Transportation Safety Board (NTSB) describing his observations. The mechanic's statement indicated that, after he checked the aft E/E bay, he saw "heavy smoke in the compartment." He reported that he "saw [a] small flame around [the] APU batt[ery]." He added that he "decided [to] discharge [the hand-held dry chemical fire] extinguisher" but could not "discharge continuously" because he believed that there was a "dangerous environment in the compartment." Further, he stated that he "tried fire extinguishing, but [the] smoke and flame (flame size about 3 inch[es]) did not stop." In addition, the mechanic gave the NTSB a drawing that showed two 3-in flames at the electrical connector on the front of the battery case. (The front of the battery case is oriented toward the front of the airplane.) The maintenance manager also provided a written statement to the NTSB, which indicated that the mechanic had seen "flames around the APU battery."

4 Eastern standard time is 5 hours behind coordinated universal time (also referred to as UTC or Zulu time).

CosMX Exhibit 1003, Page 149 of 512

the airplane. Shortly afterward, a member of the cleaning crew told the maintenance manager, who was in the cockpit, about "an electrical burning smell and smoke in the aft cabin." The maintenance manager then observed a loss of power to systems powered by the APU and realized that the APU had automatically shut down. After confirming that the airplane's electrical power systems were off, the maintenance manager turned the main and APU battery switches to the "off" position. FDR data showed that the APU battery failed at 1021:15 and that the APU shut down at 1021:37, which was also when the APU controller lost power.

A JAL mechanic in the aft cabin at the time reported that, when the airplane lost power, he went to the cockpit and learned that the APU had shut down. The mechanic then went back to the aft cabin and saw and smelled smoke. A JAL station manager arrived at the airplane and reported that, when he went into the cabin (through the door where the passenger boarding bridge is attached), he saw "intense" smoke that was concentrated 10 ft aft of the door. The turnaround coordinator for JAL flights 008 and 007,[5] who had also entered the aft cabin and observed the smoke, described the smoke as "caustic smelling." The mechanic notified the maintenance manager about the smoke, and the maintenance manager asked the mechanic to check the aft E/E bay. The mechanic found heavy smoke and flames in the compartment coming from the lid of the APU battery case. The mechanic reported that he used a dry chemical fire extinguisher (located at the base of the passenger boarding bridge) to attempt to put out the fire but that the smoke and flames did not stop.

About 1037, ARFF personnel at BOS were notified about smoke in the cabin of a JAL airplane.[6] Review of a time-stamped airport security camera video showed that the first of five ARFF trucks arrived on scene within 1 min (at 1037:50).[7] The other four ARFF trucks arrived on scene about 2.5 min after initial notification. A ladder truck, a rescue truck, an airstair truck, a hazardous materials truck, and a fire command vehicle also responded to the incident.

The JAL mechanic advised ARFF personnel that the fire was in the aft E/E bay and led a firefighter to the aft E/E bay door.[8] The firefighter reported that, after entering the compartment, he could see "a white glow about the size of a softball" on a hand-held thermal imaging camera.[9] The firefighter also reported that he applied "a shot" of Halotron (a clean fire-extinguishing agent) to knock down the fire.[10] The thermal imaging camera showed that the white glow was

[5] JAL flight 007 had been scheduled to depart BOS later that morning using the incident airplane.

[6] The JAL station manager stated that he asked a gate agent to call ARFF. The gate agent then called her supervisor, who called ARFF from a telephone at the passenger check-in counter.

[7] The airplane was located at gate 8A in terminal E. The first ARFF truck to reach the scene (after incident notification) was already in terminal E for terminal familiarization training. The airport security camera recording times were correlated to the FDR times (within 3 seconds).

[8] The term "fire" is commonly used by ARFF personnel in reference to an ARFF response or event. Although the JAL mechanic reported that flames were coming from the front of the APU battery case, none of the ARFF personnel who responded to this incident reported seeing flames.

[9] The hand-held thermal imaging cameras that ARFF personnel at BOS used had a heat-density scale portrayed as brightness and/or coloring of an object (that is, the whiter and brighter the object, the higher the heat intensity).

[10] According to the Halotron website, "Halotron is a rapidly evaporating liquid…that leaves no residue, thereby minimizing or eliminating potential agent-related damage to…assets like electronic equipment, machinery, motors

CosMX Exhibit 1003, Page 150 of 512

still present but was less intense than before. The airport security camera video showed smoke coming out of the airplane, as shown in figure 1, at 1040:26.



Source: *Boston Herald.*

Figure 1. Photograph of smoke emanating from the incident airplane's aft E/E bay.

An ARFF captain went into the aft E/E bay with the thermal imaging camera, which showed a heat signature near the APU battery. After he exited the E/E bay, another firefighter entered it. This firefighter reported no visibility because of the smoke. He did not know where the battery was located within the E/E bay, but he knew of a "hot spot" about 6 to 8 in ahead of him, so he discharged a "quick burst" of Halotron for 10 to 20 seconds. The firefighter exited and reentered the E/E bay with the thermal imaging camera. He reported that the battery case was visible and that he saw "a white glow with radiant heat waves" but no flames. An ARFF lieutenant who entered the aft E/E bay reported that the battery appeared to be rekindling.

The ARFF captain reentered the E/E bay and saw heavy white smoke (which he had seen earlier billowing through the floor of the aft cabin) but no flames. The captain applied shots of Halotron to the fire for 5 min, which he believed had knocked down the fire. He reported that the battery was emitting white smoke, creating heavy smoke conditions. The ARFF captain also reported that the battery was hissing loudly and that liquid was flowing down the sides of the battery case. A firefighter (outside the airplane) reported that he heard a "pop" sound and saw

---

and construction materials." Halotron is dispersed at a rate of 5 lbs per second. A "shot" of Halotron was estimated to last between 15 and 20 seconds, corresponding to between 75 and 100 lbs of the fire-extinguishing agent dispersed. ARFF personnel are trained to use a clean agent, such as Halotron, in electrical and avionics compartments because water would ruin electrical and avionics components.

CosMX Exhibit 1003, Page 151 of 512

smoke "pouring out of" the aft E/E bay. The ARFF captain received a minor burn on his neck when the battery, in his words, "exploded."

After additional firefighting efforts and the placement of a ventilation fan by the E/E bay door to clear smoke, the incident commander decided to remove the APU battery.[11] (The airport security camera video showed that, at 1105:58, smoke was no longer visible from the exterior of the airplane.) Firefighters reported that removing the battery was difficult because a metal kick shield installed in front of the battery prevented them from accessing the battery's quarter-turn quick disconnect knob. Also, the quick disconnect knob could not be turned because it was charred and had melted away. The airport security camera video showed that the battery was removed from the aft E/E bay at 1157:20, about 80 min after the initial notification of the event.[12] The ARFF incident report showed that the event was "controlled" about 1219 (about 1 hour 40 min after the initial notification).

1.2 Airplane Information

The Boeing 787 "Dreamliner" is a twin-engine, wide-body commercial airplane. The 787 program began in April 2004, with the 787's first flight in December 2009, certification in August 2011, and first delivery in September 2011. The incident airplane, JA829J, was delivered new to JAL on December 20, 2012. At the time of the incident, the airplane had logged 169 flight hours and 22 flight cycles. There were no abnormal indications or maintenance messages related to issues with the incident battery between the date of delivery and the date of the incident.

Boeing was responsible for the overall integration and certification of the equipment in the 787's electrical power conversion subsystem, which is part of the airplane's electrical power system. Boeing contracted with Thales Avionics Electrical Systems of Neuilly-sur-Seine, France, to design the 787 electrical power conversion subsystem, which includes the main and APU batteries. Thales subcontracted with various manufacturers for the main and APU battery system components.

1.2.1 Battery Information

The APU battery, part number LVP65-8-402, was developed, designed, and manufactured by GS Yuasa Corporation of Kyoto, Japan.[13] The battery had eight individual lithium-ion cells, all of which were from the same manufacturing lot that GS Yuasa produced in July 2012. The APU battery installed on the incident airplane, serial number 394, was manufactured in September 2012 and was delivered new to Boeing. The battery was installed in

[11] In addition, the incident commander asked a JAL mechanic and a firefighter to disconnect the main battery as a precaution in case it was feeding the APU battery fire.

[12] ARFF personnel had to cut the kick shield installed in front of the battery case to access the battery and then cut the connectors to the battery to remove it.

[13] GS Yuasa assigned this part number to the battery model at the time of the incident. Boeing's part number for the battery model at the time of the incident was B3856-901.

CosMX Exhibit 1003, Page 152 of 512

the incident airplane on October 15, 2012, and was initially charged by the airplane on or about October 19, 2012. Boeing records showed no installation issues associated with the APU battery. Boeing records also showed that, on December 6, 2012, the battery electrical connector was removed (to facilitate a routine inspection of a nearby power panel) and reinstalled the same day.

As previously stated, the APU battery (installed in the aft E/E bay) provides power to start the APU (installed in the tail of the airplane) during ground and flight operations. The aft E/E bay is an electrical equipment compartment located aft of the main landing gear and beneath approximately the third set of cabin doors (L3 and R3). The compartment is only accessible from the ground by a door in the aft cargo compartment and a set of doors in the airplane belly. The APU battery is located at floor level within the aft E/E bay.

Unique to the 787, the LVP65-8-402 battery model is also used for the 787 main battery, which is located in the forward E/E bay. The main battery, which also has eight individual lithium-ion cells, provides power to selected electrical/electronic equipment during ground and flight operations for normal and failure conditions. Table 1 shows the specifications for the LVP65-8-402 battery and LVP65 cells.

Table 1. Specifications for the main and APU battery and cells.

Specification	Battery	Cell
Nominal capacity (ampere-hours)	75	75
Nominal voltage (volts)	29.6	3.7
Operational voltage range (volts)	20 to 32.2	2.5 to 4.025
Weight (lbs)	61.8	6
Dimensions (in)		
Width	10.9	5.2
Depth	14.2	2.0
Height	8.5	7.7

Note: Battery specification information was based on information from a Thales document. Cell specification information was provided by GS Yuasa.

The 787 main and APU lithium-ion battery has primarily nonflammable components, but the electrolyte in the battery cells is flammable. The eight cells are connected in series and assembled in two rows of four cells, as shown in figure 2. Thermoplastic insulation sheets provide electrical isolation and physical separation between each cell and between the cells and the aluminum battery case, which is electrically grounded. Plastic upper and lower fixation trays secure the position and orientation of the cells in the battery case, and forward and center brace bars hold the fixation trays in place.

CosMX Exhibit 1003, Page 153 of 512

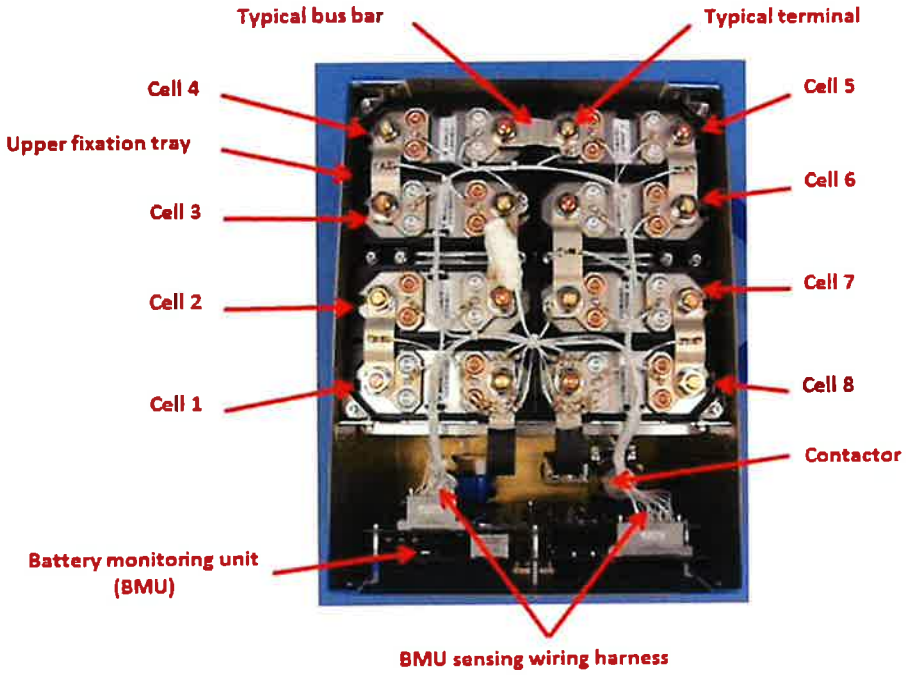


Figure 2. Main and APU exemplar battery.

In addition to the eight individual battery cells, the battery case includes two circuit boards that comprise the battery monitoring unit (BMU); cell voltage sensing wires between battery internal components and the BMU; a Hall effect current sensor for current monitoring; a contactor; bus bars for the main current pathways between the cells and to the J3 connector, which connects to the outside of the battery case; and the J1 connector, which leads outside of the battery case.[14]

Each cell has three internal electrode winding assemblies. Each winding assembly is about 30 ft long and is configured with an electrode, then a separator, then another electrode, and then another separator. One electrode—the anode—is a copper foil coated in a carbon active material; the other electrode—the cathode—is an aluminum foil coated in a lithium-cobalt-oxide compound active material. The separator material is made of polyolefin.

The three internal cell windings have been described as flattened "jelly rolls." The innermost (last) wrap of the sandwiched electrode layers is the coated copper anode layer wrapped around a thermoplastic mandrel core. The coated aluminum cathode layer begins on the

[14] A Hall effect current sensor detects and measures electrical current in a wire and generates a signal proportional to the current measured. The plastic J3 connector provides battery power to the airplane, and the aluminum J1 connector provides signal information used by the BMU and the battery charger unit.

CosMX Exhibit 1003, Page 154 of 512

second-to-last wrap and ends on the second wrap. The outermost wrap, the first wrap, is an extra layer of anode and separator. The separator extends beyond the outermost wrap of anode and winds several more times around the exterior of the winding. Figure 3 shows the electrode winding layout. Two layers of thermoplastic electrical insulation surround the electrode winding assemblies. Sheets of thermoplastic insulation (held together with thermoplastic tape) electrically isolate the stainless steel cell cases (which are not grounded) from the windings.

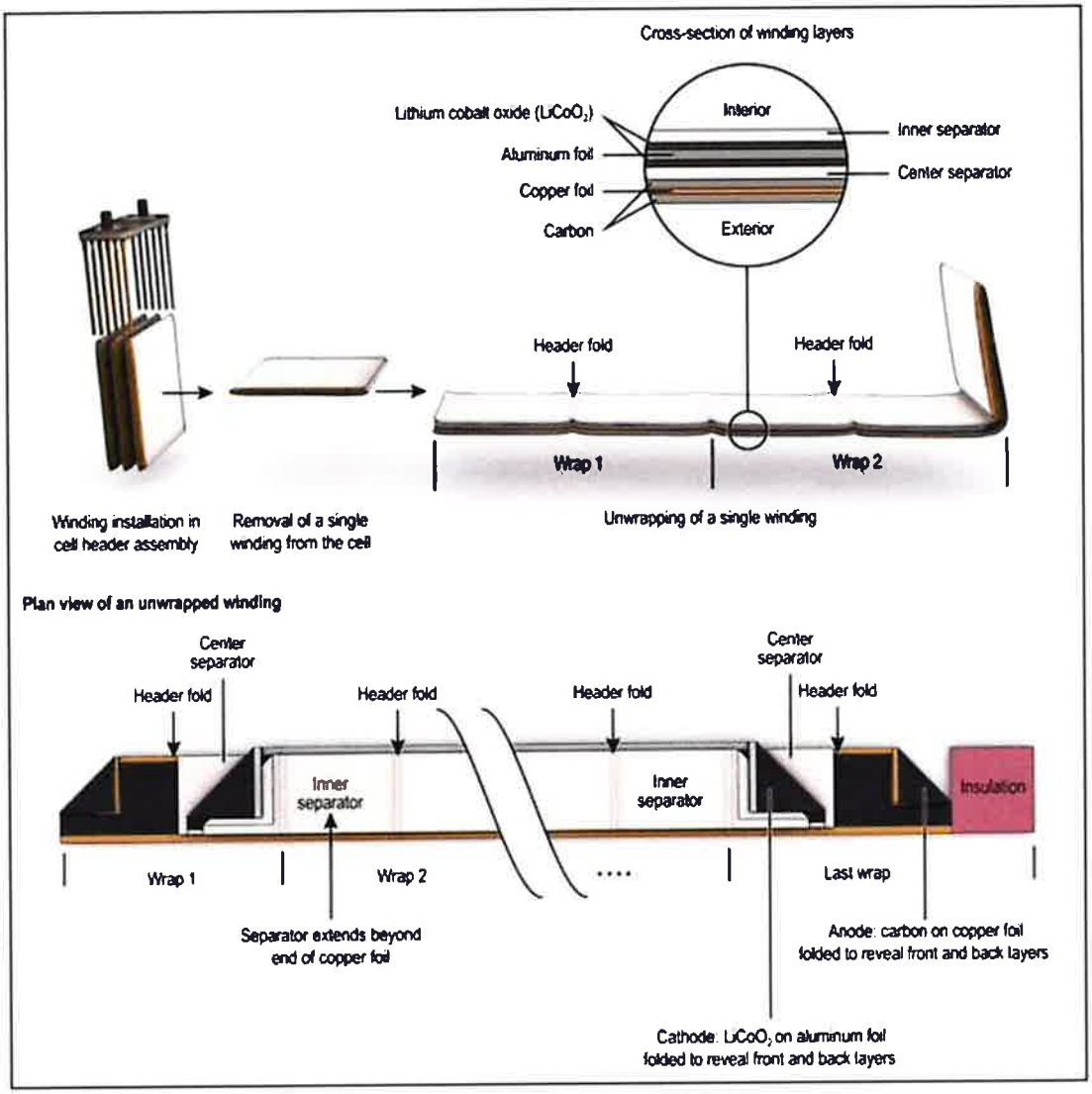


Figure 3. Electrode winding layout.

Two sets of current collectors—one set for the anode and one set for the cathode—are attached on their respective side of each winding assembly to conduct electrical current to and from the positive (cathode) and the negative (anode) terminal assemblies, which are connected to adjacent cells by bus bars. (The electrode edges, where the current collectors attach, are not coated with an active material.) Current collector "fingers" provide the electrical path between

CosMX Exhibit 1003, Page 155 of 512

the windings and the terminal plates on the exterior of each cell. According to GS Yuasa, the aluminum current collector fingers were designed to melt open under high current conditions, thereby functioning as an electrical fuse. Three pairs of copper current collector fingers are used for the anode, and three pairs of aluminum current collector fingers are used for the cathode. The fingers extend about one-half of the way down the left (anode) and right (cathode) sides of the cell. At the top of the cell's interior, the current collector fingers connect together into either copper (anode) or aluminum (cathode) bars, which connect with their respective terminal plates on the cell's exterior. Thermoplastic electrical insulating material is used between the cell case and the current collector bars and terminal plates. Figure 4 shows a diagram of the cell construction. Section 1.4 discusses the postincident examination of the APU battery and cells involved in the BOS event.

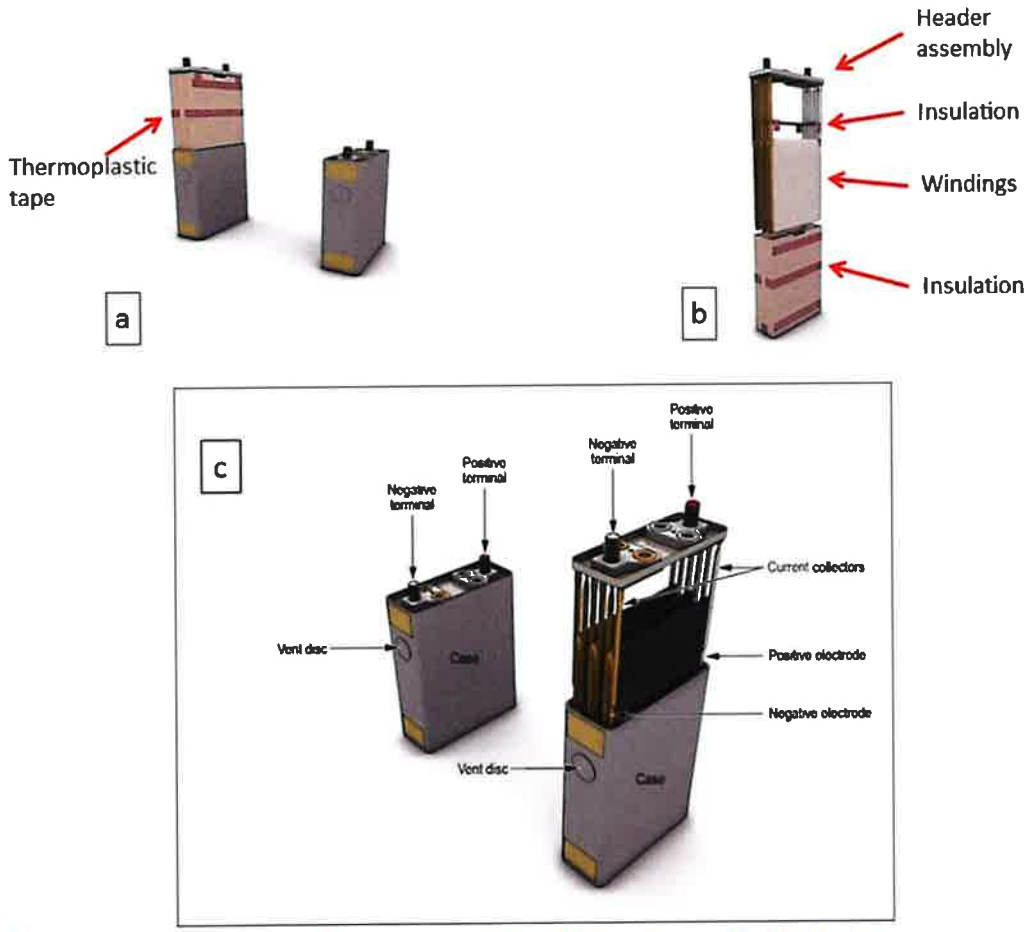


Figure 4. Exploded-view diagram of LVP65 lithium-ion cell construction.

Note: Figures 4a and 4b show the cell construction with the insulation (held together with thermoplastic tape) as installed in the cell. Figure 4c shows the cell construction without the insulation.

Each current collector attaches to two rivets that connect a collector plate with the respective terminal plate on a cell's exterior. Two aluminum rivets are installed at the positive terminal, and two copper rivets are installed at the negative terminal. The rivets provide electrical

CosMX Exhibit 1003, Page 156 of 512

continuity between the cell's exterior and interior. Figure 5 shows a photograph of a riveted header assembly. Section 1.5.5 discusses the postincident examination of riveted assemblies.



Source: Underwriters Laboratories.

Figure 5. Riveted header assembly.

Boeing's requirements for the battery, as specified in a proprietary Thales/GS Yuasa report, included the following:

- a 5-year service life under any combination of operating conditions specified within the Thales/GS Yuasa report,
- an operating temperature range of -0.4°F to 158°F,
- a specific charge acceptance capability with an internal temperature between -0.4°F to 32°F,

- a specific current capacity from a fully discharged state within 75 min at an ambient temperature of 77°F ± 18°F for 30,000 flight hours, and
- a specific current end-of-life rated capacity or greater.[15]

1.2.2 Battery and Related Component Information

The BMU is mounted inside the battery case (see figure 2). The BMU includes a main circuit card and a subcircuit card, each of which contains two independent monitoring systems: BMU1 and BMU2 (main circuit card) and BMU3 and BMU4 (subcircuit card). Each of the four BMU systems has an initiated built-in test function. BMU1 monitors for cell overcharge, overdischarge, overheating, and imbalance; controls the cell balancing function when any cell reaches a predetermined threshold; and provides voltage measurement to the battery charger unit (BCU). BMU2 provides redundant monitoring for cell overcharge. BMU3 controls the contactor and provides additional monitoring for battery and cell overcharge. BMU4 monitors for cell overdischarge and high current charge. The BMU was designed to send a signal to the BCU to discontinue charging if any of the battery monitoring thresholds were exceeded. The incident main circuit card and subcircuit card were manufactured by Kanto Aircraft Instrument Company (KAI) Ltd. The main circuit card and subcircuit card do not contain nonvolatile memory, and none of the BMU data were recorded on the FDR. Examination and testing of the BMU components, which were thermally damaged, revealed no pre-failure anomalies.[16]

The contactor is a device that can electrically isolate the battery cells from the BCU and battery bus. The contactor, which is mounted in the bottom of the battery case near the BMU (see figure 2), is normally closed during battery operations. The contactor can only be commanded to open by BMU3 if a cell overvoltage or high battery voltage is detected. The incident contactor was manufactured by Zodiac Aerospace. The damage to the contactor precluded a full functional test from being performed. X-rays and disassembly of the contactor revealed no pre-failure anomalies.

The BCU includes an electric connector for communication (among the BCU, battery, and airplane), a ground wire stud, and power terminals for the two large battery cables. The BCU of the incident APU battery was manufactured by Securaplane Technologies. At Securaplane, the National Transportation Safety Board (NTSB) performed visual examinations, preliminary electrical tests, and acceptance test procedure (ATP) functional testing of the BCU. The ATP testing revealed a previously unknown electrical oscillation in the output charge voltage, which was later determined (through additional testing at Boeing and Underwriters Laboratories [UL]) not to be related to the circumstances of the incident, as discussed in section 1.5.8.[17]

---

[15] The actual charge acceptance capability, current capacity, and current end-of-life rated capacity are proprietary.

[16] The damage to the BMU was too extensive to perform testing as a complete assembly; as a result, the testing was conducted at the component level.

[17] The NTSB contracted with UL to perform testing as part of this incident investigation. UL performed testing in its laboratories in Northbrook, Illinois; Melville, New York; and Taipei, Taiwan.

CosMX Exhibit 1003, Page 158 of 512

The APU controller operates the valves, motors, and sensors that control the operation of the APU and contains nonvolatile memory to record various APU parameters, including battery voltage. The APU controller in the 787 airplane is located near the bulk cargo door on the right side of the aft fuselage (where it is separated from the APU battery and the BCU). The incident APU controller was manufactured by Hamilton Sundstrand.[18] Examination and testing (as part of obtaining the nonvolatile memory) showed that the APU controller operated normally and that the APU's function did not affect the battery's operation at the time of the failure.

The start power unit (SPU) converts DC battery power to AC power for starting the APU and provides excitation power for the APU during startup. The SPU of the incident airplane was manufactured by Securaplane Technologies. ATP testing of the SPU found no anomalies, and the SPU's function did not affect the battery's operation at the time of the failure.

1.2.3 Postincident Airplane Examination

The aft E/E bay (the APU battery installation location) showed damage consistent with heat generated from the APU battery and smoke, hot gases, and electrolyte discharged from the battery. Evidence of material expelled from the battery (in the form of residue and thermal damage) was observed in an area that extended about 20 in from the battery installation. No primary structures (that is, those associated with airplane flight loads) exhibited damage; secondary structures—specifically, the avionics rack and the floor panel—exhibited thermal damage near the APU battery's installation location.[19]

The wires that connected to the battery case had been thermally damaged, and the front of the battery case showed thermal damage near the J1 and J3 connectors, where the mechanic's drawing indicated two small flames. The shielded bundle of signal wires, which were the circuits between the BMU and BCU, had burned away from the J1 connector. The copper conductors and shield braiding were melted, which was consistent with resistive heating due to high levels of electrical current (beyond the level that the wires were capable of carrying). The single wire designed to be the battery case ground wire (an intended electrical ground path) remained connected at each end, with the wire insulation partially melted and slightly blackened on the interior surface, which was also consistent with resistive heating due to high levels of electrical current.

The aft E/E bay contains electrical cabinets (referred to as panels) that house components used to distribute electrical power from each engine and the APU. The panel labeled P49 is the source of electrical power distribution for the APU battery bus. No physical damage was noted to the P49 panel. When the circuit breakers on the P49 panel were disengaged, continuity checks of the circuit breakers, contactors, and battery cables to the BCU and battery bus revealed no faults.

The environmental control system (ECS) on the incident airplane was designed to provide pressurized and heated or cooled air to the 787 passenger cabin and E/E bays. The ECS

[18] Hamilton Sundstrand later merged with Goodrich Corporation to form UTC Aerospace Systems.

[19] The avionics rack separated the APU battery from the BCU.

CosMX Exhibit 1003, Page 159 of 512

avionics cooling function was designed to remove smoke overboard through fans in the cooling ducts by changing supply valve positions (and using differential pressure when the airplane is in flight).[20] During this incident, the supply valves (which were electrically driven) lost electrical power after the APU shut down because the APU was the only source of electrical power being used at the time. As a result, smoke generated by the APU battery could not be effectively directed outside the cabin and aft E/E bay.

1.2.4 Additional Airplane-Related Information

According to the Japan Transport Safety Board (JTSB), on January 16, 2013, a "serious incident" involving the main battery occurred aboard a 787 airplane operated by All Nippon Airways during a flight from Yamaguchi to Tokyo, Japan.[21] The pilots received a smoke warning in the cockpit after the airplane climbed above an altitude of 32,000 ft. The airplane made an emergency landing at Takamatsu Airport (TAK), Takamatsu, Japan. Of the 137 airplane occupants, 4 passengers received minor injuries during evacuation via the emergency slides. The JTSB investigated this incident with the NTSB's support and issued its final report on the incident in September 2014 (JTSB 2014).[22]

Boeing reported that, as of the date of the TAK battery event (which occurred 9 days after the BOS battery event), the 787 fleet comprised 50 in-service airplanes that had accumulated 51,662 flight hours and 18,665 cycles.[23] After the BOS and TAK events, Boeing modified the 787 battery design and its installation configuration to include (1) additional insulation between the battery cells, (2) vents in the side of the battery case, (3) a stainless steel enclosure for the battery case, and (4) an ECS duct that vents from the interior of the stainless steel enclosure to the exterior of the airplane to prevent smoke from entering the occupiable space of the airplane. Section 1.8.1 discusses the Federal Aviation Administration (FAA) airworthiness directive (AD) mandating the installation of the new battery (part number LVP65-8-403) aboard US airplanes.[24]

---

[20] The aft E/E bay contains two smoke detectors.

[21] Chapter 1 of Annex 13, "Aircraft Accident and Incident Investigation," to the Convention on International Civil Aviation defines a serious incident as "an incident involving circumstances indicating that there was a high probability of an accident and associated with the operation of an aircraft which, in the case of a manned aircraft, takes place between the time any person boards the aircraft with the intention of flight until such time as all such persons have disembarked."

[22] The JTSB's report on the TAK incident stated that heat generation in a single cell "was probably caused by [an] internal short circuit" which developed into "thermal propagation to other cells, [which] consequently damaged the whole battery." The report also stated that possible contributing factors to the thermal propagation were that "the test conducted during the developmental phase did not appropriately simulate the on-board [battery] configuration, and the effects of internal short circuit were underestimated."

[23] One cycle comprises a complete engine startup and shutdown. The number of 787 flight hours indicated does not include about 6,000 flight test hours.

[24] GS Yuasa assigned this part number to the redesigned battery. The Boeing part number for the redesigned battery is B3856-902.

CosMX Exhibit 1003, Page 160 of 512

On January 14, 2014, an LVP65-8-403 main battery failed on a JAL 787 airplane that was parked at a gate at NRT. (The airplane was being prepared for scheduled flight.) The Japan Civil Aviation Bureau is investigating this incident with assistance from the JTSB and the NTSB. Maintenance personnel reported seeing smoke outside the cockpit window. Preliminary information indicated that one cell had overheated and vented electrolyte and that the enclosure for the battery case contained the vented electrolyte.

1.3 Flight Recorders

The BOS incident airplane was equipped with forward and aft General Electric model EAFR 2100 enhanced airborne flight recorders (EAFR), which recorded cockpit voice recorder (CVR) audio data and FDR parametric data.[25] The forward and aft recorders, which were powered by the left and right 28-volt DC buses, respectively, recorded the same set of flight data independently of each other. The forward recorder had an independent power supply to provide backup power to the recorder for about 10 min if the left 28-volt DC bus lost power.[26] (The aft recorder had no backup power supply.)

The CVR portion of the EAFR recorded 2 hours of audio data from the cockpit area microphone, the captain's audio selector panel/hot microphone, the first officer's audio selector panel/hot microphone, and the jumpseat/observer's position. The audio information from the forward recorder was used to produce a transcription summary for this incident. The summary began at 0828:21, when the airplane was level in cruise flight at 39,000 ft, and ended at 1031:35, when the forward EAFR stopped recording.

According to the transcription summary, at 1021:41, the CVR recorded sounds associated with the APU shutting down. Conversations among maintenance personnel and the turnaround coordinator about the APU shutdown began about 9 seconds later. At 1024:10, the turnaround coordinator reported smoke in the cabin. No voices were heard on the CVR from 1024:22 to the end of the recording (1031:35).

FDR data before 1021:01 showed no abnormal voltage or current indications. At 1021:01, the voltage of the APU battery decreased from 32 to 31 volts. Three seconds later, the data showed a change in current flow from 3 amperes out of the battery to between 44 and 45 amperes into the battery.[27] The current flow into the battery occurred for about 4 seconds; the remainder of the recording showed either no current flow or current flow out of the battery. Between 1021:07 and 1021:09, the battery voltage continued to decrease. At 1021:10, the battery voltage returned to 31 volts. At 1021:27, the battery voltage began decreasing again, reaching

[25] Specifically, the EAFR is a multifunction recorder that records flight (FDR) data; audio (CVR) data; and communication, navigation, and surveillance air traffic management messages. The EAFR is a new recording system with a new flight data recording format that allows multiple predefined frames of data that can vary in length and structure. This format provides more flexibility for storing data than older formats that use a single fixed-frame length and structure. The EAFR is currently installed only on 787 airplanes.

[26] A lithium-ion battery was used for the recorder independent power supply.

[27] This behavior was consistent with the BCU attempting to charge the battery.

CosMX Exhibit 1003, Page 161 of 512

28 volts at 1021:30, and the APU shut down 7 seconds later.[28] Table 2 shows selected events recorded before and after the APU shutdown. The FDR did not record any data indicating that the APU battery voltage had exceeded 32 volts.

Table 2. Events surrounding APU shutdown.

Time	Event
1000:24	Airplane touched down.
1004:10	APU started.
1006:15	Airplane completed turn into parking location.
1006:48	Parking brake set.
1006:52	Engine 1 shut down.
1006:54	Engine 2 shut down.
1021:01	APU battery bus voltage decreased from 32 to 31 volts.
1021:04	APU battery current increased from 3 amperes out of the battery to between 44 and 45 amperes into the battery.
1021:07	APU battery bus voltage decreased to 30 volts.
1021:08	APU battery current flow returned to 3 amperes out of the battery.
1021:09	APU battery bus voltage decreased to 29 volts.
1021:10	APU battery bus voltage increased to 31 volts.
1021:15	Engine indicating and crew alerting system (EICAS) message discrete indicated that the APU battery failed.
1021:27	APU battery bus voltage began decreasing 1 volt per second during the next 3 seconds.
1021:30	APU battery bus voltage reached 28 volts.
1021:37	APU battery bus voltage decreased to zero volts and returned to 28 volts three times, and APU battery current began to move between zero and 4 to 5 amperes out of the battery.
1021:37	APU controller went offline, and APU had shut down.
1021:37	Aft EAFR stopped recording. Forward EAFR continued recording for about 9 min 58 seconds.
1021:40	EICAS message discretes indicated that the left and right 1 and 2 AC buses became unpowered.
1021:41	EICAS message discrete showed that the APU battery failure was no longer indicated.
1022:00	EICAS message discrete indicated that the main battery was discharging.
1022:10	APU controller went back online.
1022:53	EICAS message discrete indicated that the main battery power switch was off.
1023:16	Airplane systems providing data to the EAFR had shut down.
1031:35	Forward EAFR stopped recording.

Note: The APU controller is the source of 32 recorded parameters, including APU shaft speed and APU battery bus voltage.

The EAFR has an integral flight data acquisition function, which receives data from various sources and then transmits those data to the FDR function according to a predetermined schedule for storage into crash-protected memory. If no new value has been received since the last time that a parameter's value was sent to the FDR function, the flight data acquisition function continues to transmit the last value received from the source. These data are referred to as "stale data."

For some parameters, the flight data acquisition function has multiple prioritized data sources from which it receives parameter values. For these parameters, a separate source index

[28] Key parameters that showed the APU battery failure and APU shutdown are presented in figure 2 of the FDR Group Chairman's Factual Report, which is available at www.ntsb.gov in the public docket for this incident (DCA13IA037). The EAFR records two parameters that indicate the APU battery voltage. Details about the sources of these parameters (APU_Batt_VDC_A and DCBus_APU_Battery_Volts) are included in addendum 1 of the FDR Group Chairman's Factual Report.

CosMX Exhibit 1003, Page 162 of 512

parameter that indicates the source being used is generated by the flight data acquisition function and then recorded.[29] For parameters with a source index, stale data are indicated by the source index being set to "no source available." Parameters that have only a single source do not have a source index parameter and thus do not have a recorded indication that the data could be stale.[30] This recording methodology can lead to cases in which apparently valid data continue to be recorded after a parameter source stops providing valid data. This problem delayed the NTSB's complete understanding of the recorded data during the initial stages of this investigation. Section 2.6.1 discusses issues associated with stale data in analyzing accidents, incidents, and maintenance events.

1.4 Incident Battery Examinations

1.4.1 External Observations

The APU battery was examined at the NTSB's materials laboratory in Washington, DC. Observations were documented using a numbering system designating the front of the battery (facing the external power connectors) as side 1, the left side as side 2, the back of the battery (facing the back wall of the aft E/E bay) as side 3, and the right side as side 4.[31]

Side 1 (forward face) of the battery case exhibited black residue and white powdery material on the exterior surface, which were consistent with thermal damage from the flames reported at the front of the case and the application of a dry chemical fire-extinguishing agent by the JAL mechanic, respectively. Side 2 (left side) of the battery case appeared to have the least visible damage of the four battery sides, with some soot residue and an area of buckling observed.

Side 3 (aft face) of the battery case appeared to be more damaged near side 4 than near side 2. Vertical black streaks, which were consistent with residue from dripping liquid, were observed toward side 4 in a location that corresponded to the right aft corner of the battery lid. A roughly oval deposit of black residue appeared on the side 3 upper portion near the side 4 edge. Side 3 had a mostly circular distortion near the lower corner adjoining sides 3 and 4. This distortion was a paint discoloration with about a 1-in diameter and a 0.25-in-wide nodular protrusion in the middle. The protrusion, which is discussed in more detail in section 1.4.4, was located about 1.5 in from the bottom and left edge of the battery case.

Side 4 (right side) of the battery case appeared to have the most extensive damage of the four battery sides. The exterior was heavily coated with black residue that was concentrated near side 3. Thicker black deposits were visible on the right side near the battery lid. Large, mostly

[29] In many cases, a source index parameter defines the source of a group of parameters that are transmitted to the EAFR from the same group of sources.

[30] Left and right radio altitude are among the mandatory parameters that do not have a recorded indication that the data could be stale.

[31] When facing aft in the airplane, the left and right sides of the battery correspond with the left and right sides of the airplane.

CosMX Exhibit 1003, Page 163 of 512

circular areas of thermal damage to the paint were located at the same elevation as the battery cell vent discs (as viewed from the exterior).[32] An area of thermal damage to the paint was adjacent to and opposite from the cell 6 vent disc. A distortion and an area of missing paint and soot were adjacent to and opposite from the cell 7 vent disc. Paint discolorations were visible at the cell 5 and 8 vent locations.

The lid on the battery case was bulged and creased. The right aft lid corner (as viewed from the front of the battery case) exhibited more soot, charring, and residue than the rest of the lid and the most damage to the lid fastening points.[33] Figure 6 shows the bulged battery case lid and side 4 of the battery case.



Figure 6. Right aft corner of the battery lid and side 4 of the battery case.

In addition, the NTSB's examination of the battery found no external fire or heat source that would have caused the battery to overheat (thermal abuse), no impact or other forces imposed on the battery from external sources (mechanical abuse), and no external shorting of wires (electrical abuse) associated with the battery system.

[32] A vent disc is a scored plate that ruptures when the internal pressure in a cell reaches a predetermined level. The battery was configured with the vent disc for each cell oriented toward the exterior of the battery.

[33] Eight mounting tabs were used to attach the battery lid to the battery case, and screws were used to fasten the mounting tabs. The two mounting tabs on side 1 remained engaged with the screws. The mounting tabs on sides 2 through 4 had torn from the screws by gross deformation and overstress. The torn mounting tabs and their fracture surfaces exhibited deposits consistent with breakage during the battery failure.

CosMX Exhibit 1003, Page 164 of 512

1.4.2 Radiographic Examinations of Incident Battery and Cells

The NTSB conducted radiographic examinations at Chesapeake Testing in Belcamp, Maryland, to examine and document the internal configuration of the incident airplane's main and APU batteries before disassembly and six of the eight APU battery cells after removal from the battery.[34] The batteries were documented using x-ray computed tomography (CT) scans and digital radiography, and the battery cells were documented using CT scans. The images of the components were examined for signs of missing or damaged parts, contamination, or other anomalies.

The CT scans of the main battery showed no anomalies outside the cells. (The main battery cells were subsequently examined for internal anomalies, as discussed in section 1.5.1.) The CT scans of the APU battery showed a breach of the battery case that corresponded with a breach of the cell 5 wall. The CT scans of the APU battery also showed that several cells were distorted with an expanded or a contracted profile, as shown in figure 7; several current collectors inside the cells had separated from their header assemblies; and some current collector fingers were out of their designed parallel alignment.

[34] Cells 2 and 8 were not included in the radiographic examinations because those cells were used to validate the cutting procedure that would be employed during the NTSB's internal examinations of all of the cells (see section 1.4.5). Cell 2 was chosen for the procedure because the cell exhibited relatively less thermal damage and cell case deformation than other cells in the battery. Cell 8 was also chosen for the procedure because, on the basis of available external cell evidence, that cell was the least likely of the more heavily damaged cells on the right side of the battery (cells 5 through 8) to have been the origination point for the event. In addition to the radiographic examinations of the batteries and cells, neutron computed tomography studies were conducted at the National Institute of Standards and Technology in Gaithersburg, Maryland, to examine and document the material distribution on the header assembly of each cell in the incident battery.

CosMX Exhibit 1003, Page 165 of 512

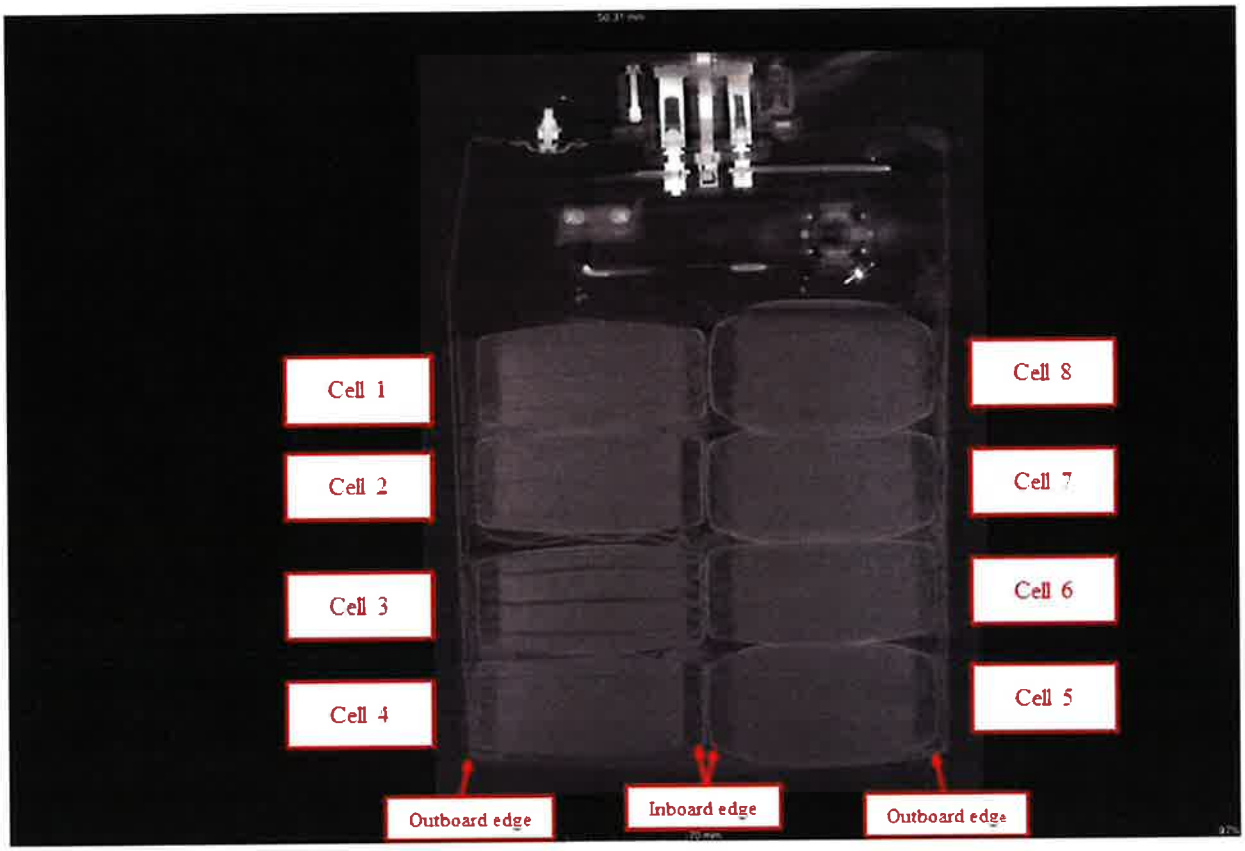


Figure 7. Cross-sectional view of the APU battery.

Note: This image was taken at the approximate midpoint of the cells. Due to the orientation of the incident APU battery during CT scanning, the resulting images appeared as mirror images of the battery. Thus, the orientation of the cells in this figure is different than the orientation of cells in other figures showing the APU battery.

The six individual APU battery cells that were examined were cells 1 and 3 through 7. The CT scans for cells 1 and 3 showed that the cells' current collectors were intact and that the windings were not uniform in some areas due to ripples and separations. The CT scans for cell 4 showed that the cell had no separations within the winding layers and that the current collectors were intact. Findings from the CT scans for cells 5, 6, and 7 included the following:

- Cell 5: Two cell wall breaches in separate locations were identified. The larger of the two breaches appeared to consist of separate smaller holes. The smaller breach appeared to consist of a single hole with some material missing from the outer cell wall around the hole. The areas inside the cell near the breaches differed from the general appearance of the cell. Also, two of the six aluminum (cathode) current collector fingers had breaks with rounded material on the ends. These breaks, as shown in figure 8, appeared as complete separations through the fingers. The current collector finger breaks occurred in the center winding. The other four aluminum current collectors and all of the copper (anode) current collectors were intact.

- Cell 6: Four of the six aluminum current collector fingers had breaks, as shown in figure 9, including one with breaks at multiple locations and another that was missing more material at the breakage location than the other current collector fingers with breaks. The current collector finger breaks occurred in the winding closest to cell 5 and the center winding. The other two aluminum current collectors and all of the copper current collectors were intact.

- Cell 7: Four of the six aluminum current collector fingers had breaks, including one with multiple breaks. All six current collector fingers appeared to be displaced from their original positions. The current collector finger breaks occurred in the winding closest to cell 6 and the center winding. The other two aluminum current collectors and all of the copper current collectors were intact.

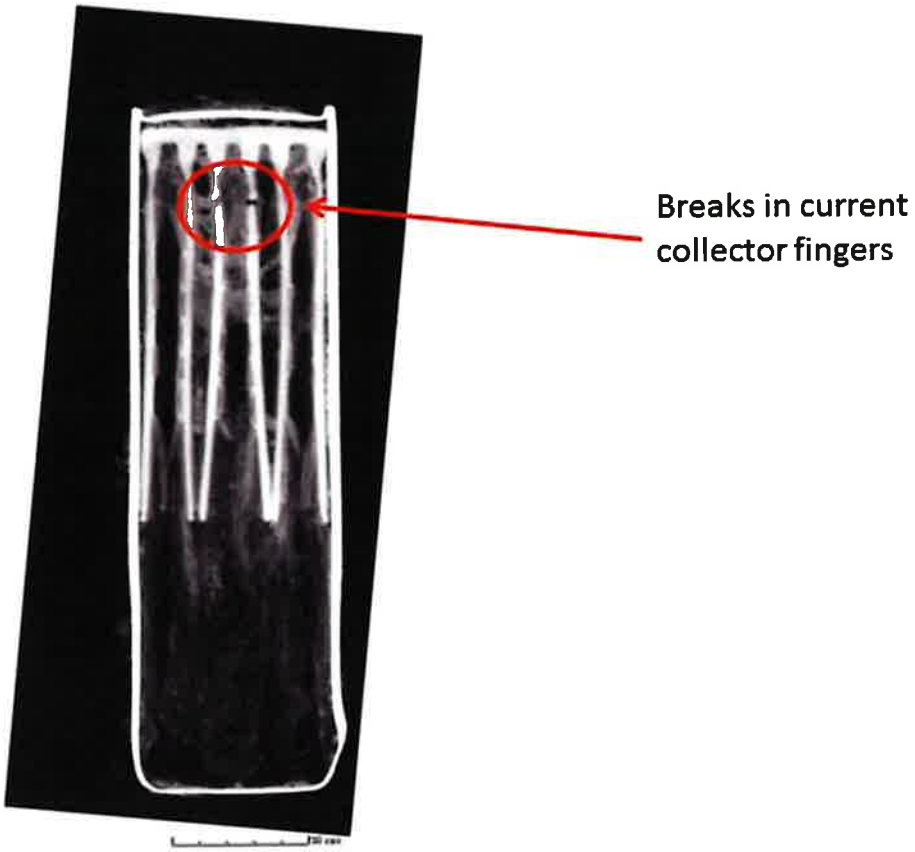


Figure 8. Cross-sectional view of cell 5 aluminum current collectors.

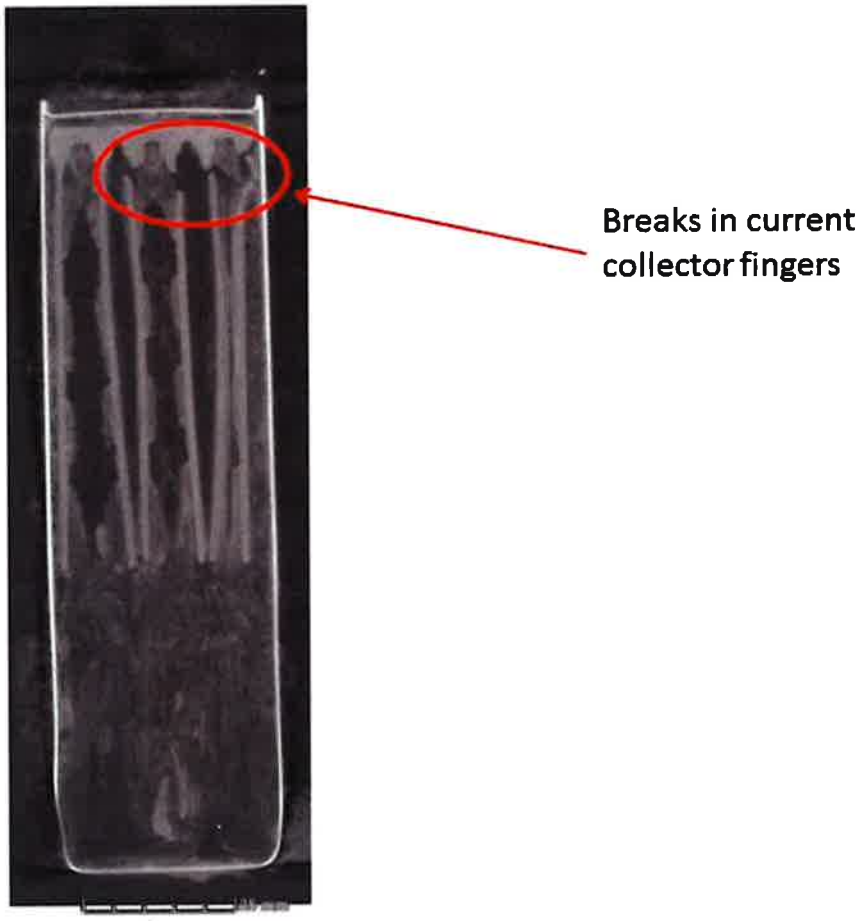


Figure 9. Cross-sectional view of cell 6 aluminum current collectors.

1.4.3 Disassembly of Incident Battery

After charred debris from the top of the battery case was removed, the physical condition of the BMU's sensing wiring harness was examined and was found to have damage consistent with exposure to a high-temperature environment. The damage to the wire insulation degraded progressively from the left side of the battery (cells 1 through 4), where the insulation was thermally discolored, to the right side of the battery (cells 5 through 8), where the insulation was missing for cells 5 and 6 (mostly in the position of cell 5), charred for cell 7, and thermally discolored for cell 8. Also, the wires above cells 5 and 6 were bare, indicating that the area of the most severe thermal damage to the wiring harness was located above cells 5 and 6.

Side 2 of the battery case was folded down to reveal cells 1 through 4. The insulation sheet adjacent to the battery cells remained in place. Behind this insulation sheet, a portion of the other insulation sheet was visible but was missing some sections. Although the insulation

between cells 1 through 4 was damaged, the material could be distinguished from other thermally damaged material in the battery case. The interior surface of side 2 had a clean area with a similar outline to that of an insulation sheet. The rest of the interior surface of side 2 was coated with residue.

Battery case side 4 was folded down to reveal cells 5 through 8. The cells exhibited a darkened, charred appearance. The insulation sheets were completely charred and could not be distinguished from each other and other thermally damaged material in the battery case, and portions of the charred insulation adhered to the cells. The interior surface of side 4 had portions of the charred insulation adhering to areas where the insulation sheets contacted the interior surface. The rest of the interior surface of side 4 was coated with residue.

Side 3 of the battery case was folded down to reveal the sides of cells 4 and 5. The side of cell 4 had staining that resembled a flowing residue. The side of cell 5 had similar staining but also had a cleaner area on the cell case without staining, combustion products, and fire-extinguishing residue. The corresponding area on the interior surface of side 3 was similarly clean and had large portions of insulation that had adhered to the case. The insulation on side 3 was thermally degraded and fragmented, and the portions of the insulation adhering to the battery case directly behind cell 5 exhibited some thinning.

The battery case contained no foreign object debris (FOD). There was no evidence of cell-to-battery case shorting before the thermal event, bus bar shorting, or resistive heating of the bus bars (including those leading to the J1 connector through the contactor and Hall effect current sensor) within the battery case. There were no loose electrical connections at terminals or on BMU wires. There was also no visible evidence of water (resulting from condensation) within the battery case or external surfaces of the battery cells.

Cells 1 through 4 exhibited the least thermal and mechanical damage. Of these cells, cell 3 appeared to be the most thermally damaged. Cells 1 through 3 had vented (with their vent discs opened slightly), and the cell 4 vent disc remained intact.[35] Even though the cell 4 vent disc did not rupture, weight measurements for the cell were lower than specifications.

Cells 5 through 8 exhibited the most thermal and mechanical damage, as shown by the thermal decomposition and degradation of the materials in contact with these cells. These materials included bisphenol A thermoplastic polyester and crystalline thermoplastic; the lowest decomposition temperature of these materials is 550°F. Thermal damage was the most severe near cells 5 and 6, as shown in figure 10. The vent discs on cells 5 through 8 had ruptured in a manner indicative of a rapid pressure release.[36] Cells 5 through 8 sustained gross mechanical plastic deformation with cells pressing into adjacent cells.

---

[35] The vent discs are scored with an "x" pattern, which enables preferential tearing when the disc ruptures, creating four independent petals. For the vent discs on cells 1 through 3, the four petals had parted slightly but remained in the same plane.

[36] For the vent discs on cells 5 through 8, the four petals were generally splayed out and positioned out of plane with each disc's original position, which was indicative of a more forceful opening than that for the vent discs for cells 1 through 4. For cell 5, the petal closest to side 1 of the cell was completely missing.

CosMX Exhibit 1003, Page 169 of 512

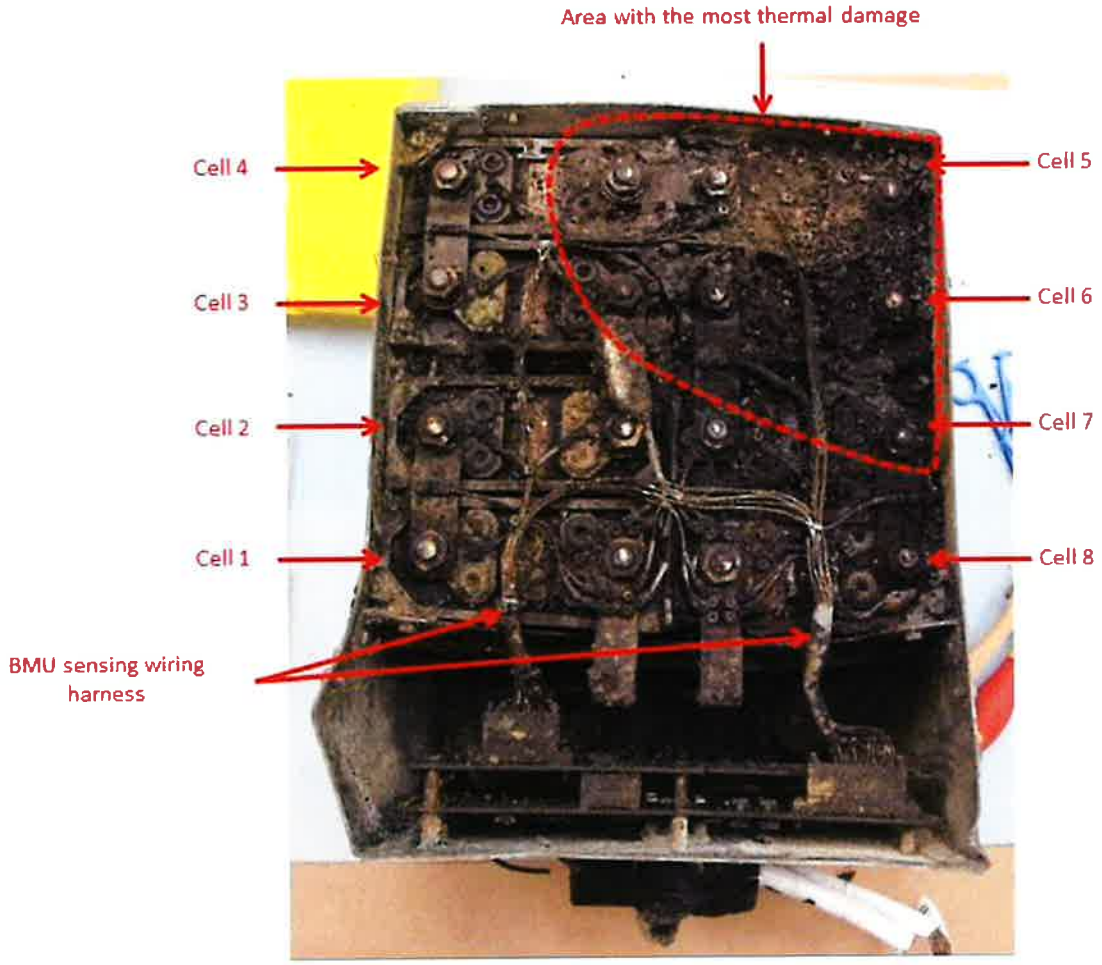
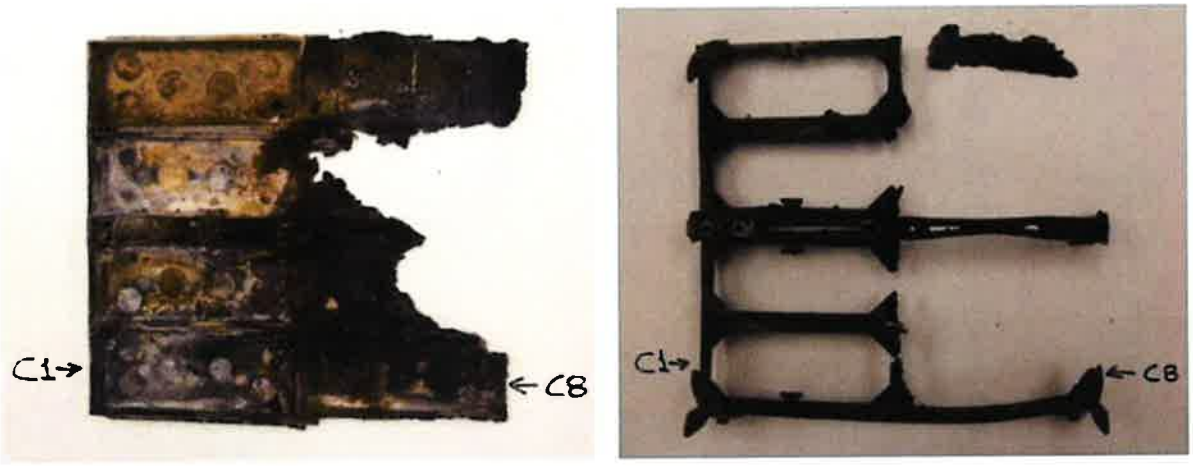


Figure 10. Thermal damage to battery.

The bus bars were removed from the cell terminal assemblies to allow extraction of the battery cells. The electrical contact surfaces of the bus bars showed no indications of localized resistive heating or arcing.

Debris and discoloration consistent with thermal damage were present on the cell 1 through 4 footprints on the lower fixation tray. The footprints of cells 5 through 8 were thermally decomposed, as shown in figure 11. Portions of the lower fixation tray under cells 5 and 6 could not be readily distinguished from other thermally damaged materials in the battery case. The portions of the upper fixation tray that contacted cells 1 through 4 sustained less damage than the portions that contacted cells 5 through 8. The cell 4 upper fixation tray imprint remained mostly intact, but the imprints for cells 1 through 3 showed progressively more damage. Minimal material remained from the portions of the upper fixation tray that contacted cells 5 through 8, which is also shown in figure 11.

CosMX Exhibit 1003, Page 170 of 512



Lower Upper

Figure 11. Lower and upper fixation trays.

The J3 connector and receptacle were also examined. The J3 connector had dark deposits on one of the blades on the positive terminal. Analysis of the dark deposits revealed the presence of a hydrocarbon. The other blades on the positive terminal and the blades on the negative terminal of the connector appeared clean with no deposits, stains, or discoloration. The J3 receptacle had thermally induced deformation in one corner. The terminals on the receptacle showed no indications of deposits, stains, or discoloration.

1.4.4 Battery Case Protrusion and Corresponding Cell Case Damage

As stated in section 1.4.1, the battery case exhibited a 0.25-in-wide nodular protrusion on the lower left of side 3, as shown in figure 12. The protrusion extended about 0.12 in from the case. The protrusion appeared metallic and had no paint. Two concentric rings surrounding the protrusion corresponded with the discoloration of exterior paint. Deposits consistent with thermally degraded materials were observed on and near the protrusion. Three holes on the periphery of the protrusion were identified. The largest of these holes was elliptical in shape, with its longest dimension measuring 0.080 in. The two other holes, which were similar in size, measured about 0.004 in. Most of the interior side of the protrusion contained dull gray flaky material consistent with spatter, as well as shiny black material consistent with charred plastics and tars.

CosMX Exhibit 1003, Page 171 of 512

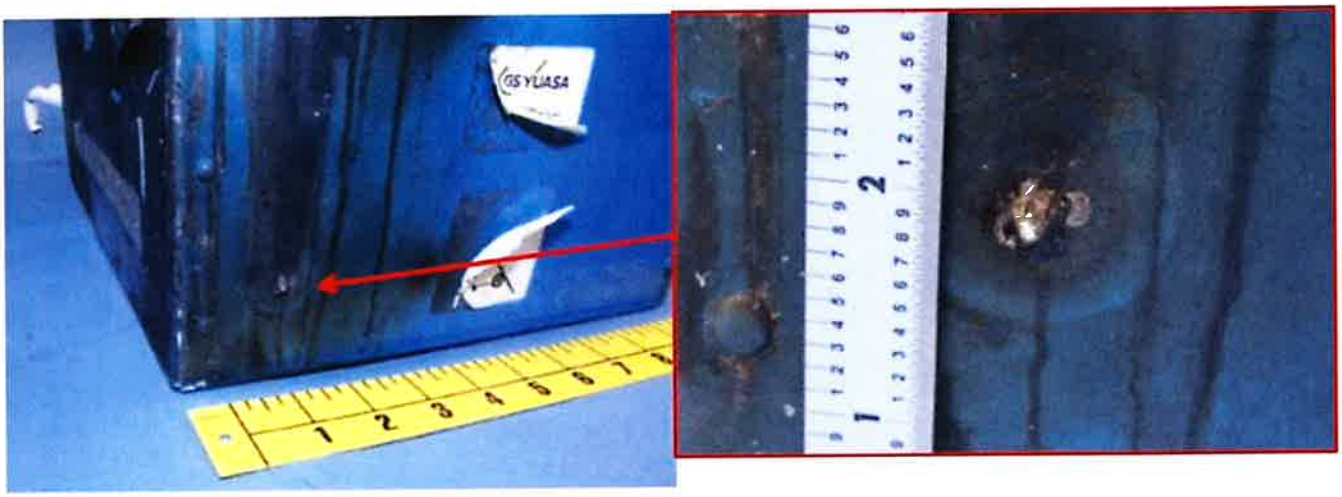


Figure 12. Protrusion on the lower left of battery case side 3.

The side of the cell 5 case that faced side 3 of the battery case had been heavily damaged, especially toward its edges and corners. Four holes were identified on the lower portions of this side of the cell case, all of which exhibited large amounts of dark, rough-appearing features consistent with decomposition products. The largest hole (in terms of size and amount of decomposition products) was about 0.2 in; this hole corresponded with the location of the protrusion on the battery case.

The battery case protrusion was examined using a scanning electron microscope (SEM) and energy dispersive x-ray spectroscopy (EDS). The examinations found that the observed damage was consistent with electrical arcing and contact between the cell 5 case and the battery case.[37] (Before contact, the cell 5 case was located about 0.2 in from the battery case with a plastic insulator in the space.) Specifically, evidence of material transfer between the cases was found on the interior surface of the battery case and the exterior surface of the cell case. Also, the battery case exhibited no inward deformation at the protrusion, but the cell case exhibited outward expansion. SEM and EDS examinations further showed that all the holes on the cell 5 case contained various compounds and alloys that were not consistent with the cell case material (a stainless steel) but were instead consistent with the battery case material (an aluminum alloy).

1.4.5 Disassembly of Incident Battery Cells

The NTSB conducted a teardown of each individual battery cell to determine whether the cells contained any anomalies.[38] The teardown, which was conducted in the NTSB's materials

[37] The other seven cells did not exhibit any evidence of electrical arcing on the exterior of the cell cases.

[38] Cell observations were documented using a numbering system that was similar to that for the battery. The front of the cell (facing the J1 and J3 power connectors) was designated as side 1, the left side was designated as side 2, the back of the cell (facing the back wall of the aft E/E bay) was designated as side 3, and the right side was designated as side 4.

CosMX Exhibit 1003, Page 172 of 512

laboratory, consisted of disassembling the cell cases, removing the electrode windings, separating the individual windings from the header assembly and current collectors, and unrolling the individual windings. Internal evaluations of each cell consisted of visual, chemical, electrical, and other observations about the overall condition of the internal cell components, the internal surface of the cell case, the current collectors, the header assembly, and the windings.

The windings had been heavily damaged as a result of the incident. The internal evaluations of the cells found no evidence of preexisting defects in, or internal damage to, the copper anode, aluminum cathode, or polyolefin separator. There was also no evidence of preexisting current collector separation, FOD of sufficient size within the cells to cause an internal failure that could lead to thermal runaway, and lithium deposits within the cell windings.

As stated in section 1.4.3, external observations of the cells showed that cells 5 through 8 were more thermally damaged than cells 1 through 4. In particular, the thermal damage to the materials near cells 5 through 8 and the opened vent discs of those cells (with the vent disc petals either missing or peeled outward from the cell cases) were consistent with a higher pressure, more energetic event in cells 5 through 8 compared with cells 1 through 4. The internal examination of the cells showed differences in the degradation of materials that were also consistent with higher temperature exposure in cells 5 through 8.

Cells 1 through 4, when opened, were generally wet and had a smell consistent with liquid electrolyte. The components of cells 1 through 4, including the anode, separator, and cathode, were found intact with most damage limited to a change in opacity in portions of the separator, which was consistent with the activation of the shutdown properties of the separator.[39] Damage patterns in cells 1 through 4 were consistent with greater external thermal exposure on battery side 4, which was closest to cells 5 through 8. The damage patterns were also consistent with less external thermal exposure on side 2, which faced the exterior of the battery case. In general, the windings for cells 1 through 4 exhibited damage consistent with greater thermal exposure on the exterior of the cells and the sides that were closer to other cells compared with the interior of the cells and the sides that were exposed to open areas within the battery case. There was no visual evidence of electrical short circuits found in the windings of cells 1 through 4.

Cells 5 through 8, when opened, were dry and did not have a smell consistent with liquid electrolyte. The components of cells 5 through 8 exhibited evidence of damage consistent with high heat exposure and localized high current, including several aluminum current collector fingers that had separated from their header assemblies. For each cell, the aluminum cathode was heavily damaged and was missing large sections of the foil. The copper anode was generally intact but contained pinholes and discolorations with areas of missing active coating material. The separator was missing, which was consistent with thermal exposure above the melting

[39] The separator is opaque but becomes more transparent as it thermally degrades. When this degradation occurs, the pores in the separator close, shutting down the lithium-ion transport between the anode and cathode. The shutdown properties of the separator activate just before melting begins.

CosMX Exhibit 1003, Page 173 of 512

temperature of the separator material. Sections 1.4.5.1 through 1.4.5.4 provide additional details about the teardown of cells 5 through 8, respectively.[40]

1.4.5.1 Cell 5

The cell 5 examination found evidence of arcing damage on the cell case interior and relatively minor damage to the winding adjacent to the protrusion in the battery case. The cell case was mostly intact. The lower half of the winding closest to battery case side 3 and adjacent to the protrusion in the battery case had adhered to the cell case. The appearance of the cell case and the adherence of the electrodes were consistent with localized heating, melting, separation, and solidification from electrical arcing. No visible portion of the thermoplastic insulation in the cell case remained. Black residue was present on the interior surfaces of the cell case and the exterior of the windings. SEM/EDS analysis found that the chemical composition of the residue was consistent with that of the thermoplastic insulation.

The condition of the aluminum cathode and the copper anode in each winding was consistent with high heat exposure. Most of the cathode material was present but was brittle. Most of the uncoated aluminum foil (at the edges of the windings) remained intact, but portions were missing. The coated aluminum foil was discolored and fractured with areas of the foil missing generally near the header (top) or footer (bottom) fold. Most of the missing aluminum foil had melted and solidified into oblong-shaped globules. The copper foil was intact but had discolorations and small pinholes that propagated through several wraps. The coating on the copper foil had mostly flaked off. The separator was not found during the examination.

For the winding that was closest to battery case side 3, the copper foil was discolored at the header fold with small ripples. The copper foil also exhibited a band of darker color adjacent to the nodular protrusion, which was consistent with high heat exposure. This band of color propagated from the exterior to interior wraps of the winding. The center winding copper foil had ripples along the header fold. This winding appeared to have more overall damage than the other two windings. The winding closest to cell 6 showed the most fragmentation of the aluminum foil and the coated material. The first and second wraps of the winding had thermally adhered to the interior of the cell case, and portions of the first wrap had also thermally adhered to subsequent wraps of the winding. One of the innermost wraps showed folds in the copper foil on the side facing cell 6, which were present through several layers of the winding, as shown in figure 13. Other notable features found during the winding examination were the lack of any sizeable repeating rifts in the windings and the greater amount of damage to the exterior wraps of the windings compared with the interior wraps.

[40] For additional information about the teardown of cells 1 through 4, see Materials Laboratory Factual Report 13-060, which is available at www.ntsb.gov in the public docket for this incident. Also, during the teardown of the eight cells, numerous specimens were excised to examine, using SEM and EDS, the physical and chemical characteristics of various internal components. Materials Laboratory Factual Report 13-060 also includes information from these examinations.

CosMX Exhibit 1003, Page 174 of 512



Figure 13. Cell 5 winding closest to cell 6.

The pair of aluminum current collectors for the center winding (which in this cell were adjacent to the vent disc) were no longer connected to the header assembly. The detachment of the current collectors occurred at the top of the current collector fingers where the collectors were designed to act as a fusible link. SEM examinations found that the breaks were consistent with thermal fracture associated with high current, as shown by the CT scans of the rounded features at the fracture surfaces (see figure 8). The two other pairs of aluminum current collectors and the three pairs of copper current collectors were intact.

1.4.5.2 Cell 6

The interior of the cell 6 case exhibited a blackened appearance. Portions of the windings and other charred materials were stuck to the bottom of the case on sides 1 and 3. There was no evidence of electrical arcing or short circuits between the windings and the cell case.

The windings exhibited varying degrees of thermal damage based on the amount of aluminum cathode material remaining and the thermal discoloration of the copper anode foil. The winding closest to cell 5 had the least cathode material remaining, and the winding closest to cell 7 had the most cathode material remaining, which was consistent with higher temperatures on side 3 of the cell that tapered off toward side 1. The separator material had melted and could not be identified in all three windings.

For the winding closest to cell 5 and the center winding, the aluminum foil was mostly missing, with the active material coating remaining. Remnants of the aluminum foil were visible as specks or small blobs of solidified aluminum. For the winding closest to cell 7, the aluminum foil was intact but was brittle. The second wrap included an area where the aluminum foil had fused to the copper foil.

CosMX Exhibit 1003, Page 175 of 512

For all three windings, large portions of the active material coating for the copper foil had delaminated, exposing large areas of the foil. Pinholes and localized areas of thermal discoloration, which were consistent with localized hot spots, were observed near the edges of the copper foil. The winding closest to cell 5 showed areas of concentrated thermal discoloration that appeared in a repeating pattern on the copper foil, as shown in figure 14. One area of thermal discoloration began on multiple exterior wraps and became lighter toward the interior wraps. Another area of thermal discoloration began about midway through the wraps and continued all of the way to the interior wraps. This pattern of thermal discoloration, which was concentrated on the side of the foil closest to the copper current collectors, exhibited a radiating pattern of wrinkles. The center winding showed an area of thermal discoloration that began at one of the outermost wraps and continued into the winding. The winding closest to cell 7 showed a repeating area of thermal discoloration at one of the outermost wraps.



Figure 14. Cell 6 winding closest to cell 5.

The current collector sides of the winding assemblies (cell sides 2 and 4) appeared blackened and charred and had no remaining insulation material. The copper current collectors were intact and attached to the windings. The aluminum current collectors exhibited fractures with areas of missing material, and two of the three pairs of aluminum current collectors (those in the winding closest to cell 5 and the center winding) had fused and were disconnected from the header assembly. The other pair of aluminum current collectors were intact.

1.4.5.3 Cell 7

The condition of the cell 7 electrodes was consistent with high heat exposure. The three windings had varying amounts of the aluminum cathode foil remaining. The winding closest to cell 8 had more aluminum foil and active material remaining than the two windings that were closer to cell 6. In each of the windings, the coated aluminum was discolored and fractured with areas of aluminum missing generally near the header or footer fold.

The copper anode foil in the winding closest to cell 6 was discolored at the header fold and had small ripples. The copper foil in the center winding was missing a section adjacent to the vent disc, which was consistent with high thermal exposure. The missing section propagated through the winding, with the most material missing from the exterior of an outermost wrap. The

CosMX Exhibit 1003, Page 176 of 512

copper foil in the winding closest to cell 8 was discolored at the header fold and contained small ripples in a radiating pattern. The separator was not found.

The pair of aluminum current collectors for the center winding and the pair for the winding closest to cell 6 were no longer connected to the header assembly. The separation in these current collectors occurred at the top of the current collector fingers where the collectors were designed to act as a fusible link. The center winding current collector fingers were separated in one location, and the current collector fingers closest to cell 6 were separated in several locations. The other pair of aluminum current collectors and the three pairs of copper current collectors were intact.

1.4.5.4 Cell 8

For cell 8, there was no discernible difference in the amount of thermal damage between the cathode and anode sides of the winding assemblies. All of the current collectors were intact and showed no readily identifiable abnormalities.

Portions of copper anode windings adhered to the side 1 and side 3 surfaces of the cell case and exhibited hues of purple and blue, consistent with exposure to high temperatures in an oxidizing environment. The cell case surfaces did not reveal any evidence of electrical arcing. The side 2 and side 4 surfaces exhibited a blackened appearance, and charred thermoplastic insulation had adhered to the surfaces. The bottom of the cell case also exhibited a blackened appearance with pieces of charred material adhering to the bottom surface.

The aluminum cathode foil in all three windings was found melted and discontinuous, but the winding closest to cell 7 appeared to be exposed to the highest temperatures because the aluminum foil in the center winding and the winding closest to the BMU had more intact aluminum remaining. (More aluminum remained on the winding closest to the BMU than on the center winding.) For each winding, the copper anode foil could be seen in the areas where the aluminum foil was missing. Small globules of solidified aluminum were interspersed throughout the remaining carbon active material. The separator material had completely melted and could not be identified.

For the winding closest to cell 7, most of the copper foil exhibited discoloration consistent with severe thermal exposure, particularly along the edge where the electrode attached to the current collector near the header fold of the winding. This discoloration continued throughout the winding. The center winding and the winding closest to the BMU showed concentrated thermal discoloration along the edge of the copper foils where they had been attached to the current collector near the header fold of the windings. This discoloration also continued throughout the windings. Areas speckled with small holes appeared throughout the copper foils, some of which continued through several wraps of the windings.

1.4.5.5 TIAX Examination of Cell Teardown Samples

The NTSB contracted with TIAX LLC of Lexington, Massachusetts, to independently examine and analyze cell 6 samples (which included remnants from all three cell windings) to determine if any internal short circuit indicators were present. TIAX's examination of the cell 6

CosMX Exhibit 1003, Page 177 of 512

evidence confirmed the findings of the NTSB's cell 6 examination (TIAX *Review* 2013). For example, TIAX determined that the winding closest to cell 5 was more thermally and physically damaged than the other two windings, with almost no aluminum cathode foil remaining; the winding closest to cell 7 had the least damage. TIAX found that most of the aluminum current collectors and all of the separators had melted and that a major portion of the copper (anode) current collectors remained.[41] TIAX also found that most of the copper current collectors had small holes, especially near wrinkled and folded areas of the copper foil. TIAX found no evidence of foreign metal.

TIAX's examination of the winding closest to cell 5 showed regions of thermal discoloration on the copper current collector. TIAX indicated that such areas could be consistent with the presence of an internal short but that it was not possible to determine whether a short could have occurred locally or developed from an external source.

TIAX's examination of the remaining copper current collectors showed that, in the winding closest to cell 7 and the center winding (which, as previously stated, were less damaged than the winding closest to cell 5), the windings' outer regions appeared more damaged thermally than the inner regions. TIAX indicated that this observation was consistent with "an origin of thermal stress" outside these windings with elevated temperatures that decreased toward the windings' inner regions.

Some abnormalities were observed in multiple regions of the windings. For example, a significant amount of beaded metal was observed around the edge of an irregularly shaped hole in a copper current collector in the winding closest to cell 5. TIAX noted that this type of formation could indicate the highest temperatures reached during the incident. The NTSB analyzed the ridges using EDS and found that the beads at the edge of the irregularly shaped hole were copper, which indicated that the hole had resulted from the melting of copper.

1.5 Exemplar Battery Examinations and Testing

1.5.1 Radiographic Examinations of Exemplar Battery Cells

Additional radiographic studies were conducted to examine and document the internal configuration of individual battery cells from five batteries. One of the batteries was the main battery installed on the incident airplane (referred to as battery 412); the other four batteries (referred to as batteries 149, 305, 344, and 376) were provided by Boeing.[42] These batteries had been installed on 787 airplanes being assembled at Boeing but were removed before any flight

[41] TIAX referred to the current collector fingers and the foils of the electrode winding assemblies as current collectors.

[42] The battery numbers reflect the battery serial numbers.

CosMX Exhibit 1003, Page 178 of 512

time because the batteries overdischarged and latched.[43] The CT scans of these cells were examined for indications of missing or damaged parts, contamination, or other anomalies.[44]

The CT scans showed that all of the cells from all five batteries contained areas of wrinkled and/or separated windings. Three batteries (149, 376, and 412) showed an anomaly (specifically, a small protrusion from the insulator) in the aluminum terminal plate for one cell; one battery (305) showed this anomaly for two cells. Battery 305 showed a measureable angle between the aluminum current collectors and the cell header in one cell; battery 149 showed this condition for two cells. (The measured angles ranged from about 1.0° to 1.7°.) Battery 149 also showed a localized bulge in one cell's wall. In addition, battery 305 showed copper current collectors that had out-of-alignment clips in two cells.

1.5.2 Cell Soft-Short Tests

A soft short can occur when the electrical isolation between the positive and negative electrodes of a cell is compromised. TIAX indicated that features creating soft shorts could reside undetected within a cell and develop slowly over time. TIAX further indicated that some soft shorts could dissipate over time, whereas others could become severe enough to result in the early failure of a battery (a loss of capacity and failure to hold a charge) or progress to "a more serious, higher-magnitude short" that could cause "catastrophic failure of the cell" (TIAX *Report* 2013).

The Naval Surface Warfare Center, Carderock Division, and TIAX performed two different types of nondestructive soft-short testing. A total of 40 cells from the incident airplane main battery and the four batteries that Boeing provided were used for the soft-short testing. The test results were used along with the radiographic examination results (discussed in section 1.5.1) to identify possible cells for TIAX's destructive physical analysis (DPA) of an exemplar battery cell, as discussed in section 1.5.3.

The Carderock soft-short testing involved a procedure that monitored cell self-discharge rate decays, which, for lithium-ion cells, occur from current leakage across the separator.[45] The test procedure discharged cells to a low state of charge, removed the discharge load, and observed the cells during a 1- to 2-week period to determine whether any anomalous decays in cell voltage occurred.[46] (Voltage decay is an indicator of a potential soft-short formation within

---

[43] Overdischarging of the battery occurs when the battery or any cell is below a predetermined voltage. If a cell's voltage drops below the predetermined level, the BMU latches a fault and prevents the battery from recharging.

[44] Before CT scanning began, the five exemplar batteries were disassembled at the Naval Surface Warfare Center, Carderock Division, US Department of the Navy. During disassembly, the batteries were evaluated for construction consistency and the presence of FOD. No anomalies were found.

[45] The Carderock soft-short testing was based on the Darcy test method, which was developed by the battery group lead for projects and integration at the National Aeronautics and Space Administration's (NASA) Johnson Space Center in Houston, Texas.

[46] State of charge is the percent of electrical potential between the designed minimum and maximum voltage potentials.

CosMX Exhibit 1003, Page 179 of 512

the cell.) None of the eight cells from the five batteries exhibited anomalous decays in cell voltage during the observation period.

The TIAX soft-short testing involved (1) charging each cell individually to the nominal voltage of 3.7 volts, (2) placing each cell test group in a pre-test configuration for 12 hours to equalize any variations in the state of charge, and (3) connecting each cell group to soft-short test instrumentation and monitoring the response of each cell for 24 hours to measure the level of self-discharge of each battery cell.[47] (According to TIAX, an internal short could have "an anomalously higher level of self-discharge" compared with other cells in the test group.) TIAX's report on the testing indicated that "all [40] cells showed normal (short-free) response characteristics."

UL conducted additional soft-short-related tests, referred to as aging sorting tests. UL conducted these tests to identify cells with possible internal anomalies because, according to UL, cells with such anomalies could exhibit higher self-discharging rates than cells without internal anomalies (Tabaddor and others 2014). The testing, which was conducted at temperatures of 77°F, 32°F, and -0.4°F, produced generally consistent results among the cells in each battery. The testing found all but one cell to be within acceptable limits. (At -0.4°F, a cell in one battery displayed a performance change in the discharge rate that differed from the other cells; this characteristic had not been displayed at other temperatures, and the specific cause of the difference was not determined.)

1.5.3 Examinations of Cells From the Incident Airplane Main Battery

TIAX and UL performed separate DPAs of cells from battery 412 to note any abnormalities in the cells. The laboratories used different methods to conduct the DPAs, but both laboratories' DPAs found areas in the cell windings that were susceptible to lithium deposits.

TIAX conducted coin cell tests before its DPA to determine the anode-to-cathode ratio in the cells and the tolerance of the electrodes to the specific charging conditions likely to lead to lithium deposits.[48] The coin cells were built from samples of electrodes and electrolyte harvested from cell 4 in battery 344. According to TIAX, the tests showed that (1) the anode-to-cathode ratio had "a large anode capacity excess," which would be consistent with a cell designed to avoid lithium deposits on the anode, and (2) voltage, charging current, and temperature extremes (within allowed operational ranges for the cell) did not produce visual evidence of lithium deposits (TIAX 2014).[49] Thus, according to the results of the coin cell tests, the LVP65 cell chemistry was not susceptible to lithium deposits under high-current or low-temperature conditions.

---

[47] The TIAX soft-short testing, which was based on a proprietary test method, was quicker and more sensitive than the Carderock soft-short testing.

[48] Coin cells are small specimens extracted from battery cells that are used to examine the electrochemical properties of the anode and cathode, excluding cell- and battery-level effects.

[49] According to GS Yuasa, the 787 battery cells were designed so that the capacity of the anode was greater than that in previous cell designs.

CosMX Exhibit 1003, Page 180 of 512

Before TIAX's DPA, cell 1 in battery 412 was charged to the maximum voltage allowed by the BMU (4.2 volts) at the maximum normal charging current (46 amperes) at 32°F to simulate the worst-case conditions for potential lithium deposits (within the airplane's specified operating envelope).[50] A fully charged cell, in which the anode appears bright gold in color, facilitated the identification of potential abnormalities. This process was repeated 20 times (with rest periods in between each charging cycle) before the DPA was performed. According to TIAX's report, the following abnormalities were observed during the DPA:

- More than 100 areas of "ingressed under-lithiation" of the anode (that is, areas of the anode that were incompletely charged) were found in each winding.

- More than 90 full creases spanning the width of the electrodes and several hundred partial creases (that is, those that did not run from one side of an electrode to its other side) were found in all three windings.[51] The full creases in the anodes were located generally where the connection to the current collectors (along the edges) ended. Many of the full and partial creases showed features consistent with underlithiation of the anode.

- A total of 61 clusters of silver-colored deposits were located in the outer two windings, with fewer clusters located in the center winding.[52] These deposits were generally adjacent to underlithiated areas on the anode. According to TIAX, these areas indicated that mechanical abnormalities in the windings resulted in uneven charging of the anode, which might have caused lithium to deposit adjacent to underlithiated areas.

Samples of the silver-colored deposits observed during TIAX's DPA were analyzed at the Naval Surface Warfare Center, Carderock Division, using x-ray photoelectron spectroscopy. The analysis showed that the deposits contained lithium along with the constituents of the electrolyte (Mansour and others 2014). No metallic elements besides lithium were found.

The DPAs that UL performed were conducted as part of testing to determine whether potential risks of cell degradation, failure, or loss of performance under specific applications, such as low temperature, existed for LVP65 cells. The DPAs involved three cells from battery 412 (cells 3, 5, and 6). All of the test cells were at 100% state of charge (4.025 volts). Cell 3 was subjected to pulse charging at -0.4°F, cell 5 was subjected to normal constant-current constant-voltage charging at 32°F, and cell 6 was subjected to pulse charging at 77°F.[53] The pulse

[50] The DPA could not be performed at the battery's minimum operating temperature (-0.4°F) because, upon charging at this temperature, the voltage reached 4.025 volts rapidly, causing the current to spike and drop. Thus, high current could not be sustained long enough to produce lithium deposits.

[51] The normal folds at the top and bottom of the windings were not considered to be creases.

[52] Each cluster represented an entire feature area and not the number of individual deposits.

[53] Pulse charging involves applying current in rapid short repetitive intervals. During the UL tests, the intervals ranged from about 0.25 to 0.50 second.

CosMX Exhibit 1003, Page 181 of 512

charging tests revealed no lithium deposits in the cell tested at 77°F and a progressive decrease in charge transfer (cell capacity) as the temperature decreased to -0.4°F.[54]

Visual examinations of the windings from cells 5 and 6 revealed features consistent with lithium deposits. (UL referred to these deposits as lithium dendrites).[55] No features consistent with lithium deposits were observed in the cell 3 windings. All observed features were found adjacent to wrinkled regions of the windings. According to UL, wrinkles can form dendrites by creating "non-uniform current density distributions" within the windings due to the "uneven contact between the electrodes and separator in a wrinkled region" (Tabaddor and others 2014).

A normal electrode assembly with consistent uniform spacing between the anode and cathode allows uniform lithium-ion transport via the shortest pathway. Thus, an assembly with wrinkled or creased regions could result in non-uniform lithium-ion transport. According to UL, non-uniform lithium-ion transport could also occur from following causes:

- localized deformations of the windings during manufacturing, such as those that occur when flattening the assemblies to the "jelly roll" shape or by stresses resulting from welding the current collectors to the electrodes;
- poor quality control of the coating and winding processes during manufacturing; and
- cell swelling during charge and contracting during discharge, which creates movement of the current collector fingers attached to the windings.

1.5.4 Cell-Level Abuse Tests

UL conducted testing to understand and compare the energy level of a thermal runaway in response to three different methods of simulating an internal short circuit within a single cell from exemplar battery assemblies.[56] The internal short circuits were initiated in a single cell winding using the indentation, nail penetration, or hot pad methods.[57] The tests were conducted at temperatures of 77°F and 158°F. Cell temperatures were measured by thermocouples at

[54] In its submission to the NTSB for this investigation, GS Yuasa stated that, after the incident, it conducted more than 100 cold charge cycle tests, all of which revealed a loss of capacity when charging repeatedly at -9.4°F.

[55] A lithium dendrite is a lithium metal deposit that can form on a coated anode surface. Lithium dendrites can grow over time and cause internal short circuiting. The lithium metal can react exothermically with electrolyte. In addition, lithium dendrites can cause the electrodes to become unstable and thus result in an exothermic reaction. Such reactions at both the anode and cathode, as well internal short circuits from lithium dendrite formation, can result in a thermal runaway (Belov and Yang 2008, 885-894).

[56] Cells 1 through 8 from batteries 149 and 241 were used for the indentation, nail penetration, and hot pad tests; cell 8 from battery 171 was also used for a hot pad test. (Boeing provided batteries 241 and 171, in addition to the previously provided battery 149, for the cell-level abuse tests). A total of 17 cells were tested.

[57] The indentation method, which UL developed, creates a localized, small-scale internal short circuit condition by stressing the electrodes without breaching the cell case. The nail penetration method involves inserting a nail through a cell case to penetrate the electrodes and induce an internal short circuit condition within the cell. The hot pad method involves placing a small electric heating pad on a cell to heat the cell to a desired temperature to induce an internal short circuit condition.

CosMX Exhibit 1003, Page 182 of 512

various locations on the cell cases, and cell voltage responses were measured by probes attached to the cell terminals.

During all tests, when the internal short circuit was induced in a single winding of a cell, the cell voltage decreased immediately.[58] The cell voltage then recovered but, within 30 seconds, decreased again and remained at a level consistent with the failure of all three windings (Wang and Wu 2014). The most significant effects observed from the tests included the temperature increase and venting as the cell entered thermal runaway, the decrease and recovery in cell voltage that occurred immediately after the induced internal short circuit, and the fused aluminum current collectors in response to the internal short circuit.[59]

Figure 15 shows the cell voltage output measured during an internal short circuit test. The test was conducted at 77°F, and the internal short circuit was induced using the indentation method. Region A in the figure shows the fully charged cell before the introduction of the simulated internal short circuit in a single winding of the cell. Region B shows the cell voltage output immediately after the initiation of the internal short circuit but before the failed winding's current collector fused open. The cell's temperature reached about 150°F at this point in the test (about 5 seconds after the initiation of the internal short circuit). Region C shows the voltage output after the failed winding's current collector fused open and the subsequent recovery of the cell with the voltage output from the two remaining windings. Region D shows the decreasing cell voltage output as the remaining two windings fail due to the heat generated by the first failed winding.[60] The cell's temperature reached about 500°F at that point in the test (about 27 seconds after the initiation of the internal short circuit). The cell's maximum temperature, about 610°F, occurred about 90 seconds after the initiation of the internal short circuit.

[58] For the 158°F tests, the voltage drop was between 0.50 to 0.75 VDC; for the 77°F tests, the voltage drop was between 1.00 and 1.25 VDC.

[59] Excessive current flow through the current collector finger causes the fuse portion of the finger to heat to the point of melting and open the electrical circuit between the winding and the other windings in a cell. Postincident discussions with GS Yuasa revealed that the current collector fingers were sized to allow for required power loads that the cell would encounter in service without fusing open.

[60] The three electrode windings in the 787 main and APU battery cell design are electrically connected in parallel. When the voltage of a single winding arranged in parallel with other windings drops below that of the adjacent windings, the remaining windings will attempt to charge the lower voltage winding to equalize the voltage across the parallel circuit. The charging currents that result could discharge the remaining windings, causing an overall drop in cell voltage or a rupture of the cell assembly. (Reddy and Linden, 2011).

CosMX Exhibit 1003, Page 183 of 512

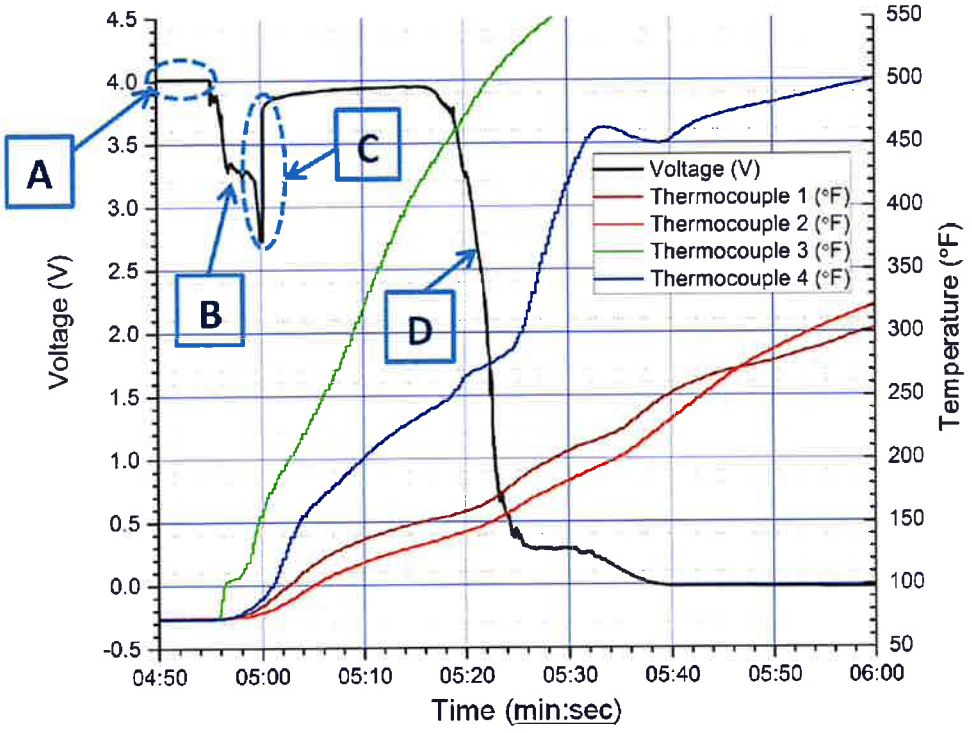


Figure 15. Results of cell-level internal short circuit abuse test.

Note: The preceding paragraph describes each region depicted in this figure. The thermocouples used to measure cell temperature were typically placed at the cell's copper (negative) rivet (thermocouple 1), the aluminum (positive) rivet (thermocouple 2), 0.2 in from the internal short circuit initiation point (thermocouple 3), and 0.1 in from the vent disc (thermocouple 4).

During all indentation and nail penetration tests conducted at 77°F and 158°F, the current collector fingers in the initiating outer winding fused open. During some of the indentation and nail penetration testing at 158°F, the current collector fingers in the center winding also fused open. During all hot pad testing conducted at 77°F and 158°F, only the current collector fingers in the initiating outer winding directly adjacent to the hot pad fused open. None of the center or far outer windings had fused current collectors.

When nail penetration testing was conducted at 158°F on two separate cells with a nail that entered the top of the cells (rather than the side of the cells) and shorted only the center winding, the center winding current collector fingers fused open, and the current collector fingers in the outer windings remained intact.[61] Data recorded during these tests showed that, after the internal short circuit was induced, the cell voltage dropped immediately, abruptly recovered, and then dropped to zero volts. For the tests in which the current collector fingers fused open in the

[61] A similar behavior involving only the center current collector fingers fusing open in the initiating cell was observed during the 158°F full-scale battery nail penetration test described in section 1.5.7. Also, as stated in section 1.4.2, CT scans of the incident battery showed that, for cell 5, the current collector fingers in only the center winding fused open as a result of the battery thermal event.

outer winding and the center winding, the recorded data showed two separate voltage decreases with two recoveries.

UL's testing showed that, with a significant internal short circuit, the current flow through a winding could reach a level sufficient to open the winding's fusible link. In addition, the testing showed that conduction of the heat generated by an internal short circuit in one winding of a parallel arrangement to adjacent windings could cause thermal damage in those windings and lead to thermal runaway of the entire cell.

Thermal abuse testing performed using accelerating rate calorimetry (ARC) showed that the cells, at zero and 100% state of charge, started to generate internal heat at temperatures as low as 144°F, which is below the maximum operational temperature of the battery (158°F).[62] When the ambient condition of a fully charged cell was increased beyond 176°F, the self-heating rate exceeded 0.04°F per minute. When the temperature of the cell was raised to about 266°F, the separator melted, and the cell entered thermal runaway and vented. None of the current collectors fused during the abuse testing using ARC.

1.5.5 Rivet Observations During Cell- and Battery-Level Testing

The aluminum and copper rivets on 787 main and APU battery cells clamp together the electrical components at the top of each cell, including a copper top plate, external and internal thermoplastic seals, and a current collector, to conduct current flow into and out of the cells.[63] The rivets also provide a hermetic seal intended to prevent leakage of electrolyte from the cell case and protect the electrolyte from external moisture. Evidence of rivet seal leakage was found in cell 4 of the incident APU battery, which had melted seals and weighed less than specifications despite the vent disc remaining intact.

During tests to determine the effects of simulated APU starts on individual cells and a complete battery assembly, UL made observations about the aluminum rivets (Wang, Chiang, and Wu 2014).[64] The APU start simulations on a full battery were performed using battery 459 at temperatures of 77°F and 32°F after the individual battery cells underwent the same levels of charge and discharge.[65] After a normal battery-level first charge/discharge cycle at 77°F, the

[62] The cells were slowly heated in an ARC chamber so that an adiabatic condition existed (that is, no heat was transferred between the cells and the surrounding environment) until the cells began to self-heat to the point that they eventually failed.

[63] The aluminum rivets conduct energy from the aluminum current collector, and the copper rivets conduct energy from the copper current collector.

[64] UL disassembled the battery before the battery-level tests to examine and test the individual cells and reassembled the battery afterward using GS Yuasa documentation provided to UL by the NTSB. (The battery could be disassembled and reassembled outside of GS Yuasa.)

[65] The APU start profile is similar to two failed starts followed by a successful start during a short time period using the APU battery as the only starting power source. An APU start discharge attempt at -0.4°F was not completed because the battery voltage dropped and the test was stopped to prevent battery damage. As shown in UL's test plan (which was distributed to the parties to the investigation before testing began), the discharge rate used during UL's testing was based on the design requirement at the time of certification, and a post-test review found that this discharge rate was not exceeded.

CosMX Exhibit 1003, Page 185 of 512

temperature of the aluminum rivets on the positive terminal of cell 5 increased progressively through 14 cycles to a maximum temperature of 315°F, which exceeded the melting temperature of the separator and the temperature at which the thermoplastic seals begin to soften.[66]

An infrared thermal image taken at 32°F during the last of the 14 battery-level test cycles showed that the aluminum rivets on cell 5 were sources of heat in addition to heat from the electrode windings. The image also showed that heat was conducted from the cell 5 aluminum rivets through the copper bus bar to the copper rivets on cell 6. Further, strain gauges placed on the sides and tops of the cell cases showed that the stresses in the cells increased during discharge, with cell 5 exhibiting the highest strain during a test at 32°F. In addition, the efficiency of the cells decreased as temperatures decreased such that 30% of the discharge energy heated the cell when the temperature was reduced to 0°F.

UL performed subsequent examinations and testing on cell 5 from battery 459, including CT scans; DC resistance measurements; cell leakage tests; and a cell DPA, which included visual inspection of the separator and compositional analysis of the electrolyte. The testing showed that the aluminum rivet seals leaked and that the DC resistance between the aluminum current collectors and the riveted joint was significantly higher (three orders of magnitude) than that of the same joint in other cells. The CT scans revealed visible gaps between the rivet and the current collector (internally) and the rivet and the copper top plate (externally). During the DPA examination, plastic seals were found deformed, and the separator material showed localized melting between the anode and cathode adjacent to the aluminum center winding current collector finger. Separator melting was not observed elsewhere in the windings.

The 787 battery was designed to measure temperature only on two cell bus bars and not at or within each cell. Infrared thermal images and thermocouple data from the UL battery-level testing showed that (1) temperatures were not even across the surfaces of individual cells, (2) the cell temperatures differed from each other, and (3) the bus bar temperatures were lower than the cell temperatures and substantially lower than the temperature at the rivets, and (4) the changes in bus bar temperatures lagged behind the changes in cell temperatures. As a result, UL conducted heat flow tests on a header assembly that had been removed from a cell to determine the internal temperatures of a cell. The interior portion of one of the aluminum rivets was heated until the exterior of the rivet reached the 315°F maximum temperature measured during the APU start simulations. At that temperature, the interior portion of the rivet measured 332°F, and the top of the internal aluminum current collector measured 277°F, which was higher than the melting temperature of the separator.[67]

The NTSB's CT scans of the rivet assemblies in cells from the main battery on the incident airplane (battery 412) revealed gaps and voids between the rivets and assembly components. After the rivet assembly in cell 5 was cross-sectioned, rinsed, and dried, water

[66] During the testing, the temperature of both aluminum rivets was measured using an infrared camera. A thermocouple was also placed on one of the rivets to further measure temperature.

[67] The interior portion of the rivet and the current collector had been within the cell before it was disassembled for the heat flow test.

CosMX Exhibit 1003, Page 186 of 512

seeped out of gaps at the edges of the plastic seals in the assembly. The water revealed gaps that were not initially seen under magnification.

Further examination of cell 5 in battery 412 revealed brown deposits that were consistent with dried electrolyte. These deposits were found around a rivet hole of the internal current collector, which had been in contact with an aluminum rivet. Closer examination of the current collector's surface showed evidence of material consistent with oxidation products under the rivet head. The current collector was bent and skewed out from the rivets, and the exterior plastic seal was deformed, diminishing the sealing surface. The deformation caused the plastic sealing surfaces to separate from the top of the stainless steel cell case. Multiple gaps between the contact surfaces were found between the rivet and copper top plate and between the rivet and current collector. The copper plate had a nickel finish, and the shoulder of the rivet had an impressed circular pattern (consistent with machining ridges) that had not been transferred into the nickel plating, which was consistent with a lack of compressive force in this area. The rest of the plating around the rivet hole showed no indications of contact with the rivet.

1.5.6 Cold Temperature Cell- and Battery-Level Testing

The airplanes involved in the BOS, TAK, and NRT events were based in Tokyo and were exposed to below-freezing temperatures during the winter months. At the time of the NRT event, the 787s based in Japan represented less than one-third of the worldwide 787 fleet. Even though other 787 airplanes had occasionally been exposed to below-freezing temperatures while at their base location, the winter temperatures in Tokyo were the coldest of the cities where 787 airplanes were based. The NTSB was concerned that cold weather exposure could be a significant risk factor for the 787 main and APU lithium-ion battery.[68] As a result, UL conducted cold temperature testing at the cell and battery levels to determine the effect that cold temperature charging could have on the battery's performance. During the cell-level testing, the cells heated significantly more when discharged at temperatures between 0°F and 32°F than at temperatures above 32°F.

As previously stated, during battery-level testing at 32°F, the aluminum rivets on a cell increased in temperature to a maximum of 315°F, which exceeded the melting temperature of the separator material. Cell disassembly found melting at the edges of the separator layers that had been adjacent to the aluminum current collector fingers. (Such melting was not found during the cell-level tests.) Measurement of the electrical resistance across rivet-to-collector joints after cell disassembly showed that the resistance in a cell that heated (cell 5 of battery 459) was 74.5 milliohms; the resistance of other cells was typically 0.03 milliohm. In its submission for this investigation, Boeing stated that it was revising the low temperature charging limit for the main and APU battery and BCU to "reduce the likelihood of an internal short circuit and improve cell and battery reliability."

[68] In its report on the TAK incident, the JTSB noted the cold temperatures that existed at the time of the three battery events and indicated that cold temperature could be related to the cause of the failures.

CosMX Exhibit 1003, Page 187 of 512

1.5.7 Battery-Level Nail Penetration Tests

UL conducted nail penetration tests on LVP65-8-402 batteries to determine the effects of a simulated short circuit within a single cell. The nail penetration tests were conducted with battery numbers 436 and 445, which Boeing provided in addition to the other 787 exemplar batteries.[69] A specially designed nail with an embedded thermocouple (which provided a single temperature within the nail-penetrated cell) was used during the tests.

In one test, the battery was electrically grounded using a single ground wire that was representative of the ground wire installed on the 787 airplane (Chapin and others, *NTSB Battery Tests [Asset 445]*, 2014).[70] The battery temperature at the start of this test was between 52°F and 57°F, which was consistent with temperatures in the E/E bay during a typical flight, as measured by Boeing.[71] In another test, the battery was not electrically grounded (similar to the test setup used by GS Yuasa in a 2006 battery development test, as described in section 1.7.3), and the test was conducted at the battery's maximum operating temperature of 158°F (Chapin and others, *NTSB Battery Tests [Asset 436]*, 2014).[72]

The test with the electrically grounded battery showed that thermal runaway occurred when a short circuit was induced into a single cell inside the battery, resulting in cell swelling and venting of the nail-penetrated cell. None of the other cells in the battery underwent thermal runaway or vented. This test also showed that the initiating cell and other cells within the battery case began to electrically discharge at an uncontrolled rate, causing a high electrical current to discharge through the ground wire circuit.[73] Within 30 seconds of the initiation of cell venting of the nail-penetrated cell, the ground wire fused open, and the current flow through the grounding path ceased. The post-test examination of the battery found evidence of arcing between the nail-penetrated cell (cell 6) and the battery case, including welding of the cell case and the center brace bar of the battery case.

The test with the ungrounded battery showed that thermal runaway of a single cell propagated to all other cells inside the battery case. This result (propagation to and venting of all cells) differed from the results of GS Yuasa's battery development test (venting of the

---

[69] Before the testing, the batteries were disassembled so that nondestructive tests could be performed. Cells 1 and 2 from battery 445 were damaged during disassembly, so they were replaced with identical cells from battery 271, which Boeing also provided.

[70] The battery case, when installed in the airplane, is grounded via the 787 common return network. The battery test setup did not include all electrical ground paths to the battery case as installed on the airplane (that is, the ground wire, shielded signal wires, and a physical connection between the battery case mounting rails and ground).

[71] APU battery temperature was not recorded on the incident EAFR. After the incident, Boeing monitored E/E bay temperatures during several flights and reported average values of 50°F to 59°F during a typical flight.

[72] UL's reports on these tests included detailed information about the test facility, test fixture, instrumentation, data acquisition, test procedures, and results.

[73] As previously stated, the incident battery ground wire was found intact with the wire insulation exhibiting an undamaged exterior surface but a slightly blackened interior surface, which was consistent with resistive heating associated with the flow of high levels of electrical current. Also, the shielded signal wires exhibited signs of internal heating that were consistent with resistive heating by high levels of electrical current.

CosMX Exhibit 1003, Page 188 of 512

nail-penetrated cell and no propagation to and venting of other cells), but the NTSB notes that GS Yuasa performed its battery test at a temperature that did not represent the battery's maximum operating temperature under normal conditions (158°F). The post-test examination of the ungrounded battery used for the UL test found no evidence of arcing between the nail-penetrated cell (or other vented cells) and the battery case.

The findings of these tests were part of the basis for Safety Recommendations A-14-32 through -36, which were issued in May 2014 (see section 1.8.2).

1.5.8 Additional Testing

Early in the investigation of the BOS incident, the NTSB performed ATP functional testing of the BCU of the incident airplane's APU battery at Securaplane's facility. At the request of the JTSB, the NTSB also performed ATP testing on both BCUs from the airplane involved in the TAK incident. As stated in section 1.2.2, the ATP testing revealed a previously unknown electrical oscillation in the output charge voltage of each BCU. Boeing and UL conducted separate detailed examinations of the BCU from the APU battery that had been installed on the BOS airplane and integrated system testing of a battery, the BCU, and battery-related components. The testing at Boeing and UL found that the oscillation could slightly diminish the battery's life but was unrelated to thermal runaway.[74] As a result of its testing, Boeing changed the BCU design to minimize the oscillation. GS Yuasa conducted testing as part of the JTSB's investigation of the TAK incident and similarly found that the BCU oscillation could shorten a cell's life.

During the investigation of the BOS and TAK incidents, Boeing developed and conducted (along with its contractors) more than 40 different laboratory and airplane tests to understand various battery failure modes. Boeing also performed tests to learn information that would support the redesign of the main and APU battery systems.[75]

Boeing performed a laboratory test to understand the effects of moisture condensing on the battery. This test subjected the battery case and internal battery components to simulated flight cycles in an environmental chamber with varying temperature, pressure, and humidity conditions.[76] After the testing was completed, small amounts of condensation were noted on the top of the cells. The condensation created an electrical short path between the cell case and the battery case. Boeing performed a subsequent laboratory test in which a single cell was placed in a container with saline solution and voltage was provided to represent the other cells of a battery.

---

[74] One of the reports that UL developed as part of this investigation refers to the BCU oscillation testing as part of the "Noisy Test Procedure" (Tabaddor and others 2014). "Noisy" electrical power refers to the lack of continuous voltage; current; and, if AC power, frequency. UL's report includes specific details about the frequency and current characteristics used for the testing.

[75] For additional information about the testing that Boeing performed, see the testing addendum to the Airworthiness Group Chairman's Factual Report, which is available at www.ntsb.gov in the public docket for this incident.

[76] The battery assembly used during this test did not use actual cells; thermally equivalent representative cells were instead used for the testing.

CosMX Exhibit 1003, Page 189 of 512

The single cell vented, and post-test examination revealed damage internal to the cell header, including evidence of arcing, shorting, and heat damage.

Another laboratory test examined the vibration environment of the battery. This test subjected the battery to vibration levels in the pitch, roll, and yaw axes in excess of the levels occurring during in-service operations. The battery's performance was monitored, and the battery was examined, before and after each vibration series. Slight changes in cell case voltages were noted, but no changes in the battery's performance were observed. Post-test examinations of the battery revealed areas of slight abrasions to battery components and one failed BMU sensing wire.[77]

In addition to the previously mentioned integrated battery/BCU system component testing, Boeing conducted flight and ground tests with an instrumented 787 airplane to determine the atmospheric and electrical environment of the system installation. During the flight and ground tests, the battery and charger performed with no anomalies, and no thermal or vibration data exceeded the design requirements. Temperatures for the main and APU battery and the forward and aft E/E bays during the flight tests were comparable with in-service temperatures. Examination of the flight test data showed oscillations during the constant-voltage charging cycle at low-current loading, which were similar to the oscillations observed during the BCU testing at Securaplane. No other abnormal electrical transients were observed in the flight and ground test data.

1.6 Battery Manufacturing Information

1.6.1 Main and Auxiliary Power Unit Battery Development

In 2003, Boeing created a statement of work to outsource the design and manufacture of the 787 power conversion subsystem and awarded this contract to Thales in May 2004. Thales then subcontracted (with concurrence from Boeing) the design and manufacture of the 787 main and APU battery to GS Yuasa and the design and manufacture of the 787 battery charging system to Securaplane Technologies.[78]

Boeing, with participation from Thales, created the specification control drawing (SCD) and interface control drawing to be used during the development and manufacture of the 787 battery and battery charging system.[79] Thales was responsible for providing these specifications to GS Yuasa and Securaplane, managing these subtier suppliers, and meeting all of the

[77] The LVP65-8-403 battery design incorporated improvements to the BMU sensing wiring installation.

[78] Outsourcing is an industry practice that can be practical and effective when all aspects of the design, manufacture, and certification of a component or system have been verified to ensure an airplane's safety of flight. Postincident interviews revealed that all of the companies involved with the design and manufacture of the 787 power conversion subsystem agreed that each would retain ownership of their associated intellectual properties.

[79] According to Boeing, the SCD depicts the performance and design requirements, functional and physical interfaces, and quality assurance requirements for the development, procurement, and configuration control of an item or assembly. The interface control drawing is a formal engineering document that defines, among other things, the interface between mating parts, connections, and signals.

CosMX Exhibit 1003, Page 190 of 512

specification requirements for the battery and battery charger system. Thales, along with its subtier suppliers, was also responsible for providing Boeing with required testing and analysis results.

The basic design of the battery began in 2005. As part of the design, GS Yuasa contracted with KAI to design and manufacture the BMU. As the battery design matured, preliminary design reviews and critical design reviews were conducted by Boeing along with Thales and GS Yuasa. Qualification testing was witnessed by delegated representatives from Boeing.[80]

In early 2007, GS Yuasa and Thales redesigned the battery (with Boeing's approval) after a November 2006 fire at Securaplane during the development of the BCU.[81] The redesigned battery included a contactor and a BMU subcircuit card to interrupt charging in an abnormal situation. Qualification testing of this redesigned battery was completed in June 2007. In October 2009, GS Yuasa and Thales redesigned the battery again (with Boeing's approval) after a July 2009 cell venting event at UTC Aerospace Systems' Airplane Power Systems Integration Facility (APSIF), where 787 power conversion subsystem components were tested as an integrated electrical system.[82] The redesigned battery included a modified BMU4 subcircuit card to avoid the subsequent recharging of the battery after overdischarge and a battery diode module (added to the electrical system) so that the main battery could be charged only by the dedicated charger and not be inadvertently charged by the airplane's electrical system. The critical design review for this battery redesign was completed in January 2010, and qualification testing was completed in June 2010.[83] (The FAA was aware of both battery events.)

Boeing required its suppliers and subtier suppliers to perform first article inspections (FAI), according to industry standards, on first production runs of any component. The FAI was the primary method for inspecting and testing vendor components and was considered to be an essential step in approving an order or a contract. The intent of the FAI was to determine if a vendor's product met acceptance and quality control requirements to ensure that all engineering, design, and specification requirements were correctly understood, accounted for, verified, and

---

[80] Qualification tests are performed to demonstrate that a design conforms to a set of requirements, such as the requirements defined in Boeing's main and APU battery SCD.

[81] On November 6, 2006, a fire occurred at the main Securaplane building when a 787 development battery was being charged for a test. The battery had been in use for about 14 months. Investigation of the incident found that thermal runaway of the battery occurred and that the BMU was not connected directly to the BCU. The cause of battery failure was unknown but was surmised to be a cell internal short circuit followed by overcharge of at least one other cell.

[82] On July 7, 2009, an APU battery experienced a loss of voltage and vented electrolyte during integrated system testing at UTC Aerospace Systems' APSIF. An investigation of the incident by Boeing, Thales, and GS Yuasa determined that the failure of the battery most likely resulted from thermal runaway of a single cell due to an internal short circuit created by repetitive overdischarge and subsequent high-rate charging operations. During the NTSB's April 2013 investigative hearing on the BOS incident, Boeing representatives testified that integrated system testing was conducted on the entire electrical system, including the APU and its grounding system, and that a number of protective (non-abuse) tests were conducted to ensure that the APU system would meet its design requirements.

[83] The changes to the battery that were made after the BOS and TAK incidents are discussed in sections 1.2.4 and 1.8.1.

CosMX Exhibit 1003, Page 191 of 512

recorded. GS Yuasa accomplished the FAI for the main and APU battery in November 2008, and Thales approved the FAI results in January 2009. GS Yuasa performed another FAI of the battery after its redesign resulting from the APSIF event. Further, in November 2010, Boeing performed an FAI on an LVP65-8-402 battery at GS Yuasa and found that the battery complied with acceptance and quality control requirements.

Boeing's surveillance of Thales was conducted in accordance with contractual specifications and requirements. Boeing also relied on the Bureau Veritas Certification to perform surveillance assessments of Thales twice a year.[84]

Thales conducted two audits of GS Yuasa between the time that battery production began and the incident. These audits, which were conducted in June 2011 and September 2012, found 11 discrepancies, all of which were subsequently closed. None of the discrepancies were directly related to battery or cell manufacturing. Thales reported the results of these audits to Boeing.

Boeing did not conduct any audits of GS Yuasa before the incident and relied on Thales to audit its subtier suppliers.[85] After the incident, Boeing sent an audit team to Thales and GS Yuasa (and KAI) to review the management of subtier suppliers, quality of manufacturing and business processes, and adherence to Boeing standards. The audit found 17 items of noncompliance with Boeing requirements. Most of the noncompliance items at GS Yuasa involved adherence to written procedures and communication with Thales and Boeing regarding authorization for proposed procedural and testing changes for the battery. The noncompliance items at Thales involved adherence to contractual requirements for Boeing's approval on drawing or procedural changes. Corrective actions for all of the noncompliance items have been completed by Thales and verified by Boeing.

The FAA did not conduct any audits of GS Yuasa before the incident.[86] In late January 2013, the FAA conducted an audit of GS Yuasa (and KAI) and found several items of noncompliance, including (1) noncompliance with component/assembly part markings and no traceability to assembly drawings and instructions and (2) noncompliance with assembly and installation instructions of battery components.[87] Corrective actions for these and other items of noncompliance have been completed by GS Yuasa and verified by the FAA.

---

[84] The Bureau Veritas Certification is an international certification organization that Boeing used to help ensure that its suppliers had an accredited quality management system in place.

[85] Boeing had a source inspector at GS Yuasa, but the inspector was contractually limited to determining whether specific inspection and checklist items, as detailed in agreements among Boeing, Thales, and GS Yuasa, met minimum quality standards. Any issues that the inspector found had to be routed to a US Boeing representative to coordinate through Thales.

[86] The FAA did not consider the 787 battery to be a critical component because the Seattle Aircraft Certification Office (which was responsible for the airplane's certification) regarded the battery as a redundant system. As a result, the FAA's automated supplier selection process, which identifies suppliers for evaluation, did not select GS Yuasa.

[87] Other items of noncompliance involved storage procedures for returned batteries and the root cause and analysis for returned batteries.

CosMX Exhibit 1003, Page 192 of 512

1.6.2 Cell Manufacturing Process

After the BOS incident, the NTSB visited GS Yuasa's production facility for the 787 main and APU battery to observe the LVP65 cell manufacturing process, including the electrode coating, winding, flattening, assembly, and postassembly inspection stages.[88] The coating process involved placing a foil roll on a reel in an enclosed case, unrolling the foil, and coating the foil (except its edges) with anode or cathode active material.[89] The machine operator checked the thickness of the coating periodically using a hand-held micrometer. The uncoated area on the edge of the foil material was monitored visually and measured periodically by the operator.[90] During operations in which the foils were unwound, the machine operator also monitored the foil roll for defects such as wrinkles.[91] After one side of the foil roll was coated, dried, and rewound, the roll was inverted, unwound, coated on the opposite side, dried, and rewound. Winding sensors in the machinery were in place to prevent misalignment of the foil roll. The machine operator visually inspected the winding edges for burrs. If defects were found during the coating process, an engineering-level review board would be convened to determine the disposition of the foil material.

Another machine used a cylindrical winding mandrel to wind the cathode and anode foils together with the separator sheets to create the cell windings. Afterward, the machine operator measured the alignment and weight of each winding. The machine operator then partially flattened each winding by hand compression, as shown in figure 16a, and positioned the three windings for final flattening. The final flattening process was accomplished using a compression jig with two flat plates facing the three windings. After final flattening, the machine operator attached heat-resistant plastic tape to the ends of the cell where the curves of the windings were located, as shown in figure 16b. Figures 16a and 16b also show perturbations of the electrode foil that were created during the flattening process.[92]

---

[88] At the time of the NTSB's visit, GS Yuasa was manufacturing LVP65-8-403 batteries.

[89] As previously stated, the current collectors are attached to the uncoated edges of the electrode winding assembly.

[90] At the time of the NTSB's visit, operators involved with cell manufacturing were working either 0800 to 2000 or 2000 to 0800 (local time) Monday through Friday unless production demands required more work hours. Operators involved in the postassembly CT inspection process received two 15-min breaks and one 45-min meal break during each shift.

[91] GS Yuasa defined "wrinkles" as visible longitudinal or diagonal surface creases in the electrode coating on the foil that occur before the winding and flattening processes.

[92] In this report, a perturbation is defined as a change in the electrode foil nominal form due to compressive buckling.

CosMX Exhibit 1003, Page 193 of 512

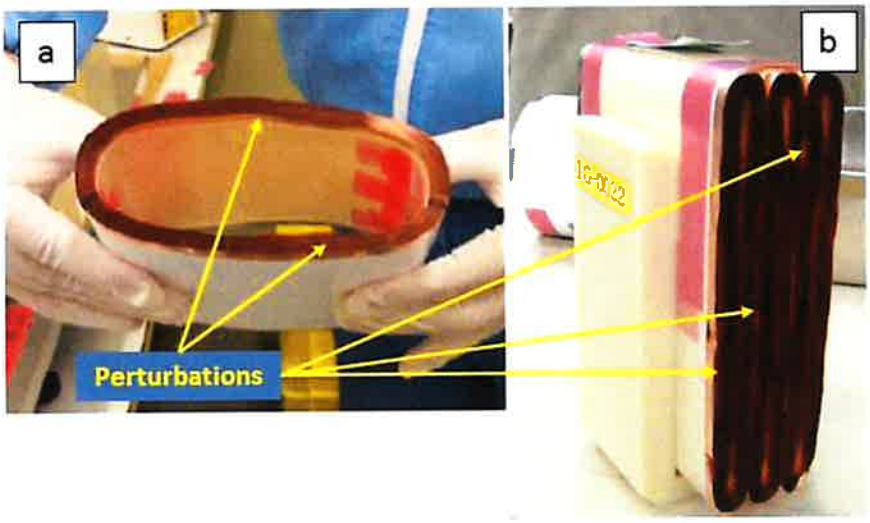


Figure 16. Winding flattening process.

Note: Figure 16a shows an electrode being hand flattened after winding and removal from the mandrel, and figure 16b shows the three-electrode assembly after final flattening and taping.

The flattened three-winding assembly was then manually attached to a prefabricated cell header assembly, which consisted of the cell header cover, two sets of current collectors attached to the cover with insulators in between, and two threaded terminals. Metallic tweezers were used to align the windings with the cell header assembly before manual ultrasonic welding.[93] A vacuum and vacuum brush on the ultrasonic welding machine (operated by a foot pedal) were in place to remove FOD generated from welding. Afterward, the cell was wrapped with an insulating polymer film and heat-resistant tape and placed inside a prismatic (rectangular-shaped) stainless steel cell case.

The next process involved manual tungsten inert gas welding of the header cover to the cell case. During this process, the welded cell was examined visually by an inspector using a magnifying glass to identify potential weld deposit defects. If a defect was identified, the cell case header cover would be welded again. The cell was also inspected for potential damage to the insulating film, excessive heat, and other defects. If such damage was found, an engineering-level review board would determine the disposition of the cell. A prefabricated small hole in the side of the cell case was used to manually fill the battery cell with liquid electrolyte. The electrolyte filling process was performed using three separate steps to prevent overflow, and the cell was precharged to low voltages in between each filling step.[94]

The postassembly inspection process involved examining a cell's interior using CT scans. An inspector viewed the CT image to identify any potential ultrasonic weld defects on the current collectors and any enclosed FOD. (The CT resolution settings were unknown because

[93] Metallic tweezers were used for processes in which precision was needed to assemble parts.

[94] The NTSB did not observe the electrolyte filling process during its visit to GS Yuasa.

CosMX Exhibit 1003, Page 194 of 512

they were not supplied to the NTSB.) If a defect was identified, the cell would be subject to further assessment.[95] GS Yuasa stated that less than 1% of manufactured cells were rejected.

1.7 System Safety and Certification

As part of its investigation of this incident, the NTSB reviewed the *Federal Aviation Regulations* and special conditions applicable to the 787 main and APU battery and battery charger system. The NTSB also reviewed the corresponding certification plan, which Boeing developed and the FAA approved. The plan defined the agreed-upon methods to be used to demonstrate that the battery and its charger system met applicable FAA and European Aviation Safety Agency (EASA) requirements.[96] In addition, the NTSB reviewed sections of Boeing's 787-8 electrical power system (EPS) safety assessment that pertained to the main and APU battery, which Boeing developed to evaluate the EPS design for compliance with safety requirements defined by the FAA and EASA.

1.7.1 Type Certification Overview and Battery Special Conditions

On March 28, 2003, Boeing applied for a type certificate for the 787-8 airplane. The FAA's aircraft certification office (ACO) in Seattle, Washington, conducted the certification oversight process. In September 2004, Boeing met with representatives from the ACO to indicate the company's intent to use lithium-ion technology for the main and APU battery on the 787 airplane.[97] At that time, the 787 was expected to be the first transport-category airplane to have permanently installed, rechargeable lithium-ion batteries.[98] In response, the FAA reviewed the adequacy of the existing regulations governing the installation of batteries in large transport-category airplanes and determined that the regulations did not sufficiently address several failure, operational, and maintenance characteristics of lithium-ion batteries that could affect the safety of the battery installations.[99]

Title 14 CFR 21.16, "Special Conditions," states that, if the FAA finds that airworthiness regulations do not contain adequate or appropriate safety standards for an aircraft because of a "novel" or an "unusual" design feature, special conditions should be issued to prescribe safety standards that establish a level of safety equivalent to that established in the regulations. Special conditions are developed by the appropriate ACO with the applicant's full participation. The ACOs use issue papers to review the adequacy of existing regulations; determine the special

---

[95] Information about other steps in the cell assembly process (and information about the battery assembly process) is detailed in the Manufacturing Data and Manufacturing Cell Group Factual Report, which is available at www.ntsb.gov in the public docket for this incident.

[96] The 787-8 FAA certification was also validated by EASA.

[97] Boeing also intended to use lithium-ion batteries in the 787's flight control electronics, emergency lighting system, and recorder independent power supply.

[98] After the incident, the FAA stated that the Cessna Citation CJ4 was the first civil airplane certificated with a lithium-ion main battery. The Citation CJ4 is not a transport-category airplane.

[99] The battery regulations that existed at the time were in 14 CFR 25.1353, "Electrical Equipment and Installations," paragraphs (c)(1) through (4).

CosMX Exhibit 1003, Page 195 of 512

conditions that would be proposed to address any inadequacies; and track the relevant technical, regulatory, and administrative issues that could arise in certifying the new technology.

In a March 31, 2006, issue paper, "Special Condition: Lithium-Ion Battery Installations" (referred to as Issue Paper SE-9), the FAA stated that, despite limited experience with the use of lithium-ion batteries in commercial aviation applications, other users of lithium-ion batteries, including wireless telephone manufacturers and electric vehicle manufacturers, had experienced safety problems with this technology. These problems included overcharging; overdischarging; and flammability of cell components as a result of the liquid electrolyte, which could serve as a source of fuel for an external fire if the battery case were breached. The FAA also noted that, in general, lithium-ion batteries are "significantly more susceptible to internal failures that can result in self-sustaining increases in temperature and pressure (thermal runaway)" than nickel-cadmium or lead-acid batteries.

On April 23, 2007, the FAA issued a notice of proposed special conditions (*Federal Register* 2007, 21162), which proposed nine safety requirements regarding the use of lithium-ion batteries for the 787 to ensure that these battery installations would not be "hazardous or unreliable." On September 28, 2007, the FAA issued Final Special Conditions 25-359-SC, "Boeing Model 787-8 Airplane; Lithium-Ion Battery Installation" (*Federal Register* 2007, 57842), which became effective on November 13, 2007. The intent of the final special conditions, which are shown in appendix B, was to establish additional safety standards that the FAA considered necessary to provide a level of safety equivalent to the existing standards for aircraft batteries.

According to the 787-8 type certificate data sheet, the airplane received transport-category approval on August 26, 2011. The type certification basis included the 14 CFR Part 25 airworthiness standards and the special conditions for the lithium-ion battery installation.[100]

1.7.2 Certification Plan

FAA Order 8110.4, "Type Certification," described the responsibilities and procedures for the FAA and the type certificate applicant to follow when evaluating and approving design data for new civil aircraft, such as the 787-8.[101] In accordance with paragraph 2-11d(1)(d) of the order, Boeing's 787 EPS certification plan presented a high-level system description of the EPS, which included the main and APU battery and battery charger system; defined the methods (for example, tests and analyses) to show compliance with applicable FAA and EASA requirements;

[100] The applicable regulations were 14 CFR Part 25 through amendment 25-119 and amendments 25-120, 25-124, 25-125, and 25-128 (with exceptions). Other applicable regulations were 14 CFR Part 26, "Continued Airworthiness and Safety Improvements for Transport Category Airplanes"; 14 CFR Part 34, "Fuel Venting and Exhaust Emission Requirements for Turbine Engine Powered Airplanes"; 14 CFR Part 36, "Noise Standards: Aircraft Type and Airworthiness Certification"; equivalent level of safety references; and special conditions for 13 other subjects.

[101] When Boeing submitted its application for the 787-8 type certificate, revision B of FAA Order 8110.4, dated April 24, 2000, was in effect. Revision C of the order was issued on October 12, 2005.

CosMX Exhibit 1003, Page 196 of 512

and defined the compliance submittals (that is, certification deliverables) to be provided to the agencies. The FAA approved the initial certification plan on December 22, 2005. Boeing was required to ensure that the certification plan was kept current throughout the 787's design, development, and certification phases, and any revisions to the certification plan were required to be approved by the FAA.

According to Boeing, on January 8, 2007, the FAA approved revision C of the certification plan and indicated that Boeing could proceed with the implementation of the proposed certification activities. Boeing conducted tests and analyses to demonstrate, among other things, that the main and APU battery and battery charger system complied with relevant 14 CFR Part 25 requirements, including sections 25.863, "Flammable Fluid Fire Protection," paragraphs (a) and (b)(3); 25.1309, "Equipment, Systems, and Installations," paragraphs (a), (b)(1), (b)(2), and (c) through (g); and Special Conditions 25-359-SC.

1.7.3 System Safety Assessment

Safety assessments are a primary means of compliance for systems that are critical to safe flight and operation. These assessments are performed by the manufacturer and its suppliers and are reviewed and accepted by the FAA. Safety assessments proceed in a stepwise, data-driven manner to ensure that all significant single-failure conditions have been identified and all combinations of failures that could lead to hazardous or catastrophic airplane-level effects have been considered and appropriately mitigated. The safety assessment process, which is outlined in FAA Advisory Circular (AC) 25.1309-1A, "System Design and Analysis," is not mandatory, but manufacturers that do not conduct safety assessments must demonstrate compliance in another manner, such as ground or flight tests. Boeing indicated in certification documents that it used a version of AC 25.1309 (referred to as the Arsenal draft) as guidance during the 787 type design certification program.[102]

Overall compliance with the applicable 787-8 main and APU lithium-ion battery safety requirements was shown through formal analyses and qualification tests. Thales and GS Yuasa performed these analyses and tests, and Boeing reviewed and approved the results.

Boeing's 787-8 EPS safety assessment, dated September 16, 2009, presented the overall safety analysis of the EPS. This analysis evaluated the design of the EPS for compliance with safety requirements derived from 14 CFR Part 25, EASA certification specifications, Special Conditions 25-359-SC, and accompanying advisory material. For the main and APU lithium-ion battery and battery charger systems, the safety assessment included a failure modes and effects analysis (FMEA) to provide a bottom-up qualitative and quantitative way to identify the effects

[102] In 1996, an FAA aviation rulemaking advisory committee (ARAC) was chartered to harmonize the FAA's practices related to 14 CFR 25.1309 with those of Europe and Canada. The committee released its final report to the FAA in August 2002, but the revised AC 25.1309, referred to as the Arsenal draft, has not yet been issued. On April 29, 2003, the FAA published a notice of availability of the ARAC-recommended proposed changes to the airworthiness standards for transport-category airplanes regarding equipment, systems, and installations as well as the current AC 25.1309 (version 1A). This notice of availability indicated that the ARAC-recommended proposed changes could be used for airplane certification programs through a request for an equivalent level of safety finding.

CosMX Exhibit 1003, Page 197 of 512

of a failure at the next (higher) level of a system; a functional hazard assessment (FHA) to determine the potential hazards that various failures of electrical system components could introduce to the airplane and its occupants; and a fault tree analysis for the hazards identified in the FHA.[103]

The FHA identified and classified two hazards associated with the main and APU lithium-ion battery: "battery vents smoke/fire," which was classified as catastrophic, and "battery vent and/or smoke (without fire)," which was classified as hazardous.[104] On the basis of the FHA's results, Boeing defined failure detection and mitigation requirements for the main and APU battery, including the following three requirements related to smoke, gas, and electrolyte release:

- The battery shall have a probability of less than 1×10^{-7} for gas emission.
- The battery shall have a probability of less than 1×10^{-7} for smoke emission.
- The battery shall be designed to prevent spilling flammable fluid, a hazardous event with a probability of less than 1×10^{-9}.

This analysis determined that overcharging was the only known failure mode that could result in cell venting with smoke and fire. As a result, Boeing established additional design requirements to ensure that the likelihood of occurrence of an overcharge event would be extremely improbable (one in 1 billion flight hours or a probability of 1×10^{-9}).[105] Boeing further determined that cell venting without fire could be initiated by several different failure modes, including external overheating, external short circuiting, internal short circuiting, recharging a battery that has been overdischarged, a high rate of charging, or charging at cold temperatures.

---

[103] A FMEA is an analytical process that postulates all known and reasonable failure modes. The FMEA assesses the effects of those failures and documents the effects that the failures could have at the airplane level. The FMEA also supports the development of fault tree basic events. An FHA examines a system's functions and purpose, identifies failure conditions that could occur with a loss or malfunction of the system, and classifies those conditions by severity (at the airplane and system levels). After the hazard classification for a system is established, the manufacturer conducts system-specific safety analyses to identify ways to mitigate the adverse effects of a failure condition. A fault tree analysis is a structured, deductive, top-down qualitative and quantitative analysis that depicts the relationship(s) between each failure condition and its primary cause(s).

[104] The harmonized requirements for 14 CFR 25.1309 define a catastrophic event as one that normally involves a hull loss with multiple fatalities. This event is assigned an allowable qualitative probability of being extremely improbable and an average quantitative probability of less than 1×10^{-9} per flight hour. The harmonized requirements for section 25.1309 define a hazardous event as one that normally involves a large reduction in functional capability or safety margins of the airplane with serious or fatal injury to a small number of passengers or cabin crew along with physical distress or excessive workload impairing the flight crew's ability. This event is assigned an allowable qualitative probability of being extremely remote and an average quantitative probability of less than 1×10^{-7} per flight hour.

[105] The risk of fire was addressed through overcharge protections. For example, Boeing required that "the battery monitoring unit when combined with the overall battery protection subsystem shall prevent undetected over-charge (over-voltage)."

CosMX Exhibit 1003, Page 198 of 512

One of the objectives of a FMEA is to support safety analyses by documenting that there are no known single-point failures that would result in catastrophic failure conditions. Boeing's 787 EPS safety assessment identified no single-point-failure catastrophic effects for the main and APU lithium-ion battery.

Boeing's FMEA was based on information contained within GS Yuasa's FMEA, which GS Yuasa developed with assistance from Boeing and Thales. GS Yuasa's FMEA included a calculation of a representative failure rate for the LVP65 cell. This calculation was based on in-service data from about 14,000 existing large-scale industrial lithium-ion cells manufactured by GS Yuasa, which had a similar design and manufacturing process as the LVP65 cell.[106] GS Yuasa's FMEA indicated that none of the industrial cells had experienced any failures, including venting, electrolyte release, or rupture of a vent disc. (GS Yuasa's FMEA did not include an analysis of usage and environmental similarities between the industrial cells and the LVP65 cells or a discussion of the hazardous effects of a lithium-ion cell failure, including overheating or venting.) On the basis of this information, Boeing determined that the rate of occurrence of cell venting for the 787 battery would be about 1 in 10 million flight hours.

Boeing's 787 EPS safety assessment also included Boeing's analysis of the results of a single development (noncertification) nail penetration test that GS Yuasa performed in November 2006.[107] This test involved driving a steel nail through a cell case to penetrate the electrodes of a fully charged single cell within a fully charged, nongrounded, preproduction battery to induce an internal short circuit within the cell. The purpose of the test, which was conducted at a temperature representative of the E/E bay operating temperature during a typical flight, was to observe the behavior of the cells near the nail-penetrated cell, observe any release of smoke or initiation of fire, and document any damage to the battery case.[108]

The nail penetration test results showed that the surface temperature of the nail-penetrated cell increased, smoke vented from the cell and the battery case, and the surface temperature of the adjacent cells increased with no venting.[109] On the basis of this development test and the in-service data of the industrial cell that GS Yuasa designed and manufactured, Boeing determined that the effects of a cell internal short circuit would be limited to (1) the

---

[106] According to GS Yuasa, failure rate data from industrial cells were used because, at that time, there were no available in-service failure history data for the LVP65 cells. According to GS Yuasa, a cell's failure rate was related more to the cell's manufacturing process and mechanical design rather than the materials used in the construction of the cell. GS Yuasa noted that some variation in chemistry existed between the LVP65 cell and the industrial cell but indicated that the difference in chemistry could impact the effect of the failure and not the probability of occurrence.

[107] Boeing collaborated with GS Yuasa and Thales about the development tests to be performed on cells and batteries. Results from this testing helped Boeing determine what types of abuse (thermal, physical, and/or electrical) certification testing and/or safety analyses needed to be performed to show compliance with the applicable battery regulations, including the special conditions. The development tests were not required by the FAA.

[108] As previously stated, Boeing reported that E/E bay temperatures during a typical flight ranged from 50°F to 59°F.

[109] Tests and analyses that GS Yuasa performed were reviewed by Boeing project engineers, safety reliability and maintainability engineers, and authorized representatives (who acted on behalf of the FAA during certification tasks).

CosMX Exhibit 1003, Page 199 of 512

release of smoke from the battery, which could be effectively handled by the airplane's ventilation system, and (2) an increase in surface temperature of the short-circuited cell with no propagation of thermal runaway to adjacent cells, damage to the battery case, fire, or explosion.

At the conclusion of the 787 testing and safety assessment process, Boeing prepared documentation for the FAA showing Boeing's proposed methods for demonstrating compliance with 14 CFR 25.1309 and each of the nine special conditions in 25-359-SC. The FAA used this information to make findings of compliance. Title 49 CFR 44702(d) allows the FAA to delegate to a qualified individual a matter related to issuing a certificate or a matter related to the examination, testing, and inspection necessary to issue a certificate. In October 2005, the FAA established the organization designation authorization (ODA) program to address delegations to organizations and standardize its oversight of organizational designees.[110] With an ODA, FAA-approved engineering designees in various technical areas act on behalf of the FAA during certification tasks. Boeing, which received ODA approval in August 2009, refers to its engineering designees as authorized representatives. They can make findings, as authorized by the FAA, for certain reports or tests in support of type certification programs, but only the FAA can issue a type certificate. Boeing's and the FAA's roles in the certification of the 787 main and APU battery are further discussed in section 2.5.

1.8 Additional Information

1.8.1 Federal Aviation Administration Actions After Battery Incidents

On January 11, 2013, 4 days after the BOS incident, the FAA announced that it would undertake a comprehensive review of the 787's critical systems with the possibility of further action pending new data and information. The FAA stated that, in addition to a review of the 787's design, manufacture, and assembly, it would verify that the 787 battery system complied with the special conditions that were part of the 787's certification (as discussed in section 1.7 and appendix B).

On January 16, 2013, after the TAK incident, the FAA issued emergency AD 2013-02-51 to address a potential battery fire risk in the 787.[111] The emergency AD "was prompted by recent incidents involving lithium-ion battery failures that resulted in release of flammable electrolytes, heat damage, and smoke on two Model 787-8 airplanes." The emergency AD indicated that these conditions "could result in damage to critical systems and structures, and the potential for fire in the electrical compartment." The emergency AD instructed owners and operators of Boeing 787-8 airplanes to, "before further flight, modify the battery system, or take other

[110] Before that time, designated engineering representatives performed certification activities that the FAA delegated.

[111] Earlier that day, JAL and All Nippon Airways had voluntarily decided to stop 787 operations as a result of the TAK battery event. On January 17, 2013, the Japan Civil Aviation Bureau issued a directive with the same content as FAA emergency AD 2013-02-51. Civil aviation authorities in other countries also required operators of 787 airplanes to temporarily cease operations.

CosMX Exhibit 1003, Page 200 of 512

actions, in accordance with a method approved by the Manager, Seattle Aircraft Certification Office."[112]

On March 12, 2013, the FAA announced that it had approved Boeing's certification plan for a redesigned 787 battery system. The FAA stated that the certification plan required Boeing to conduct "extensive testing and analysis" to demonstrate compliance with the applicable safety regulations and special conditions. Also, the FAA stated that the improvements to the battery system included "a redesign of the internal battery components to minimize initiation of a short circuit within the battery, better insulation of the cells and the addition of a new containment and venting system."

On April 19, 2013, the FAA announced that it had approved Boeing's modifications to the 787 battery system, which were designed "to address risks at the battery cell level, the battery level and the aircraft level." The FAA stated that a team of agency certification specialists observed "rigorous tests" that Boeing was required to perform and reviewed a "detailed analysis" of the design changes. The FAA also stated that it would monitor the modifications of the affected airplanes in the US fleet to ensure proper installation of the new design.

On April 22, 2013, the FAA superseded AD 2013-02-51 with AD 2013-08-12, which became effective on April 26, 2013 (*Federal Register* 2013, 24673). AD 2013-08-12 required 787 operators to (1) install main and APU battery enclosures and ECS ducts; (2) replace the main battery, the APU battery, and their respective battery chargers; and (3) revise the maintenance program to include a requirement for replacement of the main and APU battery enclosure vent burst discs.[113] The AD was intended to "allow the aircraft to return to service as soon as possible by mandating a modification that will address the unsafe condition." The AD noted that, for all future 787 airplanes, the replacement batteries, their respective chargers and enclosures, and duct installations would be incorporated before delivery.

AD-2013-08-12 detailed Boeing's measures to improve the reliability of the battery and prevent any hazardous effects on the airplane from a battery failure. According to the AD, those measures are as follows:

- Minimize the Probability of a Single Battery Cell Failure–Each main and APU battery consists of a set of individual cells within a battery case. Each battery cell will be encapsulated to isolate the cell electrically. Locking nuts with specific torque values will be used on every cell terminal to prevent overheating of the terminal due to a loose electrical connection. Drainage within the battery case will be improved to remove any condensation within the battery. The battery monitoring and charging unit will be changed to

[112] One US operator had six 787s in service when the emergency AD was issued. On February 1, 2013, the FAA issued AD 2013-02-51, which stated that emergency AD 2013-02-51 had previously been sent to all known US owners and operators of 787-8 airplanes but that "this AD is effective February 22, 2013 to all persons except those persons to whom it was made immediately effective by Emergency AD 2013-02-51" (*Federal Register* 2013, 12231).

[113] The vent burst discs are frangible discs on the battery enclosures.

CosMX Exhibit 1003, Page 201 of 512

reduce the operational voltage range to lessen electrical stress on the battery cell and to enhance overdischarge protection. Boeing has also made mandatory changes to the battery manufacturing and acceptance testing processes to improve the overall quality of the battery.

- Minimize the Probability of Multiple Cell Failure Propagation–Additional insulation will be provided between each battery cell and between each cell and the battery case to thermally and electrically isolate the individual battery cells. High temperature sleeving will also be added to the battery internal wiring harness to protect against short circuits. In addition, cell venting will be added to the battery case to allow any cell [gases], including electrolytes, to escape into the battery enclosure to minimize heat build-up within the battery case.

- Preclude Hazardous Airplane-Level Safety Effects of a Battery Failure That Might Occur–As stated previously, each main and APU battery consists of a set of individual cells within a battery case. The case containing the cells will be secured within a stainless steel, sealed enclosure. This enclosure will be connected to a titanium ECS duct that vents to the outside of the airplane. Should a battery failure occur, and generate significant heat, pressure, and [gases], a metallic frangible disc (also referred to as a vent burst disc) at the interface of the enclosure and vent duct will open and allow the heat, pressure, and [gases] to safely vent overboard through the ECS duct. This will prevent the introduction of any heat, pressure, or [gases] in the electronics equipment bays or any occupied area of the airplane.

On March 19, 2014, the FAA announced the findings of a joint FAA-Boeing team that was formed in January 2013 to review the Boeing 787's design, manufacture, and assembly processes. The team found that the 787 "was soundly designed" and "met its intended safety level" and that Boeing and the FAA had "effective processes in place to identify and correct issues that emerged before and after certification."

In the team's report on its findings, the team made recommendations to further improve Boeing processes and FAA oversight (FAA 2014). The team recommended that Boeing (1) continue to implement gated design and production processes, (2) ensure that suppliers are fully aware of their responsibilities, (3) ensure that suppliers identify realistic program risks, and (4) require suppliers to follow industry standards for personnel performing Boeing-required inspections. The team recommended that the FAA revise its orders on (1) certificate management of manufacturers to recognize new aircraft manufacturing business models; (2) production approval procedures to better address complex, large-scale manufacturers with extended supply chains; and (3) engineering conformity inspections to ensure that they are based on risk. The FAA indicated that it was taking actions to address these three recommendations.

1.8.2 Previously Issued Safety Recommendations

In response to the circumstances leading to this incident, on May 22, 2014, the NTSB issued Safety Recommendations A-14-32 through -36 to the FAA. In its letter to the FAA, the

CosMX Exhibit 1003, Page 202 of 512

NTSB stated that the type of failure that occurred during this incident—thermal runaway of a single cell as a result of an internal short circuit and the cascading thermal runaway of other cells within the battery—was not expected based on the testing and analysis of the APU battery system that Boeing performed as part of the 787 certification program (see section 1.7.3). The recommendations asked the FAA to take the following actions to (1) account for internal short circuits and thermal runaway during lithium-ion battery certification tests and (2) ensure the safe introduction of new technology into aircraft designs:

> Develop abuse tests that subject a single cell within a permanently installed, rechargeable lithium-ion battery to thermal runaway and demonstrate that the battery installation mitigates all hazardous effects of propagation to other cells and the release of electrolyte, fire, or explosive debris outside the battery case. The tests should replicate the battery installation on the aircraft and be conducted under conditions that produce the most severe outcome. (A-14-32)
>
> After Safety Recommendation A-14-32 has been completed, require aircraft manufacturers to perform the tests and demonstrate acceptable performance as part of the certification of any new aircraft design that incorporates a permanently installed, rechargeable lithium-ion battery. (A-14-33)
>
> Work with lithium-ion battery technology experts from government and test standards organizations, including US national laboratories, to develop guidance on acceptable methods to induce thermal runaway that most reliably simulate cell internal short-circuiting hazards at the cell, battery, and aircraft levels. (A-14-34)
>
> Review the methods of compliance used to certify permanently installed, rechargeable lithium-ion batteries on in-service aircraft and require additional testing, if needed, to ensure that the battery design and installation adequately protects against all adverse effects of a cell thermal runaway. (A-14-35)
>
> Develop a policy to establish, when practicable, a panel of independent technical experts to advise on methods of compliance and best practices for certifying the safety of new technology to be used on new or existing aircraft. The panel should be established as early as possible in the certification program to ensure that the most current research and information related to the technology could be incorporated during the program. (A-14-36)

Boeing's description of the certification testing performed on the redesigned battery model (LVP-8-403) before the 787 returned to service was consistent with the NTSB's certification recommendations. On August 19, 2014, the FAA responded to Safety Recommendations A-14-32 through -36. Section 2.5.3 discusses the FAA's response and the NTSB's classifications of the recommendations.

CosMX Exhibit 1003, Page 203 of 512

2. Analysis

2.1 Failure Sequence

According to the available evidence from this incident investigation, the NTSB concludes that the battery failure did not result from overcharging, overdischarging, external short circuiting, external heating, installation factors, or environmental conditions of the airplane. Specifically, EAFR data before the event did not show any evidence of the battery being charged to a level above the designed operating voltage, the battery being discharged to a level below the overdischarge threshold, or any high-current discharges that could be associated with an external short circuit. The EAFR data showed no preexisting battery failure messages indicating that the overdischarge protection circuit had activated. In addition, examination of the aft E/E bay (where the APU battery was installed) showed no evidence of external short circuits, such as chafing on the battery cables, or external sources of heat, mechanical damage, or electrical abuse that could have initiated the battery failure.

Individual component tests (including those for the BCU, SPU, and APU controller) and integrated system tests, which included a BCU and other battery-related components, found no evidence indicating that external components were related to the battery failure. Vibration testing was performed at levels that exceeded in-service levels without damage that could lead to battery failure. A battery-level test showed that condensation could occur within the battery and result in a shorting path between the cell and battery cases, and a cell-level test with moisture showed that a cell failure could occur and result in arcing, shorting, and heat damage internal to the cell header. However, the damage observed during the cell-level test was not found in the cell header from the incident APU battery. In addition, airplane flight test data did not show any abnormal electrical transients that could lead to battery failure.

External observations of the battery case showed more thermal damage on the right side of the case than the left side. The right aft corner of the battery case showed the most thermal damage and the most damage to the case lid and its fastening points. The right aft area corresponded to the positions of cells 5 and 6.

The inside of the battery case, the BMU sensing wiring harness, and the lower and upper fixation trays showed the most thermal damage in the areas near cells 5, 6, and 7. The insulating material between the cells was the most damaged in the areas adjacent to cells 5 through 8. Further, cells 5 through 8 vented, and the petals of their vent discs were splayed out, indicating that the cells vented under high pressure. Cells 1 through 3 also had ruptured vent discs, but they remained mostly in the same plane as the vent opening, indicating that the venting occurred with less force than the venting for cells 5 through 8. This evidence showed that the initiating thermal event and subsequent thermal runaway of additional cells began on the right side of the battery where cells 5 through 8 were located.

CT scans of the battery showed that the aft side of cell 8 had expanded into cell 7 and that cell 7 appeared to have expanded into cell 6, indicating that cell 8 vented after cell 7 and that cell 7 vented after cell 6. CT scans and examinations showed that side 3 of cell 6 (which was closest to cell 5) was slightly convex with a flat area in the middle of the cell. CT scans and

CosMX Exhibit 1003, Page 204 of 512

examinations also showed that side 1 of cell 5 (which was closest to cell 6) was convex with a concave-to-flat area in approximately the middle of the cell. Although the sequence of whether cell 5 or cell 6 expanded first could not be determined due to the complexity of these features, the NTSB was able to determine that the thermal event initiated in a single cell.

Cells 5 and 6 exhibited comparable internal thermal damage, including the melting of the aluminum cathode, no remaining separator or other insulating materials, and fused current collector fingers. Cells 5 and 6 also showed evidence of internal short circuiting, including pinholes, radiating patterns, and thermal discoloration. The lower and upper fixation trays were more thermally damaged in the position of cell 6, and cell 3 (across from cell 6) exhibited the most thermal damage of the cells on the left side of the battery. Cell 7 also sustained internal thermal damage similar to cells 5 and 6, including two pairs of fused current collector fingers. This thermal damage pattern, centered about the position of cell 6 and extending to cells 5, 7, and 3, is consistent with the battery thermal event originating in cell 6.

The NTSB and UL's postincident testing on individual cells showed that an internal short circuit could cause current collector fingers to fuse open and lead to failure of a cell.[114] Data recorded during these tests showed a distinctive trace in which the cell voltage initially decreased, abruptly recovered, and then decreased to zero volts. The incident EAFR recorded a decrease in battery voltage followed by a single recovery in voltage and then a drop in voltage to a level consistent with one failed cell in the battery. Visual examinations and CT scans showed that one set of cell 5 aluminum current collector fingers (in the center winding) had fused open and that two sets of cell 6 aluminum current collector fingers (in the winding closest to cell 5 and the center winding) had also fused open.

During the individual cell tests in which two sets of aluminum current collector fingers fused open as a result of an internal short circuit, the recorded data showed two separate voltage decreases with two recoveries, which were not seen in the incident EAFR data. In addition, a full battery test that simulated an internal short circuit (via nail penetration) in cell 6 showed arcing between cell 6 and the center brace bar, which was not found in the incident battery. The similarity between the voltage drop behavior observed during testing for a single pair of fused current collector fingers and the EAFR data from the incident and the lack of welding between cell 6 and the center brace bar are consistent with an internal short circuit originating in cell 5.

The NTSB concludes that the battery failure resulted from an internal short circuit that occurred in cell 5 or cell 6 and led to thermal runaway that propagated to adjacent cells. The thermal damage to the battery cells precluded a determination of the cause of the internal short circuit, and postincident laboratory testing and subsequent engineering analysis of potential failure modes were unable to determine the precise cause of the internal short circuit. Possible causes for cell internal short circuits are discussed in sections 2.3 and 2.4.

[114] The NTSB and UL's testing showed that, when current collector fingers fused open only in the center winding, that winding had to be the initiation point of the internal short circuit rather than initiation due to heat from an adjacent cell or winding.

CosMX Exhibit 1003, Page 205 of 512

2.2 Emergency Response

The response to the incident was timely. According to airport security camera video, the five BOS ARFF vehicles that responded to the incident did not experience any delay from initial notification to arrival at the scene. The ARFF truck that was positioned near the incident airplane responded to the event within 1 min of initial notification, and the four other ARFF vehicles arrived on scene within 2.5 min of initial notification. The firefighting procedures used during the incident, including the use of Halotron, were appropriate and consistent with guidance in effect at the time.[115]

The incident commander decided to have the APU battery removed from the airplane once the intensity of the battery fire diminished. ARFF personnel encountered difficulties in removing the battery from its installation location, especially given that they could not readily access the battery's quick disconnect knob. One of Boeing's postincident changes to the battery and its installation involved placing the redesigned battery into a sealed stainless steel enclosure connected to a duct that was intended to allow heat, pressure, and gases resulting from a battery failure to vent outside of the airplane. As a result of this change, Boeing created and distributed firefighting procedures for events involving the main and APU lithium-ion battery. These procedures advise ARFF personnel to allow a battery undergoing thermal runaway to vent overboard and then stand by to monitor for additional fire. Thus, during active venting of the 787 main or APU battery, it is no longer necessary for ARFF personnel to enter the E/E bay.[116]

2.3 Cell Manufacturing Concerns

GS Yuasa stated that it manufactured the incident battery according to drawing specifications provided by Thales and Boeing, and GS Yuasa's and Boeing's FAI processes showed that the battery complied with Boeing's acceptance and quality control requirements. However, the NTSB's observations of GS Yuasa's cell manufacturing process identified several concerns.

First, the manual cell winding flattening process can create perturbations (that is, electrode foil buckling) in the windings. Such perturbations (see figure 16) were visually consistent with the wrinkles found in the CT scans of LVP65-8-402 exemplar batteries and those

---

[115] On June 12, 1995, the FAA issued CertAlert 95-03, which described the approved use of Halotron in airport firefighting operations. Also, Safety Alert for Operators 09013, "Fighting Fires Caused By Lithium Type Batteries in Portable Electronic Devices," which was issued on June 23, 2009, stated that a Halon replacement (Halotron) could be used to prevent the spread of such fires to other flammable materials. At commercial airports, Halotron has been effectively used to fight fires in areas with sensitive electrical equipment, such as that in the aft E/E bay. In January 2014, the FAA issued a report indicating that, for consumer electronic devices, water was "the most effective" in suppressing lithium-ion battery fires and preventing thermal runaway propagation (FAA 2014). The report did not address the use of water for suppressing fires involving large, permanently installed, rechargeable lithium-ion batteries, such as the 787 main and APU battery.

[116] According to Boeing, if the battery is not venting or when active venting is complete, firefighters should enter the E/E bay to ensure that no visible fire source exists. If a visible flame is present, Halon (or Halotron) is the recommended agent for suppressing the fire. Boeing procedures indicated that the battery pack should not be disconnected from the airplane's electrical system by using the quick disconnect knob or cutting the battery cables.

CosMX Exhibit 1003, Page 206 of 512

observed during DPAs of the main battery on the incident airplane (as discussed later in this section). The windings are predisposed to such defects because flattening a round cylindrical object into an oval cylindrical object can cause uneven deformation and distortion due to the non-uniform distribution of stress, which results in buckling in areas of compressive stress. Also, subsequent swelling and contracting of the electrodes during charging and discharging can further exacerbate perturbations within the winding layers.

Second, two of the welding operations—ultrasonic welding of the current collectors to the winding and tungsten inert gas welding of the cell header to the cell case—occur in an area where internal cell components are also assembled. Welding can generate FOD in the form of weld spatter and small metallic particles that become airborne. No physical shielding was used at the tungsten inert gas weld station to isolate this FOD-generating process from adjacent FOD-sensitive processes, such as those involving internal components of nearby open cells. Even though the ultrasonic welding machine incorporated a vacuum system to mitigate the amount of FOD generated, this process was observed generating airborne FOD.

Third, some of the cell manufacturing processes were not consistent with industry practices.[117] For example, production of wound prismatic (rectangular-shaped) battery cells is typically performed on a flattened elliptical or rectangular mandrel, which reduces the chance for perturbations and folds during winding, but GS Yuasa used a cylindrical mandrel during the winding process.

The cell electrolyte filling process was also inconsistent with industry practices. The electrolyte was filled in three iterative steps to prevent overflow followed by a precharge to low voltages after each step. GS Yuasa stated that the cell's solid electrolyte interphase (SEI) layer does not form during the precharging process because the final precharge brings the battery to 20% state of charge.[118] Industry practices for electrolyte filling include one-step filling followed by a full charging sequence to develop the SEI layer. Developing the SEI layer is important because it allows safe cell operation during normal charging and discharging, and disruption of the SEI layer could lead to internal short circuiting. It is unknown whether GS Yuasa's precharging process affects the development of the SEI layer or the chemical properties or performance aspects of the cell. GS Yuasa representatives stated that the company has not studied the effect of its iterative electrolyte filling process on battery safety. Thus, the safety effect of GS Yuasa's precharging process during the electrolyte filling process is unknown.[119]

Last, GS Yuasa used CT equipment during the postassembly inspection process to ensure that the current collectors were properly welded to the winding edges and that FOD was not

---

[117] The industry practices discussed in this section were based on information from (1) discussions with industry personnel, including those from the Naval Surface Warfare Center, Carderock Division; the US Department of Energy; and TIAX; and (2) site visits to other battery manufacturer plants.

[118] During the full initial charge and discharge of a cell, the surface of the anode forms the SEI layer.

[119] Although the NTSB did not observe the electrolyte filling process during its visit to GS Yuasa, the NTSB did observe dried material consistent with solid electrolyte residue on the electrolyte filling container and tube, which was not consistent with industry practices because superfluous solid material introduced into a battery cell could interfere with the battery charging and discharging processes.

CosMX Exhibit 1003, Page 207 of 512

enclosed in a cell. However, the resolution settings of GS Yuasa's CT equipment was such that many internal cell features, including individual winding layers, could not be identified during the NTSB's visit to GS Yuasa's facility. As a result, perturbations in the windings and small-sized FOD and burrs might not be recognized with the CT equipment used at the time of the NTSB's visit. GS Yuasa stated that it was not aware that FOD might not be visible on the company's CT scans.

GS Yuasa's CT scans also did not detect features that the NTSB, TIAX, and UL identified during this investigation. For example, TIAX's and UL's DPAs of cells from the main battery on the incident airplane found cell windings with numerous wrinkles, folds, and creases.[120] Also, the NTSB's CT scans of the eight cells in each of the five exemplar batteries (including the main battery from the incident airplane) revealed wrinkled windings, cell-to-cell inconsistencies in the clearances between the current collector fingers and the cell case sides, and variances between the rivet heads of the terminals and the top of the cell windings. GS Yuasa indicated that it did not know whether such features could result from its LVP65 cell manufacturing process and that it did not have a process to inspect for the features.

Manufacturing defects, including FOD, burrs on component edges, and perturbations in windings (which were visually consistent with the wrinkles found in postincident CT scans and cell teardowns), are known to lead to local lithium deposits, perforation of the separator layer, or shorting between electrodes (Mikolajczak and others 2011). During the UL and TIAX DPAs of battery cells from the main battery on the incident airplane, silver-colored deposits consistent with lithium metal were observed adjacent to wrinkles (that is, those features that were visually consistent with perturbations). According to GS Yuasa representatives, the company has not studied the effects of folds and wrinkles on battery safety, performance, and reliability.

GS Yuasa monitors for "wrinkles" (that is, visible longitudinal or diagonal surface creases) in the anode and cathode foils before the winding process but does not monitor for features such as perturbations formed during the winding, flattening, and assembly processes. Further, although GS Yuasa stated that it had a formal process for actively monitoring for and controlling burrs, GS Yuasa's process for monitoring for FOD was not a formal standardized quality control process for locating, reducing, and preventing FOD generation during the cell assembly process.

GS Yuasa performed most of its quality control inspections after a cell was fully manufactured and indicated that less than 1 percent of manufactured cells were rejected. This low rejection rate could be the result of few defects to detect; however, most of the evidence (that is, poor internal manufacturing steps along with the lack of a formal inspection for manufactured defects) indicated that GS Yuasa's inspection process did not adequately screen for defects that developed during the manufacturing process. GS Yuasa's checks during the manufacturing process relied on visual inspection rather than formal sampling processes that included rejection or acceptance criteria.

[120] The wrinkles and folds can modify the anode-to-cathode ratio locally, resulting in lithium deposits on the anode surface.

CosMX Exhibit 1003, Page 208 of 512

Vigilance decrements might also have played a role in the inadequate inspection process. GS Yuasa indicated that personnel involved with cell manufacturing for LVP-8-402 batteries worked 8-hour shifts. The visual inspection tasks performed by these personnel were vigilance tasks.[121] Human factors research on inspection indicates that, as time on task increases, defects are more likely to be missed, especially if they seem to rarely occur (Fisher and others 2006, 997-1024).[122]

Industry research on lithium-ion battery hazards showed that, about the time that the LVP65 cells were being manufactured, cell failures in various industries had been caused by, among other things, internal faults resulting from manufacturing defects (Mikolajczak and others 2011). However, GS Yuasa did not establish its cell manufacturing process to minimize the potential for manufacturing defects or develop formal inspection criteria of the cells that would reliably identify any defects that were introduced during the process.

Although GS Yuasa was responsible for manufacturing the 787 main and APU battery and cells, Thales was responsible for providing Boeing with consistent and safe power conversion subsystems (which included the main and APU battery systems) for 787 airplanes. Thales audited GS Yuasa in June 2011 and September 2012, and all of the discrepancies noted in the audits were subsequently addressed. However, none of the discrepancies were related to cell features, such as perturbations created and FOD generated, from GS Yuasa's cell manufacturing process. Postincident interviews revealed that Thales did not recognize that such features could result from the cell manufacturing process or that GS Yuasa's quality controls were not established to detect these features.

Boeing and FAA personnel did not conduct any audits of GS Yuasa before the incident. (Boeing stated that it relied on Thales to audit its subtier suppliers.) Boeing, as the production approval holder (that is, the holder of a production certificate), provided oversight to ensure that its contracted suppliers of the 787 power conversion subsystem adhered to their approved quality control system for the manufacturing of subsystem components. The FAA provided oversight of Boeing to ensure that (1) its contracted suppliers followed approved procedures for the production of products, articles, and parts that conformed to Boeing's approved type design and (2) such products, articles, and parts were airworthy and safe for operations. However, given the observations discussed above about GS Yuasa's cell manufacturing process, Boeing's and the FAA's oversight of suppliers manufacturing the 787 power conversion subsystem components could have been more effective.

The NTSB concludes that GS Yuasa's cell manufacturing process allowed defects that could lead to internal short circuiting, including wrinkles and FOD, to be introduced into the

[121] The NTSB notes that visual inspection tasks performed during 8-hour workdays can lead to vigilance decrements. At the time of the NTSB's visit to GS Yuasa, personnel involved with cell manufacturing were working 12-hour shifts because of the demand for new LVP65-8-403 batteries after the 787 returned to flight.

[122] The greatest performance decrements are expected within the first 30 minutes of time on task; during that time, performance can be reduced as much as 30% but is typically reduced no more than 10% (Teichner 1974, 339-353). A 30% performance decrement is more likely for a highly detectable signal (defect) during a 3-hour period.

CosMX Exhibit 1003, Page 209 of 512

Boeing 787 main and APU battery. Therefore, the NTSB recommends that GS Yuasa (1) review its cell manufacturing processes to minimize or prevent defects that could affect cell safety and (2) ensure that its employees are properly trained to identify and eliminate these defects. The NTSB also recommends that Boeing develop or revise processes to establish more effective oversight of its suppliers (including subtier suppliers) to ensure that the product being manufactured adheres to established industry standards. Further, the NTSB recommends that the FAA develop or revise processes to establish more effective oversight of production approval holders and their suppliers (including subtier suppliers) to ensure that they adhere to established manufacturing industry standards.

2.4 Thermal Management of Large-Format Lithium-Ion Batteries

Testing performed during the investigation showed that a cell in a 787 battery assembly generated localized high-temperature conditions during maximum current discharge. This measured high temperature was above the allowable design maximum temperature, which could lead to an internal short circuit and cell thermal runaway. This section describes those test results and discusses the importance of ensuring that large-format lithium-ion battery and cells are sufficiently designed and monitored to prevent degradation that can lead to cell thermal runaway.

2.4.1 Battery Internal Heating During High-Current Discharge

The NTSB and UL performed testing on an exemplar 787 battery to evaluate the battery's performance during discharge under the highest currents that the battery was rated to carry. The testing included simulated APU starts at 77°F and 32°F with a high-current load. The battery cell design used riveted joints (part of the terminal assembly in the cell headers) as part of the current conduction path into and out of the cells. The simulated APU start tests revealed significant localized heating near the aluminum rivets of one of the test battery's cells. The temperature change was the greatest during the discharge phase of repeated battery charge and discharge cycles at lower temperatures.[123] The affected cell, located in position 5 of the test battery, began to exhibit a more substantial temperature rise in the area of the aluminum riveted joint compared with the temperature rise in other cells in the battery after the first full charge/discharge cycle of the test. During the subsequent test cycles, the affected cell's temperature increased progressively to a maximum temperature of 315°F near this joint.

Post-test measurement of the riveted joint of the affected cell showed a significant increase in contact resistance (three orders of magnitude) between the aluminum rivet and the current collector compared with the contact resistance of cells from another 787 battery.[124] Because the heating occurred during periods of maximum current draw on the

[123] In this context, a cycle comprises three high-current discharges followed by one charge. The battery was allowed to stabilize after each cycle.

[124] The affected cell's post-test contact resistance measured between the aluminum rivet and the current collector was 74.5 milliohms, whereas the resistance in the same location for a cell from another battery was 0.030 milliohm. The Boeing battery SCD required contact resistance for new components to be less than 0.025 milliohm.

CosMX Exhibit 1003, Page 210 of 512

battery and was localized to the area of the riveted joint, the NTSB and UL determined that the source was resistive heating resulting from current through the area of high contact resistance.[125] The cell's windings were also a source of resistive heating during the simulated APU start testing, with the most significant heating occurring at 32°F.[126] Although all of the battery cells would have been affected by this heating, only cell 5 showed excessive localized heating near the cell's aluminum riveted joint.

This testing also showed that the heat generated inside the battery during the heaviest current loading condition of a full APU start could expose a cell to temperatures exceeding the maximum approved operating temperature of the battery (158°F) without detection by the battery's monitoring system. Post-test disassembly and examination of the affected cell showed thermal degradation (melting) along the edges of the cell's separator in the location where the aluminum current collectors attached to the cell windings, indicating that the cell's maximum temperature (at the aluminum riveted joint) exceeded the melting temperature of the separator.[127] The post-test examination of the affected cell also showed that the excessive temperature of the cell caused (1) softening and deformation of the plastic insulator material positioned between the aluminum rivet, the aluminum current collector, and the cell case to provide a hermetic seal at each rivet and (2) electrolyte leakage through the riveted joint.[128] Moisture entering the cell and electrolyte exiting the cell due to the softening and deformation of the seal could degrade internal cell chemistry and lead to cell failure, including thermal runaway.

The NTSB reviewed the design of the 787 main and APU battery cells to determine potential causes of the resistive heating observed near the aluminum rivets. The Boeing SCD for the battery stated that "connector contacts shall be designed to carry the same or better electrical current as the equivalent wire size." However, the aluminum rivet used in the 787 main and APU battery cell had a smaller cross-sectional area than would be required, according to the American Wire Gauge standard, for a wire rated to carry an equivalent current. Further, the Boeing SCD for the battery required terminal attachments to have "a complete metal-to-metal compression system." Examination of the rivet assemblies showed that the riveted joint had no springs or

---

[125] The electrical contact resistance between mated components (such as an aluminum rivet and a current collector) is a function of the real contact surface area between interfacing parts of a joint, contact pressure between mating surfaces, surface topography, and the presence of an oxide on mating surfaces, among other factors. The smaller the contact area between interfacing parts of the joint, the higher the resistance to current flow, and the more heat generated. The heat generated when a current is passing through a conduction path is directly proportional to the square of the current multiplied by the resistance of the conduction path.

[126] Testing performed by the NTSB and UL showed that, as the 787 main and APU battery approached temperatures below 32°F, the battery's efficiency decreased such that 30% of the discharge energy was released as heat instead of usable electrical energy at 0°F. This heat loss was the result of both electrochemical and resistive heating losses in the cell windings, which increased at colder temperatures. (Lithium-ion cells normally heat during discharge as a result of the electrochemical reaction that occurs within the battery cells. Heat is also produced as a result of resistance in electrical current conduction paths within the battery and cells.)

[127] Boeing's EPS safety assessment indicated that heat-induced shrinkage of a cell separator, such as that observed after the NTSB and UL's testing, is a potential cause of cell internal short circuiting and could lead to thermal runaway.

[128] According to UL, the thermoplastic seals used between the rivets, the cell case, and the current collector can permanently deform when exposed to temperatures between about 176°F and 230°F under load.

CosMX Exhibit 1003, Page 211 of 512

other compression devices.[129] Thus, the aluminum riveted joint assembly could be a significant source of resistive heating during maximum current discharge conditions for the 787 main and APU battery. Proper sizing of electrical components and positive retention of pressure in a joint are essential in preventing resistive heating, particularly during the most severe discharge current levels for the battery (that is, those that occur during a full APU start).

Another potential cause of the resistive heating was the poor electrical connection between the rivet and current collector components in the riveted joint. During the APU start tests, the excessive heating in the joint became evident only after the affected cell had successfully completed earlier cell- and battery-level simulated APU starts, indicating that the electrical connection between the rivet and current collector components degraded with continued usage. Proper design, manufacture, and damage tolerance of electrical connections among the components of a joint intended to transmit current through the cells is critical to minimize resistive heating inside the battery under the most severe operating conditions during repeated charge and discharge cycles. Testing of large-format lithium-ion batteries designed to carry large currents (similar to the 787 main and APU battery) for other applications showed that heat generated by poorly formed joints can flow toward the internal battery and cell structure, resulting in a considerable temperature increase that can lead to thermal runaway (Taheri and others 2011, 6525-6533).

After the BOS and TAK battery incidents, Boeing modified and recertified the 787 main and APU battery design to prevent a full battery thermal runaway resulting from a cell internal short circuit. The redesign also included a stainless steel enclosure designed to mitigate the effects of a full battery thermal runaway if it were to occur, even though FAA Special Conditions 25-359-SC did not require this enhanced level of mitigation.[130] Preventing cell thermal runaway by minimizing sources of heating is critical to the safety of future lithium-ion battery designs. However, current industry standards for the design and qualification of permanently installed, large-format, rechargeable lithium-ion batteries used on civil aircraft do not include guidance on industry best practices to minimize internally generated sources of heating, such as resistive and electrochemical heating, in the design and manufacture of these batteries.

Identifying and minimizing all sources of heating generated within a large-format lithium-ion battery during operation (particularly heating that can be localized to a cell as a result of electrical current flow through components, connections, and cell windings at lower temperatures) are important parts of the battery's design and manufacturing processes. These

[129] Without such devices, additional causes of joint degradation could include thermal shock, torque applied to the terminal during assembly, bending of the current collectors during the manufacturing of the cell header assembly, manufacturing errors, or the stress created within various cells when the battery is subjected to temperature extremes. A NASA technical standard requires that clamping pressure across semipermanent joints (such as those containing rivets) be consistent with applicable mechanical engineering assembly and installation requirements (NASA 2013).

[130] According to Boeing, the redesigned battery system included changes to prevent and isolate a fault if one were to occur. The redesign incorporated multiple layers of protection, including the new enclosure, to ensure that there would be no impact to the airplane and no possibility of fire if a battery failed. The enclosure was designed to keep any amount of battery overheating from affecting the airplane.

CosMX Exhibit 1003, Page 212 of 512

actions are necessary to account for the cumulative effects of electrochemical and resistive heating within a cell or in other locations within the battery to minimize the possibility that a cell (or cells) could be exposed to temperatures above allowed operational limits during high-current, low-temperature discharging that could cause permanent damage to a cell and lead to thermal runaway.

The NTSB concludes that the thermal protections incorporated in large-format lithium-ion battery designs need to account for all sources of heating in the battery during the most extreme charge and discharge current conditions and protect cells from damage that could lead to thermal runaway. Therefore, the NTSB recommends that the FAA work with aviation industry experts to develop or modify design safety standards for large-format lithium-ion batteries to require that sources of excessive heating, including electrical contact resistance from components and connections, be identified, minimized, and documented as part of the design. The standards should include measures for identifying and minimizing potential sources of heating that consider the range of operating temperatures and the most extreme electrical currents that the battery could be expected to experience during repeated charge and discharge cycles.

2.4.2 Cell-Level Temperature and Voltage Monitoring

FAA special condition 1 (see appendix B) required the 787 main and APU battery to maintain safe cell temperatures during any foreseeable charging or discharging condition and any failure of the charging or battery monitoring system not shown to be extremely remote. Maintaining safe cell temperature is critical because, once a cell heats to the point that the SEI layer degrades or the separator becomes thermally damaged, an internal short circuit and thermal runaway can occur. Further, as shown by the affected cell in the NTSB and UL's simulated APU start tests, localized heating of the cell to excessive temperatures occurred rapidly and went undetected by the BMU when the battery was discharged at its maximum current rating. Thus, the thermal management protections incorporated into the battery did not detect the developing temperature exceedance and prevent the cell from reaching an unsafe temperature.

The 787 main and APU battery was designed to measure temperature only on two cell bus bars and not at each cell. The NTSB and UL's simulated APU start tests showed that the temperature sensors on the bus bars recorded a peak value that was less than the cell temperature at the aluminum riveted joint. Thus, the temperature measured on the bus bars did not accurately reflect actual cell temperatures. In addition, the temperatures measured on the bus bars are not recorded by the BMU or at another location in the airplane. Accurate temperature data at the cell level, when monitored and recorded, could allow the battery monitoring system to (1) detect a rise in cell temperature and take actions before the temperature exceeded safe limits and caused damage and (2) provide timely notification to the flight crew or maintenance personnel if required.

Special condition 7 addressed voltage monitoring to prevent overcharging that could lead to thermal runaway. During the NTSB and UL's simulated APU start testing on individual cells, cell voltages (in millivolts) were found to be an important indicator of battery health and could

CosMX Exhibit 1003, Page 213 of 512

thus be used to mitigate failures. Also, during cell abuse testing, a drop in voltage of an individual cell preceded thermal runaway and venting.[131] The 787 main and APU battery design incorporated provisions to monitor each cell's voltage and inhibit discharging of the battery below a specified voltage to protect the cells against overdischarge. Comparing the voltage drops of various cells during discharge could allow the BMU to inhibit subsequent charging or electrically isolate the cell to minimize further damage to the battery. The voltages measured by the sensors on the 787 cell bus bars were not recorded, and design standards do not require voltage data to be recorded. These data, if recorded, could provide maintenance or engineering personnel with trend data or other important information that could be used to determine the cause of a cell failure.

The NTSB concludes that more accurate cell temperature measurements and enhanced temperature and voltage monitoring and recording could help ensure that excessive cell temperatures resulting from localized or other sources of heating could be detected and addressed in a timely manner to minimize cell damage. Therefore, the NTSB recommends that the FAA work with aviation industry experts to develop or modify existing safety standards related to the design of permanently installed lithium-ion batteries to require monitoring of individual cell temperature and voltage and recording of exceedances to prevent internal cell damage during operations under the most extreme operating temperatures and currents. The NTSB also recommends that, once the guidance requested in Safety Recommendation A-14-115 has been issued, the FAA require type certification applicants to demonstrate that the battery monitoring system maintains each individual cell within safe temperature limits at the most extreme battery operating temperatures and the heaviest electrical current loads approved for operation. In addition, the NTSB recommends that the FAA work with lithium-ion industry experts to (1) conduct research into battery monitoring system technologies that could improve the recognition of conditions leading to thermal runaway, (2) develop active mitigation of such conditions to minimize damage, and (3) update design and safety standards accordingly.

2.4.3 Thermal Safety Limits for Cells

Boeing established the 787 main and APU battery's maximum operating temperature (158°F) at the same maximum operating temperature as that for nickel-cadmium batteries installed in other airplane models. The NTSB and UL's ARC testing on 787 main and APU lithium-ion battery cells determined that the cell began to self-heat at 144°F.[132] Maintaining cell temperature at or just above a cell's self-heating threshold for an extended period of time could

[131] For example, the testing found that about 0.8 second elapsed between the time that an initial failure in a cell (as indicated by a 20-millivolt voltage drop) was detected and the time when the cell went into thermal runaway and vented.

[132] Different types of cell-level testing are available to determine the onset of cell damage and objectively establish limits for the battery monitoring system to provide a margin of safety. The ARC test is a well-documented technique that slowly heats cells in adiabatic conditions to document the heat absorbed or generated by the cells.

CosMX Exhibit 1003, Page 214 of 512

result in thermal runaway.[133] Thus, the upper temperature limit of the 787 battery was inappropriate for the cell materials.

GS Yuasa did not use the self-heating threshold to determine the safe temperature limit for the 787 battery. Instead, GS Yuasa determined the safe cell temperature by conducting a test in which cell temperatures were elevated until cell venting occurred; in another set of tests, the cells were exposed to reduced temperatures for varying durations, and no cell venting occurred. These test methods were inadequate because the cells might not have been at elevated temperatures long enough to go into thermal runaway from the breakdown of cell materials. The temperature at which cell self-heating begins can be an objective measure for establishing a battery's margin of safety.

Thermal runaway due to overheating can occur either rapidly when a cell is exposed to temperatures that are high enough to melt the separator or slowly as the cell's SEI layer degrades when above the self-heating temperature. Research showed that SEI layer damage is cumulative and that the thermal degradation of some commercial cells, when maintained at their self-heating temperature, continued for 2 days before thermal runaway occurred (Mikolajczak and others 2011).

As previously stated, FAA special condition 1 required the 787 main and APU battery to maintain safe cell temperatures during any foreseeable charging or discharging condition and any failure of the charging or battery monitoring system not shown to be extremely remote. However, current aviation industry standards do not define methods to determine safe cell temperature limits. Such standards exist for non-aviation-related applications.[134]

The NTSB concludes that determining the initial point of self-heating in a lithium-ion cell is important in establishing thermal safety limits. Therefore, the NTSB recommends that the FAA work with industry experts to develop appropriate test methods for determining the initial point of self-heating in a lithium-ion cell to establish objective margins of thermal safety for future battery designs.

2.5 Certification Process

Type certification is a regulatory process that the FAA uses to ensure that aircraft product designs comply with applicable *Federal Aviation Regulations* and, as in this case, applicable special conditions. The 787 main and APU lithium-ion battery design was evaluated and approved as part of the Boeing 787 type design certification program. Although the investigation of this incident found that thermal runaway of a cell (due to an internal short circuit within a

---

[133] According to a NASA technical memorandum, "above a threshold temperature, a 'self-heating' condition could occur due to exothermic reactions occurring internally within the cell. Such reactions may include reactions between lithium and electrolyte and the thermal decomposition of internal cell components. If the internal heat generation is allowed to continue, a catastrophic cell 'thermal runaway' condition could occur, which would be a serious safety concern for a manned application"(Baldwin and others, 2010).

[134] For example, see Sandia National Laboratories' electrical energy storage system abuse test manual for electric and hybrid electric vehicles (Doughty and Crafts, 2006).

CosMX Exhibit 1003, Page 215 of 512

single cell of the APU battery) propagated to other cells and resulted in thermal runaway of the battery and fire, this design vulnerability was not identified during the certification of the 787 battery installation.

The NTSB's investigation of this incident found that more effective implementation of the certification process for designs incorporating new technology could be achieved through improvements in several focused areas. These areas include validation of the assumptions made and the data used in preliminary and final safety assessments developed during certification programs and the manner in which the FAA evaluates methods of compliance with special conditions during the certification process, as discussed in sections 2.5.1 and 2.5.2, respectively. Improvements in these areas could help foster better interactions between type design applicants and the FAA to ensure the completeness of data used by the applicant to demonstrate compliance with FAA requirements.

2.5.1 Validation of Assumptions and Data Used in Safety Assessments Involving New Technology

To effectively show compliance with FAA requirements during the certification process, Boeing needed to identify all foreseeable ways that 787 main and APU battery failures could cause the identified airplane-level hazards of venting with smoke and fire (classified by Boeing as a catastrophic event) or venting with or without smoke (classified by Boeing as a hazardous event). Boeing recognized that the propagation of cell-to-cell thermal runaway was a failure condition that could result from an internal short circuit in a single battery cell and evaluated this failure condition using the results of GS Yuasa's November 2006 development nail penetration test.[135] As stated in section 1.7.3, the nail penetration test results showed that the surface temperature of the nail-penetrated cell increased, smoke vented from the cell and the battery case, and the surface temperature of the adjacent cells increased with no venting. As a result of this test, Boeing, Thales, and GS Yuasa determined that an internal short circuit in a single cell that resulted in thermal runaway would not propagate to other cells within the battery case or generate a fire.

Boeing and Thales performed preliminary and final EPS safety assessments, which included fault tree analyses, FMEAs, and failure rate data provided by GS Yuasa. These assessments considered internal short circuit failures but were developed with the underlying assumption that the most severe effect of an internal short circuit within a cell would be limited to venting of only that cell without fire and propagation to other cells. Thus, the potential for an internal short circuit to lead to multiple-cell or battery thermal runaway with venting, electrolyte leakage, excessive heat, and fire was not analyzed in the safety assessment.

As shown by the circumstances of the BOS incident, the assumption that thermal runaway of a cell would not propagate to other cells within the battery case was incorrect.

[135] Boeing, Thales, and GS Yuasa indicated that other battery-level development nail penetration tests were performed, but no documentation of those tests and their results was available for the NTSB's review. For information about these tests, see the addendum to the System Safety and Certification Group Chairman's Factual Report, which is available at www.ntsb.gov in the public docket for this incident.

CosMX Exhibit 1003, Page 216 of 512

Validation of assumptions related to failure conditions that can impact safety is a critical step in the development and certification of an aircraft. The validation process must employ a level of rigor that is consistent with the potential hazard to the aircraft in case an assumption is incorrect. Society of Automotive Engineers (SAE) Aerospace Recommended Practice (ARP) 4754 provides a structured process for managing and validating assumptions with steps that include ensuring that assumptions are explicitly stated, appropriately disseminated, and justified by supporting data (SAE 2010).[136] The ARP notes that validating assumptions can be accomplished using reviews, analyses, and tests.

Development testing is often necessary to validate important design assumptions, but the nail penetration test performed by GS Yuasa did not adequately account for a number of factors that were relevant to propagation risk. For example, the test was not conducted at the battery's maximum operating temperature of 158°F, and the test setup did not fully represent the battery installation on the 787 airplane.[137] Also, the test did not include repeated trials of inducing thermal runaway of a cell in multiple batteries to understand how the repeatability of these tests could impact the validity of the test results. Further, the test was performed using a development unit that did not incorporate the final battery design certified as part the 787 type design.[138]

Other development tests were performed to evaluate various aspects of the 787 battery's performance, including the July 2009 integrated system test at UTC Aerospace Systems' APSIF. This test was not designed to evaluate internal short circuiting effects or the cell-to-cell propagation risk. During the test, the battery was unintentionally charged at an excessive rate, which resulted in the venting of a single cell. Although the thermal runaway of that cell did not propagate to other cells within the battery case, the results of this test should not have been considered to be confirmation of the results of GS Yuasa's 2006 nail penetration test because the APSIF test was not designed to examine engineering factors that could likely influence whether

---

[136] SAE ARP 4754 is an industry guideline that addresses design development for civil aircraft systems with failure modes that could affect the safety of aircraft on which the systems are installed. SAE ARP 4754 defines validation as "the determination that the requirements for a product are correct and complete." The original version of the ARP, "Certification Considerations for Highly-Integrated or Complex Aircraft Systems," was issued in November 1996 and was in use at the time of the 787 certification program. The current version of the ARP, revision A, was issued in December 2010 and was retitled, "Guidelines for Development of Civil Aircraft and Systems." The revised guideline was expanded to include all types of aircraft certification programs and not just those incorporating highly integrated or complex systems.

[137] The NTSB and UL's postincident nail penetration testing with an ungrounded battery at the battery's maximum operating temperature showed that thermal runaway of a single cell propagated to all other cells inside the battery case. Also, the JTSB conducted a heat propagation test on three 787 main and APU batteries. During all three tests, an internal short circuit was initiated in a single cell of each test battery using the nail penetration method. According to the JTSB's final report on the TAK incident, propagation of thermal runaway to multiple cells within the battery occurred during two of the three tests. For both of these tests, the battery was connected to the BCU, and the battery case was grounded, simulating the actual configuration as installed on the airplane. One of these tests was conducted at 158°F, and the other test was conducted at 86°F. The test involving the ungrounded battery case (during which no propagation occurred) was conducted at 86°F.

[138] According to Boeing, Thales, and GS Yuasa, electrolyte leakage was observed during two engineering (noncertification) cell vent tests in September 2009; as a result, the battery case design was modified to incorporate additional sealing to prevent electrolyte leakage. Also, the preproduction battery design used during GS Yuasa's testing had a different vent disc arrangement than the arrangement in the final battery design.

CosMX Exhibit 1003, Page 217 of 512

an internal short circuit would lead to propagation. As a result, the repeatability of the test result under all operating environments and usage conditions was not ensured.

Further, GS Yuasa's qualification abuse tests, which were intended to demonstrate that the battery design met the criteria established in the 787 main and APU battery SCD, did not provide adequate evidence to discount the possibility of propagation in the event of cell thermal runaway resulting from an internal short circuit.[139] Specifically, none of these tests drove a cell into thermal runaway to demonstrate that propagation would not occur or that the battery case could contain the effects of multiple-cell venting. Also, the batteries used during the tests were not grounded as installed on the airplane. Thus, the results of these tests were not relevant or sufficient for making assumptions about propagation with a grounded battery and for the full range of operating conditions.[140]

In addition to underestimating the most severe effects of a cell internal short circuit, Boeing, Thales, and GS Yuasa also underestimated the rate of occurrence for this failure mode. Boeing indicated in its EPS safety assessment that the rate of occurrence of cell venting would be about one in 10 million flight hours. However, this predicted failure rate was significantly lower than the actual failure rate observed for the 787's first 52,000 hours of service, during which time both the BOS and TAK incidents occurred.

Boeing used data from GS Yuasa to determine the rate of occurrence of cell venting. These data were based on GS Yuasa's experience with a lithium-ion battery with a similar mechanical design, which GS Yuasa manufactured for use in an industrial application. Of the more than 14,000 similarly designed lithium-ion battery cells in service at the time, GS Yuasa found that none had experienced thermal runaway or venting. Because no failures had occurred, GS Yuasa used probabilistic methods to estimate a failure rate for the industrial battery cells.[141] After accounting for capacity differences between the two battery applications and establishing that the environmental and usage conditions and the manufacturing processes for the 787 and industrial applications would be similar, GS Yuasa determined that the 787 main and APU battery cells would have a failure rate similar to that of the industrial cells.

The method that GS Yuasa used in estimating the failure rate for 787 main and APU battery cells was consistent with industry practices for components manufactured with controlled processes and subjected to similar stress conditions during normal use over time. However, the NTSB found no documented analysis comparing the duty cycle and environment expected in the

---

[139] The qualification abuse testing included two external short circuit tests (low and high impedance shorts at battery terminals), one overcharge test (charge battery to 36 volts for 25 hours), and one overdischarge test (discharge battery to zero volts). These qualification tests were conducted at the battery's maximum operating temperature of 158°F, and no thermal runaway occurred. A qualification test involving high-temperature storage (185°F for 18 hours) also resulted in no thermal runaway.

[140] During the NTSB's April 2013 investigative hearing on the BOS incident, a Boeing representative testified that Boeing used "state of the art in testing" and that no propagation of cells occurred during qualification abuse testing, nail penetration testing, and the venting event at APSIF.

[141] Probabilistic methods model and describe the random variations in systems. Probabilistic methods demonstrate compliance in the certification process using probabilistic risk analysis techniques.

CosMX Exhibit 1003, Page 218 of 512

787 application with that experienced in the industrial application. If the 787 application had higher mechanical and/or electrical stress levels than the industrial application due to differences in duty cycle and environment, the onset of certain failure modes could be accelerated, or failure modes not previously exhibited in the industrial cells, such as internal short circuiting and cell venting, could be manifested in the 787 battery cells.[142] Given the potential safety consequences of cell venting and the lack of historical data on cell and battery performance in an airplane application, Boeing, Thales, and GS Yuasa should have performed a structured engineering analysis, supplemented by testing, to compare the differences in duty cycle and environment between the two applications and measure the impact on battery and cell features that drive safety-related failure modes, effects, and rates. This level of rigor was needed to determine whether the use of the industrial cell failure rate was appropriate for the 787 application.

Boeing indicated in certification documents that it used a version of AC 25.1309 (referred to as the Arsenal draft) as guidance in preparing the EPS safety assessment for the 787 type design certification program. The draft AC addressed the treatment of assumptions and data, stating that the underlying assumptions, data sources, and analytical techniques used in safety analyses should be identified and justified to ensure the validity of the conclusions made in safety assessments. However, the analysis that Boeing presented in its EPS safety assessment did not appear to be consistent with the guidance provided in the draft AC. Specifically, the analysis did not (1) identify Boeing's assumption that thermal runaway of a cell would not propagate to other cells and (2) provide the engineering rationale needed to justify broad use of this assumption under all operating conditions. Also, the analysis did not sufficiently evaluate and justify the use of the industrial battery failure rate data in predicting the risk of a cell venting occurrence for the 787 battery. Further, even if this information had been included in the EPS safety assessment, the validity of the supporting safety analyses would have been difficult to justify given the limited data available. For example, the assumption that propagation would not occur was based on the result of GS Yuasa's single 2006 nail penetration test, and the failure rate prediction for cell venting was developed without a rigorous comparison of the most severe environmental and usage conditions between the industrial and 787 battery applications.

AC 25.1309 (Arsenal draft) also stated, "where it is not possible to fully justify the adequacy of the safety analysis and where data or assumptions are critical to the acceptability of the failure condition, extra conservatism should be built into either the analysis or the design." The assumption that the design of the main and APU battery prevented thermal runaway of a single cell from propagating to other cells inside the battery case was critical to accepting the risk of an internal short circuit in a cell because, if the assumption were incorrect, thermal runaway of the battery could occur. As a result, Boeing should have taken a more conservative approach in its safety analyses by including the possibility that propagation of thermal runaway from cell to cell could result from an internal short circuit and considering the potential effects if this failure condition were to occur. If such an approach had been taken, Boeing authorized representatives

[142] For example, stresses on the cells introduced by altitude changes would only be present in the 787 application, and these stresses applied over time in service could change the failure modes, the severity of failure effects, and increase the rates of failure for the cells and the entire battery installation. Deterministic methods that involve accelerated stress testing are commonly used to evaluate the influence of engineering factors, such as stress, design, and environment, on item reliability (Condra 1993).

CosMX Exhibit 1003, Page 219 of 512

and/or FAA certification engineers independently reviewing the EPS safety assessment would likely have required Boeing, Thales, and GS Yuasa design engineers to (1) perform more exhaustive test and analysis to properly validate claims about propagation and cell failure rate or (2) incorporate design features to safely accommodate cascading thermal runaway of all cells inside the battery case.[143]

Critical assumptions and conclusions made in GS Yuasa's and Thales' safety analyses and used in Boeing's EPS safety assessment were not fully delineated and justified with appropriate data and engineering rationale. However, multiple independent reviews of the EPS safety assessment by Boeing authorized representatives and FAA certification engineers did not reveal these deficiencies. The review process for safety assessments should be designed to closely examine the data used to support conclusions and challenge assumptions, particularly those that could result in significant safety consequences if incorrect. Also, the review process should be designed to ensure a conservative approach when available engineering data and experience are limited.

The NTSB concludes that Boeing's EPS safety assessment did not consider the most severe effects of a cell internal short circuit and include requirements to mitigate related risks and that the review of the assessment by Boeing authorized representatives and FAA certification engineers did not reveal this deficiency. Therefore, the NTSB recommends that Boeing modify its process for developing safety assessments for designs incorporating new technology to ensure that the conclusions made are validated and that any identified deficiencies are corrected. The NTSB also recommends that the FAA provide its certification engineers with written guidance and training to ensure that (1) assumptions, data sources, and analytical techniques are fully identified and justified in applicants' safety assessments for designs incorporating new technology and (2) an appropriate level of conservatism is included in the analysis or design, consistent with the intent of AC 25.1309 (Arsenal draft). Further, the NTSB recommends that, during annual recurrent training for engineering designees, the FAA discuss the need for applicants to identify, validate, and justify key assumptions and supporting engineering rationale used in safety assessments addressing new technology.

2.5.2 Validating Methods of Compliance for Designs Involving New Technology

The FAA was responsible for approving Boeing's methods of compliance and the data produced from various analyses and tests. The FAA approved Boeing's qualification test program (which was outlined in Boeing's EPS certification plan) and Boeing's EPS safety assessment as methods of demonstrating that the battery complied with the FAA's special conditions. Boeing's safety assessment was an important method of compliance because it identified the battery failure modes that could produce conditions prohibited by the FAA's special conditions and defined the safety requirements needed to mitigate the potential risks to a

[143] Regarding the process for validating assumptions, ARP 4754 stated, "where the consequences of an erroneous assumption appear to have significant potential to reduce safety, one possible validation strategy consists of showing how the system design, in fact, limits or bounds the achievable consequences of an assumption error."

CosMX Exhibit 1003, Page 220 of 512

level deemed acceptable by the FAA.[144] However, because Boeing's safety assessment did not consider the potential for cell-to-cell propagation with fire as a result of an internal short circuit, Boeing did not identify, in the 787 main and APU battery SCD or elsewhere, safety requirements directly addressing battery performance with a single cell in thermal runaway. Also, because the battery SCD did not contain a specific requirement for battery performance with a cell in thermal runaway, the need for a thermal runaway qualification test or other related verification activity as part of the battery's certification would have been less visible to Boeing authorized representatives and FAA certification engineers.[145]

Although GS Yuasa's battery design included features intended to prevent cell-to-cell propagation, such as cell spacing and thermal insulation materials between cells, these provisions were insufficient, as demonstrated by the BOS and the TAK incidents. These battery design features were not fully linked to defined, measurable performance criteria in Boeing's battery SCD, so the effectiveness of the design features in preventing propagation was not verified during battery qualification testing. The NTSB concludes that Boeing failed to incorporate design requirements in the 787 main and APU battery SCD to mitigate the most severe effects of a cell internal short circuit and that the FAA failed to uncover this design vulnerability as part of its review and approval of Boeing's EPS certification plan and proposed methods of compliance.

AC 25.1309 (Arsenal draft) noted that a safety assessment should trace the work leading to conclusions (including the basis for classification of the severity of hazards, the assumptions made, and supporting rationale for assumptions) as part of certification. However, none of the certification deliverables to which the FAA and Boeing agreed established the relationships among each individual special condition, related hazards and assumptions from the EPS safety assessment, safety requirements in the main and APU battery SCD, and the resulting data used to show compliance.[146] Thus, the FAA could not effectively use traceability principles to evaluate the completeness of Boeing's proposed methods of compliance, particularly for special condition 2, which addressed battery thermal runaway.[147] As a result, the FAA approved Boeing's proposed EPS certification plan, including qualification tests, for the 787 main and APU battery without the details necessary to demonstrate compliance with the individual special conditions.

If these relationships had been fully discussed in certification documentation or through other communications between Boeing and the FAA as part of the certification process, Boeing authorized representatives and FAA certification engineers would have had a better understanding of how the assumption regarding the propagation of thermal runaway as a result of

---

[144] AC 25.1309 (Arsenal draft) provided guidance on the acceptable failure probability per flight hour of equipment and systems installed on an airplane as a function of the severity of the resulting failure condition.

[145] ARP 4754 defines verification as "the evaluation of an implementation of requirements to determine that they have been met."

[146] Traceability is defined in revision A of ARP 4754 as "the recorded relationship established between two or more elements of the development process."

[147] Special condition 2 indicated that the "design of the lithium-ion batteries must preclude the occurrence of self-sustaining, uncontrolled increases in temperature or pressure."

CosMX Exhibit 1003, Page 221 of 512

a cell internal short circuit related to special condition 2.[148] In addition, traceability would likely have revealed the absence of safety requirements addressing cell thermal runaway and propagation in the battery SCD and the need for a thermal runaway test as part of planned qualification tests to demonstrate that the design met the requirements of special condition 2 for the internal short circuit failure condition. However, guidance used by FAA certification staff at the time of Boeing's application for the 787-8 type certificate, including FAA Order 8110.4, "Type Certification," revision B, did not include the use of traceability principles that relate each special condition to design data and compliance deliverables (such as test procedures, test reports, and safety assessments) as part of certification planning to ensure that the methods of compliance were correct and complete.

The NTSB concludes that unclear traceability among the individual special conditions, safety assessment assumptions and rationale, requirements, and proposed methods of compliance for the 787 main and APU battery likely contributed to the FAA's failure to identify the need for a thermal runaway certification test. Therefore, the NTSB recommends that the FAA develop written guidance for its certification engineers and engineering designees about the use of traceability principles to verify that the methods of compliance proposed by type certification applicants for special conditions involving new technology are correct and complete. The NTSB also recommends that, once the guidance requested in Safety Recommendation A-14-121 has been issued, the FAA provide training to its certification engineers and engineering designees on the subjects discussed in the guidance. The NTSB further recommends that the FAA require applicants to discuss key assumptions related to safety-significant failure conditions, their validation, and their traceability to requirements and proposed methods of compliance during certification planning meetings for type designs involving special conditions.

2.5.3 Certification of Lithium-ion Batteries and Certification of New Technology

As stated in section 1.8.2, the NTSB issued Safety Recommendations A-14-32 through -36 to the FAA regarding (1) insufficient testing methods and guidance for addressing the safety risks of internal short circuits and thermal runaway and (2) the need for outside technical knowledge and expertise to help the FAA ensure the safe introduction of new technology into aircraft designs. On August 19, 2014, the FAA responded to these recommendations.

In its response letter, the FAA stated that it has been working with RTCA Special Committee SC-211 to revise RTCA document DO-311, "Minimum Operational Performance Standards for Rechargeable Lithium Battery Systems," to "capture all the enhancements and lessons learned" from the BOS incident, including the need for a test that subject a single cell

[148] A review of available minutes from monthly meetings between the FAA and Boeing during the planning and implementation phases of the 787 certification program did not reveal any communications related to Boeing's assumption or proposed qualification test plan for the main and APU battery as it related to the thermal runaway propagation failure condition due to cell internal short circuiting.

CosMX Exhibit 1003, Page 222 of 512

within a lithium-ion battery to thermal runaway as a result of an internal short circuit.[149] The FAA also stated that, until these revisions are completed, it would use the issue paper process to provide new design applicants with acceptable methods of compliance for conducting tests and analyses to address the potential failure effects of permanently installed, rechargeable lithium-ion batteries. The FAA further stated that it was surveying previous approvals of rechargeable lithium battery systems to determine those existing approved designs that require additional testing and/or analysis to ensure that they can mitigate all adverse effects of a cell thermal runaway. In addition, the FAA stated that it was setting up meetings with internal stakeholders to determine how best to implement Safety Recommendation A-14-36.

The NTSB is encouraged that the FAA is taking steps to enhance RTCA document DO-311 but is concerned that aircraft installation factors might not be addressed in the document given that DO-311 is a battery-level standard. On the basis of the FAA's actions, the NTSB classifies Safety Recommendations A-14-32 through -36 "Open—Acceptable Response" pending review of future updates regarding the FAA's progress in completing the recommended actions.

2.6 Flight Recorder Issues

2.6.1 Stale Flight Data

The EAFR is a new recording system with a new flight data recording format, and the 787 is currently the only airplane that uses the EAFR to record CVR, FDR, and other data. The investigation of this incident found that the EAFR recorded stale data for some parameters (see section 1.3). The recording of stale data impacted the early stages of this investigation because significant additional effort was required to identify stale data when possible as well as those parameters for which it was not possible to determine whether the data samples were stale. This process delayed the NTSB's complete understanding of the recorded data.

Stale EAFR data could impact future investigations as well. The recording of stale data could lead to cases in which apparently valid data continued to be recorded after a parameter source stopped providing valid data, which could result in latent faults in the recording system for mandatory parameters.[150] These mandatory parameters would thus be unavailable because an EAFR's source would no longer be providing the data. In addition, the safe operation of an aircraft could be impacted if stale EAFR data were unintentionally used by an operator to assess and resolve maintenance issues.

---

[149] In 2006, the FAA chartered a federal advisory committee, known as RTCA Special Committee SC-211, to develop a standard for the design, certification, production, and use of permanently installed, rechargeable lithium-ion battery systems. The committee included representatives from the FAA, US Air Force, US Navy, US Army, commercial air carriers, and battery and aircraft manufacturers. Boeing, Thales, and GS Yuasa were also members of the RTCA special committee. The resulting standard, DO-311, which was issued in 2008, is currently considered by the FAA to be an acceptable means of compliance to the special conditions for rechargeable lithium-ion batteries and battery systems.

[150] Title 14 CFR 121.344, "Digital Flight Data Recorders for Transport Category Airplanes," details mandatory parameter requirements. Title 14 CFR Part 121 Appendix M provides supplemental information to 14 CFR 121.344.

CosMX Exhibit 1003, Page 223 of 512

The NTSB concludes that stale EAFR data could impede future accident and incident investigations by delaying the full understanding of the recorded data; stale data could also impact aircraft safety if an operator's maintenance activities were based on these data. At this time, the NTSB is concerned with the EAFR stale data recording issue on 787 airplanes because future EAFR installations might take greater advantage of the flexibility of the new recording format, which could mitigate the stale data issue. Therefore, the NTSB recommends that the FAA require Boeing 787 operators to incorporate guidance about the EAFR stale data issue in their maintenance manuals to prevent stale data from being used for maintenance activities or flight recorder maintenance. In addition, the NTSB recommends that the FAA (1) evaluate whether the recording of stale data by the Boeing 787 EAFR, including whether the data are specifically identified as stale, impacts the certification of the recording system regarding the ranges, accuracies, and sampling intervals specified in 14 CFR Part 121 Appendix M and (2) take appropriate measures to correct any problems found.

2.6.2 Poor-Quality Cockpit Voice Recording

The investigation of this incident found that the audio recording obtained from both EAFRs was poor quality. The signal levels of the three radio/hot microphone channels of the audio recording (the captain's audio selector panel, the first officer's audio selector panel, and the jumpseat/observer's position) were very low and used only about 25% of the available total dynamic range of the recorder. Further, throughout the recording, random full-deflection noise spikes could be heard. These random noise spikes were very short in duration but used the full dynamic range of the radio/hot microphone channel recording.

The recording from the cockpit area microphone channel of the EAFR was also poor quality. During the airborne portion of the flight that was captured on the recording, almost all of the individual crew conversations were completely obscured by the ambient cockpit noise. After the airplane landed, the cockpit noise was reduced, so the crew conversations became clearer. Once the airplane arrived at the gate and the engines were shut down, the crew conversations could easily be heard, and the overall quality of the recording was excellent. Thus, the issues with the EAFR audio recording did not impact this investigation because the conversations and sounds related to the circumstances of the incident occurred during the portion of the recording that was excellent quality.

The EAFR was certified under FAA Technical Standard Order (TSO) C123B, "Cockpit Voice Recorder Equipment," which was based on the European Organization for Civil Aviation Equipment (EUROCAE) ED-112A document, "Minimum Operational Performance Specification for Crash Protected Airborne Recording Systems." The installation and performance requirements in chapter I-6 of the EUROCAE document also include guidance to determine if a CVR installation would be acceptable. This guidance stated that the CVR should use all available dynamic ranges of the recorder and mitigate cockpit area background noise. The FAA took exception to this chapter of the EUROCAE ED-112A document and removed the chapter's requirements from the final TSO C123B language. As a result, the CVR certifier and installer can determine what constitutes an acceptable recording without the use of any industry-approved standard regarding specific installation guidance.

CosMX Exhibit 1003, Page 224 of 512

The NTSB concludes that the poor audio recording quality of the EAFR could impede future aircraft investigations because the recorded conversations and other cockpit sounds might be obscured. Therefore, the NTSB recommends that the FAA require Boeing to improve the quality of (1) the EAFR radio/hot microphone channels by using the maximum available dynamic range of the individual channels and (2) the cockpit area microphone airborne recordings by increasing the crew conversation signals over the ambient background noise. In addition, the NTSB recommends that the FAA either remove the current exception to ED-112A chapter I-6 in TSO 123B or provide installers and certifiers with specific guidance to determine whether a CVR installation would be acceptable.

CosMX Exhibit 1003, Page 225 of 512

3. Conclusions

3.1 Findings

1. The battery failure did not result from overcharging, overdischarging, external short circuiting, external heating, installation factors, or environmental conditions of the airplane.

2. The battery failure resulted from an internal short circuit that occurred in cell 5 or cell 6 and led to thermal runaway that propagated to adjacent cells.

3. GS Yuasa's cell manufacturing process allowed defects that could lead to internal short circuiting, including wrinkles and foreign object debris, to be introduced into the Boeing 787 main and auxiliary power unit battery.

4. The thermal protections incorporated in large-format lithium-ion battery designs need to account for all sources of heating in the battery during the most extreme charge and discharge current conditions and protect cells from damage that could lead to thermal runaway.

5. More accurate cell temperature measurements and enhanced temperature and voltage monitoring and recording could help ensure that excessive cell temperatures resulting from localized or other sources of heating could be detected and addressed in a timely manner to minimize cell damage.

6. Determining the initial point of self-heating in a lithium-ion cell is important in establishing thermal safety limits.

7. Boeing's electrical power system safety assessment did not consider the most severe effects of a cell internal short circuit and include requirements to mitigate related risks, and the review of the assessment by Boeing authorized representatives and Federal Aviation Administration certification engineers did not reveal this deficiency.

8. Boeing failed to incorporate design requirements in the 787 main and auxiliary power unit battery specification control drawing to mitigate the most severe effects of a cell internal short circuit, and the Federal Aviation Administration failed to uncover this design vulnerability as part of its review and approval of Boeing's electrical power system certification plan and proposed methods of compliance.

9. Unclear traceability among the individual special conditions, safety assessment assumptions and rationale, requirements, and proposed methods of compliance for the 787 main and auxiliary power unit battery likely contributed to the Federal Aviation Administration's failure to identify the need for a thermal runaway certification test.

10. Stale enhanced airborne flight recorder data could impede future accident and incident investigations by delaying the full understanding of the recorded data; stale data could

CosMX Exhibit 1003, Page 226 of 512

also impact aircraft safety if an operator's maintenance activities were based on these data.

11. The poor audio recording quality of the enhanced airborne flight recorder could impede future aircraft investigations because the recorded conversations and other cockpit sounds might be obscured.

3.2 Probable Cause

The National Transportation Safety Board determines that the probable cause of this incident was an internal short circuit within a cell of the auxiliary power unit (APU) lithium-ion battery, which led to thermal runaway that cascaded to adjacent cells, resulting in the release of smoke and fire. The incident resulted from Boeing's failure to incorporate design requirements to mitigate the most severe effects of an internal short circuit within an APU battery cell and the Federal Aviation Administration's failure to identify this design deficiency during the type design certification process.

CosMX Exhibit 1003, Page 227 of 512

4. Recommendations

4.1 New Recommendations

As a result of this investigation, the National Transportation Safety Board makes the following new safety recommendations:

To the Federal Aviation Administration:

Develop or revise processes to establish more effective oversight of production approval holders and their suppliers (including subtier suppliers) to ensure that they adhere to established manufacturing industry standards. (A-14-113)

Work with aviation industry experts to develop or modify design safety standards for large-format lithium-ion batteries to require that sources of excessive heating, including electrical contact resistance from components and connections, be identified, minimized, and documented as part of the design. The standards should include measures for identifying and minimizing potential sources of heating that consider the range of operating temperatures and the most extreme electrical currents that the battery could be expected to experience during repeated charge and discharge cycles. (A-14-114)

Work with aviation industry experts to develop or modify existing safety standards related to the design of permanently installed lithium-ion batteries to require monitoring of individual cell temperature and voltage and recording of exceedances to prevent internal cell damage during operations under the most extreme operating temperatures and currents. (A-14-115)

Once the guidance requested in Safety Recommendation A-14-115 has been issued, require type certification applicants to demonstrate that the battery monitoring system maintains each individual cell within safe temperature limits at the most extreme battery operating temperatures and the heaviest electrical current loads approved for operation. (A-14-116)

Work with lithium-ion industry experts to (1) conduct research into battery monitoring system technologies that could improve the recognition of conditions leading to thermal runaway, (2) develop active mitigation of such conditions to minimize damage, and (3) update design and safety standards accordingly. (A-14-117)

Work with industry experts to develop appropriate test methods for determining the initial point of self-heating in a lithium-ion cell to establish objective margins of thermal safety for future battery designs. (A-14-118)

Provide your certification engineers with written guidance and training to ensure that (1) assumptions, data sources, and analytical techniques are fully identified

CosMX Exhibit 1003, Page 228 of 512

and justified in applicants' safety assessments for designs incorporating new technology and (2) an appropriate level of conservatism is included in the analysis or design, consistent with the intent of Advisory Circular 25.1309 (Arsenal draft). (A-14-119)

During annual recurrent training for engineering designees, discuss the need for applicants to identify, validate, and justify key assumptions and supporting engineering rationale used in safety assessments addressing new technology. (A-14-120)

Develop written guidance for your certification engineers and engineering designees about the use of traceability principles to verify that the methods of compliance proposed by type certification applicants for special conditions involving new technology are correct and complete. (A-14-121)

Once the guidance requested in Safety Recommendation A-14-121 has been issued, provide training to your certification engineers and engineering designees on the subjects discussed in the guidance. (A-14-122)

Require applicants to discuss key assumptions related to safety-significant failure conditions, their validation, and their traceability to requirements and proposed methods of compliance during certification planning meetings for type designs involving special conditions. (A-14-123)

Require Boeing 787 operators to incorporate guidance about the enhanced airborne flight recorder stale data issue in their maintenance manuals to prevent stale data from being used for maintenance activities or flight recorder maintenance. (A-14-124)

Evaluate whether the recording of stale data by the Boeing 787 enhanced airborne flight recorder, including whether the data are specifically identified as stale, impacts the certification of the recording system regarding the ranges, accuracies, and sampling intervals specified in 14 *Code of Federal Regulations* Part 121 Appendix M, and take appropriate measures to correct any problems found. (A-14-125)

Require Boeing to improve the quality of (1) the enhanced airborne flight recorder radio/hot microphone channels by using the maximum available dynamic range of the individual channels and (2) the cockpit area microphone airborne recordings by increasing the crew conversation signals over the ambient background noise. (A-14-126)

Either remove the current exception to European Organization for Civil Aviation Equipment ED-112A, "Minimum Operational Performance Specification for Crash Protected Airborne Recording Systems," chapter I-6 in Technical Standard Order 123B, "Cockpit Voice Recorder Equipment," or provide installers and certifiers with specific guidance to determine whether a cockpit voice recorder installation would be acceptable. (A-14-127)

To the Boeing Company:

Develop or revise processes to establish more effective oversight of your suppliers (including subtier suppliers) to ensure that the product being manufactured adheres to established industry standards. (A-14-128)

Modify your process for developing safety assessments for designs incorporating new technology to ensure that the conclusions made are validated and that any identified deficiencies are corrected. (A-14-129)

To GS Yuasa Corporation:

Review your cell manufacturing processes to minimize or prevent defects that could affect cell safety, and ensure that your employees are properly trained to identify and eliminate these defects. (A-14-130)

4.2 Previously Issued Safety Recommendations Classified in This Report

Safety Recommendations A-14-32 through -36 are classified "Open—Acceptable Response" in section 2.5.3 of this report.

Develop abuse tests that subject a single cell within a permanently installed, rechargeable lithium-ion battery to thermal runaway and demonstrate that the battery installation mitigates all hazardous effects of propagation to other cells and the release of electrolyte, fire, or explosive debris outside the battery case. The tests should replicate the battery installation on the aircraft and be conducted under conditions that produce the most severe outcome. (A-14-32)

After Safety Recommendation A-14-32 has been completed, require aircraft manufacturers to perform the tests and demonstrate acceptable performance as part of the certification of any new aircraft design that incorporates a permanently installed, rechargeable lithium-ion battery. (A-14-33)

Work with lithium-ion battery technology experts from government and test standards organizations, including US national laboratories, to develop guidance on acceptable methods to induce thermal runaway that most reliably simulate cell internal short-circuiting hazards at the cell, battery, and aircraft levels. (A-14-34)

Review the methods of compliance used to certify permanently installed, rechargeable lithium-ion batteries on in-service aircraft and require additional testing, if needed, to ensure that the battery design and installation adequately protects against all adverse effects of a cell thermal runaway. (A-14-35)

Develop a policy to establish, when practicable, a panel of independent technical experts to advise on methods of compliance and best practices for certifying the safety of new technology to be used on new or existing aircraft. The panel should

CosMX Exhibit 1003, Page 230 of 512

be established as early as possible in the certification program to ensure that the most current research and information related to the technology could be incorporated during the program. (A 14-36)

BY THE NATIONAL TRANSPORTATION SAFETY BOARD

CHRISTOPHER A. HART
Acting Chairman

ROBERT L. SUMWALT
Member

MARK R. ROSEKIND
Member

EARL F. WEENER
Member

Adopted: November 21, 2014

CosMX Exhibit 1003, Page 231 of 512

5. Appendixes

Appendix A: Investigation and Hearing

The National Transportation Safety Board (NTSB) was notified of this incident on January 7, 2013, and sent an investigator to the scene the same day and two investigators to the scene the next day. The following investigative groups were formed: airworthiness, airport emergency response, battery and fire, manufacturing, and systems safety and certification. Also, specialists were assigned to conduct the readout of the flight data recorder and transcribe the cockpit voice recorder at the NTSB's laboratory in Washington, DC. In addition, a specialist was assigned to conduct radiographic studies of 787 batteries and cells.

The following organizations provided technical assistance to the NTSB during this investigation:

- Naval Surface Warfare Center, Carderock Division, US Department of the Navy, West Bethesda, Maryland;
- TIAX LLC, Lexington, Massachusetts;
- Underwriters Laboratories LLC, Northbrook, Illinois; Melville, New York; and Taipei, Taiwan
- US Department of Energy, Washington, DC;
- Chesapeake Testing, Belcamp, Maryland;
- National Institute of Standards and Technology, Gaithersburg, Maryland; and
- Naval Research Laboratory, Washington, DC.

Parties to the investigation were the Federal Aviation Administration (FAA) and Boeing Commercial Airplanes. In accordance with the provisions of Annex 13 to the Convention on International Civil Aviation, the Japan Transport Safety Board (JTSB) and the Bureau d'Enquêtes et d'Analyses pour la Sécurité de l'Aviation Civile (BEA) participated in this investigation. Japan Airlines and GS Yuasa Corporation participated in the investigation as technical advisors to the JTSB, and Thales Avionics Electrical Systems and the European Aviation Safety Agency participated in the investigation as technical advisors to the BEA, as provided for in Annex 13.

On April 23 and 24, 2013, the NTSB held an investigative hearing regarding the Boeing 787 battery's design and certification. The safety issues discussed were the battery system's (1) selection and certification requirements, (2) design and development, (3) design verification and validation, and (4) certification and the FAA's findings of compliance. Parties to the investigative hearing were the FAA, Boeing, Thales, and GS Yuasa.

CosMX Exhibit 1003, Page 232 of 512

Between the date of the incident and the investigative hearing, the NTSB issued an interim factual report on this incident (March 7, 2013) and held a forum on lithium-ion batteries in transportation (April 11 and 12, 2013). The interim factual report and presentations from the forum are available at www.ntsb.gov.

CosMX Exhibit 1003, Page 233 of 512

Appendix B: Boeing 787 Type Certification Special Conditions 25-359-SC

The FAA issued the following nine special conditions, in place of the electrical equipment and installation requirements of 14 *Code of Federal Regulations* (CFR) 25.1353(c)(1) through (c)(4), for the design and installation of lithium-ion batteries as part of the type certification basis for the Boeing 787-8:

(1) Safe cell temperatures and pressures must be maintained during any foreseeable charging or discharging condition and during any failure of the charging or battery monitoring system not shown to be extremely remote. The lithium-ion battery installation must preclude explosion in the event of those failures.

(2) Design of the lithium-ion batteries must preclude the occurrence of self-sustaining, uncontrolled increases in temperature or pressure.

(3) No explosive or toxic gases emitted by any lithium-ion battery in normal operation, or as the result of any failure of the battery charging system, monitoring system, or battery installation not shown to be extremely remote, may accumulate in hazardous quantities within the airplane.

(4) Installations of lithium-ion batteries must meet the requirements of 14 CFR 25.863(a) through (d).

(5) No corrosive fluids or gases that may escape from any lithium-ion battery may damage surrounding structure or any adjacent systems, equipment, or electrical wiring of the airplane in such a way as to cause a major or more severe failure condition, in accordance with 14 CFR 25.1309(b) and applicable regulatory guidance.

(6) Each lithium-ion battery installation must have provisions to prevent any hazardous effect on structure or essential systems caused by the maximum amount of heat the battery can generate during a short circuit of the battery or of its individual cells.

(7) Lithium-ion battery installations must have a system to control the charging rate of the battery automatically, so as to prevent battery overheating or overcharging, and,

(i) A battery temperature sensing and over-temperature warning system with a means for automatically disconnecting the battery from its charging source in the event of an over-temperature condition, or,

CosMX Exhibit 1003, Page 234 of 512

(ii) A battery failure sensing and warning system with a means for automatically disconnecting the battery from its charging source in the event of battery failure.

(8) Any lithium-ion battery installation whose function is required for safe operation of the airplane must incorporate a monitoring and warning feature that will provide an indication to the appropriate flight crewmembers whenever the state-of-charge of the batteries has fallen below levels considered acceptable for dispatch of the airplane.

(9) The Instructions for Continued Airworthiness required by 14 CFR 25.1529 must contain maintenance requirements for measurements of battery capacity at appropriate intervals to ensure that batteries whose function is required for safe operation of the airplane will perform their intended function as long as the battery is installed in the airplane. The Instructions for Continued Airworthiness must also contain procedures for the maintenance of lithium-ion batteries in spares storage to prevent the replacement of batteries whose function is required for safe operation of the airplane with batteries that have experienced degraded charge retention ability or other damage due to prolonged storage at a low state of charge.

The FAA noted that these special conditions were "not intended to replace 14 CFR 25.1353(c) in the certification basis of the Boeing 787-8 airplane" and that the special conditions applied "only to lithium-ion batteries and their installations." The FAA also noted that the requirements of 14 CFR 25.1353(c) remained in effect "for batteries and battery installations of the Boeing 787-8 airplane that do not use lithium-ion batteries."

CosMX Exhibit 1003, Page 235 of 512

Appendix C: Comments From the Bureau d'Enquêtes et d'Analyses pour la Sécurité de l'Aviation Civile

Ministère de l'Ecologie,
du Développement durable
et de l'Energie

BEA
Bureau d'Enquêtes et d'Analyses
pour la sécurité de l'aviation civile

Le Bourget, le 28 octobre 2014

To : David Helson
NTSB investigator

Subject : BEA comments to append to the NTSB draft report for the serious incident to the Boeing 787-8 registered JA829J

Dear David,

Thank you for having associated the BEA (Bureau d'Enquêtes et d'Analyses pour la sécurité de l'Aviation Civile) with the investigation into the serious incident to B 787-8, registered JA 829J, and for giving us the opportunity to make comments on the Draft Final Report.
We hereby present you with the comments that we would like to be appended to the final report in accordance with the provisions of Annex 13.

We are also proposing safety actions to be taken in the light of the investigation done.

The BEA remains at your disposal for any further information that you may wish to obtain.

Yours sincerely.

Emmanuel DELBARRE
BEA Accredited representative

Aéroport du Bourget
Zone Sud – Bâtiment 153
200 rue de Paris
93352 Le Bourget Cedex
France
Tél. : +33 1 49 92 72 00
Fax : +33 1 49 92 72 03
www.bea.aero

BEA proposed comments to append to the report.

The BEA agrees that an internal short circuit within a cell of the APU battery led to thermal runaway that cascaded to thermo-mechanical propagation to surrounding cells.

However, the initiating phenomenon of the internal short circuit has not been identified during the investigation and it was impossible to conclusively determine the origin of the internal short circuit. Indeed, the internal short circuit is not a root cause by itself but a "way point" in the chain of events. The reason of the development of the short circuit inside the first cell could not be determined from post incident laboratory testing and subsequent engineering analysis of potential failure modes.

The fact that the root cause couldn't be determined should also be included in the section 3.1 Findings and also in the section 3.2 Probable Causes.

In addition, the NTSB report also lists some concerns that have been observed during the investigation (refer to sections 2.3 and 2.4), namely:

- The **presence of wrinkles** generated by the manufacturing process or influenced by the manufacturing process and developed during charge and discharge due to swelling/deswelling. The report considers that "wrinkles and folds can modify anode-to-cathode ratio locally, resulting in lithium deposits at the anode surface". The BEA states that although wrinkles were observed during DPA of the incident batteries, their effect on lithium deposition hasn't been proved (no Li-metal was found by XPS analysis). The various tests performed by GSY, on LVP 65 cells didn't reveal neither Li metal dendrites nor internal short with heat generation and venting.

- The **presence of FOD** related to the manufacturing process : no FOD was identified during the teardown of the incident battery and during post incident investigation on exemplar batteries.

- The **propensity of cells to generate self-heating** below the upper operational specified temperature (70°C) (section 2.4.3): Lab in charge assessed self-heating rate in cell at 100%SOC and stated that cells self-heat at temperature as low as 60°C with a self-heating rate near 0.01°C.min-1. However the sensitivity threshold of this equipment is as high as at 0.02°C.min-1. Values below the sensitivity threshold are not relevant. The sensitivity threshold is reached at 85°C for 100%SOC cell1 which is consistent with the current state of the art on lithium-ion battery.

- The **seal assembly and rivets integrity**. Thales testing shows that when the battery is used within its specified power and temperature ranges then no anomaly occurs[2].

Proposed safety actions to be taken

The BEA suggests to take into account of the various reports and the Thales testings and to consider the following safety actions to be taken :

---

[1] UL report entitled "Multi-Level Forensic and Functional Analysis of the 787 Main/APU Lithium Ion Battery" Doc. ref. NTSBC130004 2014, p 120-123.

[2] THALES Submission to the National Transportation Safety Board For the DCA13IA037 page 17 & 18

- "As the investigation could not identify the mechanism of the internal short circuit, the aircraft manufacturer and the equipment manufacturers should :

  - continue studies of internal short circuit mechanism considering the effects of internal and external phenomenon that potentially impacts the Li-ion batteries in operational conditions, such as the aircraft electrical environment and particularly the risk associated to potential transient current and voltage ;

  - continue studies on the impact of other environmental parameters such as humidity and vibrations ;

  - continue efforts to improve Li-ion batteries quality and its reliability.

BEA detailed comments on the NTSB draft report on the serious incident to the Boeing 787-8 registered JA829J.

Page/Section:	Sentence/Comment:
	§ 1.4.3 Disassembly of the incident Battery **Existing sentence:** "There was no evidence of cell-to-battery case shorting before the thermal event, bus bar shorting or resistive heating of bus bar …".
Comment:	APU battery has demonstrate the presence of a protrusion on side 3 facing Cell 5. At the place of the protrusion the cell 5 exhibits a small hole. The Cell 5 windings also demonstrate holes that are consistent with materials that had penetrated into the cell 5 and its windings. The material found in the cell 5 and its winding were chemically analyzed and confirmed to be Battery aluminum alloy. This was interpreted by the investigation team as resulted from an arcing phenomenon between the cell 5 casing and Battery case. At this stage there is no evidence to say that arcing occurs before or during the thermal event. **Modification proposal** **"There was evidence of cell 5-to-battery case shorting during the JAL event. The exact time, at which the shorting between cell 5 and battery case occurs, is not determined. In addition there is no evidence of bus bar shorting or resistive heating of bus bar ...."**

Page/Section:	Sentence/Comment:
	§ 1.4.3 Disassembly of the incident Battery **Existing sentence:** There was also no visible evidence of water (resulting from condensation) within the battery case or external surfaces of the battery cells.
Comment:	APU battery has undergone a very significant heating during the thermal runaway. Therefore, if water, for instance from condensation, had been present, it has been vaporized during thermal runaway. Consequently, it was impossible to find any evidence of water inside the battery after the event. In order not to rule out this parameter, the following wording is proposed.

	Modification proposal **"Due to high heat exposure of the APU battery during the incident event, it was obviously not possible to conclude on water presence resulting from condensation within the battery before or during the incident event."**

Page/Section:	Sentence/Comment:
	§ 1.5.3 Examinations of main battery cells from incident airplane **Existing sentence:** "More than 100 areas of "ingressed underlithiation" of the anode (that is, areas of the anode than are incompletely charged) were found"
Comment:	Color variations in full charge carbon anode are known to be due to underlithiation. However, color is only a semi-quantitative and subjective measure of Li state of charge [1], [2]. Additionally XPS analysis from Carderock don't show any obvious difference in lithium concentration between "blue or purple areas", called "underlithiated" and gold areas, called " fully lithiated" **Modification proposal** **More than 100 areas of "ingressed" underlithiation of the anode were found (that is, areas of the anode than are incompletely charged. However Carderock XPS analysis doesn't show any significant concentration difference of lithium element between blue/purple area, called underlithiated area, and gold area, called fully lithiated area)** [1] Direct in situ measurements of Li transport in Li-ion battery negative electrodes, Harris et al, Chemical Physics Letters 485 (**2010**) 265–274 [2] Revisited structures of dense and dilute stage II lithium-graphite intercalation compounds, D. Billaud et al, J. Phys. Chem. Solids 57 (1996) 775.

Page/Section:	Sentence/Comment:
	§ 1.5.3 Examinations of main battery cells from incident airplane **Existing sentence:** "According to TIAX, these areas indicate that mechanical abnormalities in the windings results in uneven charging of the anode and might have caused lithium to deposit adjacent to underlithiated area."
Comment:	This explanation, representing TIAX' interpretation, is only based on a phenomenal description and is not supported by any technical and scientific demonstration, simulation, calculation and complete testing. **Modification proposal** **"According to TIAX, these areas indicate that, in theory, mechanical abnormalities in the windings might result in uneven charging of the anode and might have caused lithium to depose adjacent to underlithiated area. However TIAX didn't perform**

	chemical analysis, simulation, calculation and appropriate testing to validate this scenario. At the opposite, Carderock showed through deep chemical analysis (XPS) that the observed silver colored deposits didn't contain any lithium metal, invalidating the explanation proposed by TIAX"

Page/Section:	**Sentence/Comment:**
	§ 1.5.3 Examinations of main battery cells from incident airplane **Existing sentence:** "In its submission to the NTSB for this incident, GS YUASA stated that, after the incident, it conducted more than 100 cold charge cycle tests, and all of the tests revealed a loss of capacity when charging repeatedly at -9.4°F."
Comment:	The reader would surely be interested not only by the loss of capacity during charge/discharge cycles which is normal behavior of this battery technology in these specific test conditions, but it would be of greater interest to learn there from those tests that no dendrite was created during those cold charge cycles. For information, the 105 cycles of tests widely cover the time period that the incident battery was exposed onboard airplane. Such important and relevant information needs to be provided to the reader in order to have better understanding of potential dendrite presence or not according to the operating conditions specified on this airplane. **Modification proposal** **"In its submission to the NTSB for this incident, GS YUASA stated that, after the incident, it conducted more than 100 cold charge cycle tests, and all of the tests revealed a loss of capacity when charging repeatedly at -9.4°F and no lithium plating was observed".**

Page/ Section:	**Sentence/Comment:**
	§1.5.4 Cell-level abuse tests **Existing sentence:** "… cells started to generate internal heat at temperatures as low as 144°F, which is below the allowable operational temperature of the battery"
comment	As written by BEA/Thales comments on the airworthiness group report, UL used an ARC equipment to assess self-heating rate in cell at 100%SOC and 0%SOC. The sensitivity threshold of this equipment is given at 0.02°C.min^{-1} by the equipment manufacturer (cf UL report p121 and 122). However UL states that cells self-heat at temperature as low as 60°C (self-heating rate near 0.01°C.min^{-1}, but the self-heating rate at this temperature is below the sensitivity threshold of

	the equipment. Values below the sensitivity threshold are not relevant. The sensitivity threshold is reached at 110 °C for 0%SOC cell (cf p 121, UL report) and 85°C for 100%SOC cell (cf UL report 122). **Modification proposal** "...**cells started to generate internal heat at temperatures as low as 85°C (100%SOC) and 110°C (0%SOC)** (and remove the last part of the sentence as the battery is qualified for temperatures comprised between -18°C and 70°C).

Page/Section:	**Sentence/Comment:**
	§ 1.5.5 Rivet observations during cell- and battery-level testing **Existing sentence:** "the aluminum rivets on the positive terminal of cell 5 increased progressively through 14 cycles to a maximum of 157°C/315°F"
Comment:	Some precision need to be added: - In some case, the UL tests were performed with an average current of 940A. - The worst case with a battery voltage at 20Vdc corresponds to a power of 18.8KW during the simulation of APU start. - With a battery fully charged before the APU start simulation, the battery voltage is between 25 and 26Vdc the power was comprise between 23.5KW and 24.4KW. - Thales tests have demonstrated that the rivets are designed to withstand APU start with a maximum power of 18KW in all the temperature range in compliance with Boeing SCD. - In the case of APU start out of Boeing SCD (> 18KW) the rivets are damaged and this damage are irreversible. **Modification proposal** **Taking into account of Thales testing and submission, this paragraph should be amended by adding that in the operating range this phenomenon does not occur.**

Page/Section:	**Sentence/Comment:**
	§ 1.5.5 Rivet observations during cell- and battery-level testing **Existing sentence:** *""The cell leakage test showed that the seal of the cell was damaged"*
Comment:	Note that all the tests performed by UL and reported in the section refer to battery that was tested outside of the power specified domain over 18 kW as mentioned in the previous comment. Thales tests exactly showed the same results after abnormal APU start (>18KW) **BEA suggests taking into account the THALES results in this chapter or clearly indicates that tests were performed out of power specified domain.**

CosMX Exhibit 1003, Page 241 of 512

Page/Section:	Sentence/Comment:
	§ 2.1 Failure sequence **Existing sentence:** *"A battery-level test showed that condensation could occur within the battery and result in shorting path between the cell and the battery cases, and cell-level test with moisture showed that a cell failure could occur and result in arcing, shorting, and heat damage internal to cell header. However the damage observed during the cell-level test was not found in the cell header from the incident APU battery. In addition, airplane flight test data did not show any abnormal electrical transients that could lead to battery failure "*
Comment:	*During the investigation, it was not possible to show that the JAL Boston Cells, and specifically cell 5 and cell 6, had experienced or not shortings as described in the Thales submission. In addition based on information provided by NTSB, the flight test recording system was capable of recording signals that had frequency up to hundreds of Khz. The Transient phenomena that are seen as a potential contributing factor by BEA and Thales are in a range of 2 to 4 Mhz. That means that such phenomenon couldn't be captured by the aircraft flight test installation.* **The BEA suggests taking into account the THALES results in this chapter and to modify it as follows :** ***The information collected during the investigation does not allow to determine if the damages observed during the cell-level test on the cell headers were similar to the incident APU battery. In addition, during the airplane flight test, the system used to collect the electrical data had limited electrical transients recording capabilities (in the range of hundreds Kilo Hertz) and did not make it possible to capture electrical transient phenomenon that occurs with High Frequency range (Mhz).***

References

Airworthiness Directives; The Boeing Company Airplanes. *Federal Register*. Vol. 78. No. 36. February 22, 2013. 12231.

Airworthiness Directives; The Boeing Company Airplanes. *Federal Register*. Vol. 78. No. 81. April 26, 2013. 24673.

Baldwin, Richard S., William R. Bennett, Eunice K. Wong, MaryBeth R. Lewton, and Megan K. Harris. "Battery Separator Characterization and Evaluation Procedures for NASA's [National Aeronautics and Space Administration] Advanced Lithium-Ion Batteries." NASA Technical Memorandum NASA/TM-2010-216099. NASA, Washington, DC, 2010.

Belov, D. and M.H. Yang. "Failure Mechanism of Li-ion Battery at Overchage Conditions." *Journal of Solid State Electrochemistry* 12 (2008): 885-894.

Chapin, J. Thomas, Pravinray D. Gandhi, and Paul W. Brazis, Jr. "NTSB Battery Tests—Final Report for 787 Battery (Asset 436) Tested at 70°C, Ungrounded." Underwriters Laboratories LLC, Northbrook, IL, 2014.

Chapin, J. Thomas, Pravinray D. Gandhi, and Paul W. Brazis, Jr. "NTSB Battery Tests—Final Report for 787 Battery (Asset 445) Tested at 15°C, Grounded." Underwriters Laboratories LLC, Northbrook, IL, 2014.

Condra, Lloyd W. *Reliability Improvement With Design of Experiments*. New York, NY: Marcel Dekker Inc., 1993.

Doughty, Daniel H. and Chris C. Crafts. *FreedomCAR Electrical Energy Storage System Abuse Test Manual for Electric and Hybrid Electric Vehicle Applications*. SAND2005-3123, Sandia National Laboratories, Albuquerque, New Mexico, 2006.

FAA (Federal Aviation Administration), Boeing 787-8 Critical Systems Review Team. *Boeing 787-8 Design, Certification, and Manufacturing System Review*. Washington, DC: FAA, 2014. www.faa.gov/about/plans_reports/media/787_Report_Final.pdf

FAA, William J. Hughes Technical Center. *Extinguishment of Lithium-Ion and Lithium-Metal Battery Fires*. DOT/FAA/TC-13/53, Atlantic City, NJ: FAA, 2014.

Fisher, D.L., R. Schweickert, and C.G. Drury. "Mathematical Models in Engineering Psychology: Optimizing Performance." In *Handbook of Human Factors and Ergonomics*, by ed. G. Salvendy, 997-1024. Hoboken, NJ: John Wiley and Sons, 2006.

Japan Transport Safety Board. *Emergency Evacuation Using Slides, All Nippon Airways Co., Ltd., Boeing 787-8, JA804A, Takamatsu Airport, At 08:49 JST, January 16, 2013.* Aircraft Serious Incident Investigation Report AI2014-4, Tokyo, Japan: JTSB, 2014. www.mlit.go.jp/jtsb/english.html

Mansour, Azzam N., D. Fuentevilla, and Jim A. Zaykoski. *XPS [x-ray photoelectron spectroscopy] Investigation of a Carbon Anode, Separator from a Cold Charged Li-Ion Cell and a Lithium Foil Control Sample, Factual Report.* West Bethesda, MD: Naval Surface Warfare Center, Carderock Division, 2014.

Mikolajczak, C., M. Kahn, K. White, and R.T. Long. *Lithium-Ion Batteries Hazard and Use Assessment Final Report.* Quincy, MA: The Fire Protection Research Foundation, 2011.

NASA Technical Standard, "Electrical Bonding for NASA Launch Vehicles, Spacecraft, Payloads, and Flight Equipment." NASA-STD-4003A, Washington, DC, 2013.

Reddy, Thomas B. and David Linden. *Linden's Handbook of Batteries.* Fourth edition. New York, NY: McGraw-Hill, 2011.

SAE International. "Guidelines for Development of Civil Aircraft and Systems." *SAE Aerospace Recommended Practice 4754A.* Warrendale, PA: SAE, 2010.

Special Conditions: Boeing Model 787-8 Airplane; Lithium Ion Battery Installation. *Federal Register.* Vol. 72. No. 82. April 30, 2007. 21162.

Special Conditions: Boeing Model 787-8 Airplane; Lithium Ion Battery Installation. *Federal Register.* Vol. 72. No. 196. October 11, 2007. 57842.

Tabaddor, Mahmood, Helena Chiang, Dennis Grzic, and Alvin Wu. *Multi-Level Forensic and Functional Analysis of the 787 Main/APU Lithium-Ion Battery.* Northbrook, IL: Underwriters Laboratories LLC, 2014.

Taheri, Peyman, Scott Hsieh, and Majid Bahrami. "Investigating Electrical Contact Resistance Losses in Lithium-Ion Battery Assemblies for Hybrid and Electric Vehicles." *Journal of Power Sources* 196 (2011): 6525-6533.

Teichner, W.H. "The Detection of a Simple Visual Signal as a Function of Time of Watch." *Human Factors* 16 (1974): 339-353.

TIAX LLC. *Report on Soft-Short Testing of Batteries 149, 305, 344, 376, and 412.* Lexington, MA: TIAX, 2013.

—. *Review of Cell 6 Tear Down Samples of Incident APU Battery.* Lexington, MA: TIAX, 2013.

—. *Teardown of LVP65 Li-Ion Cell 1 from Battery 412.* Lexington, MA: TIAX, 2014.

Wang, Carl and Alvin Wu. *Cell-Level IIISC [indentation-induced internal short circuit], Nail Penetration, Hot Pad and ARC Tests for LVP65.* Northbrook, IL: Underwriters Laboratories LLC, 2014.

Wang, Carl, Helena Chiang, and Alvin Wu. *Analysis of Asset 459 Cell 5.* Northbrook, IL: Underwriters Laboratories LLC, 2014.

Appendix G

PERGAMON

Electrochimica Acta 48 (2002) 227–233

ELECTROCHIMICA Acta

www.elsevier.com/locate/electacta

A novel intrinsically porous separator for self-standing lithium-ion batteries

Pier Paolo Prosini *, Paola Villano, Maria Carewska

ENEA, IDROCOMB, C.R. Casaccia, S.P. 89, Via Anguillarese 301, 00060-Rome, Italy

Received 27 August 2002

Abstract

γ-$LiAlO_2$, Al_2O_3 and MgO were used as fillers in a PVdF-HFP polymer matrix to form self-standing, intrinsically porous separators for lithium-ion batteries. These separators can be hot-laminated onto the electrodes without losing their ability to adsorb liquid electrolyte. The electrochemical stability of the separators was tested by constructing half-cells with the configuration: Li/fibre-glass/filler-based separator/electrode. MgO-based separators were found to work well with both positive and negative electrodes. An ionic conductivity of about 4×10^{-4} S cm^{-1} was calculated for the MgO-based separator containing 40% 1 M solution of $LiPF_6$ in an EC/DMC 1:1 solvent. Self-standing, lithium-ion cells were constructed using the MgO-based separator and the resulting battery performance evaluated in terms of cyclability, power and energy density.
© 2002 Elsevier Science Ltd. All rights reserved.

Keywords: Lithium-ion batteries; PVdF-HFP; Polymer electrolyte

1. Introduction

Lithium-ion rechargeable batteries with $LiCoO_2$ cathodes and carbon anodes are rapidly replacing other battery systems due to their high energy and power densities. Since the introduction of lithium-ion batteries by SONY in 1991 [1], the market for these has grown to around 400 million cells per year by 2000 [2]. Energy densities of about 120–130 Wh kg^{-1} are now available in cell using metal cans, with higher values of 160–170 Wh kg^{-1} estimated for cells with light weight packaging [3]. The concept suggested by Bellcore [4,5] to construct a light weight battery is based on the preparation of a free-standing battery stack that needs no external pressure to maintain contact between the electrodes. The electrodes and separator in the Bellcore system contain a platicizer that can be extracted after lamination, leaving a porous structure, which is subsequently activated by filling the cell with a liquid electrolyte.

Recently, PEO based composite polymer electrolyte prepared using nano-scale ceramic fillers such as SiO_2, Al_2O_3, TiO_2 and MgO [6–8] have shown enhanced ionic conductivities and improved mechanical and thermal stability. The effect of inorganic oxides such as SiO_2 [9], Al_2O_3 [10], CeO_2 [11] and TiO_2 [12] on the electrochemical properties of plasticized polymer electrolytes have been also studied. It has been shown that ceramic fillers may greatly influence the characteristic and the properties of polymer electrolyte enhancing the mechanical stability and the conductivity. Furthermore, the liquid-phylic tendency of these particles may help in holding the liquid component within the membrane structure.

Abraham et al. [13] prepared ceramic-polymer composite electrolytes from Li-ion conducting ceramic PVdF gel electrolytes. They found that the nature of the ceramic did not influence the conductivity significantly.

A new concept for obtaining a porous separator that can be laminated to the electrodes in a solvent-extraction-free process to produce a battery stack was described recently [14]. The separator was produced by casting a dispersion of inert particles of $Li_{0.35}La_{0.55}TiO_3$ in a solution of high molecular weight polyethylene

* Corresponding author. Tel.: +39-6-3048-6768; fax: +39-6-3048-6357

E-mail address: prosini@casaccia.enea.it (P.P. Prosini).

0013-4686/02/$ - see front matter © 2002 Elsevier Science Ltd. All rights reserved.
PII: S0013-4686(02)00601-1

(UHMWPE) in decaline: 1 wt.% UHMWPE was sufficient to give free-standing anodes and cathodes. In paper [14], it was stated that $Li_{0.35}La_{0.55}TiO_3$, which is known as a solid-state ion conductor, does not contribute to the conductivity of the system. The particles only help to create the porous structure. Therefore, other particles such as Al_2O_3 or SiO_2 can also be used for this purpose.

In this paper we describe our results concerning the construction of self-standing plastic lithium-ion batteries based on the intrinsically porous separator concept [15]. γ-$LiAlO_2$, Al_2O_3 and MgO were used as fillers in a PVdF-HFP polymer matrix to form self-standing, intrinsically porous separators that can be laminated under heat and pressure without losing their ability to swell on the addition of liquid electrolyte. Lithium-ion battery cells were assembled, hot laminated and activated by soaking in liquid electrolyte; battery performance was then evaluated as a function of the discharge rate and cycle number.

2. Experimental

2.1. Preparation of electrodes, separators and cells

2.1.1. Cathode

$LiMn_2O_4$ powder (Merck, battery grade) was used as the cathode active material. Carbon black (Super P, MMM carbon, Belgium) was used as a conductive agent. PVdF-HFP copolymer (Aldrich) was used as a binder and cyxclohexanone (Fluka) was used as a solvent to prepare the electrode slurry. The active electrode material and the conductive agent were mixed in a weight ratio of 18:1. The polymer was dissolved in the solvent in a weight ratio of 1:19 and heated at 70 °C to facilitate dissolution. The blend of powders was added to the polymer solution in a weigh ratio of 1:1. Approximately 20% by weight of cyclohexanone was added to the mixture to regulate the viscosity. The mixture was mixed for 20 h. The paste so-obtained was spread over a glass using calibrated slits. The weight after drying of the electrode was 16 mg cm^{-2} with a thickness of 110–150 μm. The electrode was cold-calendered to reduce the thickness.

2.1.2. Anode

MCMB graphite (Osaka Gas, Japan) was used as the active anode material. Carbon black (Super P, MMM carbon, Belgium) was used as a conductive agent. PVdF-HFP copolymer (Aldrich) was used as a binder and cyxclohexanone (Fluka) was used as a solvent to prepare the electrode paste. The graphite and the carbon were mixed intimately in a weight ratio of 18:1. The blend of powders was added to the polymer solution, prepared as described above, in a weigh ratio of 1:1. About 30% by weight of cyclohexanone was added to the mixture to obtain the correct viscosity. The mixture was then mixed for 20 h, and the paste spread over a glass using calibrated slits. The weight after drying the electrode was 2–4 mg cm^{-2} with a final thickness of 40–80 μm.

Both the electrodes were dried in an oven at 110 °C for 1 day prior to use. The porosity of the electrodes was calculated using the formula:

$$\text{porosity} = 100 \times \frac{\text{true density of the active electrode material} - \text{density of the coating}}{\text{true density of the active electrode material}}$$

The resulting electrode porosities were 54 and 38% for the positive and the negative electrode, respectively.

2.1.3. Separators

Three inorganic oxide were used as the filler to make the separator. γ-$LiAlO_2$ (Cyprus Foote Mineral Co, HAS10), MgO (BDH), Al_2O_3 (Aldrich) were dried and sieved to remove larger aggregates. The polymer was dissolved in the solvent in a weight ratio of 1:19, and heated at 70 °C to facilitate dissolution. The selected powder was added to the polymer solution in a weigh ratio of 1:2. The mixture was mixed for 48 h. The paste so-obtained was spread over a glass using a calibrated slit of 100 μm, to give a thickness after drying of 30–50 μm.

2.1.4. Battery cells

The electrode (positive or negative) and the selected separator were layered and hot laminated at 80 °C. A fibre-glass disk was used as an additional separator, and lithium metal was used both as counter and reference electrode. The cells were assembled in T-shaped hydraulic connectors. The cells were soaked in a 1 M solution of $LiPF_6$ (Merck, battery grade) in EC/DMC 1:1. Stainless Steel (SS) cylinders were used as current-collectors. Hereafter, we refer to these cells as 'half-cells'.

To create lithium-ion battery cells, the layered cathode/separator/anode were hot laminated at 80 °C. The cells were soaked in a 1 M solution of $LiPF_6$ in EC/DMC 1:1, dried on blotting-paper and assembled in a T-shaped hydraulic connector. Metallic lithium, which has been considered as a suitable reference electrode for Li-based redox system [16,17] was used as reference electrode. SS cylinders were used as current-collectors. The cells were assembled in a dry-room (R.H. $< 0.1\%$ at 20 °C).

2.2. Electrochemical tests

2.2.1. Ionic conductivity

Ionic conductivities were determined from complex impedance spectra measured using a frequency response

CosMX Exhibit 1003, Page 248 of 512

analyzer (FRA Solartron, model 1260). The separator was soaked in a 1 M solution of $LiPF_6$ in EC/DMC 1:1, dried on blotting paper and sandwiched in a T-shaped hydraulic connector between two SS cylinders. The cell was assembled in a dry-room (R.H. $< 0.1\%$ at 20 °C).

2.2.2. Electrochemical compatibility

The electrochemical compatibility of the separators with the electrodes was tested by cycling the half-cells. Charge/discharge tests were performed using a Maccor Battery Cycler (Maccor 4000). Graphite/Li half-cells were discharged at C/2 rate to 5 mV and then trickle discharged at 5 mV until the current flow decreased to a C/20 rate. The cell was charged at C/2 rate to 2.5 V. $LiMn_2O_4$/Li half-cells were charged at C/6 rate and discharged at C/4 rate between 4.4 and 3.6 V. The compatibility was considered good when the half-cell cycled well with high capacity and unitary charge/discharge ratio. Alternatively, to evaluate anodic stability, a cell was prepared by sandwiching the separator, filled with the electrolyte solution, between a SS electrode and a lithium foil. The electrochemical stability was tested by slowly increasing the cell voltage until the onset of current flow. The voltage was swept from OCV towards a more anodic potential with a scan rate of 0.5 mV s^{-1} by means of an AMEL voltammetric set-up.

2.2.3. Battery performance

Lithium-ion cells were charged at C/2 rate at a constant capacity of 0.28 mAh g^{-1} based on the weight of the active anode material, and discharged at C/2 rate to 1.5 V.

To test the effect of different discharge rates, the cell was subjected to various discharge rates: C/4, C/2, 1C and 3C. The cell was always charged using the same procedure to insure identical initial conditions: a constant current step at 1C rate until the voltage reached 4.2 V, followed by a constant voltage step until the current fell below C/10 rate.

3. Results and discussion

3.1. Electrochemical compatibility

The search for the best filler to realize a self-standing plastic lithium-ion battery was quite difficult; we found that some inorganic filler are not inert with respect to the electrodes. When we started to select an appropriate filler for the separator, we concentrate our efforts on the compatibility of the filler with the anode, because we assumed that the major instability would be at the negative electrode/separator interface rather than on the positive side. This arose from the fact that the metal ions of the inorganic oxides that we selected are in a very high oxidation state, and can therefore take part in a reduction reaction when in contact with the anode, especially in its fully lithiated state. For this same reason, we assumed that the oxides could exhibit higher anodic stability. γ-$LiAlO_2$ was demonstrated to have a good stability towards a lithium metal anode in poly(ethylene oxide)-based electrolytes [18] and was selected as the first filler for the intrinsically porous separator. We made a half-cell battery by coupling a graphite electrode to the γ-$LiAlO_2$-based separator. Fig. 1 shows the voltage profile for selected cycles. The charge/discharge ratio during the initial cycles was influenced by the formation of the solid electrolyte interface [19]. After a few cycles, the charge/discharge ratio approached unit. Its value after the 20th cycle was greater than 0.992. About 50% of the total capacity was accumulated during the galvanostatic discharge at C/2 rate. The cell was cycled for 100 full cycles with good capacity retention.

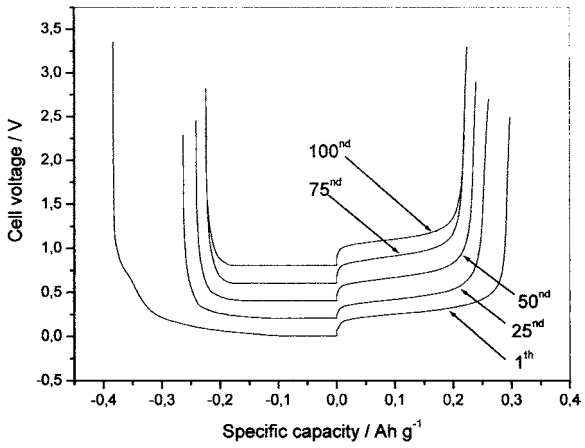


Fig. 1. Selected voltage profiles for a Li/fibre-glass/γ-$LiAlO_2$-based separator/anode cell. Discharge current was 1.27 mA cm^{-2} to 5 mV vs. Li, than the cell was left to equilibrate until the current density was less than 0.127 mA cm^{-2}. Charge current density was 1.27 mA cm^{-2}. The anode loading of graphite was 5.4 mg cm^{-2}.

This result was very encouraging and showed that γ-$LiAlO_2$ has good stability in contact with a graphite electrode. Anodic stability of γ-$LiAlO_2$-based separator was tested by sandwiching the separator between a lithium metal electrode and a blocking electrode, and slowly increasing the cell voltage until onset of current flow was observed. In Fig. 2 the current–voltage profile is reported for a γ-$LiAlO_2$-based separator containing 40 wt.% liquid electrolyte. A very low current (1.5 μA cm^{-2}) was observed in the system at the start of the experiment, becoming approximately 3 μA cm^{-2} at 4.2 V. On further increase cell voltage, a current began to flow, indicating the onset of some electrolyte decomposition process. From this we concluded that the electrochemical stability of the separator was good enough for it to be used with high-voltage cathode materials. The cathode compatibility of the separator

CosMX Exhibit 1003, Page 249 of 512

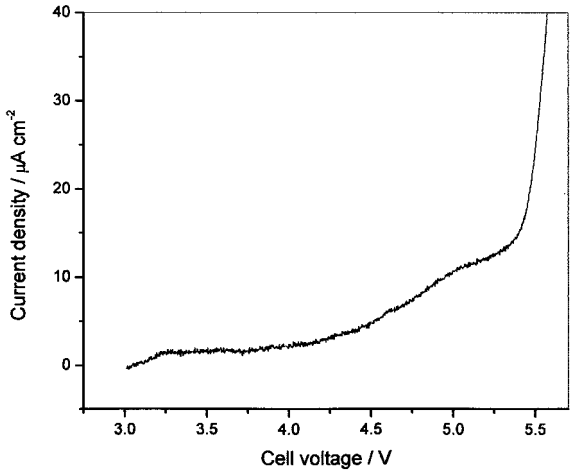


Fig. 2. Current–voltage profile for a $LiAlO_2$-based separator containing a 40 wt.% of 1 M solution of $LiPF_6$ in EC/DMC 1:1 liquid electrolyte sandwiched between lithium metal and SS electrodes. Scan rate 0.5 mV s^{-1}.

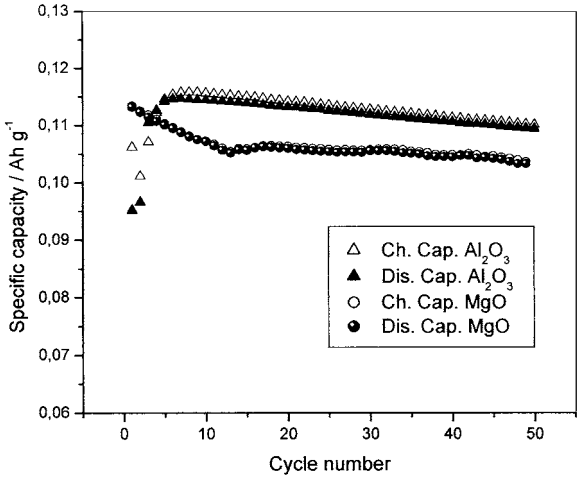


Fig. 3. Specific capacity for two half-cells realized with different separators, the fillers used to prepare the separators are reported in the figure. The insertion/release process was driven at a current density of 0.5 mA cm^{-2} in charge and 0.76 mA cm^{-2} in discharge. The cathode loading of $LiMn_2O_4$ was 15.3 mg cm^{-2}.

was also tested by cycling the half-cell formed by coupling the separator with a $LiMn_2O_4$-based electrode. Surprisingly, the half-cell did not cycle. During the first charge, the cell voltage increased initially, but then decreased after a short time, clearly indicating an electrolyte decomposition process. We conclude that the stability is strongly influenced by the nature of the separator/electrode interface, with high stability found for SS and poor stability for the composite cathode. A catalytic interaction between the electrolyte, the γ-$LiAlO_2$ particle and the cathode materials ($LiMn_2O_4$ and carbon black) at the separator/electrode interface could be responsible of the poor stability of the γ-$LiAlO_2$-based separator in contact with the cathode. On the basis of our previously reported result on PEO-based electrolyte [20], we must therefore conclude that the voltammetry test between two SS current collectors is not adequate to evaluate the stability of electrolytes, since it does not reproduce the actual cell environment.

Our interest thus shifted to other fillers with good cathode stability. Fig. 3 shows the cycling behaviour of half-cells assembled using separator membranes based on MgO and Al_2O_3. Both the membranes were found to have good stability when in contact with the high voltage cathode, with specific capacities around 120 mAh g^{-1} and good capacity retention upon cycling. Fig. 4 shows a selected charge/discharge cycle for a $LiMn_2O_4$-based cathode/MgO-based separator/fibre-glass/Li cell. It is possible to observe two well resolved lithium intercalation plateaus at 4.08 and 4.20 V vs. Li, and corresponding de-intercalation plateaus at 4.02 and 3.86 V vs. Li, in good agreement with the data reported in literature [21] and related to a two-phases intercalation/de-intercalation process.

Testing the anode compatibility for these inorganic oxides, we found that only MgO exhibited good stability upon cycling. Fig. 5 shows the voltage profile recorded for a selected cycle. The cell cycled better than for the γ-$LiAlO_2$-based separator in terms of larger reversible capacity and smaller voltage hysteresis between the charge and discharge half-cycles. About 94% of the charge was accumulated during the galvanostatic step. After a few cycles, the charge/discharge ratio approached unit. Its value after the 20th cycle was greater than 0.992.

On the other hand, the half-cells prepared with separator based on Al_2O_3 never reached the end of their first cycle (5 mV vs. Li).

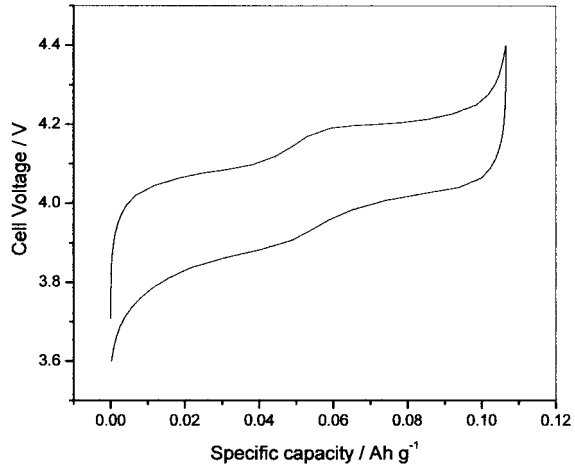


Fig. 4. Voltage profile for a Li/fibre-glass/MgO-based separator/cathode cell. The cathode loading of $LiMn_2O_4$ was 15.3 mg cm^{-2}. Discharge current was 0.76 mA cm^{-2}. Charge current density was 0.5 mA cm^{-2}.

CosMX Exhibit 1003, Page 250 of 512

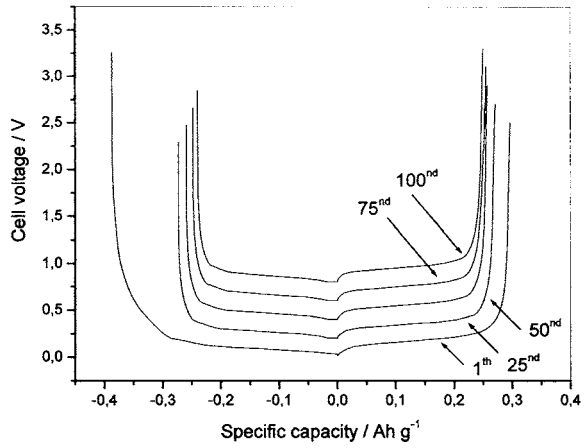


Fig. 5. Selected voltage profiles for a Li/fibre-glass/MgO-based separator/anode cell. Discharge current was 0.55 mA cm^{-2} to 5 mV vs. Li, than the cell was left to equilibrate until the current density was less than 0.055 mA cm^{-2}. Charge current density was 0.55 mA cm^{-2}. The anode loading of graphite was 2.9 mg cm^{-2}.

Finally, separators based on MgO and γ-$LiAlO_2$ have good anode stability, while those based on MgO and Al_2O_3 show good stability with respect to the cathode. Hence, only MgO is appropriate for use in a lithium-ion battery. In the follow, we report further characteristic of MgO-based separators and of lithium-ion cells prepared using them.

3.2. Ionic conductivity

Fig. 6 reports the complex impedance spectra of the separator based on MgO. Prior to the measurements, the separator was filled with the electrolyte solution by dipping it into the solution. Excess liquid electrolyte was removed with blotting-paper. The quantity of liquid electrolyte in the separator was calculated from weight difference. No thickness change was observed after soaking. Table 1 reports weights (before and after the dipping process), thickness, resistance and specific conductivity of the separator. A specific conductivity of about 4×10^{-4} S cm^{-1} was calculated for the separator with a liquid weight fraction of about 40%.

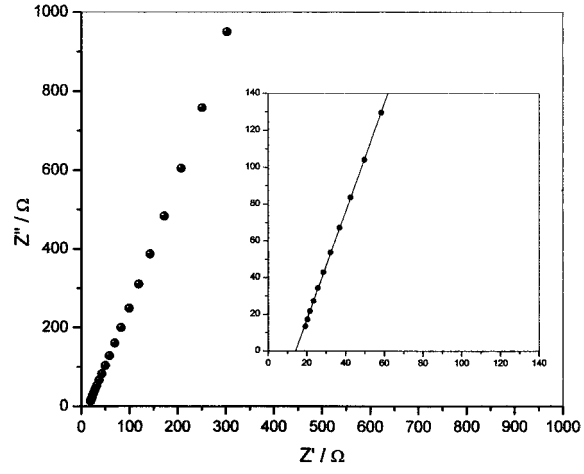


Fig. 6. Impedance spectra for a symmetrical SS/MgO-based separator/SS cell. The liquid electrolyte weight fraction in the separator was about 40%. Frequency range: 100 kHz–500 Hz. Electrode surface area: 0.785 cm^2. The insert shows the impedance spectra recorded in the frequency range from 100 kHz to 5000 Hz.

3.3. Battery performance

Anode-limited cells were fabricated with the cell Configuration anode/MgO-based separator/cathode, to demonstrate the feasibility of lithium-ion cells based on intrinsically porous separators. The layers were hot laminated to produce a self-standing stack. A scanning electron microscopy (SEM) cross-section of a cell is shown in Fig. 7. The cell battery was filled with the liquid electrolyte and cycled galvanostatically at C/2 rate. Fig. 8 shows the cell voltage and the voltage of the graphite anode measured against a Li reference electrode for a selected cycle. The large increase in the negative electrode voltage near the end of the discharge clearly suggests that the cell capacity is anode limited. The charge/discharge ratio after the 20th cycle was greater than 0.988. Representative behaviour of this cell after extensive cycling is showed in Fig. 9. The cell cycled well for the first 40 cycles, with the charge/discharge ratio approaching unit. The charge/discharge ratio then decreased and some instability was found in the voltage profile near the end of the charge. This behaviour was related to the fact that the cell was no longer anode limited. The discharge end-voltage increased with cycling and the cell after 70 cycles could not take charge. In Fig. 10, the cell voltage is plotted as a function of anode capacity during galvanostatic discharge cycles at different discharge rates (C/4, C/2, 1C and 3C). The voltage profile remained almost unchanged on increasing the discharge rate from C/4 to 1C rate, with a slight decrease in both average discharge voltage and discharged capacity. A substantial average discharge voltage decrease was observed at 3C due to the increase in ohmic drop, with a limited decrease in anode capacity. Fig. 11 shows the Ragone plot for the cell discharged at different rates. The energy and power density are based on the weight of the cell, including the liquid electrolyte, but not the current collectors. The energy density calculated at C/4 rate was about 100 Wh kg^{-1}, while the power density calculated at 3C rate was in excess at 280 W kg^{-1}. Considering that the electrodes were not optimized (the porosity was not optimized) and the cell was not properly dimensioned (it was strongly anode limited with cathode/anode capacity ratio >1.5), these values can be further improved in terms of cathode/anode ratio and electrode porosity reduction.

Table 1
Various properties of the separator

Weight before dipping (mg)	Weight after dipping (mg)	Weight difference (mg)	Thickness (μm)	Resistance (Ω)	Specific conductivity (σ)
4.2	7.2	3.0	44	14.29	3.92×10^{-4}

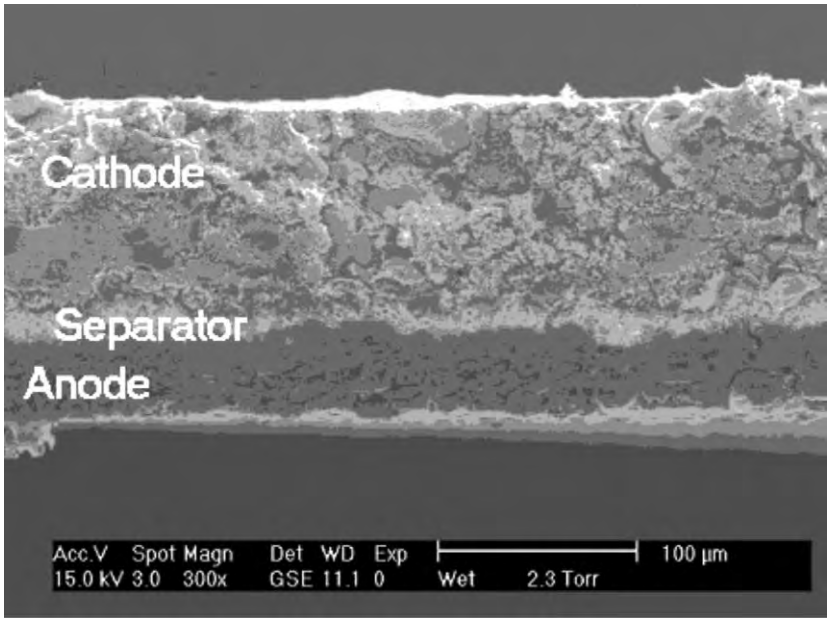


Fig. 7. SEM micrograph cross-section of an anode/MgO-based separator/cathode hot laminated cell.

4. Conclusions

Self-standing separators were made by casting a slurry of an inorganic oxide (γ-$LiAlO_2$, Al_2O_3 and MgO) and PVdF-HFP as filler and binder, respectively. These separators were found to be intrinsically porous and could swell on the addition of liquid electrolyte. Voltammetry was inadequate in evaluating electrochemical stability. Some of the fillers are not compatible with the electrodes: the separators based on MgO and γ-$LiAlO_2$ showed good anode stability, while separators based on MgO and Al_2O_3 showed good cathode stability. The MgO-based separator showed the best

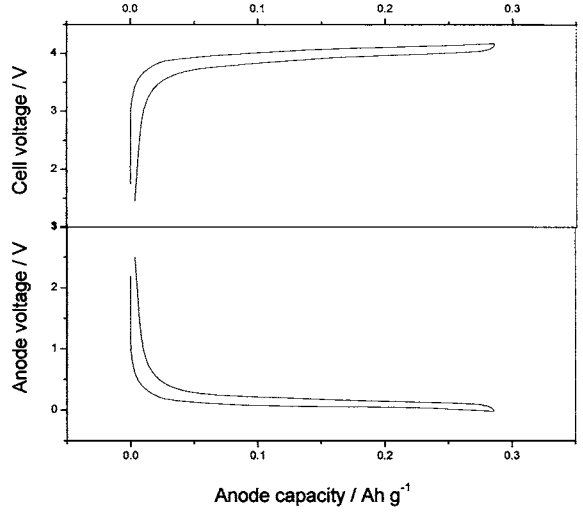


Fig. 8. Voltage profiles for a lithium-ion battery cell (top) and for the graphite anode measured against Li reference electrode (bottom). The cell was anode limited. The cell was charged at 0.5 mA cm^{-2} for 1.5 h. The cell was discharged at the same current to 1.5 V. The anode loading of graphite was 2.7 mg cm^{-2}.

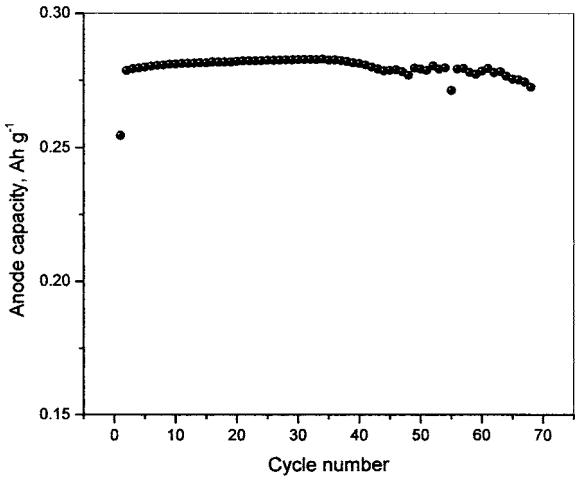


Fig. 9. Specific capacity upon discharge for the lithium-ion cell described in Fig. 8.

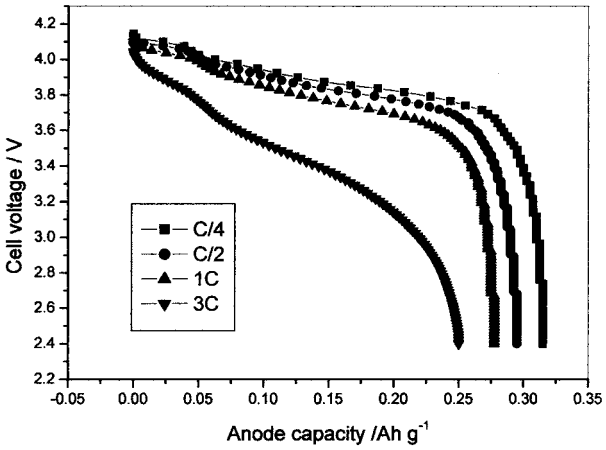


Fig. 10. Voltage profile for a lithium-ion cell cycled at different discharge rates. Discharge current densities: 0.42, 0.84, 1.65, and 4.97 mA cm^{-2}. The cell was charged at 1.65 mA cm^{-2} to 4.2 V and this voltage was applied until the current flow decreased at 1/10th of the charging current. The anode loading of graphite was 5.0 mg cm^{-2}.

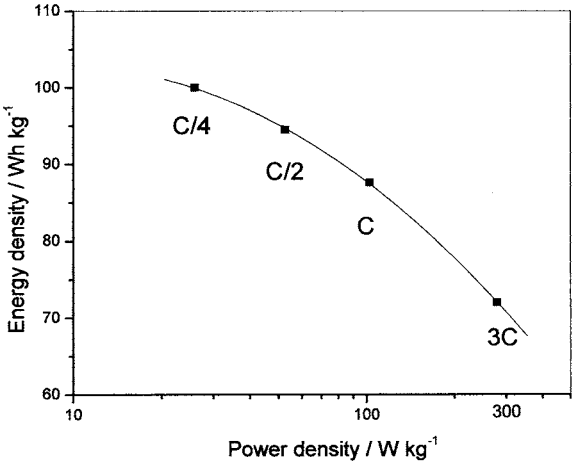


Fig. 11. Ragone plot for the lithium-ion cell described in Fig. 10. The energy and the power densities are based on the total weight of the cell, comprising the liquid electrolyte, without including the weight of the current collectors.

anode and cathode compatibilities. After activation with the liquid electrolyte, Li-ion cell cycled reversibly with good capacity retention. The energy density (at C/4 rate) was about 100 Wh kg^{-1} while the power density (at 3C rate) was >280 W kg^{-1}. These preliminary results are very encouraging and considering that the cells are not optimized, suggest that further improvements are possible.

References

[1] T. Nagaura, K. Tozawa, Prog. Batteries Solar Cells 209 (1990) 9.
[2] C. Pillot, The World-Wide Battery Market and its Main Applications, Batteries 2000, Paris (2000).
[3] T. Tanaka, The World-Wide Battery Market and its Main Applications, Batteries 2000, Paris (2000).
[4] A. Du Pasquier, J.-M. Tarascon, US Patent 5,418,091, 2001.
[5] A. Du Pasquier, G.G. Amatucci, I. Plitz, T. Zheng, A.S. Gozdz, J.-M. Tarascon, Solid State Ionics 135 (2000) 249.
[6] S.H. Chung, Y. Wang, L. Persi, F. Croce, S.G. Greenbaum, B. Scrosati, E. Plichta, J. Power Sources 97–98 (2001) 644.
[7] P.A.R.D. Jayathilaka, M.A.K.L. Dissanayake, I. Albinsson, B.-E. Mellander, Electrochim. Acta 47 (2002) 2357.
[8] B. Kumar, L. Scanlon, R. Marsh, R. Mason, R. Higgins, R. Baldwin, Electrochim. Acta 46 (2001) 1515.
[9] K.-H. Lee, Y.-G. Lee, J.-K. Park, D.-Y. Seung, Solid State Ionics 133 (2000) 257.
[10] G.B. Appetecchi, P. Romagnoli, B. Scrosati, Electrochem. Commun. 3 (2001) 281.
[11] S. Rajendran, O. Mahendran, R. Kannan, J. Phys. Chem. Solids 63 (2002) 303.
[12] A.M. Sthephan, Y. Saito, N. Muniyandi, N.G. Renganathan, S. Kalyanasundaram, R.N. Elizabeth, Solid State Ionics 148 (2002) 467.
[13] R.A.M. Hikmet, J. Power Sources 92 (2001) 212.
[14] K.M. Abraham, V.R. Koch, T.J. Blakley, J. Electrochem. Soc. 147 (2000) 1251.
[15] P.P. Prosini, M. Carewska, P. Villano, Italian Patent no. RM2001A000452 Roma (2001).
[16] A. Blyr, C. Sigala, G.G. Amatucci, D. Guyomard, Y. Chabre, J.-M. Tarascon, J. Electrochem. Soc. 145 (1998) 194.
[17] C.G. Thurston, J.R. Owen, J. Power Sources 39 (1992) 215.
[18] M.C. Borghini, M. Mastragostino, S. Passerini, B. Scrosati, J. Electrochem. Soc. 142 (1995) 2118.
[19] Y. Matsumura, S. Wang, J. Mondori, J. Electrochem. Soc. 142 (1995) 2914.
[20] P.P. Prosini, S. Passerini, Eur. Polym. J. 37 (2001) 65.
[21] J.M. Tarascon, D. Guyomard, J. Electrochem. Soc. 138 (1993) 2864.

Appendix H

ELSEVIER

Materials Science and Engineering A202 (1995) 206–217

MATERIALS SCIENCE & ENGINEERING A

Review: aqueous tape casting of ceramic powders

D. Hotza[a], P. Greil[b]

[a]*Technische Universtität Hamburg-Harburg, Arbeitsbereich Technische Keramik, Denickestrasse 15, D-21071 Hamburg, Germany*
[b]*Universtität Erlangen-Nürnberg, Institut für Werkstoffwissenchaften, Martensstrasse 5, D-91058 Erlangen, Germany*

Received 19 August 1994; in revised form 5 December 1994

Abstract

Slurry formulations and processing parameters of the water-based tape casting of ceramic powders are reviewed. Additives include binders, like cellulose ethers, vinyl or acrylic-type polymers; plasticizers, like glycols; and dispersants, like ammonium salts of poly(acrylic acids). Mostly alumina powders have been employed. Hydrophobing of ceramic powders permits the aqueous processing even of water-reactive powders, like aluminium nitride. Non-toxicity and non-inflammability of water-based systems represent an alternative to organic solvent-based ones. Aqueous slurries are, on the other hand, complex multiphase systems, very sensitive to process variations. Statistical design of experiments was used for the improvement of the process.

Keywords: Tape casting; Ceramic powders; Slurries

1. Introduction

Tape casting is a well-established technique used for large-scale fabrication of ceramic substrates and multilayered structures [1–8]. A slurry consisting of the ceramic powder in a solvent, with addition of dispersants, binders and plasticizers, is cast onto a stationary or moving surface. The cast tape, with a typical thickness in the range of 100–300 μm is then dried and finally sintered to obtain a desired final shape.

Depending on the composition of the ceramic powder a variety of non-aqueous organic solvents, such as alcohols, ketones or hydrocarbons are commonly used to prepare highly concentrated suspensions with reproducible rheological properties and drying behaviour.

In recent years, the environmental and health aspects of the tape casting process have received special attention. Therefore, slurry formulations using water as solvent instead of organic liquids have appeared in the literature [9–24]. Non-aqueous solvents have lower boiling points and avoid hydratation of the ceramic powder, but require special precautions concerning toxicity and inflammability. Typically, organic solvent recovery systems are needed to control emissions of compounds into the atmosphere. On the other hand, an aqueous system has advantages of incombustibility, non-toxicity and low cost, associated with the large amount of experience with the use of water in similar ceramic powder processes, such as slip casting. In addition, other colloidal processing methods, such as those used in paint or magnetic tape fabrication, have changed from organic to water-based systems due to safety considerations.

A tape casting slurry must be adjusted in order to yield tapes which satisfy some quality criteria, such as (i) no defects during drying; (ii) cohesion to allow the manipulation of dried sheets; (iii) microstructural homogeneity; (iv) good thermocompression (lamination) ability; (iv) easy pyrolysis (burnout); and (v) high mechanical strength after sintering. This requires careful selection of the slurry additives together with accurate control of many processing parameters.

Major differences between non-aqueous and aqueous tape casting refer to the sensitivity to process perturbations, as reported by Nahass et al. [15]. An organic solvent-based slurry is much more volatile and irritating to process, but strong, uniform green tapes are easy to achieve. An aqueous slurry has smaller tolerance to minor changes in drying conditions, casting composition or film thickness. It produces crack-free, uniform green tapes only when all variables are controlled extremely well. The aim of this work is to review the

0921-5093/95/$09.50 © 1995 — Elsevier Science S.A. All rights reserved
SSDI 0921-5093(95)09785-6

Table 1
Aqueous slurry additives for tape casting[a]

Powder	Binder	Plasticizer	Dispersant	Others	Reference
Alumina + MgO	Acrylic polymer	PEG + BBP	Condensed aryl sulfonic acid	Octylphenoxy-ethanol[b] wax emulsion[c]	[9]
Alumina + talc	PAA	Glycerol	NH_4PMA + Dispex A40[e]		[10]
	PAA	Glycerol + PVP	NH_4PM + Dispex A40[e]		
Alumina	PUR		POENPE		[11]
	PVA	Glycerol	POENPE		
	PVAc	Glycerol	POENPE		
	NH_4PA	Glycerol + DBP	Primal 850[e]		
Alumina	Cellulose ether (MC, HPMC or HBMC)		NH_4PMA		[12]
Alumina	Acrylic copolymer	BBP	NH_4 salt of a polyectrolyte		[13]
Alumina	PVAc		NaCMC	Silicon organics[c]	[14]
Alumina	Acrylic polymer (PEA + PMMA)	PPG	NH_4PMA	Pin oil[d]	[15,16]
Mullite	Acrylic polymer (PEA + PMMA)	PPG			[17]
	Acrylic polymer (PEA + PMMA)	PPG	NH_4PMA		
Alumina	HEC	PEG	NH_4PA		[18]
Alumina	AE/AA				[19,20,22,23]
	AE/AA		Acrylic dispersants		[21]
Alumina	PAA	PEG	NH_4PA		[24]

[a]BBP is benzyl butyl phthalate; DBP is dibutyl phthalate; POENPE is poly(oxyethylene nonylphenol ether); PUR is polyurethane; the remaining abbreviations are listed in Tables 2 and 3.
[b]wetting agent
[c]defoamer
[d]surfactant
[e]commercial name (no composition given)

efforts conducted to develop aqueous systems as a reliable alternative to organic solvent-based systems for the tape casting process.

2. Slurry formulation

Compared with non-aqueous solvents, the variety of water-soluble binders, plasticizers and dispersants is restricted to a few systems, which will be discussed in the following sections. Table 1 summarizes the combinations used for aqueous tape casting of alumina and mullite.

Some general rules can be inferred for the preparation of a tape casting slurry: (i) the ratio between organic components and ceramic powder must be as low as possible; (ii) the amount of solvent must be fixed at the minimum to maintain a homogeneous slurry; (iii) the amount of dispersant must be the minimum necessary to ensure the stability of the slurry; (iv) the plasticizer to binder ratio must be adjusted to make the tape flexible, resistant and easy to release.

A compilation of compositions of aqueous slurries is illustrated in Figs. 1 and 2. According to the first two mentioned criteria, the top of the triangle in Fig. 1 should be the goal to be reached. In other words, the minimal amount in water and in organic additives to prepare a slurry with satisfactory properties should be used. The ceramic powder charges vary from about 25 until almost 80 wt.%. The organic additives are always above 18 wt.%, while the water content ranges from less than 20 up to 70 wt.%.

The organic components themselves have been used in quite different ratios, as shown in Fig. 2. This

CosMX Exhibit 1003, Page 256 of 512

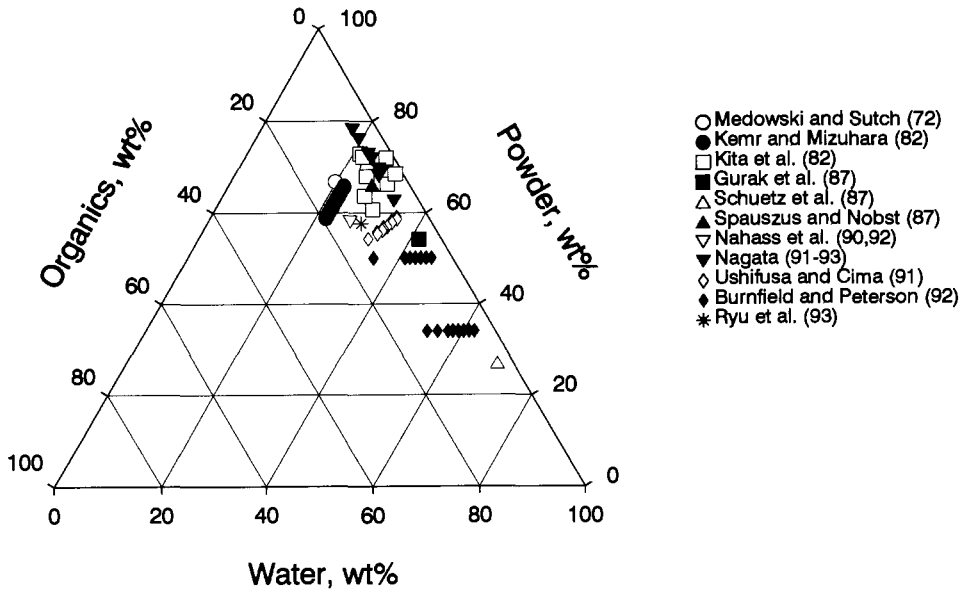


Fig. 1. Aqueous slurry formulations for tape casting. The ceramic powder is alumina, with the exception of Ushifusa and Cima [17], who used mullite.

classification, however, is not absolute: some additives have multifunctional characteristics. A certain binder, for instance, can exhibit plasticizing or dispersing effects. Two investigators use neither dispersant nor plasticizer in the slurry formulations [12,19–23]; in the other cases the binder corresponds at least to half of the organic part of the slurry. The dispersant content is in any case the lowest of all three organic additives (< 20 wt.%). Plasticizers were generally used up to around 50 wt.%, but Kemr and Mizuhara [10] have used much higher contents.

2.1. Solvent

The solvent dissolves the organic materials and distributes them uniformly throughout the slurry. It is the vehicle that carries the ceramic particles in a dispersion until it evaporates and leaves a dense tape on the carrier.

A non-aqueous suspension dries quickly and produces green sheets having a high density and a fine surface appearance. An aqueous suspension has the disadvantages of high evaporation latent heat and inferior drying characteristics, and there are many quality problems to be solved.

A comparison of aqueous and non-aqueous slurries for tape casting was made by Nahass et al. [15] to determine the effect of changing solvent systems on slurry processing and green tape quality. An alumina powder was utilized and the other slurry components as well as the processing parameters were kept constant. Green tapes from both systems had similar physical properties, although the aqueous systems were more sensitive to process perturbations.

2.2. Powder

A well-characterized powder is necessary to increase reliability in ceramic processing, and in particular in aqueous tape casting. To achieve effective particle packing, the powder must have a small particle size. However, the lower the particle size, the higher the specific surface area, which is not convenient, because higher tape shrinkages are produced and higher concentrations of additives are required [7].

Generally, alumina powders have been used (see Table 1), sometimes with addition of grain growth inhibitors and/or sintering aids, like MgO [9] or talc [10]. Aqueous tape casting of mullite has been reported by Ushifusa and Cima [17], of yttria-stabilized zirconia by Raeder et al. [25]. Surface area values from 2 up to 11 $m^2 g^{-1}$ have been mentioned for alumina powders. Average particle size from 0.3 up to 1.7 μm for alumina, or even of 3.3 μm for mullite have been cited.

A limitation of using water-based systems in tape casting should be expected to be the incompatibility with powders susceptible to hydratation, like CaO or MgO. However, even this can be overcome through the hydrophobing of ceramic powders [26]. By means of this technique water-reactive powders, like AlN [27–29], can be processed in aqueous media.

Hydrophobing of AlN powders was performed through adsorption of stearic acid on the particle surface, using cyclohexane as solvent. Adsorption data obtained indicated a Langmuir chemisorption isotherm. Even after 96 h leaching in water no crystalline phase other than AlN could be detected by XRD [29]. Tapes could be cast and sintered without significant increase in oxygen content [30].

CosMX Exhibit 1003, Page 257 of 512

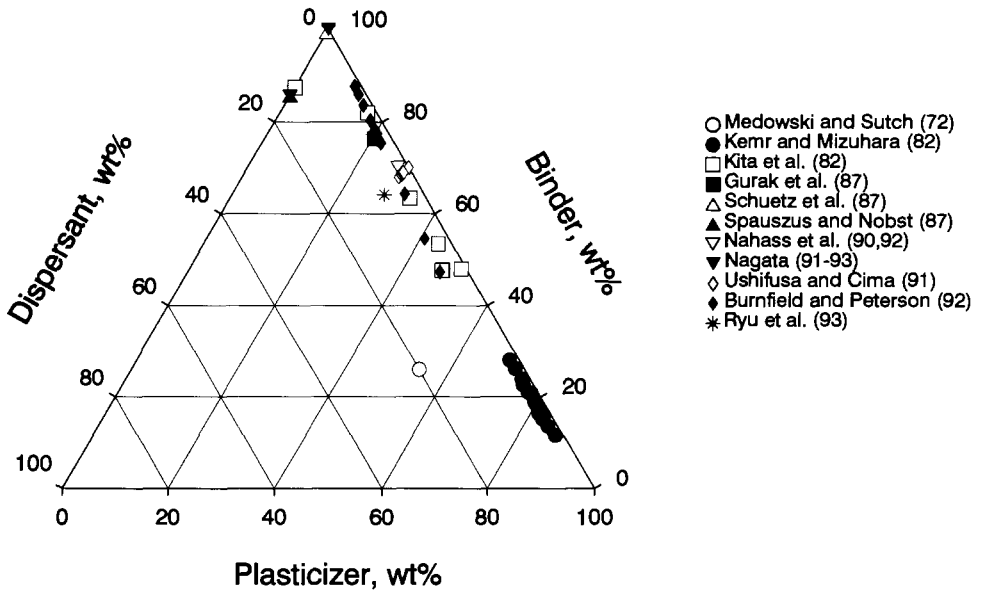


Fig. 2. Organic additive formulations used in aqueous slurries for tape casting.

2.3. Binder

The binder provides strength to green tapes after evaporation of the solvent through organic bridges between the ceramic particles. The tapes can then be easily manipulated and retained in the desired shapes before sintering.

Organic binders are either dissolved or dispersed in water as an emulsion. Most soluble binders are long-chain polymer molecules. The backbone of the molecule consists of covalently bonded atoms such as carbon, oxygen and nitrogen. Attached to the backbone are side groups located at frequent intervals along the length of the molecule. The chemical nature of the side groups determines in part which liquids will dissolve the binder. If the side groups are highly polar, solubility in water is promoted [31]. The polymeric molecules of binders consist of smaller units, the monomers. The number of monomers in a polymer is called the degree of polymerization, *DP*. The number of sites on which modifications are made in a monomer is called the degree of substitution, *DS*. The molar ratio between side groups and a monomer unit is called the average molar degree of substitution, *MS*.

Two groups of substances mainly have been used as binders for aqueous tape casting of ceramics: cellulose ethers and vinyl or acrylic-type polymers. The only remarkable exception is polyurethane, which was referred to by Kita et al. [11]. Cellulose is a natural polysaccharide formed by ring-type monomers, which have a modified glucose structure [31]. Fig. 3 shows the structure of a cellulose type molecule; it is represented as a polymeric chain that is built with a number *n* of cellobiose units. The latter ones consist of two anhydroglucose units. Each anhydroglucose ring has three free hydroxyls that can be substituted by various side groups through chemical reactions. The distribution of the substituent groups is largely determined by the corresponding reaction rate of the hydroxyls. Sometimes the reactive groups are rather attached to secondary hydroxyls present in the side chains, so that it is usual to characterize such polymers with *MS* instead of *DS*.

Cellulose ethers that have been used as additives in the tape casting technology are listed in Table 2. They are manufactured by the reaction at high temperatures and pressures of alkali cellulose with, according to the desired product, methyl chloride, ethylene oxide, propylene oxide, sodium monochloracetate and others. An idealized structure for a portion of such cellulose ethers can be obtained for a given value of *DS* or *MS* together with the general structural formula in Fig. 3. The etherification succeeds through substitution and/or addition on a part of the cellulose hydroxyls. A cellulose polymer with single substituent or several ones can be formed. In the latter case, it concerns a copolymer.

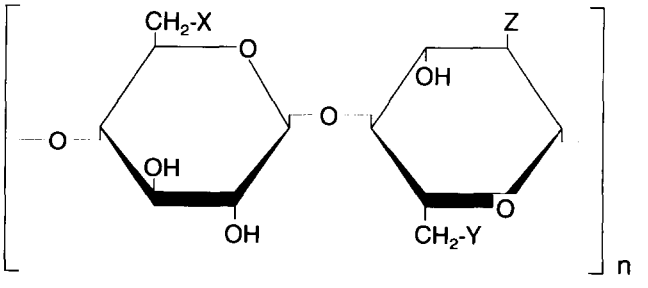


Fig. 3. Structural formula of cellulose derivatives.

CosMX Exhibit 1003, Page 258 of 512

Table 2
Cellulose derivatives used in aqueous tape casting[a]

Compound		Side groups			*DS*	*MS*
		X	Y	Z		
	Cellulose	–OH	–OH	–OH		
MC	Methyl	$-OCH_3$	$-OCH_3$	$-OCH_3$	1.5	1.5
HEC	Hydroxyethyl	$-OC_2H_4OC_2H_4OH$	$-OC_2H_4OH$	$-OC_2H_4OC_2H_4OH$	1.5	2.5
HPMC	Hydroxypropyl methyl	$-OC_3H_6OH$	$-OCH_3$	$-OCH_3$	1.5	1.5
HBMC	Hydroxybutyl methyl	$-OC_4H_8OH$	$-OCH_3$	$-OCH_3$	1.5	1.5
NaCMC	Sodium carboxymethyl	$-OCH_2COONa$	$-OCH_2COONa$	–OH	1.0	1.0

[a]Used as binders, with exception of NaCMC, used as dispersant, X, Y, Z see Fig. 3

It is usual to divide the cellulose ethers into ionic and non-ionic types. Ionic cellulose ethers, like NaCMC, contain substituents with electrical charge and are rather used as polyelectrolytes. Non-ionic cellulose ethers, like MC and HEC, carry no charge and are mainly used as binders. Copolymers with ionic and non-ionic substituents are ordered in the group, whose character predominates. Because of their different solubility, non-ionic cellulose ethers are further subdivided: for instance, MC is soluble in cold water; HEC is soluble in both cold and warm water.

The general formula for vinyl-type additives is given in Fig. 4. The vinyls are characterized by a linear backbone consisting of carbon–carbon bonds, with a side group (represented here by Y, X being a hydrogen atom) attached to every other atom. When there are two side groups (X and Y) attached to the carbon atom, they are called acrylics. Some vinyl and acrylic-type additives used in the aqueous tape casting processing are listed in Table 3. They can also be subdivided into ionic and non-ionic polymers. The former are the ammonium salts of poly(acrylic acids), which act as polyelectrolytes. The latter are used instead as binders.

Binders strongly affect the rheology of the liquid phase, increasing the viscosity and changing the characteristics from Newtonian (for pure water) to pseudoplastic in most cases. A pseudoplastic behaviour is characterized by a decreasing viscosity with increasing shear rate. The rheology of the solution for its turn directly affects the behaviour of slurries formed by adding ceramic powders and remaining organic components. The viscosity of aqueous slurries is very much lower compared with organic solvent slurries. Typical values are in the range of ≈ 0.1 to ≈ 20 Pa s for a shear rate of 50 s^{-1} at room temperature [22–24].

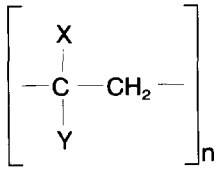


Fig. 4. General formula of vinyl and acrylic-type derivatives.

Fig. 5 shows a viscosity–shear rate relationship for a 2% aqueous solution of HEC, a typical, strongly pseudoplastic binder, with different molecular weights [31]. The pseudoplasticity of solutions is important in many technologies, including tape casting of ceramics. A suspension of solid particles tends to settle out in water if the particles are larger than 1 μm. The tape casting slips would not remain homogeneous if settling occurred. One approach to slow down the sedimentation is to increase the viscosity of the liquid. However, slips must be fluid enough to be cast. To solve this problem, a pseudoplastic solution is utilized. The sedimentation of a particle involves very small shear rates. Under these conditions a pseudoplastic solution may have a very high viscosity [31]. At high shear forces, as in casting a tape, the viscosity of the slip may be several orders of magnitude lower. Once deposited, a slip does not run and level out throughout the tape surface.

The suitable amount of binder to be added must be determined experimentally. When there is not enough

Table 3
Vinyl and acrylic-type polymers used in aqueous tape casting[a]

Compound		Side groups	
		X	Y
	Vinyl radical	–H	–
PVA	Poly(vinyl alcohol)	–H	–OH
PVAc	Poly(vinyl acetate)	–H	$-OOCCH_3$
PVP	Poly(vinyl pyrrolidine)	–H	$-NC_4H_8$
PAA	Poly(acrylic acid)	–H	–COOH
AE/AA	Copolymer of acrylic ester[b] and acrylic acid	–H	$-COOCH_3$
PEA	Poly(ethyl acrylate)	–H	$-COOCH_2CH_3$
PMAA	Poly(methacrylic acid)	$-CH_3$	–COOH
PMMA	Poly(methyl methacrylate)	$-CH_3$	$-COOCH_3$
NH_4PA	Ammonium polyacrylate	–H	$-COONH_4$
NH_4PMA	Ammonium poly(methacrylate)	$-CH_3$	$-COONH_4$

[a]Used as binders, with exception of NH_4PA, NH_4PMA and NH_4PMMA, which are generally used as dispersants of PVP, used as plasticizer. X, Y see Fig. 4

[b]In this example: a methyl ester, also called methyl acrylate

CosMX Exhibit 1003, Page 259 of 512

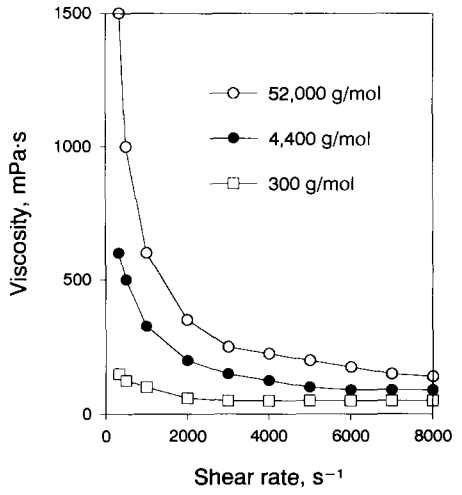


Fig. 5. Viscosity of a 2% aqueous solution of HEC with different molecular weights as a function of shear rate [31].

binder, the resulting green tape tends to develop cracks. When the amount of binder is too high, on the other hand, the tapes will contain many voids. Fig. 6 shows the dependence of green tape strength and density on a cellulose-type binder concentration for different alumina amounts [18]. Tape strength increases and green tape density decreases with increasing binder content,

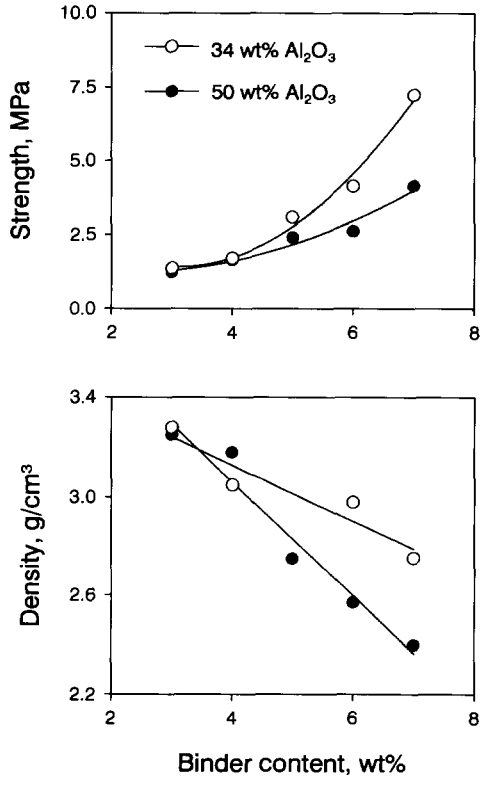


Fig. 6. Strength (top) and density (bottom) of alumina green tapes with different powder charges as a function of HEC wt.% [18].

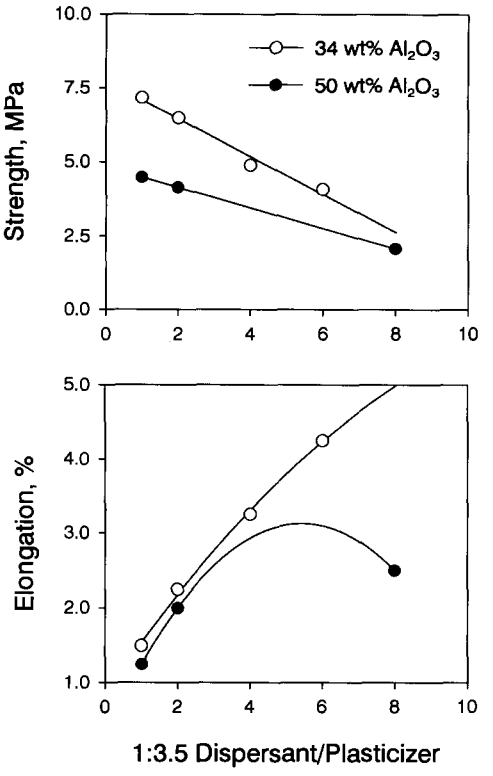


Fig. 7. Strength (top) and elongation (bottom) of alumina green tapes with different powder charges as a function of dispersant/plasticizer amount [18].

showing that a compromise must always be found.

2.4. Plasticizer

Plasticizers are additives that soften the binder in the dry or semidry state. They are organic substances with low molecular weight in comparison with binders and are soluble in the same liquid. After drying, binder and plasticizer are intimately mixed. The plasticizer breaks the close alignment and bonding of the binder molecules, thereby increasing the flexibility and workability of the tape. While softening the binder, the plasticizer tends to reduce the strength. Fig. 7 shows the results of a tensile test for alumina green tapes with a constant binder content (7 wt.% HEC) [18]. This material exhibits decreasing strength and increasing elongation with increased concentration of dispersant/plasticizer mixture (ratio dispersant/plasticizer equal to 1:3.5).

Water-soluble plasticizers used in tape casting are listed in Table 4. They generally include glycols, in a simple form like glycerol, or as polymers like PEG or PPG. Additions of phthalates like BBP and DBP that are common in organic solvent-based formulations, as well as of PVP, were instead made together with glycol-type plasticizers: PEG + BBP [9], glycerol + PVP [10], glycerol + DBP [11].

CosMX Exhibit 1003, Page 260 of 512

Table 4
Common plasticizers used in aqueous tape casting

Compound		Formula
	Glycerol	$HOCH_2CH(OH)CH_2OH$
PEG	Poly(ethylene glycol)	$HO-(CH_2CH_2O)_n-H$
PPG	Poly(propylene glycol)	$HO-(CH_2CH_2CH_2O)_n-H$
DBP	Dibutyl phthalate	$C_{16}H_{22}O_4$
BBP	Benzyl butyl phthalate	$C_{15}H_{20}O_4$

The most important effect of the plasticizer is to reduce the gel formation temperature, T_g, at room temperature or less. This is illustrated in Fig. 8, in which the variation of the T_g of PVA by adding PEG is shown [32]. Tapes having gelled liquids dry much more slowly because the liquid does not flow to the surface during drying. Water must leave the body by diffusion within the gel structure. However, one advantage of a gelled structure is that the binder does not migrate to the drying surface. It would if it were carried there by the flowing liquid as it moves to the surface.

The binder plus plasticizer system cannot strongly adhere to the casting surface after casting, and must decompose without leaving residues. In addition, there is an optimum value of flexibility, obtained when the correct binder/plasticizer system is selected and the relative concentrations are properly adjusted. If the plasticizer concentration is progressively increased to enhance the flexibility, the porosity will decrease until the pores disappear. A further addition results in increasing interparticle distances and the green density will decrease [5,33].

2.5. Dispersant

A dispersant, sometimes also called deflocculant, wetting agent or surfactant, coats the ceramics particles and keeps them in a stable suspension in the slurry due to steric and/or electrostatic repulsion. Both mechanisms have been widely discussed in the literature (for a review, see Moreno [7]). A combination of both electrostatic and steric mechanisms, referred as electrosteric, was proposed to obtain a better stabilization [34]. The electrostatic component may originate from a net charge on the particle surface and/or charges associated with the anchored polymer, called polyelectrolyte. In addition, the molecular weight of polyelectrolyte and solid loading may change the stability and rheology of aqueous slurries [35].

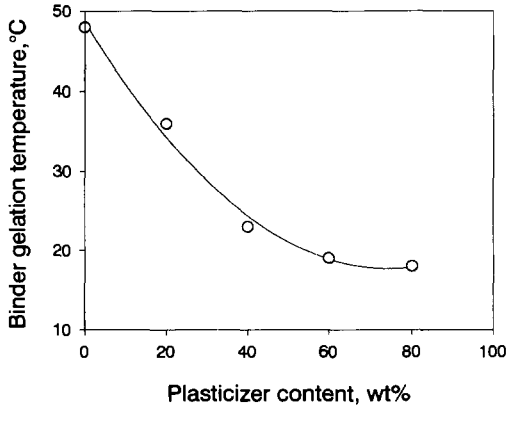


Fig. 8. Effect of the plasticizer content on the binder T_g [32]. Plasticizer is PEG, binder is PVA.

The most frequently used dispersants for aqueous tape casting are polyelectrolytes. Such additives were listed in Tables 2 and 3, respectively, as a sodium salt of a cellulose derivative, NaCMC, and ammonium salts of poly(acrylic acids), NH_4PA or NH_4PMA. The use of aryl sulphonic acid and POENPE are also mentioned as dispersants. Further additives were reported, although their function is not always clear, like a so-called surfactant (pine oil) [15,16] and a wetting agent (octylphenoxyethanol) [9]. In addition, defoamers were sometimes employed (silicon-based organics [14] or wax emulsion [9]).

In aqueous systems, the variation of pH is of particular importance due to the formation of electrostatic double layers, which can result in high surface potentials and repulsive Coulomb forces. Surface charging in aqueous environment is due to protonation or hydroxylation of surface hydroxide groups resulting in positive or negative surface charge, respectively.

Measurements of zeta potential or isoelectric point (*iep*) of an aqueous suspension can also give important information about its stability regarding pH and/or dispersant amounts [17,24]. On the other hand, measured values of *iep* for many ceramic powders may differ markedly due to surface impurity contents. Rao [36] determined the *iep* of commercial alumina powders in dilute aqueous dispersions in the pH range 4 to 10.

Relative viscosity [21], sedimentation velocity and volume [17,21], or adsorption isotherms [19–23] can be determined to find the minimum concentration of dispersant necessary to stabilize an aqueous suspension. As shown in Fig. 9, a minimum in the suspension viscosity or in the sedimentation volume represents the optimum concentration of dispersant [21]. Optionally, a maximum in the zeta potential curve or a constant plateau in an adsorption isotherm can be obtained.

3. Processing and equipment

3.1. Milling and mixing

Most of the reported aqueous tape casting processes are performed through a two-stage milling/mixing procedure [9,12–14,24]. The first stage corresponds to milling, in which a low-viscosity slurry, consisting of

CosMX Exhibit 1003, Page 261 of 512

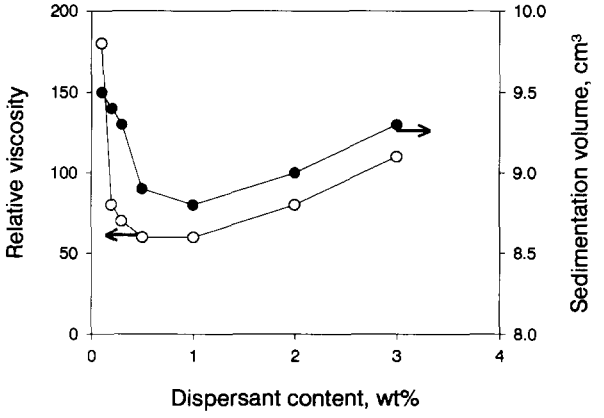


Fig. 9. Relative viscosity and sedimentation volume of an alumina/water suspension as a function of dispersant amount (adapted from Ref. [21]).

water, dispersant and powder (in this order) is prepared. During milling agglomerates are broken and dispersants are uniformly distributed on the surfaces of the ceramic particles. In the second stage, mixing and homogenization occurs in which plasticizer and binder are dissolved in the aqueous slurry.

Some modification in this standard procedure has been mentioned. A one-step milling was carried out with all components by many investigators [10,11,18–23]. Other researchers have added the plasticizer already in the first stage [9,11,13]. Ushifusa and Cima have included an ageing step (150 h) in a ball mill without milling media as second stage [17]. The order of addition of the components is critical, according to previous research with non-aqueous slurries [37–39], although the active mechanisms remain in part unexplained. Concerning aqueous slurries, there has been no specific study of it. Only Nahass et al. [15] and Ushifusa and Cima [17] describe precisely the order of addition.

Milling/mixing was mainly performed in ball mills. The milling speed was only once mentioned (60 to 120 r.p.m.) [14]. The duration varied from a total of about 5 h to about 24 h, with diverse distributions for the two stages [9,19]. An ultrasonic agitation was also cited by Nahass et al. [15,16] as the first stage of mixing, after a previous centrifuging (3500 r.p.m., >30 min) to remove excess of water.

After milling/mixing, deairing can be performed by a vacuum [11,14,24], or else by centrifugation (2000 r.p.m., 20 min) [12]. Filtering can be also applied (400 mesh) to remove large particles and bubbles [15,16].

3.2. Casting and drying

Casting of tapes is accomplished by the relative movement between a "doctor blade" and a support. Two solutions are possible: either the blade moves over a fixed support or the support moves under a fixed blade. The first technique is discontinuous and generally used in small-scale manufacture or for laboratory operations. The latter is a continuous one, used in the most production-scale tape casting processes.

Most of the investigators use the continuous process for aqueous slurries. In this case, the moving carrier is generally covered by a polymeric film, such as poly(ethylene terephthalate) [10,23], polyester [11,18] or polypropylene [13]. When the discontinuous option is used, a glass plate acts as a carrier surface, on which a releasing agent (solution of lecithin in isopropanol) can be applied [15–17]. To provide more precise control of the slurry thickness, a dual doctor blade system was sometimes employed [15–17]. Casting rates ranged from 30 to 120 cm min^{-1}, and gate openings up to 1.0 mm were adjusted [15,16,24].

Drying was performed with flowing air in a closed system or at open air, from room temperature to 85 °C, with relative humidity from 50 to 70%, for 26 min to 24 h. Spauszus and Nobst observed that the tapes tend to be fragile when the water content decreases, and recommended maintaining a residual humidity of the tapes from 2 to 5 wt.% after drying [14]. Nahass et al. [16] studied the ageing shrinkage of alumina green tapes, which was found to correlate inversely with the amount of organic phase bound to both organic and aqueous-based tapes. A detailed study about the drying of water-based tapes has not yet been made, but a theoretical model for the drying of tapes in general has been presented [2].

The density and/or the porosity of green tapes can be useful in detecting poor packing of the powder or excessive binder content, for example. Techniques for estimating the tape density were presented by Mistler et al. [2], Archimedes' principle being the most frequently employed one. Measured values of theoretical densities for aqueous-based tapes were between 42 and 63% for alumina [14,20–22], and from about 45 to 50% for mullite [17].

Nagata [19,20,22] has worked with pH variations in alumina/water slurries for tape casting in the range from pH 7.5 to 10.4. The highest value of packing density of green tapes (about 63% of the theoretical density) was obtained at pH 7.5. Ushifusa and Cima [17] described the appearance of mullite/water slurries and green tapes as a function of pH, and observed flocculation below pH 7.5. Tensile strength of alumina green tapes has also been measured [12,18–23]. Typical values for rupture strength are 0.39–10.68 MPa and for elongation to failure 1.2–80%.

3.3. Shaping, burnout and sintering

After drying, the tape can be released and cut for use in a shaping procedure, like punching [15,16] or laminating [17]. When the discontinuous process is used and the tapes are cast on glass plates, a razor blade can be

CosMX Exhibit 1003, Page 262 of 512

used to remove them from the plates [15,40]. Multilayered ceramic packages were produced by a thermocompression (lamination) at 120 °C, with a pressure of 2.5–17.5 MPa [17].

The burnout of organic slurry-based tapes has been investigated and partially modelled [41,42]. In the case of aqueous tape-casting, there is no rigorous study about it. Thermogravimetric studies performed by Burnfield and Peterson [18] showed that HEC binder in the presence of alumina burns out differently from the polymer alone. In both cases, the polymer burns out completely, but the rate and the temperature of burnout differ.

Ryu et al. [24] performed an investigation about the rheology of aqueous alumina slurries for tape casting concerning changes in pH and its influence on properties of green and sintered tapes. The bulk density of the sintered bodies followed the same tendency observed in the green bodies, Fig. 10. The variation of green and sintered tape densities on pH is a consequence of the pH-dependence of the rheological characteristics of the slurry, which presented the highest viscosity at the isoelectric point, pH 2.4. Furthermore, this isoelectric point is significantly lower in comparison to that of the aqueous alumina suspension without organic components, which lays at pH 7.8. This effect is similar to that described by Cesarano and Aksay [35] for the adsorption of a polyelectrolyte dispersant on alumina.

4. Strategies for process optimization

Aqueous slurries are a complex multiphase system, very sensitive to qualitative and quantitative changes of the components. The production of reliable, reproducible aqueous-based cast tapes requires a close control of the processing parameters or rather the identification of processing conditions to minimize variations on product quality.

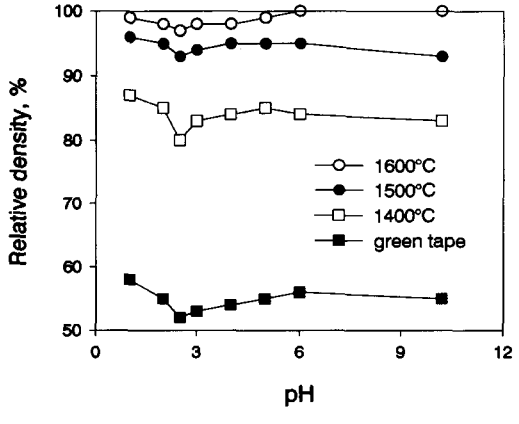


Fig. 10. Relative density as a function of slurry pH for green and sintered tapes of alumina [24].

The process optimization is dependent on many parameters, or factors, some of which can be controlled and others that are beyond the control of the manufacturer. All combinatory possibilities of varying parameters (full factorial design) cannot be normally overcome due to the extensive number of necessary experiments. Commonly, a one-factor-by-one method is used, in which one factor is varied while all the other factors are held constant. The drawback of this method is that the result of each experiment is only valid at fixed experimental conditions, and prediction of experimental results at other conditions is uncertain. In contrast to this method, a fractional factorial design, with reduced number of experiments followed by a statistical analysis, can be used to optimize ceramic processing, as related in recent investigations [29,43].

In addition, a new approach can be added to the fractional factorial design of experiments. Normally, a statistical analysis of variance is performed on the mean values of a chosen property, in order to identify a setting of controllable parameters that optimize such property. It means that the focus of traditional experimental design is therefore to determine and control the sources of variation. An alternative to this picture is to calculate a performance statistic on a property to be optimized. It means identifying a setting of process variables that reduce the sensitivity of the process to the sources of variation rather than controlling them. This approach is called *robust design* and it has been successfully applied in many research areas, including recently in ceramic processing [44].

An application to the aqueous processing for tape casting of alumina has been developed [30]. The influence of the relative amount of slurry additives on the slurry viscosity was analysed. The slurry components used were water, dispersant (ammonium polyacrylate), ceramic powder (alumina), binder (hydroxyethyl cellulose), and plasticizer (glycerol), added in this order. In every run 180 g of slurry were made. The components were mixed in a ball mill for approximately 24 h. The viscosity of the slurries was measured at 25 °C using a rotation viscometer (Rotovisco RV20, Haake, Karlsruhe, Germany). In addition, tapes were cast on a glass plate, using a double doctor blade (0.70 mm for gate height and 60 cm min^{-1} for feeding rate).

The formulations employed, according to a so-called orthogonal array L_4 [45], are summarized in Table 5. The use of this orthogonal array makes it possible to carry out four experiments (or runs) instead of 8 for a corresponding full factorial design. The factors A, B and C correspond to weight percentages of dispersant, plasticizer and binder, respectively. Two levels for each factor were chosen: a lower and a higher weight concentration. Four runs were performed, viscosity measurements for varying shear rates were made, and the signal-to-noise ratios Z, nominal-is-best type, as defined

CosMX Exhibit 1003, Page 263 of 512

Table 5
Experimental design for aqueous tape casting slurries[a]

Run No.	Factor levels			Slurry formulation (wt.%)					Viscosity (Pa s)				Z (dB)
	A	B	C	x_M	x_D	x_P	x_B	x_L	10 s^{-1}	20 s^{-1}	40 s^{-1}	50 s^{-1}	
1	1	1	1	33.3	0.0	0.0	6.7	60.0	2.50	2.00	1.80	1.80	15.75
2	1	2	2	33.3	0.0	4.2	10.0	52.5	12.00	10.00	8.50	8.00	14.58
3	2	1	2	33.3	0.8	0.0	10.0	55.8	6.00	5.00	4.25	4.00	14.58
4	2	2	1	33.3	0.8	4.2	6.7	55.0	0.40	0.30	0.28	0.26	13.95

[a] x is the weight fraction respectively of ceramic powder (M), dispersant (D), plasticizer (P), binder (B) and solvent (L). A, B and C are the factors that correspond to x_D, x_P and x_B. Z is the signal-to-noise ratio

by Taguchi [46], were calculated. The function Z, whose unit is decibels (dB), should be always maximized to make the process insensitive to variation.

The optimum viscosity can be defined as a certain value (or range of values) to produce a stable, easy-to-flow slurry and, consequently, a uniform, easy-to-handle cast tape. To find a combination of factors that permits the achievement of this goal, two analyses of variance were performed for the viscosity measurements, respectively on average and on variation, which are shown in Tables 6 and 7. The fundamentals of this statistical analysis can be found in many works about robust design of experiments [45–48].

The analysis of variance in Table 6 identifies the statistically significant factors that affect the mean value of the slurry viscosity. The main contribution is due to the factor C, binder content (about 69%). The analysis of variance in Table 7 identifies the factors that affect the variation, calculated from the signal-to-noise ratios Z, listed in Table 5. In this case, the main contributions to the total variation are due to the factors A and B, dispersant and plasticizer contents (about 43% each one).

The robust design strategy is to select the proper levels of parameters that affect variation (to reduce the process variability) and parameters that affect the average only (to adjust the average to the target value). From Table 7 in this example, the factor levels A_1 (no dispersant) and B_1 (no plasticizer) should be selected, because they yield higher average values for Z. The decreasing values of viscosity at increasing shear rates, characteristic of a pseudoplastic fluid, can be understood as a deviation of a Newtonian fluid behaviour. A Newtonian fluid should be expected to have the same viscosity, independent of the shear rate. High values of signal-to-noise ratio Z are interpreted as a low tendency to variability for viscosity measurements. In other words, high values of Z correspond to a slurry with a more pronounced Newtonian character, which can be advantageous for modelling and controlling the tape casting slurry.

Next, from Table 6, the factor C (binder content) proved to be an excellent adjustment factor, since it does not affect the process variability (in Table 6). It can then be used to adjust the viscosity value. In fact, as shown in Fig. 11, the slurry viscosity is significantly dependent on the binder concentration. The other slurry components are responsible for the deviations of an "ideal" curve that corresponds to the aqueous solution of the binder. For the same binder concentration, increasing dispersant contents decrease the slurry viscosity when compared with the binder solution viscosity.

Since a lower binder content is desirable, sufficient to maintain a workable cast tape, the factor level C_1 (6.7 wt.% binder) should be used. In this way, the combination A_1, B_1, C_1 can be identified as the optimized formulation for this system. This combination corresponds to experiment number 1. Frequently, when fractional factorial design of experiments is used the combination found to be the best one was not carried on in any run. In such a case, a verification run using the optimized combination would be necessary to confirm the statistical analysis.

In this investigation, every run produced stable slurries, which could be cast to make tapes with reasonable workability characteristics. A remarkable fact is that even in run number 1, in which dispersant and plasticizer were not added to the system, uniform slurry and tapes were produced. This has already been observed by other investigators, as mentioned before [12,19–23]. Nevertheless, other properties of the aqueous slurry and/or of the cast tape, like density, tensile strength or elongation, can be used as a quality measurement together with the slurry viscosity. A common problem is that two or more optimized properties do not always correspond to the same combination of adjustable factors. In this case, a compromise must be found to choose the best solution.

5. Summary

The use of water-based systems represents an alternative to the widespread non-aqueous tape casting. Non-toxicity and non-inflammability seem to be especially

CosMX Exhibit 1003, Page 264 of 512

Table 6
Analysis of variance on mean viscosity of aqueous tape casting slurries[a]

Factor and level	s	m	f	S	V	F	p (%)
A_1	46.60	5.83	1	42.61	42.61	41.07[d]	19.69
A_2	20.49	2.56					
B_1	27.35	3.42	1	9.59	9.59	9.25[c]	4.05
B_2	39.74	4.97					
C_1	9.34	1.17	1	146.47	146.47	141.19[c]	68.89
C_2	57.75	7.22					
Reproducibility error			12	12.45	1.04[b]		
Pooled error			12	12.45			
Total			15	211.12			

[a]s is the sum of the measured values; m is the average of the measured values; f is the degrees of freedom; S is the sum of squares; V is the variance; F is the Fisher test-value; p is the percentage contribution to variance
[b]Pooled factor into error
[c]Significant at 95% confidence
[d]Significant at 99% confidence

Table 7
Analysis of variance on signal-to-noise ratios of viscosity of aqueous tape casting slurries[a]

Factor and level	s	m	f	S	V	F	P (%)
A_1	30.32	15.16	1	0.80	0.80	10.74	43.33
A_2	28.53	14.27					
B_1	30.32	15.16	1	0.80	0.80	10.74	43.33
B_2	28.53	14.27					
C_1	29.70	14.85	1	0.07	0.07[b]		
C_2	29.19	14.58					
Pooled error			1	0.07			
Total			3	1.68			

[a]s is the sum of the signal-to-noise ratios; m is the average of the signal-to-noise; f, S, V, F and p are defined in Table 6
[b]Pooled factor into error

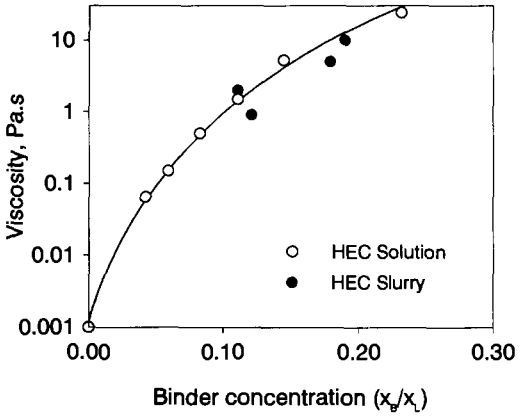


Fig. 11. Viscosity of aqueous HEC solutions and slurries at shear rate 20 s^{-1} as a function of the binder concentration [30].

advantageous. All previously reported data demonstrate, however, that many aspects of the aqueous tape casting process are yet to be understood. The use of additives has resulted from empirical observations rather than from an understanding of the physicochemical processes occurring at the particle surface and the interactions between them.

Statistically designed experiments represent a powerful tool in the improvement of ceramic processing. In aqueous tape casting, in particular, the objective of the research should be to make the product insensitive to environmental variables, product deterioration and manufacturing imperfections. This approach can be achieved by using robust design experiments.

References

[1] J.C. Williams, Doctor-blade process, in F.F.Y. Wang (ed.), *Treatise on Materials Science and Technology, Vol. 9, Ceramic Fabrication Processes*, Academic Press, New York, 1976, pp. 173–198.
[2] R.E. Mistler, D.J. Shanefield and R.B. Runk, Tape casting of ceramics, in G. Onoda Jr and L.L. Hench (eds.), *Ceramic Processing Before Firing*, Wiley, New York, 1978, pp. 411–448.
[3] E.P. Hyatt, Making thin, flat ceramics: a review, *Am. Ceram. Soc. Bull.*, *65* (4) (1986) 637–638.
[4] C. Fiori and G. de Portu, Tape casting: a technique for preparing and studying new materials, in R.W. Davidge (ed.), *Novel Ceramic Processes and Applications*, Br. Ceram. Proc., Vol. 38, The Institute of Ceramics, Stoke-on-Trent, UK, 1986, pp. 213–225.
[5] A. Roosen, Basic requirements for tape casting of ceramic powders, in G.L. Messing, E.R. Fuller and H. Hausner (eds.), *Ceramic Transactions, Vol. 1, Ceramic Powder Science II*, American Ceramic Society, Westerville OH, 1988, pp. 675–692.
[6] R.E. Mistler, Tape casting: the basis process for meeting the needs of the electronic industry, *Am. Ceram. Soc. Bull.*, *69* (6) (1990) 1022–1026.
[7] R. Moreno, The role of slip additives in tape casting technology: Part I—Solvents and dispersants, *Am. Ceram. Soc. Bull.*, *71* (10) (1992) 1521–1531.
[8] R. Moreno, The role of slip additives in tape casting technology: Part II—Binders and plasticizers, *Am. Ceram. Soc. Bull.*, *71* (11) (1992) 1647–1657.
[9] G.O. Medowski and R.D. Sutch, cited in J.C. Williams, Doctor-blade process, in F.F.Y. Wang (ed.), *Treatise on Materials Science and Technology, Vol. 9, Ceramic Fabrication Processes*, Academic Press, New York, 1976, pp. 173–198.

CosMX Exhibit 1003, Page 265 of 512

[10] M. Kemr and H. Mizuhara, Flexible Ceramic Tape and Method of Making Same, *US Patent No. 4 329 271* (1982).
[11] K. Kita, J. Fukuda, H. Ohmura and T. Sakai, Green ceramic tapes and method of producing them, *US Patent No. 4 353 958* (1982).
[12] J.E. Schuetz, I.A. Khoury and R.A. DiChiara, Water-based binder for tape casting, *Ceram. Ind.*, *66* (10) (1987) 42–44.
[13] N.R. Gurak, P.L. Josty and R.J. Thompson, Properties and uses of synthetic emulsion polymers as binders in advanced ceramics processing, *Am. Ceram. Soc. Bull.*, *66* (10) (1987) 1495–1497.
[14] S. Spauszus and P. Nobst, Das Foliengiessverfahren mit wässrig dispegierten Bindemitteln, *Silikattechinik*, *38* (8) (1987) 258–262.
[15] P. Nahass, W.E. Rhine, R.L. Pober, H.K. Bowen and W.L. Robbins, A comparison of aqueous and non-aqueous slurries for tape casting, in K.M. Nair, R. Pohanka, and R.C. Buchanan (eds.), *Ceramic Transactions, Vol. 15, Materials and Processes in Microelectronic Systems*, American Ceramic Society, Westerville OH, 1990, pp. 355–364.
[16] P. Nahass, R.L. Pober, W.E. Rhine, W.L. Robbins and H.K. Bowen, Prediction and explanation of ageing shrinkage in tape-cast ceramic green sheets, *J. Am. Ceram. Soc.*, *75* (9) (1992) 2373–2378.
[17] N. Ushifusa and M. Cima, Aqueous processing of mullite-containing green sheets, *J. Am. Ceram. Soc.*, *74* (10) (1991) 2443–2447.
[18] K.E. Burnfield and B.C. Peterson, Cellulose ethers in tape casting formulation, in M.J. Cima (ed.), *Ceramic Transactions, Vol. 26, Forming and Technology for Ceramics*, American Ceramic Society, Westerville OH, 1992, pp. 191–196.
[19] K. Nagata, Rheology and aqueous tape casting of acrylic ester–acrylic acid copolymer dispersed alumina, in S. Hirano, G.L. Messing and H. Hausner (eds.), *Ceramic Transactions, Vol. 22, Ceramic Powder Science IV*, American Ceramic Society, Westerville OH, 1991, pp. 335–340.
[20] K. Nagata, Correlation of conformation of acrylic polymers in aqueous suspensions and properties of alumina green sheets, in M.J. Cima (ed.), *Ceramic Transactions, Vol. 26, Forming and Technology for Ceramics*, American Ceramic Society, Westerville OH, 1992, pp. 205–210.
[21] K. Nagata, Rheological behaviour of suspension and properties of green sheet—effect of compatibility between dispersant and binder, *J. Ceram. Soc. Jpn.*, *101* (10) (1992) 1271–1275.
[22] K. Nagata, Dynamic viscoelastic measurements of suspension for the drying process in tape casting, *J. Ceram. Soc. Jpn.*, *100* (11) (1992) 1352–1356.
[23] K. Nagata, Effect of functionalities of binders on rheological behaviour of alumina suspensions and properties of green sheets, *J. Ceram. Soc. Jpn.*, *101* (8) (1993) 845–849.
[24] B.-H. Ryu, M. Takahashi and S. Suzuki, Rheological characteristics of aqueous alumina slurry for tape casting, *J. Ceram. Soc. Jpn.*, *101* (6) (1993) 643–648.
[25] H. Raeder, C. Simon and R. Glenne, Water-based tape casting of yttria-stabilized zirconia: influence of powder properties, presented at the conference *Ceramic Powder Science and Technology*, Friedrichshafen, Germany, 11–14 September 1994.
[26] S.M. Wolfrum and J.J. Ponjeé, Surface modification of powders with carboxylic acids, *J. Mater. Sci. Lett.*, *8* (1989) 667–669.
[27] M. Egashira, Y. Shimizu and S. Takatsuki, Chemical surface treatments of aluminium nitride powder suppressing its reactivity with water, *J. Mater. Sci. Lett.*, *10* (1991) 994–996.
[28] P. Greil, M. Kulig, D. Hotza, H. Lange and R. Tischtau, Aluminium nitride ceramics with high thermal conductivity from gas-phase synthesized powders, *J. Eur. Ceram. Soc.*, *13* (3) (1994) 229–237.
[29] D. Hotza, O. Sahling and P. Greil, Hydrophobing of aluminium nitride powders, *J. Mater. Sci.*, *30* (1995) 127–132.
[30] D. Hotza, R. Janssen, N. Claussen and P. Greil, Hydrophobing of aluminum nitride powder for aqueous tape casting, presented at the conference *Ceramic Processing Science and Technology*, Friedrichshafen, Germany, 11–14 September 1994.
[31] G.Y. Onoda Jr, The rheology of organic binder solutions, in G. Onoda Jr and L.L. Hench (eds.), *Ceramic Processing Before Firing*, Wiley, New York, 1978, pp. 235–251.
[32] C.W. Nies and G.L. Messing, Effect of glass transition temperature of polyethylene glycol-plasticized poly(vinyl alcohol) on granule compaction, *J. Am. Ceram. Soc.*, *67* (4) (1984) 301–304.
[33] T. Ueyama and N. Kaneko, Effect of agglomerated particles on properties of ceramic green sheets, in P. Vicenzini (ed.), *High Tech Ceramics*, Elsevier, Amsterdam, 1987, pp. 1451–1458.
[34] D.J. Shaw, Colloid stability, in *Colloid and Surface Chemistry*, 4th edn, Butterworth-Heinemann, Oxford, 1992, pp. 210–243.
[35] J. Cesarano III and I.A. Aksay, Processing of highly concentrated aqueous alumina suspensions stabilized with polyelectrolytes, *J. Am. Ceram. Soc.*, *71* (12) (1988) 1062–1067.
[36] A.S. Rao, Electrokinetic behaviour of commercial alumina powders in dilute dispersions, in G.L. Messing, K.S. Mazdiyasni, J.W. McCauley and R.A. Haber (eds.), *Advances in Ceramics, Vol. 21, Ceramic Powder Science*, American Ceramic Society, Westerville OH, 1987, pp. 517–523.
[37] K.R. Mikeska and W.R. Cannon, Dispersants for tape casting pure barium titanate, in J.A. Mangels and G.L. Messing (eds.), *Advances in Ceramics, Vol. 9, Forming of Ceramics*, American Ceramic Society, Columbus OH, 1983, pp. 164–183.
[38] L. Braun, J.R. Morris and W.R. Cannon, Viscosity of tape casting slips, *Am. Ceram. Soc. Bull.*, *64* (5) (1985) 727–729.
[39] W.R. Cannon, R. Becker and K.R. Mikeska, Interactions among additives used for tape casting, in M.F. Yan, K. Niwa, H.M. O'Bryan and W.S. Young (eds.), *Advances in Ceramics, Vol. 26, Ceramic Substrates and Packages for Electronic Applications*, American Ceramic Society, Westerville OH, 1989, pp. 525–541.
[40] E.P. Hyatt, Continuous tape casting for small volumes, *Am. Ceram. Soc. Bull.*, *68* (4) (1989) 869–870.
[41] M.J. Cima, J.A. Lewis and A.D. Devoe, Binder distribution in ceramic greenware during thermolysis, *J. Am. Ceram. Soc.*, *72* (7) (1989) 1192–1198.
[42] H.-W. Yan, W.R. Cannon and D.J. Shanefield, Evolution of carbon during burnout and sintering of tape-cast aluminium nitride, *J. Am. Ceram. Soc.*, *76* (1) (1993) 166–172.
[43] M.W. Weiser, D.N. Lauben, P.G. Madrid and K.B. Fong, Ceramic processing using designed partial factorial experiments, *Ceram. Eng. Sci. Proc.*, *14* (1–2) (1993) 344–359.
[44] M.W. Weiser and K.B. Fong, Applications of the Taguchi method of experimental design to improving ceramic processing, *Am. Ceram. Soc. Bull.*, *73* (1) (1994) 83–86.
[45] J. Krottmaier, Versuchsplannung—Der Weg zur Qualität des Jahres 2000, 2nd edn, Verlag Industrielle Organisation/Verlag TÜV Rheinland, Zurich/Cologne, 1991.
[46] G. Taguchi, *System of Experimental Design*, Vols. 1 and 2. UNIPUB-Kraus/ASI, New York/Dearborn MI, 1988.
[47] M.S. Phadke, *Quality Engineering Using Robust Design*, Prentice-Hall, Englewood Cliffs NJ, 1989.
[48] P.J. Ross, *Taguchi Techniques for Quality Engineering*, McGraw-Hill, New York, 1988.

CosMX Exhibit 1003, Page 266 of 512

Appendix I

J Solid State Electrochem (2011) 15:649–662
DOI 10.1007/s10008-010-1264-9

REVIEW

Separator technologies for lithium-ion batteries

Xiaosong Huang

Received: 11 October 2010 / Revised: 20 November 2010 / Accepted: 28 November 2010 / Published online: 30 December 2010
© Springer-Verlag 2010

Abstract Although separators do not participate in the electrochemical reactions in a lithium-ion (Li-ion) battery, they perform the critical functions of physically separating the positive and negative electrodes while permitting the free flow of lithium ions through the liquid electrolyte that fill in their open porous structure. Separators for liquid electrolyte Li-ion batteries can be classified into porous polymeric membranes, nonwoven mats, and composite separators. Porous membranes are most commonly used due to their relatively low processing cost and good mechanical properties. Although not widely used in Li-ion batteries, nonwoven mats have the potential for low cost and thermally stable separators. Recent composite separators have attracted much attention, however, as they offer excellent thermal stability and wettability by the nonaqueous electrolyte. The present paper (1) presents an overview of separator characterization techniques, (2) reviews existing technologies for producing different types of separators, and (3) discusses directions for future investigation. Research into separator fabrication techniques and chemical modifications, coupled with the numerical modeling, should lead to further improvements in the performance and abuse tolerance as well as cost reduction of Li-ion batteries.

Keywords Lithium-ion battery · Separator · Porous membrane · Battery abuse tolerance · Thermal runaway

Introduction

Secondary lithium-ion (Li-ion) batteries provide an attractive landscape for energy storage systems due to their high specific energy (about 150 Wh/kg), high-energy density (about 400 Wh/L), long lifetime cycle (>1,000 cycles), low self-discharge rate (2–8%/month), and high-operational voltage (2.5–4.2 V) [1]. They have been widely used in consumer electronics, such as portable computers, camcorders, and cell phones [2]. Recently, their applications have been expanding into aerospace technology, electric vehicles (EV), and hybrid-electric vehicles (HEV) [2].

Lithium-ion battery design Typically produced in either spiral wound or prismatic design, the four fundamental components of a Li-ion battery are the negative electrode (anode), the positive electrode (cathode), the electrolyte, and the separator, as shown schematically in Fig. 1. The first three components participate in the electrochemical reactions in a battery cell, while the separator is an inactive component.

Most of Li-ion batteries use carbon as the active anode material, although silicon, lithium titanate, tin dioxide, and some intermetallics have also been intensely researched [3–6]. This active material is adhered to a copper current collector with a binder, typically poly(vinylidene fluoride) (PVDF), and a high-surface-area carbon (e.g., acetylene black) is used in the electrode formulation in order to provide an electron flow path to the current collector.

Lithiated transition metal oxides have been widely used as the active materials for cathodes. Similarly to the negative electrode, the active material particles are adhered to an aluminum current collector with a binder. A high-surface-area carbon is also incorporated to provide a conductive path for the electrons to reach the active material particles.

The last active component in a Li-ion battery is the electrolyte. An electrolyte composition requires good chemical, thermal, and electrochemical stability, as well as high-ionic conductivity. Despite its known disadvantages (problematic thermal stability and susceptibility to hydrolysis with the formation of hydrofluoric acid), lithium hexafluorophosphate ($LiPF_6$) dissolved in a mixture of organic solvents represents

X. Huang (✉)
Chemical Sciences and Materials Systems Lab,
General Motors Global R&D,
30500 Mound Rd.,
Warren, MI 48090, USA
e-mail: xiaosong.huang@gm.com

CosMX Exhibit 1003, Page 268 of 512

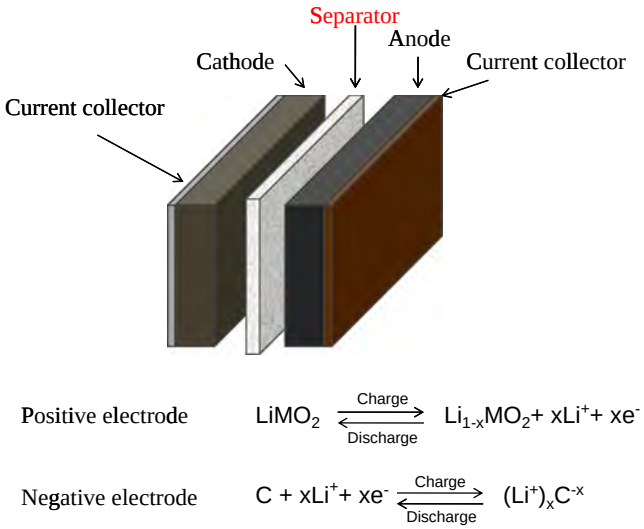


Fig. 1 Schematic of a liquid electrolyte Li-ion cell

the most widely used liquid electrolyte due to its relatively low-cost, high-ionic conductivity, and the ability of passivating the aluminum current collector for the positive electrode. Generally, the organic solvents used for dissolving $LiPF_6$ are carbonates, such as ethylene carbonate (EC), propylene carbonate (PC), dimethyl carbonate (DMC), ethyl methyl carbonate (EMC), and diethyl carbonate (DEC). During the battery operation, lithium ions (Li^+) are shuttled between the anode and cathode via the electrolyte—from the anode to the cathode during discharging and in the reverse direction during the charging of the battery.

The only inactive fundamental component of a Li-ion battery cell is the separator, necessarily sandwiched between the anode and cathode. It plays two main roles during the successful operation of a cell: (1) resting between the anode and cathode to prevent internal short circuiting and (2) providing a path for ionic conduction in the liquid electrolyte throughout the interconnected porous structure. Separators for liquid electrolyte batteries are currently engineered as porous membranes, nonwoven mats, or multilayers consisting of porous membranes and/or nonwoven mats [7, 8]. Table 1 lists the major separator manufacturers, showing that most of the commercial separators are made of porous polyolefin membranes.

Separator requirements An ideal separator should have an infinite electronic but a zero ionic resistance. In practice, the electrical resistivity of the polymers used for separators is in the order of 10^{12}–10^{14} Ω cm, i.e., they are electrical insulators. In the meantime, a low internal ionic resistance is especially important for HEV/EV applications where a battery needs to be able to offer high power. However, the existence of the separator always increases the ionic resistance of the inter-electrode medium (consisting of the separator and the liquid electrolyte) because (1) the finite porosity of a separator implies a restricted contact area between the electrolyte and the electrodes, and (2) the tortuosity of the open porous structure results in a longer mean path for the ionic current compared to when the liquid electrolyte is used alone. Generally, a thin membrane with a high porosity and a large mean pore size can minimize the ionic resistance, enabling high-specific battery power. However, too great of a porosity and a small membrane thickness can reduce the mechanical strength of the membrane and increase the risk of inner battery electrical shorting. In practice, most separators for liquid electrolyte batteries in use today are 20 to 30 μm thick, have submicron-sized pores, and possess porosity ranging from 40% to 70%.

In addition, the separator should be mechanically strong, with no skew or yield, to keep the anode and cathode from contacting each other during the whole battery lifetime. Separators also must possess dimensional stability at elevated temperatures, especially for applications in high-power batteries. Fully charged batteries have highly oxidizing and reducing environments at electrode–electrolyte interfaces, the stability of a separator in these environments is therefore critical. The specifications for a liquid electrolyte battery separator provided by the US Advanced Battery Consortium (USABC) are listed in Table 2.

Significance of separator development Despite their advantages over the alternative battery technologies, the application of large-capacity Li-ion batteries is hindered mainly due to the cost, the abuse tolerance concerns, and the loss of performance, especially at extreme operating temperatures. The further development in separator technologies will help facilitate the expansion of the application of Li-ion batteries.

Table 1 Major separator manufacturers

Manufacturer	Material	Separator design
Asahi Kasei chemicals	Polyolefin and ceramic-filled polyolefin	Biaxially orientated
Celgard LLC	PE, PP, and PP/PE/PP	Uniaxially orientated
Entek membranes	Ceramic-filled UHMWPE	Biaxially orientated
ExxonMobil/Tonen	PE and PE/PP mixtures	Biaxially orientated
SK energy	PE	Biaxially orientated
Ube industries	PP/PE/PP	Uniaxially orientated

PE polyethylene, *PP* polypropylene, *PET* poly(ethylene terephthalate), *UHMEPE* ultrahigh molecular weight polyethylene

CosMX Exhibit 1003, Page 269 of 512

Table 2 USABC requirements for Li-ion battery separators

Parameter	Goal	Test method
Sales price ($/m^2)	≤1.00	
Thickness (μm)	≤25	ASTM D5947-96, ASTM D2103
MacMullin number	≤11	N/A
Gurley (s/10 cm^3)	<35	ASTM D726
Wettability	Complete wet-out in typical battery electrolyte	N/A
Chemical stability	Stable in battery for 10 years	N/A
Pore size (μm)	<1	ASTM E128-99
Puncture strength	>300 g/25.4 μm	ASTM F1306-90
		ASTM D3763
Thermal stability	<5% shrinkage at 200 °C	ASTM D1204
Purity	<50 ppm H_2O	N/A
Tensile strength	<2% offset at 1,000 psi	ASTM D882-00
Skew (mm/m)	<2	N/A
Pin removal	Easy removal from all major brands of winding machines	N/A
Melt integrity	≥200 °C	Thermal-mechanical analysis

One of the major concerns for Li-ion batteries centers on the thermal events triggered by hard internal shorts. The cause can be traced back to the manufacturing process when defects (metal fines) are introduced into the inter-electrode space. Separators are considered to be a crucial battery component for avoiding thermal runaway conditions. Although the separators with thermal shut-down ability have been commercially available since the 1990s, they have been ineffective for preventing the hard internal shorts that originate from the manufacturing defects. Two (not necessarily incompatible) technological solutions for mitigating the internal shorting have therefore been proposed during the past several years: (1) separators exhibiting a high melting point, a low high-temperature shrinkage, and improved mechanical properties (in particular, puncture resistance) and (2) ceramic-enhanced separators, either containing ceramic layers on their surfaces or having ceramic powders dispersed in the polymeric material, where the major role of the ceramic is to prevent the collapse of the inter-electrode space and thus avoid an internal short in the event of thermal runaway conditions.

In addition, separator accounts for a large portion of the cost of a battery cell, which can exceed 20% for a high-power battery. The USABC cost target for a separator is $1/m^2 as indicated in Table 2. Research into separator fabrication techniques to develop low-cost separators is therefore critical to reduce the overall cost of the battery system.

The present paper presents an overview of separator characterization techniques, reviews existing technologies for producing different types of separators, touches upon the numerical modeling, and discusses directions for future investigation.

Separator characterization

Electrolyte resistance derating factor The incorporation of a porous separator increases the ionic resistance of the inter-electrode medium. The so-called MacMullin number (N_M), shown below in Eq. 1, is a relative value used to describe the increased resistance of the inter-electrode medium, caused by the presence of a separator, relative to the resistance of the liquid electrolyte by itself, assuming equivalent dimensions between the electrodes for each [9–11]:

$$N_M = \frac{R_s}{R_0} \tag{1}$$

where R_s is the resistance of the inter-electrode medium once a separator is sandwiched between the electrodes, and R_0 is the resistance of the liquid electrolyte.

Figure 2 is a simplified alternating current impedance spectrum (Nyquist plot), commonly used to determine the resistance. In Fig. 2, the semicircle (or overlapped semi-circles) is due to different physical electrochemical processes and the observed Warburg line in some cases can be related to the diffusion of Li^+. Ideally, N_M should be close to one, while the typical values of the N_M for Li-ion battery separators range from 5 to 15.

Besides the development of solid electrolyte interphase (SEI) on the electrode particle surface, the compatibility between the separator and the electrodes can also change the cell resistance. As indicated in Fig. 2, the total interfacial resistance (R_i or R_{SEI}) can be estimated by subtracting the bulk resistance (R_b) in the complex impedance spectrum. Jeong and Kim [12] observed that after increasing the thickness of a porous gellable poly

CosMX Exhibit 1003, Page 270 of 512

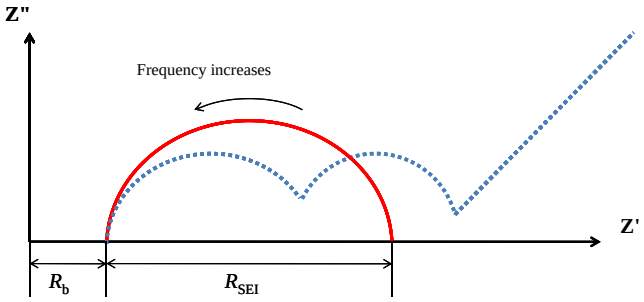


Fig. 2 Schematic of a simplified AC impedance spectrum

(acrylonitrile-*methyl* methacrylate), layered on a polyolefin separator, from 4 to 14 μm, the R_i dropped from 50.4 to 40.1 Ω cm^2. This observation in reduction was contributed to better interfacial adhesion.

Porosity, mean pore size, tortuosity, and permeability The morphology of a separator affects not only the battery performance and abuse tolerance but also the efficiency of assembling and handling of a battery through its mechanical and physical properties.

Porosity can be determined by a simple liquid absorption test according to ASTM D2873 [13], from Eq. 2,

$$P = \frac{w_T - w_s}{\rho_l \cdot V_s} \tag{2}$$

where w_s is the weight of the dry separator sample, w_T is the total weight of the separator once the liquid is fully absorbed, ρ_l is the density of the liquid, and V_s is the apparent volume of the separator sample.

Separators should have small mean pore sizes and uniform pore size distributions. Small mean pore sizes are preferred as they can effectively prevent shorts caused by dendrite growth or the migration of the active material particles between battery electrodes. Uniform pore size distributions can avoid the nonuniform current densities across the electrode-separator interfaces. A nonuniform current accelerates the formation of Li dendrites in a cell. Pore dimension and pore size distribution can be estimated from porosimetry techniques based on the Laplace equation [14] as shown below in Eq. 3:

$$d = -\frac{4\gamma \cos\theta}{\Delta P} \tag{3}$$

where d is the pore diameter, ΔP is the pressure difference across the pore, γ is the surface tension of the liquid, and θ is the contact angle. Based on this equation, different types of porometers have been developed to characterize complex porous structures as discussed in the review paper by Jena and Gupta [15]. For a more qualitative approach, cross section and surface pore morphologies can be examined simply from scanning electron microscopy images.

The tortuosity factor indicates the ratio of the mean actual path in comparison with the direct distance. Tortuosity τ [3, 16] can be estimated from Eq. 4 as shown below:

$$\tau = \sqrt{\varepsilon \frac{R_s}{R_0}} \tag{4}$$

where ε is the porosity ratio. A high tortuosity hinders the growth of Li dendrites but increases the ionic resistance of the inter-electrode medium.

The permeability is typically characterized using the Gurley number according to ASTM D726. It measures the time for a given amount of gas to flow through the membrane at a constant pressure. Clearly, the Gurley number will depend on the porosity, the fraction of open pores, and the tortuosity of a separator. The permeability can also be evaluated from the permeability coefficient B according to Darcy's law, from Eq. 5 shown below. Here, l is the sample thickness, μ is the fluid viscosity, v is the fluid velocity, and ΔP is the pressure drop across the separator [17].

$$B = \frac{l\mu v}{\Delta P} \tag{5}$$

Wettability The separator should quickly absorb and retain the electrolyte during operation. Poor wettability limits the performance of a cell by increasing the internal ionic resistance. Good wettability shortens the electrolyte filling time during the cell assembly and extends the battery's life cycle under normal operating conditions. There is no standard method for the wettability test although measuring the contact angle between the liquid electrolyte and the separator is a simple indicator. An alternative method to determine wettability is by hanging a separator vertically in a liquid electrolyte and calculating the wicking (capillary rise) rate or height.

Thermal behavior Most commercial separators provide thermal shutdown (fuse) capability at various temperatures. Upon reaching a certain temperature, the separator can flow and fuse into a film by pore collapsing, thus, minimizing the ionic conduction between the electrodes and protecting batteries from overheating or electrical shorting. Thermal shutdown must start before the occurrence of the uncontrollable thermal runaway and can be evaluated by measuring the resistance as the temperature increases. Venugopal et al. [13] tested different membranes, as shown in Fig. 3, where a polypropylene (PP) membrane exhibited shutdown at around 165 °C and the resistance increased approximately by two orders of magnitude; a polyethylene (PE) separator showed shutdown at around 135 °C and the electrical resistance increased by about three orders of magnitude. It was reported that at least a three order of magnitude

CosMX Exhibit 1003, Page 271 of 512

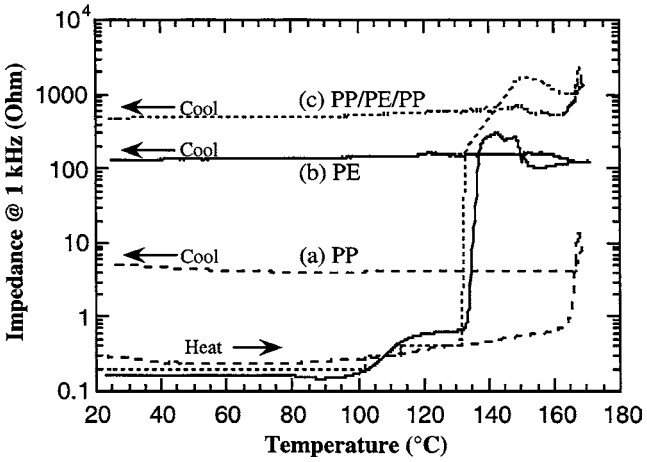


Fig. 3 Separator thermal shutdown [13]

increase in the electrical resistance was required to effectively shut down the reactions.

A separator must also prevent the electrodes from contacting one another at high temperatures. Therefore, its shrinkage at an elevated temperature needs to be minimized. Thermal-mechanical analysis can be used to characterize the high-temperature shrinkage of a separator. The separator is held under a constant load while simultaneously recording the elongation and temperature change. Porous separators that are either uniaxially or biaxially stretched usually have a large shrinkage in the stretched direction, while ceramic separators can offer high-dimensional stability at elevated temperatures.

Mechanical properties A certain mechanical strength is required for separator handling, battery assembly, and abuse tolerance consideration. The most important mechanical properties are the tensile strength and puncture strength. Tensile properties are measured by the conventional stretching process according to ASTM D882. The strength is strongly influenced by the post-extrusion stretching. Porous membranes usually show a high tensile strength in the stretched direction. The puncture strength is the load required for a needle to puncture a separator and can be tested according to ASTM F1306. The USABC puncture strength target is 300 g/25.4 μm, as indicated in Table 2. High puncture strength helps to deter dendrites or particles from penetrating the battery separators.

Polymeric porous membranes

Manufacturing processes The most widely used processes for producing porous polymeric membranes for liquid electrolyte Li-ion batteries are the dry and wet processes. Both processes are conducted through an extruder and employ stretching in one or two directions to impart/increase the porosity and improve the tensile strength. Both processes use low-cost polyolefin materials, and thus the majority of the separator cost is due to manufacturing methodologies.

In the dry process, the melt-extruded polyolefin films are annealed at an elevated temperature immediately below the polymer melting temperature to induce crystallite formation and/or to increase the size and amount of crystallites. The well-aligned crystallites have lamellae arranged in rows, perpendicular to the machine direction. Uniaxial stretching at a low temperature and a subsequent high temperature is followed. The stretching of about 150–250% in the machine direction can be achieved by utilizing nip rolls with different circumferential rates. The porous structure is formed in this step due to the fracturing of the amours phase or tearing apart of the lamellar crystallites. Heat treatment is then followed to fix the pores and relax the residual stress in the membrane. Porous membranes produced through this dry process usually show characteristic slit-like pore structures, as shown in Fig. 4a [7]. It is obvious that nanosized fibrils connect adjacent crystalline regions. The stretching ratio, speed, temperature, and other processing parameters dictate the membrane morphology. US patents 4994335, 4138459, 3801404, and 3843761 have described this process in detail. Generally speaking, a uniaxially stretched membrane exhibits good mechanical properties (>150-MPa tensile strength) but a high thermal shrinkage in the machine direction, while a low tensile strength (<15 MPa) but a negligible thermal shrinkage in the transverse direction. Dry process requires no use of solvents. However, this type of process is only applicable to polymers that can form semicrystalline structures.

In the wet process, plasticizers (or low molecular weight substances, e.g., paraffin oil and mineral oil) are added into the polymer before it is extruded or blown into a thin film at an elevated temperature. The extruded film is then calendared until a desired thickness is achieved. After solidification, the plasticizer is extracted from the film with a volatile solvent (e.g., methylene chloride and trichloroethylene) to leave submicron-sized pores. The porous membrane then passes through a solvent extractor to remove the solvent in it after it leaves the oil extraction tank. The separators fabricated through this wet process are generally stretched biaxially to enlarge the pore size and increase the porosity. Therefore, the pores are more round-like as indicated in Fig. 4b [7]. Tensile strengths in the machine and transverse directions are comparable and can both exceed 100 MPa. Compared with the dry process, this wet process can be applied on a wider range of polymers since there is no requirement on the formation of a semicrystalline structure before stretching. In addition, the application of plasticizers reduces the viscosity, thus,

CosMX Exhibit 1003, Page 272 of 512

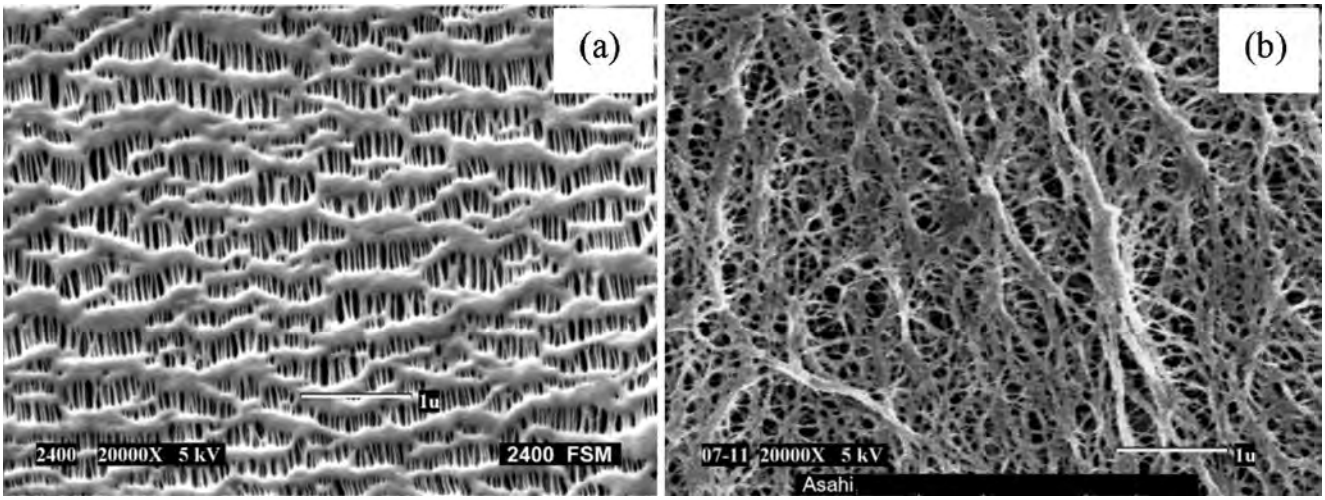


Fig. 4 Separators fabricated by the dry (**a**) and the wet (**b**) processes [7]

improving the polymer processability. However, the plasticizer extraction in this wet process adds cost to the membrane production. This step needs to be designed to prevent an undesired release of solvent from the system.

Parameters such as dope composition, quenching temperature, stretching rate, and film thickness can all influence the membrane morphology. Kim and Kim [18] investigated the pore size control by generating a phase diagram. Membranes were fabricated with PE/dioctyl phthalate (DOP), PE/isoparaffin, and PE/DOP/isoparaffin, respectively. The average pore size varied from 0.07 to 0.5 μm depending mainly on the temperature gap between the phase separation and PE crystallization. Ma et al. [19] have shown that stretching before plasticizer extraction can produce membranes with a smaller mean pore size and a narrower pore size distribution compared with stretching after the extraction. Fillers can also be used to change the morphology and improve the mechanical and thermal performance of a membrane [20, 21]. Yoneda et al. [20] investigated the phase separation behavior of a three-component system consisting of PE, nanosilica powder, and a solvent (or plasticizer). They reported that the addition of silica resulted in a greater mean pore size.

Besides the dry and wet processes, there are a couple of other techniques that have been studied to produce porous membranes for Li-ion battery applications. Phase inversion is a well-known technique to prepare porous membranes [22–28]. A polymer solution is cast into a thin film and then soaked in a nonsolvent coagulation bath. Since the solvent and nonsolvent are miscible, a rapid diffusion rate of the nonsolvent and solvent causes phase separation to take place, forming a solid-like polymer rich phase and a liquid-like polymer lean phase. In the case when the polymer rich phase is a continuous phase, a porous membrane can be formed when the polymer lean phase is replaced by the nonsolvent after a further solvent/nonsolvent exchange. The parameters that can change the membrane morphology include but are not limited to solvent, nonsolvent, composition of the polymer solution, and coagulation temperature. Zhang et al. [29] used acetonitrile as a solvent and water as a nonsolvent to fabricate a porous membrane of poly (vinylidene fluoride-co-hexafluoropropylene) (PVDF-HFP) by this phase-inversion process. They observed different morphologies on the two sides of the porous membrane as one side of the cast solution film had been in contact with a solid substrate while the other side had been exposed to the nonsolvent. Andrieu and Laurence [30] cast a PVDF solution directly onto a negative electrode and, by immersing the negative electrode in water, a porous separator membrane with a porosity of 75% was formed.

The evaporation-induced phase separation is very similar to the abovementioned phase-inversion process. It takes the advantage of the differential evaporation rates of the solvent and the nonsolvent to form a porous structure. A composition consisting of a polymer, a volatile polymer solvent, and a less volatile nonsolvent can be cast into a thin film. The solvent and the nonsolvent ideally should be completely miscible. With the evaporation of the solvent, the film solidifies and the nonsolvent is homogeneously dispersed in the matrix. The subsequent removal of the nonsolvent yields a porous structure. Similarly, solvent, nonsolvent, polymer concentration, polymer solubility, etc. can all change the membrane morphology. It has also been reported that fine fillers can be added to the polymer solution to maintain the porous structure and provide structural strength to the produced membrane [31–33].

Polymers for the fabrication of porous separators Most of the commercially available Li-ion battery separators are made of PE, PP, other polyolefins, or their mixtures, or copolymers through either a dry or wet process. Polyolefin usually provides good mechanical properties and chemical

CosMX Exhibit 1003, Page 273 of 512

stability. Most of the polyolefin separators can also provide thermal shutdown capability at various temperatures by closing the pores and turning the membrane into a nonporous film. The thermal shutdown temperature of a PP membrane is around 160 °C, while the thermal shutdown temperature of PE is between 120 and 150 °C, depending upon its morphology. Ultrahigh molecular weight PE (UHMWPE) has good melt integrity and sufficient polymer flow to cause pore collapse, thereby providing better thermal shutdown through the formation of a nonporous film.

Although polyolefin materials can provide thermal shutdown at an appropriate temperature range, the temperature in a cell may continue to increase after the pores are closed. It is possible that the separator would shrink, melt, and finally lead to the shorting of the electrodes. Therefore, to ensure good abuse tolerance, the difference between the shutdown temperature and the melting temperature should be as large as possible. Coextrusion or lamination of PP and PE to produce multilayer membranes has been used for this purpose. PP/PE bilayer separators and PP/PE/PP trilayer separators have been developed [34, 35]. The PE layer transforms into a nonporous film at a temperature lower than the thermal runway temperature, which increases the electrical resistance and provides thermal shutdown. In the meantime, the PP layers still maintain mechanical integrity and keep the electrodes separated.

Instead of lamination, Higuchi et al. [36] patented a battery separator made of a blend of PE and PP. The separator was produced by a dry process. Since PP and PE are not completely miscible, the separator showed porous regions of PE and PP. The separator provided the thermal shutdown ability at a temperature close to the melting point of PE. PP maintained the mechanical integrity of the separator up to its melting temperature.

Ihm et al. [37] made separators using the blends of a high-density polyethylene (HDPE) and an UHMWPE by a wet process. They concluded that the mechanical strength of the membranes increased with the molecular weight of UHMWPE and its content in the blends. The film consisting of 6 wt.% UHMWPE at a draw ratio of 5 showed a tensile strength of about 100 MPa. Although the tensile strength increased with the draw ratio, the puncture strength decreased. The pore size was very uniform and most of the pores arranged in size from 0.10 to 0.12 μm.

Nitto Denko Co. developed a UHMWPE separator having a crosslinked structure. UHMWPE resin blended with a crosslinkable rubber was made into a porous membrane by a wet process [38, 39]. The porous membrane was then crosslinked by air oxidation. The final structure showed high puncture strength and heat rupture resistance.

Johnson and Wilkes [40] prepared porous membranes made of an isotactic poly(4-methyl-1-pentene) (PMP) using a dry process. Compared with PP and PE, PMP has a higher melting temperature of about 235 °C. The PMP precursor film produced by a tubular extrusion process (dry process) showed a semicrystalline structure with planar-stacked lamellae. The stacked lamellar morphology and the orientation state of the membranes heavily relied on the extrusion stress and the weight-average molecular weight (M_w) of PMP. The evaluation of this type of membranes as battery separators was not presented.

Porous power technologies fabricated PVDF separators using the evaporation-induced phase separation process [41]. Acetone and water were used as the solvent and nonsolvent, respectively. The separator showed a high porosity of about 80%, and the batteries with this porous PVDF separator exhibited reduced internal resistance. However, investigations on the abuse tolerance (i.e., tolerance of short) of this type of separators need to be conducted as PVDF losses its mechanical strength in liquid electrolytes, especially when the temperature is high.

Attempts have been made to improve the battery abuse tolerance through increasing the thermal stability of the separator by using high-temperature polymers (such as polyamide and polyimide). These activities mostly remain in the research stage and the membranes are mainly being prepared using the phase-inversion approach. A paraoriented polyamide porous film comprising of fibrils having a diameter less than 1 μm has been fabricated [42]. The polyamide solution was first cast into a film and then cooled to deposit the polyamide. Next, the film was immersed in an aqueous or alcoholic solution to elute the solvent. The dry porous film exhibited good mechanical properties and a porosity ranging from 38% to 87% with good uniformity. Due to the thermal stability of the aromatic polyamide, its linear thermal expansion coefficient between 200 and 300 °C was about 50×10^{-6}/°C. However, its performance in a liquid electrolyte was not discussed.

UBE Industries, Ltd. has developed polyimide separators [43]. The polyimide precursor was a polyamic acid prepared by polymerizing a tetracarboxylic acid and a diamine. A porous precursor film was fabricated through the phase-inversion method by casting the polyamic acid solution, forming a liquid film comprising of a mixture of a solvent and a nonsolvent on a glass substrate, and immersing the cast film into a coagulating solution composed of the solvent and the nonsolvent. The precursor film was then dried and imidized into a polyimide porous film. The resulting polyimide separator showed relatively uniform pore size distribution. Although the membrane had no thermal shutdown ability, it offered excellent thermal stability.

Overcharge protection has also been investigated through the separator design [44–47]. Xiao et al. [44] prepared a composite membrane comprised of *p*-poly-

CosMX Exhibit 1003, Page 274 of 512

phenyl (PPP) and polyaniline (PAn) layers. The separator was *p*-doped at high-oxidation potentials into a conductive phase to shunt the current and returns to the de-doped isolating state at normal operating voltages. The PPP/PAn composite separator was evaluated in a Li/$LiMn_2O_4$ cell. When cycled between 3.6 and 4.3 V at 25 mA/g, the composite separator showed behaviors similar to a commercial PP porous membrane. However, upon overcharging, the voltage of the cell with the PP separator rose to 4.8 V in 8 min, while the voltage of the cell containing the composite separator showed a steady plateau at 4.31 V. Chen and Richardson [45] impregnated a PP porous separator with an electrochemically active poly(3-butylthiophene) for overcharge protection. TiS_2, Li, and 1 M $LiPF_6$ in PC/EC (1:1 by volume) were used as the cathode, the anode, and the electrolyte, respectively. When charged at a C/10 rate to a limit of 4 V, the discharge capacity of the cell with a regular PP separator degraded rapidly due to the degradation of the cathode. The cell with the poly(3-butylthiophene) impregnated separator was undamaged by overcharging up to ten times the normal capacity, since poly(3-butylthiophene) shunted the excess charge and limited the potential to about 3.2 V. However, at 1 °C rate overcharging, the overcharge protection was not achieved. Feng et al. [46] used an electroactive polytriphenylamine as the separator material. Upon testing Li/$LiFePO_4$ cells, the experimental results demonstrated that the electroactive separator produced a resistive internal short circuit to maintain the cell voltage near 3.75 V at overcharge. However, for this type of separator, the major barriers to practical applications are the battery self-discharge and the effectiveness of the overcharge protection, especially at a charge rate.

Separator modification Pristine polyolefin membranes lack sufficient compatibility with the electrodes and carbonate solvents. However, good surface contact between separators and electrodes is critical since a poor interface can cause an uneven current distribution resulting in the formation of Li dendrites and increase the battery internal resistance deteriorating the battery performance.

The modification of membranes has then been conducted to optimize the performance of the separator and the overall battery system. Grafting polymerization can attach functional groups on the membrane surface through covalent bonding so as to change the separator surface polarity permanently. Ko et al. [48] used an electron beam to attach glycidyl methacrylate on the surface of a porous PE separator. They attributed the improved life cycle of the mesocarbon microbeads/$LiCoO_2$ cell to an enhanced electrolyte holding capability and a reduced interfacial resistance. Similarly, Gao et al. [49] grafted methylmethacrylate on polyolefin separators by an electron-beam-induced polymerization; Gineste and Pourcelly [50] modified a PP membrane with acrylic acid (AA) and diethyleneglycol-dimethacrylate by electron beam irradiation; Yao and Ranby [51] developed a continuous process for the modification of polyolefin separators with AA through an ultraviolet irradiation for alkaline batteries; and Urairi et al. [52] treated polyolefin separators with plasma to improve their hydrophilicity for alkaline battery application.

Porous polyolefin membranes have also been laminated with gellable polymer films to improve their compatibility with the electrolyte and electrodes. A separator comprising of a porous polyolefin base and a porous PVDF layer on at least one surface of the base material was proposed [19, 53]. The presence of PVDF provided improved electrolyte retention and bondability to the electrodes. Polyolefin separators have also been laminated with a porous gellable poly(acrylonitrile-methyl methacrylate) layer by dipping the separator in the copolymer solution [12]. The base PE membrane was 25 μm thick, and the coated separator had a total thickness of 30–45 μm. The authors attributed the good capacity retention and rate performance to the strong bonding between the separator and the electrodes. Kim et al. [54] further incorporated ceramic particles into a gellable polymer coating by pasting a 2–3-μm thick layer of gellable polymer containing SiO_2 particles on both sides of a base separator membrane. The addition of silica particles showed improved wettability and enabled increased ionic conduction.

Other types of separators

Nonwoven mats/webs Although nonwoven mats/webs have long been used as separators for different batteries, they have very limited applications in Li-ion secondary batteries nowadays. Nonwoven mat separators have certain advantages such as low processing cost, high porosity, and lightweight. In addition, mats with different organic and inorganic fibers can be conveniently fabricated to provide high heat resistance and good mechanical properties. However, nonwoven mat separators typically have a large pore size, so to prevent dendrites from growing through the pores, their thickness must be increased. The recent technology has made the fabrication of nanofiber nonwoven mats feasible. Thin nonwoven separators can thus be produced with nanofibers, which provide the potential for Li-ion battery applications. A nonwoven mat is usually produced through a dry laid process, a wet-laid process, a melt-blown process, or an electrospinning process. These processes allow fiber adhesion by sprayed resin bonding, thermoplastic fiber bonding, fiber self bonding, or mechanical bonding.

The air-laid process is a dry process where individualized staple fibers are air conveyed onto a moving belt to form a mat. A latex binder is applied at the same time to incorporate

CosMX Exhibit 1003, Page 275 of 512

the mechanical integrity. The formed mat can also be thermally bonded through a calendaring process.

The wet-laid process can be conducted on a papermaking machine. Fibers are first suspended in water. Paper machines are used to separate water to form a uniform web, which is then bonded and dried to achieve mechanical integrity. Kritzer [55] fabricated a polyester mat using this wet-laid process. Polyester fibers together with binder fibers were suspended in water and randomly laid on a screen belt. The nonwoven mat, formed by drying the fiber suspension, was thermally bonded at 230 °C. The electrochemically and thermally stable nonwoven mat showed an average pore size of 20–30 μm and a porosity of 55–65%. Pinholes were not observed due to the labyrinth-like structure of the nonwoven material, yet, because of the large mean pore size, this nonwoven mat was not used as a separator directly, but as a support layer for battery separators. Ashida and Tsukuda [56] disclosed the fabrication of a nonwoven mat made by blending organic and up to 80 wt.% ceramic fibers through this wet-laid process showing improved heat resistance. Organic fibers such as polyolefin and polyamide fibers were used to improve formability and increase strength. The separator showed good adhesion to the electrodes, displaying no signs of slippage or gaps between the separator and the electrodes, during the fabrication of the battery. Wang et al. [57] prepared a wet-laid nonwoven separator using fibrillated aromatic polyamide fibers observing, thereafter, an improved permeability and electrolyte absorption rate compared with a conventional polyolefin separator. Capillary porometer tests showed the average pore sizes of the two mats prepared were as small as 0.180 and 0.372 μm, respectively. It should be noted that a capillary porometer measures the smallest pore constraints.

Melt-blown mats are formed by extruding molten polymers through a die and then attenuating the resulting filaments with a high-velocity air to fine diameters. This is a promising low-cost process to fabricate thermally stable thin membranes suitable for battery separator applications. The preparation of thin but strong separators made of polyester, polyamide, and polymethylpentene and its copolymers through this process has been suggested [58–60]. Mats consisting of a fibrous sheet of polymethylpentene showed a high-temperature shutdown characteristic, and those consisting of high temperature polymers such as polyester and polyamide exhibited excellent dimensional stability at elevated temperatures.

Electrospinning/electrospraying is another attractive method for preparing nonwoven mats, especially those composed of nanofibers. The electrospinning/electrospraying process is conducted by applying a strong electric field to a polymer solution and collecting a fine-charged jet from a small orifice on a grounded collector. The mat morphology is affected by the solvent evaporation rate, the polymer concentration, the distance from the nozzle tip to the target, the accelerating voltage, etc. The fibers fabricated through this process can be submicron or nanometer sized. Thus, electrospun mats can have much smaller thickness compared with those fabricated by other mat-forming processes. Due to the challenges of designing high-throughput electrojetting processes, investigation continues to be exploratory and no commercial battery separators are currently available. Porous membranes composed of submicron fibers made of polyimide [61], polyacrylonitrile (PAN) [62], and PVDF [63, 64] have been investigated. Bansal et al. [61] prepared a polyether imide nanofiber web through electrospinning. Polyimide and the blends of polyimide and PAN/PVDF-HFP were spun into mats with 65–85% porosity. However, the effect of liquid electrolytes on the properties of these mats was not discussed and their performance in a real battery was not systematically investigated. Cho et al. [62] prepared porous PAN separators using the electrospinning process. The fibers had a homogeneous diameter of 250–380 nm. Compared with the conventional porous separators, PAN nonwoven mats showed better cycling performance and rate capability at room temperature. Kim et al. [63] was able to control the pore size and porosity PVDF-HFP porous membranes by electrospinning the copolymer solutions of distinct polymer concentration. The electrospun polymer separators enabled good ionic conduction at room temperature and a wide electrochemical stability window of up to 4.5 V vs. Li^+/Li when 1 M $LiPF_6$ in EC/DMC/DEC (1/1/1 by weight) was used as the electrolyte.

In another effort, electrospinning was modified into an electroblowing process by simultaneously applying electrical force and an air shearing force [65–69]. An air-blowing system, with flow and temperature control, delivered a high-velocity air around the spinneret along the fiber spinning direction. This process resulted in higher efficiency and yield-combining characteristics of electrospinning and melt-blowing processes [65].

Currently, nonwoven mats are mainly used as a support layer for separators. Patent application WO06123811 disclosed a separator for Li-ion batteries produced by coating a nonwoven mat with porous aromatic polyamide layers on both sides [70]. The poly(ethylene terephthalate) (PET) nonwoven mat with a thickness less than 30 μm was fabricated through the wet-laid process and the polyamide coating was applied through the phase-inversion method. The separators showed high heat resistance, and no shrinkage was observed when tested at 150 °C for 2 h. Lee et al. [71, 72] coated a porous PVDF layer on the surface of a PE nonwoven mat of 20 μm thick. The PVDF coating was applied by casting a solution of PVDF in *N*-methylpyrrolidone on the PE mat and then, by the phase-

CosMX Exhibit 1003, Page 276 of 512

inversion method, converted to a 33-μm thick porous structure. The authors reported that these separators displayed sufficient mechanical properties and improved capacity retention in Li-ion cells. Pekala and Khavari [73] passed a ~18-μm thick porous UHMWPE nonwoven mat through a hot PVDF solution bath impregnating the polymer into the mat. The time required to achieve a uniform electrolyte distribution throughout the battery was reduced with this PVDF-coated mat due to increased compatibility with the battery system.

Ceramic coatings have also been applied on nonwoven mats for improved thermal performance. This topic is covered in the following section.

Composite/ceramic-enhanced separators As mentioned earlier, to improve the battery abuse tolerance, Li-ion battery separators with high thermal stability are needed, especially for applications in EVs or HEVs. This can be achieved either by using high melting temperature polymers, such as polyamide and polyimide (as described in the previous sections), or by incorporating inorganic fillers into the porous or nonwoven membranes. The latter are called composite or ceramic-enhanced separators. In general, composite separators have excellent wettability by the nonaqueous electrolyte solvents, even when the temperature is low. These separators also show excellent thermal stability, which is critical to ensure satisfactory battery abuse tolerance at high temperatures. In addition, inorganic ceramic particles have relatively high thermal conductivity, thus, dissipating heat at a fast rate. Due to the above-mentioned advantages, composite separators have attracted increasing attention recently. However, although composite separators generally offer high punch strength, their tensile strength is usually lower compared with the plain polymeric separators. Other potential issues related to ceramic-enhanced separators are increased separator weight due to the incorporation of heavy ceramic particles, unknown electrochemical stability of the ceramic and the ceramic binder in the highly oxidizing and reducing environments encountered in Li-ion batteries, and particle shedding due to the insufficient binding.

Composite separators can be produced by binding micron or submicron ceramic particles with polymeric binders. Zhang et al. [74] prepared a freestanding and flexible porous membrane by using $CaCO_3$ particles as the main component and 2–8 wt.% of polytetrafluoroethylene (PTFE) as the binder. The process for producing the membrane involved dispersing 10 μm $CaCO_3$ particles in a PTFE dispersion, casting and hot rolling the dispersion into a flexible membrane with a thickness of 175–190 μm, and drying the membrane at 120 °C under vacuum. However, to reduce the membrane thickness for realistic applications, smaller particles will need to be used. The authors evaluated the membrane with a $CaCO_3$/PTFE weight ratio of 92/8 by soaking it in a liquid electrolyte of 1 M $LiPF_6$ in a mixture of EC and EMC (3:7 by weight). The "effective ionic conductivity" of the electrolyte wetted membrane was 2.4 mS/cm at 20 °C as compared with 8.0 mS/cm for the virgin liquid electrolyte. However, the compatibility of the filler with the battery components, especially the liquid electrolyte, needs to be investigated.

Cho et al. [75] fabricated a ceramic separator by casting PE–PP sheath-core composite fibers (a fiber diameter of 2 μm) with nanosized silica particles using an air-laid process. The formed webs were thermally bonded in an oven. The cell was assembled using $LiCoO_2$ as the cathode, graphite as the anode, and 1 M $LiPF_6$ in EC/DEC (1/1 by volume) as the electrolyte. The composite separator showed improved wettability and better performance than neat polyolefin-based membranes when cycled in the voltage range of 3.0–4.2 V at a C/2 rate. The composite membrane was thermally stable, and its shrinkage at 150 °C was only 3%, as compared with the 37% shrinkage for a conventional PP separator. The authors also claimed that in order to suppress the microshorting caused by the Li dendrite growth, the Gurley number for this type of separators must be higher than 200 s/100 cm^3.

Lamination by coating a supporting porous polyolefin or nonwoven structure with a layer of inorganic particles has also been used to fabricate freestanding ceramic-enhanced separators. Shinohara et al. [76] fabricated a heat-resistant membrane by coating a mat or porous film with a dispersion of ceramic particles in a heat-resistant aromatic polymer solution of either a polyamide or a polyimide. The prepared laminate membranes typically showed a porosity of about 45% and a tensile strength of above 45 MPa.

Evonik–Degussa commercialized a ceramic separator by coating an ultrathin PET nonwoven support layer with oxides including alumina, zirconia, and silica, as shown in Fig. 5 [8, 77–79]. Oxide particles were first suspended in an inorganic binder sol that was prepared by hydrolyzing a mixture of tetraethoxysilane, methyltriethoxysilane, and (3-glycidyloxypropyl) trimethoxysilane in the presence of a HCl aqueous solution. The suspension was then coated on a nonwoven PET mat. A composite separator was obtained by drying the coated PET at 200 °C. The obtained separator had a small average pore size of 0.08 μm and a thickness of about 24 μm. For this type of separators, the PET nonwoven of about 20 μm thick provides the tensile strength and flexibility, while the fine ceramic particle coating helps avoid pinholes while providing dendrite penetration resistance and thermal stability.

LG Chem also developed ceramic-enhanced separators [80–83]. The separator was produced by coating a porous substrate (typically a polyolefin porous film) with a porous layer formed by casting a slurry of inorganic particles and a

CosMX Exhibit 1003, Page 277 of 512

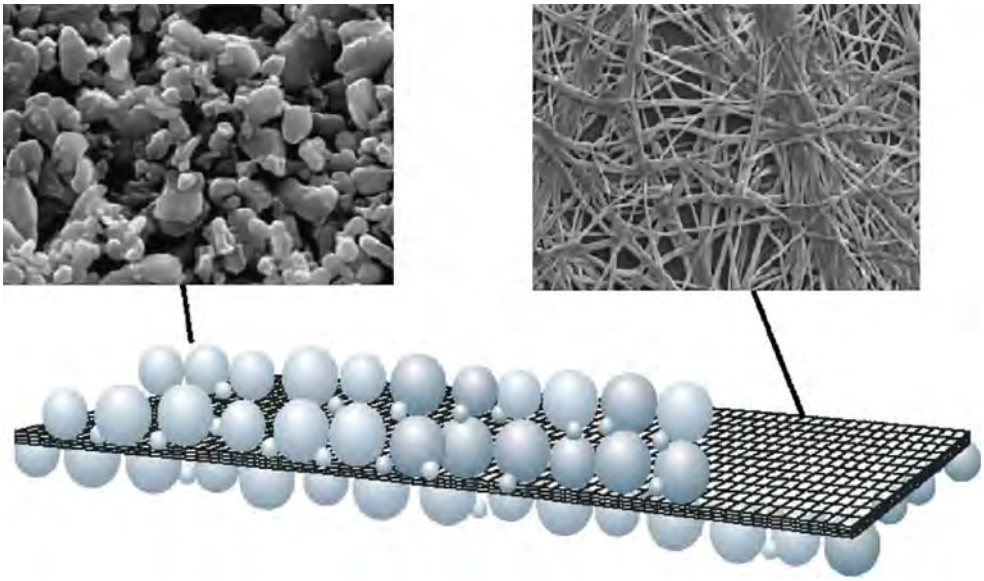


Fig. 5 Schematic of an Evonik–Degussa ceramic separator [8, 77]

polymeric binder. The membrane with a PE support and a $BaTiO_3$/butylacrylate-acrylic acid copolymer-coating layer showed less than 10% shrinkage at 150 °C for 1 h.

Hitachi Maxell Ltd. has reported the development of a thermally stable separator made by coating a polyolefin porous film with metal oxide flakes [84]. The coated separator exhibited a shrinkage of less than 5% even at 180 °C.

In addition, composite separators have been fabricated simply by adding ceramic particles into the material formulations for making separators using the wet process. Sony Corporation developed a separator composed of HDPE and fine alumina particles [85]. A mixture of PE resin, alumina particles and/or inorganic fibers, and mineral oil was kneaded into a sheet at the melting point of the polyolefin resin. A porous membrane was formed through the extraction of the mineral oils.

Besides the applications in porous separators for liquid electrolyte batteries, ceramic powders have also been used in a gel polymer electrolyte (gel polymer separator). The effects of SiO_2 [86], Al_2O_3 [87], TiO_2 [88], and MgO [89] on the electrochemical properties of gellable-polymer-based electrolytes have been studied. It has been shown that the incorporation of ceramic powder enhances the ionic conductivity, improves the mechanical and thermal stability, and provides high chemical integrity (no liquid leakage) even at elevated temperatures. The improvement has been attributed to the change of the molecular morphologies and physical properties of the polymers due to the addition of the inorganic particles. Abraham et al. [90] prepared a ceramic-PVDF electrolyte separator and Hikmet [91] obtained a porous $Li_{0.35}La_{0.55}TiO_3$-UHMWPE separator. However, they stated that addition of the ceramic particles did not significantly change the conductance.

Composite separator layers have also been coated on an electrode directly to reduce the production cost. Less et al. [92] applied separator coating on an electrode by spraying a dispersion of fumed silica in a PVDF solution. When the silica/PVDF weight ratio was 65/35, the separator coating showed a N_M similar to a commercial polyolefin separator. Kim et al. [93] formed composite separators by a dip-coating approach. The nanoalumina loading in the ceramic-coating layer was up to 94 wt.% with the rest being a PVDF binder. The cell with this separator coating showed enhanced rate performance when compared with a cell with a conventional separator.

Numerical modeling of Li-ion cells/separators

Since the porous separators have very complex pore structures, a simplified analysis has been employed to evaluate the effect of separators in practice [94, 95]. The following empirical equation (Eq. 6) has been used extensively in mathematical modeling.

$$R_s = \varepsilon^{-\alpha} \cdot R_0 \tag{6}$$

where R_s is the resistance of the separators filled with the liquid electrolyte, R_0 is the resistance of the native liquid electrolyte, ε is the void volume fraction in a separator, and α is the Bruggeman exponent. However, Patel et al. [11] found that only porous membranes with idealized morphologies (spherical or slightly prolate ellipsoids) followed the Bruggeman law with an α of about 1.3. Porous networks based on other particle morphologies resulted in either a significant increase in α, or a complete deviation from the power law, mainly due to the increased tortuosity. The models indicated that spherical or slightly prolate ellipsoidal pores should be preferred for batteries where a high-rate performance is required.

CosMX Exhibit 1003, Page 278 of 512

Thorat et al. [96] developed an empirical relationship between porosity and the tortuosity of the porous structures. Their results demonstrated that the tortuosity-dependent mass transport resistance in porous separators and electrodes was significantly higher than predicted by the frequently used Bruggeman relationship. Tye [16] investigated the effect of tortuosity on the electrolyte diffusion ingress response of a separator. He showed that separators with identical average tortuosities and porosities could have different unsteady-state behaviors due to the difference in tortuosity distributions. Newman and Srinivasan [97] studied the performance of a natural graphite/$LiPF_6$ in a mixture of EC and DEC/iron phosphate lithium-ion cell. They built a model to optimize the porosity and thickness of the positive electrode, the thickness and porosity of the separator, the electrolyte concentration, and the porosity of the negative electrode. Xiao et al. [98] attempted to evaluate the stress field in a separator during normal battery cycling. The current industrial requirement on the separator tensile property comes from the battery assembly demands. The stress distribution in a separator when the battery is under normal cycling conditions is not well understood. This work has indicated that the stress is affected by the active material properties, electrode geometries, separator wrapping patterns, charging–discharging protocols, etc.

Future work

In the light of the above discussion, the goals of the future research will be to (1) develop low-cost fabrication processes, (2) discover new materials with high thermal stability, (3) further understand the behavior of separators during the operation of the battery, and (4) extend the functions of the separator in a battery in order to improve the battery performance under all operating conditions expected in the automotive usage. Abuse tolerance and cost are especially important for large-scale applications in HEV/EV and should drive all these research directions.

The modification of commonly used polyolefin microporous separators can lead to improved separator performance. The modification can be achieved by coating and chemical crosslinking. Ceramic separators have shown excellent thermal stability and electrolyte wettability. Increasing numbers of ceramic separators have been commercialized to meet the abuse tolerance and performance requirements for HEV/EV applications. Development of modern processes, from an interdisciplinary approach, may lower the production costs. Nonwoven mats of nanosized fibers have the potential to be used as low-cost separators with good thermal stability and should be developed for battery applications. Numerical modeling should assist the design of separators for improved battery abuse tolerance and performance. Effort in this area is still needed in order to further optimize the separator performance in future battery systems.

Conclusions

Semicrystalline polyolefin-based microporous separators have dominated the Li-ion separators market. They have small thickness, excellent chemical resistance, and good mechanical properties. However, polyolefin separators generally are not thermally stable. They shrink significantly at 90–120 °C and melt at 150–200 °C depending on the type of the polymers. Ceramic-enhanced composite separators exhibit the advantages of good liquid electrolyte wettability and the ability to prevent thermal runaway conditions in the event of an internal short, which is critical in high-power applications. Although traditional nonwoven separators have a low production cost and exhibit good thermal stability, they have a large thickness, which reduces the energy and power densities of a battery, and a large mean pore size, which increases the risk of internal shorting through dendrite growth. Recent techniques for fabricating nonwoven mats comprised of nanosized fibers augment the feasibility for producing high-performance separators with high tortuosity, high porosity, and good thermal stability. The modification (including ceramic coating, crosslinking, and functionalization) of polyolefin microporous separators and the development of alternative polymers for porous membranes are also the potential directions for improving the performance of separators.

Acknowledgments The author would like to thank Ion C. Halalay, Ingrid A. Rousseau, Hamid G. Kia, and Mark W. Verbrugge at General Motors and Jonathon Hitt at Optimal Resources LLC for the valuable discussions.

References

1. Ehrlich GE (2002) In: Linden D, Reddy TB (eds) Handbook of batteries, 3rd edn. McGraw-Hill, New York
2. Johnson BA, White RE (1998) J Power Sources 70:48–54
3. Djian D, Alloin F, Martinet S, Lignier H, Sanchez JY (2007) J Power Sources 172:416–421
4. Jansen AN, Kahaian AJ, Kepler KD, Nelson PA, Amine K, Dees DW, Vissers DR, Thackeray MM (1999) J Power Sources 81–82:902–905
5. Orsini F, du Pasquier A, Beaudouin B, Tarascon JM, Trentin M, Langenhuizen N, de Beer E, Notten P (1999) J Power Sources 81–82:918–921
6. Liu HK, Wang GX, Guo Z, Wang J, Konstantinov K (2006) J Nanosci Nanotechno 6:1–15
7. Arora P, Zhang Z (2004) Chem Rev 104:4419–4462
8. Zhang SS (2007) J Power Sources 164:351–364
9. Caldwell DL, Poush KA (1984) US Patent 4464238
10. Abraham KM (1993) Electrochim Acta 38:1233–1248

CosMX Exhibit 1003, Page 279 of 512

11. Patel KK, Paulsen JM, Desilvestro J (2003) J Power Sources 122:144–152
12. Jeong YB, Kim DW (2004) J Power Sources 128:256–262
13. Venugopal G, Moore J, Howard J, Pendalwar S (1999) J Power Sources 77:34–41
14. Piatkiewicz W, Rosinski S, Lewinska D, Bukowski J, Judycki W (1999) J Membr Sci 153:1–102
15. Jena A, Gupta K (2002) Fluid Part Sep J 4:227–241
16. Tye FL (1983) J Power Sources 9:89–100
17. Liu SJ, Maslivah JH (1996) In: Schramm LL (ed) Suspensions: fundamentals and applications in the petroleum industry. American Chemical Society, Washington
18. Kim LU, Kim CK (2006) J Polym Sci Polym Phys 44:2025–2034
19. Ma JC, Megahed ES, Stachoviak TJ, Craanen SA, Schneider DA, Nestler JP (2002) US Patent 6444356
20. Yoneda H, Nishimura Y, Doi Y, Fukuda M, Kohno M (2010) Polym J 42:425–437
21. Weighall MJ (1991) J Power Sources 34:257–268
22. Strathmann H, Kock K (1977) Desalination 21:241–255
23. Yilmaz L, McHugh AJ (1986) J Membr Sci 28:287–310
24. Reuvers AJ, van der Berg JWA, Smolders CA (1987) J Membr Sci 34:45–65
25. Reuvers AJ, Smolders CA (1987) J Membr Sci 34:67–86
26. Radovanovic P, Thiel SW, Hwang ST (1992) J Membr Sci 65:213–229
27. Wienk IM, Boom RM, Beerlage MAM, Bulte AMW, Smolders CA, Strathmann H (1996) J Membr Sci 113:361–371
28. Bottino A, Camera-Roda G, Capannelli G, Munari S (1991) J Membr Sci 57:1–20
29. Zhang SS, Xu K, Foster DL, Ervin MH, Jow TR (2004) J Power Sources 125:114–118
30. Andrieu X, Laurence J (1998) US Patent 5811205
31. Dupasquier A, Tarascon JM (2003) US Patent 6537334
32. Dupasquier A, Warren PC, Culver D, Gozdz AS, Amatucci GG, Tarascon JM (2000) Solid State Ionics 135:249–257
33. Li ZH, Zhang P, Zhang HP, Wu YP, Zhou XD (2008) Electrochem Commun 10:791–794
34. Lundquist JT, Lundsager B, Palmer NI, Troffkin HJ, Howard J (1987) US Patent 4650730
35. Yu WC (1997) US Patent 5691077
36. Higuchi H, Matsushita K, Ezoe M, Shinomura T (1995) US Patent 5385777
37. Ihm DW, Noh JG, Kim JY (2002) J Power Sources 109:388–393
38. Noumi S, Yamamura Y, Nakayama S (2010) US Patent 7704597
39. Yamamoto K, Fujita S, Uetani Y, Noumi S, Emori H, Yamamura Y (2003) US Patent 6559195
40. Johnson MB, Wilkes GL (2002) J Appl Polym Sci 83:2095–2113
41. Beard KW (2006) US patent application 20060081530
42. Takahashi T, Tateno T (1999) US Patent 5856426
43. Ohya S, Fujii Y, Yao S, Asano Y, Nakayama K, Fukunaga K (2003) US Patent 6565962
44. Xiao LF, Ai XP, Cao Y, Wang YD, Yang HX (2005) Electrochem Commun 7:589–592
45. Chen G, Richardson TS (2004) Electrochem Solid-State 7:A23–A26
46. Feng JK, Ai XP, Cao YL, Yang HX (2006) J Power Sources 161:545–549
47. Thomas-Alyea KE, Newman J, Chen G, Richardson TJ (2004) J Electrochem Soc 151:A509–A521
48. Ko JM, Min BG, Kim DW, Ryu KS, Kim KM, Lee YG, Chang SH (2004) Electrochim Acta 50:367–370
49. Gao K, Hu GX, Yi TF, Dai CS (2006) Electrochim Acta 52:443–449
50. Gineste JL, Pourcelly G (1995) J Membr Sci 107:155–164
51. Yao ZP, Ranby B (1990) J Appl Polym Sci 41:1469–1478
52. Urairi M, Tachibana T, Matsumoto K, Shinomura T, Iida H, Kawamura K, Yano S, Ishida O (1996) US Patent 5558682
53. Sugiyama M, Totsuka H, Mitani S, Takahata M (2007) US Patent 7311994
54. Kim JY, Kim SK, Lee SJ, Lee SY, Lee HM, Ahn S (2004) Electrochim Acta 50:363–366
55. Kritzer P (2006) J Power Sources 161:1335–1340
56. Ashida T, Tsukuda T (2001) US Patent 6200706
57. Wang Y, Zhan H, Hu J, Liang Y, Zeng S (2009) J Power Sources 189:616–619
58. Kamei T, Yamazaki M (2004) US Patent 6730439
59. Suzuki H, Sudo Y (2003) JP-A-2003-142064
60. Sudou Y, Suzuki H, Nagami S, Ikuta K, Yamamoto T, Okijima S, Suzuki S, Ueshima H (2007) US Patent 7183020
61. Bansal D, Meyer B, Salomon M (2008) J Power Sources 178:848–851
62. Cho TH, Sakai T, Tanase S, Kimura K, Kondo Y, Tarao T, Tanaki M (2007) Electrochem Solid-State 10:A159–A162
63. Kim JR, Choi SW, Jo SM, Lee WS, Kim BC (2005) J Electrochem Soc 152:A295–A300
64. Lee SW, Choi SW, Jo SM, Chin BD, Kim DY, Lee KY (2006) J Power Sources 163:41–46
65. Chu B, Hsaio BS, Fang D (2006) US Patent application 2006049542
66. Um IC, Fang D, Hsiao BS, Okamoto A, Chu B (2004) Biomacromolecules 5:1428–1436
67. Armantrout JE, Bryner MA, Davis MC, Kim YM (2006) US Patent application 2006012084
68. Kim YM, Sung YB, Jang RS, Ahn KR (2009) US Patent 7618579
69. Peng M, Sun Q, Ma Q, Li P (2008) Microporous Mesoporous Mater 115:562–567
70. Hiroki S, Satoshi N, Hiroyuki H, Takahiro D (2006) Patent application WO 06123811
71. Lee YM, Kim JW, Choi NS, Lee JA, Seol WH, Park JK (2005) J Power Sources 139:235–241
72. Lee YM, Choi NS, Lee JA, Seol WH, Cho KY, Jung HY, Kim JW, Park JK (2005) J Power Sources 146:431–435
73. Pekala RW, Khavari M (2003) US Patent 6586138
74. Zhang SS, Xu K, Jow TR (2005) J Power Sources 140:361–364
75. Cho TH, Tanaka M, Onishi H, Kondo Y, Nakamura T, Yamazaki H, Tanase S, Sakai T (2008) J Electrochem Soc 155:A699–A703
76. Shinohara Y, Tsujimoto Y, Nakano T (1999) US Patent 6447958
77. Augustin S, Hennige VD, Horpel G, Hying C (2002) Desalination 146:23–28
78. Henninge V, Hying C, Horpel G (2010) US Patent 7807286
79. Hennige V, Hying C, Horpel G, Novak P, Vetter J (2010) US Patent 7709140
80. Kim SK, Sohn JY, Park JH, Jang HM, Shin BJ, Lee SY, Hong JH (2010) US Patent 7709152
81. Park JH, Lee SY, Hong JH, Nam MJ, Yoo JA, Kim SS, Han CH (2010) US Patent 7695870
82. Seo DJ, Kim K, Hong JH, Sohn JY, Lee SY, Ahn SH (2007) US Patent application 20070122716
83. Lee SY, Seo DJ, Sohn JY, Kim SK, Hong JH, Kim YS Jang HM (2009) US Patent 7638241
84. Katayama H, Kojima E, Aoyama S, Sato Y (2008) Patent application WO08029922
85. Tomi H, Sato E, Murayama S, Itou F, Imoto H (2006) Japan Patent JP3831017
86. Lee KH, Lee YG, Park JK, Seung DY (2000) Solid State Ionics 133:257–263
87. Appetecchi GB, Romagnoli P, Scrosati B (2001) Electrochem Commun 3:281–284
88. Chung SH, Wang Y, Persi L, Croce F, Greenbaum SG, Scrosati B, Plichta E (2001) J Power Sources 97–98:644–648
89. Kumar B, Scanlon L, Marsh R, Mason R, Higgins R, Baldwin R (2001) Electrochim Acta 46:1515–1521

CosMX Exhibit 1003, Page 280 of 512

90. Abraham KM, Koch VR, Blakley TJ (2000) J Electrochem Soc 147:1251–1256
91. Hikmet RAM (2001) J Power Sources 92:212–220
92. Less GB, Knapp A, Babinec SJ (2009) US Patent application 20090155678
93. Kim M, Nho YC, Park JH (2010) J Solid State Electrochem 14:769–773
94. Doyle M, Newman J, Gozdz AS, Schmutz CN, Tarascon JM (1996) J Electrochem Soc 143:1890–1903
95. MacMullin RB, Muccini GA (1956) AICHE J 2:393–403
96. Thorat IV, Stephenson DE, Zacharias NA, Zaghib K, Harb JN, Wheeler DR (2009) J Power Sources 188:592–600
97. Srinivasan V, Newman J (2004) J Electrochem Soc 151:A1530–A1538
98. Xiao X, Wu W, Huang X (2010) J Power Sources 195:7649–7660

CosMX Exhibit 1003, Page 281 of 512

Appendix J

Battery Separators

Pankaj Arora* and Zhengming (John) Zhang

Celgard, LLC, 13800 South Lakes Dr., Charlotte, North Carolina 28273

Received March 30, 2004

Contents

1. Introduction and Scope 4419
2. Battery and Separator Market 4420
3. Separator and Batteries 4421
4. Separator Requirements 4422
5. Separator Types 4422
5.1. Microporous Separators 4422
5.2. Nonwovens 4422
5.3. Ion Exchange Membranes 4423
5.4. Supported Liquid Membranes 4423
5.5. Polymer Electrolyte 4423
5.6. Solid Ion Conductors 4423
6. Separator for Nonaqueous Batteries 4423
6.1. Lithium Ion 4424
6.1.1. Separator Development 4424
6.1.2. Separator Requirements 4427
6.1.3. Separator Properties/Characterization 4429
6.1.4. Effect of Separator on Cell Performance and Safety 4436
6.2. Lithium Polymer 4440
6.3. Lithium-Ion Gel Polymer 4441
6.4. Lithium Primary Systems 4443
6.4.1. Separator Requirements 4443
6.4.2. Chemistries 4444
7. Separator for Aqueous Batteries 4445
7.1. Leclanche (Zinc Carbon) 4446
7.2. Alkaline Zinc MnO_2 4446
7.3. Lead-Acid Batteries 4447
7.3.1. Flooded Electrolyte Lead Acid 4447
7.3.2. Valve Regulated Lead Acid (VRLA) 4449
7.4. Nickel Systems 4450
7.4.1. Nickel–Cadmium 4450
7.4.2. Nickel–Metal Hydride 4451
7.4.3. Nickel–Hydrogen 4452
7.5. Zinc Systems 4452
7.5.1. Silver–Zinc 4452
7.5.2. Nickel–Zinc 4454
7.5.3. Zinc–Air 4455
7.5.4. Zinc–Bromine 4456
7.6. Redox Flow Batteries 4456
8. Mathematical Modeling of Batteries/Separators 4457
9. Summary 4458
10. Future Directions 4458
11. Acknowledgments 4459
12. References 4459

* Corresponding author. E-mail: pankajarora@celgard.com. Telephone: 704 587 8478. Fax: 704 588 7393



Pankaj Arora is a Senior Research Engineer at Celgard LLC in Charlotte, NC. He specializes in the design and modeling of electrochemical power sources and is currently working in the Battery Applications Laboratory of Celgard, where he helps guide separator development work for lithium batteries. He has a B.Tech. degree in Electrochemical Engineering from the Central Electrochemical Research Institute in Karaikudi, India, and a Ph.D. degree in Chemical Engineering from the University of South Carolina, Columbia, SC. Pankaj can be reached by email at pankajarora@celgard.com.



Zhengming (John) Zhang is Vice President of New Technology at Celgard LLC in Charlotte, NC. He has been working in Solid State Ionics, Batteries, and Battery Separators since 1984. He has published more than 50 papers and patents and has co-edited a book on battery. He has been a invited speaker for many professional conferences, invited lecturer for United Nations Development Program, and is a Visiting Professor at Xiamen University, Fujian, China. He has a B.S. in Mechanical Engineering from Shanghai University, Shanghai, China, an M.S. in Electrochemistry from Shandong University, Jinan City, China, and a Ph.D. in Materials Chemistry from the University of California at Santa Barbara, Santa Barbara, CA. John can be reached by email at zjzhang@celgard.com.

1. Introduction and Scope

Many advances have been made in battery technology in recent years, both through continued improvement of specific electrochemical systems and through the development and introduction of new

10.1021/cr020738u CCC: $48.50 © 2004 American Chemical Society
Published on Web 10/13/2004

CosMX Exhibit 1003, Page 283 of 512

battery chemistries. Nevertheless, there is still no one "ideal" battery that gives optimum performance under all operating conditions. Similarly, there is no one separator that can be considered "ideal" for all battery chemistries and geometries.

A separator is a porous membrane placed between electrodes of opposite polarity, permeable to ionic flow but preventing electric contact of the electrodes. A variety of separators have been used in batteries over the years. Starting with cedar shingles and sausage casing, separators have been manufactured from cellulosic papers and cellophane to nonwoven fabrics, foams, ion exchange membranes, and microporous flat sheet membranes made from polymeric materials. As batteries have become more sophisticated, separator function has also become more demanding and complex.

Separators play a key role in all batteries. Their main function is to keep the positive and negative electrodes apart to prevent electrical short circuits and at the same time allow rapid transport of ionic charge carriers that are needed to complete the circuit during the passage of current in an electrochemical cell.[1,2] They should be very good electronic insulators and have the capability of conducting ions by either intrinsic ionic conductor or by soaking electrolyte. They should minimize any processes that adversely affect the electrochemical energy efficiency of the batteries.

Very little work (relative to research of electrode materials and electrolytes) is directed toward characterizing and developing new separators. Similarly, not much attention has been given to separators in publications reviewing batteries.[1−10] A number of reviews on the on cell fabrication, their performance, and application in real life have appeared in recent years, but none have discussed separators in detail. Recently a few reviews have been published in both English and Japanese which discuss different types of separators for various batteries.[11−20] A detailed review of lead-acid and lithium-ion (li-ion) battery separators was published by Boehnstedt[13] and Spotnitz,[14] respectively, in the *Handbook of Battery Materials*. Earlier Kinoshita et al. had done a survey of different types of membranes/separators used in different electrochemical systems, including batteries.[11]

The majority of the separators currently used in batteries were typically developed as spin-offs of existing technologies. They were usually not developed specifically for those batteries and thus are not completely optimized for systems in which they are used. One positive result of adapting existing technologies is that they are produced in high volume at relatively low cost. The availability of low cost separators is an important consideration in the commercialization of batteries, because the battery industry traditionally operates with thin profit margins and relatively small research budgets.

The purpose of this paper is to describe the various types of separators based on their applications in batteries and their chemical, mechanical and electrochemical properties, with particular emphasis on separators for lithium-ion batteries. The separator requirements, properties, and characterization techniques are described with respect to lithium-ion batteries. The separators used in other batteries are only discussed briefly. Despite the widespread use of separators, a great need still exists for improving the performance, increasing the life, and reducing the cost of separators. In the following sections, an attempt is made to discuss key issues in various separators with the hope of bringing into focus present and future directions of research and development in separator technologies.

2. Battery and Separator Market

The battery industry has seen enormous growth over the past few years in portable, rechargeable battery packs. The majority of this surge can be attributed to the widespread use of cell phones, personal digital assistants (PDA's), laptop computers, and other wireless electronics. Batteries remained the mainstream source of power for systems ranging from mobile phones and PDA's to electric and hybrid electric vehicles. The world market for batteries was approximately $41 billion in 2000, which included $16.2 billion primary and $24.9 billion secondary cells.[21]

A recent study from Freedonia has predicted aggregate U.S. demand for primary and secondary batteries to climb 5.5% annually through 2007 to $14 billion. The growth will be driven by strong demand for battery-powered electronic devices like digital cameras and 3G wireless phones, and increasing production of electrical and electronic equipment. The secondary battery demand is expected to outpace the primary battery market gains through 2007 benefiting from strong growth in the use of high-drain portable electronic devices. The lead-acid batteries will account for over half of all rechargeable demand in 2007, although lithium-ion and NiMH batteries will record the strongest growth. Alkaline batteries could remain the dominant type, accounting for more than two thirds of all primary battery sales in 2007.[22]

The rechargeable battery (NiCd, NiMH, and lithium-ion) market for 2003 for portable electronics was around $5.24 billion, around 20% more then 2002. The lithium-ion battery market was around $3.8 billion (∼73%). They are now used in more than 90% of cellphones, camcorders, and portable computers, worldwide, and have also been adopted in power tools recently.[23]

The tremendous progress in lithium-ion cells is clearly visible with as much as a 2-fold increase in the volumetric and gravimetric energy density for both 18650 and prismatic cells between 1994 and 2002. In past few years the lithium-ion production has expanded to South Korea (Samsung, LG, etc.) and China (BYD, B&K, Lishen, etc.) from Japan. Several Japanese (Sanyo, Sony, MBI, NEC, etc.) and Korean (LG Chemical) manufacturers have also moved their manufacturing plants to China.[23] Japan, which controlled 94% of the global rechargeable battery market in 2000, has seen its market share drop to about 65% of the global market.[23−25] The continued growth in lithium-ion battery market has led to a strong demand for battery separators. All the

CosMX Exhibit 1003, Page 284 of 512

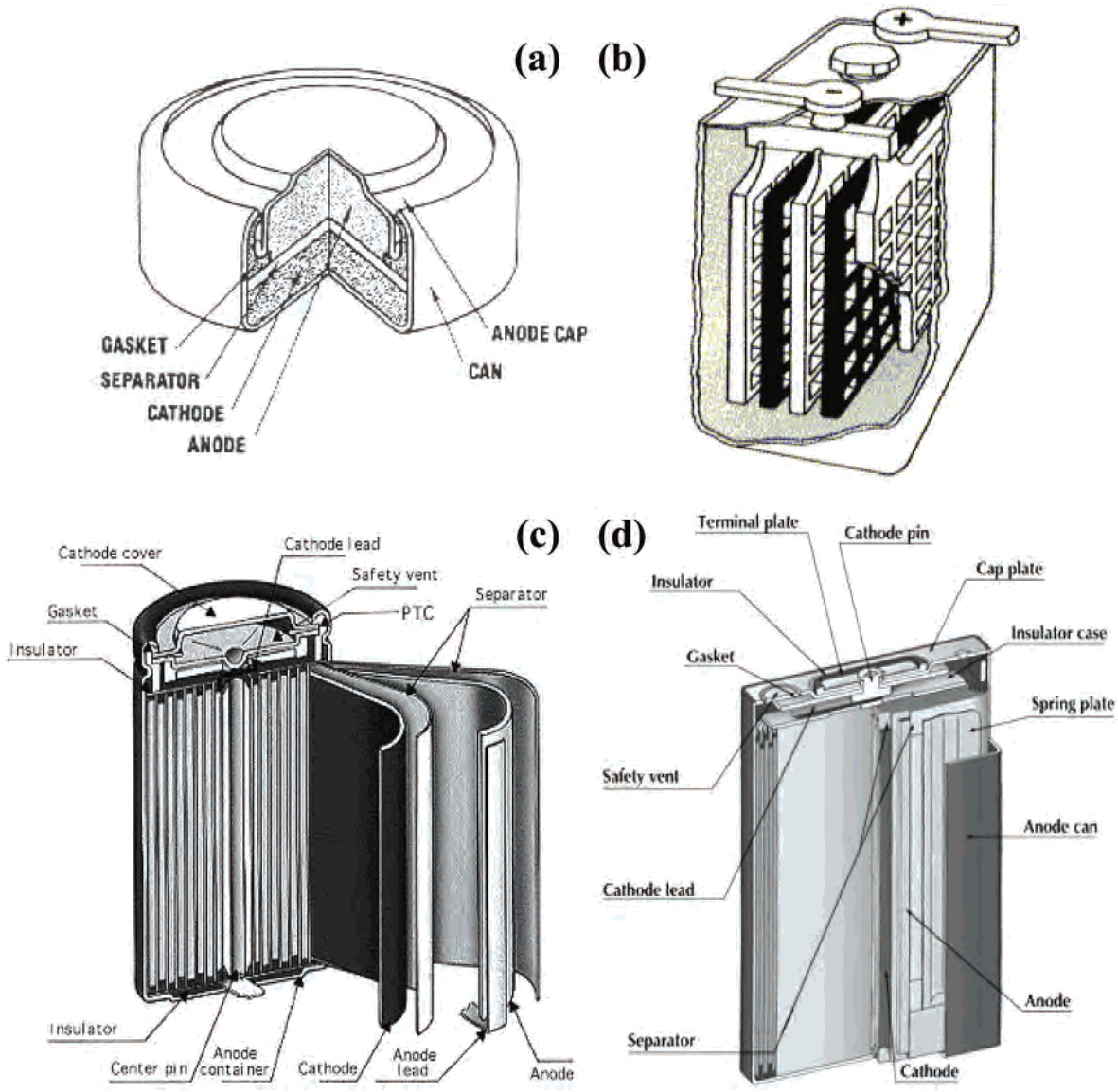


Figure 1. Typical battery configurations: (a) button cell; (b) stack lead-acid; (c) spiral wound cylindrical lithium-ion; (d) spiral wound prismatic lithium-ion.

major separator manufacturers (Celgard, Asahi, and Tonen) have either increased their capacity in 2003 or are planning to increase it in 2004.[26−28]

There is not too much information available on the battery separator market in the literature. It is estimated that about 30% of the rechargeable lithium battery market or $1.5 billion is the size of the battery materials or components market. Battery separators for lithium batteries are about a $330 million market within the total battery components market.[29,30] Recently, the Freedonia Group has reported that the U.S. demand for battery separators will increase to $410 million in 2007 from $237 million in 1977 and $300 million in 2002, respectively.[31,32]

3. Separator and Batteries

Batteries are built in many different shapes and configurations—button, flat, prismatic (rectangular), and cylindrical (AA, AAA, C, D, 18650, etc.). The cell components (including separators) are designed to accommodate a particular cell shape and design. The separators are either stacked between the electrodes or wound together with electrodes to form jellyrolls as shown in Figure 1. Stacked cells are generally held together by pressure from the cell container. The lithium-ion gel polymer stacked cells are prepared by bonding/laminating layers of electrodes and separators together. The separator properties should not change significantly during the bonding process. In some cases, the separators are coated to help in bonding process, thus reducing the interfacial resistance.[33−35]

In the conventional way of making spirally wound cells, two layers of separators are wound along with the positive and negative electrodes, resulting in a positive/separator/negative/separator configuration. They are wound as tightly as possible to ensure good interfacial contact. This requires the separators to be strong to avoid any contact between the electrodes through the separator. The separator also must not yield and reduce in width, or else the electrodes may contact each other. Once wound, the jellyroll is

CosMX Exhibit 1003, Page 285 of 512

inserted into a can, and filled with electrolyte. The separator must be wetted quickly by the electrolyte to reduce the electrolyte filling time. A header is then crimped into the cell to cover the can from top. In some prismatic cells, the jellyroll is pressed at high temperatures and pressures and then inserted into thin prismatic (rectangular) cans. A typical 18650 lithium-ion cell uses around 0.07−0.09 m^2 of separator, which is approximately 4−5% of the total cell weight.[36]

4. Separator Requirements

A number of factors must be considered in selecting the best separator for a particular battery and application. The characteristics of each available separator must be weighed against the requirements and one selected that best fulfills these needs. A wide variety of properties are required of separators used in batteries. The considerations that are important and influence the selection of the separator include the following:

- Electronic insulator
- Minimal electrolyte (ionic) resistance
- Mechanical and dimensional stability
- Sufficient physical strength to allow easy handling
- Chemical resistance to degradation by electrolyte, impurities, and electrode reactants and products
- Effective in preventing migration of particles or colloidal or soluble species between the two electrodes
- Readily wetted by electrolyte
- Uniform in thickness and other properties

The order of importance of the various criteria varies, depending on the battery applications. The above list presents a broad spectrum of requirements for separators in batteries. In many applications, a compromise in requirements for the separator must generally be made to optimize performance, safety, cost, etc. For example, batteries that are characterized by small internal resistance and consume little power require separators that are highly porous and thin, but the need for adequate physical strength may require that they be thick.

In addition to the above general requirements each battery type has other requirements essential for good performance and safety. For example, separators in sealed nickel−cadmium (NiCd) and nickel−metal hydride (NiMH) batteries should be highly permeable to gas molecules for overcharge protection, the separator in lithium-ion cells should have a shutdown feature for good safety, separators for alkaline batteries should be flexible enough to be wrapped around the electrodes, and the separator for an SLI (starting, lighting and ignition) battery could also serve as a mechanical-shock cushion.

5. Separator Types

Separators for batteries can be divided into different types, depending on their physical and chemical characteristics. They can be molded, woven, nonwoven, microporous, bonded, papers, or laminates. In recent years, there has been a trend to develop solid and gelled electrolytes that combine the electrolyte and separator into a single component.

In most batteries, the separators are either made of nonwoven fabrics or microporous polymeric films. Batteries that operate near ambient temperatures usually use separators fabricated from organic materials such as cellulosic papers, polymers, and other fabrics, as well as inorganic materials such as asbestos, glass wool, and SiO_2. In alkaline batteries, the separators used are either regenerated cellulose or microporous polymer films. The lithium batteries with organic electrolytes mostly use microporous films.

For the sake of discussion, we have divided the separators into six types—microporous films, nonwovens, ion exchange membranes, supported liquid membranes, solid polymer electrolytes, and solid ion conductors. A brief description of each type of separator and their application in batteries are discussed below.

5.1. Microporous Separators

They are fabricated from a variety of inorganic, organic, and naturally occurring materials and generally contain pores that are greater than 50−100 Å in diameter. Materials such as nonwoven fibers (e.g. nylon, cotton, polyesters, glass), polymer films (e.g. polyethylene (PE), polypropylene (PP), poly(tetrafluoroethylene) (PTFE), poly(vinyl chloride) (PVC)), and naturally occurring substances (e.g. rubber, asbestos, wood) have been used for microporous separators in batteries that operate at ambient and low temperatures (<100 °C). The microporous polyolefins (PP, PE, or laminates of PP and PE) are widely used in lithium based nonaqueous batteries (section 6.1), and filled polyethylene separators in lead-acid batteries (section 7.3), respectively.

5.2. Nonwovens

Nonwovens are textile products that are manufactured directly from fibers. They are defined as a manufactured sheet, web, or matt of directionally or randomly oriented fibers, bonded by friction, and/or cohesion, and/or adhesion excluding paper and products which are woven, tufted, stichbounded incorporating binding yarns or filaments, or felted by wetmilling whether or not additionally needed. The fibers may be of natural or manmade origin. They may be staple or continuous filaments or maybe formed in situ.[37]

The macroporous fibrous matrix is either dry laid, meltblown, or wet laid. The wet laid process is very similar to the papermaking process. The fibers are bonded together by chemical or thermal bonding. The meltblown process is a binderless process and there the polymer fiber web is extruded. Typical pore sizes of the fibrous matrix vary from 1 to 100 μm.

Nonwovens are widely utilized as separators for several types of batteries. Lightweight, wet laid nonwovens made from cellulose, poly(vinyl alcohol), and other fibers have achieved considerable success as separators for popular primary alkaline cells of various sizes. The key nonwoven attributes include consistently uniform basis weight, thickness, porosity and resistance to degradation by electrolytes. Nonwovens are also successfully employed as separators in NiCd's.

CosMX Exhibit 1003, Page 286 of 512

Table 1. Types of Separators Used in Different Type of Secondary Lithium Batteries

battery system	type of separator	composition
lithium-ion (liquid electrolyte)	microporous	polyolefins (PE, PP, PP/PE/PP)
lithium-ion gel polymer	microporous	PVdF
	microporous	polyolefins (PE, PP, PP/PE/PP) coated with PVdF or other gelling agents
lithium-polymer (e.g. $Li-V_6O_{13}$)	polymer electrolyte	poly(ethylene oxide) with lithium salt

The materials used in nonwoven fabrics include a single polyolefin, or a combination of polyolefins, such as polyethylene (PE), polypropylene (PP), polyamide (PA), poly(tetrafluoroethylene) (PTFE), polyvinylidine fluoride (PVdF), and poly(vinyl chloride) (PVC). Nonwoven fabrics have not, however, been able to compete with microporous films in lithium-ion cells. This is most probably because of the inadequate pore structure and difficulty in making thin (<25 μm) nonwoven fabrics with acceptable physical properties.

5.3. Ion Exchange Membranes

These membranes are generally fabricated from polymeric materials containing pores with diameters of less than 20 Å. The transport properties of ions in these membranes are characterized by strong interactions between the permeating species and the molecular structure of the polymer. This interaction is due to the presence of ion-exchange groups in the membrane, which allows the membrane to discriminate between permeating or migrating ions by virtue of their specific charge.

Radiation grafted membranes such as Permion manufactured by RAI Research Corporation are ion-exchange membranes. Such membranes are used as battery separators in alkaline batteries. They are made from PE, PP, or Teflon-based films, which have excellent oxidation resistance and superior chemical resistance to alkali. However, they are totally impervious to electrolyte flow, and therefore, they have almost infinite resistance as a separator in this form. By using radiation grafting and cross-linking techniques, however, selected chemical species are grafted as pendant chains to the base structure of the linear polymer without altering the inert backbone. This modification imparts desirable hydrophilic properties to the films without materially impairing their excellent chemical resistance. This paper provides a very limited discussion on ion exchange membranes, as their application in batteries is very limited.

5.4. Supported Liquid Membranes

These types of separators consist of a solid matrix and a liquid phase, which is retained in the microporous structure by capillary forces. To be effective for batteries, the liquid in the microporous separator, which generally contains an organic phase, must be insoluble in the electrolyte, chemically stable, and still provide adequate ionic conductivity. Several types of polymers, such as polypropylene, polysulfone, poly(tetrafluoroethylene), and cellulose acetate, have been used for porous substrates for supported-liquid membranes. The PVdF coated polyolefin-based microporous membranes used in gel−polymer lithium-ion battery fall into this category. Gel polymer electrolytes/membranes are discussed briefly in section 6.3.

5.5. Polymer Electrolyte

Polymer electrolytes (e.g., poly(ethylene oxide), poly(propylene oxide)) have attracted considerable attention for batteries in recent years. These polymers form complexes with a variety of alkali metal salts to produce ionic conductors that serve as solid electrolytes. Their use in batteries is still limited due to poor electrode/electrolyte interface and poor room temperature ionic conductivity. Because of the rigid structure, they can also serve as the separator. Polymer electrolytes are discussed briefly in section 6.2.

5.6. Solid Ion Conductors

They serve as both separator and electrolyte. These are generally inorganic materials that are impervious barriers to gases and liquids. They allow one or more kinds of ions to migrate through their lattice when a potential gradient or a chemical gradient is present. These types of separators are beyond the scope of this article.

6. Separator for Nonaqueous Batteries

All lithium based batteries use nonaqueous electrolytes because of the reactivity of lithium in aqueous solution and because of the electrolyte's stability at high voltage. The majority of these cells use microporous membranes made of polyolefins. In some cases, nonwovens made of polyolefins are either used alone or with microporous separators. This section will mainly focus on separators used in secondary lithium batteries followed by a brief summary of separators used in lithium primary batteries.

Lithium secondary batteries can be classified into three types, a liquid type battery using liquid electrolytes, a gel type battery using gel electrolytes mixed with polymer and liquid, and a solid type battery using polymer electrolytes. The types of separators used in different types of secondary lithium batteries are shown in Table 1. The liquid lithium-ion cell uses microporous polyolefin separators while the gel polymer lithium-ion cells either use a PVdF separator (e.g. PLION cells) or PVdF coated microporous polyolefin separators. The PLION cells use PVdF loaded with silica and plasticizer as separator. The microporous structure is formed by removing the plasticizer and then filling with liquid electrolyte. They are also characterized as plasticized electrolyte. In solid polymer lithium-ion cells, the solid electrolyte acts as both electrolyte and separator.

CosMX Exhibit 1003, Page 287 of 512

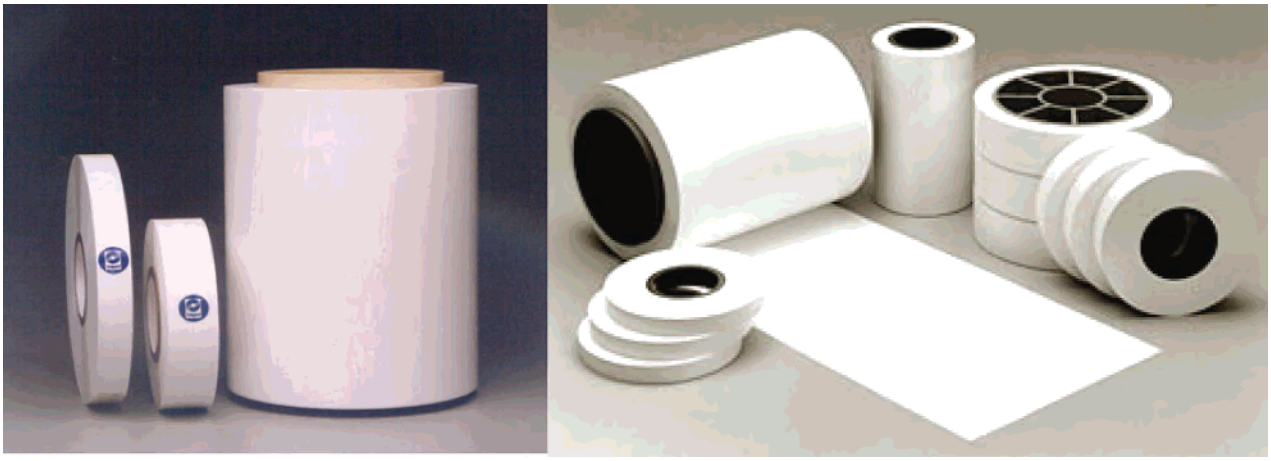


Figure 2. Polyolefin separators used in lithium-ion batteries.

6.1. Lithium Ion

The past decade has seen significant advances in the ambient temperature lithium battery technology. Lithium-ion batteries are the preferred power source for most portable electronics because of their higher energy density, longer cycle life, and higher operational voltage as compared to NiCd and NiMH systems. In 2002, 66% of the total rechargeable battery market for mobile IT and communication devices used lithium-based batteries and the rest used nickel-based batteries.[38,39]

A typical lithium-ion cell consists of a positive electrode composed of a thin layer of powdered metal oxide (e.g., $LiCoO_2$) mounted on aluminum foil and a negative electrode formed from a thin layer of powdered graphite, or certain other carbons, mounted on a copper foil. The two electrodes are separated by a porous plastic film soaked typically in $LiPF_6$ dissolved in a mixture of organic solvents such as ethylene carbonate (EC), ethyl methyl carbonate (EMC), or diethyl carbonate (DEC). In the charge/discharge process, lithium ions are inserted or extracted from the interstitial space between atomic layers within the active materials.

Sony's introduction of the rechargeable lithium-ion battery in the early 1990s precipitated a need for new separators that provided not only good mechanical and electrical properties but also added safety through a thermal shutdown mechanism. Although a variety of separators (e.g., cellulose, nonwoven fabric, etc.) have been used in different type of batteries, various studies on separators for lithium-ion batteries have been pursued in past few years as separators for lithium-ion batteries require different characteristics than separators used in conventional batteries.

A novel microporous separator using polyolefins has been developed and used extensively in lithium-ion batteries since it is difficult for conventional separator materials to satisfy the characteristics required in lithium-ion batteries. In lithium-ion batteries two layers of separators are sandwiched between positive and negative electrodes and then spirally wound together in cylindrical and prismatic configurations. The pores of the separator are filled with ionically conductive liquid electrolyte.

Microporous polyolefin membranes (see Figure 2) in current use are thin (<30 μm) and are made of polyethylene (PE), polypropylene (PP), or laminates[40] of polyethylene and polypropylene. They are made up of polyolefins materials because they provide excellent mechanical properties, chemical stability and acceptable cost.[41,42] They have been found to be compatible with the cell chemistry and can be cycled for several hundred cycles without significant degradation in chemical or physical properties.

Commercial membranes offer pore size in the range 0.03−0.1 μm, and 30−50% porosity. The low melting point of PE enables their use as a thermal fuse. As the temperature approaches the melting point of the polymer, 135 °C for PE and 165 °C for PP, porosity is lost. The trilayer material (PP/PE/PP)[43] has been developed by Celgard where a PP layer is designed to maintain the integrity of the film, while the low melting point of PE layer is intended to shutdown the cell if an over-temperature condition is reached.[108] Asahi Kasai's flat-film membrane "Hipore" is available in thicknesses ranging from 20 μm to several hundred micrometers, and with highly uniform pore sizes ranging from 0.05 to 0.5 μm.[44] The major manufacturers of lithium-ion battery separators along with their typical products are listed in Table 2.

In recent years there have been a strong demand for higher capacity lithium-ion cells because of the strong growth in portable electronics. One way to achieve higher capacity is by reducing the thickness of separators. The battery manufacturers have started using 20 and 16 μm separators in higher capacity (>2.0 A h) cylindrical cells, and 9 μm separators in lithium-ion gel polymer cells.

Nonwoven materials have also been developed for lithium-ion cells but have not been widely accepted, in part due to the difficulty in fabricating thin materials with good uniformity and high strength.[14] Nonwoven separators have been used in button cells and bobbin cells when thicker separators and low discharge rates are acceptable.

6.1.1. Separator Development

The process for making lithium-ion battery separators can be broadly divided into dry[45,46] and wet[47] processes. Both processes usually employ one or more orientation steps to impart porosity and/or increase tensile strength. The dry process involves melting a polyolefin resin, extruding it into a film, thermally

Table 2. Major Manufacturers of Lithium-Ion Battery Separators along with Their Typical Products

manufacturer	structure	composition	process	trade name
Asahi Kasai	single layer	PE	wet	HiPore
Celgard LLC	single layer	PP, PE	dry	Celgard
	multilayer	PP/PE/PP	dry	Celgard
	PVdF coated	PVdF, PP, PE, PP/PE/PP	dry	Celgard
Entek Membranes	single layer	PE	wet	Teklon
Mitsui Chemical	single layer	PE	wet	
Nitto Denko	single layer	PE	wet	
DSM	single layer	PE	wet	Solupur
Tonen	single layer	PE	wet	Setela
Ube Industries	multi layer	PP/PE/PP	dry	U-Pore

Table 3. Manufacturing Process of Typical Microporous Film

process	mechanism	raw material	properties	typical membranes	manufacturers
dry process	drawing	polymer	simple process anisotropic film	PP, PE, PP/PE/PP	Celgard, Ube
wet process	phase separation	polymer + solvent	isotropic film	PE	Asahi, Tonen
		polymer + solvent + filler	large pore size high porosity	PE	Asahi

annealing it to increase the size and amount of lamella crystallites, and precisely stretching it to form tightly ordered micropores.[48−52] In this process, a row lamellar crystal structure is generated in the polymer in the initial extrusion step. This nonporous structure is highly oriented as a result of extrusion and annealing conditions. The films are then stretched to form micropores. This microporous structure is continuous throughout the bulk interior of the membrane.[53]

Polypropylene and polyethylene microporous films obtained by this method are available from Celgard[48,50,54,55] and Ube.[56] The dry process is technologically convenient because no solvents are required. However, only a uniaxial stretching method has been successful to date, and as a result, the pores are slitlike in shape and the mechanical properties of films are anisotropic. The tensile strength in the lateral direction is relatively low.

Wet process (phase inversion process)[57,58] involves mixing of hydrocarbon liquid or some other low-molecular weight substance generally with a polyolefin resin, heating and melting the mixture, extruding the melt into a sheet, orientating the sheet either in the machine direction (MD) or biaxially, and then extracting the liquid with a volatile solvent.[45,59] Separators made by the wet process are available from Asahi Kasei,[60] Tonen,[61−63] and Mitsui Chemicals[64] and more recently from Polypore/Membrana and Entek.[65] The structure and properties of the membranes can be changed by controlling the composition of the solutions and the evaporation or subtractions of solvents in the gelation and solidification processes. The separators made by wet process use ultrahigh-molecular-weight polyethylene (UHMWPE). The use of UHMWPE gives good mechanical properties as well as some degree of melt integrity.

Ihm et al. have given a nice overview of the wet process by preparing a separator with polymer blends of high-density polyethylene (HDPE) and ultrahigh molecular weight polyethylene (UHMWPE).[58] They showed that the mechanical strength and drawing characteristics are influenced by the content and the molecular weight of the UHMWPE contained in a polyolefin blending solution. The manufacturing process of typical microporous film by dry and wet process is compared in Table 3.

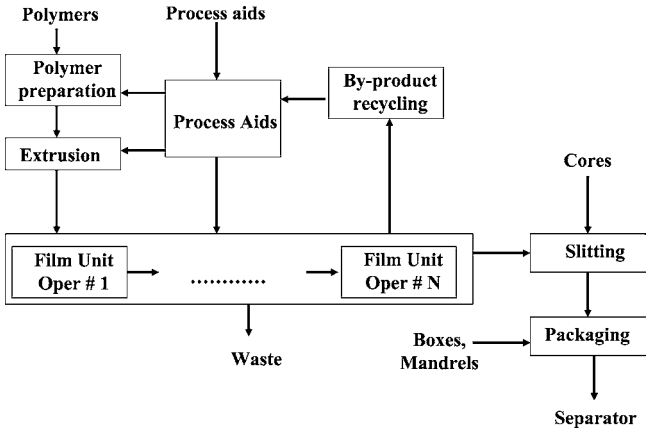


Figure 3. Generalized process for lithium-ion separator manufacturing.[66] Each step of the separator manufacturing process has online detection systems to monitor the quality of the separator.

A simplified flowchart for separator manufacturing process is shown in Figure 3.[66] The virgin polymer is prepared and mixed with processing aids (e.g., antioxidants, plasticizer, etc.) and then extruded. The extruded polymer then goes through different steps, which vary from process to process. For the dry process, it can involve film annealing and stretching, while for the wet process, it can involve solvent extraction and stretching. The finished film is then slit into required widths and packed into boxes and shipped to the battery manufacturers. With the advent of thinner separators, the film handling during manufacturing steps has become very important for the final quality of the film. Each step of the separator manufacturing process has online detection systems to monitor the quality of the separators.

Uniaxially oriented films generally have high strength in only one direction, whereas biaxially oriented films are relatively strong in both machine direction (MD) and transverse direction (TD). Although intuitively one might expect biaxially oriented films to be preferred over uniaxially oriented films,

CosMX Exhibit 1003, Page 289 of 512

Table 4. Typical Properties of Some Commercial Microporous Membranes

separator/properties	Celgard 2730	Celgard 2400	Celgard 2320	Celgard 2325	Asahi Hipore	Tonen Setela
structure	single layer	single layer	trilayer	trilayer	single layer	single layer
composition	PE	PP	PP/PE/PP	PP/PE/PP	PE	PE
thickness (um)	20	25	20	25	25	25
gurley (s)	22	24	20	23	21	26
ionic resistivity[a] (Ω cm^2)	2.23	2.55	1.36	1.85	2.66	2.56
porosity (%)	43	40	42	42	40	41
melt temp (°C)	135	165	135/165	135/165	138	137

[a] In 1 *M* $LiPF_6$ EC:EMC (30:70 by volume).

in practice biaxial orientation provides no performance advantage. In fact, biaxial orientation tends to introduce TD shrinkage. This shrinkage, at elevated temperatures, can allow electrodes to contact each other. The separator must have sufficient strength in the machine direction so that it does not decrease in width or break under the stress of winding. The strength in the transverse direction is not as important as that in the machine direction during the process of making spirally wound batteries. The minimum generally practical requirement for the mechanical strength of the 25-μm separator is 1000 kg/mm^2.[58]

The typical properties of some commercial microporous membranes are summarized in Table 4. Celgard 2730 and Celgard 2400 are single layer PE and PP separators, respectively, while Celgard 2320 and 2325 are trilayer separators of 20 and 25 μm thickness. Asahi and Tonen separators are single layer PE separators made by the wet process. Basic properties, such as thickness, gurley, porosity, melt temperature, and ionic resistivity are reported in Table 4. These properties are defined in section 6.1.3.

Efforts have been made to find a new route for dry process using biaxial stretching techniques for preparing polypropylene microporous films, which may have submicrometer pore sizes and narrow pore size distributions and high permeability to gases and liquids combined with good mechanical properties. The biaxially stretched polypropylene microporous films (Micpor) were made by using nonporous polypropylene films of high β-crystal content.[67] The porosity of these films can be as high as 30−40%, with an average pore size of approximately 0.05 μm. The pores on the surface were almost circular in shape compared to slitlike pores observed in uniaxial stretched samples and exhibited high permeability to fluids with good mechanical properties and almost circular pore shape with narrow pore size distribution.[68−70]

The PP/PE bilayers[40] and PP/PE/PP trilayer separators were developed by Celgard. Multilayer separators offer advantages by combining the lower melting temperature of PE with the high-temperature strength of PP. Nitto Denko has also patented a single-layer separator made from a blend of PE/PP by the dry stretch process.[71] According to the patent, the separator has microporous regions of PE and PP. On heating in an oven, the impedance of the separator increases near the melting point of PE and the impedance remains high until beyond the melting point of PP. However, battery performance data have not been presented.

Microporous polyethylene separator material composed of a combination of randomly oriented thick and thin fibrils of ultrahigh molecular weight polyethylene (UHMWPE), Solupur, manufactured by DSM Solutech, is also an interesting separator material for lithium-ion batteries. Solupur is fabricated in standard grades with base weights ranging from 7 to 16 g/m^2 and mean pore size ranging from 0.1 to 2.0 μm and a porosity of 80−90%.[72] Ooms et al. carried out a study on a series of DSM Solupur materials with different permeability. Rate capability and cycling tests of these materials were compared with commercial available separators in CR2320 type coin cells. Solupur materials showed low tortuosity, high strength and puncture resistance, excellent wettability, and good high rate capability and low-temperature performance because of its high porosity and UHMWPE structure.[73]

Recently Nitto Denko has developed a battery separator made by a wet process that had high puncture strength and high heat rupture resistance.[74] They used a polyolefin resin with a high molecular weight rubber as its main component materials and cross-linked through oxidation in air. The melt rupture temperature, as measured by thermomechnical analysis was over 200 °C in this material. They also tried cross-linking ultrahigh molecular weight polyethylene with electron-beam and ultraviolet irradiation, but this had the side effect of causing deterioration in the polyolefin including rupture of the main chains and therefore resulted in reduced strength.

ENTEK Membranes LLC has developed Teklon—a highly porous, ultrahigh molecular weight polyethylene separator for lithium-ion batteries. At the writing of this publication, the separator is available in small quantities. Pekala et al. characterized Celgard, Setela, and Teklon separators in terms of their physical, mechanical, and electrical properties.[75]

Celgard's separators are by far the best-characterized battery separators in the literature as they have been widely used in numerous battery systems. Bierenbam et al.[45] has described the process, physical and chemical properties, and end-use applications. Fleming and Taskier[76] described the use of Celgard microporous membranes as battery separators. Hoffman et al.[77] presented a comparison of PP and PE Celgard microporous materials. Callahan discussed a number of novel uses of Celgard membranes. Callahan and co-workers[98] also characterized Celgard membranes by SEM image analysis, mercury porosimetry, air permeability, and electrical resistivity, and later they characterized the puncture strength

CosMX Exhibit 1003, Page 290 of 512

and temperature/impedance data for Celgard membranes.[40] Spotnitz et al. reported short-circuit behavior in simulated, spirally wound cells, as well as impedance/temperature behavior and thermomechanical properties.[108] Yu[78] found that a trilayer structure of PP/PE/PP Celgard microporous membranes provided exceptional puncture strength.

Nonwoven materials such as cellulosic fibers have never been successfully used in lithium batteries. This lack of interest is related to the hygroscopic nature of cellulosic papers and films, their tendency to degrade in contact with lithium metal, and their susceptibility to pinhole formation at thickness of less than 100 μm. For future applications, such as electric vehicles and load leveling systems at electric power plants, cellulosic separators may find a place because of their stability at higher temperatures when compared to polyolefins. They may be laminated with polyolefin separators to provide high-temperature melt integrity.

Asahi Chemical Industry carried out an exploratory investigation to determine the requirements for cellulose based separators for lithium-ion batteries.[79] In an attempt to obtain an acceptable balance of lithium-ion conductivity, mechanical strength, and resistance to pinhole formation, they fabricated a composite separator (39−85 μm) that consists of fibrilliform cellulosic fibers (diameter 0.5−5.0 μm) embedded in a microporous cellulosic (pore diameter: 10−200 nm) film. The fibers can reduce the possibility of separator meltdown under exposure to heat generated by overcharging or internal short-circuiting. The resistance of these films was equal to or lower than the conventional polyolefin-based microporous separators. The long-term cycling performance was also very comparable.

Pasquier et al.[80] used paper based separators in flat pouch type lithium-ion batteries and compared the performance with cells made with Celgard type polyolefin based separators. The paper separators had good wetting properties and good mechanical properties but did not provide the shutdown effect essential for large lithium-ion batteries. Their resistance was similar to polyolefin separators, and when all water traces were removed from paper, their cycling performance was similar to that of Celgard separators. The paper-based separators can be used in small flat pouch type cells where high strength and shutdown behavior is not required. For larger spherically wound cells, which require strong separators with a shutdown feature, one can never use paper-based separators.

Recently Degussa announced that they have developed Separion separators for lithium batteries by combining the characteristics of flexible polymeric separators with the advantages of chemical and thermally resistant and hydrophilic ceramic materials. Separion is produced in a continuous coating process. Ceramic materials, e.g., alumina, silica, and/or zirconia are slip coated and hardened onto a support.[81,82] According to Degussa, Separion separators have an excellent high temperature stability, superior chemical resistance, and good wettability, especially at low temperatures. They tested the performance and safety behavior of Separion separator in 18650 cells and found the performance to be comparable to that of polyolefin-based separators.[83]

The potential use of polymeric ion-exchange membranes in the next generation single-ion secondary lithium polymer batteries was shown by Sachan et al.[84,85] Conductivities exceeding 10^{-4} S/cm with transference numbers of unity were achieved for Nafion converted to the Li^+ salt form.

To obtain a thin (less than 15 μm) separator for lithium batteries, Optodot has taken a different approach of high-speed coating of a metal oxide sol−gel coating on a smooth surface followed by a delamination step to provide the free-standing separator. Using this approach, separator with thicknesses from 6 to 11 μm was made on large-scale production coating equipment.[86] They found that the sol−gel separators with a thickness in the middle of this range of 8−9 μm have the preferred combination of thinness and strength. The metal oxide sol−gel coating is water-based with no organic solvents present. The coating formulations include a polymer and a surfactant. The polymer provides improved coating rheology, mechanical strength, and other properties. The surfactant provides improved wetting properties on the substrate. The films prepared were around 11 μm thick, with 45% porosity, and were completely wettable in nonaqueous electrolyte and had a melt temperature greater than 180 °C. These films are relatively thin and should help in increasing the capacity but may not be strong enough for tightly wound cells. Moreover, the shutdown temperature of the separator seems to be very high and thus not suitable for lithium-ion batteries.

Gineste et al. carried out the grafting of hydrophilic monomers onto PP or PE separators to improve the wettability of separators used in secondary lithium batteries with a lower content of wetting agents.[87,88] They used a PP film (Celgard 2505) of 50 μm thickness after irradiating in air by electron beams with a dose ranging from 0.5 to 4 Mrad. The irradiated film was grafted by a monofunctional monomer (acrylic acid, AA), in the presence of difunctional cross-linking agent (diethylene glycol dimethacrylate, DEGDM). The separators start loosing mechanical properties, when the grafting ratio is higher than 50%.

6.1.2. Separator Requirements

In lithium-based cells, the essential function of battery separator is to prevent electronic contact, while enabling ionic transport between the positive and negative electrodes. It should be usable on high-speed winding machines and possess good shutdown properties. The most commonly used separators for primary lithium batteries are microporous polypropylene membranes. Microporous polyethylene and laminates of polypropylene and polyethylene are widely used in lithium-ion batteries.[89] These materials are chemically and electrochemically stable in secondary lithium batteries.

The general requirements[90] for lithium-ion battery separators are given below.

6.1.2.1. Thickness. The lithium-ion cells used in consumer applications use thin microporous separators (<25 μm). The separators being developed for EV/HEV applications will require thicker (~40 μm) separators. The thicker the separator, the greater the mechanical strength and the lower the probability of punctures during cell assembly but the smaller the amount of active materials that can be placed in the can. The thinner separators take up less space and permit the use of longer electrodes. This increased both capacity and, by increasing the interfacial area, rate capability. The thinness also makes it a low resistance separator.

6.1.2.2. Permeability. The separators should not limit the electrical performance of the battery under normal conditions. Typically the presence of separator increases the effective resistivity of the electrolyte by a factor of 6−7. The ratio of the resistivity of the separator filled with electrolyte divided by the resistivity of the electrolyte alone is called MacMullin number. MacMullin numbers are as high as 10−12 have been used in consumer cells.

6.1.2.3. Gurley (Air Permeability). Air permeability is proportional to electrical resistivity, for a given separator morphology. It can be used in place of electrical resistance (ER) measurements once the relationship between gurley and ER is established. The separator should have low gurley values for good electrical performance.

6.1.2.4. Porosity. It is implicit in the permeability requirement; typically lithium-ion battery separators have a porosity of 40%. Control of porosity is very important for battery separators. Specification of percent porosity is commonly an integral part of separator acceptance criteria.

6.1.2.5. Wettability. The separators should wet out quickly and completely in typical battery electrolytes.

6.1.2.6. Electrolyte Absorption & Retention. A separator should be able to absorb and retain electrolyte. Electrolyte absorption is needed for ion transport. The microporous membranes usually do not swell on electrolyte absorption.

6.1.2.7. Chemical Stability. The separators should be stable in the battery for a long period of time. They should be inert to both strong reducing and strong oxidizing conditions and should not degrade or loose mechanical strength or produce impurities, which can interfere with the function of the battery. The separator must be able to withstand the strong oxidizing positive electrode and the corrosive nature of the electrolyte at temperatures as high as 75 °C. The greater the oxidation resistance, the longer the separator will survive in a cell. Polyolefins (e.g., polypropylene, polyethylene) exhibit high resistance to most of the conventional chemicals, good mechanical properties, and a moderate temperature range for application making them ideal polymers for lithium-ion battery separators. Polypropylene separators exhibit better oxidation resistance properties when in contact with the positive electrode in a lithium-ion cell. Thus, the oxidation resistance properties of trilayer (PP/PE/PP) separators with PP as the outside layer and PE as inner layer are superior.

6.1.2.7. Dimensional Stability. The separator should lay flat and should not curl at the edges when unrolled, as this can greatly complicate cell assembly. The separator should also not shrink when exposed to electrolyte. The cell winding should not affect the porous structure in any adverse way.

6.1.2.8. Puncture Strength. The separators used in wound cells require a high puncture strength to avoid penetration of electrode material through the separator. If particulate material from the electrodes penetrates the separator, an electrical short will result and the battery will be rejected. The separators used in lithium-ion batteries require more strength then the one used in lithium primary batteries. The primary lithium batteries have only one rough electrode, and thus it requires less strength. As empirically observed, for most applications, the puncture strength should be at least 300 g/mil for separators used in lithium-ion cells. Mix penetration strength is a better measure of separator strength in a battery compared to puncture strength.

6.1.2.9. Mix Penetration Strength. The susceptibility of separators to particle penetration is characterized by mix penetration strength.[49] During the winding of the spiral wrap construction considerable mechanical pressure is applied to the cathode−separator−anode interface. Any loose particle could be forced through the separator and short the cell. The mix penetration strength should be at least 100 kgf/mil for separators used in lithium-ion cells.

6.1.2.10. Thermal Stability. Lithium-ion batteries can be poisoned by water, and so materials going into the cell are typically dried at 80 °C under vacuum. Under these conditions, the separator must not shrink significantly and definitely must not wrinkle. Each battery manufacturer has specific drying procedures. The requirement of less than 5% shrinkage after 60 min at 90 °C (in a vacuum) in both MD and TD direction is a reasonable generalization.

6.1.2.11. Pore Size. A key requirement of separators for lithium batteries is that their pores be small enough to prevent dendritic lithium penetration through them. Membranes with submicrometer pore sizes have proven adequate for lithium batteries.

6.1.2.12. Tensile Strength. The separator is wound with the electrodes under tension. The separator must not elongate significantly under tension in order to avoid contraction of the width. A tensile strength specification is sometimes given, but the key parameter is Young's modulus in the machine direction. Since Young's modulus is difficult to measure, a 2% offset yield is a good measure; less than 2% offset at 1000 psi is acceptable for most winding machines.

6.1.2.13. Skew. Ideally, when a strip of separator is laid out, the separator should be straight and not bow or skew. In practice, however, some skew is often observed. If sufficiently extreme, the skew can cause misalignment between the electrodes and separator. Skew can be measured by laying the separator flat

CosMX Exhibit 1003, Page 292 of 512

Table 5. General Requirements for Lithium-ion Battery Separator[90]

parameter	goal
thickness[a,b] (μm)	<25
electrical resistance (MacMullin no.,[c] dimensionless)	<8
electrical resistance (ohms cm^2)	<2
gurley[d] (s)	~ 25/mil
pore size[e] (μm)	< 1
porosity (%)	~ 40
puncture strength[f] (g/mil)	>300
mix penetration strength (kgf/mil)	>100
shrinkage[g] (%)	<5% in both MD and TD
tensile strength[h] (%)	<2% offset at 1000 psi
shutdown temp (°C)	~130
high-temp melt integrity (°C)	>150
wettability	complete wet out in typical battery electrolytes
chemical stability	stable in battery for long period of time
dimensional stability	separator should lay flat; be stable in electrolyte
skew (mm/m)	<0.2

[a] ASTM D5947-96. Standard Test Methods for Physical Dimensions of Solid Plastics Specimens. ASTM International. [b] ASTM D2103. Standard Specification for Polyethylene Film and Sheeting", ASTM International. [c] Caldwell, D. L.; Poush, K. A. U.S. Patent, 4,464,238, 1984. [d] ASTM D726. Standard Test Methods for Identification of Fibers in Textiles. ASTM International. [e] ASTM E128-99. Standard test method for Maximum Pore Diameter and Permeability of Rigid Porous Filters for Laboratory Use. ASTM International. [f] ASTM D3763. Standard Test Method for High-Speed Puncture Properties of Plastics using Load and Displacement Sensors. ASTM International. [g] ASTM D1204. Standard Test methods for Linear Dimensional Changes of Nonrigid Thermoplastic Sheeting or Film at Elevated Temperatures. ASTM International. [h] ASTM D882. Standard Test Method for Tensile Properties of Thin Plastic Sheeting. ASTM International.

on a table parallel with a straight meter stick. The skew should be less than 0.2 mm/m of separator.

6.1.2.14. Shutdown. Lithium-ion batteries separators provide some margin of protection against short circuit and overcharge in lithium-ion cells. The separators exhibit a large increase in impedance at temperature about 130 °C that effectively stops ionic transport between the electrodes.[91,92] The greater the mechanical integrity of the separator above 130 °C, the greater the margin of safety the separator can provide. If the separator loses mechanical integrity, then the electrodes can come into direct contact, react chemically, and result in thermal runaway. The shutdown behavior of a separator can be characterized by heating the separator (saturated with electrolyte) to high temperatures and simultaneously monitoring the electrical resistance of the separator.[92,108]

6.1.2.15. High-Temperature Stability. A separator might provide an extra margin of safety if it can prevent the electrodes from contacting one another at high temperatures. Separators with good mechanical integrity at high temperatures can provide a greater margin of safety for lithium-ion cells. Thermal mechanical analysis (TMA) can be used to characterize the high-temperature stability of separators. Utilizing TMA, the separator is held under constant load and the degree of elongation vs. temperature is measured; at the temperature where the separator loses mechanical integrity, the elongation increases dramatically.

6.1.2.16. Electrode Interface. The separator should form a good interface with the electrodes to provide sufficient electrolyte flow.

In addition to the above properties, the separator must be essentially free of any type of defects (pinholes, gels, wrinkles, contaminants, etc.). All of the above properties have to be optimized before a membrane qualifies as a separator for a lithium-ion battery. The general requirements for lithium-ion battery separators are also summarized in Table 5.

6.1.3. Separator Properties/Characterization

Separators are characterized by structural and functional properties; the former describes what they are and the latter how they perform. The structural properties include chemical (molecular) and microcrystalline nature, thickness, pore size, pore size distribution, porosity, and various chemical and physical properties such as chemical stability, and electrolyte uptake. The functional properties of interest are electrical resistivity, permeability, and transport number. It is useful to characterize separator materials in terms of their structural and functional properties and to establish a correlation of these properties with their performance in batteries. A variety of techniques are used to evaluate separators. Some of these techniques are discussed in this section.

6.1.3.1. Gurley. Separator permeability is usually characterized by air permeability. The gurley number expresses the time required for a specific amount of air to pass through a specific area of separator under a specific pressure. The standard test method is described in ASTM-D726 (B).

The gurley number is used to characterize separators because the measurement is accurate and easy to make, and deviations from specific values are a good indication of problems. Air permeability (gurley) is proportional to electrical resistance (ER), for a given separator morphology.[98] Gurley can be used in place of ER measurements once the relationship between gurley and ER is established. A lower gurley value means higher porosity, lower tortuosity, and accordingly lower ER.

6.1.3.2. Electrical Resistance. The measurement of separator resistance is very important to the art of battery manufacture because of the influence the

separator has on electrical performance. Electrical resistance is a more comprehensive measure of permeability then the gurley number, in that the measurement is carried out in the actual electrolyte solution. The ionic resistivity of the porous membrane is essentially the resistivity of the electrolyte that is embedded in the pores of the separator. Typically, a microporous separator, immersed in an electrolyte has an electrical resistivity about 6−7 times that of a comparable volume of electrolyte, which it displaces. It is a function of the membrane's porosity and tortuosity, the resistivity of the electrolyte, the thickness of the membrane, and the extent to which the electrolyte wets the pores of the membrane.[93] The electrical resistance of the separator is the true performance indicator of the cell. It describes a predictable voltage loss within the cell during discharge and allows one to estimate rate limitations.

Classical techniques for measuring electrical resistivity of microporous separators have been described by Falk and Salkind[5] and by Robinson and Walker.[94] The resistivity of an electrolyte is more accurately determined by ac methods since dc can polarize the electrodes and cause electrolysis of the solution. Modern ac impedance measuring systems allow rapid measurements of cell resistance over a wide range or frequencies from which resistance can be calculated free of capacitance effects. Compared to the dc techniques, the equipment required and the theory necessary to interpret the ac techniques are more complex; however, ac measurements yield information about long-range migration of ions and polarization phenomena occurring within the cell. In an ac measurement, a sinusoidal voltage is applied to a cell, and the sinusoidal current passing through the cell as a result of this perturbation is determined. A four-electrode cell is usually used for resistivity measurements. The outer two electrodes serve to apply a sinusoidal potential, and the resulting current passing through the inner two electrodes is measured. This technique is employed to avoid the complications arising from a nonuniform potential field near the outer two electrodes. An excellent review of experimental techniques for measuring electrical resistivity in aqueous solution is available.[95,96]

The separator resistance is usually characterized by cutting small pieces of separators from the finished material and then placing them between two blocking electrodes. The separators are completely saturated with the electrolyte. The resistance (Ω) of the separator is measured at a certain frequency by ac impedance techniques. The frequency is chosen so that the separator impedance is equal to the separator resistance. To reduce the measurement error, it is best to do multiple measurements by adding extra layers. The average resistance of single layer is determined from multiple measurements. The specific resistivity, ρ_s (Ω cm), of the separator saturated with electrolyte is given by

$$\rho_s = \frac{R_s A}{l} \tag{1}$$

where R_s is the measured resistance of separator in Ω, A is the electrode area in cm^2, and l is the thickness of membrane in cm. Similarly, the specific resistivity of the electrolyte, ρ_e (Ω cm), is given by

$$\rho_e = \frac{R_e A}{l} \tag{2}$$

where R_e is the measured resistance of electrolyte in Ω. The ratio of the resistivity of a separator membrane to that of the electrolyte is called the MacMullin number, N_m, which can be used to predict the influence of the separator on battery performance.[97]

$$N_m = \frac{\rho_s}{\rho_e} = \frac{\tau^2}{\epsilon} \tag{3}$$

where τ is the tortuosity and ϵ is the porosity of the separator. The MacMullin number describes the relative contribution of a separator to cell resistance. It is almost independent of electrolyte used and also factors out the thickness of the material. It assumes that the separator wets completely in the electrolyte used for the test. From eqs 1 and 3, the electrical resistance of a microporous membrane is given by the following[5,114]

$$R_m = \rho_e\left(\frac{\tau^2 l}{\epsilon A}\right) \tag{4}$$

It has been shown for Celgard membranes that the membrane resistance can be related to the gurley number by[98]

$$R_m A = \frac{\rho_e}{5 \times 18 \times 10^{-3}} t_{gur} d \tag{5}$$

where R_m is the membrane resistance (Ω), A is the membrane area (cm^2), ρ_e is the specific electrolyte resistance (Ω cm), t_{gur} is the gurley number (10 cm^3 air, 2.3 mmHg), d is the pore size, and $5 \times 18 \times 10^{-3}$ is a scaling factor.

The usual procedure for characterizing battery separators is to cut several test samples from the finished material. Thus, only a small portion of the separator is actually examined. Ionov et al. has proposed an alternative technique to measure the resistance of a separator over a large separator area.[99] In this technique, the separator material is passed through an electrolyte bath between electrical resistance measuring transducers. The set of transducers installed in the bath transverse to the moving sheet of separator material examines the whole surface of the material. If the production process ensures good uniformity in the physicochemical properties of the separator material over the whole surface, the transducer outputs will clearly be close to one another. A nonuniform separator will cause significant deviations from the average value at various sections of the material. In this case, the sections having lower or higher resistance compared with the average value should be regarded as flawed.

6.1.3.3. Porosity. The porosity is important for high permeability and also for providing a reservoir of electrolyte in the cell. Higher and uniform porosity is desirable for unhindered ionic current flow. Non-

uniform porosity leads to nonuniform current density and can further lead to reduced activity of the electrodes. Cell failure can result because during discharge some areas of the electrodes work harder then other.

Porosity of a separator is defined as the ratio of void volume to apparent geometric volume. It is usually calculated (eq 6) from the skeletal density, basis weight, and dimensions of the material and so may not reflect the accessible porosity of the material.

$$\text{porosity (\%)} = \left[1 - \frac{(\text{sample weight}/\text{sample volume})}{\text{polymer density}}\right] \times 100 \quad (6)$$

The standard test method is described in ASTM D-2873. The actual or accessible porosity can also be determined by the weight of liquid (e.g., hexadecane) absorbed in the pores of the separator. In this method, the separator weight is measured before and after dipping in hexadecane solvent, and the porosity is calculated (eq 7) by assuming that volume occupied by hexadecane is equal to the porous volume of the separator.

$$\text{porosity (\%)} = \frac{\text{volume occupied by hexadecane}}{(\text{volume of polymer} + \text{volume occupied by hexadecane})} \times 100 \quad (7)$$

6.1.3.4. Tortuosity. Tortuosity is the ratio of mean effective capillary length to separator thickness. The tortuosity factor, τ of a separator can be expressed by

$$\tau = \frac{l_s}{d} \quad (8)$$

where l_s is the ion path through the separator and d is the thickness of the separating layer.

Tortuosity is a long-range property of a porous medium, which qualitatively describes the average pore conductivity of the solid. It is usual to define τ by electrical conductivity measurements. With knowledge of the specific resistance of the electrolyte and from a measurement of the sample membrane resistance, thickness, area, and porosity, the membrane tortuosity can be calculated from eq 3.

This parameter is widely used to describe the ionic transport by providing information on the effect of pore blockage. A tortuosity factor $\tau = 1$, therefore, describes an ideal porous body with cylindrical and parallel pores, whereas values of $\tau > 1$ refer to more hindered systems. Higher tortuosity is good for dendrite resistance but can lead to higher separator resistance.

6.1.3.5. Pore Size and Pore Size Distribution. For any battery applications, the separator should have uniform pore distribution to avoid performance losses arising from nonuniform current densities. The submicrometer pore dimensions are critical for preventing internal shorts between the anode and the cathode of the lithium-ion cell, particularly since these separators tend to be as thin as 25 μm or less. This feature will be increasingly important as battery manufacturers continue to increase the cell capacity with thinner separators. The pore structure is usually influenced by polymer composition, and stretching conditions, such as drawing temperature, drawing speed, and draw ratio. In the wet process, the separators produced by the process of drawing after extraction (as claimed by Asahi Chemical and Mitsui Chemical) are found to have much larger pore size (0.24−0.34 μm) and wider pore size distribution than those produced by the process of extraction (0.1−0.13 μm) after drawing (as claimed by Tonen).[58]

The testing of battery separators and control of their pore characteristics are important requirements for proper functioning of batteries. Mercury porosimetry has been historically used to characterize the separators in terms of percentage porosity, mean pore size and pore size distribution.[100] In this method, the size and volume of pores in a material are measured by determining the quantity of mercury, which can be forced into the pores at increasing pressure. Mercury does not wet most materials, and a force must be applied to overcome the surface tension forces opposing entry into the pores.

The hydrophobic (e.g. polyolefins) separators are also characterized with Aquapore (non-mercury porosimetry) technique, where water is used in place of mercury. This is a very useful technique for characterizing polyolefin-based separators used in lithium batteries.[101] Porosimetry gives pore volume, surface area, mean pore diameter, and pore size distribution. In a typical experiment, the sample is placed in the instrument and evacuated. As the pressure increase, the quantity of water forced into the pores increases in proportion to the differential pore volume, the size of the pores corresponding to the instantaneous pressure. Thus, increasing the pressure on a membrane having a given pore size distribution results in a unique volume vs pressure or pore diameter curve. The pressure required for intrusion of water in to a pore of diameter, D, is given by following equation

$$D = \frac{4\gamma \cos\theta}{p} \quad (9)$$

where D is the diameter of the pore assuming the pore to be cylindrical, p is the differential pressure, γ is the surface tension of the nonwetting liquid, water, and θ is the contact angle of water. The pores generally are not of spherical shape of a constant diameter. They usually vary in their form and size. Thus, statements of any pore diameter are always to be viewed with the above in mind.

Another technique, capillary flow porometry has been developed by Porous Materials Inc.[102] to characterize battery separators.[103,104] The instrument can measure a number of characteristics of battery separators such as size of the pore at its most constricted part, the largest pore size, pore size distribution, permeability, and envelope surface area.[109]

Scanning electron microscopy (SEM) is also used to examine separator morphology. SEM pictures of some commercial membranes are shown in Figures

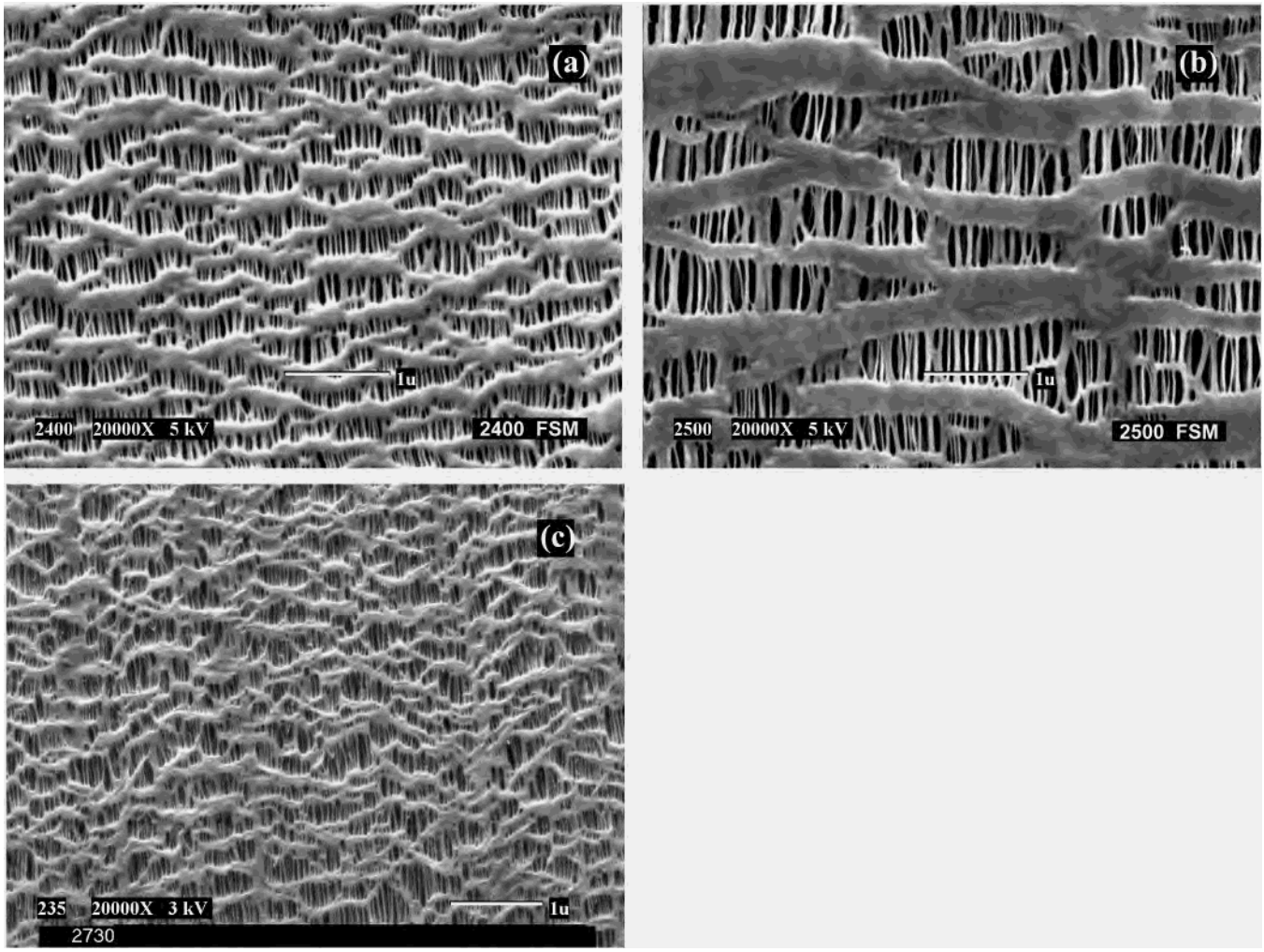


Figure 4. Scanning electron micrographs of the surface of single layer Celgard separators used in lithium batteries: (a) 2400 (PP), (b) 2500 (PP), and (c) 2730 (PE).

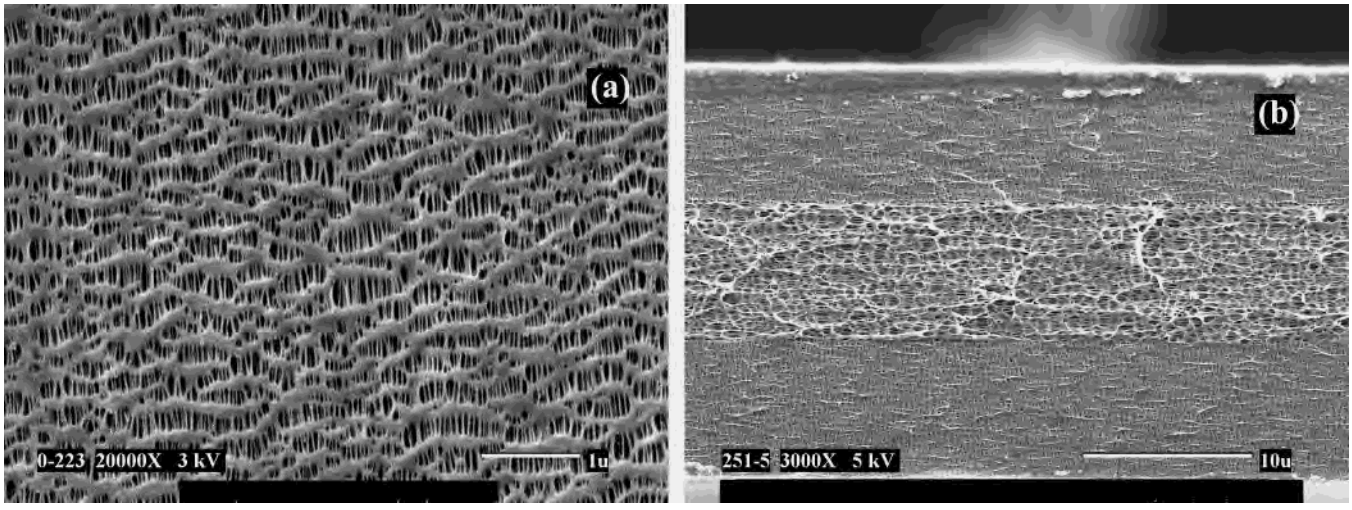


Figure 5. Scanning electron micrographs of Celgard 2325 (PP/PE/PP) separator used in lithium-ion batteries: (a) surface SEM and (b) cross-section SEM.

4−6. The surface SEM of Celgard 2400, 2500, and 2730 are shown in Figure 4. It is clear from the images that the pores are uniformly distributed. Both Celgard 2400 and 2500 are single layer PP separators, but the pore size of Celgard 2500 is substantially larger than Celgard 2400. Thus, it has lower resistance and is more suited for high rate applications. Figure 5 shows the surface SEM and cross-section SEM of Celgard 2325. The surface SEM only shows the PP pores while the PE pores are visible in the cross-section. It is clear from the image that all three layers are of equal thickness. The SEM of separators made by wet process are shown in Figure 6. The pore structure of all of these membranes is very similar.

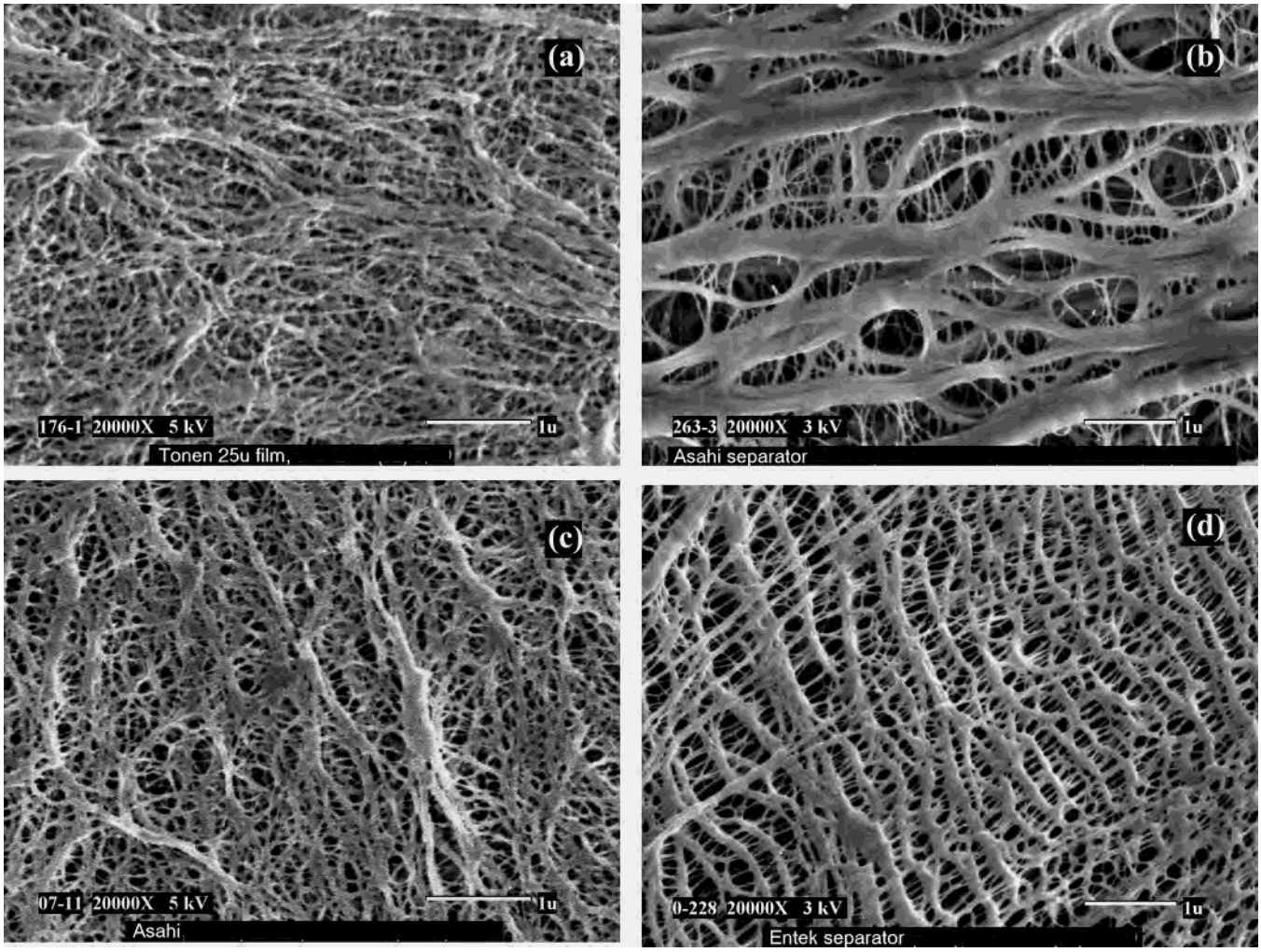


Figure 6. Scanning electron micrographs of separators made by wet process and used in lithium-ion batteries: (a) Setela (Tonen), (b) Hipore-1 (Asahi), (c) Hipore-2 (Asahi), and (d) Teklon (Entek).

Asahi-1 (Figure 6b) separator has significantly larger pores compared to the other membranes.

Image analysis has been used to characterize the pore structure of synthetic membrane materials.[105] The Celgard films have also been characterized by scanning tunneling microscopy, atomic force microscopy, and field emission scanning electron microscopy.[53,106] The pore size of the Celgard membranes can also be calculated from eq 5, once the MacMullin number and gurley values are known.

6.1.3.6. Puncture Strength. A separator is required to have sufficient physical strength to endure the rigors of cell assembly and day-to-day charge−discharge cycling. Physical strength is required to withstand basic handling, cell blocking/assembly, physical shock, punctures, abrasion, and compression.

The puncture strength (PS) is the weight that must be applied to a needle to force it completely through a separator.[45,107] It has been used to indicate the tendency of separators to allow short-circuits in a cell that may occur due to holes generated in the separator by the rough surface of an electrode during the battery assembly and charge−discharge cycle. The PS requirement for lithium-ion batteries is higher them lithium-foil batteries, because the separator must contend with two rough surfaces. Commercially available puncture strength machines made for textiles tend to give meaningless results when testing battery separator membranes. More reproducible results can be obtained with a load frame (such as an Instron Machine). The mix penetration strength is a better measure of mechanical strength for battery separators as it measures the force required to create a short through the separator when electrode mix is pushed through it.

The strength of the separator depends greatly on the materials used and the manufacturing method. The wet-biaxial method simultaneously stretches in the MD and TD directions and thus achieves a material that has tensile modulus and rupture strength in both directions. Both high polymer entanglement and stretching help increase the physical strength of the separator.

6.1.3.7. Mix Penetration Strength. The force required to create a short through a separator due to mix (electrode material) penetration defines mix penetration strength. In this test force (with a $^1/_2$ in. diameter ball) is applied on the positive electrode/separator/negative electrode sandwich, and the force at which the mix penetrates through the separator and creates an electronic short is called mix penetration force. Mix penetration strength is used to indicate the tendency of separators to allow short-

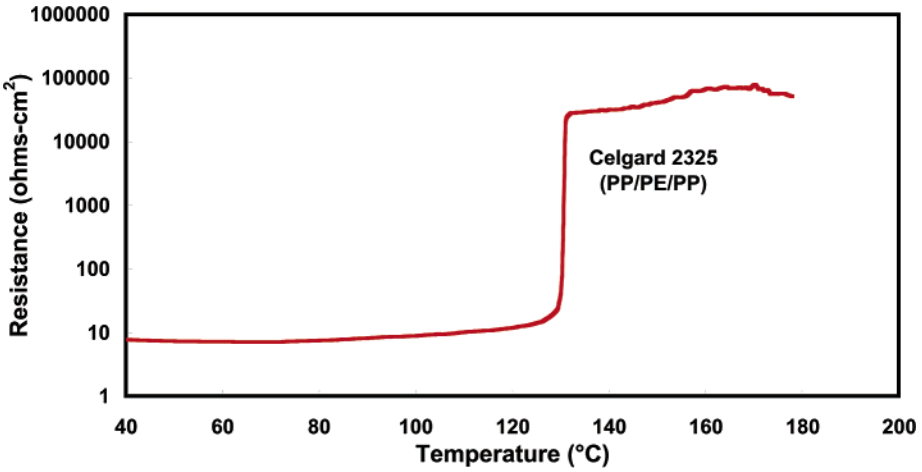


Figure 7. Internal impedance (at 1 kHz) of Celgard 2325 (PP/PE/PP) separator as a function of temperature. Heating rate: 60 °C/min.

circuits during battery assembly. The mix penetration resistance test is more closely related to particle penetration resistance compared to puncture resistance.[49]

6.1.3.8. Tensile Strength. The tensile strength measurements (e.g., Young's modulus, percent offset strength, elongation at break, and stress at break) can be made by utilizing widely known standard procedures. These tests are carried out in both MD and TD directions. The tensile properties are dependent on the manufacturing process. The uniaxially oriented films have high strength in only one direction, whereas biaxially oriented films are more uniformly strong in both MD and TD directions. ASTM test method D88-00, "Standard test method for tensile properties of thin plastic sheeting", is an appropriate test.

The separator should be strong enough to withstand mechanical handling during cell winding and assembly. It should be dimensionally stable and should not neck down during winding. The decrease in width will allow the electrodes to touch each other and create a short. Thus, the tensile property of the separator should be very strong in MD direction compared to TD direction.

6.1.3.9. Shrinkage. Shrinkage test is carried out on both MD and TD directions. In this test, the dimensions of separators are measured and then stored at 90 °C for a fixed time. The shrinkage is then calculated from the change in dimensions as shown in eq 10.

$$\text{shrinkage (\%)} = \frac{L_i - L_f}{L_i} \times 100 \qquad (10)$$

where L_i is the initial length and L_f is the final length of separator after high temperature storage. The uniaxially stretched separators tend to shrink in the MD direction only, while the biaxially stretched separators shrink in both MD and TD directions. The shrinkage of separators can also be compared by carrying out the thermal mechanical analysis (TMA) test at a constant load and rate.

6.1.3.10. Shutdown. Separator shutdown is a useful and essential mechanism for limiting temperature and preventing venting in short-circuited cells.[108] It usually takes place close to the melting temperature of the polymer when the pores collapse turning the porous ionically conductive polymer film into a nonporous insulating layer between the electrodes. At this temperature there is a significant increase in cell impedance and passage of current through the cell is restricted. This prevents further electrochemical activity in the cell, thereby shutting the cell down before an explosion can occur.

The ability of the PE based separator to shutdown the battery is determined by its molecular weight, percent crystallinity (density) and process history. Material properties and processing methods might need to be tailored so that the shutdown response is spontaneous and complete. The optimization needs to be done without affecting the mechanical properties of the material in the temperature range of interest. This is easier to do with the trilayer separators manufactured by Celgard since one material is utilized for the shutdown response and another for the mechanical properties. Polyethylene containing separators, in particular trilayer laminates of polypropylene, polyethylene, and polypropylene, appear to have the most attractive properties for preventing thermal runaway in lithium-ion cells.[109,110] The shutdown temperature of 130 °C is usually enough to control the cell heating and avoid thermal runaway in lithium-ion cells. A lower temperature shutdown will be desirable if it does not affect the separator mechanical properties or high-temperature cell performance in any adverse way.

The shutdown property of separators is measured by measuring the impedance of a separator while the temperature is linearly increased.[92,108] Figure 7 shows the actual measurement for Celgard 2325 membrane. The heating rate was around 60 °C/min, and the impedance was measured at 1 kHz. The rise in impedance corresponds to a collapse in pore structure due to melting of the separator. A 1000-fold increase in impedance is necessary for the separator to stop thermal runaway in the battery. The drop in impedance corresponds to opening of the separator due to coalescence of the polymer and/or to penetration of the separator by the electrodes; this phenomenon is

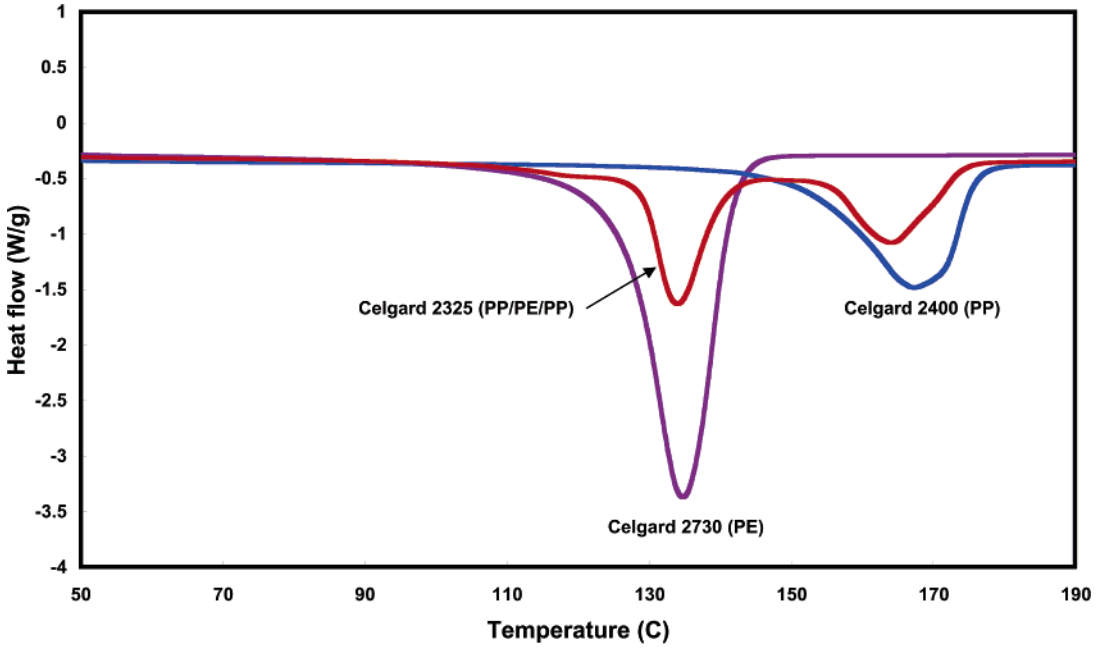


Figure 8. DSC of Celgard 2730 (PE), 2400 (PP), and 2325 (PP/PE/PP).

referred to as a loss in "melt integrity". This test is fairly reliable in indicating the temperature at which the impedance rises but shows some variability in characterizing the subsequent drop in impedance.

In Figure 7, the shutdown behavior of a multilayer (PP/PE/PP) separator (Celgard 2325) is shown. The impedance rise occurred near the melting point of polyethylene (130 °C) and remained high until such time as the melting point of polypropylene (165 °C) is attained. The shutdown temperature of the separator is governed by the melting point of the separator material. At the melting point the pores in the separator collapse to the form a relatively nonporous film between the anode and the cathode. This was confirmed by DSC as shown in Figure 8. The DSC scan in Figure 8 gives a peak melting temperature of 135 °C for Celgard 2730, 168 °C for Celgard 2400, and 135/165 °C for Celgard 2325. The shutdown behavior of thinner separators (<20 μm) is very similar to thicker separators. The battery manufacturers have been very successful in using the thinner separators without compromising on the shutdown behavior of the separators.

Laman et al. introduced the use of impedance measurements as a function of temperature to characterize shutdown separators.[92] Using a temperature scan rate of 1 °C/min, they found that the impedance increased several orders of magnitude near the melting point of the separator. They verified the patent claims of Lundquist et al.[111] that bilayer separators of PE and PP gave a temperature window of high impedance extending approximately between the melting point of the polymers. The concept of using separators consisting of distinct layers, one of which could act as a fuse, was developed by Lundquist et al.[112,113] Laman's results have been corroborated by Geiger et al.[40] and Spotnitz et al.[108,114] Spotnitz et al. developed a thin layer cell which allowed temperature scan rates of 5 °C/min and higher and obtained results similar to those of Laman et al.

Prior work related with shutdown separators also involved application of waxes on membranes.[115,116] In these cases, the wax or low melting polymers were coated on the polyolefin separator. The disadvantage of this technique is that the coating can block the pores of the separator and thus can affect the performance by increasing separator resistance. Moreover, the coating level has to be very high to get complete shutdown.

The shutdown characteristic provides protection from external short-circuit and during cell overcharge. It provides little protection from internal shorts should they occur. Should the electrodes touch each other or become shorted from a dendritic growth of soluble impurity or other dendrite forming soluble material, the separator only helps in avoiding delayed failures. In the case of an instant failure during an internal short circuit, the heating rate is too high and the separator shutdown is not fast enough to control the heating rate.

6.1.3.11. Melt Integrity. The separators used in lithium-ion batteries should have high-temperature melt integrity. The separator should maintain its melt integrity after shutdown so that the electrodes do not touch and create a short. This helps in avoiding the thermal runaway even when the cell is exposed to high temperatures. Thermal mechanical analysis (TMA) is a very good technique to measure the high-temperature melt integrity of separators.

TMA involves measuring the shape change of a separator under load while the temperature is linearly increased. Typically, separators show some shrinkage and then start to elongate and finally break as shown in Figure 9. This test utilizes a small separator samples (about 5−10 mm length (MD) and

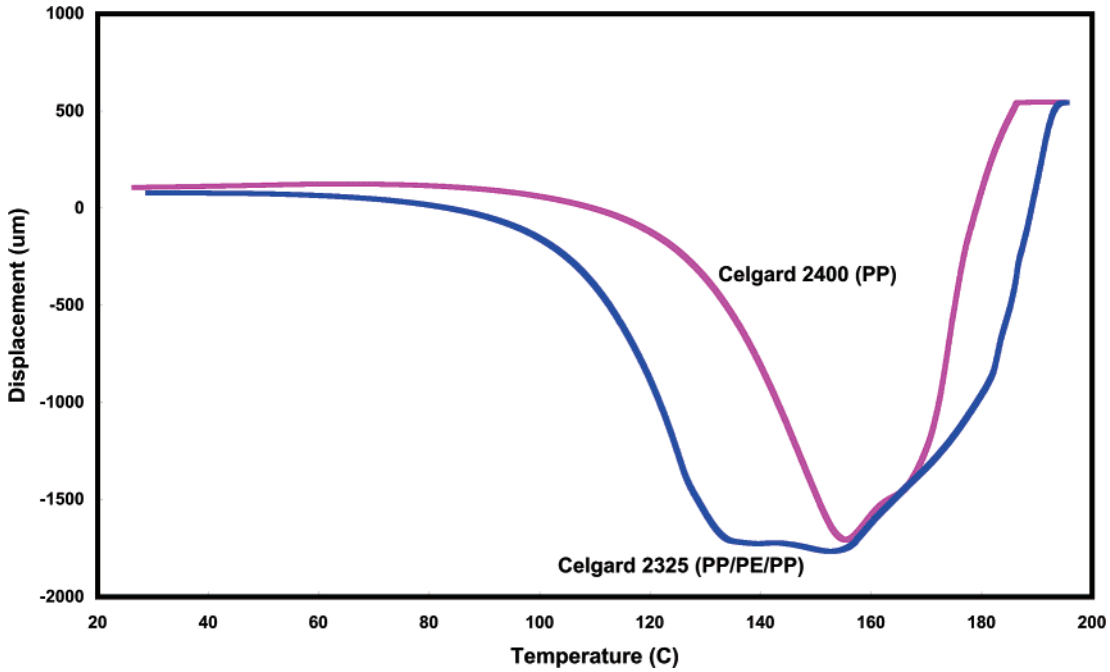


Figure 9. TMA of Celgard 2400 (PP) and 2325 (PP/PE/PP). A constant load (2 g) is applied while the temperature is ramped at 5 °C/min.

Table 6. TMA Data for Typical Celgard Separators

	Celgard 2400	Celgard 2325
shrinkage onset temp (°C)	121	106
deformation temp (°C)	156	135, 154
rupture temp (°C)	183	192

about 5 mm width), which is held in mini-instron type grips. The sample is held with a constant 2 g load while the temperature is ramped at 5 °C/min past the melting point until the tension ruptures the film. Three parameters are reported from TMA test—shrinkage onset temperature, melt temperature, and melt rupture temperature. It has proved to be a more reproducible measure of melt integrity of the separator.[108]

Figure 9 shows the TMA data for two different Celgard membranes. The shrinkage onset temperature, deformation temperature, and rupture temperature are summarized in Table 6. The single layer PP membrane (Celgard 2400) showed a higher softening temperature (~121 °C), a deformation temperature around 160 °C, and a very high rupture temperature around 180 °C. The multilayer polypropylene/polyethylene/polypropylene separator (Celgard 2325) combined the low-temperature shutdown property of polyethylene with the high-temperature melt integrity of polypropylene, resulting in a separator with softening (~105 °C) and melt temperature (~135 °C) very similar to that of PE and rupture temperature (~190 °C) very similar to that of PP.

Separators with melt integrity greater than 150 °C are desirable for lithium-ion cells. The trilayer separators with polypropylene on the outside help in maintaining the melt integrity of the separators at higher temperatures compared to single layer PE separators. This is especially important for bigger lithium-ion cells being developed for hybrid and electric vehicles.

6.1.3.12. Wettability and Wetting Speed. Two physical properties of separators, which are important to the operating characteristics of a battery, are electrolyte absorption and electrolyte retention. Any good separator should be able to absorb a significant amount of electrolyte and also retain the absorbed electrolyte when the cell is in operation. These are more important in sealed cells where no free electrolyte is present. A maximum amount of electrolyte in the separator is desirable to achieve minimum cell internal resistance.

The separator wettability can limit the performance of batteries by increasing the separator and cell resistance. Separator wetting speed can be correlated with electrolyte filling time in real cells. The wetting speed is determined by the type of polymer (surface energy), pore size, porosity, and tortuosity of the separators. There is no generally accepted test for separator wettability. However, simply placing a drop of electrolyte on the separator and observing whether the droplet quickly wicks into the separator is a good indication of wettability. The contact angle is also a good measure of wettability.

The uptake of electrolyte by many hydrophobic polymer separators can be enhanced either by wetting agents or ionic-functional groups (e.g. ion-exchange membranes).

6.1.4. Effect of Separator on Cell Performance and Safety

Although the material of a battery separator is inert and does not influence electrical energy storage or output, its physical properties greatly influence the performance and safety of the battery. This is especially true for lithium-ion cells, and thus the battery manufacturers have started paying more attention to separators while designing the cells. The cells are designed in such a way that separators do not limit the performance, but if the separator properties are

Table 7. Safety and Performance Tests for Lithium-Ion Batteries and the Corresponding Important Separator Property and Its Effect on the Cell Performance and/or Safety

cell property	separator property	comments
cell capacity	thickness	cell capacity can be increased by making the separator thinner
cell internal resistance	resistance	separator resistance is a function of thickness, pore size, porosity, and tortuosity
high rate performance	resistance	separator resistance is a function of thickness, pore size, porosity, and tortuosity
fast charging	resistance	low separator resistance will aid in overall faster charging by allowing higher and/or longer constant current charging
high-temp storage	oxidation resistance	oxidation of separators can lead to poor storage performance and reduce performance life
high-temp cycling	oxidation resistance	oxidation of separators can lead to poor cycling performance
self-discharge	weak areas, pinholes	soft shorts during cell formation and testing can lead to internal current leakage
long-term cycling	resistance, shrinkage, pore size	high resistance, high shrinkage and very small pore size can lead to poor cycling performance
overcharge	shutdown behavior; high-temp melt integrity	separator should completely shutdown and then maintain its melt integrity at high temp
external short circuit	shutdown behavior	separator shutdown stops the cells from overheating
hotbox	high-temp melt integrity	separator should be able to keep the two electrodes apart at high temp
nail crush	shutdown (to stop delayed failure)	in the case of internal shorts, the separator may be the only safety device to stop the cell from overheating
bar crush	shutdown (to stop delayed failure)	in the case of internal shorts, the separator may be the only safety device to stop the cell from overheating

not uniform, or if there are other issues, it can affect the performance and safety of cells. This section will focus on the effect of the separator properties on cell performance and safety. Table 7 shows different types of safety and performance tests for lithium-ion batteries and the corresponding important separator property and how it affects performance and/or safety.

To achieve good performance of lithium-ion cells, the separators should have low resistance, low shrinkage and uniform pore structure. The separator with high resistance will perform poorly during high rate discharge and will also increase the cell charging time. Low shrinkage is a very important characteristic for separators, especially for higher capacity cells. These cells are used in high-speed laptop computers, which can experience higher temperatures (~70−75 °C) under certain conditions.[117] This can lead to shrinkage of separators and ultimately higher cell resistance and poor long-term cycling. The shrinkage in TD direction can lead to safety issues because of an internal short between the electrodes. Larger pores can lead to shorts during cell manufacturing or can fail during hipot testing. Larger pores will allow more soft shorts and higher self-discharge, especially during high-temperature storage. Very small pore size can lead to higher resistance and poor cycle life during high-temperature cycling and storage. Thus, the pore size of the separator should be optimized to achieve good strength and performance.

One of the ways to increase cell capacity is by decreasing the thickness of separators. The newer high capacity cells (>2.0 A h) generally use 20 and 16 μm separators as compared to 25 μm separators used in cells with 1.6−1.8 A h capacity. The thinner separators offer lower resistance and help in increasing the capacity. However, they can hold less electrolyte and their mechanical strength is not as high as thicker separators. Thus, appropriate changes should be made in cell design to keep the cell safe. The handling and manufacturing of thinner separators is also a challenge for the separator manufacturers. They are required to maintain the same electrical and mechanical properties and to have better quality for thinner separators. The separator manufacturers have installed better controls and quality standards and have started offering 16-μm separators. A lot of battery experts are of the opinion that the 16-μm is the thinnest they can use and still maintain the stringent performance and safety requirements of lithium-ion cells.

The separators inside the lithium-ion batteries experience extreme oxidizing environment on the side facing the positive electrode and extreme reducing environment on the side facing the negative electrode. The separators should be stable in these conditions during long-term cycling especially at high temperatures. Separators with poor oxidation resistance can lead to poor high-temperature storage performance and poor long-term cycling behavior. The oxidation resistance properties of trilayer (PP/PE/PP) separators with PP as the outside layer and PE as inner layer is superior compared to polyethylene separators. This is because of the better oxidation resistance properties of polypropylene in contact with the positive electrode in a lithium-ion cell.

The products formed by the decomposition of the electrolyte can also block the pores of the separator, leading to increase in cell resistance. The separators with lower resistance also helps in better low temperature performance. At very low temperatures, the resistance of the electrolytes is very high and thus smaller contribution from separator helps in keeping the cell resistance lower.

CosMX Exhibit 1003, Page 301 of 512

Zeng et al.[118] has shown that small amounts of active lithium metal could be added to a lithium-ion battery via the separator by using vacuum deposition techniques. The lithium films (4−8 μm) were deposited onto a microporous PP film and showed that the lithium electrochemically reacted with either electrode and thus the intrinsic irrereversible capacity of the negative electrode was compensated for using volumetrically efficient lithium metal. This may be a novel idea to allow higher capacity designs but is likely impractical and uneconomical due to issues involved with lithium plating on polymer films and handling the resulting films.

The lithium-ion cells have demonstrated power loss when aged and/or cycled at high temperatures. Norin et al.[119] demonstrated that the separator is at least partly responsible for the power loss due to the intrinsic increase in its ionic resistance. They showed that impedance increased significantly upon cycling and/or aging of lithium-ion cells at elevated temperatures and that separators accounts for ~15% of the total cell impedance rise. They later reported that the loss in ionic conductivity of the separator was due to blocking of the separator pores with the products formed due to electrolyte decomposition, which was significantly accelerated at elevated temperatures.[120]

The U.S. Department of Transportation (DOT) classifies all lithium-ion batteries as hazardous materials for shipping in the same category as lithium metal primary batteries.[121] It grants exceptions based on the cell capacity and ability of the cells to pass specified tests. There are several groups that regulate, or provide testing, to verify safe operation of lithium-ion cells under abuse conditions. In addition, the UL Laboratories,[122,123] the International Electrotechnic Commission,[124] and the United Nations[125] have developed standardized safety testing procedures. These tests are designed to ensure that cells are safe to ship and are resistant to typical abuse conditions such as internal shorting, overcharge, overdischarge, vibration, shock, and temperature variations that may be encountered in normal transportation environments.

Underwriters Laboratories (UL) requires that consumer batteries pass a number of safety tests (UL 1642[126] and UL-2054[127]). There are similar recommendations from UN for transport of dangerous goods,[128] and from the International Electrotechnical Commission (IEC) and Japan Battery Association.[129] An abnormal increase in cell temperature can occur from internal heating caused by either electrical abuse—overcharge or short circuit—or mechanical abuse—nail penetration or crush. A higher cell temperature could also be a result of external heating. For this reason, battery packs containing lithium-ion cells are designed with safety control circuits that have redundant safety features (PTC, CID, vent, thermal fuse, etc.). Shutdown separators are one of the safety devices inside the cell and act as a last line of defense. The separator shutdown is irreversible, which is fine for polyethylene-based separators, which melt around 130 °C.

The impedance of the separator increases by 2−3 orders of magnitude due to an increase in cell temperature, which results from cell abuse (e.g., short circuit, overcharge). The separator should not only shutdown around 130 °C, but it should also maintain its mechanical integrity at higher temperatures, preferably at temperatures. If the separator does not shutdown properly then the cell will continue to heat during an overcharge test and can lead to thermal runaway. The high-temperature melt integrity of separators is also a very important property to keep the cell safe during extended overcharge or during extended exposure to higher temperatures.

Figure 10 shows a typical short-circuit curve for an 18650 lithium-ion cell with shutdown separator, $LiCoO_2$ positive electrode, and MCMB carbon negative electrode. The cell does not have other safety devices (e.g., CID, PTC), which usually work before separator shutdown. As soon as the cell is short-circuited externally through a very small shunt resistor, the cell starts heating because of the large current drained through the cell. The shutdown of the separator, which occurs around 130 °C, stops the cell from heating further. The current decrease is caused by increase of battery internal resistance due to separator shutdown. The separator shutdown helps in avoiding the thermal runaway of the cell.

Cells can be overcharged when the cell voltage is incorrectly detected by the charging control system or when the charger breaks down. When this happens, the lithium ions remaining in the cathode are removed and more lithium ions are inserted into the anode then under standard charging conditions. If the lithium insertion ability of the carbon anode is small, lithium metal in the form of dendrites may be deposited on the carbon and this causes a drastic reduction in thermal stability. At higher charging rates, the heat output increases greatly because the joule heat output is proportional to I^2R. Several exothermic reactions (e.g., reaction between lithium and electrolyte, thermal decomposition of anode and cathode, thermal decomposition of electrolyte, etc.) occur inside the cell as its temperature increases. Separator shutdown happens when the cell temperature reaches the melting point of polyethylene as shown in Figure 11. The CID and PTC of the 18650 cells was removed to test the performance of separator alone. The current decrease is caused by increase of battery internal resistance due to separator shutdown. Once the pores of the separator have closed due to softening, the battery cannot continue to be charged or discharged, and thus thermal runaway is prevented. During continued overcharge, the separator should maintain its shutdown feature and should not allow the cell to heat again. It should also maintain its melt integrity and should not allow the two electrodes to touch each other.

The separator should also not allow any dendrite to penetrate through the separator to avoid internal shorts. During an internal short, the separator is the only safety device that can stop the thermal runaway, if the failure is not instant. If the heating rate is too high, then instant failure will occur which cannot be stopped by separator shutdown. If the heating rate

CosMX Exhibit 1003, Page 302 of 512

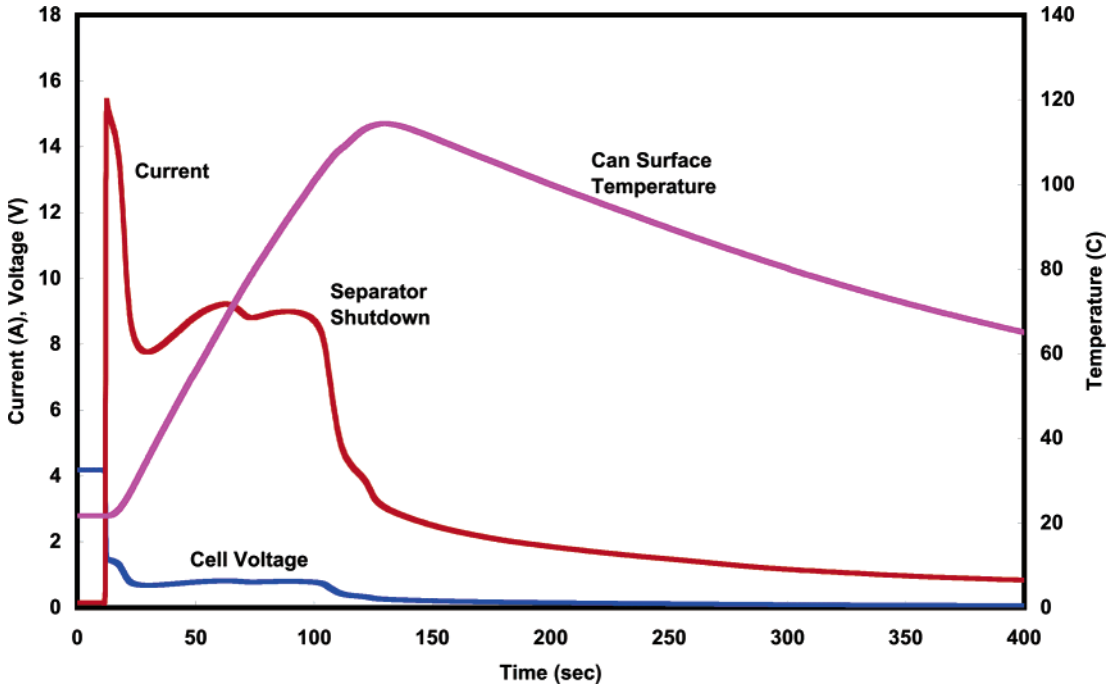


Figure 10. Typical short-circuit behavior of a 18650 lithium-ion cell with shutdown separator and without PTC (positive temperature coefficient) and CID (current interrupt device). This test simulates an external short circuit of a cell.

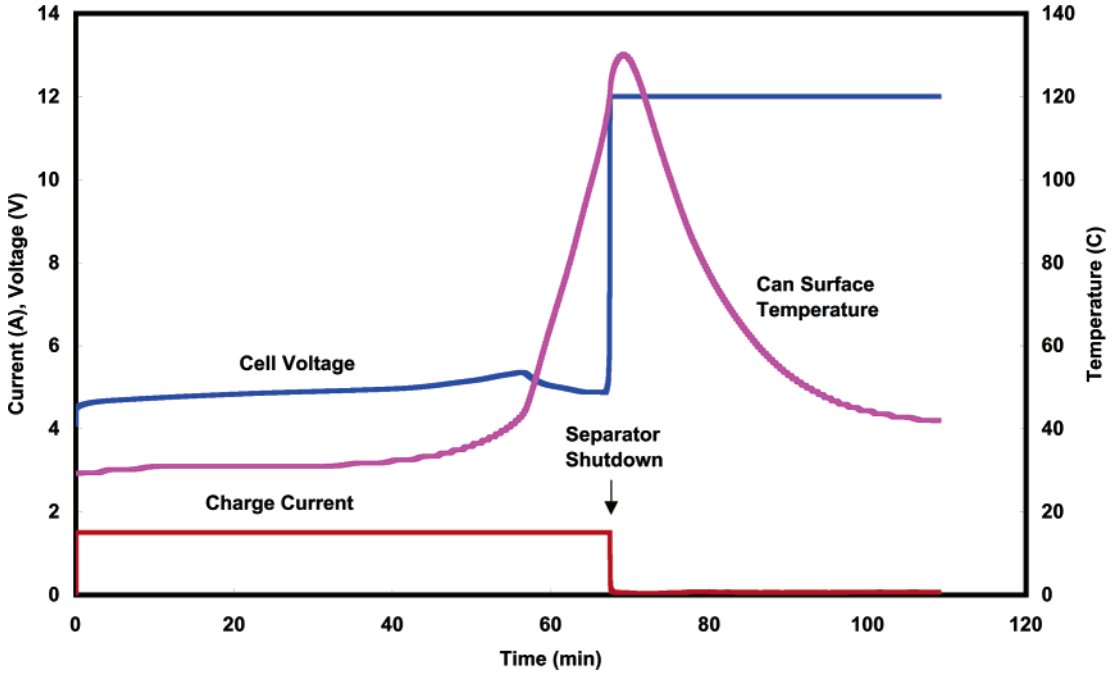


Figure 11. Typical overcharge behavior of a 18650 lithium-ion cell with shutdown separator. The PTC (positive temperature coefficient) and CID (current interrupt device) were removed from the cell header.

is not too high then the separator shutdown can help in controlling the heating rate and stop thermal runaway.

Generally in a nail penetration test, an instantaneous internal short would result the moment the nail is tucked into the battery. Enormous heat is produced from current flow (double layer discharge and electrochemical reactions) in the circuit by the metal nail and electrodes. Contact area varies according to depth of penetration. The shallower the depth, the smaller the contact area and therefore the greater the local current density and heat production. Thermal runaway is likely to take place as local heat generation induces electrolyte and electrode materials to decompose. On the other hand, if the battery is fully penetrated, the increased contact area would lower the current density, and consequently all tests would pass the nail penetration test. Internal short-circuit tests are more difficult to pass then the external short-circuit tests described earlier, because contact area between metal nail contact is smaller than the contact area between current collectors, where the current density would therefore be larger.

CosMX Exhibit 1003, Page 303 of 512

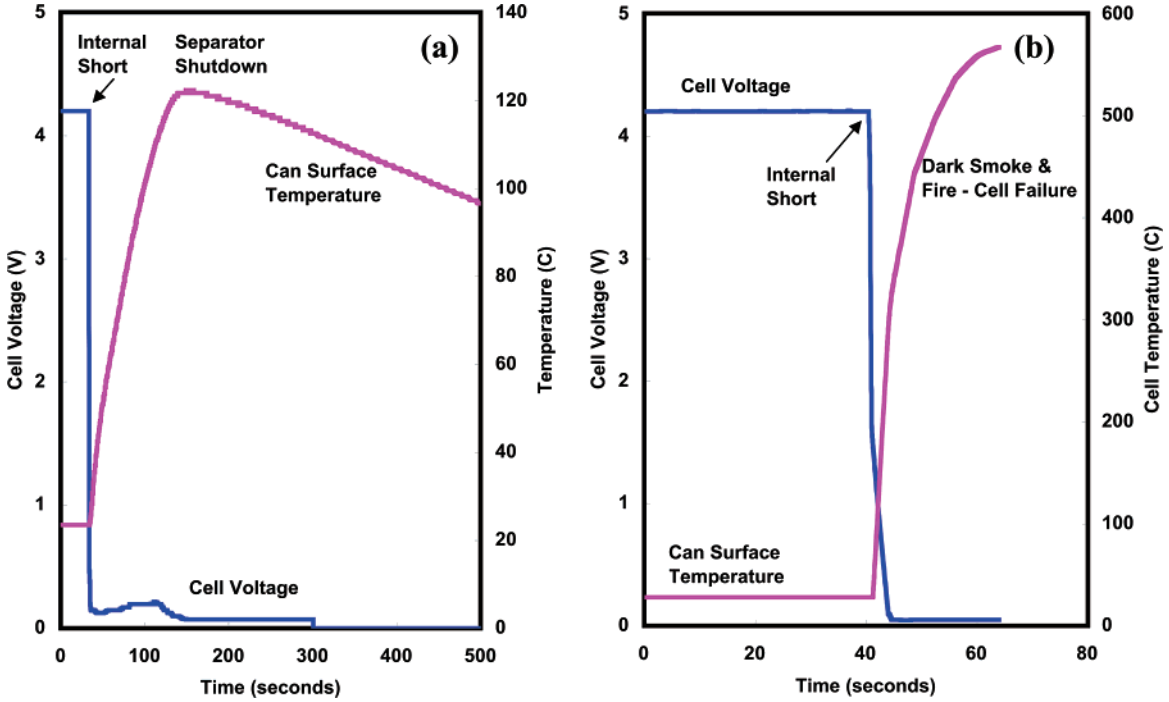


Figure 12. Typical nail penetration behavior of a 18650 lithium-ion cell with shutdown separator. This test simulates internal short circuit of a cell. Key: (a) cell passed nail penetration test; (b) cell failed nail penetration test.

Figure 12 shows the typical nail penetration behavior of a 18650 lithium-ion cell with shutdown separator, $LiCoO_2$ positive electrode, and MCMB carbon negative electrode. Clearly, there was a voltage drop from 4.2 to 0.0 V, instantaneously, as the nail penetrates through (when an internal short circuit occurs), and the temperature rose. When the heating rate is low, the cell stops heating when the temperature is close to separator shutdown temperature as shown in Figure 12a. If the heating rate is very high, then the cell continues to heat and fails the nail penetration test as shown in Figure 12b. In this case, the separator shutdown is not fast enough to stop cell from thermal runaway. Thus, the separator only helps in avoiding delayed failures in the case of internal short circuit as simulated by nail and bar crush tests. Separators with high-temperature melt integrity and good shutdown feature (to avoid delayed failures) are needed to pass the internal short-circuit test. Thinner separators (<20 μm) used in high capacity cells should offer shutdown and high-temperature melt integrity properties similar to those of thicker separators. The decrease in separator strength should be balanced with changes in cell design. The separator properties across the length and width should be very uniform to keep the cell safe during abnormal use.

The mechanism and characteristics of thermal cutoff devices in several prismatic lithium-ion cells was studied by Venugopal[130] by monitoring the impedance at 1 kHz and the open circuit voltage (OCV) of the cells as a function of temperature. All the cells studied contained PE-based separators with a shutdown temperature between 130 and 135 °C. Within this narrow temperature range, the shutdown separators caused a sharp and irreversible rise in impedance of the cell. Single layer PE separators were effective up to around 145 °C, above which they demonstrated a meltdown effect. Trilayer separators had meltdown temperatures as high as 160 °C because of the presence of additional layers of higher melting PP. It was found that the separators are not able to shutdown the cell completely. In the case of an overcharged test, the cell could continue to charge at lower currents even after the shutdown event, rendering the cell a potential hazard if not disposed immediately and safely. This usually does not become an issue in commercial cells because the cell manufacturers have addressed this issue by including multiple cutoff devices within a single cell.

Development efforts are under way to displace the use of microporous membranes as battery separators and instead use gel electrolytes or polymer electrolytes. Polymer electrolytes, in particular, promise enhanced safety by eliminating organic volatile solvents. The next two sections are devoted to solid polymer and gel polymer type lithium-ion cells with focus on their separator/electrolyte requirements.

6.2. Lithium Polymer

Because of their high theoretical capacity, lithium polymer batteries have long been identified as a very promising technology to meet the requirements of upcoming applications such as standby power and electric vehicles. Research and development of polymer electrolytes for ambient-temperature rechargeable lithium batteries has always been very active. Rapid progress for the past 2 decades in this field has led to numerous monographs and reviews.[131−137] These polymers are generally polyethers, poly(ethylene oxide) (PEO), or poly(propylene oxide) (PPO).

Solid polymer electrolytes serve two principal roles in rechargeable lithium batteries. Not only do they function as the traditional electrolyte, i.e., the me-

dium for ionic transport but also they function as the separator which insulates the cathode from the anode. Consequently, the polymer electrolyte must have sufficient mechanical integrity to withstand electrode stack pressure and stresses caused by dimensional changes, which the rechargeable electrodes undergo during charge/discharge cycling.

Lithium polymer electrolytes formed by dissolving a lithium salt LiX (where X is preferably a large soft anion) in poly(ethylene oxide) PEO can find useful application as separators in lithium rechargeable polymer batteries.[138−140] Thin films must be used due to the relatively high ionic resistivity of these polymers. For example, the lithium-ion conductivity of PEO−Li salt complexes at 100 °C is still only about $^1/_{100}$th the conductivity of a typical aqueous solution.

A polymer electrolyte with acceptable conductivity, mechanical properties and electrochemical stability has yet to be developed and commercialized on a large scale. The main issues which are still to be resolved for a completely successful operation of these materials are the reactivity of their interface with the lithium metal electrode and the decay of their conductivity at temperatures below 70 °C. Croce et al. found an effective approach for reaching both of these goals by dispersing low particle size ceramic powders in the polymer electrolyte bulk.[141,142] They claimed that this new "nanocomposite polymer electrolytes" had a very stable lithium electrode interface and an enhanced ionic conductivity at low temperature, combined with good mechanical properties. Fan et al.[143] has also developed a new type of composite electrolyte by dispersing fumed silica into low to moderate molecular weight PEO.

The gel type polymer electrolyte prepared by dispersing ceramic powders (e.g., Al_2O_3) into a matrix formed by a lithium salt solution contained in a poly(acrylonitrile) (PAN) network was reported by Appetecchi et al.[144] These new types of composite gel electrolytes had high ionic conductivity, wide electrochemical stability, and particularly, high chemical integrity even at temperatures above ambient. Kim et al.[145] used a blend of PVdF−HFP and PAN as a matrix polymer to attain high ionic conductivity and good mechanical strength. The PAN can give mechanical integrity and structural rigidity to a porous membrane without inorganic fillers. The high ionic conductivity was due to the high volume of pores and a high affinity of the membrane for electrolyte solution.[146]

6.3. Lithium-Ion Gel Polymer

The solid polymer electrolyte approach provides enhanced safety, but the poor ambient temperature conductivity excludes their use for battery applications, which require good ambient temperature performance. In contrast, the liquid lithium-ion technology provides better performance over a wider temperature range, but electrolyte leakage remains a constant risk. Midway between the solid polymer electrolyte and the liquid electrolyte is the "hybrid polymer" electrolyte concept leading to the so-called gel polymer lithium-ion batteries. Gel electrolyte is a two-component system, viz., a polymer matrix swollen with a liquid electrolyte. The gel polymer electrolyte approach to the lithium-ion technology combines the positive attributes of both the liquid (high ionic conductivity) and solid polymer electrolytes (elimination of leakage problems).

Gel polymer lithium-ion batteries replace the conventional liquid electrolytes with an advanced polymer electrolyte membrane. These cells can be packed in lightweight plastic packages as they do not have any free electrolytes and they can be fabricated in any desired shape and size. They are now increasingly becoming an alternative to liquid-electrolyte lithium-ion batteries, and several battery manufacturers, such as Sanyo, Sony, and Panasonic have started commercial production.[147,148] Song et al.[149] have recently reviewed the present state of gel-type polymer electrolyte technology for lithium-ion batteries. They focused on four plasticized systems, which have received particular attention from a practical viewpoint, i.e., poly(ethylene oxide) (PEO), poly(acrylonitrile) (PAN),[150] poly(methyl methacrylate) (PMMA),[151,152] and poly(vinylidene fluoride) (PVdF) based electrolytes.[153−157]

One particular version of the lithium-ion gel polymer cells, also known as plastic lithium-ion cell (PLION), was developed by Bellcore (now Telcordia Technologies).[158−160] In this case, Gozdz et al. developed a microporous plasticized PVdF−HFP based polymer electrolyte which served both as separator and electrolyte. In PLION cells, the anode and cathode are laminated onto either side of the gellable membrane. Good adhesion between the electrodes and the membranes is possible because all three sheets contain significant amounts of a PVdF copolymer that can be melted and bonded during the lamination step.

The PVdF−HFP separators used in PLION cells were around 3 mil thick, and had poor mechanical properties. It has been reported that the major source of rate limitation in PLION cells was the separator thickness.[161] The rate capability of these cells can be significantly improved by decreasing the separator thickness to that typically used in liquid electrolyte system. Moreover, in the absence of shutdown function, the separator does not contribute to cell safety in any way. Park et al. reported that the HFP content in separators did not have any significant impact on cell performance.[162] The Bellcore process has proven to be an elegant laboratory process but is difficult to implement in large-scale production.

To overcome the poor mechanical properties of polymer and gel polymer type electrolytes, microporous membranes impregnated with gel polymer electrolytes, such as PVdF, PVdF−HFP, and other gelling agents, have been developed as an electrolyte material for lithium batteries.[163−173] Gel coated and/or gel-filled separators have some characteristics that may be harder to achieve in the separator-free gel electrolytes. For example, they can offer much better protection against internal shorts when compared to gel electrolytes and can therefore help in reducing the overall thickness of the electrolyte layer. In addition the ability of some separators to shutdown

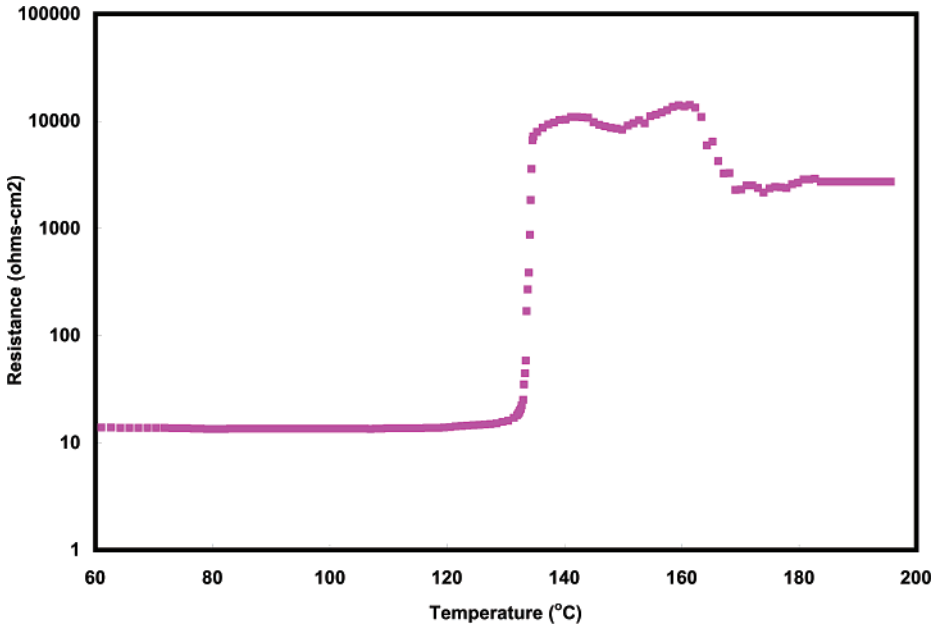


Figure 13. Internal impedance (at 1 kHz) of PVdF coated Celgard trilayer separators as a function of temperature. Heating rate: 60 °C/min.

at a particular temperature allows safe deactivation of the cell under overcharge conditions.

The shutdown behavior of PVdF coated Celgard trilayer membranes is shown in Figure 13. The shutdown is defined by the sharp increase in resistance around 130 °C. The PVdF coating should be porous and should not block the pores to maintain similar ionic conductivity. The scanning electron micrographs of the PVdF coated membrane is shown in Figure 14. The cross section SEM of Celgard 3300 provides visual evidence that the coating is porous and is not blocking the pores of the top PP layer.

Abraham et al.[174] were the first ones to propose saturating commercially available microporous polyolefin separators (e.g., Celgard) with a solution of lithium salt in a photopolymerizable monomer and a nonvolatile electrolyte solvent. The resulting batteries exhibited a low discharge rate capability due to the significant occlusion of the pores with the polymer binder and the low ionic conductivity of this plasticized electrolyte system. Dasgupta and Jacobs[163,175] patented several variants of the process for the fabrication of bonded-electrode lithium-ion batteries, in which a microporous separator and electrode were coated with a liquid electrolyte solution, such as ethylene−propylenediene (EPDM) copolymer, and then bonded under elevated temperature and pressure conditions. This method required that the whole cell assembling process be carried out under scrupulously anhydrous conditions, which made it very difficult and expensive.

More recent methods proposed by Motorola[176,177] and Mitsubishi Electric[178] researchers differ in implementation details, but they share a common feature in that a separate adhesive layer (PVdF) is applied to the separator and used to bond the electrode and the separator films, using in the first case the hot, liquid electrolyte as an in situ PVdF plasticizer. Recently, Sony[179,180] researchers described the use of a thin, liquid electrolyte-plasticized polyacrylonitrile layer directly applied either to the electrode or the separator surfaces as an effective ion-conductive adhesive. Sanyo[181,182] investigators, on the other hand, used thermally polyerizable additives to gel, or solidify, liquid electrolyte solutions in a wound, packaged battery.

The ceramic fillers (e.g. Al_2O_3, SiO_2, TiO_2) can greatly influence the characteristics and properties of polymer electrolyte by enhancing the mechanical stability and the conductivity.[141,183−186] γ-$LiAlO_2$, Al_2O_3, and MgO were used as fillers by Prosini et al.[187] in a PVdF−HFP polymer matrix to form self-standing, intrinsically porous separators for lithium-ion batteries. The MgO based separators showed the best anode and cathode compatibilities.

Liu et al.[188] has successfully prepared a PVdF−HFP/PE composite gel electrolyte by cast method. They showed that when the PE content was over 23 wt %, the electrical impedance of the composite gel electrolyte increased rapidly by several orders of magnitude, around the melting point of PE. The SEM pictures showed that the PE particles were fused and formed into a continuous film at or near the PE melting point, which cuts off the ion diffusion. This shutdown feature of the composite gel electrolyte can help in preventing the cell runaway under abusive usage. Similarly, poly(ethylene oxide) (PEO) coated separators were prepared by Kim et al.[189] by coating PEO onto a microporous PE separators. The ionic conductivity of PEO coated membranes was higher then the base film. Kim et al. prepared the polymer electrolytes by coating poly(ethylene oxide) (PEO) and poly(ethylene glycol dimethacrylate) (PEGDMA) onto a microporous polyethylene membrane (Asahi Kasei, 25 um, 40% porosity).[190] They showed that the relative weight ratio of PEO and PEGDMA coated on to the microporous membrane played a critical role in determining the uptake of electrolyte solution and ionic conductivity.

CosMX Exhibit 1003, Page 306 of 512

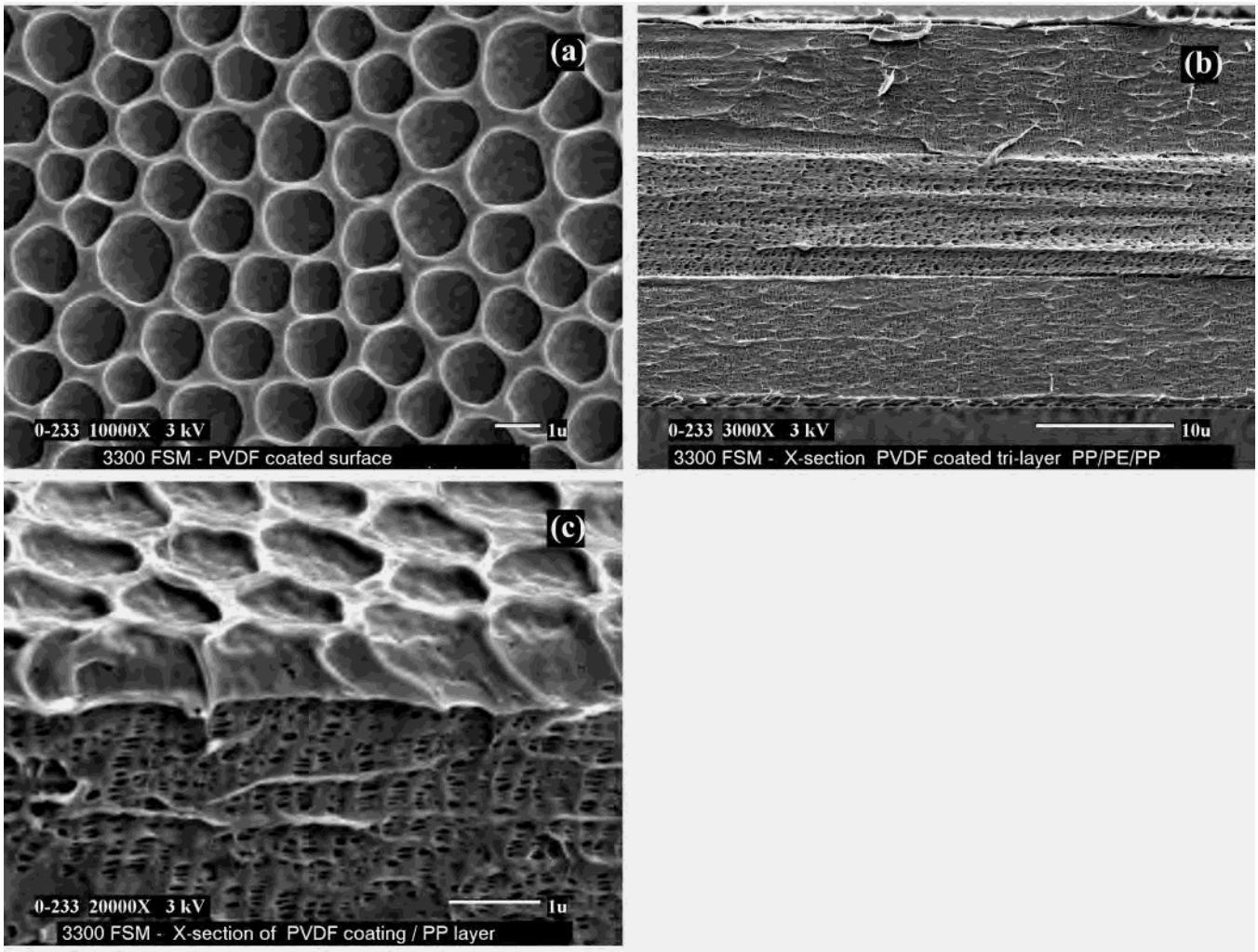


Figure 14. Scanning electron micrographs of Celgard PVdF coated separators used in lithium gel polymer batteries: (a) surface SEM, (b) cross-section SEM of coated trilayer, and (c) cross section of PVdF coating.

6.4. Lithium Primary Systems

Lithium primary batteries, with their outstanding performance and characteristics, are being used in increasing quantities in a variety of applications, including cameras, memory backup circuits, security devices, calculators, watches, etc. They were first used in early 1970s in selected military applications, but since then they have been designed using a number of different chemistries, in a variety of sizes and configurations, and have been used in different consumer applications. They are attractive because of their high voltage, high specific energy, good power density, flat discharge characteristic, good low temperature performance, and superior shelf life.

The term "lithium battery", applies to many different types of chemistries, each using lithium as the anode but differing in cathode material, electrolyte, and chemistry as well as in design and other physical and mechanical features. Lithium primary batteries can be classified into several categories, based on the type of electrolyte (or solvent) and cathode material used—soluble cathode cells (e.g., SO_2, $SOCl_2$, SO_2Cl_2), solid cathode cells (e.g., V_2O_5, MnO_2, $(CF)_n$, FeS_x, CuO), and solid electrolyte cells (I_2 (P_2VP)). The Li−I_2 system is unique as the cell reaction product, LiI, forms the separator in situ. In the large cylindrical size batteries, three chemistries are currently available for consumer applications: Li−MnO_2, Li−CF_x, and Li−FeS_2. Li−MnO_2 and Li−CF_x cells are 3 V cells that come in special sizes and are typically used in cameras, safety devices, industrial applications, etc. Li−FeS_2 is a 1.5 V battery that is a drop-in replacement for primary alkaline and C/Zn batteries.

As the separator requirements for most of the above batteries are very similar, they will not be dealt with in detail. In this section, we will generally describe the separator requirements followed by a brief discussion on few selected systems.

6.4.1. Separator Requirements

The requirements for the separator properties are generally lower in lithium primary cells compared to lithium secondary cells. The lack of a charging process helps avoid undesirable electrochemical deposits (e.g., dendrites) as well as the generation of oxidizing substances. The mechanical strength requirements are less severe because the negative electrode is made of lithium foil, which is relatively smooth. Further, the shutdown behavior of separator is not mandatory because the thermal runaway occurs only when the cell temperatures goes beyond 180 °C (melting point of lithium). The basic require-

Table 8. Separators and Their Manufacturers for Major Primary Lithium Battery Systems

battery system	type of separator	compositions (manufacturer)
Li/SO_2	microporous	glass fiber;[a] polypropylene;[b] Tefzel
$Li/SOCl_2$	microporous	glass fiber;[c] glass mat or filter paper
Li/MnO_2	microporous	polypropylene[d] (Celgard); polyethylene (Asahi Kasei)
$Li/(CF)_n$	microporous	polypropylene[e]
Li/CuO	microporous	nonwoven glass
Li/V_6O_{13}	microporous	polypropylene (Celgard 2400)[f]
	solid-ion conductor	poly(ethylene oxide)−lithium salt[g]
Li/V_2O_5	microporous	polypropylene[h]
Li/FeS_2	microporous	polypropylene[i]
$Li/CuCl_2$	microporous	Tefzel
solid electrolyte (Li−I_2 (P2VP))	solid ion conductor	LiI film (self-healing)[j]

[a] Walk, C. R. In *Lithium Batteries*; Gabano, J. P., Ed.; Academic Press: New York, 1983, p 281. [b] Linden, D.; McDonald, B. *J. Power Sources* **1980**, *5*, 35. [c] Klinedinst, K. A. *J. Electrochem. Soc.* **1984**, *131*, 492. [d] Moses, P. R.; Turchan, M. J.; Taylor, A. H.; Mank, R. M. In *Lithium Batteries;* Gabano, J. P., Ed.; Academic Press: New York, 1983, p 333. [e] Morita, A.; Iijima, T.; Fujii, T.; Ogawa, H. *J. Power Sources* **1980**, *5*, 111. [f] Abraham, K. M.; Goldman, J. L.; Holleck, G. L. *Lithium Batteries*; Venkatasetty, H. V., Ed.; The Electrochemical Society, Inc.: Pennington, NJ, 1981; p 271. [g] Armand, M. B. Second International Meeting on Lithium Batteries, Extended Abstracts No. 2, Paris, France. *Solid State Ionics* **1983**, *9/10*, 745. [h] Walk, C. R. In *Lithium Batteries*; Gabano, J. P., Ed.; Academic Press: New York, 1983, p 265. [i] Uetani, Y.; Yokoyama, K.; Okamoto, O. J. *Power Sources* **1980**, *5*, 89. [j] Liang, C. C.; Holmes, C. F. J. *Power Sources* **1980**, *5*, 3.

ments are very generic—low electrical resistance, thin, high strength, low shrinkage, relatively small pore size, and no defects. As is true for separators for use in lithium-ion batteries, all the properties of separators for primary lithium batteries should be very uniform.

The most common separator by far used in these cells is the single layer PP separator made by Celgard (Celgard 2400) as shown in Table 8.

6.4.2. Chemistries

The separators used in major lithium primary systems are listed in Table 8. The majority of the lithium primary systems shown in Table 8 use microporous membranes (single layer PP or PE) as separators. Some of the systems are discussed below.

6.4.2.1. Lithium MnO_2. The Li/MnO_2 battery is the most widely used primary lithium battery. It is used in a wide variety of applications such as long-term memory backup, safety and security devices, cameras, many consumer devices, and military electronics. It uses a lithium anode, microporous polypropylene separator impregnated with electrolyte, and MnO_2 cathode. It is available in many configurations (including coin, bobbin, spirally wound cylindrical, and prismatic configurations in multicell batteries) and in designs for low, moderate, and moderately high drain application.

The Li/MnO_2 coin cells use a lithium anode disk, which is separated from the manganese dioxide pellet cathode by a nonwoven polypropylene separator, impregnated with the electrolyte. The bobbin-type design contains a central lithium anode core surrounded by the manganese oxide cathode, separated by a polypropylene separator impregnated with the electrolyte. The bobbin design maximizes the energy density due to the use of thick electrodes and the maximum amount of active materials. In the spirally wound cells, the lithium anode and the cathode are wound together with a microporous polypropylene separator to form the jelly roll. These cells are designed for high-current pulse applications as well as continuous high-rate operation.

The lithium MnO_2 system has been preferred over lithium CF_x for the primary lithium cell market for its lower cost and essentially equivalent performance for camera (cylindrical cells), watch (coin cells), and memory applications. Dan et al. published results for an AA size rechargeable size cell based on Li/MnO_2 chemistry with energy density of 125−140 W h/kg and 280−315 W h/L. The cell used a polypropylene separator and was able to pass all safety tests (short circuit, overcharge, deep discharge, crush, and nail penetration).[191] Ikeda[192] and co-workers reported the development of "long life and high reliability Li/MnO_2 cell for back up" and demonstrated how the microporous structure of Celgard flat sheet membranes reduced self-discharge to provide reliable operation for up to 10 years.

6.4.2.2. Lithium CF_x. The Li/CF_x battery consists of a lithium anode, polycarbon monofluoride cathode, and microporous polypropylene separator saturated with organic electrolyte. These batteries are used as power sources for watches, portable calculators, memory applications, and so on.

6.4.2.3. Lithium Iron Sulfide. Energizer has marketed Li−FeS_2 (L91) AA-size cells since 1990.[193] These cells usually have a high surface area jellyroll construction, using pyrite (FeS_2) coated onto aluminum foil as the cathode, a polyolefin (polypropylene) microporous separator, and a lithium foil anode. This system is particularly well suited for high drain and constant power applications, where its higher operating voltage extends service time.

6.4.2.4. Lithium SO_2. The lithium SO_2 systems are mainly used in military and some industrial and space applications. This system is particularly known for its capability to handle high current and high power requirements, for its excellent low-temperature performance, and for its long shelf life. They are typically fabricated in cylindrical structure by spirally winding rectangular strips of lithium foil, a microporous polypropylene separator, the cathode electrode, and a second separator layer.

CosMX Exhibit 1003, Page 308 of 512

6.4.2.5. Lithium $SOCl_2$. The lithium $SOCl_2$ battery has one of the highest cell voltages (~3.6 V) and energy densities of the practical battery systems. These batteries have been fabricated in a variety of sizes and designs, ranging from wafer or coin cells with capacities as low as 400 mA h to cylindrical cells in bobbin and spirally wound electrode structures and to large 10 000 A h prismatic cells. Li/$SOCl_2$ bobbin batteries are manufactured in a cylindrical configuration. The anode is made of lithium foil, which is swaged against the inner wall of the can, the separator is made of nonwoven glass fibers, and the cathode is made of Teflon-bonded acetylene black.

6.4.2.6. Lithium TiS_2. In 1990, W. R Grace & Co developed rechargeable Li−TiS_2 cells with high energy density, and excellent cycle life. To improve the safety, they developed a fusible separator (SafeTsep) for use in both primary and secondary lithium batteries.[112] The separator consists of two or more microporous layers with at least one of the layers capable of transforming to a nonporous membrane at a temperature between 100 and 150 °C. The additional layers maintain the dimensional stability of the separator during this transformation.[113]

6.4.2.7. Lithium Bromine. Ultrafine porous polymer membranes were prepared by Weininger et al.[194] by adding sodium benzoate or other salts of benzoic acid to the melted polymer in a weight ratio of 70−85 parts of benzoate to 30−15 parts of polymer. The salt does not dissolve in the polymer but forms a dispersion or colloidal suspension. Processing the polymer involved milling on differential rolls with the benzoate salt at 140−160 °C for PE or 170−180 °C for PP. The mixtures are then cooled close to the softening point of the polymer and sheeted into 0.0005 in thick films. The final leaching of the sheets is done in water at 20−55 °C. The salt was generally extracted over a period of 1−16 h. However, leaching is almost complete within 5−10 min. The polymers are also irradiated with high-energy electrons of 20 Mrad at a dose rate of 10 Mrad/min before or after extraction of the salt. This irradiation step is employed to improve the thermal and mechanical properties of the porous polymer. Irradiation after leaching is more effective in strengthening mechanical and thermal properties, but by this treatment, the smallest pores are closed by cross-linking. These membranes are flexible, about 50% porous, have extremely fine pore sizes (40−120 Å), and are used as separators in rechargeable lithium bromine batteries. The lithium bromine system is not a commercial system. A lot of developmental work has gone into developing the system, but it still is not commercialized.

6.4.2.8. Lithium Iron Sulfide (High Temperature). High-temperature molten salt Li−Al/LiCl−KCl/FeS_x cells are known for their high energy density and superior safety. At one point they were being actively pursued for electric vehicle and pulse-power applications. Historically, boron nitride (BN) cloth or felt has been used as the separator in flooded-electrolyte cells, while MgO pressed-powder plaques have been used in starved-electrolyte cells.

Martino et al. have demonstrated the use of BN felt separators in engineering tests.[195] They have high porosity (~90%), and hence, low ionic resistance, in addition to excellent compatibility with other cell materials at the operating temperature of 470 °C. However, this separator is too expensive and has poor mechanical properties and so cannot prevent electrode shape change during cell operation.[196]

MgO, Y_2O_3, and AlN powder-based separators are substantially less expensive.[197,198] Cell assembly with such powder separators is simple and amenable to mass production. Although powder separators were shown to maintain their integrity and conform to small dimensional changes of electrodes, their porosity (~50%) is considerably lower than that of BN felt and this drawback can limit their application to stationary load-leveling systems operating at low current densities.[197]

Shimizu et al. has developed a low-cost MgO porous particle separator, which possessed both the high porosity (~85%) of the BN felt and the high mechanical resistance of powder separators.[199] The separator was prepared by loosely sintering fine MgO powder with $Mg(NO_3)_2$ as the binder. The particles thus formed showed excellent performance as separators in Li−Al/FeS_x cells.

The state of development of the BN-felt separator is more advanced than that of the MgO powder separator. However, the ceramic powder separator has the potential for lower cost than the felt separator.

7. Separator for Aqueous Batteries

The aqueous batteries use water based electrolytes (e.g., KOH electrolyte for NiCd and NiMH and H_2SO_4 electrolyte for lead acid), which are less resistive then nonaqueous electrolytes. Polyolefin materials are generally suitable for use in the manufacture of separators for these batteries, but they are not inherently wettable by aqueous electrolytes. Such electrolytes are therefore unable to penetrate the pores of a separator formed from such a material, so that ion migration through the pores in solution will not occur without modification. This problem is sometimes overcome by treating the polyolefin material with a surfactant, which allows an aqueous electrolyte to wet the material. However, such surfactant can be removed from the surfaces of the polyolefin material when electrolyte is lost from the device, for example during charging and discharging cycles, and it is not subsequently replaced on the material when the electrolyte is replenished.

This problem has also been more durably addressed by modifying the surface properties of the polyolefin materials used to form polymeric sheets, by graft-copolymerizing to those surfaces a monomeric substance which, after copolymerization, confers hydrophilic properties and, in some cases, ion exchange properties. This technique has been found to be practical when the porous substrate is formed from PE, which has been found to lend itself well to a graft-copolymerization reaction of this kind. However, it has been found that when such a reaction is

attempted using polyolefin materials other than PE, the rate of the grafting reaction is reduced significantly.

Graft polymerization is a convenient method for the modification of the physical and chemical properties of polymer materials and is of particular interest for synthesis of the hydrophilic membranes. Graft copolymerization can be achieved by various methods such as an exposure to ionizing radiation or ultraviolet light and the use of chemical initiators. Ionizing radiation is one of the most promising methods because of its rapid and uniform formation of active sites for initiating grafting throughout the matrix. Under appropriate experimental conditions, modifications of polymer properties can be accomplished not only on the surface but also throughout the polymer.

There have been several reports on radiation grafting of acrylic and methacrylic acid onto various substrates. These include both the direct grafting method and the preirradiation method to synthesize ion-exchange membranes. Two cation exchange membranes modified with the carboxylic acid group for a battery separator were prepared by radiation-induced grafting of acrylic acid (AA) and methacrylic acid (MA) onto a polyethylene film by Choi et al.[200] They found that KOH diffusion flux of AA-grafted PE membrane and MA-grafted PE membrane increased with an increase in the degree of grafting. AA-grafted PE membrane had a higher diffusion flux then MA-grafted PE membrane. Electrical resistance of both membranes decreased rapidly with an increase in the degree of grafting up to 120% and then leveled off.

Battery separators having carboxylic acid group were prepared by radiation induced grafting of acrylic acid onto a polyolefin nonwoven fabric (PNF). The PNF comprised approximately 60% polyethylene and 40% polypropylene. It was found that the wetting speed, electrolyte retention, thickness, and ion-exchange capacity increased, whereas the electrical resistance decreased with increasing grafting yield.[201] The surface characteristics of the separators can also be modified by plasma discharge.

This subsequent section discusses different types of aqueous batteries and the separators used in those batteries. The recent work in the development of new separators for aqueous batteries will also be discussed in detail.

7.1. Leclanche (Zinc Carbon)

Dry cells have been well-known for over 100 years and form the technical basis of today's modern dry cell industry. Zinc carbon cells are the most widely used of all the primary batteries worldwide because of their low cost, availability, and acceptability in various situations. The two major separator types ever used or in use are gelled paste and paper coated with cereal or other gelling agents such as methylcellulose.[202] The paste type is dispensed into the zinc can, and the preformed bobbin is inserted, pushing the paste up the can walls between the zinc and the bobbin. A typical paste electrolyte uses zinc chloride, ammonium chloride, water, and starch or flour as the gelling agents. The coated-paper type uses a special paper coated with flour, starch, regenerated cellulose, or other gelling agent on one or both sides.[203] The paper selected must be of low metallic impurity. A kraft paper separator provides thinner separator spacing, lower internal resistance, and increased active materials volume.[204] One of the critical functions of the separator is to keep the zinc can surface properly wetted.

As the paste separator is relatively thick compared with the paper liner, about 10% or more manganese dioxide can be accommodated in a paper-lined cell, resulting in a proportional increase in capacity.[205] The pasted separator carbon−zinc cells were phased out more then a decade ago. All the cells made since then are paper-lined constructions.

The performance and capacity advantages of alkaline batteries vs carbon−zinc is resulting in the continuous decline of this battery. The low cost of the carbon zinc cell is a major reason for its continued use. Thus, cost is a major consideration in the development and selection of separators for this system.

7.2. Alkaline Zinc MnO_2

Since its introduction in the early 1960s, the alkaline manganese dioxide (Zn/MnO_2) cell has advanced to a dominant position in the portable battery market. It gets its name from the use of alkaline solutions as electrolyte. Alkaline cells have many acknowledged advantages over zinc−carbon, including a higher energy density, longer shelf life, superior leakage resistance, better performance in both continuous and intermittent duty cycles, and lower internal resistance, which allows them to operate at high discharge rates over a wider temperature range.

In general, alkaline MnO_2 cells use "macroporous" nonwoven separators made from fibrous materials and binders. Various blends of fibers including cellulose, synthetic fiber, such as PVA fiber, nylon rayon, etc. are used in producing this type of separator. Other types such as gelled, inorganic, and radiation-grafted separators have been tried, but they have not gained much practical use. Some of the more advanced nonwoven separators are made by coating fibers made of an acrylonitride polymer with a surface layer of an acrylic acid which has carboxyl groups, that are then mixed with polypropylene fiber and bound by a PVA fiber. The carboxyl group is partially cross-linked, resulting in swelling, but remains insoluble in the electrolyte. This demonstrates the complexity of today's separators in contrast to earlier separator materials, which were primarily cellulosic.

Techniques commonly used to produce fibrous webs include the wet laid, dry laid carded, and meltblown processes. The wet laid or paper making process is the predominant method for several reasons. The wet laid process, configured properly, allows for the blending of cellulosic and polymeric components. Also, the ability to use short cut length and fine denier fiber provides for consistent blending, uniform formation, and controlled pore structure.[12]

Because of the removal of mercury from the alkaline MnO_2 cell, there has been a re-formulation in the anode paste. Because of this change, theses cells

now use a nonwoven laminated to cellophane as the separator to ensure against shorting due to zinc solubility and migration. This can lead to higher separator resistance. The key to success of such a lamination is to use an adhesive (e.g., PVA) that will not interfere with the ionic movement of the electrode. Some manufacturers of the mercury free cells use nonwoven mat of much smaller pore size made possible by the availability of 0.1−0.3 denier man-made fiber. The smaller diameter fiber allows for more uniform web formation at low ream weight and thickness resulting in improved high rate performance. Often a compromise must be struck between wicking rate and average pore size.

The rechargeable $Zn-MnO_2$ battery is an outgrowth of the primary battery. In these type of batteries, a "microporous" type separator is required to resist dendritic growth more likely to evolve as a result of numerous recharges. Materials like cellophane, grafted membrane, or polymeric films can be used as laminates to absorptive substrates. Another approach providing a similar effect is to coat a fibrous base with a layer of viskose. Both cellophane and viskose materials have remarkable properties in that they are electropermeable when wetted with KOH. To produce the functional laminate, the base nonwoven is designed for wicking and absorbency while the cellophane or membrane provides the short resistance. The adhesive used in laminating the separator must not adversely affect electrical resistance and should not interfere with the electrochemical behavior of the cell. On the basis of sales, the alkaline $Zn-MnO_2$ market is about 3−4 times larger than the lithium-ion battery market.[2] As this particular article is mainly focused on separators used in lithium-based batteries, we will not be discussing $Zn-MnO_2$ separators in more detail.

7.3. Lead-Acid Batteries

It has been a long time since the invention of the lead-acid battery, but it still represents the most important secondary chemical power source—both in number of types and diversity of application. The lead-acid battery has maintained its leading role for so many decades due to its competitive electrical characteristics and price and due to its adaptability to new applications. It is manufactured in a variety of sizes and designs, ranging from less than 1 to over 10 000 A h.[206]

Lead-acid batteries can be classified into three major types or categories, namely, automotive (SLI), stationary, and motive power (industrial). In addition, there are many special batteries that cannot be easily categorized as either of the above types. As these types of batteries are constructed with different materials and design to meet the requirements of their intended end uses, each requires a particular separator with specific material composition, mechanical design, and physical, chemical, and electrochemical properties that are tailored for the battery and its relevant specific uses. These batteries are generally available in flooded electrolyte or valve regulated (sealed) versions. In this section the types and properties of separators used for lead-acid batteries are reviewed. The reader is referred to recent reviews published by Boehnstedt[13,207,208] and others[209−211] for detailed descriptions of lead-acid separators.

7.3.1. Flooded Electrolyte Lead Acid

Separators currently used in lead-acid batteries can be classified based on their materials of construction into four major types: plastic (PE/silica, PVC/silica, sintered PVC), paper (phenolic resin impregnated cellulose), glass (glass fiber mat), and rubber (hard rubber/silica, flexible rubber/silica, coated rubber/silica) separators. Table 9 shows the different types of separators used in batteries along with their manufacturing process and main features. Glass, paper, and sintered PVC separators can be classified as macroporous separators having an average pore diameter greater than 10 μm while all other separators can be classified as microporous separators having an average pore diameter smaller than 1 μm. All of these separators can be utilized as leaf separators in battery construction. Polyethylene can be used also for enveloped separators around either the positive or the negative plate. The use of "envelope" separators is popular in small, sealed cells, SLI, motive power, and standby batteries to facilitate production and to control lead contamination during manufacturing.

The environment concerns surrounding the lead-acid battery (e.g., the automotive battery) have been increasing in severity in recent years. The improvements and development of the separators have proceeded in accordance with the changes in the specifications for the batteries which were first made with wooden separators (the preferred wood was Oregon cedar as it contained small amounts of lignin that enhanced the performance of lead negative), then progressed through microporous rubber separators, cellulose separators, and synthetic pulp separators (SPG) with glass mats, to PVC separators, and now polyethylene separators have evolved. This sequential change in separator technology has provided continuous improvements in the charge and discharge efficiency of batteries and has given high vehicle-starting capability and reliability. Moreover, short circuits (caused by particles of active material dislodged from the battery plates) are prevented due to the smaller pores and excellent electrochemical oxidation resistance of the PE separator. These features contributed greatly to the improvement in battery life.

Rubber separators have good voltage characteristics, the ability to retard antimony transfer, properties to retard dendrite growth, and good electrochemical compatibility.[212] Due to the hydrophilic properties of the rubber composition, the separators are highly wettable and renewable for the dry-charging process. Paik et al. showed that ACE-SIL (sulfur cured, hard rubber) separators performed well in industrial stationary or traction batteries, FLEX-SIL (electron-beam-cured, flexible rubber separator) separators are suited for deep-cycling batteries, and MICROPOR-

Table 9. Typical Separators Used in Lead-Acid Battery Systems

separator	class	manufacturing process	properties
wood	paper	cellulosic separators made from cotton linters or craft pulp and generally coated with phenolic resin for acid resistance and strength	comparatively large pore size and relatively high electrical resistance
hard-rubber[213]	rubber	made by mixing natural rubber, rehydrated precipitated silica, and sulfur, which is then extruded and calendared, vulcanized under water, and dried	finer pore diameter (0.2 μm average), relatively lower electrical resistance, excellent oxidation resistance, retards antimony transfer
flexible rubber[213]	rubber	made by mixing natural rubber, rehydrated precipitated silica, which is then extruded and calendared, irradiated with an ionizing electron beam, and dried	flexible, fine pore structure (0.06 μm average), retards antimony transfer
glass-mat rubber[213]	rubber/glass mat	made by mixing a polymeric emulsion, precipitated silica, and rubber, which is then coated on a fiberglass mat and finally cured and dried	finer pore diameter (<0.2 μm average), high porosity, excellent thermal dimensional stability
sintered PVC	plastic	made by sintering PVC powder of a particle size ranging between 10 and 20 μm	medium pore size (10−20 μm), generally good chemical resistance
synthetic PVC	plastic	made from mixture of PVC, silica fine powder, and a solvent, and then extruded, calandered, and extracted	small to medium average pore size and relatively low electrical resistance
synthetic pulp with glass mat	plastic/glass	made from blending PE synthetic pulp, synthetic fiber, and fine silica powder and then heat treated	medium pore size, low electrical resistance, and long service life at high temp; more difficult to process and assemble
polyethylene (PE)	plastic	made from a mixture of UHMW PE powder, fine silica powder and mineral oil, which is extruded as a film, calendered, and made porous by extraction	fine pore size, low electrical resistance, high puncture resisatance, and strongly resistant to oxidation
glass fiber mat	glass	deposition on a single sheet, a mixture of fibers dispersed in an aqueous solution	excellent wettability, durable in an acid environment, good resiliency, high temp stability, more difficult to process and assemble

SIL (a coated, glass mat and rubber separator) separators have been found to be good choice for high rate discharging or cranking applications and for various types of gel cells.[213] Recently Daramic DC UHMW PE has demonstrated excellent performance in these applications, as well.

Poly(vinyl chloride) (PVC) and polyethylene (PE) separators have been the most commonly used separators in automotive batteries for the last 20 years. Polyethylene separators have a narrow pore size distribution. The PVC separator is built up by sintering PVC powder in general of a particle size ranging between 10 and 20 μm. The decrease of particle size in the sintered product is negligible compared to the particle size of the raw materials. The pores are dispersed homogeneously with a medium size ranging between 10 and 20 μm. Since a PVC separator exclusively consists of PVC, it exhibits advantageously good chemical resistance against acid and alkaline solutions. Unlike PE, PVC is disadvantaged due to its brittleness. The decline in PVC separators in recent years is in part due to their tendency to yield chloride ions from chemical attack.

The battery separator currently used by most flooded cell type lead-acid battery manufacturers are of the microporous PE type. It was invented in the late 1960s by W. R. Grace & Co.[214] The term "polyethylene separators" is somewhat misleading, since such a separator consists mainly of agglomerates of precipitated silica, being held within a network of extremely long-chain UHMW PE.[215] A typical PE separator formulation comprises precipitated silica (~60 wt %), UHMW PE (~20 wt %), and mineral process oil (~15 wt %), as well as some processing aids, like antioxidants and/or proprietary surface tension modifiers.[216,217]

The microporous PE separator is commercially manufactured by passing the ingredients through a heated extruder, passing the extrudate generated by the extruder through a die and into the nip formed by two heated calendar rolls to form a continuous web, extracting a substantial amount of the processing oil from the web by use of a solvent, drying the extracted web, slitting the web into lanes of predetermined width, and winding the lanes into rolls.[216]

The PE separators have excellent microporous structure for electrolyte flow with minimal lead particle deposits; excellent ductility, strength, and toughness for envelopability and plate puncture resistance; excellent oxidation, chemical and thermal resistance to resist premature deterioration; and good manufacturability with high production efficiency and relatively low raw material cost, which reduces overall manufacturing costs.[218] The PE pocket sepa-

CosMX Exhibit 1003, Page 312 of 512

Table 10. Comparison of Properties of Different Separators Used in Lead-Acid Batteries

property	rubber	cellulose	PVC	PE	glass fiber
year available	1930	1945	1950	1970	1980
electrical resistance	very poor	poor	poor	very good	very good
porosity	sufficient	good	poor	good	very good
battery performance (cold crank)	poor	sufficient	sufficient	very good	very good
maximum pore size	good	poor	sufficient	very good	poor
mean pore diameter	good	poor	poor	very good	poor
purity	good	fair	good	good	good
resistance to shorting	good	poor	poor	very good	poor
corrosion resistance	very good	poor	good	very good	good
oxidation resistance	fair	poor	good	very good	very good
envelopable (sealability)	very poor	very poor	sufficient	very good	very poor
flexibility	brittle	brittle	brittle	excellent	good

ration is in almost all aspects significantly superior to leaf separation. Only PE separators can be enveloped and can develop good sealability. It has low electrical resistance, sufficient porosity, small pore size, and great resistance to both shorting and corrosion. The PE separator, by virtue of its low electrical resistance, generally provides better cold cranking performance. These separators are very flexible and offer excellent oxidation resistance if the residual oil content is controlled and/or proprietary chemical modifiers have been incorporated. A comparison of the properties of different types of separators is given in Table 10.

PE separators have contributed to improved battery specific energy and specific power, increased battery cycle life, and higher temperature operating capabilities. PE separators have gained in popularity and have generally replaced PVC, cellulose, glass fiber, and other conventional separators. The transition to microporous PE envelope separators started in the U.S. in the 1970s, followed by Europe in 1980s. Today, PE separators have captured almost 100% of the U.S. market and more than 70% of the remaining worldwide automotive markets.[219]

In a flooded cell type lead-acid battery, the battery separator typically has "ribs" or protrusions extending from at least one planar face of the separator. Such ribs are either formed integrally with the backweb of the separator or can be subsequently applied to the backweb as a bead of same or different material as the backweb, or they can be formed by embossing the backweb. The ribs function is to provide proper spacing between the plates and to provide a space wherein free electrolyte resides. The ribs also provides pressure to hold the electrodes in contact with the separator. This reduces the need for precise dimensional control on the cell components. Microporous PE separators typically have a configuration comprising a backweb having a predetermined thickness and a plurality of parallel or patterned ribs spaced apart by a predetermined distance and extending outwardly from one planar surface of the backweb. The ribs extend continuously in a longitudinal direction parallel to the edges of the separator material. The thickness of the backweb and height and spacing of the ribs is specified to the separator manufacturer by the battery manufacturer; based on specifications designed to maximize certain battery characteristics desired by the battery manufacturer. SLI batteries tend to have separators that are thinner than "industrial" lead-acid batteries used for standby power sources and traction devices.

Endoh[220] has reported that one reason for the occasionally shortened life of batteries assembled with PE pocket separators is the development of internal short circuits at the bottom part of the PE separator due to anodic corrosion causing active material to shed from the positive plates and leak through the separators. He also found that when synthetic pulp (SP) separators with glass mats are used, it is possible not only to restrain the shedding from positive plates but also to protect the separators against intensive oxidation so that no internal short circuits take place. He concluded that the use of SP separators with a glass mat is required to produce long service-life batteries, especially in tropical regions.

Higashi et al.[221] carried out endurance test under high-temperature conditions on automotive batteries made with three different types of separators. One group was assembled with PE pocket separators for the negative plates, another with PE pocket separators with glass mats for the positive plates, and a third with leaf-type synthetic pulp separators with glass mats. They concluded that battery assembly with PE pocket separators with a glass mat is an effective way to achieve good endurance (i.e. life extension at high temperature), and leaf-type synthetic pulp separators with glass mats are the best approach for hot climatic conditions.

7.3.2. Valve Regulated Lead Acid (VRLA)

An important development in lead-acid battery technology is the valve regulated lead-acid battery. These batteries operate on the principle of oxygen recombination, using a "starved" or immobilized electrolyte. The oxygen generated at the positive electrode during charge can, in these battery designs, diffuse to the negative electrode, where it can react, in the presence of sulfuric acid, with freshly formed lead. The separator material should provide innumerable gas channels between the plates through which oxygen can migrate from the positive to the negative electrode. These batteries differ from its flooded electrolyte precursor in a number of important ways.[222] They have been manufactured for many years with microfiber glass separators, also called absorptive glass mat (AGM). They are inherently resistant to acid stratification and have the additional important advantage of being essentially

Table 11. Separators and Their Manufacturers for Nickel and Zinc Based Battery Systems

battery system	type of separator	manufacturer and composition
nickel−cadmium	microporous	nylon, Pellon 2505, Polypropylene
nickel−metal hydride	microporous	polypropylene (Scimat, Freudenberg)
nickel−hydrogen	microporous	polymer-inorganic compounds, asbestos, zirconium oxide cloth, Celgard 3501, polypropylene
nickel−zinc	supported liquid membrane, microporous, ion-exchange	polypropylene (Celgard 3400, 3501), PVA
silver−zinc	ion exchange	Permion (RAI); Silvergard (RAI); cross-linked PVA
	microporous	pellon, cellophane, Celgard 3400
zinc−HgO	microporous	cellulose, poly(vinyl alcohol), polyolefins, poly(vinyl chloride)
zinc−air	ion-exchange	PVA cross-linked with dimethylolurea
	microporous	asbestos, nonwoven/polypropylene laminate
zinc/bromine	microporous	polyolefins (Daramic)
	ion-exchange	nafion (DuPont)

maintenance free. The separator is a crucial component in determining the useful life of a VRLA cell. While a prime function of the VRLA cell separator is to hold the cell's electrolyte in place, it must also offer characteristics that prevent major failure mechanisms occurring in the cell's positive and negative plates.

The microglass separator, since its discovery by McClelland and Devitt, has been the material of choice for VRLA designs.[223,224] It is a wet laid nonwoven (glass fiber) "paper" and is manufactured on a paper machine. The type of paper machine used by the manufacturer can influence the separator properties. Three properties—porosity, uniformity, and fiber directionality—are important attributes that can be influenced by the type of fiber used. The glass fiber, which has a zero contact angle with the acid, is durable in the acid environment, and the fine fiber structure also has good resiliency to allow for a sustained pressure against the plate. The microglass separator has a high porosity in the 90−95% range and is very conformable. The separator can adapt to imperfections in the plate surface. The separator also has high-temperature stability. Recent studies have shown that higher levels of fine fiber and higher separator compression provide improved cycle performance in VRLA batteries.[225−228]

On the other hand, AGM separators offer little control over the oxygen transport rate or the recombination process. The arrival of too much oxygen to the negative plate could result in overheating, hindrance of the battery's ability to recharge, or even a loss of capacity. Furthermore, AGM separators exhibit low puncture resistance.

7.4. Nickel Systems

The nickel-based systems include the flowing systems: nickel−iron (Ni/Fe), nickel−cadmium (NiCd), nickel−metal hydrides (NiMH), nickel−hydrogen (Ni/H_2), and nickel−zinc (Ni/Zn). All nickel systems are based on the use of a nickel oxide active material (undergoing one valence change from charge to discharge or vice versa). The electrodes can be pocket type, sintered type, fibrous type, foam type, pasted type, or plastic roll-bonded type. All systems use an alkaline electrolyte, KOH.

The separators may be simple absorbent material except in Ni/Zn where zinc solubility creates zinc electrode shape change and zinc dendrites, resulting in shorts. The fundamental cause for zinc electrode shape change is nonuniform current distribution across the electrode surface. This leads to concentration gradients, which in turn give rise to densification and dendrite formation. In the other systems, solubility of the negative materials is minimal, and therefore, failure by shorting is nonexistent or delayed for a large number of cycles. The vented Ni/Fe, Ni/Cd, and Ni/Zn cells are mostly constructed in a prismatic configuration. Systems built in a sealed cylindrical pressurized configuration are NiCd, NiMH, and Ni−H_2. The pressure configuration in the NiCd and NiMH differs from the Ni−H_2. In the former, pressure is used to hold the electrodes and separator in contact. In the latter pressure is the result of storage of a gaseous reactant. The type of separators and their manufacturers for nickel-based systems are listed in Table 11

7.4.1. Nickel–Cadmium

The NiCd secondary battery is the most popular alkaline secondary battery, and it is available in several cell designs and in a wide range of sizes. It is a very reliable, sturdy, long-life battery, which can be operated effectively at relatively high discharge rates and over a wide temperature range.

7.4.1.1. Vented NiCd. The vented NiCd battery is one of the best-known power sources in the commercial and military fields, particularly for aircraft and communication applications. It has excellent high rate and low temperature performance capabilities. It also has a long useful life capability and is both physically and electrochemically rugged.

Early separators used in NiCd cells for space applications consisted of materials as ordinary as Whatman filter paper[5] and eventually nonwoven nylon felt (Pellon 2505). Pellon 2505 was more stable than cellulosic separators, but it too had stability limitations. In the late 1960s and early 1970s, nonwoven polypropylene saw limited use in NiCd cells. The PP separators were quite useful where sterilization (heating the cell to 135 °C) was required.[229,230] The major difficulty with nonwoven polypropylene was that it was only marginally wettable, and the amount of electrolyte that can be placed in the cell was limited.

In the early 1980s, Pellon Corporation (now Freudenberg) discontinued the manufacturing of Pellon 2505. This led to the qualification of Pellon

CosMX Exhibit 1003, Page 314 of 512

2536 in 1984 as the new separator material for the major portion of NiCd applications in the U.S.[231,232] Hughes Aircraft took a different approach by evaluating Freudenberg FS2117 (a nonwoven nylon fabric), nonwoven polypropylene impregnated with polybenzimidazole (PBI) and zirconium oxide material (Zircar) impregnated with either PBI or polysulfone (PS).[233] Their objective was to develop a separator that is chemically stable for a minimum of 10 years and has a better electrolyte retention and gas permeability than the state-of-the-art Pellon 2505 separator. The main purpose of the polymer impregnation of the zirconia material was to improve the mechanical strength of the fabric, which was too fragile for easy handling in the fabrication of the NiCd cells. The purpose of the PBI impregnation of the polypropylene felt was to improve the wettability in the electrolyte. They found that Zircar impregnated with PBI was the best separator for geosynchronous orbit applications while Zircar impregnated with PS was best for low earth orbit applications. The PP impregnated with PBI found to be as good as Pellon 2505 separator in some cell designs but had longer life because of excellent chemical stability and was additionally less expensive than zirconia material.

The separator used in vented NiCd's is a thin, multiple ply combination. It consists of a cloth (woven or felted nylon) that electrically separates the positive and negative plates and an ion-permeable plastic membrane (microporous polypropylene, Celgard 3400, a wettable variant of Celgard 2400) that serves as the gas barrier. This thin gas barrier, which becomes relatively soft when wetted, is frequently placed between two layers of cloth separators and receives significant mechanical support from them. Previously, cellophane has also been used as the gas barrier layer. Studies done by Hill[234] and Feldman and Verville[235] showed superior performance of NiCd batteries with Celgard microporous polypropylene separators as compared to cellophane. The authors attribute this improvement to the better chemical and thermal stability of the polyolefin sheet membrane. The outer nylon separator degrades with use by undergoing hydrolysis in the KOH electrolyte, thus seriously degrading the battery life.[236] It involves a slow hydrolysis reaction followed by fast electrochemical oxidations of the hydrolysis reaction products.

7.4.1.2. Sealed NiCd. In sealed cells, the positive and negative electrodes are wound together in a jelly roll with a separator material between them. The working principle of sealed NiCd batteries is based on internal oxygen consumption. As a prerequisite the separator has to be permeable to gaseous oxygen, which is achieved by separator pores being of a specific minimum size and not all of them being filled with electrolyte at the same time, so as to leave some gas channels. Nonwovens (fleeces) made of polyamide, PE, and PP fibers have proven themselves in these cells. With their porosity they can absorb sufficient electrolyte, and due to their pore size distribution, they can simultaneously bind electrolyte and allow oxygen transfer.

Mechanical strength is an important criterion for sealed NiCd cells, because wound cells (spiral type construction) are manufactured automatically at very high speeds. Melt blown PP fleeces, with their excellent tensile properties, are good for these cells. Frequently two layers of the same or different materials are used, to gain increased protection against shorts. For higher temperature applications (up to about 60 °C) PP fleeces are preferred since they offer better chemical stability, though at lower electrolyte absorption.[12]

The nylon-based separators tend to degrade by undergoing hydrolysis in the KOH electrolyte. The products formed by the hydrolysis reaction are believed to cause a charge imbalance between positive and negative electrodes in a sealed NiCd cell leading to a loss of overcharge protection. The harmful products include carbonates, which accumulate in the electrolyte. The nylon degradation also gives rise to ammonia and hydroxylamine redox couple, which can increase the self-discharge rate. The rate of the hydrolysis of Nylon-66 separator material was approximately one-half of that of the nylon-6 material.[237] It is well-known that in sealed NiCd cells a separator weight loss of 10% is often sufficient to cause internal shorting.[238]

7.4.2. Nickel–Metal Hydride

The sealed nickel−metal hydride battery has characteristics very similar to those of the sealed NiCd battery. The main difference is that the NiMH battery uses hydrogen, absorbed in a metal alloy, for the active negative material in place of the cadmium used in the NiCd battery. The NiMH batteries have a higher energy density and are considered more environmentally friendly than the NiCd battery. The sealed NiMH battery, however, does not have the very high rate capability of NiCd battery, and is less tolerant of overcharge.

The self-discharge rate of a Ni/MH battery is generally much higher than that of NiCd battery, especially when conventional nylon separators are used.[239] The presence of oxygen and hydrogen gases cause the polyamide materials to decompose, producing corrosion products which poison the nickel hydroxide, promoting premature oxygen evolution and also forming compounds capable of a redox shuttle between the two electrodes which further increases the rate of self-discharge.[240] In the case of the NiMH battery, ammonia and amine participate in the shuttle reaction in the same way that the nitrate ion does in the NiCd battery.

Ikoma et al. carried out a detailed investigation to study the self-discharge mechanism and contribution of separators.[241] They used nonwoven fabric made of conventional polyamide (PA), PP (with surfactant), and a nonwoven fabric whose main material was sulfonated-PP (hydrophilic) as separators. When nonwoven fabric made of chemically stable sulfonated-PP is used as a separator instead of a conventional polyamide separator, the self-discharge rate of the NiMH battery was strongly depressed, to the same level as that of NiCd battery.[240,242,243]

Recently Nagarajan et al.[244] characterized three different commercial AA cells and compared the

materials and cell performance. They used a differential scanning calorimeter (DSC) to determine the materials used as separators. Toshiba cells contained both polyethylene and polypropylene, while the Sanyo and Matsushita cells separators were identified as nonwoven fabrics fabricated from conventional polyamide. Since the Sanyo and Matsushita cells used the conventional polyamide separator, the self-discharge in these cells was substantially higher due to the shuttle reaction of the ammonia and amine, which expedite self-discharge. They also characterized the commercial cells and determined that separators contribution to the overall weight of the AA cell was around 3%.

Scimat Ltd. has shown that acrylic acid grafted nonwoven polyolefin separators have the ability to absorb chemical impurities, for example ammonia, from the alkaline environments. It has been shown that by using a grafted polyolefin separator, the free ammonia present inside a NiMH cell is trapped by the separator, resulting in a reduction in self-discharge to levels normally associated with NiCd cells.[245] In October 2002, Scimat Ltd. announced the launch of the next generation of separators for NiMH and NiCd cells using its second-generation grafting technology.[246]

The commonly used separator material now is the surface treated polypropylene. The surface treatment helps in making the polypropylene permanently wettable. Surface treatments involve the grafting of a chemical such as acrylic acid to the base fibers to impart wettability and is accomplished using a variety of techniques such as UV or cobalt radiation. Another method of imparting wettability to the polypropylene is a sulfonation treatment where the base fiber material is exposed to fuming sulfuric acid. The separator surface is designed to be made hydrophilic to the electrolyte.

Cheng et al.[247] carried out the impedance study on a foam-type NiMH battery with nonwoven PP separator to determine the main causes of early cycle deterioration. Their data indicated that the decrease in the voltage characteristic of the battery was due to drying out of the separator that increases the ohmic resistance of the battery and that decay of the total discharge capacity is due to an inactive surface that increases the charge-transfer of the battery.

7.4.3. Nickel–Hydrogen

Nickel−hydrogen batteries offer long cycle life that exceeds that of other maintenance-free secondary battery systems and accordingly makes it suitable for many space applications. Three types of separator materials have been used for aerospace $Ni-H_2$ cells—asbestos (fuel-cell-grade asbestos paper), Zircar (untreated knit ZYK-15 Zircar cloth),[248] and nylon.[1,249] In year 2000, Japan supplied over 90% of the nickel−hydrogen battery separators globally.[250]

Fuel-cell-grade asbestos is a nonwoven fabric with a thickness of 10−15 mil. The asbestos fibers are made into a long roll of nonwoven cloth by a carding or paper-making process. Asbestos is a controversial material with respect to health considerations in addition to potentially being a source of corrosion at high temperatures. Although asbestos is still in use, there is a trend to replace it with Zircar (zirconium oxide cloth). Zircar fibrous ceramic separators are available in textile product forms (Zircar Products, Inc.). These textiles are composed of zirconium oxide fibers stabilized with approximately 10% yttrium oxide.[251] These materials offer the extreme temperature and chemical resistance of ceramic zirconia. They are constructed of essentially continuous individual filaments fabricated in flexible textile forms. Zircar has the drawback of being expensive and delicate from an assembly perspective. Aerospace cells have shown excellent medium term performances with their nylon separators, but it is known that nylon is weak in terms of its stability over time and its temperature sensitivity.[249]

Zirfon separator is a new alternative for $Ni-H_2$ batteries. It is a porous composite separator material composed of a polysulfone matrix and ZrO_2, which is present in a powder form. The manufacturing is based on the film-casting technique. It is very stable in concentrated KOH solutions at elevated temperatures. These films are around 300 μm thick.[252] SORAPEC has tested Zirfon in $Ni-H_2$ cells and has indicated that it is one of the best separators.[249]

7.5. Zinc Systems

Zinc is a nontoxic, relatively inexpensive, and abundant material. It is the most electropositive metal which is fully compatible with aqueous electrolytes. Its low (negative) electrode potential and its high hydrogen overpotential make it a very suitable negative electrode material for use in aqueous electrolytes.[253]

Although primary cells with zinc electrodes are widespread, secondary systems based on the same materials still suffer from a short lifetime arising from problems caused by zinc mass redistribution, undesirable changes in zinc morphology, and the influence of zinc ions on the opposite electrodes. Because nickel−zinc and manganese dioxide systems are otherwise suitable for electric vehicle propulsion, an effort to develop a long-lasting secondary storage battery is very desirable. One avenue would be to find a better separator for such systems. A lot of work has been done by different groups in developing new separators for zinc-based secondary systems, but none of them have been very successful in developing long cycle life zinc systems. The type of separators and their manufacturers for zinc-based systems are listed in Table 11.

7.5.1. Silver–Zinc

The first practical silver−zinc battery was developed more then 60 years ago. Since then, primary and secondary silver−zinc batteries have attracted a variety of applications due to their high specific energy, proven reliability and safety, and the highest power output per unit weight and volume of all commercially available batteries. However, they find very limited use in commercial applications, because of their high price and limited cycle life. Development of a battery separator which will improve the performance and life of zinc based alkaline cells has been

CosMX Exhibit 1003, Page 316 of 512

and continues to be the focus of concerted efforts in many battery groups, both in industry and academia.

The separator used in silver−zinc cells should be permeable to water and hydroxyl ions, stable in strong alkaline solutions, and not oxidized by the solid silver oxide or dissolved silver ions and should retard the migration of dissolved ions to the anode.[203] A sophisticated separator system is needed to avoid short-circuits resulting from growth of dendrites.[5] Because of the slight solubility of silver oxides in alkaline electrolyte, little work had been done with zinc/silver oxide cells until 1941 when Andre[254] suggested the use of a cellophane barrier. Cellophane prevents migrating silver ions from reaching the anode[255] by reducing them to insoluble silver metal. The cellophane is oxidized and destroyed in the process, making it less effective for long-life cells. Cycle life is very limited, even with the best separators known to date.

In general, secondary silver−zinc cells require a minimum of three different separators. The inner separator, or positive interseparator, serves both as electrolyte reservoir and as a barrier to minimize oxidation of the main separator by the highly oxidative silver electrode. This separator is usually made of a relatively inert fiber such as nylon or polypropylene. The outer separator, or negative interseparator also serves as an electrolyte reservoir and can also, ideally, serve to stabilize the zinc electrode and retard zinc penetration of the main separator, thus minimizing the dendrite growth. Improvement in cell life has been reported with improved inorganic negative electrode interseparators utilizing such materials as asbestos and potassium titanate.[256] Asbestos helps in preventing or reducing the magnitude of short circuits and also acts as a silver "stopper", but it is bulky and reacts with silver oxide. It may also contaminate the cell with iron and posts a health risk during fabrication. A potassium titanate mat helps to reduce zinc shape changes as well as the magnitude of short circuits. It is also bulky and more expensive.[1]

The primary ion exchange separator remains the key to the life of the secondary silver cell. The cellulosics (cellophane, treated cellophane, and fibrous sausage casing) are usually employed in multiple layers as the primary separators for these cells.[257] Cellophane has to be specifically treated as battery grade, meaning a very low content of glycerine (or deglycerinated), since glycerine is an organic material that causes fast degradation of the cell performance by weakening the texture of the cellulosic material under the influence of the strong oxidants (silver peroxide and silver monoxide) present in colloidal form.[258] Cellophane prevents migrating silver ions from reaching the anode by reducing them to insoluble silver metal.[259] The cellophane is oxidized and destroyed in the process, making it less effective for long-life cells. It also physically inhibits the zinc dendrite formation.[260] Cellophane film is typically drawn to a thickness of 1 mil, and usually five or six layers are used to wrap the cathode (silver plate) in the cell.[261]

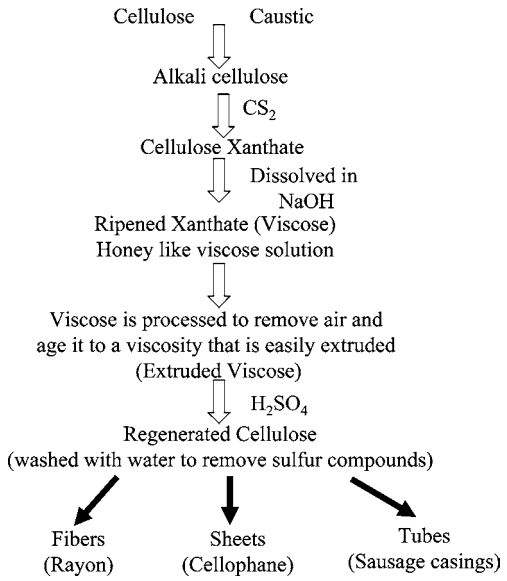


Figure 15. Viscous process for regenerated cellulose.[263]

The tendency for cellulose to degrade in alkaline solutions has been addressed by using multiple layers of the separator in the battery. Lewis et al.[262] showed that double-ply UCB cellophane films were less subject to dendritic hard shorting by zinc and retained some degree of polymerization "DP" after extended cycling. Another way to minimize cellulose degradation in alkaline solutions has been to keep the KOH concentration high (around 45%). The rate of degradation reaction slows down due to the KOH tying up the water used in the hydrolysis reaction.[263] The silver-treated cellophane gives improved life performance, reduction in rates of silver migration, and promotes a longer performance life, compared to plain cellophane.[264] However, cellophane still has significant disadvantages in terms of poor resistance to attack by the alkaline electrolyte and by active materials in the electrodes. These limit the wet life of cells, even when used in multiple layers. Cellophane is also ineffective in preventing shape change, which curtails cycle life.

Thomas Danko has described the manufacturing process and properties of cellulose in detail.[263] The term regenerated cellulose refers to cellulose that has been converted from a solubilized cellulose derivative back into a pure cellulose derivative. The most notable of these processes is the viscous process in which cellulose of fairly high DP can be dissolved and maintained at viscosities that are easy to handle (up to 300000 cps). Figure 15 describes the viscous process in detail.[263] The molecular weight of cellulose is described by the degree of polymerization (DP), which is the number of glucose units in the molecular chain. The final DP is selected based on desired properties and a balance of the regeneration process conditions. Purity of the cellulose plays an important role in the production of regenerated cellulose. The impurities (hemicellulose which is a low DP polysaccharide) in the cellulose reduces the strength of the final film. The properties of the regenerated cellulose can vary depending on the source of wood pulp used (purity) and the regeneration conditions used to

CosMX Exhibit 1003, Page 317 of 512

convert the xanthate derivative back in to cellulose. By using a high purity wood pulp, a stronger and less porous film can be made.

For battery separators, regenerated cellulose is placed on the surface of nonwoven so that the nonwoven is available to promote the wicking of the electrolyte. The nonwovens should not allow the penetration of viscose into itself. Suitable nonwovens are made from polypropylene, poly(vinyl alcohol), and hardwood hemps. Regenerated cellulose films are commonly used in alkaline manganese cells, both primary and secondary, in NiCd industrial batteries, as well as in silver−zinc batteries.

A variety of other separators have been proposed and developed to replace or complement the cellulosics, such as poly(vinyl alcohol) (PVA),[265] radiation-grafted polyethylene,[260] microporous polypropylene, inorganic separators,[256] and other synthetic polymer membranes. The inorganic separators are stable at higher temperatures (~150 °C), and also resist attack by silver oxides and electrolyte, but it leads to higher cell resistance and they are more expensive. Modified polyethylene films are thinner then standard materials leading to higher energy density. They also provide a greater resistance to attachment by silver oxides and electrolyte but are more expensive, more difficult to handle and provide lower resistance to zinc penetration.[1] It requires a coating of the appropriate material(s) to improve the resistance to zinc and silver.

The degradation in mechanical properties of nonwoven battery separator was studied by Danko[266] by storing the separators in 40% KOH for long period of time. The test showed that among the nonwovens, the polyamide retained about 93% of its initial tensile strength whereas poly(vinyl alcohol) and cellulosic nonwovens retained only 55% and 35%, respectively. Adding the viscose coating to the nonwovens improved tensile strength retention by 20−25% for the poly(vinyl alcohol) and cellulosic materials. The viscose-coated polyamide retained more than 98% of its initial tensile strength.

Recently Serenyl used a flexible alkaline separator (FAS) in Silver−Zinc cells, which consists of a microporous polyolefin film, with inorganic filler.[267] This can be folded around the silver and/or zinc electrodes to form conventional "U" wraps or heat sealed bags. They showed that the FAS was not attacked by the electrolyte and helps in inhibiting the "shape change" of zinc electrode.

Another commonly used alternate separator material is prepared from a radiation graft of methacrylic acid onto a polyethylene membrane such as Permion.[259] The graft makes the film wettable and permeable to the electrolyte. The low resistance Permion 2192 barrier membrane is suitable for high-rate KOH cells while higher resistance Permion 2193 is suitable for low rate NaOH cells. Cellophane is still often used in conjunction with the grafted separator as a sacrificial barrier. The lamination of cellophane to either side of the Permion membrane results in a synergistic action for stopping silver migration.[268] Lee and co-workers[269] reported that Permion extended the service life of Zn/AgO button cells from 2 to up to as much as 4−5 years. RAI Research Corporation also developed an improved ion-exchange membrane (Silvergard), which has better selectivity toward silver-ion diffusivity than other ion-exchange membranes.

7.5.2. Nickel–Zinc

The nickel−zinc (NiZn) system is attractive as a secondary cell because of its high energy density and low material cost and the low level of potential pollutants contained. The widespread use of nickel−zinc batteries, particularly as electric vehicle power sources, would be strongly enhanced by significantly extending the deep-discharge cycle life beyond the current level of 100−300 cycles.[270] Considerable work has been done in the past to develop a suitable separator for nickel− and silver−zinc batteries.[271,272] An excellent discussion of separator development is contained in a comprehensive review.[273]

These cells generally fail because of zinc dendrite shorting or zinc electrode shape changes.[274] To mitigate the problem of dendrite growth and subsequent shorting, battery separators should contain submicrometer-size pores, longer pore paths, increased thickness, and multiple layers.[275] As these solutions all lead to increased resistance losses in batteries, a compromise in the properties of separators is necessary. The separator can also influence shape change. Separators with rapid mass transfer properties will reduce the electro-osmosis effects and concentration gradients within the battery, thus slowing the rate of shape change. A lot of developmental work has been done on the nickel−zinc system, but it is still not a commercial system.

The most common material used is cellophane, which is a cellulose film, which acts as a membrane and is capable of resisting zinc penetration. The cycle life of cells utilizing this material is severely limited due to the hydrolysis of the cellophane in alkaline solution. Various methods have been tried to stabilize cellulose materials, such as chemical treatment and radiation grafting to other polymers, but none have, as of now proved economically feasible. The most successful zinc migration barrier material yet developed for the nickel−zinc battery is Celgard microporous polypropylene film.[1] It is inherently hydrophobic so it is typically treated with a wetting agent for aqueous applications.

There are two broad classes of separators employed in nickel−zinc batteries; a main separator, which exhibits resistance to dendrite penetration, and an interseparator, which principally acts as an electrolyte reservoir and wicking layer. Both main and interseparator should be resistant to chemical attack by the alkaline electrolyte and resistant to oxidative attack by nascent oxygen, permanently wettable by the electrolyte, flexible, heat sealable, tear resistant, and inexpensive.

The two basic kinds of nickel−zinc main separators are the membranes and the microporous separators. Membrane separators are those in which ionic transport occurs through the interaction of the hydrophilic groups attached to the polymer with the ionic groups in the electrolyte. Ionic transport through mi-

CosMX Exhibit 1003, Page 318 of 512

croporous separators, on the other hand, occurs by diffusion through discrete pores. Other than wetting, there is essentially no interaction of this type of main separator with the electrolyte.

An important advantage of the microporous separator is that it has high water and electrolyte permeability leading to less electrode shape change. They can be prepared from chemically inert polymers, and hence have good chemical and oxidation resistance. The disadvantages of the microporous membranes are risk of dendrites shorting through the discrete pores and greater scope for zinc oxide to deposit within the separator pores. Membrane separators should provide greater resistance to zinc dendrite penetration, much lower rates of active material migration away from the negative electrode, and probably no deposition of zinc oxide within the separator. Their main disadvantages are the higher rates of negative electrode shape change resulting from poor mass transfer properties and the greater vulnerability to chemical attack.[276]

Lundquist[276] compared the performance of membrane separators with microporous separators and found that the rate of zinc electrode shape change is greater in batteries with membrane separators although in either case shape change was the primary failure mode. Batteries containing separators with the lowest electrolytic resistivity and highest water permeability gave the longest cycle life. The results favored the use of microporous separators since its superior mass transfer characteristics minimize the rate of shape change.

Studies made by several authors, such as Poa,[277] Wagner,[278] and Brown,[279] have shown significant improvement in the performance of NiZn rechargeable batteries, when microporous polyolefin flat sheet membranes were used as separators. Poa and coworkers examined the diffusion of the OH^- electrolyte through candidate separator materials, including microporous polypropylene, Celgard 3501 (Celgard 2500 coated with a proprietary surfactant). The OH^- diffusional flow for Celgard 3501 was found to be greater than either the traditional swollen, nonporous cellophane separator used in the battery or a nonporous methacrylic acid grafted and cross-linked polyethylene.[277]

Krejci et al. studied the transport of zincate ions through modified microporous PP separators (Celgard 3401, Celgard 3501) using polarography and conductometry.[280] Celgard 3401 and 3501 were chosen because they are proven to have slow redistribution of zinc material, good mechanical properties, and low electrical resistivity. Soluble Nafion as an ion exchange modifying agent was applied to the PP microporous separators. They studied the influence of Nafion and surfactant (coated on 3401 and 3501) on transport of zinc ions through the membrane. It was found that the zincate ions transport through the membrane was higher for higher conductivity membranes and vice versa. Higher amounts of surfactant and Nafion coating increase both the membrane conductivity and the membrane's ability to allow zinc ions to pass.

Castle Technology Corporation had developed a supported liquid membrane battery separator to prevent zinc dendrite growth and decrease the shape changes on zinc electrode.[281] These membranes use a highly specific organic transport reagent contained in a microporous membrane support to transport hydroxyl ions while rejecting zincate ions. Several materials (polyvinyl chloride (PVC), PVC copolymer, nylon, nonwoven PP, and microporous PP) were tested, and Celgard 2500 was found to be the best material because of its larger pore size and higher porosity.

The nickel zinc system would be a suitable power source for many portable devices if the cells were tightly sealed and had a prolonged life. In sealed nickel−zinc batteries, oxygen, which is formed on the positive electrode, has to recombine with metallic zinc at the negative electrode. The microporous membrane must have some degree of permeability to oxygen.[282] Sato et al. developed a separator which consisted of nylon nonwoven cloth coated with poly(vinyl alcohol) (PVA) containing boric acid. The separator has a high ionic conductivity and is resistant to zincate ion penetration.[283]

To address the zinc dendrite problem in nickel−zinc cells, eVionyx claims to have developed a proprietary membrane system that is nonporous, has very high ionic conductivity, is of low cost, and can block zinc dendrite penetration even in high concentrations of KOH.[284−286] The polymeric membrane has an ionic species contained in a solution phase thereof. The ionic species behaves like a liquid electrolyte, while at the same time the polymer-based solid gel membrane provides a smooth impenetrable surface that allows the exchange of ions for both discharging and charging of the cell.

7.5.3. Zinc–Air

For many applications zinc−air technology offers the highest available energy density of any primary battery system. It also offers a flat discharge voltage, long shelf life, safety and ecological benefits, and low energy cost. Since these cells are open to the ambient atmosphere, a factor limiting universal applications of zinc−air technology is the trade off between long service life and maximum power capability.

The separator materials used in zinc−air batteries should be inert to oxidation, stable in cells at high potentials, chemically inert to KOH at high temperatures, have a fine porous capillary structure to hold the electrolyte in the pores (and limit diffusion of oxygen gas), have a high bubble pressure, and exhibit low electrical resistance. Usually a polypropylene membrane such as treated Celgard 2500 or Celgard 3501 is used as separator in these cells. The function of the separator is to prevent cross mixing of the positive and negative electrolytes but to still allow the transport of ions. Because of its porosity, the cationic compound produced in the anode reaction can easily pass through the separator to cathode that leads to an increased polarization and decreased capacity and battery life. The separator should be able to stop the passage of these cationic compounds to increase the cell life. The commercial Zn−air cells

also use laminated separators (e.g. Celgard 4560 and Celgard 5550), which have a microporous membrane laminated with a nonwoven.

Dewi et al. used a cationic polysulfonium membrane as a separator in a zinc−air cell. They showed that the polysulfonium membranes were highly effective in preventing zinc cation permeation from the anode to the cathode compared to the commercially available PP separators.[287]

A new polymeric separator membrane has been developed for alkaline electrochemical systems (e.g. metal/air, Zn/Ni, Zn/MnO_2, Zn/HgO etc.) by Schubert et al.[288,289] It is a water-soluble copolymer of acrylic acid and sodium styrenesulfonate monomers (PAASS). The monomer ratio is varied to manipulate electrolyte absorption and ionic resistivity of the copolymer. Processes have been developed to coat PAASS onto conventional nonwoven separator papers to produce composite membranes. The monomer ratio and the coating weight can be adjusted to balance ionic resistivity and shorting protection to provide adequate overall performance. PAASS coated separators demonstrate good barrier properties to soluble zincate and silver species. Preliminary use of PAASS separator materials in a rechargeable Zn/air system showed a significant improvement in shorting protection over microporous materials such as Celgard 3401.

The primary zinc−air cells have captured the hearing aid market, but the rechargeable zinc−air battery is still in the developmental stage.

7.5.4. Zinc–Bromine

The zinc−bromine battery is an attractive technology for both utility-energy storage and electric-vehicle applications. The technology has been limited in use and not commercialized due to two major drawbacks, the tendency of zinc to form dendrites and the high solubility of bromine in the aqueous zinc bromide electrolytes. Dendritic zinc deposits could easily short circuit the cell, and the high solubility of bromine allows diffusion and direct reaction with the zinc electrode, resulting in self-discharge of the cell.

Various materials have been used as separators in zinc−bromine cells. Ideally a material is needed which allows the transport of zinc and bromide ions but does not allow the transport of aqueous bromine, polybromide ions, or complex phase structures. Ion selective membranes are more efficient at blocking transport then nonselective membranes.[290] These membranes, however, are more expensive, less durable, and more difficult to handle then microporous membranes (e.g., Daramic membranes).[291] The use of ion selective membranes can also produce problems with the balance of water between the positive and negative electrolyte flow loops. Thus, battery developers have only used nonselective microporous materials for the separator.[292]

Microporous separators have the advantage of being relatively low-cost and adequately stable in the electrolyte, but unfortunately they contribute to energy-efficiency losses in the battery. Rapid transport of bromine through microporous separators and accumulation of a bromine−oil complex in the separator lead to efficiency losses. Thus, improved separators with lower bromine mass transport and higher electrolytic conductivity would be beneficial for improving the energy efficiency of zinc−bromine batteries.

7.6. Redox Flow Batteries

The redox flow battery (RFB) concept was first proposed by L. H. Thaller at the NASA Lewis Research Center, Cleveland, OH.[293,294] Since then, it has been investigated as one of the energy storage systems for solar power, nuclear power, load leveling purposes, and electric vehicles.[295]

The all-vanadium RFB developed by the University of New South Wales has the advantage of a higher electromotive force (1.4 V in a vanadium system compared to 1.1 V in an Fe/Cr system) and a higher energy density compared with other RFB systems.[296] It employs V(II)/V(III) and V(IV)/V(V) redox couples in the negative and positive half-cell electrolytes. The ideal membrane for this system should exhibit low permeation rates of the active species to minimize self-discharge and also have low area resistivity to minimize losses in internal energy. Further, the membrane should also exhibit good chemical stability for long cycle life. The energy losses in a V−RFB are partly caused by the undesired transport of vanadium ions of different oxidation states across the membrane, which separates the anolytic from the catholytic solution in the battery system.[297]

Ion exchange membranes of cation and anion selectivity are usually used as the membrane separators for V−RFB. Commercially available cation selective CMV membrane (Asahi Glass) degrades by the fully charged anolyte,[298] but the Nafion membrane (Dupont) does not appear to degrade. However, the current efficiency of the V−RFB using Nafion decreases due to self-discharge of the vanadium ions, which permeated through the membrane.[298] Furthermore, the cost of Nafion is exceptionally high. Chlorosulfonated polyolefin membrane shows a good resistivity to oxidation and its resistivity in the RFB, almost equal to Nafion.[299] It has also been reported that a cross-linked chlorosulfonated homogeneous membrane formed by accelerated electron radiation at 2.5 Mrad/pass had a longer lifetime than the non cross-linked membrane because of the increase in the chemical stability.[300,301]

Microporous membranes perform poorly in V−RFB compared to ion exchange membranes due to their poor selectivity. Modification of low cost microporous separators to impart perm-selective properties could lead to significant cost reduction. Chieng et al. developed a composite membrane from Daramic (a microporous separator), treated with Amberlite 400CG (an ion-exchange resin), and cross-linked using divinylbenzene.[302,303] The separator selectivity was improved by partially blocking or by reducing the pore size or by incorporating some ion exchange capability to the separator. The chemical stability of the membrane was found to be excellent, and the membrane was not susceptible to fouling.[304] Sulfonation of the

CosMX Exhibit 1003, Page 320 of 512

cross-linked Daramic separators was done to impart some cation-exchange capacity, and it was successful in reducing the amount of water transport across the membrane in V−RBC.[305] The scale-up of sulfonation process is both difficult and expensive due to the very corrosive nature of concentrated sulfuric acid. Incorporation of cation-exchange groups using poly(sodium 4-styrenesulfonate) (PSSS) has been studied, and results show that the method reduces the water transport across the membrane. The PSSS treatment step can be easily scaled up.[306]

Diffusion coefficients of vanadium ions in CMS (Neosepta made by Tokuyama Soda), CMV (Selemion made by Asahi Glass), and CMX (Neosepta made by Tokuyama Soda) cation exchange membranes were determined by measuring the ion-exchange fluxes of the vanadium ions with H_3O^+ ions using a dialysis cell.[297] The lowest diffusion coefficients were observed in the CMS membrane for all vanadium ions. CMS membranes were found to be most suitable for V−RFB, as it was expected to prevent cross contamination of vanadium ions.[307]

One of the most important requirements that must be met is the membrane's ability to prevent excessive transfer of water from one half cell to the other. The preferential transfer of water can be a problem in the vanadium battery as one half-cell (the negative half cell in the case of cation exchange membranes) is flooded and becomes diluted, while the other becomes more concentrated, adversely affecting the overall operation of the cell. Most of the membranes show good initial water transfer properties, but their performance deteriorates with exposure to the vanadium solutions. Sukkar et al.[308] evaluated various polyelectrolytes to determine whether they could improve the selectivity and stability of the membranes in the vanadium redox cell solutions. Both the cationic and anionic polyelectrolytes evaluated improved the water transfer properties of the membranes, although upon extended exposure to the vanadium electrolyte the modified membranes did not maintain their improved water transfer properties. The solvent based Nuosperse 657 modified membrane displayed exceptional properties initially but also failed to maintain its performance with extended exposure to the vanadium solutions.

Another system under investigation is the iron/chromium redox flow battery (Fe/Cr RFB) developed by NASA. The performance requirements of the membrane for Fe/Cr RFB are severe. The membrane must readily permit the passage of chloride ions, but should not allow any mixing of the chromium and iron ions. An anionic permselective membrane CDIL-AA5-LC-397, developed by Ionics, Inc., performed well in this system.[309] It was prepared by a free radical polymerization of vinylbenzyl chloride and dimethylaminoethyl methacrylate in a 1:1 molar ratio. One major issue with the anionic membranes was its increase in resistance during the time it was exposed to a ferric chloride solution. The resistance increase termed "fouling" is related to the ability of the ferric ion to form ferric chloride complexes, which are not electrically repelled by the anionic membrane. An experiment by Arnold and Assink indicated that fouling decreased when the degree of cross-linking of the anion-exchange membrane was increased.[310]

Hruska et al.[311] evaluated various microporous materials (Celgard 5511 composed of porous polypropylene and Daramic W0733 composed of porous polyethylene) to reduce the columbic efficiency loss caused by the oxidation of the iron plate. The chemical resistances of both Celgard and Daramic membranes in iron electrolytes were excellent at pH = 0. Celgard separators with very low resistivity offered some improvement in columbic efficiency but the Daramic separators gave very high columbic efficiencies in a laboratory size redox cell. Daramic separators also limited the ferric ion diffusional loss to about 3% for both charge and discharge modes of operation. Two commercial ion exchange membranes were also evaluated in this study: Neosepta ACH-45T (Tokuyama Soda Company Ltd.) and Selemion DMV (Asahi Glass Company Limited). In laboratory cells, the membranes discolored, giving evidence of deterioration, and the resistivity of the membrane increased significantly. The increased resistivity was attributed to $FeCl_4^-$ fouling. Thus, attempts at lowering the polarization by maintaining a pH differential across the cell with commercial anion membranes were unsuccessful because of membrane fouling. In spite of the poor voltaic performance of the membrane, the overall Coulombic efficiency was found to be exceptionally good.

8. Mathematical Modeling of Batteries/Separators

Computer simulations have been used as a tool for understanding and optimizing battery performance since the 1970s.[312−314] Continued progress in computational tools has enabled ever-increasing sophistication in battery modeling and a steady increase in the number of systems to which modeling has been applied. Today it is possible to obtain simulation codes for all of the major rechargeable batteries, some of which are available for free.[315]

The mathematical models of different types of batteries (lead-acid,[316,317] NiMH,[318] lithium-ion[319,320]) have been developed during the past few years.[315] This has led to a better understanding of those systems. The present models consider only the thickness and porosity of the separators. Not much work has been done in incorporating the effect of physical and chemical properties of separators on the performance and safety of batteries. This is also because the microstructure of separators and their effect on transport properties in batteries are generally known only qualitatively. A thorough understanding of the microstructure of separators would be beneficial for modeling studies and optimization of electrochemical systems. This will help in making the battery model predictions more practical and reliable.

The separator pore structure is usually very complex. It consists of a porous network of interconnected pores, which are filled with liquid electrolyte. A complete description of the pore structure would require a very intricate model. Simulations are only practically possible if the structure is represented by a simplified quasi-continuum involving a few param-

eters. In such an approach, the "effective" electrolytic conductivity, σ_{eff}, is often defined by[97]

$$\sigma_{eff} = \epsilon^{\alpha}\sigma_0, \quad \alpha \approx 1.5 \tag{11}$$

where σ_0 is the bulk ionic conductivity of the electrolyte, ϵ is the void volume fraction of separator filled with electrolyte, and α is the Bruggeman exponent. The general applicability of $\alpha \sim 1.5$, appears questionable because separator pores are never of an ideal shape. Fan and White[321] chose a α value of 2.5 for separators in NiCd batteries, and Doyle et al.[322] used 3.3 for lithium-ion batteries. Arora et al.[323] measured the value as 2.4 for PVdF based separators by measuring the separator and electrolyte conductivity at different salt concentrations. Doyle et al. used an even higher Bruggeman exponent of 4.5 for quantifying the ionic conductivity of their plasticized electrolyte membrane.[322]

Patel et al. showed that a Bruggeman exponent of 1.5 is often not valid for real separator materials, which do not have uniform spherical shape.[324] Porous networks based on other morphologies such as oblate (disk-type) ellipsoids or lameller increase the tortuous path for ionic conductivity and result either in a significant increase of the exponent α, or in a complete deviation from the power law. They showed that spherical or slightly prolate ellipsoidal pores should be preferred for separators, as they lead to higher ionic conductivity separators.

Tye[325] explained that separator tortuosity is a key property determining transient response of a separator and steady-state electrical measurements do not reflect the influence of tortuosity. He recommended that the *distribution of tortuosity* in separators be considered; some pores may have less tortuous paths than others. He showed mathematically that separators with identical average tortuosities and porosities could be distinguished by their unsteady-state behavior if they have different distributions of tortuosity.

Doyle et al.[322] used a mathematical model to examine the effect of separator thickness for the PVdF:HFP gel electrolyte system and found that decreasing separator thickness below 52 μm caused only a minor decrease in ohmic drop across the cell. The voltage drops in the electrodes were much more significant. Mao and White[326] developed a mathematical model for discharge of a Li/TiS_2 cell. Their model predicted that increasing the thickness of the separator from 25 to 100 μm decreased the discharge capacity from 95% to about 90%; further increasing separator thickness to 200 μm reduced discharge capacity to 75%. These theoretical results indicate that conventional separators (25−37 μm thick) do not significantly limit mass transfer of lithium.

The use of electroactive polymers for overcharge protection has been recently reported for lithium-ion batteries.[327,328] The electroactive polymer incorporated into a battery's separator is an attractive new option for overcharge protection. Thomas et al.[329] developed a mathematical model to explain how electroactive polymers such as polythiophene can be used to provide overcharge protection for lithium-ion batteries. The model shows that, as the cell potential exceeds the oxidation potential of the polymer, the cell is transformed, over a time scale of a few minutes, from a battery into a resistor, after which a steady-state overcharge condition is attained.

9. Summary

The ideal battery separator would be infinitesimally thin, offer no resistance to ionic transport in electrolytes, provide infinite resistance to electronic conductivity for isolation of electrodes, be highly tortuous to prevent dendritic growths, and be inert to chemical reactions. Unfortunately, in the real world the ideal case does not exist. Real world separators are electronically insulating membranes whose ionic resistivity is brought to the desired range by manipulating the membranes thickness and porosity.

It is clear that no single separator satisfies all the needs of battery designers, and compromises have to be made. It is ultimately the application that decides which separator is most suitable. We hope that this paper will be a useful tool and will help the battery manufacturers in selecting the most appropriate separators for their batteries and respective applications. The information provided is purely technical and does not include other very important parameters, such as cost of production, availability, and long-term stability.

There has been a continued demand for thinner battery separators to increase battery power and capacity. This has been especially true for lithium-ion batteries used in portable electronics. However, it is very important to ensure the continued safety of batteries, and this is where the role of the separator is greatest. Thus, it is essential to optimize all the components of battery to improve the performance while maintaining the safety of these cells. Separator manufacturers should work along with the battery manufacturers to create the next generation of batteries with increased reliability and performance, but always keeping safety in mind.

This paper has attempted to present a comprehensive review of literature on separators used in various batteries. It is evident that a wide variety of separators are available and that they are critical components in batteries. In many cases, the separator is one of the major factors limiting the life and/or performance of batteries. Consequently, development of new improved separators would be very beneficial for the advanced high capacity batteries.

10. Future Directions

Up until more recent history, most of the separators and membranes historically used had not been specifically developed for battery applications. Thus, future research should be aimed at developing separators that are specifically tailored for battery applications. The general objectives of separator research should be as follows: (a) to find new and cost-effective separators, (b) to understand the separator properties in batteries, and (c) to optimize separator properties related to specific cell performance, life,

and safety. One way to achieve some of these goals will be to develop mathematical models that reflect the effects of separator resistance, thickness, pore size, shrinkage, tortuosity, and mechanical strength on the final performance and safety of batteries. The battery separators for tomorrow will demand more than just good insulation and mechanical filtration; they will require unique electrochemical properties.

11. Acknowledgments

The authors would like to acknowledge numerous colleagues and staff members at Celgard, LLC., and Polypore, International, Inc., for their help with the preparation and publication of this paper.

12. References

(1) Linden, D.; Reddy, T. B. *Handbook of Batteries*, 3rd ed.; McGraw-Hill: New York, 2002.
(2) Besenhard, J. O. Editor, *Handbook of Battery Materials*; Wiley-VCH: Weinheim, Germany, 1999.
(3) Berndt, D. *Maintenance Free Batteries*, 3rd ed., Research Studies Press Ltd.: Taunton, Somerset, England, 2003.
(4) Bode, H. *Lead-Acid Batteries*; John Wiley: New York, 1977.
(5) Falk, S. U.; Salkind, A. J. *Alkaline Storage Batteries*; John Wiley: New York, 1969.
(6) Fleischer, A.; Lander, J. J. *Zinc−Silver Oxide Batteries*; John Wiley: New York, 1971.
(7) Brodd, R. J., Friend, H. M., Nardi, J. C., Eds. *Lithium Ion Battery Technology*: ITE-JEC Press: Brunswick, OH, 1995.
(8) Wakihara, M., Yamamoto, O., Eds. *Lithium Ion Batteries, Fundamentals and Performance*; Wiley-VCH: New York, 1998.
(9) Yoshino, A. *Chem. Ind.* **1995**, *146*, 870.
(10) Schalkwijk, W. A. V., Ed. *Advances in Lithium Ion Batteries*; Kluwer Academic: New York, 2002.
(11) Kinoshita, K.; Yeo, R. *Survey on Separators for Electrochemical Systems*; LBNL: January 1985.
(12) Benett, J.; Choi, W. M. Developments in small cell separators. In *Proceedings of the 10th Annual Battery Conference on Applications & Advances*; IEEE: New York, 1995; p 265.
(13) Boehnstedt, W. In *Handbook of Battery Materials*; Besenhard, J. O., Ed.; VCH Wiley: Amsterdam and New York, 1999.
(14) Spotnitz, R. In *Handbook of Battery Materials*; Besenhard, J. O., Ed.; VCH Wiley: Amsterdam and New York, 1999.
(15) Shirai, H.; Spotnitz, R. *Lithium Ion Secondary Battery−Materials and Applications*; Yoshio, K, Ed.; Nikkan Kogyo Shin-bun: Tokyo, 1996; p 91 (in Japanese).
(16) Shirai, H.; Spotnitz, R.; Atsushi, A. *Chem. Ind.* **1997**, *48*, 47 (in Japanese).
(17) Hiroshi, T. In *The Latest Technologies of the New Secondary Battery Material*; Ogumi, Z., Ed.; CMC: Tokyo, 200X; p 99 (in Japanese).
(18) Hiroshi, T. In *Advanced Technologies for Polymer Battery*; Oyama, N., Ed.; CMC: Tokyo, 200X; p 165 (in Japanese).
(19) Koichi, K. In *Advanced Technologies for Polymer Battery*; Oyama, N., Ed.; CMC: Tokyo, 200X; p 174. (In Japanese).
(20) Kiyoshi, K. In *Lithium Secondary Battery Technology for the 21st Century*, Kanamura, K., Ed.; CMC: Tokyo, 200X; p 116.
(21) Brodd, R. J.; Bullock, K. R.; Leising, R. A.; Middaugh, R. L.; Miller, J. R.; Takeuchi, E. *J. Electrochem. Soc.* **2004**, *151*, K1.
(22) *Battery Power Prod. Technol.* **2003**, *7* (May), 15.
(23) Takeshita, H. Presented at The 21st International Seminar & Exhibit on Primary & Secondary Batteries, Fort Lauderdale, FL, Florida Educational Seminars Inc., March 8, 2004.
(24) *Battery EV Technol.* **2004**, *28* (Jan), 2.
(25) Pilot, C. The Worldwide Rechargeable Battery Market. Presented at Batteries 2004, 6th ed.; Paris, June 2−4, 2004.
(26) Celgard LLC http://www.celgard.com.
(27) Celgard completes capacity expansion, Global Sources, http://www.globalsources.com, February 04, 2004.
(28) Asahi Kasei adding battery membrane capacity. *Nikkei Net Interact.* http://www.nni.nikkei.co.jp/AC/TNKS/Nni20030806D06JFA23.htm, August 7, 2003.
(29) Advanced Rechargeable Battery Industry 2001/2002, Nomura Research Institute Limited, 2002.
(30) About Edison Batteries, Inc., http://www.optodot.com/sys-tmpl/htmlpage/.
(31) *Battery and Fuel Cell Components*; The Fredonia Group: 2003.
(32) *Adv. Battery Technol.* **2004**, *40* (Feb), 22.
(33) Hamano, K.; Yoshida, Y.; Shiota, H.; Shiraga, S.; Aihara, S.; Murai, M.; Inuzuka, T. U.S. Patent 6,664,007, B2, 2003.
(34) Sun, L.; Chen, G.; Xu, D.; Abe, T. Presented at the 204th Meeting of The Electrochemical Society, 2003; Abstract 423.
(35) Sun, L. U.S. Patent 2003/0152828A1, 2003.
(36) Johnson, B. A.; White, R. E. *J. Power Sources* **1998**, *70*, 48.
(37) Hoffman, H. G. *Proceedings of the Tenth Annual Battery Conference on Applications and Advances*; IEEE: New York, 1995; p 253.
(38) Bradford, S. M. *Battery Power Prod. Technol.* **2004**, (Mar), 17.
(39) Frost & Sullivan Research World Rechargeable Battery Markets for Mobile IT and Communication Devices (A575−27); 2002.
(40) Geiger, M.; Callahan, R. W.; Diwiggins, C. F.; Fisher, H. M.; Hoffman, D. K.; Yu, W. C.; Abraham, K. M.; Jillson, M. H.; Nguyen, T. H. Presented at The Eleventh International Seminar on Primary and Secondary Battery Technology and Application, Fort Lauderdale, FL, Florida Educational Seminars Inc., Feb 28−Mar 3, 1994.
(41) Tanba, H. *Molding Process* **1999**, *11*, 759.
(42) Adachi, A.; Spotnitz, R. M.; et al. *Osaka Chem. Marketing Center* **1997**, 69−80.
(43) Yu, W. C.; Hux, S. E. U.S. Patent, 5,952,120, 1999.
(44) Hipore, Asahi Kasai, http://www.asahi-kasai.co.jp/memrbane/english/tradenm/t07.html.
(45) Bierenbaum, H. S.; Isaacson, R. B.; Druin, M. L.; Plovan, S. G. *Ind. Eng. Chem. Prod. Res. Dev.* **1974**, *13*, 2.
(46) *Jpn. Ind. News* **1996**, *91*.
(47) Kim, S. S.; Lloyd, D. R. *J. Membr. Sci.* **1991**, *64*, 13.
(48) Druin, M. L.; Loft, J. T.; Plovan, S. G. U.S. Patent 3,801,404. 1974.
(49) Schell, W. J.; Zhang, Z. *The Fourteenth Annual Battery Conference on Applications and Advances, Long Beach, CA*; IEEE: New York, 1999; p 161.
(50) Isaacson, R. B.; Bierenbaum, H. S. U.S. Patent 3,558,764, 1971.
(51) Kamei, E.; Shimomura, Y. U.S. Patent 4,563,317, 1986.
(52) Yu, T. H. Processing and Structure−Property Behavior of Microporous Polyethylene−From Resin to Final Film Ph.D. Dissertation, Virginia Polytechnic Institute and State University, Blacksburg, VA, 1996.
(53) Sarada, T.; Sawyer, L. C.; Ostler, M. I. *J. Membr. Sci.* **1983**, *15*, 97.
(54) Bierenbaum, H. S.; Daley, L. R.; Zimmerman, D.; Hay, I. L. U.S. Patent, 3,843,761, 1974.
(55) Hamer, E. A. G. U.S. Patent, 4,620,956, 1986.
(56) Hiroshi, K.; Tetuo, A.; Akira, K. U.S. Patent 5,691,047, 1997.
(57) Kesting, R. E. *Synthetic Polymeric Membranes*, 2nd ed.; John Wiley & Sons Inc.: New York, 1985; Chapter 2.
(58) Ihm, D. W.; Noh, J. G.; Kim, J. Y. *J. Power Sources* **2002**, *109*, 388.
(59) Takita, K.; kono, K.; Takashima, T.; Okamoto, K. U.S. Patent, 5,051,183, 1991.
(60) Michiyuki, A.; Jpn. Patent 8064194, 1996.
(61) Kotaro, T.; Koichi, K.; Tatsuya, T.; Kenkichi, O. U.S. Patent 5,-051,183, 1991.
(62) Koichi, K.; Kotaro, T.; Mamoru, T.; Tatsuya, T. Jpn. Patent 8012799, 1996.
(63) Norimitsu, K.; Kotaru, T.; Koichi, K.; Hidehiko, F. U.S. Patent 6,153,133, 2000.
(64) Akinao, H.; Kazuo, Y.; Hitoshi, M. U.S. Patent 6,048,607, 2000.
(65) Pekala, R. W.; Khavari, M. U.S. Patent 6,586,138, 2003.
(66) Userguide, FreedomCar Separator Costing Document, February 2003.
(67) Xu, M.; Hu, S.; Guan, J.; Sun, X.; Wu, W.; Zhu, W.; Zhang, X.; Ma, Z.; Han, Q.; Liu, S. U.S. Patent 5,134,174, 1992.
(68) Fisher, H. M.; Wensley, C. G. U.S. Patent 6,368,742, 2002.
(69) Zhu, W.; Zhang, X.; Zhao, C.; Zu, W.; Hou, J.; Xu, M. *Polym. Adv. Technol.* **1996**, *7*, 743.
(70) Sadamitsu, K.; Ikeda, N.; Hoki, Manabu, Nagata, K.; Ogino, K. World Patent Application 02066233A1, 2002.
(71) Higuchi, H.; Matsushita, K.; Ezoe, M.; Shinomura, T. U.S. Patent 5,385,777, 1995.
(72) Calis, G. H. M.; Daemen, A. P. M.; Gerrits, N. S. J. A.; Smedinga, J. T. *J. Power Sources* **1997**, *65*, 275.
(73) Ooms, F. G. B.; Kelder, E. M.; Schoonman, J.; Gerrits, N.; Smedinga, J.; Calis, G. *J. Power Sources* **2001**, *97−98*, 598.
(74) Yamamura, Y.; Ooizumi, S.; Yamamoto, K. Separator for rechargeable lithium ion batteries with high puncture strength and high melt rupture temperature. *Nitto Denko Technol. Rep.* (http://www.nitto.com/rd/rd6_1.html), **2001**, *39*, 39.
(75) Pekala, R. W.; Khavari, M.; Dobbie, G.; Lee, D.; Fraser-Bell, G. Presented at the 17th International Seminar & Exhibit on Primary and Secondary Batteries, Fort Lauderdale, FL, Florida Educational Seminars, Inc., March 6−9, 2000.
(76) Fleming, R.; Taskier, H. *Prog. Batteries Solar Cells* **1990**, *9*, 58.
(77) Hoffman, D.; Fisher, H.; Langford, E.; Diwiggins, C. *Prog. Batteries Solar Cells* **1990**, *9*, 48.
(78) Yu, W. C.; Callahan, R. W.; Diwiggins, C. F.; Fischer, H. M.; Geiger, M. W.; Schell, W. J. Presented at the North America Membrane Society Conference, Breckenridge, CO, 1994.
(79) Kuribayashi, I. *J. Power Sources* **1996**, *63*, 87.

CosMX Exhibit 1003, Page 323 of 512

(80) Pasquier, A. D.; Gozdz, A.; Plitz, I.; Shelburne, J. Presented at the 201st meeting of The Electrochemical Society, Philadelphia, PA, May 12−17, 2002.
(81) Augustin, S.; Volker, H.; Gerhard, H.; Christian, H. *Desalination* **2002**, *146*, 23.
(82) http://www.separion.com.
(83) Hying, C. Separion separators for lithium batteries−safety & performance. Presented at Batteries 2004, 6th Ed.; Paris, June 2−4, 2004.
(84) Sachan, S.; Ray, C. A.; Perusich, S. A. *Polym. Eng. Sci.* **2002**, *42*, 1469.
(85) Sachan, S.; Perusich, S. Electrochemical Society Meeting, Seattle, 1999.
(86) Carlson, S. A. *Membr. Sep. Technol. News* **2004**, *22*, 8.
(87) Abraham, K. M. *Electrochim. Acta* **1993**, *38*, 1233.
(88) Gineste, J. L.; Pourcell, G. *J. Membr. Sci.* **1995**, *107*, 155.
(89) Hoffman, D. K.; Abraham, K. M. In *Proceedings of the Fifth International Seminar on Lithium Battery Technology and Applications*; Florida Educational Seminars, Inc.: Deerfield Beach, FL, 1991.
(90) USABC "Development of low cost separators for lithium-ion batteries", RFPI 2001.
(91) Laman, F. C.; Sakutai, Y.; Hirai, T.; Yamaki, J.; Tobishima, S. *Ext. Abstr., 6th Int. Meet. Lithium Batteries* **1992**, 298−300.
(92) Laman, F. C.; Gee, M. A.; Denovan, J. *J. Electrochem. Soc.* **1993**, *140*, L51.
(93) Abraham, K. M. *Electrochim. Acta* **1993**, *38*, 1233.
(94) Robinson, R. G.; Walker, R. L. In *Batteries*; Collins, D. H., Ed.; The MacMillan Company: New York, 1963; p 15.
(95) Lander, J. J.; Weaver, R. D.; Salkind, A. J.; Kelley, J. J. In *Characteristics of Separators for Alkaline Siver Oxide Zinc Secondary Batteries. Screening Methods*; Cooper, J. E., Fleischer, A., Eds.; NASA Technical Report NAS 5-2860, 1964.
(96) Kilroy, W. P.; Moynihan, C. T. *J. Electrochem. Soc.* **1978**, *125*, 520.
(97) MacMullin, R. B.; Muccini, G. A. *AIChE J.* **1956**, *2*, 393.
(98) Callahan, R. W.; Nguyen, K. V.; McLean, J. G.; Propost, J.; Hoffman, D. K. *Proceedings of the 10th International Seminar on Primary and Secondary Battery Technology and Application*; Florida Educational Seminars, Inc.: Fort Lauderdale, FL, 1993.
(99) Ionov, V. V.; Isakevitch, V. V.; Katalevsky, E. E.; Chernokoz, A. J. *J. Power Sources* **1990**, *30*, 321.
(100) Lowell, S.; Shields, E. *Powder Surface Area and Porosity*, 3rd ed.; Chapman and Hall: New York, 1991.
(101) PMI Conference 2000 Proceedings, PMI short course, Ithaca, NY, Oct 16−19, 2000.
(102) Porous Materials Inc, http://www.pmiapp.com.
(103) Jena, A. K.; Gupta, K. M. *J. Power Sources* **1999**, *80*, 46.
(104) Jena, A. K.; Gupta, K. M. *J. Power Sources* **2001**, *96*, 214.
(105) Zeman, L.; Denault, L. *J. Membr. Sci.* **1992**, *71*, 221.
(106) Chen, R. T.; Saw, C. K.; Jamieson, M. G.; Aversa, T. R.; Callahan, R. W. *J. Appl. Polym. Sci.* **1994**, *53*, 471.
(107) Fujii, T.; Mochizuki, T. U.S. Patent, 5, 759, 678, 1998.
(108) Spotnitz, R.; Ferebee, M.; Callahan, R. W.; Nguyen, K.; Yu, W. C.; Geiger, M.; Dwiggens, C.; Fischer, H.; Hoffman, D. *Proceedings of the 12th International Seminar on Primary and Secondary Battery Technology and Applications*; Fort Lauderdale, FL, Florida Educational Seminars, Inc.: Fort Lauderdale, FL, 1995.
(109) Venugopal, G.; Moore, J.; Howard, J.; Pendalwar, S. *J. Power Sources* **1999**, *77*, 34.
(110) Venugopal, G. The role of plastics in lithium-ion batteries. *Proceedings of the 3rd Annual Conference on Plastics for Portable and Wireless Electronics*; Philadelphia, PA, 1997; p 11.
(111) Lundquist, J. T.; Lundsager, C. B.; Palmer, N. L.; Troffkin, H. J.; Howard, J. U.S. Patent 4,731,304, 1998.
(112) Lundquist, J. T.; Lundsager, C. B.; Palmer, N. I.; Troffkin, H. J. U.S. Patent 4,650,730, 1987.
(113) Zuckerbrod, D.; Giovannoni, R. T.; Grossman, K. R. *Proceedings of the 34th International Power Sources Symposium*; Cherry Hill, NJ, 1990; p 172.
(114) Spotnitz, R.; Ferebee, M. W. *Meeting Abstracts, The Electrochemical Society Inc., Volume 96−2, Fall Meeting, San Antonio, TX, October 6−11*; The Electrochemical Society: New York, 1996.
(115) Faust, M. A.; Suchanski, M. R.; Osterhoudt, H. W. U.S. Patent No. 4,741,979, 1988.
(116) Matthias, U.; Dieter, B.; Heinrich, R.; Thomas, B.; U.S. Patent, 6,511,517, 2003.
(117) Maleki, H.; Shamsuri, A. K. *J. Power Sources* **2003**, *115*, 131.
(118) Zeng, S.; Moses, P. R. *J. Power Sources* **2000**, *90*, 39.
(119) Norin, L.; Kostecki, R.; McLarnon, F. *Electrochem. Solid State Lett.* **2002**, *5*, A67.
(120) Kostecki, R.; Norin, L.; Song, X.; McLarnon, F. *J. Electrochem. Soc.* **2004**, *151*, A522.
(121) *Hazardous Materials Regulations*; Code of Federal Regulations, CFR49 173.185.
(122) UL1640, Lithium Batteries. Underwriters Laboratories, Inc.
(123) UL2054, Household and Commercial Batteries. Underwriters Laboratories, Inc.
(124) Secondary Lithium Cells and Batteries for Portable Applications. International Electrotechnic Commission, IEC 61960-1 and IEC 61960-2.
(125) Recommendations on the Transport of Dangerous Goods, Manual of Tests and Criteria. United Nations: New York, 1999.
(126) Safety Standard for Lithium Batteries, UL 1642, Underwriters Laboratories Inc, Third Edition, 1995.
(127) Standard for Household and Commercial Batteries, UL 2054, Underwriter Laboratories, Inc., 1993.
(128) UN Recommendations on the Transport of Dangerous Goods, December 2000.
(129) A Guideline for the Safety Evaluation of Secondary Lithium Cells. Japan Battery Association, 1997.
(130) Venugopal, G. *J. Power Sources* **2001**, *101*, 231.
(131) Alamgir, M.; Abraham, K. M. In *Lithium Batteries: New Materials, Developments and Perspectives*; Industrial Chemistry Library 5; Pistoia, G., Ed.; Elsevier: New York, 1994; Chapter 3.
(132) Gray, F. M. *Polymer Electrolytes*; RSC Materials Monograph; The Royal Society of Chemistry: Cambridge, U.K., 1997.
(133) Fauteux, D.; Massucco, A.; McLin, M.; Van Buren, M.; Shi, J. *Electrochim. Acta* **1995**, *40*, 2185.
(134) North, M.; Markin, T. L.; Hooper, A.; Tofield, B. C. Second International Meeting on Lithium Batteries, Paris, France, April 25−27, 1984;Extended Abstracts # 19.
(135) *Chem. Int.* **1982**, (June, No. 3), 14.
(136) Appetecchi, G. B.; Dautzenberg, G.; Scrosati, B. *J. Electrochem. Soc.* **1996**, *143*, 6.
(137) Armand, M. *Solid State Ionics* **1983**, *9 & 10*, 745.
(138) Lightfoot, P.; Mehta, M. A.; Bruce, P. G. *Science* **1993**, *262*, 883.
(139) Vincent, C. A.; Scrosati, B. *Modern Batteries. An Introduction to Electrochemical Power Sources*; Arnold: London, 1993.
(140) Appetecchi, G. B.; Passerini, S. *J. Electrochem. Soc.* **2002**, *149*, A891.
(141) Croce, F.; Appetecchi, G. B.; Persi, L.; Scrosati, B. *Nature (London)* **1998**, *394*, 4496.
(142) Croce, F.; Persi, L.; Ronci, F.; Scrosati, B. *Solid State Ionics* **2000**, *135*, 47.
(143) Fan, J.; Fedkiw, P. S. *J. Electrochem. Soc.* **1997**, *144*, 399.
(144) Appetecchi, G. B.; Romagnoli, P.; Scrosati, B. *Electrochem. Commun.* **2001**, *3*, 281.
(145) Kim, D. W.; Sun, Y. K. *J. Power Sources* **2001**, *102*, 41.
(146) Chojnacka, J.; Acosta, J. L.; Morales, E. *J. Power Sources* **2001**, *97−98*, 819.
(147) Nishi, Y. *Advances in Lithium Ion Batteries*; van Schalkwijk, W., Scrosati, B., Eds.; Kluwer Academic/Plenum Publishers: New York, 2002.
(148) EE Times.com: http://www.eet.com/story/OEG19990121S0013.
(149) Song, J. Y.; Wang, Y. Y.; Wan, C. C. *J. Power Sources* **1999**, *77*, 183.
(150) Min, H. S.; Ko, J. M.; Kim, D. W. *J. Power Sources* **2003**, *119−121*, 461.
(151) Jo, S. I.; Sohn, H. J.; Kang, D. W.; Kim, D. W. *J. Power Sources* **2003**, *119−121*, 478.
(152) Kim, H. S.; Kum, K. S.; Cho, W. I.; Cho, B. W.; Rhee, H. W. *J. Power Sources* **2003**, *124*, 221.
(153) Abraham, K. M.; Alamgir, M. *Solid State Ionics* **1994**, *70−71*, 20.
(154) Schmutz, C.; Tarascon, J. M.; Gozdz, A. S.; Schumtz, C. N.; Warren, P. C.; Shokoohi, F. K. *Proc. Electrochem. Soc.* **1995**, *94* (28), 330.
(155) Murata, K.; Izuchi, S.; Yoshihisa, Y. *Electrochim. Acta* **2000**, *45*, 1501.
(156) Jiang, Z.; Carroll, B.; Abraham, K. M. *Electrochim. Acta* **1997**, *42*, 2667.
(157) Song, J. Y.; Cheng, C. L.; Wang, Y. Y.; Wan, C. C. *J. Electrochem. Soc.* **2002**, *149*, A1230.
(158) Gozdz, A. S.; Schmutz, C. N.; Tarascon, J. M.; Warren, P. C. U.S. Patent, 5,456,000, 1995.
(159) Gozdz, A. S.; Tarascon, J. M.; Schmutz, C. N.; Warren, P. C.; Gebizlioglu, O. S.; Shokoohi, F. *Tenth Annual Battery Conference on Advances and Applications, Long Beach, CA, January 10−13*; IEEE: New York, 1995; 301.
(160) Tarascon, J. M.; Gozdz, A. S.; Schumtz, C. N.; Shokoohi, F. K.; Warren, P. C. *Solid State Ionics* **1996**, *86−88*, 49.
(161) Pasquier, A. D.; Waren, P. C.; Culver, D.; Gozdz, A. S.; Amatucci, G.; Tarascon, J. M. *Proc. Electrochem. Soc.* **1999**, *99* (24), 360.
(162) Park, C. K.; Kakirde, A.; Ebner, W.; Manivannan, V.; Chai, C.; Ihm, D. J.; Shim, Y. J. *J. Power Sources* **2001**, *97−98*, 775.
(163) Dasgupta, S.; Jacobs, J. K. U.S. Patent, 5,437,692, 1995.
(164) Abraham, K. M.; Alamgir, M.; Hoffman, D. K. *J. Electrochem. Soc.* **1995**, *142*, 683.
(165) Pendalwar, S. L.; Howard, J. N.; Venugopal, G.; Oliver, M. U.S. Patent, 5,716,421, 1998.
(166) Gozdz, A. S.; Plitz, I.; Du Pasquier, A.; Zheng, T. *Proceedings of the 200th ECS Meeting, Fall 2001, Phoenix, AZ*, 2001; Vol. 2000−2001, pp 336−351.
(167) Gozdz, A. S. U.S. Patent 6,328,770, 2001.

(168) Kim, D. W.; Oh, B.; Park, J. H.; Sun, Y. K. *Solid State Ionics* **2000**, *138*, 41.
(169) Wang, Y.; Sejdic, J. T.; Steiner, R. *Solid State Ionics*, **2002**, *148*, 443.
(170) Gozdz, A. S.; Plitz, I.; DuPasquier, A.; Zheng, T. Presented at the 198th Meeting of the Electrochemical Society, Phoenix, AZ, Oct 22−27, 2000.
(171) Spotnitz, R. M.; Wensley, C. G. U.S. Patent 6,322,923, 2000.
(172) Fabrice, C.; Bradford, R. WO 02/50929 A2, 2002.
(173) Jeong, Y. B.; Kim, D. W. *J. Power Sources* **2004**, *128*, 256.
(174) Abraham, K. M.; Alamgir, M.; Hoffman, D. K. *J. Electrochem. Soc.* **1995**, *142*, 683.
(175) Dasgupta, S.; Jacobs, J. K. U.S. Patent 5,498,489, 1996.
(176) Gies, P.; Charles, R. A.; Dieken, J. World Patent 00/13248, 2000.
(177) Eschbach, F. O.; Oliver, M. U.S. Patent, 5,681,357, 1997.
(178) Hamano, K.; Shiota, H.; Shiraga, S.; Aihara, S.; Yoshida, Y.; Murai, M,; Inuzuka, T. U.S. Patent, 5, 981, 107, 1999.
(179) Akashi, H. U.S. Patent, 5,658,686, 1997.
(180) Akashi, H. Paper presented at the International Symposium on Polymer Electrolytes, ISPE-5, Uppsala, Sweden, Aug 11−16, 1996.
(181) Fujii, T. *Proceedings of the 17th International Seminar & Exhibit on Primary and Secondary Batteries*; Florida Educational Seminars, Inc.: Boca Raton, FL, 2000.
(182) Nakane, I.; Narukawa, S. Presented at Power 2000, The 8th Annual International Conference on Power Requirements for Mobile Computing and Wireless Communications, San Diego, CA, Sept 24−27, 2000.
(183) Kim, K. M.; Ryu, K. S.; Kang, S. G.; Chang, S. H.; Chung, I. J. *Macromol. Chem. Phys.* **2001**, *202*, 866.
(184) Kim, K. M.; Park, N. G.; Ryu, K. S.; Chang, S. H. *Polymer* **2002**, *43*, 3951.
(185) Kim, K. M.; Ko, J. M.; Park, N. G.; Ryu, K. S.; Chang, S. H. *Solid State Ionics* **2003**, *161*, 121.
(186) Scrosati, B.; Croce, F.; Persi, L. *J. Electrochem. Soc.* **2000**, *147*, 1718.
(187) Prosini, P. P.; Villano, P.; Carewska, M. *Electrochim. Acta* **2002**, *48*, 227.
(188) Liu, X.; Kusawake, H.; Kuwajima, S. *J. Power Sources* **2001**, *97−98*, 661.
(189) Kim, D. W.; Ko, J. M.; Chun, J. H.; Kim, S. H.; Park, J. K. *Electrochem. Commun.* **2001**, *3*, 535.
(190) Kim, D. W.; Noh, A.; Chun, J. H.; Kim, S. H.; Ko, J. M. *Solid State Ionics* **2001**, *144*, 329.
(191) Dan, P.; Mengeritski, E.; Geronov, Y.; Aurbach, D.; Weisman, I. *J. Power Sources* **1995**, *54*, 143.
(192) Ikeda, H.; et al. *Proceedings of the Symposium on Lithium Batteries*; The Electrochemical Society: Pennington, NJ, 1984; Vol. 84, 311.
(193) Grady, J. P. Presented at the 20th International Seminar and Exhibit on Primary and Secondary Batteries, Fort Lauderdale, Florida, Florida Educational Seminars, Inc., Mar 17−20, 2003.
(194) Weininger, J. L.; Holub, F. F. *J. Electrochem. Soc.* **1970**, *117*, 340.
(195) Martino, F. J.; Gay, E. C.; Moore, W. E. *J. Electrochem. Soc.* **1982**, *129*, 2701.
(196) Swaroop, R. B.; Battles, J. E. *J. Electrochem. Soc.* **1981**, *128*, 1873.
(197) Mathers, J. P.; Boquist, C. W.; Olszanski, T. W. *J. Electrochem. Soc.* **1978**, *125*, 1913.
(198) Bandyopadhyay, G.; Swaroop, R. B.; Battles, J. E. *J. Electrochem. Soc.* **1982**, *129*, 2187.
(199) Shimizu, Y.; Terasaki, M.; Kashihara, S. *J. Power Sources* **1984**, *13*, 235.
(200) Choi, S. H.; Park, S. Y.; Nho, Y. C. *Radiat. Phys. Chem.* **2000**, *57*, 179.
(201) Choi, S. H.; Kang, H. J.; Ryu, E. N.; Lee, K. P. *Radiat. Phys. Chem.* **2001**, *60*, 495.
(202) Navy Primary and Secondary Batteries, Design and Manufacturing Guidelines, Department of the Navy, Sept 1991; p 85.
(203) Linden, D. *Handbook of Batteries*, 2nd ed.; McGraw-Hill: New York, 1994.
(204) Vinal, G. *Primary Batteries*; Wiley: New York, 1950.
(205) Mantell, C. L. *Batteries & Energy Systems*, 2nd ed. McGraw-Hill: New York, 1983.
(206) Mardegain, S. B. *Battery Power Prod. Technol.* **2003**, (Jan).
(207) Boehnstedt, W. *J. Power Sources* **1996**, *59*, 45.
(208) Boehnstedt, W. *J. Power Sources* **2004**, *133*, 59.
(209) Lander, J. J. *Proceedings of the Symposium on Battery Separators*; The Electrochemical Society: Columbus, OH, 1974; p 4.
(210) Prout, L. *J. Power Sources* **1993**, *46*, 117.
(211) Vinal, G. W. *Storage Batteries*; Wiley: New York, 1945.
(212) Butherus, A. D.; Lindenberger, W. S.; Vaccaro, F. J. *Bell Syst. Technol. J.* **1970**, 1377.
(213) Paik, S. L.; Terzaghi, G. *J. Power Sources* **1995**, *53*, 283.
(214) Kung, J. *J. Power Sources* **1994**, *48*, 129.
(215) Wang. L. C.; Harvey, M. K.; Stein, H. L.; Scheunemann, U. The Role of UHMW−PE in Microporous PE Separators. *Proceedings of the 12th Annual Battery Conference on Applications & Advances*; IEEE: New York, 1997; p 69.
(216) Larsen, D. W.; Kehr, C. L. U.S. Patent 3,351,495, 1996.
(217) Boehnstedt, W. *J. Power Sources* **2001**, *95*, 234.
(218) Wang, L. C.; Harvey, M. K.; Ng, J. C.; Scheunemann, U. *J. Power Sources* **1998**, *73*, 74.
(219) Boehnstedt, W. *J. Power Sources* **1996**, *59*, 45.
(220) Endoh, H. *J. Power Sources* **1996**, *599*, 51.
(221) Higashi, T.; Endoh, H. *J. Power Sources* **1998**, *73*, 110.
(222) Rand, D. A. J.; Woods, R.; Dell, R. M. *Batteries for Electric Vehicles*; Research Studies Press: 1998; ISBN 0-86380-205-0.
(223) McClelland, D. H.; Devitt, J. L. U.S. Patent 3,862,861, 1975.
(224) Zguris, G. C. *J. Power Sources* **1998**, *73*, 60.
(225) Zguris, G. C. *J. Power Sources* **1997**, *67*, 307.
(226) Zguris, G. C. *J. Power Sources* **1996**, *59*, 131.
(227) Pavlov, D.; Ruevski, S.; Naidenov, V.; Sheytanov, G. *J. Power Sources* **2000**, *85*, 164.
(228) Ferreira, A. L. *J. Power Sources* **1999**, *78*, 41.
(229) Britting, A. O. *Proceedings of the 1981 Goddard Space Flight Center Battery Workshop*; NASA Conference Publication 2217; NASA: Washington, DC, 1981; p 327.
(230) Britting, A. O. *J. Power Sources* **1984**, *12*, 305−316.
(231) Morrow, G. W. *J. Power Sources* **1987**, *21*, 313.
(232) Francis, R. W.; Haag, R. L. *J. Power Sources* **1986**, *18*, 147.
(233) Lim, H. S.; Pickett, D. F. Separator Evaluation in NiCd Cells. *Proceedings of the Intersociety Energy Conversion Engineering*; IEEE: New York, 1990; Vol. 3, p 61.
(234) Hill, J. M. U.S. Army ERADCOM, Devet-TR-75-F, 1979.
(235) Feldman, K.; Verville, G. DREO Technical Note, 78-6, 1978.
(236) Lim, H. S.; Margerum, J. D.; Verzwyvelt, S. A.; Lackner, A. M. *Proceedings of the 27th Power Sources Conference, Atlantic City, NJ, June 21−24*; 1976; p 83.
(237) Lim, H. S.; Margerum, J. D.; Verzwyvelt, S. A.; Lackner, A. M.; Knechtli, R. C. *J. Electrochem. Soc.* **1989**, *136*, 605.
(238) Scott, W. R.; Rusta, D. W. NASA RP 1052, 1979.
(239) Fetcenko, M. A.; Venkatesan, S.; Ovshinsky, S. *Proceedings of the Symposium on Hydrogen Storage Materials, Batteries & Electrochemistry*; 1992; p 141.
(240) Wada, M. *Polym. Adv. Technol.* **1994**, *5*, 645.
(241) Ikoma, M.; Hoshina, Y.; Matsumoto, L.; Iwakura, C. *J. Electrochem. Soc.* **1996**, *143*, 1904−1907.
(242) Ikoma, M.; Takahashi, O.; Tsuboi, R.; Matsumoto, L. *Denki Kagaku* **1993**, *61*, 997.
(243) Furukawa, N. *J. Power Sources* **1994**, *51*, 45.
(244) Nagarajan, G. S.; Van Zee, J. W. *J. Power Sources* **1998**, *70*, 173−180.
(245) Cook, J. A.; Lancaster, I. M. *Proc. Electrochem. Soc.* **1998**, *98* (15), 55.
(246) Scimat's latest separators. *Batteries Int.* **2002** (Oct).
(247) Cheng, S.; Zhang, J.; Liu, H.; Leng, Y.; Yuan, A.; Cao, C. *J. Power Sources* **1998**, *74*, 155−157.
(248) Hamling, P.; Hamling, B. H. Zirconia Battery Separators—An historical perspective and development update. *Proceedings of the 11th Annual Battery Conference on Applications & Advances*; IEEE: New York, 1996; p 15.
(249) Vermeiren, P. H.; Adriansens, W.; Moreels, J. P.; Leysen, R. *Int. J. Hydrogen Energy* **1998**, *23*, 5, 321−324.
(250) *Chem. Business Newsbase* **2001** (July 25).
(251) http://www.zircarzirconia.com.
(252) Vermeiren, P. H.; Adriansens, W.; Leysen, R. *Int. J. Hydrogen Energy* **1996**, *21*, 8, 679−684.
(253) Barak, M., Ed. *Electrochemical Power Sources*; Peter Peregrinus: London, 1980.
(254) Andre, H. *Bull. Soc. Fr. Elect.* **1941**, *6* (1), 132.
(255) Agostino, V. D.; Lee, J.; Orban, G. In *Grafted Membranes in Zinc−Silver Oxide Batteries*; Fleisher, A., Lander, J. J., Eds.; Wiley: New York, 1971; p 271.
(256) Charkey, A. *Proc. 26th Annual Power Sources Symp.* **1976**, 87.
(257) Karpinski, A. P.; Makovetski, B.; Russell, S. J.; Serenyi, J. R.; Williams, D. C. *J. Power Sources* **1999**, *80*, 53−60.
(258) Himy, A. *Silver Zinc Battery—Phenomena & Design Principles*, 1st ed.; Vantage Press: New York, 1986.
(259) Agostino, V. D.; Lee, J.; Orban, G. In *Grafted Membranes in Zinc−Silver Oxide Batteries*; Fleisher, A., Lander, J. J., Eds.; Wiley: New York, 1971; p 271.
(260) Himy, A. *Silver−Zinc Batteries: Phenomena and Design Principles*, 1st ed.; Vantage Press: New York, 1983; p 31.
(261) Lewis, H.; Grun, C.; Salkind, A. *J. Power Sources* **1997**, *65*, 29.
(262) Lewis, H.; Jackson, P.; Salkind, A.; Danko, T.; Bell, R. *J. Power Sources* **2001**, *96*, 128.
(263) Danko, T. Properties of cellulose separators for alkaline secondary batteries. *Proceedings of the 10th Annual Battery Conference on Applications & Advances*; IEEE: New York, 1995; p 261.
(264) Lewis, H. L.; Hammersley, V. L.; Wharton, S. P. NSWC: evaluation of cellophane separation in model rechargeable silver−zinc cell. Presented at the 38th Power Sources Conference, Cherry Hill, NJ, 1998.

CosMX Exhibit 1003, Page 325 of 512

(265) Lewis, H.; Henderson, S.; Danko, T. Separator composition evaluation in model rechargeable silver zinc cells. *Proceedings of the 16th Annual Battery Conference on Applications & Advances*; IEEE: New York, 2001.
(266) Danko, T. Strength Properties of Separators in Alkaline Solutions. *Proceedings of the 11th Annual Battery Conference on Applications & Advances*; IEEE: New York, 1996; p 283.
(267) Serenyl, R. *Proceedings of the 41st Power Sources Conference, Philadelphia, June 14−17, 2004*; 2004; p 465.
(268) Megahed, E. A.; Davig, D. C. *Power Sources*; Academic: London, 1981; Vol. 8.
(269) Lee, J.; Agostino, V. D.; Zapisek, S.; Freid, R.; Cannizzaro, J. *Membranes and Ionic and Electronic Conducting Polymers*; Yeager, E. B., Ed.; The Electrochemical Society Inc.: Pennington, NJ, 1983; p 245.
(270) Drumm, J. J. British Patent 365,125, 1930.
(271) Kishimoto, T.; Yamane, M.; Bogauchi, T.; Eguchi, Y. U.S. Patent 5,320,916, 1994.
(272) Kishimoto, T.; Yamane, M.; Bogauchi, T.; Eguchi, Y. U.S. Patent 5,547,779, 1996.
(273) McLarnon, F. R.; Cairns, E. J. *J. Electrochem. Soc.* **1991**, *138* (Feb).
(274) McBreen, J.; Cairns, E. J. In *Advances in Electrochemistry & Electrochemical Engineering*; Gerischer, H., Tobias, C. W., Eds.; Wiley: New York, 1978; Vol. 11; pp 273−351.
(275) Bennion, D. N. A review of membrane separators and Zinc−Nickel oxide battery development. Prepared for Argonne National Laboratory under Contract No. 31-109-38-5455, October 1980.
(276) Lundquist, J. T. *J. Membr. Sci.* **1983**, *13*, 337.
(277) Poa, D. S.; Cook, G. M.; Yao, N. P. ANL/OEPM-83−4. National Technical Information Service: 1983.
(278) Wagner, C. A.; Almerini, A.; Smith, R. L. *Proceedings of the 29th International Power Sources Symposium*; The Electrochemical Society Inc.: Pennington, NJ, 1980.
(279) Brown, R. A.; Cloyd, J. S. *Proceedings of the 29th International Power Sources Symposium*; The Electrochemical Society Inc.: Pennington, NJ, 1980.
(280) Krejci, I.; Vanysek, P.; Trojanek, A. *J. Electrochem. Soc.* **1993**, *140*, 2279.
(281) *J. Power Sources* **1984**, *11*, 242−243.
(282) Bugnet, B.; Doniat, D.; Rouget, R. *Proc. 40th Power Sources Conf.* **2002**, *10* (13), 535.
(283) Sato, Y.; Kanda, M.; Niki, H.; Ueno, M.; Murata, K.; Shirogami, T.; Takamura, T. *J. Power Sources* **1983**, *9*, 147.
(284) Chen, M.; Tsai, T. U.S. Patent 6,605,391, 2003.
(285) Chen, M.; Li, L. F.; Tsai, T. U.S. Patent, 6,358,651, 2002.
(286) Chen, M.; Cao, F.; Liang, L.; Tsai, T.; Faris, S. *Proc. 41st Power Sources Conf.* **2004**, 473.
(287) Dewi, E. L.; Oyaizu, K.; Nishide, H.; Tsuchida, E. J. *Power Sources* **2003**, *115*, 149−152.
(288) Schubert, M. A.; Myers, J. P.; Thrasher, G. T. Acrylic Acid-Sodium Styrene Sulfonated Copolymer Separator Coatings for Alkaline Electrolytes. Presented at the 202nd Meeting of the Electrochemical Society, Salt Lake City, UT.
(289) Schubert, M. A.; Myers, J. P. *Proc. 41st Power Sources Conf.* **2004**, 122.
(290) Will, F. G. *J. Electrochem. Soc.* **1979**, *126*, 36.
(291) Bellows, R.; Einstein, H.; Grimes, P.; Kantner, E.; Malachesky, P.; Newby, K.; Tsein, H. Development of a Circulating Zn−Br_2 Battery Phase I. Final Report, Exxon Research and Engineering Company and Sandia National Laboratories, SAND82-7022, Jan 1983.
(292) Cathro, K. J.; Constable, D. C.; Hoobin, P. M. *J. Power Sources* **1988**, *22*, 29−57.
(293) Thaller, L. H. U.S. Patent 3,996,064, 1976.
(294) Jorne, J. *Am. Sci.* **1983**, *71* 507.
(295) Sum, E.; Skyllas-Kazacos, M. *J. Power Sources* **1985**, *15*, 179.
(296) Skyllas-Kazacos, M.; Grossmith, F. *J. Electrochem. Soc.* **1987**, *134*, 2950.
(297) Wiedemann, E.; Heintz, A.; Lichtenthaler, R. N. *J. Membr. Sci.* **1998**, *141*, 207.
(298) Skyllas-Kazacos, M.; Kasherman, D.; Hong, D. R.; Kazacos, M. *J. Power Sources* **1991**, *35*, 399.
(299) Ohya, H.; Kawahara, T.; Kang, A. S.; Aihara, M.; Negishi, Y. *Denki kagaku* **1994**, *62*, 863.
(300) Hwang, G. H.; Ohya, H. *J. Membr. Sci.* **1997**, *132*, 55.
(301) Hwang, G. J.; Ohya, H. *J. Membr. Sci.* **1996**, *120*, 55.
(302) Chieng, S. C.; Kazacos, M.; Skyllas-Kazacos, M. *J. Power Sources* **1992**, *39*, 11.
(303) Chieng, S. C.; Kazacos, M.; Skyllas-Kazacos, M. *J. Membr. Sci.* **1992**, *75*, 81.
(304) Mohammadi, T.; Skyllas-Kazacos, M. *J. Membr. Sci.* **1995**, *98*, 77.
(305) Mohammadi, T.; Skyllas-Kazacos, M. *J. Membr. Sci.* **1995**, *107*, 35.
(306) Mohammadi, T.; Skyllas-Kazacos, M. *J. Power Sources* **1995**, *56*, 91.
(307) Wiedemann, E.; Heintz, A.; Lichtenthaler, R. N. *J. Membr. Sci.* **1998**, *141*, 215.
(308) Sukkar, T.; Kazacos, M. S. *J. Membr. Sci.* **2003**, *222*, 249.
(309) Assink, R. A. *J. Membr. Sci.* **1984**, *17*, 205.
(310) Arnold, C.; Assink, R. A. *J. Appl. Polym. Sci.* **1984**, *29*, 2318.
(311) Hruska, L. W.; Savinell, R. F. *J. Electrochem. Soc.* **1981**, *128*, 18.
(312) Newman, J.; Tiedemann, W. *AIChE J.* **1975**, *21*, 25.
(313) Newman, J. S. *Electrochemical Systems*, 2nd ed.; Prentice Hall Inc.: Englewood Cliffs, NJ, 1991.
(314) Vidts, P. D.; White, R. E. *J. Electrochem. Soc.* **1997**, *144*, 1343.
(315) Ceder, G.; Doyle, M.; Arora, P.; Fuentes, Y. *MRS Bull.* **2002**, *27*, 619.
(316) Newman, J.; Tiedemann, W. *J. Electrochem. Soc.* **1997**, *144*, 3081.
(317) Gu, H.; Nguyen, T. V.; White, R. E. *J. Electrochem. Soc.* **1987**, *134*, 2953.
(318) Vidts, P. D.; Delgado, J.; White, R. E. *J. Electrochem. Soc.* **1995**, *142*, 4006.
(319) Doyle, M.; Fuller, T. F.; Newman, J. *J. Electrochem. Soc.* **1993**, *140*, 1526.
(320) Fuller, T. F.; Doyle, M.; Newman, J. *J. Electrochem. Soc.* **1994**, *141*, 1.
(321) Fan, D.; White, R. E. *J. Electrochem. Soc.* **1991**, *138*, 17.
(322) Doyle, M.; Newman, J.; Gozdz, A. S.; Schumtz, C. N.; Tarascon, J. M. *J. Electrochem. Soc.* **1996**, *143*, 1890.
(323) Arora, P.; Doyle, M.; Gozdz, A. S.; White, R. E.; Newman, J. *J. Power Sources* **2000**, *88*, 219.
(324) Patel, K. K.; Paulsen, J. M.; Desilvestro, J. *J. Power Sources* **2003**, *122*, 144.
(325) Tye, F. L. *J. Power Sources* **1983**, *9*, 89.
(326) Mao, Z.; White, R. E. *J. Power Sources* **1993**, *43−44*, 181.
(327) Denton, F.; Howard, J. N.; Anani, A. A.; Fernandez, J. M. U.S. Patent 6,228,516, 2001.
(328) Mao, H.; Wainwright, U.S. Patent 6,074,766, 1990.
(329) Thomas-Alyea, K. E.; Newman, J.; Chen. G.; Richardson, T. J. *J. Electrochem. Soc.* **2004**, *151*, A509.

CR020738U

CosMX Exhibit 1003, Page 326 of 512

Appendix K

ELSEVIER

Journal of Power Sources 77 (1999) 34–41

JOURNAL OF POWER SOURCES

Characterization of microporous separators for lithium-ion batteries

Ganesh Venugopal *, John Moore, Jason Howard, Shekhar Pendalwar

Motorola Energy Systems Group, Lawrenceville, GA 30043, USA

Received 28 July 1998; accepted 4 October 1998

Abstract

Several properties including porosity, pore-size distribution, thickness value, electrochemical stability and mechanical properties have to be optimized before a membrane can qualify as a separator for a lithium-ion battery. In this paper we present results of characterization studies carried out on some commercially available lithium-ion battery separators. The relevance of these results to battery performance and safety are also discussed. Porosity values were measured using a simple liquid absorption test and gas permeabilities were measured using a novel pressure drop technique that is similar in principle to the Gurley test. For separators from one particular manufacturer, the trend observed in the pressure drop times was found to be in agreement with the Gurley numbers reported by the separator manufacturer. Shutdown characteristics of the separators were studied by measuring the impedance of batteries containing the separators as a function of temperature. Overcharge tests were also performed to confirm that separator shutdown is indeed a useful mechanism for preventing thermal runaway situations. Polyethylene containing separators, in particular trilayer laminates of polypropylene, polyethylene and polypropylene, appear to have the most attractive properties for preventing thermal runaway in lithium ion cells. © 1999 Elsevier Science S.A. All rights reserved.

Keywords: Lithium-ion; Batteries; Microporous; Separators; Membranes

1. Introduction

Lithium-ion batteries are rapidly becoming the preferred choice for powering portable electronic products, particularly laptop computers and cellular phones [1,2]. This choice is primarily driven by the demand for batteries having higher energy densities than that offered by nickel cadmium (NiCd) and nickel metal hydride (NiMH) systems. The energy density for a lithium-ion battery is anywhere between 30–60% higher than that demonstrated by the nickel based systems. In addition, lithium-ion cells can also provide longer cycle life and higher voltages. Lithium-ion batteries operate on the same principle as lithium metal batteries but do not have many of the problems that are associated with the latter, particularly the unstable lithium metal interface. This is because lithium-ion technology utilizes lithium-intercalated or lithium-inserted compounds of graphite, amorphous carbon or low voltage metal oxides as the negative electrode instead of the highly reactive metallic lithium. The cathodes are usually higher voltage metal oxides, chosen from a list that includes lithium cobalt oxide ($LiCoO_2$), lithium nickel oxide ($LiNiO_2$) and lithium manganese oxide ($LiMn_2O_4$). Interposed between the anode and the cathode is a porous sheet or film commonly referred to as the *separator*. The pores in the separator are filled with an ionically conductive liquid electrolyte—a solution of lithium salt in non-aqueous solvents. Electrode and separator combinations are wound into tight rolls to be fitted into rigid cylindrical or prismatic (rectangular) metal cans. The main functions of a separator are: (I) to isolate the anode and the cathode so that no electrons can flow between them within the cell and (II) to allow the ions that are contained in the liquid electrolyte unrestricted passage between anode and cathode.

The next generation of the lithium-ion batteries, commonly referred to as *lithium-ion polymer* [1], utilizes gel electrolytes—gels of liquid electrolytes with a gellable polymer such as poly(vinylidene fluoride) (PVDF). Lithium-ion polymer batteries are expected to provide battery makers with the flexibility for designing cells with unique shapes and sizes. Furthermore, plastic lithium-ion batteries may not require the rigid metal cans that are

* Corresponding author. Tel.: +1-770-338-3315; Fax: +1-700-338-3321

0378-7753/99/$19.00 © 1999 Elsevier Science S.A. All rights reserved.
PII: S0378-7753(98)00168-2

required for conventional lithium ions to ensure stack pressure between electrodes and separator. This allows one to pack the cell in flexible foil packaging material and achieve a significant improvement in gravimetric energy density of the battery.

In one version of the lithium-ion polymer, or *plastic lithium-ion*, battery that is being developed by Bellcore, the anode and the cathode are laminated onto either side of a gellable membrane [3]. Lamination is carried out in the presence of a plasticizer, which is subsequently extracted to give the required porous structure in the battery. Good adhesion between the electrodes and the membranes is possible because all three sheets contain significant amounts of a poly(vinylidenefluoride-co-hexafluoropropylene) copolymer that can be melted and bonded during the lamination step. Due to the presence of the plasticizer, the lamination can be done at relatively low temperatures.

Recently, there have been a number of reports of lithium-ion polymer batteries in which the gel electrolyte layer contains an inert microporous separator. These microporous separators are similar to the separators that are used in a conventional lithium-ion battery [4–7]. Gel-covered and/or gel-filled separators have some characteristics that may be harder to achieve in the separator-free gel electrolytes. For example, they can offer much better protection against internal shorts when compared to gel electrolytes and can therefore help in reducing the overall thickness of the electrolyte layer. In addition, the ability of some separators to shutdown at a particular temperature allows safe deactivation of the cell under overcharge conditions [8,9]. Until the appearance of truly robust liquid-free polymer electrolytes, inert microporous separators may be an important component of lithium-ion polymer batteries as well.

2. Experimental

2.1. Materials

Samples of separators were obtained from four different suppliers. Due to the confidential nature of Motorola's relationships with these suppliers their names are not disclosed. Instead, samples from the four suppliers will be referred to as A, B, C and D. Seven samples (A1–A7) were received from supplier A, two (B1 and B2) from supplier B, two (C1 and C2) from supplier C and one (D1) from supplier D. Table 1 gives a list of the separator samples that were studied, along with the composition and thickness values.

Mineral oil [CAS # 8020-83-5] was used for membrane porosity determination. It was purchased from Aldrich Chemical (Milwaukee, WI) and has a density of 0.86 g/ml. Porewick® [CAS # 86508-42-1], a non-volatile per-fluorinated liquid was used for pore size measurements. Porewick® has a surface tension of 16 dynes/cm and was purchased from Porous Materials (PMI).

Table 1
Composition and thickness values of separators studied

Separator type	Composition	Thickness (μm)
A1	PP//PE//PP	25
A2	PP	25
A3	PP//PP	50
A4	PP	25
A5	PP//PP	50
A6	PE	25
A7	Surfactant coated PP	25
B1	PE	25
B2	PE	30
C1	PP	25
C2	PE	25
D1	PP/PE/PP	25

Prismatic Li-ion cells containing a $LiCoO_2$ cathode, a graphite anode and a PVDF coated polyolefin separator were used for studying the shutdown characteristics of different separators. Apart from variations in the separators, the cells were identical in all respects and are hence expected to have identical thermal transport properties. Further details about the cell assembly can be obtained from Ref. [7].

2.2. Methods

Pore dimensions were measured using a Model MFP1500A capillary flow porometer (CFP) manufactured by PMI. This instrument is designed to handle pressures of up to 500 psi. Most experiments described in this manuscript however were carried out at pressure values under 250 psi. In a typical CFP experiment, a porous membrane is filled with Porewick® and subjected to gas pressure. The pressure on the membrane is increased in a controlled fashion while the flow rate of the gas through the membranes is simultaneously monitored. Pore size information can be obtained from these two values as described later.

Membrane porosity was determined by a simple liquid absorption test. The liquid chosen for this test was mineral oil. Permeability studies were carried out using the *pressure drop test*, which was also carried out by utilizing the CFP. In the pressure-drop test, the separator is subjected to compressed gas pressure of around 100 psi in a closed sample chamber. Permeability information can be obtained by monitoring the rate at which the gas escapes through the pores of the separator.

A Rheometrics Scientific STA625 differential scanning calorimeter (DSC) was used to determine the melting points of the separators. Impedance measurements were made at a frequency of 1 kHz using a Tegam Model 252 Impedance meter. Mechanical measurements were carried out with a Rheometrics Scientific Minimat (MMT2000)

CosMX Exhibit 1003, Page 329 of 512

mechanical tester working in the tensile mode. The Minimat was equipped with a 200 N load cell.

3. Results and discussion

Commercially available Li-ion battery separators are made out of polyolefins like polyethylene and polypropylene. These materials have been found to be compatible with the cell chemistry and can be cycled for several hundred cycles without significant degradation in chemical or physical properties. Polyolefin separators have existed long before the advent of lithium-ion technology, either in the form of microporous membranes or as non-woven materials [10]. They have been and continue to be used in batteries with other chemistries, including lithium primaries and lead-acid. With the recent surge of activity in the lithium-ion polymer area, poly(vinylidenefluoride) homopolymers and copolymers have also emerged as suitable candidates for separator material [3]. Unlike the polyolefin separators, however, the PVDF ones are used in a partially or completely gelled state as discussed earlier in this manuscript.

Most separator manufacturing is done by some combination of extrusion and stretching/drawing [11]. This process allows one to achieve relatively low (≤ 75 μm) film thickness values. Furthermore, in some cases the stretching operation also creates the necessary porous structure in the membrane. For example, the pores in the Hoechst Celgard® line of separators are produced by a process that involves high melt-stress extrusion and elevated temperature annealing [11]. If multiple layers are desired in the separator element, co-extrusion and/or lamination processes may also become involved [12]. The stretching process gives the separators an anisotropy in mechanical properties. Fig. 1 shows the results from tensile tests that were carried out on sample A2. As is clear from the results shown, the tensile strength for break is much higher for the sample in the machine (stretching) direction (~ 50 N) when compared to the transverse direction (~ 5 N).

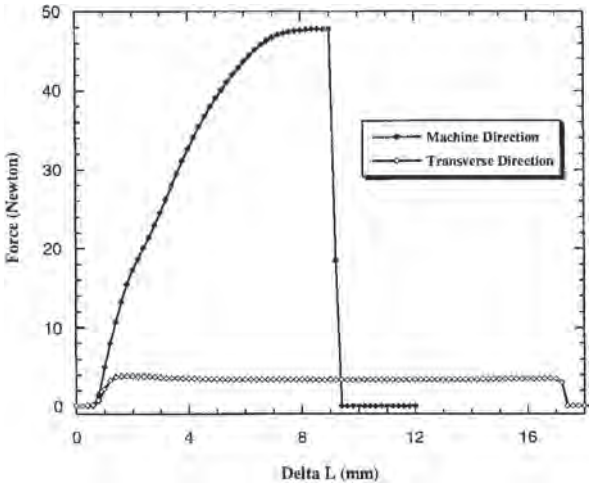


Fig. 1. Tensile force at break for separator A2 in the machine direction and the transverse direction.

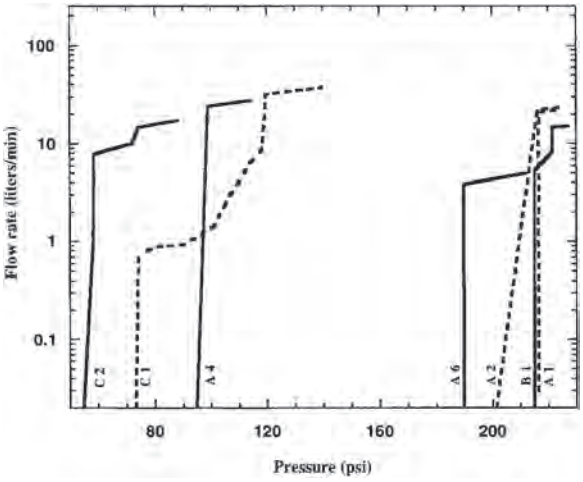


Fig. 2. Flow rate vs. pressure curves for commercial Li-ion battery separators.

Some separator manufacturers utilize plasticizers during the extrusion process. After extrusion the plasticizer is removed through an extraction process, to generate micropores in the film [13,14]. Plasticizers are particularly useful for making filler containing separators because they reduce the viscosity of the filler containing melt. Fillers are used to give the separator a skeletal structure, which prevents the pores and the film from shrinking or collapsing during plasticizer extraction. In addition, fillers could improve the mechanical strength of the separators, making them more effective for preventing electrical shorts. Filled separators are used mainly in lead acid batteries [13] and are also being considered for the lithium-ion polymer batteries [14,15]. Lithium-ion polymer battery separators can be processed either by extrusion or by solvent casting [14].

3.1. Pore dimensions

Fig. 2 shows the pressure vs. flow rate plot for liquid filled separators from three different suppliers. The curves in this plot can be used to collect information about the dimensions of the pores in the separator. The pressure, p, required to displace the liquid from a circular pore of diameter d is given by the equation:

$$p = C\frac{\tau}{d} \quad (1)$$

where τ is the surface tension of the liquid and C is a capillary constant [16]. As suggested by Eq. (1), liquid from the larger pores in the separator is expelled before the liquid from the smaller pores. The pressure required to expel liquid from the largest pore in the separator is usually referred to as the *bubble point pressure*, P_{bp}. The

CosMX Exhibit 1003, Page 330 of 512

diameter, d_1, for the largest pore in the separator can hence be given by the relationship:

$$d_1 = C\frac{\tau}{P_{bp}} \quad (2)$$

Pores in lithium-ion battery separators were detected in the pressure range 50–230 psi (see Fig. 2). In general, lower pressures are preferred for analysis since they are less likely to deform the pores. Porewick® was chosen as the wetting liquid for this reason. It has a lower surface tension relative to other possible candidates such as mineral oil or the alcohols and allows pore size detection at lower pressures (see Eq. (1)). Separators A1, B1, A2 and A6 have pore sizes in the range 0.03–0.05 μm. Separators A4, C1 and C2 have pore sizes in the range 0.09 to 0.12 μm. For any curve in Fig. 2, the height of the flow rate jump can be taken to be a measure of the number of pores detected at that pressure range. In most of the separators shown in Fig. 2, the largest pore diameter was found to be within 0.01 μm from the average pore diameter, suggesting relatively narrow distributions of pore sizes. Separator C1 showed the broadest distribution of pore sizes. The multi-step nature of the C1 curve suggests a bimodal pore size distribution.

Sub-micron pore dimensions are critical for preventing internal 'shorts' between the anode and the cathode of the Li-ion battery, particularly since these separators tend to be as thin as 25 μm. This feature will be increasingly important as separator manufacturers continue to make the membranes thinner. Thinner membranes are desired for increasing the energy density and decreasing the impedance of batteries, particularly those designed for portable electronic products. A more quantitative investigation of average pore diameters and pore size distributions is underway in our laboratory. These studies will be done by comparing the flow rate vs. pressure curve for a liquid-filled membrane with that of a liquid-free membrane. A wider range of liquids will be used for these studies and the results will be published as a separate manuscript.

3.2. Porosity

Fig. 3 shows the porosities for a number of polyolefin separators. The porosities were calculated by measuring the mass of mineral oil absorbed by the separator. A density value of 0.90 g/cm^3 was used for polypropylene materials and 0.95 g/cm^3 was used as the density value for the polyethylene separators. Trilayer separators were also assumed to have a materials density of 0.90 g/cm^3.

Most of the separators that were studied had porosity values between 40 and 50%. Only separators C1 and C2 have higher porosities, around 55%. Significantly low porosity values were observed in the A7 separators. This may be either because the pores in these surfactant-coated separators are partially filled with the surfactant or because the mineral oil was inefficient at wetting these modified materials.

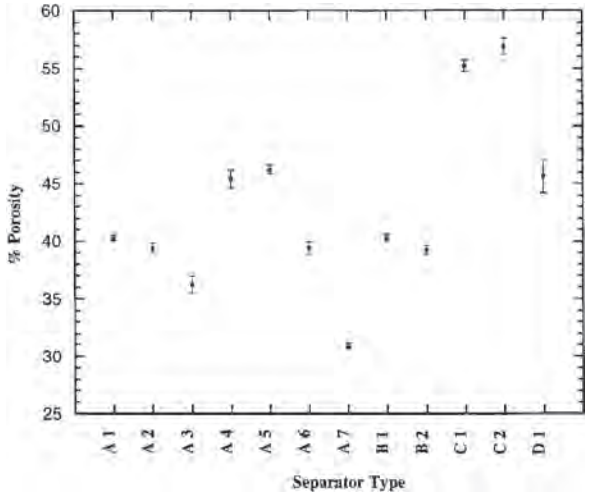


Fig. 3. Percent porosity for Li-ion battery separators as measured by liquid absorption.

High rate capability of a battery depends on, among other factors, the ionic conductivity of the liquid electrolyte filled separator. Typical non-aqueous liquid electrolyte compositions, of the type used in Li-ion batteries, demonstrate ionic conductivity values in the range, 10^{-2} to 10^{-3} S/cm. Although separators are effective in preventing electrical shorts between anode and cathode, their presence in between the two electrodes decreases the effective conductivity of the electrolyte, raising cell impedance. Some separators will reduce the ionic conductivity values by as much as one order of magnitude. However, separators enable the battery manufacturer to minimize the distance between the anode and cathode thereby reducing the impedance of the cell. For any given electrolyte, lower impedance values are observed when separators have higher porosities and/or lower thickness values. It is possible to commercially manufacture separators with porosities significantly greater than 50%. However, such materials may not be desirable since their puncture resistance and other mechanical characteristics tend to be poorer than those of the separators with lower porosities. In some cases separators with similar porosity and thickness values may contribute differently to the overall impedance of the battery. This would probably be expected if there is a significant difference in the tortuousity of the pores.

3.3. Permeability

A qualitative understanding of both porosity and tortuosity of the separator can be achieved by measuring the gas permeability of the separators. As described earlier, the permeability of the separators to gas was measured by using a novel pressure drop technique. In the pressure drop technique, a sample chamber containing the separator is pressurized to a predetermined 'upper pressure'. The

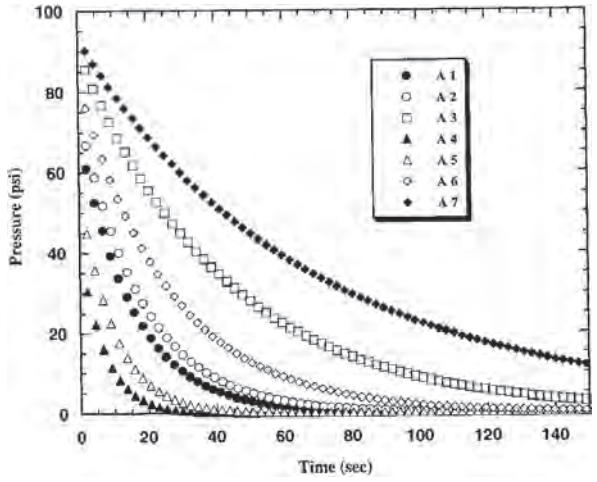


Fig. 4. Pressure drop curves for separators from supplier A.

chamber is then isolated from the gas source. As the gas in the chamber escapes through pores of the membrane, the chamber pressure drops. This pressure drop across the membrane is monitored as a function of time. Membranes with higher permeability demonstrate a more rapid drop in pressure than membranes with lower permeability. Fig. 4 shows the pressure vs. time curves for a number of separators manufactured by supplier A. The long pressure drop time for sample A7 suggests that this sample does indeed have a relatively low porosity value. Samples A4 and A5 have the shortest pressure drop times because of the higher porosity values in these separators. The bilayer separators A3 and A5 have slightly lower permeability values when compared to their single layer counterparts A2 and A4, respectively. Some separators with similar porosity numbers, like A1 and A2, have pressure drop curves that look fairly similar. However, other separators that have similar porosities, like A2 and A6, have significantly different pressure drop profiles. The pressure drop in separator A6 is much slower than the pressure drop in separator A2. This suggests that the pores in separator A6 are significantly more tortuous than the pores in separator A2.

From the data in Fig. 4 it is possible to estimate the time required for the pressure across each of these separators to drop from 100 psi to an arbitrary lower value (20 psi). These times, henceforth referred to as the *pressure drop times*, are given in Table 2 for all the separators from supplier A. In summary, an increase in porosity and/or a decrease in tortuosity leads to higher permeabilities and lower pressure drop times.

The most commonly used test method for gauging permeability is the Gurley method [17]. This test is similar in principle to the pressure drop technique that is described above, except that it measures the time taken for a fixed volume of gas to be forced through a membrane at constant pressure. This time is frequently referred to as the *Gurley number*. The third column in Table 2 shows the Gurley numbers for separators from supplier A. These numbers are average values of the Gurley number range that was reported by the supplier in the product datasheets. No numbers were available for sample A7. For samples A1 to A6, the trend observed in the pressure drop times for the separators is identical to the trend in the Gurley numbers reported by the supplier in the product data sheets.

Fig. 5 shows the pressure vs. time curves for separators from suppliers B, C and D. The pressure drop times for these samples are also included in Table 2. Gurley numbers for these separators are not included however, since every supplier does not use the same conditions to do the test. Samples C1 and C2 have relatively low pressure drop times because of their high porosities. Samples B1 and B2 have higher pressure drop times when compared to samples A1 and A2, in spite of the fact that all four of these separators have porosity values of around 40%. Again, this suggests that the pores in samples B1 and B2 have higher tortuosity than the pores in samples A1 and A2.

Table 2
Comparison of pressure drop times and Gurley numbers for microporous separators

Separator type	Pressure drop time (s)[a]	Gurley Number (s)[b]
A1	20	28
A2	24	33
A3	64	65
A4	5	10
A5	10	20
A6	37	37
A7	108	n/a
B1	31	–
B2	38	–
C1	5	–
C2	<5	–
D1	28	–

[a] For pressure to drop from 100 to 20 psi (sample area = 1.25 in.^{2}).
[b] Average value of range from supplier A datasheets (sample area = 1 in.^{2}).

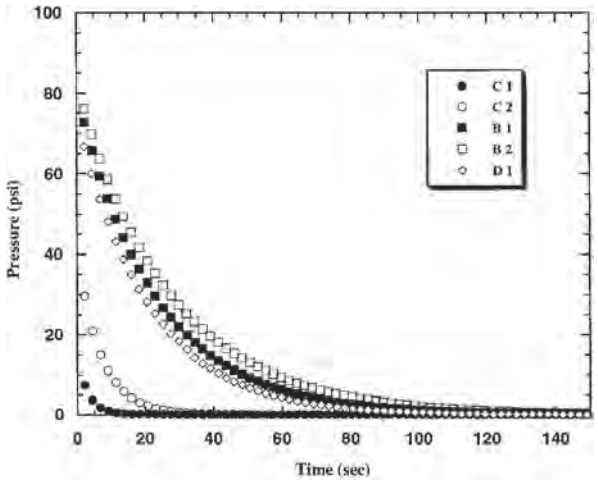


Fig. 5. Pressure drop curves for separators from suppliers B, C and D.

CosMX Exhibit 1003, Page 332 of 512

3.4. Thermal properties and shutdown mechanism

Like most batteries, Li-ion will generate heat if overcharged [18]. Above a threshold temperature the battery starts to 'self-heat' because of exothermic reactions within the components of the cell [18]. Accidental overcharging may occur during any one of the following situations: a malfunctioning charger, malfunctioning safety circuit, electrical misuse/abuse of battery pack. Separator 'shutdown' is a useful safety feature for preventing thermal runaway reactions in Li-ion batteries [8,9]. Separator shutdown is also a useful mechanism for limiting temperature and preventing venting in short-circuited cells [19,20]. Shutdown usually takes place close to the melting temperature of the polymer when the pores collapse, turning the porous ionically conductive polymer film into a non-porous insulating layer between the electrodes. At this temperature there is a significant increase in cell impedance and passage of current through the cell is restricted. This prevents further electrochemical activity in the cell thereby shutting the cell down before an explosion can occur. In principle most polyolefinic separators are shutdown separators since they melt at reasonable (< 200°C) temperatures. Fig. 6 shows the DSC thermograms for separators made out of (a) polypropylene, PP (b) polyethylene, PE and (c) a trilayer combination of the PP/PE/PP. Polypropylene separators melt at around 170°C and may be effective for shutting down cells that have relatively high thermal runaway temperatures. However, most commercial lithium-ion cells use separators with a lower shutdown temperature. For example polyethylene (PE) separators have shutdown temperatures between 130 and 140°C (see Fig. 6). In some cases, even after shutdown the cell temperature may continue to increase before actually beginning to cool. This is a likely scenario for a cell in a battery pack where heat dissipation is expected to be slow. Robust mechanical properties are therefore expected of the separator even above the shutdown temperature. If the separator undergoes a *meltdown*, i.e., if the mechanical properties of the separator deteriorate greatly after shutdown, the cell may internally short creating a safety hazard. More recently, some separator manufacturers have started offering products which have the porous PE layer sandwiched between two porous PP layers (see Fig. 6 for DSC of PP/PE/PP). The PE layer offers lower shutdown temperature while the PP provides the mechanical stability at and above the shutdown temperature. These multi-ply separators are expected to provide a wider shutdown window and may be safer than the single layer separators for some applications.

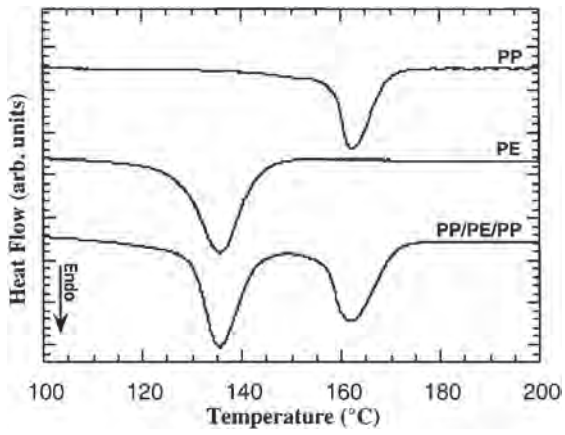


Fig. 6. DSC thermograms of representative polyolefin separators. PP represents polypropylene, PE represents polyethylene and PP/PE/PP represents a trilayer separator.

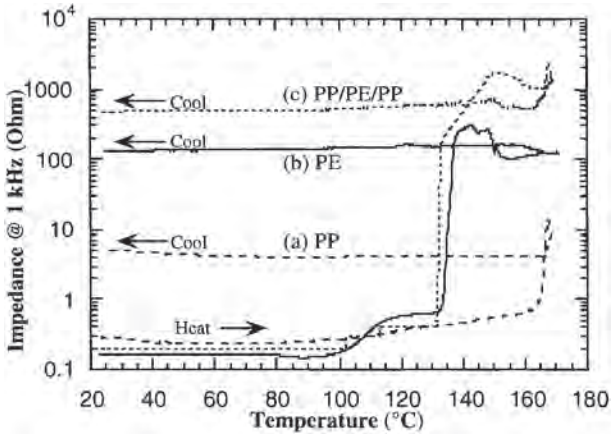


Fig. 7. Impedance vs. temperature curves for cells containing polyolefin separators: (a) polypropylene, (b) polyethylene and (c) polypropylene/polyethylene/polypropylene multiple layer.

Fig. 7 shows the impedance vs. temperature curves for three cells each containing a different separator. All cells contained a $LiCoO_2$ cathode, a graphite anode and a PVDF coating on the separator. The cells were assembled and formed under identical conditions, as described in Ref. [7]. As indicated on the figure, impedance values for each cell were collected and plotted as the cells were heated up to 170°C and then cooled back down to ambient temperature. Fig. 7a corresponds to a cell containing a single layer polypropylene separator. The shutdown in this cell occurs at around 165°C, as is indicated by the sharp rise in impedance at this temperature. However, the impedance increase is approximately two orders of magnitude which may not be large enough for 'complete' shutdown i.e., cells may continue to overcharge albeit at lower rates and this will continue to be a safety hazard. As expected the shutdown temperature for the cell containing a polyethylene separator is at around 135°C (Fig. 7b). The impedance increases by about three orders of magnitude at this temperature. The lower shutdown temperature and the higher impedance of the cell after shutdown would make the polyethylene separator the preferred one for most lithium-ion cells. The shutdown behavior of the cell containing the PP/PE/PP multi-ply separator (Fig. 7c) is very similar to the one containing the PE separator. The impedance increase for this cell at the shutdown temperature is larger than that seen in Fig. 7b and may also be a result of the additional layers of PP that are present in the multi-ply separator.

CosMX Exhibit 1003, Page 333 of 512

The voltage, current and skin temperature data of two prototype cells were collected during an overcharge test and plotted as a function of time in Fig. 8a and b. Both cells contained a $LiCoO_2$ cathode, a graphite anode and a PVDF coated polyolefin separator. The cells were assembled and formed under identical conditions as described in Ref. [7]. The overcharge test was performed by charging an optimally charged cell at a constant current value of 1.5 A. A 10 V (maximum) power supply was used to deliver the current. No additional voltage cut-off was used. The data shown in Fig. 8a is for a cell containing a trilayer PP/PE/PP separator. As is evident from the temperature profile in the figure, the cell starts to heat up because of the overcharge process. The heating rate increases significantly after 12 min. After about 19 min the applied current drops from 1.5 A to around 0.04 A. The current value stays at around 0.04 A even after the power supply voltage is increased to the 10 V limit. The low current value and high voltage value is an indication of high cell impedance arising from timely separator shutdown. After the drop in the current value, the cell skin temperature reaches a maximum and then begins to revert back to ambient. The maximum skin temperature is around 80°C. The internal temperature, however, is expected to be greater than 135°C. Typically, post-mortem analysis of a cell that demonstrated this kind of shutdown behavior revealed a deformed jelly roll in which the separator had been transformed into a translucent film. Both these observations indicate that separator shrinkage and pore closure is the most likely shutdown mechanism in these cells.

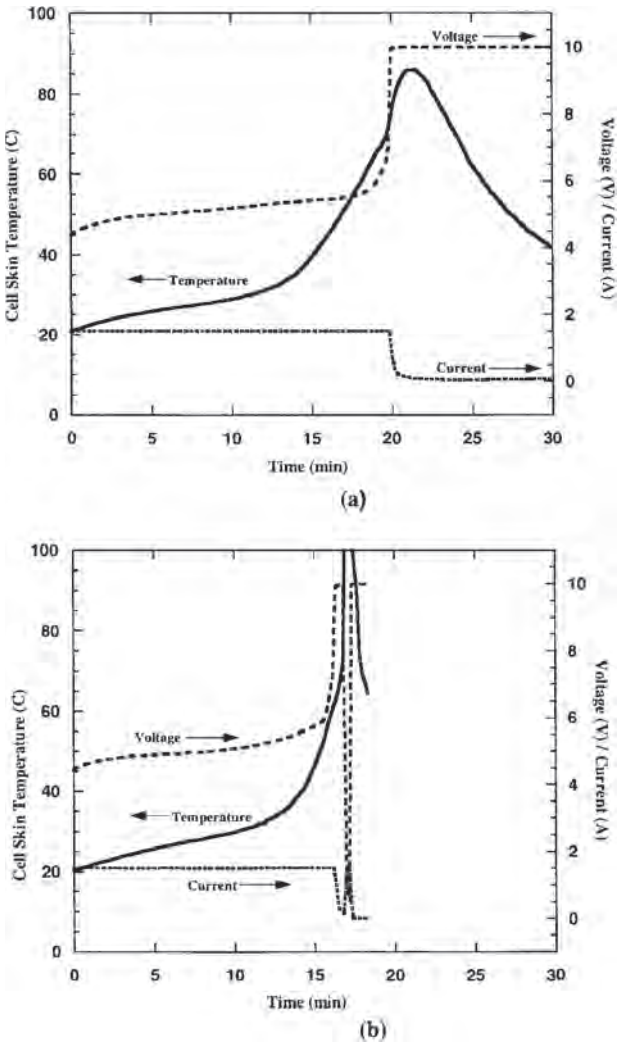


Fig. 8. (a) Overcharge test results for a cell containing a polypropylene/polyethylene/polypropylene trilayer separator. (b) Overcharge test results for a cell containing a polypropylene separator.

Fig. 8b shows the voltage, current and temperature vs. time profiles for a cell containing a single layer PP separator. As is evident from the temperature profile in this figure, the cell temperature reaches the thermal runaway point before the cell can actually shutdown. [1] This thermal runaway condition resulted in violent venting and ignition of the cell. This illustrates the potential safety advantage of separators with lower shutdown temperatures like the PE-based material. It is essential to point out, however, that not all PE containing separators are capable of demonstrating the same shutdown behavior. The ability of the PE-based separator to shutdown the battery is determined by its molecular weight, percent crystallinity (density) and process history. Materials properties and processing methods might need to be tailored so that the shutdown response is fast and complete. This optimization needs to be done without effecting the mechanical properties of the material in the temperature range of interest and is easier to do with the trilayer separators since one material is utilized for the shutdown response and another for the mechanical properties.

4. Conclusion

Porosity, pore-size, gas permeability, thermal properties and shutdown characteristics of commercial Li-ion battery separators were studied. Most lithium-ion battery separators were found to have porosity values between 40 and 50%. Average pore sizes were typically less than 0.1 μm. The relatively low porosity and pore size values allow these separators to be efficient at preventing internal shorts between the electrodes even when their thickness values are as low as 25 μm. The permeability of these separators to nitrogen gas was measured using a novel pressure drop method that is similar in principle to the Gurley method. As was expected, the pressure drop times were strongly influenced by the porosity and the size of the pores in the separators. Comparison of pressure drop times on separators with similar porosities gave qualitative information about the tortuosity of the pores in those separators. For

[1] The applied voltage and the current for this cell after thermal runaway are 10 V and 0 A, respectively. This happens because the power supply is now connected to an open circuit, which was formed during cell disassembly.

CosMX Exhibit 1003, Page 334 of 512

one particular series of separators, the trend observed in the pressure drop times was in agreement with the trend in the Gurley numbers reported by the supplier. Separator shutdown properties were studied by measuring the impedance of a Li-ion cell containing the separator as a function of temperature. Overcharge tests were also performed to check the efficiency of the shutdown behavior. Polyethylene containing separators, in particular trilayer separators, appear to be efficient at timely prevention of thermal runaway in lithium ion cells. This is made possible by the lower melting/shutdown temperature of the polyethylene layer, and also the improved mechanical stability rendered to the trilayer construction by the polypropylene layer at the higher temperatures. The ability of separators to provide shutdown capability coupled with their ability to prevent shorts while maintaining thickness values of less than 30 μm also make these materials very attractive for use in the gel-electrolyte layer of lithium-ion polymer batteries.

References

[1] S. Megahead, B. Scrosati, Interface 4 (1995) 34.
[2] H. Takeshita, Nikkei Electronics Asia (1997) March issue.
[3] A.S. Gozdz, C.N. Schmutz, J.M. Tarascon, P.C. Warren, 5,456,000, U.S. Patent, 1995.
[4] K. Morigaki, N. Kabuto, H. Kazunori, 5,597,659, U.S. Patent, 1997.
[5] S. Dasgupta, J.K. Jacobs, 5,437,692, U.S. Patent, 1995.
[6] K.M. Abraham, M. Alamgir, D.K. Hoffman, J. Electrochem. Soc. 142 (1995) 683.
[7] S.L. Pendalwar, J.N. Howard. G. Venugopal, M. Oliver, 5,716,421, U.S. Patent, 1998.
[8] F.C. Laman, M.A. Gee, J. Denovan, J. Denovan, J. Electrochem. Soc. 140 (1993) L51.
[9] K.M. Abraham, Electrochim. Acta 38 (1) (1993) 1233.
[10] M.J. Weighall, Sixth International ILZRO Lead Acid Battery Seminar, 1992.
[11] R. Fleming, H. Taskier, Progress in Batteries and Solar Cells 9 (1990) 58.
[12] H.J. Troffkin, M.R. Burton, R.M. Spotnitz, R.T. Giovannoni, Y. Guo, 5,240,655, U.S. Patent, 1993.
[13] M.J. Weighall, Fourth International ILRZO Lead Acid Battery Seminar, 1990.
[14] A.S. Gozdz, C.N. Schmutz, J.M. Tarascon, P.C. Warren, 5,607,485, U.S. Patent, 1997.
[15] F.O. Eschbach, M. Oliver, G. Venugopal, S.L. Pendalwar, 5,631,103, U.S. Patent, 1997.
[16] J.S. Dixon, Proceedings of the INDEX '96 Conference, 1996.
[17] ASTM Test # D726.
[18] J.R. Dahn, E.W. Fuller, M. Obrovac, U. von Sacken, Solid State Ionics 69 (1994) 265.
[19] R. Spotnitz, M. Ferebee, R. Callahan, K. Nguyen, W.C. Yu, M. Geiger, C. Dwiggens, H. Fisher, D. Hoffman, Proceedings of the 12th International Seminar on Primary and Secondary Battery Technology and Application, 1995.
[20] R. Spotnitz, M. Ferebee, Proceedings of the 191st Meeting of the Electrochemical Society, 1997, p. 109.

CosMX Exhibit 1003, Page 335 of 512

Appendix L

US007709152B2

(12) **United States Patent**
Kim et al.

(10) **Patent No.: US 7,709,152 B2**
(45) **Date of Patent: May 4, 2010**

(54) **ORGANIC/INORGANIC COMPOSITE SEPARATOR HAVING POROUS ACTIVE COATING LAYER AND ELECTROCHEMICAL DEVICE CONTAINING THE SAME**

(75) Inventors: **Seok-Koo Kim**, Daejeon (KR); **Joon-Yong Sohn**, Busan (KR); **Jong-Hyeok Park**, Daejeon (KR); **Hyun-Min Jang**, Daejeon (KR); **Byoung-Jin Shin**, Busan (KR); **Sang-Young Lee**, Daejeon (KR); **Jang-Hyuk Hong**, Daejeon (KR)

(73) Assignee: **LG Chem, Ltd.**, Seoul (KR)

(*) Notice: Subject to any disclaimer, the term of this patent is extended or adjusted under 35 U.S.C. 154(b) by 0 days.

(21) Appl. No.: **12/158,934**

(22) PCT Filed: **Feb. 5, 2008**

(86) PCT No.: **PCT/KR2008/000706**

§ 371 (c)(1),
(2), (4) Date: **Jun. 23, 2008**

(87) PCT Pub. No.: **WO2008/097013**

PCT Pub. Date: **Aug. 14, 2008**

(65) **Prior Publication Data**

US 2009/0111026 A1 Apr. 30, 2009

(30) **Foreign Application Priority Data**

Feb. 5, 2007 (KR) 10-2007-0011818

(51) **Int. Cl.**
H01M 2/16 (2006.01)
H01M 4/58 (2006.01)

(52) **U.S. Cl.** **429/251**; 429/247; 429/249; 429/231.95

(58) **Field of Classification Search** 429/251, 429/249, 247
See application file for complete search history.

(56) **References Cited**

U.S. PATENT DOCUMENTS

6,328,770	B1	12/2001	Gozdz	
6,492,295	B2 *	12/2002	Hitomi et al.	502/159
6,746,803	B1	6/2004	Bauer et al.	
6,821,680	B2	11/2004	Tanaka et al.	
6,878,484	B2 *	4/2005	Tanaka et al.	429/145
2002/0187401	A1 *	12/2002	Lee et al.	429/303

FOREIGN PATENT DOCUMENTS

KR	10-2006-0003665	A	1/2006
KR	10-2006-0072065	A	6/2006
KR	10-2007-0000231	A	1/2007

* cited by examiner

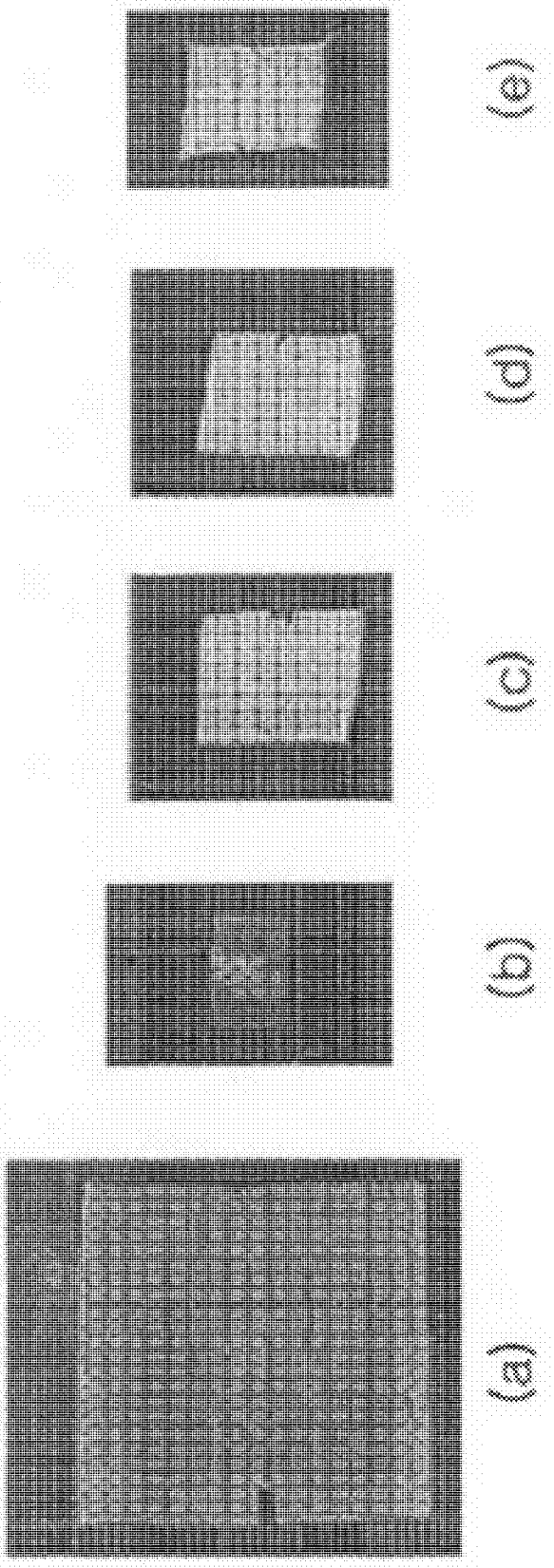
Primary Examiner—Patrick Ryan
Assistant Examiner—Julian Mercado
(74) *Attorney, Agent, or Firm*—Birch, Stewart, Kolasch & Birch, LLP

(57) **ABSTRACT**

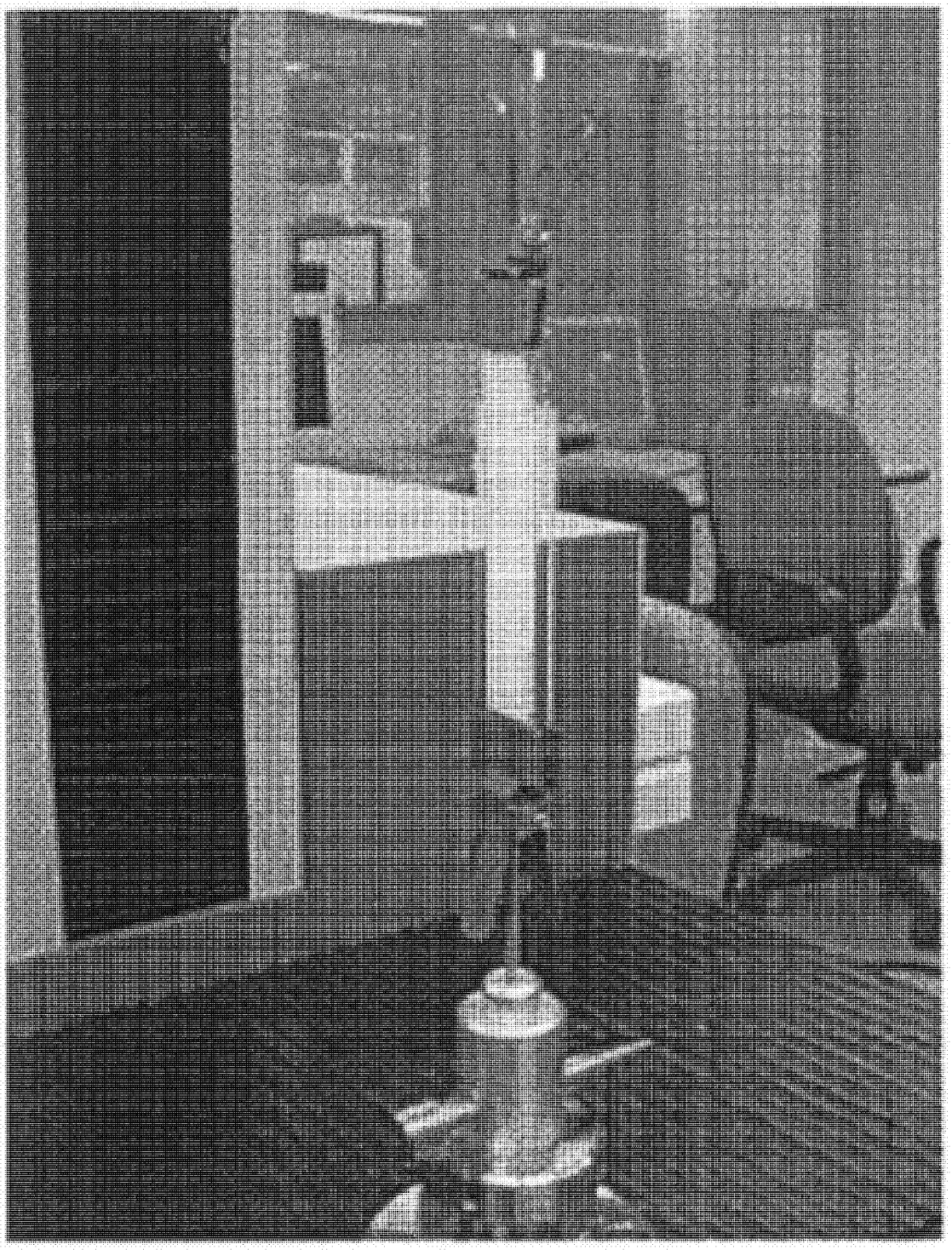
An organic/inorganic composite separator includes (a) a polyolefin porous substrate having pores; and (b) a porous active layer containing a mixture of inorganic particles and a binder polymer, with which at least one surface of the polyolefin porous substrate is coated, wherein the porous active layer has a peeling force of 5 gf/cm or above, and a thermal shrinkage of the separator after being left alone at 150° C. for 1 hour is 50% or below in a machine direction (MD) or in a transverse direction (TD). This organic/inorganic composite separator solves the problem that inorganic particles in the porous active layer formed on the porous substrate are extracted during an assembly process of an electrochemical device, and also it may prevent an electric short circuit between cathode and anode even when the electrochemical device is overheated.

20 Claims, 2 Drawing Sheets

[Fig. 1]



[Fig. 2]



ORGANIC/INORGANIC COMPOSITE SEPARATOR HAVING POROUS ACTIVE COATING LAYER AND ELECTROCHEMICAL DEVICE CONTAINING THE SAME

TECHNICAL FIELD

The present invention relates to a separator of an electrochemical device such as a lithium secondary battery and an electrochemical device containing the same. More particularly, the present invention relates to an organic/inorganic composite separator in which a porous active layer is coated with a mixture of an inorganic particle and a polymer onto a surface of a porous substrate, and an electrochemical device containing the same.

BACKGROUND ART

Recently, there has been an increasing interest in energy storage technology. Batteries have been widely used as energy sources in the fields of cellular phones, camcorders, notebook computers, PCs and electric cars, resulting in intensive research and development into them. In this regard, electrochemical devices are one of the subjects of great interest. Particularly, development of rechargeable secondary batteries has been the focus of attention. Recently, the research and development into a novel electrode and a novel battery that can improve capacity density and specific energy have been made intensively in the field of the secondary batteries.

Among currently used secondary batteries, lithium secondary batteries developed in early 1990's have a higher drive voltage and a much higher energy density than those of conventional batteries using a liquid electrolyte solution such as Ni-MH batteries, Ni—Cd batteries, and H_2SO_4—Pb batteries. For these reasons, the lithium secondary batteries have been advantageously used. However, such a lithium secondary battery has disadvantages in that organic electrolytes used therein may cause safety-related problems such as ignition and explosion of the batteries and that processes for manufacturing such a battery are complicated. Recently, lithium-ion polymer batteries have been considered as one of the next-generation batteries since the above disadvantages of the lithium ion batteries are solved. However, the lithium-ion polymer batteries have a relatively lower battery capacity than those of the lithium ion batteries and an insufficient discharging capacity in low temperature, and therefore these disadvantages of the lithium-ion polymer batteries remain to be urgently solved.

Such electrochemical devices have been produced from many companies, and the battery stability has different phases in the electrochemical devices. Accordingly, it is important to evaluate and ensure the stability of the electrochemical batteries. First of all, it should be considered that errors in operation of the electrochemical device should not cause damage to users. For this purpose, the Safety Regulation strictly regulates ignition and explosion in the electrochemical devices. In the stability characteristics of the electrochemical device, overheating of the electrochemical device may cause thermal runaway, and explosion may occur when a separator is pierced. In particular, a polyolefin porous substrate commonly used as a separator of an electrochemical device shows extreme thermal shrinking behavior at a temperature of 100° C. or above due to the features of its material and its manufacturing process such as elongation, so there may occur an electric short circuit between cathode and anode.

In order to solve the above safety-related problems of the electrochemical device, there has been proposed an organic/inorganic composite separator having a porous active layer formed by coating at least one surface of a polyolefin porous substrate having many pores with a mixture of inorganic particles and a binder polymer (see Korean Laid-open Patent Publication No. 10-2006-72065 and 10-2007-231, for example). The inorganic particles in the porous active layer formed on the polyolefin porous substrate act as a kind of spacer that keeps a physical shape of the porous active layer, so the inorganic particles restrain thermal shrinkage of the polyolefin porous substrate when the electrochemical device is overheated. In addition, interstitial volumes exist among the inorganic particles, thereby forming fine pores.

As mentioned above, at least a certain amount of inorganic particles should be contained such that the porous active layer formed on the organic/inorganic composite separator may restrain thermal shrinkage of the polyolefin porous substrate. However, as the content of inorganic particles is increased, a content of binder polymer is relatively decreased, which may cause the following problems.

First, due to the stress generated in an assembly process of an electrochemical device such as winding, inorganic particles may be extracted from the porous active layer, and the extracted inorganic particles act as a local defect of the electrochemical device, thereby giving a bad influence on the stability of the electrochemical device.

Second, an adhesion between the porous active layer and the polyolefin porous substrate is weakened, so the ability of the porous active layer to restrain thermal shrinkage of the polyolefin porous substrate is deteriorated. Thus, it is difficult to prevent an electric short circuit between cathode and anode even when the electrochemical device is overheated.

On the contrary, if the content of binder polymer in the porous active layer is increased in order to prevent extraction of inorganic particles, the content of inorganic particles is relatively decreased, so thermal shrinkage of the polyolefin porous substrate may not be easily restrained. Accordingly, it is hard to prevent an electric short circuit between cathode and anode, and also the performance of the electrochemical device is deteriorated due to the decrease of porosity in the porous active layer.

DISCLOSURE OF INVENTION

Technical Problem

The present invention is designed to solve the problems of the prior art, and therefore an object of the invention is to provide an organic/inorganic composite separator capable of preventing extraction of inorganic particles in a porous active layer formed on a porous substrate during an assembly process of an electrochemical device, and also capable of restraining an electric short circuit between cathode and anode even when the electrochemical device is overheated.

Technical Solution

In order to accomplish the first object, the present invention provides an organic/inorganic composite separator, which includes (a) a polyolefin porous substrate having pores; and (b) a porous active layer containing a mixture of inorganic particles and a binder polymer, with which at least one surface of the polyolefin porous substrate is coated, wherein the porous active layer has a peeling force of 5 gf/cm or above, and a thermal shrinkage of the separator after being left alone

at 150° C. for 1 hour is 50% or below in a machine direction (MD) or in a transverse direction (TD).

The organic/inorganic composite separator of the present invention may solve the problem that inorganic particles in the porous active layer are extracted during an assembly process of an electrochemical device, though inorganic particles are sufficiently contained over certain content. In addition, an adhesive force between the porous active layer and the polyolefin porous substrate is strong, so thermal shrinkage is restrained to some extent though the electrochemical device is overheated, thereby preventing an electric short circuit between the cathode and the anode. Accordingly, the stability of the electrochemical device is greatly improved.

In the organic/inorganic composite separator according to the present invention, the binder polymer is preferably a mixture of a first binder polymer having a contact angle to a water drop of 70° to 140° and a second binder polymer having a contact angle to a water drop of 1° to 69°. Since the first and second binder polymers with different hydrophile properties are used in a blend form to control the hydrophile property of the polymer blend, there may be obtained a synergistic effect in improvement of thermal stability of the organic/inorganic composite separator.

The first binder mentioned above may be any one polymer or a mixture of at least two polymers selected from the group consisting of polyvinylidene fluoride, polyvinylidene fluoride-co-hexafluoropropylene, polyvinylidene fluoride-co-trichloroethylene, polymethylmethacrylate, polyacrylonitrile, polyvinylacetate, polyethylene-co-vinyl acetate, polyimide and polyethylene oxide.

Also, the second binder polymer mentioned above may be any one polymer or a mixture of at least two polymers having at least one polar group selected from the group consisting of hydroxyl group (—OH), carboxyl group (—COOH), maleic anhydride group (—COOOC—), sulphonate group ($—SO_3H$) and pyrrolidone group (—NCO—). These second binder polymer may be cyanoethylpullulan, cyanoethylpolyvinylalcohol, cyanoethylcellulose, cyanoethylsucrose, carboxyl methyl cellulose, polyvinylalcohol, polyacrylic acid, polymaleic anhydride, or polyvinylpyrrolidone, for example.

BRIEF DESCRIPTION OF THE DRAWINGS

These and other features, aspects, and advantages of preferred embodiments of the present invention will be more fully described in the following detailed description, taken accompanying drawings. In the drawings:

FIGS. **1***a* to **1***e* are photographs showing a separator manufactured according to embodiments of the present invention and comparative examples, which illustrate heat shrinkage after the separator is left alone for 1 hour in an oven of 150° C.; and

FIG. **2** is a photograph showing a test device for measuring a peeling force of a porous active layer formed on an organic/inorganic composite separator manufactured according to embodiments of the present invention and comparative examples.

BEST MODE

Hereinafter, preferred embodiments of the present invention will be described in detail referring to the accompanying drawings. Prior to the description, it should be understood that the terms used in the specification and appended claims should not be construed as limited to general and dictionary meanings, but interpreted based on the meanings and concepts corresponding to technical aspects of the present invention on the basis of the principle that the inventor is allowed to define terms appropriately for the best explanation. Therefore, the description proposed herein is just a preferable example for the purpose of illustrations only, not intended to limit the scope of the invention, so it should be understood that other equivalents and modifications could be made thereto without departing from the spirit and scope of the invention.

The present invention provides an organic/inorganic composite separator, which includes (a) a polyolefin porous substrate having pores; and (b) a porous active layer containing a mixture of inorganic particles and a binder polymer, with which at least one surface of the polyolefin porous substrate is coated, wherein the porous active layer has a peeling force of 5 gf/cm or above, and a thermal shrinkage of the separator after being left alone at 150° C. for 1 hour is 50% or below in a machine direction (MD) or in a transverse direction (TD).

In the organic/inorganic composite separator of the present invention, the porous active layer has a peeling force of 5 gf/cm or above, so the porous active layer has an excellent peeling resistance, thereby solving the problem that inorganic particles in the porous active layer are extracted while assembling a charger chemical device. In addition, an adhesive force between the porous active layer and the polyolefin porous substrate is strong. Thus, though the battery is overheated, the porous active layer and the polyolefin porous substrate are not separated, and thermal shrinkage of the polyolefin porous substrate may be restrained. That is to say, since the organic/inorganic composite separator shows a thermal shrinkage of 50% or below in a machine direction (MD) or in a transverse direction (TD), it is possible to prevent an electric short circuit between cathode and anode. In addition, though the porous substrate is overheated in the electrochemical device, both electrodes are not entirely short-circuited due to the porous active layer. Even if there occurs a short circuit, the short-circuited area is not enlarged, thereby improving stability of the electrochemical device.

In the organic/inorganic composite separator of the present invention, more preferably, the porous active layer has a peeling force of 10 gf/cm or above, and a thermal shrinkage of the separator after being left alone at 150° C. for 1 hour is preferably 30% or below in a machine direction (MD) or in a transverse direction (TD), in aspect of stability of the electrochemical device and peeling resistance of the porous active layer.

In the organic/inorganic composite separator of the present invention, the binder polymer preferably uses a mixture of a first binder polymer having a contact angle to a water drop of 70° to 140° and a second binder polymer having a contact angle to a water drop of 1° to 69°. In the present invention, after a sample film was made using a corresponding binder polymer, a distilled water drop was fallen thereon, and then a contact angle formed on the water drop was set as 23 degrees. Also, the contact angle to a water drop was measured using a contact angle measurer model CA-DT-A (mfd. produced by Kyowa Kaimen Kagaku KK) under the condition of 50% RH. Contact angles were measured at two points (namely, left and right points) of each of three sample films, and six measured values are averaged and set as a contact angle. The distilled water drop has a diameter of 2 mm, and the contact angle value displayed on the measurer shows a contact angle measured 1 minute after the distilled water drop is fallen.

Since the first and second binder polymers having different hydrophile properties are used in a blend form to control a hydrophile property of the polymer blend as mentioned

above, it is possible to realize a synergistic effect in improving thermal stability of the organic/inorganic composite separator.

More preferably, the first binder polymer has a contact angle to a water drop of 90° to 110° and the second binder polymer has a contact angle to a water drop of 20° to 40°. Also, the first binder polymer and the second binder polymer are preferably mixed in a weight ratio of 95:5 to 5:95, but not limitedly.

The first binder polymer mentioned above may be any one polymer or a mixture of at least two polymers selected from the group consisting of polyvinylidene fluoride, polyvinylidene fluoride-co-hexafluoropropylene, polyvinylidene fluoride-co-trichloroethylene, polymethylmethacrylate, polyacrylonitrile, polyvinylacetate, polyethylene-co-vinyl acetate, polyimide, and polyethylene oxide, but not limitedly.

Also, the second binder polymer is preferably a polymer or a mixture of at least two polymers having at least one polar group selected from the group consisting of hydroxyl group (—OH), carboxyl group (—COOH), maleic anhydride group (—COOOC—), sulphonate group (—SO_3H) and pyrrolidone group (—NCO—). The second binder polymer may be cyanoethylpullulan, cyanoethylpolyvinylalcohol, cyanoethylcellulose, cyanoethylsucrose, carboxyl methyl cellulose, polyvinylalcohol, polyacrylic acid, polymaleic anhydride, or polyvinylpyrrolidone.

In addition, in the organic/inorganic composite separator according to the present invention, the number of inorganic particles per a unit area of the porous active layer is preferably 1×10^{15} to $1\times10^{30}/m^2$ in consideration of a common thickness of the porous active layer. If the number of inorganic particles per a unit area of the porous active layer is less than 1×10^{15}, the thermal stability obtained by the inorganic particles may be deteriorated. Meanwhile, if the number of inorganic particles per a unit area of the porous active layer is greater than $1\times10^{30}/m^2$, dispersion in a coating solution and coating workability, required for forming the porous active layer, may be deteriorated. Also, a weight of the inorganic particles per a unit area of the porous active layer is preferably 5 to 100 g/m^2.

In the organic/inorganic composite separator according to the present invention, the inorganic particle used for forming the porous active layer is not specifically limited if it is electrically chemically stable. That is to say, an inorganic particle usable in the present invention is not specially limited if oxidation or reduction reaction does not occur in an operating voltage range (for example, 0 to 5V based on Li/Li^+) of an applied electrochemical device. In particular, in case an inorganic particle with ion transferring capability is used, it is possible to enhance the performance by increasing ion conductivity in the electrochemical device.

In addition, in case an inorganic particle with a high dielectric constant is used, it contributes to the increase of dissociation of electrolyte salt, for example lithium salt, in the liquid electrolyte, thereby improving ion conductivity of the electrolyte.

Due to the above reasons, it is preferred that the inorganic particles are selected from the group consisting of inorganic particles having a dielectric constant of 5 or above, preferably 10 or above, inorganic particles having lithium-ion transferring capability, or their mixtures. The inorganic particle having a dielectric constant of 5 or above is any one inorganic particle or a mixture of at least two inorganic particles selected from the group consisting of $BaTiO_3$, $Pb(Zr,Ti)O_3$ (PZT), $Pb_{1-x}La_xZr_{1-y}Ti_yO_3$ (PLZT), $PB(Mg_3Nb_{2/3})O_3$—$PbTiO_3$ (PMN-PT), hafnia (HfO_2), $SrTiO_3$, SnO_2, CeO_2, MgO, Nil, CaO, ZnO, ZrO_2, SiO_2, Y_2O_3, Al_2O_3, SiC and TiO_2, but not limitedly.

In particular, the inorganic particles such as of $BaTiO_3$, $Pb(Zr,Ti)O_3$ (PZT), $Pb_{1-x}La_xZr_{1-y}Ti_yO_3$ (PLZT), $PB(Mg_3Nb_{2/3})O_3$—$PbTiO_3$ (PMN-PT) and hafnia (HfO_2) show a high dielectric constant of 100 or above and have piezoelectricity since charges are generated to make a potential difference between both surfaces when a certain pressure is applied to extend or shrink them, so the above inorganic particles may prevent generation of an internal short circuit of both electrodes caused by an external impact and thus further improve the stability of the electrochemical device. In addition, in case the inorganic particles having a high dielectric constant are mixed with the inorganic particles having lithium ion transferring capability, their synergistic effect may be doubled.

In the present invention, the inorganic particle having lithium ion transferring capability means an inorganic particle containing lithium atom and having a function of moving a lithium ion without storing the lithium. The inorganic particle having lithium ion transferring capability may transfer and move lithium ions due to a kind of defect existing in the particle structure, so it is possible to improve lithium ion conductivity in the battery and also improve the performance of the battery. The inorganic particle having lithium ion transferring capability is any one inorganic particle or a mixture of at least two inorganic particles selected from the group consisting of lithium phosphate (Li_3PO_4), lithium titanium phosphate ($Li_xTi_y(PO_4)_3$, $0<x<2$, $0<y<3$), lithium aluminum titanium phosphate ($Li_xAl_yTi_z(PO_4)_3$, $0<x<2$, $0<y<1$, $0<z<3$), $(LiAlTiP)_xO_y$ type glass ($0<x<4$, $0<y<13$), lithium lanthanum titanate ($Li_xLa_yTiO_3$, $0<x<2$, $0<y<3$), lithium germanium thiophosphate ($Li_xGe_yP_zS_w$, $0<x<4$, $0<y<1$, $0<z<1$, $0<w<5$), lithium nitrides (Li_xN_y, $0<x<4$, $0<y<2$), SiS_2 ($Li_xSi_yS_z$, $0<x<3$, $0<y<2$, $0<z<4$) type glass, and P_2S_5 ($Li_xP_yS_z$, $0<x<3$, $0<y<3$, $0<z<7$) type glass, but not limitedly.

In the organic/inorganic composite separator according to the present invention, the size of inorganic particles in the porous active layer is not specially limited, but it is preferably in the range from 0.001 to 10 μm, if possible, in order to form a coating layer in a uniform thickness and ensure suitable porosity. If the particle size is less than 0.001 μm, a dispersing property is deteriorated, so it is not easy to control properties of the organic/inorganic composite separator. If the particle size exceeds 10 μm, the thickness of the porous active layer is increased, which may deteriorate mechanical properties. In addition, due to excessively great pore size, the possibility of internal short circuit is increased while charging or discharging a battery.

In the organic/inorganic composite separator coated with the porous active layer according to the present invention, a weight ratio of the inorganic particles and the binder polymer is in the range from 50:50 to 99:1, more preferably from 70:30 to 95:5. If the weight ratio of the organic particles to the binder polymer is less than 50:50, the content of polymer is so great that the thermal stability of the organic/inorganic composite separator may not be much improved. In addition, pore size and porosity may be decreased due to the decrease of interstitial volume formed among the inorganic particles, thereby causing deterioration of the performance of a battery. If the weight ratio exceeds 99:1, the peeling resistance of the porous active layer may be weakened since the content of binder polymer is so small. The thickness of the porous active layer composed of the inorganic particles and the binder polymer is not specially limited but preferably in the range from 0.01 to 20 μm. Also, pore size and porosity are not specially limited, but the pore size is preferably ranged from 0.001 to 10 μm and a porosity is preferably ranged from 10 to 90%. The pore size and porosity are mainly dependent on the

size of inorganic particles. For example, in case inorganic particles have a diameter of 1 μm or less, the formed pore is also approximately 1 μm or less. The pores as mentioned above are filled with electrolyte later, and the filled electrolyte plays a role of transferring ions. In case the pore size and porosity are respectively less than 0.001 μm and 10%, the porous active layer may act as a resistance layer. In case the pore size and porosity are respectively greater than 10 μm and 90%, mechanical properties may be deteriorated.

The organic/inorganic composite separator according to the present invention may further include other additives as components of the active layer, in addition to the inorganic particles and the polymer.

In addition, in the organic/inorganic composite separator according to the present invention, the polyolefin porous substrate may adopt any kind of polyolefin porous substrate if it is commonly used as a separator of an electrochemical device, particularly a lithium secondary battery. For example, the polyolefin porous substrate may be a membrane formed using any one polyolefin polymer or a mixture of at least two polyolefin polymers selected from the group consisting of polyethylene, polypropylene, polybutylene and polypentene. The polyolefin porous substrate preferably has a thickness of 1 to 100 μm, though not limited thereto, and also the pore size and porosity of the porous substrate are preferably 0.01 to 50 μm and 10 to 95%, respectively, though not limited thereto.

Hereinafter, a method for manufacturing an organic/inorganic composite separator coated with a porous active layer according to the present invention is explained based on the case that a mixture of the first and second binder polymers with different contact angles to a water drop is used as an example, but the present invention is not limited thereto.

First, the first and second binder polymers with the aforementioned contact angles to a water drop are dissolved in a solvent to make a binder polymer solution.

Subsequently, inorganic particles are added to the binder polymer solution and then dispersed therein. The solvent preferably has a solubility parameter similar to that of the used binder polymer and a low boiling point. It will help uniform mixture and easy removal of the solvent afterward. A non-limiting example of usable solvent includes acetone, tetrahydrofuran, methylene chloride, chloroform, dimethylformamide, N-methyl-2-pyrrolidone (NMP), cyclohexane, water and mixtures thereof. It is preferred that the inorganic particles are pulverized after being added to the binder polymer solution. At this time, the time required for pulverization is suitably 1 to 20 hours, and the particle size of the pulverized particles ranges preferably from 0.001 and 10 μm, as mentioned above. Conventional pulverization methods may be used, and a method using a ball mill is particularly preferred.

After that, the polyolefin porous substrate is coated with the binder polymer solution in which the inorganic particles are dispersed, under the humidity condition of 10 to 80%, and then dried.

In order to coat the porous substrate with the binder polymer solution in which the inorganic particles are dispersed, a common coating method well known in the art may be used. For example, various methods such as dip coating, die coating, roll coating, comma coating or their combinations may be used. In addition, the porous active layer may be formed selectively on both surfaces or only one surface of the porous substrate.

The organic/inorganic composite separator manufactured as mentioned above may be used as a separator of an electrochemical device, preferably a lithium secondary battery. At this time, in case a gellable polymer is used as a binder polymer component when a liquid electrolyte is impregnated, after a battery is assembled using the separator, the injected electrolyte and polymer may be reacted and then gelled, thereby forming a gel-type organic/inorganic composite electrolyte.

In addition, the present invention provides an electrochemical device, which includes (a) a cathode; (b) an anode; (c) an organic/inorganic composite separator interposed between the cathode and the anode and coated with the above-mentioned porous active layer; and (d) an electrolyte.

The electrochemical device may be any device in which electrochemical reactions may occur, and a specific example of the electrochemical devices includes all kinds of primary batteries, secondary batteries, fuel cells, solar cells or capacitors. In particular, among the secondary batteries, lithium secondary batteries including a lithium metal secondary battery, a lithium ion secondary battery, a lithium polymer secondary battery or a lithium ion polymer secondary battery are preferred.

The electrochemical device may be manufactured according to common methods well known to the art. As one embodiment of the method for manufacturing an electrochemical device, an electrochemical device may be manufactured by interposing the above-mentioned organic/inorganic composite separator between a cathode and an anode and injecting an electrolyte solution therein.

There is no special limitation in the electrodes that may be used together with an organic/inorganic composite separator of the present invention, and the electrodes may be manufactured by settling electrode active materials on a current collector according to one of common methods well known in the art. Among the electrode active materials, a non-limiting example of cathode active materials may include any conventional cathode active materials currently used in a cathode of a conventional electrochemical device. Particularly, lithium manganese oxides, lithium cobalt oxides, lithium nickel oxides, lithium iron oxides or lithium composite oxides thereof are preferred as the cathode active materials. Also, a non-limiting example of anode active materials may include any conventional anode active materials currently used in an anode of a conventional electrochemical device. Particularly, lithium intercalation materials such as lithium metal, lithium alloys, carbon, petroleum coke, activated carbon, graphite or other carbonaceous materials are preferred as the anode active materials. A non-limiting example of a cathode current collector includes a foil formed of aluminum, nickel or a combination thereof. A non-limiting example of an anode current collector includes a foil formed of copper, gold, nickel, copper alloys or a combination thereof.

The electrolyte solution that may be used in the present invention includes a salt represented by the formula of A^+B^-, wherein A^+ represents an alkali metal cation selected from the group consisting of Li^+, Na^+, K^+ and combinations thereof, and B^- represents an salt containing an anion selected from the group consisting of PF_6^-, BF_4^-, Cl^-, Br^-, I^-, ClO_4^-, AsF_6^-, $CH_3CO_2^-$, $CF_3SO_3^-$, $N(CF_3SO_2)_2^-$, $C(CF_2SO_2)_3^-$ and combinations thereof. The salt may be dissolved or dissociated in an organic solvent selected from the group consisting of propylene carbonate (PC), ethylene carbonate (EC), diethyl carbonate (DEC), dimethyl carbonate (DMC), dipropyl carbonate (DPC), dimethyl sulfoxide, acetonitrile, dimethoxyethane, diethoxyethane, tetrahydrofuran, N-methyl-2-pyrrolidone (NMP), ethylmethyl carbonate (EMC), gamma-butyrolactone (γ-butyrolactone) and mixtures thereof. However, the electrolyte solution that may be used in the present invention is not limited to the above examples.

More particularly, the electrolyte solution may be injected in a suitable step during the manufacturing process of a bat-

tery, according to the manufacturing process and desired properties of a final product. In other words, the electrolyte solution may be injected before a battery is assembled or during a final step of the assembly process of a battery.

In order to apply the organic/inorganic composite separator according to the present invention to a battery, a stacking (or, laminating) process or a folding process may be used in addition to a winding process that is most commonly used. The organic/inorganic composite separator of the present invention has an excellent peeling resistance, so the inorganic particles are not easily extracted during the battery assembly process.

MODE FOR INVENTION

Hereinafter, various preferred examples of the present invention will be described in detail for better understandings. However, the examples of the present invention may be modified in various ways, and they should not be interpreted as limiting the scope of the invention. The examples of the present invention are just for better understandings of the invention to persons having ordinary skill in the art.

Example 1

Preparation of Organic/Inorganic [(PVdF—HFP/Cyanoethylpolyvinylalcohol)/Al_2O_3] Composite Separator

5 weight % of polyvinylidene fluoride-co-hexafluoropropylene (PVdF-HFP, a contact angle to a water drop is 100°) and 5 weight % of cyanoethylpolyvinylalcohol (a contact angle to a water drop is 30°) were respectively added to acetone and dissolved at 50° C. for about 12 hours to make a binder polymer solution. Al_2O_3 powder was added to the prepared binder polymer solution at a weight ratio that polymer mixture/Al_2O_3=10/90, and then the Al_2O_3 powder was pulverized and dispersed for 12 hours or more by ball milling to make a slurry. In the prepared slurry, the diameter of Al_2O_3 may be controlled according to a size (or, diameter) of used beads and the time for the ball milling, but in this example 1, the Al_2O_3 powder was pulverized into about 400 nm to make the slurry. The prepared slurry was used for coating a polyethylene separator (having a porosity of 45%) with a thickness of 16 μm by means of dip coating, and a coating thickness was controlled to be about 4 μm on one surface of the separator. A pore size in the porous active layer formed on the polyethylene separator was in the level of 0.5 μm, and a porosity was 58%. The weight of the porous active layer was about 16 g/m^2 per a unit area, and the number of only inorganic particles in the porous active layer was estimated as about 5×10^{19}/m^2, considering the size (400 nm) and density (4.123 g/cc) of the inorganic particles.

Example 2

An organic/inorganic [(PVdF-CTFE/Cyanoethylpolyvinylalcohol)/Al_2O_3] composite separator was prepared in the same way as the example 1, except that polyvinylidene fluoride-co-trichloroethylene (PVdF-CTFE, a contact angle to a water drop is 95°) was used instead of PVdF-HFP.

Example 3

An organic/inorganic [(PVdF-HFP/Cyanoethylpolyvinylalcohol)/$BaTiO_3$] composite separator was prepared in the same way as the example 1, except that $BaTiO_3$ powder was used instead of Al_2O_3 powder. The active layer had a weight of about 22 g/m^2, and the number of only inorganic particles in the active layer was estimated as about 4×10^{19}/m^2, considering the size (400 nm) and density (5.7 g/cc) of the inorganic particles.

Comparative Example 1

A polyethylene (PE) separator not coated with a porous active layer is selected as a comparative example 1.

Comparative Example 2

An organic/inorganic [PVdF-HFP/Al_2O_3] composite separator was prepared in the same way as the example 1, except that cyanoethylpolyvinylalcohol is not used but a binder polymer composed of only PVdF-CTFE was used.

Comparative Example 3

An organic/inorganic [(PVdF-HFP/PVdF-CTFE)/Al_2O_3] composite separator was prepared in the same way as the example 1, except that PVdF-CTFE was used instead of cyanoethylpolyvinylalcohol and thus binder polymer composed of PVdF-HFP and PVdF-CTFE was used.

Comparative Example 4

An organic/inorganic [PVdF-HFP/Al_2O_3] composite separator was prepared in the same way as the comparative example 2, except that the content of PVdF-HFP was increased to 50 weight % (PVdF-HFP/Al_2O_3=50/50).

Analysis of Properties of Organic/Inorganic Composite Porous Separator

In order to measure thermal shrinkage of the separators prepared according to the examples 1 to 3 and the comparative examples 1 to 4, experiments were conducted in a way that a corresponding separator is stored in an oven heated to 150° C. for 1 hour and then taken out. As a test piece, the organic/inorganic [(PVdF--HFP/Cyanoethylpolyvinylalcohol)/Al_2O_3] composite separator prepared according to the example 1 was used, and the separators of the comparative examples 1 to 3 were used as a control group.

It would be understood that the separator of the example 1 shows thermal shrinkage of about 20% in both TD and MD directions, so it gives an excellent thermal shrinkage restraining effect (see FIG. **1***a*).

Meanwhile, the polyethylene separator of the comparative example 1, to which a coating layer is not introduced, shows extreme thermal shrinkage of about 90% (see FIG. **1***b*), and the separators of the comparative examples 2 and 3 show thermal shrinkage of about 60% (see FIGS. **1***c* and **1***d*), which is better than that of the comparative example 1 but still significantly high. In addition, the separator of the comparative example 4 shows a peeling resistance improved rather than that of the comparative examples 2 and 3 but shows a deteriorated thermal shrinkage restraining effect (see FIG. **1***e*), and its reason is guessed as the content of inorganic particles is relatively seriously lowered rather than the content of binder polymer.

Meanwhile, in order to evaluate a peeling resistance of the porous active layer with which the organic/inorganic composite separators according to the examples and the comparative examples were coated, the following test was conducted. The term 'a peeling force of a porous active layer' used herein means a peeling force measured according to the following test.

The organic/inorganic composite separators of the embodiments 1 to 3 and the comparative examples 2 to 4 were respectively firmly attached to a glass plate using a transparent double-sided tape (3M). At this time, the test piece had a width of 1.5 cm and a length of 6 to 8 cm. Subsequently, a force required for separating the porous active layer from a base film was measured using a tensile force measuring device (UTM, LLOYD LF PLUS) as shown in FIG. **2** to evaluate a peeling force of the porous active layer. Thermal shrinkages of the separator of the examples and comparative examples and peeling forces of the porous active layers, measured as mentioned above, are listed in the following table 1.

TABLE 1

	Thermal shrinkage [%] (after 150° C./1 hour preservation)	Peeling force [gf/cm]
Example 1	~20	28
Example 2	~20	31
Example 3	~20	25
Comparative example 1	~90	—
Comparative example 2	~60	2
Comparative example 3	~60	3
Comparative example 4	~70	22

INDUSTRIAL APPLICABILITY

As described above, the organic/inorganic composite separator of the present invention prevents the problem that inorganic particles in a porous active layer are extracted during an assembling process of an electrochemical device, though the content of inorganic particles contained in the porous coating layer is sufficient over a certain level. In addition, since an adhesive force between the porous active layer and the polyolefin porous substrate is strong, thermal shrinkage of the electrochemical device is restrained though the electrochemical device is overheated, thereby preventing an electric short circuit between cathode and anode. According, the stability of the electrochemical device is greatly improved.

In particular, if the porous active layer is formed using two kinds of binder polymers having predetermined contact angles to a water drop according to the preferred embodiment of the present invention, it is possible to realize a synergistic effect in improving thermal stability of the organic/inorganic composite polymer.

The invention claimed is:

1. An organic/inorganic composite separator, comprising:

(a) a polyolefin porous substrate having pores; and

(b) a porous active layer containing a mixture of inorganic particles and a binder polymer, with which at least one surface of the polyolefin porous substrate is coated,

wherein the porous active layer has a peeling force of 5 gf/cm or above, and a thermal shrinkage of the separator after being left alone at 150° C. for 1 hour is 50% or below in a machine direction (MD) or in a transverse direction (TD),

wherein the inorganic particles and the binder polymer are mixed in a weight ratio of 50:50 to 99:1.

2. The organic/inorganic composite separator according to claim **1**, wherein the porous active layer has a peeling force of 10 gf/cm or above, and a thermal shrinkage of the separator after being left alone at 150° C. for 1 hour is 30% or below in a machine direction (MD) or in a transverse direction (TD).

3. The organic/inorganic composite separator according to claim **1**, wherein the binder polymer is a mixture of a first binder polymer having a contact angle to a water drop of 70° to 140° and a second binder polymer having a contact angle to a water drop of 1° to 69°.

4. The organic/inorganic composite separator according to claim **3**, wherein the first binder polymer has a contact angle to a water drop of 90° to 110° and the second binder polymer has a contact angle to a water drop of 20° to 40°.

5. The organic/inorganic composite separator according to claim **3**, wherein the first binder polymer and the second binder polymer are mixed in a weight ratio of 95:5 to 5:95.

6. The organic/inorganic composite separator according to claim **3**, wherein the first binder polymer is any one polymer or a mixture of at least two polymers selected from the group consisting of polyvinylidene fluoride, polyvinylidene fluoride-co-hexafluoropropylene, polyvinylidene fluoride-co-trichloroethylene, polymethylmethacrylate, polyacrylonitrile, polyvinylacetate, polyethylene-co-vinyl acetate, polyimide and polyethylene oxide.

7. The organic/inorganic composite separator according to claim **3**, wherein the second binder polymer has at least one polar group selected from the group consisting of hydroxyl group (—OH), carboxyl group (—COOH), maleic anhydride group (—COOOC—), sulphonate group (—SO_3H) and pyrrolidone group (—NCO—).

8. The organic/inorganic composite separator according to claim **7**, wherein the second hinder polymer is any one polymer or a mixture of at least two polymers selected from the group consisting of cyanoethylpullulan, cyanoethylpolyvinylalcohol, cyanoethylcellulose, cyanoethylsucrose, carboxyl methyl cellulose, polyvinylalcohol, polyacrylic acid, polymaleic anhydride and polyvinylpyrrolidone.

9. The organic/inorganic composite separator according to claim **1**, wherein the number of inorganic particles per a unit area of the porous active layer is 1×10^{15} to $1\times10^{30}/m^2$.

10. The organic/inorganic composite separator according to claim **1**, wherein a weight of the inorganic particles per a unit area of the porous active layer is 5 to 100 g/m^2.

11. The organic/inorganic composite separator according to claim **1**, wherein a size of the inorganic particles is 0.001 to 10 μm.

12. The organic/inorganic composite separator according to claim **1**, wherein the inorganic particles are selected from the group consisting of inorganic particles having a dielectric constant of 5 or above, inorganic particles having lithium-ion conductivity, or their mixtures.

13. The organic/inorganic composite separator according to claim **12**, wherein the inorganic particle having a dielectric constant of 5 or above is any one inorganic particle or a mixture of at least two inorganic particles selected from the group consisting of $BaTiO_3$, $Pb(Zr,Ti)O_3$ (PZT), $Pb_{1-x}La_xZr_{1-y}Ti_yO_3$ (PLZT), $PB(Mg_3Nb_{2/3})O_3$—$PbTiO_3$ (PMN-PT), hafnia (HfO_2), $SrTiO_3$, SnO_2, CeO_2, MgO, NiO, CaO, ZnO, ZrO_2, SiO_2, Y_2O_3, Al_2O_3, SiC and TiO_2.

14. The organic/inorganic composite separator according to claim **13**, wherein the inorganic particle having a dielectric constant of 5 or above is any one piezoelectric inorganic particle or a mixture of at least two piezoelectric inorganic particles selected from the group consisting of $BaTiO_3$, $Pb(Zr,Ti)O_3$ (PZT), $Pb_{1-x}La_xZr_{1-y}Ti_yO_3$ (PLZT), $PB(Mg_3Nb_{2/3})O_3$—$PbTiO_3$ (PMN-PT) and hafnia (HfO_2).

15. The organic/inorganic composite separator according to claim **12**, wherein the inorganic particles having lithium-ion conductivity is any one inorganic particle or a mixture of at least two inorganic particles selected from the group consisting of lithium phosphate (Li_3PO_4), lithium titanium phosphate ($Li_xTi_y(PO_4)_3$, $0<x<2$, $0<y<3$), lithium aluminum titanium phosphate ($Li_xAl_yTi_z(PO_4)_3$, $0<x<2$, $0<y<1$, $0<z<3$),

$(LiAlTiP)_xO_y$ type glass ($0<x<4$, $0<y<13$), lithium lanthanum titanate ($Li_xLa_yTiO_3$, $0<x<2$, $0<y<3$), lithium germanium thiophosphate ($Li_xGe_yP_zS_w$, $0<x<4$, $0<y<1$, $0<z<1$, $0<w<5$), lithium nitrides (Li_xN_y, $0<x<4$, $0<y<2$), SiS_2($Li_xSi_yS_z$, $0<x<3$, $0<y<2$, $0<z<4$) type glass, and P_2S_5 ($Li_xP_yS_z$, $0<x<3$, $0<y<3$, $0<z<7$) type glass.

16. The organic/inorganic composite separator according to claim **1**, wherein the porous active layer has a thickness of 0.01 to 20 μm, a pore size of 0.001 to 10 μm and a porosity of 10 to 90%.

17. The organic/inorganic composite separator according to claim **1**, wherein the polyolefin porous substrate has a thickness of 1 to 100 μm, a pore size of 0.01 to 50 μm and a porosity of 10 to 95%.

18. The organic/inorganic composite separator according to claim **1**, wherein the polyolefin porous substrate is formed using any one polymer or a mixture of at least two polymers selected from the group consisting of polyethylene, polypropylene, polybutylene and polypentene.

19. An electrochemical device including a cathode, an anode, a separator and an electrolyte,

wherein the separator is the organic/inorganic composite separator defined in claim **1**.

20. The electrochemical device according to claim **19**, wherein the electrochemical device is a lithium secondary battery.

* * * * *

Appendix M

US007695870B2

(12) **United States Patent**
Park et al.

(10) **Patent No.: US 7,695,870 B2**
(45) **Date of Patent: *Apr. 13, 2010**

(54) **ORGANIC/INORGANIC COMPOSITE SEPARATOR AND ELECTROCHEMICAL DEVICE CONTAINING THE SAME**

(75) Inventors: **Jong-Hyeok Park**, Daejeon (KR); **Sang-Young Lee**, Daejeon (KR); **Jang-Hyuk Hong**, Daejeon (KR); **Moon-Ja Nam**, Daejeon (KR); **Jung-A Yoo**, Daejeon (KR); **Sang-Seop Kim**, Seoul (KR); **Chang-Hun Han**, Daejeon (KR)

(73) Assignee: **LG Chem, Ltd.**, Seoul (KR)

(*) Notice: Subject to any disclaimer, the term of this patent is extended or adjusted under 35 U.S.C. 154(b) by 0 days.

This patent is subject to a terminal disclaimer.

(21) Appl. No.: **12/158,936**

(22) PCT Filed: **Mar. 6, 2008**

(86) PCT No.: **PCT/KR2008/001263**

§ 371 (c)(1),
(2), (4) Date: **Mar. 23, 2009**

(87) PCT Pub. No.: **WO2008/108583**

PCT Pub. Date: **Sep. 12, 2008**

(65) **Prior Publication Data**

US 2009/0246613 A1 Oct. 1, 2009

(30) **Foreign Application Priority Data**

Mar. 7, 2007 (KR) 10-2007-0022320

(51) **Int. Cl.**

H01M 2/16	(2006.01)
H01M 2/18	(2006.01)
H01M 10/04	(2006.01)
H01M 4/48	(2006.01)
B05D 5/12	(2006.01)
B05C 5/00	(2006.01)

(52) **U.S. Cl.** **429/251**; 429/252; 429/30; 429/44; 429/137; 429/231.1; 429/134; 427/115; 502/101; 252/511

(58) **Field of Classification Search** 429/30, 429/44, 137, 231.1, 34, 249, 251, 252; 427/115; 502/101; 252/511; *H01M 2/16, 2/18, 10/04, H01M 4/48*

See application file for complete search history.

(56) **References Cited**

U.S. PATENT DOCUMENTS

5,256,503 A * 10/1993 Cook et al. 429/249

(Continued)

FOREIGN PATENT DOCUMENTS

CN 1569318 * 1/2005

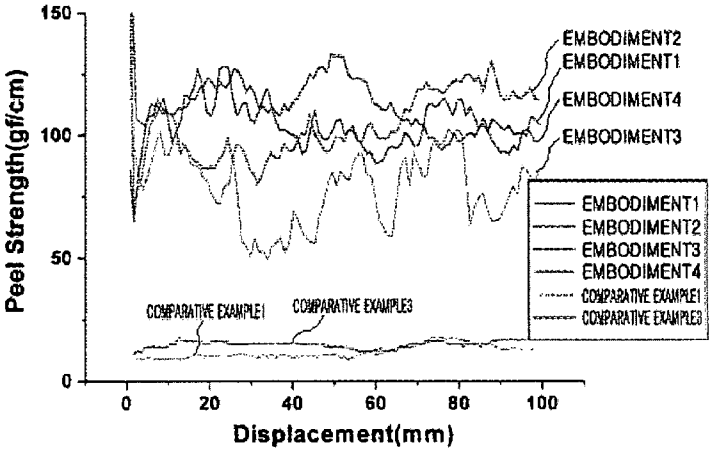
(Continued)

Primary Examiner—Melvin C Mayes
Assistant Examiner—Jun Li
(74) *Attorney, Agent, or Firm*—Birch, Stewart, Kolasch & Birch, LLP

(57) **ABSTRACT**

An organic/inorganic composite separator includes a porous substrate having a plurality of pores; and a porous coating layer formed on at least one surface of the porous substrate with a plurality of inorganic particles and a binder polymer. The binder polymer is a copolymer including: (a) a first monomer unit having a contact angle to a water drop in the range from 0° to 49°; and (b) a second monomer unit having a contact angle to a water drop in the range from 50° to 130°. This organic/inorganic composite separator has excellent thermal stability, so it may restrain an electric short circuit between a cathode and an anode. In addition, the separator may prevent inorganic particles in the porous coating layer from being extracted during an assembling process of an electrochemical device, thereby improving stability of an electrochemical device.

19 Claims, 3 Drawing Sheets



U.S. PATENT DOCUMENTS

6,048,641	A *	4/2000	Ohmory et al.	429/142
2002/0029465	A1	3/2002	Shida et al.	
2004/0115499	A1	6/2004	Tani et al.	
2005/0048367	A1	3/2005	Igaki et al.	
2006/0121329	A1	6/2006	Shishitani et al.	

FOREIGN PATENT DOCUMENTS

KR	10-2001-0082058	A	8/2001
KR	10-2001-0082059	A	8/2001
KR	10-2006-0072065	A	6/2006
KR	10-2007-0000231	A	1/2007
WO	WO 2006068428	A1 *	6/2006

* cited by examiner

Fig. 1

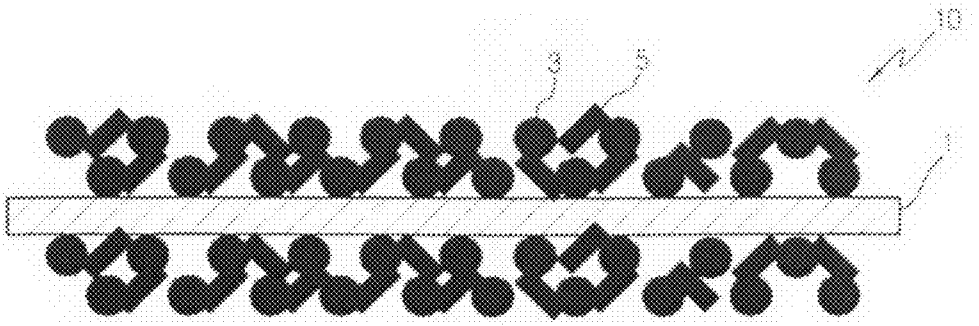
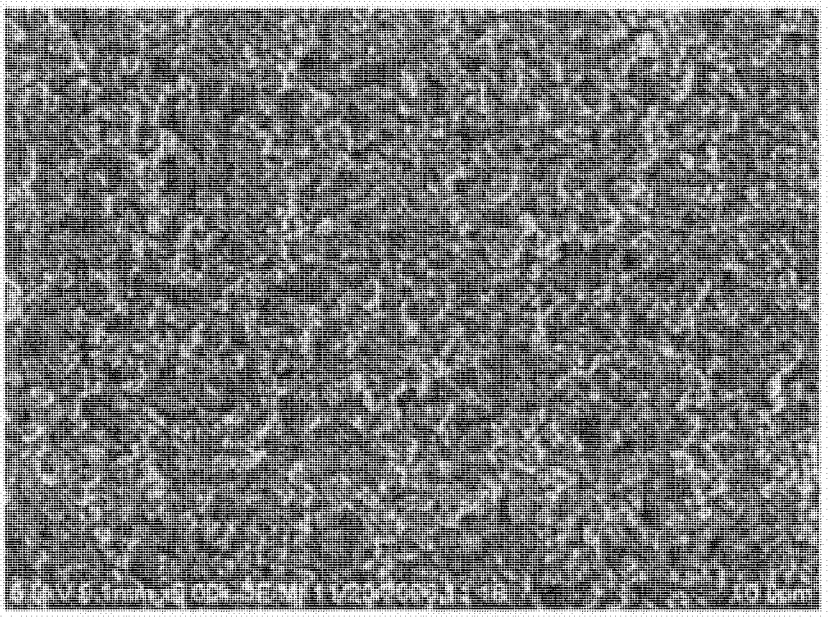


Fig. 2



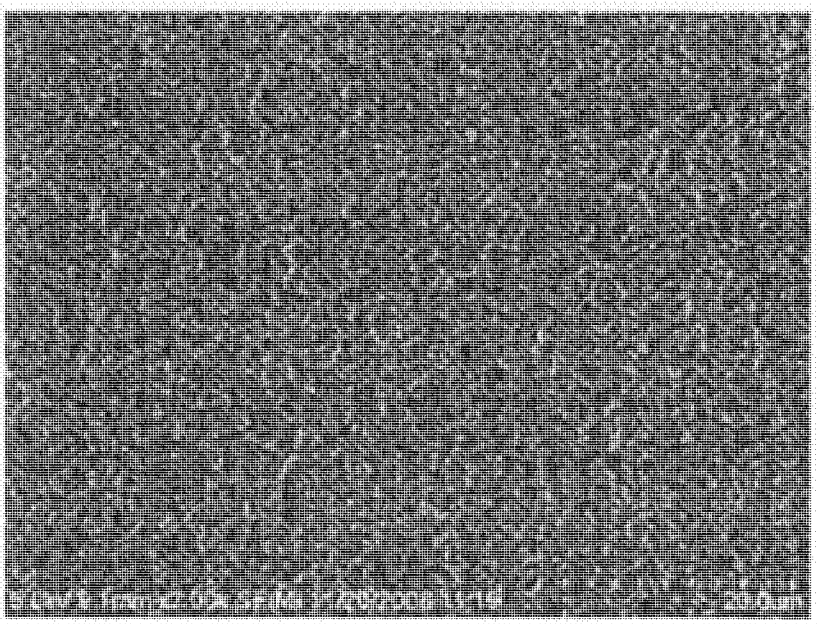


Fig. 3

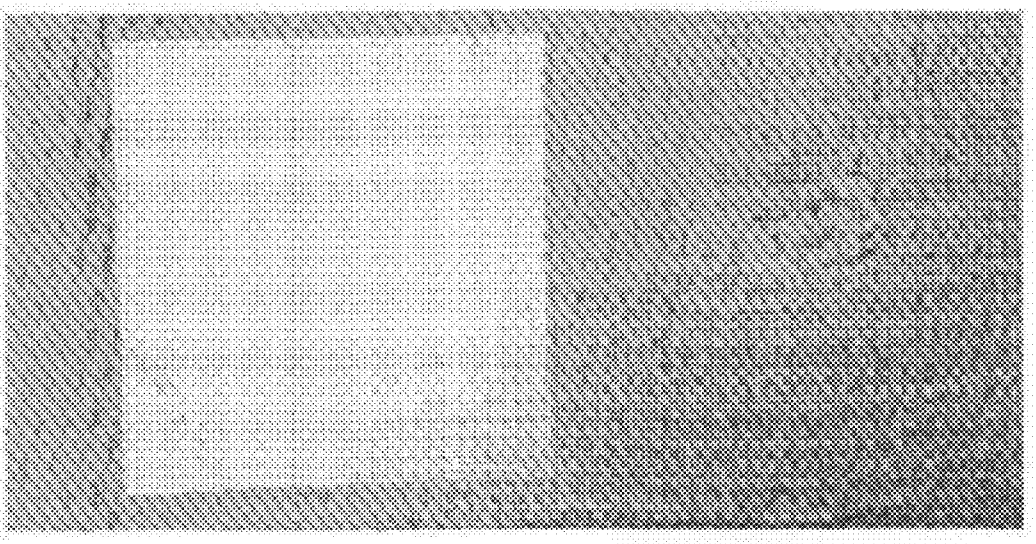


Fig. 4

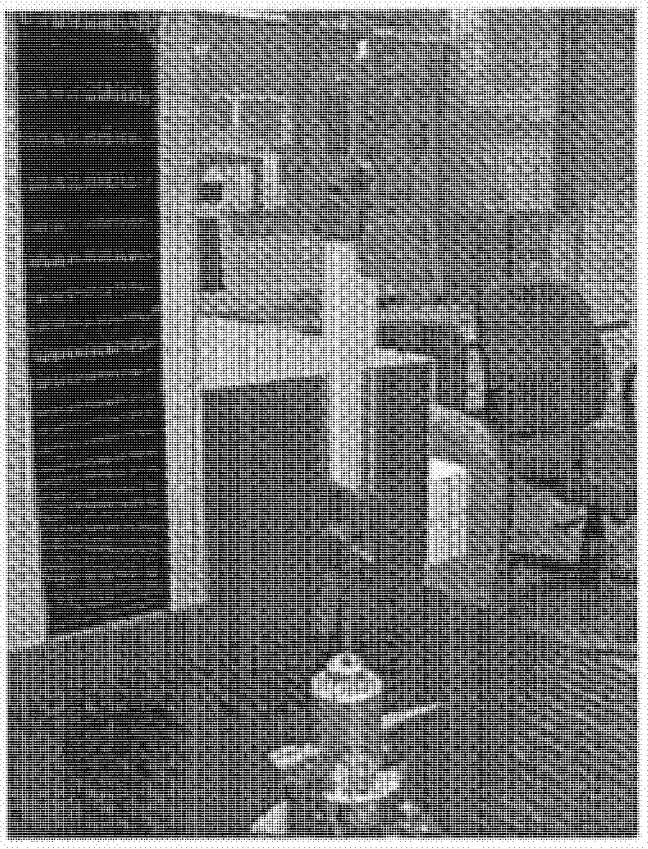
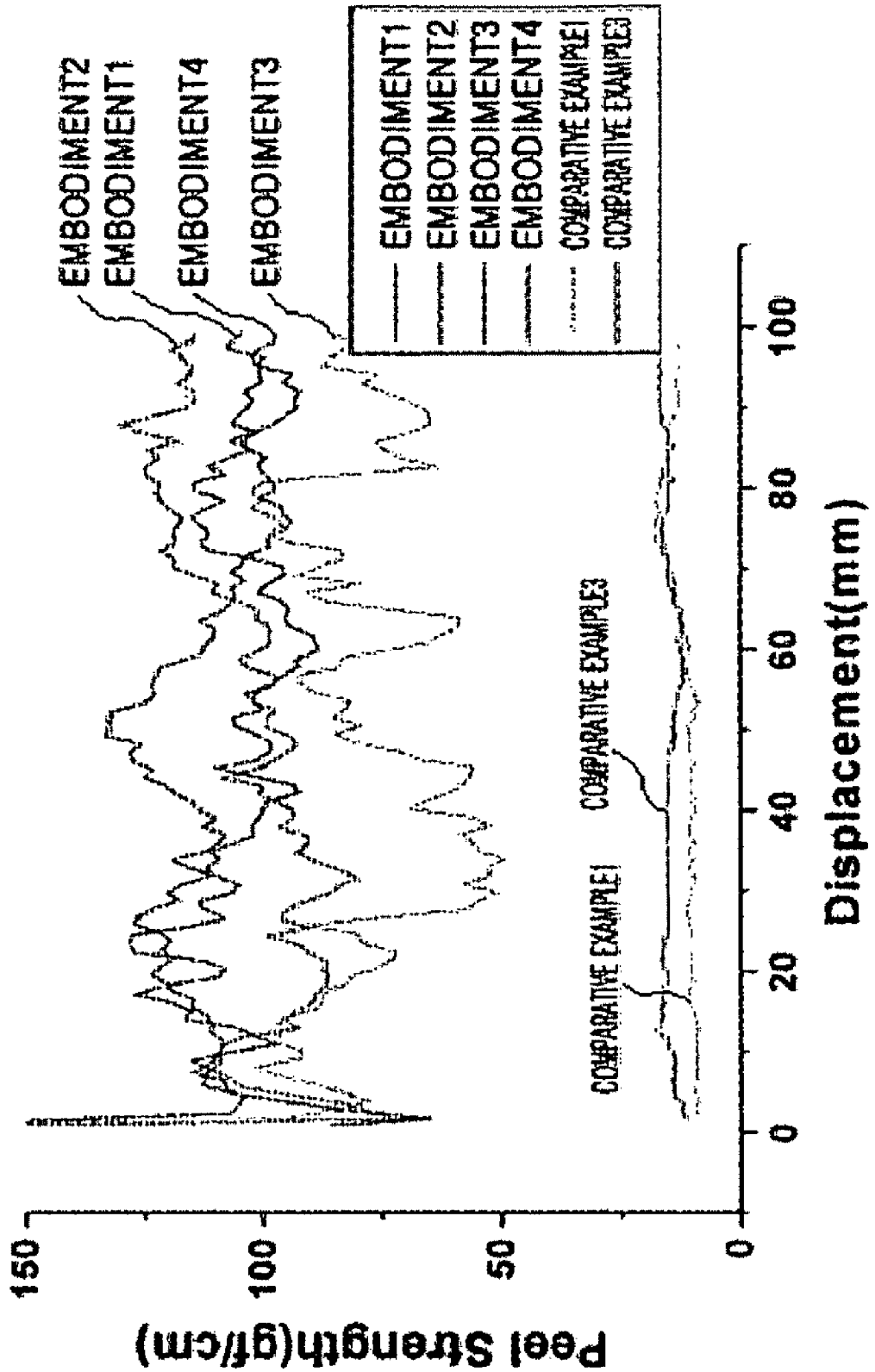


Fig. 5


EMBODIMENT1
EMBODIMENT2
EMBODIMENT3
EMBODIMENT4
COMPARATIVE EXAMPLE1
COMPARATIVE EXAMPLE3
EMBODIMENT2
EMBODIMENT1
EMBODIMENT4
EMBODIMENT3
COMPARATIVE EXAMPLE1
COMPARATIVE EXAMPLE3
Peel Strength(gf/cm)
150
100
50
0
Displacement(mm)
0
20
40
60
80
100

ORGANIC/INORGANIC COMPOSITE SEPARATOR AND ELECTROCHEMICAL DEVICE CONTAINING THE SAME

TECHNICAL FIELD

The present invention relates to a separator of an electrochemical device such as a lithium secondary battery and an electrochemical device containing the same. More particularly, the present invention relates to an organic/inorganic composite separator having a porous coating layer formed with a mixture of inorganic particles and polymer on a surface of a porous substrate, and an electrochemical device containing the same.

BACKGROUND ART

Recently, there has been an increasing interest in energy storage technology. Batteries have been widely used as energy sources in the fields of cellular phones, camcorders, notebook computers, PCs and electric cars, resulting in intensive research and development into them. In this regard, electrochemical devices are one of the subjects of great interest. Particularly, development of rechargeable secondary batteries has been the focus of attention. Recently, the research and development into a novel electrode and a novel battery that can improve capacity density and specific energy have been made intensively in the field of the secondary batteries.

Among currently used secondary batteries, lithium secondary batteries developed in early 1990's have a higher drive voltage and a much higher energy density than those of conventional batteries using a liquid electrolyte solution such as Ni-MH batteries, Ni—Cd batteries, and H_2SO_4—Pb batteries. For these reasons, the lithium secondary batteries have been advantageously used. However, such a lithium secondary battery has disadvantages in that organic electrolytes used therein may cause safety-related problems such as ignition and explosion of the batteries and that processes for manufacturing such a battery are complicated. Recently, lithium-ion polymer batteries have been considered as one of the next-generation batteries since the above disadvantages of the lithium ion batteries are solved. However, the lithium-ion polymer batteries have a relatively lower battery capacity than those of the lithium ion batteries and an insufficient discharging capacity in low temperature, and therefore these disadvantages of the lithium-ion polymer batteries remain to be urgently solved.

Such electrochemical devices have been produced from many companies, and the battery stability has different phases in the electrochemical devices. Accordingly, it is important to evaluate and ensure the stability of the electrochemical batteries. First of all, it should be considered that errors in operation of the electrochemical device should not cause damage to users. For this purpose, the Safety Regulation strictly regulates ignition and explosion in the electrochemical devices. In the stability characteristics of the electrochemical device, overheating of the electrochemical device may cause thermal runaway, and explosion may occur when a separator is pierced. In particular, a polyolefin porous substrate commonly used as a separator of an electrochemical device shows extreme thermal shrinking behavior at a temperature of 100° C. or above due to the features of its material and its manufacturing process such as elongation, so there may occur an electric short circuit between cathode and anode.

In order to solve the above safety-related problems of the electrochemical device, Korean Laid-open Patent Publication No. 10-2006-72065 and No. 10-2007-231 disclose an organic/inorganic composite separator **10** having a porous coating layer formed by coating at least one surface of a porous substrate **1** having many pores with a mixture of inorganic particles **3** and a binder polymer **5** (see FIG. **1**). In the organic/inorganic composite separator, the inorganic particles **3** in the porous coating layer formed on the porous substrate **1** act as a kind of spacer that keeps a physical shape of the porous coating layer, so the inorganic particles restrain thermal shrinkage of the porous substrate when the electrochemical device is overheated. In addition, interstitial volumes exist among the inorganic particles, thereby forming fine pores.

As mentioned above, at least a certain amount of inorganic particles should be contained such that the porous coating layer formed on the organic/inorganic composite separator may restrain thermal shrinkage of the porous substrate. However, as the content of inorganic particles is increased, a content of binder polymer is relatively decreased, which may cause inorganic particles to be extracted from the porous coating layer due to the stress generated in an assembly process of an electrochemical device such as winding. The extracted inorganic particles act as a local defect of the electrochemical device, thereby giving a bad influence on the stability of the electrochemical device.

DISCLOSURE OF INVENTION

Technical Problem

The present invention is designed to solve the problems of the prior art, and therefore an object of the invention is to provide an organic/inorganic composite separator, which has good thermal stability so as to restrain an electric short circuit between cathode and anode even when an electrochemical device is overheated, and also which may improve stability of the electrochemical device by preventing extraction of inorganic particles in a porous coating layer formed on a porous substrate during an assembly process of the electrochemical device.

Technical Solution

In order to accomplish the first object, the present invention provides an organic/inorganic composite separator, which includes a porous substrate having a plurality of pores; and a porous coating layer formed on at least one surface of the porous substrate with a plurality of inorganic particles and a binder polymer, wherein the binder polymer is a copolymer including: (a) a first monomer unit having a contact angle to a water drop in the range from 0° to 49°; and (b) a second monomer unit having a contact angle to a water drop in the range from 50° to 130°.

The organic/inorganic composite separator according to the present invention has an excellent peeling resistance, so it may prevent inorganic particles in the porous coating layer from being extracted during an assembling process of an electrochemical device. Also, though an electrochemical device is overheated, thermal shrinkage is restrained, which allows to prevent any electric short circuit between cathode and anode. Accordingly, the safety of the electrochemical device is greatly improved.

In the organic/inorganic composite separator according to the present invention, the first monomer unit is preferably a monomer unit having at least one functional group selected from the group consisting of OH, COOH, MAH (maleic anhydride) and SO_3H, and the second monomer unit is preferably a monomer unit having at least one functional group selected from the group consisting of F, Cl, CN, acrylate, acetate and ester.

The copolymer may be a copolymer selected from the group consisting of acrylonitrile-maleic anhydride copolymer, acrylonitrile-vinylalcohol copolymer, cyanoethylene-vinylalcohol copolymer, cyanoethylene-cellulose copolymer, cyanoethylene-sucrose copolymer, acrylonitrile-acrylic acid copolymer, acrylonitrile-anhydrous maleic acid copolymer, acrylate-acrylic acid copolymer and acrylate-anhydrous maleic acid copolymer, or their mixtures.

The organic/inorganic composite separator according to the present invention may be used for an electrochemical device such as a lithium secondary battery or a super capacity device as being interposed between a cathode and an anode.

BRIEF DESCRIPTION OF THE DRAWINGS

These and other features, aspects, and advantages of preferred embodiments of the present invention will be more fully described in the following detailed description, taken accompanying drawings. In the drawings:

FIG. **1** is a sectional view schematically showing an organic/inorganic composite separator;

FIG. **2** a photograph showing a surface of a porous coating layer and a surface of a polyethylene porous film of an organic/inorganic composite separator according to one embodiment of the present invention, taken by a SEM (Scanning Electron Microscope);

FIG. **3** is a photograph showing an organic/inorganic composite separator according to one embodiment of the present invention, taken after the separator is left alone in an oven at 150° C. for 1 hour;

FIG. **4** is a photograph showing a test device used for measuring a peeling force of a porous coating layer of the organic/inorganic composite separator; and

FIG. **5** is a graph showing measurement results of peeling forces of porous coating layers according to embodiments of the present invention and comparative examples.

BEST MODE

Hereinafter, preferred embodiments of the present invention will be described in detail referring to the accompanying drawings. Prior to the description, it should be understood that the terms used in the specification and appended claims should not be construed as limited to general and dictionary meanings, but interpreted based on the meanings and concepts corresponding to technical aspects of the present invention on the basis of the principle that the inventor is allowed to define terms appropriately for the best explanation. Therefore, the description proposed herein is just a preferable example for the purpose of illustrations only, not intended to limit the scope of the invention, so it should be understood that other equivalents and modifications could be made thereto without departing from the spirit and scope of the invention.

An organic/inorganic composite separator of the present invention includes a porous substrate having a plurality of pores; and a porous coating layer formed with a plurality of inorganic particles and a binder polymer. Here, the binder polymer is a copolymer including (a) a first monomer unit having a contact angle to a water drop in the range from 0° to 49°; and (b) a second monomer unit having a contact angle to a water drop in the range from 50° to 130°. This copolymer may be expressed as follows: $(\text{first monomer unit})_m$-$(\text{second monomer unit})_n$ ($0<m<1$, $0<n<1$). At this time, the copolymer including the first monomer unit and the second monomer unit may be any kind of copolymer such as random copolymer and block copolymer. The first monomer unit preferably has a molar ratio in the range from 1 to 20 mol % based on the entire copolymer, and the entire copolymer preferably has a contact angle to a water drop in the range from 30° to 80°. It would be apparent to those having ordinary skill in the art that the above copolymer may further include another monomer unit without obstructing the object of the present invention, and another binder polymer may be mixed thereto in addition to the above copolymer without obstructing the object of the present invention.

In the present invention, after a sample film was made using a single monomer of a corresponding binder polymer, a distilled water drop was fallen thereon, and then a contact angle formed on the water drop was set as 23 degrees. Also, the contact angle to a water drop was measured using a contact angle measurer model CA-DT-A (mfd. produced by Kyowa Kaimen Kagaku KK) under the condition of 50% RH. Contact angles were measured at two points (namely, left and right points) of each of three sample films, and six measured values were averaged and set as a contact angle. The distilled water drop has a diameter of 2 mm, and the contact angle value displayed on the measurer shows a contact angle measured 1 minute after the distilled water drop was fallen.

Among the monomer units that constitute the copolymer, the first monomer unit having a contact angle to a water drop in the range from 0° to 49°, preferably from 5° to 30°, shows a relatively greater hydrophile property than the second monomer unit, so the first monomer unit attributes to improving an adhering characteristic among inorganic particles. Also, the second monomer unit having a contact angle to a water drop in the range from 50° to 130°, preferably from 70° to 120°, shows a relatively greater hydrophobic property than the first monomer unit, so the second monomer unit attributes to improving an adhering characteristic between inorganic properties and the porous substrate. Thus, when the above copolymer is used as a binder polymer for the porous coating layer, it is possible to increase a peeling resistance of the porous coating layer rather than the case using a conventional polymer binder. Accordingly, it is possible to lower a content ratio of the binder polymer of the porous coating layer and increase a content ratio of inorganic particles, which allows to further restrain thermal shrinkage of the organic/inorganic composite separator. In addition, a porosity of the porous coating layer is increased, which attributes to improving the performance of an electrochemical device. Also, since an adhesive force between the porous coating layer and the porous substrate is strong, the porous coating layer may sufficiently exhibit its function to restrain thermal shrinkage of the porous substrate even though the electrochemical device is overheated. Accordingly, the stability of the electrochemical device is greatly improved.

In the organic/inorganic composite separator according to the present invention, the porous coating layer preferably has a peeling force of 5 gf/cm or above in view of preventing extraction of inorganic particles in the porous coating layer during the assembling process of the electrochemical device.

In the organic/inorganic composite separator according to the present invention, the first monomer unit is preferably a monomer unit having at least one functional group selected from the group consisting of OH, COOH, MAH (maleic anhydride) and SO_3H, and the second monomer unit is preferably a monomer unit having at least one functional group selected from the group consisting of F, Cl, CN, acrylate, acetate and ester.

The copolymer including the first monomer unit and the second monomer unit may employ acrylonitrile-maleic anhydride copolymer, acrylonitrile-vinylalcohol copolymer, cyanoethylene-vinylalcohol copolymer, cyanoethylene-cellu-

lose copolymer, cyanoethylene-sucrose copolymer, acrylonitrile-acrylic acid copolymer, acrylonitrile-anhydrous maleic acid copolymer, acrylate-acrylic acid copolymer or acrylate-anhydrous maleic acid copolymer, in single or in combination.

In the organic/inorganic composite separator according to the present invention, the inorganic particle used for forming the porous coating layer is not specially limited if it is electrically and chemically stable. That is to say, an inorganic particle usable in the present invention is not specially limited if oxidation or reduction reaction does not occur in an operating voltage range (for example, 0 to 5V based on Li/Li^+) of an applied electrochemical device. In particular, in case an inorganic particle with ion transferring capability is used, it is possible to enhance the performance by increasing ion conductivity in the electrochemical device.

In addition, in case an inorganic particle with a high dielectric constant is used, it contributes to the increase of dissociation of electrolyte salt, for example lithium salt, in the liquid electrolyte, thereby improving ion conductivity of the electrolyte.

Due to the above reasons, it is preferred that the inorganic particles include inorganic particles having a dielectric constant of 5 or above, preferably 10 or above, inorganic particles having lithium-ion transferring capability, or their mixtures. The inorganic particle having a dielectric constant of 5 or above is for example $BaTiO_3$, $Pb(Zr,Ti)O_3$ (PZT), $Pb_{1-x}La_xZr_{1-y}Ti_yO_3$ (PLZT), $PB(Mg_3Nb_{2/3})O_3$-$PbTiO_3$ (PMN-PT), hafnia (HfO_2), $SrTiO_3$, SnO_2, CeO_2, MgO, NiO, CaO, ZnO, ZrO_2, SiO_2, Y_2O_3, Al_2O_3, SiC and TiO_2, but not limitedly.

In particular, the inorganic particles such as of $BaTiO_3$, $Pb(Zr,Ti)O_3$ (PZT), $Pb_{1-x}La_xZr_{1-y}Ti_yO_3$ (PLZT), $PB(Mg_3Nb_{2/3})O_3$-$PbTiO_3$ (PMN-PT) and hafnia (HfO_2) show a high dielectric constant of 100 or above and have piezoelectricity since charges are generated to make a potential difference between both surfaces when a certain pressure is applied to extend or shrink them by applying a certain pressure thereto, so the above inorganic particles may prevent generation of an internal short circuit of both electrodes caused by an external impact and thus further improve the stability of the electrochemical device. In addition, in case the inorganic particles having a high dielectric constant are mixed with the inorganic particles having lithium ion transferring capability, their synergistic effect may be doubled.

In the present invention, the inorganic particle having lithium ion transferring capability means an inorganic particle containing lithium atom and having a function of moving a lithium ion without storing the lithium. The inorganic particle having lithium ion transferring capability may transfer and move lithium ions due to a kind of defect existing in the particle structure, so it is possible to improve lithium ion conductivity in the battery and also improve the performance of the battery. The inorganic particle having lithium ion transferring capability is any one inorganic particle or a mixture of at least two inorganic particles selected from the group consisting of lithium phosphate (Li_3PO_4), lithium titanium phosphate ($Li_xTi_y(PO_4)_3$, $0<x<2$, $0<y<3$), lithium aluminum titanium phosphate ($Li_xAl_yTi_z(PO_4)_3$, $0<x<2$, $0<y<1$, $0<z<3$), $(LiAlTiP)_xO_y$ type glass ($0<x<4$, $0<y<13$), lithium lanthanum titanate ($Li_xLa_yTiO_3$, $0<x<2$, $0<y<3$), lithium germanium thiophosphate ($Li_xGe_yP_zS_w$, $0<x<4$, $0<y<1$, $0<z<1$, $0<w<5$), lithium nitrides (Li_xN_y, $0<x<4$, $0<y<2$), SiS_2 ($Li_xSi_yS_z$, $0<x<3$, $0<y<2$, $0<z<4$) type glass, and P_2S_5 ($Li_xP_yS_z$, $0<x<3$, $0<y<3$, $0<z<7$) type glass, but not limitedly.

In the organic/inorganic composite separator according to the present invention, the size of inorganic particles in the porous coating layer is not specially limited, but it is preferably in the range from 0.001 to 10 μm, if possible, in order to form a coating layer in a uniform thickness and ensure suitable porosity. If the particle size is less than 0.001 μm, a dispersing property is deteriorated, so it is not easy to control properties of the organic/inorganic composite separator. If the particle size exceeds 10 μm, the thickness of the porous coating layer is increased, which may deteriorate mechanical properties. In addition, due to excessively great pore size, the possibility of internal short circuit is increased while charging or discharging a battery.

In the organic/inorganic composite separator coated with the porous coating layer according to the present invention, a weight ratio of the inorganic particles and the hinder polymer is in the range from 50:50 to 99:1, more preferably from 70:30 to 95:5. If the weight ratio of the organic particles to the binder polymer is less than 50:50, the content of polymer is so great that the thermal stability of the organic/inorganic composite separator may not be much improved. In addition, pore size and porosity may be decreased due to the decrease of interstitial volume formed among the inorganic particles, thereby causing deterioration of the performance of a battery. If the weight ratio exceeds 99:1, the peeling resistance of the porous coating layer may be weakened since the content of binder polymer is so small. The thickness of the porous coating layer composed of the inorganic particles and the binder polymer is not specially limited but preferably in the range from 0.01 to 20 μm. Also, pore size and porosity are not specially limited, but the pore size is preferably ranged from 0.001 to 10 μm and a porosity is preferably ranged from 10 to 90%. The pore size and porosity are mainly dependent on the size of inorganic particles. For example, in case inorganic particles have a diameter of 1 μm or less, the formed pore is also approximately 1 μm or less. The pores as mentioned above are filled with electrolyte later, and the filled electrolyte plays a role of transferring ions. In case the pore size and porosity are respectively less than 0.001 μm and 10%, the porous coating layer may act as a resistance layer. In case the pore size and porosity are respectively greater than 10 μm and 90%, mechanical properties may be deteriorated.

The organic/inorganic composite separator according to the present invention may further include other additives as components of the porous coating layer, in addition to the inorganic particles and the polymer.

In addition, in the organic/inorganic composite separator according to the present invention, the porous substrate having a plurality of pores may adopt any kind of porous substrate if it is commonly used as a separator of an electrochemical device like a polyolefin porous substrate. For example, the porous substrate may be a non-woven fabric or a membrane formed using a polyolefin polymer containing polyethylene such as HDPE (high density polyethylene), LLDPE (linear low density polyethylene, LDPE (low density polyethylene) and UHMWPE (ultra high molecular weight polyethylene), polypropylene, polybutylene or polypentene, in single or in combination. The porous substrate preferably has a thickness of 5 to 50 μm, though not limited thereto, and also the pore size and porosity of the porous substrate are preferably 0.01 to 50 μm and 10 to 95%, respectively, though not limited thereto.

Hereinafter, a method for manufacturing an organic/inorganic composite separator having a porous coating layer according to the present invention is explained as an example, but the present invention is not limited thereto.

First, a copolymer including the first and second monomer units with the aforementioned contact angles to a water drop is dissolved in a solvent to make a binder polymer solution.

Subsequently, inorganic particles are added to the binder polymer solution and then dispersed therein. The solvent preferably has a solubility parameter similar to that of the used binder polymer and a low boiling point. It will help uniform mixture and easy removal of the solvent afterward. A non-limiting example of usable solvent includes acetone, tetrahydrofuran, methylene chloride, chloroform, dimethylformamide, N-methyl-2-pyrrolidone (NMP), cyclohexane, water and mixtures thereof. It is preferred that the inorganic particles are pulverized after being added to the binder polymer solution. At this time, the time required for pulverization is suitably 1 to 20 hours, and the particle size of the pulverized particles ranges preferably from 0.001 and 10 μm, as mentioned above. Conventional pulverization methods may be used, and a method using a ball mill is particularly preferred.

After that, the polyolefin porous substrate is coated with the binder polymer solution in which the inorganic particles are dispersed, under the humidity condition of 10 to 80%, and then dried.

In order to coat the porous substrate with the binder polymer solution in which the inorganic particles are dispersed, a common coating method well known in the art may be used. For example, various methods such as dip coating, die coating, roll coating, comma coating or their combinations may be used. In addition, the porous coating layer may be formed selectively on both surfaces or only one surface of the porous substrate.

The organic/inorganic composite separator manufactured as mentioned above may be used as a separator of an electrochemical device. Namely, the organic/inorganic composite separator may be usefully used as a separator interposed between a cathode and an anode. At this time, in case a gellable polymer is used as a binder polymer component when a liquid electrolyte is impregnated, after a battery is assembled using the separator, the injected electrolyte and polymer may be reacted and then gelled, thereby forming a gel-type organic/inorganic composite electrolyte.

The electrochemical device may be any device in which electrochemical reactions may occur, and a specific example of the electrochemical devices includes all kinds of primary batteries, secondary batteries, fuel cells, solar cells or capacitors such as a super capacitor. In particular, among the secondary batteries, lithium secondary batteries including a lithium metal secondary battery, a lithium ion secondary battery, a lithium polymer secondary battery or a lithium ion polymer secondary battery are preferred.

The electrochemical device may be manufactured according to common methods well known to the art. As one embodiment of the method for manufacturing an electrochemical device, an electrochemical device may be manufactured by interposing the above-mentioned organic/inorganic composite separator between a cathode and an anode and injecting an electrolyte solution therein.

There is no special limitation in the electrodes that may be used together with an organic/inorganic composite separator of the present invention, and the electrodes may be manufactured by settling electrode active materials on a current collector according to one of common methods well known in the art. Among the electrode active materials, a non-limiting example of cathode active materials may include any conventional cathode active materials currently used in a cathode of a conventional electrochemical device. Particularly, lithium manganese oxides, lithium cobalt oxides, lithium nickel oxides, lithium iron oxides or lithium composite oxides thereof are preferred as the cathode active materials. Also, a non-limiting example of anode active materials may include any conventional anode active materials currently used in an anode of a conventional electrochemical device. Particularly, lithium intercalation materials such as lithium metal, lithium alloys, carbon, petroleum coke, activated carbon, graphite or other carbonaceous materials are preferred as the anode active materials. A non-limiting example of a cathode current collector includes a foil formed of aluminum, nickel or a combination thereof. A non-limiting example of an anode current collector includes a foil formed of copper, gold, nickel, copper alloys or a combination thereof.

The electrolyte solution that may be used in the present invention includes a salt represented by the formula of A^+B^-, wherein A^+ represents an alkali metal cation selected from the group consisting of Li^+, Na^+, K^+ and combinations thereof, and B^- represents an salt containing an anion selected from the group consisting of PF_6^-, BF_4^-, Cl^-, Br^-, I^-, ClO_4^-, AsF_6^-, $CH_3CO_2^-$, $CF_3SO_3^-$, $N(CF_3SO_2)_2^-$, $C(CF_2SO_2)_3^-$ and combinations thereof. The salt may be dissolved or dissociated in an organic solvent selected from the group consisting of propylene carbonate (PC), ethylene carbonate (EC), diethyl carbonate (DEC), dimethyl carbonate (DMC), dipropyl carbonate (DPC), dimethyl sulfoxide, acetonitrile, dimethoxyethane, diethoxyethane, tetrahydrofuran, N-methyl-2-pyrrolidone (NMP), ethylmethyl carbonate (EMC), gamma-butyrolactone (y-butyrolactone) and mixtures thereof. However, the electrolyte solution that may be used in the present invention is not limited to the above examples.

More particularly, the electrolyte solution may be injected in a suitable step during the manufacturing process of a battery, according to the manufacturing process and desired properties of a final product. In other words, the electrolyte solution may be injected before a battery is assembled or during a final step of the assembly process of a battery.

In order to apply the organic/inorganic composite separator according to the present invention to a battery, a stacking (or, laminating) process or a folding process may be used in addition to a winding process that is most commonly used. The organic/inorganic composite separator of the present invention has an excellent peeling resistance, so the inorganic particles are not easily extracted during the battery assembly process.

MODE FOR INVENTION

Hereinafter, various preferred examples of the present invention will be described in detail for better understandings. However, the examples of the present invention may be modified in various ways, and they should not be interpreted as limiting the scope of the invention. The examples of the present invention are just for better understandings of the invention to persons having ordinary skill in the art.

EXAMPLE 1

5 weight % of butylacrylate-acrylic acid copolymer containing 5 mol % of acrylic acid unit (a contact angle of the butylacrylate unit to a water drop was 80° and a contact angle of the acrylic acid unit to a water drop was 10°) was added to acetone and dissolved at 50° C. for about 12 hours to make a binder polymer solution. $BaTiO_3$ powder was added to the prepared binder polymer solution at a weight ratio of polymer mixture/$BaTiO_3$=10/90, and then the $BaTiO_3$ powder was pulverized and dispersed for 12 hours or more by ball milling to make a slurry. In the prepared slurry, the diameter of $BaTiO_3$ may be controlled according to a size (or, diameter) of used beads and the time for the ball milling, but in this example 1, the $BaTiO_3$ powder was pulverized into about 400 nm to make the slurry. The prepared slurry was used for

coating a polyethylene porous separator (having a porosity of 45%) with a thickness of 12 μm by means of dip coating, and a coating thickness was controlled to be about 8 μm. A pore size in the porous coating layer formed on the polyethylene porous separator was in the level of 0.4 μm, and a porosity was in the level of 57%.

EXAMPLE 2

An organic/inorganic composite separator was prepared in the same way as the example 1, except that acrylonitrile-acrylic acid copolymer containing 5 mol % of acrylic acid unit (a contact angle of the acrylonitrile unit to a water drop was 85°) was used instead of the butylacrylate-acrylic acid copolymer.

EXAMPLE 3

An organic/inorganic composite separator was prepared in the same way as the example 1, except that Al_2O_3 powder was used instead of $BaTiO_3$ powder.

EXAMPLE 4

An organic/inorganic composite separator was prepared in the same way as the example 1, except that a content ratio of binder polymer/$BaTiO_3$ was changed into 5/95.

COMPARATIVE EXAMPLE 1

An organic/inorganic composite separator was prepared in the same way as the example 1, except that butylacrylate homopolymer was used instead of the butylacrylate-acrylic acid copolymer.

COMPARATIVE EXAMPLE 2

An organic/inorganic composite separator was prepared in the same way as the example 1, except that acrylic acid homopolymer was used instead of the butylacrylate-acrylic acid copolymer. However, since the acrylic acid homopolymer was not dissolved in acetone that is a solvent, it was impossible to make a slurry for forming a porous coating layer.

COMPARATIVE EXAMPLE 3

An organic/inorganic composite separator was prepared in the same way as the example 1, except that acrylonitrile homopolymer was used instead of the butylacrylate-acrylic acid copolymer.

Preparation of Anode

96 weight % of carbon powder as an anode active material, 3 weight % of polyvinylidene fluoride (PVdF) as coupling agent and 1 weight % of carbon black as a conductive material were respectively added to N-methyl-2 pyrrolidone (NMP) as a solvent to make an anode mixture slurry. The anode mixture slurry was applied to a copper (Cu) film, which is an anode current collector with a thickness of 10 μm, and then dried to make an anode, and then roll pressing was conducted thereto.

Preparation of Cathode

92 weight % of lithium cobalt composite oxide as a cathode active material, 4 weight % of carbon black as a conductive material and 4 weight % of PVdF as a coupling agent were respectively added to N-methyl-2 pyrrolidone (NMP) as a solvent to make a cathode mixture slurry. The cathode mixture slurry was applied to an aluminum (Al) film, which is a cathode current collector with a thickness of 20 μm, and then dried to make a cathode, and then roll pressing was conducted thereto.

Manufacture of Battery

A battery was manufactured using the organic/inorganic composite separator and the electrodes prepared as above, and then its performance and safety were tested.

The battery was assembled in a way of stacking the anode, the cathode and the porous organic/inorganic composite separator, and then an electrolyte (ethylenecarbonate (EC)/ethylmethylcarbonate (EMC)=½ (a volume ratio), 1 mol of lithiumhexafluorophosphate (LiPF6).

Analysis of Surface of Organic/Inorganic Composite Separator

FIG. **2** is a photograph showing a surface of the porous coating layer and a surface of the polyethylene porous film of the organic/inorganic composite separator manufactured according to the example 1, taken using SEM (Scanning Electron Microscope). Seeing FIG. **2**, it would be found that the porous coating layer and the polyethylene porous film show a uniform pore size of about 1 μm or less.

Evaluation of Thermal Shrinkage of Organic/Inorganic Composite Separator

The organic/inorganic composite porous films coated with electrode active material, manufactured according to the examples 1 to 4 and the comparative examples 1 to 3, were stored at 150° C. for 1 hour, and then their thermal shrinkages were evaluated and then listed in the following table 1.

As a result of the experiment, the examples 1 to 4 showed a thermal shrinkage substantially less than 10%, but the comparative examples 1 to 3 showed a thermal shrinkage of 60% or above. Meanwhile, FIG. **3** is a photograph showing the organic/inorganic composite separator according to the example 1 of the present invention, taken after the separator is left alone in an oven at 150° C. for 1 hour.

TABLE 1

	Examples				Comparative Examples	
Condition	1	2	3	4	1	3
Thermal shrinkage	<10%	<10%	<10%	<5%	60%	60%

Evaluation of Peeling Resistance of Organic/Inorganic Composite Separator

The following experiment was conducted in order to evaluate peeling resistances of the porous coating layers formed in the organic/inorganic composite separators according to the examples and the comparative examples. The term 'peeling force of the porous coating layer' used herein means a peeling force measured according to the following test.

A double-sided adhesive tape was used to fix each organic/inorganic composite separator according to the examples 1 to 4 and the comparative examples 1 to 3 on a glass plate, and then a tape (a transparent tape produced by 3M) was firmly attached to the exposed porous coating layer.

Subsequently, as shown in FIG. **4**, a force required for detaching the tape was measured using a tensile force measuring device to evaluate a peeling force of the porous coating layer. FIG. **5** shows a graph obtained accordingly.

Test for Battery Performance

The batteries respectively having cathode and anode capacities of 30 mAh were charged by 0.5 C and then discharged by 1.0 C, and their discharging capacities are listed in the following table 2. It would be understood that the perfor-

mance of the cells according to the examples 1 to 4 are greatly improved in comparison to the comparative examples 1 to 3.

TABLE 2

	Examples				Comparative Examples	
Condition	1	2	3	4	1	3
Capacity	30.14	30.12	30.18	30.21	28.43	28.50

INDUSTRIAL APPLICABILITY

As described above, the organic/inorganic composite separator coated with a porous coating layer according to the present invention has excellent thermal stability, so it may restrain an electric short circuit between a cathode and an anode. In addition, the problem that inorganic particles in the porous coating layer formed on a porous substrate are extracted during an assembling process of an electrochemical device may be solved. Also, since an adhesive force between the porous coating layer and the porous substrate is strong, the porous coating layer may sufficiently exhibit its function to restrain thermal shrinkage of the porous substrate even though the electrochemical device is overheated. Accordingly, the present invention allows to greatly improve safety of the electrochemical device and attributes to improving battery performance.

What is claimed is:

1. An organic/inorganic composite separator, which includes a porous substrate having a plurality of pores, and a porous coating layer formed on at least one surface of the porous substrate with a plurality of inorganic particles and a binder polymer,

wherein the binder polymer is a copolymer including:

(a) a first monomer unit having a contact angle to a water drop in the range from 0° to 49°; and

(b) a second monomer unit having a contact angle to a water drop in the range from 50° to 130°.

2. The organic/inorganic composite separator according to claim **1**,

wherein the first monomer unit has a contact angle to a water drop in the range from 5° to 30°, and the second monomer unit has a contact angle to a water drop in the range from 70° to 120°.

3. The organic/inorganic composite separator according to claim **1**,

wherein the first monomer unit has a molar ratio in the range from 1 to 20 mol % based on the entire copolymer.

4. The organic/inorganic composite separator according to claim **1**,

wherein the copolymer has a contact angle to a water drop in the range from 30° to 80°.

5. The organic/inorganic composite separator according to claim **1**,

wherein the first monomer unit is a monomer unit having at least one functional group selected from the group consisting of OH, COOH, MAH (maleic anhydride) and SO_3H, and the second monomer unit is a monomer unit having at least one functional group selected from the group consisting of F, Cl, CN, acrylate, acetate and ester.

6. The organic/inorganic composite separator according to claim **1**,

wherein the copolymer is a copolymer selected from the group consisting of acrylonitrile-maleic anhydride copolymer, acrylonitrile-vinylalcohol copolymer, cyanoethylene-vinylalcohol copolymer, cyanoethylene-cellulose copolymer, cyanoethylene-sucrose copolymer, acrylonitrile-acrylic acid copolymer, acrylonitrile-anhydrous maleic acid copolymer, acrylate-acrylic acid copolymer and acrylate-anhydrous malcic acid copolymer.

7. The organic/inorganic composite separator according to claim **1**,

wherein the porous coating layer has a peeling force of 5 gf/cm or above.

8. The organic/inorganic composite separator according to claim **1**,

wherein the inorganic particles have a size in the range from 0.001 to 10 μm.

9. The organic/inorganic composite separator according to claim **1**,

wherein the inorganic particles are selected from the group consisting of inorganic particles having a dielectric constant of 5 or above, inorganic particles having lithium-ion transferring capability, or their mixtures.

10. The organic/inorganic composite separator according to claim **9**,

wherein the inorganic particle having a dielectric constant of 5 or above is an inorganic particle selected from the group consisting of $BaTiO_3$, $Pb(Zr,Ti)O_3$ (PZT), $Pb_{1-x}La_xZr_{1-y}Ti_yO_3$ (PLZT), $PB(Mg_3Nb_{2/3})O_3$-$PbTiO_3$ (PMN-PT), hafnia (HfO_2), $SrTiO_3$, SnO_2, CeO_2, MgO, NiO, CaO, ZnO, ZrO_2, SiO_2, Y_2O_3, Al_2O_3, SiC and TiO_2.

11. The organic/inorganic composite separator according to claim **10**,

wherein the inorganic particle having a dielectric constant of 5 or above is an piezoelectric inorganic particle selected from the group consisting of $BaTiO_3$, $Pb(Zr,Ti)O_3$ (PZT), $Pb_{1-x}La_xZr_{1-y}Ti_yO_3$ (PLZT), $PB(Mg_3Nb_{2/3})O_3$-$PbTiO_3$ (PMN-PT) and hafnia (HfO_2).

12. The organic/inorganic composite separator according to claim **9**,

wherein the inorganic particle having lithium ion conductivity is an inorganic particle selected from the group consisting of lithium phosphate (Li_3PO_4), lithium titanium phosphate ($Li_xTi_y(PO_4)_3$, $0<x<2$, $0<y<3$), lithium aluminum titanium phosphate ($Li_xAl_yTi_z(PO_4)_3$, $0<x<2$, $0<y<1$, $0<z<3$), $(LiAlTiP)_xO_y$ type glass ($0<x<4$, $0<y<13$), lithium lanthanum titanate ($Li_xLa_yTiO_3$, $0<x<2$, $0<y<3$), lithium germanium thiophosphate ($Li_xGe_yP_zS_w$, $0<x<4$, $0<y<1$, $0<z<1$, $0<w<5$), lithium nitrides (Li_xN_y, $0<x<4$, $0<y<2$), SiS_2 ($Li_xSi_yS_z$, $0<x<3$, $0<y<2$, $0<z<4$) type glass, and P_2S_5($Li_xP_yS_z$, $0<x<3$, $0<y<3$, $0<z<7$) type glass.

13. The organic/inorganic composite separator according to claim **1**,

wherein a weight ratio of the inorganic particles and the binder polymer is in the range from 50:50 to 99:1.

14. The organic/inorganic composite separator according to claim **1**,

wherein the porous coating layer has a thickness of 0.01 to 20 μm a pore size of 0.001 to 10 μm and a porosity of 10 to 90%.

15. The organic/inorganic composite separator according to claim **1**,

wherein the porous substrate is a polyolefin porous substrate.

16. The organic/inorganic composite separator according to claim **1**,

wherein the polyolefin porous substrate is famed using a polymer selected from the group consisting of polyethylene, polypropylene, polybutylene and polypentene.

17. The organic/inorganic composite separator according to claim 1,

wherein the porous substrate has a thickness of 5 to 50 μm, a pore size of 0.01 to 50 μm and a porosity of 10 to 95%.

18. An electrochemical device including a cathode, an anode, and a separator interposed between the cathode and the anode,

wherein the separator is the organic/inorganic composite separator defined in claim 1.

19. The electrochemical device according to claim 18, wherein the electrochemical device is a lithium secondary battery.

* * * * *

Appendix N

US007638241B2

(12) **United States Patent**
Lee et al.

(10) **Patent No.: US 7,638,241 B2**
(45) **Date of Patent: Dec. 29, 2009**

(54) **ORGANIC/INORGANIC COMPOSITE SEPARATOR HAVING MORPHOLOGY GRADIENT, MANUFACTURING METHOD THEREOF AND ELECTROCHEMICAL DEVICE CONTAINING THE SAME**

(75) Inventors: **Sang-Young Lee**, Daejeon (KR); **Dae-Jong Seo**, Daejeon (KR); **Joon-Yong Sohn**, Busan (KR); **Seok-Koo Kim**, Daejeon (KR); **Jang-Hyuk Hong**, Daejeon (KR); **Young-Soo Kim**, Yangsan-si (KR); **Hyun-Min Jang**, Daejeon (KR)

(73) Assignee: **LG Chem, Ltd.**, Seoul (KR)

(*) Notice: Subject to any disclaimer, the term of this patent is extended or adjusted under 35 U.S.C. 154(b) by 23 days.

(21) Appl. No.: **11/997,948**

(22) PCT Filed: **Dec. 6, 2006**

(86) PCT No.: **PCT/KR2006/005222**

§ 371 (c)(1),
(2), (4) Date: **Feb. 5, 2008**

(87) PCT Pub. No.: **WO2007/066967**

PCT Pub. Date: **Jun. 14, 2007**

(65) **Prior Publication Data**

US 2008/0292968 A1 Nov. 27, 2008

(30) **Foreign Application Priority Data**

Dec. 6, 2005 (KR) 10-2005-0118315

(51) **Int. Cl.**
H01M 2/16 (2006.01)
H01M 2/14 (2006.01)

(52) **U.S. Cl.** **429/251**; 429/129; 429/247

(58) **Field of Classification Search** 429/129, 429/232, 247; 29/623.1, 623.5; 428/212, 428/218, 304.4, 306.6, 307.3, 312.2
See application file for complete search history.

(56) **References Cited**

U.S. PATENT DOCUMENTS

4,322,524	A *	3/1982	Onda et al.	536/55
6,242,135	B1 *	6/2001	Mushiake	429/304
2002/0102455	A1	8/2002	Daroux et al.	
2004/0200355	A1	10/2004	Kim et al.	
2004/0214089	A1	10/2004	Lee et al.	

FOREIGN PATENT DOCUMENTS

JP	6-236752	*	8/1994
KR	10-2004-0089186 A	*	10/2004
KR	10-2004-0089187 A	*	10/2004

OTHER PUBLICATIONS

International Search report for PCT/KR2006/005222 dated Mar. 19, 2007.
Written Opinion for PCT/KR2006/005222 dated Mar. 19, 2007.

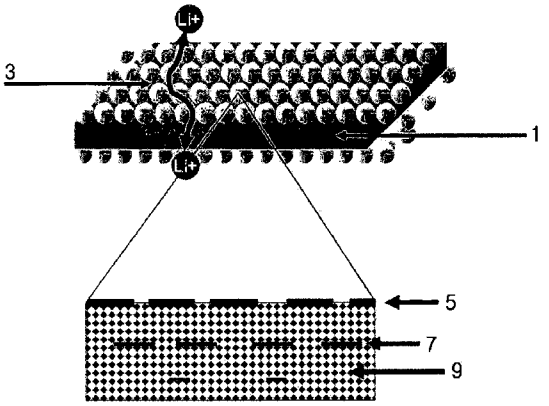
* cited by examiner

Primary Examiner—Patrick Ryan
Assistant Examiner—Julian Mercado
(74) *Attorney, Agent, or Firm*—Birch, Stewart, Kolasch & Birch, LLP

(57) **ABSTRACT**

Disclosed is an organic/inorganic composite separator including: a porous substrate having pores; and a porous active layer containing a mixture of inorganic particles and a binder polymer with which at least one surface of the porous substrate is coated. The organic/inorganic composite separator of the present invention may be useful to enhance peeling and scratch resistances and improve a lamination characteristic by introducing a porous active layer onto a porous substrate having pores, the porous active layer having heterogeneity of morphology toward a thickness direction in which a content ratio of the binder polymer/inorganic particles present in a surface layer is higher than that of the binder polymer/inorganic particles present inside the surface layer. Accordingly, the stability and performances of a battery can be improved together since the detachment of inorganic particles from the porous active layer may be reduced during the assembly process of the electrochemical device.

36 Claims, 2 Drawing Sheets





(A) (B)

FIG. 1

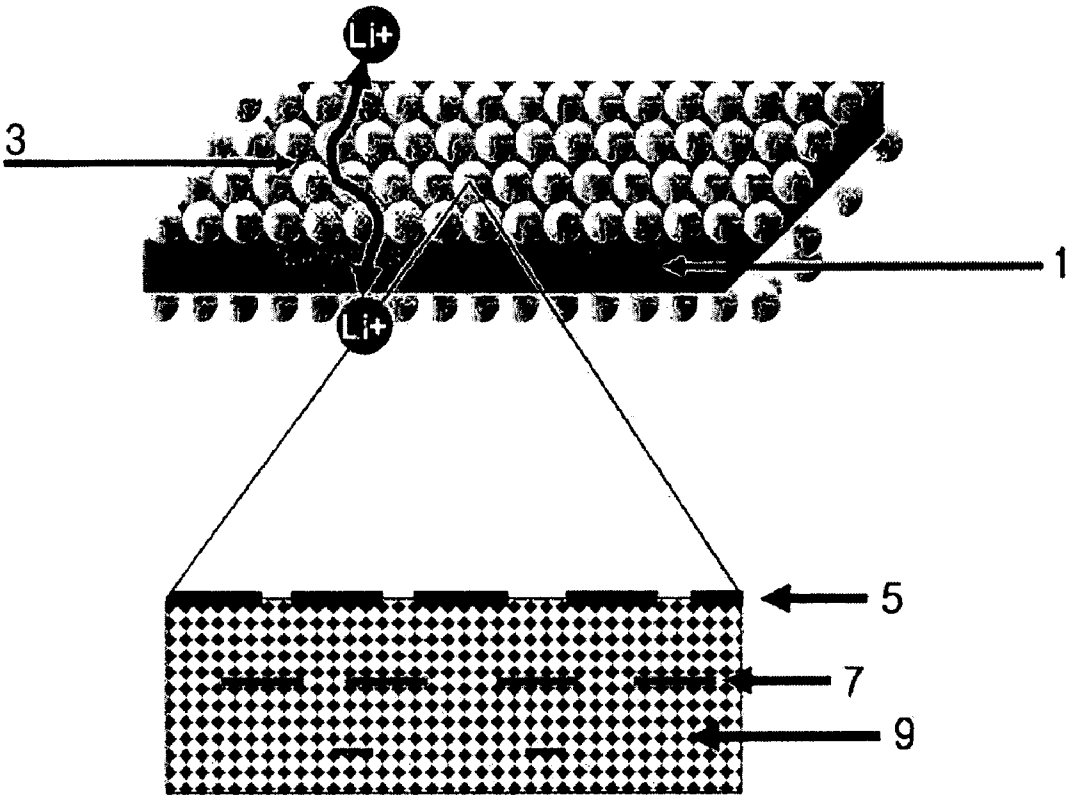
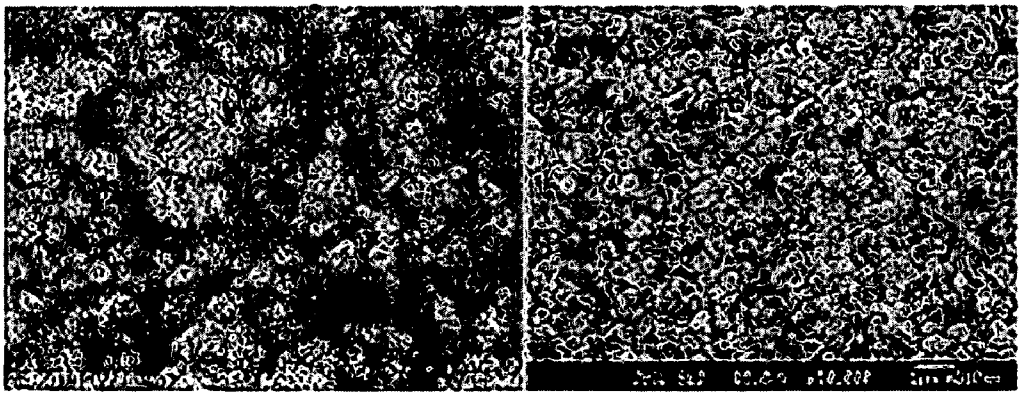
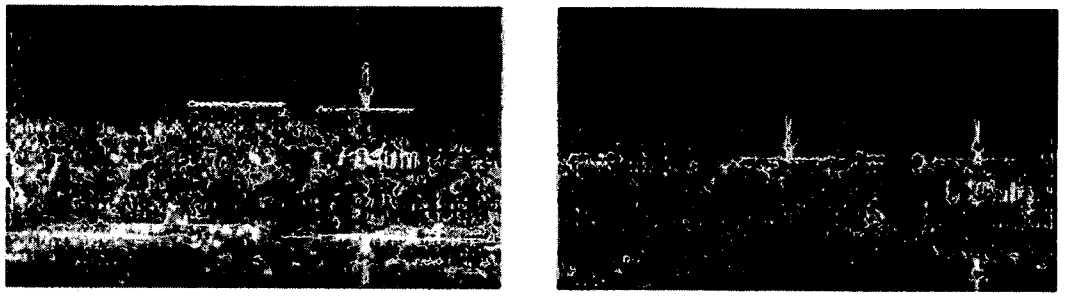


FIG. 2



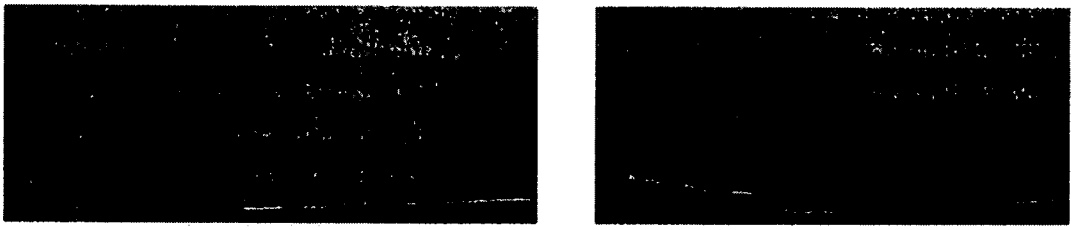
(A) (B)

FIG. 3



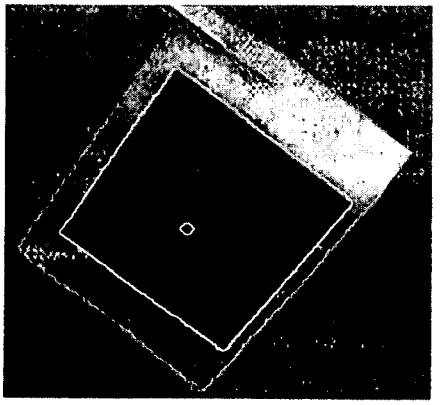
(A) (B)

FIG. 4



(A) (B)

FIG. 5



ORGANIC/INORGANIC COMPOSITE SEPARATOR HAVING MORPHOLOGY GRADIENT, MANUFACTURING METHOD THEREOF AND ELECTROCHEMICAL DEVICE CONTAINING THE SAME

TECHNICAL FIELD

The present invention relates to a separator of an electrochemical device such as a lithium secondary battery, a manufacturing method thereof and an electrochemical device containing the same, and more particularly to an organic/inorganic composite separator in which a porous active layer is coated with a mixture of an inorganic material and a polymer onto a surface of a porous substrate, a manufacturing method thereof and an electrochemical device containing the same.

BACKGROUND ART

Recently, there has been an increasing interest in energy storage technology. Batteries have been widely used as energy sources in the fields of cellular phones, camcorders, notebook computers, PCs and electric cars, resulting in intensive research and development into them. In this regard, electrochemical devices are one of the subjects of great interest. Particularly, development of rechargeable secondary batteries has been the focus of attention. Recently, the research and development into a novel electrode and a novel battery that can improve capacity density and specific energy have been made intensively in the field of the secondary batteries.

Among currently used secondary batteries, lithium secondary batteries developed in early 1990's have a higher drive voltage and a much higher energy density than those of conventional batteries using an aqueous electrolyte solution (such as Ni-MH batteries, Ni—Cd batteries, H_2SO_4—Pb batteries, etc). For these reasons, the lithium secondary batteries have been advantageously used. However, such a lithium secondary battery has disadvantages in that organic electrolytes used therein may cause safety-related problems resulting in ignition and explosion of the batteries and that processes for manufacturing such a battery are complicated.

Recently, lithium-ion polymer batteries have been considered as one of the next-generation batteries since the above disadvantages of the lithium ion batteries were solved. However, the lithium-ion polymer batteries have a relatively lower battery capacity than those of the lithium ion batteries and an insufficient discharging capacity in low temperature, and therefore these disadvantages of the lithium-ion polymer batteries remain to be urgently solved.

Such a battery has been produced from many companies, and the battery stability has different phases in the lithium-ion polymer batteries. Accordingly, it is important to evaluate and ensure the stability of the lithium-ion polymer batteries. First of all, it should be considered that errors in operation of the batteries should not cause damage to users. For this purpose, the Safety and Regulation strictly regulate the ignition and the explosion in the batteries.

In order to solve the above battery safety-related problem, there has been proposed an organic/inorganic composite separator having a porous active layer formed by coating at least one surface of a porous substrate having pores with a mixture of inorganic particles and a binder polymer. The porous active layer formed of this conventional organic/inorganic composite separator shows homogeneous composition morphology toward a thickness direction, as shown in FIG. **2**B and FIG. **3**B. However, if the electrochemical device is

assembled with the organic/inorganic composite separator, it has disadvantages in that inorganic particles in the porous active layer are detached and a lamination characteristic toward electrodes is deteriorated during a winding process, etc. If a content of a binder polymer in the porous active layer is increased so as to solve the above disadvantages, characteristics such as the peeling and scratch resistances, the lamination characteristic toward electrodes, etc. in the assembly process of the electrochemical device may be rather improved, but porosities in the porous active layer are decreased since the inorganic particles are present in a relatively lower content, resulting in deterioration in performances of the electrochemical device, and the safety of the separator is also reduced due to the introduction of the porous active layer.

DISCLOSURE OF INVENTION

The present invention is designed to solve the problems of the prior art, and therefore the first object of the invention is to provide an organic/inorganic composite separator capable of improving characteristics in an assembly process of an electrochemical device without any increase in the content of a binder polymer so that a porous active layer with which at least on surface of the organic/inorganic composite separator is coated can maintain sufficient porosities, a manufacturing method thereof and an electrochemical device containing the same.

The present invention is designed to solve the problems of the prior art, and therefore the second object of the invention is to provide a method for manufacturing an organic/inorganic composite separator having characteristics as described in the first object by undergoing only a single coating process.

In order to accomplish the first object, the present invention provides an organic/inorganic composite separator including: (a) a porous substrate having pores; and (b) a porous active layer containing a mixture of inorganic particles and a binder polymer with which at least one surface of the porous substrate is coated, wherein the porous active layer shows heterogeneity of composition morphology toward a thickness direction in which a content ratio of the binder polymer/inorganic particles present in a surface region of the porous active layer is higher than that of the binder polymer/inorganic particles present inside the porous active layer, a manufacturing method thereof and an electrochemical device containing the organic/inorganic composite separator.

The above-mentioned organic/inorganic composite separator of the present invention may enhance peeling and scratch resistances of the porous active layer and improve a lamination characteristic toward electrodes by introducing a porous active layer onto a porous substrate having pores, the porous active layer having heterogeneity of morphology toward a thickness direction in which a content ratio of the binder polymer/inorganic particles present in a surface layer is higher than that of the binder polymer/inorganic particles present inside the surface layer. Accordingly, stability and performances of the battery can be all improved together since the detachment of inorganic particles from the porous active layer may be reduced in the assembly process of the electrochemical device.

In the organic/inorganic composite separator of the present invention, a first binder polymer is preferably used as the binder polymer, the first binder polymer containing together at least one functional group selected from the group consisting of carboxy, maleic anhydride and hydroxy; and at least one functional group selected from the group consisting of cyano and acrylate. Such a first binder polymer includes

cyanoethylpullulan, cyanoethylpolyvinylalcohol, cyanoethylcellulose, cyanoethylsucrose, etc.

In the organic/inorganic composite separator of the present invention, a second binder polymer having a solubility parameter of 17 to 27 $MPa^{1/2}$ is preferably used as the binder polymer together with the above-mentioned binder polymer in the aspect of electrochemical stability of the porous coating layer. Such a second binder polymer includes polyvinylidene fluoride-co-hexafluoropropylene, polyvinylidene fluoride-co-trichloroethylene, polymethylmethacrylate, polyacrylonitrile, polyvinylpyrrolidone, polyvinylacetate, polyethylene-co-vinyl acetate, polyimide, polyethylene oxide, cellulose acetate, cellulose acetate butyrate, cellulose acetate propionate, etc.

In order to accomplish the second object, the present invention provides a method for manufacturing an organic/inorganic composite separator including a porous active layer, the method including: (S1) preparing a solution of a first binder polymer containing together at least one functional group selected from the group consisting of carboxy, maleic anhydride and hydroxy; and at least one functional group selected from the group consisting of cyano and acrylate; (S2) adding inorganic particles to the solution of the first binder polymer and dispersing the inorganic particles in the solution of the first binder polymer; (S3) coating the solution of the first binder polymer having inorganic particles dispersed therein with a film and drying the coated film, wherein the porous active layer shows heterogeneity of morphology toward a thickness direction in which a content ratio of the first binder polymer/inorganic particles present in a surface region of the porous active layer is higher than that of the first binder polymer/inorganic particles present inside the porous active layer.

In the method for manufacturing an organic/inorganic composite separator of the present invention, the second binder polymer having a solubility parameter of 17 to 27 $MPa^{1/2}$ is preferably further dissolved in the solution of the first binder polymer in the aspect of electrochemical stability of the porous coating layer.

BRIEF DESCRIPTION OF THE DRAWINGS

These and other features, aspects, and advantages of preferred embodiments of the present invention will be more fully described in the following detailed description, taken accompanying drawings. In the drawings:

FIG. **1** is a diagram showing a cross-sectional view of an organic/inorganic composite separator according to the present invention and a schematic view of an active layer having heterogeneity of morphology toward a thickness direction.

FIG. **2** is a photograph, taken by a scanning electron microscope (SEM), showing the organic/inorganic composite separator. Here, FIG. **2**A is a magnified photograph showing a surface of the porous active layer having heterogeneity of morphology toward a thickness direction prepared in Example 1, and FIG. **2**B is a magnified photograph showing a surface of a conventional porous active layer.

FIG. **3** is a photograph, taken by a scanning electron microscope (SEM), showing the organic/inorganic composite separator. Here, FIG. **3**A is a magnified photograph showing a surface of the porous active layer having heterogeneity of morphology toward a thickness direction prepared in Example 1, and FIG. **3**B is a magnified photograph showing a surface of a conventional porous active layer.

FIG. **4**A is a photograph showing a peeling characteristic in a surface of an organic/inorganic composite separator prepared in Example 1, wherein the organic/inorganic composite separator has a porous active layer formed therein, the porous active layer having heterogeneity of morphology toward a thickness direction, and FIG. **4**B is a photograph showing a peeling characteristic in a surface of a conventional organic/inorganic composite separator, wherein the organic/inorganic composite separator has a composite coating layer formed therein, the composite coating layer being composed of an inorganic material and a polymer.

FIG. **5** is a photograph taken after an organic/inorganic composite separator prepared in Example 1 is laminated into an electrode, wherein the organic/inorganic composite separator has a porous active layer formed therein, the porous active layer having heterogeneity of morphology toward a thickness direction.

BEST MODES FOR CARRYING OUT THE INVENTION

Hereinafter, preferred embodiments of the present invention will be described in detail referring to the accompanying drawings. Prior to the description, it should be understood that the terms used in the specification and appended claims should not be construed as limited to general and dictionary meanings, but interpreted based on the meanings and concepts corresponding to technical aspects of the present invention on the basis of the principle that the inventor is allowed to define terms appropriately for the best explanation. Therefore, the description proposed herein is just a preferable example for the purpose of illustrations only, not intended to limit the scope of the invention, so it should be understood that other equivalents and modifications could be made thereto without departing from the spirit and scope of the invention.

Unlike conventional composite separators, such as a polyolefin separator having a porous active layer, wherein the porous active layer has homogeneous morphology toward a thickness direction is simply formed on a porous substrate, the present invention provides an organic/inorganic composite separator including a porous active layer having heterogeneity of composition morphology toward a thickness direction in which a content ratio of the binder polymer/inorganic particles present in a surface region of the porous active layer is higher than that of the binder polymer/inorganic particles present inside the porous active layer.

1) The organic/inorganic composite separator of the present invention includes a porous substrate **1** and a porous active layer **3** formed in at least one surface of the porous substrate **1**, wherein the porous active layer **3** includes a polymer **5** and inorganic particles **9**, the content ratios of the a polymer **5** and the inorganic particles **9** are varied toward a thickness direction, as shown in FIG. **1**. Accordingly, the organic/inorganic composite separator has increased resistances to external stimuli such as a peeling resistance, a scratch resistance, etc. and an improved lamination characteristic toward electrodes due to adhesion characteristic of the polymer present in a large amount in the surface of the active layer. Therefore, the organic/inorganic composite separator of the present invention may exhibit very excellent characteristics in the assembly process of a battery such a winding process, a lamination process, etc. (see FIG. **4**A). Also, the organic/inorganic composite separator of the present invention may have excellent ion conductivity since the heterogeneity of morphology toward a thickness direction enables the porosity of the active layer to become increased from its surface to its inside, thereby resulting in improved battery performances.

2) Also, the complete internal short-circuit between the electrodes is hard to occur because of the presence of an organic/inorganic composite porous active layer even if the porous substrate is ruptured inside of the battery, and the short-circuited area is not enlarged any more although a short-circuited phenomenon appears in the battery, resulting in improvement in safety of the battery.

In the application of the present invention, the expression "heterogeneity of morphology toward a thickness direction in which a content ratio of binder polymer/inorganic particles present in a surface region of a porous active layer is higher than that of binder polymer/inorganic particles present inside the porous active layer" should be understood to include all aspects if the organic/inorganic composite separator of the present invention is formed so that a content ratio of binder polymer/inorganic particles present in a surface of a porous active layer is higher than that of binder polymer/inorganic particles present beneath (inside) the surface of the porous active layer. For example, by the expression, it is meant that the organic/inorganic composite separator of the present invention includes all porous active layers including a porous active layer formed so that the content ratio of the binder polymer/inorganic particles is linearly decreased toward a direction from a surface of the porous active layer to the porous substrate; a porous active layer formed so that the content ratio of the binder polymer/inorganic particles is non-linearly decreased toward a direction from a surface of the porous active layer to the porous substrate; a porous active layer formed so that the content ratio of the binder polymer/inorganic particles is non-continuously decreased toward a direction from a surface of the porous active layer to the porous substrate, etc.

In the application of the present invention, the content ratio of the binder polymer/inorganic particles is also determined on the basis of the entire surface region of the porous active layer since the binder resin present in the surface region of the porous active layer may not be partially homogenously mixed with the inorganic particles.

One of major components in the organic/inorganic composite separator according to the present invention are inorganic particles generally used in the art. The inorganic particles are the major components used to manufacture a final organic/inorganic composite separator, and serve to form micropores due to the presence of interstitial volumes among the inorganic particles. Also, the inorganic particles also serve as a kind of a spacer capable of maintaining a physical shape of a coating layer.

The inorganic particles used in the organic/inorganic composite separator of the present invention are stable in the electrochemical aspect, but the present invention is not particularly limited thereto. That is to say, the inorganic particles, which may be used in the present invention, is not limited if oxidation and/or reduction reactions do not take place within the operation voltage range (for example, 0~5V in a Li/Li^+ battery) of a battery to be applied. In particular, the inorganic particles having ion conductivity may improve performances of the organic/inorganic composite separator by enhancing ion conductivity in the electrochemical device.

Further, when inorganic particles having high dielectric constant are used, they can contribute to increasing the dissociation degree of an electrolyte salt in a liquid electrolyte, such as a lithium salt, thereby improving the ion conductivity of the electrolyte.

For these above reasons, the inorganic particles preferably include inorganic particles having a high dielectric constant of 5 or more, and more preferably 10 or more, inorganic particles having lithium conductivity or mixtures thereof. A non-limiting example of the inorganic particles having a dielectric constant of 5 or more include $BaTiO_3$, $Pb(Zr,Ti)O_3$ (PZT), $Pb_{1-x}La_xZr_{1-y}Ti_yO_3$ (PLZT), $PB(Mg_3Nb_{2/3})O_3$—$PbTiO_3$ (PMN-PT), hafnia (HfO_2), $SrTiO_3$, SnO_2, CeO_2, MgO, NiO, CaO, ZnO, ZrO_2, Y_2O_3, Al_2O_3, TiO_2, SiC or mixtures thereof.

In particular, the above-described inorganic particles, for example $BaTiO_3$, Pb $(Zr,Ti)O_3$ (PZT), $Pb_{1-x}La_xZr_{1-y}Ti_yO_3$ (PLZT), PB $(Mg_3Nb_{2/3})O_3$—$PbTiO_3$ (PMN-PT) and hafnia (HfO_2), has a high dielectric constant of 100 or more. The inorganic particles also have piezoelectricity so that an electric potential between both surfaces can be generated in the presence of the generated charges when pressure is applied over a critical level. Therefore, the inorganic particles can prevent internal short circuit between both electrodes, thereby contributing to improving the safety of a battery. Additionally, when such inorganic particles having a high dielectric constant are mixed with inorganic particles having lithium ion conductivity, synergic effects may be obtained.

As used herein, "inorganic particles having lithium ion conductivity" are referred to as inorganic particles containing lithium ions and having a capability of transferring lithium ions without storing lithium. The inorganic particles having lithium ion conductivity can conduct and move lithium ions due to defects in their particle structure, and thus can improve lithium ion conductivity and contribute to improving battery performance. A non-limiting example of such inorganic particles having lithium ion conductivity includes: lithium phosphate (Li_3PO_4), lithium titanium phosphate ($Li_xTi_y(PO_4)_3$, $0<x<2$, $0<y<3$), lithium aluminum titanium phosphate ($Li_xAl_yTi_z(PO_4)_3$, $0<x<2$, $0<y<1$, $0<z<3$), $(LiAlTiP)_xO_y$ type glass ($0<x<4$, $0<y<13$) such as $14Li_2O$-$9Al_2O_3$-$38TiO_2$-$39P_2O_5$, lithium lanthanum titanate ($Li_xLa_yTiO_3$, $0<x<2$, $0<y<3$), lithium germanium thiophosphate ($Li_xGe_yP_zS_w$, $0<x<4$, $0<y<1$, $0<z<1$, $0<w<5$) such as $Li_{3.25}Ge_{0.25}P_{0.75}S_4$, lithium nitrides ($Li_xN_y$, $0<x<4$, $0<y<2$) such as Li_3N, SiS_2 type glass ($Li_xSi_yS_z$, $0<x<3$, $0<y<2$, $0<z<4$) such as Li_3PO_4—Li_2S—SiS_2, P_2S_5 type glass ($Li_xP_yS_z$, $0<x<3$, $0<y<3$, $0<z<7$) such as Lil-Li_2S—P_2S_5, or mixtures thereof.

Micropores may be formed by adjusting the sizes and contents of the inorganic particles and content of the binder polymer as the components of the organic/inorganic composite separator according to the present invention. And, the pore size and porosity of the micropores may also be adjusted.

Although there is no particular limitation in size of the inorganic particles, the inorganic particles preferably have a size of 0.001-10 μm for the purpose of forming a coating layer having a uniform thickness and providing a suitable porosity. If the size is less than 0.001 μm, physical properties of the porous active layer cannot be controlled with ease since the inorganic particles have poor dispersibility. If the size is greater than 10 μm, the resultant porous active layer has an increasing thickness, resulting in degradation in mechanical properties. Furthermore, such excessively large pores may increase a possibility of generating internal short circuit during repeated charge/discharge cycles.

As one of the major components in the organic/inorganic composite separator having heterogeneity of morphology toward a thickness direction according to the present invention, a first binder polymer is preferably used as the binder polymer, the first binder polymer including together at least one functional group selected from the group consisting of carboxy, maleic anhydride and hydroxy; and at least one functional group selected from the group consisting of cyano and acrylate. More preferably, first binder polymers containing a hydroxy group and a cyano group together, such as cyanoethylpullulan, cyanoethylpolyvinylalcohol, cyanoeth-

ylcellulose, cyanoethylsucrose, are used alone or in combinations thereof. If a coating solution using the first binder polymer having two predetermined functional groups is used herein, an organic/inorganic composite separator having heterogeneity of morphology toward a thickness direction is easily formed by only one coating by means of control of phase inversion, and a cohesion force among the inorganic particles, an adhesion force between the porous active layer and the porous substrate and a lamination characteristic toward electrodes are further improved.

In the manufacturing process of a battery, one of the very important characteristics is particularly the lamination to electrodes of the porous active layer formed in the organic/inorganic composite separator. The lamination characteristic toward electrodes is evaluated by measuring an adhesion force between separators, namely an adhesion force between two separators after a separator is adhered to another separator at 100° C. under a pressure of 5.0 kgf/cm^2. The porous active layer, formed in the organic/inorganic composite separator of the present invention under the above-mentioned conditions, preferably has an adhesion force of 5 gf/cm or more.

Also, it is not essential to use a binder polymer having ion conductivity, used in the porous active layer having heterogeneity of morphology toward a thickness direction of the present invention. However, when the binder polymer has ion conductivity, it can further improve performances of an electrochemical device. Therefore, the binder polymer preferably has a dielectric constant as high as possible. Because a dissociation degree of a salt in an electrolyte depends on a dielectric constant of a solvent used in the electrolyte, the polymer having a higher dielectric constant can increase the dissociation degree of a salt in the electrolyte used in the present invention. The dielectric constant of the polymer may range from 1.0 to 100 (as measured at a frequency of 1 kHz), and is preferably 10 or more.

Also, the above mentioned first binder polymer is preferably used in combination with a second binder polymer having a solubility parameter of 17 to 27 MPa$^{1/2}$ in the aspect of electrochemical safety of the porous coating layer. Such a second binder polymer includes polymers having a functional group selected from the group consisting of halogen, acrylate, acetate and cyano. More particularly, an example of the second binder polymer includes polyvinylidene fluoride-co-hexafluoropropylene, polyvinylidene fluoride-co-trichloroethylene, polymethylmethacrylate, polyacrylonitrile, polyvinylpyrrolidone, polyvinylacetate, polyethylene-co-vinyl acetate, polyimide, polyethylene oxide, cellulose acetate, cellulose acetate butyrate, cellulose acetate propionate, etc.

If the first binder polymer and the second binder polymer are used together in the porous active layer having heterogeneity of morphology toward a thickness direction according to the present invention, a content ratio of the first binder polymer:the second binder polymer ranges from 0.1:99.9 to 99.9:0.1, and more preferably from 20.0:80.0 to 80.0:20.0.

There is no particular limitation in mixing ratio of inorganic particles to a binder polymer. However, the mixing ratio of inorganic particles to a binder polymer preferably ranges from 10:90 to 99:1, and more preferably ranges from 50:50 to 99:1. If the content of the inorganic particles is less than 10 parts by weight, interstitial volumes formed among inorganic particles may be decreased due to the presence of an excessively large amount of the polymer, thereby reducing the pore size and porosity of a coating layer, resulting in degradation in battery performance. If the content of the inorganic particles is greater than 99 parts by weight, an excessively low content of the polymer may cause the adhesion among inorganic particles to be weakened, resulting in degradation in mechanical properties of the resultant organic/inorganic composite separator.

There is no particular limitation in thickness of the active layer composed of the inorganic particles and the binder polymer, but the active layer preferably has a thickness of 0.01 and 100 μm. Also, there are no particular limitations in pore size and porosity of the active layer, but the active layer preferably has a pore size of 0.001 to 10 μm and a porosity of 5 to 95%. The active layer serve as a resistant layer if the pore size and the porosity of the active layer is less than 0.001 μm and 5%, respectively, while it is difficult to maintain mechanical properties of the active layer if the pore size and the porosity of the active layer is greater than 150 μm and 95%, respectively.

The organic/inorganic composite separator of the present invention further may include other additives, in addition to the inorganic particles and the polymer as the components in the active layer.

There is no particular limitation in selection of a porous substrate including the active layer having homogeneous composition morphology according to the present invention, as long as it includes a porous substrate having pores. A non-limiting example of the porous substrate includes polyethyleneterephthalate, polybutyleneterephthalate, polyester, polyacetal, polyamide, polycarbonate, polyimide, polyetheretherketone, polyethersulfone, polyphenyleneoxide, polyphenylenesulfidro, polyethylenenaphthalene, high-density polyethylene, low-density polyethylene, linear low-density polyethylene, ultrahigh molecular weight polyethylene, polypropylene and mixtures thereof, and other heat-resistant engineering plastics may be used without any limitation.

There is no particular limitation in thickness of the porous substrate, but the porous substrate preferably has a thickness of 1 to 100 μm, and more preferably 5 to 50 μm. It is difficult to maintain a mechanical property of the porous substrate if the thickness of the porous substrate is less than 1 μm, while the porous substrate serve as a resistant layer if the thickness of the porous substrate is greater than 100 μm.

There are no particular limitations in pore size and porosity of the porous substrate, but the porous substrate preferably has a porosity of 5 to 95%. The porous substrate preferably has a pore size (a diameter) of 0.01 to 50 μm, and more preferably 0.1 to 20 μm. The porous substrate serve as a resistant layer if the pore size and the porosity of the active layer is less than 0.01 μm and 10%, respectively, while it is difficult to maintain mechanical properties of the active layer if the pore size and the porosity of the active layer is greater than 50 μm and 95%, respectively.

The porous substrate may be in a form of a non-woven fabric or a membrane. If a non-woven fabric is used as the porous substrate, it can form a porous web. At this time, the non-woven fabric is preferably in a spunbond or melt blown shape composed of long fibers.

A spunbond process is carried out by undergoing a series of continuous procedures, for example by applying heat to a polymer to form a long fiber and stretching the long fiber with the hot air to form a web. A melt blown process is a process for spinning a polymer through a spinneret, wherein the polymer can form a fiber and the spinneret is formed of hundreds of small orifices. At this time, the resultant fiber is a three-dimensional fiber having a spider-web structure in which microfibers having a diameter of 10 μm or less are interconnected.

The organic/inorganic composite separator of the present invention, which is formed by coating the porous substrate with a mixture of the inorganic particles and the binder poly-

mer, includes pores in the porous substrate and also has pores in the active layer formed on the porous substrate, as described above. A binder polymer preferably interconnects and fixes the inorganic particles, and the micropores are formed in the porous active layer due to the presence of interstitial volumes among the inorganic particles. The pore size and the porosity of the organic/inorganic composite separator depend mainly on the size of the inorganic particles. For example, if inorganic particles having a particle diameter of 1 μm or less are used, the pores formed thereby also have a size of 1 μm or less. The pore structure is filled with an electrolyte injected during a subsequent process and the injected electrolyte serves to transfer ions. Therefore, the pore size and the porosity are important factors in controlling the ion conductivity of the organic/inorganic composite separator. Preferably, the pores size and the porosity of the organic/inorganic composite separator according to the present invention preferably range from 0.001 to 10 μm and from 5 to 95%, respectively.

Also, there is no particular limitation in thickness of the organic/inorganic composite separator of the present invention, but the thickness of the organic/inorganic composite separator may be controlled depending on the performance of a battery. The organic/inorganic composite separator preferably has a thickness of 1 to 100 μm, and more preferably a thickness of 2 to 30 μm. The performance of a battery may be improved by controlling the thickness range of the organic/inorganic composite separator.

The organic/inorganic composite separator of the present invention may be used in a battery with a microporous separator, for example a polyolefin separator, depending on the characteristic of the resultant battery.

The organic/inorganic composite separator including a porous active layer having heterogeneity of composition morphology toward a thickness direction according to the present invention may be manufactured according to the following methods, but the present invention is not limited thereto.

As the first method, a method for manufacturing an organic/inorganic composite separator having a porous active layer is described, as follows. In this manufacturing method, the porous active layer is formed in the organic/inorganic composite separator so that a content ratio of binder polymer/inorganic particles is non-continuously decreased from a surface of porous active layer toward the porous substrate.

First, a binder polymer is dissolved in a solvent to form a polymer solution, and inorganic particles are added and dispersed in the polymer solution to prepare various coating solutions having different contents of the inorganic particles. At this time, kinds of the binder polymer and the inorganic particles may be same or different in each of the coating solutions. A porous active layer having heterogeneity of morphology toward a thickness direction is prepared by repeatedly applying and drying each of the coating solutions on a surface of a porous substrate with a thin thickness, wherein the binder polymer/inorganic particles have different content ratios in the coating solutions. Binder polymer/inorganic particles in a finally applied coating solution should have a sufficiently high content ratio to improve characteristics of a battery during an assembly process of the battery. Then, binder polymer/inorganic particles in the coating solution, applied beneath the finally applied coating solution, should have a lower content ratio than that of binder polymer/inorganic particles present in the coating solution in a surface of the porous active layer. Meanwhile, polymer/inorganic particles in the coating solution, with which a surface of the porous substrate is coated so that the surface can be in contact to the coating solution, may have a higher content ratio than that of binder polymer/inorganic particles present in the coating solution of the intermediate layer. Such a non-continuous multiple coating layer may be formed of 2 layers, 3 layers or more, and the entire thickness of the multiple coating layer should be controlled within the known range so that the performances of a separator cannot be degraded.

All conventional binder polymers may be used as the binder polymer capable of being used to form the above-mentioned multiple coating layer, as long as they can be used to form a porous active layer. In particular, the binder polymer is preferably gelled when swelled with a liquid electrolyte, thereby to shows a high degree of swelling. Therefore, it is preferred to use a binder polymer having a solubility parameter of 15 to 45 $MPa^{1/2}$, and more preferably a solubility parameter of 15 to 25 $MPa^{1/2}$ and 30 to 45 $MPa^{1/2}$. Accordingly, hydrophilic polymers having a large number of polar groups are more advisable as the binder polymer compared to hydrophobic polymers such as polyolefin polymers. The binder polymer cannot be swelled sufficiently in a conventional aqueous electrolyte solution for a battery if the solubility parameter of the binder polymer is less than 15 $MPa^{1/2}$ or greater than 45 $MPa^{1/2}$.

As the second method, there is a method for forming a porous active layer having heterogeneity of morphology toward a thickness direction through a single coating process.

First, the above-mentioned first binder polymer is dissolved in a solvent to prepare a first polymer solution (S1). The first binder polymer includes together at least one functional group selected from the group consisting of carboxy, maleic anhydride and hydroxy; and at least one functional group selected from the group consisting of cyano and acrylate. Therefore, it is possible to improve physical properties of the resultant organic/inorganic composite separator, and to control phase inversion.

Subsequently, inorganic particles added and dispersed in a first binder polymer solution (S2). The solvent having a solubility parameter similar to that of the binder polymer as well as a low boiling point is preferred. This is why the solvent is uniformly mixed with the polymer and removed easily after coating the binder polymer. A non-limiting example of the solvent that may be used include, but is not limited to, acetone, tetrahydrofuran, methylene chloride, chloroform, dimethylformamide, N-methyl-2-pyrrolidone (NMP), cyclohexane, water and mixtures thereof. It is preferred to perform a step of pulverizing inorganic particles after adding the inorganic particles to the polymer solution. At this time, the time required for pulverization is suitably 1-20 hours, and the particle size of the pulverized particles ranges preferably from 0.001 and 10 μm, as described above. Conventional pulverization methods may be used, and a method using a ball mill is particularly preferred. There are no particular limitations in composition of the mixture composed of the inorganic particles and the polymer. Therefore, it is possible to control thickness, pore size and porosity of the finally produced organic/inorganic composite separator of the present invention. That is to say, the porosity of the organic/inorganic composite separator according to the present invention is increased with increase in a ratio (ratio=I/P) of inorganic particles (I) to a polymer (P), indicating that the thickness of the organic/inorganic composite separator is improved in the same solid content (weight of inorganic particles+weigh of a binder polymer). Also, the pore size of the organic/inorganic composite separator is increased with increase in an ability to form pores among the inorganic particles. At this time, the pore size of the organic/inorganic composite separator is

increased since an interstitial distance among inorganic materials is increased with increase in a size (a diameter) of the inorganic particles.

Then, a porous substrate is directly coated with, or a separate support is coated with a solution of a first binder polymer having inorganic particles dispersed therein, and the coated porous substrate or support is dried. Here, the heterogeneity of morphology toward a thickness direction is determined according to components and coating conditions of the binder polymer. That is to say, the heterogeneity of morphology in the porous active layer is formed according to the components and the suitable coating condition (in particular, moisture) of the binder polymer. If a polymer having a high polarity, for example the first binder polymer, is mixed with inorganic materials to prepare a mixed solution of the binder polymer/inorganic particles and the porous substrate is then coated with the mixed solution under a suitable moisture condition, the polymer having a high polarity is present in a surface of the porous active layer as a result of a phase inversion. That is to say, a relative density of the binder polymer is gradually decreased from a surface of the active layer toward a thickness direction. At this time, the moisture condition, required for coating the porous substrate, ranges from 5 to 80% (a relative moisture, room temperature), and preferably from 20 to 50%. The heterogeneity of morphology in the active layer is not accomplished if the moisture condition is less than 5%, while the formed active layer has a very loose adhesion force and an excessively high porosity if the moisture condition is greater than 80%, resulting in easy peeling of the active layer.

In order to improve electrochemical stability of a porous active layer to be formed, it is preferred to further dissolve a second binder polymer having a solubility parameter of 17 to 27 $MPa^{1/2}$ in the above-mentioned first binder polymer solution. Specific kinds and preferred content ratios of the first binder polymer and the second binder polymer are the same as described above.

As the method for coating a porous substrate with the solution of the binder polymer having inorganic particles dispersed therein, conventional methods well known to the art may be used. For example, the conventional methods include a dip coating, a die coating, a roll coating, a comma coating or combination thereof. Also, the porous active layer may be selectively formed in one side or both sides of the porous substrate.

The organic/inorganic composite separator of the present invention, prepared thus, may be used as an electrochemical device, preferably a separator of a lithium secondary battery. At this time, if a polymer, which can be swelled by uptake of liquid electrolytes, is used as the component of the binder polymer, it can act as a gel-type polymer electrolyte since the polymer is gelled by reaction of the polymer to the electrolyte solution injected after assembly process of a battery using the separator.

Also, the present invention provides an electrochemical device including: (a) a cathode; (b) an anode; (c) an organic/inorganic composite separator interposed between the cathode and the anode and having a porous active layer formed therein according to the present invention, wherein the porous active layer has heterogeneity of composition morphology toward a thickness direction; and (d) an electrolyte.

The electrochemical devices include any devices in which electrochemical reactions may occur, and a specific example of the electrochemical devices includes all kinds of primary batteries, secondary batteries, fuel cells, solar cells or capacitors. In particularly, it is preferred to use lithium secondary batteries among the secondary batteries including a lithium metal secondary battery, a lithium ion secondary battery, a lithium polymer secondary battery or a lithium ion polymer secondary battery.

The electrochemical device may be manufactured according to conventional methods well known to the art. According to one embodiment of the manufacturing method of the electrochemical device, an electrochemical device may be manufactured by interposing the above-mentioned organic/inorganic composite separator between a cathode and an anode and injecting an electrolyte solution into a battery.

There is no limitation in the electrodes which may be used together with an organic/inorganic composite separator of the present invention, and the electrodes may be manufactured by settling electrode active materials on a current collector according to one of the conventional methods known to one skilled in the art. Among the electrode active materials, a non-limiting example of cathode active materials may include any conventional cathode active materials currently used in a cathode of a conventional electrochemical device, and particularly preferably includes lithium manganese oxides, lithium cobalt oxides, lithium nickel oxides, lithium iron oxides or lithium composite oxides thereof. Additionally, a non-limiting example of anode active materials may include any conventional anode active materials currently used in an anode of a conventional electrochemical device, and particularly preferably include lithium intercalation materials such as lithium metal, lithium alloys, carbon, petroleum coke, activated carbon, graphite or other carbonaceous materials. A non-limiting example of a cathode current collector includes foil formed of aluminum, nickel or a combination thereof. A non-limiting example of an anode current collector includes foil formed of copper, gold, nickel, copper alloys or a combination thereof.

The electrolyte solution that may be used in the present invention includes a salt represented by the formula of A^+B^-, wherein A^+ represents an alkali metal cation selected from the group consisting of Li^+, Na^+, K^+ and combinations thereof, and B^- represents an salt containing an anion selected from the group consisting of PF_6^-, BF_4^-, Cl^-, Br^-, I^-, ClO_4^-, AsF_6^-, $CH_3CO_2^-$, $CF_3SO_3^-$, $N(CF_3SO_2)_2^-$, $C(CF_2SO_2)_3^-$ and combinations thereof, the salt being dissolved or dissociated in an organic solvent selected from the group consisting of propylene carbonate (PC), ethylene carbonate (EC), diethyl carbonate (DEC), dimethyl carbonate (DMC), dipropyl carbonate (DPC), dimethyl sulfoxide, acetonitrile, dimethoxyethane, diethoxyethane, tetrahydrofuran, N-methyl-2-pyrrolidone (NMP), ethylmethyl carbonate (EMC), gamma-butyrolactone (y-butyrolactone) and mixtures thereof. However, the electrolyte solution that may be used in the present invention is not limited to the above examples.

More particularly, the electrolyte solution may be injected in a suitable step during the manufacturing process of a battery, according to the manufacturing process and desired properties of a final product. In other words, the electrolyte solution may be injected before a battery is assembled or in a final step of the assembly process of a battery.

In addition to the general winding process, a stacking process and a folding process may be used as the process using the organic/inorganic composite separator of the present invention in a battery, wherein the stacking process is laminating an electrode on a separator. In particular, the organic/inorganic composite separator of the present invention has an advantage that it may be easily used during the assembly process of a battery since a binder polymer is present in a relatively large amount in a surface region of an organic/inorganic composite active layer. At this time, adhesion force may be controlled according to the content of main compo-

nents, for example inorganic particles and a polymer, or the physical properties of the polymer, and the organic/inorganic composite separator of the present invention is easily adhered to an electrode especially if the above-mentioned first binder polymer is used as the binder polymer.

Hereinafter, preferred embodiments of the present invention will be described in detail for better understandings, with reference to the accompanying drawings. However, the description proposed herein is just a preferable example for the purpose of illustrations only, not intended to limit the scope of the invention.

EXAMPLES 1 TO 6

Preparation of Organic/Inorganic Composite Separator and Lithium Secondary Battery

Example 1

1-1. Preparation of Organic/Inorganic [(PVdF-CTFE/Cyanoethylpullulan)/$BaTiO_3$] Composite Separator

A polyvinylidene fluoride-chlorotrifluoroethylene copolymer (PVdF-CTFE) and cyanoethylpullulan were added to acetone at contents of 10% by weight and 2% by weight, respectively, and dissolved at 50 □ for about 12 hours to prepare a polymer solution. A $BaTiO_3$ powder was added to the prepared polymer solution to a weight ratio of 20/80 weight ratio of the polymer mixture/$BaTiO_3$, and then the $BaTiO_3$ powder was ground and dispersed for at least 12 hours using a ball mill, thereby to prepare a slurry. A particle diameter (particle size) of $BaTiO_3$ in the slurry prepared thus may be adjusted according to the size of a bid used in the ball mill and the time used in the ball mill, but the $BaTiO_3$ powder was ground to a particle diameter of about 400 nm to prepare a slurry in this Example 1. A polyethylene separator (porosity of 45%) having a thickness of 18 μm was coated with the prepared slurry under a moisture condition of 30% relative humidity using a dip coating process, and a coating thickness of the polyethylene separator was adjusted to a thickness of about 4 μm. An average size of pores in the active layer of the coated polyethylene separator was about 0.4 μm, and its porosity was 57%.

1-2. Preparation of Lithium Secondary Battery

(Preparation of Anode)

To N-methyl-2-pyrrolidone (NMP) as a solvent, 96% by weight of carbon powder as an anode active material, 3% by weight of PVDF (polyvinylidene fluoride) as a binder and 1% by weight of carbon black as a conductive agent were added to prepare a mixed slurry for an anode. A Cu thin film having a thickness of 10 μm as an anode collector was coated with the missed slurry and dried to prepare an anode. Then, the anode was subject to a roll press.

(Preparation of Cathode)

To N-methyl-2-pyrrolidone (NMP) as a solvent, 92% by weight of lithium cobalt composite oxide ($LiCoO_2$) as a cathode active material, 4% by weight of carbon black as a conductive agent and 4% by weight of PVDF (polyvinylidene fluoride) as a binder were added to prepare a mixed slurry for a cathode. An Al thin film having a thickness of 20 μm as a cathode collector was coated with the mixed slurry and dried to prepare a cathode. Then, the cathode was subject to a roll press.

(Preparation of Battery)

The cathode, the anode and the organic/inorganic composite separator, as obtained as described above, were stacked to form an assembly. Then, an electrolyte solution (ethylene carbonate (EC)/ethylene methyl carbonate (EMC)=½ (by volume ratio) containing 1 M of lithium hexafluorophosphate ($LiPF_6$)) was injected into the battery assembly to prepare a lithium secondary battery.

Example 2

Example 1 was repeated to prepare an organic/inorganic [(PVdF-CTFE/cyanoethylpolyvinylalcohol)/$BaTiO_3$] composite separator and a lithium secondary battery having the separator, except that cyanoethylpolyvinylalcohol was used instead of cyanoethylpullulan.

Example 3

Example 1 was repeated to prepare an organic/inorganic [(PVdF-CTFE/cyanoethylsucrose)/$BaTiO_3$] composite separator and a lithium secondary battery having the separator, except that cyanoethylsucrose was used instead of cyanoethylpullulan.

Example 4

Example 1 was repeated to prepare an organic/inorganic [(PVdF-HFP/cyanoethylpullulan)/$BaTiO_3$] composite separator and a lithium secondary battery having the separator, except that PVdF-HFP was used instead of PVdF-CTFE.

Example 5

Example 4 was repeated to prepare an organic/inorganic [(PVdF-HFP/cyanoethylpullulan)/PMNPT] composite separator and a lithium secondary battery having the separator, except that a PMNPT powder was used instead of the $BaTiO_3$ powder.

Example 6

Example 4 was repeated to prepare an organic/inorganic [(PVdF-HFP/cyanoethylpullulan)/$BaTiO_3$-Al_2O_3] composite separator and a lithium secondary battery having the separator, except that a mixed powder of $BaTiO_3$ and Al_2O_3 (a weight ratio: 90/10) was used instead of the $BaTiO_3$ powder.

Comparative Example 1

Example 1 was repeated to prepare a lithium secondary battery, except that a conventional polyethylene (PE) separator was used herein.

Analysis of Physical Properties of Organic/Inorganic Composite Separator

In order to analyze a surface of the organic/inorganic composite separator prepared according to the present invention, and a cross section of the active layer, a test was carried out, as described in the following.

The organic/inorganic composite separator [(PVdF-CTFE/cyanoethylpullulan)/$BaTiO_3$] prepared in Example 1 was used as a test sample, and a separator having a porous active layer was used as a control, the separator being formed so that it is not capable of having heterogeneity of morphology toward a thickness direction using PVdF-CTFE alone instead of the 2-compoment binder polymer prepared in Example 1.

The surfaces of the separators were analyzed using a scanning electron microscope (SEM). As a result, it was revealed that the organic/inorganic composite separator of the present invention includes an active layer and a support, wherein regular pores having a diameter of 1 μm or less are present in both of the active layer and the support (see FIG. **2**A and FIG. **3**A). Unlike the control separators in which most inorganic

materials are observed on the surfaces (see FIG. **2**B, FIG. **3**B), it was seen that the inorganic particles and the polymer layer are well-distributed in a quite amount on the surface of the organic/inorganic composite separator prepared in Example 1 (see FIG. **2**A).

FIG. **3** shows an SEM result showing a cross section of the organic/inorganic composite separators prepared in Example 1 and the control, respectively. It was seen that the polymer is present in a higher amount on a surface of the active layer than inside of the active layer in the case of the organic/inorganic composite separator of Example 1 (see FIG. **3**A). On the contrary, it was seen that the control has a homogenous composition on the surface as well as inside of the active layer (see FIG. **3**B). From the photographic results of the surfaces and cross sections of the above-mentioned separators, it was revealed that the organic/inorganic composite separator of the present invention has morphology heterogeneity, namely a morphology gradient formed in the active layer. Also, it was seen that the organic/inorganic composite separator of Example 1 has an improved surface peeling resistance due to the specific composition morphology (see FIG. **4**A), compared to that of the separator including the composite coating layer composed of conventional inorganic materials and a polymer (see FIG. **4**B).

Meanwhile, in order to objectively evaluate a lamination characteristic toward electrodes in the separator, two separators were adhered to each other at 100° C. under a pressure of 5.0 kgf/cm^2 to measure an adhesion force between the separators. As a result, it was revealed that an adhesion force of the control organic/inorganic composite separator is proven to be 3 gf/cm or less. Actually, the control separator was not easily laminated to the electrodes.

On the contrary, it was revealed that an adhesion force between the organic/inorganic composite separators prepared in Example 1 is high (10 gf/cm or more). Actually, the separator of Example 1 has a good lamination characteristic toward electrodes (see FIG. **5**).

Evaluation for Performance of Lithium Secondary Battery

The lithium secondary batteries including the organic/inorganic composite separator prepared in the present invention were evaluated for a high rate discharge characteristic, as follows.

The lithium secondary batteries prepared in Examples 1 to 6 and the control battery prepared in Comparative example 1 were used herein.

Each of the batteries having a battery capacity of 960 mAh was subject to cycling at a discharge rate of 0.5C, 1C and 2C. The discharge capacities of the batteries are listed in the following Table 1, wherein the capacity is expressed on the C-Rate basis.

From the experimental results, it was revealed that each of the batteries of Examples 1 to 6 including the separator having a morphology gradient shows a high-rate discharge (C-rate) characteristic comparable to that of the battery of Comparative example 1 including the conventional polyolefin separator in which the active layer is not coated until the discharge rate of 2C (see Table 1).

TABLE 1

Discharge Rate	Example 1	Example 2	Example 3	Example 4	Example 5	Example 6	Comparative example 1
0.5C	954	955	953	954	952	956	956
1C	944	945	942	943	944	945	945
2C	891	892	889	891	893	892	893

INDUSTRIAL APPLICABILITY

As described above, the organic/inorganic composite separator of the present invention may be useful to enhance peeling and scratch resistances of the porous active layer and improve a lamination characteristic toward electrodes by introducing a porous active layer onto a porous substrate having pores, the porous active layer having heterogeneity of morphology toward a thickness direction in which a content ratio of the binder polymer/inorganic particles present in a surface layer is higher than that of the binder polymer/inorganic particles present inside the surface layer. Accordingly, the stability and performances of a battery can be improved together since the detachment of inorganic particles from the porous active layer may be reduced during the assembly process of the electrochemical device.

What is claimed is:

1. An organic/inorganic composite separator comprising:

(a) a porous substrate having pores; and

(b) a porous active layer containing a mixture of inorganic particles and a binder polymer with which at least one surface of the porous substrate is coated,

wherein the porous active layer shows heterogeneity of composition morphology toward a thickness direction in which a content ratio of the binder polymer/inorganic particles present in a surface region of the porous active layer is higher than that of the binder polymer/inorganic particles present inside the porous active layer.

2. The organic/inorganic composite separator according to claim **1**, wherein the binder polymer interconnects and fixes the inorganic particles and pores are formed in the porous active layer due to the presence of interstitial volumes among the inorganic particles.

3. An electrochemical device comprising a cathode, an anode, a separator and electrolytes, wherein the separator is the organic/inorganic composite separator as defined in claim **2**.

4. The organic/inorganic composite separator according to claim **1**, wherein the inorganic particles are selected from the group consisting of inorganic particles having a dielectric constant of 5 or more, inorganic particles having lithium ion conductivity, and a mixture thereof.

5. The organic/inorganic composite separator according to claim **4**, wherein the inorganic particles having a dielectric constant of 5 or more are selected from the group consisting of $BaTiO_3$, $Pb(Zr,Ti)O_3$ (PZT), $Pb_{1-x}La_xZr_{1-y}O_3$ (PLZT), $PB(Mg_3Nb_{2/3})O_3$—$PbTiO_3$ (PMN-PT), hafnia (HfO_2), $SrTiO_3$, SnO_2, CeO_2, MgO, NiO, CaO, ZnO, ZrO_2, SiO_2, Y_2O_3, $A1_20_3$, SiC, TiO_2, and mixtures thereof.

6. The organic/inorganic composite separator according to claim **5**, wherein the inorganic particles having a dielectric

constant of 5 or more are selected from the group consisting of $BaTiO_3$, Pb(Zr,Ti)O_3 (PZT), $Pb_{1-x}La_xZr_{1-y}Ti_yO_3$(PLZT), $PB(Mg_3Nb_{2/3})O_3$—$PbTiO_3$(PMN-PT), hafnia (HfO_2), and mixtures thereof.

7. An electrochemical device comprising a cathode, an anode, a separator and electrolytes, wherein the separator is the organic/inorganic composite separator as defined in claim **6**.

8. The organic/inorganic composite separator according to claim **4**, wherein the inorganic particles having lithium ion conductivity are selected from the group consisting of lithium phosphate (Li_3PO_4), lithium titanium phosphate ($Li_xTi_y(PO_4)_3$, 0<x <2, 0<y<1, 0<z y<3), lithium aluminum titanium phosphate ($Li_xAl_yTi_z(PO_4)_3$, 0<x<2, 0<y<1, 0<z <3), (LiAlTiP)$_xO_y$ type glass (0<x<4, 0<y<13), lithium lanthanum titanate ($Li_xLa_yTiO_3$, 0<x<2, 0<y<3), lithium germanium thiophosphate ($Li_xGe_yP_zS_w$, 0<x<4, 0<y<1, 0<z<1, 0<w<5), lithium nitrides (Li_xN_y, 0<x<4, 0<y<2), SiS_2 ($Li_xSi_yS_z$, 0<x<3, 0<y<2, 0<z<4) type glass, P_2S_5 ($Li_xP_yS_z$, 0<x<3, 0<y<3, 0<z<7) type glass, and mixtures thereof.

9. An electrochemical device comprising a cathode, an anode, a separator and electrolytes, wherein the separator is the organic/inorganic composite separator as defined in claim **4**.

10. The organic/inorganic composite separator according to claim **1**, wherein the inorganic particles have a particle diameter of 0.001 to 10 μm.

11. The organic/inorganic composite separator according to claim **1**, wherein the binder polymer comprises a first binder polymer containing together at least one functional group selected from the group consisting of carboxy, maleic anhydride and hydroxy; and at least one functional group selected from the group consisting of cyano and acrylate.

12. The organic/inorganic composite separator according to claim **11**, wherein the first binder polymer contains a hydroxy group and a cyano group together.

13. The organic/inorganic composite. separator according to claim **12**, wherein the first binder polymer is selected from the group consisting of cyanoethylpullulan, cyanoethylpolyvinylalcohol, cyanoethylcellulose, cyanoethylsucrose and mixtures thereof.

14. An electrochemical device comprising a cathode, an anode, a separator and electrolytes, wherein the separator is the organic/inorganic composite separator as defined in claim **12**.

15. The organic/inorganic composite separator according to claim **11**, wherein the binder polymer further comprises a second binder polymer having a solubility parameter of 17 to 27 $MPa^{1/2}$.

16. The organic/inorganic composite separator according to claim **15**, wherein the second binder polymer contains a functional group selected from the group consisting of halogen, acrylate, acetate and cyano.

17. The organic/inorganic composite separator according to claim **15**, wherein the second binder polymer is selected from the group consisting of polyvinylidene fluoride-co-hexafluoropropylene, polyvinylidene fluoride-co-trichloroethylene, polymethylmethacrylate, polyacrylonitrile, polyvinylpyrrolidone, polyvinylacetate, polyethylene-co-vinyl acetate, polyimide, polyethylene oxide, cellulose acetate, cellulose acetate butyrate and cellulose acetate propionate.

18. The organic/inorganic composite separator according to claim **15**, wherein a content ratio of the first binder polymer the second binder polymer ranges from 0.1:99.9 to 99.9:0.1.

19. An electrochemical device comprising a cathode, an anode, a separator and electrolytes, wherein the separator is the organic/inorganic composite separator as defined in claim **15**.

20. An electrochemical device comprising a cathode, an anode, a separator and electrolytes, wherein the separator is the organic/inorganic composite separator as defined in claim **11**.

21. The organic/inorganic composite separator according to claim **1**, wherein a gel polymer electrolyte is formed by swelling the binder polymer in an electrolyte solution to be used.

22. The organic/inorganic composite separator according to claim **1**, wherein the porous active layer has an adhesion force of 5 gf/cm or more when the organic/inorganic composite separators adhere to each other at a temperature of 100°C. under a pressure of 5.0 kgf/cm_2.

23. An electrochemical device comprising a cathode, an anode, a separator and electrolytes, wherein the separator is the organic/inorganic composite separator as defined in claim **22**.

24. The organic/inorganic composite separator according to claim **1**, wherein the porous active layer has a thickness of 0.01 to 100 μm, a pore size of 0.001 to 10 μm and a porosity of 5 to 95%.

25. An electrochemical device comprising a cathode, an anode, a separator and electrolytes, wherein the separator is the organic/inorganic composite separator as defined in claim **24**.

26. The organic/inorganic composite separator according to claim **1**, wherein the porous substrate having pores is a polymer selected from the group consisting of

polyethyleneterephthalate, polybutyleneterephthalate, polyester, polyacetal, polyamide, polycarbonate, polyimide, polyetheretherketone, polyethersulfone, polyphenyleneoxide, polyphenylenesulfidro, polyethylenenaphthalene, high-density polyethylene, low-density polyethylene, linear low-density polyethylene, ultrahigh molecular weight polyethylene and polypropylene.

27. An electrochemical device comprising a cathode, an anode, a separator and electrolytes, wherein the separator is the organic/inorganic composite separator as defined in claim **26**.

28. The organic/inorganic composite separator according to claim **1**, wherein the porous substrate has a thickness of 1 to 100 μm, a pore size of 0.01 to 50 μm and a porosity of 10 to 95%.

29. An electrochemical device comprising a cathode, an anode, a separator and electrolytes, wherein the separator is the organic/inorganic composite separator as defined in claim **1**.

30. A method for manufacturing an organic/inorganic composite separator comprising a porous active layer, the method comprising:

(S1) preparing a solution of a first binder polymer containing together at least one functional group selected from the group consisting of carboxy, maleic anhydride and hydroxy; and at least one functional group selected from the group consisting of cyano and acrylate;

(S2)adding inorganic particles to the solution of the first binder polymer and dispersing the inorganic particles in the solution of the first binder polymer;

(S3)coating the solution of the first binder polymer having inorganic particles dispersed therein with a film and drying the coated film,

wherein the porous active layer shows heterogeneity of composition morphology toward a thickness direction in which a content ratio of the first binder polymer/inorganic particles present in a surface region of the porous active layer is higher than that of the first binder polymer/inorganic particles present inside the porous active layer.

31. The method for manufacturing an organic/inorganic composite separator according to claim **30**, wherein the first binder polymer contains a hydroxy group and a cyano group together.

32. The method for manufacturing an organic/inorganic composite separator according to claim **31**, wherein the first binder polymer is selected from the group consisting of cyanoethylpullulan, cyanoethylpolyvinylalcohol, cyanoethylcellulose, cyanoethylsucrose and mixtures thereof.

33. The method for manufacturing an organic/inorganic composite separator according to claim **30**, further comprising: dissolving a second binder polymer having a solubility parameter of 17 to 27 $MPa^{1/2}$ in the solution of the first binder polymer.

34. The method for manufacturing an organic/inorganic composite separator according to claim **33**, wherein the second binder polymer contains a functional group selected from the group consisting of halogen, acrylate, acetate and cyano.

35. The method for manufacturing an organic/inorganic composite separator according to claim **34**, wherein the second binder polymer is selected from the group consisting of polyvinylidene fluoride-co-hexafluoropropylene, polyvinylidene fluoride-co-trichloroethylene, polymethylmethacrylate, polyacrylonitrile, polyvinylpyrrolidone, polyvinylacetate, polyethylene-co-vinyl acetate, polyimide, polyethylene oxide, cellulose acetate, cellulose acetate butyrate, cellulose acetate propionate, pullulan and polyvinylalcohol.

36. The method for manufacturing an organic/inorganic composite separator according to claim **33**, wherein a content ratio of the first binder polymer : the second binder polymer ranges from 0.1:99.9 to 99.9:0.1.

* * * * *

Appendix O

A basic guide to particle characterization

PARTICLE SIZE

PARTICLE SHAPE

Introduction

The aim of this guide is to provide you with a basic grounding in the main particle characterization techniques currently in use within industry and academia. It assumes no prior knowledge of particle characterization theory or instrumentation and should be ideal for those new to particle characterization, or those wishing to reinforce their knowledge in the area. The guide covers introductory basics, particle characterization theory and particle characterization instrumentation, as well as a quick reference guide to help you decide which techniques might be most appropriate for your particle characterization needs.

What is a particle?

At the most basic level, we can define a particle as being a discrete sub-portion of a substance. For the purposes of this guide, we shall narrow the definition to include solid particles, liquid droplets or gas bubbles with physical dimensions ranging from sub-nanometer to several millimeters in size.

The most common types of materials consisting of particles are:

- powders and granules e.g. pigments, cement, pharmaceutical ingredients
- suspensions, emulsions and slurries e.g. vaccines, milk, mining muds
- aerosols and sprays e.g. asthma inhalers, crop protection sprays.

Why measure particle properties?

There are two main reasons why many industries routinely employ particle characterization within their businesses.

1. Better control of product quality

In an increasingly competitive global economy, better control of product quality delivers real economic benefits such as:

- ability to charge a higher premium for your product
- reduce customer rejection rates and lost orders
- demonstrate compliance in regulated markets.

©2015 Malvern Instruments Limited

2. Better understanding of products, ingredients and processes

In addition to controlling product quality, a better understanding of how particle properties affect your products, ingredients and processes will allow you to:

- improve product performance
- troubleshoot manufacturing and supply issues
- optimize the efficiency of manufacturing processes
- increase output or improve yield
- stay ahead of the competition.

Which particle properties are important to measure?

In addition to chemical composition, the behavior of particulate materials is often dominated by the physical properties of the constituent particles. These can influence a wide range of material properties including, for example, reaction and dissolution rates, how easily ingredients flow and mix, or compressibility and abrasivity. From a manufacturing and development perspective, some of the most important physical properties to measure are:

- particle size
- particle shape
- surface properties
- mechanical properties
- charge properties
- microstructure.

Depending upon the material of interest, some or all of these could be important and they may even be interrelated: e.g. surface area and particle size. For the purposes of this guide, we will concentrate on two of the most significant and easy to measure properties - particle size and particle shape.

Particle Properties

Particle size

By far the most important physical property of particulate samples is particle size. Particle size measurement is routinely carried out across a wide range of industries and is often a critical parameter in the manufacture of many products. Particle size has a direct influence on material properties such as:

- reactivity or dissolution rate e.g. catalysts, tablets
- stability in suspension e.g. sediments, paints
- efficacy of delivery e.g. asthma inhalers
- texture and feel e.g. food ingredients
- appearance e.g. powder coatings and inks
- flowability and handling e.g. granules
- viscosity e.g. nasal sprays
- packing density and porosity e.g. ceramics.

Measuring particle size and understanding how it affects your products and processes can be critical to the success of many manufacturing businesses.

How do we define particle size?

CosMX Exhibit 1003, Page 376 of 512

Particles are 3-dimensional objects, and unless they are perfect spheres (e.g. emulsions or bubbles), they cannot be fully described by a single dimension such as a radius or diameter.

In order to simplify the measurement process, it is often convenient to define the particle size using the concept of equivalent spheres. In this case the particle size is defined by the diameter of an equivalent sphere having the same property as the actual particle such as volume or mass for example. It is important to realize that different measurement techniques use different equivalent sphere models and therefore will not necessarily give exactly the same result for the particle diameter.

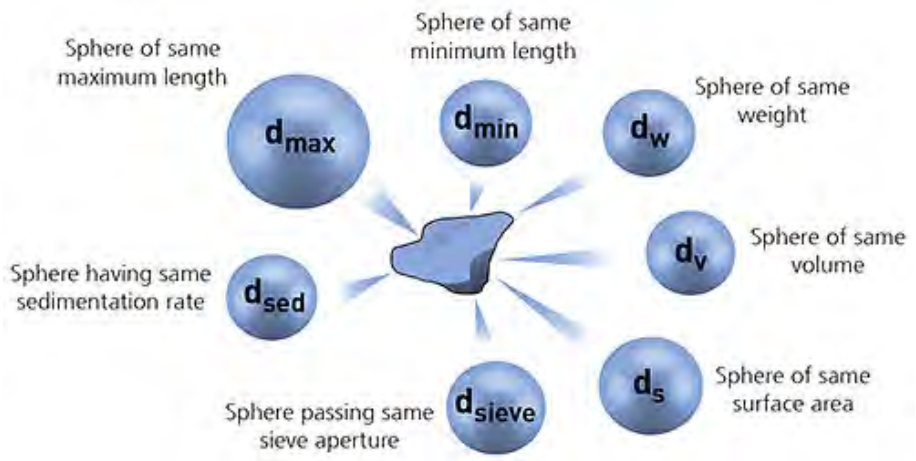


Figure 1: Illustration of the concept of equivalent spheres.

The equivalent sphere concept works very well for regular shaped particles. However, it may not always be appropriate for irregular shaped particles, such as needles or plates, where the size in at least one dimension can differ significantly from that of the other dimensions.

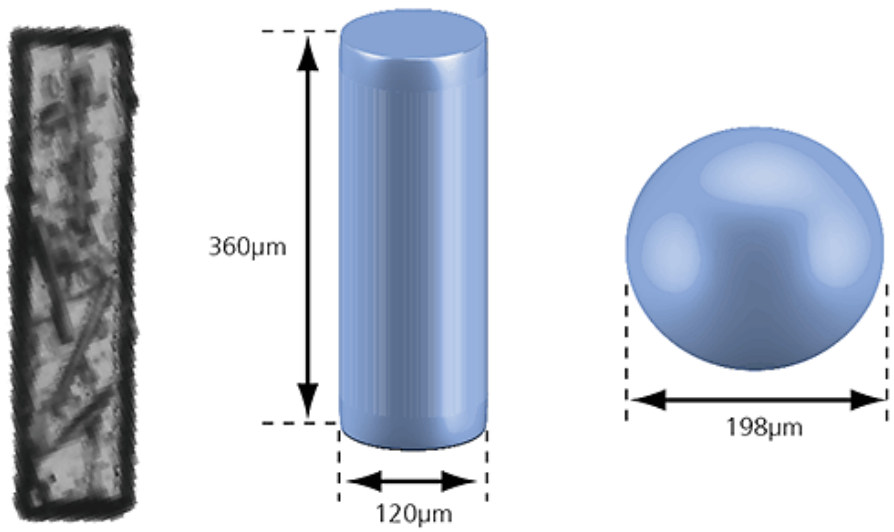


Figure 2: Illustration of the volume equivalent rod and sphere of a needle shaped particle.

In the case of the rod shaped particle shown in the image above, a volume equivalent sphere would give a particle diameter of 198µm, which is not a very accurate description of its true dimensions. However, we can also define the

CosMX Exhibit 1003, Page 377 of 512

particle as a cylinder with the same volume which has a length of 360µm and a width of 120µm. This approach more accurately describes the size of the particle and may provide a better understanding of the behavior of this particle during processing or handling for example.

Many particle sizing techniques are based on a simple 1-dimensional sphere equivalent measuring concept, and this is often perfectly adequate for the required application. Measuring particle size in two or more dimensions can sometimes be desirable but can also present some significant measurement and data analysis challenges. Therefore careful consideration is advisable when choosing the most appropriate particle sizing technique for your application.

Particle size distributions

Unless the sample you wish to characterize is perfectly mono disperse, i.e. every single particle has exactly the same dimensions, it will consist of a statistical distribution of particles of different sizes. It is common practice to represent this distribution in the form of either a frequency distribution curve, or a cumulative (undersize) distribution curve.

Weighted distributions

A particle size distribution can be represented in different ways with respect to the weighting of individual particles. The weighting mechanism will depend upon the measuring principle being used.

Number weighted distributions

A counting technique such as image analysis will give a number weighted distribution where each particle is given equal weighting irrespective of its size. This is most often useful where knowing the absolute number of particles is important - in foreign particle detection for example - or where high resolution (particle by particle) is required.

Volume weighted distributions

Static light scattering techniques such as laser diffraction will give a volume weighted distribution. Here the contribution of each particle in the distribution relates to the volume of that particle (equivalent to mass if the density is uniform), i.e. the relative contribution will be proportional to (size)3. This is often extremely useful from a commercial perspective as the distribution represents the composition of the sample in terms of its volume/mass, and therefore its potential $ value.

Intensity weighted distributions

Dynamic light scattering techniques will give an intensity weighted distribution, where the contribution of each particle in the distribution relates to the intensity of light scattered by the particle. For example, using the Rayleigh approximation, the relative contribution for very small particles will be proportional to (size)6.

When comparing particle size data for the same sample measured by different techniques, it is important to realize that the types of distribution being measured and reported can produce very different particle size results. This is clearly illustrated in the example below, for a sample consisting of equal numbers of particles with diameters of 5nm and 50nm. The number weighted distribution gives equal weighting to both types of particles, emphasising the presence of the finer 5 nm particles, whereas the intensity weighted distribution has a signal

CosMX Exhibit 1003, Page 378 of 512

one million times higher for the coarser 50nm particles. The volume weighted distribution is intermediate between the two.

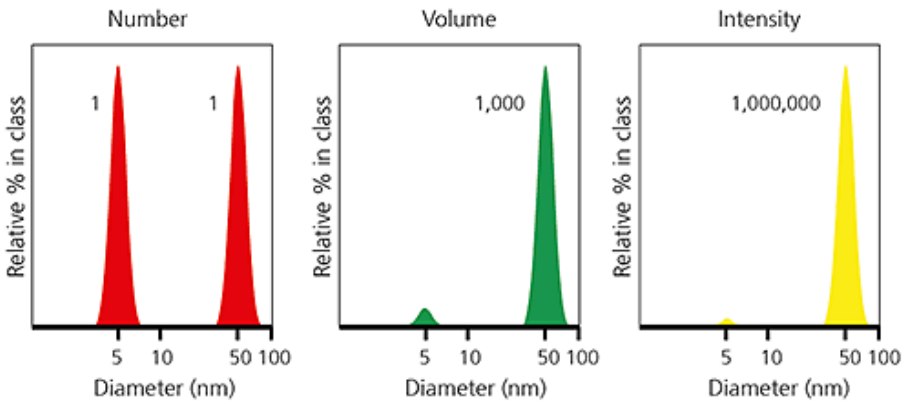


Figure 3: Example of number, volume and intensity weighted particle size distributions for the same sample.

It is possible to convert particle size data from one type of distribution to another, however this requires certain assumptions about the form of the particle and its physical properties. One should not necessarily expect, for example, a volume weighted particle size distribution measured using image analysis to agree exactly with a particle size distribution measured by laser diffraction.

Distribution statistics

"There are three kinds of lies: lies, damned lies, and statistics."

Twain, Disraeli

In order to simplify the interpretation of particle size distribution data, a range of statistical parameters can be calculated and reported. The choice of the most appropriate statistical parameter for any given sample will depend upon how that data will be used and what it will be compared with. For example, if you wanted to report the most common particle size in your sample you could choose between the following parameters:

• mean - 'average' size of a population

• median - size where 50% of the population is below/above

• mode - size with highest frequency.

If the shape of the particle size distribution is asymmetric, as is often the case in many samples, you would not expect these three values to be exactly equivalent, as illustrated below.

CosMX Exhibit 1003, Page 379 of 512

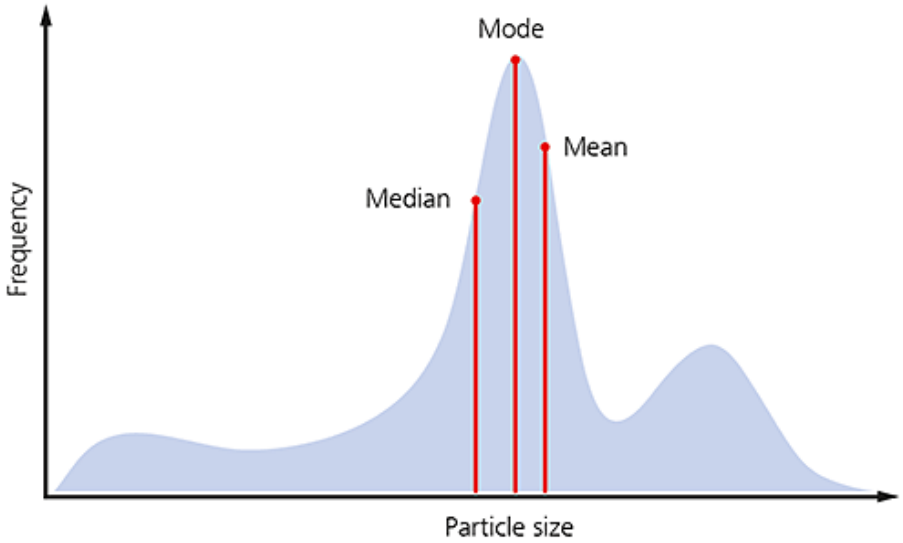


Figure 4: Illustration of the median mode and mean for a particle size distribution.

Means

There are many different means that can be defined depending upon how the distribution data are collected and analyzed. The three most commonly used for particle sizing are described below.

1. Number length mean D[1,0] or Xnl

The number length mean, often referred to as the arithmetic mean, is most important where the number of particles is of interest e.g. in particle counting applications. It can only be calculated if we know the total number of particles in the sample and is therefore limited to particle counting applications.

2. Surface area moment mean D[3, 2] or Xsv

The surface area mean (Sauter Mean Diameter) is most relevant where specific surface area is important e.g. bioavailability, reactivity, dissolution. It is most sensitive to the presence of fine particulates in the size distribution.

3. Volume moment mean D[4, 3] or Xvm

The volume moment mean (De Brouckere Mean Diameter) is relevant for many samples as it reflects the size of those particles which constitute the bulk of the sample volume. It is most sensitive to the presence of large particulates in the size distribution.

An example of the surface area and volume moment means is shown in the particle size distribution below. If the aim is to monitor the size of the coarse particulates that make up the bulk of this sample, then the D[4,3] would be most appropriate. If, on the other hand, it is actually more important to monitor the proportion of fines present, then it might be more appropriate to use the D[3,2].

CosMX Exhibit 1003, Page 380 of 512

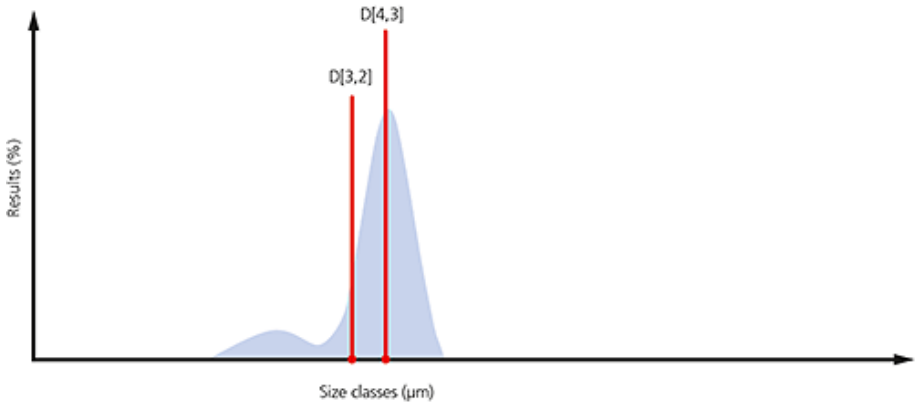


Figure 5: Illustration of the D[4,3] and D[3,2] on a particle size distribution where a significant proportion of fines are present.

Percentiles

For volume weighted particle size distributions, such as those measured by laser diffraction, it is often convenient to report parameters based upon the maximum particle size for a given percentage volume of the sample.

Percentiles are defined as XaB where:

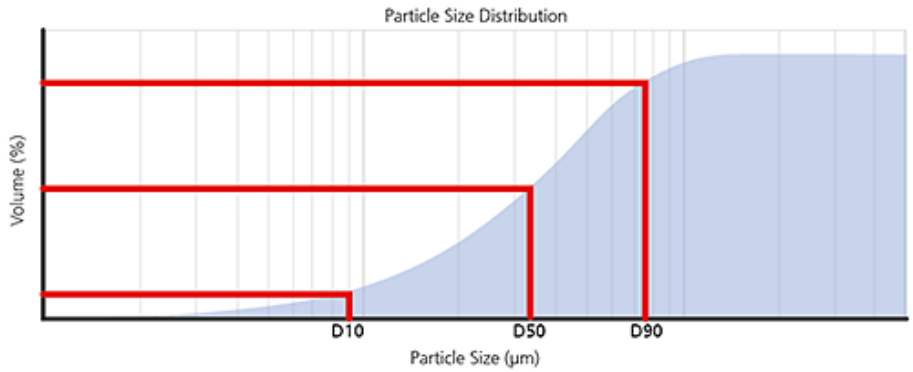
X= parameter, usually D for diameter

a = distribution weighting, e.g. n for number, v for volume, i for intensity

B = percentage of sample below this particle size e.g. 50%, sometimes written as a decimal fraction i.e. 0.5

For example, the Dv50 would be the maximum particle diameter below which 50% of the sample volume exists - also known as the median particle size by volume.

The most common percentiles reported are the Dv10, Dv50 and Dv90, as illustrated in the frequency and cumulative plots below.



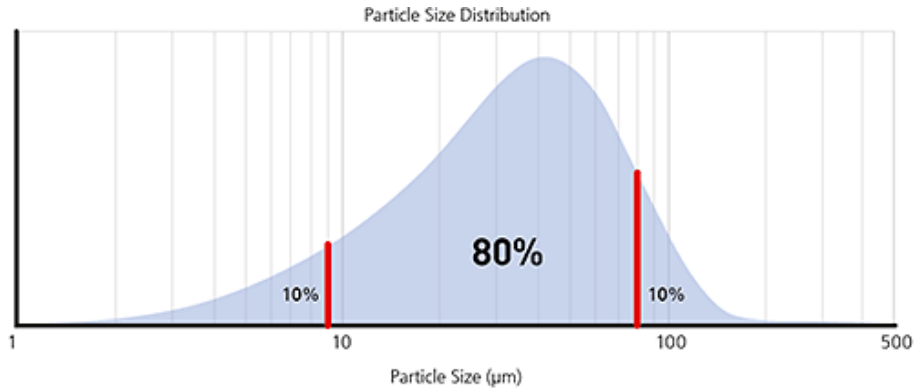


Figure 6: Illustration of volume percentiles in terms of cumulative and frequency plots.

By monitoring these three parameters it is possible to see if there are significant changes in the main particle size, as well as changes at the extremes of the distribution, which could be due to the presence of fines, or oversized particles/ agglomerates as shown in the particle size distribution below.

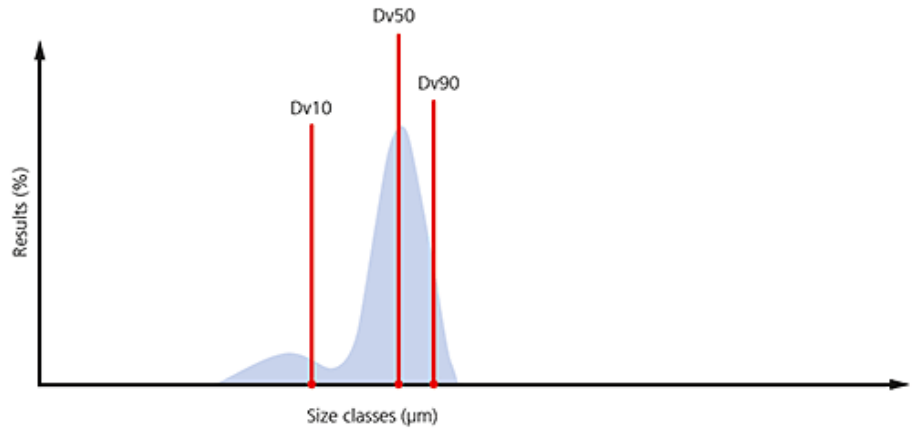


Figure 7: Illustration of the Dv10, Dv50 and Dv90 on a typical particle size distribution where a significant proportion of fines are present.

Particle shape

As well as particle size, the shape of constituent particles can also have a significant impact upon the performance or processing of particulate materials. Many industries are now also making particle shape measurements in addition to particle size in order to gain a better understanding of their products and processes. Some areas where particle shape can have an impact include:

- reactivity and solubility e.g. pharmaceutical actives
- powder flow and handling e.g. drug delivery systems
- ceramic sinter properties e.g. ceramic filters
- abrasive efficiency e.g. SiC wire saws
- texture and feel e.g. food ingredients.

Particle shape can also be used to determine the state of dispersion of particulate materials, specifically if agglomerates or primary particles are present.

How do we define particle shape?

CosMX Exhibit 1003, Page 382 of 512

Particles are complex 3-dimensional objects and, as with particle size measurement, some simplification of the description of the particle is required in order to make measurement and data analysis feasible. Particle shape is most commonly measured using imaging techniques, where the data collected is a 2-dimensional projection of the particle profile. Particle shape parameters can be calculated from this 2-dimensional projection using simple geometrical calculations.

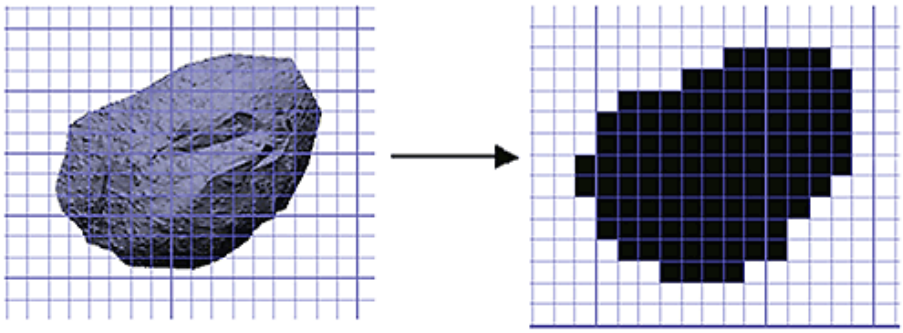


Figure 8: Conversion of a particle image into a 2D binary projection for shape analysis.

Particle form

The overall form of a particle can be characterized using relatively simple parameters such as aspect ratio. If we take as an example the image of the particle below, the aspect ratio can simply be defined as:

Aspect ratio =width/length

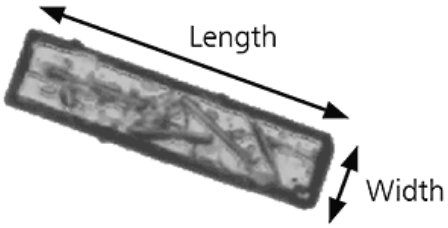


Figure 9: Illustration of length and width on a needle shaped particle image.

Aspect ratio can be used to distinguish between particles that have regular symmetry, such as spheres or cubes, and particles with different dimensions along one axis, such as needle shapes or ovoid particles. Other shape parameters that can be used to characterize particle form include elongation and roundness.

Particle outline

As well as detecting agglomerated particles, the outline of a particle can provide information about properties such as surface roughness. In order to calculate particle outline parameters, a concept known as the convex hull perimeter is used. In simple terms the convex hull perimeter is calculated from an imaginary elastic band which is stretched around the outline of the particle image, as shown in the image below.

CosMX Exhibit 1003, Page 383 of 512

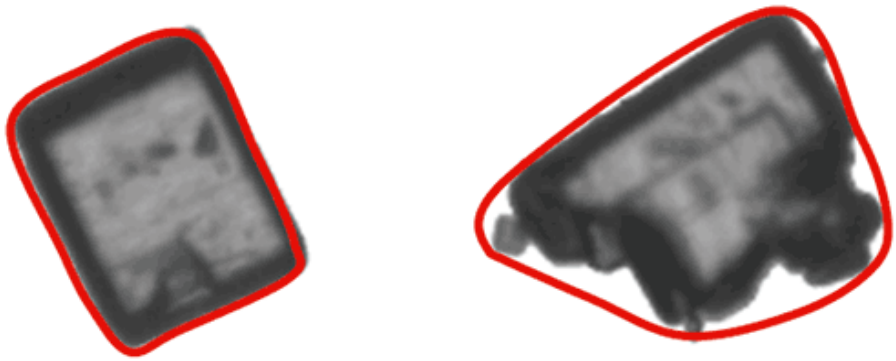


Figure 10: Illustration of the convex hull for two different shapes of particle.

Once the convex hull perimeter has been calculated we can then define parameters based upon it, such as convexity or solidity where:

• convexity = convex hull perimeter/actual perimeter

• solidity = area bound by actual perimeter/area bound by convex hull perimeter

Particles with very smooth outlines will have a convexity/solidity value close to 1, whereas particles with rough outlines, or agglomerated primary particles, will have consequently lower convexity/solidity values.

Universal shape parameters

Some shape parameters capture changes in both particle form and outline. Monitoring these can be useful where both form and outline may influence the behaviour of the material being measured. The most commonly used parameter is circularity where

• Circularity* = perimeter/perimeter of an equivalent area circle

*This is sometimes defined as:

(perimeter/perimeter of an equivalent area circle)2

where it is also referred to as HS circularity to avoid confusion with the above definition.

Circularity is often used to measure how close a particle is to a perfect sphere, and can be applied in monitoring properties such as abrasive particle wear. However, care should be exercised in interpreting the data, since any deviations could be due to either changes in surface roughness or physical form, or both.

While circularity can be very useful for some applications, it is not suitable for all situations. To date, there is no definition of a universal shape parameter that will work in every case. In reality, careful consideration is necessary to determine the most suitable parameter for each specific application.

Zeta potential

Zeta potential is a measure of the magnitude of the electrostatic or charge repulsion or attraction between particles in a liquid suspension. It is one of the fundamental parameters known to affect dispersion stability. Its measurement brings detailed insight into the causes of dispersion, aggregation or flocculation,

CosMX Exhibit 1003, Page 384 of 512

and can be applied to improve the formulation of dispersions, emulsions and suspensions.

The speed with which new formulations can be introduced is the key to product success. Measuring zeta potential is one of the ways to shorten stability testing, by reducing the number of candidate formulations and hence minimizing the time and cost of testing as well as improving shelf life.

In water treatment, monitoring dosage using zeta potential measurements can reduce the cost of chemical additives by optimizing dosage control.

Zeta potential measurement has important applications in a wide range of industries including: ceramics, pharmaceuticals, medicine, mineral processing, electronics and water treatment.

Particle Characterization Techniques

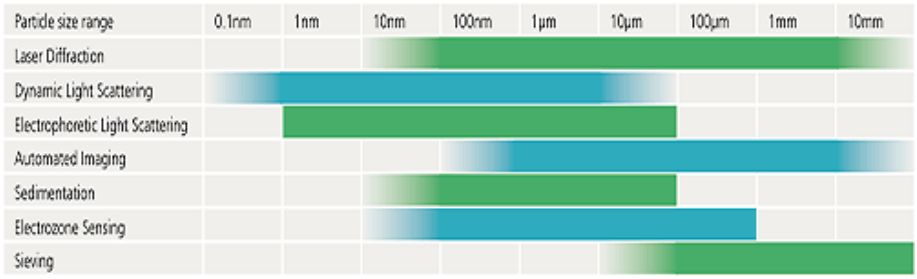
There is a wide range of commercially available particle characterization techniques that can be used to measure particulate samples. Each has its relative strengths and limitations and there is no universally applicable technique for all samples and all situations.

Which particle characterization techniques do I need?

A number of criteria must be considered when deciding which particle characterization techniques you need:

- which particle properties are important to me?
- what particle size range do I want to work over?
- are my samples polydisperse i.e. do I need a wide dynamic range?
- how quickly do I need to be able to make measurements?
- do I need to measure at high resolution?
- do I need good statistical sampling for robust QC measurement?
- do I need to disperse my sample wet or dry?
- how much money am I prepared to spend?

The following table is designed to provide some basic guidelines to help you decide which of some of the commonly used techniques could be most suitable for a particular application. The particle size ranges indicated are a guide only and exact specifications may vary from one instrument to another.



CosMX Exhibit 1003, Page 385 of 512

Technique	Size	Shape	Zeta potential	Dynamic range	Rapid	Resolution	Sampling	Wet	Dry
Laser Diffraction	●			●●●●	●●●	●●	●●●	●	●
Dynamic Light Scattering	●			●●●	●●●	●●	●●	●	
Electrophoretic Light Scattering			●	●●●	●●●	●●	●●	●	
Automated Imaging	●	●		●●	●●	●●●	●●	●	●
Sedimentation	●			●●	●	●●	●●	●	
Electrozone Sensing	●			●	●●	●●●	●	●	
Sieving	●			●	●	●	●	●	●

Sampling

Virtually all particle characterization techniques will involve a degree of subsampling in order to make a measurement. Even particle counting applications where the entire contents of a syringe are measured, for example, will only examine a small fraction of all the syringes on a production line.

It is worth pointing out that the root cause of issues around unreliable measurements is very often related in some way to sampling. It is therefore essential that the subsample measured by the instrument is as representative as possible of the whole.

Where instruments (laser diffraction for example) require presentation of the sample as a stable dispersion, the effects of any sampling issues are minimized by homogenizing, stirring and recirculating the material. This does not, however, deal with the challenge of taking a representative 10g aliquot from a 10,000 kg batch for example.

One common method that is widely used to increase the robustness of powder sampling is a device known as a spinning riffler.

CosMX Exhibit 1003, Page 386 of 512

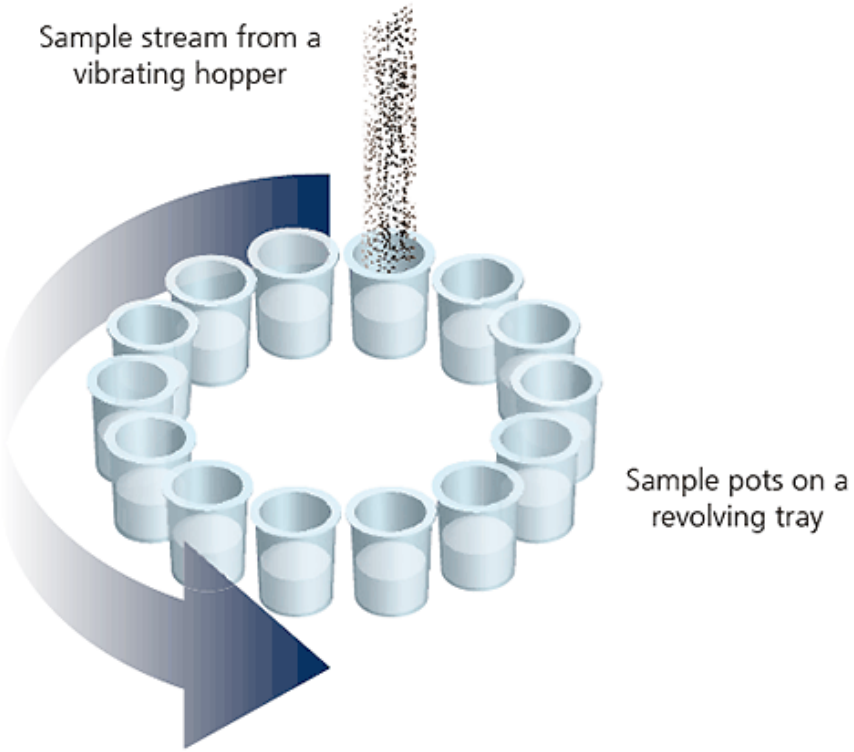


Figure 11: Illustration of a spinning riffler device.

In the spinning riffler, a number of subsamples are taken at regular intervals from powder flowing through a hopper into a rotating array of containers. This ensures that if any sample segregation takes place within the hoppers each container should contain a representative subsample.

Sample dispersion

Many particle characterization techniques require the sample to be analyzed in some sort of dispersed form where the individually particles are spatially separated. In order to do this there are two basic approaches:

- wet dispersion - particles dispersed in a liquid
- dry dispersion - particles dispersed in a gas (usually air).

Wet dispersion

In a wet dispersion, individual particles are suspended in a liquid dispersant. The wetting of the particle surfaces by the dispersant molecules lowers their surface energy, reducing the forces of attraction between touching particles. This allows them to be separated and go into suspension.

For dispersants with high surface tension, such as water, the addition of a small amount of surfactant can significantly improve the wetting behavior and subsequent particle dispersion.

In order to disperse individual particles it is usual to apply some energy to the sample. Often this is through stirring or agitation, but for very fine materials or strongly bound agglomerates ultrasonic irradiation is sometimes used.

CosMX Exhibit 1003, Page 387 of 512

In microscopy based techniques, wet sample preparation methods can be used to initially disperse the sample onto a microscope slide. Subsequent evaporation of the dispersant then allows analysis of the dispersed particles in the dry state.

Dry dispersion

In a dry powder dispersion, the dispersant is usually a flowing gas stream, most typically clean dry air. The nature of the dry dispersion process means this is normally a higher energy process than wet dispersion. As shown below, three different types of dispersion mechanism act upon the sample. In order of increasing energy input they are:

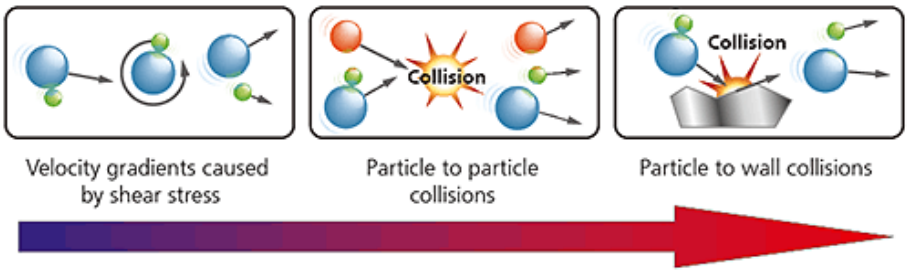


Figure 12: Illustration of the three dry powder dispersion mechanisms with increasing energy/ aggressivity.

The dispersion mechanism that is most dominant will depend upon the design of the disperser, with particle-wall impaction providing a more aggressive high energy dispersion than particle-particle collisions or shear stresses.

By eliminating the need to dispose of costly and potentially harmful solvents, dry dispersion is often an attractive option. However, dry dispersion is not suitable for very fine powders (<1 micron) because the high particle-particle forces of attraction in these materials are very difficult to overcome. Care is also needed with fragile particles to ensure that only sufficient energy is applied to the sample to obtain dispersion and that particles are not being broken during the dispersion process. In such cases a wet dispersion method should be used as a method validation reference.

Techniques : Laser Diffraction Particle Sizing

Laser diffraction is a widely used particle sizing technique for materials ranging from hundreds of nanometers up to several millimeters in size. The main reasons for its success are:

- wide dynamic range - from submicron to the millimetre size range
- rapid measurements - results generated in less than a minute
- repeatability - large numbers of particles are sampled in each measurement
- instant feedback - monitor and control the particle dispersion process
- high sample throughput - hundreds of measurements per day
- calibration not necessary - easily verified using standard reference materials
- well-established technique - covered by ISO13320 (2009).

Principles

Laser diffraction measures particle size distributions by measuring the angular variation in intensity of light scattered as a laser beam passes through a dispersed particulate sample. Large particles scatter light at small angles relative to the laser beam and small particles scatter light at large angles, as illustrated below.

CosMX Exhibit 1003, Page 388 of 512

The angular scattering intensity data is then analyzed to calculate the size of the particles responsible for creating the scattering pattern, using the Mie theory of light scattering. The particle size is reported as a volume equivalent sphere diameter.

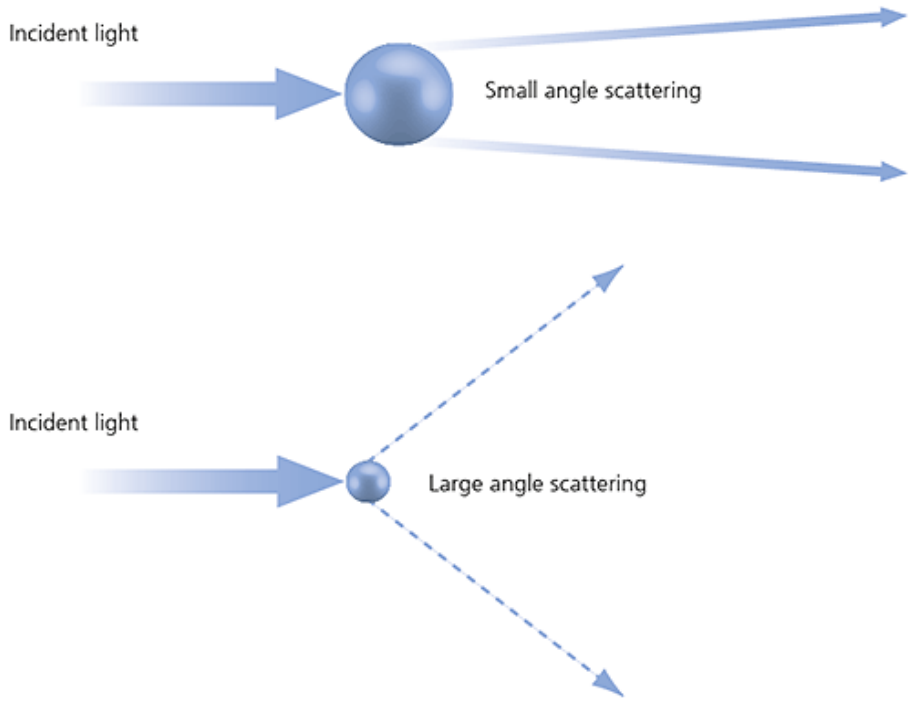


Figure 13: Scattering of light from small and large particles.

Optical properties

Laser diffraction uses Mie theory of light scattering to calculate the particle size distribution, assuming a volume equivalent sphere model.

Mie theory requires knowledge of the optical properties (refractive index and imaginary component) of both the dispersant and the sample being measured.

Usually the optical properties of the dispersant are relatively easy to find from published data, and many modern instruments will have in-built databases that include common dispersants.

For samples where the optical properties are not known, the user can either measure them or make an educated guess and use an iterative approach based upon the fit of the modelled data versus the actual.

A simplified approach is to use the Fraunhofer approximation, which does not require the optical properties of the sample. However it should be used with caution whenever working with samples which might have particles below 50µm or where the particles are relatively transparent.

Instrumentation

A typical laser diffraction system is made up of three main elements:

1. Optical bench. A dispersed sample passes though the measurement area of the optical bench, where a laser beam illuminates the particles. A series of detectors

CosMX Exhibit 1003, Page 389 of 512

then accurately measure the intensity of light scattered by the particles within the sample over a wide range of angles.

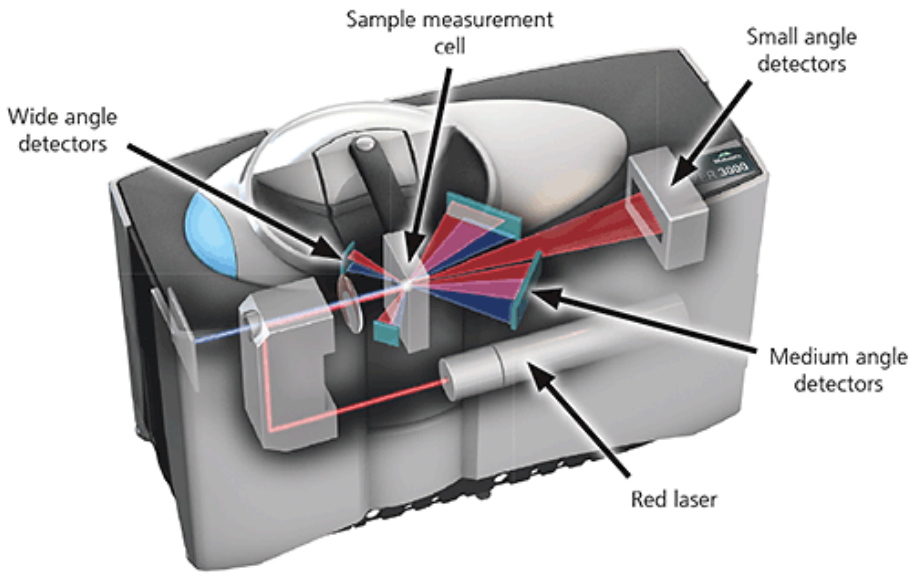


Figure 14: Optical layout of a state-of the-art laser diffraction instrument.

2. Sample dispersion units. Sample handling and dispersion are controlled by sample dispersion units designed to either measure the sample wet or dry. These ensure the particles are delivered to the measurement area of the optical bench at the correct concentration and in a suitable, stable state of dispersion.

Wet sample dispersion units use a liquid dispersant, aqueous or solvent based, to disperse the sample. In order to keep the sample suspended and homogenized it is recirculated continuously through the measurement zone.

Dry powder sample dispersion units suspend the sample in a flowing gas stream, usually dry air. Normally the entire sample passes once only through the measuring zone, therefore it is desirable to capture data at rapid speeds, typically up to 10kHz, in order to ensure representative sample measurement.

3. Instrument software. The instrument software controls the system during the measurement process and analyzes the scattering data to calculate a particle size distribution. In more advanced instrumentation it also provides both instant feedback during method development and expert advice on the quality of the results.

The application of laser diffraction is covered by the international standard ISO 13320: 2009, which is highly recommended reading for anyone who uses this technique on a routine basis.

CosMX Exhibit 1003, Page 390 of 512

Techniques : Dynamic Light Scattering

Dynamic light scattering (DLS), sometimes referred to as Photon Correlation Spectroscopy (PCS) or Quasi-Elastic Light Scattering (QELS), is a non-invasive, well-established technique for measuring the size of particles and macromolecules typically in the submicron region down to below 1 nanometre. It can be used to measure samples which consist of particles suspended in a liquid e.g. proteins, polymers, micelles, carbohydrates, nanoparticles, colloidal dispersions, and emulsions

Key advantages include:

- particle size range ideal for nano and biomaterials
- small quantity of sample required
- fast analysis and high throughput
- non-invasive allowing complete sample recovery.

Principles

Particles in suspension undergo Brownian motion caused by thermally induced collisions between the suspended particles and solvent molecules.

If the particles are illuminated with a laser, the intensity of the scattered light fluctuates over very short timescales at a rate that is dependent upon the size of the particles; smaller particles are displaced further by the solvent molecules and move more rapidly. Analysis of these intensity fluctuations yields the velocity of the Brownian motion and hence the particle size using the Stokes-Einstein relationship.

The diameter measured in Dynamic Light Scattering is called the hydrodynamic diameter and refers to the way a particle diffuses within a fluid. The diameter obtained by this technique is that of a sphere that has the same translational diffusion coefficient as the particle being measured.

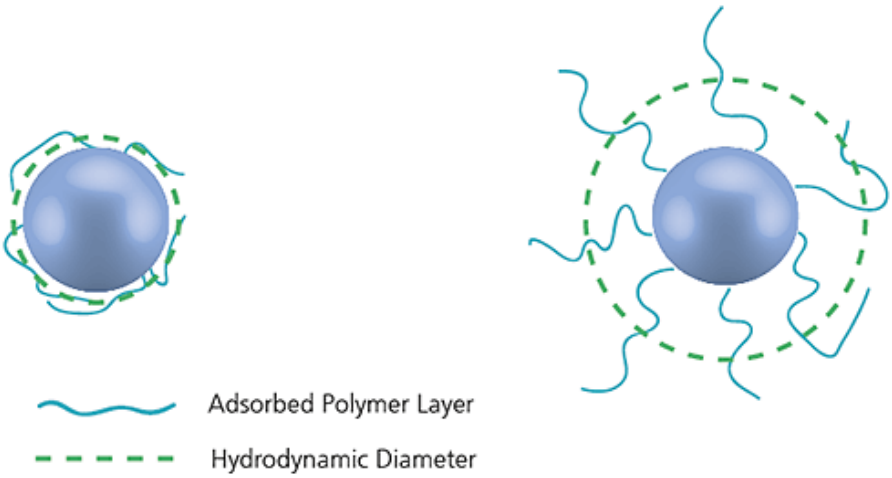


Figure 15: Illustration of the reported hydrodynamic diameter in DLS being larger than the 'core' diameter.

The translational diffusion coefficient will depend not only on the size of the particle 'core', but also on any surface structure, as well as the concentration and type of ions in the medium. This means that the size will be larger than measured

CosMX Exhibit 1003, Page 391 of 512

by electron microscopy, for example, where the particle is removed from its native environment.

It is important to note that dynamic light scattering produces an intensity weighted particle size distribution, which means that the presence of oversized particles can dominate the particle size result.

Instrumentation

A conventional dynamic light scattering instrument consists of a laser light source, which converges to a focus in the sample using a lens. Light is scattered by the particles at all angles and a single detector, traditionally placed at 90° to the laser beam, collects the scattered light intensity. The intensity fluctuations of the scattered light are converted into electrical pulses, which are fed into a digital correlator. This generates the autocorrelation function, from which the particle size is calculated.

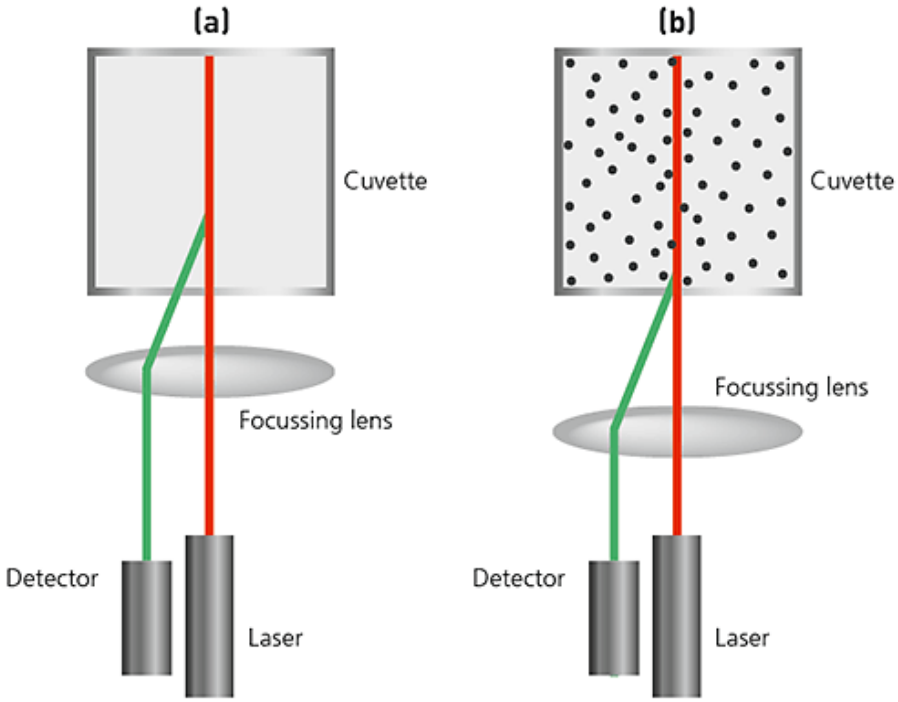
NIBS

In state-of-the art instruments, NIBS (Non-Invasive Back-scatter) technology extends the range of sizes and concentrations of samples that can be measured.

The sizing capability in these instruments detects the light scattered at 173° as shown below. This is known as backscatter detection. In addition, the optics are not in contact with the sample and hence the detection optics are said to be non-invasive.

There are many advantages of using non-invasive backscatter detection:

- sensitivity is improved
- a wider range of sample concentrations can be measured
- sample preparation is simplified



(a) For small particles, or samples at low concentrations, it is beneficial to maximize the amount of scattering from the sample. As the laser passes through

CosMX Exhibit 1003, Page 392 of 512

the wall of the cuvette, the difference in refractive index between the air and the material of the cuvette causes 'flare'. This flare may interfere with the signal from the scattering particles. Moving the measurement position away from the cuvette wall towards the centre of the cuvette will remove this effect.

(b) Large particles or samples at high concentrations scatter much more light. Measuring closer to the cuvette wall reduces the effect of multiple scattering by minimizing the path length through which the scattered light has to pass.

Techniques: Automated Imaging

Automated imaging is a high resolution direct technique for characterizing particles from around 1 micron up to several millimeters in size. Individual particle images are captured from dispersed samples and analyzed to determine their particle size, particle shape and other physical properties. Statistically representative distributions can be constructed by measuring tens to hundreds of thousands of particles per measurement.

Static imaging systems require a stationary dispersed sample whereas in dynamic imaging systems the sample flows past the image capture optics. The technique is often used in conjunction with ensemble based particle sizing methods such as laser diffraction, to gain a deeper understanding of the sample or to validate the ensemble based measurements. Typical applications include:

- measurement of shape differences where particle size alone does not give differentiation
- detection and/or enumeration of agglomerates, oversized particles or contaminant particles
- size measurement of non-spherical particles such as needle shaped crystals
- validation of ensemble based particle size measurements such as laser diffraction.

Instrumentation

A typical automated imaging system is composed of three main elements;

1. Sample presentation and dispersion

This step is critical to getting good results: spatial separation of individual particles and agglomerates in the field of view is the goal. A range of sample presentation methods is available depending upon the type of sample and instrumentation employed. Dynamic imaging instrumentation uses a flow cell through which the sample passes during the measurement. Static imaging techniques use a flat surface such as a microscope slide, a glass plate or a filter membrane, for example. Automated dispersion methods are desirable to avoid potential operator variability.

CosMX Exhibit 1003, Page 393 of 512

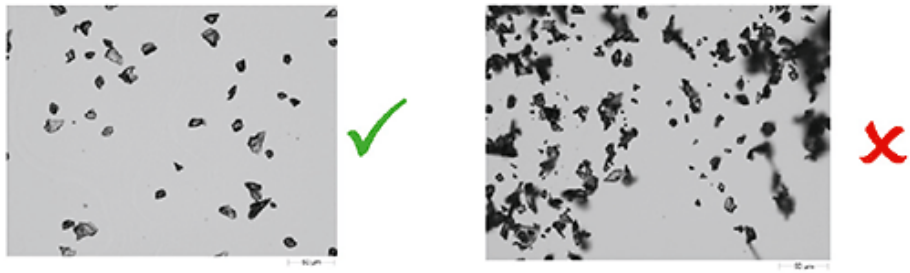


Figure 17: Illustration of the importance of sample dispersion for automated particle imaging.

2. Image capture optics

Images of individual particles are captured using a digital ccd camera with appropriate magnification optics for the sample in question. In dynamic imaging systems the sample is typically illuminated from behind the sample whereas static imaging systems offer more flexibility in terms of the sample illumination e.g. episcopic, diascopic, darkfield, etc. Polarizing optics can also be used for birefringent materials such as crystals. The most advanced dynamic imaging systems use a hydrodynamic sheath flow mechanism to achieve consistent focus for even very fine particles.

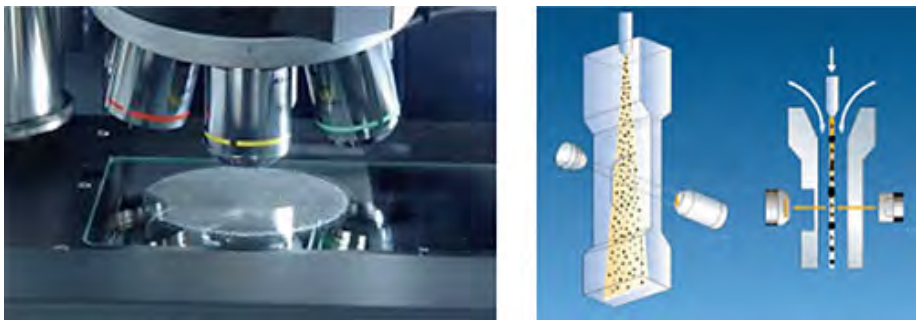


Figure 18: Illustration of static imaging (left) and dynamic imaging (right) optical arrangements.

3. Data analysis software

Typical instruments measure and record a range of morphological properties for each particle. In the most advanced instruments, graphing and data classification options in the software ensure that extracting the relevant data from your measurement is as straightforward as possible, via an intuitive visual interface. Individually stored grayscale images for each particle provide qualitative verification of the quantitative results.

CosMX Exhibit 1003, Page 394 of 512

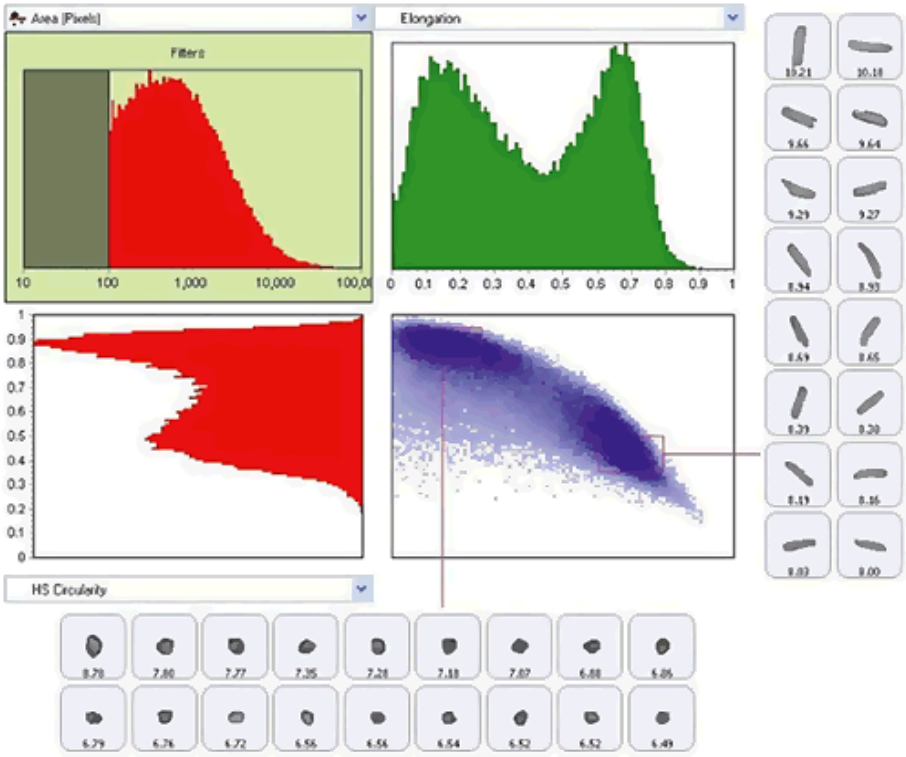


Figure 19: Use of scattergram tool to show classification of the sample by both size (elongation) and shape (HS Circularity).

Techniques: Electrophoretic Light Scattering (ELS)

Electrophoretic Light Scattering (ELS) is a technique used to measure the electrophoretic mobility of particles in dispersion, or molecules in solution. This mobility is often converted to zeta potential to enable comparison of materials under different experimental conditions.

The fundamental physical principle is that of electrophoresis. A dispersion is introduced into a cell containing two electrodes. An electrical field is applied to the electrodes and any charged particles or molecules will migrate towards the oppositely charged electrode. The velocity with which they migrate is known as the electrophoretic mobility and is related to their zeta potential.

This velocity is measured by the laser Doppler technique, of which there are two implementations: one to determine a frequency shift, which can give a full zeta potential distribution, and a second, phase analysis light scattering (PALS), where the phase shift is measured. PALS is a more sensitive method, but only gives an average zeta potential value.

State-of-the art instruments often combine DLS and ELS into one instrument giving the capability to measure both particle size and zeta potential.

Particle related properties: Rheology

The physical properties of particulate based materials also have an influence on the bulk or macro properties of products and materials.

For instance, the rheological (flow/deformation) behavior of a formulated product can be related directly to properties of its ingredients, such as particle size,

CosMX Exhibit 1003, Page 395 of 512

particle shape and suspension stability. Therefore measuring the rheology of a formulation gives an indication of its colloidal state and interactions between the different constituents. Rheology based measurements can help predict formulation behaviors such as;

- shear thinning or thickening
- flocculation or aggregation
- coagulation or coalescence
- settling, separation or creaming.

Therefore when working with particulate based formulations it is also important to consider macro properties, such as rheology, in order to better understand the behavior of formulated materials. The details of rheology theory and application are outside the scope of this publication, but many introductory materials are available on the Malvern website.

Useful References

Particle Size

App Note : Basic principles of particle size analysis

Webinar : An introduction to particle size

Particle Shape

Article: Particle shape an important parameter in pharmaceutical manufacturing

Webinar : Imaging Masterclass 1 Basic principles of particle characterization by automated image analysis

Zeta Potential

Zeta Potential : An Introduction in 30 Minutes

Sampling

P Gy 'Sampling of Particulate Material, Theory and Practice' 2nd Edition Elsevier, Amsterdam (1982)

Webinar : Sampling for particle size analysis

Laser diffraction

Laser diffraction masterclass

ISO 13320:2009 Particle size analysis -- Laser diffraction methods

Dynamic light scattering

Dynamic Light Scattering : An Introduction in 30 Minutes

Automated imaging

Webinar : Imaging Masterclass 1 Basic principles of particle characterization by automated image analysis

CosMX Exhibit 1003, Page 396 of 512

ISO 13322-1:2004 Particle size analysis -- Image analysis methods -- Part 1: Static image analysis methods

ISO 13322-2:2006 Particle size analysis -- Image analysis methods -- Part 2: Dynamic image analysis methods

Electrophoretic light scattering

Electrophoretic light scattering overview

Rheological properties of particulates

Understanding the links between rheology and particle parameters

CosMX Exhibit 1003, Page 397 of 512



Malvern Instruments Limited
Grovewood Road, Malvern,
Worcestershire, UK. WR14
1XZ

Tel: +44 1684 892456
Fax: +44 1684 892789
www.malvern.com

Malvern Instruments is part of Spectris plc, the Precision Instrumentation and Controls Company.

Spectris and the Spectris logo are Trade Marks of Spectris plc.



All information supplied within is correct at time of publication.

Malvern Instruments pursues a policy of continual improvement due to technical development. We therefore reserve the right to deviate from information, descriptions, and specifications in this publication without notice. Malvern Instruments shall not be liable for errors contained herein or for incidental or consequential damages in connection with the furnishing, performance or use of this material.

Malvern Instruments owns the following registered trademarks: Bohlin, FIPA, Insitec, ISYS, Kinexus, Malvern, Malvern 'Hills' logo, Mastersizer, MicroCal, Morphologi, Rosand, 'SEC-MALS', Viscosizer, Viscotek, Viscogel and Zetasizer.

©2015 Malvern Instruments Limited

WP120620BasicGuidePartChar

Appendix P

Journal of Power Sources 195 (2010) 6192–6196

Contents lists available at ScienceDirect

Journal of Power Sources

journal homepage: www.elsevier.com/locate/jpowsour

Short communication

Enhancement of thermal stability and cycling performance in lithium-ion cells through the use of ceramic-coated separators

Ji-Ae Choi[a], Sa Heum Kim[b], Dong-Won Kim[a,*]

[a] Department of Chemical Engineering, Hanyang University, 17 Haengdang-dong, Seungdong-Gu, Seoul 133-791, Republic of Korea
[b] Corporate Research & Development Division, Hyundai-Kia Motors, Gyeonggi-Do 446-912, Republic of Korea

ARTICLE INFO

Article history:
Received 16 September 2009
Received in revised form 3 November 2009
Accepted 3 November 2009
Available online 11 November 2009

Keywords:
Ceramic-coated separators
Cycling performance
Lithium-ion cells
Polyethylene membrane
Thermal stability

ABSTRACT

Ceramic-coated separators are prepared by coating the sides of a porous polyethylene membrane with nano-sized Al_2O_3 powder and hydrophilic poly(lithium 4-styrenesulfonate) binder. These separators exhibit an improved thermal stability at high temperatures without significant thermal shrinkage. Due to the high hydrophilicity of the polymer binder and large surface area of the small ceramic particles, the separators show good wettability in non-aqueous liquid electrolytes. By using the ceramic-coated separators, lithium-ion cells composed of a carbon anode and a $LiCoO_2$ cathode are assembled and their cycling performance is evaluated. The cells are proven to have better capacity retention than for cells prepared with polyethylene membrane. It is expected that the ceramic-coated separator in this study can be potential candidate as a separator for rechargeable lithium-ion batteries that require thermal safety and good capacity retention.

© 2009 Elsevier B.V. All rights reserved.

1. Introduction

Lithium-ion batteries have rapidly dominated the power-source market for portable electronic devices, power tools, and electric vehicles due to their high energy density and excellent cycle life. For lithium-ion batteries, a separator is a critical component that prevents physical contact of the positive and negative electrodes while permitting free ionic transport within the cell. Proper selection of the separator is very important for achieving good battery performance with respect to cycle life, energy density, power density, and safety [1]. Most of the separators currently used in lithium-ion batteries are based on microporous polyolefin membranes, including polyethylene and polypropylene, as well as various combinations of the two [2,3]. Although such membranes offer excellent mechanical strength and chemical stability, they exhibit large thermal shrinkage at high temperatures [4–6], which causes a short circuit between electrodes in cases of unusual heat generation. In order to solve this problem, inorganic composite separators have been developed by combining the characteristics of polymeric nonwoven and ceramic materials [7–9]. Separators should be also wet in the electrolyte and permanently retain the electrolyte solution; however, the large difference in polarity between the non-polar polyolefin separator and the highly polar organic electrolyte leads to poor wettability. As a result of this poor wettability, there is a high resistance when the pores in the separator are not completely filled with the liquid electrolyte [10]. Therefore, separators with enhanced thermal stability and good wettability in organic liquid electrolytes are highly desirable for the development of lithium-ion batteries with enhanced safety and good cycling performance.

In the present study, we tried to improve the thermal stability and wettability of a microporous polyethylene (PE) membrane by coating both sides of the membrane with nano-sized ceramic powders and a hydrophilic polymer binder. Due to the presence of a heat-resistant ceramic powder with a high surface area and a hydrophilic polymer binder, the ceramic-coated separator exhibited good thermal stability and wettability in non-aqueous liquid electrolytes. Using these ceramic-coated separators, we assembled lithium-ion cells composed of a carbon anode and a $LiCoO_2$ cathode, and their cycling performances were evaluated.

2. Experimental

2.1. Preparation of the ceramic-coated separator

Ceramic-coated separators were prepared from nano-sized ceramic powder and a hydrophilic polymer binder. Poly(lithium 4-styrenesulfonate) (PLSS, Aldrich Chem. Co.) and aluminum oxide (Al_2O_3) powder with a particle size of 2–4 nm (Aldrich Chem. Co.) were used as the raw materials for making the ceramic-coated separators. These materials were put into a water/*N*,*N*-dimethylacetamide solvent mixture (5/95, v/v), and uniformly dispersed by ball milling overnight. The resulting slurry

* Corresponding author. Tel.: +82 2 2220 2337; fax: +82 2 2298 4101.
E-mail address: dongwonkim@hanyang.ac.kr (D.-W. Kim).

0378-7753/$ – see front matter © 2009 Elsevier B.V. All rights reserved.
doi:10.1016/j.jpowsour.2009.11.020

Table 1
Composition and thickness of the ceramic-coated separators.

Thickness (μm)	Al_2O_3: PLSS (w/w ratio)	Sample designation
25	None	PE
28	1:1	ACS[a]-1
	1:2	ACS-2
30	1:1	ACS-3
	1:2	ACS-4

[a] Alumina-coated separator.

was then coated onto both sides of a microporous PE membrane substrate with a thickness of 25 μm and a porosity of 40%. Next, the separator was dried at room temperature for 10 min to allow the solvent to evaporate, followed by additional drying in a vacuum oven at 80 °C for more than 24 h. The thickness of the ceramic-coated separator was controlled by changing the content of polymer binder and ceramic powder in the slurry. The total thickness of the ceramic-coated separator was kept at less than 30 μm in order to avoid losing the high energy density, which is one of the most important advantages of lithium-ion batteries. The weight ratios of Al_2O_3 powder and polymer binder that were coated onto the PE substrate, as well as the resulting thicknesses of the respective ceramic-coated separators, are given in Table 1.

2.2. Electrode preparation and cell assembly

The cathode was prepared by coating the *N*-methyl pyrrolidine (NMP)-based slurry containing $LiCoO_2$ (Japan Chemical), poly(vinylidene fluoride) (PVdF), and super-P carbon (MMM Co.) on an aluminum foil. The carbon anode was prepared similarly by coating the NMP-based slurry of mesocarbon microbeads (MCMB, Osaka gas), PVdF, and super-P carbon on a copper foil. The thicknesses of the electrodes ranged from 50 to 60 μm after roll pressing, and their active mass loading corresponded to a capacity of about 2.84 mAh cm^{-2}. Lithium-ion cells were assembled by sandwiching the ceramic-coated separator between the carbon anode and the $LiCoO_2$ cathode. The cell was then enclosed in a pouch bag and injected with the same amount of electrolyte solution, which consisted of 1.0 M $LiPF_6$ in ethylene carbonate (EC)/dimethyl carbonate (DMC) (1:1, v/v, Techno Semichem Co., Ltd.). All cells were assembled in a dry box filled with argon gas.

2.3. Measurements

The surface morphologies of the PE membranes and ceramic-coated separators were examined using a scanning electron microscope (JEOL, JSM-6300). Thermal shrinkage of the ceramic-coated separators in the form of dimensional change was measured before and after being kept at 105 °C for 1 h. In order to measure electrolyte uptake and ionic conductivity, the ceramic-coated separator was immersed in 1.0 M $LiPF_6$ in EC/DMC for 1 h. Afterward, the separator was taken out from the electrolyte solution and excess electrolyte solution on the surface of separator was removed by wiping with filter paper. The uptake of electrolyte solution was determined using the following relationship:

$$\text{uptake}\,(\%) = \frac{W - W_o}{W_o} \times 100$$

Here, W_o and W are the weights of the separator before and after soaking in the liquid electrolyte, respectively. The wetted separator was sandwiched between two stainless steel (SS) electrodes for conductivity measurements. AC impedance measurements were performed to measure ionic conductivity using an impedance analyzer over the frequency range of 10 Hz to 100 kHz with an amplitude of 10 mV. Charge and discharge cycling tests of the lithium-ion cells were conducted at a current density of 1.42 mA cm^{-2} (0.5 C rate) over a voltage range of 2.8–4.2 V with battery test equipment.

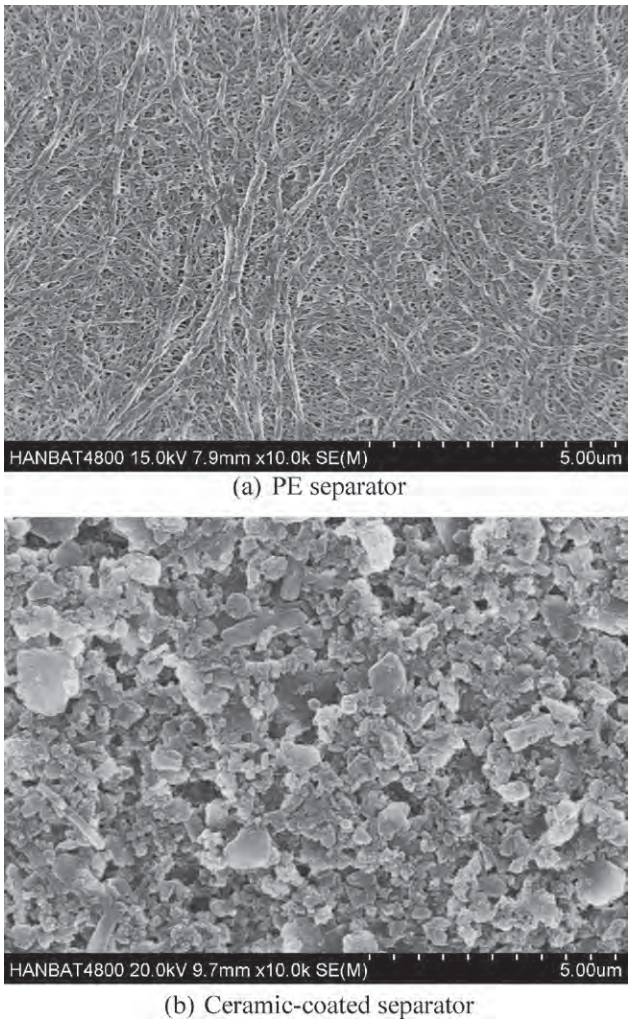


Fig. 1. Scanning electron micrographs of the surface of a porous PE membrane and ceramic-coated separator (ACS-3).

3. Results and discussion

Scanning electron micrographs of the surface of the porous PE membrane and the ceramic-coated separator (ACS-3) are presented in Fig. 1. The PE membrane exhibited a uniformly interconnected submicron pore structure. As the Al_2O_3 powder with polymer binder was coated onto the PE substrate, the ceramic particles were covered the polymer binder, due to the high volumetric ratio of polymer binder to ceramic powder. We also observed the formation of large pores in the coating layer of the ceramic-coated separator, the presence of which was expected to lead to efficient uptake of the liquid electrolyte upon immersion in an electrolyte solution.

The uptake of an electrolyte solution in the ceramic-coated separator and the ionic conductivity after soaking in the liquid electrolyte (1.0 M $LiPF_6$–EC/DMC) were measured and are summarized in Table 2. Ionic conductivity of liquid electrolyte used in soaking the separators is 1.1×10^{-2} S cm^{-1} at room temperature. For comparison purposes, a microporous PE membrane was soaked in the same electrolyte solution, and the resulting experimental data is included in Table 2. As expected, the non-polar PE membrane exhibited poor wettability and electrolyte retention

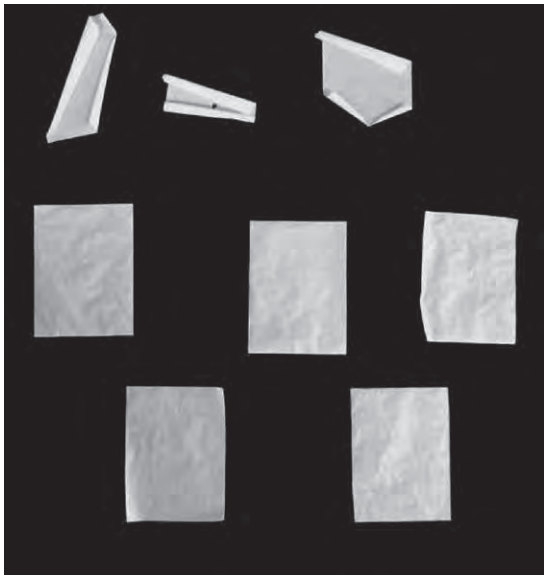


Fig. 2. Photographs of PE membranes and ceramic-coated separators (ACS-3) after being kept at 105 °C for 1 h.

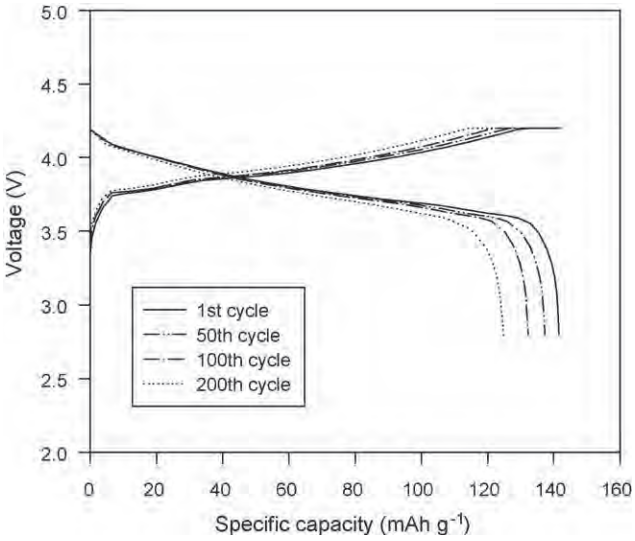


Fig. 3. Charge and discharge curves of lithium-ion cell assembled with the ceramic-coated separators (ACS-3) (0.5 C CC and CV charge, 0.5 C CC discharge, cut-off: 2.8–4.2 V).

due to its inherent hydrophobic properties. For the ceramic-coated separators, the amount of electrolyte absorbed was greater than the amount absorbed by the PE membrane, which resulted in higher ionic conductivity. This result was due to the high hydrophilicity of the polymer binder and the high surface area of the nano-sized Al_2O_3 particles. In addition, since the poly(lithium 4-styrenesulfonate) had a large number of lithium ions in the side chains and had a high affinity for the electrolyte solution, a higher amount of electrolyte solution was expected to be retained by the separator. Indeed, the wettability and ionic conductivity of the ceramic-coated separator were found to increase slightly with increasing thickness of the coating layer and the relative composition of polymer binder to Al_2O_3 particles. Ionic conductivity of PE separator filled with electrolyte solution is lower than that of electrolyte solution, which is due to the fact that the specific resistivity of the separator saturated with liquid electrolyte is increased by the combination of tortuosity and porosity of the separator [3]. Ionic conductivities of the ceramic-coated separators after soaking in the electrolyte solution ranged from 7.2×10^{-4} to 8.3×10^{-4} S cm^{-1} at room temperature.

In order to evaluate the heat-resistant properties of the ceramic-coated separators, we measured thermal shrinkage after storing the separators at 105 °C for 1 h (Table 2). Photographs of the PE membranes and the ceramic-coated separators (ACS-3) after being kept at 105 °C for 1 h are shown in the top and bottom of Fig. 2, respectively. The photographs clearly show that the PE membranes underwent a high degree of shrinkage (13.8%) during exposure to the high temperature conditions. Since the manufacturing process of microporous PE membranes includes a drawing step, membranes shrinks easily when exposed to high temperature, due to internal stress [1]. Consequently, PE membranes would lose mechanical stability upon exposure to high temperatures, which may result in physical contact between the anode and the cathode. On the other hand, thermal shrinkage was significantly reduced by coating both sides of the PE membrane with Al_2O_3 powder and polymer binder. It is considered that coating heat-resistant ceramic particles onto both sides of the porous PE membrane can prevent dimensional changes by thermal deformation because of the frame structure of the heat-resistant ceramic powder with polymer binder. The lowest degree of shrinkage was obtained with ACS-3, suggesting that thermal stability of a PE membrane can indeed be enhanced by increasing either the content of the ceramic particles or the thickness of the coating layer.

We evaluated the cycling performance of lithium-ion cells prepared with the ceramic-coated separator. Assembled cells were initially subjected to a preconditioning cycle in the voltage range of 2.8–4.2 V at constant current rates of 0.05, 0.1 and 0.2 C, consecutively. After three cycles, cells were charged at a current density of 1.42 mA cm^{-2} (0.5 C rate) up to a target voltage of 4.2 V. This was followed by a constant voltage charge with a decline of current until a final current was reached to 20% of the charging current. The cells were then discharged to a cut-off voltage of 2.8 V at the same current density (0.5 C rate). Fig. 3 shows the charge–discharge curves of the 1st, 50th, 100th and 200th cycles of the lithium-ion cell assembled with the ceramic-coated separator (ACS-3). The cell had an initial discharge capacity of 141.6 mAh g^{-1} based on active $LiCoO_2$ material in the cathode. The discharge capacity of the cell declined to 124.8 mAh g^{-1} after 200 charge/discharge cycles, which corresponded to 88.1% of the initial discharge capacity. The coulombic efficiency of the cell increased steadily and stabilized with cycle number and was maintained at greater than 99.0% after the initial few cycles.

Fig. 4 shows the discharge capacities of lithium-ion cells assembled with different separators as a function of cycle number. The cycling characteristics of the cells were found to depend on the

Table 2
Electrolyte uptakes, ionic conductivities, and thermal shrinkage of the ceramic-coated separators.

Separator	Electrolyte uptake (%)	Ionic conductivity (S cm^{-1})	Thermal shrinkage (%)
PE	116.5	2.5×10^{-4}	13.8
ACS-1	206.7	7.2×10^{-4}	6.1
ACS-2	237.8	8.1×10^{-4}	7.6
ACS-3	218.5	7.6×10^{-4}	3.8
ACS-4	248.4	8.3×10^{-4}	4.5

CosMX Exhibit 1003, Page 402 of 512

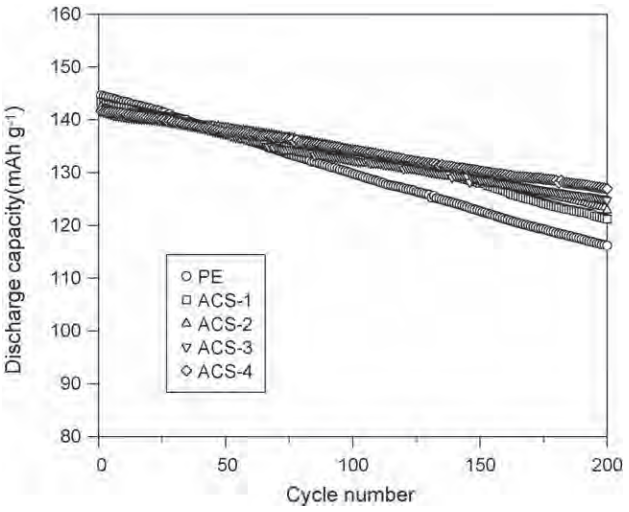


Fig. 4. Discharge capacities of the lithium-ion cells prepared with a PE membrane and ceramic-coated separators (0.5 C CC and CV charge, 0.5 V CC discharge, cut-off: 2.8–4.2 V).

type of separator. The initial discharge capacity of the cell was slightly decreased by coating the PE membrane with Al_2O_3 powder and polymer binder. Presence of an additional coating layer on the porous PE membrane may have increased the resistance of ion migration in the separator, giving rise to a reduced discharge capacity; however, the capacity retention was improved by coating Al_2O_3 powder and polymer binder onto the porous PE membrane. It was thought that the ability to retain electrolyte solution in the pores of the ceramic-coated separator was higher than in the hydrophobic PE membrane alone, and thus helped to prevent a lack or leak of electrolyte during repeated cycling. When examining the effect of the ratio of Al_2O_3 powder and polymer binder on the cell performance, the cell assembled with ceramic-coated separator containing high content of polymer (PLSS) exhibited better capacity retention.

The rate capability of the lithium-ion cell prepared with the ceramic-coated separator was evaluated. Cells were charged to 4.2 V at a constant current of 0.2 C and discharged at different current rates ranging from 0.1 to 2.0 C. The discharge curves of the lithium-ion cell assembled with ACS-2 are given in Fig. 5. Both the voltage and the capacity decreased gradually with increasing

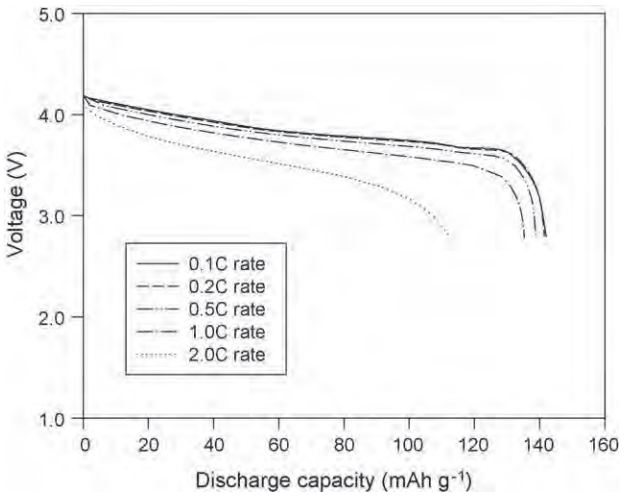


Fig. 5. Discharge profiles of lithium-ion cell prepared with ceramic-coated separator (ACS-2) as function of C rate. The charge rate was 0.2 C with a 4.2 V cut-off.

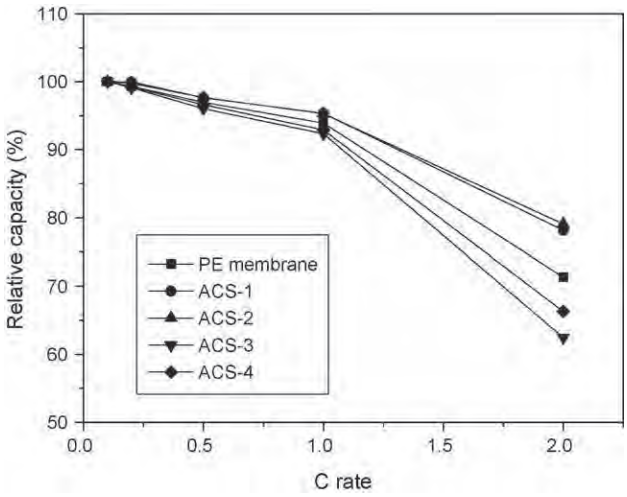


Fig. 6. Relative capacities of lithium-ion cells prepared with PE membrane or ceramic-coated separators as a function of C rate.

rates of current. Fig. 6 compares the relative discharge capacities of lithium-ion cells prepared with different separators as a function of current density, where relative capacity was defined as the ratio of the discharge capacity at a specific C rate to the discharge delivered at a rate of 0.1 C. The results showed that the coating layer thickness affected high rate performance. The high rates of performance of the cells assembled with ACS-1 or ACS-2 could be ascribed to favorable interfacial charge transport between the electrodes and the electrolytes in the cell, because the coating layer on both sides of the PE membrane was able to assist in adhering the separator to the electrodes after soaking in the electrolyte solution. In the case of ACS-3 or ACS-4, the thick coating layer on the porous PE membrane may have hampered the ion migration in the separator even if the coating layer on the PE membrane improved interfacial adhesion, the result of which was a decreased discharge capacity at high current rates.

4. Conclusions

Ceramic-coated separators were prepared by coating nano-sized Al_2O_3 powder and hydrophilic poly(lithium 4-styrenesulfonate) onto both sides of a porous PE membrane. These separators exhibited enhanced thermal stability by retaining stable dimensions at high temperatures. Due to the high hydrophilicity of the polymer binder and high surface area of the small inorganic particles, the coated membranes exhibited good wettability in non-aqueous liquid electrolytes. As a result, the lithium-ion cells assembled with the ceramic-coated separators exhibited better capacity retention than did the cells prepared with only a PE membrane. It is expected that the ceramic-coated separators described in this study may be useful as separators for rechargeable lithium-ion batteries that require thermal safety and good capacity retention.

Acknowledgements

This work was supported by NGV and the Hyundai Motor Company.

References

[1] S.S. Zhang, J. Power Sources 164 (2007) 351.
[2] D. Linden, T.B. Reddy, Handbook of Batteries, third ed., McGraw-Hill, New York, 2002.
[3] P. Arora, Z. Zhang, Chem. Rev. 104 (2004) 4419.

CosMX Exhibit 1003, Page 403 of 512

[4] I. Uchida, H. Ishikawa, M. Mohamedi, M. Umeda, J. Power Sources 119–121 (2003) 821.
[5] G. Venugopal, J. Moore, J. Howard, S. Pendalwar, J. Power Sources 77 (1999) 34.
[6] M.S. Wu, P.C.J. Chiang, J.C. Lin, Y.S. Jan, Electrochim. Acta 49 (2004) 1803.
[7] S. Augustin, V.D. Hennige, G. Horpel, C. Hying, Desalination 146 (2002) 23.
[8] S. Augustin, V.D. Hennige, G. Horpel, C. Hying, J. Tarabocchia, J. Swoyer, M.Y. Saidi, Meet. Abstr.: Electrochem. Soc. 502 (2006) 80.
[9] P. Kritzer, J. Power Sources 161 (2006) 1335.
[10] J. Saunier, F. Alloin, J.Y. Sanchez, G. Caillon, J. Power Sources 119–121 (2003) 454.

CosMX Exhibit 1003, Page 404 of 512

Appendix Q

US006447958B1

(12) **United States Patent**
Shinohara et al.

(10) **Patent No.: US 6,447,958 B1**
(45) **Date of Patent: Sep. 10, 2002**

(54) **NON-AQUEOUS ELECTROLYTE BATTERY SEPARATOR**

(75) Inventors: **Yasuo Shinohara**, Niihara-mura; **Yoshifumi Tsujimoto**, Tsuchiura; **Tsuyoshi Nakano**, Tsukuba, all of (JP)

(73) Assignee: **Sumitomo Chemical Co., Ltd.**, Osaka (JP)

(*) Notice: Subject to any disclaimer, the term of this patent is extended or adjusted under 35 U.S.C. 154(b) by 0 days.

(21) Appl. No.: **09/299,077**

(22) Filed: **Apr. 26, 1999**

(30) **Foreign Application Priority Data**

Apr. 27, 1998 (JP) 10-116838

(51) **Int. Cl.**[7] **H01M 2/16**

(52) **U.S. Cl.** **429/248**; 429/251; 429/252; 429/254; 429/249

(58) **Field of Search** 429/142, 144, 429/248, 249, 251, 252, 254, 255, 231.95

(56) **References Cited**

U.S. PATENT DOCUMENTS

5,023,065 A * 6/1991 Ohno et al.

5,741,608 A * 4/1998 Kojima et al.

FOREIGN PATENT DOCUMENTS

JP	59-36939	9/1984
JP	59-14494	12/1984
JP	60-52	1/1985
JP	60-136161	7/1985
JP	62-37871	2/1987
JP	63-276868	11/1988
JP	2-46649	2/1990
JP	3-291848	12/1991
JP	4-1692	1/1992
JP	4-112452	4/1992
JP	5-335005	12/1993
JP	7-37571	2/1995
JP	7-78608	3/1995

* cited by examiner

Primary Examiner—John Kim
Assistant Examiner—David Sorkin
(74) *Attorney, Agent, or Firm*—Sughrue Mion, PLLC

(57) **ABSTRACT**

A non-aqueous electrolyte battery separator comprising a heat-resistant nitrogen-containing aromatic polymer and a ceramic powder.

18 Claims, No Drawings

NON-AQUEOUS ELECTROLYTE BATTERY SEPARATOR

BACKGROUND OF THE INVENTION

1. Field of the Invention

The present invention relates to a non-aqueous electrolyte battery separator comprising a heat-resistant nitrogen-containing aromatic polymer and a ceramic powder, and a lithium secondary battery.

2. Description of the Related Art

A lithium primary battery or lithium secondary battery using a non-aqueous electrolyte is highly useful due to its property that high capacity and high energy density are obtained. As a main structure of these batteries, a separator composed of an electrically insulating porous film is intercalated between positive and negative electrodes, an electrolyte solution containing a lithium salt dissolved is impregnated into pores of the film, and the positive electrode and negative electrode and the separator are laminated, or wound in the form of a roll. It is required for a lithium secondary battery to make various safe measures against problems derived from its high capacity and high energy density, for example, large increase in battery temperature because of short-circuit inside and outside of a battery. For solving such problems, there have been made various ideas for the separator.

Particularly, as a safety precaution to which a separator can contribute, shut down property and short circuit property are under notice. Herein, the term shut down (also referred to as fuse) means that battery temperature increases by troubles such as overcharge, external or internal short, a part of a separator is melted to obstruct pores, and current is cut off, and the temperature in this phenomenon is called shut down temperature. The term short circuit means that temperature further increases from the shut down temperature, the separator is melted and a large hole is formed to cause short again, and the temperature in this phenomenon is called short circuit temperature. Decrease in the shut down temperature and increase in short circuit temperature are required for a non-aqueous electrolyte battery separator.

Conventionally, as a separator of a lithium secondary battery, a thin porous film is used, and for example, Celgard (registered trade mark) manufactured by Hoechst Co. is preferably used as a separator of a lithium secondary battery. However, a non-aqueous electrolyte battery separator having further excellent heat-resistance and higher short circuit temperature has been desired.

Regarding a raw material of such a non-aqueous electrolyte battery separator, use of a whole aromatic polyamide-based polymer having excellent heat-resistance has been investigated. For example, Japanese Patent Application Publication (JP-B) No. 59-36939 describes a method for producing a porous film made of an aromatic polymer, that is aromatic polyamide or aromatic polyimide, JP-B No. 59-14494 describes that a method for producing a porous film made of an aromatic polyamide and that it can be used as a battery separator. Further, Japanese Patent Application Laid-Open (JP-A) No. 5-335005 describes use of Normex (registered trade mark) paper (meta-aramid paper) manufactured by du Pont Co. as a separator of a lithium secondary battery. Likewise, JP-A Nos. 7-78608 and 7-37571 also suggest use of non-woven fabric or paper-like sheet made of meta-aramid as a battery separator. Further, JP-A Nos. 62-37871 and 2-46649 describes use of polyimide as a separator of a non-aqueous electrolyte solution battery. In these publications, a material is employed which exhibits excellent ion permeability and battery property while maintaining heat-resistance.

On the other hand, regarding shut down and short circuit, JP-A No. 3-291848 and JP-B No. 4-1692 suggest, for securing safety of a battery when short is occurred inside or outside of a battery, that a battery separator is allowed to have shut down function which cut off current, by providing an obstruction material which can be heat-melted on a porous film made of a thermoplastic resin and by covering the surface of a micro porous film by heat-melting of this obstruction material. Further, JP-A Nos. 60-52 and 60-136161 suggest that a battery separator is allowed to have shut down function, by adhering a polyethylene-based resin powder onto polypropylene non-woven fabric and by heat-melting the resin to obstruct pores of the non-woven fabric. However, in these suggestions, thermoplastic resins are used, therefore, heat-resistance is not sufficient and short circuit temperature is low, and use is restricted in view of safety.

The present inventors have intensively investigated a separator which does not have problems as described above, and found that a separator containing ceramic powder in a heat-resistant nitrogen-containing aromatic polymer is highly heat-resistant and has high short circuit temperature, and further has excellent ion permeability.

SUMMARY OF THE INVENTION

An object of the present invention is to provide a non-aqueous electrolyte battery separator having excellent ion permeability and battery property while maintaining merits of a heat-resistant nitrogen-containing aromatic polymer that heat-resistance is high and short circuit temperature is high.

Another object of the present invention is to provide a non-aqueous electrolyte battery separator which has such safety that shut down occurs in over-heating, has so high short circuit temperature that it is not melted when heated, and further has excellent safety. Further object of the present invention is to provide a lithium secondary battery having high short-circuit temperature and excellent safety by using such as separator.

Namely, the present invention relates to (1) a non-aqueous electrolyte battery separator comprising a heat-resistant nitrogen-containing aromatic polymer and a ceramic powder.

Further, the present invention relates to (2) a non-aqueous electrolyte battery separator comprising a heat-resistant nitrogen-containing aromatic polymer, a ceramic powder, and a substrate made of woven fabric, non-woven fabric, paper or porous film.

Further, the present invention relates to (3) a non-aqueous electrolyte battery separator according to (1) or (2), wherein the non-aqueous electrolyte battery separator contains a thermoplastic polymer which is melted at a temperature of 260° C. or less in an amount of 10% by weight or more based on the whole separator, and said thermoplastic polymer is melted when temperature increases and obstructs pore of said separator.

Moreover, the present invention relates to (4) a non-aqueous electrolyte battery separator comprising a coated film obtained by a method comprising the following steps of:

(a) preparing a slurry solution which may contain a thermoplastic resin which is melted at a temperature of 260° C. or less, by dispersing a ceramic powder in a

solution of a polar organic solvent containing a heat-resistant nitrogen-containing aromatic polymer in an amount of 1 to 1500 parts by weight based on 100 parts by weight of said heat-resistant nitrogen-containing aromatic polymer,

(b) producing a coated film by coating said slurry solution,

(c) depositing said heat-resistant nitrogen-containing aromatic polymer on said coated film,

(d) removing the polar organic solvent from said coated film, and

(e) drying said coated film.

Furthermore, the present invention relates to (5) a non-aqueous electrolyte battery separator comprising a coated film obtained by a method comprising the following steps of:

(a) preparing a slurry solution which may contain a thermoplastic resin which is melted at a temperature of 260° C. or less, by dispersing a ceramic powder in a solution of a polar organic solvent containing a heat-resistant nitrogen-containing aromatic polymer in an amount of 1 to 1500 parts by weight based on 100 parts by weight of said heat-resistant nitrogen-containing aromatic polymer,

(b) producing a coated film by coating said slurry solution on a substrate made of woven fabric, non-woven fabric, paper or porous film,

(c) depositing said heat-resistant nitrogen-containing aromatic polymer on said coated film,

(d) removing the polar organic solvent from said coated film, and

(e) drying said coated film.

Also, the present invention relates to (6) a lithium secondary battery comprising a non-aqueous electrolyte battery separator of any of the inventions (1) to (5).

DETAILED DESCRIPTION OF THE PREFERRED EMBODIMENTS

The non-aqueous electrolyte battery separator of the present invention comprises a heat-resistant nitrogen-containing aromatic polymer and a ceramic powder.

The heat-resistant nitrogen-containing aromatic polymer of the present invention is a polymer containing a nitrogen atom and an aromatic ring in the backbone, and examples thereof include an aromatic polyamide (hereinafter, may sometimes be referred to as "aramid"), aromatic polyimide (hereinafter, may sometimes be referred to as "polyimide"), aromatic polyamideimide and the like.

Examples of the aramid include a meta-oriented aromatic polyamide ((hereinafter, may sometimes be referred to as "meta-aramid") and para-oriented aromatic polyamide (hereinafter, may sometimes be referred to as "para-aramid"), and a para-aramid is preferable since it tends to become porous.

The para-amide is obtained by polycondensation of a para-oriented aromatic diamine with a para-oriented aromatic dicarboxylic halide, and substantially consists essentially of repeating units in which amide bonds are bonded in para-orientation or corresponding orientation (for example, orientation extending co-axially or in parallel to reverse direction such as 4,4'-biphenylene, 1,5-naphthalene, 2,6-naphthalene and the like).

Specifically, there are exemplified para-aramids having structure of para-orientation or orientation corresponding to para-orientation, such as poly(p-phenyleneterephthalamide), poly(p-benzamide), poly(4,4'-benzanilideterephthalamide), poly(p-phenylene-4,4'-biphenylenedicarboxylic amide), poly(p-phenylene-2,6-naphthalenedicarboxylic amide), poly(2-chloro-p-phenyleneterephthalamide), p-phenyleneterephthalamide/2,6-dichloro p-phenyleneterephthalamide copolymer and the like.

The para-aramid of the present invention can be dissolved in polar organic solvent to prepare a solution having low viscosity, and has an intrinsic viscosity preferably of 1.0 dl/g to 2.8 dl/g, further preferably of 1.7 dl/g to 2.5 dl/g for excellent coating property. A satisfactory film strength may not be obtained when the intrinsic viscosity is less than 1.0 dl/g. When the intrinsic viscosity is over than 2.8 dl/g, a stable para-amide solution may not be easily obtained, and it may be difficult to form a film because a para-amide is deposited.

The polar organic solvent herein used is for example a polar amide-based solvent or polar urea-based solvent, and specific examples thereof include N,N-dimethylformamide, N,N-dimethylacetoamide, N-methyl-2-pyrrolidone, tetramethylurea and the like, but are not limited to these examples.

The para-aramid of the present invention is preferably a porous polymer in the form of fibril. The fibril-like polymer is microscopically in the form of non-woven cloth and in the form of a porous layer containing pore and forms a so-called para-aramid porous resin.

The polyimide used in the present invention is not particularly restricted and preferably a whole aromatic polyimide produced by polycondensation of an aromatic diacid anhydride with a diamine. Specific examples of the diacid anhydride include pyromellitic dianhydride, 3,3'-4,4'-diphenylsulfonetetracarboxylic dianhydride, 3,3'-4,4'-benzophenonetetracarboxylic dianhydride, 2,2'-bis(3,4-dicarboxyphenyl)hexafluoropropane, 3,3'-4,4'-biphenyltetracarboxylic dianhydride and the like, but are not limited to these examples. Specific examples of the diamne include oxydianiline, p-phenylenediamine, benzophenonediamine, 3,3'-methylenedianiline, 3,3'-diaminobenzophenone, 3,3'-diaminodiphenylsulfone, 1,5'-naphthalenediamine and the like, but are not limited to these examples. In the present invention, when a porous film is made directly from a polyimide solution, a polyimide soluble in a solvent can be suitably used. As this polyimide, there is for example listed a polyimide, that is a polycondensate of 3,3'-4,4'-diphenylsulfonetetracarboxylic dianhydride with an aromatic diamine.

As the polar organic solvent used in the polyimide, dimethylsulfoxide, cresol, o-chlorophenol and the like can be suitably used in addition to those exemplified for the aramid.

In the present invention, a porous polyimide is preferable. Example, a solid film can be subjected to boring by mechanical process, laser process and the like to be made into porous material. When a polyimide film is made by a solution casting method, a porous film can be produced by controlling molding conditions of the polyimide such as polymer concentration in coating and the like. Further, a uniform and fine porous film can be produced using a solution having any polymer concentration by combining ceramic powders. Also, gas permeability can be controlled by added amount of a ceramic powder.

The non-aqueous electrolyte battery separator of the present invention is required to contain a ceramic powder. The ceramic powder is entangled and arrested by a heat-resistant nitrogen-containing aromatic polymer, and situated

being totally or partially dispersed in the non-aqueous electrolyte battery separator.

The ceramic powder used in the present invention has an average particle size of the primary particle of preferably 1.0 μm or less, more preferably 0.5 μm or less in view of influence on strength of a non-aqueous electrolyte battery separator and smoothness on coated surface. The average particle size of the primary particle is measured by analyzing a photograph made by an electron microscope with a particle size measuring apparatus. When the average particle size of the primary particle of a ceramic powder is over 1.0 μm, the separator may become fragile and also coated surface may become fragile. The content of the ceramic powder is preferably from 1% by weight to 95% by weight, more preferably from 5% by weight to 50% by weight based on the weight of the non-aqueous electrolyte battery separator. When the content of the ceramic powder is less than 1% by weight based on the weight of the non-aqueous electrolyte battery separator, effect for promoting ion permeability and battery property may not be sufficient, and when over 95% by weight, the separator may become fragile and handling thereof may become difficult. The form of the ceramic powder is not particularly restricted, and sphere and random forms can also be used.

As the raw material of the ceramic powder in the present invention, metal oxide, metal nitride, metal carbide and the like having electrically insulating property are listed, and for example, alumina, silica, titanium dioxide, zirconium oxide and the like are preferably used.

As the substrate of the present invention, there are listed porous woven fabric, non-woven fabric, paper and porous films made of electrically insulating organic, inorganic fiber or pulp. Among them, non-woven fabric, paper or porous films are preferable in view of cost and small thickness.

The raw material of said substrate may be organic or inorganic, synthetic or natural material providing it has electrically insulating property, and materials containing organic fiber and/or inorganic fiber and/or organic fiber pulp and/or inorganic fiber pulp are listed. Specifically, natural fiber such as a fiber comprising a Manila hemp, thermoplastic polymer fiber and the like are listed as the organic fiber. As the fiber comprising a thermoplastic polymer, fibers such as polyolefins like polyethylene, polypropylene and the like, rayon, vinylon, polyester, acryl, polystyrene, nylon and the like are listed. As the inorganic fiber, glass fiber, alumina fiber and the like are listed.

The non-aqueous electrolyte battery separator (2) of the present invention comprises a heat-resistant nitrogen-containing aromatic polymer, a ceramic powder and a substrate made of woven fabric, non-woven fabric, paper or porous film.

The non-aqueous electrolyte battery separator (2) of the present invention is preferably one in which the substrate is coated with the above-described heat-resistant nitrogen-containing aromatic polymer containing a ceramic powder, or pore of the substrate is filled with the above-described heat-resistant nitrogen-containing aromatic polymer, or the substrate is coated with the above-described heat-resistant nitrogen-containing aromatic polymer and pore of the substrate is filled with the above-described heat-resistant nitrogen-containing aromatic polymer.

When used in the non-aqueous electrolyte battery separator (2) of the present invention, the weight per unit area of a substrate is preferably 40 g/m^2 or less, more preferably 15 g/m^2 or less. The pore percentage of the substrate is preferably 40% or more, further preferably 50% or more. The thickness of the substrate is preferably 70 μm or less, further preferably 25 μm or less.

The non-aqueous electrolyte battery separator (3) of the present invention contains a thermoplastic polymer which is melted at a temperature of 260° C. or less in an amount of 10% by weight or more, preferably 30% by weight or more, more preferably 40% by weight or more based on the whole separator, and the thermoplastic polymer is melted when temperature increases to obstruct pore of the separator. The above-described thermoplastic polymer may advantageously be a polymer which is melted in temperature increase, if it is used as a battery separator. The thermoplastic polymer is preferably a polymer which is melted at a temperature of 260° C. or less, more preferably 200° C. or less in view of shut down function, when it is used as a separator in a lithium secondary battery. The melting temperature is preferably about 100° C. or more because it is suitable for shut down.

As the thermoplastic polymer, polyolefin resins, acrylic resins, styrene resins, polyester resins, nylon resins and the like are listed. In particular, polyethylenes such as low density polyethylene, high density polyethylene, linear polyethylene and the like, or low molecular weight wax components thereof, or polyolefin resins such as polypropylene and the like are suitably used since they have an appropriate melting temperature and are available easily. These may be used alone or in a mixture thereof.

The thermoplastic polymer used in the present invention is preferably a powder having an average particle size of preferably 10 μm or less, more preferably 6 μm or less in view of dispersibility into a solvent and smoothness of the coated surface. The form of the powder particle is not particularly restricted, and any of spherical and random forms can be used.

In the non-aqueous electrolyte battery separator (3) of the present invention, a thermoplastic polymer is totally or partially dispersed in the form of a particle in a non-aqueous electrolyte battery separator, and the dispersion embodiment is not particularly restricted providing the thermoplastic polymer is melted when temperature increases to block pore of the separator.

The non-aqueous electrolyte battery separator (4) of the present invention comprises a coated film obtained by a method comprising the following steps (a) to (e) of:

(a) preparing a slurry solution which may contain a thermoplastic resin which is melted at a temperature of 260° C. or less, by dispersing a ceramic powder in a solution of a polar organic solvent containing a heat-resistant nitrogen-containing aromatic polymer in an amount of 1 to 1500 parts by weight based on 100 parts by weight of said heat-resistant nitrogen-containing aromatic polymer,

(b) producing a coated film by coating said slurry solution,

(c) depositing said heat-resistant nitrogen-containing aromatic polymer on said coated film,

(d) removing the polar organic solvent from said coated film, and

(e) drying said coated film.

The method for producing a non-aqueous electrolyte battery separator (4) of the present invention will be specifically described.

Step (a): Preparation of Slurry Solution

Cases using a para-aramid and a polyimide as a heat-resistant nitrogen-containing aromatic polymer will be exemplified.

When a para-aramid is used, for example, in a polar organic solvent containing 2 to 10% by weight of an alkaline metal chloride or alkaline earth metal chloride dissolved, a para-oriented aromatic dicarboxylic dihalide is added in an amount of 0.94 to 0.99 mol per 1.00 mol of a para-oriented aromatic diamine and is poly-condensed at a temperature of −20 to 50° C. to prepare a polar organic solvent solution of an aramid in which the concentration of the produced para-oriented aromatic polyamide is from 1 to 10% (by weight) and the intrinsic viscosity is from 1.0 to 2.8 dl/g.

As the para-oriented aromatic diamine used in polycondensation of a para-aramid, p-phenylenediamine, 4,4'-diaminobiphenyl, 2-methyl-p-phenylenediamine, 2-chloro-p-phenylenediamine, 2,6-dichloro-p-phenylenediamine, 2,6-naphthalenediamine, 1,5-naphthalenediamine, 4,4'-diaminobenzanilide, 3,4'-diaminodiphenyl ether and the like are listed. The para-oriented aromatic diamines can be used alone or in a mixture thereof and subjected to polycondensation.

As the para-oriented aromatic dicarboxylic dihalide used in polycondensation of a para-aramid, terephthalic dichloride, biphenyl-4,4'-diarboxylic dichloride, 2-chloroterephthalic dichloride, 2,5-dichloroterephthalic dichloride, 2-methylterephthalic dichloride, 2,6-naphthalenedicarboxylid dichloride, 1,5-naphthalenedicarboxylid dichloride, and the like are listed. The para-oriented aromatic dicarboxylic dihalide can be used alone or in a mixture thereof and subjected to polycondensation.

For the purposed of improving solubility of a para-aramid into a solvent, an alkaline metal chloride or alkaline earth metal chloride is preferably used. Specific examples include, lithium chloride and calcium chloride, but are not limited to these examples.

The added amount of the above-described chloride into the polymer system is preferably in the range from 0.5 to 6.0 mol, more preferably in the range from 1.0 to 4.0 mol based on 1.0 mol of an amide group produced in polycondensation. When the amount of the chloride is 0.5 mol or less, the solubility of a para-aramid produced may become insufficient, and when the amount is over 6.0 mol, it substantially may exceed the amount dissolved of the chloride into a solvent.

In general, when the amount of an alkaline metal chloride or alkaline earth metal chloride is less than 2% by weight, solubility of a para-aramid may be insufficient, and when over 10% by weight, an alkaline metal chloride or alkaline earth metal chloride may not be dissolved in a polar organic solvent such as a polar amide-based solvent, polar urea-based solvent or the like.

When the para-amide concentration is 0.5% by weight or less, productivity remarkably may decrease to cause industrial disadvantage. When the amount of a para-aramid is over 10% by weight, the para-aramid may be deposited and a stable para-aramid solution may not be easily obtained.

As the polar organic solvent solution of a polyimide, for example, N-methyl-2-pyrrolidone solution of a polyimide in which imidation has been completed is listed. N-methyl-2-pyrrolidone solution is prepared by polycondensation reaction of 3,3',4,4'-diphenylsulfonetetracarboxylic dianhydride with an aromatic diamine such as 4,4'-bis(p-aminophenoxy) diphenylsulfone and the like. When a polyimide is used as this polar organic solvent, cresol, o-chlorophenol and the like are listed in addition to the above-exemplified compounds.

A ceramic powder is dissolved in the above-described polar organic solvent solution in an amount of 1 to 1500 parts by weight, preferably 5 to 100 parts by weight per 100 parts by weight of a heat-resistant nitrogen-containing aromatic polymer. When the amount of the ceramic powder less than 1 parts by weight, improvement of in ion permeability and battery property is not sufficient. When the amount over 1500 parts by weight, the separator becomes fragile and handling thereof becomes difficult. optionally, a thermoplastic polymer may be added to the slurry solution.

Step (b): Production of a Coated Film

This slurry solution is coated on a base film, steel belt, roll, drum and the like to form a wet coated film.

As the base film, there are listed, for example, polyethylene terephthalate, paper subjected to releasing treatment, and the like. It is industrially often conducted to coat a solution on a steel belt having corrosion resistance which has been subjected to mirror finish. In small scale system, it can also be possible to coat a solution on a roll or a drum having corrosion resistance which has been subjected to mirror finish.

As the coating method, coating methods such as knife coating, blade coating, bar coating, gravure coating, die coating and the like are listed. In small scale system, bar coating, knife coating and the like are convenient. However, industrially, die coating is preferable in which a solution is not brought in contact with outer air.

Step (c): Deposition of Heat-resistant Nitrogen-containing Aromatic Polymer

The resulted coated film is placed in atmosphere controlled under constant humidity at a temperature of preferably 20° C. or more, and a heat-resistant nitrogen-containing aromatic polymer is allowed to deposit, then, immersed in a coagulation solution. Alternatively, it is immersed in a coagulation solution, deposition and coagulation of a polymer are conducted simultaneously to obtain a wet coated film. For uniform and quick coagulation, it is also possible that a poor solvent, for example, water or the like is previously added to a slurry solution, to prepare deposited condition.

In the case of a para-aramid, it is also possible that a part or all of a solvent is evaporated and simultaneously a polymer is deposited, namely, solvent removal process and deposition process are conducted simultaneously to obtain a semi-dried or dried coated film.

As the coagulation solution, an aqueous solution, alcoholic solution or the like may advantageously be used. Though the solution is not particularly limited, it is preferable to use an aqueous solution or alcoholic solution containing a polar organic solvent since solvent removal process can be industrially simplified.

Step (d): Removal of Polar Organic Solvent

Then, a polar organic solvent is removed from this coated film on which a heat-resistant nitrogen-containing aromatic polymer is deposited. For this removal, a part or all of the polar organic solvent may be evaporated, or it may be removed by using a solvent which can dissolve the polar organic solvent such as water, aqueous solution, alcoholic solution or the like. When the removal is conducted using water, it is preferable to use ion-exchanged water. Further it is also industrially preferable that washing is conducted in an aqueous solution containing the polar organic solvent in certain amount, then, washing with water is conducted. For drying, a solvent used for washing is evaporated by heating to be removed. When a thermoplastic polymer which is melted is contained, the drying temperature in this procedure is preferably not more than the temperature for the melting.

When, a para-aramid is prepared using an alkaline metal chloride or alkaline earth metal chloride, the alkaline metal

chloride or alkaline earth metal chloride is washed and removed together with a solvent from a wet coated film on which the para-aramid has been deposited. Alternatively, the alkaline metal chloride or alkaline earth metal chloride is washed and removed from a dried coated film. For this removal, there is adopted a method in which a coated film is immersed in a solution and a solvent and a chloride are eluted. As the solution for eluting a solvent or a chloride, water, aqueous solution or alcoholic solution is preferable since it can dissolve both of the solvent and the chloride.

(e): Drying

The coated film from which a polar organic solvent has been removed can be preferably dried at the melting temperature or less of a polymer which is heat-melted to produce an intended dried coated film.

This dried coated film can be used as a non-aqueous electrolyte battery separator without any other treatment. For imparting shut down property, it is preferable to contain a thermoplastic polymer, this thermoplastic polymer may be added in any step. Also, it is preferable that a fine particle-like suspension of the thermoplastic polymer is coated on the dried coated film and dried to form a fine particle layer of the thermoplastic resin.

As the coating method, coating methods such as knife coating, blade coating, bar coating, gravure coating, die coating and the like are listed. In small scale system, bar coating, knife coating and the like are convenient.

The non-aqueous electrolyte battery separator (5) of the present invention comprises a coated film obtained by a method comprising the following steps (a) to (e) of:

(a) preparing a slurry solution which may contain a thermoplastic resin which is melted at a temperature of 260° C. or less, by dispersing a ceramic powder in a solution of a polar organic solvent containing a heat-resistant nitrogen-containing aromatic polymer in an amount of 1 to 1500 parts by weight based on 100 parts by weight of said heat-resistant nitrogen-containing aromatic polymer,

(b) producing a coated film by coating said slurry solution on a substrate made of woven fabric, non-woven fabric, paper or porous film,

(c) depositing said heat-resistant nitrogen-containing aromatic polymer on said coated film,

(d) removing the polar organic solvent from said coated film, and

(e) drying said coated film.

The method for producing a non-aqueous electrolyte battery separator (5) of the present invention will be specifically described.

The method for producing a non-aqueous electrolyte battery separator (5) of the present invention is in the same manner as for the separator (4) of the present invention except that a substrate made of woven fabric, non-woven fabric, paper or porous film is used.

The step (a) is the same as the step (a) for the separator (4) of the present invention.

The step (b) is the same as the step (b) for the separator (4) of the present invention except that coating is conducted on a substrate made of woven fabric, non-woven fabric, paper or porous film. Alternatively, it is also permissible that a slurry solution is coated on a roll or drum, then, the substrate is mounted to be impregnated with the solution.

The steps (c), (d) and (e). can be carried out in the same manners as in the steps (c), (d) and (e) for the separator (4) of the present invention.

This dried coated film can be used as a non-aqueous electrolyte battery separator without any other treatment. For imparting or reinforcing shut down property, it is preferable to contain a thermoplastic polymer, this thermoplastic polymer may be added in any step. Also, it is preferable that a fine particle-like suspension of the thermoplastic polymer is coated on the dried coated film and dried to form a fine particle layer of the thermoplastic resin. The coating method is the same as that for the separator (4) of the present invention.

The thickness of the non-aqueous electrolyte battery separator of the present invention is preferably from 5 to 100 μm. When the thickness is less than 5 μm, strength as a non-aqueous electrolyte battery separator may lack and handling thereof may be difficult. As a non-aqueous electrolyte battery separator, higher thickness provides easier handling, however, a separator having so smaller thickness as not to cause short circuit is desirable for making internal resistance as low as possible in the case of a lithium secondary battery thought there is no strict restriction regarding thickness in the case of a nickel-cadmium battery. That is, in a lithium secondary battery separator, the thickness is preferably from 5 to 100 μm, further preferably from 5 to 50 μm, particularly preferably from 5 to 30 μm.

It is known that the heat-resistant nitrogen-containing aromatic polymer used in the present invention exhibits almost no degradation in strength at a temperature from room temperature to about 200° C., and has excellent heat resistance. Further, it has self-extinguishing property, is not decomposed and keeps its shape up to about 300° C., and heat-decomposed at a temperature over this range. Further, it is known that a ceramic powder exhibits almost no degradation in strength at a temperature up to about 1000° C., and has excellent heat resistance. Therefore, in a non-aqueous electrolyte battery using the separator of the present invention, even if the battery temperature increases due to short circuit inside or outside of the battery and the like, shut down function works, and even if the temperature further increases, it keeps the shape until high temperature, that is, it keeps insulation property between positive and negative electrodes and manifests excellent safety.

Pore size of the non-aqueous electrolyte battery separator of the present invention, or a diameter of the sphere (hereinafter, sometimes referred to as pore size) when the void can be approximated to sphere, is preferably about 1 μm or less. When the average size of the pore size is over 1 μm, there is possibility of occurrence of such problems that when a carbon powder which is a main component of positive and negative electrodes or a fragment thereof drops, short circuit and the like tends to occur.

The non-aqueous electrolyte battery separator of the present invention can be suitably used in a lithium secondary battery. In the non-aqueous electrolyte battery separator of the present invention, film form of the non-aqueous electrolyte battery separator is maintained even when temperature increases since it contains a heat-resistant nitrogen-containing aromatic polymer and a ceramic powder. Further, in the case of the non-aqueous electrolyte battery separator of the present invention containing a thermoplastic resin, when the battery is locally or totally heated, the thermoplastic polymer is melted, and introduced into fine pores of the separator to obstruct the fine pores, preventing current. Further, even when temperature increases, the polymer does not flow out since it is introduced in the fine pores. Thus, shut down of the battery is accomplished.

The non-aqueous electrolyte battery separator of the present invention manifests excellent ion permeability and battery property while keeping the feature of a heat-resistant nitrogen-containing aromatic polymer that heat-resistance is

high and short circuit temperature is high. Further, the non-aqueous electrolyte battery separator of the present invention has safety property that shut down occurs in overheat, and further, is not melted when heated and has high short circuit temperature, providing more excellent safety. Moreover, the lithium battery of the present invention has higher short circuit temperature and more excellent safety by using the above-described separator.

EXAMPLE

The following examples further illustrate the present invention specifically, but do not limit the scope thereof. In the examples and comparative examples, test and evaluation methods or judging methods are as follows.

(1) Intrinsic Viscosity

Intrinsic viscosity in the present invention is defined as a value measured by the following measuring method. A solution prepared by dissolving 0.5 g of a para-aramid polymer into 100 ml of 96 to 98% sulfuric acid, and 96 to 98% sulfuric acid were respectively subjected to measurement of flow time at 30° C. using a capillary viscometer, and the intrinsic viscosity was calculated according to the following formula using ratio of the measured flow times.

$$\text{Intrinsic viscosity} = \ln(T/T_0)/C \text{ [unit: dl/g]}$$

T and T_0 represent flow times of a para-aramid sulfuric acid solution and sulfuric acid, respectively, and C represents the para-aramid concentration (dl/g) in the para-aramid sulfuric acid solution.

(2) Measurement of Thickness of a Coated Film and the Like

The thickness of the obtained coated film and the like were measured according to JIS K7130-1992.

(3) Pore Ratio

Coated films and the like were cut into squares having an edge length of 10 cm, and weights (wg) and thickness (D cm) were measured. The weights of materials in the sample were calculated, weight of each material (Wi) was divided by true specific gravity, volume of each material was hypothesized, and void ratio (% by volume) was calculated.

$$\text{Pore ratio (\%)} = 100 - \{(W1/\text{true specific gravity 1}) + (W2/\text{true specific gravity 2}) + \ldots + (Wn/\text{true specific gravity } n)\}/(100D)$$

$$W = \sum_{i=1}^{n} Wi$$

Regarding an aerial weight of coated films and the like, coated films and the like were cut into squares having an edge length of 10 cm, and weights were measured according to the following formula.

$$\text{Aerial weight (g/m}^2\text{)} = \text{weight of sample (g)}/0.01\ (\text{m}^2)$$

Aerial weight of each material was calculated from amount used for film forming, and ratio.

(4) Gas Permeability

The flow amount of air through a sample having a measuring area of 11.3 cm^2 (diameter: 38 mm) at a pressure of 3 kg/cm^2 was measured as air permeability by using Perm Porometer manufactured by Porous Materials Inc., U.S. according to ASTM F316-86.

In general, it is judged that when air permeability is higher, ion permeability is more excellent and battery property is also more excellent in the same material system.

(5) Tensile Strength

A specimen was cut out from the resulted coating films and the like by using a dumbbell cutter manufactured by Dumbbell Corp., and tensile strength, elastic modulus and strain at break were measured according to JIS K-7127 using Instron Universal Tester model4301 manufactured by Instron Japan Corp.

(6) Measurement of Tearing Strength

A specimen was cut out from the resulted coating films and the like by using a dumbbell cutter for JIS K-7128-1991 C method (right angle tearing method) manufactured by Dumbbell Corp., and tearing strength was measured according to JIS K-7128-1991 C method (right angle tearing method using Instron Universal Tensile Tester model 4301 manufactured by Instron Japan Corp. Both ends of the sample were clamped with chucks of the universal tensile tester, drawn at a speed of 200 mm/minute, and load and change during the tension were recorded by a recorder. Tearing strength was calculated from load when tearing of the sample started. Then, tearing transmission resistance was calculated from average value of loads until the sample was completely broken.

The tearing strength and tearing transmission resistance were calculated according to the following formulae.

$$\text{Tearing strength (kg/mm)} = \text{maximum load when tearing of sample start/sample thickness}$$

$$\text{Tearing transmission strength (kg/mm)} = \text{average value of loads after initiation of tearing of sample until complete break/sample thickness}$$

(7) Measurement of Internal Electric Resistance in Flat Battery (Intended for Measuring Electric Resistance, Evaluating Shut Down Action and Evaluating Heat-resistance of Separator)

Coated films and the like were cut into squares having an edge length of 25 mm, and impregnated with an electrolyte solution of a 1N propylene carbonate solution of $LiPF_6$. This was sandwiched between two platinum disk electrodes having a thickness of 0.5 mm and a diameter of 18 mm, 1 volt was applied at 1 KHz between these electrodes to measure internal electric resistance of the flat battery, and the internal electric resistance at a temperature of 25° C. was used as an electric resistance of the separator. This flat battery was placed on a heat plate, and heated at a rate of 4° C./minute from 25° C. to 200° C. The temperature at which internal electric resistance increases in this process was recognized as shut down working temperature.

(8) Evaluation as Non-aqueous Electrolyte Battery Separator

For preparing an anode, a lithium nickelate powder, a carbonaceous conductive powder and polyvinylidene fluoride were mixed at a ratio by weight of 87:10:3 using a N-methylpyrrolidone solvent to prepare a paste, this paste was coated on a 20 μm aluminum foil, dried and pressed to form a sheet having a thickness of 85 μm. For preparing a cathode, a graphite powder and polyvinylidene fluoride were mixed at a ratio by weight of 90:10 using a N-methylpyrrolidone solvent to prepare a paste, this paste was coated on a 10 μm copper foil, dried and pressed to form a sheet having a thickness of 100 μm. Lithium phosphate hexa-fluoride was dissolved (1 mol/L concentration) in a mixed solvent of ethylene carbonate, dimethyl carbonate and ethylmethyl carbonate (ratio weight; 30:35:35) to obtain a solution used as an electrolyte solution. The non-aqueous electrolyte battery separator described in the examples of the present invention was us ed as a separator.

The battery used had flat structure having an anode area of 2.34 cm^2 . The cathode sheet, separator, anode sheet as prepared above were laminated in this order in a box under argon atmosphere, then, the separator is fully impregnated

with the electrolyte solution. The flat battery produced was subjected to 8 cycles of a charge voltage of 4.2 V and a discharge voltage of 2.75 V, and discharge capacity (discharge current: 1.5 mA) was measured at 8 cycle, defined as discharge capacity at 0.2 C. Also, cycle degratation was measured. Charging was conducted under the above-described conditions and discharge capacity (discharge current: 22.5 mA) was measured to be defined as discharge capacity at 3 C. Load property of the battery at 3 C was calculated according to the following formula.

Load property (%) of battery at 3 *C*=discharge capacity at 3 *C*/discharge capacity at 0.2×100

"C." is defined as discharge is occurred for one hour, also "3C" is defined as discharge is occurred for 20 minutes.

(9) Safety Test in Cylindrical Battery

Anode sheet electrodes and cathode sheet electrodes produced in the same manner as in the procedure (8) were laminated via the above-described separator in the order of cathode, separator, anode and separator, and the resulted laminate was wound from one end to obtain an electrode element having roll form.

The above-described electrode element was inserted into a battery can, impregnated with the above-described non-aqueous electrolyte solution, and a battery lid also acting as an anode terminal having safety was fastened via a gasket to obtain a cylindrical battery having 18650 size.

(10) Method for Measuring Average Particle Size of Ceramic Powder

The average particle size was obtained by analyzing a photography obtained by an electron microscope using a particle size measuring apparatus TGZ 3 manufactured by Karl Zeiss Corp.

Example 1

1. Production of poly(p-phenyleneterephthalamide)

Poly(p-phenyleneterephthalamide) (hereinafter, sometimes referred to as PPTA) was produced using a 3 liter separable flask equipped with a stirrer, thermometer, nitrogen introducing tube and powder addition port. The flask was fully dried, charged with 2200 g of N-methyl-2-pyrrolidone, and 151.07 g of a calcium chloride powder which had been dried in vacuo at 200° C. for 2 hours was added, the resulted mixture was heated to 100° C. for completion dissolution. The temperature was lowered to room temperature again, and 68.23 g of p-phenylenediamine was added and dissolved completely. Then, 124.97 g of terephthalic dichloride was added in ten portions at an interval of about 5 minutes while maintaining this solution at 20° C.±2° C. One portion of ten-divided terephthalic dichloride was dissolved in the same weight of N-methyl-2-pyrrolidone (hereinafter, sometimes referred to as NMP) as that of the terephthalic dichloride before the final addition. The solution was filtered through a 1500 mesh stainless wire gauze. The resulted solution was liquid crystal phase having a PPTA concentration of 6%, and exhibited optical anisotropy. A part of the PPTA solution was sampled, and precipitated again in water to obtain PPTA having an intrinsic viscosity of 2.01 dl/g.

2. Preparation of PPTA Slurry Solution for Coating

65 g of the PPTA solution in the above-described process 1. in Example 1 was weighed into a 500 ml separable flask equipped with a stirrer, thermometer, nitrogen introducing tube and liquid addition port, to this was added 235 g of NMP, and the mixture was processed finally into an isotropic solution having a PPTA concentration of 1.3% by weight and stirred for 60 minutes.

Into the above-described solution was mixed 3.9 g of an alumina fine particle (manufactured by Nippon Aerosil Corp.; Alumina C, average particle size 0.013 μm), and the mixture was stirred for 240 minutes. The slurry solution in which the alumina fine particle had been sufficiently dispersed was filtered through a 1000 mesh wire gauze, then, defoamed under reduced pressure to obtain a slurry solution for coating.

3. Production of Coating Film

A polyethylenetelephthalate (hereinafter, sometimes referred to as PET) film having a thickness of 100 μm was wound on a drum having a diameter of 550 mm and a length of 350 mm. Onto the PET film, a substrate (polyester paper, trade name 0132TH-8 narrow denier type, aerial weight 8 g/m^2, thickness 20 μm; manufactured by Japan Vilene Co., Ltd.) was wound. One end of the substrate was fixed on the drum with a tape. On another end, a weight of 0.6 g was suspended so that the load was applied uniformly to the substrate. A stainless coating bar having a diameter of 20 mm was mounted on the top of the drum in parallel so that clearance between it and the drum was 0.3 mm. Drum was so rotated that the end fixed with tape was situated between the drum and the coating bar, and stopped. The drum was rotated at 0.5 rpm while supplying the PPTA slurry solution for coating as prepared above to the substrate in front of the coating bar, to conduct coating on the substrate.

When the whole substrate was coated, the rotation of the drum was stopped, and left under atmosphere of a temperature of 23° C. and a humidity of 50% for 10 minutes to allow PPTA to deposit. The 100 μm PET film and the coated film prepared by coating the slurry solution on the substrate and allowing it to deposit were removed in integrated form from the drum and immersed in ion-exchanged water, and washed for 12 hours while ion-exchanged water was being flown. After the washing, the PET film was taken up, and the wet coated film was sandwiched with polyester clothes from both sides, further sandwiched by aramid felts, plated on an aluminum flat plate having a thickness of 3 mm, and onto this was placed a nylon film having a thickness of 0.1 mm, and the surrounding area was sealed with a sealing material, and dried at 150° C. for 2 hours with evacuating inside thereof, to obtain a dried coated film.

4. Coating of Polyolefin Suspension

Suspensions of polyolefin (hereinafter, referred to as "PO")(Chemipearl WF 640 and Chemipearl WP 100 (manufactured by Mitsui Petrochemical Industries, Ltd.)) were mixed in the same amount, and to this was added ion-exchanged water so that the solid contend was 30% to prepare a polyolefin suspension for coating.

Chemipearl WF 640 and Chemipearl WP 100:Lower molecular weight polyolefin having a particle size of 1 μm (measured by Colter.Counter method).

A PET film having a thickness of 25 μm which had been subjected to releasing treatment was wound on a drum having a diameter of 550 mm and a length of 350 mm. Onto the PET film, the above-described dried coated film cut into a width of 300 mm and a length of 900 mm was wound, and one end was fixed on the drum with a tape. On another end, a weight of 0.6 g was suspended so that the load was applied uniformly to the dried coated film. A stainless coating bar having a diameter of 20 mm was mounted on the top of the drum in parallel so that clearance between it and the drum was 0.075 mm. Drum was so rotated that the end fixed with tape was situated between the drum and the coating bar, and stopped. The drum was rotated at 0.5 rpm while supplying the polyolefin suspension for coating as prepared above onto the dried coated film in front of the coating bar, to conduct

coating of the polyolefin suspension onto the dried coated film. When the whole dried coated film was coated, the rotation of drum was stopped, left and dried for 60 minutes to obtain a non-aqueous electrolyte separator.

5. Physical Properties of Non-aqueous Electrolyte Battery Separator

The above-described non-aqueous electrolyte separator had a thickness of 26.3 μm, an aerial weight of 19.2 g/m^2 (PET paper; 8 g/m^2, PPTA; 3.1 g/m^2, alumina; 3.1 g/m^2, PO; 5.0 g/m^2), and a void ratio of 44.8%. The separator was observed with a scanning electron microscope to find that one surface was a porous layer which was made of a PPTA resin in the form of fibril, layer having a thickness of about 0.1 μm or less, in which an alumina fine particle having a particle size of about 0.013 μm was dispersed between the fibrils and which had voids having a pore size of 0.05 to 0.2 μm. Another surface carried polyolefin particles having a particle size of about 1 μm in the form of a layer having a thickness of about 5 μm. The section was observed to find that an alumina fine particle having a particle size of about 0.013 μm was filled between the polyester fiber of the substrate paper so that the alumina fine particle was dispersed between the PPTA resin in the form of fibril having a thickness of about 0.1 μm or less.

The separator of the present invention had an air permeability of 105 cc/sec, a tensile strength of 4.9 kg/mm^2, a strain at break of 2.8%, a tearing strength of 4.9 kg/mm and a tearing transmission resistance of 2.5 kg/mm.

6. Measurement of Shut Down Ability and Evaluation of Heat-resistance

The internal electrical resistance at 25° C. before heating of the above-described separator was 25Ω. When the temperature of the sample increased gradually, the internal electric resistance decreased gradually, however, from around 100° C. on, the internal electric resistance started to increase and reached to 100Ω at about 120° C. The temperature was further increased to 200° C. to find no reduction in electric resistance by melt down. Form the above-described results, it was found that the separator of the present invention had shut down function which cut off current in temperature increase, and heat-resistance.

7. Evaluation as Non-aqueous Electrolyte Battery Separator

The resulted separator had a discharge capacity at 8th cycle of 188 mAH/g (discharge current 1.5 mA), and operated normally without cycle degradation. Load property was 41% at 3 C. From the above-described results, it was found that the separator of the present invention had function as a non-aqueous electrolyte battery separator.

8. Safety Test on Cylindrical Battery

Two cylindrical batteries obtained in the above-described method were made into overcharged condition by conducting 150% charging base on rated capacity, then needle piercing test was conducted. The needle piercing test was conducted according to lithium secondary battery safety evaluation standard guideline of Nippon Chikudenchi Battery Association(Nippon Chikudenchi Kogyokai Guideline SBA-G1101-1995).

In spite of such severe condition as overcharge, the battery subjected to the test did not manifest neither breakage nor ignition.

Example 2

1. Preparation of PPTA Slurry Solution for Coating

It was prepared in the same manner as in Example 1 except that the weight of the alumina fine particle mixed was 39 g.

2. Production of Coated Film

It was made in the same manner as process 3 in Example 1 except that the stainless coating bar was placed in parallel so that the clearance between it and the drum was 0.1 mm.

3. Coating of Polyolefin Suspension Layer

A non-aqueous electrolyte battery separator was obtained in the same manner as process 4 in Example 1. (0081)

4. Physical Properties of Non-aqueous Electrolyte Battery Separator

The above-described non-aqueous electrolyte separator had a thickness of 24.1 μm, an aerial weight of 17.8 g/m^2 (PET paper; 8 g/m^2, PPTA; 0.42 g/m^2, alumina; 4.2 g/m^2, PO; 5.0 g/m^2), and a void ratio of 45.3%. The separator was observed with a scanning electron microscope to find that one surface was a porous layer which was made of a PPTA resin in the form of fibril, said layer having a thickness of about 0.1 μm or less, in which an alumina fine particle having a particle size of about 0.013 μm was dispersed between the fibrils and which had voids having a pore size of 0.05 to 0.2 μm. Another surface carried polyolefin particles having a particle size of about 1 μm in the form of a layer having a thickness of about 5 μm. The section was observed to find that an alumina fine particle having a particle size of about 0.013 μm was filled between the polyester fiber of the substrate paper so that the alumina fine particle was dispersed between the PPTA resin in the form of fibril having a thickness of about 0.1 μm or less.

The separator of the present invention had an air permeability of 750 cc/sec.

5. Measurement of Shut Down Ability and Evaluation of Heat-resistance

The internal electrical resistance at 25° C. before heating of the above-described separator was 20Ω. When the temperature of the sample increased gradually, the internal electric resistance decreased gradually, however, from around 100° C., the internal electric resistance started to increase and reached to 252Ω at about 120° C. The temperature was further increased to 200° C. to find no reduction in electric resistance by melt down. Form the above-described results, it was found that the separator of the present invention had shut down function which cut off current in temperature increase, and heat-resistance.

6. Evaluation as Non-aqueous Electrolyte Battery Separator

The resulted separator had a discharge capacity at 8 cycle of 193 mAH/g (discharge current 1.5 mA), and operated normally without cycle degradation. Load property was 47% at 3 C. From the above-described results, it was found that the separator of the present invention had function as a non-aqueous electrolyte battery separator.

Example 3

1. Preparation of Polyimide Resin Slurry Solution for Coating

100 g of a NMP solution of a polyimide resin soluble in a solvent having a polymer concentration of 20% (Ricacoat PN-20; manufactured by New Japan Chemical Co., Ltd.) and 2 g of an alumina fine particle (manufactured by Nippon Aerosil Corp.; Alumina C, average particle size 0.013 μm) were weighed into a 500 ml separable flask equipped with a stirrer, thermometer, nitrogen introducing tube and liquid addition port, and the mixture was stirred for 120 minutes. To this was added 45 ml of NMP, and the mixture was stirred for 120 minutes. The slurry solution in which the alumina fine particle had been sufficiently dispersed was filtered through a 1000 mesh wire gauze, then, defoamed under reduced pressure to obtain a slurry solution for coating.

2. Production of Coating Film

It was prepared in the same manner as process 3 in Example 1 except that the stainless coating bar was placed in parallel so that the clearance between it and the drum was 0.1 mm.

3. Coating of Polyolefin Suspension

A non-aqueous electrolyte battery separator was obtained in the same manner as in Example 1.

4. Physical Properties of Non-aqueous Electrolyte Battery Separator

The above-described non-aqueous electrolyte separator had a thickness of 27.4 μm, an aerial weight of 18.1 g/m^2 (PET paper; 8 g/m^2, polyimide; 4.4 g/m^2, alumina; 0.44 g/m^2, PO; 5.3 g/m^2), and a void ratio of 45.4%. The section of the separator was observed with a scanning electron microscope to find one layer in which an alumina fine particle having a particle size of about 0.013 μm was filled between the polyester fiber of the substrate paper so that the alumina fine particle was dispersed to form open cell in the porous polyimide resin and a layer containing polyolefin particles having a particle size of about 1 μm, and having a thickness of about 5 μm.

5. Measurement of Shut Down Ability and Evaluation of Heat-resistance

The internal electrical resistance at 25° C. before heating of the above-described separator was 35Ω. When the temperature of the sample increased gradually, the internal electric resistance decreased gradually, however, from around 100° C., the internal electric resistance started to increase and reached to 70Ω at about 120° C. The temperature was further increased to 200° C. to find no reduction in electric resistance by melt down. Form the above-described results, it was found that the separator of the present invention had shut down function which cut off current in temperature increase, and heat-resistance.

6. Evaluation as Non-aqueous Electrolyte Battery Separator

The resulted separator had a discharge capacity at 8 cycle of 183 mAH/g (discharge current 1.5 mA), and operated normally without cycle degradation. Load property was 8% at 3 C. From the above-described results, it was found that the separator of the present invention had function as a non-aqueous electrolyte battery separator.

Example 4

1. Preparation of Polyimide Resin Slurry Solution for Coating

100 g of a NMP solution of a polyimide resin soluble in a solvent having a polymer concentration of 20% (Ricacoat PN-20; manufactured by New Japan Chemical Co., Ltd.) and 7 g of an alumina fine particle (manufactured by Nippon Aerosil Corp.; Alumina C, average particle size 0.013 μm) were weighed into a 500 ml separable flask equipped with a stirrer, thermometer, nitrogen introducing tube and liquid addition port, and the mixture was stirred for 120 minutes. To this was added 28 ml of NMP, and the mixture was stirred for 120 minutes. The slurry solution in which the alumina fine particle had been sufficiently dispersed was filtered through a 1000 mesh wire gauze, then, defoamed under reduced pressure to obtain a slurry solution for coating.

2. Production of Coating Film

It was prepared in the same manner as process 3 in Example 1 except that the stainless coating bar was placed in parallel so that the clearance between it and the drum was 0.1 mm.

3. Coating of Polyolefin Suspension

A non-aqueous electrolyte battery separator was obtained in the same manner as process 4 in Example 1.

4. Physical Properties of Non-aqueous Electrolyte Battery Separator

The above-described non-aqueous electrolyte separator had a thickness of 26.7 μm, an aerial weight of 17.7 g/m^2 (PET paper; 8 g/m^2, polyimide; 3.4 g/m^2, alumina; 1.2 g/m^2, PO; 5.1 g/m^2), and a void ratio of 46.5%. The section of the separator was observed with a scanning electron microscope to find one layer in which an alumina fine particle having a particle size of about 0.013 μm was filled between the polyester fiber of the substrate paper so that the alumina fine particle was dispersed to form open cell in the porous polyimide resin and a layer containing polyolefin particles having a particle size of about 1 μm, and having a thickness of about 5 μm.

The separator of the present invention had an air permeability of 680 cc/sec.

5. Measurement of Shut Down Ability

The internal electrical resistance at 25° C. before heating of the above-described separator was 25Ω. When the temperature of the sample increased gradually, the internal electric resistance decreased gradually, however, from around 100° C., the internal electric resistance started to increase and reached to 79Ω at about 120° C. The temperature was further increased to 200° C. to find no reduction in electric resistance by melt down. Form the above-described results, it was found that the separator of the present invention had shut down function which cut off current in temperature increase, and heat-resistance.

6. Evaluation as Non-aqueous Electrolyte Battery Separator

The resulted separator had a discharge capacity at 8 cycle of 190 mAH/g (discharge current 1.5 mA), and operated normally without cycle degradation. Load property was 24% at 3 C. From the above-described results, it was found that the separator of the present invention had function as a non-aqueous electrolyte battery separator.

Example 5

1. Preparation of Polyimide Resin Slurry Solution for Coating

100 g of a NMP solution of a polyimide resin soluble in a solvent having a polymer concentration of 20% (Ricacoat PN-20; manufactured by New Japan Chemical Co., Ltd.) and 10 g of an alumina fine particle (manufactured by Nippon Aerosil Corp.; Alumina C, average particle size 0.013 μm) were weighed into a 500 ml separable flask equipped with a stirrer, thermometer, nitrogen introducing tube and liquid addition port, and the mixture was stirred for 120 minutes. To this was added 40 ml of NMP, and the mixture was stirred for 120 minutes. The slurry solution in which the alumina fine particle had been sufficiently dispersed was filtered through a 1000 mesh wire gauze, then, defoamed under reduced pressure to obtain a slurry solution for coating.

2. Production of Coating Film

It was prepared in the same manner as process 3 in Example 1 except that the stainless coating bar was placed in parallel so that the clearance between it and the drum was 0.1 mm.

3. Coating of Polyolefin Suspension

A non-aqueous electrolyte battery separator was obtained in the same manner as process 4 in Example 1 except that the stainless coating bar was placed in parallel so that the clearance between it and the drum was 0.05 mm. (0097)

4. Physical Properties of Non-aqueous Electrolyte Battery Separator

The above-described non-aqueous electrolyte separator had a thickness of 29.6 μm, an aerial weight of 20.5 g/m^2 (PET paper; 8 g/m^2, polyimide; 4.9 g/m^2, alumina; 2.5 g/m^2, PO; 5.1 g/m^2), and a void ratio of 48.1%. The section of the separator was observed with a scanning electron microscope to find one layer in which an alumina fine particle having a particle size of about 0.013 μm was filled between the polyester fiber of the substrate paper so that the alumina fine particle was dispersed to form open cell in the porous polyimide resin and a layer containing polyolefin particles

having a particle size of about 1 μm, and having a thickness of about 5 μm.

The separator of the present invention had an air permeability of 3200 cc/sec, a tensile strength of4.5 kg/mm^2, a strain at break of 14.0%, a tearing strength of 7.5 kg/mm and a tearing transmission resistance of 3.3 kg/mm.

5. Measurement of Shut Down Ability and Evaluation of Heat-resistance

The internal electrical resistance at 25° C. before heating of the above-described separator was 35Ω. When the temperature of the sample increased gradually, the internal electric resistance decreased gradually, however, from around 100° C., the internal electric resistance started to increase and reached to 221Ω at about 120° C. The temperature was further increased to 200° C. to find no reduction in electric resistance by melt down. Form the above-described results, it was found that the separator of the present invention had shut down function which cut off current in temperature increase, and heat-resistance.

6. Evaluation as Non-aqueous Electrolyte Battery Separator

The resulted separator had a discharge capacity at 8 cycle of 187 mAH/g (discharge current 1.5 mA), and operated normally without cycle degradation. Load property was 63% at 3 C. From the above-described results, it was found that the separator of the present invention had function as a non-aqueous electrolyte battery separator.

7. Safety Test on Cylindrical Battery

Two cylindrical batteries obtained in the above-described method were made into overcharged condition by conducting 150% charging base on rated capacity, then needle piercing test was conducted. The needle piercing test was conducted according to lithium secondary battery safety evaluation standard guideline of Nippon Chikudenchi Battery Association (Nippon Chikudenchi Kogyokai Guideline SBA-G1101-1995)

In spite of such severe condition as overcharge, the battery subjected to the test did not manifest neither breakage nor ignition.

Example 6

1. Preparation of Polyimide Resin Slurry Solution for Coating

100 g of a NMP solution of a polyimide resin soluble in a solvent having a polymer concentration of 20% (Ricacoat PN-20; manufactured by New Japan Chemical Co., Ltd.) and 10 g of an alumina fine particle (AMS-12;manufactured by Sumitomo Chemical Co., Ltd.) having a particle size of 0.4 μm were weighed into a 500 ml separable flask equipped with a stirrer, thermometer, nitrogen introducing tube and liquid addition port, and the mixture was stirred for 120 minutes. To this was added 45 ml of NMP, and the mixture was stirred for 120 minutes, then, defoamed under reduced pressure to obtain a slurry solution for coating. This slurry solution was allowed to stand still for 24 hours to find deposition of the alumina fine particle.

2. Production of Coating Film

It was prepared in the same manner as process 3 in Example 1 except that the stainless coating bar was placed in parallel so that the clearance between it and the drum was 0.1 mm.

3. Coating of Polyolefin Suspension

A non-aqueous electrolyte battery separator was obtained in the same manner as process 4 in Example 1.

4. Physical Properties of Non-aqueous Electrolyte Battery Separator

The above-described non-aqueous electrolyte separator had a thickness of 26.5 μm, an aerial weight of 17.8 g/m^2 (PET paper; 8 g/m^2, polyimide; 3.0 g/m^2, alumina; 1.5 g/m^2, PO; 5.3 g/m^2), and a void ratio of 46.0%. The section of the separator was observed with a scanning electron microscope to find one layer in which an alumina fine particle having a particle size of about 0.4 μm was filled between the polyester fiber of the substrate paper so that the alumina fine particle was dispersed to form open cell in the porous polyimide resin and a layer containing polyolefin particles having a particle size of about 1 μm, and having a thickness of about 5 μm.

The separator had air permeabilities from 120 cc/sec to 270 cc/sec, and unevenness depending on site was observed.

Comparative Example 1

1. Preparation of Polyimide Resin Slurry Solution for Coating

1100 g of a NMP solution of a polyimide resin soluble in a solvent having a polymer concentration of 20% (Ricacoat PN-20; manufactured by New Japan Chemical Co., Ltd.) was weighed into a 500 ml separable flask equipped with a stirrer, thermometer, nitrogen introducing tube and liquid addition port, and the mixture was defoamed under reduced pressure to obtain a solution for coating.

2. Production of Coating Film

It was prepared in the same manner as process 3 in Example 1 except that the stainless coating bar was placed in parallel so that the clearance between it and the drum was 0.05 mm.

3. Coating of Polyolefin Suspension

A non-aqueous electrolyte battery separator was obtained in the same manner as process 4 in Example 1.

4. Physical Properties of Non-aqueous Electrolyte Battery Separator

The above-described non-aqueous electrolyte separator had a thickness of 28.0 μm, an aerial weight of 17.7 g/m^2 (PET paper; 8 g m^2, polyimide; 4.6 g/m^2, PO; 5.1 g/m^2) and a pore ratio of 47.3%. The section of the separator was observed with a scanning electron microscope to find one layer in which a porous polyimide resin was filled between the polyester fiber of the substrate paper and a layer containing polyolefin particles having a particle size of about 1 μm, and having a thickness of about 5 μm.

The separator had an air permeabilities of as low as 3 cc/sec.

5. Measurement of Shut Down Ability and Evaluation as Battery Separator

It is impossible to measure because of poor impregnation of electrolyte.

Example 7

1. Preparation of PPTA Dope for Coating PPTA Dope for Coating ①

100 g of the PPTA dope in the above-described process 1. in Example 1 was weighed into a 500 ml separable flask equipped with a stirrer, thermometer, nitrogen introducing tube and liquid addition port, to this was added 140 g of NMP, and the mixture was processed finally into an isotropic solution having a PPTA concentration of 2.5% by weight and stirred for 60 minutes. Into the above-described solution having a PPTA concentration of 2.5% by weight was mixed 6 g of an alumina fine particle (manufactured by Nippon Aerosil Corp.; Alumina C), and the mixture was stirred for 240 minutes. The coating dope was passed through a nanomizer three times to fully disperse the alumina fine particle and was filtered through a 1000 mesh wire gauze. Then, defoamed under reduced pressure to obtain a dope for coating.

2. Production of Porous Film Layer

A PET film having a thickness of 100 μm was wound on a drum having a diameter of 550 mm and a length of 350

mm. Onto the PET film, a substrate (polyethylene separator, aerial weight 10.5 g/m^2, thickness 16 μm; pore ratio 40%) was wound. One end of the substrate was fixed on the drum with a tape. On another end, a weight of 0.6 g was suspended so that the load was applied uniformly to the substrate. A stainless coating bar having a diameter of 25 mm was mounted on the top of the drum in parallel so that clearance between it and the drum was 0.15 mm. Drum was so rotated that the end fixed with tape was situated between the drum and the coating bar, and stopped. The drum was rotated at 0.5 rpm while supplying the PPTA slurry solution for coating as prepared above to the substrate in front of the coating bar, to conduct coating on the substrate.

The whole substrate was coated, the drum was left under atmosphere of a temperature of 23° C. and a humidity of 50% for 10 minutes while the drum was being rotated to allow PPTA to deposit. The 100 μm PET film and the film prepared by coating and depositing the dope on the substrate were removed in integrated form from the drum and immersed in ion-exchanged water, and washed for 12 hours while ion-exchanged water was being flown. After the washing, the PET film was taken up, and the wet coated film was sandwiched with polyester clothes from both sides, further sandwiched by aramid felts, plated on an aluminum flat plate having a thickness of 3 mm, and onto this was placed a nylon film having a thickness of 0.1 mm, and the surrounding area was sealed with a sealing material, and dried at 70° C. for 6 hours with evacuating inside thereof, to obtain a non-aqueous electrolyte battery separator.

3. Physical Properties of Non-aqueous Electrolyte Battery Separator

The above-described non-aqueous electrolyte separator had a thickness of 24.0 μm, an aerial weight of 17.0 g/m^2 (polyethylene separator 10.5 g/m^2, PPTA; 3.2 g/m^2, alumina; 3.2 g/m^2), and a void ratio of the heat-resistant layer of 59.4%. The film was observed with a scanning electron microscope to find that one surface was a porous layer which was made of a PPTA resin in the form of fibril, layer having a thickness of about 0.1 μm or less, in which an alumina fine particle having a particle size of about 0.013 μm was dispersed between the fibrils and which had voids having a pore size of 0.05 to 0.2 μm. The section was observed to find two-layer structure in which the PPTA resin invaded into and adhered to the substrate polyethylene separator.

The separator of the present invention had an air permeability of 43 cc/sec.

4. Measurement of Shut Down Ability

The internal electrical resistance at 25° C. before heating of the above-described separator was 20Ω. When the temperature of the sample increased gradually, the internal electric resistance decreased gradually, however, from around 130° C., the internal electric resistance started to increase and reached to 2KΩ at about 135° C. The temperature was further increased to 200° C. to find no reduction in electric resistance by melt down. Form the above-described results, it was found that the separator of the present invention had shut down function which cut off current in temperature increase, and heat-resistance.

5. Evaluation as Non-aqueous Electrolyte Battery Separator

The resulted separator had a discharge capacity at 8th cycle of 193 mAH/g (discharge current 1.5 mA), and operated normally without cycle degradation. Load property was 53% at 3 C. From the above-described results, it was found that the separator of the present invention had function as a non-aqueous electrolyte battery separator.

Example 8

1. Preparation of Polyimide Resin Dope for Coating

100 g of a NMP solution of a polyimide resin having a polymer concentration of 20% (PN-20; manufactured by New Japan Chemical Co., Ltd.) and 10 g of an alumina fine particle (manufactured by Nippon Aerosil Corp.; Alumina C) were weighed into a 500 ml separable flask equipped with a stirrer, thermometer, nitrogen introducing tube and liquid addition port, and the mixture was stirred for 120 minutes. To this was added 60 ml of NMP, and the mixture was stirred for 120 minutes. The mixture was passed through a nanomizer three times to fully disperse the alumina fine particle and the coating dope was filtered through a 1000 mesh wire gauze. Then, defoamed under reduced pressure to obtain a dope for coating.

2. Production of Porous Film Layer

A PET film having a thickness of 100 μm was wound on a drum having a diameter of 550 mm and a length of 350 mm. Onto the PET film, a substrate (polyethylene separator, aerial weight 10.5 g/m^2, thickness 16 μm; pore ratio 40%) was wound. One end of the substrate was fixed on the drum with a tape. On another end, a weight of 0.6 g was suspended so that the load was applied uniformly to the substrate. A stainless coating bar having a diameter of 25 mm was mounted on the top of the drum in parallel so that clearance between it and the drum was 0.03 mm. Drum was so rotated that the end fixed with tape was situated between the drum and the coating bar, and stopped. The drum was rotated at 0.5 rpm while supplying the PPTA slurry solution for coating as prepared above to the substrate in front of the coating bar, to conduct coating on the substrate.

The whole substrate was coated, the drum was left under atmosphere at a temperature of 23° C. and a humidity of 50% for 10 minutes while the drum was being rotated to allow PPTA to deposit. The 100 μm PET film and the film prepared by coating and depositing the dope on the substrate were removed in integrated form from the drum and immersed in ion-exchanged water, and washed for 12 hours while ion-exchanged water was being flown. After the washing, the PET film was taken up, and the wet coated film was sandwiched with polyester clothes from both sides, further sandwiched by aramid felts, plated on an aluminum flat plate having a thickness of 3 mm, and onto this was placed a nylon film having a thickness of 0.1 mm, and the surrounding area was sealed with a sealing material, and dried at 70° C. for 6 hours with evacuating inside thereof, to obtain a non-aqueous electrolyte battery separator.

3. Physical Properties of Non-aqueous Electrolyte Battery Separator

The above-described dried film had a thickness of 28.0 μm, an aerial weight of 17.5 g/m^2 (polyethylene separator 10.5 g/m^2, PI; 4.7 g/m^2, alumina; 2.3 g/m^2), and a void ratio of the heat-resistant layer of 65.9%. The film was observed with a scanning electron microscope to find that the alumina fine particle was dispersed in the porous polyimide resin to form open cell and this dispersion invaded into and adhered to the substrate polyethylene separator, forming two-layer structure.

The separator of the present invention had an air permeability of 60 cc/sec.

4. Measurement of Shut Down Ability The internal electrical resistance at 25° C. before heating of the above-described separator was 35Ω. When the temperature of the sample increased gradually, the internal electric resistance decreased gradually, however, from around 130° C., the internal electric resistance started to increase and reached to 2.5KΩ at about 135° C. The temperature was further

increased to 200° C. to find no reduction in electric resistance by melt down. Form the above-described results, it was found that the separator of the present invention had shut down function which cut off current in temperature increase, and heat-resistance.

5. Evaluation as Non-aqueous Electrolyte Battery Separator

The resulted separator had a discharge capacity at 8 cycle of 183 mAH/g (discharge current 1.5 mA), and operated normally without cycle degradation. Load property was 61% at 3 C. From the above-described results, it was found that the separator of the present invention had function as a non-aqueous electrolyte battery separator.

Example 9

1. Preparation of Polyimide Resin Dope for Coating

50 g of a NMP solution of a polyimide resin having a polymer concentration of 20% (PN-20; manufactured by New Japan Chemical Co., Ltd.) and 150 g of an alumina fine particle (manufactured by Sumitomo Chemical Co., Ltd.; Sumicorumdum, having an average particle size of 0.3 μm and a particle size distribution of 0.1 to 1.0 μm) were weighed into a 500 ml separable flask equipped with a stirrer, thermometer, nitrogen introducing tube and liquid addition port, and to this was added 350 ml of NMP, and the mixture was stirred for 120 minutes. The mixture was passed through a nanomizer three times to fully disperse the alumina fine particle and the coating dope was defoamed under reduced pressure to obtain a dope for coating.

2. Production of Porous Film Layer

A PET film having a thickness of 100 μm was wound on a drum having a diameter of 550 mm and a length of 350 mm. Onto the PET film, a substrate (polyethylene separator, aerial weight 10.5 g m^2, thickness 16 μm; pore ratio 40%) was wound. One end of the substrate was fixed on the drum with a tape. On another end, a weight of 0.6 g was suspended so that the load was applied uniformly to the substrate. A stainless coating bar having a diameter of 25 mm was mounted on the top of the drum in parallel so that clearance between it and the drum was 0.05 mm. Drum was so rotated that the end fixed with tape was situated between the drum and the coating bar, and stopped. The drum was rotated at 0.5 rpm while supplying the PPTA slurry solution for coating as prepared above to the substrate in front of the coating bar, to conduct coating on the substrate.

The whole substrate was coated, then, the drum was heated at a temperature of 70° C. for 2 hours to evaporate the solvent, obtaining a non-aqueous electrolyte battery separator.

3. Physical Properties of Non-aqueous Electrolyte Battery Separator

The above-described dried film had a thickness of 24.0 μm, an aerial weight of 28.1 g/m^2 (polyethylene separator 10.5 g/m^2, PI; 1.1 g/m^2, alumina; 16.5 g/m^2), and a void ratio of the heat-resistant layer of 25.7%. The section of the film was observed with a scanning electron microscope to find that the alumina fine particle was dispersed in the porous polyimide resin to form open cell and this dispersion invaded into and adhered to the substrate polyethylene separator, forming two-layer structure.

The separator of the present invention had an air permeability of 38 cc/sec.

4. Measurement of Shut Down Ability

The internal electrical resistance at 25° C. before heating of the above-described separator was 31Ω. When the temperature of the sample increased gradually, the internal electric resistance decreased gradually, however, from around 130° C., the internal electric resistance started to increase and reached to 2.8KΩ at about 135° C. The temperature was further increased to 200° C. to find no reduction in electric resistance by melt down. Form the above-described results, it was found that the separator of the present invention had shut down function which cut off current in temperature increase, and heat-resistance.

5. Evaluation as Non-aqueous Electrolyte Battery Separator

The resulted separator had a discharge capacity at 8 cycle of 183 mAH/g (discharge current 1.5 mA), and operated normally without cycle degradation. Load property was 40% at 3 C. From the above-described results, it was found that the separator of the present invention had function as a non-aqueous electrolyte battery separator.

What is claimed is:

1. A non-aqueous electrolyte battery separator comprising a heat-resistant nitrogen-containing aromatic polymer and a ceramic powder that has a spherical form and an average particle size of a primary particle of 1.0 μm or less, and the amount of the ceramic powder is from 1% by weight to 95% by weight based on the weight of the whole separator.

2. A non-aqueous electrolyte battery separator comprising a heat-resistant nitrogen-containing aromatic polymer, a ceramic powder and a substrate made of woven fabric, non-woven fabric, paper or porous film, wherein the ceramic powder has a spherical form and an average particle size of a primary particle of 1.0 μm or less, and the amount of the ceramic powder is from 1% by weight to 95% by weight based on the weight of the whole separator.

3. The non-aqueous electrolyte battery separator according to claim **2**, wherein the substrate has a weight per unit area of 40 g/m^2 or less and a thickness of 70 μm or less.

4. The non-aqueous electrolyte battery separator according to claim **2** or **3**, wherein the substrate comprises organic fiber and/or inorganic fiber.

5. The non-aqueous electrolyte battery separator according to claim **4**, wherein the organic fiber is made of a thermoplastic polymer.

6. The non-aqueous electrolyte battery separator according to claim **4**, wherein the inorganic fiber is glass fiber.

7. The non-aqueous electrolyte battery separator according to claim **1**, wherein the non-aqueous electrolyte battery separator contains a thermoplastic polymer which is melted at a temperature of 260° C. or less in an amount of 10% by weight or more based on the whole separator, and said thermoplastic polymer is melted when temperature increases and obstructs void of said separator.

8. A non-aqueous electrolyte battery separator comprising a film obtained by a method comprising the following steps of:

(a) preparing a slurry solution which may contain a thermoplastic resin which is melted at a temperature of 260° C. or less, by dispersing a ceramic powder in a solution of a polar organic solvent containing a heat resistant nitrogen-containing aromatic polymer in an amount of 1 to 1500 parts by weight based on 100 parts by weight of said heat-resistant nitrogen-containing aromatic polymer, wherein the ceramic powder has a spherical form and an average particle size of a primary particle of 1.0 μm or less, and the amount of the ceramic powder is from 1% by weight to 95% by weight based on the weight of the whole separator,

(b) coating said slurry solution on a support,

(c) depositing said heat-resistant nitrogen-containing aromatic polymer from said slurry solution to produce a film coated,

(d) removing the polar organic solvent from said film, and

(e) drying said film.

9. A non-aqueous electrolyte battery separator comprising a film obtained by a method comprising the following steps of:

(a) preparing a slurry solution which may contain a thermoplastic resin which is melted at a temperature of 260° C. or less, by dispersing a ceramic powder in a solution of a polar organic solvent containing a heat resistant nitrogen-containing aromatic polymer in an amount of 1 to 1500 parts by weight based on 100 parts by weight of said heat-resistant nitrogen-containing aromatic polymer, wherein the ceramic powder has a spherical form and an average particle size of a primary particle of 1.0 μm or less, and the amount of the ceramic powder is from 1% by weight to 95% by weight based on the weight of the whole separator,

(b) coating said slurry solution on a substrate made of woven fabric, non-woven fabric, paper or porous film,

(c) depositing said heat-resistant nitrogen-containing aromatic polymer from said slurry solution to produce a coated film,

(d) removing the polar organic solvent from said film, and

(e) drying said coated film.

10. A non-aqueous electrolyte battery separator obtained by coating a fine particle-like suspension of a thermoplastic polymer on the non-aqueous electrolyte battery separator according to claim **8** or **9** and drying the suspension to form a fine particle layer of the thermoplastic polymer.

11. The non-aqueous electrolyte battery separator according to claim **1**, wherein the heat-resistant nitrogen-containing aromatic polymer is an aromatic polyimide or aromatic polyamide.

12. The non-aqueous electrolyte battery separator according to claim **11**, wherein the aromatic polyamide is a para-oriented aromatic polyamide having an intrinsic viscosity of 1.0 to 2.8 dl/g.

13. The non-aqueous electrolyte battery separator according to claim **11**, wherein the aromatic polyimide is an aromatic polyimide which is soluble in a solvent.

14. The non-aqueous electrolyte battery separator according to claim **1**, wherein the ceramic powder is selected from the group consisting of a metal oxide, metal nitride and metal carbide.

15. The non-aqueous electrolyte battery separator according to claim **14**, wherein the metal oxide is selected from the group consisting of alumina, silica, titanium oxide and zirconium oxide.

16. A lithium secondary battery comprising the non-aqueous electrolyte battery separator of claim **1**.

17. The non-aqueous electrolyte battery separator according to claim **1**, wherein the separator has a pore size of about 1 μm or less.

18. The non-aqueous electrolyte battery separator according to claim **2**, wherein the separator has a pore size of about 1 μm or less.

* * * * *

Appendix R

Available online at www.sciencedirect.com
ScienceDirect
Journal of Power Sources 164 (2007) 351–364
JOURNAL OF POWER SOURCES
www.elsevier.com/locate/jpowsour

Review

A review on the separators of liquid electrolyte Li-ion batteries

Sheng Shui Zhang *

U.S. Army Research Laboratory, AMSRD-ARL-SE-DC, Adelphi, MD 20783-1197, USA

Received 21 September 2006; received in revised form 16 October 2006; accepted 17 October 2006
Available online 22 November 2006

Abstract

This paper reviews the separators used in liquid electrolyte Li-ion batteries. According to the structure and composition of the membranes, the battery separators can be broadly divided as three groups: (1) microporous polymer membranes, (2) non-woven fabric mats and (3) inorganic composite membranes. The microporous polymer membranes are characterised by their thinness and thermal shutdown properties. The non-woven mats have high porosity and a low cost, while the composite membranes have excellent wettability and exceptional thermal stability. The manufacture, characteristics, performance and modifications of these separators are introduced and discussed. Among numerous battery separators, the thermal shutdown and ceramic separators are of special importance in enhancing the safety of Li-ion batteries. The former consists of either a polyethylene (PE)–polypropylene (PP) multilayer structure or a PE–PP blend which increases safety by allowing meltdown of the PE to close the ionic conduction pathways at a temperature below that at which thermal runway occurs. Whereas the latter comprises nano-size ceramic materials coated on two sides of a flexible and highly porous non-woven matrix which enhances the safety by retaining extremely stable dimensions even at very high temperatures to prevent the direct contact of the electrodes.
Published by Elsevier B.V.

Keywords: Separator; Microporous membrane; Polyolefin; Non-woven; Thermal shutdown; Safety

Contents

1. Introduction 352
2. Requirements and characterization 352
   2.1. Chemical stability 352
   2.2. Thickness 352
   2.3. Porosity 352
   2.4. Pore size 352
   2.5. Permeability 352
   2.6. Mechanical strength 353
   2.7. Wettability 353
   2.8. Dimensional stability 353
   2.9. Thermal shrinkage 353
   2.10. Shutdown 353
   2.11. Cost 353
3. Type and manufacture of the separators 353
   3.1. Microporous polymer membrane 353
   3.2. Non-woven fabric mat 356
   3.3. Inorganic composite separator 358
4. Property improvement of the separators 360
   4.1. Surface modification 360

* Tel.: +1 301 394 0981; fax: +1 301 394 0273.
E-mail address: szhang@arl.army.mil.

0378-7753/$ – see front matter. Published by Elsevier B.V.
doi:10.1016/j.jpowsour.2006.10.065

4.2. Surface polymer coating 361
4.3. Impregnation of gel polymer electrolyte 361
5. Concluding remarks 362
References 363

1. Introduction

The separator is a critical component in liquid electrolyte batteries, and is placed between the positive electrode and the negative electrode to prevent physical contact of the electrodes while enabling free ionic transport and isolating electronic flow. It mostly is a microporous layer consisting of either a polymeric membrane or a non-woven fabric mat. Essentially, it must be chemically and electrochemically stable towards the electrolyte and electrode materials, and must be mechanically strong to withstand the high tension during the battery assembly operation. Structurally, the separator should have sufficient porosity to absorb liquid electrolyte for the high ionic conductivity. However, the presence of the separator adds electrical resistance and takes up limited space inside the battery, which adversely affects battery performance. Therefore, selection of an appropriate separator is critical to the battery performance, including energy density, power density, cycle life and safety. For high energy and power densities, the separator is required to be very thin and highly porous while still remaining mechanically strong. For battery safety, the separator should be able to shut the battery down when overheating occurs, such as the occasional short circuit, so that thermal runaway can be avoided. The shutdown function can be obtained through a multilayer design of the separator, in which at least one layer melts to close the pores below the thermal runaway temperature and the other layer provides mechanical strength to prevent physical contact of the electrodes. In this paper, the separators used in non-aqueous liquid electrolyte Li and Li-ion batteries will be reviewed in terms of the separator type, manufacture, function and structural modification.

2. Requirements and characterization

The essential function of a separator is to prevent physical contact of the positive and negative electrodes while permitting free ion flow. The separator itself does not participate in any cell reactions, however, its structure and properties considerably affect the battery performance, including the energy and power densities, cycle life and safety. The requirements for use in rechargeable Li and Li-ion batteries are generally listed below.

2.1. Chemical stability

The separator material must be chemically stable against the electrolyte and electrode materials, especially under the strongly reductive and oxidative environments when the battery is fully charged. Meanwhile, it should not degrade and lose mechanical strength. An easy method to verify chemical stability is by calendar life testing.

2.2. Thickness

A low thickness is required for high energy and power densities. However, this adversely affects the mechanical strength and safety. In the current technologies, 25.4 μm (1 mil) seems to be the standard thickness for consumer rechargeable batteries. In addition, a uniform thickness is critical for long cycle life of the batteries. The thickness can be measured using the T411 om-83 method developed under the auspices of the Technical Association of the Pulp and Paper Industry.

2.3. Porosity

An appropriate porosity is necessary to hold sufficient liquid electrolyte for the ionic conductivity between the electrodes. However, too high porosity will adversely impact the shutdown performance because in this case the pores cannot be closed effectively and the membrane tends to shrink as it melts or softens. The porosity can be measured using liquid or gas absorption methods according to American Society for Testing and Materials (ASTM) D-2873. Typically, the Li-ion battery separators have a porosity of 40%.

2.4. Pore size

The pore size must be smaller than the particle size of the electrode components, including the electrode active materials and the conducting additives. In practical cases, membranes with sub-micron pore sizes have proven adequate to block the penetration of particles since the tortuous structure of the pores assists in blocking the particles from reaching the opposite electrode. The distribution and structure of pores can be analyzed using a Capillary Flow Porometer (Porous Materials Inc.) or scanning electron microscopy based on ASTM 1294 standard. Uniform distribution and a tortuous structure of the pores are both highly desirable since the former ensures a uniform current distribution throughout the separator and the latter suppresses the growth of dendritic lithium.

2.5. Permeability

Separator should not limit the electrical performance of the battery. Typically the presence of a separator increases the effective resistance of the electrolyte by a factor of 4–5. The ratio of the resistance of the separator filled with electrolyte divided by the resistance of the electrolyte alone is called MacMullin number. MacMullin numbers as high as 8 have been used in high power Li-ion batteries. For batteries used in hybrid electric vehicles (HEV) and in power tools, the MacMullin number should be lower for the purpose of safety and a long cycle life. Air permeability can be used indirectly to estimate the MacMullin

CosMX Exhibit 1003, Page 422 of 512

number. Air permeability is expressed by a terms of the Gurley value, which is defined as the time required for a specific amount of air to pass through a specific area of the separator under a specific pressure. The Gurley value can be measured according to ASTM D726. When the porosity and thickness of the separators are fixed, the Gurley value reflects the tortuosity of the pores. The separator with uniform permeability is essential for the long cycle life of a battery. Variations in permeability will result in uneven current density distribution, which has been verified as the main reason for the formation of dendrite Li on the negative electrode.

2.6. Mechanical strength

This is characterized in terms of the tensile strength along the machine direction (MD) and the transverse direction (TD) (ASTM D-638), the tear resistance (ASTM D-1004) and the puncture strength (ASTM D-822). All these parameters are described by Young's modulus. The separator must be mechanically strong, especially in the MD, and enough to withstand the tension of the winding operation during battery assembly. The puncture strength is defined as the maximum load required for a given needle to puncture a given separator and it can be measured with a tensile tester. The minimum requirement for the mechanical and puncture strengths is 1000 kg cm^{-2} and 300 g, respectively, for a 25 μm membrane.

2.7. Wettability

The separator should wet easily in the electrolyte and retain the electrolyte permanently. The former facilitates the process of electrolyte filling in battery assembly and the latter increases cycle life of the battery. There is no generally accepted test for separator wettability. However, placing a droplet of electrolyte on the separator and observing whether or not the droplet quickly wicks into the separator is an easy way to indicate sufficient wettability.

2.8. Dimensional stability

The separator should lay flat and not bow or skew when it is laid out and soaked with liquid electrolyte. The separator should remain stable in dimensions over a wide temperature range.

2.9. Thermal shrinkage

When the temperature rises to the softening temperature, the membrane tends to shrink, even if the porosity is very low, because of the difference in the density between the crystalline and amorphous phases of polyolefin materials. For example, the PE can shrink as much as 10% when exposed to a temperature of 120 °C for only 10 min. The thermal shrinkage should be minimized. For the Li-ion battery, the shrinkage is required to be not more than 5% after 60 min at 90 °C.

2.10. Shutdown

In a Li-ion battery, the separator is required to be capable of battery shutdown at the temperature below that at which thermal runaway occurs, and the shutdown should not result in loss of mechanical integrity. Otherwise, the electrodes could come into direct contact and the resulting chemical reactions cause thermal runaway. The shutdown characteristics can be examined by differential scanning calorimetry or by observing the resistance change of the electrolyte-soaked membrane with temperature increase. For the PE–PP bilayer separators used currently in Li-ion batteries, they have ∼130 °C shutdown temperature and ∼165 °C melting temperature.

2.11. Cost

According to the current material prices and Li-ion technology, the cost of the separator can be over 20% of the total cost of a Li-ion battery. The majority of the separator cost is in the manufacturing process. Therefore, a cost-effective process is necessary for the reduction of separator cost.

Many of the properties above are associated with each other and may be in a trade-off relationship. For example, reducing the separator thickness increases battery energy and power densities, but it inevitably lowers the mechanical strength of the separator. In practical applications, the requirements above should be appropriately weighed among the performance, safety and cost.

3. Type and manufacture of the separators

According to the structure and composition, battery separators can be broadly divided into three types: (1) microporous polymer membranes, (2) non-woven fabric mats and (3) inorganic composite membranes. These three types of separators are, respectively, featured by the thinness, high porosity and excellent thermal stability. Among them, the microporous polyolefin membranes have been most widely used in liquid electrolyte batteries due to their comprehensive advantages of performance, safety and cost [1,2]. These three types of separators are reviewed below with focus on the relationships of the material, process, structure and properties.

3.1. Microporous polymer membrane

Nearly all microporous polymer membranes used in the current Li-ion batteries are based on semi-crystalline polyolefin materials, including polyethylene (PE) [3,4], polypropylene (PP) [5–10] and their blends such as PE–PP [11–14] and high density polyethylene (HDPE)-ultrahigh molecular polyethylene (UHMWPE) [15,16]. The methods for manufacturing the microporous membranes can be divided into dry process and wet process. Both methods include an extrusion step to make thin films and employ one or more orientation steps to impart porosity and increase the tensile strength. Separators made by the dry process generally show a distinct slit-pore and straight microstructure, while those made by the wet process exhibit interconnected spherical or elliptical pores.

CosMX Exhibit 1003, Page 423 of 512

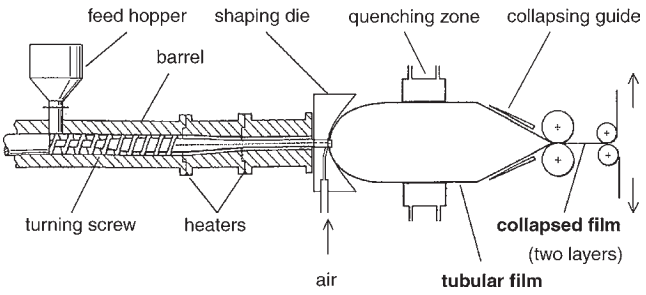


Fig. 1. Schematic chart of a screw extrusion process. Polyolefin pellets are fed from a hopper into the barrel of the extruder, where the pellets are gradually melted by mechanical energy generated by a turning screw and by heaters arranged along the barrel. The molten polymer is forced through a shaping (tubing) die to expand into a balloon shape by a stream of air, which subsequently shapes and quenches into a tubular film, followed by collapsing and drawing forward by rollers to get a collapsed film (two layers), whose two sides are trimmed to obtain two identical films.

The dry process can be generally described as three steps [3,5,7–10,12,13,19–28]: (1) extruding, (2) annealing and (3) stretching. The first step, as shown in Fig. 1, is operated at a temperature higher than the melting point of polymer resins. In this step, the polymer resins are melt-extruded into a uniaxially oriented tubular film or called precursor film, whose morphology and orientation depend on the processing conditions and the characteristics of the polymer resins. Generally, the resulting film is required to have a crystalline row structure with lamellae arranged in rows with their long axis perpendicular to the MD. Such a structure is critical for the formation of micropores because only stacked lamellae are able to "open" in the next stretching process.

The second step is to anneal the extruded precursor film at a temperature slightly lower than the melting point of the polymer. Its purpose is to improve the crystalline structure so as to facilitate the formation of micropores in the subsequent stretching step. Variables of this step include annealing temperature and time. In the third step, the annealed film is deformed along the MD by a process consisting of a cold stretch, a hot stretch and a relaxation. The cold stretch is to create the pore structure by stretching the film at a lower temperature with a faster strain rate, and the hot stretch is to increase the size of the pores by further stretching the film at a higher temperature with a slower strain rate. The relaxation is a heat treatment to reduce internal stresses within the film. The porosity of the final film depends on the morphology of the precursor film, annealing conditions and the stretching ratios/conditions. Both uniaxial [5,10,13,24–26] and biaxial [3,7,8,9,12,20] stretches have been adopted in the third step. In the former, the precursor film is stretched only in the MD, while in the latter the film is stretched in the MD at a lower temperature (70–10 °C, depending on the melting point of polymer), followed by stretching of the film in the TD at a higher temperature (110–140 °C). The tensile strength and its orientation of the final microporous film depend on the ratio of the MD and TD stretches. Both the pore shape and the tensile strength of the uniaxially stretched films are strongly MD-oriented since the film is stretched only in the MD. Significant difference between the MD and TD strengths may result in a splitting problem, i.e. tearing as a result of puncture, which increases difficulties in handling the separators during battery assembly.

Fig. 2 shows the microstructure of a melt extruded HDPE film before and after a uniaxial stretch. Before the stretch, the film shows a stacked lamellar morphology with the lamellae oriented along the TD (Fig. 2a). On stretching, the film is deformed along the MD, during which some of the stacked lamellae separate to form a microporous structure while others remain with their initial morphology. Obviously, the pores formed by a uniaxial stretch are MD-oriented, which is almost perpendicular to the TD (Fig. 2b). As described above, the formation of pores by stretching is based on a lamellae-arranged crystalline structure. Therefore, the dry process is only applicable to the polymers with high crystallinity. Apart from semi-crystalline polyolefins, other polymers such as polyoxymethylene [24,25] and isotactic poly(4-methyl-1-pentene) [26] also have been reported to make microporous membranes. In addition, the dry process also is

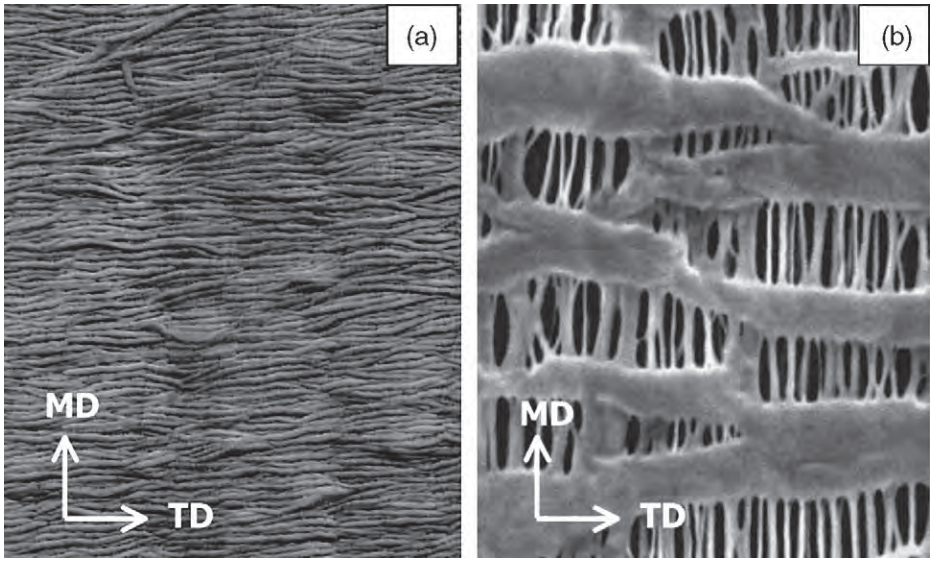


Fig. 2. Microstructure of a uniaxially oriented HDPE film before (a) and after (b) uniaxial stretch.

applicable to the blends of two immiscible polymers, in which at least one polymer has a crystalline structure, such as PE–PP [13], polystyrene (PS)–PP [27] and poly(ethylene terephthalate) (PET)–PP blends [27]. The membranes thus obtained exhibit such microporous structures with two polymer phases interconnected throughout the membrane.

The wet process for the manufacture of microporous PE membranes was reviewed by Weighall [29], and since then, the technology has moved forward [4,6,11,14–17,29–34]. The wet process generally consists of these steps: (1) mixing of polymer resins, paraffin oil, antioxidant and other additives and heating to make a homogenous solution, (2) extruding the heated solution through a sheet die into a gel-like film and (3) extracting the paraffin oil and other additives with a volatile solvent to form the microporous structure. In the second step, the same extrusion process as described in the dry process can be used. In most cases, methylene chloride is used in the last extraction process. The wet process is applicable to both crystalline and amorphous polymers, and its resulting membrane is non-oriented for both pore structure and mechanical strength. For semi-crystalline polymers, a stretching step is often added before or after the extraction in order to achieve high porosity and a large pore size [4,11,15,16]. It has been proven that the membranes produced by the process of stretching after extraction have a much larger pore size and a wider pore-size distribution than those produced by the process of stretching before extraction [16]. Fig. 3 shows a distinct difference in the orientation of the pore structure for two microporous polyolefin membranes made by the dry and wet processes, respectively. In consistence with the pore structure, other physical properties also exhibit a distinct difference between the membranes made by the dry and wet processes. Table 1 summarizes the properties of the microporous polyolefin membranes made by these two different processes. It is obvious that the membranes made by the dry process distinguish themselves by a high orientation-dependent tensile strength and a low Gurley value. The low Gurley value reflects their less tortuous pore structures. From the viewpoint of microporous structure, the membranes made by the dry process seem to be more suitable for a high power density battery due to their open and straight porous structure, while those made by the wet process are more suitable for a long cycle life battery because of their tortuous and interconnected porous structure that is helpful in suppressing the growth of dendritic Li on the graphite anode during fast charging or low temperature charging.

Most of microporous polyolefin membranes used in Li-ion batteries have a thickness below 50 μm and an average pore size below 1 μm. Typical thickness is 25 μm or even lower with a tendency towards 10 μm for the higher energy density batteries. However, reducing the thickness may raise the safety risk regarding mechanical penetration. Thermal properties of the membranes are dependent on the properties of the polyolefin materials. Membranes made from an HDPE melt at 135 °C and have no mechanical integrity above the melting point. Membranes made by laminating layers of PP and PE have mechanical integrity up to 165 °C (the melting point of PP). An extensive study on the structure–property relations of the microporous polyolefin separators can be found in the work by Venugopal et al. [35].

A thermal shutdown separator has been manufactured based on the difference in the melting point of PE (120–130 °C) and PP (165 °C). The shutdown separators are generally designed as a multilayer structure, in which one or more PE layers serve to shutdown the battery and at least one PP layer as the mechanically dimensional support. Typically, PE–PP bilayer [17,20] and PP–PE–PP trilayer [18,21–23,28,36,37] structures have been widely adopted by many separator manufacturers. With such structures, the PE layer is capable of melting and filling the pores at a temperature lower than thermal runway,

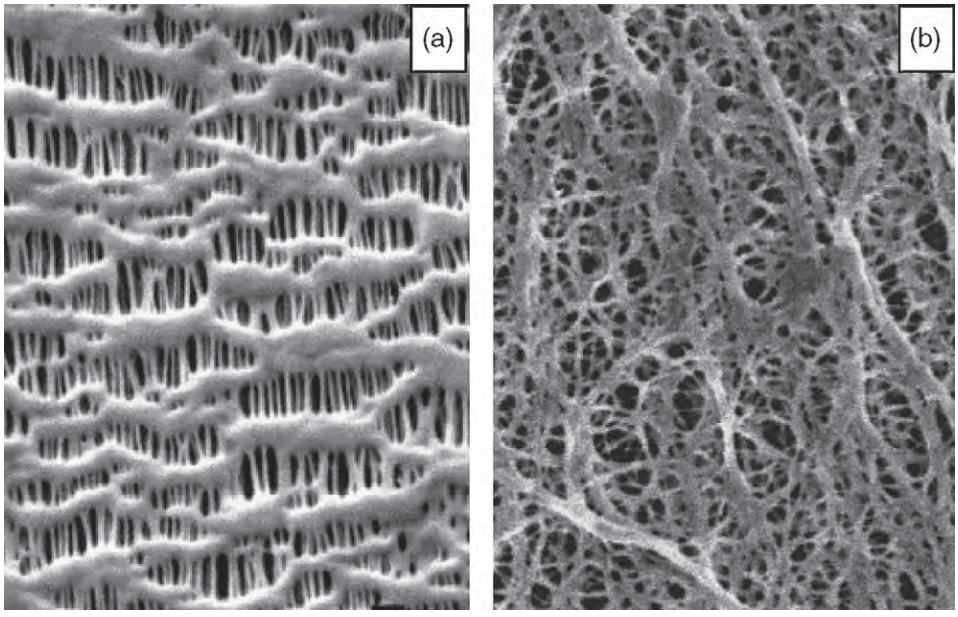


Fig. 3. Microstructure of the microporous polyolefin membranes made by dry process (a) and wet process (b), respectively. This figure was edited from Figs. 4 and 6 of ref. [2], with permission from American Chemical Society.

Table 1
Comparison of the properties of the microporous polyolefin membranes by different processes

Manufacturer	Celgard	Celgard	Exxon Mobil	Exxon Mobil
Membrane name	Celgard 2325	Celgard 2340	Tonen-1	Tonen-2
Process	Dry	Dry	Wet	Wet
Composition	PP–PE–PP	PP–PE–PP	PE	PE
Thickness (μm)	25	38	25	30
Porosity (%)	41	45	36	37
Pore size (μm)	0.09 × 0.04	0.038 × 0.9		
Gurley value [a] (s) per 100 cm^3	575	775	650	740
Tensile strength (MD) (kg cm^{-2})	1900	2100	1500	1500
Tensile strength (TD) (kg cm^{-2})	135	130	1300	1200
Melting temperature (°C)	134/166	135/163	135	135
Thermal shrinkage[b] (%)	2.5	5	6.0/4.5[c]	6.0/4.0[c]
Reference	Data sheet	Date sheet	[34]	[34]

[a] Gurley value was based on per gauge (piece of membrane) [34].
[b] The shrinkage was measured at 90 °C for a fixed time for Celgard membranes according to ref. [2] and at 105 °C for 8 h for Tonen membranes [34], respectively.
[c] The numbers show MD and TD shrinkage, respectively.

which, as a result, considerably increases the resistance of the electrolyte layer between the two electrodes to terminate the operation of the battery, while the PP layer still has sufficient mechanical strength to prevent a short circuit between the electrodes. About a 35 °C buffer between the PE shutdown and PP melting may be enough for the protection of most Li-ion batteries. However, it cannot provide protection against serious safety tests, such as nail penetration and overcharge at a high current density, since the local overheating under these conditions can cause separator shrinking or even melting, which results in physical contact between the strongly oxidative cathode and the strongly reductive anode, and the resulting chemical reactions then would lead to thermal runaway. The multilayer separators usually are made by laminating different functional layers together by calendaring, adhesion or welding. Preferably, a cross-plied lamination, where the axis of one ply is angularly biased relative to the axis of another ply, can increase the mechanical strength and puncture resistance. Alternatively, multilayer separators can be made through a co-extrusion processes, in which all the precursor layers are extruded simultaneously and then are annealed and stretched to form a multilayer microporous structure [28,36]. In consideration of the impurities brought in by the resin materials, antioxidants, and other possible additives during extrusion, Kinouchi et al. [37] claimed that dispersing a small amount of metal oxide particles into the two PP layers of the PP–PE–PP trilayer membrane could effectively adsorb these impurities and consequently reduce their negative impact on battery performance. Meanwhile, the presence of the inorganic fillers favors increasing the wettability and retention of the liquid electrolyte.

By the same principle as the solvent extraction, a microporous structures can be formed through a phase inversion or selective solvent evaporation. The phase inversion method [38–43] generally consists of: (1) dissolving the polymer into a good solvent, (2) applying the polymer solution as a thin doping layer and (3) precipitating the polymer to form a porous membrane through solvent exchange between the good solvent in the polymer dope and the non-solvent in a coagulation bath by immersing the polymer dope into a coagulation bath. The selective solvent evaporation or thermally induced liquid–liquid phase separation [44–46] uses a mixture of a good solvent and a non-solvent to dissolve polymer, in which the good solvent is required to be more volatile than the non-solvent. The resulting polymer solution is coated or cast onto a flat substrate to form a thin polymer dope layer, which is left to evaporate the volatile good solution until a porous membrane is formed due to the phase separation and solidification of the polymer. It has been proven that both the methods above lead to an asymmetrical porous structure, depending on many factors such as the properties and concentration of the polymer, the type of the good solvent and the non-solvent, solution temperature, dope thickness and so forth. In most cases, the membranes thus made show an open-pored structure on the top surface (the side facing air), a dense surface on the bottom (the side in contact with the substrate) and a sponge-like layer sandwiched between them, as shown in Fig. 4. Such asymmetric porous structures greatly restrict the application of these membranes as a battery separator due to the concerns that the dense surface blocks electrolyte absorption and the path of ionic conduction. To eliminate this adverse effect, the polymers that are able to swell or dissolve in the liquid electrolytes, such as polyvinylidene fluoride (PVDF) based homo- and co-polymers [41,47], polyacrylonitrile [42], and their related blends [43], have been selected to prepare asymmetric porous membranes because such membranes can be gelled by the liquid electrolyte to form in situ a microporous gel polymer electrolyte inside the batteries [41].

3.2. Non-woven fabric mat

A non-woven separator is a fibrous mat made by bonding numerous fibers together through chemical, physical or mechanical methods. Both natural and synthetic materials have been used to manufacture the fibers for non-woven separators. Natural materials include celluloses and their chemically modified derivatives [48–50]. The synthetic materials include polyolefin [51–56], polyamide (PA) [57,58], polytetrafluoroethylene (PTFE) [59], PVDF [60], polyvinyl chloride (PVC) [60], polyester [61,62] and so forth. The principal bonding methods

CosMX Exhibit 1003, Page 426 of 512

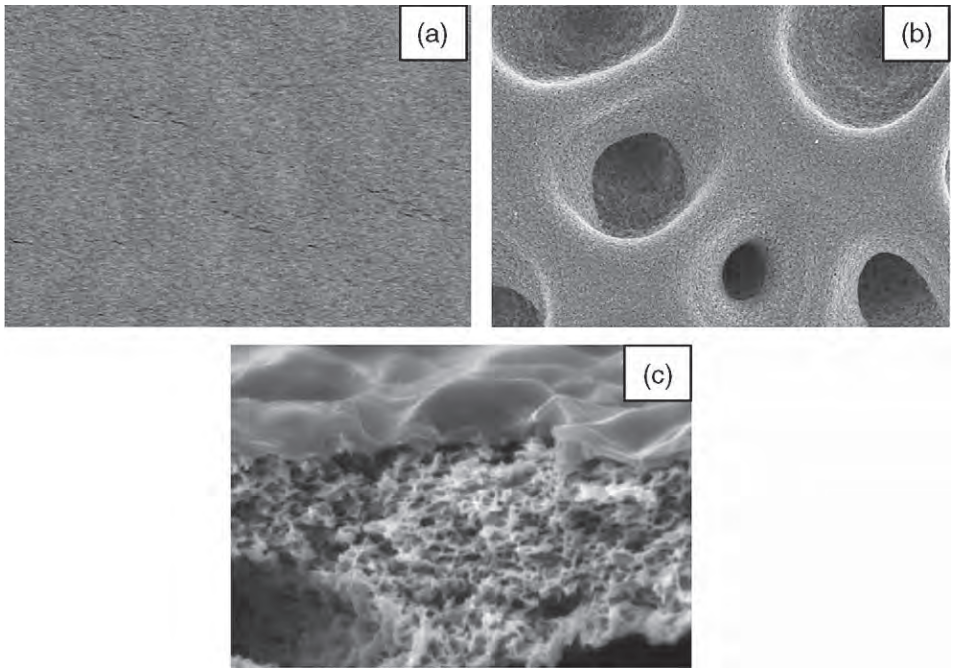


Fig. 4. Typical structures of a microporous membrane made by the phase inversion method. (a) Bottom surface facing the substrate, (b) top surface facing air and (c) cross-sectional view.

for the battery separators are resin bonding and thermoplastic fiber bonding. In the former, the resin as an adhesive is sprayed onto the web of fibers, and then dried, heat-cured and in some instances pressed. In the latter, a fusible (thermoplastic) fiber having a lower melting point than the base fiber as the bonding agent is blended with the base fiber to form a web, followed by pressing between two heated rollers to promote bonding of the thermoplastic fibers and the base fibers. To minimize the adverse effect of foreign adhesives on the battery performance, the thermoplastic bonding method is most preferable for the manufacture of battery separator [53–55,63]. The fibrous webs can formed either by a wet process such as a paper-making process [51,60], a solution extrusion method using a spinning jet [49] and wet-laid method [48,60,61,63] or by a dry process such as a melt blowing method [53,55,56,64]. As an example, the melt blowing process can be described as two steps: (1) forming fabric web and (2) boning of the web. In the first step, both base polymer resin and fusible polymer are molten and blown to form a non-woven fabric web. In the second step, the resulting web is thermally bonded by calendaring it at a temperature higher than the melting point of the fusible polymer to form a non-woven mat with sufficiently high mechanical strength. Beside the polymers and their composition, the blowing conditions such as temperature, spinning speed and the parameters of the fiber-forming die greatly affect the properties of the final non-woven mats. In order to reduce thickness while still remaining good mechanical strength, an electrospinning method has been adopted to prepare the highly porous non-woven separators by applying a high voltage between the solution capillary jet and the membrane-collecting substrate [65,66]. By optimizing the correlation among the polymer concentration, deposition distance, applied electric field strength, feed rate of the solution, Kim et al. [66] successfully made a poly(vinylidene fluoride-co-hexafluoropropylene) (PVDF–HFP) membrane composed of fibers with an average diameter of 0.5–2.3 μm, a thickness of 30 μm and a porosity of 68–82%.

Non-woven separators are featured by a high porosity (60–80%) and a large pore size (20–50 μm). Fig. 5 shows the microstructure of typical non-woven mats made by different process and used in exploratory research for a Li-ion battery separator. Their structures are featured by the labyrinth-like pores, which are very helpful in preventing the growth of dendritic Li in rechargeable Li and Li-ion batteries. These separators generally have a thickness of 100–200 μm and a base density of 9–30 g cm^{-2}. In an effort to reduce the thickness, recent technology has made it possible to produce non-woven mats with a thickness of 20 μm or less [61]. The diameter of the fibers is a critical parameter to determine the evenness of the non-woven surfaces, and must not exceed 5 μm. When the fiber diameters are in the range of the non-woven thickness, the thickness only allows one layer of fibers. Such a structure might result in the presence of locally “open” areas when two or more of fibers are neighbored, so that the separator cannot effectively prevent a short circuit between the two electrodes. Except for a few exploratory investigations by Kuribayashi [67], the non-woven separators are mainly used in rechargeable alkaline batteries such as nickel–cadmium and nickel–metal–hydride batteries. They have not been used in Li-ion batteries mainly because their “open” structure and the rough surface cannot effectively prevent short circuits unless their thickness is increased to at least 6 mils at a considerable expense to the battery energy density.

In Li-ion batteries, the non-woven mats are mainly used as the supporting framework to make gel polymer electrolyte (GPE) batteries. Due to the high porosity and large pore size of

CosMX Exhibit 1003, Page 427 of 512

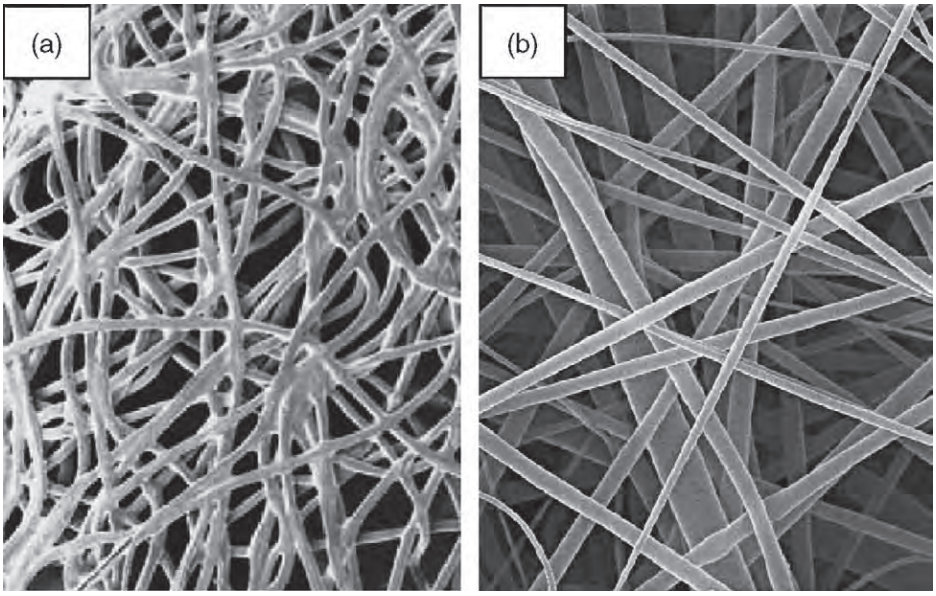


Fig. 5. Microstructure of the non-woven mats made by: (a) wet-laid method and (b) electrospinning method, respectively.

non-woven separators, the GPE can be readily impregnated into the non-woven separator and fill up the uneven surface. Thus, the non-woven nature serves as the mechanical support while the GPE provides the necessary ionic conductivity between the electrodes. Based on this concept, Song et al. [68] impregnated a blend of polyethylene glycol diacrylate (PEGDA), PVDF and poly(methyl methacrylate) (PMMA) into a 85 μm PET non-woven by ultraviolet (UV) cross-linking method. Beside the improved mechanical strength and surface integrity, they found that the resulting separator exhibited a very stable conductivity and liquid electrolyte retention at high temperatures, as compared with the untreated gel polymer electrolyte. More simply, Pekala and Khavari [52] employed a continuous coating machine to pass a porous UHMWPE non-woven mat having a thickness of 18 ± 0.5 μm through a hot PVDF solution bath. Due to the reduced viscosity of the hot polymer solution, the polymer (PVDF) not only coated on the surface, but also was impregnated into the web. Such a structure improved the overall permeability of the liquid electrolyte and resulted in a reduction of the time required to achieve a uniform electrolyte distribution throughout the separator. In order to increase the permeability of the liquid electrolyte through the polymer coating layer, Lee et al. [69] coated a microporous PVDF layer on the rough surface of a 20 μm PE non-woven mat by the phase inversion method. Thus, the PE non-woven matrix imparted mechanical strength and a thermal shutdown property to the separator, while the PVDF layer provided a hydrophilic ionic conducting phase. Their results showed a good improvement in the capacity retention of the Li-ion cells using such separators. In their continued efforts [70], they applied a poly(vinyl acetate) (PVAc) to the surface of the PVDF-coated separator and found that the additional PVAc layer resulted in a small increase of the ionic conductivity, as compared to the bare separator. Due to the increased evenness of the separator surface and the improved adhesion of the separator to the electrodes, the Li-ion cells using such separators presented a lower resistance and a higher capacity than those using bare separators. Microporous structure of the surface coatings also can be created by a method of removing the plasticizer [71]. In this method, an acetone solution of PVDF and diethylsuccinate (as a plasticizer) was spread onto the surfaces of a porous non-woven mat. Upon evaporation of acetone, the plasticizer-contained separator was laminated with the electrodes, and the resulting cell stack was heated under vacuum to remove the residual placticizer, which in turn created a "dry" cell stack with highly porous structure.

Aiming at increased safety and cycle life of the polymer battery, Kritzer [61] proposed polyester non-woven as the mechanical supporting matrix. The suggested non-woven matrixes are made using the conventional wet-laid method, and they have a thickness of below 20 μm, a porosity of 55–65%, a pore size of 20–30 μm, and an average fabric diameter of 3–4 μm. Due to the high melting point of polyester, such non-woven matrixes can tolerate temperatures up to 180 °C with very low shrinkage. Furthermore, the homogeneous and labyrinth-like non-woven structures offer an increased safety and cycle life in relation to the formation of Li dendrite because such structures can more effectively prevent the growth of dendrite Li.

3.3. Inorganic composite separator

An inorganic composite separator, or "ceramic separator", is a porous mat made of ultrafine inorganic particles bonded using a small amount of binder. Due to the high hydrophilicity and high surface of the small inorganic particles, such separators exhibit exceptional wettability with all non-aqueous liquid electrolytes, especially those containing a high content of cyclic carbonate solvents such as ethylene carbonate (EC), propylene carbonate (PC) and γ-butyrolactone (GBL), which have a high dielectric constant and are known to be unable to wet the

non-polar polyolefin separators. Meanwhile, these separators have extreme thermal stability and show zero-dimensional shrinkage at high temperatures. The outstanding wettability allows one to use a high content of PC and EC in the liquid electrolytes, which is very helpful to increase the cycleability of the Li-ion batteries at high temperatures, while the extreme thermal stability offers the batteries excellent temperature tolerance, which is critical to large-size Li-ion batteries. In fact, temperature-related safety issues are mostly related to the dimensional shrinking or melting of the separator. Both shrinking and melting of the separator could result in physical contact of the electrodes so that direct chemical reactions between the strongly oxidative cathode material and the strongly reductive anode material occur, and the generated heat causes thermal runaway. Therefore, the inorganic composite separators with excellent wettability and zero shrinkage are highly desirable for the development of large-size Li-ion batteries, especially these for hybrid electric vehicles and power tools.

Early reports about the composite separators were given by Prosini et al. who dispersed metal oxides powders (γ-$LiAlO_2$, Al_2O_3, MgO, respectively) into a PVdF–HFP solution in a 1:2 (w/w) ratio of the inorganic filler to polymer, and spread the resulting suspension over a glass substrate to obtain a free-standing and intrinsically porous film with a thickness of 30–50 μm [72]. They examined the resultant separators using Li half-cells of $LiMn_2O_4$ and MCMB, respectively, and found that the performance of such separators depended on the type of inorganic fillers. Among the separators made of these three fillers, the one made of MgO showed the best capacity retention. Since the solution method used by Prosini et al. [72] resulted in the formation of a dense polymer phase, which inevitably increased the difficulty in filling with electrolyte, especially when the content of the polymer is high. To solve this problem, Kim et al. [73] adopted a phase inversion method to make a TiO_2/PVDF–HFP composite separator. Due to the formation of a highly porous polymer phase, the membranes thus obtained not only facilitated the electrolyte filling process, but also were superior in electrochemical properties, such as ionic conductivity and interfacial stability with a Li electrode. Regarding the composition–property correlation of the membranes, Takemura et al. [74] systematically studied the impact of particle size and the powder–binder (P/B) ratio on the Al_2O_3–PVDF composite. It was shown that the pore size of the composite membrane was nearly equal to the powder particle size, and that the small powder particle size and high P/B ratio favored increasing electrolyte retention in the membrane pores and air permeability through the membrane. For example, a Li-ion cell using a 0.01 μm powder membrane exhibited almost the same capacity retention as that using a PE separator. On the other hand, aiming at reducing the acid-induced dissolution of $LiMn_2O_4$ active materials, Zhang et al. [75,76] proposed alkali $CaCO_3$ power as the main component of the composite separator so that the acidic products formed due to the hydrolysis of $LiPF_6$ can be neutralized in situ. They adopted the thermal pressing (calendaring) method to make a freestanding and flexible porous membrane by using 2–8 wt.% of Teflon as the binder. The obtained separators were wetted with a 1.0 M $LiPF_6$ 3:7 (w/w) EC/ethylmethyl carbonate (EMC) electrolyte, and their ionic conductivities at 20 °C were measured to be 2.5–4 mS cm^{-1} (depending on the content of Teflon) versus 3.4 S cm^{-1} of the Celgard membrane. They also found that the cells using alkali $CaCO_3$ composite separator showed better capacity retention, as compared with the one using Celgard membrane. They attributed such an improvement to the removal of acidic impurities such as HF by the alkali $CaCO_3$.

The small solid particles tend to aggregate and theoretically the thickness of the composite separators cannot be less than the diameter of the aggregated particles. To reduce the thickness of the composite separators, Carlson et al. [77] used a sol–gel method, which allows the making of less than 10 μm thick membranes. In their method, a water suspension of a Boehmite sol and polyvinyl alcohol in a 10:1 solid weight ratio was prepared and then coated onto a PET sheet, followed by drying at 130 °C to obtain a composite film, which was subsequently soaked in a water–isopropanol solution to delaminate the film. They claimed that the thickness of the membranes could be easily controlled by multiple coating and drying processes. Since each coating led to a 12.5 μm thick membrane, a 25 μm membrane could be obtained by a second coating after the first coating was dry. The apparent porosity of such membranes was measured to be 65% versus 48% of Celgard 2500 membrane when the same measuring method was used.

Although the composite separators described above offer excellent wettability and extremely thermal stability, they are not mechanically strong enough to withstand handling in cell winding and assembly. To solve this problem, Degussa developed a series of Separion (a trade name) separator by combining the characteristics of polymeric non-woven and ceramic materials [78–82]. The Separion separator is a flexible perforated non-woven mat coated with a porous ceramic layer on its each side, as illustrated in Fig. 6. The pore size of Separion separator can be selectively set by an appropriate choice of the ceramic materials. Generally, the ceramic materials used in these separators are alumna, silica, zirconia, or their mixture, and their particle size is required to be of nano-size. To keep the excellent hydrophilic properties of the ceramic materials, an inorganic binder is highly recommended for the production of such separators. As an example [82], the inorganic binder sol can be prepared by hydrolyzing a mixture of tetraethoxysilane, methyltriethoxysilane and (3-glycidyloxypropyl) trimethoxysilane in the presence of HCl aqueous solution. The resulting sol was used to suspend aluminum oxide powders, and then the homogenized suspension was coated on a porous non-woven PET, followed by drying at 200 °C to obtain the separator. This method resulted in a separator having an average pore size of 0.08 μm, a thickness of about 24 μm and a Gurley value of about 65 s, and the separator thus made was thermally stable up to 210 °C, which is limited by the melting point of PET non-woven matrix. Typical physical properties of the Separion and Celgard membranes are summarized in Table 2, which clearly shows that the Separion separators have excellent wettability, high permeability (i.e. low Gurley value), a high meltdown temperature and negligible shrinkage at high temperatures. Remarkable improvements of the Separion separators on the battery safety have been demonstrated by a

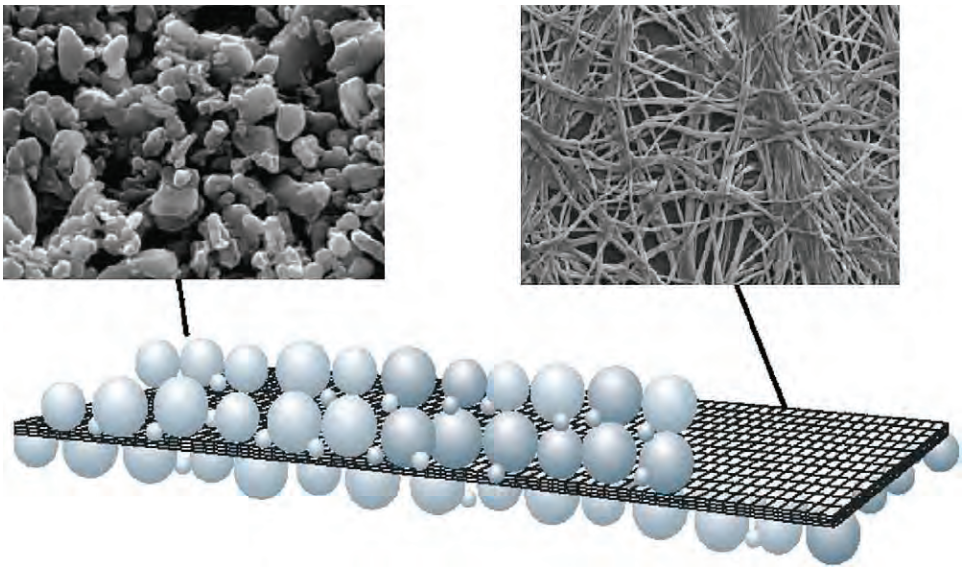


Fig. 6. Schematic structure of the Separion separators. This figure was redrawn based on Fig. 1 of ref. [78] and product brochure of Separion separators.

Table 2
Comparison of the properties of the Separion and Celgard separators[a]

Trade name	Separion	Separion	Celgard	Celgard
Separator brand	S240-P25	S240-P35	Celgard 2340	Celgard 2500
Composition	Al_2O_3/SiO_2	Al_2O_3/SiO_2	PP–PE–PP	PP
Support matrix	PET non-woven	PET non-woven	N/A	N/A
Thickness (μm)	25 ± 3	25 ± 3	38	25
Average pore size (μm)	0.24	0.45	0.038×0.90	0.209×0.054
Gurley value[b] (s)	10–20	5–10	31	9
Porosity (%)	>40	>45	45	55
Temperature stability (°C)	210	210	135/163	163
Thermal shrinkage[c] (%)	<1	<1	5	3
Tensile strength (MD)[d]	>3 N cm^{-1}	>3 N cm^{-1}	2100 kg cm^{-2}	1200 kg cm^{-2}
Tensile strength (TD)			100 kg cm^{-2}	115 kg cm^{-2}
Wettability for PC, EC, GBL	Excellent	Excellent	Not wet	Good

[a] The data were cited directly from the product brochures.
[b] Gurley value was expressed as the time in seconds required to pass 100 ml of air through 6.45 cm^2 (1 in.^{2}) of membrane under a pressure of 31.0 cm (12.2 in.) of water.
[c] Separion shows a value measured at 200 °C for 24 h, while Celgard a value measured at 90 °C for a fixed time according to ref. [2].
[d] Different units were used to express tensile strength by two companies.

series of abuse tests [80,81]. During a hot oven test on the 1.1 Ah Li-ion pouch cells by heating the cells at 5 °C min^{-1} to 150 °C and holding at 150 °C for 30 min, the cells with Separion separators had no change while the cells with PE separators showed numbers of short circuit voltage peaks as a result of the shrinkage of the separator [80]. In a nail penetration test on the 8 Ah Li-ion pouch cells, it was shown that the maximum temperature of the cell using Separion separators was only 58 °C with a weight loss of 0.4% after nail penetration test, while that of the control cell using PE separators reached over 500 °C with a weight loss as high as 56.1% [81]. Since the maximum temperature (58 °C) in the nail penetration test is far from the melting point of the PE materials, one may assume that the exceptional safety behavior of the Separion separator is more related to the nano-size ceramic materials, instead of the PET non-woven matrix. Therefore, a composite separator that combines both characteristics of the thermal shutdown and ceramic zero-shrinkage could be made by replacing PET matrix with a highly porous PE non-woven matrix if the Separion separators can be produced at the temperature below the softening temperature of the PE.

4. Property improvement of the separators

4.1. Surface modification

Due to the inherent hydrophobic properties of non-polar polyolefin separators, the electrolytes containing a high content of polar solvents, such as EC, PC, GBL, etc., exhibit a poor wettability and electrolyte retention. In this case, surface modification is necessary to make the polyolefin separators hydrophilic [83]. The modification either treats the separator with a wetting agent (mostly a surfactant) [84,85] or grafts hydrophilic functional

groups onto the surface and pore wells of the separators [86–93]. The use of a surfactant generally improves wettability, but it is unable to increase electrolyte retention. To increase the electrolyte retention, Taskier [84] combined a surfactant and a hydrophilic polymer (cellulose acetate) together to treat the polyolefin membranes. He found that the membrane thus treated exhibited much better wettability and electrolyte retention. In general, the surfactant treatment only makes the membrane hydrophilic temporarily since the surfactant is subjected to washing away by the liquid electrolyte upon cycling or storage. Therefore, permanent grafting of hydrophilic functional groups is preferable for the modification of the polyolefin membranes. Physically, the hydrophilic groups can be grafted onto polyolefin membranes by a means of plasma treatment, which usually is carried out between two electrode plates and applied with a radio-frequency field in a gas atmosphere [87,94]. By selecting the appropriate gas, the hydrophilic groups of hydroxyl, carbonyl, carboxyl, amino, imino, sulfonyl, etc., can be grafted. Chemically, the polyolefin membranes can be modified through sulfonation, fluorination and grafting polymerization. The sulfonation [94,95] has been used mainly for the treatment of these membranes used in aqueous alkali batteries. An additional benefit of the sulfonated membranes is that the introduced sulfonic groups are able to trap unwanted ammonia, which is present in NiMH batteries and has been identified to be the main source of self-discharge [94,95]. Due to the extreme reactivity of fluoride gas, fluorination can be carried out by exposing directly the membrane to fluorine gas for a short time [53]. The grafting polymerization can be initiated by high-energy radiation [86,89–93] and UV-irradiation [88], respectively. In the former, the polyolefin is radiation-induced to cleave the C–C or C–H bonds to generate polymeric radicals and the resulting polymeric radicals subsequently initiate the hydrophilic monomer to polymerize. In the latter, a photo-initiator should be used to increase the sensitivity of the polymer to UV-irradiation, and with the aid of the photo-initiator the monomer polymerizes and grafts onto the membrane surface. In these efforts, Senyarich and Viaud [88] developed a device that allowed the UV-induced grafting process to be operated continuously. In their method, the polyolefin membrane was first passed through a solution bath containing the monomer and photo-initiator, and then the wetted membrane was moved into a UV-chamber where the polymerization was initiated by the UV-irradiation. According to the chemical structure, the monomers bearing carboxylic acid, such as acrylic acid [86,88–91] and methacrylic acid [90], are suitable for the treatment of the membranes used in aqueous electrolyte batteries, while the monomers being polar but aprotic such as glycidyl methacrylate [92] and methylmethacrylate [93] are suitable for those used in non-aqueous electrolyte batteries. In both cases, the uptake and retention of the liquid electrolytes are affected by the degree of grafting and the type of monomer.

4.2. Surface polymer coating

Compact contact of the separator and electrodes is critical to the long-term reliable performance of a rechargeable battery. Even a small failure at the interface can give rise to a significantly uneven current distribution due to the high contact resistance in failure areas, which can cause the formation of dendritic Li on the negative electrode and further can contribute to an increase in battery impedance. To improve the interfacial contact, a thin polymer layer that can be gelled by the liquid electrolyte has been proposed to coat the surfaces of the microporous membranes [96–99]. The polymers that are suitable for this purpose include PEO [96,97], PVDF and its related copolymers such as PVDF–HFP [98,99]. Upon gelling with the liquid electrolyte, the polymer becomes a gel electrolyte and it in turn serves as an adhesive to bond the separator and electrodes together, which meanwhile increases uptake and retention of the liquid electrolyte. In practical processes, the polymer coating can be applied to the microporous membrane by a means of dipping or spraying. A heating step is required to promote the in situ formation of the gel polymer electrolyte when the polymer-coated membranes are used as the separator.

A negative effect of the approaches above is that the polymer layer made by the solution method is structurally dense, which inevitably blocks the penetration of liquid electrolyte into the pores of the microporous membrane. Therefore, the polymer layer with a porous structure is highly desirable so as to facilitate the electrolyte filling process. In such efforts, Jeong and Kim [100] employed a phase inversion method to replace the solvent evaporation step to form the microporous polymer layer. In their method, they first applied a dilute dimethylformamide (DMF) solution of acrylonitrile–methyl methacrylate copolymer (AMMA, AN:MMA = 84:16) to the micropouous PE membrane with a thickness of 25 μm and a porosity of 40%, and then immersed the coated PE membrane into a water bath to induce phase inversion. Due to the fast solvent exchange between the good solvent (DMF) in the polymer solution and non-solvent (water), the polymer layer with highly microporous structure is formed. They found that a Li-ion cell using the separator with a 14 μm polymer coating layer exhibited a very stable capacity retention and excellent rate performance, which is attributed to the strong bonding between the separator and electrodes. Based on the work above, Kim et al. [101] introduced different amounts of an inorganic filler, SiO_2, into the polymer coating layer, and they found that the presence of hydrophilic SiO_2 significantly reduced the contact angle of the liquid electrolyte and accelerated the wetting of electrolyte to the separator. As a result of the improved interfacial characteristic, the Li-ion cell using such a separator exhibited excellent capacity retention and rate performance. As a comparison, Fig. 7 exhibits the surface images of a microporous PE membrane before and after the polymer coating by different methods. The differences in the surface morphology of the polymer layers coated by the solution and phase inversion methods are very clear.

4.3. Impregnation of gel polymer electrolyte

In the same manner as described in the non-woven section, the microporous polyolefin membrane can be employed as a dimensional support to enhance the mechanical strength of the GPE. The impregnation of GPE into the pores of membranes is

CosMX Exhibit 1003, Page 431 of 512

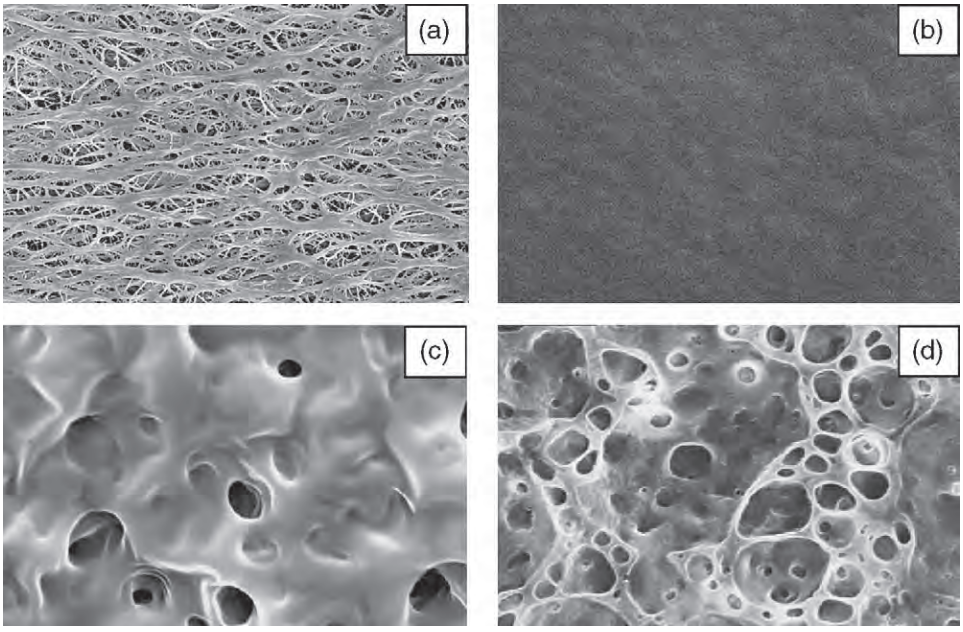


Fig. 7. Micrographs of the surface structure of a microporous PE membrane before and after polymer coating treatment. (a) Bare membrane, (b) with polymer coating by solution method, (c) with polymer coating by phase inversion and (d) with polymer/silica coating by phase inversion. This figure was reprinted selectively from Figs. 4, 1 and 2c of refs. [104,70,101], respectively, with permission from Elsevier.

carried out mainly through dipping [102–104] and in situ polymerization [105,106]. In the former, the operation is required to conduct at elevated temperature to reduce the viscosity of GPE so that the GPE can be easily impregnated into the small pores of the membrane. It has been reported [102] that when a copolymer is used, the composition of the copolymer plays a critical role in determining the electrolyte uptake and ionic conductivity due to the different functions of the copolymeric components. Alternatively, the GPE-impregnation can be conducted by diluting GPE in a volatile aprotic solvent to reduce the viscosity, and then applying the solution onto the porous membrane, followed by evaporation of the volatile solvent to obtain GPE-impregnated membrane [104]. This method generally is applicable to the GPE composed of the placitizer with high boiling point, such as EC, PC and GBL. In the latter, the GPE is formed in situ by a means of polymerization. In this approach, Abraham et al. [105] first reported the impregnation of GPE by UV-irradiation of the microporous membrane soaked with a solution containing a lithium salt, an oligo(oxyethylene) monomer, a non-volatile electrolyte solvent and a photoinitator. Due to the combined advantages of the GPE and microporous membrane, the GPE-impregnated membrane offers better protection against internal short circuit than the GPE alone, and the cells using it exhibit more stable capacity retention than the ones using the microporous membrane as the separator and the plasticizer as the solvent of liquid electrolyte.

5. Concluding remarks

The separator is a critical component of a battery, its main function is to prevent physical contact of the electrodes while permitting ions to flow freely. The separator itself does not participate in any cell reactions, however, its properties significantly determine the performance and safety of the batteries. For high energy and power densities, the separator is required to be very thin and highly porous, while it adversely affects the safety and cycle life of the battery as a result of the reduced mechanical strength. The safety requirement is a top priority for rechargeable Li-ion batteries, especially these used in hybrid electric vehicles and power tools. The PE-based shutdown separators are able to protect the battery in the temperature range of 90–130 °C, depending on the properties, such as average molecular weight and distribution, of PE and the composition of the blend if a blend is used. However, none of polyolefin separators can withstand temperatures above the melting point (near 165 °C) of PP. The melting of the polyolefin separator results in a direct contact of the electrodes, which induces very dangerous chemical reactions between the strongly oxidative cathode materials and the strongly reductive anode materials. When stored near the softening temperature of polyolefin, the polyolefin separator is subjected to shrinking, and therefore a safety concern is present as a result of a potential internal short circuit. The ceramic separator, which combines the characteristics of flexible polymers and hydrophilic ceramic materials, exhibits exceptional thermal stability and excellent wettability. Therefore, the ceramic separator exhibits overwhelming advantages in terms of safety and electrolyte wettability. In the view of battery safety, Separion separators could be very promising for high energy and power Li-ion batteries if their other performances and their cost can be made competitive with the current polyolefin separators. Future development of Li-ion battery separators will be made by balancing the performance against safety and cost. The high cost of separators is mainly due to their production process, therefore, developing a more cost-effective process is very important for the reduction of battery separator cost. The separators that combine the features of thermal shutdown and ceramic separators

are highly desirable, and such separators could be developed based on the Degussa Separion separators by replacing the PET matrix with a porous PE shutdown matrix.

References

[1] D. Linden, T.B. Reddy, Handbook of Batteries, third ed., McGraw-Hill, New York, 2002.
[2] P. Arora, Z. Zhang, Chem. Rev. 104 (2004) 4419.
[3] A. Hashimoto, K. Yagi, H. Mantoku, U.S. Patent 6,048,607 (2000).
[4] N. Kaimai, K. Takita, K. Kono, H. Funaoka, U.S. Patent 6,153,133 (2000).
[5] S. Nagou, S. Nakamura, U.S. Patent 4,791,144 (1988).
[6] P. Jacoby, C.W. Bauer, U.S. Patent 4,975,469 (1990).
[7] M. Xu, S. Hu, J. Guan, X. Sun, W. Wu, W. Zhu, X. Zhang, Z. Ma, Q. Han, S. Liu, U.S. Patent 5,134,174 (1992).
[8] F. Chu, T. Yamaoka, Polymer 37 (1996) 537.
[9] H.M. Fisher, C.G. Wensley, U.S. Patent 6,368,742 (2002).
[10] S.Y. Lee, B.I. Ahn, S.G. Im, S.Y. Park, H.S. Song, Y.J. Kyung, U.S. Patent 6,830,849 (2004).
[11] K. Takita, K. Kono, T. Takashima, K. Okamoto, U.S. Patent 5,051,183 (1991).
[12] P. Jacoby, C.W. Bauer, S.R. Clingman, W.T. Tapp, U.S. Patent 5,317,035 (1994).
[13] H. Higuchi, K. Matsushita, M. Ezoe, T. Shinomura, U.S. Patent 5,385,777 (1995).
[14] H. Sogo, U.S. Patent 5,641,565 (1997).
[15] P. Jacoby, C.W. Bauer, S.R. Clingman, W.T. Tapp, U.S. Patent 5,176,953 (1993).
[16] D.W. Ihm, J.G. Noh, J.Y. Kim, J. Power Sources 109 (2002) 388.
[17] J.T. Lundquist, B. Lundsager, N.I. Palmer, H.J. Troffkin, J. Howard, U.S. Patent 4,650,730 (1987).
[18] J.T. Lundquist, C.B. Lundsager, N.I. Palmer, H.J. Troffkin, U.S. Patent 4,731,304 (1988).
[19] H.M. Fisher, D.F. Leone, J.J. Lowery, U.S. Patent 5,013,439 (1991).
[20] W.C. Yu, M.W. Geiger, U.S. Patent 5,565,281 (1996).
[21] W.C. Yu, C.F. Dwiggins, U.S. Patent 5,667,911 (1997).
[22] W.C. Yu, U.S. Patent 5,691,077 (1997).
[23] T.H. Yu, U.S. Patent 6,080,507 (2000).
[24] M.B. Johnson, G.L. Wilkes, J. Appl. Polym. Sci. 81 (2001) 2944.
[25] M.B. Johnson, G.L. Wilkes, J. Appl. Polym. Sci. 84 (2002) 1762.
[26] M.B. Johnson, G.L. Wilkes, J. Appl. Polym. Sci. 83 (2002) 2095.
[27] C. Chandavasu, M. Xanthos, K.K. Sirkar, C. Gogos, U.S. Patent 6,824,680 (2004).
[28] W.C. Yu, U.S. Patent 6,878,226 (2005).
[29] M.J. Weighall, J. Power Sources 34 (1991) 257.
[30] L.K. Yankov, S.K. Filipova, I.Y. Zlatanov, E.B. Budevski, U.S. Patent 4,959,396 (1990).
[31] Y.L. Yen, G. Lopatin, H. Malarkey, D. Soane, U.S. Patent 5,032,274 (1991).
[32] T.S. Chung, P. Foley, E.R. Kafchinski, J. Mater. Sci.-Mater. Electron. 4 (1993) 259.
[33] J.J. Kim, S.S. Kim, J.R. Hwang, S.B. Suh, U.S. Patent 5,250,240 (1993).
[34] K. Kimishima, Y. Yaniyama, M.E. Lesniewski, P. Brant, K. Kono, Advanced Automotive Battery and Ultracapacitor Conference (AABC-06), Baltimore, MD, May 15–19, 2006.
[35] G. Venugopal, J. Moore, J. Howard, S. Pendalwar, J. Power Sources 77 (1999) 34.
[36] R.W. Callahan, R.W. Call, K.J. Harleson, T.H. Yu, U.S. Patent 6,602,593 (2003).
[37] M. Kinouchi, T. Akazawa, T. Oe, R. Kogure, K. Kawabata, Y. Nakakita, U.S. Patent 6,627,346 (2003).
[38] D.R. Lloyd, K.E. Kinzer, H.S. Tseng, J. Membr. Sci. 52 (1990) 239.
[39] A. Bottino, G. Camera-Roda, G. Capannelli, S. Munari, J. Membr. Sci. 57 (1991) 1.
[40] H. Strathmann, K. Kock, Desalination 21 (1977) 241.
[41] S.S. Zhang, K. Xu, D.L. Foster, M.H. Ervin, T.R. Jow, J. Power Sources 125 (2004) 114.
[42] H.S. Min, J.M. Ko, D.W. Kim, J. Power Sources 119–121 (2003) 469.
[43] A. Subramania, N.T.K. Sundaram, G.V. Kumar, J. Power Sources 153 (2006) 177.
[44] D.R. Lloyd, S.S. Kim, K. Kinzer, J. Membr. Sci. 64 (1991) 1.
[45] E. Kessler, T. Batzilla, F. Wechs, F. Wiese, U.S. Patent 6,375,876 (2002).
[46] E. Kessler, T. Batzilla, F. Wechs, F. Wiese, U.S. Patent 6,497,752 (2002).
[47] A. Magistris, E. Quartarone, P. Mustarelli, Y. Saito, H. Kataoka, Solid State Ionics 152–153 (2002) 347.
[48] W.F. Schortmann, U.S. Patent 5,204,165 (1993).
[49] S.J. Law, H. Street, G.J. Askew, U.S. Patent 6,358,461 (2002).
[50] J.F. Audebert, H.J. Feistner, G. Frey, R. Farer, G.L. Thrasher, European Patent WO 03/043103 (2003).
[51] T. Ashida, T. Tsukuda, U.S. Patent 6,200,706 (2001).
[52] R.W. Pekala, M. Khavari, US6,586,138 (2003).
[53] M. Masanao, H. Yamazaki, Y. Kondo, K. Takahashi, T. Takase, S. Oota, U.S. Patent 6,586,137 (2003).
[54] J.K. Whear, J.G. Yaritz, U.S. Patent 6,537,696 (2003).
[55] J. Zucker, U.S. Patent 6,692,868 (2004).
[56] Y. Sudou, H. Suzuki, S. Nagami, K. Ikuta, T. Yamamoto, S. Okijima, S. Suzuki, H. Ueshima, U.S. Patent Appl. 20060073389 (2006).
[57] A.L. Benson, D.A. Jordan, U.S. Patent 4,279,979 (1981).
[58] R.P. Schwobel, H. Hoffmann, U.S. Patent 5,401,594 (1995).
[59] R. Sassa, R. Winkelmayer Jr, U.S. Patent 5,324,579 (1994).
[60] A. Mathur, U.S. Patent 6,517,676 (2003).
[61] P. Kritzer, J. Power Sources 161 (2006) 1335.
[62] T. Takahashi, S. Terazono, R. Kamei, E. Takiyama, U.S. Patent 5,525,409 (1996).
[63] M. Tanaka, T. Nobutoshi, U.S. Patent 6,030,727 (2000).
[64] A.S. Fabbricante, G.F. Ward, T.J. Fabbricante, U.S. Patent 6,114,017 (2000).
[65] S.S. Choi, Y.S. Lee, C.W. Joo, S.G. Lee, J.K. Park, K.S. Han, Electrochim. Acta 50 (2004) 339.
[66] J.R. Kim, S.W. Choi, S.M. Jo, W.S. Lee, B.C. Kim, J. Electrochem. Soc. 152 (2005) A295.
[67] I. Kuribayashi, J. Power Sources 63 (1996) 87.
[68] M.K. Song, Y.T. Kim, J.Y. Cho, B.W. Cho, B.N. Popov, H.W. Rhee, J. Power Sources 125 (2004) 10.
[69] Y.M. Lee, J.W. Kim, N.S. Choi, J.A. Lee, W.H. Seol, J.K. Park, J. Power Sources 139 (2005) 235.
[70] Y.M. Lee, N.S. Choi, J.A. Lee, W.H. Seol, K.Y. Cho, H.Y. Jung, J.W. Kim, J.K. Park, J. Power Sources 146 (2005) 431.
[71] J.C. Ma, E.S. Megahed, T.J. Stachoviak, S.A. Craanen, D.A. Schneider, J.P. Nestler, U.S. Patent 6,444,356 (2002).
[72] P.P. Prosini, P. Villano, M. Carewska, Electrochim. Acta 48 (2002) 227.
[73] K.M. Kim, N.G. Park, K.S. Ryu, S.H. Chang, Electrochem. Acta 51 (2006) 5636.
[74] D. Takemura, S. Aihara, K. Hamano, M. Kise, T. Nishimura, H. Urushibata, H. Yoshiyasu, J. Power Sources 146 (2005) 779.
[75] S.S. Zhang, K. Xu, T.R. Jow, J. Solid State Electrochem. 7 (2003) 492.
[76] S.S. Zhang, K. Xu, T.R. Jow, J. Power Sources 140 (2005) 361.
[77] S.A. Carlson, Q. Ying, Z. Deng, T.A. Skotheim, U.S. Patent 6,306,545 (2001).
[78] S. Augustin, V.D. Hennige, G. Horpel, C. Hying, Desalination 146 (2002) 23.
[79] S. Augustin, V.D. Hennige, G. Horpel, C. Hying, J. Tarabocchia, J. Swoyer, M.Y. Saidi, Meet. Abstr.-Electrochem. Soc. 502 (2006) 80.
[80] S. Augustin, V.D. Hennige, G. Horpel, C. Hying, P. Haug, A. Perner, M. Pompetzki, T. Wohrle, C. Wurm, D. Ilic, Meet. Abstr.-Electrochem. Soc. 502 (2006) 84.
[81] S. Augustin, Advanced Automotive Battery and Ultracapacitor Conference (AABC-06), Baltimore, MD, May 15–19, 2006.
[82] V. Hennige, C. Hying, G. Horpel, P. Novak, J. Vetter, U.S. Patent Appl. 20,060,078,791 (2006).
[83] W.M. Choi, The 17th Annual IEEE Battery Conference on Applications and Advances, Long Beach, CA, January 14–18, 2002, pp. 83–88.
[84] H.T. Taskier, U.S. Patent 4,359,510 (1982).
[85] Product brochure of Celgard microporous membrane 3400.
[86] J.L. Gineste, G. Pourcelly, J. Membr. Sci. 107 (1995) 155.

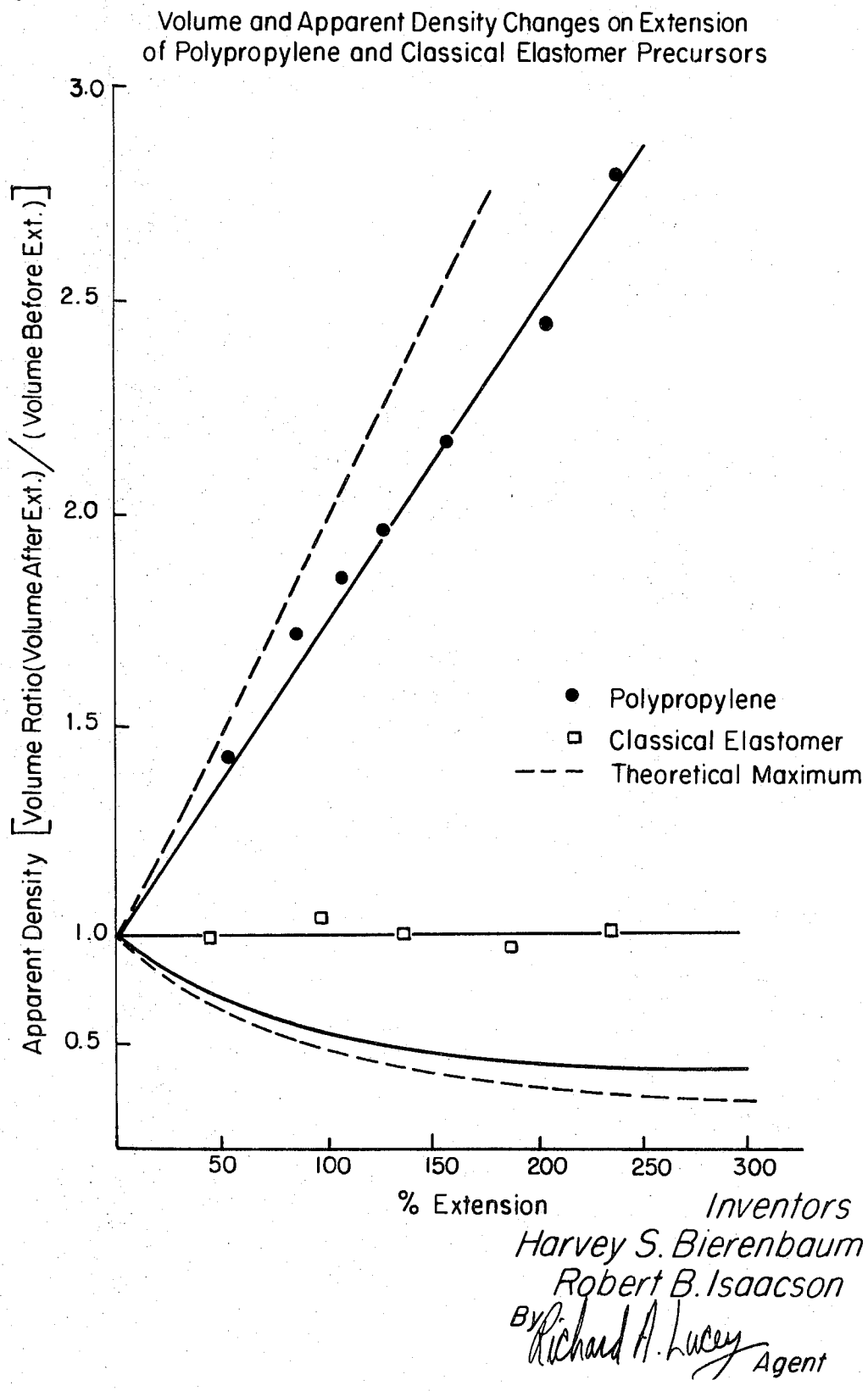
[87] M. Urairi, T. Tachibana, K. Matsumoto, T. Shinomura, H. Iida, K. Kawamura, S. Yano, O. Ishida, U.S. Patent 5,558,682 (1996).
[88] S. Senyarich, P. Viaud, U.S. Patent 6,042,970 (2000).
[89] S.H. Choi, K.P. Lee, J.G. Lee, Y.C. Nho, J. Appl. Polym. Sci. 77 (2000) 500.
[90] S.H. Choi, S.Y. Park, Y.C. Nho, Radiat. Phys. Chem. 57 (2000) 179.
[91] S.H. Choi, H.J. Kang, E.N. Ryu, K.P. Lee, Radiat. Phys. Chem. 60 (2001) 495.
[92] J.M. Ko, B.G. Min, D.W. Kim, K.S. Ryu, K.M. Kim, Y.G. Lee, S.H. Chang, Electrochim. Acta 50 (2004) 367.
[93] K. Gao, X.G. Hu, T.F. Yi, C.S. Dai, Electrochem. Acta 52 (2006) 443.
[94] Y. Takeuchi, M. Kawabe, H. Yamazaki, M. Kaneko, G. Anan, K. Sato, U.S. Patent 6,171,708 (2001).
[95] T. Tanaka, H. Yamaguchi, N. Takimoto, M. Yamashita, S, Hamamoto, U.S. Patent 6,821,680 (2004).
[96] D.W. Kim, J.M. Ko, J.H. Chun, S.H. Kim, J.K. Park, Electrochem. Commun. 3 (2001) 535.
[97] D.W. Kim, K.A. Noh, J.H. Chun, S.H. Kim, J.M. Ko, Solid State Ionics 144 (2001) 329.
[98] F.O. Eschbach, M. Oliver, U.S. Patent 5,681,357 (1997).
[99] K. Hamano, H. Shiota, S. Shiraga, S. Aihara, Y. Yoshida, M. Murai, T. Inuzuka, U.S. Patent 5,981,107 (1999).
[100] Y.B. Jeong, D.W. Kim, J. Power Sources 128 (2004) 256.
[101] J.Y. Kim, S.K. Kim, S.J. Lee, S.Y. Lee, H.M. Lee, S. Ahn, Electrochim. Acta 50 (2004) 363.
[102] D.W. Kim, B. Oh, J.H. Park, Y.K. Sun, Solid State Ionics 138 (2000) 41.
[103] Y. Wang, J. Travas-Sejdic, R. Steiner, Solid State Ionics 148 (2002) 443.
[104] J.S. Oh, Y.K. Kang, D.W. Kim, Electrochim. Acta 52 (2006) 1567–1570.
[105] K.M. Abraham, M. Alamgir, D.K. Hoffman, J. Electrochem. Soc. 142 (1995) 683.
[106] K. Morigaki, N. Kabuto, K. Haraguchi, U.S. Patent 5,597,659 (1997).

Appendix S

PROCESS FOR PREPARING MICROPOROUS FILM

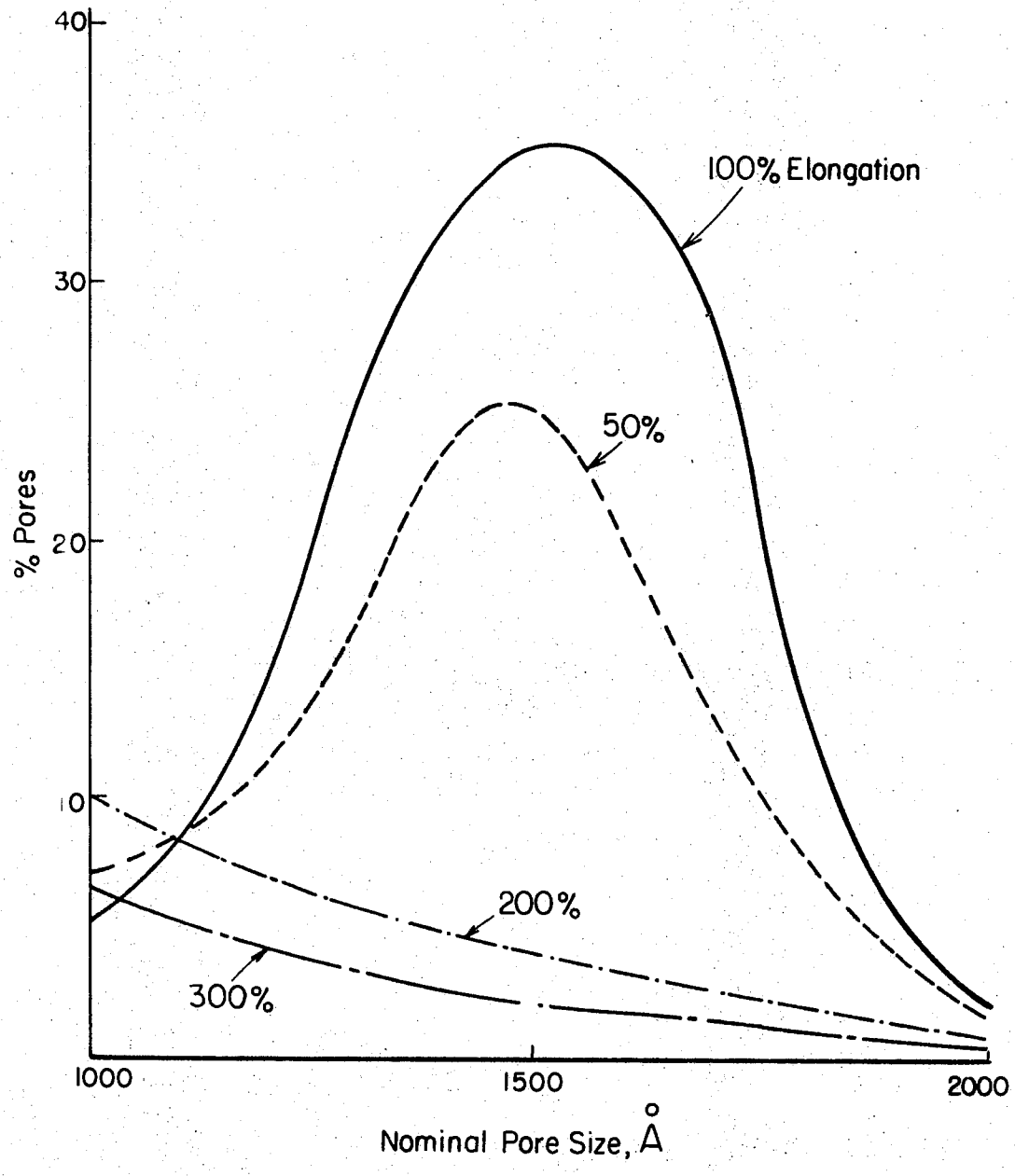
Filed June 23, 1969 4 Sheets-Sheet 1

FIG. 1



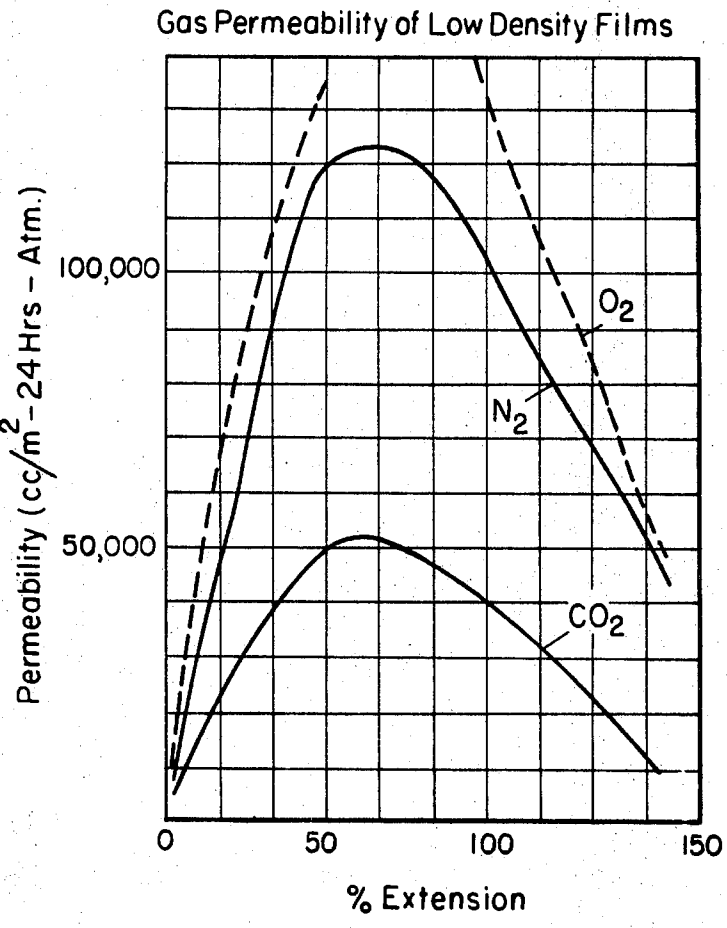
Inventors
Harvey S. Bierenbaum
Robert B. Isaacson
By Richard A. Lucey Agent

FIG. 2



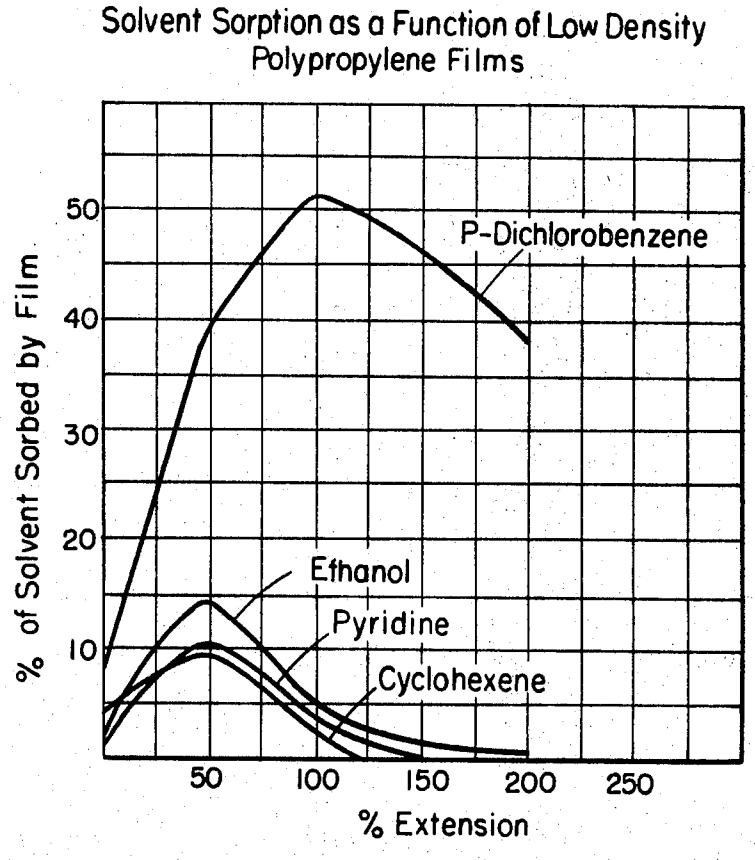
Inventors
Harvey S. Bierenbaum
Robert B. Isaacson
By Richard A. Lucey Agent

FIG. 3



Inventors
Harvey S. Bierenbaum
Robert B. Isaacson
By Richard A. Lacey
Agent

FIG. 4



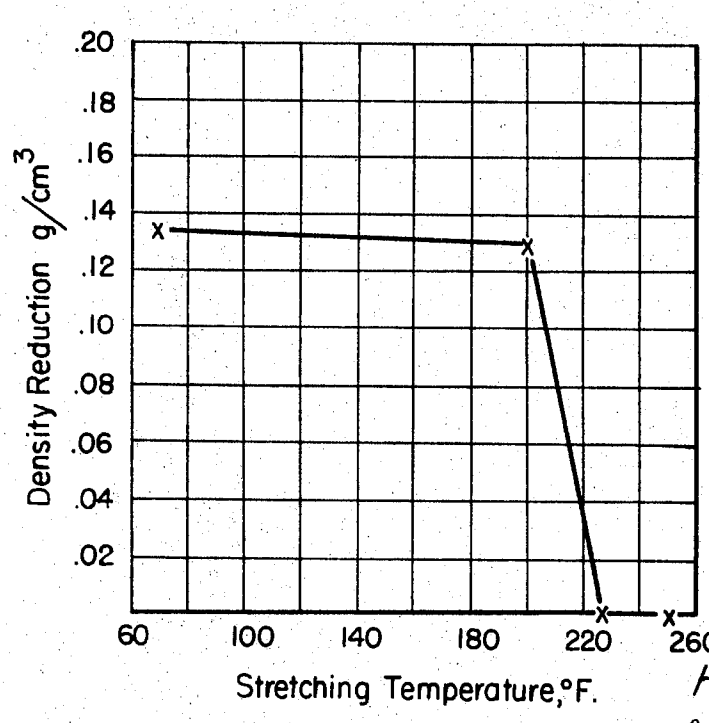


FIG. 5

Inventors
Harvey S. Bierenbaum
Robert B. Isaacson
By Richard A. Lucey Agent

United States Patent Office 3,558,764
Patented Jan. 26, 1971

3,558,764

PROCESS FOR PREPARING MICROPOROUS FILM

Robert B. Isaacson, Rahway, N.J., and Harvey S. Bierenbaum, Worcester, Mass., assignors to Celanese Corporation, New York, N.Y., a corporation of Delaware

Continuation-in-part of application Ser. No. 577,439, Sept. 6, 1966. This application June 23, 1969, Ser. No. 835,367

Int. Cl. D01d 5/12

U.S. Cl. 264—210 7 Claims

ABSTRACT OF THE DISCLOSURE

A method is disclosed and claimed for the production of polymeric films (e.g. polyethylene, polypropylene or polyacetal films) characterized by an open-cell structure and an apparent density lower than the actual density of the original polymers. Such products are prepared by first extruding a film, next drawing down this film at a high rate, then annealing it and cold drawing it and finally heat-setting the cold drawn film. The thus-produced polymeric films are particularly useful for such applications as microporous membranes.

INVENTION

This invention is a continuation-in-part of applicants' co-pending application Ser. No. 577,439 filed on Sept. 6, 1966, now abandoned.

This invention relates to novel films characterized by an open-celled structure and by a low apparent density and to a process for preparing same from crystalline polymers. More particularly, this invention relates to novel films having an open-celled structure evidencing an optimum pore size distribution and to a process for preparing same.

Porous compositions are of two general types; one type in which the pores are not interconnected, and which constitute foams or cellular plastics, and the other type in which the pores are essentially interconnected through tortuous paths which may extend from surface to surface of the structure. The microporous structures of the present invention are of the latter type.

The development of plastic materials possessing outstanding physical qualities has resulted in an extensive search for plastic materials which evidence a microporous structure in addition to their other desirable qualities. Generally, however, the plastic sheet or film materials encountered in the prior art have been unsatisfactory in this connection due to the problem of obtaining materials having optimum porosity which problem is mainly attributable to the difficulty in obtaining a microporous structure having uniform pore sizes in a desired range.

It has been proposed to prepare porous filters from thermoplastic synthetic resin by sintering the substances in the form of powders or granules, using a moderate pressure so that they will adhere together. Instead of heat, solvents can be used. In either case, the object is to adhere the particles together, forming aggregates, but while the aggregates must be tightly bonded, the interstices between them must be retained to form pores. However, neither of these procedures has been satisfactory, because it has been found to be quite impossible to prepare uniform structures by this means. When thermoplastic synthetic resins are heated above their softening point, even under slight pressures they tend to deform readily and even to flow, with the result that it is easy for the aggregates to be displaced, forming non-uniform pores in various sections, and even to collapse and bond to such an extent that the mass is actually non-porous. Naturally, the smaller the particle size of the synthetic plastic, the more

difficult it is to prepare a porous material by this means. As a practical matter, it has been found to be impossible to prepare by this method structures of significant porosity from plastic materials smaller in size than 150 mesh.

In order to overcome the problems heretofore encountered, it has been proposed to employ film materials which unlike the structures of the prior art, possess apparent densities lower than the polymer materials from which this type of material is formed, usually no greater than 90%, preferably about 50 to 75% of the densities of the corresponding polymer materials and which, surprisingly, evidence a porous, open-celled structure. The sizes of the passageways to the voids or pore spaces of said open-celled structure accessible to the outside of the film are under 5000 angstrom units, and generally range from between about 150 to 5000 angstrom units, as determined by mercury penetration porosymmetry which measurement also determines the volume of such void or pore space.

While these structures exhibit the desired microporous structure, i.e., about 99% of the pores are accessible from the outer surface of the porous structure, said structures generally have been unsatisfactory due to the non-uniformity of the pore sizes of the structure. This lack of uniformity has in many instances almost negated the permeability of the microporous structure. Surprisingly, however, it has been found that the pore sizes of the structure can be optimized, i.e., rendered uniform in size, if certain critical process variables are practiced during fabrication of the microporous structure. Hence, it has been discovered that if the sheets or films of the present invention are stretched to a critical degree during the processing thereof, a microporous structure of an essentially uniform pore size results.

Broadly, the films suitable for use herein are prepared by extruding in the form of a film an extrudable molten polymer, e.g., a polymer having a crystallinity of at least about 40% at a suitable melt temperature. The thus-extruded film is taken up at a prescribed drawdown ratio and is annealed, e.g., at a temperature in the range of about 5 to 100° C. below the crystalline melting point of the polymer. This annealing step is found to impart the desired elasticity to the film so as to characterize same as a precursor for forming the desired open-celled product. Such precursor film is then drawn, e.g., at a draw ratio which preferably ranges from about 1.3:1 to about 2.5:1 (i.e. 30 to 150% extension) and is subsequently heat-set or annealed to stabilize the resultant product.

The unconventional characteristic of the above-discussed film is that when such precursor is subjected to a degree of stretch below its breaking point, the ratio of the total gross volume of the stretched film to that of the unstretched film is significantly greater than 1. This is surprising and totally unexpected since the ratio of total gross volume of a given mass of an article of an elastic material such as rubber, i.e., a classical elastomer in the stretched state to that of said article in the unstretched state has been found to be substantially 1, i.e., there is no increase of total gross volume of these articles when they are stretched. Moreover, when a conventional article, e.g., an article synthesized of nylon, polyester, polypropylene, and the like, is inelastically stretched, i.e., "cold drawn," the ratio of total gross volume of stretched to unstretched material is generally less than 1, i.e., the apparent density of the stretched article is higher than that of the unstretched article. Expressed another way, the cross section of an elastic article of rubber or classical elastomer, or of an ordinary inelastic article which is stretched, e.g., to increase orientation, decreases on stretch to the extent that the length of the article increases so that the total gross volume of the stretched article is approximately equal to or less than that of the

unstretched article. This is in contrast to what occurs when an elastic crystalline precursor contemplated by this invention is suitably stretched or drawn and is subsequently heat set or annealed.

In the present instance, the decrease in the cross section of the article on stretch is either zero or extremely small and such decrease in cross section does not make up for the increase in length on stretching, so that the total gross volume of the stretched article is substantially higher than that of the unstretched article. As the total gross volume of the fiber being stretched increases, its apparent density decreases proportionately.

As used herein, the term "apparent density" signifies the weight per unit of "gross volume" of the film where "gross volume" is determined by the amount of mercury infused into the film by high pressure, see R. G. Quynn et al. in Journal of Applied Polymer Science, vol. 2, No. 5, pages 166–173 (1959).

As used herein, the term "open-celled structure" signifies that the major portion of the void or pore space of the structure within the geometric confines of the film is accessible to the outside planar surfaces of the film.

In order to illustrate the above-discussed behavior, the volume changes of stretched articles, e.g., polypropylene and typical classical elastomer, were determined by measuring the cross section of the articles. The volume at any degree of stretch or extension could then be compared with the original volume. The results are shown in the accompanying FIG. 1, which is incorporated herein by reference.

In interpreting FIG. 1 the dashed line represents the maximum theoretical volume increase that could be caused by extension. For no volume increase the volume ratio is unity, and the classical elastomer manifests such behavior. However, the polypropylene precursor exhibits extremely great increases in volume upon stretching, i.e., close to the theoretical maximum.

The densities of the same articles in the stretched state were porosimetrically determined by mercury penetration and are also shown on FIG. 1. Here, again, the dashed line represents the maximum theoretical decrease in apparent density. For no decrease in the apparent density, the value is unity, and the typical classical elastomer evidences such behavior. However, the propylene precursor exhibits a surprising decrease in the apparent density upon stretching, close to the theoretical maximum. Further, examination of the low density polypropylene article under an optical microscope showed it to be highly porous.

From the foregoing, it is logical to conclude that the pore size distribution in the stretched polypropylene article would be dependent on, and be directly proportional to, the degree of extension of said article. Hence, it is also logical to conclude that as the volume ratio increased and the apparent density decreased, the porosity of the extended article would increase and the concomitant characteristics, e.g., gas permeability (to water vapor, O_2, CO_2, N_2), dye receptivity, penetration by salts and other chemicals, rates of topochemical reaction, and the like would also be affected in a directly proportional relationship. Surprisingly, however, it was discovered that while pore size distribution, as well as the characteristics dependent thereon, is strongly dependent on the extension of the article, optimum pore size distribution is found at extensions less than 150%, i.e., at intermediate extensions and extensions less than intermediate rather than at higher extensions. Further, it was found that at extensions falling within a narrow range, i.e., between about 50% and about 100%, a disproportionately high percentage of pores in the 1000–2000 angstrom range (as measured by mercury intrusion porosymmetry) was encountered. This high percentage of pores in the 1000–2000 angstrom range was also manifested in the physical characteristics, permeability, etc. of the films. Thus, contrary to expectation, it was found that the amount of solvent absorbed into the articles was a maximum at 50–100% extension

and also, contrary to expectation, the amount fell off at higher extensions. This same unconventional behavior was observed with the rates of various topochemical reactions, gas permeability, dye receptivity, penetration of salts and other chemicals, etc. Hence, the present invention is predicated on the surprising discovery that the open-celled low density articles described above behave as a more porous substrate at intermediate extensions, i.e., less than about 150% and most preferably about 50–100%, for polypropylene articles, than at higher extensions. It is, of course, understood that higher and lower extensions may be employed, however, the desired optimum pore size distribution will not be achieved as demonstrated in FIG. 2.

The films of the present invention are formed from precursor films of a relatively crystalline film-forming polymer having an elastic recovery at zero recovery time (hereinafter defined) at 25° C. and 65% relative humidity, of about 50 to about 90% when subjected to a standard strain (extension) of 50%, and preferably an elastic recovery at zero recovery time of at least about 80% when subjected to a strain of 50%. These precursor films, as well as the preparation thereof, are further defined in copending application Ser. No. 572,601, filed on Aug. 15, 1966.

It should be noted that although a standard strain of 50% is used to identify the elastic properties of the precursor films of this invention, such strain is merely exemplary. Such precursor films will, of course, generally have elastic recoveries even higher at strains less than 50% than they do at 50% strain, and such films also have relatively high elastic recoveries at strains substantially higher than 50%, e.g., from strains of say 100%.

The precursor film utilized in the preparation of the low density film of the present invention must be differentiated from film formed from classical elastomers. With such classical elastomers the stress-strain behavior, and particularly the stress-temperature relationship, is governed by an entropy-mechanism of deformation (rubber elasticity). The positive temperature coefficient of the retractive force, i.e., decreasing stress with decreasing temperature and complete loss of elastic properties at the glass transition temperature are particular consequences of entropy-elasticity. The elasticity of the precursor films utilized herein, on the other hand, is of a different nature. In qualitative thermodynamic experiments with these precursors, increasing stress with decreasing temperature (negative temperature coefficient) may be interpreted to mean that the elasticity of said materials was not governed by entropy effects but depended on an energy term. More significantly, it was found that the precursor films of this invention retained their "stretch" properties at temperatures where entropy-elasticity could no longer be operative. Thus, it may be concluded that the "stretch" mechanism of the precursor films is based on energy-elasticity and may be referred to as "non classical" elastomers.

The above characteristics necessary to the precursor films can be accomplished by employing a critical combination of process variables and process steps. Broadly the necessary process steps comprise the forming, i.e., extrusion of the films under critical conditions followed by an annealing step to impart the desired degree of elasticity. The necessary process conditions comprise: (1) a rapid rate of drawdown, (2) a high drawdown ratio and, (3) a low melt temperature, i.e., a melt temperature substantially closer to the melt temperature of the film-forming polymer than in conventional extrusion processes.

The rapid rate of drawdown may be accomplished, for example, in slit die extrusion by providing the take-up roll or spool for the extruded film at a distance not more than two inches, and preferably not more than one inch, from the extrusion slit or orifice. At the same time, said takeup roll must be operated at a high rate, e.g., a speed

of at least 25 feet/min. of the film, measured at said roll since the takeup rate of the film actually varies at the extrusion slit (where the film is relatively thick) and at the takeup roll (where the film is comparatively thinner).

The drawdown ratios suitably employed to prepare the precursors range from about 20:1 to about 180:1 and preferably range from about 30:1 to about 125:1.

The melt temperature for extrusion of the precursors is in general no higher than 100° C. above the melting point of the polymer and most suitably in the range of 10 to 40° C. above such melting point, while the drawdown ratio of extrusion, i.e., ratio of linear velocity of the take-up roll to the linear velocity of extrusion is at least 20:1. The annealing step is generally carried out at a temperature in the range of about 5 to 100° C. below the melting point of the polymer for a period of at least 10 seconds.

The first of two essential steps of the present invention is drawn or stretched. This can be done continuously in connection with an extrusion unit or the film may be drawn in a separate step. Regardless of which procedure is followed, the extruded film must be drawn to accomplish the objects of the invention. By "extruded" film is meant film as it first solidifies on emergence from the extruder. The extruded film is drawn to impart the open-celled structure and to reduce the apparent density of same. The precise degree of drawing is critical to this invention in that an optimization of useful properties takes place at extensions intermediate or less than intermediate rather than at extensions greater than intermediate.

In order to obtain optimum levels of the characteristics mentioned hereinbefore, the extruded films should not be drawn or extended to an amount greater than 150% of their original length. As hereinbefore set forth, extensions of from about 30% to about 150% (i.e., draw ratios of from 1.3:1 to about 2.5:1) are preferred to achieve the optimized distribution of pore sizes of the subject low density films. Extensions of as low as 10% and as high as 1,000% may be employed, but the desireable quality of the films (e.g., their optimized low density distribution) will not be achieved. This result is set forth in FIG. 2 which is incorporated herein by reference. In order to attain maximization of the desired utility of the invention, e.g., maximum gas permeability, dye receptivity, etc., optimum pore size and the like, it is preferred to extend the film from about 30% to about 150% of their original lengths and it is most preferred to extend the film about 50 to 100% of their original lengths.

In accordance with the present invention, the film is preferably "cold drawn" to impart the desired voidy structure. In this operation the film is drawn at the above draw ratios at ambient or near-ambient temperatures. The drawing per se may be performed in any convenient manner using known techniques where a film is positively forwarded by one moving means to a second moving means operating at a higher speed. The temperature of the film per se being drawn is referred to herein as the draw temperature.

The present invention also contemplates drawing the film at sub-ambient temperatures as well as at temperatures above ambient. However the upper limit of the draw temperature ranges has been found to be critical and it is essential that this limit not be exceeded. This criticality is illustrated by graphical means in FIG. 5 of the drawings which is incorporated herein by reference. The graph presented compares the density reduction of a typical polypropylene film with the drawing or stretching temperature utilized. From the graph it is easily discernible that substantial reduction in the apparent density of the film can be effected up to a temperature of about 200° F. (93.3° C.) but when this temperature is exceeded there is a marked decrease in the reduction of the apparent density of the film. Surprisingly in this instance essentially no reduction can be accomplished when the upper limit of the drawing operation is exceeded by even a small amount. For instance see FIG. 5 wherein at the stretching temperature of 200° F. a density reduction of about 0.13 g./cm.^{3} was achieved as compared to a stretching temperature of 220° F. wherein a density reduction of only about 0.03 was achieved. Accordingly with respect to polypropylene films the critical stretching temperature of 200° F. may be exceeded but at the expense of achieving a final product with a poor microporous quality. Accordingly the polypropylene films of the present invention are preferably not drawn at a temperature in excess of the 200° F. upper limit and the polyethylene film not in excess of the 220° F. If acetal films are contemplated they are not drawn at a temperature in excess of 255° F. Although graphs relating to the latter two species have not been included herein similar results would be achieved at their respective critical temperatures.

When the film is drawn at temperatures above ambient said film may be heated by any conventional means. Preferably the film is heated by heated moving rolls. However the film may also be heated by passage over a heated plate through a heated liquid a heated gas or the like.

The second essential step in the process of this invention is the step of heat setting or annealing the film, after the drawing thereof, while said film is in the tensioned state. It has been found that heating the drawn film in a tensioned state at a temperature of 80° C. or above has a remarkable influence on the dimensional stability of the open-celled, low density characteristics of same. Accordingly, the drawn film is stabilized against excessive shrinkage, etc. by heating at a temperature which may be somewhat higher than the drawing temperature and while being held under a tension such that the film is not free to shrink or can shrink to only a controlled extent, e.g., not greater than 15% of the initial length. In order to insure maximum relaxation of the strains introduced into the films during the earlier processing thereof and thus impart the desired stability, the heat treatment is preferably carried out at a temperature within the range of from about 100° C. to about 150° C. for polypropylene, 100 to 150° C. for acetal polymers, 100 to 135° C. for polyethylene, etc. The upper limit of the temperature parameters is seen to be critical in that some dissipation of the voidy structure especially the voids of the herein desired pore space, is encountered at temperatures above the foregoing limits. The period of heat treatment should be longer than about 0.1 second at the higher annealing temperatures and may be within the range of about 0.5 second to about 30 minutes at the lower annealing temperatures, preferably about 2 seconds to 15 minutes. The drawing operation and the heat treatment is preferably carried out sequentially. As may be surmised from the foregoing discussions, the apparent density of the resulting heat treated low density film is significantly below that of the precursor film.

The resultant film, in a tensionless state, has an apparent density lower than the density of the polymeric precursor material from which it is formed, usually no greater than 95%, preferably about 50 to 75% of the densities of the corresponding polymer material. The sizes of the passageways to the void or pore spaces of the open-celled film structure accessible to the outside planar surfaces of the film are generally under 5000 angstrom units, e.g., 150 to 5000 angstrom units and optimized in the 1000–2000 angstrom unit range, as determined by mercury penetration porosymmetry, which measurement also determines the volume of such void or pore space. The final crystallinity of these films is preferably at least 30%, more preferably at least 40% and more suitably at least 50%, e.g., 50 to 100%.

As stated, the elastic precursor films employed in this invention are composed of a polymer of a type capable of developing a significant degree of crystallinity, as contrasted with more conventional or "classical" elastic ma-

terials such as a rubber which are substantially amorphous in the unstretched or tensionless state.

The significant group of polymers to which this invention may be applied are the olefin polymer, e.g., polypropylene, poly-3-methyl butene-1, poly-4-methyl pentene-1, polyethylene as well as copolymers of propylene, 3-methyl butene-1, 4-methyl pentene-1, or ethylene with each other or with minor amounts of other olefins, e.g., copolymers of propylene and ethylene, copolymers of a major amount of 3-methyl butene-1 and a minor amount of a straight chain n-alkene such as n-octene-1, n-hexadecene-1, n-octadecene-1, or other relatively long chain alkenes, as well as copolymers of 3-methyl pentene-1 and any of the same n-alkenes mentioned previously in connection with 3-methyl butene-1. These polymers in the form of films generally have a percent crystallinity of at least 50%, e.g., 50 to 60%.

While the present disclosure and examples are directed primarily to the aforesaid polyolefin polymers, the invention also contemplates the high molecular weight acetal polymers. While both acetal (or oxymethylene) homopolymers and copolymers are contemplated, the preferred oxymethylene polymer is a "random" oxymethylene copolymer, i.e., one which contains recurring oxymethylene, i.e, —CH_2—O—, units interspersed with —OR— groups in the main polymer chain where R is a divalent radical containing at least two carbon atoms directly linked to each other and positioned in the chain between the two valences, with any substituents on said R radical being inert, that is, those which do not include interfering functional groups and which will not induce undesirable reactions, and wherein a major amount of the —OR— units exists as single units attached to oxymethylene groups on each side. Examples of preferred polymers include copolymers of trioxane and cyclic ethers containing at least two adjacent carbon atoms such as the copolymers disclosed in U.S. Pat. No. 3,027,352 of Walling et al. These polymers in film form also have a crystallinity of at least 50%, e.g., 50 to 60%.

Other relatively crystalline polymers to which the invention may be applied are polymethylene sulfide, polyethylene sulfide, polyphenylene oxide, polyamides such as polyhexamethylene adipamide (nylon 66) and polycaprolactam (nylon 6) and polyesters such as polyethylene terephthalate.

The types of apparatus suitable for forming the precursor film products of this invention are well known in the art. For example, a conventional film extruder equipped with a shallow channel metering screw and coathanger die, is satisfactory. Generally, the resin is introduced into a hopper of the extruder which contains a screw and a jacket fitted with heating elements. The resin is melted and transferred by the screw in the die from which it is extruded through a slot in the form of a film from which it is drawn by a take-up roll. Obviously, more than one take-up roll in various combinations may be used.

Using this type of apparatus, film may be extruded at a drawdown ratio of about 20:1 to about 180:1, preferably about 30:1 to about 125:1. The die opening or slot width may be in the range, for example, of about 30 to 200 mils. Polypropylene may be extruded at a melt temperature of about 180° to 260° C., preferably 195° to 225° C. Polyethylene may be extruded at a melt temperature of about 175° to 225° C. while acetal polymers, e.g., of the type disclosed in U.S. Pat. No. 3,027,352, may be extruded at a melt temperature of about 185° C. to 235° C., preferably 195° to 215° C.

The extrusion operation is necessarily carried out with rapid cooling and rapid drawdown in order to obtain maximum elasticity. This may be accomplished by having the take-up roll relatively close to the extrusion slot, e.g., within two inches and, preferably, within one inch, and rotating as fast as possible without breakage. An "air knife" may be employed within one inch of the slot. The take-up roll may be rotated, for example, at a speed of 20–1000 ft./min., preferably 50 to 500 ft./min.

While the present invention has been directed to slit die extrusion methods, an alternative method of forming the precursor films contemplated by this invention is the blown film extrusion method wherein a hopper and an extruder are employed which are substantially the same as in the slot extruder described above. From the extruder, the melt enters a die from which said melt is extruded through a round slot to form a tubular film having an initial diameter D_1. Air enters the system through an inlet and is distributed by means of air ring or similar means through an opening into the interior of said tubular film and has the effect of blowing up the diameter of the tubular film to a diameter D_2. A second source of air is also provided and impinging means direct this air about the extruded tubular film so as to quickly and effectively cool same. After a short distance during which the film is allowed to completely cool and harden, it is wound up on a take-up roll.

Using the blown film method, the drawdown ratio is preferably 20:1 to 180:1, the slot opening 20 to 200 mils, the D_2/D_1 ratio 0.5 to 6.0 and the take-up speed 30 to 700 ft./min. The melt temperature may be within the ranges given previously for straight slot extrusion.

As stated previously, the extruded precursor film may be initially annealed in order to develop the desired range of elasticity. Generally, this first annealing is carried out at a temperature in the range of about 5° to 100° C. below the crystalline melting point of the polymer for a period of at least 5 seconds. Thus, for polypropylene, the preferred annealing temperature is about 100 to 155° C., while for oxymethylene (acetal) copolymers, the preferred annealing temperature is about 110 to 165° C.

One method of carrying out the annealing step is through the use of hot rolls wherein the annealing time is generally in the range of about 5 to 90 seconds or longer. Another method is by placing the film in the tensionless state in an oven at the desired temperature in which case the residence time is preferably in the range of about 30 seconds to 1 hour.

In accordance with the invention, the extruded and annealed, film passes over a roll and into suitable stretching means. This may be accomplished by passage between a first pair of rolls and then a second pair of rolls; and said second pair of rolls being rotated at higher peripheral speeds than said first pair of rolls so as to effect stretching of the film to the predetermined extent. For example, the first rolls may be rotated at a peripheral speed of about 10 to 1000 feet per minute and the second rolls may be rotated at a peripheral speed of 12 to 1350 feet per minute to impart the desired stretch to the film as it proceeds through the drawing operation. The drawn film then passes from the rolls into a heater and over a roll to a windup means. The peripheral speed of this latter roll may be lower than, the same as, or somewhat higher than that of the second pair of rolls so that the film passing through the heater is held against shrinkage or shrinks to a controlled extent. The rate of feed of the film to the heaters and the heating times are correlated so that at the selected drawing and stabilizing temperature, the desired objectives are accomplished.

The heater, as mentioned, may be heated in any suitable manner, for example, by a heated plate, heated liquid, a heated gas, etc. These, obviously, may be substituted by any equivalent heating medium.

Generally, the polypropylene precursor film of this invention has, at 25° C. and 65% relative humidity, an elastic recovery from 50% extension of about 50 to about 90%, a tensile strength of 10,000 to 35,000 p.s.i., a breaking elongation of 200 to 350%, a modulus of 100,000 p.s.i. (all the foregoing in the machine direction), a haze of 20% to opaque, a void volume .565 to .075 $cm.^3/gm.$, and a density .60 to .85 $gm./cm.^3$, the values of the last

two properties being determined by mercury porosymmetry.

More pertinent to the utility of the invention, however, the present polypropylene film exhibits properties in the following ranges: O_2 transmittance as high as 150,000, generally 110,000 to 150,000; N_2 transmittance as high as 130,000, generally 100,000 to 125,000; CO_2 transmittance as high as 60,000, generally 40,000 to 55,000; and water vapor transmittance as high as 400, generally 150 to 350, the units of transmittance being given in cc./24 hours, m.^{2}, atm. Advantageously, the distribution of pore sizes in the 1000–2000 angstrom unit range represents 20%–50% of the pores present.

The invention is further illustrated by the following examples.

EXAMPLE I

This example illustrates the affect the amount of extension (percent increase in length of original structure) has on the apparent density (gm./cm.^{3}) and the pore volume (cm.^{3}/gm.) of a polypropylene film.

In this example, crystalline polypropylene of melt index 4.0 and density .905 g./cc. was melt extruded at 380° F. through an 8" slit die of the coat hanger type using a 1¾" extruder with a shallow channel metering screw. The length to diameter ratio of the extruder barrel was 24:1. The extrudate was drawn down very rapidly to a draw-down ratio of 180:1, contacted with a rotating casting roll maintained at 185° F. and ¼" from the lip of the die. The film produced in this fashion was found to have the following properties:

Thickness—.0005 inch
Recovery from 50% elongation at 25° C.—48%

A sample of this film was oven-annealed in the tensionless state of 125° C. for one hour, removed from the oven and allowed to cool. It was then found to have the following properties:

Recovery from 50% elongation at 25° C.—90%

Samples of both films, annealed and unannealed, were extended at room temperature to a series of different elongations, and heat set in the extended state for 5 minutes at 125° C. All samples were then allowed to cool and found to have the following apparent densities and void volumes by mercury porosymmetry.

	Apparent density, gm./cm^3		Pore volume, cm.^{3}/gm.	
	Annealed prior to stretching	Not annealed priot to stretching	Annealed prior to stretching	Not annealed prior to stretching
Percent extension:				
50	.804	.853	.144	.070
100	.784	.834	.174	.087
200	.755	.831	.224	.094
300	.734	.829	.263	.096

The above apparent density and pore volume comparative data illustrate the respective definite decreasing trend and increasing trend of each characteristic. Hence it would be expected that the more porous films (high pore volume, etc.) would consequently exhibit high permeability, a pore size distribution of large size (in angstrom units) etc. This as hereinbefore disclosed and as herein later illustrated is not the case.

EXAMPLE II

The polymer described in Example I was melt extruded and oven-annealed substantially as per Example I. The resulting precursor was extended to various lengths, i.e., elongations of 50%, 100%, 200% and 300%, and heat set in the extended state for 5 minutes at 135° C. At the end of this period the film was removed from the oven, allowed to cool and the pore sizes present were measured.

The pore sizes present in the film were measured by mercury porosymmetry by the Quynn method in the Journal of Applied Polymer Science, cited hereinbefore.

FIG. 2, incorporated herein by reference, illustrates the unexpected pore size distribution of 1000–2000 angstrom units resulting from the various elongations. Thus it was found that the desired 1000–2000 angstrom unit range was extremely pronounced at an intermediate elongation than at the higher elongations.

EXAMPLE III

A series of polypropylene films similar to those employed in Examples I and II were subjected to a solvent sorption test. In this test pre-weighed samples were immersed completely in a particular solvent for a period of 24 hours. After such period the samples were removed and surfaces of each were carefully wiped clean. The thus-treated samples were then weighed with the difference in weights being noted.

FIG. 3 incorporated herein by reference illustrates the marked effect the elongation has on the solvent sorption of the polypropylene films. The extreme decrease in the sorption slope when 100% elongation is reached is readily apparent. The complete lack of utility in some instances at 150% clearly manifests the criticality of the amount of drawing or extension which must be applied to the films to accomplish the objects of this invention.

This phenomena was also experienced, and to the same significant degree, with other solvents such as methanol, xylene, acetone, benzene, heptane, toluene and carbon tetrachloride.

EXAMPLE IV

In order to illustrate the effect that elongation has on the gas permeability characteristics of various polypropylene films a number of films were extended in a manner similar to that in the preceding examples. The resulting sample films treated so as to observe their respective behaviors with regard to rates of gas permeability, in this instance: O_2, N_2, CO_2 and water vapor.

The tests employed were:

Moisture vapor transmittance—ASTM #9663T—Method B Procedure B

O_2, N_2, CO_2 transmittance—ASTM #D1434–63, Dow Cell Method, except that because of exceedingly high gas permeability, two pieces of film were laminated together with Interchemical Coating #NB483C which was less than .0001 inch in thickness.

FIG. 4, clearly illustrates the pronounced effect the elongation has on the gas permeability of the films. The almost complete absence of permeability at an elongation of as low as 150% readily emphasizes the necessity for extending the films within the parameters of this invention. The moisture vapor transmittance was found to conform to this behavior with a transmittance of as high as 400 cc./24 hours, m.^{2}, atm.

EXAMPLE V

In order to observe the effect elongation has on the pore size distribution as concerned with penetration by salts or other chemicals, polypropylene films similar to the preceding were stretched and annealed at various elongations and silver was then incorporated into the pores thereof.

Table I which follows indicates the criticality of the amount of elongation has on the pore size distribution and hence on the amount of extraneous matter which may be incorporated. This behavior was similarly encountered when sodium chloride and nickel chloride-dimethylglyoxime was tested in a like manner.

TABLE I

Incorporation of Ag into K film

Sample treatment:	Percent Ag incorporated
Stretched 50% under liquid surface	3.2
K film:	
50% extended	6.3
100% extended	11.6
250% extended	3.5

The values of "recovery" hereinbefore referred to are elastic recovery determined as follows at 25° C. and 65% relative humidity:

A sample 15 mm. in width was placed in an Instron tensile property testing machine with the jaw separation being 2" apart. The sample was extended at the rate of 1"/min. until 50% extension was reached. The sample was held at that extension for 1 minute and then relaxed at the same rate as extended. A reading was recorded as soon as a no load condition was indicated by the Instron. The elastic recovery is then calculated as follows:

$$\text{Elastic recovery} = \frac{\left(\begin{matrix}\text{Totol length}\\ \text{when extended}\end{matrix}\right) - \left(\begin{matrix}\text{Final distance}\\ \text{between jaws}\end{matrix}\right)}{\text{Length added when extended}} \times 100$$

EXAMPLE VI

The film-forming polymer of this example was a copolymer having a melt index of 2.5, of trioxane and 2 weight percent based on the weight of the polymer of ethylene oxide of the type described in U.S. Pat. No. 3,027,352, after-treated to remove unstable groups as described in Pat. No. 3,219,623, and suitably stabilized.

The above-described polymer was melt extruded at 375° F. through an 8" slit of the coat hanger type as illustrated in FIG. 2 at a shear rate of approximately 46 reciprocal seconds using a 1" extruder with a shallow channel metering screw. The length to diameter ratio of the extruder barrel was 24:1. The extrudate was drawn down very rapidly to a drawdown ratio of 270:1, contacted with a rotating casting roll maintained at 289° F. and about ¼" from the lip of the die. The film produced in this manner was wound up and found to have the following properties:

Thickness—.0005 inch
Recovery from 50% strain—46%

The polymer was then oven annealed in the tensionless state at 145° C. for 16 hours. At the end of the annealing period it was removed from the oven, allowed to cool and found to have the following properties:

Thickness—.0005 inch
Recovery from 50% elongation at 25° C.—92%
Density as determined by mercury porosymmetry—1.40 g./cm.^{3}

The film was extended at room temperature to 89% of its original length, held in the extended state by metal clamps and heat set in an oven at 150° C. for two minutes. At the end of this period it was removed from the oven, allowed to cool and found to have the following properties:

Void volume as determined by mercury porosymmetry—.18 cm.^{3}/gm.
Density as determined by mercury porosymmetry—1.12 gm./cm.^{3}
Pore size as determined by mercury porosymmetry—100–900 A.

EXAMPLE VII

This example illustrates one of the utilities to which the films of the present invention may be applied; in this instance as a microporous membrane for the desalinization of a saline solution.

The polymer described in Example I was melt extruded as per that example and oven annealed at 145° C. for 16 hours. At the end of this period it was removed from the oven and allowed to cool. One film (No. One) was extended 91% at room temperature and heat set in an oven in the tensioned state at 142° C. for 8 minutes. Film No. Two was unchanged after the first annealing step.

Piece No. One was placed in a supported cell and contacted on one side with a pressurized salt solution (.5 weight percent NaCl at 600 p.s.i.). A solution flux through the film was obtained due to the external pressure gradient and was recorded as 4.2 gal./day/ft.^{2}. The salt concentration of the solution that has been forced through the membrane was found to have been reduced to .17 weight percent. The film was then reversed, i.e., the other side was made to initially contact the flowing pressurized salt solution. Flux and salt content were then found to be 1.8 gal./day/ft.^{2} and .27 weight percent.

The above procedure was repeated with Piece No. Two. No flux was obtained with either side facing upstream.

EXAMPLE VIII

Crystalline polypropylene of melt index 4.0 and density .905 g./cm.^{3} was melt extruded at 380° F. through an 8" slit die of the coat hanger type using a 1¾" extruder with a shallow channel metering screw. The length to diameter ratio of the extruder barrel was 24:1. The extrudate was drawn down very rapidly to a drawdown ratio of 90:1, contacted wtih a rotating casting roll maintained at 185° F. and ¼" from the lip of the die. The film produced in this fashion was found to have the following properties:

Thickness—.001 inch
Elastic recovery from 50% strain—49%

The resulting film was divided into two pieces which then were oven annealed at 130° C. for 15 minutes. At the end of this period they were removed from the oven and allowed to cool. Piece No. 1 was stretched 190% at room temperature and heat set in the extended state for 15 minutes at 130° C. Piece No. 2 was unchanged after the first annealing step. Mercury porosymmetry (infusion) analysis of both samples gave the following results:

	Sample No. 1	Sample No. 2
Penetration volume (cm.^{3}/g.)	.15	.01
Density (g./cm.^{3})	.79	.89
Pore size, A	100–1,000	

EXAMPLE IX

A polyethylene sample having a density of 0.960 and a melt index of 0.7 was melt extruded at 380° F. through a thin annular opening die of 0.040 inch and 4" diameter. The hot tube thus formed was expanded 1.5 times by internal air pressure and cooled by an air stream impinging on the film from an air ring located around above the die. The extrusion was accomplished with an extruder of 20:1 length to a diameter barrel ratio and a hollow channel metering screw. The extrudate was drawn down very rapidly to a drawdown ratio of 100:1 and passed

through a series of rollers which collapsed the tube and maintained internal air pressure. After windup at 100 ft./min. the film was found to have the following properties:

EXAMPLE IX

Thickness—.0005 inch
Recovery from 50% strain—45%

The film was then oven annealed in the tensionless state at 115° C. for 16 hours.

After removal from the oven the film was allowed to cool, stretched 50% at room temperature, and heat set in an oven in the extended state under tension for 5 minutes at 120° C. The film treated in this manner was found to have the following properties by mercury porosymmetry.

Apparent density—.785 g./cm.^{3}
Pore volume—.25 cm.^{3}/gm.
Pore size range—100–2000 A.

The values of "recovery" given above are elastic recovery determined as follows at 25° C. and 65% relative humidity:

A sample 15 mm. in width was placed in an Instron tensile property testing machine with the jaw separation being 2" apart. The sample was extended at the rate of 1"/min. until 50% extension was reached. The sample was held at that extension for 1 minute and then relaxed at the same rate as extended. A reading was recorded as soon as a no load condition was indicated by the Instron. The elastic recovery is then calculated as hereinbefore set forth.

EXAMPLE X

The process described in Example VIII was repeated except instead of stretching "Piece No. 1" at room temperature, a higher temperature (200° F.) was employed, and the resultant denstiy was 0.78 g./cm.^{3} (i.e., a density reduction from 0.905 g./cm.^{3} of about 0.13).

EXAMPLE XI

The process described in Example X was repeated except that a stretching temperature of 220° F. was employed and the resultant density was 0.88 g./cm.^{3}.

The other properties mentioned were determined with standard ASTM methods as follows:

Tensile strength—ASTM #D882—Method A sample width 15 mm.
Breaking elongation—ASTM #D882—Method A sample width 15 mm.
Modulus—ASTM #D882—Method A sample width 1 inch
Moisture vapor transmittance—ASTM #9663T—Method B, Procedure B
O_2, N_2, CO_2 transmittance—ASTM #D1434–63, Dow Cell Method, except that because of exceedingly high gas permeability, two pieces of film were laminated together with Interchemical Coating #NB483C which was less than .0001 inch in thickness.
Density—As determined by mercury penetration. See Textile Research Journal, vol. 33, pp. 21 et seq. (1963) by R. G. Quynn.
Haze—ASTM #D1003, Procedure A as per FIG. 2.

The values of percent crystallinity given above are determined using the procedure described in an article by R. G. Quynn et al. in Journal of Applied Polymer Science, vol. 2, No. 5, pp. 116–173 (1959).

The elastic films of this invention are useful as printable wrappers, microporous membranes for dialysis operations, etc.

It is to be understood that the foregoing detailed description is given merely by way of illustration and that many variations may be made therein without departing from the spirit of the invention.

What is claimed is:

1. A process for the production of a film characterized by a microporous, open-celled structure, said film having an apparent density no greater than about 90 percent of the density of the polymer comprising the film, said polymer having a crystallinity when solid of at least 40 percent and being selected from the group consisting of polyethylene, polypropylene and polyacetal, and said film being characterized by an open-celled structure comprising pore spaces wherein the size distribution of said pore spaces is optimized in the 1000–2000 angstrom range, said process comprising:

(a) extruding said polymer at a melt temperature no higher than about 100° C. above the crystalline melting point of said polymer, so as to form a film,
(b) taking up the resulting film at a drawdown ratio of from 20:1 to about 180:1
(c) rapidly cooling the extruded film while it is being drawn down,
(d) annealing the resulting film at a temperature in the range of about 5 to 100° C. below the crystalline melting point of said polymer for a period of at least 5 seconds in order to develop in the resulting film an elastic recovery from a 50° strain of at least 50 percent at 25° C.,
(e) cold drawing the film at a draw ratio of from about 30 percent to about 150 percent of its total length at a temperature no greater than about 200° F. when said film comprises polypropylene, no greater than about 220° F. when said film comprises polyethylene and no greater than about 255° F. when said film comprises polyacetal,
(f) heat setting the thus cold drawn film at a temperature of from about 80° C. to about 150° C. while under tension.

2. The process of claim **1** wherein the film having an elastic recovery from a 50 percent strain of at least 50 percent at 25° C., is cold drawn at a draw ratio of from about 50 to about 100 percent of its total length.

3. A process for the production of a film characterized by a microporous, open-celled structure, said film having an apparent density no greater than about 90 percent of the density of the polymer comprising the film, said polymer having a crystallinity when solid of at least 40 percent and being selected from the group consisting of polyethylene, polypropylene and polyacetal, and said film being characterized by an open-celled structure comprising pore spaces wherein the size distribution of said pore spaces is optimized in the 1000–2000 angstrom range, said process comprising:

(a) cold drawing an elastic film of said polymer, said elastic film having an elastic recovery from 50 percent strain of at least 50 percent at 25° C., at a draw ratio of from about 30 percent to about 150 percent of its total length at a temperature no greater than about 200° F. when said film comprises polypropylene, at a temperature no greater than about 220° F. when said film comprises polyethylene, and at a temperature no greater than about 255° F. when said film comprises polyacetal, and
(b) heat setting the thus cold drawn film at a temperature of from about 80° C. to about 150° C. while under tension.

4. The process of claim **3** wherein said elastic film is cold drawn at a draw ratio of from about 50 to about 100 percent of its total length.

5. The process of claim **1** wherein said polymer is extruded in the form of a tubular film with air pressure in its interior which expands the tubular film to a large diameter, the ratio of diameter of the blow up film to the diameter of the film as extruded being in the range of 0.5 to 6.0, at a draw down ratio of 20:1 to about 180:1.

6. The process of claim **1** wherein said polymer is

extruded at a melt temperature in the range of 10 to 40° C. above the melting point of the polymer.

7. The process of claim 6 wherein the extruded film is taken up at a drawdown ratio of from about 50:1 to about 125:1.

References Cited

UNITED STATES PATENTS

2,325,060	7/1943	Ingersoll	8—115.5
2,799,896	7/1957	Grow et al.	18—8BX
2,948,583	8/1960	Adams et al.	264—210F
3,048,467	8/1962	Roberts et al.	264—210F
3,215,486	11/1965	Hada et al.	264—210FUX
3,323,190	6/1967	Boltuiew	264—176FUX
3,330,897	7/1967	Tessier	264—176F
3,377,415	4/1968	Oppenlander	264—210F
3,382,306	5/1968	Oppenlander	264—178
3,413,397	11/1968	Bierbaum et al.	264—346X
3,426,754	2/1969	Biernbaum et al.	128—156
3,432,590	3/1969	Papps	264—210F

JULIUS FROME, Primary Examiner

J. H. WOO, Assistant Examiner

U.S. Cl. X.R.

264—209, 235, 288, 290, 346

Appendix T

United States Patent Office 3,351,495 Patented Nov. 7, 1967

3,351,495

BATTERY SEPARATOR

Donald Wayne Larsen, Bowie, and Clifton Leroy Kehr, Ednor, Md., assignors to W. R. Grace & Co., Cambridge Mass., a corporation of Connecticut

No Drawing. Filed Nov. 22, 1966, Ser. No. 596,056
11 Claims. (Cl. 136—146)

This application is a continuation-in-part of application Ser. No. 300,682, filed Aug. 7, 1963, now abandoned, and copending application Ser. No. 373,824, filed June 9, 1964, now abandoned.

This invention is directed to a battery separator and to the method of making such. In one particular aspect, this invention is related to a novel battery separator of excellent chemical and physical properties which is comprised of a microporous sheet of very high molecular weight polyolefin. In another particular aspect, it relates to a microporous sheet comprised of very high molecular weight oplyolefin and an inert filler material.

Storage batteries employ an acid or an alkaline electrolyte. Two widely used batteries are a lead-acid type and an alkaline type, e.g., silver-cadmium. Separators are included in the batteries to prevent direct contact between plates of opposite polarity while freely permitting electrolytic conduction. The separator for the acid type of battery is generally comprised of a sheet or web with ribs on at least one side. The separator for the alkaline type of battery is usually a thin sheet or film. The method of the instant invention may be used to form separators for acidic or alkaline batteries.

The battery separator of the present invention comprises a microporous sheet of polyolefin having a molecular weight of at least 300,000, a standard load melt index of substantially 0 and a reduced viscosity of not less than 4.0. The battery separator preferably comprises a homogenous mixture of 8 to 100 volume percent of very high molecular weight polyolefin, 0 to 40 volume percent of a plasticizer, and 0 to 92 volume percent of inert filler material.

In a preferred embodiment, the battery separator comprises 8 to 93 volume percent polyolefin, 7 to 92 volume percent filler and 0 to 15 volume percent plasticizer. A more preferred composition comprises 40 to 60 volume percent polyolefin, 40 to 60 volume percent filler and 1 to 10 volume percent plasticizer and, more particularly, 46.5 volume percent polyolefin, 46.5 volume percent filler and 7 volume percent plasticizer. The battery separator also contains 0 to 15 weight percent antioxidant, based on the weight of the polyolefin. In a preferred embodiment, 0.1 percent by weight is employed.

The microporous battery separators of this invention have a pore size which is generally less than 1 micron in diameter, preferably with greater than 50 percent of the pores being 0.5 micron or less in diameter. In most cases, at least 90 percent of the pores have a diameter smaller than 0.5 micron.

According to this invention, the battery separator is produced by a process which comprises blending a composition of from 5 to 65 volume percent of high molecular weight polyolefin, 5 to 60 volume percent of an inert

filler material, and the volume percent difference between the total amount of the polyolefin and the inert filler and 100 percent being a plasticizer (a minimum of 30 volume percent plasticizer is required), forming said composition into sheet form, and subsequently extracting from said sheet by means of a suitable solvent at least a portion of a component selected from the group consisting of the inert filler and the plasticizer.

In a preferred embodiment, 15 volume percent polyolefin, 15 volume percent filler and 70 volume percent plasticizer are blended together, extruded to provide a flat sheet and then sufficient plasticizer is extracted to provide a finished separator composed of 46.5 volume percent polyolefin, 46.5 volume percent filler and 7 volume percent plasticizer.

It is an object of this invention to use such a blend in the production of microporous battery separator. It is a further object of this invention to provide a process for producing such battery separators from a very high molecular weight, polyolefin-filler-plasticizer blend. Other objects, features, and advantages of this invention will be apparent to those skilled in the art in view of the following more detailed description of the invention.

In this invention, it is necessary to use polyolefin having a standard load melt index of 0, an average molecular weight of at least 300,000 and a reduced viscosity of not less than 4.0 in order to be able to tolerate significant amounts of filler without producing a composition which is excessively brittle. For example, polyethylene having a standard load melt index of 0 is very unlike conventional polyethylene having a standard load melt index of 0.7 to 5.0 and an average molecular weight of about 100,000 to 90,000 which yields brittle products at relatively low filler concentrations. Moreover, the high molecular weight polyolefin confers strength and flexibility to the final composition.

The polyolefin can be comprised of a mixture of a high molecular weight polyolefin with a standard load melt index of 0 and a compatible lower molecular weight polyolefin with a standard load melt index higher than 0. An amount of the lower molecular weight polyolefin can be used a long as such amount does not remove the polyolefin from above-set forth minimum molecular weight, standard load melt index and reduced viscosity values. Ordinarily, the standard load melt index of the lower molecular weight polyolefin will range from about 0.1 to about 5. Representative of the polyolefins of high and low molecular weight operable in the instant invention are polyethylene, polypropylene, polybutene, ethylene-propylene copolymers, ethylene-butene copolymers, propylene-butene copolymers and ethylene-propylene-butene copolymers.

The term "high molecular weight polyolefin" as employed herein is intended to refer to a polyolefin having an average molecular weight of at least 300,000, a standard load melt index of substantially 0, and a reduced viscosity of not less than 4.0. The employment of a polymer having the above minimum properties is critical in the present invention. Polymers having characteristics outside of these limits have been found to be unsatisfactory. For example, a polyolefin (polyethylene) having an average molecular weight of 200,000,

CosMX Exhibit 1003, Page 449 of 512

a standard load melt index of 0.2 and a reduced viscosity of 2.6 was found to be unsatisfactory for the present invention, in that it produced a separator which was too brittle and too weak. Severe processing difficulties were also encountered. In a particularly preferred embodiment, polyethylene having an average molecular weight of 2,000,000, a standard load melt index of 0 and a reduced viscosity of 15 is employed.

The standard load melt index (SLMI) was measured as specified in ASTM D 1238–57T (Condition E) using a standard load of 2,160 grams. The high load melt index (HLMI) was measured as specified in ASTM D 1238–57T (Condition F) using a load of 21,600 grams.

Reduced viscosity was determined in a solution of 0.02 g. of the polyolefin in 100 g. of decalin at 130° C.

The instant process produces microporous battery separators which meet minimum electrical resistance requirements and posses acceptable tensile strength and porosity. When the battery separator is provided with rib members, these members can be formed from a number of polymeric compositions known to the art. For example, they can be formed from the same composition as that of the battery separator or from such materials as other polyolefins, polyvinyl chloride, as well as filled and/or foamed compositions thereof. Alternatively, the sheet is also grooved or embossed to provide ribs. In still another alternative, a rib of the above-described character is applied to the up-thrust portion of the embossing or on the flat portion of the sheet beside the up-thrust portion.

The usage of inorganic fillers and extenders for rubbers and some other resins is well known by the prior art. Most attempts to use these fillers to extend polyolefiins have met with failure due to the increased crystallinity of these resins. Products are obtained which are too brittle to be useful as general purposes resins or as base compositions. In our copending application, U.S. S.N. 285,181, filed May 20, 1963, now abandoned, and U.S. S.N. 354,064, filed Mar. 23, 1964, we disclosed a polyolefin-filler composition which overcomes the aforementioned deficiencies such as brittleness. In that application, a composition of matter and a method are disclosed for producing inexpensive blends of fillers and polyolefins which retain to a surprising extent much of the flexibility, impact resistance, and strength of the base polymers.

The polyolefin must be substantially insoluble in the solvents used and at the temperatures used to extract the plasticizer or filler from the polyolefin-filler-plasticizer composition. Such insolubility or inertness to the action of solvents is imparted to the polyolefin by its crystallinity content or by the judicious choice of solvent used in the extraction procedure. The partially crystalline polyolefin such as polyethylene, and isotactic polypropylene, are ideally suited to such an application because they are substantially insoluble in common hydrocarbons and other organic and aqueous solvents at low temperatures.

Conventional stabilizers or antioxidants are employed in the compositions of the present invention to prevent thermal and oxidative degradation of the polyolefin component. Representative of the stabilizers are 4,4 thiobis (6 - tert - butyl - m - cresol) ("Santonox"), and 2,6-di-tert-butyl-4-methylphenol ("Ionol").

The filler provides the primary means by which the plasticizer is absorbed and held in the instant composition. It should, therefore, not be soluble in the plasticizer. The capacity of the filler particles to absorb and hold the plasticizer in the composition is proportional to its surface area. Highsurface area fillers are either materials of very small particle size or materials of a high degree of porosity. Generally, the size of the filler particles can range from an average of about 0.01 micron to about 10 microns in diameter depending upon the porous character of the filler. The surface of the area of the filler can range from about 30 to 950 square meters per gram. Preferably, the surface area of the filler should be at least

100 square meters per gram. Ordinarily, amounts of filler used in the instant composition can range from about 5 to 60 volume percent. While the high surface areas are preferred, fillers having relatively low surface areas, e.g., 1 square meter per gram or less are also employed satisfactorily, particularly for alkaline battery separators. The specfic amount of filler used will depend primarily on its surface area and the amount of plasticizer used.

The filler can be soluble or insoluble in water. Representative of the fillers which are substantially water insoluble and operable in the instant invention are carbon black, coal dust and graphite; metal oxides and hydroxides such as those of silicon, aluminum, calcium, magnesium, barium, titanium, iron, zinc, and tin; metal carbonates such as those of calcium and magnesium; minerals such as mica, montmorillonite, kaolinite, attapulgite, asbestos, talc, diatomaceous earth and vermiculite; synthetic and natural zeolites; portland cement; precipitated metal silicates such as calcium silicate and aluminum polysilicate; alumina silica gels; wood flour, wood fibers and bark products; glass particles including microbeads, hollow microspheres, flakes and fibers; and salts such as molybdenum disulfide, zinc sulfide and barium sulfate.

Illustrative of the water-soluble fillers operable in the present invention are inorganic salts such as the chlorides of sodium, potassium, and calcium; acetates such as those of sodium, potassium, calcium, copper and barium; sulfates such as those of sodium, potassium and calcium; phophates such as those of sodium and potassium; nitrates such as those of sodium and potassium; carbonates such as those of sodium and potassium and sugar.

In the embodiment of this invention in which the battery separator contains unextracted filler, the filler should be preselected with respect to end use, which is to say, battery separators with alkali insoluble fillers should be used only in alkaline batteries, and acid insoluble fillers should be used only in acid batteries. If so used, the filler is not extracted by the battery electrolyte. Neutral fillers, or fillers that do not react with either acid or alkaline electrolytes, can of course be used with either acid or alkaline batteries. Examples of neutral fillers are carbon black, coal dust, graphite and barium sulfate. Representative of the fillers suitable for use in alkaline batteries are the oxides, hydroxides and carbonates of calcium, magnesium, barium and iron. A typical filler for acid batteries is silica.

The preferred filler is dry, finely divided silica. It has been found that separators produced from compositions containing this filler have unusually small pore size, e.g., as low as 0.002 micron and void volume and are readily wet by electrolyte.

It should be understood that any of the commercially available wetting agents known to the art, such as sodium alkyl benzene sulfonate, sodium lauryl sulfate, dioctyl sodium sulfosuccinate, and isooctyl phenyl polyethoxy ethanol, can be used to enhance the wettability of the battery separator by electroylte. These wetting agents can also be used to enhance the wettability of the filler prior to its inclusion in the composition.

The plasticizer of the instant composition improves the processability of the composition, i.e., lower the melt viscosity, or reduces the amount of power input which is required to comopund and to fabricate the composition. In addition, since the plasticizer is the component which is easiest to remove from the polymer-filler-plasticizer composition, it is useful in imparting porosity to the battery separators.

The plasticizer can be soluble or insoluble in water. Representative of the water-insoluble plasticizers are organic esters such as the sebacates, phthalates, stearates, adipates and citrates; epoxy compounds such as epoxidized vegetable oil; phosphate esters such as tricresyl phosphate; hydrocarbon materials such as petroleum oil including lubricating oils and fuels oils, hydrocarbon resin and asphalt and pure compounds such as eicosane; low

molecular weight polymers such as polyisobutylene, polybutadiene, polystyrene, atactic polypropylene, ethylene-propylene rubber; ethylene-vinyl acetate copolymer, oxidized polyethylene, coumarone-indene resins and terpene resins; tall oil and linseed oil.

Illustrative of the water-soluble plasticizers are ethylene glycol, polyethylene glycol, polypropylene glycol, glycerol, and ethers and esters thereof; alkyl phosphates such as triethyl phosphate; polyvinyl alcohol; polyacrylic acid and polyvinyl pyrrolidone.

When a plasticizer is used which is not removed from the composition during the extraction step but forms part of the battery separator, it imparts flexibility, high elongation and imparts resistance to the battery separator.

There are a number of water-insoluble, normally solid plasticizers which are sufficiently inert to form a part of the battery separator. Typical examples of these plasticizers are polyisobutylene, polybutadiene, polystyrene, atactic polypropylene, ethylene - propylene rubber and ethylene vinyl acetate copolymer. Generally, when this type of plasticizer is used, it can be included in the battery separator in an amount as high as 40 percent by volume of the battery separator composition.

The preferred ranges for the components employed in forming the battery separator comprises from 7.5 to 40 volume percent of polyolefin, from 10 to 40 volume percent filler, and the difference between the total amount of polyolefin and filler and 100 percent being the plasticizer. The minimum amount of plasticizer which must be present in all compositions is 30 percent by volume. Examples of particularly preferred compositions are as follows:

Polyolefin (Vol. Percent)	Filler (Vol. Percent)	Plastixizer (Vol. Percent)
20	20	60
20	15	65
17	18	65
15	15	70
10	15	75

The above amounts are based upon the processing requirements of the composition, the physical properties necessary in the final product, and the cost of the composition. Based on these factors, the indicated amounts have been found to be acceptable. By specifying the amounts as percentages by volume, the percent by volume of the various ingredients expressed in terms of the specific gravity of the components is referred to. To determine the percent by volume, the individual components are weighed and the volume calculated from the known specific gravities.

A particularly preferred composition consists essentially of polyethylene having at least 50 percent by weight crystallinity, finely-divided silica and petroleum oil.

The components of the instant composition can be mixed by any conventional manner which will produce a substantially uniform mixture. To produce a particularly uniform mixture, the components can be premixed at room temperature in a blender. The polyolefin-filler-plasticizer dry blends are then fluxed in a conventional mixer such as a Banbury mixer or melt homogenized in a conventional two roll mill.

After being suitably mixed, the composition is molded or shaped in any conventional manner. Specifically, it can be fed to an extrusion, calendering, injection moldiug, or compression molding machine to be processed into its final form.

As used in this application, the terminology "sheet" is intended to define a unitary article, i.e., a battery separator consisting of a base web and a plurality of rib members. The web and rib members can be of the same material or of different materials. The terminology "film" is used to define a battery separator which does not have rib members and which can be very thin. Such a film is particularly suitable for use in alkaline batteries where it generally has a thickness of about 5 mils or less. The terminology "essentially flat surface" is intended to be generic to sheets and films and to refer to battery separators suitbale for usage in acid or alkaline batteries.

The rib members of the battery separator can also be formed by a conventional method such as by extrusion. In order to reduce the expense of fabrication, the rib members are preferably of the same composition as the base web or of foamed polypropylene, foamed filled polyvinyl chloride, or foamed filled polyethylene. The terminology "foamed polyethylene" or "foamed polypropylene" defines a polyolefin which has been foamed by conventional techniques, e.g., dry blended with a foaming agent such as azobisformamide plus zinc stearate, pelletized, and extrusion-foamed at a temperature of approximately 375° F. The terminology "foamed filled polyolefins" or "foamed filled polyvinyl chloride" is intended to define a polymer which has been dry blended with a foaming agent and a filler material such as carbon black or any of the other materials mentioned in this application. This dry blend is then pelletized and foamed. It is to be understood that the polyethylene used in the ribs need not be the same type used in the web, but may be of lower molecular weights and densities which may process more readily in the rib forming operation. It is also to be understood, however, that the rib members can be made of the same material as the base web. When this is desired, the web and rib members are extruded as a unitary article. This is achieved by replacing the regular die member of the extruder with a die which has been especially designed to mold the composition into the desired configuration. Alternatively, the rib members may be formed by embossing. By this procedure, a web is formed from the base composition. This web is then passed through a pair of embossing rollers to form the ribs on the web as a unitary article. The web can also be extracted with solvent before being passed through a pair of embossing rolls to form ribs on the web.

When the rib members are molded separately, they can be bonded to the base web by a number of methods well known in the art such as heat sealing or by means of an adhesive. The bonding of the rib members to the web can occur either before or after the inert filler and/or plasticizer are extracted. It has been found that if the extraction is carried out after the bonding, there are no material adverse effects upon the physical properties of the battery separator.

The specific extraction procedure and medium employed depends upon the component which is to be extracted. For example, if the plasticizer or the filler is to be extracted, a single stage extraction is used. However, if the plasticizer and the filler are to be extracted, a two-stage extraction may necessarily be required. Similarly, if two or more dissimilar plasticizers are used in the same composition, a multiple stage extraction may be required. Numerous extracting solvents are suitable for usage in this invention with the particular solvent depending upon the particular ingredient to be extracted. The solvent or extraction conditions should be chosen so that the polyolefin is essentially insoluble. For example, when petroleum oil to to be extracted from the molded composition, the following solvents are suitable: chlorinated hydrocarbons, such as trichloroethylene, tetrachloroethylene, carbon tetrachloride, methylene chloride, tetrachloroethane, etc.; hydrocarbon solvents such as hexane, benzene, petroleum ether, toluene, cyclohexane, gasoline, etc. If polyethylene glycol is to be extracted, the extraction medium can be water, ethanol, methanol, acetone, etc. If finely ground silica is to be extracted, the following solvents are suitable: aqueous or alcoholic sodium hydroxide, potassium hydroxide, etc., hydrofluoric acid solution. Generally, acids such as hydrochloric acid, can be used to extract metal oxides and metal carbonates.

CosMX Exhibit 1003, Page 451 of 512

The extraction temperature can range anywhere from room temperature up to the melting point of the polyolefin as long as the polyolefin does not dissolve.

The time of the extraction will vary depending upon the temperature used and the nature of the plasticizer or filler being extracted. For example, when a higher temperature is used, the extraction time for an oil of low viscosity can be only a few minutes, whereas if the extraction is performed at room temperature, the time requirement for a polymeric plasticizer can be in order of several hours.

The final composition of the separator will depend upon the original composition and the component or components extracted. When the plasticizer and the inert filler are removed from the molded composition, the microporous battery separator will consist essentially of a polyolefin.

Unless otherwise stated, the pore size and the pore volume of the battery separator were measured using the mercury intrusion method described in Ritter, H. L., and Drake, L. C., Ind. Eng. Chem. Anal. Ed., 17, 787 (1945).

According to this method, mercury is forced into different sized pores by varying the pressure exerted on the mercury, i.e., low pressures being used to fill large sized pores and higher pressures being used to fill small sized pores. The total pore volume is then determined and the pore volume distribution calculated from a measure of mercury in the various sized pores and the pressures exerted. Such a determination was accomplished in the instant invention by using a standard commercial mercury porosimeter, (Aminco-Winslow Porosimeter). The pore diameter entered by the mercury under pressure is stated in the equation

$$D=\frac{175}{P}$$

where D equals the diameter of the pore in microns and P equals absolute pressure in pounds per square inch. According to the equation, 350 p.s.i. is required to force the mercury into pores having a diameter of 0.5 micron. Since pressures higher than 350 p.s.i. may collapse some pores and compress the samples in the instant invention, pores having a diameter smaller than 0.5 micron may not be accurately measured by this method.

Mercury intrusion date for commercial battery separators of various materials were compared to data obtained for battery separators prepared according to the instant invention. The results are shown in Table I.

TABLE I.—MERCURY INTRUSION OF BATTERY SEPARATORS

Pore Diameter Microns	Volume Percent of Pores					
	Microporous Polyvinyl Chloride	Rubber Silica Hydrogel	Sintered Polyvinyl Chloride	Polyethylene Cellulose	Example 1	Example 5
.035-.05	0	3.6	0	0	25.0	11.9
.05-.1	1.05	5.1	1.2	0.5	33.9	27.0
.1-.3	0	10.3	1.2	0.5	26.8	53.8
.3-.5	1.05	8.7	0	0.5	7.1	2.3
.5-.7	0	7.4	0	0.5	1.8	1.1
.7-1.0	2.1	10.2	0	0.5	1.8	1.1
1.0-2.0	16.0	23.2	0	1.4	1.8	1.1
2.0-3.0	71.3	15.4	0	1.9	1.8	0.9
3.0-4.0	7.4	6.0	0	1.4	0	0
4.0-5.0	1.1	2.9	1.2	2.4	0	0.9
5.0-10	0	3.5	3.3	10.0	0	0
10-50	0	2.3	82.0	77.5	0	0
50-100	0	1.4	11.1	2.9	0	0
Mean Pore Diameter Microns	2.58	1.18	36.7	16.6	0.084	0.14

In Example 1 of Table I the composition employed in preparing the battery separator consisted of 20 volume percent of polyethylene, 20 volume percent of silica and 60 volume percent of polyethylene glycol. The polyethylene glycol was extacted with water. In Example 5 of Table I the composition employed in preparing the battery separator consisted of 15 volume percent of polyethylene, 15 volume percent of silica and 70 volume percent of petroluem oil. The petroleum oil was extracted with trichloroethylene.

To show the presence of exceedingly small pores in the structure of the battery separators of the instant invention, i.e. pores having a diameter in the range of 0.002 to 0.06 micron in diameter, the nitrogen absorption method described by S. Brunauer, P. Emett and E. Teller in J. Am. Chem. Soc., 60, 309 (1938) was used.

The nitrogen absorption test was used to determine the surface area and pore diameter of battery separators of various materials including battery separators prepared according to the instant invention. The results are shown in Table II.

TABLE II

Battery Separator Material	Nitrogen Absorption Test	
	Surface Area (Sq. meters/gram)	Mean Pore Diameter (Microns)
Rubber Silica hydrogel	92	0.27
Sintered Polyvinyl Chloride	9	(1)
Example 5 (15% by vol. polyethylene, 15% by vol. silica and 70% by vol. petroleum oil before extraction)	135	.011

[1] Pores too large to measure.

As illustrated in Table II, the battery separator prepared according to this invention has a larger surface area and a smaller mean pore diameter than battery separators prepared from two conventional materials. The smaller mean pore diameter shows clearly the presence of exceedingly small pores in the structure of the battery separators prepared according to the instant invention.

The size of the pores of the battery separator of the present invention satisfies the requirements of battery separators in general that the size of the pores be small enough to prevent the passage of solid materials such as lead or lead sulfate crystals but sufficiently large to permit the electrolyte to pass through. In addition, the pores of the instant battery separator are small enough to hinder the passage of antimony ions which frequently are introduced into the electrolyte by the positive plate and which migrate to the negative plate and thereby shorten the life of the battery.

The minute pore size of the separators of the instant invention is in distinct contrast (see Table II) to that of presently available commercial microporous separators. The microporous separators of this invention also distinguish over the prior art in that the void volume of the separator can be greater than that of most commercial separators, (see Table III).

It should be understood, however, that the void volume

CosMX Exhibit 1003, Page 452 of 512

can vary to a considerable extent depending upon the particular ingredients and thickness of the separator. For example, if the separator is very thin, a void volume as low as 30% is acceptable. It is normally desirable, however, that the void volume of the separator be at least 50%, preferably at least 60%, and more preferably 70 to 80%. The combination of extremely small pore size while maintaining a high void volume in a battery separator which provides good electrical resistance requirements and which possesses excellent physical and chemical properties is very unexpected. These unexpectedly superior properties are believed to be the result of the usage of the above-described very high molecular weight polyolefin. In this respect, compare Examples 4 and 9 of this application to note the good results obtained with polyethylene having a standard load melt index of 0, as compared to those obtained with a low molecular weight polyethylene having a standard load melt index of 0.7.

Table III is a comparison of the average pore diameter and void volume of the separator of this invention prepared as described in Example 2 of the instant application and commercial separators. In Example 2 of the composition employed in preparing the battery separator consisted of 10% by volume of polyethylene 15% by volume of silica and 75% by volume of petroleum oil. The petroleum oil was extracted from the molded composition with petroleum ether and the percent void volume shown in Table III is based on the extracted amount of petroleum oil. The average pore diameter of the separator of Example 2 was measured by mercury intrusion on an Aminco-Winslow Porosimeter.

TABLE III

Separator	Average Pore Diameter, Microns	Void Volume,* Percent
Sintered Polyvinyl Chloride	36.7	48
Sintered Polyethylene	*50	47
Microporus Polyvinyl Chloride	2.58	87
Rubber/Silica Hydrogel	1.18	66
Polyethylene Cellulose	*33.0	70
Standard Cellulose	40.0	67
Example 2	0.11	75

*Values are taken from a paper by Robinson and Walker, Third International Battery Symposium, Bournemouth, England, October 1962, except for the value for Example 2.

The thickness of the battery separators will vary depending upon the type of battery in which they are used. In general, the thickness of the base web can range from 1 to 50 mils. For lead-acid batteries the preferred thickness range is usually 10 to 40 mils. The height of the rib members for lead-acid battery separators vary over a wide range depending upon the plate spacing requirements, generally ribs from 5 to 200 mils in height from the base web are employed with the preferred range being 10 to 100 mils. For alkaline type batteries, the preferred thickness is generally about 1 to 10 mils.

In order to be commercially acceptable, battery separators must meet minimum electrical resistance requirements. Generally, the acceptable range is from 1 to 100 milliohms-square inch, with the preferred range being from 10 to 75 milliohms-square inch.

Battery separators should possess chemical properties such as resistance to oxidation, and resistance to loss of weight in acid in order to be suitable for commercial usage. To demonstrate the superior qualities of the separators of this invention, samples made from a polyethylene-filler-plasticizer blend were subjected to these tests and compared with other commercial separators. The results are summarized in Table IV.

TABLE IV

Separator	Oxidation Test [1] (hours)	Acid Weight Loss [2] (percent)	Fast Acid Weight Loss [3] (percent)
4	227+	1.6	0.5
5	227+	0.6	
Sintered Polyvinyl Chloride	227+	1.5	2.7
Microporous Polyvinyl Chloride	227+	61.3	28.6
Rubber/Silica Hydrogel	208	8.6	Destroyed
Polyethylene Cellulose	114	31.0	44.8

[1] Oxidation test was made at ambient temperatures by placing the separator between electrodes, immersing the resulting assembly in a sulfuric acid solution having a specific gravity of 1.400, passing a current of 9 amperes through the circuit which provided a current density of 3 amperes per square inch, and maintaining the current of 9 amperes until short circuiting occurs.

[2] 168 hours in 1.3000 sp. gr. H_2SO_4 at 165° F.

[3] 3 hours at 140° F. in 3% potassium dichromate in 1.200 sp. gr. H_2SO_4

[4] This is Example 18: 17 vol. percent polyethylene (SLMI=0, HLMI=0), 18 vol. percent finely ground silica, 44 vol. percent glycerin and 21 vol. percent petroleum oil was processed into a sheet 0.028" thick and the glycerin and paraffin oil were extracted with water and petroleum ether.

[5] Same as 4, but thickness was 0.020".

As noted in Table IV, there is significantly less loss of material in acid with the separators made from the polyethylene-filler-plasticizer blends of the instant invention than with the commercial separators.

Acceptable battery separators must also possess certain physical properties, such as tensile strength, puncture strength, break angle strength, and pore volume.

This invention is further illustrated by the following examples. Unless otherwise stated, tests in the following examples were made as follows: the tensile strength of the samples was measured by a standard commercial tensile tester which continually records stress as it pulls the sample at a constant rate of strain. Unless otherwise specified, the tensile strength of the sample was measured in the extrusion direction of the sample.

The resistance to puncture of the samples was measured as follows: A ¼ inch diameter probe (connected via a lever arm to a container) with a rounded end is placed on the sample. Water is added to the container above the probe on the lever arm until the sample is punctured. The weight of water added is recorded.

The samples were also subjected to a break angle test. The purpose of this test is to determine the flexibility of the samples by measuring the angle at which the sheet breaks when bent by hand.

The samples were also tested to determine their pore volume and average pore diameter. Unless otherwise stated these were determined according to the mercury intrusion method on an Aminco-Winslow Porosimeter.

The crystallinity of the polyolefins was determined by an X-ray diffraction method described by J. L. Matthews, H. S. Pieser and R. B. Richards in Acta Crystallographica 2, 85–90 (1949). According to this method, the crystal-

	Percent by weight
Polyethylene ("Grex FF–60–018")	
Particle form	72 to 75
Polyethylene ("Hifax 1901")	
Particle form	83.3
Pressed sheet	58.4
Polypropylene	
Particle form	45.6
Pressed sheet	45.7
Annealed sheet	51.5
Quenched sheet	35.8

Example I

The polyethylene ("Grex FF–60–018") used in this example had an average molecular weight of 350,000, a standard load melt index of 0, a high melt index of 1.8, a density of 0.95, and a reduced specific viscosity of 4.0. The filler was a finely divided silica ("HiSil 233") having

CosMX Exhibit 1003, Page 453 of 512

an average particle diameter of about 0.02 micron and a surface area of 165 square meters per gram.

Using the system described, a composition consisting of 20 volume percent of the polyethylene, 20 volume percent of the silica, 60 volume percent polyethylene glycol of 4,000 molecular weight ("Polyglycol E, 4000"), and the antioxidant, phenothiazine, in an amount of 0.05 percent by weight of the composition (0.36 percent by weight of the polyethylene), was mixed in a two-roll mill for a period of about 10 minutes and removed in sheet form. After grinding in a Wiley mill, the composition was fed to the hopper of a one-inch extruder which was operating at a speed of 70 r.p.m. and at a pressure of 400 p.s.i. Attached to the extruder was an eight inch sheeting die. The temperature profile which was progressively spaced along the length of the extruder from the feed end to the die end was 200° F., 350° F. and 350° F. The extruder was adjusted so as to operate at a speed of approximately 1½ feet per minute. The extruded composition was then immersed in water for 20 hours at 130° F. to extract the polyethylene glycol plasticizer. The thickness of the composition was found to be 49 mils. The extracted sheet was composed of 50 volume percent polyethylene and 50 volume percent of silica.

The polyethylene-silica sample was then analyzed by standard techniques to determine its electrical resistance which was found to be 70 milliohms-square inch. When subjected to the puncture test, it was found that the sample was able to withstand a force of 673 grams. The tensile strength of the sample was 210 lbs. per square inch. The break angle of the sample was 85 degrees. The pore volume was found to be 0.30 cc./g. The mean pore diameter was 0.084 micron.

Example 2

The procedure of Example 1 was followed. The polyethylene and the silica of Example 1 was also used. A composition consisting of 10 percent by volume of the polyethylene, 15 percent by volume of the silica, 75 percent by volume of petroleum oil ("Shellflex 411," 547 SSU at 110° F.) and the antioxidant, 2,6-di-tert-butyl-4-methylphenol ("Ionol") in an amount of 0.1 percent by weight of the composition (1.15 percent by weight of the polyethylene), was blended on a two-roll mill for about 5 minutes and removed as sheet. After grinding on a Wiley mill, the composition was fed into the hopper of a standard one-inch extruder to which was attached an eight inch sheeting die. The pressure within the extruder was 500 p.s.i. The temperature profile along the length of the extruder from the feed end to the die end progressively decreased from 400 to 300° F. with the die at 350° F. The extrusion rate was again approximately 1½ feet per minute. The extruded composition was then immersed in petroleum ether for 60 minutes at room temperature to extract the petroleum oil. The thickness of the final product was 26 mils, and the composition was 40 volume percent polyethylene and 60 volume percent silica.

This sample was then tested to determine its properties. The electrical resistance of this sample was found to be 22 milliohms-square inch. The puncture test indicated that this sample could withstand a force of 366 grams. The tensile strength was 220 lbs. per square inch. The break angle was found to be greater than 110°. The pore volume was determined to be 0.71 cc./g. The mean pore diameter was 0.11 micron.

Example 3

The procedure of Example 1 was generally followed. The polyethylene, silica and petroleum oil used in this example were the same as that used in Example 2. A composition consisting of 20 volume percent of the polyethylene, 15 percent by volume of the silica, and 65 percent by volume of petroleum oil was mixed in a two-roll mill for about 5 minutes and removed as sheet. The product was immersed in trichloroethylene for 60 minutes at room temperature to remove the petroleum oil. The thickness of the final product was 23 mils and the composition was 60 volume percent polyethylene and 40 volume percent silica.

The electrical resistance of this sample was found to be 66 milliohms-square inch. This sample was able to withstand a force of 1313 grams. The tensile strength was 580 lbs. per square inch. The break angle was greater than 110°. The pore volume was found to be 0.76 cc./g. The mean pore diameter was 0.12 micron.

Example 4

The polyethylene, silica and petroleum oil used in this example were the same as that used in Example 2.

A composition consisting of 17 percent by volume of the polyethylene, 18 percent by volume of the silica, 21 percent by volume of petroleum oil, 44 percent by volume glycerol and 2,6-di-tert-butyl-4-methylphenol ("Ionol") in an amount of 0.1 percent by weight of the composition was pelletized by extrusion. This composition was then fed to an extruder to which was attached an eight inch sheeting die. The extruder was operated at a speed of 60 r.p.m. and at a pressure of 550 p.s.i. The temperature profile from the feed end to the die end progressively increased from 300° F. to 350° F. The extruded product was immersed in water for 6 hours at room temperature to extract the glycerol. The resulting product was then immersed for 1 hour in petroleum ether to extract the petroleum oil. The thickness of the final product was approximately 37 mils and the composition was 48.5 volume percent of polyethylene and 51.5 volume percent silica.

The electrical resistance of this product was 64 milliohms-square inch. This product was able to withstand a force of 1573 grams. The tensile strength of the product was 535 lbs. per square inch. The percent elongation at failure was 35 percent. The break angle was greater than 150°. The pore volume was found to be 0.41 cc./g. The mean pore diameter was 0.10 micron.

Example 5

The polyethylene, silica and petroleum oil used in this example were the same as that used in Example 2.

A composition consisting of 15 percent by volume of the polyethylene, 15 percent by volume of the silica, 70 percent by volume of the petroleum oil, and 2,6-di-tert-butyl-4-methylphenol ("Ionol") in an amount of 0.1 percent by weight of the composition (0.77 percent by weight of polyethylene), was mixed on a two-roll mill for about 5 minutes, and removed as sheet. After grinding, the composition was fed to an extruder which was operating at approximately 60 r.p.m. and at a pressure of 400 p.s.i. An eight inch sheeting die was attached to the extruder. The temperature profile within the extruder progressively decreased from a temperature of 375° F. at the feed end to 300° F. with the die at 325° F. The extrusion rate was again approximately 1½ feet per minute. The extruded product was then immersed in trichloroethylene at 180° F. for 90 minutes to extract the oil. The thickness of the final product was found to be 32 mils.

The electrical resistance of this product was found to be 36 milliohms-square inch. This product was able to withstand a force of 1013 grams. The tensile strength of the product was 375 lbs. per square inch. The break angle was greater than 110°. The pore volume was found to be 0.88 cc./g. The mean pore diameter was 0.14 micron.

Example 6

The silica and petroleum oil used in this example were the same as that used in Example 2. The polyethylene ("Hifax 1901") had an average molecular weight of 2,000,000, a standard load melt index of 0, a high load melt index of 0, a density of 0.94 grams/cc. and a reduced specific viscosity of 15.

A composition consisting of 10 volume percent of the polyethylene, 15 volume percent of the silica, 75 percent by volume petroleum oil, and the antioxidant, 2,6-di-tert-butyl-4-methylphenol ("Ionol") in an amount of 0.1 percent by weight of the composition was mixed in a Brabender Plastograph for 15 minutes. This composition was then compression molded. The product was then immersed in petroleum ether for 60 minutes at room temperature to remove the petroleum oil. The thickness of the final product was 33 mils.

The electrical resistance *e* of this sample was 32 milliohms-square inch. The sample could withstand a force of 1973 grams. The tensile strength was 430 lbs. per square inch. Break angle was greater than 110°.

Example 7

The polyethylene, silica and petroleum oil used in this example were the same as that used in Example 2.

Using the system described, a composition consisting of 14.5 volume percent of the polyethylene, 14.5 percent by volume of the silica, 2.5 percent by volume of carbon black ("Elftex 8") having an average particle size of 0.03 micron in diameter, and 68.5 percent by volume of petroleum oil was mixed in a two-roll mill for about 5 minutes and removed as sheet. After grinding the sheet, the composition was fed into the hopper of an extruder which was operating under approximately the same conditions as in Examples 2 and 3. The extruded product was then immersed in trichloroethylene for 10 minutes at 180° F. to extract the petroleum oil. The thickness of the final product was 32 mils.

The electrical resistance of this product was determined to be 48 milliohms-square inch. The product was able to withstand a force of 1143 grams. The tensile strength of the product was 415 lbs. per square inch. The break angle was greater than 110°.

Example 8

The polyethylene used in this example was the same as that used in Example 6.

A composition consisting of 20 volume percent polyethylene, 12 percent by volume of carbon black ("Elftex 8") having an average particle size of 0.03 micron in diameter, and 68 percent by volume paraffin oil ("Primol," 335 SSU at 100° F.) was mixed in a Brabender Plastograph for 15 minutes. The composition was compression molded and a thin film blown on a Cryovac hat tester. Briefly stated, this operation comprised securing the outer periphery of the 20-mil thick film in the apparatus, heating the film and then projecting compressed air against one wall of the heated film to form a bubble to draw its wall to the desired thickness.

The sample was immersed in petroleum ether at room temperature to extract the paraffin oil. The thickness of the final product was about 1 mil. The product had an electrical resistance of 4 milliohms-square inch after treatment with wetting agent.

Example 9

To illustrate the importance of the polyethylene having a high molecular weight and a standard load melt index of 0, this run was conducted using a commercial pelletized polyethylene ("Grex 60007 E") having a standard load melt index of 0.7, an average molecular weight of 112,000 and a reduced viscosity of 2.2. Except for the polyethylene component, this composition was the same as that of Example 4. Seventeen volume percent of the polyethylene of standard load melt index of 0.7, 18 percent by volume silica, 21 percent by volume petroleum oil and 44 percent by volume glycerol was mixed in a Brabender Plastograph for 15 minutes. This composition was then compression molded and immersed first in water and then in petroleum ether as described in Example 4 to extract the glycerol and petroleum oil. The thickness of the product was 31 mils.

The electrical resistance of the sample was 60 milliohms-square inch. The tensile strength was 287 lbs. per square inch. The percent elongation at failure was only 1 percent. The break angle was less than 45°. When subjected to the puncture test, it was found that the sample failed completely; that is, it was unable to withstand even the slightest force, crumbling under pressure. It is concluded from the foregoing that this sheet is too brittle to be employed.

Example 10

The procedure of Example 1 was generally followed. The polyethylene and petroleum oil used in this example were the same as that disclosed in Example 2. The composition consisted of 15 volume percent of polyethylene, 69 volume percent of petroleum oil, 15 volume percent of diatomaceous earth ("Celite Filter Cel") having an average particle diameter of 4 microns and a surface area of 25 square meters per gram. 1 volume percent of carbon black ("Sterling MT") having an average particle diameter of 0.47 micron and a surface area of 6 square meters per gram and the antioxidant, 4,4-thiobis(6-tert-butyl-m-cresol) ("Santonox") in an amount of 0.1 percent by weight of the polyethylene.

The composition was blended, ground and extruded substantially as described in Example 1. The extruded composition was then immersed in petroleum ether for 30 minutes at room temperature to extract the petroleum oil. The thickness of the final product was 18 mils.

The product was then tested to determine its properties. It was able to withstand a force of 1260 grams of water. The product had a tensile strength of 500 p.s.i. in the extrusion direction and 910 p.s.i. in the cross extrusion direction. It had a break angle greater than 110°. The electrical resistance of the product was greater than 100 milliohms-square inch. However, after the product was soaked in a 1 percent solution of a standard commercial wetting agent for 60 minutes, its resistance was 27 milliohms-square inch.

Example 11

The procedure of Example 1 was generally followed. The polyethylene, silica and petroleum oil used in this example were the same as that used in Example 2. The composition consisted of 15 volume percent of polyethylene, 69 volume percent of petroleum oil, 15 volume percent of silica, 1 volume percent of carbon back ("Sterling MT") having an average particle diameter of 0.47 micron and a surface area of 6 square meters per gram and the antioxidant 4,4-thiobis(6-tert-butyl-m-cresol) ("Santonox") in an amount of 0.1 percent by weight of the polyethylene.

The composition was blended, ground and extruded substantially as described in Example 1. The extruded composition was then immersed in petroleum ether for 30 minutes at room temperature to extract the petroleum oil. The thickness of the final product was 29 mils.

The product was then tested to determine its properties. It was able to withstand a force of 1100 grams of water. The product had a tensile strength of 430 p.s.i. in the extrusion direction and 510 p.s.i. in the cross extrusion direction. It had a break angle greater than 110°. The electrical resistance of the product was 44 milliohms-square inch. However, after the product was soaked in a 1 percent solution of a standard commercial (e.g., sodium dodecyl benzene sulfonate) wetting agent for 60 minutes, its resistance was 28 milliohms-square inch.

Example 12

The polyethylene and petroleum oil used in this example were the same as those disclosed in Example 2. The composition consisted of 20 volume percent of polyethylene, 60 volume percent of petroleum oil, 20 volume percent of precipitated calcium carbonate ("Purecal U") having an average diameter of 0.040 micron and 2,6-di-

tert-butyl-4-methylphenol ("Ionol") in an amount of 1.0 percent by weight of the polyethylene.

The composition was blended in a Banbury and then placed in a platen press and pressed at about 350° F. at a pressure of 40,000 lbs. for about 3 minutes. The resulting film, which was 20 mils thick, was then blown into a thin film by means of a Cryovac hat tester as described in Example 8.

The resulting film was less than 5 mils thick. This thin film was then immersed in petroleum ether for 30 minutes at room temperature to extract the petroleum oil. The resulting product had an electrical resistance of 8 milliohms-square inch.

Example 13

The procedure and composition used in this example were the same as that described in Example 12 except that 15 volume percent of polyethylene, 15 volume percent of precipitated calcium carbonate and 70 volume percent of petroleum oil were used. The resulting product, a film less than 5 mils thick, had an electrical resistance of 35 milliohms-square inch.

Example 14

The polyethylene and petroleum oil used in this example were the same as those disclosed in Example 2. The composition consisted of 30 volume percent of polyethylene, 40 volume percent of petroleum oil, 30 volume percent of a very finely divided kaolin clay ("Clemson Clay") ordinarily used as filler in paper, and 2,6-di-tert-butyl-4-methylphenol ("Ionol") in an amount of 0.1 percent by weight of the polyethylene.

The composition was blended in a Banbury and then blown into a thin film. In this blowing operation, the blend was extruded into a tube, and while the tube was still hot, compressed air was injected into it to form a bubble to draw its wall to the desired thickness. The bubble was then collapsed and slit.

The blown thin film was about one mil thick. It was immersed in petroleum ether for 30 minutes at room temperature to extract the petroleum oil. The resulting film had an electrical resistance of over 100 milliohms-square inch. However, after the film was soaked in a 1 percent solution of a standard commercial wetting agent solution (e.g., sodium dodecyl benzene sulfonate) for 60 minutes, its electrical resistance was 15 milliohms-square inch.

Example 15

The petroleum oil and silica used in this example were the same as those disclosed in Example 2. A composition consisting of 15 volume percent polypropylene having a standard load melt index 0, a reduced viscosity of 20 and a molecular weight in excess of 1,000,000, 15 volume percent of silica, 70 volume percent of petroleum oil and an antioxidant were thoroughly mixed in a Brabender Plastograph. The antioxidant was comprised of 2,6-di-tert-butyl-4-methylphenol ("Ionol") in an amount of 0.5 percent by weight of the polypropylene, dilaurylthiodipropionate in an amount of 0.5 percent by weight of the polypropylene and calcium stearate in an amount of 0.2 percent by weight of the polypropylene.

The mixture was placed in a platen press and pressed at about 350° F., at a pressure of 40,000 lbs. for about 3 minutes. The resulting film was immersed in petroleum ether at room temperature for 60 minutes to extract the petroleum oil. The thickness of the final product was 25 mils.

The electrical resistance of the product was determined to be 47 milliohms-square inch.

Example 16

The petroleum oil and silica used in this example were the same as those disclosed in Example 15. The procedure used in this example was the same as that disclosed in Example 15.

The composition consisted of 15 volume percent of a 99 mole percent ethylene–1 mole percent butene copolymer having a standard load melt index of 0, a high load melt index of 1.7 and a crystallinity of over 50 percent by weight, 15 volume percent of silica, 70 volume percent of petroleum oil and 2,6 - di - tert - butyl - 4 - methylphenol ("Ionol") in an amount of 1.0 percent by weight of the copolymer. The thickness of the final product was 22 mils.

The resistance of this product was determined according to the standard technique except that it was presoaked under a vacuum of 27 inches of mercury. The electrical resistance was 30 milliohms-square inch. The product had a tensile strength of 440 p.s.i. It was able to withstand a force of 486 grams in the puncture resistance test.

Example 17

In this experiment, the battery separator prepared as described in Example 11 was provided on one side with a plurality of ribs of foamed polyethylene.

A composition consisting of 100 parts of a polyethylene having a density of 0.92, 1 part of a blowing agent, azo-bis-formamide, ("Kempore 150"), 0.5 part zinc stearate and 1.6 parts of carbon black was mixed thoroughly. The mixture was extruded at a temperature of about 155° C. i.e., a temperature below the decomposition temperature of the blowing agent which was 175° C. The extruded mixture was cooled and cut to form pellets.

The pellets were then passed through an extruder maintained at a temperature above the decomposition temperature of the blowing agent, i.e., 180° C. to form a plurality of thin ribs of foamed polyethylene. The ribs were deposited on one side of the battery separator which had been preheated to a temperature of about 80° C. The composite was allowed to cool to room temperature. Good adhesion of the ribs to the separator was obtained.

Example 18

The polyethylene, petroleum oil and silica used in this example were the same as that disclosed in Example 6.

A composition comprised of 17 volume percent of polyethylene, 18 volume percent glycerol, and 2,6-di-tert-butyl-4-methyl-penol ("Ionol") in an amount of 0.12 percent by weight of the composition (0.95 percent by weight of the polyethylene) was mixed in a Banbury for about five minutes. A portion of the resutling composition was compression molded to form a sheet 28 mils thick. A second portion of the resulting composition was compression molded to form a sheet 20 mils thick.

Each sheet was immersed in petroleum ether for one hour at room temperature to remove the petroleum oil. The sheet was then immersed in water at room temperature for about 16 hours to extract the glycerol.

The electrical resistance of the 28 mil thick sheet was determined to be 49 millohms-square inch. The electrical resistance of the 20 mil thick sheet was determined to be 20 milliohms-square inch.

Example 19

The composition used in this example was the same as that described in Example 18. It was mixed and compression molded to form a sheet as disclosed in Example 19.

The sheet was immersed in petroleum ether for one hour at room temperature to remove the petroleum oil. The sheet was then immersed in water at room temperature for about 16 hours to remove the gylcerol. At the end of this time, it was removed from the water and immersed in about 25% potassium hydroxide solution for about 16 hours to extract the silica. The sheet was then washed off with water.

The sheet was 27 mils thick and had an electrical resistance of 7 milliohms-square inch. It was able to withstand a force of 510 grams of water. The tensile strength of the sheet was 160 p.s.i.

Example 20

The polyolefin, the silica and the petroleum oil were the same as that employed in Example 16. A composition consisting of 15 volume percent of the ethylene-butene copolymer, 15 volume percent of silica (HiSil 233) and 70 volume percent of the petroleum oil was prepared. In addition, an antioxidant, 4,4-thiobis(6-tert-butly-m-cresol), was added to the composition at a level of 0.1 percent by weight based on the weight of the composition and carbon black having an average particle size of 0.47 microns and a surface area of six square meters per gram was added in an amount 1.5 percent based on the weight of the composition. The above components were premixed in a ribbon blender and then fed to a twin screw extruder and the composition was continuously extruded to form a sheet. The sheet was then fed to counter current extractor containing a solution of hexane and petroleum oil whereby all but 7 volume percent of the petroleum was extracted.

The sheet was 20 mils in thickness, had an electrical resistance of 30 milliohms-square inch and a puncture resistance of 800 grams. When subjected to SAE Life Cycle Tests, the separator was found to survive the lives of five automotive (SLI) batteries.

Example 21

The polyolefin employed in this example was the same as that employed in Example 6 and the petroleum oil and silica were the same as that employed in Example 15.

The ratio of ingredieints and the method of processing was the same as that disclosed in Example 20 except that subsequent to the premixing and prior to the extrusion, the composition was fed to a twin screw extruder, extruded into strands and pelletized. The pelletized material was then fed to the twin screw extruder for extrusion into sheet form. The composition was then extracted in accordance with the procedure of Example 20.

The sheet was 20 mils in thickness, had an electrical resistance of 30 milliohms-square inch, and a puncture resistance of 2000 grams. The separator was found to survive five automotive (SLI) batteries when tested according to SAE Life Cycle Methods.

Example 22

The effectiveness of a separator in preventing loss in battery capacity as a result of antimony migration from the positive plate to the negative plate through the separator was determined in a conventional 12 volt 60 ampere hour lead acid battery.

During the charge discharge cycles of the battery, the antimony dissolves from the positive grid, migrates through the sulfuric acid electrolyte and the battery separator, and deposits on the negative plate which results in a loss in capacity of the battery. At least part of the lead sulfate produced during this self discharge is formed irreversibly. Thus the battery loses some of its capacity permanently.

The battery separator used in this example was prepared substantially as described in Example 17. This separator was placed in the lead storage battery and its effectiveness in preventing antimony ion transfer during "charge" "discharge" cycles of the lead storage battery was tested according to the procedure. The procedure employed is described in Robinson, R. G., and Walker, R. L., "Separators and Their Effect on Lead-Acid Battery Performance," in Collins, D. H., Ed., Batteries, MacMillan Co., N.Y., 1963, p. 28. One complete cycle of this test is comprised of the following:

(a) 4½ days' continuous charge at the normal rate of 3 amperes at 70° F.

(b) 7 days' stand on open circuit at 100° F.

(c) A discharge at the 10 hour rate to 1.8 volts per cell at 70° F.

(d) A full recharge

(e) A discharge at the 10 hour rate to 1.8 volts per cell at 70° F. From the discharges under (c) and (e) the percentage loss in capacity during the 7 days' open circuit stand was calculated.

The percent capacity loss at the end of the sixth cycle was determined and the results were as follows:

Battery separator	Percent capacity loss at end of sixth cycle
Battery separator prepared substantially as described in Example 17	17
Microporous rubber	28
Microporous polyvinyl chloride ("Porvic 1")	21
Sintered polyvinyl chloride ("Porvic 2B")	75
Rubber and diatomaceous silica backed with spun fiber mat ("Permalife")	43

The above results show a significantly lower loss in capacity for the battery using the separator prepared according to the instant invention.

It is thus seen that a novel and relatively inexpensive battery separator of superior quality has been disclosed. This battery separator of superior quality has been disclosed. The battery separator is suitable for usage in batteries employing an acid electrolyte as, for example the lead acid type, and also in batteries employing an alkaline electrolyte such as the silver-zinc, air zinc or nickel-cadmium types.

It is to be understood that many equivalent modifications will be apparent to those skilled in the art from a reading of the foregoing disclosure without a departure from the intended concept of the invention. For example, it is to be clearly understood that the process of this invention will be operated in a continuous manner when in actual production and that this is within the scope of this invention.

Although the instant invention is described in connection with battery separators, it can easily be adapted for other uses such as fuel cells, selective filtration or purification membranes, e.g., for use in water purification or biomedical applications, and breathable coatings for textile fabrics such as rainwear.

What is claimed is:

1. A battery separator having an essentially flat surface and comprising a microporous polyolefin having a molecular weight of at least 300,000, a standard load melt index of substantially 0, and a reduced viscosity of not less than 4.0.

2. A battery separator according to claim **1** wherein said polyolefin is polyethylene.

3. A battery separator as defined in claim **1** wherein said polyolefin is an ethylene-butene copolymer.

4. A battery separator according to claim **1** wherein the web has pores at least 50 percent of which are less than 0.5 micron in diameter and a void volume of at least 50 percent.

5. A battery separator according to claim **1** wherein at least 90 percent of the pores are less than 0.5 micron in diameter.

6. A microporous battery separator having an essentially flat surface comprising a homogeneous mixture of 8 to 100 volume percent of polyolefin having a molecular weight of at least 300,000, a standard load melt index of 0 and a reduced viscosity of not less than 4.0, 0 to 40 volume percent of a plasticizer and 0 to 92 volume percent of inert filler material.

7. A product as defined in claim **6** wherein said polyolefin is present at a level of 40 to 60 volume percent, said plasticizer is present at a level of 1 to 10 percent and said filler is present at a level of 40 to 60 volume percent.

8. A product as defined in claim **6** wherein said polyolefin is polyethylene, said filler is finely divided silica, and said plasticizer is petroleum oil.

9. A battery separator according to claim **6** wherein the base web has pores at least 50 percent of which are less than 0.5 micron in diameter and a void volume of at least 50 percent.

10. A battery separator according to claim **9** wherein at least 90 percent of the pores are less than 0.5 micron in diameter.

11. A microporous battery separator comprising a homogeneous mixture of 46.5 volume percent of polyolefin having a molecular weight of at least 300,000, a standard load melt index of 0 and a reduced viscosity of not less than 4.0, 46.5 volume percent of finely divided silica and 7 volume percent of the petroleum.

References Cited

UNITED STATES PATENTS

2,700,694	1/1955	Fernald	136—146
3,026,366	3/1962	Comeau et al.	136—145
3,045,058	7/1962	Martinak	136—146

WINSTON A. DOUGLAS, *Primary Examiner.*

D. L. WALTON, *Assistant Examiner.*

Appendix U

United States Patent [19]

Lundquist et al.

[11] **Patent Number: 4,650,730**

[45] **Date of Patent: Mar. 17, 1987**

[54] **BATTERY SEPARATOR**

[75] Inventors: **Joseph T. Lundquist,** Jessup; **Christian B. Lundsager,** Ashton, both of Md.; **Nigel I. Palmer,** Lexington, Mass.; **Howard J. Troffkin,** Potomac, Md.

[73] Assignee: **W. R. Grace & Co.,** New York, N.Y.

[21] Appl. No.: **734,431**

[22] Filed: **May 16, 1985**

[51] **Int. Cl.**[4] **H01M 10/50**

[52] **U.S. Cl.** **429/62;** 429/145

[58] **Field of Search** 429/62, 145

[56] **References Cited**

U.S. PATENT DOCUMENTS

4,075,400	2/1978	Fritts	429/62
4,351,888	9/1982	Dampier et al.	429/62
4,407,910	10/1983	Catanzarite	429/62

Primary Examiner—Donald L. Walton

Attorney, Agent, or Firm—Howard J. Troffkin

[57] **ABSTRACT**

A multiply sheet product useful as a battery separator having at least two plies each in the form of a microporous sheet of predetermined length and breadth and a thickness of less than 10 mils wherein (a) at least one of said ply being a sheet capable of transforming to a substantially non-porous membrane at a temperature between about 80° and 150° C. while essentially maintaining its length and breadth dimensions and (b) at least one ply being a sheet capable of maintaining its dimensions and porosity at temperatures from ambient to at least about 10° C. greater than the transformation temperature of sheet (a).

30 Claims, No Drawings

BATTERY SEPARATOR

BACKGROUND OF THE INVENTION

The subject invention is directed to a sheet product which is useful as separators in batteries, in particular, separators in lithium batteries to prevent the occurence of overheating and thermal-runaway.

Storage batteries have at least one pair of electrodes of opposite polarity and, generally, have a series of adjacent electrodes of alternating polarity. The current flow between these electrodes is maintained by an electrolyte which can be acid, alkaline or substantially neutral depending on the nature of the battery system. Separators are located in the batteries between adjacent electrodes of opposite polarity to prevent direct contact between the oppositely charged electrode plates while freely permitting electrolytic conduction. The separator is normally in the form of a thin sheet or film or in certain designs can be in the form of an envelope surrounding each electrode plate of one polarity. It is generally agreed that separators should be (a) thin and light weight to aid in providing a battery of high energy density, (b) resistant to degradation and instability with respect to the battery components with which it is in contact, (c) capable of exhibiting a high degree of electrolytic conductivity (low electrolytic resistance) and (d), in battery systems where appropriate, capable of inhibiting formation and growth of dendrites.

Lithium batteries have distinct advantages over other storage batteries. These batteries are capable of providing much higher power storage densities than other types of batteries, excellent shelf life, high energy density (power capability per unit weight) due to the low atomic weight of lithium metal, and high potential for forming a battery in conjunction with positive electrodes far removed from the lithium electrode in the electromotive series. The battery can be formed in any conventional physical design-cylindrical, rectangular or disc-shaped "button" cells—normally of a closed cell configuration. Such batteries are generally composed of a negative lithium electrode, a positive electrode and a non aqueous electrolyte. The negative electrode is conventionally lithium metal or its alloy on a support, such as a nickel coated screen. Positive electrodes of various types have been suggested, including metal oxides such as manganese dioxide or transition metal sulfides such as sulfides of cobalt, nickel, copper, titanium, vanadium, chromium, cerium and iron. The positive electrode may further contain carbon and a current collector. The electrolyte is formed of a non aqueous solvent containing a lithium salt. For example, solvents may be acetonitrile, tetrahydrofuran, propylene carbonate, and various sulfones. The lithium salts may be lithium perchlorate, iodide or hexafluroarsenate and the like. An additional, normally passive, component of the battery is a separator membrane located between plates of opposite polarity to prevent contact between such plates while permitting electrolytic conduction.

Separators conventionally used in present battery systems are formed of polymeric films which when placed in an electrolyte or electrolyte system, are capable of exhibiting a high degree of conductivity while being stable to the environment presented by the battery. The films may be macroporous or microporous to thus permit transporation of electrolyte. Examples of such separators include polypropylene sheet which has been stretched and annealed to provide microporosity in the sheet. Such sheets are normally highly oriented and shrink when subjected to heat. Other examples are filled polymeric sheets such as those disclosed in U.S. Pat. Nos. 3,351,495 and 4,287,276 in which the electrolyte is capable of passing through the separator through microporous channels and by the wicking of the filler.

Due to the reactivity of lithium, a major problem encountered with these batteries involves overheating of the cell due to improper use of the cell, e.g. placed in inverted position causing plating out of electrolyte onto an anode; contact between electrodes of opposite polarity such as by dendrite formation or shrinkage of separator; formation of high surface spongy lithium which exothermally reacts with the solvent-electrolyte; as well as other known conditions. Such overheating tends to cause thermal runaway and potentially explosive effects as the system continues to act in its defective mode. This must be controlled to provide a battery having commercial acceptability.

Polymeric films presently employed as separators in lithium batteries are generally not capable of preventing any uncontrolled overheating. Some separator films are inert to heat and, therefore, do not trigger any preventative mechanism. Other presently used separators, such as microporous polyolefins, when subjected to elevated temperatures exhibit dimensional instability and/or degradation permitting contact between electrodes of opposite polarity. Such instability only accelerates the thermal-runaway of a battery.

SUMMARY OF THE INVENTION

The present invention is directed to a sheet product having at least two plies coextensively bonded together, to provide a product capable of exhibiting low electrolytic resistivity at normal operating temperatures and when subjected to a predetermined elevated temperatures, to irreversibly transform to a product having high electrolytic resistivity while maintaining its overall length and breath dimensions.

DETAILED DESCRIPTION OF THE INVENTION

The sheet product of the present invention, in addition to exhibiting conventionally desired properties for use as a battery separator as described above, is uniquely suitable for use as a separator in lithium batteries as a means of reducing or stopping the electrochemical activity of the battery cell when encountering elevated temperatures. This unique feature provides the ability to produce a lithium battery having an internal means to prevent undesired thermal-runaway and/or explosive reaction.

For purposes of clarity some of the terms used herein and in the appended claims to describe the instant invention are defined herein below:

A "sheet" is intended to define a unitary article having a large surface with respect to its length and breath and having a thickness of about 0.025 cm. or less, preferably less than about 0.01 cm.

A "ply" is a sheet which is microporous and is a component of a sheet product.

A "sheet product" is intended to define a multiply structure formed from (a) at least one ply capable of transforming to a substantially non-porous membrane at a predetermined temperature selected between about 80° C. and 150° C. and (b) at least one ply capable of maintaining its dimensions and porosity at temperatures

of from ambient to at least about 10° C. greater than the transformation temperature of ply (a); all plies are bonded together to form a unitary structure which is capable of maintaining its length and breath dimensions.

The term "first" is intended to modify terms to reference them to ply (a) of a sheet product, or sheets, materials or components used to form a ply (a).

The term "second" is intended to modify terms to reference them to ply (b) of a sheet product, or sheets, materials or components used to form a ply (b).

The term "polymer composition" is intended to refer to a thermoplastic polymer which may contain substantially uniformly distributed therein other material such as plasticizer, antioxidants, solid particulate fillers and the like.

The term "fluidity" is intended to refer to the ability of a polymer composition to flow, that is to have polymer molecules of the composition capable of sliding over one another. This ability will depend upon the polymer's particular configuration, i.e. linear or branched, crystalline or amorphous, degree of cross-link, temperature of the composition and the like. The fluidity can be measured by conventional techniques such as using Standard Load Melt Index or High Load Melt Index tests (ASTM D-1238-57T) modified to be measured at varying temperatures.

The term "viscosity" is intended to refer to the ability of a polymer composition to resist flow. Viscosity is inversely related to fluidity.

A "separator" is a component of a battery, in particular a storage battery, by which the component maintains a separation between adjacent electrode plates of opposite polarity. A separator of the present invention is formed from a sheet product and may be in various configurations such as, flat, ribbed, corrugated sheet product in the form of a membrane or envelope capable of maintaining separation between electrodes.

The multiply sheet product of the present invention must be composed of (a) at least one first ply in the form of a microporous sheet of a predetermined length and breath and of a thickness of less than about 10 mils (0.025 cm) preferably less than 5 mils (0.013 cm) and most preferably from 0.1 to 4 mils. The pores of the sheet must be of sufficient size and amount to permit the resultant sheet product of the present invention to exhibit low electrolytic resistivity i.e. 500 ohm-cm or less depending on the particular application. It is understood that the thinner the sheets dimensions are, the lower the overall volume percent of the sheet needs to be occupied by the pores to sustain the desired low electrolytic resistance. The pores of the first ply will normally have average pore size of from about 0.005 to about 5 microns in diameter and the pores normally occupy at least about 10 volume percent and preferably at least about 25 volume percent of the total volume of the sheet. The first sheet is formed of a composition capable of transforming to a substantially non-porous membrane sheet at a predetermined temperature within the range of from about 80° to 150° C. while substantially maintaining its predetermined length and breath dimensions when a component of the multiply sheet product; and (b) at least one second ply in the form of a microporous sheet of a predetermined length and breath and a thickness of less than 10 mil (0.025 cm), preferably less than 5 mils (0.013 cm) and most preferably from 1 to 4 mils (0.025–0.01 cm) having average pore size of from about 0.005 to about 5 microns in diameter wherein the pores occupy at least about 25 volume percent and preferably at least about 40 volume percent of the sheet's volume and the sheet is substantially stable (minor shrinkage of less than 10 percent may occur over conventional battery life and can be accommodated for in initial design) in form and dimensions at temperatures ranging from ambient to at least about 10° C., preferably at least 20° C. greater than the transformation temperature of sheet (a).

The transformation temperature of a sheet materials is the temperature at which the sheet, when in a battery cell, exhibits a large increase in electrolytic resistivity to provide resistivity sufficient to substantially shut down a battery system or a portion of such a system (for example one cell or a localized portion to prevent undesired thermal runaway. Electrolytic resistivity of at least about 1500 ohm-cm is normally sufficient to shut down a battery system although greater or lesser resistance may be sufficient for a particular battery or for a particular application. The transformation temperature substantially coincides with the temperature at which the composition of the first ply exhibits sufficient fluidity and ability to collapse into its pores to provide a substantially non-porous membrane while a component of the sheet product.

The microporous sheets forming (a) and (b) are each formed from polymeric compositions. The polymer matrix must be selected from polymers which are inert under the conditions encountered in a battery especially with respect to the electrolyte composition. In addition, each polymer composition must be capable of exhibiting microporosity and must also be capable of being formed into a thin sheet of less than 10 mils preferably less than 5 mils and most preferably less than 4 mils. With respect to the first ply, it may be in the form of a sheet or, alternately, a thin coating of from about 0.01 to 4 mils contained on ply (b). Ply (b), in turn, is of equal or greater thickness than that of the first ply and, most preferably has a thickness ranging from about 1 to 4 mils.

The first ply is formed from a polymeric composition comprising a polymer, as described fully herein below, and may, in addition, have uniformly distributed therein plasticizers, stabilizers, antioxidants and the like for said polymer. The polymer composition used to from a first ply should contain substantially no particulate filler although small amounts of up to about 15 weight percent, preferably less than 10 weight percent may be contained in the compositions as residue from processing and formation.

The second ply is formed from a polymeric composition comprising a polymer, as described fully herein below, and, in addition, may have uniformly distributed therein plasticizers, stabilizers, antioxidants and the like and, preferably contains a large (greater than 20) weight percentage of solid, particulate filler.

The sheet products of the present invention utilize first and second polymeric compositions which have different profiles of viscosity and flow with respect to temperature. These properties can be readily determined by known methods such as by a modified Standard Load Melt Index or High Load Melt Index test to make the determinations over a range of temperature, particularly a range of from 80° to 150° C. The viscosity of the composition forming the first ply should be substantially equal to or less than that of the composition of the second ply at all temperatures. It is understood that both the first and second polymer compositions exhibit very high viscosity at low and moderate temperatures

where they are solid materials. At these temperatures, both solid compositions have substantially equal (approach infinite values) viscosities as they do not exhibit any pronounced flow. However, at some predetermined elevated temperatures of from about 80° C. or greater, as directed by the application for the sheet product, the ply formed from the first polymeric composition must be capable of having a sufficient change in viscosity (decrease) or released elastic energy (exhibiting plastic memory) to exhibit flow and ability to collapse into its pores. This temperature is the transformation temperature of the first composition. At this transformation temperature, the second polymer composition must maintain sufficient high viscosity and thus retain its elastic energy, i.e. show substantially no flow.

The present sheet product has been found useful as a battery separator for lithium type batteries because, in addition to exhibiting the normally desired electrolytic conductivity at operating temperatures, it is capable of irreversibly transforming to a sheet product having high electrolytic resistivity at an elevated temperature of at least about 80° C., preferably from about 80° to 150° C. while maintaining its overall length and breath dimensions.

The polymeric compositions useful in forming each of the sheets of the multiply sheet product of the present invention can be selected from known classes of polymers capable of forming a microporous sheet as, for examples, polyolefins, polysulfones, polyvinyl chloride, polyvinyl fluoride, polytetrafluoroethylene-propylene copolymers, polyamides, polyphenyleneoxide-polystyrene copolymers, polycarbonates and the like. The polymers used to form the first and second sheets of the multiply sheet product are preferably selected from the same class of polymeric material to best provide the properties described above.

A preferred class of polymers are the polyolefins due to their inertness with respect to the other battery components with which they come in contact. The remainder of this description shall illustrate the present invention by combinations of the most preferred embodiment wherein polyolefin compositions are used to form the present sheet materials and separators therefrom. It has been found that when forming a product having at least one first ply of an unfilled microporous polyolefin composition which normally exhibits the undesired properties of shrinkage in length and breath in combination with at least one second ply of a higher viscosity profile polyolefin composition (most preferably a filled polyolefin composition) one unexpectedly attains a product of low transformation temperature while exhibiting and maintaining high stability.

The instant invention is directed to a multiply sheet product in which the plys are formed from at least two different classes of sheet materials.

A polymer composition found useful to form a second ply of the subject sheet product and separators formed therefrom are a substantially homogeneous admixture of from 5 to 30 weight percent of polyolefin, from 10 to 60 weight percent of a plasticizer for the polyolefin and from 30 to 75 weight percent of a particulate filler. The preferred range of each component, respectively, is: 10 to 20; 20 to 40; and 45 to 65.

The second polyolefin should have a high weight average molecular weight of at least 100,000 and can be selected from polyolefins having weight average molecular weight of from 100,000 to about 2,000,000. The second polyolefin can be selected from homopolymers such as polyethylene or polypropylene or from copolymers formed from a mixture of hydrocarbon olefinic monomers, such as ethylene, propylene, butene and the like, or from a mixture of at least 90 percent by weight of hydrocarbon olefinic monomer with other olefinic monomer, such as acrylic acids and esters, vinyl acetate, styrene and the like. This polyolefin can also be formed from a mixture of a high molecular weight and a low molecular weight polyolefin. The mixture can be formed from about 5 to 95 weight percent high molecular weight polymer (at least about 500,000 weight average molecular weight) with the corresponding about 95 to 5 weight percent of low molecular weight polymer (weight average molecular weight of from 100,000 to 500,000). It is preferred that the lower molecular weight polymer be the major component of the polyolefin mixture. When only one polyolefin is used in forming the second sheet, the weight average molecular weight of the polyolefin component should preferably be greater than 150,000 and, more preferably, greater than 200,000.

The second plasticizer can be soluble or insoluble in water. Representative of the water-insoluble plasticizers are organic esters, such as the sebacates, phthalates, stearates, adipates, and citrates; epoxy compounds such as epoxidized vegetable oil; phosphate esters such as tricresyl phosphate; hydrocarbon materials such as petroleum oil including lubricating oils and fuel oils, hydrocarbon resin and asphalt and pure compounds such as eicosane; low molecular weight polymers such as polyisobutylene, polybutadiene, polystyrene, atactic polypropylene, ethylene-propylene rubber; ethylene-vinyl acetate copolymer, oxidized polyethylene, coumarone-indene resins and terpene resins; tall oil and linseed oil. Illustrative of the water-soluble plasticizers useful as first plasticizers are ethylene glycol, polyethylene glycol, polypropylene glycol, glycerol, and ethers and esters thereof; alkyl phosphates such as triethyl phosphate; polyvinyl alcohol, polyacrylic acid and polyvinyl pyrrolidone. In addition, there are a number of useful water-insoluble, normally solid plasticizers. Typical examples of these plasticizers are polyisobutylene, polybutadiene, polystyrene, atactic polypropylene, ethylene-propylene rubber, and ethylene/vinyl acetate copolymer. Generally, when this type of plasticizer is used, it can be included into the composition forming the second sheet material in an amount as high as 40 percent by volume of the second sheet's composition.

The filler used in forming the second sheet should generally be a high surface area particulate material. The particle size of the second filler should be less than about 0.01 cm and preferably less than about 0.0025 cm in diameter. The surface area of the filler may be from about 1 to 950 square meters while 10 to 500 square meters per gram is preferred. The pore volume (BET) of the filler is preferably at least about 0.07 cc/gm with from 0.07 to 0.8 cc/gm being most preferred.

The second filler and second plasticizer must have distinctly different solubilities taking into account the solvent intended to be used to remove the plasticizer from the formed sheet as more fully described below. The second filler may be soluble or insoluble in water. Representative of particulate filler material which are insoluble in water and which may be used, singly or in combination, to form the first sheet are carbon black, coal dust and graphite; metal oxides and hydroxides such as those of silicon, aluminum, calcium, magnesium, barium, titanium, iron, zinc, and tin; metal carbonates

such as those of calcium and magnesium; minerals such as mica, montmorillonite, kaolinite, attapulgite, asbestos, talc, diatomaceous earth and vermiculite; synthetic and natural zeolites; portland cement; precipitated metal silicates such as calcium silicate and aluminum polysilicate; alumina silica gels; wood flour, wood fibers and bark products; glass particles including microbeads, hollow microspheres, flakes and fibers; and salts such as molybdenum disulfide, zinc sulfide and barium sulfate.

Illustrative of the water-soluble fillers are inorganic salts such as the chlorides of sodium, potassium, and calcium; acetates such as those of sodium, potassium, calcium, copper and barium; sulfates such as those of sodium, potassium and calcium; phophates such as those of sodium and potassium; nitrates such as those of sodium and potassium; carbonates such as those of sodium and potassium.

In addition to the above combination of polyolefin-plasticizer-filler, the mixture used to form the second sheet may contain conventional stabilizers, antioxidants, additives and processing aids as known to those skilled in the art. Representative of the stabilizers include 4,4-thiobis (6-tert-butyl-m-cresol), 2,6-ditert-butyl-4-methylphenol and the like. Representatives of antioxidants include hydroquinone and the like. Representatives of other additives include conductive carbon black which may have high surface area (1000 m^2/gm) and the like. Representatives of processing aids include zinc stearate and the like. The processing aids, stabilizers antioxidants are used in conventional low amounts such as up to about 2 percent. The conductive carbon black additive may be used in up to 10 percent by weight.

A preferred composition useful in forming the second sheet comprises from 10 to 20 weight percent of a polyolefin, in particular a high density polyethylene or a polypropylene having a high degree of crystallinity, preferably of at least about 30 and most preferably at least about 50 percent crystallinity; from 20 to 40 weight percent of a petroleum oil; and from 45 to 65 weight percent of a first filler selected from carbon or a metal oxide or hydroxide such as those of silicon, aluminum, calcium, magnesium and titanium and mixtures thereof.

The sheet product of the present invention must also have a first ply capable of transforming to a substantially non-porous membrane which is superimposed and bonded to the second ply described above. This ply can be first formed as a separate sheet or can be formed while part of a multi-ply structure or can be formed as a coating on a second sheet which may or may not require further treatment. The particular mode depends on the particuilar polymer composition used, the desired thickness of the first ply and the bonding abilities of the compositions as can be readily determined. The resultant first ply is a substantially unfilled microporous sheet of less than about 10 mils (0.025 cm) thickness.

One method of forming the first ply is by initially forming a filled sheet material similar to that described above for the second sheet. The first sheet is initially a substantially uniform mixture of polyolefin and plasticizer or polyolefin, plastilcizer and filler in amounts within the ranges described above for the second sheet. The first and second sheets are bonded together and a substantial portion, if not all, of the plasticizers and filler are removed. The second polyolefin can be substantially the same as described above with respect to the second polyolefin or may be a low density polyethylene or an atactic, isotactic or syndiotactic polypropylene. Therefore, in general, the polyolefin used in forming both the first and second sheets may be high density, highly crystalline, polymers. However, the first polyolefin may also be chosen from low density or low or non-crystalline polymer. The weight average molecular weight of the first polyolefin may be equal to or less than the range described above for the second polyolefin. The particular polyolefin chosen will depend on the temperature at which one desires to have the electrolytic resistivity of the resultant battery markedly increase to cause reduced electrochemical activity therein. However, the fluidity at and below the transformation temperature of the first polyolefin should always be substantially the same or greater (the viscosity is substantially the same or lower) than that of the second polyolefin used in forming a particular sheet product. The first polyolefin most suitable for a particular application can be readily determined by laboratory scale tests.

The plasticizers suitable for use in forming the first sheet are the same as those described with respect to the second sheet herein above. When forming the first sheet from an initially filled sheet the only limitation in selecting the first plasticizer is that (a) it is the same as the second plasticizer or (b) the first plasticizer and the second plasticizer are mutually soluble in a common solvent or in solvents (which is to be used in extraction as described below) which are inert with respect to the first and second polyolefins and the second filler.

The first fillers can be selected from those fillers described above with respect to forming the second sheet. However, the first filler and the second filler must be chosen in a manner so they have distinctly different and separate solubility characteristics. While the selection of the second filler must be done so it is inert with respect to the other components of the battery the first filler must be soluble in a substantial non-solvent with respect to the second filler. This is necessary when forming the sheet product from two filled sheets, wherein it will be required to remove the filler of the first sheet while retaining the filler in the second sheet. Each filler is thus chosen both with respect to end use to be compatable with the other battery components and with respect to solubility to provide a means of removing the first filler while retaining the second filler. In a lithium battery, which has a substantially neutral electrolyte, the second filler can be any of the above described fillers and is preferably the above-described metal oxides or hydroxides, in particular, may be selected from titanium dioxide, calcium oxide, aluminum oxide, calcium hydroxide, or silica or the like while the first filler should be a water soluble, preferably an aqueous acid soluble, filler as described above such as metal chlorides, acetates, carbonates and the like and, in particular, sodium, potassium or calcium carbonate.

The two classes of sheets are separately formed by mixing the selected components for that sheet in any conventional manner to produce a substantially uniform mixture. For example, the components can be premixed at room temperature in a blender and the polyolefin-filler-plasticizer dry blends can then be fluxed in a conventional mixer such as a Banbury mixer or melt homogenized in a conventional two roll mill. After being suitably mixed, each composition is molded or shaped in any conventional manner, such as by extrusion, calendering, injection molding, or compression molding to form separate sheets which can be bonded by use of heated nip rollers or the like.

Where one starts with a multilayer filled sheet material, the sheet product is formed by subjecting the multilayer sheet material to extraction to remove certain components from each layer. The plasticizer is removed from the first and second sheets and, in addition, the filler is removed from the first sheet. The specific extraction procedure and medium(s) employed depend upon the nature of the components to be extracted. For example, if the first and second plasticizer and first filler are soluble in a mutual solvent, a single stage extraction is employed. If the first and second plasticizers are mutually soluble in a common solvent but the filler has dissimilar solvency, a two stage extraction may well be required. The solvent and extraction conditions should be chosen so that the first and second polyolefins and the second filler are essentially insoluble. Numerous extracting solvents are suitable for forming the sheet materials of this invention with the particular solvent depending upon the particular component to be extracted. For example, if petroleum oil is used as the first and/or second plasticizer, the following solvents are suitable to extract it from the multilayer sheet material: chlorinated hydrocarbons, such as trichloroethylene, tetrachloroethylene, carbon tetrachloride, methylene chloride, tetrachloroethane, and the like; hydrocarbon solvents such as hexane, benzene, petroleum ether, toluene, cyclohexane, gasoline, and the like. If polyethylene glycol is the plasticizer of the first and/or second sheet material, the extraction medium can be water, ethanol, methanol, acetone, and the like. If finely ground silica is to be extracted, the following solvents are suitable: aqueous or alcoholic sodium hydroxide, potassium hydroxide, and the like or hydrochloric or hydrofluoric acid, can be used to extract metal oxides and metal carbonates.

The conditions under which the extraction is conducted will depend on the particular components. The time of the extraction will vary depending upon the temperature used and the nature of the plasticizer or filler being extracted. For example, when higher temperatures are used, the extraction time for an oil of low viscosity can be less than a minute, whereas if the extraction is performed at room temperature, the time requirement for extraction of a polymeric plasticizer may be in the order of a half hour or even longer. In order to permit easy removal of the first filler, it is preferred that ply or plies of first sheet be outer or surface ply of the sheet product. A multilayer sheet material of two ply (one of the second class and one of the first) or of three ply (one of the first class with two outer sheets of the second class) are, therefore, preferred.

The microporous, substantially unfilled polyolefin sheet comprising the first ply of the subject sheet product can, alternately, be formed in other manners known to those skilled in the art. For example, it is well known that microporous polyolefin sheets, especially polyethylene and polypropylene, can be formed by extruding, as by blown film extrusion method, a film of polyolefin with a rapid drawdown rate and ratio, uniaxially cold stretching the film, such as at a temperature in the range of from about −20° C. to about 25° C. below the crystalline melt temperature of the polyolefin to impart microporosity to the film. The resultant microporous sheet may be further processed by hot stretching, in the same direction as it was cold stretched, the previously cold stretched film at a temperature normally from about 25° C. below to 5° C. below the crystalline melt temperature. The formed microporous sheet is normally annealled by exposing the sheet under tension without stretching to a temperature normally ranging from about 40° C. below to about 5° C. below the sheets crystalline melt temperature. The resultant sheet may be further treated to increase its wetting properties in manners known in the art. Sheets formed in this manner are non-filled microporous polyolefin, preferably of polyethylene or polypropylene (most preferably, polypropylene), which normally exhibit crystallinity of at least about 30 and preferably at least about 50 percent, an average pore size of from about 10^{-6} cm to about 10^{-4} cm and a void volume of about 20 to 45 percent. Various modifications for forming microporous polyolefin sheet by extrusion-stretching-annealing processes are described in U.S. Pat. Nos. 3,558,764; 3,679,538; 3,843,761; and 3,853,601, the teachings of which are incorporated herein by reference.

A multiply sheet product having at least one first ply and at least one second ply can be formed in conventional manners such as by coextensively overlaying at least one first sheet with at least one second sheet and subjecting them to nip rollers, calendering or the like. Alternatively, the sheet product can be formed by coating a second sheet with a first composition, normally of polymer and plasticizer, and then removing the first and second plasticizers.

In the instance where one starts with a multilayer sheet material in which the first layer is formed from a preformed substantially unfilled, non-plasticized microporous polyolefin sheet as described above, the subject sheet product is formed by extraction of the plasticizer from the second sheet composed of polyolefin, plasticizer and filler. The extraction can use solvents and conditions described above which provide removal of the plasticizer of the second sheet material while being inert to the polyolefins and filler materials.

The final sheet product is a multiply structure in which all plies of the sheet product are coextensive and bonded together. The most preferred sheet product is composed of two ply. The second ply is most preferably a highly filled polyolefin in which substantially all of the plasticizer has been removed. Normally, the extracted second ply has polymer/filler/plasticizer in wt. percent of 7-35/50-93/0-15. The first ply is most preferably composed essentially of polyolefin. When initially formed from a filled and/or plasticized polymer composition, it may contain residual amounts (10% or less) of the filler and of the plasticizer.

The exact final composition of each ply will depend on the original composition. Each ply exhibits microporosity. The size of the pores of the present sheet product have a substantial proportion which are less than of 0.5 micron diameter (Mercury Intrusion Method) and are generally tortuous in nature.

The resultant sheet products have been found to be capable of exhibiting inhibition to dendrite growth, high conductivity at ambient temperatures, capability to be formed into a very thin sheet products, and stability to the environment produced by and components of the battery. In addition, the present sheet products are dimensionally stable and do not exhibit unacceptable and detrimental shrinkage in its length and breath dimensions when subjected to elevated temperatures. The sheet product, therefore, when used as a separator does not permit contact of electrodes even at temperatures where conventional polyolefin separators would degrade and/or shrink.

It has further been unexpectedly found that separators formed from the present sheet product has the ability to drastically reduce its degree of porosity. The reduced porosity causes a "shut-down" of the battery's electrical system by being a barrier to the passage of ions in the electrolyte between electrodes of opposite polarity. This "shut-down" ability can, in lithium batteries, act as a "safety switch" which in effect, turns off the circuit prior to harm being done through thermal runaway or explosion of the defective battery.

The following examples are given for illustrative purposes only and are not meant to be a limitation on the invention described herein and in the claims appended hereto. All parts and percentages given below are by weight unless otherwise stipulated.

EXAMPLE I

A two ply sheet product was formed and used as a separator in an environment simulating a lithium battery system. A second ply of the sheet product was formed by initially introducing into a Brabender Plastograph mixer 6% of commercially available high density polyethylene (MW of 250,000) and 29% of low aromatic, saturated hydrocarbon petroleum oil (Shellflex 411; 547 SSU at 100° F.) and 0.1% of Santonox followed by 52.7% of titanium dioxide (Unitane OR-573; BET surface area 53 m^2/gm). Finally, 2% carbon black (Vulcan XC-72) and 0.2% zinc stearate are added. After complete addition of the components, they were compounded in the mixer at 175° C. for about 15 minutes. The resultant composition was removed from the mixer, cooled, and ground to a coarse powder in a Wiley mill. The powder was fed into a one inch single screw extruder, operated at 175° C., and extruded through two 40 mesh (U.S. Standard) screens to remove any large aggolmerates and pelletized. The pellets were subjected to a second extruder similar to the first, except that it was equipped with a two inch tubing die and formed into a blown film of approximately 0.005 to 0.0075 cm thick.

A first ply of the sheet product was formed in the same way as described above for the second ply except the materials used were 17.9 parts of a commercially available high density polyethylene (MW of 250,000), 14.1 parts of low aromatic saturated petroleum oil (Shellflex 411), 61.3 parts of finely ground calcium carbonate, 4.7 parts of titanium dioxide (Unitane OR-573), 1 part zinc stearate and 0.01 part of an antioxidant Santonox.

The first and second sheet materials formed above were superimposed and pressed (110 psi) together at 150° C. for about one minute to form a bonded sheet product. The 2 ply sheet product was immersed in 1,1,1-trichloroethane for about 30 minutes and air dried. Samples of the extracted sheet separator were analyzed and showed that greater than 90 percent of the plasticizer was removed. The sheet product was then wet with acetone and immersed in a dilute hydrochloric acid solution for about 30 minutes to remove substantially all of the calcium carbonate from the first sheet.

The resultant sheet product was subjected to propylene carbonate at various temperatures. Propylene carbonate is a typical electrolyte composition carrier used in lithium batteries and therefore exemplifies a battery environment to which separators are exposed. The exposed sheet product was subsequently tested for electrolytic resistance (ER) in 33 wt % KOH solution according to the ER determination described in Cooper and Fleischer, "Characteristics of Separators for Alkaline Silver oxide, Zinc Secondary Batteries: Screening Methods" Air Force Aero Propulsion Laboratory, September, 1965. The results were: 15 ohm-cm at 25° C.; 14.7 ohm-cm after exposure at 110° C.; and greater than 4000 ohm-cm after exposure at 135° C. The separator formed from the prepared sheet product exhibited a large electrical resistance capable of shutting down a battery system when exposed to a temperature between 110° C. and 135° C.

EXAMPLE II

A separator capable of exhibiting very high resistivity upon exposure to heat was prepared from a 2 ply sheet product. The second ply was formed in the same manner as described for the second ply of Example I above.

The first ply was formed in the same manner as the first ply of Example I except that the components were 22.9 parts of a commercial low density polyethylene (DYNH-1) 57.2 parts calcium carbonate (Baker Reagent Grade) 18.8 parts of low aromatic petroleum oil (Sunthene 255) with 0.1 part Santonox and 1 part zinc stearate. The pelletized material was pressed between Teflon sheets at 150° C. and 1000 psi for about 5 minutes to form a first sheet material 3.1 mil (0.0079 cm) thick.

The first and second sheet materials were superimposed and pressed between heated plates (125° C. at 110 psi) to form a bonded sheet product and then subjected to the extraction steps described in Example I above.

The thickness of the 2 ply sheet product was 5.1 mil (0.013 cm) (2 mil (0.005 cm) first ply and 3.1 mil (0.0079 cm) second ply) which upon exposures above 110° C. reduced to a thickness of 3.7 mil (0.0094 cm) while exhibiting essentially no reduction in the sheet products length and breath dimensions. The separator formed from the sheet product exhibited an ER-temperature profile as follows: 103 ohm-cm at 22° C.; 149 ohm-cm after exposure at 100° C.; greater than 3400 ohm-cm after exposure at 110° C.; and greater than 3400 ohm-cm after exposure at 120° C.

EXAMPLE III

A separator capable of exhibiting very high resistivity upon exposure to heat was prepared from a 2 ply sheet product. The second ply was formed in the same manner as described for the second ply of Example I above.

The first ply was a commercial non-filled microporous polypropylene sheet believed formed by blown film extrusion to produce a non-porous crystalline film which was sequentially cold stretched, hot stretched and annealed to provide its microporous character (Celanese Corp, Celguard 3401).

The first and second sheets were laminated together by pressing at elevated temperature for 20 seconds at 140 psi to form a bonded sheet product.

The plasticizer was extracted from the second sheet material by immersing the sheet product into 1,1,1-trichloroethane for 30 minutes and drying. The resultant sheet product, when tested as a battery separator as described in Example I above exhibited an ER- temperature profile as follows: 27 ohm-cm at ambient temperature; 28 ohm-cm after exposure at 100° C.; 36 ohm-cm after exposure at 110° C., 31 ohm-cm after exposure at 120° C. and 2000 ohm-cm after exposure at 140° C.

What is claimed is:

1. A sheet product having at least two plies comprising:

(a) at least one first ply in the form of a microporous sheet having pores of average pore size of from about 0.005 to about 5 microns in diameter and the pores occupy at least about 10 volume percent of the total volume of the first ply and of a predetermined length and breadth and a thickness of less than 10 mils (0.025 cm), said ply being capable, while a component of the sheet product, of transforming to a substantially non-porous membrane sheet at a transformation temperature of between about 80° C. and 150° C. while substantially maintaining the predetermined length and breadth dimensions; and

(b) at least one second ply in the form of a microporous sheet of a predetermined length and breadth and a thickness of less than 10 mils (0.025 cm) having pores of average pore size of from about 0.005 to about 5 microns in diameter wherein said pores occupy at least about 25 percent of the total volume of said sheet, said second ply being capable, while a component of the sheet product of substantially maintaining said microporous structure and said determined length, breadth and thickness at temperatures of from about ambient to at least about 10° C. greater than the transformation temperature of said first ply; each of said first and second ply being bonded together to provide a unitary sheet product.

2. The sheet product of claim 1 wherein the second ply is stable in form and dimensions at temperatures of from ambient to about 20° C. above the transformation temperature of the first ply and the sheet product exhibits an increase in electrolytic resistivity to at least about 1500 ohm-cm. at the transformation temperature of the first ply of said sheet product.

3. The sheet product of claim 2 wherein the first ply is from abut 0.01 to 4 mils thick.

4. The sheet product of claim 2 wherein the first ply and the second ply are each formed from polymer compositions such that the viscosity of the first ply's composition is substantially equal to or less than the viscosity of the second ply's composition at temperatures ranging from ambient to about 150° C.

5. The sheet product of claim 4 wherein each polymeric composition forming a first ply and a second ply comprise polymers selected from the group consisting essentially of polyolefins, polysulfones, polyvinyl chloride, polyvinyl fluoride, polytetrafluoroethylenepolypropylene copolymer, polyamides, plophenylene oxidi-polystyrene and polycarbonate.

6. A sheet product having at least two plies comprising

(a) at least one firat ply in the form of a microporous sheet having pores of average pore size of from about 0.005 to about 5 microns in diameter and the pores occupy at least about 10 volume percent of the total of the first ply and of a predetermined length and breadth and a thickness of less than 10 mils (0.025 cm) composed of a substantially non-filled polyolefin polymer composition; and

(b) at least one second ply in the form of a microporous sheet of a predetermined length and breadth and of less than 10 mils (0.025 cm) thickness and having pores of average pore size of from 0.005 to about 5 microns in diameter occupying at least about 25 percent of the total volume of said sheet, said sheet composed of a substantially homogeneous admixture of from about 7 to 40 weight percent of a high density polyolefin having a weight average molecular weight of at least 100,000, from 0 to 10 weight percent of a plasticizer for said polyolefin, and from about 50 to 93 weight percent of an inert particulate filler having a particle size of less than about 0.01 cm;

each of said first and second ply being bonded together to provide a unitary sheet product and the viscosity of the polymer composition of each of said first ply being substnatially equal to or less than that of the polymer composition of said second ply at temperatures ranging from ambient to about 150° C. and, at a transformation temperature of between about 80° and 150° C., being sufficiently decreased to exhibit flow to provide a substantially non-porous sheet while substantially maintaining its predetermined length and breadth dimensions.

7. The sheet product of claim 6 wherein the polyolefin of component (b) is a mixture of from 5 to 95 weight percent of a high molecular weight polyolefin and from 95 to 5 weight percent of a low molecular weight polyolefin and the polyolefin of component (a) is a low density polyolefin.

8. The sheet product of claim 6 wherein the polyolefin of component (b) is selected from a polyethylene or polypropylene having a standard load melt index of less than about 0.5 and the polyolefin of component (a) is selected from a polyethylene or polypropylene.

9. The sheet product of claim 6 wherein the plasticizer of component (b) is selected from a petroleum oil and low molecular weight polymers and mixtures thereof; the filler of component (b) is selected from carbon black, coal dust, graphite, oxides and hydroxides of silicon, aluminium, calcium, magnesium, boron, titanium, or mixtures thereof; and the polyolefin is selected from polyethylene or polypropylene.

10. The sheet product of claim 8 wherein the plasticizer of component (b) is selected from a petroleum oil and low molecular weight polymers and mixtures thereof; the filler of component (b) is selected from carbon black, coal dust, graphite, oxides and hydroxides of silicon, aluminium, calcium, mangesium, boron, titanium, or mixtures thereof; and the polyolefin is selected from polyethylene or polypropylene.

11. The sheet product of claim 6 wherein component (b) further has substantially uniformly distributed therein a conductive carbon black in amounts of up to 10 weight percent.

12. The sheet product of claim 7 wherein component (b) further has substantially uniformly distributed therein a conductive carbon black in amounts of up to 10 weight percent.

13. The sheet product of claim 8 wherein component (b) further has substantially uniformly distributed therein a conductive carbon black in amounts of up to 10 weight percent.

14. The sheet product of claim 8 wherein the microporous polyolefin sheet of component (a) is a highly crystalline polypropylene sheet.

15. In a storage battery having positive electrodes, negative electrodes, an electrolytic composition and separators positioned between adjacent electrodes of opposite polarity, wherein the improvement comprises that the separator is a sheet product having at least two plies composed of

(a) at least one first ply in the form of a non-filled microporous sheet having pores of average pore size of from about 0.005 to about 5 microns in diam-

eter and the pores occupy at least about 10 volume percent of the total volume of the first ply and of a predetermined length and breadth and a thickness of less than 10 mils composed of a substantially non-filled polyolefin polymer composition; said sheet being capable, while a component of the sheet product, of transforming to a substantially non-porous membrane sheet at a transformation temperature between about 80° C. and 150° C. while substantially maintaining the predetermined length and breadth dimensions; and

(b) at least one second ply in the form of a microporous sheet of a predetermined length and breadth and a thickness of less than 10 mils having pores of average pore size of from about 0.005 to about 5 microns in diameter wherein said pores occupy at least about 25 percent of the total volume of said sheet, said second sheet composed of a substantially homogeneous admixture of from about 7 to 40 weight percent of a high density polyolefin having a weight average molecular weight of at least 100,000, from 0 to 10 weight percent of a plasticizer for said polyolefin, and from about 50 to 93 weight percent of an inert particulate filler having a particle size of less than 0.01 cm; each of said first and second ply being bonded together into a unitary sheet product and said second ply being capable while contained in a storage battery, of substantially maintaining said microporous structure and said determined length, breadth and thickness at temperatures of from about ambient to at least about 10° C. greater than the transformation temperature of said first ply.

16. The storage battery of claim **15** wherein the battery has at least one electrode containing lithium.

17. The storage battery of claim **16** wherein the polyolefin of component (b) is a mixture of from 5 to 95 weight percent of a high molecular weight polyolefin and from 95 to 5 weight percent of a low molecular weight polyolefin and the polyolefin of component (a) is a low density polyolefin and wherein component (b) having pores of from about 0.005 to about 5 microns in diameter wherein said pores occupy at least about 25 percent of this total volume of said sheet, and component (a) having pores of average pore size of from about 0.005 to about 5 microns in diameter and the pores occupy at least about 10 volume percent of the total volume of the first sheet.

18. The storage battery of claim **16** wherein the polyolefin of component (b) is selected from a polyethylene or polypropylene having a standard load melt index of less than about 0.5 and the polyolefin of component (a) is selected from a polyethylene or polypropylene.

19. The storage battery of claim **16** wherein component (b) is formed from a plasticizer selected from a petroleum oil and low molecular weight polymers and mixtures thereof; a filler selected from carbon black, coal dust, graphite, oxides and hydroxides of silicon, aluminium, calcium, magnesium, boron, titanium, or mixtures thereof; and a polyolefin selected from a polyethylene or polypropylene.

20. The storage battery of claim **17** wherein component (b) is formed from a plasticizer selected from a petroleum oil and low molecular weight polymers and mixtures thereof; a filler selected from carbon black, coal dust, graphite, oxides and hydroxides of silicon, aluminium, calcium, magnesium, boron, titanium, or mixtures thereof; and a polyolefin selected from a polyethylene or polypropylene.

21. The storage battery of claim **15** wherein component (b) further has substantially uniformly distributed therein a conductive carbon black in amounts of up to 10 weight percent.

22. The storage battery of claim **16** wherein component (b) further has substantially uniformly distributed therein a conductive carbon black in amounts of up to 10 weight percent.

23. The storage battery of claim **17** wherein component (b) further has substantially uniformly distributed therein a conductive carbon black in amounts of up to 10 weight percent.

24. A process of forming a sheet product useful as a battery separator comprising

(a) forming a first substantially homogeneous admixture of from 5 to 30 weight percent of a first polyolefin, from about 10 to 60 weight percent of a first plasticizer for said polyolefin and from 30 to 75 weight percent of a first particulate filler; said first plasticizer being soluble in a material which is substantially a non-solvent with respect to the first polyolefin, the second polyolefin and the second filler; said first filler being soluble in a material which is a non-solvent with respect to the first polyolefin, the second polyolefin and the second filler;

(b) forming a second substantially homogeneous admixture of from about 5 to 30 weight percent of a second polyolefin, from about 10 to 60 weight percent of a second plasticizer for said polyolefin and from about 30 to 75 weight percent of a second particulate filler said second polyolefin being selected from high density polyolefins having a weight average molecular weight of at least 100,000; said second plasticizer being soluble in a material which is a substantial non-solvent with respect to the second polyolefin and second filler; said second filler having a particle size of less than 0.01 cm, a surface area of from about 10 to 950 square meters per gram and a pore volume of at least about 0.07 cc/gm;

(c) forming a first sheet of less than 10 mils (0.025 cm) thickness from the first substantially homogeneous admixture;

(d) forming a second sheet of less than 10 mils (0.025 cm) thickness from the second substantially homogeneous admixture;

(e) forming a multilayered sheet having at least one layer composed of the first sheet and at least one layer composed of the second sheet, each layer being bonded to, substantially coextensive with and superimposed on the other layers of the multilayer sheet material; and

(f) extracting from the multilayer sheet material substantially all of the first and second plasticizers and substantially all of the first filler therein to provide a sheet product.

25. The process of claim **22** wherein the polyolefin selected for forming the first homogeneous mixture, the second homogeneous mixture or both comprises a major amount of a polyolefin having a weight average molecular weight of from 100,000 to 500,000 and a minor amount of a polyolefin having a weight average molecular weight of from 500,000 to 2,000,000 and wherein the olefin of the first mixture are polyethylene.

26. The process of claim 24 wherein the first and second plasticizers are soluble in a common material and wherein said multiply sheet product is contacted with said common material to coextract the first and second plasticizers therefrom.

27. The process of claim 24 wherein the multilayer sheet comprises one layer of a first sheet material and one layer of a second sheet material and wherein said first and second sheets are formed simultaneously by coextrusion.

28. The process of claim 24 wherein the first and the second sheet materials each are formed in a thickness of from about 1 to 4 mils (0.0025 to 0.01 cm) thickness.

29. A process of forming a sheet product useful as a battery separator comprising

(a) forming a first sheet comprising an unfilled microporous polyolefin composition of less than 10 mils thickness;

(b) forming a second substantially homogeneous admixture of from about 5 to 30 weight percent of a second polyolefin, from about 10 to 60 weight percent of a second plasticizer for said polyolefin and from about 30 to 75 weight percent of a second particulate filler which is inert with respect to the components of the battery system in which it is to be used; said second polyolefin being selected from high density polyolefins having a weight average molecular weight of at least 100,000; said second plasticizer being soluble in a material which is a substantial non solvent with respect to the second polyolefin and said second filler; said second filler having a particle size of less than 0.01 cm, and surface area of from about 10 to 950 square meters per gram and a pore volume of at least about 0.07 cc/gm; said second composition having a viscosity substantially equal or greater than that of the first composition at temperatures from ambient to about 150° C.,

(c) superimposing and bonding at least one first sheet onto a second sheet to form a multilayer sheet wherein each layer is bonded to, substantially coextensive with and superimposed on the other layers of the multilayer sheet; and

(d) extracting from the multilayer sheet material substantially all of the second plasticizer from the second sheet material to provide a sheet product.

30. The process of claim 29 wherein said substantially non-filled microporous polyolefin sheet bonded to said first sheet is formed from polypropylene, exhibits at least about 30 percent crystallinity, has an average pore size of from about 10^{-6} cm to about 10^{-4} cm and a void volume of at least about 20 percent.

* * * * *

Appendix V

US005565281A

United States Patent [19]

Yu et al.

[11] Patent Number: 5,565,281

[45] Date of Patent: Oct. 15, 1996

[54] **SHUTDOWN, BILAYER BATTERY SEPARATOR**

[75] Inventors: **Wei-Ching Yu**; **Margaret W. Geiger**, both of Charlotte, N.C.

[73] Assignee: **Hoechst Celanese Corporation**, Somerville, N.J.

[21] Appl. No.: **348,630**

[22] Filed: **Dec. 2, 1994**

[51] **Int. Cl.**[6] **H01M 2/18**

[52] **U.S. Cl.** **429/62**; 429/145

[58] **Field of Search** 429/62, 144, 145, 429/254; 204/252, 296; 428/316.6, 421, 422, 913

[56] **References Cited**

U.S. PATENT DOCUMENTS

3,426,754	2/1969	Bierenbaum et al.	128/156
3,558,764	1/1971	Isaacson et al.	264/210
3,679,538	7/1972	Druin et al.	161/159
3,801,404	4/1974	Druin et al.	156/229
3,801,692	4/1974	Zimmerman	264/210
3,843,761	10/1974	Bierenbaum et al.	264/210
3,853,601	12/1974	Taskier	117/98
4,138,459	2/1979	Brazinsky et al.	264/154
4,539,256	9/1985	Shipman	428/315.5
4,650,730	3/1987	Lundquist et al.	429/62
4,726,989	2/1988	Mrozinski	428/315.5
4,731,304	3/1988	Lundquist et al.	429/62
4,994,335	2/1991	Kamei et al.	429/254
5,240,655	8/1993	Troffkin et al.	264/28
5,281,491	1/1994	Rein et al.	429/62
5,385,777	1/1995	Higuchi et al.	429/254 X
5,389,433	2/1995	Chang et al.	429/145 X
5,409,588	4/1995	Mushiake et al.	429/144 X

FOREIGN PATENT DOCUMENTS

0577387A1	1/1994	European Pat. Off. .
55-105968	11/1981	Japan .
57-095070	6/1982	Japan .
57-172657	10/1982	Japan .
06020671	11/1986	Japan .
6-20671	1/1994	Japan .

Primary Examiner—Anthony Skapars

Attorney, Agent, or Firm—R. H. Hammer, III

[57] **ABSTRACT**

The present invention is directed to a shutdown, bilayer battery separator and a process for making the same. A first microporous membrane with shutdown capability and a second microporous membrane with strength capability are joined together in face-to-face contact. The face of the first membrane being adhered by calendaring, adhesives, or welding, to the face of the second membrane, and the separator having a thickness of less than 3 mils, and a puncture strength, as measured from the second microporous membrane, of greater than 1900 g-mm, and a peel strength of greater than 1 grams/centimeter.

11 Claims, No Drawings

SHUTDOWN, BILAYER BATTERY SEPARATOR

FIELD OF THE INVENTION

The present invention is directed to a shutdown, bilayer battery separator.

BACKGROUND OF THE INVENTION

Shutdown, bilayer battery separators are known. For example, see U.S. Pat. Nos. 4,650,730; 4,731,304; 5,240,655; 5,281,491; and Japanese Kokai No. 6-20671, each of the foregoing is incorporated herein by reference.

In batteries, the anode and cathode are separated from one another by a separator. Today, "lithium batteries" are very popular because they are able to generate high energy outputs. The lithium battery market can be divided into two groups, the "primary" lithium battery and the "secondary" lithium battery. The primary lithium battery is a disposable battery, while the secondary lithium battery, is a rechargeable battery. A problem associated with the secondary lithium battery is its potential for short circuiting. Short circuiting arises when the separator ruptures and allows the anode and the cathode to come into direct electrical communication with one another. This short circuit may manifest itself with a rapid evolution of heat. This rapid evolution of heat can cause the battery to explode. Accordingly, the shutdown battery separator was developed.

The shutdown battery separator generally comprises two polymerically dissimilar and juxtaposed microporous membranes. One microporous membrane is chosen for its relatively low melting point and the other for its relative strength. For example, the low melting point membrane may be a polyethylene material and the strength membrane may be a polypropylene material. The polyethylene microporous membrane has a melting point of about 130° C. This is sufficiently low that, in the event of a short circuit in a lithium battery, the heat generated will melt the polyethylene so that it shuts down, or fills in the pores of the separator, and thereby stops or inhibits the likelihood of a short circuit. The polypropylene membrane, which has a substantially higher melting point, approximately 160° C., provides strength to the separator so that it maintains the separator's integrity in the event of a short circuit.

In U.S. Pat. No. 4,650,730 and 4,731,304, shutdown, bilayer battery separators of the foregoing type are disclosed. In the examples, separator thicknesses of 3–4 mils are disclosed. The methods of making these battery separators are disclosed as: 1) two discrete films containing extractable fillers are made, then bonded together, and then the fillers are extracted; 2) a bilayer film, containing extractable fillers, is coextruded and the fillers are subsequently extracted; 3) one film made by an extrusion, annealing and stretching process, and a second film made with extractable fillers are bonded together, and then the fillers are subsequently extracted; 4) a first film is coated with a second material. In U.S. Pat. No. 5,240,655, a shutdown, bilayer battery separator, of the above-mentioned type, is made by coextruding the discrete layers, and then stretching and annealing the extruded bilayer film. In U.S. Pat. No. 5,281,491, the shutdown, bilayer battery separator, of the above-mentioned type, is made by coextruding the first and second films that contain an extractable material, and the extractable material is subsequently removed.

In Japanese Kokai 6-20671, a shutdown, bilayer battery separator, of the above-mentioned type, has a thickness of about 1 to 2 mils, a penetration energy (from FIG. 1) of about 1660 g-mm (this value is equivalent to about 1800 g-mm when converted into units comparable with the test method disclosed herein), and a peel strength of 0.1 to 1 gram/centimeter. The separator is made by a process in which two discrete films, made by the process set forth in U.S. Pat. Nos. 3,679,538 or 3,801,404, are bonded together by calendaring at a temperature of 134° C.

A problem with the foregoing battery separators is that, while they provide the necessary shutdown characteristics, they are deficient in one or more of the following qualities: thinness or penetration energy for puncture strength) or peel strength. In the manufacture of batteries, it is important to have extremely thin separators, so that: the energy density of the battery maybe increased; and the size of the battery, as well as, the electrical resistance across the separator, may be reduced. Good penetration energy is important in battery manufacture, particularly in the manufacture of "jelly roll" type batteries because the surfaces of the anode and the cathode can be sufficiently rough that they can puncture these extremely thin separators during manufacture. Good peel strength is important in battery manufacture because it prevents delamination of the separator. Accordingly, there is a need to produce an extremely thin, shutdown battery separator that has a sufficient penetration energy and peel strength to withstand the rigors of battery manufacture.

SUMMARY OF THE INVENTION

The present invention is directed to a shutdown, bilayer battery separator. A first microporous membrane with shutdown capability and a second microporous membrane with strength capability are joined together in face-to-face contact. The face of the first membrane being adhered by calendaring, adhesives, or welding, to the face of the second membrane, and the separator having a thickness of less than 3 mils, and a puncture strength, as measured from the second microporous membrane, of greater than 1900 g-mm, and a peel strength of greater than 1 grams/centimeter.

Additionally, the present invention is directed to a process for making a shutdown, bilayer battery separator comprising the steps of:

1) forming a first microporous membrane by
   a) extruding a first polymer to form a first sheet,
   b) annealing the first sheet,
   c) stretching the first sheet;
2) forming a second microporous membrane by
   a) extruding a second polymer to form a second sheet,
   b) annealing the second sheet,
   c) stretching the second sheet; and
3) bonding the first membrane in face-to-face contact with the second membrane by a method comprising calendaring at a temperature less than 134° C., adhering with adhesives, and welding.

DESCRIPTION OF THE INVENTION

The present invention shall be described in further detail below by way of the following detailed description and the non-limiting examples.

Shutdown battery separator, as used herein, refers to the type of separator described in U.S. Pat. Nos. 4,640,730; 4,731,304; 5,240,655; 5,281,491; Japanese Kokai No. 6-20671; and U.S. patent application Ser. No. 08/341,239,

filed Nov. 17, 1994. now abandoned, and entitled "Methods of Making Cross-ply Microporous Membrane Battery Separators, and the Battery Separators Made Thereby", each of which is incorporated herein by reference.

These battery separators are preferably bilayer, i.e., have two different layers, one that provides the shutdown characteristics and the other that provides the strength characteristics. These separators, however, are not so limited and they may have more than two layers. Since the bilayer separator is preferred, it shall be discussed hereinafter.

These separators are made with at least two layers, one being a microporous membrane having shutdown capabilities and the other being a microporous membrane having strength capabilities. The shutdown capabilities refer to the principal, but not necessarily the sole, function of the layer which is the ability to close the micropores of the separator in the event of a short circuit. This typically means that the shutdown layer will melt, at some temperature, blind the pores of the separator, and thereby terminate the short circuit by prohibiting ion migration across the separator. Preferably, in lithium batteries, the shutdown capabilities can be provided by a material that will melt at a temperature at least 20° C. below the melting temperature of the lowest melting electrode (e.g., the lithium material, the melting point of lithium is about 180° C.). An example of such a material is polyethylene or a blend comprising substantially polyethylene, or a copolymer of polyethylene. The strength capabilities refer to the principal, but not necessarily the sole, function of the layer which is the ability to maintain the integrity of the separator in the event of a short circuit, as well as, to facilitate the manufacture of the battery. Preferably, in lithium batteries, the strength capabilities can be provided by a material that will melt at a temperature at about or greater than the melting temperature of the lowest melting electrode (e.g., the lithium material). An example of such a material is polypropylene or a blend comprising substantially polypropylene, or a copolymer of polypropylene.

The thickness of these separators is less than 3 mils (about 75 microns). These separators preferably range in thickness from about 0.9 mils (about 22 microns) to less than 3 mils (about 75 microns). Measurement details are set forth below.

The puncture strength (penetration energy) should be greater than 1900 grams-millimeters, when measured from the strength enabling side of the separator. Preferably, the puncture strength should be greater than 2000 gram-millimeters and, most preferably, the puncture strength should be greater than 2400 grams-millimeters. Measurement details are set forth below. The strength enabling side of a shutdown, bilayer battery separator made of a polyethylene layer and a polypropylene layer is the polypropylene side.

The peel strength should be greater than 1 gram/centimeter. Preferably, the peel strength should be greater than or equal to 4 grams/centimeters and, most preferably, the peel strength should be greater than or equal to 8 grams/centimeter. Measurement details are set forth below.

The process, by which the inventive separators are made, broadly comprises making a first microporous membrane, making a second microporous membrane, and bonding together the first membrane and the second membrane. Regarding the preferred method for making the first and the second membranes, the process requires the following steps: extruding a polymer to form a sheet; annealing the sheet; and stretching the annealed sheet. The specific methods for making these sheets, particularly polyethylene or polypropylene, are within the skill of the art. By way of non-limiting example, the following references, each of which is incorporated herein by reference, illustrate possible routes for making the sheets: U.S. Pat. Nos: 3,426,754; 3,558,764; 3,679,538; 3,801,404; 3,801,692; 3,843,761; 3,853,601; 4,138,459; 4,539,256; 4,726,989; 4,994,335; and U.S. patent application Ser. No. 08/341,239, filed Nov. 17, 1994. Further specifics regarding the preferred method fir making these sheets may be found in the non-limiting examples below.

The first and second membranes are preferrably oriented, with respect to one another in the same direction. Cross-plying, as set forth in U.S. application Ser. No. 08/341,239, incorporated by reference, is also contemplated.

Regarding the preferred methods for bonding the first membrane to the second membrane, several bonding methods are contemplated. Broadly, the bonding methods include calendaring at a temperature less than 134° C., adhering with adhesives, and welding. Preferably, bonding is accomplished by calendaring, with nips closed, at a temperature of about 130° C. (a peel strength of greater than 1 gram/centimeter is thereby obtained). The application of adhesives may include: air atomizing; gravure/screen printing; hydraulic spraying; and ultrasonic spraying. The choice of adhesive and the rate of adhesive application must be chosen so that the separator's porosity is not adversely effected. The welding technique includes thermal welding and ultrasonic welding. The amount of energy for either welding procedure and the pattern of welds should be chosen so that the separator's porosity is not adversely effected.

Further information about the foregoing inventions may be obtained from the following non-limiting examples. The test methods referenced to herein are set forth below.

Test Methods	
Gurley	ASTM-D726(B) Gurley is a resistance to air flow measured by the Gurley densometer (e.g. Model 4120). Gurley is the time in seconds required to pass 10 cc of air through one square inch of product under a pressure of 12.2 inches of water.
Basis Weight	Basis weight is determined by cutting three - one square foot samples across the width of the sample and weighing them on a precision balance with accuracy to 0.0001 grams. The three (3) samples are averaged and compared to tolerance limits.
Thickness	Method: T411om-83 developed under the auspices of the Technical Association of the Pulp and Paper Industry. Thickness is determined using a precision micrometer with a ½inch diameter, circular shoe contacting the sample at seven (7) PSI. Ten (10) individual micrometer readings taken across the width of the sample are averaged.
Shrinkage, MD	ASTM D-1204 (60 min. @ 90° C.) Three (e) separate lengths of stretched product of approximately ten centimeters are measured across the width of the sample in the machine direction (MD). The sample is exposed to air at 90° C. for one hour, the lengths are re-measured, the percentage shrinkage of the original length is calculated for each sample, and the results averaged.
Tensile Strength	ASTM D-882
Puncture Strength	Ten measurements are made across the width of the stretched product and averaged. A Mitech Stevens LFRA Texture Analyzer is used. The needle is 1.65 mm in diameter with 0.5 mm radius. The rate of descent is 2 mm/sec and the amount of deflection is 6 mm. The film is held tight in the clamping device with a central hole of 11.3 mm. The displacement (in mm) of the film that was pierced by the needle was recorded against the resistance force (in gram force) developed by the film. The

-continued

Test Methods	
	penetration energy (puncture strength) was defined as the product of the resistance force and the displacement at the maximum point.
Peel Strength	Peel strength is measured using a tension and compression tester to determine the force in grams required to separate two one-inch wide sections of bonded membrane. The peel rate is 6 inches/minute. Three measurements are taken across the web and averaged.
Melt Index	ASTM D 1238, (P); PP: 230° C., 2.16 Kg; PE: 190° C., 2.16 Kg

EXAMPLE 1

A polyethylene sheet product is formed by extruding a high density polyethylene with a melt index of 0.6 g/10 min and a density of 0.96 g/cc. Extrusion conditions are summarized in Table 1.

A polypropylene sheet product is formed by extruding an isotactic polypropylene homopolymer having a melt index of 1.5 g/10 min and a density of 0.90 g/cc. Extrusion conditions are summarized in Table 1.

TABLE 1

Extrusion conditions		
	Polyethylene	Polypropylene
Die Temperature, °C.	195	212
Melt Temperature, °C.	220	228
Air ring height, inches	0.75	2.25
Take up speed, fpm	80	80
Draw down ratio	90 to 1	82 to 1
Blow up ratio	1	1
Air plenum pressure, inches of water	3.5	2.5
Weighted gauge, mil	0.58	0.63
Birefringence	0.031	0.016

The sheet products are annealed in an oven under slight tension at a constant temperature for 10 minutes. The annealing temperature for polypropylene is 140° C. and for polyethylene, 115° C.

The annealed material is then subjected to a cold stretch at room temperature, followed by a hot stretch at elevated temperatures, and then by heat setting with relaxation of the film. Stretching conditions are summarized in Table 2. The stretched products are microporous films with the properties summarized in Table 3.

TABLE 2

Stretching Conditions		
	Polyethylene (PE)	Polypropylene (PP)
Cold Stretch, %	30	50
Hot Stretch, %	200	150
Hot Stretch Temperature, °C.	115	140
Relaxation, %	50	50
Relaxation Temperature, °C.	120	140

The two ply stretched film is slit along the edges and deplied. Using four unwind stands, two plies of polyethylene and two plies of polypropylene are mounted in the sequence of polyethylene on the top, the two polypropylene plies, and a polyethylene ply on the bottom. The four plies are passed through the oven under slight tension at 130° C. with nips closed. Two polyethylene-polypropylene bilayers are produced after separating the polypropylene plies. Adhesion between the polyethylene and polypropylene is about 8 grams/cm (the peel strength, at these values, does not appear to be significantly dependent upon peel rate of 0.25 inch/min to 6 inch/min). The properties of the bilayer separator are summarized in Table 3.

TABLE 3

Stretched Microporous Film and Bilayer Properties			
	PE	PP	Bilayer
Gurley, sec-in^2	10	16	25
Thickness, mil	0.51	0.50	1.06
Basis Weight, mg/cm^2	0.77	0.73	
Porosity, %	36	38	
Machine direction shrinkage, %	1	2	3
Machine direction stress, kpsi	24	25	25
Machine direction elongation, %	62	48	43
Transverse direction stress, kpsi	1.8	2.0	1.8
Transverse direction elongation, %	860	690	800
Electrical resistance, mOhms-in$_2$	5	4	6
Puncture strength, grams-mm			2400

EXAMPLE 2

A polyethylene sheet product is formed by extruding a high density polyethylene with a melt index of 0.3 g/10 min and a density of 0.96 g/cc. Extrusion conditions are summarized in Table 4.

A polypropylene sheet product is formed by extruding an isotactic polypropylene homopolymer having a melt index of 1.5 g/10 min and a density of 0.90 g/cc. Extrusion conditions are summarized in Table 4.

TABLE 4

Extrusion conditions		
	PE	PP
Die Temperature, °C.	180	210
Melt Temperature, °C.	204	224
Air ring height, inches	1.75	2.0
Take up speed, fpm	60	50
Draw down ratio	115 to 1	120 to 1
Blow up ratio	1	1
Air plenum pressure, inches of water	1.2	1.2
Weighted gauge, mil	0.61	0.57
Birefringence	0. 035	0.016

The sheet products are annealed in an oven under slight tension at a constant temperature for 10 minutes. The annealing temperature for polypropylene is 140° C. and for polyethylene, 115° C. The annealing step increases the crystallinity of the sheet products.

The annealed material is then subjected to a cold stretch at room temperature, followed by a hot stretch at elevated temperatures, and then by heat setting with relaxation of the film. Stretching conditions are summarized in Table 5. The stretched products are microporous films with the properties summarized in Table 6.

TABLE 5

	Stretching Conditions	
	Polyethylene	Polypropylene
Cold Stretch, %	45	25
Hot Stretch, %	150	140
Hot Stretch Temperature, °C.	115	140
Relaxation, %	50	50
Relaxation Temperature, °C.	115	140

The two ply stretched film is slit along the edges and deplied. Using four unwind stands, two plies of polyethylene and two plies of polypropylene are mounted in the sequence of polyethylene on the top, the two polypropylene plies, and a polyethylene ply on the bottom. The four plies are passed through the oven under slight tension at 130° C. with nips closed. Two polyethylene-polypropylene bilayers are produced after separating the polypropylene plies. Adhesion between the polyethylene and polypropylene is about 8 grams/cm (the peel strength, at these values, does not appear to be significantly dependent on peel rate OF 0.25 inch/min to 6 inch/min). The properties of the bilayer are summarized in Table 6.

TABLE 6

Stretched Microporous Film and Bilayer Properties			
	Poly-ethylene	Poly-propylene	Bilayer
Gurley, sec-in^2	8	10	16
Thickness, mil	0.50	0.50	1.03
Basis Weight, mg/cm^2	0.75	0.74	
Porosity, %	40	39	
Puncture strength, grams-mm			2060

The present invention maybe embodied in other specific forms without departing from the spirit or essential attributes thereof, and, accordingly, reference should be made to the appended claims, rather than to the foregoing specification, as indicating the scope of the invention.

We claim:

1. A shutdown, bilayer battery separator comprising:

a first microporous membrane having shutdown capability and having a face; and

a second microporous membrane having strength capability and having a face; and

said first membrane and said second membrane being joined together in face-to-face contact; and

said separator having a thickness less than 3 mils; a puncture strength, as measured from said second microporous membrane, of greater than 1900 grams-millimeters; and a peel strength of greater than 1 gram/centimeter.

2. The separator according to claim **1** wherein said puncture strength is greater than 2000 grams-millimeter.

3. The separator according to claim **1** wherein said puncture strength is greater than or equal to 2400 grams-millimeter.

4. The separator according to claim **1** wherein said peel strength is greater than or equal to 4 grams/centimeter.

5. The separator according to claim **1** wherein said peel strength is greater than or equal to 8 grams/centimeter.

6. The separator according to claim **1** wherein said thickness ranges from about 0.9 mils to less than 3 mils.

7. The separator according to claim **1** wherein said first membrane's melting temperature is at least 20° C. less than said second membrane's melting temperature.

8. The separator according to claim **1** wherein said first membrane is made from a polyethylene material and said second membrane is made from a polypropylene material.

9. A battery comprising the separator set forth in claim **1**.

10. A shutdown, bilayer battery separator comprising:

a polyethylene, microporous membrane having a face;

a polypropylene, microporous membrane having a face;

said polyethylene membrane and said polypropylene membrane being joined together in face-to-face contact; and

said separator having a thickness less than 3 mils; a puncture strength, as measured from the polypropylene membrane, greater than or equal to 2400 gram-millimeter; and a peel strength greater than or equal to 8 grams/centimeter.

11. A battery comprising the separator set forth in claim **10**.

* * * * *

Appendix W

US005952120A

United States Patent [19]

Yu et al.

[11] Patent Number: 5,952,120

[45] Date of Patent: Sep. 14, 1999

[54] **METHOD OF MAKING A TRILAYER BATTERY SEPARATOR**

[75] Inventors: **Wei-Ching Yu**, Charlotte; **Shawn E. Hux**, Gastonia, both of N.C.

[73] Assignee: **Celgard LLC**, Charlotte, N.C.

[21] Appl. No.: **08/839,664**

[22] Filed: **Apr. 15, 1997**

[51] **Int. Cl.**[6] **H01M 2/14**

[52] **U.S. Cl.** **429/144**; 29/623.4; 264/171.11; 264/175; 264/288.4

[58] **Field of Search** 429/144, 247; 29/623.1, 623.4; 264/171.1, 173.11, 175, 288.4, 291

[56] **References Cited**

U.S. PATENT DOCUMENTS

4,650,730	3/1987	Lundquist et al.	429/62
4,731,304	3/1988	Lundquist et al.	429/62
5,240,655	8/1993	Troffkin et al.	429/254 X
5,281,491	1/1994	Rein et al.	429/145 X
5,691,077	11/1997	Yu	429/62

FOREIGN PATENT DOCUMENTS

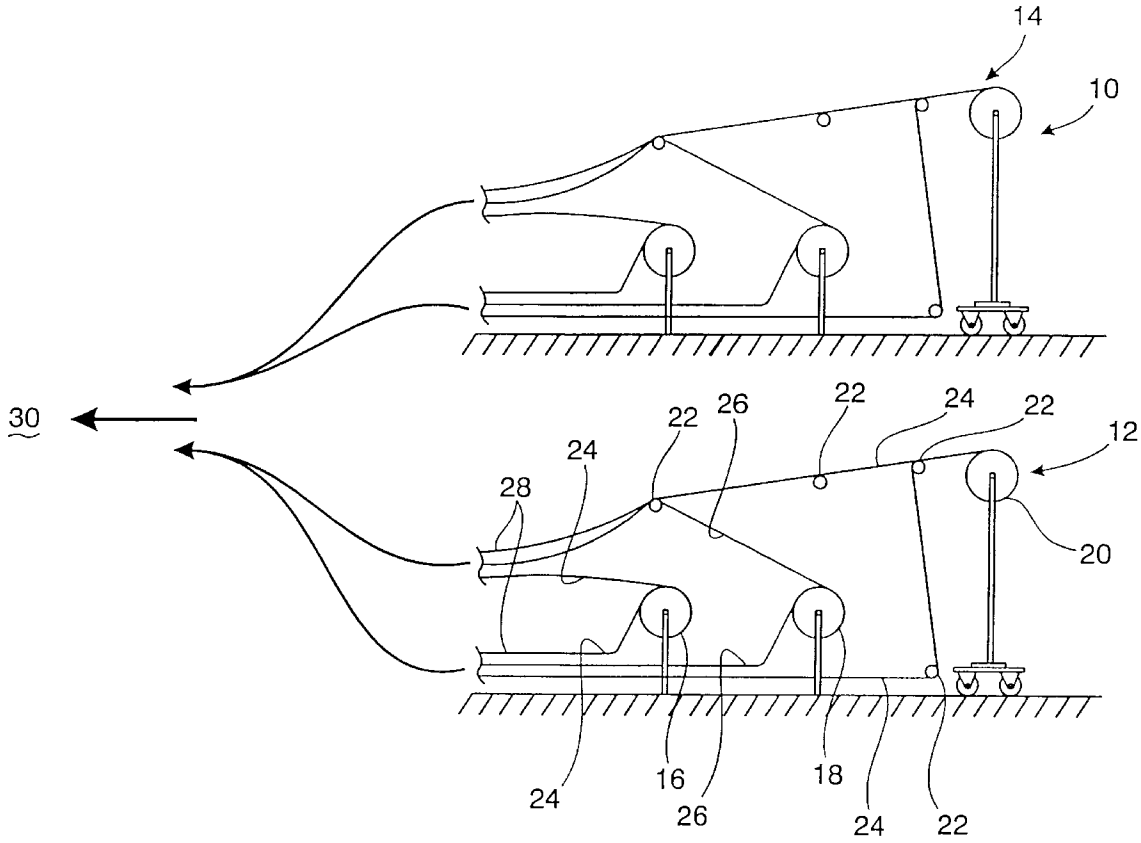
6-98394	5/1994	Japan .
6-98395	5/1994	Japan .
5-56320	3/1995	Japan .
2298 817	9/1996	United Kingdom .

Primary Examiner—Steven J. Kalafut
Attorney, Agent, or Firm—Robert H. Hammer III

[57] **ABSTRACT**

A method of making a trilayer, shutdown battery separator has the following steps: extruding a polyethylene precursor; extruding a polypropylene precursor; forming a trilayer precursor, the trilayer precursor having the polyethylene precursor sandwiched between two polypropylene precursors; bonding the trilayer precursor; annealing the trilayer precursor; stretching the trilayer precursor; and forming thereby the battery separator.

14 Claims, 2 Drawing Sheets



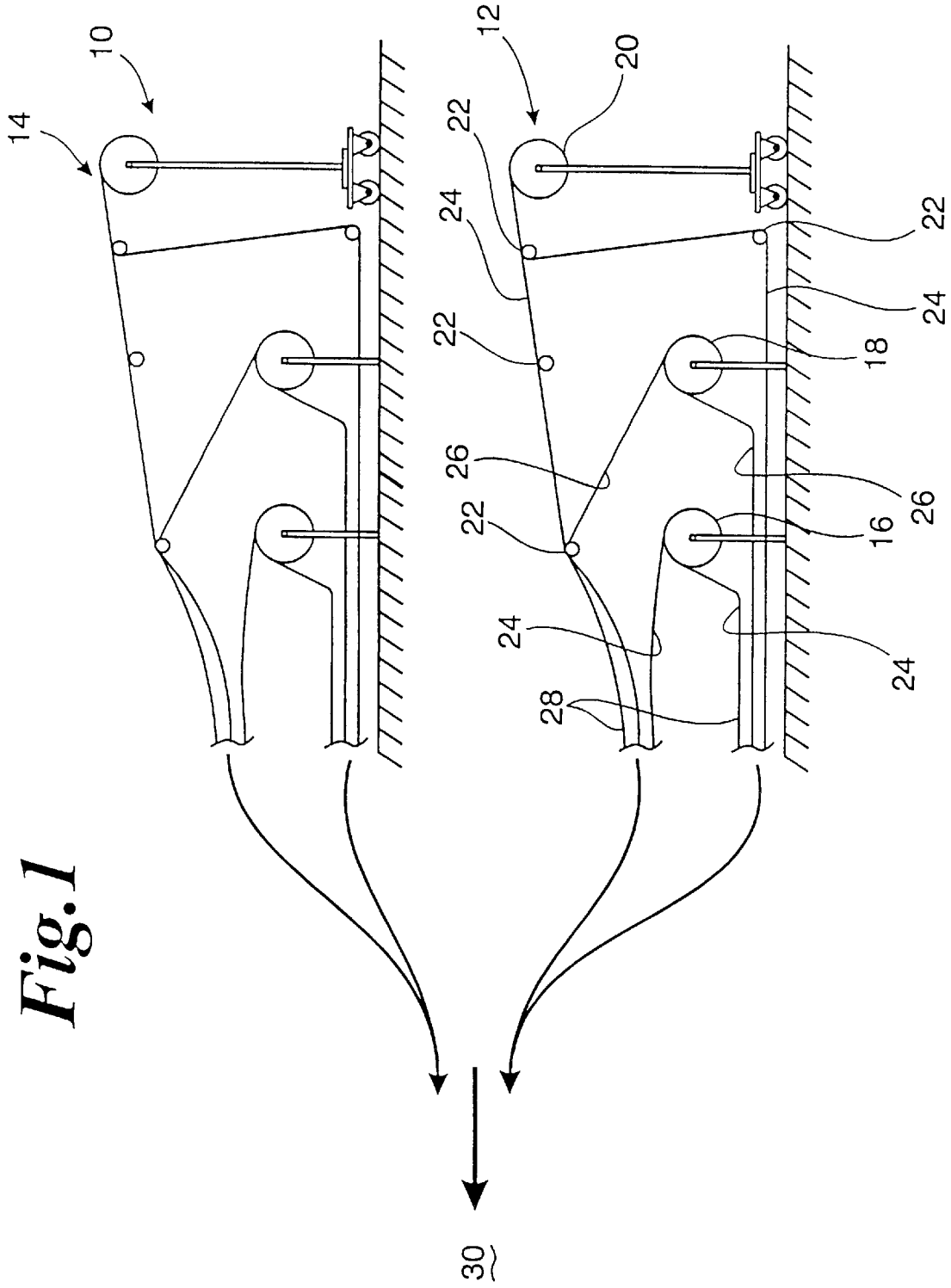


Fig. 1

Fig.2

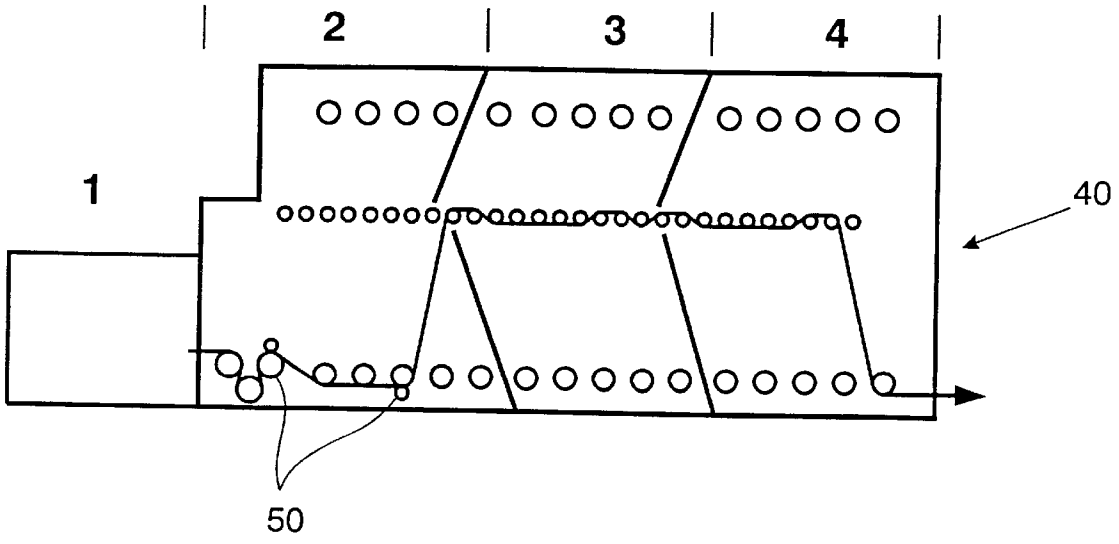
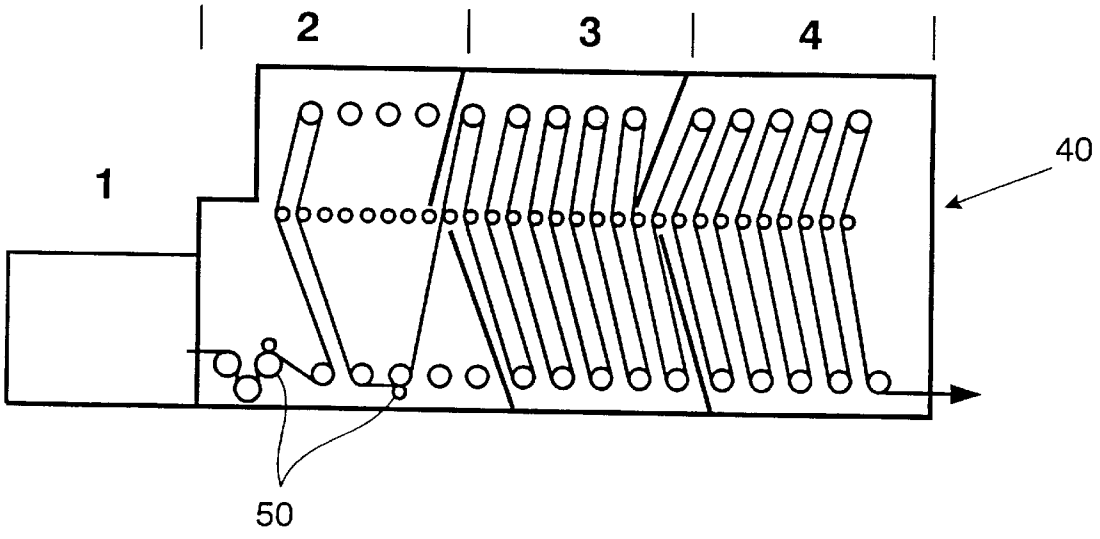


Fig.3



METHOD OF MAKING A TRILAYER BATTERY SEPARATOR

FIELD OF THE INVENTION

The invention is directed to a method of making a trilayer, shutdown battery separator.

BACKGROUND OF THE INVENTION

Trilayer, shutdown battery separators are known. See: Japanese Patent Application Nos. 98395/1994 and 98394/1994 both filed May 20, 1994 by Ube Industries, Ltd. (the Ube trilayer separator); U.S. patent application Ser. No. 359,772 filed Dec. 20, 1994, now abandoned, by Hoechst Celanese Corporation (the CELGARD® Separator); Japanese Patent Application No. 55550/1995 filed Mar. 15, 1995 by Nitto Denko Kogyo K.K. (the Nitto Denko trilayer separator); and Japanese Patent Application No. 56320/1995 filed Mar. 15, 1995 by Kureha Chemical Industry Co., Ltd. (the Kureha trilayer separator).

Trilayer, shutdown battery separator are porous films and have become a commercial success, within the battery industry, particularly within the secondary (or rechargeable) lithium battery industry. The success is believed to be due, in part, to the separator's puncture strength and the separator's ability to reduce the risk of internal short circuit within the battery. The separator's puncture strength is, at least, important because it enables the separator to withstand the rigors of battery manufacture. The separator's ability to reduce the risk of internal short circuit is believed to be important because internal short circuit may lead to unexpected battery rupture.

The Ube trilayer separator is a porous trilayer film having a polypropylene-polyethylene-polypropylene construction. Ube's process includes the steps of: extruding a polypropylene non-porous precursor; extruding a polyethylene non-porous precursor; forming the polypropylene-polyethylene-polypropylene non-porous trilayer precursor; bonding the trilayer precursor together at a temperature ranging from 120–140° C. between nip rollers and then taking up the precursor for subsequent processing; heat-treating (annealing) the bonded precursor at a temperature range from 110–140° C.; and stretching the bonded, annealed precursor to form the porous, trilayer separator. The stretching step consisted of three discrete steps: cold-stretching (temperature ranging from −20° to 50° C. and a draw ratio of 5–200%); hot-stretching (temperature ranging from 70–130° C. and a draw ratio of 100–400%); and heat-treating, also believed to be referred to as annealing and/or relax (temperature ranging from 75–175° C. and a draft ratio of −10 to −50% or 0%).

The CELGARD® separator is a porous trilayer film having a polypropylene-polyethylene-polypropylene construction. The CELGARD separator process includes the steps of: forming a porous polypropylene precursor; forming a porous polyethylene precursor; forming a porous trilayer precursor; and bonding the porous trilayer precursor to form the trilayer battery separator.

The Nitto Denko separator is a porous trilayer film having polypropylene-polyethylene-polypropylene construction. The Nitto Denko separator process includes the steps of: co-extruding a trilayer precursor having a polypropylene-polyethylene-polypropylene non-porous construction; annealing (heat-treating) the trilayer precursor; and stretching the annealed trilayer precursor to form the porous trilayer battery separator.

The Kureha separator is a porous trilayer film having a polypropylene-polyethylene-polypropylene construction. The Kureha separator process includes the steps of: co-extruding a trilayer precursor, the precursor containing a pore forming aid (e.g., a fine inorganic particle or a solvent extractable material); and forming the pores in the precursor by stretching the particle-loaded precursor or by solvent extraction of the extractable-laden precursor.

There is a need to continue to improve the process for making trilayer shutdown separators so that: manufacturing throughput can be increased while minimizing the capital investment; and manufacturing cost can be minimized by minimizing material handling costs and increasing production quality.

SUMMARY OF THE INVENTION

A method of making a porous, trilayer, shutdown battery separator has the following steps: extruding a non-porous polyethylene precursor; extruding a non-porous polypropylene precursor; forming a non-porous trilayer precursor, the trilayer precursor having the polyethylene precursor sandwiched between two polypropylene precursors; simultaneously bonding and annealing the trilayer precursor to form a bonded and annealed trilayer precursor; stretching the bonded and annealed trilayer precursor; and forming thereby the porous battery separator.

A method of making a trilayer, shutdown battery separator has the following steps: extruding a non-porous polyethylene precursor; extruding a non-porous polypropylene precursor; forming a non-porous trilayer precursor, the trilayer precursor having the polyethylene precursor sandwiched between two polypropylene precursors; bonding the trilayer precursor to form a bonded precursor; annealing the bonded precursor; and stretching the bonded, annealed precursor to form the battery separator. The annealing step further includes annealing in two zones, each zone at a different temperature.

DESCRIPTION OF THE DRAWINGS

For the purpose of explaining the invention, there is shown in the drawings various preferred aspects of the invention; it being understood, however, that this invention is not limited to the precise arrangements and instrumentalities shown.

FIG. **1** is a schematic illustration of trilayer precursor formation set-up.

FIG. **2** is a schematic illustration of a bonding/annealing string-up configuration.

FIG. **3** is a schematic illustration of another bonding/annealing string-up configuration.

DETAILED DESCRIPTION OF THE INVENTION

A trilayer, shutdown battery separator refers to a porous film for use in electrochemical cells, e.g., batteries, particularly secondary (or rechargeable) batteries, such as lithium batteries. This trilayer separator has a polypropylene-polyethylene-polypropylene construction. The separator has a thickness of less than 3 mils (about 75 microns). The separator's thickness preferably ranges between 0.5 mils (about 12 microns) and 1.5 mils (about 38 microns). Most preferably, the separator's thickness is about 1 mil (about 25 microns). Preferably, the separator has a permeability, as measured by Gurley, of less than 50 sec. Preferably, the separator has a puncture strength of at least 300 grams. Preferably, the separator has an interply adhesion strength of at least 5 grams/inch. The separator's pores have an average area in the range of 0.003 to 0.010 square microns with an aspect ratio ranging from 3 to 5.

The method of making the trilayer, shutdown battery separator generally comprises the steps of: extruding a

non-porous polypropylene precursor; extruding a non-porous polyethylene precursor; forming a non-porous trilayer precursor where the polyethylene precursor is sandwiched between the polypropylene precursors; bonding the trilayer precursor; annealing the trilayer precursor; and stretching the bonded and annealed, non-porous trilayer precursor to form the porous battery separator. Each of the steps shall be discussed in greater detail below.

Extruding the polypropylene or a polyethylene precursor refers to the conversion of resin into a non-porous film. Extrusion is performed in a conventional manner, preferably through a circular dye, so that the parison may be collapsed for subsequent processing (e.g. to form a 2-ply structure). Varying the precursor thickness, to obtain the desired final separator thickness, is well known. Polypropylene refers to polypropylene, or a blend comprising primarily polypropylene, or a copolymer of polypropylene. An exemplary polypropylene is Escorene PP 4292 commercially available from Exxon Chemical Company, Houston, Tex. Polyethylene refers to polyethylene, or a blend comprising primarily polyethylene, or a copolymer of polyethylene. An exemplary polyethylene is Fina HDPE 7208 commercially available from Fina Oil and Chemical Company, Dallas, Tex., and Hizex HDPE 5202B commercially available from Mitsui Petrochemical Industries, Ltd.

Forming the trilayer precursor may be accomplished as shown in FIG. **1**. Scheme **10** includes a first level layout **12** and a second level layout **14**. Layouts **12** and **14** are identical, but for elevation (to efficiently use space), so only layout **12** will be discussed in detail. Layout **12** comprises three unwind stations **16**, **18**, and **20**. Stations **16** and **20** support rolls of polypropylene precursor (i.e., one roll—2 plies), and station **18** supports a roll of polyethylene precursor (i.e., one roll—2 plies). To avoid wrinkling or creasing , these precursors are handled (as much as possible), in 2-ply form. The polypropylene precursors **24** and polyethylene precursor **26** are unwound from their rollers, deplyed, in some cases with the assistance of guide rollers **22**, and then replied to form trilayer precursors **28**. From scheme **10**, four (4) trilayer precursors **28** are formed.). A minimum of at least two trilayer precursors is preferred for process economics. At least four trilayer precursors are preferred so to avoid the wrinkle problem and to more efficiently use equipment (economic reasons to facilitate production efficiency, at least four trilayer precursors are (and preferably eight or more) simultaneously passed through the following steps of bonding, annealing and stretching. The precursors **28** are forwarded to the next processing operation (not shown).

Bonding and annealing of the trilayer precursor may be performed in a multizone oven **40**, each zone capable of maintaining a distinct temperature. See, for example, FIGS. **2–3**. Bonding is for joining together the polypropylene-polyethylene-polypropylene precursors to form the trilayer precursor. The interply adhesion should be at least 5 gram/inch. Bonding may be performed at a temperature ranging from 125–135° C. and between nip rollers. Preferably, bonding is performed at a temperature ranging from 128–130° C. Annealing is to form crystal structures in the polymers to facilitate pore formation in the stretching step. Annealing is influenced by temperature and time. Accordingly, the multizoned oven capable of maintaining several distinct temperatures may be advantageous. Annealing of the trilayer precursor should be conducted within the temperature range of 105–135° C., preferably in the range of 110–130° C. If annealing is conducted at a single temperature, that temperature should be in the range of 125–132° C., preferably about 128° C. If annealing is conducted at more than a single temperature, e.g., to separately influence annealing in the differing polymer layers, then the higher temperature, e.g., the temperature influencing the polypropylene, should be in the range of 125–132° C., preferably 128–132° C.; and the lower temperature, e.g., the temperature influencing the polyethylene, should be in the range of 105–125° C., preferably about 110° C.

Stretching the bonded and annealed trilayer precursor forms the microporous structure of battery separators. Stretching generally includes several steps, e.g., a cold drawing step, a hot drawing step, and a relax or heat-treating step. The relax or heat-treating step is to reduce internal stress within the separator and may be accomplished with either negative draw ratio or substantially no draw tension at various heat profiles. Stretching is a continuous process performed in ovens containing a draw frame.

The cold drawing step is conduced at ambient temperature (i.e., no energy is input into the precursor) and at a draw ratio in the range of 15–40%. Preferably the draw ratio is in the rang of 20–35%.

The hot drawing step is conduced at temperatures ranging from 110–125° C. and at draw ratios ranging from 105–130%. Preferably, hot drawing is conducted at temperatures ranging from 115–123° C. and at draw ratios ranging from 110–125%.

The relax or heat-treating step is conducted at temperatures ranging from 110–125° C. and at draw ratios ranging from −30 to −50%. Preferably, relax or heat-treatment is conducted at temperatures ranging from 115–123° C. and at draw ratios of −30 to −50%.

After stretching, the trilayer battery separators are wound up and slit to desired widths.

The invention is further illustrated with reference to the following examples:

Test Methods

Gurley ASTM-D726(B)

Gurley is a resistance to air flow measured by the Gurley Densometer (e.g. Model 4120). Gurley is the time in seconds required to pass 10 cc of air through one square inch of product under a pressure of 12.2 inches of water.

Thickness

Method: T411 om-83 developed under the auspices of the Technical Association of the Pulp and Paper Industry. Thickness is determined using a precision micrometer with a ½ inch diameter, circular shoe contacting the sample at seven (7) PSI. Ten (10) individual micrometer readings taken across the width of the sample are averaged.

Porosity ASTM D-2873

Puncture Strength

Ten measurements are made across the width of the stretched product and averaged. A Mitech Stevens LFRA Texture Analyzer is used. The needle is 1.65 mm in diameter with 0.5 mm radius. The rate of descent is 2 mm/sec and the amount of deflection is 6 mm. The film is held tight in the clamping device with a central hole of 11.3 mm. The displacement (in mm) of the film that was pierced by the needle was recorded against the resistance force (in gram force) developed by the tested film. The maximum resistance force is the puncture strength.

Peel Strength

Peel strength is measured using a tension and compression tester to determine the force in grams required to separate two one-inch wide sections of bonded membrane. The peel rate is 6 inches/minute. Three measurements are taken across the web and averaged.

Shrinkage

The sample in the machine direction is marked L_i (L_i= 9.99 cm) apart, and then suspended in a convection oven set at 90° C. for one hour. After taking out of the oven, the sample is then measured the distance, L_f, between the marks. The shrinkage is calculated as follows.

(%) Shrinkage=$(L_i-L_f)\times 100/L_f$

EXAMPLE 1

The polyethylene precursor was extruded from Fina HDPE 7208 resin to form a 0.38 micron thick film. The polypropylene precursor was extruded from Escorene PP 4292 to form a 0.37 micron thick film. The trilayer precursor was formed as shown in FIG. **1**.

The bonding and annealing of the precursor was accomplished as follows: the precursor was strung-up with the oven configured as shown in FIG. **2**; the oven has 4 zones. The nip rollers **50** are located in zone 2. Zones 2, 3 and 4 were set at a temperature of 128° C. and the line speed was 30 ft./min. The adhesion of the trilayer precursor was 5.7 g/in. The trilayer precursor was then stretched under various conditions (note Table 1) to yield the battery separator, the results are set in Table 1.

TABLE 1

Sample	Oven Temp (° C.)	Cold Stretch (%)	Hot Stretch (%)	Relax (-%)	Gurley (Sec)	Thickness (mil)	Punct. Strength (g)	Shrinkage (%)
1	115	35	115	50	32.9	1.02	388	25.5
2	120	35	115	50	29.3	1.02	396	15.3
3	120	30	115	45	28.3	0.97	400	17.3
4	120	25	115	40	29.5	0.99	421	18
5	120	25	115	35	100+	—	—	—
6	120	30	115	40	66	.99	435	2.6
7	120	35	115	45	50	.95	428	3.0
8	120	35	115	30	40	.98	442	7.0
9	120	25	125	30	162	.94	441	7.0
10	118	35	115	30	22	1.01	439	13.0

The bonding and annealing of the precursor was accomplished as follows: the precursor was strung-up with the oven configured as shown in FIG. **3**. Zone 1 is at ambient temperature, zone 2 at 128–130° C., and zones 3 and 4 at 110° C. The line speed was 40 ft./min. The interply adhesion for the precursor was greater than 30 g/in. The trilayer precursors were then stretched under various conditions (note Table 2) and at speeds ranging from 20–30 ft/min. (feed speed) to 40–60 ft/min. (output speed) to yield the battery separator; the results are set forth in Table 2.

TABLE 2

	Oven Temp (° C.)			Cold Stretch	Hot Stretch	Relax	Gurley	Thickness	Shrinkage
Sample	2	3	4	(%)	(%)	(-%)	(Sec)	(mil)	(%)
4	118	118	118	35	115	50	28.8	1.00	10.0
6	118	118	128	35	115	50	31.6	1.00	3.0
7	118	118	123	35	115	50	28.9	1.00	6.0
8	118	118	123	30	120	50	31.8	1.00	7.0
9	118	118	123	25	115	40	26.6	1.00	5.0
10	118	118	123	20	120	40	25.4	1.00	5.0
101	118	118	123	20	120	40	25.4	1.00	3.0
102	118	118	123	20	120	40	24.6	1.02	3.1
11	118	118	123	20	110	30	25.8	1.02	5.6
12	118	118	123	20	110	30	27.0	1.02	6.9
13	123	123	123	20	120	40	24.0	0.99	2.2
14	123	123	123	20	120	40	25.4	1.01	3.5

EXAMPLE 2

The polyethylene precursor was extruded from Fina HDPE 7208 resin to form a 0.38 micron film. The polypropylene precursor was extruded from Escorene PP 4292 to form a 0.37 micron film. The trilayer precursor was formed as shown in FIG. **1**.

EXAMPLE 3

The polyethylene precursor was extruded from Hizex HDPE 5202 B resin to form a 0.65 micron film. Otherwise, the procedures of Example 2 were followed except as noted in Table 3.

TABLE 3

The polyethylene precursor was extruded from Hizex HDPE 5202 B resin to form a 0.65 micro film. Otherwise, the procedures of Example 2 were followed except as noted in Table 3.

Sample	Oven Temp (° C.)	Hot Stretch (%)	Cold Stretch (%)	Relax– (–%)	Gurley (Sec)	Thickness (mil)	Shrinkage (%)
1	118	35	115	40	31.6	1.24	10
2	118	35	115	50	33.8	1.24	7.4

We claim:

1. A method of making a trilayer, shutdown battery separator comprising the steps of:

extruding a polyethylene precursor;

extruding a polypropylene precursor;

forming a nonporous trilayer precursor, the trilayer precursor having the polyethylene precursor sandwiched between two polypropylene precursor;

simultaneously bonding and annealing the trilayer precursor to form a bonded and annealed trilayer precursor, the annealing being preformed at temperatures ranging from 105 to 135° C., and the annealing further comprising two zones, each zone at a different temperature;

stretching the bonded and annealed trilayer precursor; and

forming thereby the battery separator.

2. The method according to claim **1** where bonding is performed at a temperature ranging from 125 to 135° C.

3. The method according to claim **1** where bonding is performed by nip rollers.

4. The method according to claim **1** where stretching is performed in several steps.

5. The battery made with the separator produced by the method of claim **1**.

6. A method of making a trilayer, shutdown battery separator comprising the steps of:

extruding a polyethylene precursor;

extruding a polypropylene precursor;

forming a nonporous trilayer precursor, the trilayer precursor having the polyethylene precursor sandwiched between two polypropylene precursors;

bonding the trilayer precursor, to form a bonded trilayer precursor;

annealing the bonded trilayer precursor, to form a bonded, annealed trilayer precursor, the annealing being performed at temperatures ranging from 105° to 135° C., and further comprising two zones, each zone at a different temperature within the range;

stretching the bonded, annealed trilayer precursor; and

forming thereby the battery separator.

7. The method according to claim **6** where bonding is performed at a temperature ranging from 125 to 135° C.

8. The method according to claim **6** whereby bonding is performed by nip rollers.

9. The method according to claim **8** where bonding and annealing are initiated simultaneously.

10. The method according to claim **6** where stretching is performed in several steps.

11. The battery made with the separator produced by the method of claim **6**.

12. A method of making a trilayer, shutdown battery separator comprising the steps of:

extruding a polyethylene precursor;

extruding a polypropylene precursor;

forming a nonporous trilayer precursor, the trilayer precursor having the polyethylene precursor sandwiched between two polypropylene precursors;

bonding, annealing and stretching the trilayer precursor in a multizone oven, the annealing being performed at temperatures ranging from 105° to 135° C. and further comprising two zones, each zone at a different temperature; and

forming thereby the battery separator.

13. A method of making a trilayer, shutdown battery separator comprising the steps of:

providing a nonporous trilayer precursor, the trilayer precursor having a polyethylene layer sandwiched between two polypropylene layers;

annealing the trilayer precursor, to form an annealed trilayer precursor, the annealing being performed at temperatures ranging from 105° to 135° C., and further comprising two zones, each zone at a different temperature within the range;

stretching the annealed trilayer precursor; and

forming thereby the battery separator.

14. A method of making a trilayer, shutdown battery separator comprising the steps of:

providing a nonporous trilayer precursor, the trilayer precursor having a polyethylene layer sandwiched between two polypropylene layers;

annealing and stretching the trilayer precursor in a multizone oven, the annealing being performed at temperatures ranging from 105° to 135° C. and further comprising two zones, each zone at a different temperature; and

forming thereby the battery separator.

* * * * *

Appendix X

US006306545B1

(12) **United States Patent**
Carlson et al.

(10) **Patent No.: US 6,306,545 B1**
(45) **Date of Patent: *Oct. 23, 2001**

(54) **SEPARATORS FOR ELECTROCHEMICAL CELLS**

(75) Inventors: **Steven A. Carlson**, Cambridge, MA (US); **Qicong Ying**, Tucson, AZ (US); **Zhongyi Deng**, Tucson, AZ (US); **Terje A. Skotheim**, Tucson, AZ (US)

(73) Assignee: **Moltech Corporation**, Tucson, AZ (US)

(*) Notice: Subject to any disclaimer, the term of this patent is extended or adjusted under 35 U.S.C. 154(b) by 0 days.

This patent is subject to a terminal disclaimer.

(21) Appl. No.: **09/215,112**

(22) Filed: **Dec. 17, 1998**

Related U.S. Application Data

(63) Continuation-in-part of application No. 08/995,089, filed on Dec. 19, 1997, now Pat. No. 6,153,337.

(51) **Int. Cl.**[7] **H01M 2/16**; C04B 35/10

(52) **U.S. Cl.** **429/247**; 429/251; 501/153

(58) **Field of Search** 429/247, 251; 501/153

(56) **References Cited**

U.S. PATENT DOCUMENTS

3,647,554		3/1972	Arrance et al. .	
4,361,620		11/1982	Newton .	
4,664,991		5/1987	Perichaud et al. .	
5,178,849		1/1993	Bauer .	
5,194,341		3/1993	Bagley et al. .	
5,312,789	*	5/1994	Wood	501/153 X
5,326,391		7/1994	Anderson et al.	428/317.9
5,418,091		5/1995	Gozdz et al.	429/252
5,529,860		6/1996	Skotheim et al.	429/213
5,538,812		7/1996	Lee et al. .	
5,549,989		8/1996	Anani .	
5,597,659		1/1997	Morigaki et al. .	
5,601,947		2/1997	Skotheim et al.	429/213
5,605,750		2/1997	Romano et al.	428/304.4
5,690,702		11/1997	Skotheim et al.	29/623.1
5,691,005		11/1997	Morigaki et al.	427/508
5,782,940		7/1998	Jayan et al. .	
5,824,434		10/1998	Kawakami et al.	429/209
5,882,721		3/1999	Delnick	427/77

FOREIGN PATENT DOCUMENTS

0 144 097	6/1985	(EP) .
250518 B1	11/1991	(EP) .
0 523 840	1/1993	(EP) .
0 524 626	1/1993	(EP) .
600718 A2	6/1994	(EP) .
814520 A2	12/1997	(EP) .
875950 A2	11/1999	(EP) .
WO 91/02385	2/1991	(WO) .
WO 91/03080 A1	3/1991	(WO) .

OTHER PUBLICATIONS

Chemical Abstracts, Columbus, OH, U.S., Abstract No. 114:167903, "High–energy sodium–sulfur battery" corresponding to German Patent Publication No. DE 3,926,977 A1 (Month unknown) (1991).

Mori, Kazutaka. (Sep. 24, 1984), "Manufacturing porous diaphragm for gas separation," *Chemical Abstracts* 101, No.13, abstract No. 112848t.

Turkovic et al., (1995). "Measurements of the electrical properties of transparent gamma–A100H film" *Advances in Science and Technology, 3D Ceramics: Charting the Future,* pp. 2655–2662 (Month unknown).

Udagawa, Shigekazu. (Apr. 27, 1984), "Porous Diaphragm" *Patent Abstracts of Japan* 8, No.93 (C–220).

* cited by examiner

Primary Examiner—Stephen Kalafut
(74) *Attorney, Agent, or Firm*—Jacqueline M. Nicol; Steven A. Carlson

(57) **ABSTRACT**

This invention pertains to separators for electrochemical cells which comprise a microporous pseudo-boehmite layer; electrolyte elements comprising such separators; electrical current producing cells comprising such separators; and methods of making such separators, electrolyte elements and cells.

103 Claims, No Drawings

SEPARATORS FOR ELECTROCHEMICAL CELLS

This application is a continuation-in-part of U.S. patent application Ser. No. 08/995,089, filed Dec. 19, 1997, now U.S. Pat. No. 6,153,337 the contents of which are incorporated herein by reference in their entirety.

TECHNICAL FIELD

This invention is in the field of separators for electrochemical cells. More particularly, this invention pertains to separators for electrochemical cells which comprise a microporous pseudo-boehmite layer; electrolyte elements comprising such separators; electrical current producing cells comprising such separators; and methods of making such separators, electrolyte elements, and cells.

BACKGROUND

Throughout this application, various publications, patents, and published patent applications are referred to by an identifying citation. The disclosures of the publications, patents, and published patent specifications referenced in this application are hereby incorporated by reference into the present disclosure to more fully describe the state of the art to which this invention pertains.

An electroactive material that has been fabricated into a structure for use in a battery is referred to as an electrode. Of a pair of electrodes used in a battery, herein referred to as an electric current producing cell, the electrode on the electrochemically higher potential side is referred to as the positive electrode, or the cathode, while the electrode on the electrochemically lower potential side is referred to as the negative electrode, or the anode.

An electrochemically active material used in the cathode or positive electrode is referred to hereinafter as a cathode active material. An electrochemically active material used in the anode or negative electrode is hereinafter referred to as an anode active material. An electric current producing cell or battery comprising a cathode with the cathode active material in an oxidized state and an anode with the anode active material in a reduced state is referred to as being in a charged state. Accordingly, an electric current producing cell comprising a cathode with the cathode active material in a reduced state, and an anode with the anode active material in an oxidized state, is referred to as being in a discharged state.

Discharging an electric current producing cell in its charged state by allowing electrons to flow from the anode to the cathode through an external circuit results in the electrochemical reduction of the cathode active material at the cathode and the electrochemical oxidation of the anode active material at the anode. To prevent the undesirable flow of the electrons in a short circuit internally from the anode to the cathode, an electrolyte element is interposed between the cathode and the anode. This electrolyte element must be electronically non-conductive to prevent the short circuiting, but must permit the transport of positive ions between the anode and the cathode. The electrolyte element should also be stable electrochemically and chemically toward both the anode and the cathode.

Typically, the electrolyte element contains a porous material, referred to as a separator (since it separates or insulates the anode and the cathode from each other), and an aqueous or non-aqueous electrolyte, which typically comprises an ionic electrolyte salt and ionically conductive material, in the pores of the separator. A variety of materials

have been used for the porous layer or separator of the electrolyte element in electric current producing cells. These porous separator materials include polyolefins such as polyethylenes and polypropylenes, glass fiber filter papers, and ceramic materials. Usually these separator materials are supplied as porous free standing films which are interleaved with the anodes and the cathodes in the fabrication of electric current producing cells. Alternatively, the porous separator layer can be applied directly to one of the electrodes, for example, as described in U.S. Pat. No. 5,194,341 to Bagley et al.

Porous separator materials have been fabricated by a variety of processes including, for example, stretching combined with special heating and cooling of plastic films, extraction of a soluble plasticizer or filler from plastic films, and plasma oxidation. The methods for making conventional free standing separators typically involve extrusion of melted polymeric materials either followed by a post-heating and stretching or drawing process or followed by a solvent extraction process to provide the porosity throughout the separator layer. U.S. Pat. No. 5,326,391 to Anderson et al. and references therein, describe the fabrication of free standing porous materials based on extraction of a soluble plasticizer from pigmented plastic films. U.S. Pat. No. 5,418,091 to Gozdz et al. and references therein, describe forming electrolyte layers by extracting a soluble plasticizer from a fluorinated polymer matrix either as a coated component of a multilayer battery structure or as an individual separator film. U.S. Pat. No. 5,194,341 to Bagley et al. describes an electrolyte element with a microporous silica layer and an organic electrolyte. The silica layer was the product of the plasma oxidation of a siloxane polymer. These manufacturing methods for free standing separators are complex and expensive and are not effective either in providing ultrafine pores of less than 1 micron in diameter or in providing separator thicknesses of less than 15 microns.

The methods for making a separator coated directly on another layer of the cell typically involve a solvent extraction process after coating to provide the porosity throughout the separator layer. As with the free standing separators, this solvent extraction process is complex, expensive, and not effective in providing ultrafine pores of less than 1 micron in diameter.

As the electrolyte in the pores of the separator in the electrolyte element, a liquid organic electrolyte containing organic solvents and ionic salts is typically used. Alternatively, a gel or solid polymer electrolyte containing an ionically conductive polymer and ionic salts, and optionally organic solvents, might be utilized instead of the liquid organic electrolyte. For example, U.S. Pat. Nos. 5,597,659 and 5,691,005 to Morigaki el al. describe a separator matrix formed of a microporous polyolefin membrane impregnated in its pores with an ionic conductive gel electrolyte.

In addition to being porous and chemically stable to the other materials of the electric current producing cell, the separator should be flexible, thin, economical in cost, and have good mechanical strength. These properties are particularly important when the cell is spirally wound or is folded to increase the surface area of the electrodes and thereby improve the capacity and high rate capability of the cell. Typically, free standing separators have been 25 microns (μm) or greater in thickness. As batteries have continued to evolve to higher volumetric capacities and smaller lightweight structures, there is a need for separators that are 15 microns or less in thickness with a substantial increase in the area of the separator in each battery. Reduc-

ing the thickness from 25 microns to 15 microns or less greatly increases the challenge of providing porosity and good mechanical strength while not sacrificing the protection against short circuits or not significantly increasing the total cost of the separator in each battery.

This protection against short circuits is particularly critical in the case of secondary or rechargeable batteries with lithium as the anode active material. During the charging process of the battery, dendrites can form on the surface of the lithium anode and can grow with continued charging. A key feature of the separator in the electrolyte element of lithium rechargeable batteries is that it have a small pore structure, such as 10 microns or less in pore diameter, and sufficient mechanical strength to prevent the lithium dendrites from contacting the cathode and causing a short circuit with perhaps a large increase in the temperature of the battery leading to an unsafe explosive condition.

Another highly desirable feature of the separator in the electrolyte element is that it is readily wetted by the electrolyte materials which provide the ionic conductivity. When the separator material is a polyolefinic material which has nonpolar surface properties, the electrolyte materials (which typically have highly polar properties) often poorly wet the separator material. This results in low capacities in the battery due to the nonuniform distribution of electrolyte materials in the electrolyte element.

Further it would be highly advantageous to be able to prepare free standing separators by a relatively simple process of coating which directly provides ultrafine pores as small as 1 nm in diameter and can readily provide a range of thicknesses from 50 microns or greater down to 1 micron. Also, it would be advantageous to be able to prepare separators with ultrafine pores and a wide range of thicknesses coated directly on another layer of the electric current producing cell by a process of coating without requiring any subsequent solvent extraction or other complex process which is costly, difficult to control, and not effective in providing ultrafine pores.

A separator, particularly one with a thickness less than 25 microns, which is applicable for electric current producing cells, and which can avoid the foregoing problems often encountered with the use of polyolefinic and other conventional porous materials made using extrusion, extraction, or other processes would be of great value to the battery industry.

SUMMARY OF THE INVENTION

The separator of the present invention for use in an electric current producing cell comprises a microporous pseudo-boehmite layer. In one embodiment, the pseudo-boehmite layer has a pore volume from 0.02 to 2.0 cm^3/g. In a preferred embodiment, the pseudo-boehmite layer has a pore volume from 0.3 to 1.0 cm^3/g. In a more preferred embodiment, the pseudo-boehmite layer has a pore volume from 0.4 to 0.7 cm^3/g.

In one embodiment, the pseudo-boehmite layer of the separator has an average pore diameter from 1 to 300 nm. In a preferred embodiment, the pseudo-boehmite layer has an average pore diameter from 2 to 30 nm. In a more preferred embodiment, the pseudo-boehmite layer has an average pore diameter from 3 to 10 nm.

In another embodiment of the invention, the pseudo-boehmite layer further comprises a binder. In one embodiment, the binder is present in the amount of 5 to 70% by weight of the pseudo-boehmite in the separator. In a preferred embodiment, the binder comprises polyvinyl alcohol, polyethylene oxide, polyvinyl pyrrolidone, copolymers of the foregoing, or a combination thereof. In another preferred embodiment, the pseudo-boehmite layer is impregnated with an ionic conductive polymer. In a most preferred embodiment, the ionic conductive polymer comprises a polymer resin cured with heat, ultraviolet light, visible light, infrared radiation, or electron beam radiation.

In one embodiment, the pseudo-boehmite layer of the separator has a thickness of from 1 micron to 50 microns. In a preferred embodiment, the pseudo-boehmite layer has a thickness of from 1 micron to 25 microns. In a more preferred embodiment, the pseudo-boehmite layer has a thickness of from 5 microns to 15 microns.

In another embodiment of the invention, a method for forming a separator for use in electric current producing cells is provided. The method comprises coating onto a substrate a liquid mixture comprising a boehmite sol and then drying the coating to form the microporous pseudo-boehmite layer, as described herein. In one embodiment, the liquid mixture comprising a boehmite sol further comprises a binder and then is dried to form the microporous pseudo-boehmite layer with binder present, as described herein. In a preferred embodiment, there is a subsequent step of delaminating the pseudo-boehmite layer from the substrate, thereby providing a free standing separator comprising the pseudo-boehmite layer with binder present. In a most preferred embodiment, the substrate comprises a cathode coating layer on at least one outermost surface and the liquid mixture comprising the boehmite sol is coated onto the cathode coating layer.

Another aspect of the separators and of the methods of forming the separator of this invention pertains to a method of making the separator comprising a microporous layer, which microporous layer comprises pseudo-boehmite and a binder, and to a separator formed by such method, wherein the method comprises the steps of: (a) coating onto a substrate a liquid mixture comprising a boehmite sol, a binder, and a liquid medium; and, (b) drying the coating formed in step (a) to yield the microporous layer. In one embodiment, the liquid medium comprises water. In one embodiment, the liquid medium comprises one or more organic solvents. In one embodiment, the liquid medium comprises one or more protic organic solvents selected from the group consisting of: alcohols and glycols. Suitable organic solvents for the liquid medium include, but are not limited to, methanol, ethanol, isopropanol, 1-propanol, 1-butanol, 2-butanol, ethylene glycol, propylene glycol, 2-methoxyethanol, 2-ethoxyethanol, and 2-butoxyethanol. In a preferred embodiment, the liquid medium comprises ethanol. In one embodiment, the liquid medium comprises water and one or more organic solvents.

A wide variety of binders that are compatible with the liquid mixture of the methods of this invention may be utilized in the present invention. In one embodiment, the binder is an organic binder. Suitable organic binders include, but are not limited to, polyvinyl alcohols, polyethylene oxides, alkylated polyethylene oxides, polyvinyl pyrrolidones, polyvinyl butyrals, cellulosics, polymers comprising quaternary ammonium groups, polyacrylamides and non-hydrolyzed derivatives and partially hydrolyzed derivatives, polyvinyl ethers, polyethyleneimines, polyurethanes, epoxies, melamine formaldehydes, urea formaldehydes; copolymers thereof; copolymers of maleic anhydride and derivatives and esters thereof; gelatin; starch; and mixtures of the foregoing binders. In one embodiment, the binder is an inorganic binder. Suitable inorganic binders include, but are not limited to, colloidal silicas, colloidal

non-hydrated aluminum oxides, colloidal tin oxides, colloidal titanium oxides, colloidal zirconium oxides, and colloidal zinc oxides. In one embodiment, the binder further comprises one or more additives. Suitable additives include, but are not limited to, pigments, crosslinking agents, catalysts for non-radiation curing, sensitizers for radiation curing, plasticizers, surfactants, and dispersants. Since the densities of some binders, especially those comprising inorganic binders and pigments with high specific gravities, may be high, in one embodiment, the binder is present in an amount of 3 to 200% of the weight of the pseudo-boehmite in the microporous layer. In a preferred embodiment, the binder is present in an amount of 5 to 70% by weight of the pseudo-boehmite in the microporous layer. In one embodiment, the microporous layer has a thickness of from 1 micron to 50 microns, preferably from 1 micron to 25 microns, and, more preferably, from 2 to 15 microns.

In one embodiment of the methods of forming the separator of the present invention, at least one outermost surface of said substrate comprises a cathode layer and said liquid mixture is coated onto said cathode layer.

In one embodiment of the methods of forming the separator of the present invention, the substrate comprises a release layer on at least one outermost surface, and the liquid mixture is coated onto the release layer. In one embodiment, after step (b) of drying the coating to yield the microporous layer, there are subsequent steps of: (c) contacting a surface of the microporous layer with a coating solution comprising a solid material and a liquid medium; and, (d) drying the coating formed in step (c) to yield a coating layer comprising the solid material. In one embodiment, the coating layer in step (d) is a cathode layer. In one embodiment, there is a subsequent step of delaminating the microporous layer, as described herein, from the substrate comprising the release layer.

In one embodiment of the methods of forming the separator of the present invention, pores of said microporous layer are impregnated with a composition comprising a polymer, preferably the polymer is ionically conductive. In one embodiment of the methods of forming the separator of the present invention, after step (b) of drying the coating to yield the microporous layer, there are subsequent steps of: (c) contacting a surface of said microporous layer with a solution comprising heat- or radiation-curable monomers or oligomers, thereby causing infusion of said monomers or said oligomers into pores of said microporous layer; and, (d) curing said monomers or said oligomers with an energy source selected from the group consisting of: heat, ultraviolet light, visible light, infrared radiation, and electron beam radiation; thereby forming a polymer.

In another embodiment of the methods of forming the separator of this invention, there is a subsequent step of contacting the surface of the pseudo-boehmite layer with a solution comprising heat- or radiation-curable monomers or oligomers to thereby cause the infusion of the monomers or oligomers into the pores of the pseudo-boehmite layer and then curing the monomers or oligomers with heat, ultraviolet light, visible light, infrared radiation, or electron beam radiation to form a composition comprising a polymer, preferably an ionically conductive polymer. In one embodiment, the solution further comprises a crosslinking agent, thereby forming a composition further comprising the crosslinking agent. In one embodiment, after the infusion and curing of the heat- or radiation-curable monomers or oligomers, there is a subsequent step of delaminating the pseudo-boehmite layer from the substrate, thereby providing a free standing separator comprising the pseudo-boehmite layer with a polymer present, preferably an ionically conductive polymer, in the pores of the pseudo-boehmite layer.

In another embodiment of the invention, an electrolyte element for use in an electric current producing cell comprises the separator comprising a microporous pseudo-boehmite layer, as described herein, and an organic electrolyte contained within the pores of the microporous pseudo-boehmite layer. Suitable materials for use as the organic electrolyte include liquid electrolytes, gel polymer electrolytes, and solid polymer electrolytes.

In another embodiment of the invention, a method of making an electrolyte element for an electric current producing cell is provided. The method comprises the methods of forming the separator comprising a microporous pseudo-boehmite layer, as described herein, and then contacting the surface of the microporous pseudo-boehmite layer with an organic electrolyte thereby causing the infusion of the electrolyte into the pores of the microporous pseudo-boehmite layer. In one embodiment, the organic electrolyte comprises heat- or radiation-curable monomers or oligomers. In a preferred embodiment, there is a subsequent step of curing the heat- or radiation-curable monomers or oligomers of the organic electrolyte with heat, ultraviolet light, visible light, infrared radiation, or electron beam radiation to form a polymer, preferably an ionically conductive polymer. In a most preferred embodiment, at least an outermost surface of the substrate is a cathode coating layer, and the pseudo-boehmite layer is coated on the cathode layer.

Another aspect of the invention pertains to a method of making an electrolyte element for an electric current producing cell, wherein the electrolyte element comprises a microporous layer comprising pseudo-boehmite and a binder, wherein the method comprises the steps of: (a) coating onto a substrate a liquid mixture comprising a boehmite sol, a binder, and a liquid medium; (b) drying the coating formed in step (a) to yield said microporous layer; and, (c) contacting a surface of said microporous layer with an organic electrolyte, thereby causing infusion of said electrolyte into pores of said microporous layer.

In another embodiment of the invention, an electric current producing cell is provided. The cell is comprised of a cathode and an anode, and an electrolyte element interposed between the cathode and the anode, wherein the electrolyte element comprises the separator comprising a microporous pseudo-boehmite layer, as described herein, and an organic electrolyte contained within the pores of the microporous pseudo-boehmite layer. In one embodiment, the cell is a secondary battery. In one embodiment, the cell is a primary electric current producing cell. In a preferred embodiment, the anode active material of the cell is selected from the group consisting of: a lithium metal, lithium-aluminum alloys, lithium-tin alloys, lithium-intercalated carbons, and lithium-intercalated graphites.

Suitable cathode active materials for the electric current producing cells of this invention include, but are not limited to, transition metal chalcogenides, conductive polymers, and sulfur-containing materials. In a preferred embodiment, the cathode of the cell comprises a sulfur-containing material.

In one embodiment, the sulfur-containing material comprises elemental sulfur. In one embodiment, the sulfur-containing material comprises a sulfur-containing polymer, wherein the electroactive sulfur-containing polymer, in its oxidized state, comprises a covalent polysulfide moiety of the formula, —S_m—, wherein m is an integer equal to or greater than 3, preferably m is an integer from 3 to 10, most preferably m is an integer equal to or greater than 6, and

particularly most preferably m is an integer equal to or greater than 8. In one embodiment, the sulfur-containing polymer has a polymer backbone chain comprising conjugated segments. In one embodiment, the sulfur-containing polymer has a polymer backbone chain and the polysulfide moiety, —S_m—, is covalently bonded by one or both of its terminal sulfur atoms on a side group to the polymer backbone chain. In one embodiment, the sulfur-containing polymer has a polymer backbone chain and the polysulfide moiety, —S_m—, is incorporated into the polymer backbone chain by covalent bonding of terminal sulfur atoms of the polysulfide moiety. In one embodiment the sulfur-containing polymer comprises greater than 75 weight percent of sulfur.

In one embodiment, the electroactive sulfur-containing material comprises a sulfur-containing polymer comprising an ionic polysulfide moiety selected from the group of consisting of: ionic —S_m^- moieties and ionic S_m^{2-} moieties, wherein m is an integer equal to or greater than 3, and preferably m is an integer equal to or greater than 8. In one embodiment, the sulfur-containing polymer comprising an ionic polysulfide moiety has a polymer backbone comprising conjugated segments. In one embodiment, the polysulfide moiety, —S_m^-, is covalently bonded by one of its terminal sulfur atoms on a side group to the polymer backbone chain. In one embodiment, the sulfur-containing polymer comprising an ionic polysulfide moiety comprises greater than 75 weight percent of sulfur.

In a preferred embodiment, the cathode of the secondary battery comprises an electroactive sulfur-containing cathode material, wherein the electroactive sulfur-containing cathode material, in its oxidized state, comprises a polysulfide moiety of the formula, —S_m—, wherein m is an integer equal to or greater than 3, preferably m is an integer from 3 to 10, and most preferably m is an integer equal to or greater than 6, and particularly most preferably m is an integer equal to or greater than 8. In a most preferred embodiment, the electroactive sulfur-containing cathode material is selected from the group consisting of: elemental sulfur; carbon-sulfur polymer materials with their —S_m— groups covalently bonded by one or more of their terminal sulfur atoms on a side group on the polymer backbone chain; carbon-sulfur polymer materials with their —S_m— groups incorporated into the polymer backbone chain by covalent bonding of their terminal sulfur atoms; and carbon-sulfur polymer materials with greater than 75 weight percent of sulfur in the carbon-sulfur polymer material. In one embodiment, the carbon-sulfur polymer materials comprise conjugated segments in the polymer backbone chain.

In another embodiment of the cell of this invention, the organic electrolyte in the electrolyte element comprises one or more materials selected from the group consisting of: liquid electrolytes, gel polymer electrolytes, or solid polymer electrolytes.

In another embodiment of the invention, a method for forming an electric current producing cell is provided. The method comprises providing an anode and a cathode, and enclosing an electrolyte element, as described herein, interposed between the anode and the cathode. In one embodiment of the method, the organic electrolyte of the electrolyte element comprises one or more materials selected from the group consisting of: liquid electrolytes, gel polymer electrolytes, and solid polymer electrolytes. In a preferred embodiment of the method, after the step of enclosing the electrolyte element between the anode and the cathode, there is a subsequent step comprising the imbibition of a solution comprising one or more ionic electrolyte salts and one or more electrolyte solvents into the electrolyte element. In a most preferred embodiment, after the step of enclosing the electrolyte element between the anode and the cathode, there is substantially no ionic electrolyte salt present in the electrolyte element, and there is a subsequent step comprising the imbibition of a solution comprising one or more ionic electrolyte salts and one or more electrolyte solvents into the electrolyte element.

As will be appreciated by one of skill in the art, features of one aspect or embodiment of the invention are also applicable to other aspects or embodiments of the invention.

DETAILED DESCRIPTION OF THE INVENTION

The separators of the present invention provide superior electric current producing cell properties, particularly in cells utilizing separators with thicknesses below about 25 microns. Conventional separators, such as porous polyolefins, porous fluoropolymers where the porosity is provided by a solvent extraction process, and glass fiber papers, and the like, are difficult and costly to manufacture, especially at thicknesses below about 25 microns. Due to the nature of the processes used to manufacture these separators and the relatively large pore sizes intrinsic to these separators, electrical shorting may be a significant challenge at separator thicknesses of below about 25 microns, especially at thicknesses below about 15 microns. To overcome these limitations, the separators of the present invention for use in electric current producing cells comprise a microporous pseudo-boehmite layer.

Separators Comprising Microporous Pseudo-Boehmite

Upon heating, $Al(OH)_3$ (which occurs naturally as gibbsite) transforms to a mixed oxide hydroxide, AlO•OH (which occurs naturally as diaspore and boehmite). Upon further heating above about 450° C., it further transforms to gamma-alumina, Al_2O_3. The term "pseudo-boehmite," as used herein, pertains to hydrated aluminum oxides having the chemical formula Al_2O_3•xH_2O wherein x is in the range of from 1.0 to 1.5. Terms used herein, which are synonymous with "pseudo-boehmite," include "boehmite," "AlOOH," and "hydrated alumina." The materials referred to herein as "pseudo-boehmite" are distinct from anhydrous aluminas (Al_2O_3, such as alpha-alumina and gamma-alumina), and hydrated aluminum oxides of the formula Al_2O_3•xH_2O wherein x is less than 1.0 or greater than 1.5.

The term "microporous," is used herein to describe the material of a layer, which material possesses pores of diameter of about 10 microns or less which are connected in a substantially continuous fashion from one outermost surface of the layer through to the other outermost surface of the layer. Porous separators which are made from fibers, such as glass, TEFLON (a trademark for polytetrafluoroethylene available from DuPont Corporation, Wilmington, Del.), and polypropylene, are generally characterized as non-woven separator materials and typically have pore diameters too large to be called microporous, thereby making them unacceptable for rechargeable cells where dendrite formation is a potential concern.

The amount of these pores in the layer may be characterized by the pore volume, which is the volume of pores per unit weight of the layer. The pore volume may be measured by filling the pores with a liquid having a known density and then calculated by the increase in weight of the layer with the liquid present divided by the known density of the liquid and then dividing this quotient by the weight of the layer with no liquid present, according to the equation:

$$\text{Pore Volume} = \frac{[W_1 - W_2]/d}{W_2} \quad \text{I}$$

where W_1 is the weight of the layer when the pores are completely filled with the liquid of known density, W_2 is the weight of the layer with no liquid present in the pores, and d is the density of the liquid used to fill the pores. Also, the pore volume may be estimated from the apparent density of the layer by subtracting the reciprocal of the theoretical density of the materials (assuming no pores) comprising the microporous layer from the reciprocal of the apparent density or measured density of the actual microporous layer, according to the equation:

$$\text{Pore Volume} = \left(\frac{1}{d_1} - \frac{1}{d_2}\right) \quad \text{II}$$

where d_1 is the density of the layer which is determined from the quotient of the weight of the layer and the layer volume as determined from the measurements of the dimensions of the layer, and d_2 is the calculated density of the materials in the layer assuming no pores are present or, in other words, d_2 is the density of the solid part of the layer as calculated from the densities and the relative amounts of the different materials in the layer. The porosity or void volume of the layer, expressed as percent by volume, can be determined according to the equation:

$$\text{Porosity} = \frac{100(\text{Pore Volume})}{[\text{Pore Volume} + 1/d_2]} \quad \text{III}$$

where pore volume is as determined above, and d_2 is the calculated density of the solid part of the layer, as described above.

In one embodiment, the pseudo-boehmite layer of the present invention has a pore volume from 0.02 to 2.0 cm^3/g. In a preferred embodiment, the pseudo-boehmite layer has a pore volume from 0.3 to 1.0 cm^3/g. In a more preferred embodiment, the pseudo-boehmite layer has a pore volume from 0.4 to 0.7 cm^3/g. Below a pore volume of 0.02 cm^3/g, the transport of ionic species is inhibited by the reduced pore volume. Above a pore volume of 2.0 cm^3/g, the amount of voids are greater which reduces the mechanical strength of the microporous pseudo-boehmite layer.

In contrast to conventional microporous separators which typically have pore diameters on the order of 1 to 10 microns, the separators of the present invention have pore diameters which range from about 1 micron down to less than 0.002 microns. In one embodiment, the separator of the present invention has an average pore diameter from 0.001 microns or 1 nm to 0.3 microns or 300 nm. In a preferred embodiment, the separator of the present invention has an average pore diameter from 2 nm to 30 nm. In a more preferred embodiment, the separator of the present invention has an average pore diameter from 3 nm to 10 nm.

The pore diameters of the separators of the present invention can be measured by preparing a sample of a cross-section of the layer by conventional techniques and viewing this cross-section through a microscope having the necessary resolution. For the ultrafine pore diameters of 2 to 30 nm, a transmission electron microscope (TEM) can provide the necessary resolution. The average pore diameter of the separators of the present invention may be determined by mercury porosimetry using conventional techniques.

One distinct advantage of separators with much smaller pore diameters on the order of 0.001 to 0.03 microns is that insoluble particles, even colloidal particles with diameters on the order of 0.05 to 1.0 microns, can not pass through the separator because of the ultrafine pores. In contrast, colloidal particles, such as the conductive carbon powders often incorporated into cathode compositions, can readily pass through conventional separators, such as microporous polyolefins, and thereby can migrate to undesired areas of the cell.

Another significant advantage of the pseudo-boehmite separators of the present invention over conventional separators is that the nanoporous structure of the layer may function as an ultrafiltration membrane and, in addition to blocking all particles and insoluble materials, may block the diffusion of soluble materials of relatively low molecular weights, such as 2,000 or higher, while permitting the diffusion of soluble materials with molecular weights below this cutoff level. This property may be utilized to advantage in selectively impregnating or imbibing materials into the separator during manufacture of the electric current producing cell or in selectively permitting diffusion of very low molecular weight materials through the separator during all phases of the operation of the cell while blocking or significantly inhibiting the diffusion of insoluble materials or of soluble materials of medium and higher molecular weights.

Another important advantage of the extremely small pore diameters of the separators of the present invention is the strong capillary action of these tiny pores which enhances the capability of the separators to readily take up or imbibe electrolyte liquids and to retain these materials in the pores.

The microporous pseudo-boehmite layer may optionally further comprise a binder, preferably an organic polymer binder. The binder is usually selected on the basis of improving the mechanical strength of the layer without significantly impacting the properties of the microporous structure, which includes transport of low molecular weight materials through the layer while blocking the transport of colloidal or larger particles and high molecular weight materials. The preferred amount of binder is from 5% to 70% of the weight of the pseudo-boehmite in the layer. Below 5 weight per cent, the amount of binder is usually too low to provide a significant increase in mechanical strength. Above 70 weight per cent, the amount of binder is usually too high and fills the pores to an excessive extent which may interfere with the transport of ionic species and other low molecular weight materials through the microporous layer.

Any binder that is compatible with the boehmite sol during mixing and processing into the microporous layer and provides the desired mechanical strength and uniformity of the layer without significantly interfering with the desired microporosity is suitable for use in this invention. Examples of suitable binders include, but are not limited to, polyvinyl alcohols, polyethylene oxides, polyvinyl pyrrolidones, copolymers thereof, and mixtures thereof. Preferred binders are water soluble polymers and have ionically conductive properties.

The microporous layer comprising pseudo-boehmite and binder may further comprise an ionic conductive polymer which is impregnated into the microporous layer. The term "ionic conductive polymer," as used herein, denotes a polymer which, when combined with an appropriate ionic electrolyte salt, may provide ionically conductive properties to a gel polymer electrolyte or a solid polymer electrolyte. The ionic conductive polymer may further increase mechanical strength, in addition to providing ionically conductive properties to the microporous layer. Since the microporous layer of the present invention typically blocks insoluble materials and soluble materials above a low molecular weight such as

2,000, the ionic conductive polymer is preferably formed by impregnating the microporous layer with suitable heat- or radiation-curable monomers or oligomers with molecular weights below 2,000 and then crosslinking these monomers or oligomers in situ to form an ionic conductive polymer resin by exposure to an energy source. Suitable energy sources include heat, ultraviolet light, visible light, infrared radiation, and electron beam radiation. Where the monomers or oligomers are not sensitive to the radiation (such as ultraviolet light), sensitizers may be added to the monomers or oligomers to activate the crosslinking or curing to form a polymer resin.

The thickness of the microporous pseudo-boehmite layer, with or without additional binder, for use as a separator may vary over a wide range since the basic properties of microporosity and mechanical integrity are present in layers of a few microns in thickness as well as in layers with thicknesses of hundreds of microns. For various reasons including cost, overall performance properties as a separator, and ease of manufacturing, the desirable thicknesses are in the range of 1 micron to 50 microns. Preferred are thicknesses in the range of 1 micron to 25 microns. More preferred are thicknesses in the range 2 to 15 Microns. The most preferred thicknesses are in the range of 5 microns to 15 microns. Conventional separators, such as the porous polyolefin materials, are typically 25 to 50 microns in thickness so it is particularly advantageous that the microporous separators of this invention can be effective and inexpensive at thicknesses well below 25 microns.

The present invention provides a method of forming a separator for use in electric current producing cells which overcomes the disadvantages of the aforementioned conventional methods for forming separators. One aspect of the method of the present invention comprises the steps of coating a liquid mixture comprising a boehmite sol onto a substrate and subsequently drying the coating to form a microporous pseudo-boehmite layer. This pseudo-boehmite layer has a pore volume from 0.02 to 2.0 cm^3/g and has an average pore diameter from 1 nm to 300 nm, as described previously for the microporous pseudo-boehmite separator.

If increased mechanical strength or some other improvement in the properties of the separator are desired, the liquid mixture comprising the bochmite sol may further comprise a binder, and the resulting liquid mixture is then dried to form the microporous pseudo-boehmite layer with binder present.

One aspect of the separators and of the methods of forming the separator of this invention pertains to a method of making the separator comprising a microporous layer, which microporous layer comprises pseudo-boehmite and a binder, and to a separator formed by such method, wherein the method comprises the steps of: (a) coating onto a substrate a liquid mixture comprising a boehmite sol, a binder, and a liquid medium; and, (b) drying the coating formed in step (a) to yield the microporous layer. In one embodiment, the liquid medium comprises water. In one embodiment, the liquid medium comprises one or more organic solvents. In one embodiment, the liquid medium comprises one or more protic organic solvents selected from the group consisting of: alcohols and glycols. Suitable organic solvents for the liquid medium include, but are not limited to, methanol, ethanol, isopropanol, 1-propanol, 1-butanol, 2-butanol, ethylene glycol, propylene glycol, 2-methoxyethanol, 2-ethoxyethanol, and 2-butoxyethanol. In a preferred embodiment, the liquid medium comprises ethanol. In one embodiment, the liquid medium comprises water and one or more organic solvents. The use of organic solvents in the liquid medium may be advantageous in allowing a wider choice and amount of binders to be utilized with the boehmite sol, in providing a faster rate of drying, and in reducing the presence of water in the microporous layer, where the water may lead to undesirable reactions in the electric current producing cell.

A wide variety of binders that are compatible with the liquid mixture of the methods of this invention may be utilized in the present invention. In one embodiment, the binder is an organic binder. Suitable organic binders include, but are not limited to, polyvinyl alcohols, polyethylene oxides, alkylated polyethylene oxides such as the dimethyl ethers of polyethylene oxides, polyvinyl pyrrolidones, polyvinyl butyrals, cellulosics such as hydroxyethyl cellulose and alcohol-soluble cellulose acetate propionate, polymers comprising quaternary ammonium groups, polyacrylamides and non-hydrolyzed derivatives and partially hydrolyzed derivatives, polyvinyl ethers, polyethyleneimines, polyurethanes, epoxies, melamine formaldehydes, urea formaldehydes; copolymers thereof; copolymers of maleic anhydride and derivatives and esters thereof; gelatin; starch; and mixtures of the foregoing binders. In one embodiment, the binder is an inorganic binder. Suitable inorganic binders include, but are not limited to, colloidal silicas, colloidal non-hydrated aluminum oxides, colloidal tin oxides, colloidal titanium oxides, colloidal zirconium oxides, and colloidal zinc oxides. These colloidal oxide materials have the typical colloidal particle sizes of less than 1 micron and typically are present in the liquid mixture as colloidal sols which form inorganic gel networks with binder properties upon drying. In one embodiment, the binder further comprises one or more additives, as are known in the art of coatings with organic or inorganic binders. Suitable additives include, but are not limited to, pigments, crosslinking agents such as isocyanates, catalysts for non-radiation curing such as organic acids, sensitizers for radiation curing, plasticizers, surfactants, and dispersants.

Since the densities of some binders, such as, for example, those comprising inorganic binders and pigments with high specific gravities, may be high, in one embodiment, the binder is present in an amount of 3 to 200% of the weight of the pseudo-boehmite in the microporous layer. In a preferred embodiment, the binder is present in an amount of 5 to 70% by weight of the pseudo-boehmite in the microporous layer. In one embodiment, the microporous layer has a thickness of from 1 micron to 50 microns, preferably from 1 micron to 25 microns, and, more preferably, from 2 to 15 microns.

These methods of forming a microporous pseudo-boehmite layer with or without a binder present may be used to produce either a free standing separator or a separator coated directly onto a layer of an electric current producing cell. In a most preferred embodiment of the methods of forming the separators of this invention, the separator is coated directly onto the cathode layer of the electric current producing cell by application of a liquid mixture comprising a boehmite sol and a binder onto the outermost surface of a cathode coating layer on a suitable current collector substrate and then drying this liquid mixture to form the microporous pseudo-boehmite separator layer. The term "cathode coating layer" or "cathode layer," as used herein, refers to an outer most layer or surface of a cathode of an electric current producing cell. Typically, the outer most layer of the cathode is the cathode active layer. However, the cathode active layer may have another layer over it such that the cathode active layer is an intermediate layer in the cathode and not an outer most layer. The term "cathode

active layer," as used herein, pertains to any layer of the cathode that comprises the cathode active material.

A further distinct advantage of this coating method to produce a separator is that it is flexible in the pattern in which the separator layer may be applied to the substrate. For example, the separator layer may be applied over the entire outermost surface of the cathode including the top surface and sides of the cathode coating on the current collector and cathode substrate. The cathode may thus be completely encapsulated on all outermost surfaces, including the edges or sides of the cathode coating which are not contacted or covered by conventional free standing polyolefin or other porous separators, by coating the separator layer in a pattern over all the outermost, exposed surfaces of the cathode. This complete encapsulation by the separator layer of the present invention is very advantageous to safety and battery performance in providing an insulating surface to prevent any short circuits by the cathode during fabrication and during use of the electric current producing cell. This encapsulation is also very advantageous to high cell capacity and long cycle life in acting as a total barrier in inhibiting the migration of any insoluble or high molecular weight species in the cathode to outside the cathode area and similarly in retarding the diffusion of any low molecular weight species, such as soluble polysulfides, in the cathode to outside the cathode area.

In a preferred embodiment, a free standing separator is formed by application of a liquid mixture comprising a boehmite sol and a binder onto a substrate, subsequently drying the liquid mixture to form the microporous pseudo-boehmite layer, and then delaminating this pseudo-boehmite layer from the substrate to provide a free standing microporous pseudo-boehmite separator with binder present. The substrate is selected to have weak adhesion to the pseudo-boehmite layer so that the coating can be readily delaminated from the substrate without damaging the separator. Suitable substrates include papers with release coatings on the surface that receives the pseudo-boehmite liquid mixture and flexible plastic films, such as polyester and polystyrene films, which have weak adhesion to the coating of boehmite sol and binder. The width of the separator layer when it is delaminated from the substrate may be the full width as coated on the substrate or the coated separator may be cut to a narrower width, such as the width desired for use in the specific electric current producing cell. In a most preferred embodiment, before delaminating the microporous pseudo-boehmite layer with binder present from the substrate, the surface of the pseudo-boehmite layer is contacted with heat- or radiation-curable monomers or oligomers, as described herein, to impregnate the pores of the pseudo-boehmite layer. After curing the monomers or oligomers with heat or radiation to form a polymer, the pseudo-boehmite layer is delaminated from the substrate to provide a free standing separator with polymer present, preferably an ionically conductive polymer.

In one embodiment of the methods of forming the separator of the present invention, the substrate comprises a release layer on at least one outermost surface, and the liquid mixture is coated onto the release layer. In one embodiment, after step (b) of drying the coating to yield the microporous layer, there are subsequent steps of: (c) contacting a surface of the microporous layer with a coating solution comprising a solid material and a liquid medium; and, (d) drying the coating formed in step (c) to yield a coating layer comprising the solid material. In one embodiment, the coating layer in step (d) is a cathode layer. In one embodiment, there is a subsequent step of delaminating the microporous layer, as described herein, from the substrate comprising the release layer.

In one embodiment of the methods of this invention for producing a separator coated directly on the cathode active layer, the surface of the pseudo-boehmite layer is contacted with a solution comprising heat- or radiation-curable monomers or oligomers, as described herein, to impregnate the pores of the pseudo-boehmite layer. Curing the monomers or oligomers with heat or radiation to form a composition comprising a polymer provides a microporous pseudo-boehmite separator with polymer, preferably an ionically conductive polymer, present coated directly on the cathode active layer. In one embodiment, the solution further comprises a crosslinking agent, thereby forming a composition further comprising the crosslinking agent. Suitable crosslinking agents include, but are not limited to, isocyanates and polyaziridines.

Electrolyte Elements

The present invention provides an electrolyte element for use in an electric current producing cell by combining the separator of the present invention, as described herein, with an electrolyte contained within the pores of the pseudo-boehmite layer of the separator. The electrolyte may be any of the types of non-aqueous and aqueous electrolytes known in the art.

The methods of making electrolyte elements for an electric current producing cell of the present invention comprise the steps of first coating a liquid mixture comprising a boehmite sol and a liquid medium, and optionally a binder, onto a substrate and then drying the coating to form a microporous pseudo-boehmite layer, as described herein in the methods of making a separator, and subsequently contacting a surface of this pseudo-boehmite layer with an electrolyte, preferably an organic electrolyte, to cause the electrolyte to infuse into the pores of the pseudo-boehmite layer. Prior to the infusion of the electrolyte, the pseudo-boehmite layer has a pore volume from 0.02 to 2.0 cm^3/g and an average pore diameter from 1 nm to 300 nm, as described herein for the microporous pseudo-boehmite separator.

If increased mechanical strength or some other improvements such as improved adhesion to the substrate or coating uniformity are desired, the liquid mixture comprising the boehmite sol may further comprise a binder and then is dried to form a microporous pseudo-boehmite layer with binder present. The types of the binders such as polyvinyl alcohols, the amounts of the binder materials in the range of 3 to 200% of the weight of the pseudo-boehmite in the layer, and the thicknesses of the pseudo-boehmite layer with binder in the range of 1 to 50 microns, preferably 1 to 25 microns, more preferably 2 to 15 microns, and most preferably 5 to 15 microns, are as described herein for the microporous pseudo-boehmite separator and the methods of making the microporous pseudo-boehmite separator.

Examples of suitable electrolytes for use in the electrolyte elements of the present invention include, but are not limited to, organic electrolytes comprising one or more materials selected from the group consisting of: liquid electrolytes, gel polymer electrolytes, and solid polymer electrolytes.

Examples of useful liquid electrolyte solvents include, but are not limited to, those comprising electrolyte solvents selected from the group consisting of: N-methyl acetamide, acetonitrile, carbonates, sulfones, sulfolanes, aliphatic ethers, cyclic ethers, glymes, siloxanes, dioxolanes, N-alkyl pyrrolidones, substituted forms of the foregoing, and blends thereof; to which is added an appropriate ionic electrolyte salt.

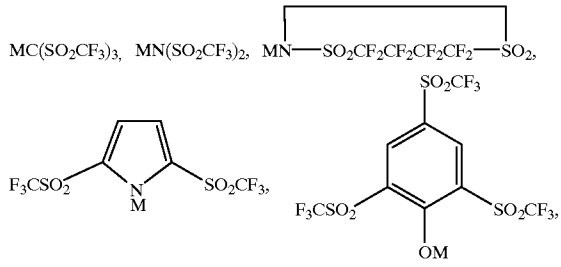
The electrolyte solvents of these liquid electrolytes are themselves useful as plasticizers for semi-solid or gel poly-

mer electrolytes. Examples of useful gel polymer electrolytes include, but are not limited to, those comprising, in addition to the electrolyte solvents sufficient to provide the desired semi-solid or gel state, ionic conductive polymers selected from the group consisting of: polyethylene oxides (PEO), polypropylene oxides, polyacrylonitriles, polysiloxanes, polyimides, polyphosphazenes, polyethers, sulfonated polyimides, perfluorinated membranes (NAFION™ resins), polydivinyl polyethylene glycols, polyethylene glycol diacrylates, polyethylene glycol dimethacrylates, derivatives of the foregoing, copolymers of the foregoing, crosslinked and network structures of the foregoing, and blends of the foregoing; to which is added an appropriate ionic electrolyte salt.

Examples of useful solid polymer electrolytes include, but are not limited to, those comprising ionic conductive polymers selected from the group consisting of: polyethers, polyethylene oxides (PEO), polypropylene oxides, polyimides, polyphosphazenes, polyacrylonitriles (PAN), polysiloxanes, polyether grafted polysiloxanes, derivatives of the foregoing, copolymers of the foregoing, crosslinked and network structures of the foregoing, and blends of the foregoing; to which is added an appropriate ionic electrolyte salt. The solid polymer electrolytes suitable for use in this invention may optionally further comprise one or more electrolyte solvents, typically less than 20% by weight.

To improve the ionic conductivity and other electrochemical properties of the electrolyte element, the organic electrolyte typically comprises one or more ionic electrolyte salts. As used herein, liquid electrolytes, gel polymer electrolytes, and solid polymer electrolytes comprise an ionic electrolyte salt.

Examples of ionic electrolyte salts for use in the present invention include, but are not limited to, $MClO_4$, $MAsF_6$, MSO_3CF_3, MSO_3CH_3, MBF_4, $MB(Ph)_4$, MPF_6, MSCN, MI MBr,



and the like, where M is Li or Na. Other electrolyte salts useful in the practice of this invention are lithium polysulfides, lithium salts of organic ionic polysulfides and those disclosed in U.S. Pat. No. 5,538,812 to Lee et al. Preferred ionic electrolyte salts are LiI, LiSCN, $LiSO_3CF_3$ (lithium triflate) and $LiN(SO_2CF_3)_2$ (lithium imide).

Since the microporous pseudo-boehmite layer of this invention is usually impermeable to high molecular weight materials such as the ionic conductive polymers typically used in gel polymer electrolytes and solid polymer electrolytes, it is preferable to introduce the ionic conductive polymer component of the electrolyte in a low molecular weight monomer or oligomer form into the pores of the pseudo-boehmite layer. Subsequently, the low molecular weight monomer or oligomer may be cured into an ionic conductive polymer to provide the desired type of polymer electrolyte. Suitable monomers or oligomers include, but are not limited to, heat- or radiation-curable monomers or oligomers. Examples include divinyl ethers such as tetraethyleneglycol divinyl ether. To provide sensitivity to ultraviolet (UV) or visible radiation where the monomers or oligomers do not absorb significantly, a conventional photosensitizer may be added to cause curing of the monomers or oligomers into a polymeric material. For example, a small amount, such as 0.2% by weight of the monomers or oligomers, of a UV sensitizer, such as ESCURE KTO (a trademark for a photosensitizer available from Sartomer Inc., Exton, Pa.), may be added to the monomers or oligomers.

The fraction of the pores of the pseudo-boehmite layer that are filled with ionic conductive polymer may vary from 2 to 100% depending on the type of polymer electrolyte desired. For gel polymer electrolytes, it is preferred to fill 15 to 80% of the pores with the ionic conductive polymer and then to fill the remainder of the pores with electrolyte solvents and ionic electrolyte salts. Typically, the ionic conductive polymer swells in the presence of the electrolyte solvents and ionic electrolyte salts to form a semi-solid or gel polymer electrolyte. A particular advantage of the ultrafine pores and strong capillary action of the pseudo-boehmite separator of the present invention is its excellent wetting by a broad variety of electrolytes and retention of these electrolytes in the pores. Accordingly, it is possible to incorporate liquid or tacky electrolyte materials into the nanoporous matrix of the pseudo-boehmite separator without having a significant excess of liquid or tacky material on the surface. Preferably, the electrolyte material is held below the outermost surface of the pseudo-boehmite separator during the cell fabrication process. For example, this is useful in preventing the tacky surfaces of solid or gel polymer electrolytes from interfering with the fabrication processes of winding or layering a multiple layer construction of an electric current producing cell. For liquid organic electrolytes, no polymer is required, and the electrolyte composition may consist of only electrolyte solvents and ionic electrolyte salts.

In a most preferred embodiment, the method of producing the electrolyte element comprises a substrate with a cathode coating layer on at least one of its outermost surfaces, and the liquid mixture comprising the boehmite sol is coated onto this cathode coating layer and, after drying, the surface of the pseudo-boehmite layer is contacted with an organic electrolyte to cause the infusion of the electrolyte into the pores of the pseudo-boehmite layer.

Electric Current Producing Cells

The present invention provides an electric current producing cell comprising a cathode and an anode and an electrolyte element interposed between the cathode and the anode, wherein the electrolyte element comprises a microporous pseudo-boehmite layer and an electrolyte, preferably an organic electrolyte, contained within the pores of the pseudo-boehmite layer, as described herein for the microporous pseudo-boehmite layer or separator and the electrolyte element of the present invention. This pseudo-boehmite layer has a pore volume from 0.02 to 2.0 cm^3/g, before the introduction of the electrolyte, and has an average pore diameter from 1 nm to 300 nm, as described herein for the microporous pseudo-boehmite separator.

Although the electric current producing cell of the present invention may be utilized for a wide variety of primary and secondary batteries known in the art, it is preferred to utilize these cells in secondary or rechargeable batteries where the many features of a free standing or directly coated microporous pseudo-boehmite separator may be employed to help control the chemistry of the active materials through many repeated discharge and charge cycles.

Suitable anode active materials for the electric current producing cells of the present invention include, but are not limited to, one or more metals or metal alloys or a mixture of one or more metals and one or more alloys, wherein said metals are selected from the Group IA and IIA metals in the Periodic Table. Examples of suitable anode active materials of the present invention include, but are not limited to, alkali-metal intercalated conductive polymers, such as lithium doped polyacetylenes, polyphenylenes, polypyrroles, and the like, and alkali-metal intercalated graphites and carbons. Anode active materials comprising lithium are especially useful. Preferred anode active materials are lithium metal, lithium-aluminum alloys, lithium-tin alloys, lithium-intercalated carbons, and lithium-intercalated graphites.

Suitable cathode active materials for use in the cathode active layers of the cathodes for the electric current producing cells of this invention include, but are not limited to, electroactive transition metal chalcogenides, electroactive conductive polymers, and electroactive sulfur-containing materials. The term "sulfur-containing material," as used herein, relates to cathode active materials which comprise the element sulfur in any form, wherein the electrochemical activity involves the breaking or forming of sulfur-sulfur covalent bonds. In one embodiment, the electroactive sulfur-containing material comprises elemental sulfur. In one embodiment, the electroactive sulfur-containing material is organic, that is, it comprises both sulfur atoms and carbon atoms. In one embodiment, the electroactive sulfur-containing material comprises a sulfur-containing polymer, wherein the electroactive sulfur-containing polymer, in its oxidized state, comprises a covalent polysulfide moiety of the formula, —S_m—, wherein m is an integer equal to or greater than 3, preferably m is an integer from 3 to 10, most preferably m is an integer equal to or greater than 6, and particularly most preferably m is an integer equal to or greater than 8.

Cathode active materials for use in the cathodes for the electric current producing cells of the present invention include, but are not limited to, electroactive sulfur-containing cathode materials which, in their oxidized state, comprise a polysulfide moiety of the formula, —S_m—, wherein m is an integer equal to or greater than 3, preferably m is an integer from 3 to 10, most preferably m is an integer equal to or greater than 6, and particularly most preferably m is an integer equal to or greater than 8. Examples of these preferred cathode materials include elemental sulfur and carbon-sulfur polymer materials, as described in U.S. Pat. Nos. 5,529,860; 5,601,947;and 5,690,702;in U.S. patent application Ser. No. 08/602,323, all by Skotheim et al.; and in U.S. patent application Ser. No. 08/995,112 to Gorkovenko et al., all to the common assignee.

In a most preferred embodiment, the polysulfide moiety, —S_m—, of the carbon-sulfur polymer material is covalently bonded by one or both of its terminal sulfur atoms on a side group to the polymer backbone chain of the polymer material. In another most preferred embodiment, the polysulfide moiety, —S_m—, of the carbon-sulfur polymer material is incorporated into the polymer backbone chain of the polymer material by covalent bonding of the polysulfide moiety's terminal sulfur atoms. In another most preferred embodiment, the carbon-sulfur polymer material with polysulfide, —S_m—, groups, wherein m is an integer equal to or greater than 3, comprises greater than 75 weight percent of sulfur.

In one embodiment, the electroactive sulfur-containing material comprises a sulfur-containing polymer comprising an ionic polysulfide moiety selected from the group consisting of: ionic —S_m^- moieties and ionic S_m^{2-} moieties, wherein m is an integer equal to or greater than 3, and preferably m is an integer equal to or greater than 8. Examples of these sulfur-containing materials include sulfur-containing polymers comprising ionic —S_m^- moieties, as described in U.S. Pat. No. 4,664,991 to Perichaud et al, and sulfur-containing polymers comprising ionic S_m^{2-} moieties, as described in the aforementioned U.S. Pat. No. 4,664,991 and in European Pat. No. 250,518 B1 to Genies. In one embodiment, the polymer backbone chain of the sulfur-containing polymer having an ionic polysulfide moiety comprises conjugated segments. In one embodiment, the polysulfide moiety, —S_m^-, is covalently bonded by one of its terminal sulfur atoms on a side group to the polymer backbone chain of the sulfur-containing polymer. In one embodiment, the sulfur-containing polymer having an ionic polysulfide moiety comprises greater than 75 weight percent of sulfur.

In another embodiment of the electric current producing cell of the present invention, the electrolyte of the electrolyte element is an organic electrolyte comprising one or more materials selected from the group consisting of: liquid electrolytes, gel polymer electrolytes and solid polymer electrolytes.

A method for forming the electric current producing cell of the present invention comprises providing an anode and a cathode and interposing an electrolyte element of the present invention, as described herein, between the anode and the cathode.

In one embodiment of the methods of forming the electric current producing cell, the electrolyte of the electrolyte element is an organic electrolyte comprising one or more materials selected from the group consisting of: liquid electrolytes, gel polymer electrolytes, and solid polymer electrolytes.

The flexibility of the product designs and methods of forming the separators and electrolyte elements of the present invention provide the option of effectively incorporating the ionic electrolyte salt into the electric current producing cell at a later or final stage of fabricating materials into the electrochemically active cell. This may be advantageous when the ionic electrolyte salt is hygroscopic and difficult to coat as part of a gel polymer or solid polymer electrolyte composition and then difficult to keep from absorbing water before fabrication and hermetic sealing of the cell in a dry room facility. This may also be advantageous when the ionic electrolyte salt increases the viscosity and otherwise interferes with the wetting and penetration of a liquid or polymer electrolyte into the separator and cathode layers during the filling of the cell. In a preferred embodiment, after the electrolyte element is enclosed between the anode and cathode, there is a subsequent step comprising the imbibition of a solution comprising one or more ionic electrolyte salts and one or more electrolyte solvents into the electrolyte element. In a most preferred embodiment, the electrolyte element that is enclosed between the anode and the cathode initially comprises the microporous layer and electrolyte solvents, but contains no ionic electrolyte salt; and the ionic electrolyte salts as may be required for the electrolyte element are provided by a subsequent step of imbibing a solution comprising one or more ionic electrolyte salts and one or more electrolyte solvents into the electrolyte element. To achieve the desired final concentration of ionic electrolyte salts in the organic electrolyte, the concentration of ionic electrolyte salts in the imbibed solution will be correspondingly much greater than this desired final concentration.

EXAMPLES

Several embodiments of the present invention are described in the following examples, which are offered by way of illustration and not by way of limitation.

Example 1

A microporous layer of pseudo-boehmite with polyvinyl alcohol binder present was prepared according to the following procedure. A coating mixture with a solids content of about 8% comprising 7 weight per cent (solid content) of CATALOID AS-3 (a tradename for boehmite sol available from Catalysts & Chemicals Ind. Co., Ltd., Tokyo, Japan) and 0.7 weight per cent (solid content) of AIRVOL 125 (a trademark for polyvinyl alcohol polymer available from Air Products, Inc., Allentown, Pa.) in water was prepared. This coating mixture was coated on 100 micron thick MELINEX 516 film (a trademark for polyethylene terephthalate (PET) film available from ICI Polyester, Wilmington, Del.) using a gap coater so that the dry pseudo-boehmite coating thickness would be 25 microns and followed by drying at 130° C. Alternatively, the dry coating thickness of 25 microns was obtained by multiple passes of coating application and drying such as two consecutive coating applications with thicknesses of about 12.5 microns of dry coating. After drying, the coated film was soaked in a solution of 67:33 by volume of water:isopropanol. This lowered the adhesion of the coating to the PET film so that the 25 micron pseudo-boehmite coating could be delaminated from the PET film substrate.

The pore volume of this 25 micron free standing pseudo-boehmite film was determined by the method of soaking a piece of film with a known area in liquid polyethylene glycol dimethyl ether, wiping the excess liquid from the film surface, and weighing the film before and after imbibing the liquid. By this method, using Equation I:

$$\text{Pore Volume} = \frac{[W_1 - W_2]/d}{W_2} \qquad \text{I}$$

wherein W_1 is the weight of the film when the pores are completely filled with the liquid, W_2 is the weight of the film with no liquid present in the pores, and d is the density of the liquid, the pore volume of the 25 micron pseudo-boehmite film was measured to be 0.67 cm^3/g. The porosity was calculated as 65% using Equation III. Using the same method, the porosity of CELGARD 2500 polyethylene separator film (trademark for porous polyolefin films, such as this 25 micron thick polyethylene film, available from Hoechst Celanese Corporation, Charlotte, N.C.) was calculated as 48%. As an alternative method, the actual density of the 25 micron pseudo-boehmite film was measured as 1.0 g/cm^3, and the theoretical density (assuming no pores) was calculated as 2.8 g/cm^3. From this, by subtracting the reciprocal of the theoretical density from the reciprocal of the measured density as in Equation II, the pore volume was estimated as 0.64 cm^3/g. The porosity was calculated as 64%.

Example 2

A 5% by weight solution of a 1:1 ratio by weight of PHOTOMER 4028 (a trademark for radiation curable oligomers, such as this ethoxylated bisphenol A diacrylate, available from Henkel Corp., Ambler, Pa.) and PHOTOMER 6210 (an ethoxylated aliphatic urethane diacrylate also available from Henkel Corp., Ambler, Pa.) was prepared by dissolving these oligomers in methyl acetate. To this solution, 0.2% by weight (based on the total weight of the oligomers) of ESCURE KTO (a trademark for photosensitizers available from Sartomer Inc., Exton, Pa.) was added and dissolved by stirring to give the final solution for treatment of the pseudo-boehmite film.

A 25 micron thick free-standing pseudo-boehmite film, prepared according to Example 1, was dipped in the above solution of oligomers and photosensitizer so that the pores of the pseudo-boehmite film were completely filled with the solution. Excess liquid was removed from the surface of the pseudo-boehmite film by using a smooth coating blade. The film was then dried at 25° C. in a laboratory hood with moderate exhaust air flow. The dried film was then cured by placing it on the conveyor belt of a FUSION Model P300 UV exposure unit (a tradename for radiation curing equipment available from Fusion Systems Company, Torrance, Calif.) and exposing it to the UV lamps for 30 seconds. The resulting 25 micron thick pseudo-boehmite separator film with polymer treatment was insoluble in water and in 1,3-dioxolane, methyl acetate, and dimethoxyethane (DME). By weighing the pseudo-boehmite separator film before and after the polymer treatment, the increase in weight from a single dipping process and subsequent cure, as described above, corresponded to filling about 18% of the available void volume of the pseudo-boehmite layer with cured polymer materials. Since the porosity or void volume of the pseudo-boehmite layer of Example 1 is about 65%, the void volume of the pseudo-boehmite layer remaining after this polymer treatment was calculated to be about 53%.

Comparative Example 1

A cathode was prepared by coating a mixture of 55 parts of elemental sulfur, 15 parts of CAB-O-SIL TS-530 silica (a trademark for silica pigment available from Cabot Corporation, Tuscola, Ill.), 15 parts of conductive carbon pigment (Shawingan Acetylene Black or SAB-50, a trademark for carbon pigments available from Chevron Corporation, Baytown, Tex.), and 15 parts of polyethylene oxide (PEO) binder (5,000,000 molecular weight available from Polysciences Inc., Warrington, Pa.) in acetonitrile as the solvent onto an 18 micron thick nickel foil substrate to give a cathode coating thickness of about 25 microns. The anode was lithium foil of about 175 microns in thickness. The electrolyte was a 1.0 M solution of lithium triflate in tetraethylene glycol dimethyl ether (tetraglyme). The porous separator used was CELGARD 2500.

The above components were combined into a layered structure of cathode/separator/anode with the liquid electrolyte filling the void areas of the separator and cathode to form disc-shaped CR2032 coin cells of 2 cm^2 in area.

Discharge-charge cycling on these cells was done at 0.2 mA or 0.1 mA/cm^2 for the first two cycles and then at 1 mA or 0.5 mA/cm^2 for additional cycles. The average capacity for 4 coin cells was 1.9 mAh on the first cycle and 1.3 mAh on the fifth cycle.

Two different coin cells were cycled at 0.4 mA (0.2 mA/cm^2) discharge and charge from the first cycle. The average capacity for these 2 coin cells with CELGARD 2500 polyethylene separator was 0.8 mAh (specific capacity of 466 mAh/g of elemental sulfur in the cell) on the fifth cycle and was 0.7 mAh (specific capacity of 408 mAh/g) on the 15th cycle.

Example 3

Coin cells were constructed as in Comparative Example 1 except that the 25 micron pseudo-boehmite separator film

from Example 1 was substituted for the 25 micron CELGARD 2500 polyethylene film. Discharge-charge cycling was done under the same first set of conditions (0.2 mA for first two cycles and then 1 mA) as in Comparative Example 1. The average capacity for 2 coin cells with the 25 micron pseudo-boehmite separator of Example 1 was 1.9 mAh on the first cycle and 1.4 mAh on the fifth cycle. This shows cell performance and cycling similar to Comparative Example 1 with the conventional porous polyethylene separator (CELGARD 2500).

Another coin cell was cycled at a second set of conditions, namely 1.0 mA (0.5 mA/cm^2) discharge and charge from the first cycle. The capacity of this coin cell with pseudo-boehmite separator was 1.0 mAh (specific capacity of 633 mAh/g of elemental sulfur in the cell) on the fifth cycle and was 0.7 mAh (specific capacity of 466 mAh/g) on the 33rd cycle. Although the significantly higher discharge and charge rates for this cell would be expected to lower its capacity and cycling stability compared to the two coin cells in Comparative Example 1 with lower discharge-charge rates, this cell with pseudo-boehmite separator had better capacity and cycle stability than the two cells with the porous polyethylene separator tested at 0.4 mA charge and discharge in Comparative Example 1.

Comparative Example 2

A cathode was prepared by coating a mixture of 80 parts of a carbon-sulfur polymer with an average polysulfide chain length of about 5 and with about 90% sulfur content (made by the process described in Example 2 in a copending U.S. patent application Ser. No. 08/995,112 to Gorkovenko et al. to the common assignee); 10 parts of a conductive carbon pigment, PRINTEX XE-2 (a trademark for carbon pigments available from Degussa Corporation, Akron, Ohio); 5 parts of PYROGRAF-III carbon nanofiber (a trademark for carbon filaments available from Applied Sciences, Inc., Cedarville, Ohio); and 5 parts of a 4:1 by weight ratio of poly(acrylamide-co-diallyldimethylammonium chloride) (available from Aldrich Chemical Company, Milwaukee, Wis.) and of polyethylene oxide or PEO (as described in Comparative Example 1) at about 12% solids in a blend of 13:1 ethanol:water onto a 17 micron thick conductive carbon and resin coated aluminum foil substrate (Product No. 60303 available from Rexam Graphics, South Hadley, Mass.). The cathode coating thickness was about 25 microns. The anode was lithium foil of about 75 microns in thickness. The electrolyte was a 0.75 M solution of lithium imide (available from 3M Corporation, St. Paul, Minn.) in a 50:50 by volume mixture of 1,3-dioxolane and dimethoxyethane (DME). The porous separator used was E25 SETELA (a trademark for polyolefin separators available from Tonen Chemical Corporation, Tokyo, Japan, and also available from Mobil Chemical Company, Films Division, Pittsford, N.Y.).

The above components were combined into a layered structure of cathode/separator/anode with the liquid electrolyte filling the void areas of the separator and cathode to form vial cells of about 40 cm^2 in area. Discharge-charge cycling on these cells was done at 8 mA or 0.2 mA/cm^2 with discharge cutoff at a voltage of 1.3 V and charge cutoff at 150% overcharge of the previous discharge capacity or 2.8 V, whichever came first. Typical capacity of these cells was 32 mAh (specific capacity of 575 mAh/g of carbon-sulfur polymer in the cell) at the fifth cycle with a total capacity fade of about 25% over the next 25 cycles. The charging at each cycle was to the 150% overcharge limit. The 2.8 V cutoff was not reached on the charging half of the cycle. Thus, charging was relatively inefficient and required at least a 50% extra charge on each cycle to recharge after the discharge.

Comparative Example 3

Vial cells were constructed as in Comparative Example 2 except that 80 parts of elemental sulfur were substituted for the 80 parts of carbon-sulfur polymer in the mixture used to prepare the cathode. Discharging of the cells was done at 0.33 mA/cm^2, and charging of the cells was done at 0.22 mA/cm^2. The discharge and charge cutoff conditions were the same as in Comparative Example 2. Typical specific capacity of these cells was 460 mAh/g of elemental sulfur in the cell at the 5th cycle with no significant loss in specific capacity out to 70 cycles. As in Comparative Example 2, the charging at each cycle on these cells was to the 150% overcharge limit. The 2.8 V cutoff was not reached on the charging half of the cycle.

Example 4

Vial cells were constructed as in Comparative Example 2 except that the 25 micron pseudo-boehmite separator film with polymer treatment from Example 2 was substituted for the 25 micron E25 SETELA separator film. Discharge-charge cycling was done under the same set of conditions as in Comparative Example 2. Typical capacity of these cells was 25 mA (specific capacity of 613 mAh/g of carbon-sulfur polymer in the cell) at the fifth cycle with a total capacity fade of about 14% over the next 25 cycles and of about 28% over the next 65 cycles. The charging at each cycle was to the 2.8 V cutoff. The 150% overcharge limit was not reached on the charging half of the cycle. The amount of overcharge before reaching the 2.8 V cutoff remained in the range of 105 to 120% during the cycling. This data shows the specific capacities, capacity fading, and charging conditions and efficiencies of the cells with the pseudo-boehmite separator to be significantly better than that of the cells with the conventional polyolefin separator of Comparative Example 2.

A self-discharge test was performed by resting the cells for 24 hours after the 5th, 10th, and 30th cycles and then measuring the loss in capacity. The self-discharge was 5.8%, 2.6%, and 2.7% after the 5th, 10th, and 30th cycles, respectively. By contrast, the self-discharge of cells from Comparative Example 2 was in the range of 10 to 20%.

Example 5

Vial cells were constructed as in Comparative Example 3 except that the 25 micron pseudo-boehmite separator film with polymer treatment from Example 2 was substituted for the 25 micron E25 SETELA separator film. Discharge-charge cycling was done under the same set of conditions as in Comparable Example 3. Typical specific capacity of these cells was 600 mAh/g of elemental sulfur in the cell at the 5th cycle with a total capacity fade of about 15% out to 70 cycles. The charging at each cycle was to the 2.8 V cutoff. The 150% overcharge limit was not reached on the charging half of the cycle. The amount of overcharge before reaching the 2.8 V cutoff remained in the range of 110 to 140% during the cycling. This data shows the specific capacities and charging conditions and efficiencies of the cells with the pseudo-boehmite separator to be significantly better than that of the cells with the conventional polyolefin separator of Comparative Example 3. The capacity fade of the cells with the pseudo-boehmite separator is greater than in Comparative Example 3, but the specific capacity at the 70th cycle

and the accumulated capacity out to 70 cycles are significantly better than Comparative Example 3.

Example 6

Vial cells were constructed as in Example 5 except that an 11 micron thick pseudo-boehmite separator film with polymer treatment was used instead of the 25 micron thick pseudo-boehmite separator film with polymer treatment. The 11 micron pseudo-boehmite separator film with polymer treatment was prepared as in Examples 1 and 2, except that DISPAL 11N7-12 (a trademark for boehmite sol available from CONDEA Vista Company, Houston, Tex.) was used instead of CATALOID AS-3, and the gap of the gap coater was reduced so that the dry pseudo-boehmite coating thickness was 11 microns. Discharge-charge cycling performed under the same set of conditions as in Example 5 gave similar specific capacities, capacity fading, and charging properties as in Example 5. This shows that the large reduction in thickness in the pseudo-boehmite separator from 25 to 11 microns still provides satisfactory performance and retains significant advantages over the thicker 25 micron polyolefin separators. No formation of short circuits was observed during cycling of these cells to over 100 cycles. This is further evidence that the pseudo-boehmite separator is stable during cycling and is not degrading such that the formation of short circuits occurs.

Example 7

Vial cells were constructed as in Example 6, except that a 12 micron thick pseudo-boehmite separator layer was coated directly on the cathode instead of using the free standing separator of Example 6; the oligomer treatment with curing was done after the direct coating of the separator; and changes were made in the cathode and the electrolyte. As in Example 6, DISPAL 11N7-12 instead of CATALOID AS-3 was used for the boehmite sol. The approximately 8% by weight solids mixture of 10:1 DISPAL 11N7-12:AIRVOL 125 in water was applied in two coating passes of approximately equal coating weight application to give a total pseudo-boehmite layer thickness of 12 microns. The cathode used was the same as in Comparative Example 3, except that 85 parts of elemental sulfur was used instead of 80 parts; the amount of conductive carbon pigment, PRINTEX XE-2, was increased to 12 parts; the amount of PYROGRAF-III carbon nanofiber was reduced to 2 parts; and no polymeric binder was present. The cathode coating thickness was about 16 microns. The UV curable oligomer and photosensitizer solution was the same as in Example 2. This solution was applied by a blade coating to the outermost surface of the pseudo-boehmite separator layer coated on the cathode so that the pores of the pseudo-boehmite layer were completely filled with the solution. The excess liquid was removed from the surface and the pseudo-boehmite layer then dried and cured by UV radiation, as described in Example 2. The electrolyte was a 1.0 M solution of lithium triflate (available from 3M Corporation, St. Paul, Minn.) in a 50:35:10:5 by volume mixture of 1,3-dioxolane:diethylene glycol dimethyl ether (diglyme) :DME:o-xylene.

Discharge-charge cycling was done under the same set of conditions as in Example 5. Typical specific capacities of these cells were 550 mAh/g of elemental sulfur in the cell at the 5th cycle with a total capacity fade of about 20% out to 100 cycles. The charging at each cycle was to a 3.0 V cutoff. The 150% overcharge limit was not reached on the charging half of the cycle. The amount of overcharge before reaching the 3.0 V cutoff remained in the range of 125 to 145% during the cycling. This data shows that cells with a pseudo-boehmite separator layer coated directly on the cathode provided comparable specific capacities, capacity fading, and charging properties to cells with a free standing pseudo-boehmite separator of similar composition and had satisfactory performance at a dry thickness of only 12 microns.

Example 8

Vial cells were constructed as in Example 7, except that a 50:50 by weight mixture of PEO (600,000 molecular weight):PEO (5,000,000 molecular weight), both available from Polysciences Inc., Warrington, Pa., was used instead of the AIRVOL 125 polyvinyl alcohol polymer; and the electrolyte as described in Comparative Example 2 was used. Discharge, charge, and cutoff conditions were the same as in Example 7. The specific capacities, capacity fading, and charging properties were similar to those reported in Example 7. This illustrates that other polymeric binders, such as polyethylene oxides, can be used instead of polyvinyl alcohol to form the microporous separator of the present invention.

Comparative Example 4

The carbon electrode was prepared using 85 parts of graphite powder (MCMB 10-28 available from Osaka Gas, Osaka, Japan), 5 parts of conductive carbon (SAB-50), and 10 parts of KYNAR 500LVD binder (a trademark for vinylidene fluoride-tetrafluoroethylene copolymer available from Elf Atochem North America, Inc., Philadelphia, Pa.) in N-methyl pyrrolidone as the solvent to give a coating thickness of about 75 microns on a 13 micron thick copper foil substrate. The other electrode was lithium foil of about 175 microns in thickness. The electrolyte was a 1.0 M solution of $LiPF_6$ in an 1:1 by volume mixture of ethylene carbonate (EC): dimethyl carbonate (DMC). The porous separator used was CELGARD 3401, a special grade of polyolefin separator with a wetting agent treatment present.

The above components were combined into a layered structure of carbon electrode/separator/lithium foil with the liquid electrolyte filling the void areas of the separator and cathode to form disc-shaped CR2032 coin cells of 2 cm^2 in area.

Discharge-charge cycling on these cells was done at 0.2 mA or 0.1 mA/cm^2 for the first two cycles and then at 1 mA or 0.5 mA/cm^2 for additional cycles. The average capacity for 8 of these coin cells was 8.9 mAh on the second cycle.

Example 9

A coin cell was constructed as in Comparative Example 4, except that the 25 micron pseudo-boehmite separator film from Example 1 was substituted for the 25 micron CELGARD 3401 polyolefin film. Discharge-charge cycling was done under the same conditions as in Comparative Example 4. The carbon-lithium coin cell with the 25 micron pseudo-boehmite separator of Example 1 had a capacity of 6.0 mAh on the second cycle and a capacity of 6.2 mAh on the sixth cycle. Although the capacity with the pseudo-boehmite separator is lower on the second charge-discharge cycle than with the CELGARD 3401 polyolefin separator, the capacity is still good. The lack of capacity fade upon charge-discharge cycling with the pseudo-boehmite separator is also positive.

The pseudo-boehmite separator of this invention with its excellent wetting properties exhibits flexibility in its broad

compatibility with various cathode and electrolyte solvent/lithium salt combinations, such as sulfur-based cathodes and electrolyte compositions for both sulfur-based and for lithium ion type batteries, without requiring a special treatment with a wetting agent. In particular, the wettability of the separator to the different electrolytes commonly used in batteries is often problematical. For example, the combination of electrolyte solvent and lithium salt of Comparative Example 4 does not wet conventional polyolefin separators, such as CELGARD 2500, adequately so a surfactant or wetting agent treatment must be applied to the separator surface. However, there is a concern about possible negative effects of a surfactant treatment on battery performance.

Comparative Example 5

A cathode was prepared by coating a mixture of 75 parts of elemental sulfur (available from Aldrich Chemical Company, Milwaukee, Wis.), 20 parts of PRINTEX XE-2 conductive carbon pigment, and 5 parts of PYROGRAF-III carbon nanofibers dispersed at 10% solids in isopropanol onto a 17 micron thick conductive carbon and resin coated aluminum foil substrate (Product No. 60303). After heating at 130° C. for 1 minute and calendering, the thickness of the cathode active layer was about 10 microns. The anode was lithium foil of about 50 microns in thickness. The electrolyte was a 1.424 M solution of lithium imide in a 41.5:58.5 volume ratio of 1,3-dioxolane and dimethoxyethane. The porous separator used was 16 micron thick E25 SETELA polyolefin separator.

The above components were combined into a layered structure of cathode/separator/anode, which was wound and compressed, with the liquid electrolyte filling the void areas of the separator and cathode active layer to form prismatic cells of 500 cm^2 in area. Discharge/charge cycling on these cells was done at 0.5/0.3 mA/cm^2, respectively, with discharge cutoff at 1.3 V and charge cutoff at 3 V or 120% of the discharge capacity of the last cycle, whichever came first. Typical capacity of these cells was about 500 mAh (specific capacity of 1030 mAh/g of the elemental sulfur in the cell) at the 10th cycle with a total capacity fade of about 14% over the next 50 cycles.

Example 10

A microporous layer comprising pseudo-boehmite with binder present was prepared according to the following procedure. A water-based coating mixture with a solids content of about 8% comprising 86 parts by weight (solid content) of DISPAL 11N7-12 boehmite sol, 6 parts by weight (solid content) of AIRVOL 125 polyvinyl alcohol polymer, 3 parts by weight of polyethylene glycol (molecular weight of 900,000 available from Aldrich Chemical Company, Milwaukee, Wis.), and 5 parts by weight of polyethylene glycol dimethylether, M-250 (available from Fluka Chemical Company, Ronkonkoma, N.Y.), in water was prepared. This coating mixture was coated directly on a cathode with a cathode active layer prepared as described in Comparative Example 5, using a slot die extrusion coating application with two successive coating applications of similar thickness to provide a total dry pseudo-boehmite coating thickness of about 12 microns.

A 5% by weight solution of a 3:2 ratio by weight of CD 9038 (a tradename for ethoxylated bisphenol A diacrylate available from Sartomer Inc., Exton, Pa.) and CN 984 (a tradename for a urethane acrylate available from Sartomer Inc., Exton, Pa.) was prepared by dissolving these oligomers in ethyl acetate. To this solution, 0.2% by weight (based on the total weight of acrylate oligomers) of ESCURE KTO was added. This coating solution also contained 5% by weight of CAB-O-SIL TS-530 silica pigment, which was dispersed in the oligomer solution by sonication. The oligomer solution was coated on the 12 micron thick microporous layer comprising pseudo-boehmite and binder and then dried to remove the solvent present. The coating thickness of the dried coating on top of the pseudo-boehmite layer was about 4 microns. The dried film was then cured by UV curing using a Model F450T UV exposure unit (available from Fusion Systems Corporation, Rockville, Md.). After heating at 110° C. for 4 minutes, these cathodes were ready for assembly into electric current producing cells.

Prismatic cells of 500 cm^2 in area were constructed as described in Comparative Example 5. The electrolyte was the same as that used in Comparative Example 5. Discharge/charge cycling was performed on these cells at the same current densities as described in Comparative Example 5. The specific capacity of the cells was about 850 mAh/g for the elemental sulfur in the cell at the 5th cycle with a total capacity fade of about 17% over the next 80 cycles. After 100 cycles, the average capacity of these cells was 77% of the specific capacity at the 5th cycle.

Example 11

18% by weight of DISPAL 11N7-80 boehmite powder (available from CONDEA Vista Company, Houston, Tex.) was added slowly into ethanol solvent under stirring by a 1 horsepower laboratory mixer and emulsifier (Ross Model ME-100LX) and stirred at about 2500 rpm for 5 minutes followed by additional stirring for 15 minutes at 4750 rpm.

A microporous layer comprising pseudo-boehmite was prepared according to the following procedure. A coating mixture with a solid content of about 14% comprising 85 parts by weight (solid content) of DISPAL 11N7-80 boehmite powder (18% solids dispersion in ethanol), 12 parts by weight (solid content) of MOWITAL B60H (a trademark for polyvinyl butyral binders available from Hoechst Celanese Corporation, Charlotte, N.C.), and 3 parts by weight of M-250 polyethylene glycol dimethyl ether in ethanol was prepared and then coated as described in Example 10.

Prismatic cells were prepared as described in Example 10, except that the microporous layer comprising pseudo-boehrnite was obtained by using the above ethanol-based boehmite coating mixture. The electrolyte used was the same as that used in Example 10. Discharge/charge cycling was performed on these cells at the same current densities as in Example 10. The specific capacity of the cells was about 1030 mAh/g of the elemental sulfur in the cell at the 10th cycle with a total capacity fade of only about 13% over the next 130 cycles. After 150 cycles, the average capacity of these cells was above 85% of the specific capacity at the 10th cycle.

While the invention has been described in detail and with reference to specific and general embodiments thereof, it will be apparent to one skilled in the art that various changes and modifications can be made therein without departing from the spirit and scope thereof.

What is claimed is:

1. A separator for use in an electric cunent producing cell for separating an anode and a cathode, wherein said separator comprises a microporous layer comprising pseudo-boehmite and a binder;

wherein said binder is an inorganic binder.

2. The separator of claim **1**, wherein said binder is present in an amount of 3 to 200% of the weight of pseudo-boehmite in said microporous layer.

3. The separator of claim 1, wherein said binder is present in an amount of 5 to 70% of the weight of pseudo-boehmite in said microporous layer.

4. The separator of claim 1, wherein said binder is selected from the group consisting of colloidal silicas, colloidal non-hydrated aluminum oxides, colloidal tin oxides, colloidal titanium oxides, colloidal zirconium oxides, and colloidal zinc oxides.

5. The separator of claim 1, wherein pores of said microporous layer are impregnated with a composition comprising a polymer.

6. The separator of claim 1, wherein said microporous layer has a thickness of from 1 micron to 50 microns.

7. A separator for use in an electric current producing cell for separating an anode and a cathode, wherein said separator comprises a microporous layer comprising pseudo-boehmite and a binder;

wherein pores of said microporous layer are impregnated with a composition comprising a polymer; and

wherein said polymer is ionically conductive.

8. The separator of claim 7, wherein said binder is an organic binder.

9. The separator of claim 7, wherein said binder is selected from the group consisting of polyvinyl alcohols, polyethylene oxides, alkylated polyethylene oxides, polyvinyl pylTolidones, polyvinyl butyrals, hydroxyethyl cellulose, cellulose acetate propionate, polymers comprising quaternary ammonium groups, polyacrylamides, polyvinyl ethers, polyethyleneimines, polyurethanes, epoxies, melamine formaldehydes, urea formaldehydes; copolymers thereof; copolymers of maleic anhydride and derivatives and esters thereof; gelatin; starch; and mixtures of the foregoing binders.

10. The separator of claim 7, wherein said binder is an inorganic binder.

11. The separator of claim 7, wherein said binder further comprises one or more additives selected from the group consisting of pigments, crosslinking agents, catalysts for non-radiation curing, sensitizers for radiation curing, plasticizers, surfactants, and dispersants.

12. The separator of claim 7, wherein said composition further comprises a crosslinking agent.

13. The separator of claim 7, wherein said microporous layer has a thickness of from 1 micron to 25 microns.

14. The separator of claim 7, wherein said microporous layer has a thickness of from 2 microns to 15 microns.

15. An electrolyte element for use in an electric current producing cell for separating an anode and a cathode, wherein said electrolyte element comprises:

(a) a separator comprising a microporous layer comprising pseudo-bochmite and a binder; and

(b) an organic electrolyte contained within pores of said microporous layer.

16. The electrolyte element of claim 15, wherein said binder is present in an amount of 3 to 200% of the weight of pseudo-boehmite in said microporous layer.

17. The electrolyte element of claim 15, wherein said binder is present in an amount of 5 to 70% of the weight of pseudo-boehmite in said microporous layer.

18. The electrolyte element of claim 15, wherein said binder is an organic binder.

19. The electrolyte element of claim 15, wherein said binder is selected from the group consisting of polyvinyl alcohols, polyethylene oxides, alkylated polyethylene oxides, polyvinyl pyrrolidones, polyvinyl butyrals, hydroxyethyl cellulose, cellulose acetate propionate, polymers comprising quartemary ammonium groups, polyacrylamides polyvinyl ethers, polyethyleneimines, polyurethanes, epoxies, melamine formaldehydes, urea formaldehydes; copolymers thereof; copolymers of maleic anhydride and derivatives and esters thereof; gelatin, starch; and mixtures of the foregoing binders.

20. The electrolyte element of claim 15, wherein said binder is an inorganic binder.

21. The electrolyte clement of claim 15, wherein said binder is selected from the group consisting of colloidal silicas, colloidal non-hydrated aluminum oxides, colloidal tin oxides, colloidal titanium oxides, colloidal zirconium oxides, and colloidal zinc oxides.

22. The electrolyte element of claim 15, wherein said binder further comprises one or more additives selected from the group consisting of pigments, crosslinking agents, catalysts for non-radiation curing, sensitizers for radiation curing, plasticizers, surfactants, and dispersants.

23. The electrolyte element of claim 15, wherein said organic electrolyte comprises one or more materials selected from the group consisting of liquid electrolytes, gel polymer electrolytes, and solid polymer electrolytes.

24. The electrolyte element of claim 15, wherein said microporous layer has a thickness of from 2 microns to 15 microns.

25. A method of making a separator for use in an electric current producing cell for separating an anode and a cathode, said separator comprising a microporous layer comprising pseudo-boehmite and a binder, wherein said method comprises the steps of:

(a) coating onto a substrate a liquid mixture comprising a boehmite sol, a binder, and a liquid medium; and

(b) drying the coating formed in step (a) to yield said microporous layer;

wherein said binder is an inorganic binder.

26. The method of claim 25, wherein said liquid medium comprises water.

27. The method of claim 25, wherein said liquid medium comprises one or more organic solvents.

28. The method of claim 25, wherein said liquid medium comprises one or more protic organic solvents selected from the group consisting of alcohols and glycols.

29. The method of claim 25, wherein said liquid medium comprises one or more protic organic solvents selected from the group consisting of methanol, ethanol, isopropanol, 1-propanol, 1-butanol, 2-butanol, 2-methoxyethanol, 2-ethoxyethanol, 2-butoxyethanol, ethylene glycol, and propylene glycol.

30. The method of claim 25, wherein said liquid medium comprises ethanol.

31. The method of claim 25, wherein said liquid medium comprises water and one or more organic solvents.

32. The method of claim 25, wherein said binder is present in an amount of 3 to 200% of the weight of pseudo-boehmite in said microporous layer.

33. The method of claim 25, wherein said binder is present in an amount of 5 to 70% of the weight of pseudo-boehmite in said microporous layer.

34. The method of claim 25, wherein said binder is selected from the group consisting of colloidal silicas, colloidal non-hydrated aluminum oxides, colloidal tin oxides, colloidal titanium oxides, colloidal zirconium oxides, and colloidal zinc oxides.

35. The method of claim 25, wherein pores of said microporous layer are impregnated with a composition comprising a polymer.

36. The method of claim 25, wherein said microporous layer has a thickness of from 1 micron to 50 microns.

37. A method of making a separator for use in an electric current producing cell for separating an anode and a cathode, said separator comprising a microporous layer comprising pseudo-boehmite and a binder, wherein said method comprises the steps of:

(a) coating onto a substrate a liquid mixture comprising a boehmite sol, a binder, and a liquid medium; and

(b) drying the coating formed in step (a) to yield said microporous layer;

wherein pores of said microporous layer are impregnated with a composition comprising a polymer; and

wherein said polymer is ionically conductive.

38. The method of claim 37, wherein said binder is an organic binder.

39. The method of claim 37, wherein said binder is selected from the group consisting of polyvinyl alcohols, polyethylene oxides, alkylated polyethylene oxides, polyvinyl pyrrolidones, polyvinyl butyrals, hydroxyethyl cellulose, cellulose acetate propionate, polymers comprising quaternary ammonium groups, polyacrylamides, polyvinyl ethers, polyethylenieimines, polyurethanes, epoxies, melamine formaldehydes, urea formaldehydes; copolymers thereof; copolymers of maleic anhydride and derivatives and esters thereof; gelatin; starch; and mixtures of the foregoing binders.

40. The method of claim 37, wherein said binder is an inorganic binder.

41. The method of claim 37, wherein said binder further comprises one or more additives selected from the group consisting of pigments, crosslinking agents, catalysts for non-radiation curing, sensitizers for radiation curing, plasticizers, surfactants, and dispersants.

42. The method of claim 37, wherein said composition further comprises a crosslinking agent.

43. The method of claim 37, wherein said microporous layer has a thickness of from 1 micron to 25 microns.

44. The method of claim 37, wherein said microporous layer has a thickness of from 2 microns to 15 microns.

45. A method of making a separator for use in an electric current producing cell for separating an anode and a cathode, said separator comprising a microporous layer comprising pseudo-boehmite and a binder, wherein said method comprises the steps of:

(a) coating onto a substrate a liquid mixture comprising a boehmite sol, a binder, and a liquid medium; and

(b) drying the coating formed in step (a) to yicld said microporous layer;

wherein at least one outermost surface of said substrate comprises a cathode layer and said liquid mixture is coated onto said cathode layer.

46. The method of claim 45, further comprising, subsequent to step (b), the steps of:

(c) contacting a surface of said microporous layer with a solution comprising heat- or radiation-curable monomers or oligomers, thereby causing infusion of said monomers or said oligomers into pores of said microporous layer; and,

(d) curing said monomers or said oligomers with an energy source selected from the group consisting of: heat, ultraviolet light, visible light, infrared radiation, and electron beam radiation; thereby forming a polymer.

47. The method of claim 46, wherein said polymer formed in step (d) is an ionic conductive polymer.

48. A method of making a separator for use in an electric current producing cell for separating an anode and a cathode, said separator comprising a microporous layer comprising pseudo-boehmite and a binder, wherein said method comprises the steps of:

(a) coating onto a substrate a liquid mixture comprising a boehmite sol, a binder, and a liquid medium;

(b) drying the coating formed in step (a) to yield said microporous layer; and

(c) delaminating said microporous layer from said substrate;

wherein at least one outermost surface of said substrate comprises a release layer and said liquid mixture is coated onto said release layer.

49. The method of claim 48, further comprising, subsequent to step (b) and prior to step (c), the steps of:

(i) contacting a surface of said microporous layer with a solution comprising heat- or radiation-curable monomers or oligomers, thereby causing infusion of said monomers or said oligomers into pores of said microporous layer; and

(ii) curing said monomers or said oligomers with an energy source selected from the group consisting of heat, ultraviolet light, visible light, infrared radiation, and electron beam radiation; thereby forming a polymer.

50. The method of claim 49, wherein said polymer formed in step (ii) is an ionic conductive polymer.

51. A method of making a separator for use in an electric current producing cell for separating an anode and a cathode, said separator comprising a microporous layer comprising pseudo-boehmite and a binder, wherein said method comprises the steps of:

(a) coating onto a substrate a liquid mixture comprising a boehmite sol, a binder, and a liquid medium; and

(b) drying the coating formed in step (a) to yield said microporous layer;

(c) contacting a surface of said microporous layer with a coating solution comprising a solid material and a liquid medium; and

(d) drying the coating formed in step (c) to yield a coating layer comprising said solid material;

wherein at least one outermost surface of said substrate comprises a release layer and said liquid mixture is coated onto said release layer.

52. The method of claim 51, wherein said binder is an organic binder.

53. The me thod of claim 51, wherein said binder is an organic binder.

54. The method of claim 51, further comprising, subsequent to step (d), the step of:

(e) delaminating said microporous layer from said substrate.

55. The method of claim 51, wherein said coating layer formed in step (d) is a cathode layer.

56. The method of claim 55, further comprising, subsequent to step (d), the step of:

(e) delaminating said microporous layer from said substrate.

57. A method of making an electrolyte element for an electric current producing cell, said electrolyte element comprising a microporous layer comprising pseudo-boehmite and a binder, wherein said method comprises the steps of:

(a) coating onto a substrate a liquid mixture comprising a boehmite sol, a binder, and a liquid medium;

(b) drying the coating formed in step (a) to yield said microporous layer; and,

(c) contacting a surface of said microporous layer with an organic electrolyte, thereby causing infusion of said electrolyte into pores of said microporous layer.

58. The method of claim **57**, wherein said liquid medium comprises water.

59. The method of claim **57**, wherein said liquid medium comprises one or more organic solvents.

60. The method of claim **57**, wherein said liquid medium comprises one or more protic solvents selected from the group consisting of: alcohols and glycols.

61. The method of claim **57**, wherein said liquid medium comprises water and one or more organic solvents.

62. The method of claim **57**, wherein said binder is present in an amount of 3 to 200% of the weight of pseudo-boehmite in said microporous layer.

63. The method of claim **57**, wherein said binder is present in an amount of 5 to 70% of the weight of pseudo-boehmite in said microporous layer.

64. The method of claim **57**, wherein said binder is an organic binder.

65. The method of claim **57**, wherein said binder is selected from the group consisting of polyvinyl alcohols, polyethylene oxides, alkylated polyethylene oxides, polyvinyl pyrrolidones, polyvinyl butyrals, hydroxyethyl cellulose, cellulose acetate propionate, polymers comprising quarternary ammonium groups, polyacrylamides, polyvinyl ethers, polyethyleneimines, polyurethanes, epoxies, melamine formaldehydes, urea formaldehydes; copolymers thereof; copolymers of maleic anhydride and derivatives and esters thereof; gelatin, starch; and mixtures of the foregoing binders.

66. The method of claim **57**, wherein said binder is an inorganic binder.

67. The method of claim **57**, wherein said binder is selected from the group consisting of:

colloidal silicas, colloidal non-hydrated aluminum oxides, colloidal tin oxides, colloidal titanium oxides, colloidal zirconium oxides, and colloidal zinc oxides.

68. The method of claim **57**, wherein said binder further comprises one or more additives selected from the group consisting of:

pigments, crosslinking agents, catalysts for non-radiation curing, sensitizers for radiation curing, plasticizers, surfactants, and dispersants.

69. The method of claim **57**, wherein said organic electrolyte comprises one or more materials selected from the group consisting of:

liquid electrolytes, gel polymer electrolytes, and solid polymer electrolytes.

70. The method of claim **57**, wherein said organic electrolyte comprises heat- or radiation-curable monomers or oligomers.

71. The method of claim **70**, further comprising, subsequent to step (c), the step of:

(d) curing said monomers or said oligomers with an energy source selected from the group consisting of: heat, ultraviolet light, visible light, infrared radiation, and electron beam radiation.

72. The method of claim **57**, wherein at least one outermost surface of said substrate comprises a cathode layer and said liquid mixture is coated onto said cathode layer.

73. The method of claim **72**, further comprising, subsequent to step (b) and prior to step (c), the steps of:

(i) contacting a surface of said microporous layer with a solution comprising heat- or radiation-curable monomers or oligomers, thereby causing infusion of said monomers or said oligomers into pores of said microporous layer; and,

(ii) curing said monomers or said oligomers with an energy source selected from the group consisting of: heat, ultraviolet light, visible light, infrared radiation, and electron beam radiation; thereby forming a polymer.

74. The method of claim **72**, further comprising, subsequent to step (b) and prior to step (c), the steps of:

(i) contacting a surface of said microporous layer with a coating solution comprising a solid materi al and a liquid medium; and,

(ii) drying the coating formed in step (i) to yield a coating layer comprising said solid material.

75. An electric current producing cell comprising a cathode, an anode, and an electrolyte element interposed between said cathode and said anode, wherein said electrolyte element comprises:

(a) a separator comprising a microporous layer, which microporous layer comprises pseudo-boehmite and a binder; and,

(b) an organic electrolyte contained within pores of said microporous layer.

76. The cell of claim **75**, wherein said binder is present in an amount of 3 to 200% of the weight of pseudo-boehmite in said microporous layer.

77. The cell of claim **75**, wherein said binder is an organic binder.

78. The cell of claim **75**, wherein said binder is an inorganic binder.

79. The cell of claim **75**, wherein said cell is a secondary electric current producing cell.

80. The cell of claim **75**, wherein said cell is a primary electric current producing cell.

81. The cell of claim **75**, wherein said anode comprises one or more anode-active materials selected from the group consisting of:

lithium metal, lithium-aluminum alloys, lithium-tin alloys, lithium-intercalated carbons, and lithium-intercalated graphites.

82. The cell of claim **75**, wherein said cathode comprises one or more cathode active materials selected from the group consisting of:

transition metal chalcogenides, conductive polymers, and sulfur-containing materials.

83. The cell of claim **75**, wherein said cathode comprises a sulfur-containing materials.

84. The cell of claim **83**, wherein said sulfur-containing material comprises elemental sulfur.

85. The cell of claim **83**, wherein said sulfur-containing material comprises a sulfur-containing polymer comprising a covalent polysulfide moiety of the formula, —S_m—, wherein m is an integer equal to or greater than 3.

86. The cell of claim **83**, wherein said sulfur-containing material comprises a sulfur-containing polymer comprising a covalent polysulfide moiety of the formula, —S_m—, wherein m is an integer equal to or greater than 8.

87. The cell of claim **85**, wherein said sulfur-containing polymer has a polymer backbone chain comprising conjugated segments.

88. The cell of claim **85**, wherein said sulfur-containing polymer has a polymer backbone chain and said polysulfide moiety, —S_m—, is covalently bonded by one or both of its terminal sulfur atoms on a side group to said polymer backbone chain.

89. The cell of claim **85**, wherein said sulfur-containing polymer has a polymer backbone chain and said polysulfide

moiety, —S_m—, is incorporated into said polymer backbone chain by covalent bonding of terminal sulfur atoms of said polysulfide moiety.

90. The cell of claim **85**, wherein said sulfur-containing polymer comprises greater than 75 weight percent of sulfur.

91. The cell of claim **83**, wherein said sulfur-containing material comprises a sulfur-containing polymer comprising an ionic polysulfide moiety selected from the group consisting of:

ionic —S_m^- moieties and ionic S_m^{2-} moieties; wherein m is an integer equal to or greater than 3.

92. The cell of claim **83**, wherein said sulfur-containing material comprises a sulfur-containing polymer comprising an ionic polysulfide moiety selected from the group consisting of:

ionic —S_m^- moieties and ionic S_m^{2-} moieties; wherein m is an integer equal to or greater than 8.

93. The cell of claim **91**, wherein said sulfur-containing polymer has a polymer backbone chain comprising conjugated segments.

94. The cell of claim **91**, wherein said sulfur-containing polymer has a polymer backbone chain and said polysulfide moiety, —S_m—, is covalently bonded by one or both of its terminal sulfur atoms on a side group to said polymer backbone chain.

95. The cell of claim **91**, wherein said sulfur-containing polymer comprises greater than 75 weight percent of sulfur.

96. The cell of claim **75**, wherein said organic electrolyte comprises one or more materials selected from the group consisting of:

liquid electrolytes, gel polymer electrolytes, and solid polymer electrolytes.

97. The cell of claim **75**, wherein said organic electrolyte comprises a liquid electrolyte.

98. The cell of claim **75**, wherein said organic electrolyte comprises a gel polymer electrolyte.

99. The cell of claim **75**, wherein said organic electrolyte comprises a solid polymer electrolyte.

100. A method of forming an electric current producing cell, said method comprising the steps of:

(a) providing an anode;

(b) providing a cathode; and

(c) interposing an electrolyte element between said anode and said cathode, wherein said electrolyte element comprises:

(i) a separator comprising a microporous layer comprising pseudo-boehmite and a binder; and

(ii) an organic electrolyte contained within pores of said microporous layer.

101. The method of claim **100**, wherein the organic electrolyte of said electrolyte element comprises one or more materials selected from the group consisting of:

liquid electrolytes, gel polymer electrolytes, and solid polymer electrolytes.

102. The method of claim **100**, further comprising, subsequent to step (c), the step of:

(d) imbibing a solution comprising one or more ionic electrolyte salts and one or more electrolyte solvents into said electrolyte element.

103. The method of claim **101**, wherein said organic electrolyte after step (c) and prior to step (d) does not comprise an ionic electrolyte salt.

* * * * *

Appendix Y

Available online at www.sciencedirect.com
ScienceDirect
Electrochimica Acta 51 (2006) 5636–5644
ELECTROCHIMICA Acta
www.elsevier.com/locate/electacta

Characteristics of PVdF-HFP/TiO_2 composite membrane electrolytes prepared by phase inversion and conventional casting methods

Kwang Man Kim [a,*,1], Nam-Gyu Park [b], Kwang Sun Ryu [a], Soon Ho Chang [a]

[a] *Ionics Devices Team, Basic Research Lab., Electronics & Telecommunications Research Institute (ETRI), 161 Gajong, Yusong, Daejon 305-700, South Korea*

[b] *Materials Science & Technology Division, Korea Institute of Science & Technology (KIST), 39-1 Hwaolgok, Seongbuk, Seoul 136-791, South Korea*

Received 2 January 2006; received in revised form 20 February 2006; accepted 27 February 2006
Available online 3 April 2006

Abstract

Porous poly(vinylidene fluoride-*co*-hexafluoropropylene) (PVdF-HFP)-based polymer membranes filled with various contents of titania (TiO_2) nanocrystalline particles are prepared by phase inversion technique and, along with conventional casting method for comparison. *N*-methyl-2-pyrrolidone (NMP) as a solvent is used to dissolve the polymer and to make the slurry with TiO_2. Cast film is obtained by spreading the slurry and evaporating NMP in a dry oven, while phase inversion membrane by promptly immersing the spread slurry into flowing water as a non-solvent. Physical and electrochemical characterizations, such as morphology, thermal and crystalline behavior, and other transport properties of lithium ionic species, are carried out for the polymer films/membranes and the polymer electrolytes with absorbing an electrolyte solution. Phase inversion polymer electrolytes are proved to show superior behaviors in electrochemical properties, such as ionic conductivity, electrochemical and interfacial stability, than cast film electrolytes. This is greatly owed to highly porous structure of phase inversion membranes. Even including the feature of interfacial resistance with lithium electrode, phase inversion polymer electrolytes of PVdF-HFP/(5–20 wt.% TiO_2) can be optimized as the adequate ones in applying to the electrolyte medium of lithium rechargeable batteries.
© 2006 Elsevier Ltd. All rights reserved.

Keywords: Polymer electrolytes; Poly(vinylidene fluoride); Titanium oxide nanoparticles; Phase inversion technique; Cast films

1. Introduction

Poly(vinylidene fluoride-*co*-hexafluoropropylene) (PVdF-HFP) is a copolymer consisting of crystalline vinylidene fluoride (VdF) and amorphous hexafluoropropylene (HFP) units. It has been known that the PVdF-HFP is very useful as the polymer matrix material in the polymer electrolyte of lithium rechargeable battery, due to its excellent chemical stability mainly supported by VdF unit, as well as due to the enhanced plasticity (somewhat associated with high ionic conductivity) by HFP unit. Moreover, the inclusion of inorganic nanoparticles to the PVdF-HFP leads not only to the improvement of mechanical strength but also to the advantageous features of better lithium cation (Li^+) transport properties such as the enhancement of electrochemical stability and interfacial compatibility with lithium electrode. Nanoparticles that have been used for these purposes were, e.g., fumed silica (SiO_2) [1], nanocrystalline titania (TiO_2; anatase [2] and rutile [3]), alumina (Al_2O_3), and so on. Several roles of such nanoparticles in the PVdF-based electrolyte have been known as the enhancement of transport property by the suppression of Li^+–F interactions (for Al_2O_3) [4] and considerable effects in polymer matrix structure (for SiO_2) [5]. TiO_2 nanoparticles have been also used to improve transport properties, particularly for the lithium ionic conduction and cationic diffusivity in poly(ethylene oxide)-lithium ionic salt systems [6–11]. Lewis acid–base interactions between the TiO_2 surface and polymer chains or lithium salt anions are recently considered as a promising mechanism for the increase in ionic conductivity [12].

On the other hand, the matrix structure in polymer electrolyte medium can be modified to yield a great number of pores with a wide range of pore sizes. The porous structure may be useful in obtaining the improved electrochemical properties of

* Corresponding author. Tel.: +82 42 860 6829; fax: +82 42 860 6836.
E-mail address: kwang@etri.re.kr (K.M. Kim).
[1] ISE member.

0013-4686/$ – see front matter © 2006 Elsevier Ltd. All rights reserved.
doi:10.1016/j.electacta.2006.02.038

polymer electrolyte. There exists an effective method of making highly porous membrane, called phase inversion technique, using both solvent and non-solvent simultaneously. Many examples of phase inversion PVdF-HFP electrolytes were reported for the application to rechargeable lithium batteries [13–26]. Phase inversion membrane can be formed by the immersion precipitation in a non-solvent bath, promptly occurring mutual diffusion between solvent and non-solvent to make highly porous structure in polymer matrix. In other words, two kinds of diffusion with opposite directions are competing in that the solvent component is going to evaporate (or escape) from the spread slurry while the non-solvent to penetrate into (or solidify) it. This method is very beneficial in obtaining planned morphology by controlling preparation conditions such as the kind of solvent and non-solvent, their concentration and even the crystallinity of polymer matrix [27].

In this paper, we prepare porous PVdF-HFP/TiO_2 membranes by varying the amounts of TiO_2 and by using phase inversion technique. *N*-methyl-2-pyrrolidone (NMP) is used as a good solvent for the polymer and water as a non-solvent. For comparison, we also prepare PVdF-HFP/TiO_2 cast films with corresponding TiO_2 contents by conventional casting method. The development of highly porous structure is precisely observed by adopting phase inversion method and also by changing the TiO_2 content. As a first step, some basic characterizations such as morphology, thermal and crystalline properties are performed for the PVdF-HFP/TiO_2 cast films and phase inversion membranes without adding electrolytic solution. Electrochemical properties measured for the liquid-filled PVdF-HFP/TiO_2 electrolytes also provide useful information on ionic conduction, electrochemical stability, and interfacial reaction with lithium electrode. All these works are essential to using the PVdF-HFP/TiO_2 polymer electrolytes in lithium rechargeable batteries.

2. Experimental

The PVdF-HFP and TiO_2 used were, respectively, a commercial fluoro-copolymer KynarFlex 2801 (Atofina Chemicals, 12 mol% HFP) and an anatase-type titanium oxide nanoparticles PC-101 (Japan Titan Kogyo, average particle size of 20 nm). Viscous slurry was prepared by mixing PVdF-HFP and TiO_2 in NMP with fixing the PVdF-HFP:NMP ratio of 1:9 (w/w). The TiO_2 content was varied as 0–70 wt.% based on the total weight of PVdF-HFP/TiO_2 composite film. It was difficult to make the slurry having more than 65 wt.% of TiO_2 because of overdosing nanoparticles to give a powder-like mass. Viscous slurries with 0–60 wt.% of TiO_2 were then spread on a clean glass plate by using doctor blade apparatus with a gap of 300 μm. Phase inversion membranes were obtained by promptly dipping the glass plate into a flowing water bath, on time by peeling off the membrane from the glass plate just after the onset of solidification, and finally by drying the solidified membranes under ambient condition for 24 h. Flowing in the water bath was very significant because it might provide the efficient removal of NMP escaped from the spread slurry and simultaneously the helpful penetration of water into the membrane. The prompt peeling of membrane under flowing water was also an important factor to provide the penetration of water molecules in any direction, as well as to avoid the formation of asymmetric pore structure (e.g., finger-like pore at the surface and large cavity at the bottom) due to the one-dimensional diffusion of water from the membrane surface. All the membranes made by the phase inversion procedure were also confirmed to have no moisture from a thermogravimetric test up to 150 °C. For comparison, cast films were also obtained by drying the slurries spread on the glass plate in a vacuum oven at 120 °C for 12 h. However, the cast films with compact structure were much thinner (20–40 μm) than the phase inversion membranes (80–100 μm).

For the PVdF-HFP/TiO_2 cast films and phase inversion membranes, surface and cross-sectional morphologies were observed by a scanning electron microscope (Jeol JSM 5610). Image magnifications were 20,000× and 5000× for surface and cross-sectional views, respectively. Thermal properties were measured by using a differential scanning calorimeter (du Pont 2100 Thermal Analyst with a 910 Cell Base) under the conditions of heating run (25–250 °C) at the scan rate of 10 °C min^{-1} and the subsequent cooling run (250–60 °C) at −5 °C min^{-1}. From the results, thermal parameters of T_m (melting point), T_c (crystallization temperature), ΔH_m (heat of fusion), and ΔH_c (heat of crystallization) were analyzed in terms of TiO_2 content and preparation method of PVdF-HFP/TiO_2 samples. Crystalline properties of the films and membranes were investigated by an X-ray diffractometer (Philips X'Pert Pro) equipped with a Cu $K\alpha_1$ target X-ray tube and a fast X-ray detector (X'Celerator).

Electrolyte solution of 1M $LiPF_6$ dissolved in the mixture of ethylene carbonate (EC) and dimethyl carbonate (DMC) (1:1 w/w) was used as a swelling liquid for the pieces (2 cm × 2 cm) of cast films and phase inversion membranes to give PVdF-HFP/TiO_2 polymer electrolytes. Liquid uptake was measured as a function of time by weighing the polymer electrolyte before and after absorbing the electrolyte solution. The liquid uptake (%) was determined using the relation $(W_2 - W_1) \times 100/W_1$, where W_1 and W_2 denote the weights of polymer electrolytes before and after absorbing the electrolyte solution, respectively. A conductivity cell (2 cm × 2 cm) comprising two stainless steel electrodes on each side of the polymer electrolyte was used to obtain the ionic conductivity of PVdF-HFP/TiO_2 polymer electrolytes, which was determined from complex impedance spectra obtained by a frequency response analyzer (Solartron HF 1225 Gain-Phase Analyzer) in the frequency range of 0.1 Hz to 100 kHz. Temperature dependence of the ionic conductivity was obtained over the range of 0–80 °C. The ionic conductivity σ was calculated from the bulk resistance (R) using the relation $\sigma = l/(R \times A)$, where l and A were the thickness of polymer electrolyte and the cell area, respectively. The bulk resistance was directly obtained from the diameter of semicircle (at moderate temperature) or Z' axis intercept of straight line (at elevated temperature) in the impedance spectrum. Cyclic voltammetry was performed to investigate the electrochemical window of PVdF-HFP/TiO_2 polymer electrolytes by using a non-blocking cell (2 cm × 2 cm) in which a stainless steel served as working electrode and lithium as both counter and reference electrodes. MacPile-II potentiostat/galvanostat system was used under the scan rate of 0.1 mV s^{-1} in the range of 0–5 V (versus

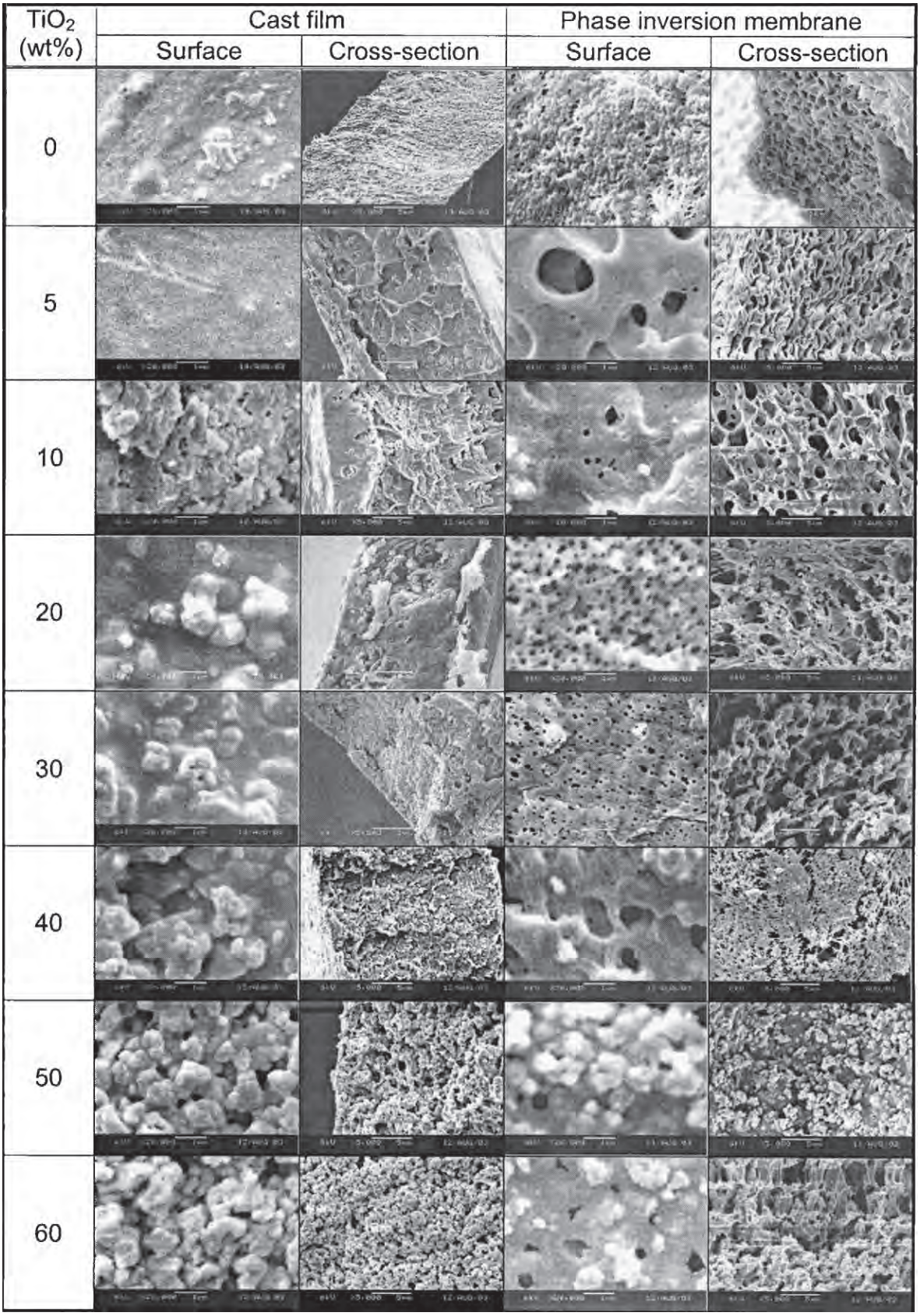


Fig. 1. Scanning electron microscope images of PVdF-HFP/TiO_2 films, with varying TiO_2 content, prepared by casting and phase inversion methods. Image magnifications were 20,000× and 5000× for surface and cross-sectional views, respectively.

Li/Li^+). In addition, the interfacial stability between lithium and polymer electrolyte was examined as a function of time by monitoring the impedance of a blocking cell (2 cm × 2 cm) with two lithium sheets at room temperature.

3. Results and discussion

3.1. Morphology

Surface and cross-sectional images of cast films and phase inversion membranes of PVdF-HFP/TiO_2 are shown in Fig. 1. It seems that porous structure can be obviously observed in the phase inversion membranes whereas relatively compact structure in the cast films. In the cast film with 20 wt.% TiO_2, the nanoparticles are hardly dispersed and thus a form of aggregates begins to appear with polymer component. Further increase in TiO_2 content easily leads to the more roughened surface by the growth of aggregates and the cross-section having many macro- and micro-pores distributed irregularly. However, these pores do not necessarily contribute to high liquid uptake and ionic conductivity (see Fig. 4) because the aggregates do not always exhibit the liquid-holding property like the inorganic fillers such as surface-treated SiO_2 and TiO_2. On the other hand, the phase inversion membranes show highly porous surface and cross-section at about 5–30 wt.% TiO_2, which are produced by the mutual diffusion between solvent and non-solvent, not by the aggregates. Further addition of TiO_2, however, can provide that such the porous structure suffers the short- and/or long-range breakage within the membrane and then it easily becomes brittle by overdosing particulate feature.

Particularly for the samples with low TiO_2 content (e.g., about 0–20 wt.%), the phase inversion membrane shows a porous structure with a slightly distorted honeycomb cross-sectional view, whereas the cast film provides a compact structure with hardly distributed pores. Aggregates formed by the insufficient dispersion of TiO_2 nanoparticles are not seen for the phase inversion membrane with low TiO_2 content, but actually they may exist as a form of fine granules distributed at the inner-wall of pores if observing with high resolution. It can be thought that the granules composed of TiO_2 and polymer component can play some roles of capturing liquid electrolyte and providing it as a medium for carrier migration. With further addition of TiO_2, however, the roles may be easily failed by the appearance of highly roughened surface with big aggregates and broken pore structure in cross-section.

It should be mentioned that the present membranes by phase inversion method do not show finger-like or sponge-like morphology which was reported by others [17,18,21,27], but exhibit a honeycomb-like structure at low TiO_2 content and then the broken honeycomb skeleton with irregularly distributed aggregates by higher loading of TiO_2. It seems that for low TiO_2 membranes, the mutual diffusion between water non-solvent and NMP solvent occurs rapidly and efficiently to yield highly porous structure just after the impregnation. For high TiO_2 membranes, the porous structure starts to be distorted and finally to be broken down by the superimposed bulky aggregates of overdosing TiO_2 nanoparticles.

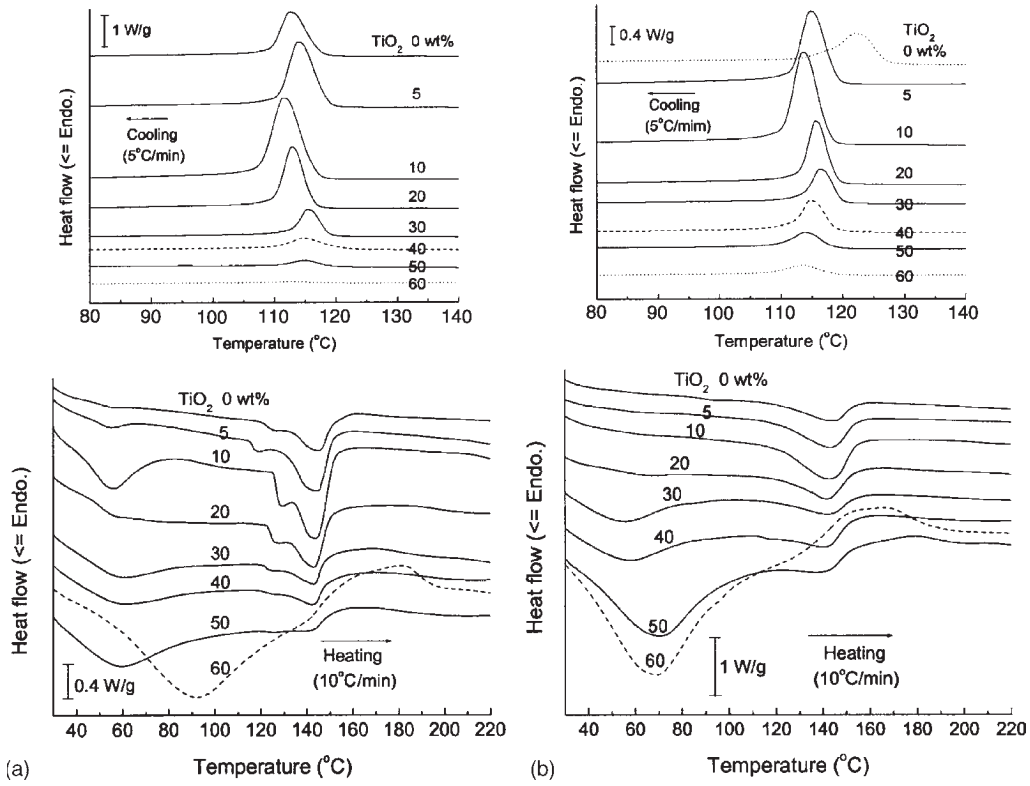


Fig. 2. Differential scanning calorimetric thermograms of PVdF-HFP/TiO_2 films, with varying TiO_2 content, prepared by (a) casting and (b) phase inversion methods. Small figures in upper part are the results of cooling run at $-5\,^{\circ}C\,min^{-1}$, examined after heating run from room temperature to 250 °C at $10\,^{\circ}C\,min^{-1}$.

CosMX Exhibit 1003, Page 507 of 512

Table 1
Thermal properties of PVdF-HFP/TiO_2 cast films and phase inversion membranes

TiO_2 content (wt.%)	Cast films				Phase inversion membranes			
	T_m (°C)	ΔH_m (J g^{-1})	T_c (°C)	ΔH_c (J g^{-1})	T_m (°C)	ΔH_m (J g^{-1})	T_c (°C)	ΔH_c (J g^{-1})
0	144.9	16.4	112.5	4.5	144.3	8.7	122.2	4.8
5	144.3	16.6	114.0	8.3	143.0	9.1	114.9	6.5
10	143.5	21.7	111.7	10.8	142.6	12.8	113.7	8.0
20	142.9	16.7	113.0	6.6	141.5	12.9	115.8	5.0
30	142.8	7.4	115.5	3.3	141.8	7.3	116.5	3.1
40	142.2	6.2	114.8	2.3	140.1	11.3	114.9	2.4
50	141.7	3.9	115.0	1.9	141.5	6.7	114.0	2.9
60	140.7	1.2	112.8	0.4	141.2	3.9	113.5	3.4

3.2. Thermal and crystalline properties

Fig. 2 shows differential scanning calorimetric thermograms of the cast films and phase inversion membranes, obtained by melting in heating run and crystallization processes in the subsequent cooling run. Thermal data such as melting point (T_m), heat of melting (ΔH_m), crystallization temperature (T_c), and heat of crystallization (ΔH_c) are also summarized in Table 1. As the TiO_2 content increases, the T_m of cast film slightly shifts downward whereas the phase inversion membrane suffers an irregular T_m pattern of decrease/increase. These T_m behaviors would be rather better to understand in association with VdF crystal phase corresponding to the melting peak. The cast films exhibit some melting peaks corresponding to VdF crystals (e.g., α- and γ-phase [28]) in the range of 120–150 °C whereas the phase inversion membranes just a broad melting peak around 140 °C corresponding to the melting of α-phase (big spherulite) crystals [29,30]. Further addition of TiO_2, however, yields a broad endothermic peak around 60 °C in both the films and membranes. We think that the broad peak around 60 °C may be probably regarded as the nanocrystalline phase change of TiO_2. The absence of the endothermic peak at 60 °C in the case of using amorphous SiO_2 nanoparticles [31] may be an evidence for the nanocrystalline phase change of TiO_2.

Compared to the high crystallinity appeared when using SiO_2/acetone solvent (40–60%) and TiO_2/acetone (20–60%) [2,3], the present case of using TiO_2/NMP solvent exhibits very low crystallinity (about 1–20%). The crystallinity can be calculated from the ΔH_m with a basis (104.7 J g^{-1}) [32] for pure α-phase PVdF crystal. The low crystallinity may be originated from the usage of NMP as a solvent, which can interact with VdF chain (particularly, the interaction between N-atom of NMP and VdF chain [33]) and consequently inhibit chain rearrangement. Moreover, it seems that the degree of TiO_2 association with the interaction leads to the small change within the low crystallinity. Contrary to the general effect of lowering the crystallinity by the addition of inorganic fillers to the polymer films, the present case of using TiO_2 shows increasing and subsequent decreasing trend of crystallinity with the increase in TiO_2 content. Most of the crystalline phase formed by polymer chain rearrangement may disappear when more than 60 wt.% TiO_2 is filled, and this tendency is more enhanced in the cast film than the phase inversion membrane.

Cooling run for cast films produces small range of T_c (112–115 °C) with the increase in TiO_2 content, but the phase inversion membrane has wide range of T_c (113–122 °C). Moreover, the cast films filled with TiO_2 have similar T_c to the film without filler, whereas the phase inversion membranes with TiO_2 give much lower T_c than the membrane without filler. This means that TiO_2 in the phase inversion membrane plays a role of delaying the crystallization due to the interaction with polymer chains. The interaction of TiO_2 with the polymer chain is possible if sufficient free volume is given to permit chain rearrangement. Highly porous structure of phase inversion membrane may be associated with the interaction. Contrary to this, it seems that TiO_2 in the cast film does not interact with the polymer chain by the compact structure during cooling run to yield the comparable T_c to the film without filler.

As shown in Fig. 3, X-ray diffraction results for the films and membranes apparently exhibit the gradual reduction of VdF crystalline phases with the increase in TiO_2 content, which is consistent with the reduction in ΔH_m value in Table 1, corresponding to VdF crystallinity. At low TiO_2 content, some characteristic peaks at $2\theta = 18°$, 26.8°, and 38° corresponding to big spherulites of VdF α-phase crystals ((1 0 0), (0 2 1), and (1 3 1) planes, respectively) [29,30] are obviously shown. Small spherulites of VdF γ-phase crystals may co-exist with the α-phase crystals at $2\theta \approx 18.6°$ and 20.2° ((0 2 0) and (1 1 0) planes, respectively) [30]. It is very difficult to distinguish the diffraction patterns between cast films and phase inversion membranes, but the intensity ratio of $I(1\,1\,0)_{(\alpha+\gamma)}/I(1\,0\,0)_\alpha$ can explain the difference in terms of distribution degree of VdF γ-phase crystals in the co-existed phases of (α + γ) crystals [30]. From Gaussian line shape fitting, the values of $I(1\,1\,0)_{(\alpha+\gamma)}/I(1\,0\,0)_\alpha$ can be calculated as 1.45, 1.56, 1.23, 1.50, 1.37, 1.50, 1.45, and 1.38 for the cast films with 0, 5, 10,20, 30, 40, 50, and 60 wt.% of TiO_2, respectively. For the phase inversion membranes, the values are 1.28, 1.33, 1.13, 1.31, 1.50, 1.45, 1.29, and 1.18. These values of $I(1\,1\,0)_{(\alpha+\gamma)}/I(1\,0\,0)_\alpha$ support the fact that the phase inversion membrane holds slightly less γ-phase crystals than the cast films. In addition, the distribution degree of VdF γ-phase crystals increases and then decrease with the increase in TiO_2 content.

3.3. Liquid absorption and ionic conductivity

Phase inversion membranes with highly porous structure are expected to absorb more liquid electrolyte solution than cast

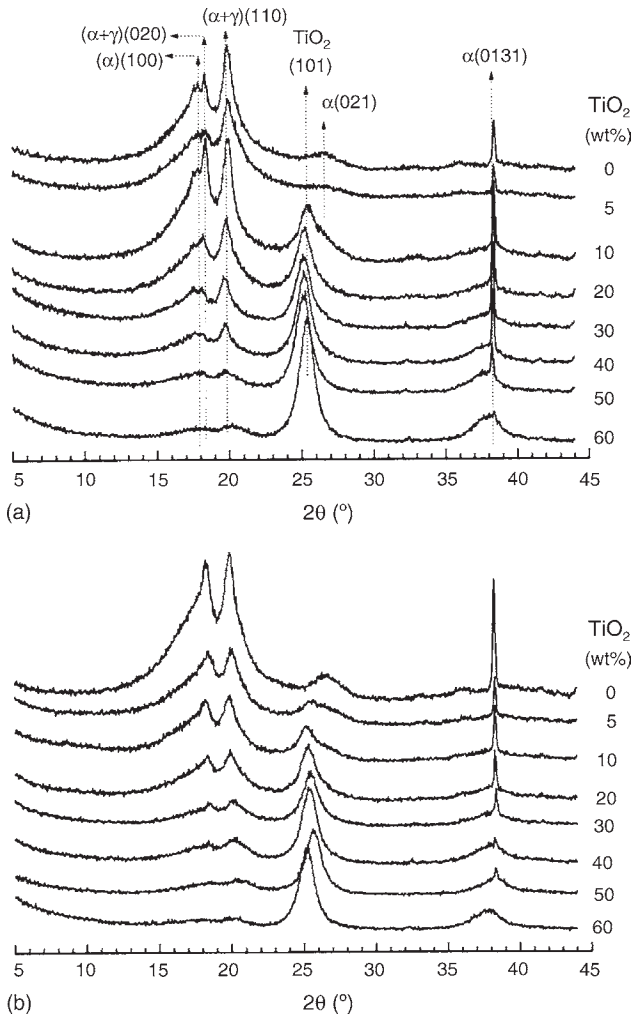


Fig. 3. X-ray diffraction spectra of PVdF-HFP/TiO_2 films, with varying TiO_2 content, prepared by (a) casting and (b) phase inversion methods.

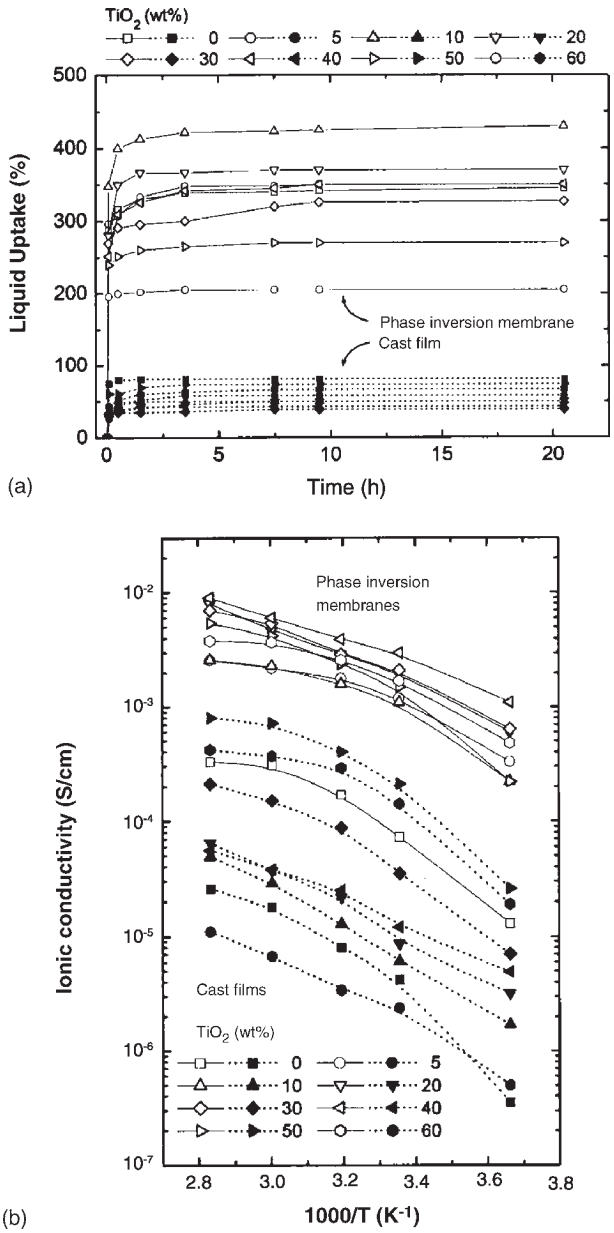


Fig. 4. (a) Liquid uptake and (b) Arrhenius plot for the ionic conductivities of PVdF-HFP/TiO_2 films, with varying TiO_2 content, prepared by casting (filled symbol) and phase inversion (hollow symbol) methods. The electrolyte solution used was 1 M $LiPF_6$ dissolved in EC/DMC (1:1 w/w).

film with compact morphology. As shown in Fig. 4(a), the phase inversion membranes exhibit greater amount of liquid absorption than the cast films, particularly exceeding 400% of liquid uptake for the membrane with 10 wt.% TiO_2. In Fig. 4(b), the ionic conductivity of phased inversion membrane electrolyte is highly increased over the temperature range of 0–80 °C except the sample without TiO_2, compared with the cast film electrolytes. All phase inversion membrane electrolytes have the room-temperature ionic conductivity higher than 10^{-3} S cm^{-1} which is an appropriate value as the electrolyte medium of lithium rechargeable battery. Temperature dependence of the ionic conductivity obeys the empirical Vogel–Tammann–Fulcher (VTF) rule in both the cast films and phase inversion membranes. Small deviation from the Arrhenius behavior is also given by the steep decrease in ionic conductivity in the low temperature region (<25 °C), which is commonly occurred by the freezing of EC-based electrolyte solution. As the temperature increases, the ionic conduction takes place very fast by the liquid-like electrolyte medium in the absence of solid constituents.

Comparing Fig. 4(a) and (b), however, the general trend that higher uptake leads to higher ionic conductivity can not exactly employed in this case of having different pore structure and TiO_2 content. For instance, the phase inversion membrane with 10 wt.% TiO_2 shows highest liquid uptake, but its ionic conductivity is somewhat lower than other membranes with different TiO_2 contents. This is due to the fact that all liquids absorbed do not necessarily contribute to the ionic conduction by the existence of different pore structures within the membranes. Ionic conduction in the phase inversion membranes can be separated into more than two modes with respect to some factors of carrier migration, cavity barrier, interaction with swelled polymer [19,20], and pore connectivity (or tortuosity). Ionic conduction or carrier migration mechanism in these membranes should be further studied by some precise characterizations, e.g., a pulsed

CosMX Exhibit 1003, Page 509 of 512

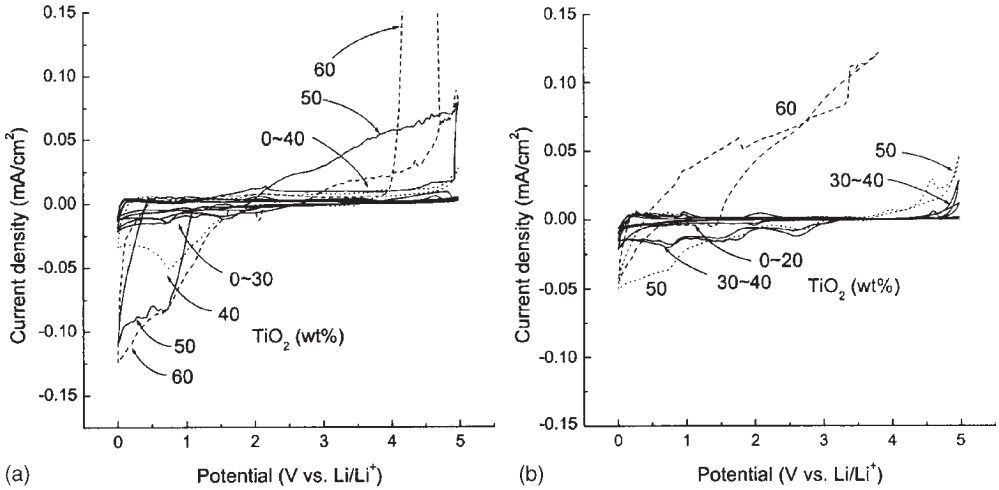


Fig. 5. Electrochemical window of PVdF-HFP/TiO_2 electrolyte films, with varying TiO_2 content, prepared by (a) casting and (b) phase inversion methods. The electrolyte solution used was 1 M $LiPF_6$ dissolved in EC/DMC (1:1 w/w).

field gradient spin-echo NMR measurement using cationic (^{7}Li) and anionic (^{19}F) probes to determine the diffusivity and/or mobility of ions and ion pairs [19].

3.4. Electrochemical stability and interfacial resistance

Fig. 5 shows cyclic voltammograms of the PVdF-HFP/TiO_2 electrolytes containing 1 M $LiPF_6$/(EC:DMC 1:1 w/w) solution to characterize the electrochemical stability (window) under the potential range of 0–5 V versus Li/Li^+. The cast film electrolytes with 0–30 wt.% TiO_2 easily achieve the cathodic and anodic stabilities over 0–5 V versus Li/Li^+, but those with 40–60 wt.% TiO_2 exhibit big oxidation and reduction peaks corresponding to lithium stripping and plating, respectively. Particularly, the cast film electrolyte with 60 wt.% TiO_2 is highly reactive by lithium stripping oxidation in high potential

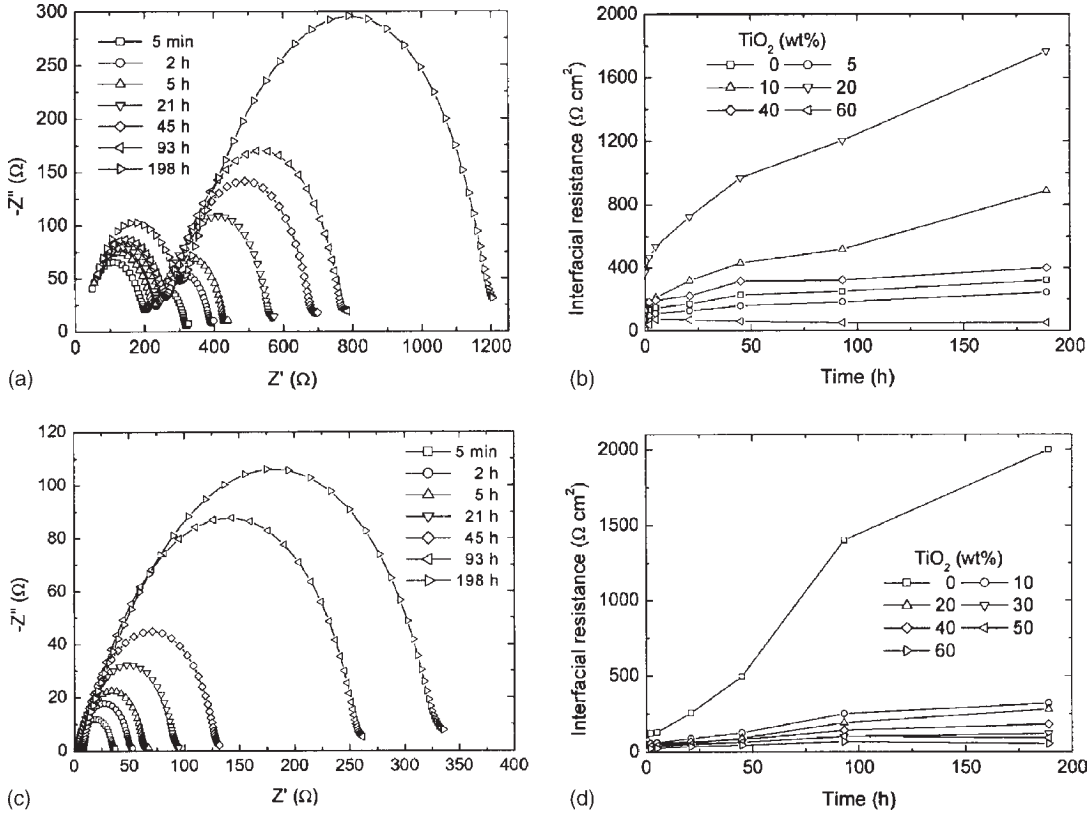


Fig. 6. Impedance spectra of PVdF-HFP/TiO_2 (10 wt.%) electrolytes on lithium electrodes as a function of time, which are prepared by (a) cast and (c) phase inversion techniques. Time evolutions of interfacial resistance between polymer electrolytes of (b) cast film and (d) phase inversion membrane, and lithium electrodes. The electrolyte solution used was 1 M $LiPF_6$ dissolved in EC/DMC (1:1 w/w).

Table 2
Qualitative summary of physical and electrochemical characteristics of PVdF-HFP/TiO_2 polymer electrolytes

Method	TiO_2 (wt.%)	Mechanical strength[a]	Ionic conductivity[b]	Electrochemical stability[c]	Interfacial resistance[d]
Cast	0	O	$>10^{-5}$	O	O
	5	O	$>10^{-6}$	O	O
	10	O	$>10^{-5}$	O	X
	20	O	$>10^{-5}$	O	X
	30	O	$>10^{-4}$	O	X
	40	X	$>10^{-5}$	X	O
	50	X	$>10^{-4}$	X	O
	60	X	$>10^{-4}$	X	O
Phase inversion	0	O	$>10^{-4}$	O	X
	5	O	$>10^{-3}$	O	O
	10	O	$>10^{-3}$	O	O
	20	O	$>10^{-3}$	O	O
	30	O	$>10^{-3}$	O	O
	40	O	$>10^{-3}$	O	O
	50	X	$>10^{-3}$	X	O
	60	X	$>10^{-3}$	X	O

[a] "O" if preserving the shape of self-supporting film when usual light extension by two hands is applied; "X" if breaking.
[b] Ionic conductivity (S cm^{-1}) at room temperature (25 °C).
[c] "O" if the absolute value of maximum current density in cathodic and/or anodic peaks is lower than 0.025 mA cm^{-2}; "X" if higher than 0.025 mA cm^{-2}.
[d] "O" if the interfacial resistance after 200 h is lower than 400 Ω cm^2; "X" if higher than 400 Ω cm^2.

region (4–5 V), as well as by lithium plating reduction in low potential region (0–2 V). Contrary to the cast film electrolytes, the phase inversion membrane electrolytes with 0–40 wt.% TiO_2 behaves with more stabilized cathodic window except a small oxidation wave at 4.8 V versus Li/Li^+. The samples with 30–40 wt.% TiO_2 have some anodic peaks appeared at about 0.7, 1.6, and 2.7 V with low absolute current densities (<0.025 mA cm^{-2}). However, this value of current density is comparatively higher than the case of using SiO_2 as filler [31]. That is, the nanocrystalline TiO_2 particle is more electrochemically active than the SiO_2 nanoparticle with an amorphous nature. This is also true in both electrolytes made from the phase inversion membrane and the cast film. Nonetheless, it is very fortunate that other electrolyte samples with 0–20 wt.% TiO_2 have a good electrochemical stability over 0–5 V (versus Li/Li^+) to be used as the electrolyte medium in lithium rechargeable battery.

Interfacial stability of the PVdF-HFP/TiO_2 electrolytes with the lithium metal electrode can be investigated by the analysis of impedance spectra, e.g., shown in Fig. 6, as a function of time. Impedance spectra for the cast film electrolytes are obviously distinguished from those of phase inversion membrane electrolytes: a small semi-circle at high frequency region, corresponding to the bulk resistance of polymer electrolyte, is followed by a large semi-circle at low frequency region, relating to the interfacial resistance formed on lithium electrode by the reaction with electrolyte components [1,34]. Nearly constant bulk resistance in Fig. 6(a) is due to the compact structure of cast film electrolytes whereas the gradual increase of interfacial resistance reflects the development of passivation layer formed between polymer electrolyte and lithium electrode. As an example of phase inversion membrane electrolytes, the impedance spectra of 10 wt.% TiO_2 sample electrolyte (see Fig. 6(c)) show just one semi-circle that seems to be associated with the interfacial layer formed on inner wall of large pores. Consequently, the resistance of bulk-phase polymer electrolyte becomes so small to be neglected, though its bulk thickness is roughly two to four times higher than the cast film.

Through the time evolution of interfacial resistance, as shown in Fig. 6(b) and (d), one can consider the gradual increase of passivation layer (the increase in resistance) by the reaction continuation with electrolyte components as the time proceeds. Some cast film electrolytes preserve lower interfacial resistance than 400 Ω cm^2 even after 200 h, but the samples with 10–30 wt.% TiO_2 shows much higher resistance that cannot be applied as the electrolyte medium of lithium rechargeable battery. In contrast, all the phase inversion membrane electrolytes have lower interfacial resistance than 400 Ω cm^2 after 200 h except the sample with no TiO_2, which can be estimated as somewhat lower than the case of using SiO_2 [1,31]. It may be due to the pore structure of phase inversion membrane electrolytes filled with TiO_2, in which the growth of passivation layer is getting adjusted to have a proper pore size, so that the interfacial resistance no longer increases or the rate of increasing resistance diminishes with time.

4. Concluding remarks

In the present study, we report comparison of physical and electrochemical properties of PVdF-HFP/TiO_2 electrolytes prepared by casting and phase inversion methods to examine the usability to lithium rechargeable battery. Physical and electrochemical properties of phase inversion samples are proved to have superior characteristics than the cast samples. Comprehensively summarizing such results as shown in Table 2, the phase inversion PVdF-HFP/(5–20 wt.% TiO_2) polymer electrolytes may be the best for the application to lithium rechargeable battery.

Acknowledgement

The authors thank the Korea Ministry of Information and Communication (MIC) for supporting this work through the Contract 2005-S-067.

References

[1] K.M. Kim, K.S. Ryu, S.-G. Kang, S.H. Chang, I.J. Chung, Macromol. Chem. Phys. 202 (2001) 866.
[2] K.M. Kim, N.-G. Park, K.S. Ryu, S.H. Chang, Polymer 43 (2002) 3951.
[3] K.M. Kim, J.M. Ko, N.-G. Park, K.S. Ryu, S.H. Chang, Solid State Ionics 161 (2003) 121.
[4] Z. Li, G. Su, D. Gao, X. Wang, X. Li, Electrochim. Acta 49 (2004) 4633.
[5] M. Wachtler, D. Ostrovskii, P. Jacobsson, B. Scrosati, Electrochim. Acta 50 (2004) 357.
[6] F. Croce, G.B. Appetecchi, L. Persi, B. Scrosati, Nature 394 (1998) 456.
[7] F. Croce, R. Curini, A. Martinelli, L. Persi, F. Ronci, B. Scrosati, R. Caminiti, J. Phys. Chem. B 103 (1999) 10632.
[8] G.B. Appetecchi, F. Croce, L. Persi, F. Ronci, B. Scrosati, Electrochim. Acta 45 (2000) 1481.
[9] B. Scrosati, F. Croce, L. Persi, J. Electrochem. Soc. 147 (2000) 1718.
[10] A.S. Best, J. Adebahr, P. Jacobsson, D.R. MacFarlane, M. Forsyth, Macromolecules 34 (2001) 4549.
[11] J. Adebahr, A.S. Best, N. Byrne, P. Jacobsson, D.R. MacFarlane, M. Forsyth, Phys. Chem. Chem. Phys. 5 (2003) 720.
[12] A.S. Aricò, P. Bruce, B. Scrosati, J.-M. Tarascon, W. van Schalkwijk, Nat. Mater. 4 (2005) 366.
[13] F. Boudin, X. Andrieu, C. Jehoulet, I.I. Olsen, J. Power Sources 81/82 (1999) 804.
[14] T. Michot, A. Nishimoto, M. Watanabe, Electrochim. Acta 45 (2000) 1347.
[15] H. Kataoka, Y. Saito, T. Sakai, E. Quartarone, P. Mustarelli, J. Phys. Chem. B 104 (2000) 11460.
[16] Y. Saito, H. Kataoka, T. Sakai, S. Deki, Electrochim. Acta 46 (2001) 1747.
[17] A. Magistris, P. Mustarelli, E. Quartarone, P. Piaggio, A. Bottino, Electrochim. Acta 46 (2001) 1635.
[18] A. Magistris, P. Mustarelli, F. Parazzoli, E. Quartarone, P. Piaggio, A. Bottino, J. Power Sources 97/98 (2001) 657.
[19] Y. Saito, H. Kataoka, E. Quartarone, P. Mustarelli, J. Phys. Chem. B 106 (2002) 7200.
[20] A. Magistris, E. Quartarone, P. Mustarelli, Y. Saito, H. Kataoka, Solid State Ionics 152/153 (2002) 347.
[21] D.J. Jin, C.L. Chang, F.M. Huang, L.P. Cheng, Polymer 44 (2003) 413.
[22] A. du Pasquier, P.C. Warren, D. Culver, A.S. Gozdz, G.G. Amatucci, J.-M. Tarascon, Solid State Ionics 135 (2000) 249.
[23] C. Capiglia, Y. Saito, H. Kataoka, T. Komada, E. Quartarone, P. Mustarelli, Solid State Ionics 131 (2000) 291.
[24] Y. Saito, H. Kataoka, A.M. Stephan, Macromolecules 34 (2001) 6955.
[25] H. Huang, S.L. Wunder, J. Power Sources 97/98 (2001) 649.
[26] H. Huang, S.L. Wunder, J. Electrochem. Soc. 148 (2001) A279.
[27] A. Bottino, G. Camera-Rota, G. Capannelli, S. Munari, J. Membr. Sci. 57 (1991) 1.
[28] P. Sajkiewicz, Eur. Polym. J. 35 (1999) 1581.
[29] W.M. Prest Jr., D.J. Luca, J. Appl. Phys. 49 (1978) 5042.
[30] H.L. Marand, R.S. Stein, G.M. Stack, J. Polym. Sci. Part B: Polym. Phys. 26 (1988) 1361.
[31] K.M. Kim, N.-G. Park, K.S. Ryu, S.H. Chang, J. Appl. Polym. Sci. (in press).
[32] Y. Rosenberg, A. Sigmann, M. Narkis, S. Shkolnik, J. Appl. Polym. Sci. 43 (1991) 535.
[33] M. Tazaki, R. Wada, M. Okabe, T. Homma, J. Appl. Polym. Sci. 65 (1997) 1517.
[34] G.B. Appetecchi, F. Croce, A. de Paolis, B. Scrosati, J. Electroanal. Chem. 463 (1999) 248.